Proceedings

5th International Scientific and Expert Conference of the International TEAM Society

ISSN 1847-9065 | TEAM 2013, Vol.V, No.1, November 2013.

5th International Scientific and Expert Conference of the International TEAM Society

TEAM 2013

Editors:
Lehocká Dominika
Cárach Ján
Knapčíková Lucia
Hloch Sergej

TEAM

Participants states:
| Austria | Bosnia and Herzegovina | Bulgaria | Croatia | Czech Republic | Hungary | India |
| Iran | Italy | Poland | Romania | Serbia | Slovakia | Slovenia | South Africa | Turkey | Ukraine |

5th International Scientific and Expert Conference of the International TEAM Society

(Technique, Education, Agriculture & Management)

Dominika Lehocká

Ján Cárach

Lucia Knapčíková

Sergej Hloch

Editors

Prešov 4th – 6th November 2013

This book contains the papers suggested by the reviewers for publishing and presentation at the 5th International Scientific and Expert Conference of the International TEAM society to be held during 4th – 6th November 2013 in Prešov, Slovak Republic, EU.

Note

This publication was reproduced from the manuscripts supplied by authors and co-authors. The layout, the figures and tables of some papers did not conform exactly to the standard requirements. In some cases was the layout of the manuscripts rebuild. The editors are not responsible either for the statements made or for the opinion expressed in those papers, published in the proceedings of 5th International Scientific and Expert Conference of the International TEAM society.

Editors:	LEHOCKÁ Dominika
	CÁRACH Ján
	KNAPČÍKOVÁ Lucia
	HLOCH Sergej
Publisher:	TEAM Society
Volume:	V
Number:	1

ISSN 1847-9065

Brief Contents

Chairman Foreword

There is (no) I in TEAM or how to unlock our doubts

Dear Reader,

somewhere I read that there is on „I“ in the TEAM. I think that there is very important I hidden in A – Interdisciplinary.

Angela F. Orviz remarked in her study “Effective Collaboration in Multidisciplinary Teams following „Usually project is not only related just to one area or study. They can be analysed from the perspective of different disciplines. If they are working independently, they can only see the information related to their piece of work. That can have two negative effects in the process. It the pieces of work cannot be joint, it is a waste of time. If the results are similar, it is waste of resources.“

Clean lines, which are kept straightforward by supplemented graduated education, lose their creative fertility. By the way, original discoveries are made by people who stand on the border line and have yet each leg in another space. These border areas are today very frequent. Best researchers are derived from two or more professional fields.

How do we effective create reality? It depends on readiness and kindness, novelty, and mentioned Interdisciplinary.

Crucial milestone on the way to discovery is an idea. It is said that “one” gets the idea. During intellectual adventure, in science, nothing is obtained for free. Everything is paid by talent, education, experience, hard work and interpersonal relationships. If that did not exist, scientific research would look like undemanding moments in the meanwhile.

Even so-called coincidence, e.g. when an apple dropped to Newton´s head, someone had to notice it, to make good conclusions, to understand what was going on and to estimate what could be. Louis Pasteur said that coincidences served only to a ready man. The work of a scientist is a detective work, it is a form of adventure. We discover reality and the “truth”. But the truth is like a coffee bean. Boiled beans after the second and third times: weak smell impresses anyone.

Einstein said "Most people say that it is the intellect which makes a great scientist. They are wrong: it is the character." We are missing the nature, that of unaffected children. Children are not afraid to try their luck. If they do not know, they try. They are not worried to doubt. What is really wrong today? Myth of truth and different opinion. Do not fear about a different opinion. Truth is temporary. Problem is only a challenge. Be sure that no one is perfect. The truth is something we still have to find and improve. Being true is not fixed to academic title or position. If we want to do good research first we have to break all the rules. If we are not prepared to make mistakes, to see the problems we‘ll come out with anything original.

It happened in 2005 in one “innocent” e-mail from Prof. Dražan Kozak during ATDC conference held in Slavonski Brod. This minor incident caused an explosion of the cooperation between Mechanical Engineering Faculty in Slavonski Brod signed by Prof. Dr. Ivan Samardžić and the Faculty of Manufacturing Technologies, Technical University of Košice with a seat in Prešov signed by Prof. Dr. Jozef Novák-Marcinčin. Almost daily communication, many hours spent in scientific discussion, joint meetings, realized incoming and outcoming mobility (Erasmus, Ceepus), projects for industry, collaboration with other institutions, and taking part in the conferences gave as a result 13 joint papers in Journals referred in Web of Knowledge database, 3 monographs, 1 university handbook, and 7 papers published in the International Conference Proceedings.

Currently the great success of the cooperation of Mechanical Engineering Faculty in Slavonski Brod and the Faculty of Manufacturing Technologies is the implementation of approved international scientific project IPA IIIC project OrtoFlex - Flexible manufacturing of customized spinal orthoses, thanks to great work of Prof. Dr. Pero Raos and his project manager assistant Assoc. Prof. Dr. Tomislav Galeta.

Because of a very successful cooperation between the Faculty of Manufacturing Technologies TUKE with a seat in Prešov and two out of three International TEAM Society founders (Mechanical Engineering Faculty and the University of Applied Sciences from Slavonski Brod) our Faculty was invited to host this year TEAM Conference by the president of TEAM Society Prof. Dr. Sc Antun Stoić.

On behalf of TEAM 2013 organization committee, I am pleased to invite You to the 5th International Scientific and Expert Conference of the International TEAM Society (Technique, Education, Agriculture & Management) which will take place on November 4 - 6, 2013, in one of the most dynamic cities of Slovakia - Prešov with a beautiful restored city center and youthful atmosphere under patronage Prof. Dr. Jozef Zajac, the Dean of Faculty of Manufacturing Technologies TUKE with a seat in Prešov.

We would be delighted to have You, Dear reader, present at this conference to hear about the advancements of Your researches and their impact on our daily lives. We would also love to hear Your thoughts and opinions in this direction. Presented papers will be selected for publishing in Technical Gazette and the Journal of Manufacturing and Industrial Engineering. The cooperation between Mechanical Engineering Faculty in Slavonski Brod, Faculty of Manufacturing Technologies TUKE with a seat in Prešov and other mentioned institutions summarizes the words of Henry Ford. “Coming together is a beginning. Keeping together is progress. Working together is success”.

This book includes the proceeding of the 5th International Scientific and Expert Conference of the International TEAM Society, where the latest findings in science and engineering concerned with the technology systems operation are reported. TEAM 2013 conference is arranged under the patronage Dean of the Faculty of the Manufacturing Technologies Technical University of Košice with a seat in Prešov Prof. Dr. Jozef Zajac and TEAM president Prof. Dr.Sc. Antun Stoić.

This year, TEAM organizing committee received more than 110 submissions which authors and co-authors and participants are from 17 different countries of the world. Reviewers and members of the Program committee and their recommendations used for a selection of carefully reviewed all submissions in the spirit of Dražan´s words "Do not prove, but improve". According their advices were accepted more than 100 papers. In addition to the contributed papers, prominent researches were invited to give keynote lectures in their respective fields of competence. For running a conference of this magnitude, financial support is essential. We would like to thank you to LPH, Ltd. Vranov, 1PN Ltd., Prešov, MERCATOR DMS, Ltd. Bratislava, Interprofis v.m., Ltd., Prešov.

This conference bears all the hall marks of success. This is due to the great TEAM work. I would like to thank all those who helped in organization of the TEAM conference especially our colleagues Dr. Lucia Knapčíková, Assoc. Prof. Dr. Tomislav Galeta, Dr. Krunoslav Mirosavljevic, Assoc. Prof. Dr. Peter Monka, Prof. Dr.Sc. Dražan Kozak, Eng. Dominika Lehocká, Eng. Ján Cárach, Eng. Svetlana Radčenko and Eng. Alena Mihaľovová. Smooth running of the conference can be hardly imagined without the devoted presence of Dr. Lucia Knapčíková, Jozef Chomanič the owner of Via Magna and Metropolis.

Thanks belong to the reviewers for their diligence and expert reviewing. Last but not least are the authors who deserve big thank you, their research and development efforts are recorded in those proceedings. We wish you warm welcome and hope that your participation in TEAM 2013 will be enjoyable and also professionally rewarding and we are hoping that the proceedings will be helpful to all scientists and engineers.

To all who came in contact with TEAM in the role of the author or the reader I wish a lot of inspiring results during contact of sport with reality, a fair-play game the outcomes of which will be useful for future generations, papers which will be more than a record in scientific databases.

Instead conclusion I would like to address You some inspiriting words in fantastically written e-mail to me from Prof. Dr.Sc. Damir Markulak: „..it is so easy to recognize bright and motivating mind in today's mostly gloomy (unfortunately) surroundings, where the (even young) people are trying to cut corners, focus on satisfying the form only, engage only a small percent of their creativity that is necessary for acquiring of minimum demands...but, on the other hand, how can we blame them taking into account a role models set as examples of contemporary successful persons, where the only important things (too) often are just acquaintances or affiliations, prior to real skills and knowledge."

Dear reader, how do we want to create our reality?

Hloch Sergej, Assoc., Prof., Ing., PhD.

Foreword of the Mayor of the City of Prešov

Dear Ladies and Gentlemen,

I am delighted to attend today the fifth International Scientific and Expert Conference of the International TEAM society. I believe that this conference will be beneficial not only for the participants but also for the development of cooperation between University and the City of Prešov.

This Conference has encouraged us to see the future of the city and the faculty as a one entity on its way to become a modern and prospering ecological city that uses the advanced technologies.

Prešov has the great potential of the utilizable natural energy. Our main objective is especially the utilization of geothermal energy for heating and also using of the energy for development of tourism and for production of electricity. The unique sources of the geothermal energy are opening big opportunities for our citizens how to cut down energy costs and for its further usage. We would like to utilize the other alternative energy sources like solar energy and biomass. Clean and healthy environment belongs to the main priorities when we are talking about the City of Prešov.

After discussion in Energy-Cites Prešov has been selected as a pilot city for the IMAGINE Campaign. Energie-Cités is the association of European local authorities for the promotion of local sustainable energy policies. Ladies and Gentlemen, Prešov is a seat of the University of Prešov. The students from all parts of Slovakia are studying at the University. There are also other faculties in the city and one of them is the Faculty of Manufacturing Technologies, Technical University of Kosice. The city has an ambition to establish an environment that can offer opportunities for high-class education and also for students' employment. That is the reason why there must be connection between the city, educational institutions and industrial parks. The city needs educated and ambitious people in order to become a prominent European centre. It needs people who will not leave the city but people who will stay in the city that can care of them.

I hope that our collaboration will help us to establish a strong base for the graduates and their potential employers. The relationship with industrial parks will improve the level of the high education not only at this particular Faculty but also it is good opportunity for the other educational institutions in our city. It is also one of the solutions for students to gain experience in the field of their studies and it is the opportunity for the university to get feedback on their education programs directly from the practice. To become a professional, one has to be educated and have a good experience in the field of his study program. The connection of the city and the University will secure not only opportunity for graduates, but also opportunity for students to practice during their studies and see how the technologies are used in industry.

One of the ideas of the cooperation between the city of Prešov and the Faculty of Manufacturing Technologies is to make suitable environment for students in our city. One of the major aims of the city on this successful way is to help students to resolve the problem with an accommodation by building up of new flats. The Municipality has further ambition to build up wellness centres for students and for inhabitants of Prešov. We expect that the University graduates will fulfil the requirements and expectations of the growing city and new coming investors. Education will remain one of the priorities of the city's development. The cooperation of the City and the Faculty is a significant step forwards by reason that they lived independently until this time. Their connection is an important element for the experience of the graduates and for students.

At the present time, the City of Prešov makes an effort to belong to these fast growing cities that will be able to respond to solving such a big challenge as the climate changes and global warming are. The citizens of Prešov do understand the need to cut down energy usage and the importance of combat against climate changes. Municipality of Prešov has clear priorities to achieve concrete results for which the connection between the Faculty and the City will be beneficial.

The City of Prešov has an ambitious aim to be a leader in the Eastern Slovakia region. Prešov is on the best way to become modern and dynamic city that is interesting for its inhabitants as well as it is attractive for tourists. There are also OPAL MINES in our region that are very attractive touristic attraction with its unique "nobel opal". Our plan is to connect OPAL MINES, SALT MINES and GOLDEN MINES together under the open-air mine's museum and to create a great place to visit. We are pleased by the attention of foreign visitors, officials and representatives of the authorities of the European Union that we regularly welcome at our City Hall.

The message of this Conference would be to bring together Faculty and the City and thus enable Prešov to become the ecological and technological city. We look forward to our cooperation with Technical University in Kosice through its Faculty of Manufacturing Technologies with seat in Prešov.

I wish we will meet again on the further Conference in 2014.

JUDr. Pavel Hagyari

Mayor of the City of Presov

TEAM^{2013}

5TH International Scientific and Expert Conference of the International TEAM society

Idea for establishment of international TEAM Society was initiated in year 2009. The TEAM Society funders are Faculty of Mechanical Engineering and Automation, Kecskeméti Föiskola, Hungary, Faculty Mechanical Engineering in Slavonski Brod, University of Osijek and University of Applied sciences of Slavonski Brod.

TEAM Society offers a new identity for Conferences by joining together, networking the institution and changing the forms and importance of the events, since TEAM conferences are organised in the framework of international cooperation and by changing the country and host institution. TEAM Conference is organised to gather scientists and experts of European countries in fields of Technics, Education, Agriculture and Management (the first letter of fields are acronym TEAM) and it is based on results of fruitful international cooperation between institutions in recent years.

Organised by:

Faculty of Manufacturing Technologies with a seat in Prešov, Technical University of Košice |SK

In cooperation

International TEAM society | HR
Kecskemet College, Faculty of Mechanical Engineering and Automation | HU
Institute of Geonics AS CR, v.v.i., Ostrava-Poruba | CZ

Financially supported by (in alphabetical order)**:**

1st Presov tool making company, **Ltd.,** Prešov, Slovak Republic (http://www.1pn.sk)

INTERPROFIS, **Ltd.,** Prešov, Slovak republic

MERCATOR DMS, Ltd., Bratislava, Slovak Republic (http://www.mercator.sk/)

Metropolis Bistro Restaurant, Prešov, Slovak Republic

VIA MAGNA, Prešov, Slovak Republic

Scientific Committee | in alphabetical order

BARTOLOVIČ VIŠNJA	VUSB SLAVONSKI BROD	HR
BEŇO PAVEL	FEMT UNI ZVOLEN	SK
BOŠNJAKOVIĆ MLADEN	VUSB SLAVONSKI BROD	HR
CAR ZLATAN	TF – UNI RIJEKA	HR
ČEP ROBERT	VŠB – TU OSTRAVA	CZ
DIMKOW SVETOSLAV	TECHNICAL UNIVERSITY, SOFIA	BG
DURAKBASA NUMAN M.	VIENNA UNIVERSITY OF TECHNOLOGY	A
FOLDYNA JOZEF	INSTITUTE OF GEONICS AS CR	CZ
GALIĆ RADOSLAV	ETFOS, UNI OSIJEK	HR
GUBELJAK NENAD	FS, UNI MARIBOR	SLO
HATALA MICHAL	FVT TUKE	SK
HERZOG MICHAEL	TH WILDAU	D
HODOLIČ JANKO	UNIVERSITY OF NOVI SAD	RS
CHATTOPADHYAYA SOMNATH	INDIAN SCHOOL OF MINES, DHANBAD	IN
HOLEŠOVSKY FRANTIŠEK	FPTM UNI J. E. PURKYNĚ ÚSTÍ NAD LABEM	CZ
HVIZDOŠ PAVOL	SLOVAK ACADEMY OF SCIENCE	SK
IVANDIĆ ŽELJKO	MEFSB UNI OSIJEK	HR
JOSIPOVIC MARKO	AGRICULTURAL INSTITUTE OSIJEK	HR
JURAGA IVAN	FAMENA UNI ZAGREB	HR
KANDÁR MILAN	SLOVAK AGRICULTURE UNIVERSITY NITRA	SK
KLADARIĆ IVICA	MEFSB UNI OSIJEK	HR
KLJAJIN MILAN	MEFSB UNI OSIJEK	HR
KOLEDA PETER	TECHNICAL UNIVERSITY IN ZVOLEN	SK
KOVÁCZ BEATRIX	GAMF KECSKEMET	HU
KOVÁCZ LÓRANT	GAMF KECSKEMET	HU
KOZAK DRAŽAN	MEFSB UNI OSIJEK	HR
LACATUS ELENA	POLITECHNICA UNIVERSITY BUCHAREST	RO
LEE HO-SUNG	KOREA AEROSPACE RESEARCH INSTITUTE, DAEJUN	KR
LEGUTKO STANISLAW	POZNAN UNIVERSITY OF TECHNOLOGY	PL
MAGLIĆ LEON	MEFSB UNI OSIJEK	HR
MARKOVIČ MONIKA	UNI OSIJEK	HR
MARÔNEK MILAN	FMSTSUT TRNAVA	SK
MILKOVIĆ MARIN	VELV VARAŽDIN	HR
MIROSAVLJEVIĆ KRUNOSLAV	VUSB SLAVONSKI BROD	HR
MLÁDKOVÁ LUDMILA	UNIVERSITY OF ECONOMICS, PRAGUE	CZ
MODRÁK VLADIMÍR	FVT TUKE	SK
MONKA PETER	FVT TUKE	SK
MONKOVÁ KATARÍNA	FVT TUKE	SK
MULLER MIROSLAV	CZECH UNIVERSITY OF LIFE SCIENCE	CZ
NOVÁK MARCINČIN JOZEF	FVT TUKE	SK
OBAR MILENKO	FEC UNI MOSTAR	BA
OHLÍDAL MILOSLAV	SF VÚT BRNO	CZ
PAŠKO JÁN	FVT TUKE	SK
PAVIĆ ZLATKO	MEFSB UNI OSIJEK	HR
PETROPOULOS GEORGE	UNIVERSITY OF THESSALAY	GR
PIŠTORA JAROMÍR	VŠB – TU OSTRAVA	CZ
PLANCAK MIROSLAV	UNIVERSITY OF NOVI SAD	HR
PREINER DARKO	UNIVERSITY OG ZAGRED	HR
RAOS PERO	MEFSB UNI OSIJEK	HR
RUGGIERO ALESSANDRO	UNIVERSITY OF SALERNO	I
RUŽBARSKÝ JURAJ	FVT TUKE	SK
SAMARDŽIĆ IVAN	UNI OSIJEK	HR
ŠARIĆ TOMISLAV	MEFSB UNI OSIJEK	HR
SEDMAK ALEKSANDAR	MF UNI BELEGRADE	RS
SEGOTA SUZANA	RUDER BOSKOVIC INSTITUTE	HR

SENNAROĞLU BAHAR	MARMARA UNIVERSITY, ISTANBUL	TR
ŠERCER MLADEN	FAMENA UNI ZAGREG	HR
SHARMA VINAY	BIRLA INSTITUTE OF TECHNOLOGY, MESRA	IN
SIMUNOVIC KATICA	SFSB SLAVONSKI BROD	HR
ŠIMUNOVIĆ GORAN	MEFSB UNI OSIJEK	HR
ŠOSTARIĆ JASNA	PFOS UNI OSIJEK	HR
STOIĆ ANTUN	VUSB SLAVONSKI BROD	HR
ŠUGAR PETER	FACILTY OF MAT. SCI. AND RECHN. IN TRNAVA	SK
SURZENKOV ANDREI	TALLINN UNIVERSITY OF TECHNOLOGY	EE
TÓTH ÁKOS	GAMF KECSKEMET	HU
TOZAN HAKAN	TURKISH NAVAL ACADEMY, ISTANBUL	TR
TRAUSSNIGG UDO	CAMPUS 02 TU GRAZ	A
TROPŠA VLADO	VELV VARAŽDIN	HR
VÁCLAVÍK VOJTECH	VŠB – TU OSTRAVA	CZ
VALÍČEK JAN	VŠB – TU OSTRAVA	CZ
VASILKO KAROL	FVT TUKE	SK
VAYVAY ÖZALP	MARMARA UNIVERSITY, ISTANBUL	TR
VINAY SHARMA	BIRLA INSTITUTE OF TECHNOLOGY	IN
YASHAR JAVADI	ISLAMIC AZAD UNIVERSITY – SEMNAN BRANCH	IR
ŽIVIĆ MARIJA	MEFSB UNI OSIJEK	HR

Proceedings Contents

Keynote Lectures | in presentation order

Regular Section | in received order

Authors Index

I

J

K

L

M

N

O

P

Q

R

S

T

U

V

Z

Keynote Lectures

INFILTRANTS AND ROUGHNESS OF 3D PRINTED MODELS

Tomislav Galeta[1*], Goran Šimunović[1] and Ante Ćurić[1]

[1]Mechanical Engineering Faculty in Slavonski Brod, J. J. Strossmayer University of Osijek, Croatia
* *Corresponding author e-mail: tgaleta@sfsb.hr*

Abstract
3D printing developers persistently introduces new base materials and various strengthening infiltrants. Professional users need detailed information about properties of 3D printed models and they often ask about surface roughness. Therefore in this paper we have tested roughness of 3D printed samples strengthened with usual but also with alternative infiltrants.
In order to estimate possible enhancement, after initial roughness measurement raw samples were sanded and roughness were measured again
The lowest average roughness was obtained for samples infiltrated by cyanoacrylate, followed by wax and Protektin. The highest average roughness was for water and for epoxy resin.
Sanding of samples had lowered roughness significantly for water and epoxy resin, thereby leveling it to values of other infiltrants. For other infiltrants, sanding had not provided noteworthy improvement of roughness.

Keywords:
3D printing, roughness, strengthening infiltrants

1. Introduction

What surface quality can be achieved for models printed on 3D printer? Could it complies with the user requirements so 3D printed models could have a wide application? Does the quality of the surface change if it inflicts some reinforcements? These are all questions that have been arisen, especially the last few years as technology of 3D printing has advanced and the increased use of such objects in everyday life [1]–[3].
In this paper we have tried to answer previous questions with the study that was conducted on specimens printed on a 3D printer. The base material for models used in our study was plaster-based and models were reinforced with different infiltrates. Then we made roughness measurement using a suitable device to original raw specimens, and again on the same specimens after sanding.

2. Method

Samples used in this study were printed on Z Corporation's 3D printer model ZPrinter 310 [4]. It is a low-cost monochrome 3D printer suitable for education or for small and medium sized companies. The printer firmware version was 10.158 and test samples were prepared in a printer software ZPrint version 7.10.

The considered 3D printer combines a layered approach from rapid prototyping technologies and a conventional ink-jet printing. It prints a binder fluid through the conventional ink-jet print head into a powder, one layer onto another, from the lowest model's cross-section to the highest (Figure 1). After printing, the printed models are dried in the building box, then removed from the powder bed, de-powdered by compressed air, dried in the oven and infiltrated for maximum strength.

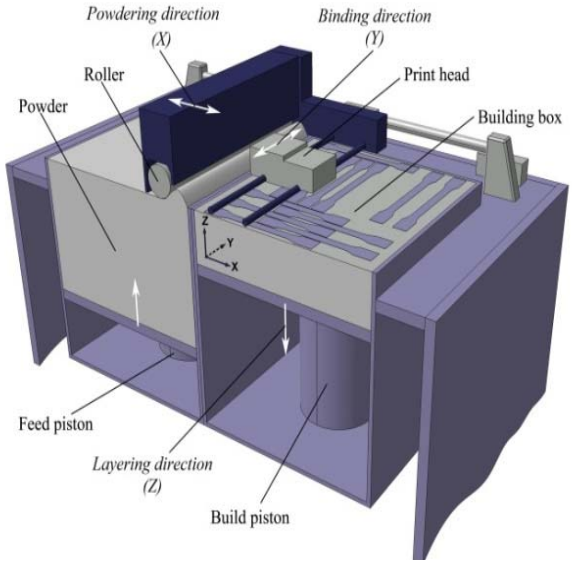

Figure 1. 3D Printer - section view

The base material from which samples were printed was the ZP150 powder [5]. Following strengthening infiltrants were used: water based Epsom salt water solution; wax; acrylate resin Protectine [6]; cyanoacrylate Loctite 406 and epoxy resin Loctite Hysol 9483. One set of 3D printed samples were left without strengthening infiltrants. Standard shape type 1A of tensile test samples was selected in order to reuse samples in planned further researches [7].
Device used for roughness measuring was Rugosurf 10G with related equipment for calibration and with software for data processing [8]. Before the measurement, device was calibrated to the corresponding standards and connected to a computer with installed belonging software Rugosoft 10G [9].

Figure 2. Measuring procedure

Roughness measurements were performed on every specimen, three times for each observed side of sample. Observed sides were named conveniently as Front, Top and Side, as shown in Figure 3.

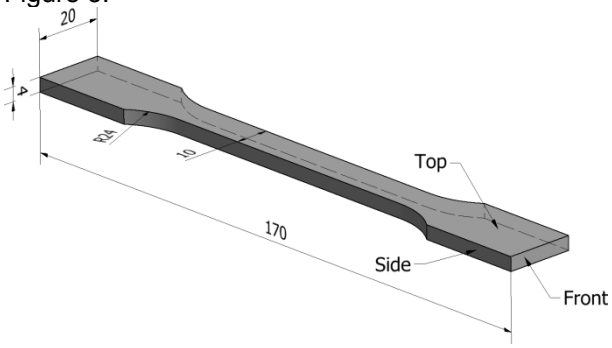

Figure 3. Test sample and side naming

In doing so, the roughness on the top i.e. the greatest upper side was measured in both longitudinal (L) and transversal (T) directions. On the device selected standard was ISO4287/JIS B0601 for measuring roughness with the cut-off length λ of 0,80 mm and the number of displacements 7. Such combination gives an overall length of 5,6 mm on which roughness were measured, Figure 4.

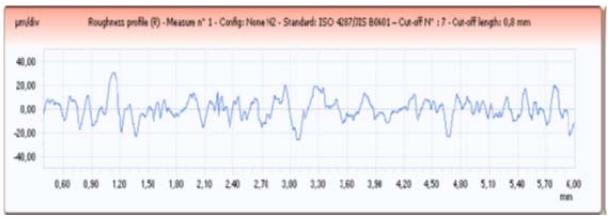

Figure 4: Roughness profile for sample N2 top side longitudinal direction

After initial measurements, raw samples were sanded with 800 grit sandpaper and the complete measurement process was repeated.

3. Results

As results of measurements we present: maximum height of profile *Rz* [μm] and the average deviations from the estimated profile *Ra* [μm]. Values presented in following tables and later graphs are arithmetic mean of the results obtained by three measuring for each sample and each side.

Table 1. Roughness of raw samples [μm]

		Top L	Top T	Side	Front
None	*Ra*	8,43	8,03	15,88	14,72
	Rz	46,03	44,55	76,93	73,46
		Top L	Top T	Side	Front
Water	*Ra*	11,70	7,91	15,12	20,83
	Rz	62,52	44,28	74,60	95,29
		Top L	Top T	Side	Front
Wax	*Ra*	7,10	6,84	12,50	13,64
	Rz	39,14	35,14	62,09	64,25
		Top L	Top T	Side	Front
Protektin	*Ra*	7,42	11,82	15,35	17,54
	Rz	37,51	57,61	73,87	83,75
		Top L	Top T	Side	Front
Cyanocrylate	*Ra*	5,32	6,65	8,29	9,47
	Rz	25,42	32,16	38,28	45,32
		Top L	Top T	Side	Front
Epoxy resin	*Ra*	11,72	9,47	16,01	18,49
	Rz	62,33	49,85	75,59	88,96

Table 2. Roughness of sanded samples [μm]

		Top L	Top T	Side	Front
None	*Ra*	13,75	12,89	9,40	11,20
	Rz	68,79	56,11	66,41	60,19
		Top L	Top T	Side	Front
Water	*Ra*	6,18	4,23	12,44	12,99
	Rz	32,91	33,00	24,18	60,07
		Top L	Top T	Side	Front
Wax	*Ra*	5,84	3,17	5,88	5,17
	Rz	29,57	29,57	16,82	27,11
		Top L	Top T	Side	Front
Protektin	*Ra*	6,64	8,31	13,65	10,80
	Rz	32,13	32,13	39,83	52,45
		Top L	Top T	Side	Front
Cyanocrylate	*Ra*	4,75	7,48	9,43	3,92
	Rz	22,11	22,11	36,68	20,37
		Top L	Top T	Side	Front
Epoxy resin	*Ra*	6,50	3,89	10,38	6,18
	Rz	35,01	35,01	22,60	33,97

4. Discussion

In next few charts we can see the relationship of measured values due to variety of reinforcements and surface condition (raw/sanded).

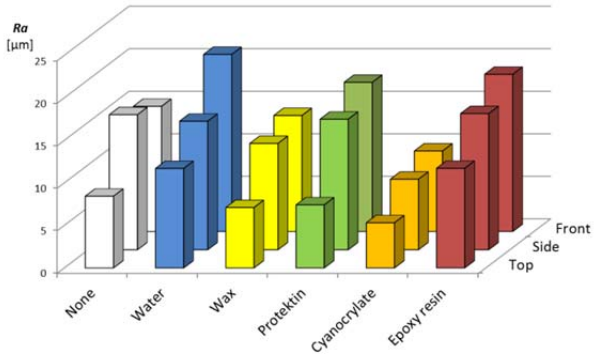

Figure 5. Average roughness of raw samples

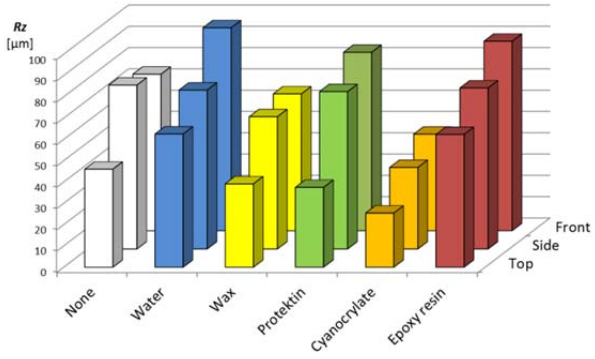

Figure 6. Maximum profile height of raw samples on top face in longitudinal direction

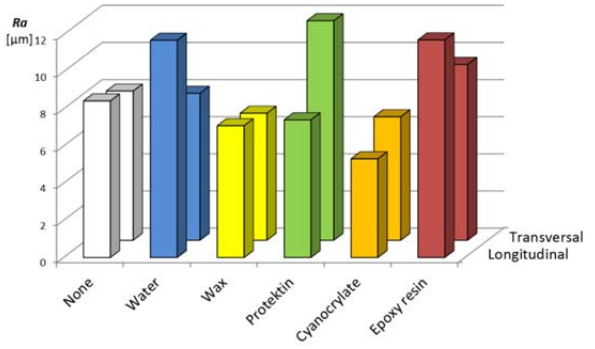

Figure 7. Average roughness of raw samples on top face in longitudinal and transversal directions

Comparison of average roughness of raw samples on top face in longitudinal and transversal directions reveals significant deviations for all samples except for those strengthened with wax. Following charts show comparison of values *Ra* and *Rz* for the sanded samples.

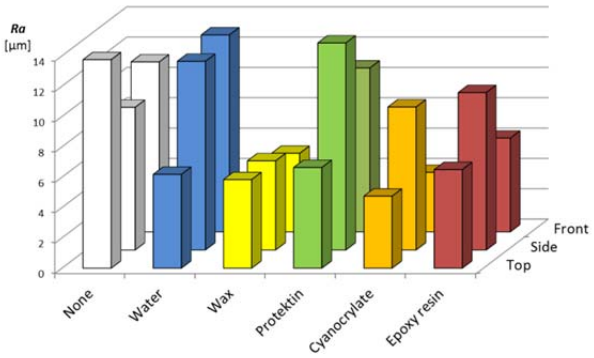

Figure 8. Average roughness of sanded samples

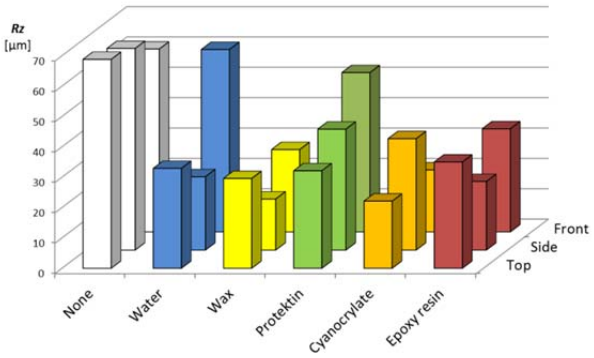

Figure 9. Maximum profile height of sanded samples

From previous figures could be noticed decrease of both average roughness and maximum profile height after the samples were sanded. The only exception is sample that was not treated with hardener since in this case roughness was increased compared to the raw state. For better evaluation, comparison is presented in separate figure.

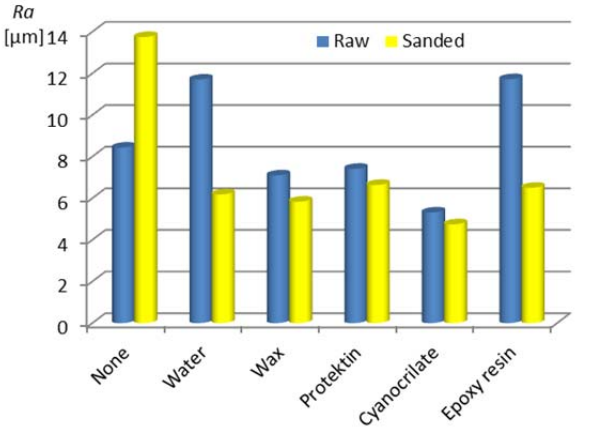

Figure 10. Comparison of average roughness for raw and sanded samples, top face, longitudinal direction

Graph on Figure 10 clearly shows significant difference between average roughness of raw and sanded specimens. However, average roughness of unreinforced sanded sample is greater than original raw sample. This phenomenon could be explained with appearance of the lamellas during sanding of unreinforced samples. It occasionally leads to removal of multiple layers of material and the surface becomes wavy.

5. Conclusion

Strengthening infiltrants have a significant influence on roughness of 3D printed model. Therefore it is necessary to carefully select appropriate infiltrant if roughness is dominant required properties of model.

The best surface roughness for 3D printed models provides cyanoacrylate, followed by wax and then other infiltrants.

Sanding provides better surface quality, especially for faces printed in direction of layer deposition, here faces named Front and Side. However, here one should pay attention to the other properties of 3D printed models. It is possible that with the desire for higher quality of surface sanding remove too much reinforced material and therefore decrease other mechanical properties. In order to avoid undesired degradation of other properties, cross-section of 3D printed models should be investigated under the microscope to determine how deep selected infiltrant penetrates. Such research will help to determine whether sanding leads to a significant decrease in mechanical properties.

6. Acknowledgement

Authors wish to thank engineers Miroslav Mazurek and Vladimir Pecić for their assistance in experiments; to Ivan Sertić, director of Industrial Park Nova Gradiška Ltd for providing measuring equipment. The work presented in this paper was financially supported by the Ministry of Science, Education and Sports of the Republic of Croatia through the several scientific research projects.

7. References

[1] D. Ahn, J.-H. Kweon, J. Choi, and S. Lee, “Quantification of surface roughness of parts processed by laminated object manufacturing,” *J. Mater. Process. Technol.*, vol. 212, no. 2, pp. 339–346, Feb. 2012.

[2] A. Butscher, M. Bohner, N. Doebelin, L. Galea, O. Loeffel, and R. Müller, “Moisture based three-dimensional printing of calcium phosphate structures for scaffold engineering,” *Acta Biomater.*, vol. 9, no. 2, pp. 5369–5378, Feb. 2013.

[3] A. Butscher, M. Bohner, S. Hofmann, L. Gauckler, and R. Müller, “Structural and material approaches to bone tissue engineering in powder-based three-dimensional printing,” *Acta Biomater.*, vol. 7, no. 3, pp. 907–920, Mar. 2011.

[4] D. E. Webster, “ZPRINTER 310 PLUS HARDWARE MANUAL.” Z Corporation, Aug-2007.

[5] “zp150 powder MATERIAL SAFETY DATA SHEET.” Z Corporation, Jun-2009.

[6] A. Mikus, “Protektin Tehnična Informacija.” SAMSON KAMNIK d.o.o., Apr-2004.

[7] “ISO 527-2-2012 Plastics — Determination of tensile properties — Part 2 Test condition for moulding and extrusion plastics.pdf.” ISO, Mar-2012.

[8] “TESA RUGOSURF 10G Surface roughness gage.” TESA –TECHNOLOGY, Jul-2007.

[9] Reichert, “User manual Rugosoft 10 / 10G Software for Rugosurf 10 / 10G.” TESA – TECHNOLOGY, Jul-2007.

PULSATING WATER JET – A TOOL FOR THE FUTURE?

Josef Foldyna[1*]

[1]Institute of Geonics of the ASCR, Ostrava, Czech Republic
** Corresponding author e-mail: josef.foldyna@ugn.cas.cz*

Abstract
Phenomenon arising during the impact of a droplet on the solid surface and its utilization to enhance effects of water jetting is described in the paper. Some examples of superior performance of pulsating water jets over the continuous ones are presented.

Keywords:
Pulsating water jet, pressure pulsations, impact pressure, erosion effects.

Motto: "Gutta cavat lapidem non vi, sed saepe cadendo" - A drop of water hollows a stone, not by force, but by continuously dripping (Ovid, Epistulae ex Ponto).

1. Introduction

Effects of high-speed water jets in the material disintegration are well known to the professional public. A pure water compressed up to the pressure of 415 MPa using commonly used high-pressure pumps and discharged through a very small opening (i.e. the nozzle orifice having the internal diameter from tenths to units of millimetres) has enough energy to cut soft and/or thin materials, such as paper, wood, plastics, rubber, thin metal sheets. The area of usability of water jets is extended significantly when abrasive particles are added to the high-speed water jet either downstream the nozzle exit (abrasive water jets) or upstream the nozzle exit (abrasive suspension jets). The abrasive jets are able to cut, drill, turn or mill not only metals but also hard to work materials such as composites, load-bearing ceramics, high-strength alloys, glass and rocks. At present, there is not known any material that could not be disintegrated by abrasive water jets.
However, despite the impressive technological advances made recently in the field of water jetting applications, there is permanent worldwide demand for further development of technologies utilizing pure water jets only. Therefore, substantial attention of number of research teams throughout the world is still paid to the improvement of the performance of the technology, its adaptation to environmental requirements and making it more beneficial from the economic point of view.
One of possible approaches to the improvement of the pure water jetting performance is generation of the jets at ultra-high pressures. The feasibility of cutting metals with pure water jets at pressures close to 690 MPa was investigated already in early nineties of the last century [1]. At present, high-pressure pumps capable to pressurize water up to 700 MPa are commercially available for water jet cutting. Such a high pressure, however, induces extreme overtension of high-pressure parts of the cutting system which has adverse effect on their lifetime.
An alternate approach was taken by researchers from the Institute of Geonics of the ASCR in Ostrava. The approach can be characterized by the effort to eliminate need for such extreme pressures by the utilization of a physical phenomenon arising during the impact of a droplet on the solid surface.

2. Background

The collision of a high-velocity liquid mass with a solid generates transient accompanied with substantial increase in pressure at the point of impingement of the liquid on the surface. The phenomenon can cause serious damage both to the surface and interior of the material exposed to effects of the impinging liquid. An understanding of the dynamics of liquids undergoing collisions with solids is needed in a number of technological situations. In the past, the erosion of steam turbine blades stimulated interested in the study of effects occurring during liquid impact on the solid surface. At present, there is considerable research on the rain erosion of aircraft and missiles, particularly the ''window'' materials. Cavitation damage is also closely linked to the liquid impact.
The liquid impact on a solid surface consists of two main stages (see Figure 1). During the first stage, the liquid behaves in a compressible manner generating the so-called ''water-hammer'' pressures. These high pressures are responsible for most of the damage resulting from liquid impact on the solid surface.

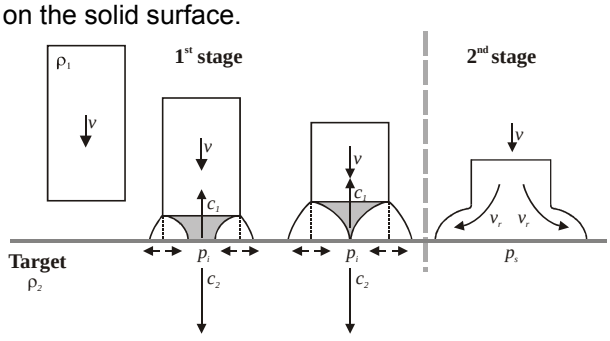

Figure 1. Two stages of liquid impact on a solid target

The situation shortly after the initial impact of the liquid on the solid surface is illustrated in Figure 2.

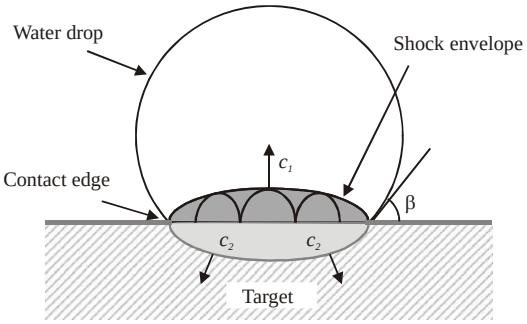

Figure 2. Initial stage of impact between a water drop and a solid target with the contact edge moving faster than the shock velocity in the liquid. The liquid behind the shock envelope is compressed and the target beneath this area subjected to high pressure. [2]

The force distribution on liquid jet impact on the solid surface can be summarized as follows: initially a small central area of the first contact is compressed under a uniform pressure. The magnitude of the impact pressure p_i on the central axis is given by

$$p_i = \frac{v\rho_1 c_1 \rho_2 c_2}{\rho_1 c_1 + \rho_2 c_2} \quad (1)$$

where v is the impact velocity and ρ_1, ρ_2 and c_1, c_2 are the densities and the shock velocities in the liquid and the solid, respectively [3].
The magnitude of the impact pressure is independent of the geometry of the drop [4], but the duration of the pressure is affected by the size and shape of the drop.
The impact pressure lasts for the short period, Δt, that takes a release wave, generated at the contact edge of the jet, to reach the impact axis. This time can be expressed as

$$\Delta t = \frac{3rv}{2c_1^2} \quad (2)$$

where r is the radius of curvature of the drop or cylinder (liquid mass) in the region of contact.
After the release of the impact pressure, the second stage of the liquid impact begins. Once incompressible stream line flow is established, the pressure on the central axis falls to the much lower Bernoulli stagnation pressure, p_s, that lasts for relatively long time. The stagnation pressure is given by

$$p_s = \frac{1}{2}\rho_1 v^2 \quad (3)$$

The outward flow of the liquid becomes possible when the limit of the compressible deformation of the liquid is exceeded. The limit is given by

$$\frac{v}{c_1} = \sin\beta \quad (4)$$

where β is the liquid/solid interface angle [2].
When the liquid begins to flow away from the point of impact, there is evidence that the velocity of this tangential flow may be as much as five times the impact velocity [4]. The velocity increase is thought to be connected with the shape of the head of the jet. It has been observed that an increase in velocity along the surface occurs only in cases where the jet head is inclined at an angle to the surface. Since spherical drops (and/or spherical heads of a train of pulses of pulsating jet) always provide a sloping interface to a plane solid surface it might be expected that high radial velocities will occur on impact. Therefore, there are additional shear forces associated with the high speed flow across the surface acting on the surface in addition to the normal forces. If the surface is stepped, roughened or broken in any way, very large shear forces are produced by the impingement of the flow against the projections in the surface. For example, for impact velocities which are as low as 90 m s^{-1}, the shear forces acting on a roughened surface are large enough to cause local shear fractures, even in high strength materials [2].
When one compares values of impact and stagnation pressures, the impact pressure can be 4 to 10 times higher than the stagnation pressure at jet velocities commonly used in water jetting technology. Because the continuous water jet generates basically only stagnation pressure at the point of contact with solid surface, it is desirable to divide continuous stream of water into train of "droplets" that will be able to generate also impact pressures and thus utilize all of above described effects accompanying the droplet impact on the solid material to enhance effects of high-speed water jets.

3. Pulsating water jets

The researchers from the Institute of Geonics verified experimentally in laboratory conditions the idea to create pulsating water jet by generating of sufficiently high pressure pulsations upstream from the nozzle exit. The pulsating water jet emerges from the nozzle as a continuous liquid jet but owing to the variable pressure at the nozzle exit jet velocity also changes. Faster parts of the jet tends to „catch up" slower ones and, as a result, originally continuous jet forms into pulses at certain standoff distance from the nozzle exit. The impacts of individual pulses on the solid surface then generates cyclically all the above mentioned effects connected with droplet impact. In addition, the action of pulsating jet induces also fatigue stress in the target material due to the cyclic loading of the target surface. This further improves the efficiency of the pulsating liquid jet in comparison with the continuous one [5].
An intensive research on pulsating water jets at the Institute of Geonics started in 2000. An original

method of generation of pulsating liquid jet was gradually developed and tested extensively under the laboratory conditions. The method is based on the generation of acoustic waves by the action of the acoustic transducer on the pressure liquid and their transmission via pressure system to the nozzle. The method described in detail in [6] can be used to create puslating jet generating tens of thousands pulses per second.

4. Effect of pulsating water jets on materials

Effects of pulsating water jets with the frequencies of pulses of 20 and 40 kHz were tested in laboratory conditions on various types of materials, such as metals, rocks and concrete. Tested materials were exposed to the action of diverse types of jets: single round and fan pulsating jets as well as rotating pulsating jets. The effects of pulsating jets were evaluated in terms of cutting depth, rate of mass-loss or volume removal rate respectively and compared with the effects of continuous water jets under the same operating conditions.

Obtained results show clearly the supremacy of pulsating water jets over continuous ones in terms of their effects on material. Figure 3 illustrates the effects of round pulsating water jet on brass and mild steel samples. The pulsating jet eroded deep grooves in both samples, as can be seen in figure. The continuous jet acting on the same metal samples under the same operating conditions does not produce any visible erosion traces on the sample surface.

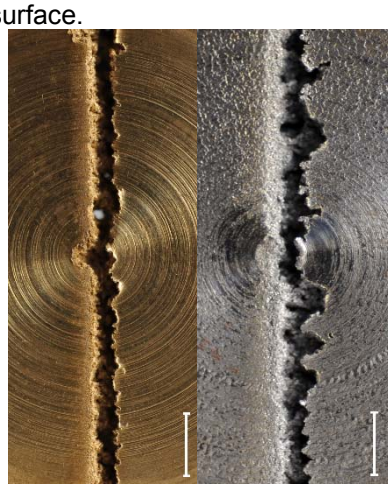

Figure 3. Grooves eroded by pulsating water jet in brass (left) and mild steel (right) samples. Pressure 70 MPa, nozzle diameter 1.2 mm, traversing velocity 1 mm.s^{-1} (white section of a line represents 5 mm)

The comparison of effects of flat continuous and pulsating water jets on concrete sample can be seen in Figure 4. While continuous jets removed only the upper part of the cement paste, pulsating jets penetrated deeper and removed cement paste to aggregates under given testing conditions. A higher roughness of the concrete substrate treated by pulsating jets leads to the better adhesion of newly applied layers of repair coatings and mortars.

Figure 4. Example of surfaces created by three passes (side by side) of both flat continuous (left) and flat pulsating (right) jets on concrete sample (water pressure 30 MPa, equivalent nozzle diameter 2.05 mm, stand off distance 40 mm, traversing velocity 0.2 m.min^{-1})

The application of pulsating water jets in ornamental stone surface treatment was tested on three different types of rocks (granite, basalt, and marble). Characteristics of rock surfaces created by acting of pulsating water jets were compared to those created by traditional methods, namely polishing, bush hammering and flaming. Results obtained up to now indicate that the application of pulsating water jets in surface treatment of ornamental stones can reduce (or even eliminate) disadvantages of traditional techniques because it creates surface with required roughness but preserves its aesthetical appearance.

The possibility of use of pulsating water jets for surface treatment (so called pulsating water jet peening) was tested on Almen strips samples [7]. The results of the experiments performed so far show that pulsating water jet can be an effective tool for the surface treatment. As can be seen in Figure 5, efficiency of pulsating water jet is more than ten times higher in comparison with continuous water jet for pressures of around 20 MPa. Subsurface residual stress gradients resulting from pulsating water jet peening are also a significant element of the surface integrity and will be identified in future studies.

Tests of disintegration of bone cement proved the potential of the use of pulsating ware jets also in medical applications [8]. Results from performed experiments show that the pulsating water jet is a viable technology for bone cement removal due to very low pressures necessary for disintegration of bone cement – see Figure 6.

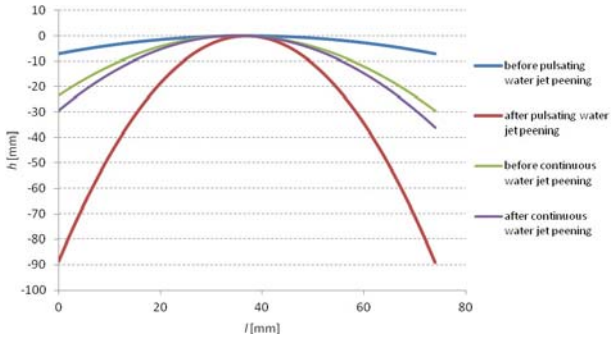

Figure 5. Comparison of peening intensity of continuous water jet peening versus pulsating water jet peening (t_p = 2 s·mm^{-1}; p = 20 MPa)

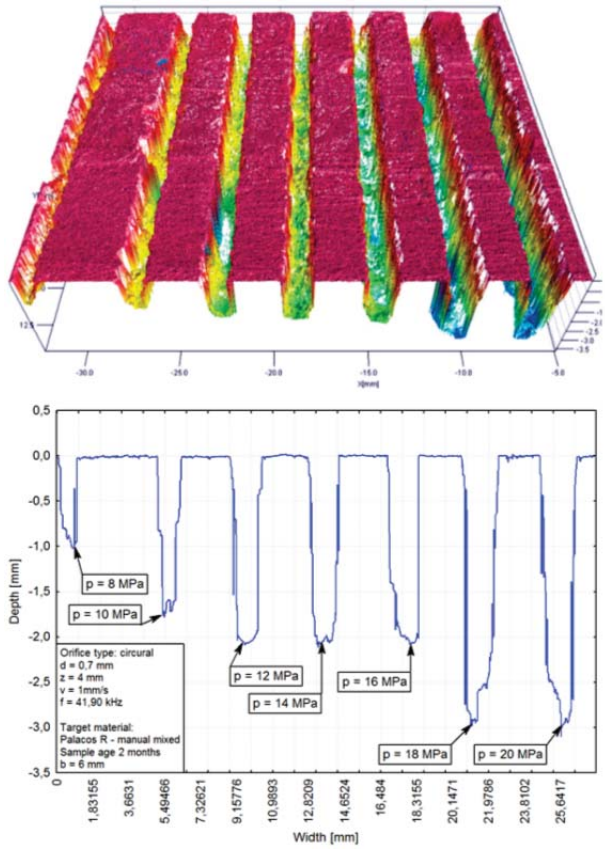

Figure 6. Bone cement Palacos R+G® surface 3D profile (top) and 2D depth profile (bottom) measured by MicroProf FRT – Traces created by pulsating water jet with circular orifice MVT d = 0,7 mm

Further research in this area will be aimed at the evaluation of disintegration of different kinds of bone cements commercially used in orthopaedic practise.

5. Conclusion

Designed and realized proprietary systems for generation of pulsating water jets using the acoustic generator to produce pressure pulsations in the high-pressure system at frequencies of 20 and 40 kHz proved significant improvement of effects of pulsating water jets on various materials compared to continuous ones. The results obtained so far show that pulsating water jets have a great potential to replace continuous ones in many applications and even to spread the use of water jetting technology to new areas where the technology is not used yet.

6. Acknowledgement

The article was written in connection with project Institute of clean technologies for mining and utilisation of raw materials for energy use, reg. no. CZ.1.05/2.1.00/03.0082, which is supported by the Research and Development for Innovations Operational Programme financed by the Structural Founds of the Europe Union and the state budget of the Czech Republic. Presented work was supported also by the Academy of Sciences of the Czech Republic, project RVO: 68145535. Authors are thankful for the support.

7. References

[1] C. Raghavan, E. Ting, “Hyper pressure waterjet cutting of thin sheet metal”, *Proceedings of 6th American Water Jet Conference*, 1991.

[2] N. L. Hancox, J. H. Brunton, “The erosion of solids by the repeated impact of liquid drops”, *Philosophical Transactions of the Royal Society of London, Series A, Mathematical and Physical Sciences*, Vol. 260, No. 1110, 1966.

[3] P. de Haller, “Untersuchungen über die durch Kavitation hervorgerufenen Korrosionen”, *Schweizerische Bauzeitung*, Vol. 101, No. 21& 22, 1933.

[4] G. P. Thomas & J. H. Brunton, “Drop impingement erosion of metals”, *Proceedings of the Royal Society of London. Series A, Mathematical and Physical Sciences*, Vol. 314, No. 1519, 1970.

[5] J. Foldyna, L. Sitek, B. Švehla, Š. Švehla, “Utilization of ultrasound to enhance high-speed water jet effects”, *Ultrasonics Sonochemistry*, Vol 11/3-4, 2004

[6] J. Foldyna, B. Švehla, “Method of generation of pressure pulsations and apparatus for implementation of this method”, *US patent No. 7,934,666*, 2011.

[7] P. Hlaváček, J. Klich, J. Foldyna, L. Sitek, “Measurement and evaluation of pulsating water jet peening intensity”, Proceedings of the Conference on Water Jetting Technology Water Jet 2013 – Research, Development, Applications, 2013.

[8] S. Hloch et al., „Disintegration of Bone Cement by Continuous and Pulsating Water Jet“, Technicki vjesnik - Technical Gazette, vol. 20, No. 4, 2013.

INVESTIGATION INTO COAL CUTTING OPERATION BY USING SHAPER MACHINE AS A LINEAR CUTTING RIG

Saurabh Dewangan, Somnath Chattopadhyaya

Department of Mechanical Engineering, Indian School of Mines, Dhanbad, India
Email:somuismu@gmail.com

Abstract
This paper presents the analysis of coal fragmentation due to cutting action of a tool bit. An experiment was performed with the aid of a shaper machine using conical cutting pick to simulate the cutting action of the tool of the excavating machines. A shaper machine was used as a linear cutting rig. During the tests the number of parameters such as depth of cut, average cutting velocity, force, material removal rate, and angle of attack were monitored. The test results were analyzed and plotted considering different parameters like weight of coal removed, depth of cut, angles of attack to obtain fragmentation behaviour of coal.

Keywords: Conical cutting pick; Depth of cut; Attack angle; Material removal rate; Tool life.

1. Introduction

In recent year the application of mechanical excavators for rock and coal excavation has increased significantly in mining engineering field. Shearer, continuous miner, road headers are the few of these machines which have found their wide application in the field of excavation for higher rate of production. Tool bits and their operational life and cutting parameters associated with them have great impact on the performance of these machines. The analysis of tool bit cutting performance becomes a necessity in order to provide basic data for machine selection, design and performance prediction. A number of researchers have studied about theoretical aspect of coal and rock cutting process. *Roxborough et al. (1981)* concluded that cutting efficiency improves markedly as the depth of cut per revolution of the drum increases, and that the best spacing of picks on the drum is twice the depth of cut. Pick shape is of secondary importance in terms of cutting efficiency, only small differences have been found between the performances of conical and chisel shaped tools[1, 2]. However, the most comprehensive and accepted theories are those of *Evans* [3-6] for chisel and conical picks.

Conical picks are the essential cutting tools which are used on many mechanical excavators. During cutting action of conical picks, its shape remained sharp due to symmetrical wear [7]. Conical tool bit provides better efficiency due to lowest specific energy for penetration [8]. In this paper, conical shaped cutting pick was chosen for the coal cutting purpose. The cutting action of conical pick and continuous miner machine are given in fig.1 and fig.2 respectively.

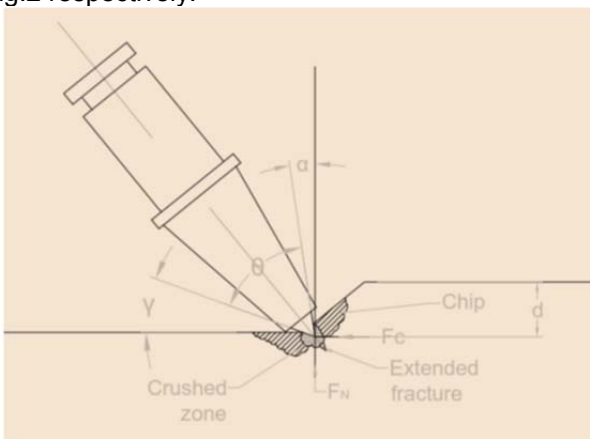

Figure 1. Cutting action of conical cutting pick

Where,
F_C = Cutting force
F_N = Normal force
d = Depth of cut
θ = Tip angle
α = rake angle
Y = clearance angle

Figure 2. Cutting action of continuous miner machine

2. Experimental work and set up

Experiment was performed on a shaper machine ('BATLIBOI' (GEARED) SHAPING MACHINE MODEL BSH-63) by converting it into a linear cutting rig. The coal sample was cut and trimmed to get the shape of 14×14×9 cm^3 so that proper fitting of the coal can be done on the shaper machine. The conical pick was joined with

rectangular cross section bar to fit it properly on tool post. The coal was cut in linear forward direction at different depth of cut and at different tilt angle. In each case removed coal was collected and weighed. The experimental setup is given in fig.3.

Figure 3. Shaper machine as a linear cutting rig

The conical cutting pick of following specification was used for experiment (given in table 1)

Table 1. specification of conical pick

Pick type Kennametal U85HD
J30 series
conical shape
1-3/16" square shoulder
sleeve type - press fit
collar length -0.630mm
bit gauge -3.345mm

3. Investigation and analysis

Experimental data on coal cutting with the help of shaper machine is given in following table no.2.

Weight of coal	2.28 kg
Stroke length	5 inch = 12.7 cm
No. of stroke per minute	24
Cutting width of coal	9 cm
Dimension of specimen	14 x 14 x 9 cm^3
Time of forward stroke	1.4 sec
Time of backward stroke	1 sec

Table 3. Experimental data of weight removal rate at different depth of cut when tilting angle is zero

S. No.	Depth of cut(mm)	Tilting Angle (deg)	Time (seconds)	Weight of cut coal (gm)
1	0.5mm	0^o	112	5.511
2	1.0mm	0^o	133	9.843
3	0.5mm	0^o	119	3.665
4	1.0mm	0^o	112	7.076
5	1.5mm	0^o	175	12.930
6	0.05mm	0^o	100	1.231
7	0.10mm	0^o	117	1.472
8	0.15mm	0^o	117	2.263
9	0.2mm	0^o	117	2.725
10	0.25mm	0^o	117	4.641
11	0.3mm	0^o	122	3.950
12	0.35mm	0^o	116	5.857
13	0.4mm	0^o	119	5.617
14	0.6mm	0^o	123	14.420

Table 4. Experimental data of weight removal rate at different depth of cut when tilting angle is 5°

S. No.	Depth of cut(mm)	Tilting Angle (deg)	Time (seconds)	Weight of cut coal(gm)
1	0.1mm	5^o	112	5.511
2	0.2mm	5^o	118	2.110
3	0.3mm	5^o	122	5.490
4	0.4mm	5^o	119	3.160
5	0.5mm	5^o	118	6.370
6	0.6mm	5^o	121	4.068
7	0.7mm	5^o	117	11.367

Table 5. Experimental data of weight removal rate at different depth of cut when tilting angle is 10^0

S. No	Depth of cut(mm)	Tilting Angle (deg)	Time (seconds)	Weight of cut coal (gm)
1	0.1	10^o	120	2.084
2	0.2	10^o	113	8.248
3	0.3	10^o	120	3.671
4	0.4	10^o	117	0.850
5	0.5	10^o	122	0.732
6	0.6	10^o	119	1.540
7	0.7	10^o	116	2.221
8	0.8	10^o	118	1.963
9	0.9	10^o	116	1.527

After collecting, calculating and measuring all the parameters the various graphs had been plotted and analyzed to observe the variation trend between the rate of the weight loss and the depth of cut at various tilt angles. The cutting surface of coal was made flat, smooth and horizontal by performing cutting action with shaping machine. After the surface was prepared again the coal sample was weighed and recorded.
One can observe that the rate of weight loss of coal increases with the increase in the depth of cutting at cutting angle 0°. (Fig. 4)

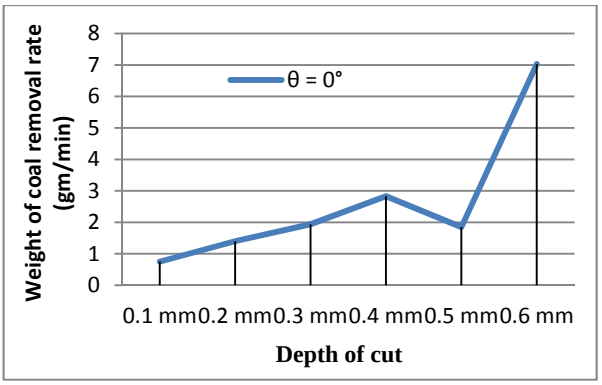

Figure 4. Graph showing weight of coal removal rate Vs depth of cut at θ=0°

Similarly from table 4, at 5^0 tilt angle, the material removal rate follows both increasing and decreasing behaviour and a very fluctuating character with increment in depth of cut (Fig.5).

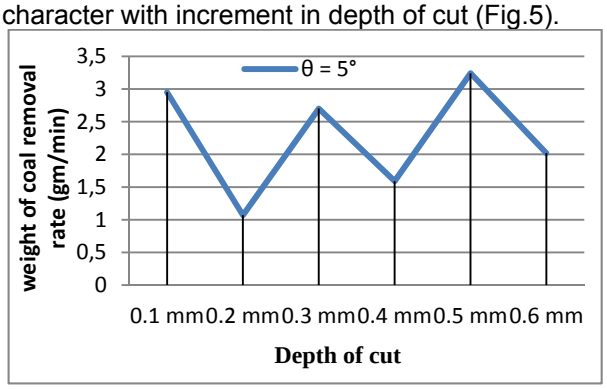

Figure 5. Graph showing weight of coal removal rate Vs depth of cut at θ=5°

At 10^0 tilt angle, the material removal rate decreases with the increment in the depth of cut. From table 5, by analysing the two parameters depth of cut and material removal rate on a graph. It is observed that the material removal rate increases and then decreases with the increment in depth of cut as shown in fig.6.

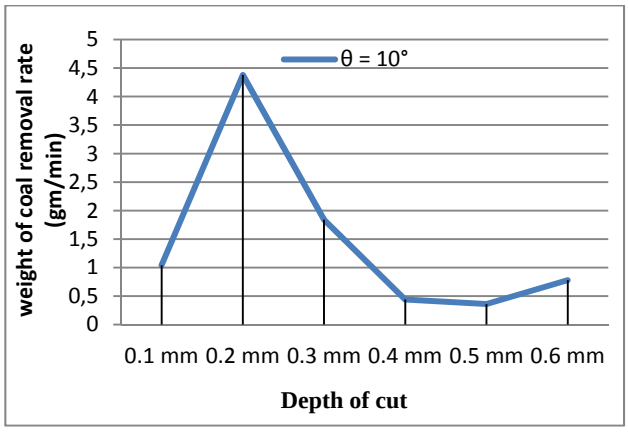

Figure 6. Graph showing weight of coal removal rate Vs depth of cut at θ=10°

A combined graph was plotted with 0^0, 5^0, 10^0 angle of attack, depth of cut and material removal rate. Fig.7 shows the behaviour of material removal rate with depth of cut at different angles of attack. A comparison among the different angle of attack shows that the material removal rate is greater with 0^0 angle of attack.

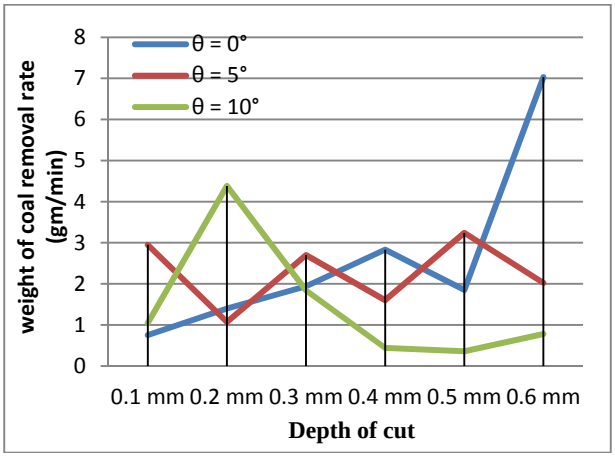

Figure 7. Graph showing weight of coal removal rate Vs depth of cut at θ=0°, θ=5° & θ=10°

4. Cutting mechanism

When a pick cuts across the surface of a block of coal, it is seen that it always produce a groove that is much wider than the width of the pick. The depth of the cut is also sometimes greater than the depth of the pick.

The cutting of coal is considered by increase in the cutting force acting on the pick as it penetrates. When this force exceeds the strength of coal, then a coal fragment or chip is produced with immediate reduction of pick force. The coal chip extends to the front of the pick, the later then advancing under negligible force until it re-engages a fresh coal surface, and then the chip formation process is repeated. Coal is known to have time-dependent stress-strain properties; these are of no practical significance when cutting, even at the lowest speed.

From this perspective, coal can be regarded as a brittle and heterogeneous material. According to Evan's theory, the cutting force acting on a pick is linearly proportional to the depth of cut.

$$F_C \alpha d$$

$$F_C = K \times d \quad \text{.....(K= constant)}$$

The generalized cutting force F_C acting on a pick can be resolved into two mutually perpendicular components. F_C is the cutting force that acts in the direction of cutting and F_N is normal force acting perpendicular to the direction of cutting. The normal force (F_N) is the force required to maintain the pick at a constant depth of cut.

Work done for coal cutting = $F_C \times l$

$$W = F_C \times l$$

$$W = K \times d \times l$$

Where, F_C = mean cutting force
d = depth of cut
l = cutting distance
K = a constant depending on the shape of the pick and the coal strength
W = width of cut
θ = breakout angle

Fig. 8 shows mechanism of cutting

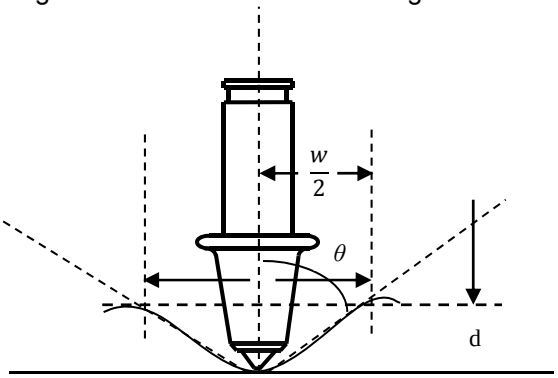

Figure 8. Cutting mechanism

V = *a* × *l*

$$V = \frac{1}{2} \times w \times d \times l$$

Since, $\tan\theta = \frac{w}{2d} l$

$$\boldsymbol{V = d^2 \tan\theta \times l}$$

Specific energy=work done (W)/ volume of coal removed (V)

$$\boldsymbol{S.E = \frac{F_C \times l}{d^2 \times \tan\theta \times l} = \frac{F_C}{d^2 \times \tan\theta} = \frac{K}{d \tan\theta}}$$

$$\boldsymbol{S.E \propto \frac{1}{d} \propto \frac{1}{\tan\theta}}$$

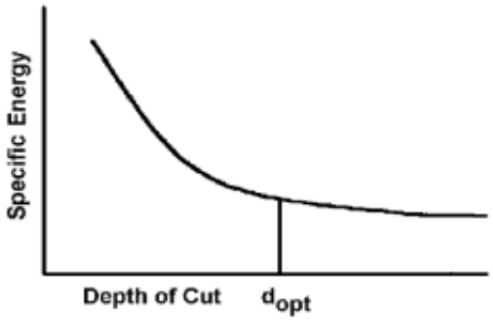

Figure 9. Specific energy Vs depth of cut [9]

5. Conclusion

On the basis of theoretical and experimental data, one can observe that the fragmentation of coal is much quicker around its edges and the fragmented particles are greater when the depth of cut is larger. Very fine particles were produced when the depth of cut are small. The material removal rate increases as the depth of cut increases. At 0^0 tilt angle, the material removal rate increases with the increment in depth of cut. At 5^0 tilt angle, the material removal rate follows both the increasing and decreasing behaviour. This condition shows very fluctuating nature with increment in depth of cut. When tilt angle equals 10^0, the material removal rate decreases with the increment in the depth of cut.
Conical cutting pick is to be found efficient for cutting purpose because of its symmetrical wear phenomenon and it requires lowest specific energy for penetration.

6. References

[1] Roxborough et al. 1981. Applied Rock and Coal Cutting Mechanic. Australia Mineral Foundation.
[2] Roxborough F.F., King P., Pedroncelli E.J., 1981.,Journal of the South African Institute of Mining and Metallurgy, 9-25.
[3] Evans I. Line spacing of picks for efficient cutting. Int J Rock Mech Min Sci 1972; 9: 355–9.
[4] Evans I. Optimum line spacing for cutting picks. Min Eng 1982; Jan.:433–4.
[5] Evans I. A theory of the cutting force for point attack picks. Int J Min Eng 1984; 2:63–71.
[6] Evans I. Basic Mechanics of the point attack pick. Colliery Guardian, 1984; May: 189–193.
[7] A.W.Khair; Research and Innovations for Continuous Miner's Cutting Head, for Efficient Cutting process of rock /coal. Department of Mining Engineering, West Virginia University, Morgantown, U.S A. 17* International Mining Congress and Exhibition of Turkey-IMCET2001, ©2001, ISBN 975-395-417-4.
[8] Miller, M.H. and D.L. Sikarskie, 1968, On the penetration of rock by three-dimensional indentors: International Journal 0/ Rock Mechanics and Mining Sciences, v. 5, no.5, pp. 375-398.
[9] N. Bilgin et al.(2006), Dominant rock properties affecting the performance of conical picksand the comparison of some experimental and theoretical results, International Journal of Rock Mechanics & Mining Sciences 43 (2006) 139–156.

APPLICATION OF NUMERICAL AND LUMPED CAPACITANCE METHOD FOR COOLING OF BODIES IMMERSED IN WATER

Marija Živić[1]*, Antun Galović[2] and Zdravko Virag[2]

[1]Mechanical Engineering Faculty in Slavonski Brod, J. J. Strossmayer University of Osijek, Croatia
[2]Faculty of Mechanical Engineering and Naval Architecture, University of Zagreb, Croatia
*Corresponding author e-mail: mzivic@sfsb.hr

Abstract
Transient cooling of solid bodies (sphere and vertical plate) due to natural convection in water is simulated using the CFD softwares FLUENT and AVL FIRE and in house developed FORTRAN code based on the lumped capacitance method. The time variation of the body temperature and the heat transfer rate between the bodies and water, obtained by the three methods, are compared.

Keywords
natural convection, vertical plate, sphere, lumped capacitance method, finite-volume method

1. Introduction

In many engineering applications, such as heat treatment, heat storage, as well as in everyday life, cooling or heating of solid bodies immersed in fluid are present. These processes are mainly driven by laminar or turbulent natural convection; they are unsteady problems due to continuous change of the body and the surrounding fluid temperature. The most commonly used body geometries in the heat transfer calculations are flat plate, circular cylinder and sphere.
Early experimental, analytical and numerical work related to the heat transfer from sphere immersed in fluid can be found in [1, 2, 3]. In more recent works [4, 5], a numerical approach based on solving Navier-Stokes and energy equations, for a wide range of Grashof number, can be found.
In terms of computer time, the approach based on solving of simultaneous equations in solid and liquid is still expensive, and an approach based on a simplified lumped model is more suitable for engineers because the set of partial differential governing equations from conjugate formulation are reduced to an ordinary differential equation that may be easily solved by the Runge-Kutta method. The lumped model approach is based on the assumption that the temperature of the solid is spatially uniform at any instant during the transient process. The goal of this paper is to describe cooling of a body immersed in water defined by the lumped capacitance method, and to compare the results of this model with the results obtained by solving Navier-Stokes and energy equations. Hence, it is important to determine under what conditions the lumped capacitance method may be used with reasonable accuracy.

2. Problem definition

We consider a cooling process of resting solid body at initial uniform temperature T_{p0}=90 °C immersed in unbounded water at uniform initial temperature T_0=20 °C . The water is initially at rest, and due to temperature difference between the body and water, natural convection develops. Close to the body, there is a thin boundary layer in which the water temperature varies from 90 °C to the far field value T_0=20 °C. The problem of cooling of solid body has been solved by using the following three approaches: 1) Full approach with heat conduction in the body and laminar natural convection in the water. For this purpose AVL FIRE and FLUENT software were used, 2) Approach using the lumped capacitance method taking into account the time dependent value of the heat transfer coefficient, 3) Analytical solution of the lumped capacitance method with constant value of the heat transfer coefficient.

3. Mathematical model

The problem is governed by the continuity, the momentum and the energy equation applied for the liquid and for the solid body. Boundary conditions are set at infinity (sufficiently far from the body) where the velocity of the liquid is equal to zero, and the temperature is equal to the initial temperature. At the solid body, the fluid velocity is equal to zero, and conduction heat fluxes in the solid and the fluid are equal. Heat radiation is neglected. The equations for water are:

$$\frac{\partial(\rho)}{\partial t}+\nabla\cdot(\rho\vec{v})=0 \quad (1)$$

$$\frac{\partial(\rho\vec{v})}{\partial t}+\nabla\cdot(\rho\vec{v}\vec{v})=\nabla\cdot\left[\mu\left(\nabla\vec{v}+(\nabla\vec{v})^{\mathrm{T}}\right)\right]-\nabla p+\rho\vec{g} \quad (2)$$

$$\frac{\partial(\rho cT)}{\partial t}+\nabla\cdot(\rho c\vec{v}T)=\nabla\cdot(\lambda\nabla T) \quad (3)$$

and the energy equation for solid body is

$$\frac{\partial\left(\rho_s c_s T\right)}{\partial t} = \nabla\cdot\left(\lambda_s \nabla T\right) \tag{4}$$

where, t is the time, v is the velocity of water, ρ is the temperature dependent water density, μ is the viscosity of water, c and c_p are the specific heat capacities of water and of the body, respectively, λ and λ_p are the thermal conductivities of the water and of the body, T is the temperature, p is the pressure, ∇ is the del operator and $(\nabla\vec{v})^T$ denotes the transpose of velocity gradient. The described set of equations with the prescribed boundary conditions is solved by means of the FLUENT software and AVL FIRE software. As a result, we have obtained time varying the surface and volume averaged body temperature, as well as the heat transfer rate between the body and the water.

Lumped capacitance method

The same problem is solved by using a simplified approach which is based on problem decoupling. In such an approach, only the energy equation for the body is considered, and the heat transfer rate between the body and water is modeled by the heat transfer coefficient.

After volume integration of equation (4), over the body domain V_s bounded by the body surface S_s, it follows

$$\int_{V_s} \rho_s c_s \frac{\partial T}{\partial t}\mathrm{d}V = \int_{S_s} \lambda_s \nabla T\cdot\vec{n}\mathrm{d}S \tag{5}$$

where $\vec{n}$ denotes the outward normal to the sphere surface. The integral on the right hand side of above equation denotes the heat transfer rate ($\dot{Q}$) from the surrounding fluid to the sphere. $\dot{Q}$ is modeled by the following expression

$$\dot{Q} = \alpha A_s\left(T_0 - T_s\right) \tag{6}$$

where α is the heat transfer coefficient, A_s is the area of the body surface and T_s is the body average surface temperature. For small values of Biot number (0<Bi<0.1) defined as

$$Bi = \frac{\alpha D}{\lambda_s} \tag{7}$$

it is appropriate to neglect the temperature variation within the body (to consider it as uniform T=T_s) and in that case, equation (5) takes the form

$$\rho_s V_s c_s \frac{\mathrm{d}T_s}{\mathrm{d}t} = \alpha A_s\left(T_0 - T_s\right) \tag{8}$$

Generally speaking, α is the time varying quantity and depends on the strength of natural convection in the fluid.

As an approximation, α can be considered as a constant, and in that case, equation (8) has the analytical solution in the form

$$\frac{T_s(t) - T_0}{T_{s,0} - T_0} = \exp\left(-\frac{t}{\tau}\right) \tag{9}$$

where τ is the thermal time constant defined as

$$\tau = \frac{\alpha A_s}{\rho_s V_s c_s} \tag{10}$$

Sphere

The heat transfer coefficient α can be calculated from the correlation function for spheres, suggested by Churchill [6]

$$Nu = 2 + \frac{0.589 Ra^{1/4}}{\left[1+\left(0.469/Pr\right)^{9/16}\right]^{4/9}} \tag{11}$$

for $Pr \geq 0.7$, $Ra \leq 10^{11}$

where Nusselt, Rayleigh and Prandtl numbers are defined by the following expressions:

$$Nu = \frac{\alpha\lambda}{D},\ Ra = \frac{\rho^2 c\beta\left(T_s - T_0\right)gD^3}{\lambda\mu},\ Pr = \frac{\mu c}{\lambda} \tag{12}$$

where, $\beta = -\frac{1}{\rho}\left(\frac{\partial\rho}{\partial T}\right)_p$ is the volumetric thermal expansion coefficient of the fluid. All of the temperature dependent fluid properties are defined at the mean temperature

$$T_m = \frac{T_s + T_0}{2} \tag{13}$$

Vertical plate

The heat transfer coefficient for the vertical plate is defined in [6] and it can be calculated from the expression:

$$Nu = \frac{\alpha H}{\lambda} = 0.678\left(Gr\,Pr\right)^{1/4}\left(\frac{Pr}{0.952 + Pr}\right)^{1/4} \tag{14}$$

where Grashof number, and Prandtl number are:

$$Gr = \frac{g\beta\left(T_p - T_0\right)H^3}{\nu^2} = \frac{g\beta\Delta T H^3}{\nu^2},\ Pr = \frac{\mu c}{\lambda} \tag{15}$$

The correlation functions (11) and (14) define the steady state heat transfer coefficient. Using this steady state coefficient in an unsteady cooling process implies that the temperature field changes so slowly that it can be supposed that the natural convection is fully developed at any time.

4. Numerical method for lumped capacitance method

Equation (5) with the initial condition $T_s(0)$=$T_{s,0}$ was solved by using the fourth order Runge–Kutta method.

5. Results and discussion

Here, results of cooling of the sphere and the vertical plate immersed in water will be compared.

Sphere

The sphere diameter is D=20 mm, ρ_s=7800 kg/m^3, c_s=380 J/(kg·K) and λ_s=16.27 W/(m·K).

The FLUENT solution is obtained in the spherical calculation domain of size 45D. The problem is considered as a symmetric with respect to the vertical midline, with no slip isothermal conditions at the outer boundary. The computational grid is refined near the sphere according to the expected solution, as described in [5]. Such a grid ensures a grid independent solution. The total number of grid cells was 67273. The segregated SIMPLE algorithm and the second order implicit time integration were used. A variable integration time step was used. The lowest time step was $5\cdot10^{-3}$ s (at the beginning of the cooling process), and the greatest was 0.1 s. Fig. 1 shows the temperature field obtained by FLUENT after 4 s from the start of cooling process.

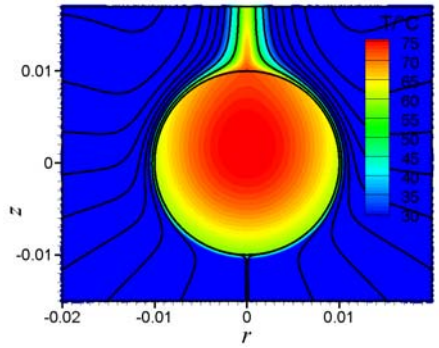

Figure 1. Results at t=4 s of cooling process of sphere

The average heat transfer coefficient for the analytical solution is defined in a way that the temperature at the end of integration obtained by the Churchill's correlation function is the same as the temperature defined by the analytical solution.

Fig. 2 shows the time variation of the sphere temperature and Fig. 3 shows the heat transfer rate between the sphere and the water obtained by the three approaches. In the considered case, the Prandtl number lies within the range from 3.15 to 6.2, the Rayleigh number varies from $3.47\cdot10^7$ to $1.5\cdot10^6$ and the Biot number varies from 0.80 (at the beginning of the process) to 0.037. Since the Biot number is not small enough, at least at the beginning of cooling process, a certain difference between the surface averaged and volume averaged sphere temperatures obtained by FLUENT exists. The result from the second approach (based on the Churchill's correlation function) is in good agreement with the FLUENT results, while the analytical solution, based on the average α, is not useful if the rate of cooling is of interest. The same conclusion can be derived from Fig. 3 which shows the heat transfer rate between the sphere and the water. The analytical solution underestimates the heat transfer rate at the beginning of the cooling process, and overestimates it after that.

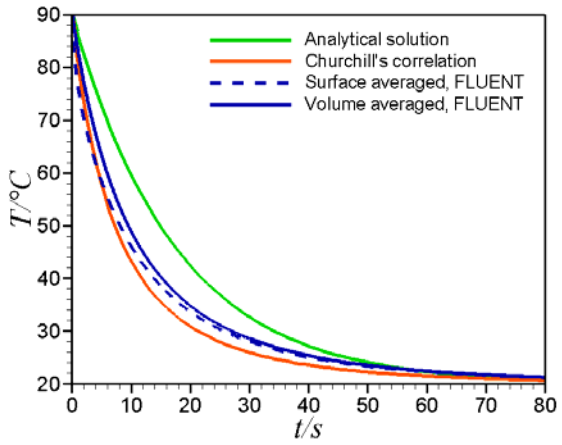

Figure 2. Time variation of the sphere temperature

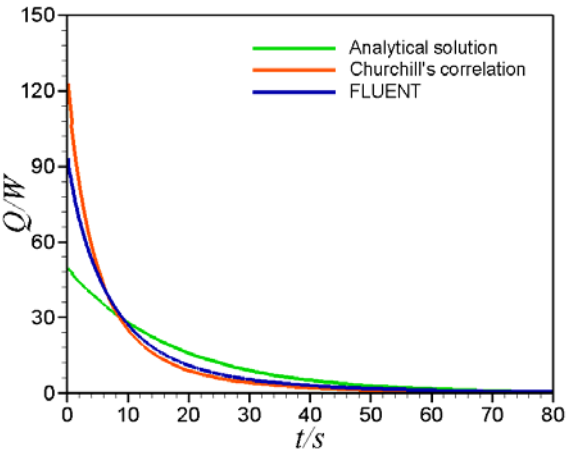

Figure 3. Time variation of the heat transfer rate

Vertical plate

We consider a vertical steel plate of height H=0.2 m, and H=1.0 m of thickness 10 mm.

The AVL FIRE solution is obtained in a rectangular calculation domain of size 12 m x 1 m. The computational grid is refined near the plate. The total number of grid cells was 72486. The SIMPLE algorithm and the implicit time integration with time step of 0.1 s are used.

The temperature field in time (10, 20, 30, 40, 50 s) for the plate of the height H=0.2 m, obtained by FIRE is shown in Fig. 4. It can be seen that the cooling of the plate starts from the bottom of the plate, and the natural convection in water around the plate develops.

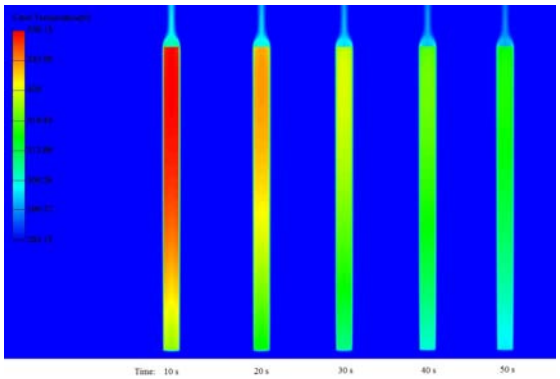

Figure 4. Temperature field in the plate (10, 20, 30, 40, 50 s) obtained by AVL FIRE for the plate H=0.2 m

Fig. 5 and Fig.6 show a comparison of time variations of the plate temperature obtained by the lumped capacitance method (blue line) and the volume averaged temperature obtained by AVL FIRE (red line) for the two values of the plate heights: *H*=0.2 m and *H*=1 m, respectively.
The discrepancy between the results is practically negligible, in the case of the plate height *H*=0.2 m; and relatively small in the case of the plate height *H*=1 m.

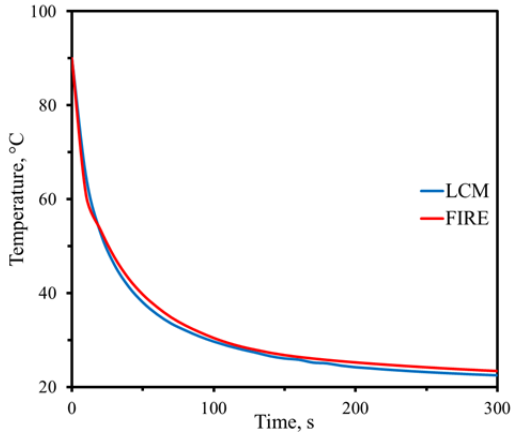

Figure 5. Plate temperature variation in time for H=0.2 m obtained by LCM and AVL FIRE

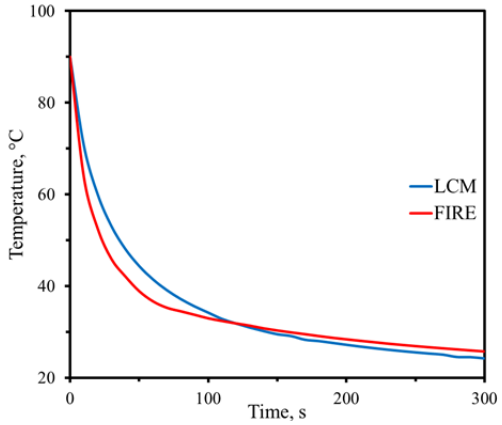

Figure 6. Plate temperature variation in time for H=1 m obtained by LCM and AVL FIRE

In the case of cooling of sphere, the smaller difference between LCM and FLUENT solution is obtained in the case of higher Rayleigh number which is opposite to the case of cooling of plate where the smaller difference is observed in the case of smaller Rayleigh number (*H*=0.2 m). This points to a need for a more detailed analysis of the existing correlations functions.

6. Conclusion

In the case of small Biot number and an available heat transfer correlation, the lumped parameter model results in a fast and accurate method for predicting of cooling processes.
The discrepancy between the results obtained by the lumped parameter model and by FLUENT could be explained by three reasons: (i) the influence of Biot number (at large Biot numbers, the temperature in the sphere is not uniform), (ii) differences in the heat transfer coefficients defined by the correlation function and obtained by FLUENT (in a steady state case, the maximal discrepancy is 4.5 %), and (iii) neglecting the transition of natural convection in the lumped parameter model (the correlation function for the steady state condition was used.)

7. Acknowledgement

The authors are grateful to AVL List GmbH for the use of AVL FIRE software.

8. Reference

[1] Amato, W.S., Tien C.,"Free convection heat transfer from isothermal spheres in water", Int. J. Heat Mass Transfer, 15 (1972), pp. 327-339.
[2] Jafarpur, K., Yovanovich, M.M,"Laminar free convective heat transfer from isothermal spheres: a new analytical method", Int. J. Heat Mass Transfer", 35, pp.2195-2201, 1992.
[3] Geoola, F., Cornish, A.R.H." Numerical solution of steady-state free convective heat transfer from a solid sphere", Int. J. Heat Mass Transfer, 24, pp. 1369-1379, 1981.
[4] Jia, H., Gogos, G. "Laminar natural convection heat transfer from isothermal spheres, Int. J. Heat Mass Transfer, 39, pp.1603-1615,1996.
[5] S. Yang, V. Raghavan, G. Gogos, „Numerical study of transient laminar natural convection over an isothermal sphere", Int. J. Heat Fluid Flow, 28, pp.821–837, 2007.
[6] Churchill, S.W., "Free convection around immersed bodies", in E.U. Schlunder, Ed-in-Chief Heat Exchanger Design Handbook, Section 2.5.7 Hemisphere Publishing, New York, 1983.
[7] W. H. Press. S.A. Teukolsky. W.T Vetterling. B.P. Flannery, "Numerical Recipes in FORTRAN", Cambridge University Press, New York, 1994.

A PROBABILISTIC APPROACH FOR ADMISSION CONTROL OF SMART APPLIANCES IN SMART GRIDS

Lorant Kovacs[1*], Janos Levendovszky[4], Andras Olah[1,2], Rajmund Drenyovszki[1,3], David Tisza[1,2], Kalman Tornai[1,2] and Istvan Pinter[1]

[1]Kecskemet College, Faculty of Mechanical Engineering and Automation,
Izsaki ut 10, H-6000 Kecskemet, HUNGARY
[2]Pazmany Peter Catholic University, Faculty of Information Technology
Prater utca 50/a, H-1083 Budapest, HUNGARY
[3]University of Pannonia, Department of Computer Science and Systems Technology,
Egyetem u. 10, H-8200 Veszprem, HUNGARY
[4]Budapest University of Technology and Economics, Dept. of Telecommunications
** Corresponding author e-mail: lorant.kovacs@gamf.kefo.hu*

Abstract
New generation electricity network called Smart Grid is a recently conceived vision for a cleaner, more efficient and cheaper electricity system. One of the major challenges of electricity network is that generation and consumption should be balanced at every moment. This paper introduces a new concept for controlling the demand side by the means of automatically enabling/disabling electric appliances to make sure that the demand is in match with the available supplies, based on the statistical characterization of the need. In our new approach instead of using hard limits we estimate the tail probability of the demand distribution and control system by using the principles and the results of statistical resource management.

Keywords:
Smart grid, Demand Side Management, Admission Control

1. Introduction

The main issue in electricity networks is keeping an almost perfect balance must be kept between electricity generation and consumption in every minute. Balance between demand and supply is crucial since oversupply means waste of energy, while undersupply causes performance degradation of the grid parameters (e.g. phase, voltage level, etc.). The balance can be satisfied by the control of the supply side, or by the demand side. Balance of the electricity generation and consumption can be maintained by utilizing several techniques. For instance, generation volume can be set according to predicted day-to-day consumption information. Random differences between real and predicted consumption can be dealt with only at the expense of deficit: on the one hand in case of oversupply, extra energy is dissipated, on the other hand, in the case of undersupply, costly auxiliary diesel generators are turned on. Financially, generation can be done in the most feasible way when power plants generate constant electricity in time; consequently it would be desirable to have a constant level of consumption as well. Unfortunately the control of the supply side is slow because of the large time constants of the fossil and nuclear plants. Additionally, the percentage of renewable resources should be increased which gives rise to uncertainty in the generation side. Hence, it turns out that the only way to keep the balance is to manage the demand side. Even though aggregate volume of the consumption can be predicted, it is basically also a stochastic process. Methods used today cannot take into account the stochastic nature of the demand side. It is clear that it is a great challenge due to its hard predictable nature.

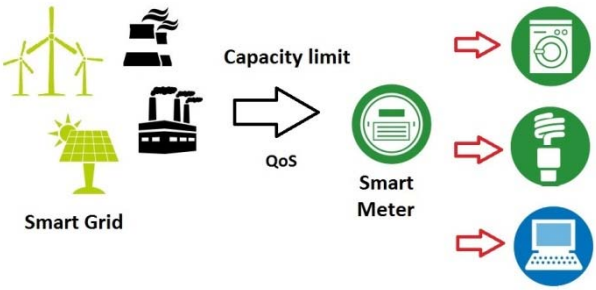

Figure 1. The structure of smart grid

Algorithmic solutions are used in Smart Grids, for instance the Direct Control of Smart Appliances. Its aim is to control consumption in short term (typically several minutes)[1]. Direct control can be used to remove the extreme values in electricity consumption (peak shaving, valley filling). Constant level of daily consumption can be also achieved by utilizing different pricing programs, for example Time Of Use tariffs [2]. In Smart Grid a new kind of pricing method is also emerging, called Real Time Pricing, which can affect the users' consumption by an indirect way. A new tariff is communicated with the households in the beginning of 15-60 minutes periods and the instantaneous price is in direct relation with the current wholesale prices (which also depends on the demand level). Demand side management with a longer time constant is also possible by using

load scheduling (e.g. charging of the batteries of electric vehicles).
Our current approach tries to give a solution to the short time balance problem of the electricity generation, in a way that capacity limits and quality criteria of the whole network are controlled by algorithms running automatically on consumer level and requiring minimal user interactions. The proposed method estimates the statistical parameters with relatively low algorithmic complexity (these parameters are obtained from intelligent appliances or from measurements) taking into account the probabilistic nature of the consumption.

2. The Model

In the model the following assumptions have been made. All subscribers have a Smart Meter (SM). The SM has the following properties:

- 2-way communication to the service provider;
- 2-way measurement capability of energy consumption;
- the SM can measure the consumption of every connection points individually;
- the SM can enable/disable every connection points;
- the SM communicates with smart appliances;
- the SM can register the consumption statistics of the appliances (both smart and traditional ones);

In this paper, we assume that the service provider can calculate and communicate the parameters regarding the consumption of a subscriber in order to make balance between energy generation and consumption in the system level. Using these parameters, the subscriber's SM can enable/disable the appliances at a local level, resulting in a fully distributed solution to the problem. The parameters coming from the service provider are as follows: a capacity upper limit C_u in every time slot, which is allowed to be overloaded only by probability p. p is called the Quality of Service (QoS) parameter, because it can satisfy the stability of the grid parameters (such as frequency, voltage level, etc.). There is a capacity lower limit C_l as well, which is allowed to be underloaded only by probability p. The task of the SM is the admission control (enabling/disabling) of the appliances by such a way, that the probability distribution function (pdf) of the aggregate consumption satisfies the prescription of the service provider. (The cooperative attitude of the subscriber can be motivated by rewards). The underlying model is depicted in Figure 1.
The probability distribution function of the aggregate consumption of the appliances connected to a given SM can be influenced by shifting the consumption of appliances. Many type of appliances can tolerate some delay (e.g. executing the program of a washing machine later). Further possibility is the application of the batteries of PHEVs (Plug-in Hybrid and Electric vehicles) as electric energy storage devices (when vehicles are parked). As a result, there are (time) shiftable and non-shiftable demands in the system.
On the other hand most of the devices show very high level of uncertainty of consumption (neither the level of power nor the execution time of the device is known at the moment of switch on), that's why only a statistical approach can efficiently solve the control task. In this paper, the stochastic and deterministic behavior of appliances will be also used for categorization. (The devices executing a fixed program can be seen as deterministic). The reason of this categorization is the different method, by which these appliances are handled by the admission algorithm.
The defined categories and examples of appliances can be seen in Table 1.

	stochastic	deterministic
shiftable	electric heating, air conditioner, refrigerator	washing machine, dishwasher
non-shiftable	circulation pump	lighting, vacuum cleaner

Table 1. Device categories used in the model

In the model both stochastic and deterministic, shiftable and non-shiftable appliances are taken into consideration as described in Section 3 in details.

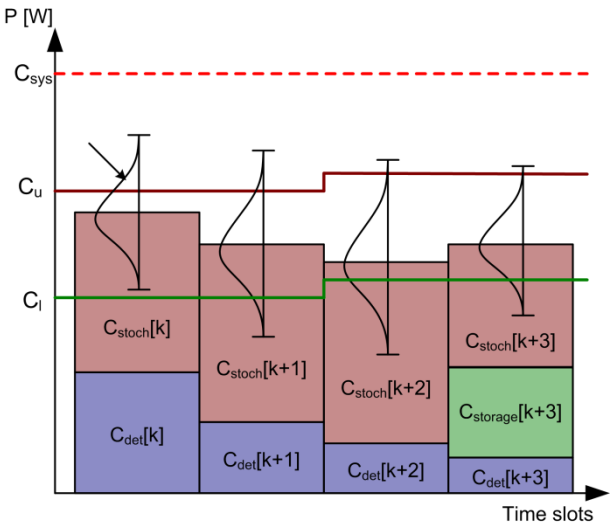

Figure 2. Measures used in the model

The admission control algorithm uses discrete time slots (denoted by k in Figure 2.), in which the

enabled/disabled status of the appliances and the system parameters (capacity limits and QoS) are supposed to be unchanged – except the handling of new enable requests that must be handled continuously.

In Figure 2. the measures used in the model are depicted. In all time slots there is a deterministic component of the consumption and as well as a stochastic one (the possible consumption of enabled appliances). The stochastic part is descripted by its estimated (or calculated) probability distribution function (for details see Section 3.) The capacity limits C_u and C_l can be changed in every time slots by the service provider. In time slot k the upper tail probability of the aggregate consumption is larger than the legal value p, i.e. the probability of overload is larger than allowed. Hence, shiftable appliances will be disabled temporarily in time slot $k+1$, satisfying the system requirements. In time slot $k+2$ the probability of underload is larger than required, etc. C_{sys} denotes the system capacity. Note that C_u not equals C_{sys}. C_{sys} builds a natural upper limit on C_u.

3. Consumption and Storage Admission Control Algorithm

The Smart Meter calculates the aggregate p.d.f. from the individual p.d.f.-s of the appliances. The individual p.d.f. can be communicated to the SM by smart appliances, or it can be measured in the case of traditional ones.
Let X_j denote the random variable of the consumption of the jth appliance, while

$$X = \sum_{j=1}^{N} X_j \qquad (1)$$

is the aggregate consumption random variable and N is the number of enabled appliances. The upper tail probability of the aggregate consumption should be kept under the limit p, which can be formulated as

$$\Pr(X > C_u) \le p = e^{-\gamma} \qquad (2)$$

where Pr denotes the probability and $\gamma = -\log p$ is introduced for mathematical convenience. Note that the probability $\Pr(X > C_u)$ can be calculated using its pdf $f(X)$, which can be determined by the terms of convolution [3]

$$f(X) = f(X_1) * f(X_2) * \ldots * f(X_N). \qquad (3)$$

This calculation can be very time consuming in the case of large N, that is why it is suggested to estimate the tail probability by the terms of Large Deviation Theory, using the Chernoff-bound:

$$\Pr\left(\sum_{j=1}^{N} X_j > C_u\right) \le e^{\sum_{j=1}^{N}\mu_j(s^*) - s^* C_u} \le e^{-\gamma} \qquad (4)$$

where $\mu_j(s) = \lg E\{e^{sX_j}\}$ are the so called logarithmic momentum generating functions and s^* is the parameter that satisfies the possibly tightest bound (5).

$$s^* : \inf_{s>0} \sum_{j=1}^{J} \mu_j(s) - sC \qquad (6)$$

When a new demand of a shiftable appliance appears enabling or disabling will be calculated using the Chernoff-bound:

$$\operatorname{sgn}\left\{\sum_{i=1}^{N+1} \mu_i(s^*) - s^* C + \gamma\right\} = \begin{cases} -1 & \text{Accept} \\ +1 & \text{Reject} \end{cases} \qquad (6)$$

where N is the number of the enabled (both shiftable and non-shiftable) appliances, but the test should be calculated taking into consideration the incoming appliance (N+1).
Algorithm (6) checks the upper capacity limit when a new consumption demand appears. The lower limit can be checked by the same manner at the beginning of each time slot. If the probability of underload is higher than p, The goal can be expressed as

$$\Pr(X < C_l) \ge p,$$

using the complementary probability

$$1 - \Pr(X > C_l) \ge p$$

and as a result

$$\Pr(X < C_l) \le p$$

for which the Chernoff bound can be used as given in (4).

4. Modules of the algorithm

The aim of our algorithm is to establish an automatic and distributed solution for enabling/disabling smart appliances in a smart grid environment in order to satisfy short-term balance between electricity supply and demand. The accept/reject decision is based on the CAC algorithm. The functional diagram of the algorithm can be seen on Figure 3. Modules of the algorithm are the followings:
Update Statistics – Updating probability distribution functions using prediction techniques. (The probability of usage depends on parameters such as date, time, temperature, light, etc.)
New Demand – In this point the algorithm checks whether a new appliance wants to start operating.

CAC algorithm – Checks whether the aggregate consumption of the currently enabled appliances satisfy the Quality of Service parameter of overloading; SAC – Storage Admission Control: Checks whether the aggregate consumption of the currently enabled appliances satisfy the Quality of Service parameter of underloading;
Switch On Storage Device: in the case of underloading storage capacities can be charged (PHEV batteries, or electric water heaters).
UPDATE Priority levels – Updating operation priority levels of appliances.
UPDATE Consumption vector – Updating consumption vector which contains the number of different type of appliances and its nominal consumption.
UPDATE Cdet[k+i] – Updating the sum of deterministic consumption value in time slot k+i.

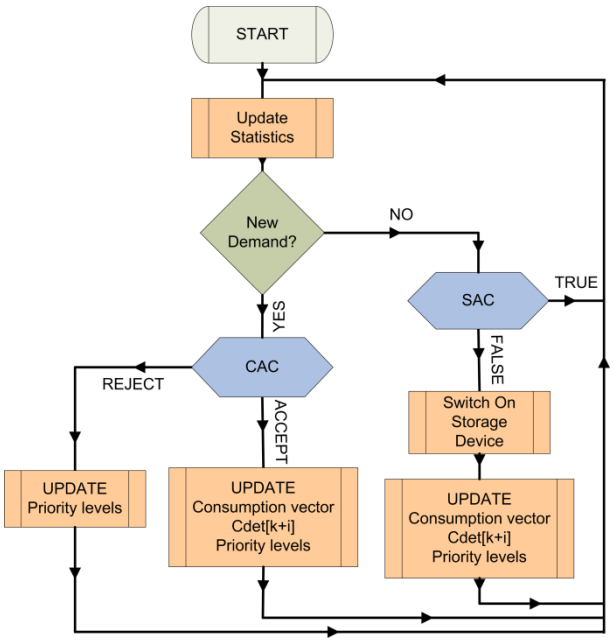

Figure 3. Functional diagram of the algorithm

Working of the algorithm can described as follows: In every iteration of the algorithm the statistics are updated first and that the CAC or SAC algorithm is running according to the existence of new demand. The CAC module can reject or accept the new demand. In case of rejection only the priority levels are updated, otherwise the consumption vector and the value of deterministic consumption also. The SAC module can return with true or false. In the latter case it tries to switch on storage devices to use the extra energy and updates the priority levels, the consumption vector and the value of deterministic consumption.

5. Conclusions

In this paper a new statistical approach has been introduced for managing the balance between demand and available supplies in smart grids. The smart meter of the subscriber performs the task of enabling/disabling of shiftable appliances based on three parameters, obtained from the supplier: lower and upper capacity thresholds and a probability value. The smart meter controls the probability distribution function of the aggregate consumption in order to keep the tail probabilities under a given threshold p. The new approach takes the uncertainty of the consumption into account, and furthermore it can work in a fully distributed manner, since the calculations can be performed in the smart meter. As a result the introduced consumption admission control method is a promising candidate for demand side management in smart grids.

6. Acknowledgement

This publication/research has been supported by the European Union and the Hungarian Republic through the project TÁMOP-4.2.2.A-11/1/KONV-2012-0072 – Design and optimization of modernization and efficient operation of energy supply and utilization systems using renewable energy sources and ICTs.

7. References

[1] Costanzo, G.T.; Guchuan Zhu; Anjos, M.F.; Savard, G., A System Architecture for Autonomous Demand Side Load Management in Smart Buildings, IEEE Transactions on Smart Grid, vol.3, no.4, 2012, pp.2157,2165.
[2] Torriti J., Price-based demand side management: Assessing impacts of time-of-use tariffs on residential electricity demand and peak shifting in Northern Italy, Energy, Vol 44., 2012, pp. 576-583.
[3] D.L. Evans, L.M. Leemis, Algorithms for computing the distributions of sums of discrete random variables, Mathematical and Computer Modelling, Volume 40, Issue 13, December 2004, Pages 1429-1452, ISSN 0895-7177
[4] J. Levendovszky, Zs. Elek, Cs. Vegso: "Integrated Neural Call Admission Control for Cell Loss Probability and Mean Cell Delay", Proceedings of the 8th IFIP ATM & IP 2000 Workshop, pp. R45/1-10, Ilkely, West Yorkshire, UK, July 2000.
[5] J. Levendovszky, Cs. Vegso, E. C. van der Meulen: "Nonparametric decision algorithms for CAC in ATM networks", Performance Evaluation, 41 (2-3) (2000) pp. 133-147.
[6] Levendovszky, J, E.C. van der Meulen,: "Tail Distribution Estimation for Call Admission Control in ATM Networks", Proccedings of IFIP, Third Workshop on Performance Modelling and Evaluation of ATM Networks, Ilkley, West Yorkshire, UK, 2-6th July 1995.

DESIGN ASPECTS AND FRACTURE BEHAVIOUR OF TITANIUM ALLOY ARTIFICIAL HIP IMPLANT

Katarina Colic[1*], Aleksandar Sedmak[2], Nenad Gubeljak[3], Sergej Hloch[4], Aleksandar Veg[2]

[1] University of Belgrade, Innovation Center of Faculty of Mechanical Engineering, Belgrade, Serbia
[2] University of Belgrade, Faculty of Mechanical Engineering, Belgrade, Serbia
[3] University of Maribor, Faculty of Mechanical Engineering, Maribor, Slovenia
[4] Faculty of Manufacturing Technologies of Technical University of Kosice with seat in Presov, Slovakia
Institute of Geonics Academy of Science of Czech Republic, v.v.i., Ostrava Poruba, Czech Republic
** Corresponding author e-mail: kbojic@mas.bg.ac.rs*

Abstract

In this paper an experimental investigation of hip replacement implant is presented. The long-term stability of hip implants depends, among other things, on the loads acting across the joint. The force magnitudes are of interest, and the modified standard investigation of an implant was performed. The results indicate that forces occurring *in vivo* can be much greater than the recommended test values, and can cause implant stress field changes and implant stability problems.

An analysis of titanium alloys that are used as biomaterials in biomedical applications, such as artificial joint implants, is also presented from a fracture mechanics perspective. It is shown that it is necessary to understand the fatigue crack initiation and propagation characteristics in order to prevent catastrophic failure of the implant. The fracture behaviour of Ti-6Al-4V is investigated by means of standard fracture mechanics tests. The results indicate that this new optical stereometric measurement methodology produces good results in investigation of fracture behaviour of bimetallic materials.

Keywords:
fracture behaviour, biomedical applications design, Ti-6Al-4V alloy, digital image correlation

1. Introduction

Total hip replacement is a surgical procedure in which parts of the hip joint are removed and replaced with artificial parts, known as the prosthesis. [1] Currently, titanium-based alloys, especially Ti-6Al-4V & Ti-6Al-7Nb, are the most commonly used materials for joint prostheses, being registered in ASTM standard as biomaterials.

There are many potential hazards that can affect the long-term outcome of the operation, once an implant surgery is performed. In orthopaedic applications, such as knee and hip joint prostheses, fatigue fracture and wear have been identified as some of the major problems associated with implant loosening, stress-shielding and ultimate implant failure. [2] [3] [4] [5]

While it is not possible to avoid failure, recent work has focused on predictive and design tools to enable more accurate prediction so as to avoid catastrophic failure *in vivo*. *In vivo*, each prosthesis component is subjected to a different set of loads that is specific to the individual patient. In addition, the anchoring conditions vary depending on the patient's pre-existing diseases, prosthesis design, quality of the bone and surgical implantation techniques. [1] [6] [7] [8]

Figure 1 shows the devastation that can occur to an improperly designed artificial hip implant.

Figure 1. Artificial hip prosthesis failure

During surgery and general handling of the prosthesis, scratches will inevitably appear on its surface, which will result in an intensification of the stress at those points and provide a location for crack growth propagation.

Late failure of cemented implants, designed for interlocking mechanical fixation, is commonly related to formation of wear particle debris, resulting from the cement fracture and fragmentation due to high stress, and enhanced by interface micromotions. High amount of wear particle debris is suspected to induce peri-prosthetic osteolysis, probably due to debris migration along the bone-implant interface. [6] [7] [8] [9]

The main goal of this investigation was to experimentally examine hip replacement implants from a mechanical perspective, considering stability and forces acting on a prosthesis and fracture behaviour of the implant biomaterial.

2. Research methodology

The goal of the hip implant design is to mimic the design of the hip. [1] The human hip is a ball and socket joint, which allows for movement in all directions. To accomplish this, a total hip implant is composed of three sections, the acetabulum, femoral head and femoral stem.

During walking and jogging, the forces acting across the hip joint are several times higher than the body weight. [10] The loads depend on the walking speed and the weight of the subject.

Throughout normal activity there are a variety of loads acting on the femoral stem and the acetabulum. The femoral stem is a loaded column, and the loads applied to it can be resolved into orthogonal loads acting along vertical, mediolateral, and anteroposterior axes. [10] [11]

Despite the progress in design and testing, fatigue fractures of hip stems continue to be reported. The ISO 7206 standard defines a laboratory test for determining the endurance properties of femoral components of hip prostheses. [12] This method is based on several hypotheses to reduce the complexity of problem to a reproducible setup. The current ISO 7206 standard defines that the load applied has to be at an angle of 10° in adduction and 9° in flexion to the stem axis, as shown in Figure 2.

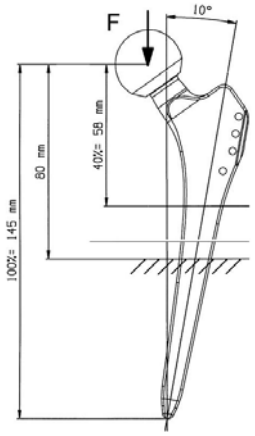

Figure 2. ISO standard fatigue test arrangement for hip stems

Furthermore, the test conditions are fixed on the conservative assumption that the stem becomes unsupported proximally, remaining restrained at 80 mm from the centre of the head of the prosthesis. This assumption is consistent with the clinical observation that failures generally occur in the middle third of the stem. [8] [9] [10]

To analyse the mechanical behaviour of the prosthesis under physiological loading, the experimental route was based on the ISO 7206 standard, which is used to evaluate the endurance properties of femoral components of hip prostheses. This standard defines a maximum load of 2.3 kN that should be applied as shown in Figure 2. This vector corresponds to the maximum joint load on an implant during normal walking. However, if a person decides to stand on one foot, the load may multiply six times and more, if the person is heavy. Therefore, the goal of this investigation was to analyse the effect of higher loads on the implant stability, as could be the case *in vivo*. Thus, a maximum load that was applied on the implant in this investigation was 6000 N.

To perform the experiment, an adapter to constrain the implant was constructed and used with the HB250 testing machine. During pre-testing investigation, a solid model of the adapter was made, as shown in Figure 3.

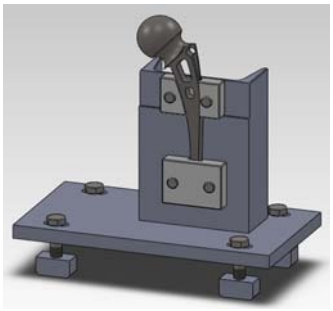

Figure 3. Solid model of testing arrangement

This test arrangement was developed to model a proximally loosened hip stem, the clinical situation that has led to hip stem fatigue fracture.

The purpose of these experimental tests was to determine precise correlation between deflections of the implant and load, in order to analyse implant stability.

The crack propagation characteristics are important in achieving a fail-safe design for structural materials. While titanium alloys are superior to pure titanium in terms of their significantly better fatigue properties, fatigue failure still remains a problem. In order to prevent the catastrophic failure of biomaterial, it is necessary to understand the fatigue crack initiation and fatigue crack propagation characteristics. [6] [3] [13] [14] [15]

Titanium alloys are known for their high sensitivity to fatigue induced by notches. Accordingly, prosthesis components must be designed in a way that minimizes stress concentration. Considering this, a sharp–notch tension test was performed. The fatigue behavior of Ti–6Al–4V alloys was investigated by means of ASTM International Standard Test for Materials E338–03. [16]

Experimental analysis of titanium alloys for biomedical applications presented in this paper is based on an optical methodology measuring system. This 3D system for experimental analysis is useful in analyzing structural integrity and determining properties of materials. The method is also suitable for analysis of irregular object geometries made of various materials, as is often the case in biomedical applications. [14] [17] [18]

3. Experimental analysis results. Discussion

In this experimental analysis Ti6Al4V alloy implant stability and fracture behaviour of specimens was analysed at room temperature (20°C). For the experimental testing of artificial hip implants a servo hydraulic dynamic and static material testing machine ZWICK ROELL HB250 was used. Experimental testing arrangement for titanium alloy implant is presented in Figure 4.

Figure 4. Servo-hydraulic dynamic and static material testing machine ZWICK ROELL HB250

Artificial hip prosthesis that was removed during revision surgery was used as a testing specimen. The prosthesis that was investigated is of cemented type with a conical stem and a spherical head. It is standardized as Austin Moore prosthesis and presented in Figure 5.

Figure 5. Testing specimen

The femoral head of the prosthesis is made of cobalt-chromium alloy, while the stem component is made of Ti-6Al-4V alloy.

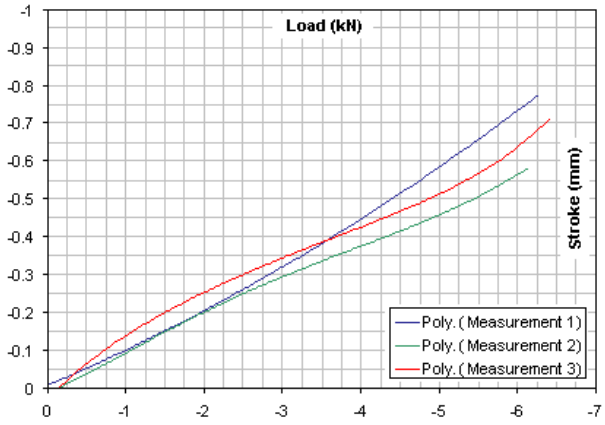

Figure 6. Diagram of force and stroke

In the laboratory test three different time rate loading conditions on the implant were simulated, for 0.01 kN/s, 0.05 kN/s and 0.1 kN/s. During the test, the forces and the stroke were recorded. The results of the experiment are shown in Figure 6.

The experimental system for digital image correlation uses two matched digital cameras that provide a synchronized stereo view of the specimen. It also includes the stand that provides stability of the sensors, an image recording and power control unit, and the data processing system. [10]

The experiment was performed to evaluate fracture behaviour and crack propagation in two Ti-6Al-4V alloy specimens. The titanium alloy specimens were machined to the dimensions given for standard Sharp Edge-Notch Specimen, DE(T).

In crack initiation testing, specimens were subjected to a number of stress cycles required for the fatigue crack to initiate and subsequently to grow large enough to produce failure.

After the system and the specimens were calibrated, the experimental measurement procedure was successfully performed. The procedure included creating a new project, setting recording speed and lighting around the object. After the measuring project was created in the software, the images were recorded during various loading stages of the object. After the computations, the results of fracture analysis were processed and prepared for the final report.

The results indicate that the force action of 2200 N was sufficient for fatigue cracking of titanium alloys used in biomedicine. After that, the failure of the specimen occurred at applied force of 490 N, as shown in Figure 7.

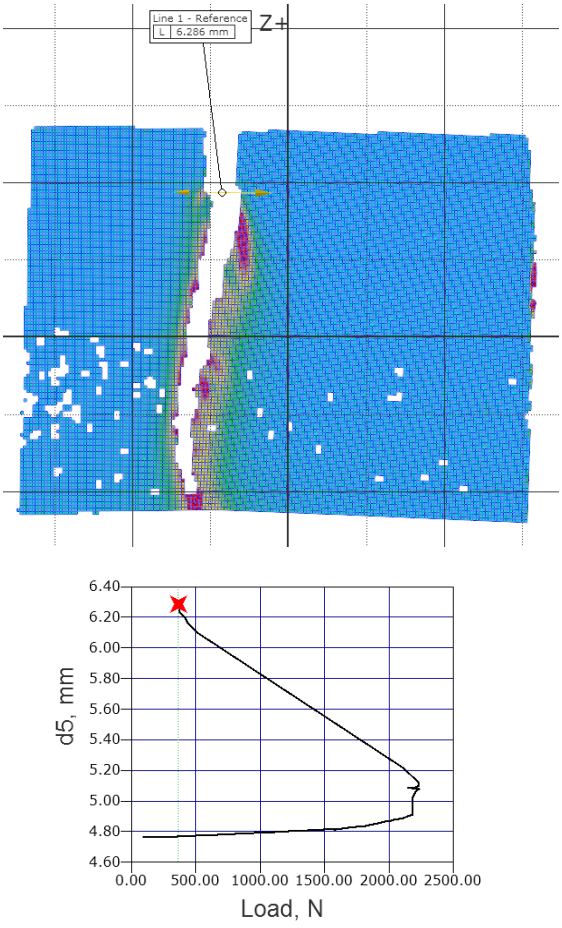

Figure 7. Major strain field - Ti alloy specimen

The results indicate that greater loading forces that occur *in vivo* can lead to impairment of implant stability. In such a condition the loading direction changes, causing changes to the stress field not anticipated by implant design. In this situation, even the normal loading conditions during the gait cycle can lead to initial crack formation, or even ultimate implant failure.

4. Conclusions

The results of this study show that understanding of physiological mechanical loadings on the implant is very important. Applied loads in standards are defined in order to correspond with mean values for daily activity. The aim of this study was to investigate how peak values of forces and torques acting at the hip joint during human gait cycle influence implant stability. In this experiment it was shown that the loads that can occur *in vivo* can be much higher than the standardized values, and that they can make much greater deflections, leading to impairment of implant stability.

Impaired implant stability and, as its consequence, the changed implant stress field, can lead to implant failure. In this case, when there is an initial crack formed in the biomaterial, crack growth and failure can occur even under standard loading conditions.

Prevention of premature failure of orthopedic hip implants has been a constant struggle for engineers. Mechanical testing of total joint replacement components must be performed as part of design approval. *In vivo*, each prosthesis component is subjected to a different set of loads that is specific to the individual patient. Moreover, the actual *in vivo* mechanisms are complex and involve the hostile body environment. Materials used in biomedical implants are subjected to high stresses and high cycle loading. This very demanding condition, coupled with the aggressive body environment, leads to fatigue failure of metallic implants.

Fatigue fracture and stability considerations have been identified as major problems associated with implant failure of biomedical devices. Numerous other mechanisms, such as aseptic loosening, wear, fretting and corrosion may contribute to fatigue and biomedical application failures. In addition, combined effects of material failure modes working together should be considered.

5. Acknowledgement

The research work is funded by the support of the Ministry of Education and Science of the Republic of Serbia - Contract grants: TR 35040.

6. References

[1] Jeffrey N Katz, „Total joint replacement in osteoarthritis“, *Best Practice & Research Clinical Rheumatology* Vol. 20, No. 1, pp. 145–153, 2006.

[2] A. Buford, T. Goswami, “Review of wear mechanisms in hip implants: Paper I–General”, *Materials and Design*, vol. 25(2004), 385–393.

[3] M. Niinomi, „Fatigue Characteristics of Metallic Biomaterials“, *International Journal Of Fatigue*, Vol. 29, pp. 992–1000, 2007.

[4] Manish Paliwal, D. Gordon Allan, Peter Filip, „Failure analysis of three uncemented titanium-alloy modular total hip stems“, *Engineering Failure Analysis* Volume 17, Issue 5, pp. 1230–1238, 2010.

[5] Jesus Chao, Victor Lopez, „Failure analysis of a Ti6Al4V cementless HIP prosthesis“, *Engineering Failure Analysis* 14, pp. 822–830, 2007.

[6] A. Sargeant, T. Goswami, „Hip implants: Paper V. Physiological effects“, *Materials & Design* Volume 27, Issue 4, pp. 287–307, 2006.

[7] George F. Chimento, Thomas P. Sculco, „Minimally Invasive Total Hip Arthroplasty“, *Operative Techniques in Orthopaedics*, Vol 11, No 4 (October), pp. 270-273, 2001.

[8] Michael J. Archibeck et al., „Cementless Total Hip Arthroplasty in Patients 50 Years or Younger“, *The Journal of Arthroplasty* Vol. 21 No. 4, 2006.

[9] S. Griza et al., „Design aspects involved in a cemented THA stem failure case“, *Engineering Failure Analysis* Volume 16, Issue 1, pp. 512–520, 2009.

[10] G. Bergmann et al., “Hip contact forces and gait patterns from routine activities”, *Jour. of Biomechanics* 34(2001),859-871.

[11] M. Hernandez-Rodriguez, J. A. Ortega-Saenz, G. R. Contreras-Hernandez, „Failure analysis of a total hip prosthesis implanted in active patient“, *Journal of the Mechanical Behavior of Biomedical Materials* 3, pp. 619–622, 2010.

[12] ISO 7206/4. „Determination of endurance properties of stemmed femoral components with application of torsion, Implants for surgery – partial and total hip joint prostheses“, Geneva (CH): International Standards Organization; 2002.

[13] S.H. Teoh, „Fatigue of biomaterials: a review“, *International Journal of Fatigue* 22, pp. 825–837, 2000.

[14] K. Colic, A. Sedmak, N. Gubeljak, M. Burzic, S. Petronic, „Experimental analysis of fracture behavior of stainless steel used for biomedical applications“, *Integritet i vek konstrukcija* (*Structural Integrity and Life*). 2012, Vol. 12 No. 1, pp. 59-63, 2012.

[15] A. Sedmak, K. Čolić, Z. Burzić, S. Tadić, „Structural Integrity Assessment of Hip Implant Made of Cobalt-Chromium Multiphase Alloy“, *Structural Integrity and Life*, 10(2) : pp. 161-164, 2010.

[16] ASTM, International Standard E338-03.“Standard Test Method of Sharp-Notch Tension Testing.” ASTM, Philadelphia, 2003.

[17] D. Zhang, D. Arola. „Applications of digital image correlation to biological tissues“, *Journal of Biomedical Optics*, 9(4), pp. 691-699, 2004.

[18] P. Sztefek et al. „Using digital image correlation to determine bone surface strains during loading and after adaption of the mouse tibia“, *Journal of Biomechanics*, 43, pp. 599-605, 2010.

MECHANICAL PROPERTIES OF POLYAMIDE 12/CLAY NANOCOMPOSITES

Pero Raos[1], Josip Stojšić[1*], Mladen Šercer[2], Ana Pilipović[2] and Marija Somolanji[3]

[1]Mechanical Engineering Faculty in Slavonski Brod, J. J. Strossmayer University of Osijek, Croatia
[2] Faculty of Mechanical Engineering and Naval Architecture, University of Zagreb, Croatia
[3] HEP-Trade Ltd, Zagreb, Croatia
* *Corresponding author e-mail: jstojsic@sfsb.hr*

Abstract
The paper deals with mechanical properties of polyamide 12/clay nanocomposites prepared by a melt-intercalation technique. The aim of the investigation was to determine the influence of compounding conditions, screw rotation speed and mixing temperature on mechanical properties (tensile and flexural strength, and toughness) of the nanocomposite.

Keywords:
Polymer nanocomposite, polyamide 12, montmorillonite, mechanical properties

1. Introduction

Nanocomposites are materials which study had been started in 90th years of last century, but manufacture of nanoscale materials is at least a 100 year old industry (particles of carbon black as fillers in automotive tires). The field of nanotechnology is one of the most popular areas for current research and development in basically all technical disciplines. Seeking for new materials with better properties, scientists are lately more and more dealing with nanocomposites. By definition, the nanocomposites are materials in which at least one phase is in nanometer dimensions, (dimensions of the particle, platelet or fibre modification are in the range of 1–100 nm), whereby is achieved higher specific interfacial area. Therefore the properties of obtained nanocomposites depend more on interactions at the phase boundary than on the phase itself.

2. Polymer nanocomposites

Polymer nanocomposites are composed of polymer matrix and nanofiller. Typical nanofiller / reinforce filler includes: layered filler (with nanometre layer thickness and sheet structure, fibre reinforcing filler (carbon nanotubes and nanofibres) and nanoparticles (SiO_2 nanometre dimensions particles). Layered silicates used in the synthesis of nanocomposites are natural or synthetic minerals, consisting of very thin layers that are usually bound together with counter-ions. For decades, the clay minerals in the sheet form of nanometer thickness are used as filler during the production of polymer nanocomposites. For this purpose, today are most commonly used natural clay minerals: montmorillonite, hectorite and saponite [1].

The name of Montmorillonite is derived from the deposit Montmorillon which is in France. Montmorillonite is clay mineral which is classified in class of dioctahedral smectite.
The structure of montmorillonite is 2:1 The crystal lattice of 2:1 layered silicates (or 2:1 phyllosilicates), consists of two dimensional layers where a central octahedral sheet of alumina is fused to two external silica tetrahedra by the tip, so that the oxygen ions of the octahedral sheet also belong to the tetrahedral sheets, as shown in Fig. 1 [2].

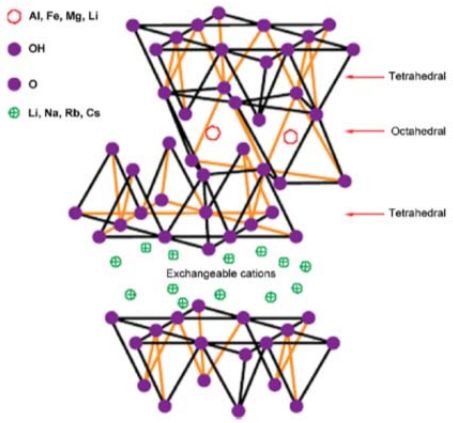

Figure 1. The structure of a 2:1 layered silicate [2]

The thickness of such layer is in the order of magnitude 1 nm and the blank between nearby layers is about 0,3 nm. The reason why the clay is used to produce nanocomposites is very high specific layer surface, more than 100 m^2 per gram, which allows, together with very small mass ratios (2-6%), uniformly dispersed filler in the polymer matrix with the large interactive matrix-filler surface that result in improvements of the obtained composite properties.

3. Production of polymer nanocomposites by melt intercalation process

The most common and simple method, particularly useful for thermoplastic polymers is melt intercalation. In melt intercalation, fillers are mechanically dispersed into a polymer matrix using a high temperature and high shear force mixer or compounder. This approach is simple and compatible with current industrial practices. The biggest challenge in getting nanocomposite reinforced with clay layers is the separation and

dispersal of an individual layer in the polymer matrix. Unless there is no separation of clay layers, common micro composite is obtained (Figure 3a). Nanocomposites with a few polymer molecules inserted in the interlayer between the clay sheets can occur depending on the strength of interfacial interactions (Figure 3b). In the above mentioned dependence can also occur stratified nanocomposite where the clay layers are completely separated and evenly dispersed in the polymer matrix (Figure 3c). Stratified polymer composite is preferred because it produces the largest matrix-filler contact area, which leads to the best nanocomposite properties.

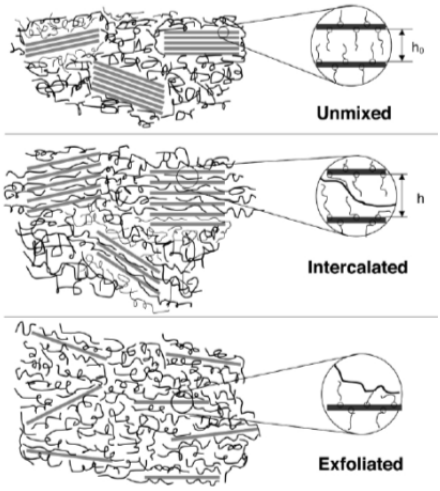

Figure 3. Schematic diagrams of the possible layered silicate based nanocomposite structures [3]

4. Influence of mixing parameters on mechanical properties of PA12/clay nanocomposite

Material used for the nanocomposite matrix is PA12 in the powder form (made in Eos Company), known under the trade name "PA 2200 Balance 1.0". This material is used for the production of laser-sintered fully functional products, which are replacing typical injection moulding products due to their excellent mechanical properties. The main material properties are given in Table 1.

Table 1. PA 2200 Balance 1.0 properties [4]

Properties	Value	Unit	Test Standard
Tensile Modulus	1650	MPa	ISO 527-1/-2
Tensile Strength	48	MPa	ISO 527-1/-2
Charpy impact strength (+23°C)	53	kJ/m²	ISO 179/1eU
Shore D hardness (15s)	75	-	ISO 868
Melting temperature (10°C/min)	176	°C	ISO 11357-1/-3
Density (lasersintered)	930	kg/m³	EOS Method

Cloisite 93A of Southern Clay Products are the nanofiller used in the experiment. Based on previous studies this type of nanofiller is selected as optimal for PA 2200 [5], [6]. Cloisite 93A is a natural montmorillonite modified with a ternary ammonium salt. This filler is designed for use as an additive for plastics and rubber to improve various physical properties, such as reinforcement, HDT, CLTE, synergistic flame retardant and barrier.

Table 2. Typical Cloisite properties [7]

Nanofiler	Organic Modifier	Modifier concentration	Denisity
Cloisite 93A	M2HT	95 meq/100 g clay	1,88 g/cm^3

Nanocomposite compounds were prepared on Brabender extruder line which has two-screw extruder, cooling paths and granulator. Previously weighed and mixed powder (PA 12 + Cloisite 93A) is inserted into the two-screw extruder which mixes melt, pushes it forward and after mixing extrudes it through a nozzle. Nanocomposite mixture is put down on the cooling strip which transports it and cools it in the granulation thread (Figure 4).

Figure 4. Brabender two-screw extruder

Based on previous researches and pre-experiments the three main parameters were selected: content of nanoclay, screw rotation frequency and mixing temperature. Lower and upper limits were determinate for three selected specific factors: content of nanoclay from 3 to 9%, screw rotation frequency from 20 to 40 min^{-1} and mixing temperature from 210 to 230 °C.

Analysis of nanostructure was made by X-ray diffraction and scanning electron microscopy. The results showed that not all the samples exfoliated. For samples with a higher content of nanoclay (9%) intercalation of polymer chains occurred between nanoclay layers while samples with lower

proportion of nanoclay (3%) were fully exfoliated (Figure 5. and 6.). The distance between the layers of Cloisite 93A amounts 2,36 nm by the manufacturer declaration which results with diffraction angle (2*θ*) of 3,7 ° (indicated in Figure 5 with vertical direction).

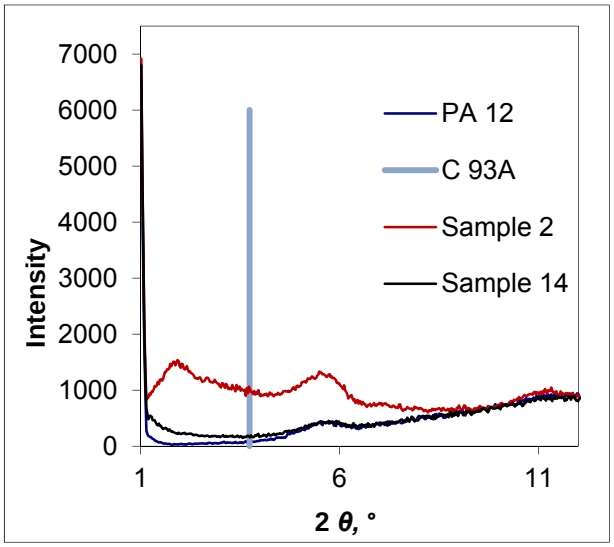

Figure 5. XRD patterns of neat PA12 and samples 2 and 14

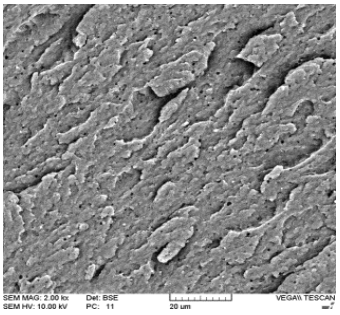

a) sample 2

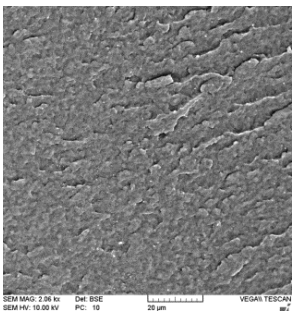

a) sample 14

Figure 6. SEM images of samples 2 and 14

Messphysik Beta 50 – 5 tensile testing machine was used for testing flexural properties. Five specimens of each experimental state were used for testing (95 samples) + 5 samples made of pure PA12 for comparison. The testing speed was 2 mm/min. Charpy device with a mallet of 5 kpcm (≈ 0,5 J) (manufactured by Karl Frank GmbH company) was used in order to determine the Charpy notced impact strength. The distance between supporters was 62 mm. The investigation results are presented in Table 3 and figures 7 and 8.

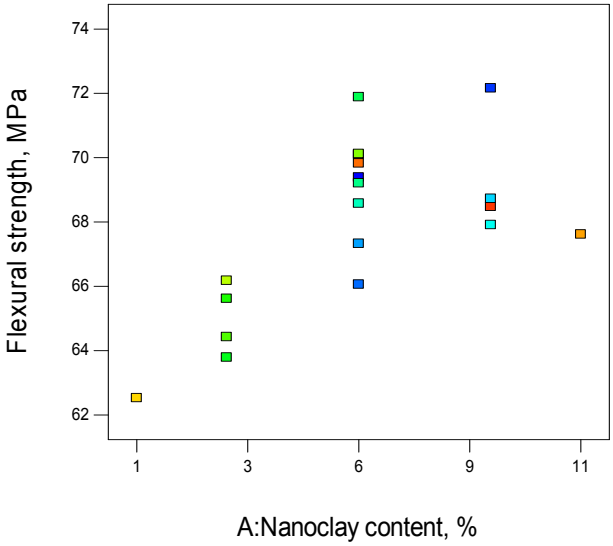

Figure 7. Dependence of flexural strength on the content of nanoclay (with the impact of remaining 2 factors)

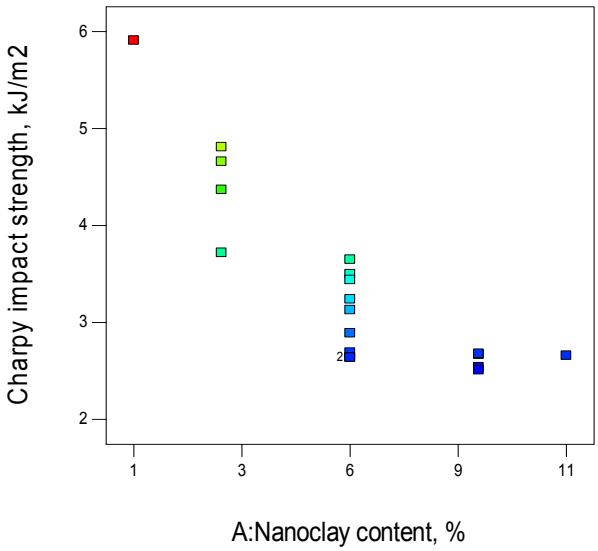

Figure 8. Dependence of Charpy impact strength on the content of nanoclay (with the impact of remaining 2 factors)°

Table 3. Investigation results

Number of samples	Factor 1 A: contnet of nano-clay, %	Factor 2 B: screw rotation frequency, min^{-1}	Factor 3 C: temperature, °C	Flexural strength σ_{fM}, MPa	Charpy notched impact strength, a_{cN}, kJ/m^2
1	3	20	210	65,62	4,81
2	9	20	210	67,91	2,67
3	3	40	210	64,43	4,37
4	9	40	210	68,48	2,68
5	3	20	230	66,18	4,66
6	9	20	230	68,73	2,54
7	3	40	230	63,79	3,72
8	9	40	230	72,16	2,51
9	0,95	30	220	62,53	5,91
10	11,05	30	220	67,62	2,66
11	6	13,18	220	71,89	2,69
12	6	46,82	220	70,09	3,13
13	6	30	203,18	68,58	3,5
14	6	30	236,82	69,83	3,65
15	6	30	220	69,39	3,24
16	6	30	220	67,33	2,64
17	6	30	220	70,12	3,44
18	6	30	220	69,21	2,89
19	6	30	220	66,06	2,64
PA12	X	X	X	60,72	5,98

5. Conclusion

The experimental part investigated the dependence of mechanical properties (flexural strength, toughness) on the mixing parameters PA12/layered clay nanocomposites. It is evident from the results that increasing the content of nanoclay from 1% to 6% (with the impact of the other two parameters) significantly increases the flexural strength. Furthermore, increasing the content of nanoclay has no significant effect on the flexural toughness. Increasing the content of nanoclay (with the impact of the other two parameters) significantly decreases Charpy´s notched impact strength. Further research will go in the direction of getting the appropriate mathematical model that will determine the dependence of mechanical properties (flexural strength, Charpy impact strength) on the mixing parameters while making nanocomposite mixture of PA 12/layered clay needed to specifically define mixing parameters in order to achieve desired properties.

6. References

[1] M. Ivanković, *Polimerni nanokompoziti*, Polimeri 28(2007)3, pp. 156-167
[2] S. Pavlidou; C.D. Papaspyrides, A review on polymer–layered silicate nanocomposites. Progress in Polymer Science 33 (2008), pp.1119–1198
[3] R. Krishnamoorti; K. Yurekli, *Rheology of polymer layered silicate nanocomposites*. Current Opinion in Colloid & Interface Science 6(2001), pp. 464-470
[4] EOS GmbH, Electro Optical Systems, München, http://eos.materialdatacenter.com/eo/en, 16.06.2011.
[5] J. Stojsic, A. Kalendova, P.Raos, M. Somolanji, Compounding of PA12/clay nanocomposites. TEAM 2011, 3rd International scientific conference TEAM 2011, October 19-21, 2011 Trnava, Slovakia
[6] J. Stojsic, A. Kalendova, P.Raos, M. Somolanji, Compounding of PA12/clay nanocomposites, 2nd International conference on manufacturing engineering & management ICMEM 2012, December 5-7, 2012 Prešov, Slovakia
[7] Rockwood Additives LTD., Product Bulletins http://www.rockwoodadditives.com/product_bulletins.asp, 16.06.2011.

BIOTRIBOLOGY RESEARCHES IN NATURAL LUBRICATION OF HUMAN SYNOVIAL JOINTS

A. Ruggiero[1*], S. Hloch[2]

[1]Department of Industrial Engineering, University of Salerno, Italy
[2] Faculty of Manufacturing Technologies, of TUKE with a seat in Prešov |SK
* *Corresponding author e-mail: ruggiero@unisa.it*

Abstract
The aim of this paper is to present a record of early major lubrication concepts developed for natural synovial joints up to the 1970s; to present a recent study focused on the analytical modeling of the lubrication phenomena acting in the human synovial joints, with particular reference to the ankle joint. It should also be pointed out that the focus of this paper was on the development of major lubrication concepts, and therefore only selected studies were presented, rather than a detailed, comprehensive account of all literature.

Keywords:
Biotribology, natural lubrication, synovial joint, mathematical modeling

1. Introduction

According to the Concise Oxford English Dictionary, 'Tribo' is derived from the Greek word 'Tribos', meaning rubbing and friction, and Tribology is 'the study of friction, wear and lubrication, and design of bearings, science of interacting surfaces in relative motion'. Tribology was introduced in 1966 in the Jost Report (Lubrication (tribology) Education and Research, Department of Education and Science, HMSO, 1966) and was formally defined as ''The science and technology of interacting surfaces in relative motion and the practices related thereto''[1]. In short, tribology deals with lubrication, friction and wear, which can be involved with a number of basic engineering subjects such as solid mechanics, fluid mechanics, lubricant chemistry, material science, heat transfer, etc. The importance of tribology in engineering is self-evident since virtually all engineering components and systems are involved with relative motion. Typical examples include ball bearings, gears, tyres, etc. The importance of tribology in biological systems is also clear. The term *bio-tribology* was introduced by Dowson and Wright [2] in 1973 to cover ''all aspects of tribology related to biological systems''. The best-known example of the subject is the numerous studies of natural synovial joint lubrication and the design, manufacture and performance of various forms of total joint replacements. Wear of bearing surfaces in humans and animals can result in pain and restricted movement. The consequences of excessive wear of the bearing material (articular cartilage) in synovial joints are well known.

Typical examples of tribology applied to biology include:

- Tribology of natural synovial joints and artificial replacements;
- Wear of dentures;
- Tribology of contact lenses and ocular tribology;
- The wear of replacement heart valves;
- The lubrication of the pump in total artificial hearts;
- The wear of screws and plates in bone fracture repair;
- Cutting of biomaterials in surgery [3,4];
- Lubrication in pericardium and pleural surfaces
- Friction of skin and garments;

The mechanism of synovial joints have attracted the interest of individuals and groups in several countries [5] , all of whom are trying to find how synovial joints functions in health and how this functioning is disturbed in the early stages of osteoarthrosis. In view of the considerable and increasing burden placed on individuals and on yhe health and social services by joint deseas, this aspect of research is perhaps the one from which there may come sufficient understanding to lead to methods of preventing, arresting, or reversing the process of degeneration.
Natural synovial joints such as ankle, hips and knees are remarkable bearings in engineering terms (biobearings [6]). The bearing materials are articular cartilage, supported by subchondral bone and lubricated by synovial fluid. The load experienced in hip joints during normal steady walking can reach up to 3 to 5 times body weight, while a wide range of motions are encountered. Furthermore, the high load is often accompanied with slow speed in the stance phase, which is not suited for hydrodynamic lubrication in engineering practice. Despite these harsh environments, healthy synovial joints can last for more than 70 years with minimum friction and wear. However, disease or trauma can severely impair the normal function of synovial joints, resulting in the loss of articular cartilage, consequently causing pain and restricted movements, and requiring artificial joint replacements. The current understanding of joint diseases such as osteoarthritis (OA) is still incomplete, although the role of mechanical factors is clearly recognized. OA is often associated with loss of articular cartilage and therefore lubrication

plays an important role. Understanding of the lubrication mechanism is also important for developing interventions to treat cartilage degeneration and loss. This is particularly timely due to the clinical problems associated with current total joint replacements after their extensive introduction since the1960s. Consequently, early interventions and minimally invasive approaches are required and articular cartilage may become one of the bearing surfaces. Significant lubrication studies of synovial joints have been carried out, particularly in the 1990s and 2000s.
In the last years the Authors of the present paper focused their research activities principally in the field of mathematical modelling of some human synovial joints, starting from the ankle joint [7,8,9] , and in the field of the cutting of bio materials by using water jet, with related tribolocical aspects.
In this paper some principal results will be shown with particular reference to a new proposed analytical model to describe, in simplified way, the synovial pressure field and fluid film force acting in the human ankle joint during the motion.

2. Structure of natural joint and early lubrication concepts

Man has over three hundred joints in his body [10]. Through the centuries they have been classified in two main groups, synarthroses and diarthroses. Diarthroses have a cavity between the bones, containing synovial fluid. They are therefore commonly called synovial joints. It is often thought that only the joints of the leg are load-bearing, but in fact those of the arm also bear load. The elbow, for instance, is subjected to forces of 3.2kN during maximal isometric efforts.
From an engineering point of view synovial joints are remarkable bearings. In a most general sense, the function of the synovial joint is to facilitate artic- ulating motion of a creature supported by an internal skeleton. To do this it must permit the relative motion of one segment of bone past another while support- ing the considerable load involved.The ability of weight-bearing oints to provide trouble-free operation for the lifespan of most users is even more remarkable when the size of the forces encountered is considered. These may be many times body weight in certain activities and, depending on the geometry, may be entirely borne by an area as small as 500mm^2.

Moreover, the large loads applied to the cartilage surfaces are not static. They are applied while the opposing diarthroses are sliding over one another or approaching each other normally. Throughout this relative motion the magnitude and direction of the applied force is changing as well. In walking, for example, flexion, extension, adduction, and abduction may occur, together with a consider-able degree of medial and lateral rotation of the femur. During all these activities adequate lubrication must be maintained to protect the cartilage from wear.
In their simplest form, joints may be considered as simple or compound. This is a numerical classification which describes the number of joint surfaces within the capsule. A simple joint contains two surface. A compound joint has more than two surfaces and is well illustrated by the radio-carpal joint.
Sometimes an intra-articular structure subdivides the joint cavity, e.g. the knee and temporo-mandibular joints, and this is called two-chambered or bicameral.
Cartilage is a permeable, soft tissue, 70% of which (by weight) is made of water. The remaining tissue is composed (again by weight) of 40% chondrocytes (cartilage cell), 35% collagen fibres and 25% proteoglycon. Interstitial fluid in the articular cartilage contains water and positively charged solutes. The proteoglycon gel has glycosaminoglycon branches with fixed negatively charged groups in the protein core. Although these weak electrostatic forces are not sufficient to hold the interstitial fluid when the cartilage is loaded they are sufficiently strong to hold the fluid in place when there is no load and to return it to place when a load is released.
Porosity affects the material properties. Collagen fibres are of the order of 1 μm in diameter and form a fine mesh network. If dry articular cartilage is compressed the elasticity of the whole cartilage layer (i.e. the complete layer including cartilage and the gaps between the fibres) should increase with increased load. During the initial loading period the gaps between the fibres decrease while the fibres themselves are compressed. After sufficient load has been applied, the inter-fibre spaces will diminish to an extent where they will have little effect on the elasticity of the cartilage as a whole. The elasticity at this stage will be characterized by the material properties of the fibres themselves. This will clearly result in an elasticity which will vary with applied load. However, when load is applied to a saturated cartilage, not only are the fibres compressed but the fluid between the fibres must be squeezed out, or compressed, to compress the fluid-filled gaps.
Surface properties of the articular cartilage are important in determining the nature of the lubrication between the upper and lower cartilage. Most research to date suggests that, with sufficient magnification, the surface roughness consists of a series of rounded peaks and valleys. Studies of casts of cartilage with a stylus profilometer indicate that the surface is composed of repeating ridged patterns. McCutchen [3] suggests that, in young humans, these patterns have peak to valley heights of 2 μm with a wavelength of 25 μm and

range up to 15 μm peak to valley heights with a wavelength of 250 μm in old arthritic humans.
Synovial joint fluid is a mucinous material of high and variable viscosity. It is a light yellowish liquid contained within synovial joints in the region bounded between the synovial membrane and the articular cartilage surfaces. The relative importance of the fluid as a lubricant or as a supplier of nutrients to the adjacent cartilage has not been clearly established. Nevertheless, experiments on cartilage with the surface wiped dry and on cartilage moistened with synovial fluid have clearly demonstrated that the fluid, or one of its components, does lubricate the joint and does protect the joint against wear. It has also been established that the fluid acts as a fluid film which has a variable viscosity depending partly on the concentration of hyaluronate macromolecules contained in the fluid. These macromolecules are too large (larger than 1 μm) to enter the pores of the cartilage.
The earliest concept of a lubrication mechanism proposed for natural synovial joints was fluid film, probably because of the remarkable tribological performance of these natural bearings. The development of this early concept was based largely on simple observations of anatomical and structural similarities between natural synovial joints and engineering counterparts. Reynolds, in his classical paper which established the scientific foundation of fluid film lubrication, wrote: *..."This plays an important part in certain mechanisms, as in the steam engine, and is as fundamental to animal mechanics as the lubricating action of the journal is to mechanical contrivances".* Further support for the fluid film lubrication concept was offered by MacConaill [5] who noted the similarities between the anatomical structure of some synovial joints, such as the meniscus between the femoral and tibial cartilages in the knee, and the "physical wedge" shown by Reynolds for generating hydrodynamic pressure. He suggested that the intra-articular cartilages set themselves at a slight inclination and thus presented wedge-shaped lubricant films similar to those developed in Michell titling pad thrust bearings well known in engineering. This concept was later indirectly confirmed experimentally by Jones [5].
The fluid film lubrication concept for synovial joints was challenged by the late Sir John Charnley10) who argued that the slow speed and large dynamic load would not favour the generation of a hydrodynamic lubricating film and he proposed boundary lubrication instead.
Although different lubrication concepts were developed separately in early studies of synovial joints, it was clearly recognized by Dowson [] that a combination of some form of fluid film lubrication, due to entraining and squeeze-film actions, with boundary lubrication providing the surface protection in cases of severe loading and little movement, was probably responsible for the remarkable tribological performance of these natural bearings.

3. The human ankle joint approximate squeeze film and closed-form mathematical model

The human ankle joint can be simply taken as cylindrical, enabling rotation in the sagittal plane only. The joint is represented by two rigid circular cylinders in the inner contact (a cylinder encased in a cylindrical cavity), coated with thin layers of cartilage. The coupling model is assumed by two infinite rigid circular cylinders [7,8,9] (subchondral bone) in the internal contact (a cylinder encased in a cylindrical cavity), covered with thin layer (articular cartilage) of uniform thickness; the lower (talar) articular surface is supposed stationary while the upper (tibial) surface is assumed to have pure squeeze motion $\dot{\varepsilon}(t)$

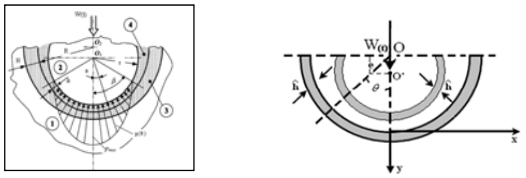

Figure 1. a) Geometry of ankle joint. (1), (2)-Bone, (3)-cartilage layer, (4)-synovial fluid; b) Human ankle joint equivalent bearing

The long chain polysaccharide hyaluronic acid molecules present in the synovial fluid give us the motivation for modeling of the synovial fluid as a Stokes [5] couple-stress fluid.

Making the usual assumptions of hydrodynamic lubrication applicable to thin films [6], and considering the flow of a viscous fluid in a porous matrix governed by modified Darcy's law (1) [7], the modified Reynolds equation, considering the nomenclature in table 1, written in a non-dimensional form is (2):

$$v(x,h,z,)=\frac{\Phi H}{\mu(1-\alpha)}\left(\frac{\partial^2 p}{\partial x^2}\right)=0 \qquad (1)$$

$$\frac{\partial}{\partial x}\left[f(h,l)\frac{\partial p}{\partial x}\right]=12\mu\frac{dh}{dt}+\frac{12\Phi H}{(1-\alpha)}\left(\frac{\partial^2 p}{\partial x^2}\right) \qquad (2)$$

where:

$$f(h,l)=h^3-12l^2h+24l^3\tanh\left(\frac{h}{2l}\right);\quad l=\left(\frac{\eta}{\mu}\right)^{\frac{1}{2}}; \qquad (3)$$

and μ has the dimensions of viscosity, whereas η has the dimensions of momentum. The ratio η/μ has the dimensions of length squared.
It is convenient to analyse the problem by using the non-dimensional variables and parameters as follows[8].

$$\theta=\frac{x}{R},\ L^*=\frac{L}{c},\ l^*=lc,\ \varepsilon=\frac{e}{c}, \qquad (4)$$

$$h^* = \frac{h}{c} = 1 + \varepsilon\cos(\theta),$$

$$H^* = \frac{H}{c}, \phi^* = \frac{\phi}{c^2}, p^* = \frac{pc^2}{\mu R^2 \left(d\varepsilon/dt\right)}$$

Consequently, one has the modified Reynolds equation written in a non-dimensional form as:

$$\frac{\partial}{\partial\theta}\left\{\frac{\partial p^*}{\partial\theta}\left[f^*\left(h^*, l^*\right) + \frac{12\Phi^* H^*}{(1-\alpha)}\right]\right\} = 12\cos(\theta) \quad (5)$$

As regards the determination of the thickness of the fluid film can be estimated that the same can be assessed as the sum of a component linked to the geometry of the system and another related to the elastic deformation of the thin coating cartilage, namely:

$$h = h_g + h_e, \quad h_g = c - e\cos\theta \quad (6)$$

In which *e* represents the radial clearance, while the term h_e takes into account the influence of elastic deformation of the porous matrix of thickness, and depends on the physical characteristics of the material (cartilage).

As can be seen from the drawing, in both cases, the term related to the deformability of the surfaces he is added to the geometric h_g. In approximating way the deformation of the matrix layer can ce be calculated:

$$h_e = Kp_e \qquad K = \frac{H(1-\nu^2)}{E} \quad (7)$$

,

Switching to a non-dimensional formula we will :

$$h^* = 1 + \varepsilon\cos\theta + C_0\overline{P},$$

with

$$C_0 = \frac{\mu R^2 \left(d\varepsilon/dt\right) H(1-\nu^2)}{Ec^3} \quad (8)$$

The showed formulation allow to solve analitically the equation 5 in order to have the closed form solution of the non-stationary SF pressure field and subsequently, by integration, the SF film force.

8. Conclusion

The paper summarize, in the limits of the available pages, the early major lubrication concepts developed for natural synovial joints up to the 1970s and presents some results obtained by the Authors in the recent studies, focused mainly on the analytical modeling of the lubrication phenomena acting in the human synovial joints, with particular reference to the ankle joint. It should also be pointed out that the focus of this paper was on the development of major lubrication concepts, and therefore only selected studies were presented, rather than a detailed, comprehensive account of all literature.

9. References

[1] Z.M. Jina, M. Stoneb, E. Inghamc, J. Fishera, "Biotribology," *Current Orthopaedics (2006) 20, 32-40, Elsevier*.

[2] Dowson D, Wright V. Bio-tribology. In: Proceedings of the conference on the rheology of lubrication. The Institute of Petroleum, The Institution of Mechanical Engineers and the British Society of Rheology; 1973. p. 81–8.

[3] Sergej Hloch, Alessandro Ruggiero(2013). Online Monitoring and Analysis of Hydroabrasive Cutting by Vibration. Advances In Mechanical Engineering. Vol. 203. Pag.1-10 ISSN:1687-8132.

[4] Pavol Hreha, Sergej Hloch, Dagmar Magurová, Jan Valíček, Dražan Kozak, Marta Harničárová, Marko Rakin Water Jet Technology Used In Medicine Technical Gazette 17, 2(2010), 237-240 ISSN 1330-3651

[5] "Jin Z., Dowson D. , Development of Early Concepts of Lubrication in Natural Synovial Joints, Tribology Online, 6, 3 (2011) 168-173. ISSN 1881-2198.

[6] Walicki E. and Walicka A., Mathematical modelling of some biological bearings, Smart Mater. Struct. 9 (2000) 280–283. Printed in the UK.

[7] Ruggiero A., Gòmez E. , D'Amato R. Approximate Analytical Model for the Squeeze-Film Lubrication of the Human Ankle Joint with Synovial Fluid Filtrated by Articular Cartilage. Tribology Letters. Vol. Volume 41-N.2. Pag.337-343 ISSN:1023-8883.

[8] Alessandro Ruggiero, Emilio Gòmez, Roberto D'Amato(2012). Approximate Closed-Form Solution Of The Synovial Fluid Film Force In The Human Ankle Joint With Non Newtonian Lubricant. Tribology International. Vol. 57. Pag.157-161 ISSN:0301-679X.

[9] A. Ruggiero, R. D'Amato, E. Gòmez, S. Hloch(2013). Approximate closed-form solution of the synovial pressure field in the human ankle joint with non newtonian lubricant and deformable cartilage layer. In: Biomodlore 2013 Palanga, LT 20-22 Sept. 2013 Vilnius Vilnius Gediminas Technical University Press Pag.14-16 ISBN:9786094575488.

[10] J. H. Dumbleton, Tribology of Natural and Artificial Joints, Elsevier 1981. SBN: 0-44441898-9 (Val.3) ISBN: 0-444-416773 (Series).

ASSESSMENT OF THE INDUSTRIAL ENTERPRISES CHANGEABILITY

Svetoslav Dimkow [1]

[1] Technical University – Sofia, Business Faculty, Bulgaria, sdim@tu-sofia.bg

Abstract
This work discusses a developed by the author system for evaluating industrial enterprises changeability. The system assesses the degree of maturity of 30 related to industrial enterprise changeability business processes which are structured into three groups: Integrated product design; Factory planning; Production operations planning. Evaluation system has been piloted in few Bulgarian manufacturing SMEs.

Keywords:
Mass customization; Collaborative manufacturing; Responsive manufacturing; Changeable manufacturing systems; SMEs

1. Introduction

The last decade has brought forth enormous changes in world economy. Markets in industrial countries have reached a level of maturity, where quality, technical superiority and short delivery lead times of products have become mere prerequisites for market success. Companies today can only compete if they offer products and services that meet the customer's individual needs.
This has lead to an increasing number of products, product variants and configurations offered. Concepts such as mass customization and individualization promise the creation of unique items for nearly every customer. Decreasing product lifecycles leave only short and transient windows of opportunity for companies to profitably produce and sell a particular product or service using a given value chain. Corporate managements had to accept the fact that market forecasts turned more complex and that rapid changes in the marketplace cannot be controlled. At the same time, globalization has intensified the worldwide competition and imposed a permanently growing pressure on production costs.
The above mentioned challenges have led to the development of an innovative strategy and a new industrial paradigm is now essential in order to guarantee competitiveness with a sustainable business vision. From a manufacturing perspective it is becoming progressively clearer that the next generation of factories needs to be modular, scalable, flexible, open, agile and knowledge-based in order to be able to adapt, in real time, to the continuously changing market demands, technology options and regulations.
The main objective of this work is the identification of changeability related Business processes and development of a system for assessing the maturity of these processes.

2. Changeable manufacturing systems

Changeability as the 'ability to change' and to adapt the company to new circumstances describes a concept which is popular especially in German literature. Although the concept of changeability is widely accepted, the notion is not yet defined in a uniform way.
It seems not advisable to use the term flexibility on all levels of a factory. In addition, the level of product to be changed must be taken into account as well. If the five structuring levels are combined with the associated product levels, a hierarchy emerges that allows the definition of five types of changeability [1]. Any type at a higher level subsumes the types below it.
The hierarchy of product levels starts from the top with the product portfolio a company offers to the market. Then the product or a product family follows downwards. The product is usually structured into sub products or assembly groups that contain work pieces. The work pieces themselves consist of features.
Five classes of changeability evolve from this matrix [2].
Changeover ability designates the operative ability of a single machine or workstation to perform particular operations on a known work piece or subassembly at any desired moment with minimal effort and delay.
- Reconfigurability describes the operative ability of a manufacturing or assembly system to switch with minimal effort and delay to a particular family of work pieces or subassemblies through the addition or removal of functional elements.
- Flexibility refers to the tactical ability of an entire production and logistics area to switch with reasonably little time and effort to new - although similar - families of components by changing manufacturing processes, material flows and logistical functions.
- Transformability indicates the tactical ability of an entire factory structure to switch to another product family. This calls for structural interventions in the production and logistics systems, in the structure and facilities of the buildings, in the organization structure and process, and in the area of personnel.
- Agility means the strategic ability of an entire company to open up new markets, to develop the requisite products and services, and to build up necessary manufacturing capacity.

Multiple requirements on both an organizational and an operative level have to be met in the strive for changeability.

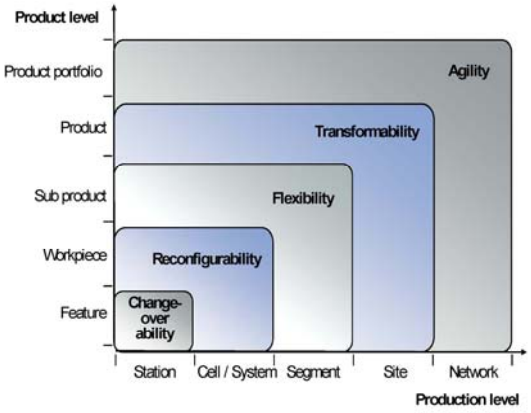

Figure 1. Classes of Factory Changeability
Source: [1]

A thorough analysis is necessary to identify the extent to which the fulfillment of these needs can be supported through today's digital factory approaches. The concept of the digital factory and its current implementation in industry supports mainly product and process design. From the perspective of production engineering, the central enhancements gained through the digital factory can be summarized as follows:

- Efficient and fast planning;
- Virtual ramp-up decoupled from real factory;
- Reusability;
- Evaluation of discrete alternative concepts.

As discussed in the previous section, changeability requires the ability to frequently changeover, to adapt to unplanned situations, to support planning on all levels of a production system and to combine both centralized and decentralized action. Frequent changeovers are facilitated by the digital factory in terms of allowing fast and efficient planning as well as a virtual ramp-up. Reducing cost and time required for preparing and implementing a changeover, companies are enabled to reorganize their production more often. Virtual ramp-ups decoupled from the real factory strongly contributed to the vision of a digital ramp-up, where production down-time and financial losses due to introduction of a new product or production process are minimized.

The ability to adapt to unplanned situations is a characteristic of changeable systems. Hence, the design and evaluation of such systems is focused on the potential that is inherent to a production system. On the other hand, the digital factory is aimed on planning and detailing a discrete solution to a complex manufacturing problem. When it comes to evaluation, the digital factory therefore only offers the possibility to manually detail several discrete alternative solutions and compare them against each other. Consequently, the digital factory can help to evaluate known alternatives, but it provides little aides for finding them.

3. Assessment model of the industrial enterprises readiness for changeability

The authors propose the assessment of the industrial enterprises readiness to be performed by determining the degree of maturity of the changeability related Business processes.

The concept of process maturity proposes that a process has a lifecycle that is assessed by the extent to which the process is explicitly defined, managed, measured and controlled. It also implies growth in process capability, richness and consistency across the entire organization [3]. As an organization increases its process maturity, institutionalization takes place via policies, standards and organizational structures [4].

Building an infrastructure and a culture that supports Business processes estimation methods, practices and procedures, enables process maturity to survive and endure long after those who have created it. Continuous process improvement, an important aspect of Business processes estimation, is based on many small evolutionary rather than revolutionary steps. Continuous process improvement serves as the energy that maintains and advances process maturity to new maturity levels.

As processes mature, they move from an internally-focused perspective to an externally-focused system perspective. A maturity level represents a threshold that, when reached, will institutionalize a total systems view necessary to achieve a set of process goals [3]. Achieving each level of maturity establishes a higher level of process capability for an organization.

According to the model developed by the authors, the evaluation is performed through adoption of five levels maturity of the changeability related Business processes:

Level 1. Unstructured and undocumented Process. Being associated with changeability related Business process and practices it is unstructured and ill-defined. There are no measures for evaluating the process. Activities and organizational structures do not account for Changeability Concept. Process performance is unpredictable. Targets, if defined, are often missed. Process costs are high. Customer satisfaction is low. Functional cooperation is also low.

Level 2. Defined and documented Process. The main activities associated with changeability related Business proces are defined and documented. Traditional hierarchical methods are used to manage the activities in the process. Process performance is more predictable. Targets are defined but still missed more often than not.

Overcoming the functional hierarchies takes considerable effort. Process costs remain high. Customer satisfaction has improved, but is still low.

Level 3. Process Linked to other processes in the enterprise. There has been a breakthrough for Changeability Concept. Managers of the organization use the process in the strategic plans and pursue strategic outcomes. There are joint activities and structures, which extend out of the process, but remain within the enterprise. The cooperation between intra-company functions is in the form of teams that share common measures and goals reached horizontally across the product life cycle. Process performance becomes more predictable and targets are often achieved. Continuous improvement efforts take shape focused on root cause elimination and performance improvements. Supply Chain Management costs start decreasing.

Level 4. Process Linked to processes outside the enterprise. There are joint activities that extend outside the organization. The enterprise, its vendors and suppliers, cooperate on the process level. Organizational structures and activities are based on Changeability Concept procedures. Traditional functions, as they relate to the Changeability Concept, start disappearing altogether. Changeability measures and management systems are deeply imbedded in the organization. Advanced management practices, such as collaborative forecasting and planning with customers and suppliers, take shape. Process performance becomes very predictable and targets are successfully achieved. Process improvement goals are set by the teams and achieved with confidence. Process costs are dramatically reduced and customer satisfaction becomes a competitive advantage.

Level 5. Process as part of cooperation in business networks. The organization functions as a part of the business network. Collaboration between legal entities is routine to the point where advanced Changeability practices which allow transfer of responsibility without legal ownership are in place. Multi-firm Changeability teams with common processes, goals and broad authority take shape. Trust, mutual dependency are the glue holding the extended supply chain together. A horizontal, customer-focused, collaborative culture is firmly in place. Process performance and reliability of the extended system are measured and joint investments in improving the system are shared, as are the returns.

Based on literature studies related to the development of sections 2 to 6 of this work, the authors have identified 30 business processes that can be assessed. According to the developed model these business processes are structured in three groups of 10 business process as follows:

Integrated Product Planning: Computer aided product design - CAD; Computer-aided engineering calculations - CAE; Modular product development - the use of group technologies, standardization of components, reuse of components.; Study of consumer satisfaction in the development of new products; Optimizing the design of products - according to customer satisfaction; design excellence (for manufacturing;, for assembly; for costs, for six sigma etc.).; Collaborative product design; Product design mock up; Use of Reverse Engineering in the design of products; Using creative methods in the design of products (TRIZ, USIT); Use of Rapid Prototyping in the design of products.

Factory Planning: Use of Responsive manufacturing systems; Use of Collaborative manufacturing systems - suppliers, vendors, subcontractors, outsourcers.; Use of continuous improvement (KAIZEN) in the operation of manufacturing systems; Use of Total Productive Maintenance in the operation of manufacturing systems; Use of rapid adjustment (SMED) in the operation of manufacturing systems; Using the methods of Business Processes Management in the design of manufacturing systems; Using the methods of Visual Management in the operation of manufacturing systems; Using the methods of Virtual Reality in the operation of manufacturing systems; Using the methods of Virtual Cells in the operation of manufacturing systems; Cost optimization in the operation of manufacturing systems - Activity Based Costing

Production Operations Planning: Use of Computer Aided Production Operations Planning - CAPP - Process engineering, Process Validation.; Use of product data management systems in the planning of Production Operations - PDM systems.; Use of organizational resources management systems in Production Operations planning - ERP systems - resources modelling and simulation.; Use of Computer Aided Quality Management - CAQQ systems - Inspection planning.; Use of systems for operational control of the Production Operations - MES, RFID, SCADA etc.; Using a collaborative planning and scheduling in the planning of Production Operations - APS systems, Vendor Managed Inventories etc.; Using a pull-type production strategies in planning Production Operations - JIT, Kanban,; Optimizing WIP planning of Production Operations - Line Design, CONWIP; Use singly movement of material flow in the planning of Production Operations - One Piece Flow (One Piece Machining, One Piece Assembly); Using the principles of Theory of Constraints (TOC) in the management of Production Operations;

3. Concluding Remarks

The main objective of this study was to evaluate the industrial enterprises changeability of the SMEs participating in the project, in order to estimate the possibilities for forming competitive behavior based on different forms of partnership.

This research has allowed us to investigate the activity of 4 manufacturing SMEs. If we analyze the research results, we may come to the conclusion that the processes in the group "Production Operations Planning" have the highest level of readiness to implement industrial enterprises changeability, followed by the processes of the group "Factory Planning". The lowest readiness of processes is in the group "Integrated Product Planning".

This is understandable because the researched manufacturing SMEs are of the „Rough Cutting Company" type, but in future if these companies want to maintain their high competitiveness, the main effort should be directed towards improving the processes of the group "Integrated Product Planning" at the expense of integrating the existing software application and implementing advanced software applications for Rapid Prototyping, Reverse Engineering, etc.

4. References

[1] H. P. Wiendahl, Wandlungsfahigkeit, Werkstattstechnik online, 92/4: 122-127, 2002.

[2] H.A. El Maraghy, "Flexible and reconfigurable manufacturing systems paradigms". International Journal of Flexible Manufacturing Systems, Special Issue on Reconfigurable Manufacturing Systems, Vol. 17, pp. 261-276, 2005, ISSN (printed): 0920-6299. ISSN (electronic): 1572-9370.

[3] M. Dorfman, and R.H. Thayer, "The capability maturity model for software", in M. Dorfman, and R.H. Thayer, Eds, Software Engineering, IEEE Computer Society Press, Los Alamitos, CA, 1997, pp. 427-38.

[4] M. Hammer, Beyond Reengineering: How the Process-Centered Organization Is Changing Our Lives, Harper Business, New York, NY, 1996.

Sections

THE EVALUATION OF DOWN-MILLING WITH DIFFERENT RADIAL CUTTING DEPTH

Veronika Fecova[1*], Peter Michalik[1], Jozef Zajac[1] and Erik Hanisko[1]

[1]Faculty of Manufacturing Technologies with a seat in Presov, Technical University of Kosice, Slovakia
* veronika.fecova@tuke.sk

Abstract
The aim of this article is the monitoring of the temperature during the down-milling with different radial cutting depth and subsequently the surface roughness. Contribution describes the state of art in the coherencies between temperature and surface roughness. A main part of this article is realization of experiment, its description, evaluation of results and making a conclusion and recommendations.

Keywords:
down-milling, surface roughness, temperature in milling

1. Introduction

For the function components is the lowest surface roughness of the machined surfaces commonplace. Finding out what effect the temperature of the surface roughness during milling process is an appropriate choice of topic. Milling acquired important place in engineering productions, thanks to the wide applications and precision manufacturing options. Milling with high speed cutting speeds in most cases allows more cost – effective and productive material removal, than using tools with just one cutting edge such as shaping and planning. Milling is in some particularly difficult cases the only way of machining. [1]- [3]

This article describes the experiment about temperature and surface roughness in the milling process with the different radial depth of cut. In [4] author claims, that the higher temperature is achieved by machining with the higher cutting speed. And author in [5] claims, that the lower surface roughness is achieved by higher cutting speed. So, is possible to claim, that higher temperature causes the lower surface roughness? And it is possible to claim, that different radial cutting depth causes the different temperature in the milling and so the different surface roughness according the above claims? It is aim of this article. And for the surface roughness the cooling is very important [6]. Nowadays, the researchers want to find a relation between cutting conditions and temperature. For example, the contribution written by Mr. Cui [7] is focused on the analysis of temperature in the machining – what conditions the user need to set for achieved a defined temperature. It is one of possibilities how we can achieve the needed temperature and so the needed surface roughness in the machining.

2. Implementation of the experiment

This paper deals with the monitoring of the temperature during the down-milling. The radial cutting depth of the milling was 0.8mm on the right side of rib and 0.5mm on the left side of this rib. Realization of this experiment was performed at the Faculty of Manufacturing Technologies of Technical University of Kosice with a seat in Presov. Temperature monitoring was performed on the rib of workpiece. Its dimensions are shown in Figure 1. For experiment the C45 material (12 050) was used.

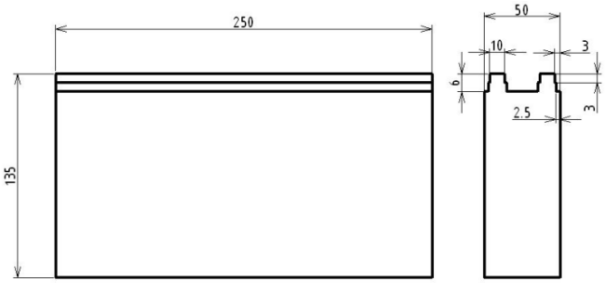

Figure 1. Dimensions of product

First the roughing milling was performed on workpiece, where was achieved the shape of the ribs and then the smoothing was performed, which was captured by using infrared (IR) camera. The experiment was performed by vertical milling CNC machining center Pinnacle VMC 650 S (Figure 2) and the temperature was monitored by the IR camera FLIR T425 (Figure 3).

Figure 2. Vertical CNC milling machining center Pinnacle VMC 650S

Figure 3. FLIR T425

During the experiment was used smoothing tool:

- tool holder AMM15020HR – M10,
- modular adapter – with carbide cylindrical shank,
- cutting blades APMT 0903PDSR – MM PC 3530 VBD with carbide coating KOR.

The working smoothing tool and workpiece on the start of machining are shown in Figure 4.

Figure 4. Smoothing tool and workpiece

The smoothing process was performed with these cutting conditions:

- dry machining,
- n = 2 600 min^{-1},
- f = 260 mm.min^{-1},
- a_p = 3 mm,
- d = 20 mm,
- a_e = 0.5 mm / 0.8mm.

The temperature in workroom was 20.5°C and humidity was 48%. Resolution of camera is 320x240 pixels. Emissivity was set according the table of materials included in IR camera. Distance between IR camera and workpiece was approximately 450 mm.

3. Realization of the experiment

Thermal images were made at the beginning of milling, during the milling and on the end of milling. During the realization of this experiment, the suspicion of break of cutting blade occurred. The process was finished but afterwards the suspicion was confirmed. The following images show the temperature during the machining, which was mentioned before. It can be seen that the temperature at the end of machining is approximately 140-150°C (Figure 5), which confirms the damage of the cutting blade. That was reflected in the machined surface, because the machined surface had the high surface roughness visible to the eye. It is very important to say, that it is not temperature of cutting zone, but it is temperature only of tool. But if the temperature of tool is increasing, the temperature in cutting tool is increasing, too.

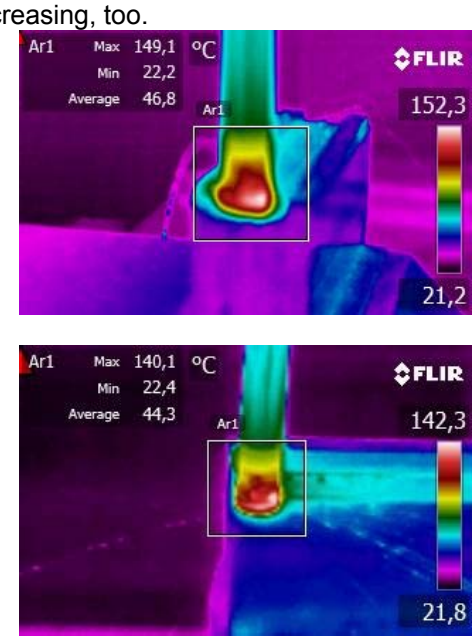

Figure 5. Down-milling – tool breakage

Subsequently the replacement of cutting blade and the correction of the tool were performed and then the smoothing process was started again. During the smoothing process an additional error occurred once again also visible to the eye. The tool path was not correct. The tool at the one side went below the defined path (Figure 6).

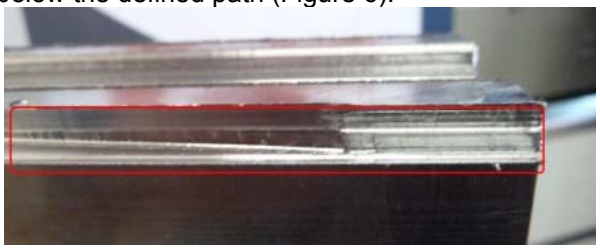

Figure 6. The tool path on the workpiece

The probable cause of this situation was that the broking of blade created bigger oscilation of the tool. It caused peak-to-peak of workpiece in clamp and subsequently the minor feed in clamp and extension of tool from the chuck. All of these effects reflected in the fact that the tool during the process slide below and the resulting surface roughness was very high. After the removing of all errors, the experiment continued.

4. The results of IR camera

Images of the down–milling with the radial cutting depth 0.8mm are shown in Figure 7. These figures display also the value of the highest temperature in the area which is marked.

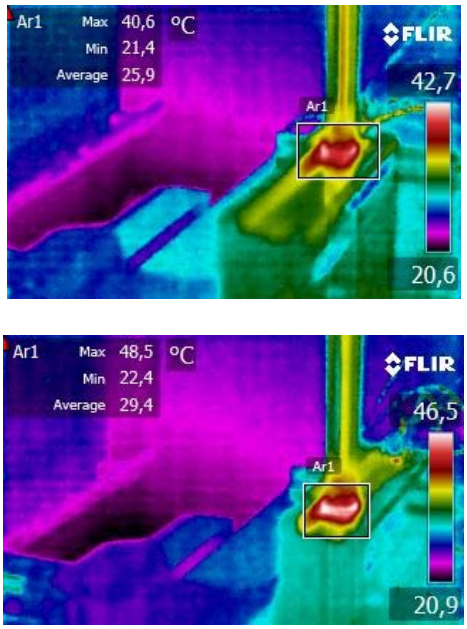

Figure 7. Down–milling with radial cutting depth 0.8mm

In the records are shown substantially lower temperatures as temperatures which were captured at the start of the experiment, respectivelly during the machining with the broken cutting blade. After properly re-set of the all necessary settings the results of the temperature were significantly lower. The following figures show the temperatures during down – milling with the radial cutting depth 0.5 mm (Figure 8).

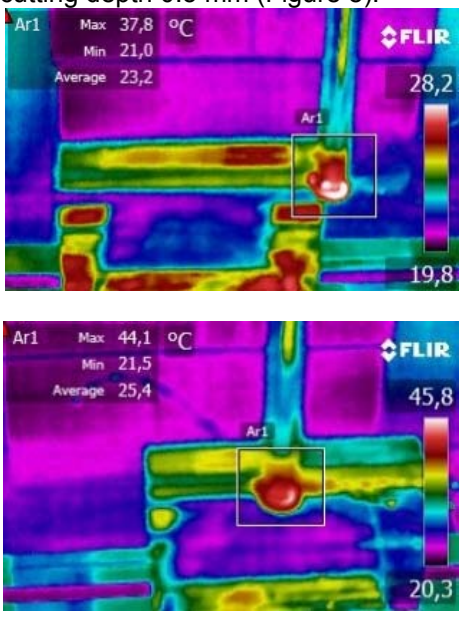

Figure 8. Down – milling with radial cutting depth 0.5mm

From the results of both radial cutting depths can be evaluated, that difference between radial cutting depths in the temperatures is minimal. Both of the milling methods achieve at the end the working temperature of 45 – 49 °C. The final quality of the surface is not affected with this minimal temperature difference.

5. Measurement of surface roughness

Surface roughness measuring of the machined surfaces was followed after milling process and capturing of temperature. This measuring was also performed at FVT with a seat in Presov in metrology laboratory with the standard temperature in room (20.5°C). The digital equipment SJ – 401 was used for measuring (Figure 9).

Figure 9. Digital surface roughness tester

Measurement was performed 10 times for each surface and then was performed the Grubbs test. The surftest SJ-401 measures 5mm from surface and the filter Gauss – 0.8mm was used. The surface roughness was measured only at the ends of the workpiece. Roughness values *Ra* and *Rz* were evaluated (Table 1).

Table 1: Measured values of surface roughness

a_e [mm]	surface roughness [µm]
0.5mm	*Ra* = 0.82 µm
	Rz = 3.7 µm
0.8mm	*Ra* = 1.37 µm
	Rz = 6.4 µm

Due the unexpected events during the machining is necessary to take into the account that the surface roughness in the table will show some deviation.
For evaluation of coherencies of radial cutting depth, temperature and surface roughness, the surface roughness was measured on the start and on the end of rib made by down milling with 0,5mm radial cutting depth (Table 2).

Table 2: Measured values of surface roughness-radial cutting depth 0.5mm

Surface roughness [µm]		
	Ra	*Rz*
Start of milling	0.93	3.9
End of milling	0.82	3.7

6. Evaluation of the experiment

Based on the measured values can be said that with rising temperature value is the value of

surface roughness decreasing. The experiment was unexpected affected by various factors. In consideration was taken also errors which occurred during the measurement. On the basis of only these measurements it is not enough to clearly identify the end of this experiment. It is necessary to have more extensive measurements to determine the end of this experiment. So the experiment would be useful only for this material, tool and cutting conditions after adding additional milling, measuring and testing operations.

Table 3: Comparison of surface roughness and temperature

a_e [mm]	*Ra /Rz* [µm]	*t* [°C]
0.5mm	*Ra* = 0.82 µm	45.2°C
	Rz = 3.7 µm	
0.8mm	*Ra* = 1.37 µm	48.5
	Rz = 6.4 µm	

Table 4 shows the coherencies of temperature and surface roughness from the down milling with the 0.5mm radial cutting depth. It does not confirm theory, that lower surface roughness is achieved by milling with higher temperature. In this case the temperature different is small, but surface roughness different is high, therefore the radial cutting depth has important factor for surface roughness.

Table 4: Measured values of surface roughness-radial cutting depth 0.5mm

Temperature [°C]		Surface roughness [µm]		
Start of milling	End of milling	Ra	Rz	
37.8	45.2	0.93	3.9	Start of milling
		0.82	3.7	End of milling

7. Conclusion

The main aim of this article was to monitor the effect of radial cutting depth on the temperature and surface roughness of machined surface during the down-milling process. The task was to take images of the temperatures, which was created in down- milling with radial cutting depth 0.5mm and 0.8mm. Then the surface roughness of these surfaces was measured and subsequently the evaluation of these parameters was created. After these measurements we can see, that the surface with a higher temperature has a lower surface roughness as surface with a lower temperature, but only if the radial cutting depth is same. Contribution [4] claims, that the higher temperature is achieved in the machining by higher cutting speed. Contribution [5] claims, that the lower surface roughness is achieved by higher cutting speed. Is possible to claim, that higher temperature causes the lower surface roughness? This experiment confirms this claim, because in the machining with higher temperature achieved the lower surface roughness. And how influence the radial cutting depth on the temperature and surface roughness in the milling? According this experiment, the radial cutting depth 0.5mm causes the lower temperature as radial cutting depth 0.8mm. And surface roughness with a_e 0.5mm was lower as surface roughness machined by a_e 0.8mm. So, the radial cutting depth has important influence for achieved surface roughness. But for the more reliable claim about this coherence we recommend to extend the experiment.

8. References

[1] J. Duplak, I. Orlovsky, M. Cuma, "Comprehensive expression of durability for the selected cutting tools in comparison with standard ISO 3685", In: Advanced Science Letters, Volume 19, Issue 2, February 2013, pp. 460-463, ISSN: 19366612.

[2] Z. Hutyrova, J. Zajac, A. Tarasovicova, "Assessment of Statistical Signification of Factors by Machining Inhomogeneous Materials – WPC" In: Applied Mechanics and Materials, Vol. 308 (2013), pp. 165-169, ISSN 1662-7482.

[3] J. Novak-Marcincin, M. Janak, L. Novakova-Marcincinova, V. Fecova, "Possibility of quick check on milling strategy suitability", In: Tehnički Vjesnik, Vol. 19, no. 4 (2012), pp. 959-964, ISSN 1330-3651.

[4] K. Vasilko, E. Ragan, "Theory of Manufacturing Technologies". Technical University of Kosice, Faculty of Manufacturing Technologies with seat in Presov, Prešov, 2010, p. 241, ISBN 978-80-553-0367 (in Slovak)

[5] A. Czan, M. Neslusan, "Chip Machining of Hard to Machine Materials". 2005. p. 156. ISBN 80-969395-2-1. (in Slovak)

[6] M. S. Shahrom, N. M. Yahya, A. R. Yusoff, "Taguchi Method Approach on Effect of Lubrication Condition on Surface Roughness in Milling Operation", Procedia Engineering, vol. 53, 2013, p. 594-599, ISSN 1877-7058

[7] X. Cui, J. Zhao, Z. Pei, "Analysis of transient average tool temperatures in face milling", International Communications in Heat and Mass Transfer, Vol. 39, 2012, p. 786-791, ISSN: 0735-1933

[8] J. Jurko, A. Panda, M. Behún, "Prediction of a new form of the cutting tool according to achieve the desired surface quality". In: Applied Mechanics and Materials, Trans Tech Publications, Zurich, Switzerland, 2013, Vol. 268-270 (2013), p.473-476., ISSN 1660-9336,

A SET COVERING APPROACH TO NAVAL LOGISTICS

Ü.T. Tuzlacı[1], H. Tozan[2*] and T. Altınalev[2]

[1]Naval Science and Engineering Institute, Turkish Naval Academy, Tuzla, İstanbul, Turkey
[2]Department of Industrial Engineering, Turkish Naval Academy, Tuzla, İstanbul, Turkey
* *Corresponding author e-mail: htozan@dho.edu.tr*

Abstract
Naval Logistics has become one of the important subjects nowadays. Set covering problems (SCP) also has become one of widely studied subjects in recent years. In this study, a mathematical model is developed for solving a naval logistic problem by using the maximal covering location problem (MCLP) model, which is a special case of set covering problems. Optimal solution and genetic algorithm solutions are applied to the problem by using MATLAB Global Optimization Toolbox.

Keywords:
Naval logistics, set covering problem, genetic algorithm.

1. Introduction

The aim of this study is to develop a new model in order to locate oil tanker ships for maximal covering of any particular sea area. In this location model when a new oil request comes from fishing boats in the area, an oil tanker ship will certainly interfere in an hour.
The problem "maximal covering location of oil tanker ships at the Mediterranean Sea" is dealt in this study. This problem is evaluated as the maximal covering location problem, which is a special case of set covering problems. An appropriate mathematical model based on maximal covering location model is obtained by integrating unique constraints of the problem.
In the developed model, certain number and qualification of ships are intended to appoint certain pre-defined ports providing the prescribed constraints in order to minimize the cost. The model is also solved with genetic algorithm by using MATLAB Global Optimization Toolbox, optimal and genetic algorithm solutions are compared with analysis.
The main concept of covering problems is originally expressed by Toregas et al. (1971) and then it is extended by Berlin and Liebman (1974). In a classic covering problem, a demand point is called covered if it is within a defined distance, covering radius, from one of the closest facilities [1].
Covering models is used for location of emergency warning sirens, location of ambulance bases, ecological reserve selection and the location of retail facilities [2]. It is obvious that improving of covering models can result in savings in terms of cost of operations [3].
While covering models are not new, they have always been very attractive for research. This is due to its applicability in real-world life, particularly for service and emergency facilities. In some covering problems, a demand point should be served by at least one facility within a given critical distance. In most of the covering problems, customers take services by facilities depending on the distance between the customer and the facilities. The customer can take service from each facility, which its distance from customer is equal or less than a defined number [4].
Set covering problems and maximal covering problems are known as NP-hard problems in the literature [5,6].
This study is actually based on maximal covering location problem (MCLP). To date, scarce application of the MCLP to locate ships for maximal covering has encountered in the literature. In the case of this study, it is shown that covering models can result in savings in terms of fuel cost and reduced time. That's why it is very important for naval logistics. The maximal covering location problem seeks the maximum population, which can be served within a particular service distance known a restricted number of facilities [7].
Some assumptions for MCLPs are as follows:
1. Various demand nodes may have various quantities of demand.
2. All facilities have a covering distance and only demand points within the covering distance are fulfilled.
3. There is no capacity limitation on facilities.
4. The number of facilities to be located is prearranged and the purpose is to maximize the demand covered.
Because the MCLP is really complicated, some heuristic solutions are developed [8]. Additionally, the MCLP is a different formulation of other major location models. The solution of maximal covering location problem is approached by exact and heuristic methods. Church and ReVelle propose three methods for solution of the problem. These are greedy adding method, greedy adding with substitution, and relaxed linear programming [9].
Genetic Algorithm (GA) is used firstly in 1975 by Holland and it attempts to find a result nearest to the best solution. GA is a heuristic method [10]. Different types of GA are used in problems such as vehicle routing problems, covering problems, facility location, scheduling and quadratic

assignment problems from the mid 70s to date [11].

2. Methodology

In order to locate oil tanker ships, a 0-1 integer programming model is defined. Assumptions and mathematical model of the problem are given below.

Assumptions:

1. All the ships sail always with maximum speed.
2. All the ships begin sailing immediately without any preparation time.
3. All the ships are always full of fuel and never break down.
4. Safety drafts of all the ships are 1 meter more of own draft for secure location.

Mathematical Model:

Minimize $\sum_{i=1}^{n} \sum_{j=1}^{m} m_{ij} x_{ij}$ (1)

Subject to $d_i x_{ij} - b_j \le M y_{ij}$ $\forall i \in I, \forall j \in J$ (2)

$x_{ij} \le M (1 - y_{ij})$ $\forall i \in I, \forall j \in J$ (3)

$u_j - t s_i x_{ij} \le M y_{ij}$ $\forall i \in I, \forall j \in J$ (4)

$x_{ij} \le M (1 - y_{ij})$ $\forall i \in I, \forall j \in J$ (5)

$\sum_{i=1}^{n} x_{ij} \ge 1$ $\forall j \in J$ (6)

$\sum_{j=1}^{m} x_{ij} = 1$ $\forall i \in I$ (7)

$\sum_{i=1}^{n} \sum_{j=1}^{m} x_{ij} = N$ (8)

$x_{ij} \in \{0,1\}$ $\forall i \in I, \forall j \in J$ (9)

$y_{ij} \in \{0,1\}$ $\forall i \in I, \forall j \in J$ (10)

Where

I : set of ships $\in \{1,2,\ldots,n\}$

J : set of ports $\in \{1,2,\ldots,m\}$

N : total number of ships

m_{ij}: cost of assignment of ships to ports (Million Turkish Liras – TL)

b_j : depth of port j (meter - M)

d_i : safety draft of ship I (meter)

s_i : speed of ship i (knots - KTS)

u_j : covering distance (nautical mile – NM)

t : reaction time for the emergency situation

x_{ij} : $\begin{cases} 1, & \text{if ship I is assigned to port j} \\ 0, & \text{otherwise} \end{cases}$

y_{ij} : auxiliary binary variables for providing if-then structure

Objective (1) minimizes the cost of ship assignment to a port. All the ships are assigned to ports by considering both features of the ships and location costs of the ports. Constraint (2) and constraint (3) imply ship assignment to a port for suitable draft and depth values. Constraint (2) and constraint (3) ensure "**if** $x_{ij} > 0$ **then** $d_i x_{ij} \le b_j$" constraint. If a ship assigns to a port then safety draft of the ship must be equal or less than depth of the port. Constraint (4) and constraint (5) guarantee ship assignment to a port for suitable covering distance and speed values. Constraint (4) and constraint (5) ensure "**if** $x_{ij} > 0$ **then** $t s_i x_{ij} \ge u_j$" constraint. If a ship is assigned to a port then the product of the reaction time and the speed of the ship must be greater than or equal to maximum covering distance of the port. Constraint (6) ensures all ports to be assigned to at least one ship. Therefore, all ports are fulfilled. Constraint (7) guarantees a ship can be assigned only to one port. So, a ship is located in only one port. Constraint (8) implies using certain number of ships because the ships on hand are pre-known. Constraint (9) and constraint (10) are binary variables imposed to the model.

Upon reviewing the solution approaches in the literature, genetic algorithm that is proved to be generating confident results in location problems [5] is used.

Binary Integer Programming Tool in MATLAB Global Optimization Toolbox is used for optimal solutions. For big sizes of problems, MATLAB cannot solve the problem optimally. Therefore, the problem is solved by using genetic algorithm. Genetic Algorithm Tool in MATLAB Global Optimization Toolbox is used for genetic algorithm solutions.

3. Experimental Study

Default parameters of MATLAB Binary Integer Programming Tool values are used for optimal solution of all experiments. All experiments are computed in computer with Intel N450 CPU 1.67 GHz and 2 GB RAM properties. Genetic Algorithm Tool parameters that are used for genetic algorithm solutions are shown in Table 1 below:

Table 1.Parameters of Genetic Algorithm Tool

Population size	100
Creation function	Constraint dependant
Selection	Stochastic Uniform
Elite Count	2
Mutation	Constraint dependent – Adaptive feasible
Crossover	Scattered
Crossover Fraction	0.8
Migration	Forward Direction
Generations	100
Stall Generation	100

Cost of assignment of a ship to a port, covering distances of the ports and drafts of the ports in Mediterranean Sea are shown in Table 2.

Table 2.Data Related with Mediterranean Sea Ports

PORT NAME	COST OF ASSIGNMENT (TL)	COVERAGE DISTANCE (NM)	DEPTH OF PORT(M)
FINIKE	3	12	3
ANTALYA	2	12	5
ALANYA	4	12	3
BOZYAZI	3	12	3
MERSIN	2	12	5
ISKENDERUN	2	12	3
CEVLIK	3	12	4

Maximum speeds and safety drafts of the ships to be assigned to the ports in Mediterranean Sea are given in the Table 3 below:

Table 3.Data Related with The Ships

CLASS OF SHIP	ID OF SHIP	SPEED OF SHIP (KTS)	SAFETY DRAFT OF SHIP (M)
6	70	17	4
7	73	17	4
8	89	17	3
8	92	17	3
1	102	27	3
1	103	27	3
1	104	27	3
1	105	27	3
1	108	47	3
3	304	45	3
3	305	45	3
3	306	45	3
3	309	45	3

The problem cannot be solved by MATLAB optimally under reasonable time limit because of variable and constraint number. Best lower bound on objective value, which is 37, is accepted as best solution.
After the genetic algorithm, the final assignment of the ships to the ports are shown in Table 4 below:

Table 4.The Assignment of Ships to The Ports

Cost=31
Gap=0 %
Time:37 sec.

	70	73	89	92	102	103	104	105	108	304	305	306	309
FINIKE	0	0	0	0	0	0	0	0	0	1	0	0	0
ANTALYA	0	0	0	0	0	0	0	1	1	0	0	0	0
ALANYA	0	0	0	1	0	0	0	0	0	0	0	0	0
BOZYAZI	0	0	0	0	0	0	0	0	0	0	0	1	0
MERSIN	1	0	1	0	0	0	1	0	0	0	1	0	0
ISKENDERUN	0	1	0	0	0	1	0	0	0	0	0	0	1
CEVLIK	0	0	0	0	1	0	0	0	0	0	0	0	0

In Figure 1, the assignment of ships to the ports in Mediterranean Sea is shown on the map. On the arrows in the figure, the IDs of the ships, which are assigned to the related port, are listed.

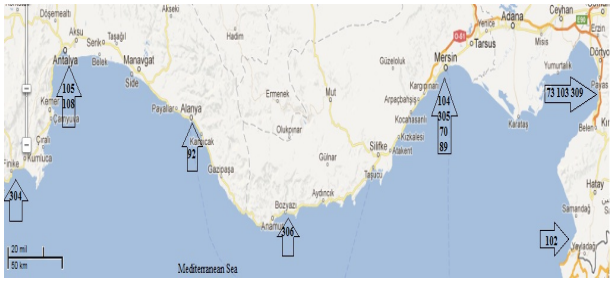

Figure 1. The Assignment of Ships to The Ports

It is clearly shown that genetic algorithm solution of naval logistic coverage of Mediterranean Sea is the same as best solution. The optimality gap ((GA-Op)/Op) between best solution and genetic algorithm solution for Mediterranean Sea is 0 %.

4. Conclusion

A new mathematical model is developed for a type of maximal covering location problem, which is an NP-hard problem in the naval logistic point of view. In particular, it is applied to locating oil tanker ships in Mediterranean Sea. Even though It is solved optimally in small instances, the larger ones can not be solved optimally. Therefore, genetic algorithm is applied to the larger optimal problems. the near optimal solutions obtained by the genetic algorithm are compared with the best IP solutions in two hours. In most cases, the same results are yielded. The study contributes to the literature in terms of ensuring the comparison of genetic algorithm as a fast solution method for these types of coverage problems.

5. References

[1] M. Jabalamelia, B. Tabrizia and M. Javadia, "A Simulated Annealing Method to Solve a Generalized Maximal Covering Location Problem", International Journal of Industrial Engineering Computations 2, 2011, pp.439-448.

[2] K. Curtin, K. Hayslett-Mc.Call and F. Qiu, "Determining Optimal Police Patrol Areas with Maximal Covering and Backup Covering Location Models", Netw Spat Econ , 2007, pp.125–145.

[3] R. Galvao and C. ReVelle, "A Lagrangean Heuristic for the Maximal Covering Location Problem, European Journal of Operational Research 88, 1996, pp. 114-123.

[4] R. Farahani, N. Asgari, N. Heidari, M. Hosseininia and M. Goh, "Covering Problems in Facility Location: A Review", Computers & Industrial Engineering 62, 2012, pp. 368–407.

[5] M. Karaman, "A Genetic Algorithm for the Multi-Level Maximal Covering Ambulance Location Problem", Master of Science Thesis, The Graduate School Of Natural And Applied Sciences, Middle East Technical University, 2008.

[6] P. Yin and L. Mu, "Modular Capacitated Maximal Covering Location Problem for the Optimal Siting of Emergency Vehicles", Applied Geography 34, 2012, pp. 247-254.

[7] R. Church and C. ReVelle, "The Maximal Covering Location Problem", Papers of the Regional Science Association, Vol. 32, 1974, pp. 101-118.

[8] L. Xia, M. Xie, W. Xu, J. Shao, W. Yin and J. Dong, "An Empirical Comparison of Five Efficient Heuristics for Maximal Covering Location Problems", Institute of Electrical and Electronics Engineers, 2009, pp.747-753.

[9] C. ReVelle, M. Scholssberg and J. Williams,"Solving the Maximal Covering Location Problem with Heuristic Concentration", Computers & Operations Research 35, 2008, pp. 427 – 435.

[10] A. Altay, "Genetik Algoritma ve Bir Uygulama", Master of Science Thesis, Institute Of Science, Istanbul Technical University, 2007.

[11] B. Gülsün, G. Tuzkaya and C. Duman, "Facility Layout Design with Genetic Algorithms and an Application", Journal of Dogus University, vol.10, no.1, 2009, pp.73-87.

COMPARISON OF FUZZY LOT-SIZING METHODS

E. Olcaytu[1] and H. Tozan[2*]

[1]Naval Science and Engineering Institute, Turkish Naval Academy, Tuzla, Istanbul, Turkey
[2]Department of Industrial Engineering, Turkish Naval Academy, Tuzla, Istanbul, Turkey
** Corresponding author e-mail: htozan@dho.edu.tr*

Abstract
The aims of the paper are: incorporate uncertain demands and uncertain costs into single level lot-sizing methods, create a software tool that can work for both crisp and fuzzy environments, and compare fuzzy lot-sizing methods with generated benchmark problems. The selection of the fuzzy lot-sizing method is important to improve the performance of MRP systems in an uncertain environment.

Keywords:
Lot-sizing method, Fuzzy set theory; Triangular fuzzy number

1. Introduction

The Material Requirements Planning (MRP) is a tool that performs the function of detailed material planning in a manufacturing system. MRP takes into account the dimension of supply/production times while realizing the main production program. It specifies order/production amounts to cover the independent demand items. Lot-sizing methods play an important role in MRP systems. Various lot-sizing methods have been developed in the literature according to demand characteristics, system dynamic, and nature of the systems interested in. These methods are classified basically in three groups: (i) Methods based on optimization, (ii) Methods based on heuristic rules, and (iii) Methods based on empirical factors.

There have been different well known methods existing. Wagner and Whitin developed an algorithm as a dynamic approach [1]. The Wagner-Whitin (W-W) algorithm evaluates all possible combinations of ordering to meet the needs of each period. It ensures minimum cost assignment and results optimum solution for the state of not allowed depletion of stock and discrete time variable demands. The deficit of the algorithm is high amount of computation. The square rooted formula is not proper for MRP systems [2]. Part Period Balancing (PPB) method was introduced by DeMatties & Mendoza in 1968 [3][4]. Part period means, holding items for a number of periods. It determines order quantities by balancing ordering costs and holding costs. The Silver–Meal (S-M) method was composed in 1975 by E.A. Silver and H.C. Meal [5]. It refers to production planning in manufacturing and its aim is to determine production quantities to meet the requirement of operations at minimum cost. Groff's Marginal Cost (GMC) method was introduced by Groff in 1979 [6]. It is based on balancing the marginal costs rather than total costs. Drexl & Kimms [7] and Ullah & Parveen [8] are recommended to reader for a comprehensive literature review on lot-sizing methods.

The objective is to compare three heuristic methods under fuzzy demand and fuzzy costs of the MRP environment. When determining the lot sizes fuzzy inputs are available, related to human judgments and evaluations. These fuzzy inputs with terms "about", "around" and "close to" can be well represented by fuzzy numbers. Fuzzy sets theory can be applied in this vagueness. Many times demand vagueness is not well expressed by random variables chosen from probability distributions. Fuzzy set theory which is introduced by Zadeh in 1965 can be used in these situations [9]. In fuzzy set theory demand vagueness is modeled by possibility distributions else probability distributions [10].

Three widely used algorithms: PPB, S-M and W-W are modified by Lee and investigated under fuzzy demands [11]. To reach our objectives, shortly mentioned in abstract section, Crisp/Fuzzy Lot-Sizing Tool (CFLST 1.0) is developed, supporting both crisp and fuzzy methods. Nine data sets (benchmark problems) are generated to compare performance of the three fuzzy lot-sizing methods which are fuzzy GMC (FGMC), fuzzy PPB (FPPB), and fuzzy S-M (FS-M).

2. Methodology

In this study triangular fuzzy numbers (TFNs) are used to illustrate uncertainty and generalized mean value is also used for defuzzification method.

A TFN, $\tilde{A}$, can be defined by a triplet $\tilde{A}=(a_1,a_2,a_3)$, the membership function of $\tilde{A}$ can be expressed in Equation(1) as follows:

$$\mu_{\tilde{A}}(x)=\begin{cases}0, & x<a_1\\ \dfrac{x-a_1}{a_2-a_1}, & a_1\le x\le a_2\\ \dfrac{a_3-x}{a_3-a_2}, & a_2\le x\le a_3\\ 0, & x>a_3\end{cases} \quad (1)$$

where, a_1,a_3 are the most extreme values whose membership degrees, $\mu_{\tilde{A}}(a_1),\mu_{\tilde{A}}(a_3)=0$, a_2 is the value whose membership degree, $\mu_{\tilde{A}}(a_2)=1$.

Lee and Li used generalized mean value and standard deviation to rank the fuzzy numbers [12].

When TFN is used, the generalized mean value and standard deviation expressed in Equation (2) and (3) as follows:

$$m\left(\tilde{A}\right)=\frac{1}{3}\left(a_1+a_2+a_3\right) \quad (2)$$

$$d\left(\tilde{A}\right)=\frac{1}{18}\left(a_1^2+a_2^2+a_3^2-a_1a_2-a_1a_3-a_2a_3\right) \quad (3)$$

Suppose that $\tilde{A}\left(a_1,a_2,a_3\right)$, $\tilde{B}\left(b_1,b_2,b_3\right)$ are two fuzzy numbers, if $m\left(\tilde{A}\right)>m\left(\tilde{B}\right)$ then $\tilde{A}>\tilde{B}$. When $m\left(\tilde{A}\right)=m\left(\tilde{B}\right)$, the spread $d\left(\tilde{A}\right),d\left(\tilde{B}\right)$ is used to compare two fuzzy numbers. The smaller spread value is chosen [12].

The notations used in the illustrations are: $\tilde{S}$: Fuzzy order/setup cost per order, $\tilde{D}_i$: Fuzzy demand at period i, $\tilde{h}$: Fuzzy holding cost per unit per period, $E\tilde{P}P$: Fuzzy economic part periods, $P\tilde{P}_i$: Fuzzy part periods in period i, $C\tilde{P}P_i$: Fuzzy cumulative part periods in period i, $\tilde{C}_{ij}$: Fuzzy cost for all periods i to j when an order placed in period i, $\tilde{F}_i$: Minimum fuzzy cost for period 1 through i, and $\tilde{Z}_k$: Minimum fuzzy total cost for period k.

The FGMC methods marginal cost decrease is expressed in Equation (4) and marginal cost increase in Equation (5) as follows:

$$\frac{\tilde{S}}{i-1}-\frac{\tilde{S}}{i}=\frac{\tilde{S}}{i(i-1)} \quad (4)$$

$$\frac{\tilde{D}_i\tilde{h}}{2} \quad (5)$$

Thus the $\tilde{D}_i$ in period i is added if the Equation (6) is true.

$$\frac{\tilde{D}_i\tilde{h}}{2}<\frac{\tilde{S}}{i(i-1)} \quad (6)$$

Equation (7) is gathered by rearranging the Equation (6).

$$\tilde{D}_i i(i-1)<\frac{2\tilde{S}}{\tilde{h}} \quad (7)$$

Fuzzy demands, fuzzy holding costs and fuzzy ordering costs are TFNs with the highest membership function value 1 ($\mu_{\tilde{A}}=1$). According to TFN, multiplication approximation and division approximation, Equation (7) is rearranged and Equation (8) is obtained.

$$m\left[i(i-1)d_{i1},i(i-1)d_{i2},i(i-1)d_{i3}\right]<m\left[\frac{2s_1}{h_3},\frac{2s_2}{h_2},\frac{2s_3}{h_1}\right] \quad (8)$$

When the Equation (8) is not true, order is placed in period i.

The PPB method is modified as follows [10]:
$E\tilde{P}P$ is obtained by TFN division approximation. $E\tilde{P}P$ formula shown in Equations (9) and (10).

$$E\tilde{P}P=\frac{\tilde{S}}{\tilde{h}} \quad (9)$$

$$E\tilde{P}P=\left(\frac{S_1}{h_3},\frac{S_2}{h_2},\frac{S_3}{h_1}\right) \quad (10)$$

Part periods for period i can be determined by multiplying operation of TFN. $\tilde{D}_i$ multiplies with the number of periods that holds before used. Fuzzy part periods and fuzzy cumulative part periods can be calculated in Equations (11) and (12).

$$P\tilde{P}_i=\left((i-1)\tilde{D}_{i1},(i-1)\tilde{D}_{i2},(i-1)\tilde{D}_{i3}\right) \quad i=1,2,3,... \quad (11)$$

$$C\tilde{P}P_i=\sum_{n=1}^{i}P\tilde{P}_n \quad (12)$$

When $m\left[C\tilde{P}P_i\right]$ first exceeds the $m\left[E\tilde{P}P\right]$ order is placed in period i.

The FS-M algorithm steps are as follows [11]:
Step 1: Set $i=1$, calculate fuzzy proportion expressed in Equation (13).

$$\tilde{G}_i=\frac{\tilde{S}}{\tilde{h}}=\left(\frac{S_1}{h_3},\frac{S_2}{h_2},\frac{S_3}{h_1}\right) \quad (13)$$

Step 2: Calculate the Equation (14). If the Equation (15) is true then go to Step 4 else go to Step 3.

$$i^2\tilde{D}_{i+1} \quad (14)$$

$$m\left[i^2\tilde{D}_{i+1}\right]>m\left[\tilde{G}_i\right] \quad (15)$$

Step 3: Set $i=i+1$, calculate the Equation (16) then go to Step 2.

$$\tilde{G}_i=\tilde{G}_{i-1}(+)\left(i-1\right)\tilde{D}_i \quad (16)$$

Step 4: Find lot size expressed in Equation (17).

$$\tilde{Q}_i=\sum_{j=1}^{i}\tilde{D}_j \quad i=1,2,3... \quad (17)$$

The FW-W algorithm steps are as follows:

$$\tilde{C}_{ik} = \tilde{S}(+)\left[\sum_{t=i}^{k-1}\tilde{h}_t(\bullet)\sum_{j=t+1}^{k}\tilde{D}_J\right] \qquad (18)$$

Let, the Equation (18) and minimum total cost can be determined as follows:

$$\tilde{Z}_k = \min_{1<i<k}\left\{\tilde{F}_i(+)\tilde{C}_{ik}\right\} \qquad for\ k=1,2,...,n. \qquad (19)$$

If $j_t = k$ then the last period in which production occurs in an optimal $t+1$ period policy must be in the set $k,\ k+1,...,\ t+1$.

3. Experimental Study

To compare performances of the fuzzy lot-sizing methods, data sets from Berry [13] are fuzzified to have the form of TFNs. Fuzzification function in Equation (20) is used to transform crisp data into TFN data. In Equation (13) x_0 is a crisp value, $\tilde{x}$ is a fuzzy set, and $fuzzifier(x_0)$ represents a fuzzification operator.

$$fuzzifier(x_0) = \tilde{x} = [x_0 - (p-left.x_0), x_0, x_0 + (p-right.x_0)]$$
$$p-right,\ p-left \in [0,1] \qquad (20)$$

When transforming crisp value to TFN, the p-left value is chosen at 0.08 and p-right value is chosen at 0.12 for all data, arbitrarily. Skewed on the right hand side TFNs are gathered by this fuzzification operator. These TFNs are shown in Table 1 and Table 2 as follows.

Table 1. Fuzzy Demand Data Sets

Period	Data Set 1	Data Set 2	Data Set 3
1	(73.6, 80, 89.6)	(46, 50, 56)	(9.2, 10, 11.2)
2	(92, 100, 112)	(73.6, 80, 89.6)	(9.2, 10, 11.2)
3	(115, 125, 140)	(165.6, 180, 201.6)	(13.8, 15, 16.8)
4	(92, 100, 112)	(73.6, 80, 89.6)	(18.4, 20, 22.4)
5	(46, 50, 56)	(0, 0, 0)	(64.4, 70, 78.4)
6	(46, 50, 56)	(0, 0, 0)	(165.6, 180, 201.6)
7	(92, 100, 112)	(165.6, 180, 201.6)	(230, 250, 280)
8	(115, 125, 140)	(138, 150, 168)	(248.4, 270, 302.4)
9	(115, 125, 140)	(9.2, 10, 11.2)	(211.6, 230, 257.6)
10	(92, 100, 112)	(92, 100, 112)	(36.8, 40, 44.8)
11	(46, 50, 56)	(165.6, 180, 201.6)	(0, 0, 0)
12	(92, 100, 112)	(87.4, 95, 106.4)	(9.2, 10, 11.2)

Table 2. Fuzzy Cost Data

Ordering Cost (per order)	Inventory Holding Cost (per unit per week)
(110.4, 120, 134.4)	(1.84, 2, 2.24)
(189.52, 206, 230.72)	(1.84, 2, 2.24)
(276, 300, 336)	(1.84, 2, 2.24)

Three data sets with three different ordering costs equal nine benchmark problems are used to solve by Crisp/Fuzzy Lot Sizing Tool (CFLST 1.0). CFLST 1.0 is a new single level lot-sizing tool which is an open source application and implemented with Microsoft Visual Studio C# language. The program interface shown in Figure 1, can solve lot-sizing problems with Economic Order Quantity (EOQ), Fixed EOQ, GMC, Lot for Lot, Least Total Cost, Least Unit Cost, Period Order Quantity, PPB, S-M, W-W methods. And also it can solve problems with fuzzified versions of these methods in MRP systems with fuzzy environments.

As seen in Figure 1, user can able to create triangular fuzzy numbers (TFNs) using crisp data with fuzzification function. After selecting the method, lot-sizing plan of a planning horizon is seen in grid and generalized mean values of the demands/lot-sizes are seen in bar chart as shown in Figure 2.

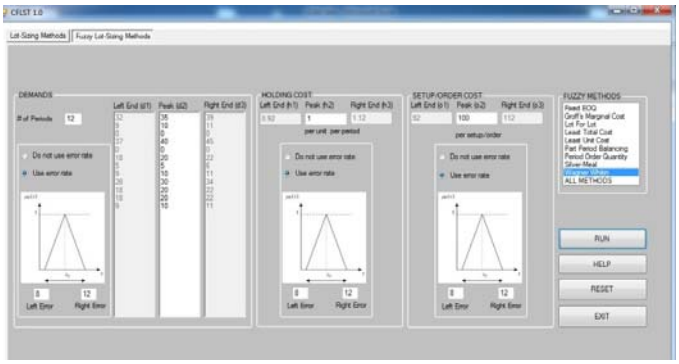

Figure 1. User Interface of CFLST 1.0

Figure 2. Result of the Selected Fuzzy Method

FW-W method is assumed as optimal method and it used for benchmarking. Deviations over FW-W solutions are calculated to test performances of FGMC, FPPB, and FS-M methods.

Generalized mean values of fuzzy total costs are shown in Table 3. According to generalized mean values, average deviations over FW-W solutions are shown in Table 4.

As shown in Table 3 and 4, FGMC, FPPB and FS-M methods obviously give better solutions within 2% of deviation over FW-W solution.

Table 3. Mean Values of Fuzzy Total Costs

Order Cost = $(110.4, 120, 134.4)			
	Data Set 1	Data Set 2	Data Set 3
FW-W	1422.72	1114.80	1056.56
FGMC	1422.72	1114.80	1078.32
FPPB	1422.72	1114.80	1138.72
FS-M	1422.72	1114.80	1078.32
Order Cost = $(189.52, 206, 230,72)			
	Data Set 1	Data Set 2	Data Set 3
FW-W	2290.13	1800.56	1602.00
FGMC	2391.47	1800.56	1623.76
FPPB	2391.47	1800.56	1602.00
FS-M	2492.8	1800.56	1623.76
Order Cost = $(276, 300, 336)			
	Data Set 1	Data Set 2	Data Set 3
FW-W	3006.56	2372.08	2173.52
FGMC	3012.64	2372.08	2173.52
FPPB	3012.64	2372.08	2173.52
FS-M	3012.64	2372.08	2173.52

Table 4.Average Percentage Deviation Over FW-W Solution

Modified Methods	Average Percent Deviation over FW-W Solution
FGMC	0.89%
FPPB	1.38%
FS-M	1.39%

4. Conclusion

This research shows that a fuzzy set theory approach can successfully incorporate uncertainty, fuzziness, and subjectivity into lot sizing methods. This research tried to answer two main issues are: Representation of demand and cost uncertainty in the MRP system, and Modification of lot-sizing methods for fuzzy environment.

The developed CFLST 1.0 software tool can solve both crisp and fuzzy lot-sizing problems by ten lot-sizing methods and fuzzified versions of them. Three widely used algorithms: PPB, S-M and W-W are modified by Lee and investigated under fuzzy demands [10]. The nine lot-sizing methods are modified to be use under not only fuzzy demand but also under fuzzy holding cost and fuzzy setup cost. When the all information is imprecise, fuzzy set theory can be applied to lot-sizing algorithms so the decision maker can make more real judgments for the real systems. Results of this research can be benefited before selecting the modified method in the MRP systems when the environment is fuzzy. FGMC, FPPB and FS-M methods are tested against the FW-W and the average performances are resulted within 2% of FW-W solution.

A larger set of benchmark problems provide more certain results. Developed fuzzy lot-sizing methods can be extended to other lot-sizing methods. Different types of fuzzy numbers (trapezoidal fuzzy numbers, exponential fuzzy numbers etc.) can be used in methods. Ranking of fuzzy numbers has become an important component, thus different types of defuzzification methods can be used for ranking. Measurement of the membership functions for fuzzy parameters can be studied with extended examples. And final recommendation is to study the use of different lot-sizing methods with the combination of lead time uncertainty.

5. References

[1] H. M. Wagner, and T. M. Whitin, “Dynamic Version of the Economic Lot Size Model,” *Management Science (informs)*, 50(12), 1770-1774 (2004, reprint from 1958).

[2] F. Chyr, S. Huang, and S. Lai, “A Dynamic Lot-Sizing Model with Quantity Discount,” *Production Planning & Control*, 10(1), 67-75, 1999.

[3] J. J. DeMatties, “An economic lot-sizing technique I: The part-period algorithm,” *IBM Systems Journal*, 7(1), 30-38, 1968.

[4] A. G. Mendoza, “An economic lot-sizing technique II: Mathematical analysis of the part-period algorithm,” *IBM Systems Journal*, 7(1), 39-46, 1968.

[5] E. A. Silver, and H. C. Meal, “A Heuristic for Selecting Lot Sizing Quantities for The Case of A Deterministic Time-Varying Demand Rate and Discrete Opportunities for Replenishment,” *Production and Inventory Management*, 2, 64-74, 1973.

[6] G. K. Groff, “A lot-sizing rule for time phased component demand,” *Production and Inventory Management*, 20(1), 46-53, 1979.

[7] A. Drexl, and A. Kimms, “Lot Sizing and Scheduling - Survey and Extensions,” *European Journal of Operational Research*, 99, 221-235, 1997.

[8] H. Ullah, and S. A. Parveen, “A Literature Review on Inventory Lot Sizing Problems,” *Global Journal of Reseaches in Engineering*, 10(5), 21-36, 2010.

[9] L. A. Zadeh, “Fuzzy Sets,” *Information and Control*, 8, 338-353, 1965.

[10] Y. Y.Lee, B. A. Kramer, and C. L. Hwang, “Part-Period Balancing with Uncertainty: A Fuzzy Sets Theory Approach,” *Int. J. Prod. Res.*, 28(10), 1771-1778, 1990.

[11] Y. Y. Lee, B.A. Kramer, and C. L. Hwang, “A Comparative Study of Three Lot-Sizing Methods for The Case of Fuzzy Demand,” *International Journal of Operations & Production Management*, 11(7), 72 – 80, 1991.

[12] E. S. Lee, and R. J. Li “Comparison of fuzzy numbers based on the probability measure of fuzzy events,” *Computer and Mathematics with Applications*, 15(10), 887-896, 1988.

[13] W. L. Berry,“Lot Sizing Procedures for Requirements Planning Systems: A Framework for Analysis,” *Production and Inventory Management*, 2nd Quarter, 1972.

GEOMETRIC AND DIMENSIONAL ACCURACY OF TURNED CYLINDRICAL SURFACES

Z. Murčinková*, K. Vasilko

Faculty of Manufacturing Technologies with seat in Prešov, Bayerova 1, Prešov, Technical University in Košice, Slovakia

** Corresponding author e-mail: zuzana.murcinkova@tuke.sk*

Abstract

The paper dealt with geometric and dimensional accuracy of turned cylindrical surfaces. The paper identifies inaccuracies as a result of deformation of elastic component joints of cutting machine during acting the cutting forces. Moreover, the numerical experiments analyse the clamping as fixed or pined constraint regarding the measured final shape of cylindrical workpiece surface. The experimental data are compared with data of numerical simulation by FEM. The paper provides the shapes of turned cylindrical surfaces for case of a centre lathe.

Keywords:

accuracy, turning, machine tool, workpiece clamping, elastic pin

1. Introduction

Each construction of cutting machine tool activates during machining the geometric and dimensional inaccuracies of the workpieces as a result of different stiffness of its joints. The acting of cutting force and the moving of its position leads to the deformation of the elastic joints of cutting machine and the elastic deformation of the workpiece appears. The aim is to maintain geometric modifications of the workpiece in required tolerances.

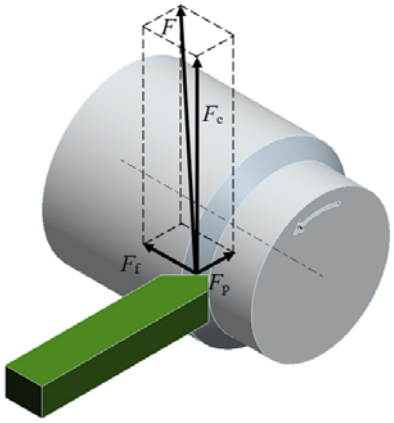

Figure 1. Division of cutting force during turning

The workpiece is loaded by the cutting force F during cutting. This force can be divided into three components according to Fig. 1. [1, 4, 10, 11]. Force F_p causes the displacements and deflection of the workpiece. The centre of cutting edge, which is in feed together with the workpiece, is considered the force effect point. During turning, the force moves from tailstock to headstock.

Tangential, main, cutting force F_c lies in the direction of cutting force. The value of force F_c is necessary for the calculation of the power of the main movement, tool stiffness and machine mechanism parts. It determines torsion moment M_k on the spindle. If the centre of the force effect point is considered to be in the centre of the cutting edge, the following equation is valid:

$$M_k = F_c\left(\frac{D}{2} - \frac{a_p}{2}\right) \quad (1)$$

where:

D is diameter of workpiece, mm,

a_p is cut depth, mm.

Because D is usually much larger than a_p, therefore a_p can be neglected in practical conditions, so:

$$M_k = F_c \frac{D}{2} \quad (2)$$

The radial cutting force F_p influences the movement of parts and the stiffness of turning machine and cutting tool. Its values are necessary for the calculation of the accuracy of turned parts and the stiffness of technological system.

2. Experimental measurement

The diameter of the workpiece was measured after turning from tailstock to headstock by dial indicator with accuracy in μm (Fig. 2).

Figure 2. Measuring

3. Numerical experiment by FEM

The aim of this calculation is to find out the values of displacements when the centre of force F_p is moving during turning. Moreover, the aim is to draw the shape of the curve, which presents the resulting surface shape of the workpiece, which was found out experimentally. The values of the displacements cause shape inaccuracy of turned cylindrical surface, [7].

Computational model used p-version of the Finite Element Method, one-dimensional finite elements with the polynomial shape function of 4th order, [2, 9]. The oscillation of the system machine-tool-workpiece is not considered. The mentioned oscillation was eliminated to minimum during experiment.

During real experiment the workpiece was clamped into a chuck and centre, the stiffness of which was unknown. During numerical experiment, their stiffness and the mechanical type of workpiece clamping was determine, i.e. fix-fix (Fig. 3), fix-pin constraint. The curves in Fig. 3 show the surface shapes of workpiece profile for the case if the clamping into the chuck is recognised as elastic fix and the clamping into the centre is recognised as elastic fix. If clamping into the centre is considered as an elastic pin, than the curves of the profile have different shape as measured. The experimentally found values show considerable difference in comparison with the curves found out numerically for the constraint of elastic fix-elastic pin even in case of different ratios of stiffness of the tailstock and headstock therefore this type of constraint is not considered in further solution.

The best fitting with the experimentally measured curve ♦ in Fig. 3 is shown by ◊ with the ratio of stiffness of the headstock c_h and the tailstock c_t 1.7:1 (c_h =1700 N/mm, c_t =1000 N/mm). Maximum difference in values is 0.012 mm what is 4.8%.

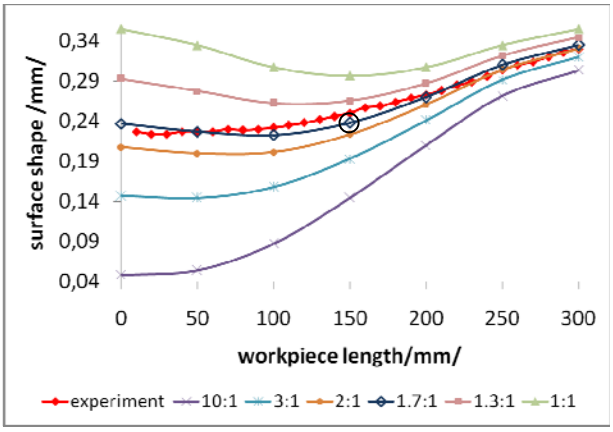

Figure 3. Constaint: elastic fix – elastic fix

Fig. 4 presents comparison of final surface shape for rigid and elastic fixes. The difference is obvious. The deformations are shown 100times larger as calculated ones. The circle on the face surface in lower side of Fig. 4 is original cross-section and dimension of workpiece before turning. The real clamps are elastic as the each component joint of machine structure. We determined the stiffness of clamps by numerical experiment described lower.

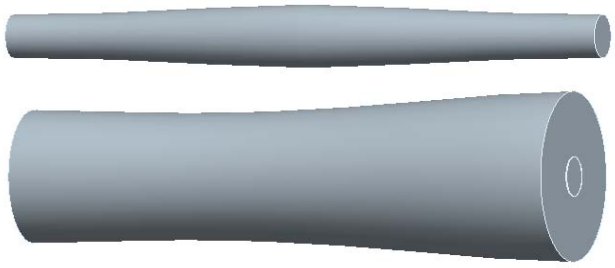

Figure 4. Final surface shape: rigid (up) and elastic constraints

Fig. 5 shows deflection curves of the workpiece with changing position of tool during turning so that the position of working force F_p is changing. The deflection curves (shape of workpiece axis) are being changed in individual phases of turning and they are considerably different. The ratios of stiffness of headstock and tailstock as well as their values contribute to the differences of deflection curves. The resulting curve presenting the shape of workpiece final profile is obtained from the deflections (shape differencies) in the places where force F_p acts. The effect point of the force is presented by a circle. In Fig. 5 the ratio of the stiffness of the headstock c_h and the tailstock c_t is 3:1 (c_h =3000 N/mm, c_t =1000 N/mm).

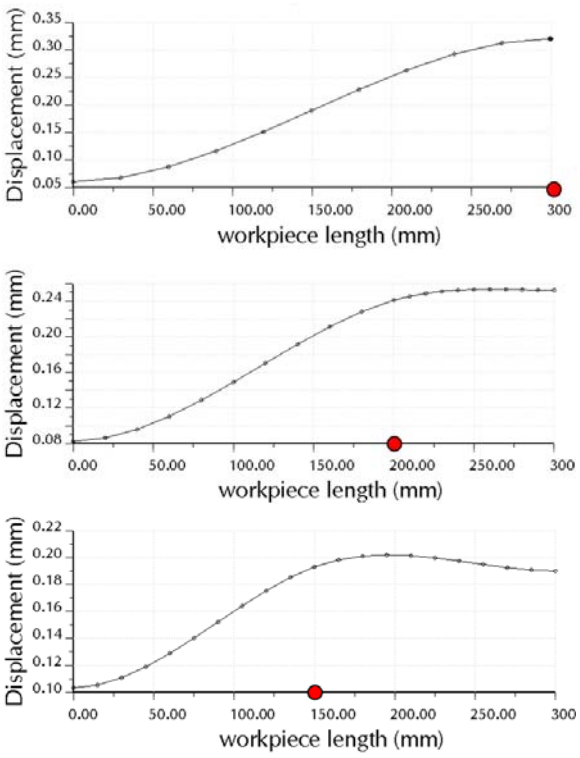

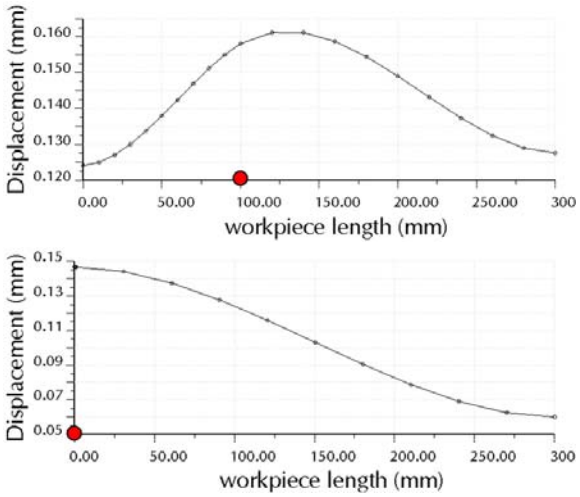

Figure 5. *Deflection curves during turning - elastic fixes*

4. Analytical accuracy determination

By the consideration of elastic fixes it is necessary to solve three times statically indeterminate beam with elastic fixes according to Fig. 6 with given stiffness. By the use of the method of canonic equations the values of reactions, distribution of shear forces and bending moments of this statically indeterminate task have been obtained. One of the methods for the calculation of deflection is used for determination of deflection (more [8]).

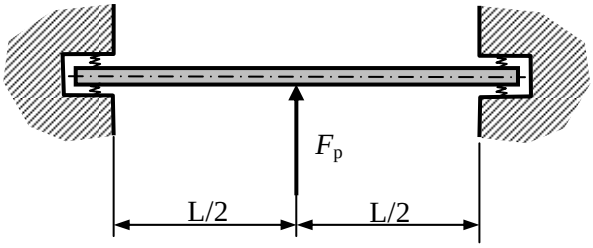

Figure 6. Calculation model

For the presentation of the process of analytical calculation of the fixed-fixed beam (workpiece), the deflection is calculated in the middle of the beam for the ratio of the rigidity of headstock c_h and the tailstock c_t 1.7:1 (c_h=1700 N/mm, c_t=1000 N/mm). The force F_p=500 N, the length of workpiece L=300 mm and the diameter d=20 mm, material: steel. The reciprocal value of stiffness is headstock elasticity w_h and tailstock elasticity w_t (w_h=1/c_h=0.588x10^{-3} mm/N, w_t=1/c_t=10^{-3} mm/N). The displacement of the headstock y_h and tailstock y_t can be calculated as follows:

$$y_h = H\,w_h = 283.92\,\mathrm{N}\,\mathrm{x}\,0.588\,\mathrm{x}\,10^{-3}\,\mathrm{mm/N} = 0.1669\ \mathrm{mm} \quad (3)$$

$$y_t = T\,w_t = 216.08\,\mathrm{N}\,\mathrm{x}10^{-3}\,\mathrm{mm/N} = 0.2161\,\mathrm{mm}$$

where H and T are reactions in headstock and tailstock, N.

For the first step, we consider rigid workpiece (Fig. 7a). The displacement of the workpiece axis y_{ax} in the middle of the workpiece considering different elasticity of the headstock and the tailstock can be determined from the parallelism of triangles:

$$\frac{y_{ax}-y_h}{L/2}=\frac{y_t-y_h}{L}\Rightarrow y_{ax}=\frac{y_t+y_h}{2}= =\frac{1}{2}\left(H\,w_h+T\,w_t\right)=0.1915\ \mathrm{mm} \quad (4)$$

where y_{ax} is displacement of loaded and unloaded rigid workpiece axes in its middle, mm, L is length of workpiece, mm.

In the next step of calculation, the elasticity of workpiece is considered. The displacement (deflection) y in the middle of the workpiece is:

$$y = y_{work} + y_{ax} = 0.04476\ \mathrm{mm} + 0.1915\ \mathrm{mm} = 0.23626\ \mathrm{mm} \quad (5)$$

where y_{work} is displacement (deflexion) of loaded elastic workpiece, mm. y_{work} is calculated according [8] as follows:

$$y_{work}=\frac{F\,L^3}{192\,E\,J}=0.04476\ \mathrm{mm} \quad (6)$$

where E is Young's modulus of elasticity, MPa, J is moment of inertia: $J=\pi\,r^4/4$.

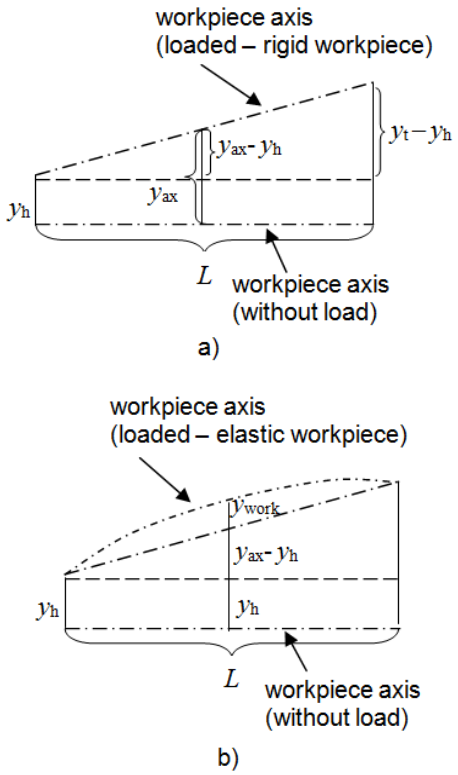

Figure 7. Scheme for calculation of displacement

Value y_{work} is the same for the workpiece without regard to elasticity of constraints. Value y_{ax} is changing in dependence on clamping. If the influence of shear force is considered and y_{work} according equation (6) is in perpendicular direction

to axis, then y_{work}= 0.0465 mm. From the above mentioned formulas and calculations, the displacement y in the middle of workpiece is 0.23800 mm (0.0465 mm + 0.1915 mm) what corresponds with the numeric solution according to Finite Element Method (point marked by circle in Fig. 3). The mentioned value according Finite Element Method is 0.23803 mm.

5. Fixing into the chuck

For the fixation into the chuck the situation is more complicated (Fig. 8). The stiffness of the chuck is higher than the one of the tailstock, but different jaws have different flexibility. During measurement of the roundness of the workpiece in fixing by minimal fixing force $F_{u\ min}$, a shift of the workpiece axis, which corresponds with spindle wobbling (chuck) (e), has been identified. Deformed triangle profile, shifted by wobbling, is measured in the application of fixing force. The different elasticity of individual jaws is visible.

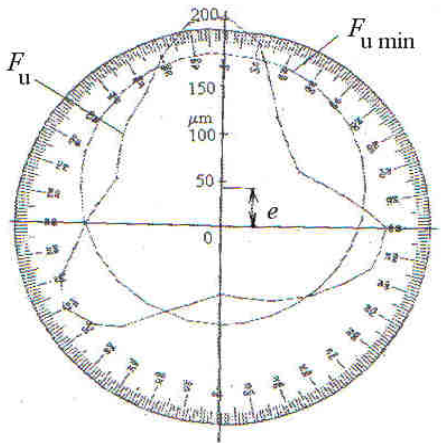

Figure 8. Workpiece profile in the vicinity of three-jaw chuck

The size of the deflection depends on the size of fixing force therefore its value has great importance. The real shape of the workpiece is shown in Fig. 9 with the consideration of flexibility of workpiece deflection and flexibility of headstock jaws.

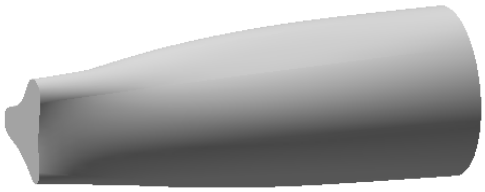

Figure 9. Final shape of workpiece turned with fixation in chuck

6. Conclusion

It is obvious that the stiffness of technological system considerably influences workpiece accuracy. Moreover, the productivity of turning also depends on the stiffness of technological system. If the stiffness is not sufficient, subsequently the cutting conditions have to be adjusted. It caused the increasing the number of removal material cuttings to apply minimal displacement. Similarly, the geometric inaccuracies for other types of turning machines (miller, grinder etc.) can be identified by presented approach. For their evaluation it is needful to modify the calculation according to individual design of cutting machine

7. References

[1] J. Buda, J. Békés, "*Teoretické základy obrábania kovov"*, pp. 698, ALFA, Bratislava, 1967.
[2] P. Demeč, J. Svetlík, J. Semjon, "*Vitrtuálne prototypovanie obrábacách strojov z hľadiska dynamiky procesov obrábania"*, pp. 182, Technical University in Košice, Košice, 2011.
[3] A. Dugin, A. Popov, "Effect of the processing materials on the ploughing force values", In: *Manufacturing Technology*, Vol. 12, No. 13, pp. 102-105, J. E. Purkyně University in Ústí nad Labem, Ústí nad Labem, 2012.
[4] W. Grzesik, "*Podstawy skawania materialow metalowych"*. pp. 526, Wydawnictwa Naukowo-Techniczne, Warszawa, 2010.
[5] J. Kundrák, K. Gyáni, I. Deszpoth, "The effect of the borehole diameter on the machining times in hard machining", In: *Manufacturing Technologies*, Vol. 12, No. 13, pp. 144-150, J. E. Purkyně University in Ústí nad Labem, Ústí nad Labem, 2012.
[6] J. Mádl, J. Kvasnička, "*Optimalizace obráběcího procesu"*, pp. 168, Czech Technical University in Prague, Prague, 1998.
[7] J. Murčinko, "The Application of MFG Templates in CAD/CAM Systems", In: Proceedings of 4th IEEE International Symposium on Logistics and Industrial Informatics LINDI 2012, pp. 17-20, Óbuda University, Budapest, 2012.
[8] Z. Murčinková, "*Pružnosť a pevnosť 1 Mechanika poddajných tellies"*, pp. 121, Technical University in Košice, Prešov, 2011.
[9] P. Novák, J. Meško, M. Žmindák, "Finite Element Implementation of Multi-Pass Fillet Weld with Phase Changes", In: *Manufacturing Technology*, Vol. 13, No.1, pp.79-85, J. E. Purkyně University in Ústí nad Labem, Ústí nad Labem, 2013.
[10] Z. Přikryl, R. Musílková, "*Teorie obrábění"*, pp. 235, SNTL, Prague, 1982.
[11] K. Vasilko, J. Mádl, "*Teorie obrábění"*, pp. 526, J. E. Purkyně University in Ústí nad Labem, Ústí nad Labem, 2013.

EFFECTIVENESS OF TOOL PROFILE IN SHEET METAL INCREMENTAL FORMING

Manish Oraon[1], Vinay Sharma[2]

University Polytechnic; B.I.T. Mesra, Ranchi, India
Department of Production Engg.; B.I.T. Mesra, Ranchi, India
Manish_oraon@yahoo.com: vinay1970@gmail.com

Abstract
The present study is an analytical study and formulation which predict the effectiveness of tool profile in the part during the Microforming process. The main area of the study is the effectiveness of tool and its optimized shape, size of the tool, lubrication media, applied force, tool feed rate and the rpm of the tool. The materials parameters and other function of the working conditions (sheet thickness, wall angle, temperature and step down) take as with a good precision. Moreover, a general model has been deduced which allow to simulate an approximate size and shape of the tool and other tool profile helps to find the precise part.

Keywords
Microforming, Rapid prototyping, Sheet metal forming, Forces, Process modeling

1. Introduction

In recent years new sheet metal forming processes have been developed and introduced to industry in order to increase the flexibility and meet the present day challenge of manufacturing prototypes with flexible forming technologies. The trend in sheet metal forming industry is to manufacture more complex parts and faster introduction of new and individual products in small lot series (Fig 1).

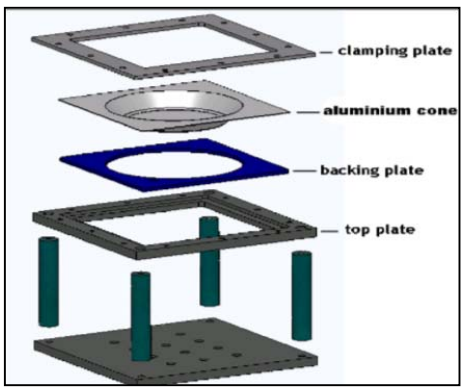

Fig.1. (Ref 7) The schematic view of Microforming process

Incremental forming (ISF) is suitable for this kind of manufacturing and has great potential in flexible production. Due to its manufacturing procedure, the process is also called 'Microforming' because a small hemispherical end tool with end diameter of few mm is used to deform the sheet at a particular point at a time. In this order to form the sheet into the desired shape, a suitable hemispherical end tool, mounted on the numerically controlled machine end, moved accordingly to a predefined path.

2. Analysis of force

The application of force depends upon the sheet material properties and thickness. The sound knowledge of these forming forces can contribute to the preservation of the tooling and the machinery used in the process. Previous research work in this field has been performed by different researchers. Ambrogio et al. [1] studied the influences of the tool diameter, the wall angle, and the sheet thickness on the axial force used in the aluminum. Jeswiet et al. and Szekeres et al. [2-3] developed a dedicated force sensor for measuring the three components of the SPIF force with encouraging initial results. The measuring system, however, seems to need further enhancements to assure systematic output. Petek et al. [4] studied the influences of the wall angle, tool rotation, tool diameter, feed rate, step down, and lubrication on the axial force for a single material. Iseki [5] developed an approximate formula to compute the axial and radial forces based on a simplified membrane analysis. Here the target was to form the pyramid form a 3mm thin AA3003 sheet. The sheet was initially clamped in the set. The parameters for the formation of pyramid was taken as with the wall angle of 45^0 and 60^0.

The present studies are focused on the tool-sheet metal interface where the plastic deformation takes place. At the contacting area, Material will be drawn out along the radial direction, sheet thickness will be reduced, and little change will take place along tangential direction as the forming tool acting on the

sheet material during the forming process. The state of force at contacting deformation area can be shown in Fig. 2

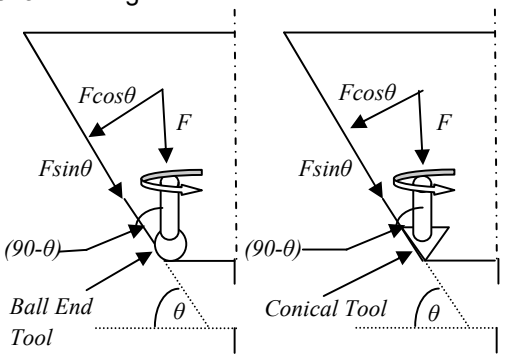

Fig 2. State of force at deformation zone

3. Deformation Force prediction

When the forming tool move forward on the surface of the parts with constant feed rate *f*, the ball end tool descend in the surface of sheet metal along the Z axis. The aluminum sheets start to deform along the radius of the ball end tool.

The axial force *Fz* in steady state can be predicted by the experimental parameters. The tensile strength R_m of AA3003 sheet metal, the sheet thickness '*t*', the tool diameter '*d*' , the step height '*Δh*' and the wall angle *θ* following the formula established by Aerens et al. [8] for the hemispherical end tool which validates the tool with ball end because the end shape was similar to the previous experimented by the authors.

$$F_z = 0.0716 \cdot R_m \cdot t^{1.57} \cdot d^{0.41} \cdot \Delta h^{0.09} \cdot \theta \cos\theta \qquad (1)$$

Where F_z is in Newton (N)
R_m in N/mm^2
t, d and *Δh* in mm

In conical end tool, all the parameters will be same as above equation only change because of the end of tool (cone) shape. The equation may be modified as

$$F_z = 0.0716 \cdot R_m \cdot H \cdot t^{1.57} \cdot d^{0.41} \cdot \Delta h^{0.09} \cdot \theta \cos\theta \qquad (2)$$

Where 'H' is the height of cone in mm

4. Infuence of Tool Profile

As the concern of surface finish, tool profile plays an important role during the deformation of sheet metal. The various experimentations were carried out with different tool profile. The details of material properties are presented in Table 1.

Table1: Properties of Al sheet metal

Material	Aluminum (AA3003)
Tensile stress (MPa)	119
Yield stress (MPa)	60
Young's modulus (GPa)	70
Elongation (%)	26.4

5. Shape of tool tip (ball end tool)

The shape of forming tool which directly contacted with the sheet during the deformation, the tool plays an important role in the surface roughness of the final part. During deformation, the thinning of sheet depends upon the contact area of the tool end. For experiment two types of tool were used ball end tool and conical end tool. Firstly the ball end tool of diameters 05 mm and 10 mm were used for the deformation of sheet.

The process parameter for the experimentation was set according to the Table2.

Table 2: Process parameters for the experiment

Wall angle	**45^0, 60^0**
Forming depth 'h'	30mm
Tool Rotation speed	500 r.p.m
Tool diameter (ball end tool)	05 mm, 10mm
Tool diameter (conical tool)	15 mm
Tool hight (conical tool)	10mm
Vertical step depth	0.2 mm
Tool Feed rate	1000-3000mm/min
Lubricant	Grease, graphite

The forming process was carried out in two different environments called with lubricant and without lubrication. The outcome of the experiment found that, with the bigger diameter ball end tool (10mm) locally deforms more than the small diameter ball end tool (5mm). On the other hand, the better surface profile was achieved with the small ball end tool but the total time for processing was almost double due to small contact area at the sheet and the small ball end tool needs more force to deform the sheet metal.

The FEM simulation result of the square pyramid of total height 24.6 mm can be seen in fig.3. Commercial software (COMSOL multiphysics version

4.1, explicit formulation) based on a combined kinematic/isotropic hardening model was used for the simulation. The results comes out from the simulation validates the experimental results (force, surface roughness, total deformation depth) to close proximity.

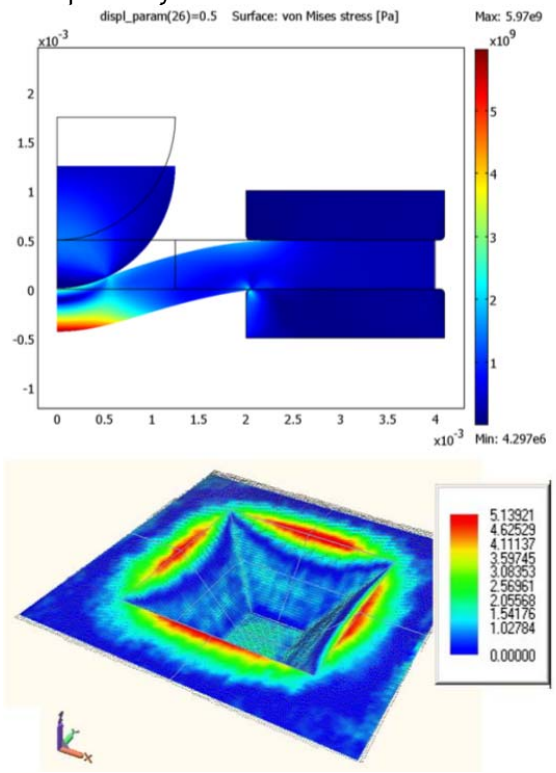

Fig. 3. Simulation of thin sheet on COMSOL multiphysics

The next observation is the effect of lubrication on the tool and final part. The result founds that the aluminum sheet get cracked before achieving the final step due to high frictional resistance and tool wears out. These two complicacies are reduced with the application of the lubricating media as mentioned in the Table 1 at the tool-sheet metal interface. The lubricant grease reduces the above problem efficiently the graphite.

6. Shape of tool tip (Conical end tool)

The new area of investigation carried out by the deformation of sheet using a conical end tool (Fig 4). The experimental analysis was concentrated on the applied forces and the deformation steps. The tool used for this purpose was with and without lubrication of grease. The experimental result found that the applied force greatly reduced in comparison to ball end tool. But the probability of crack formation will increased due to the sharp corner at the end of conical tool.

Fig. 4. (a) Ball end tool (b) Conical end tool

It has been found that more local deformation (Figure 5) takes place at the side of the sheet. On the other hand the tool with lubricant forms a smooth surface finish rather than without lubricant tool.

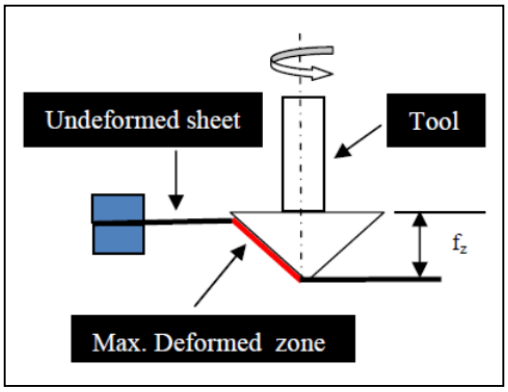

Fig.5. Deformation through conical end tool

The graph of deformation time against strain rate of the sheet material is plotted for the ball end tool diameter and the conical end tool shown in Graph A. It shows that the relative effect on deformation of sheet with the application of constant force 5N.

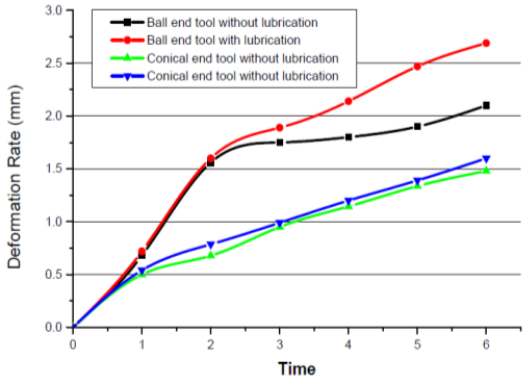

Graph A: Time of deformation Vs deformation Rate

From the above curves, which plotted against predetermined depth of deformation, It can be easily seen that, for equal forming depth of the final part, ball end with larger diameter (10mm) tool gives the larger rate of deformation with respect to time just because of the more contact area at tool and work sheet interface whereas ball end with small diameter (5mm) tool results the larger forming depth of the final part without breakage of work sheet just because of the small local contact area at tool and work sheet interface. On the other hand, it has been found that, the more local deformation of sheet occurs at the contact zone using with the conical end tool but the crack occurs on the specimen at the forming depth of 10mm because of the excessive thinning of the sheet (fig.5).
The deformation of work sheet also affect by the application of lubrication media. In the environment of lubricant, the surface roughness of the final part is also improved.
Due to the rotation of tool at high speed (Graph B) the friction force develops at the tool-sheet interface which causes local heat dissipation in contact area. This results the excessive thinning of the work material can be achieve but a very rough surface is formed. On the other hand, the chances of cracks may increase on the part without achieving final depth.

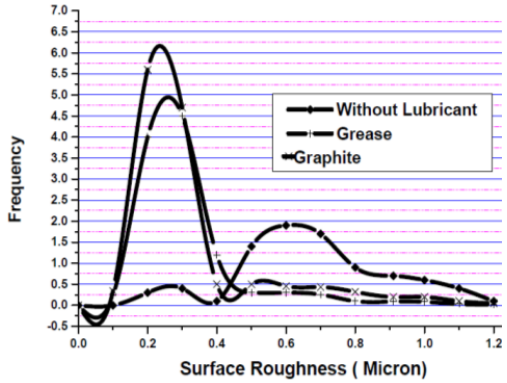

Graph B. Surface roughness vs. frequency

It has been also found that with the use of different lubrication media, the surface roughness may vary as shown in the graph. Vertical side of the graph indicates the frequency (Hz) of the forming force which is recorded through three axes, eight channel kistler force dynamometer. This frequency indicates the force developed at the tool- work interface. Without using any lubricant, the force dynamometer records maximum frequency during the process and lesser in case of liquid lubricant (high speed sapphire grease).

The tip of the tool wears out and the adherence of thin aluminum sheet to tool tip was significantly increased without the application of lubricant. This validates the experimentation carried out by the *R. de Bruyn et at.* [10]. therefore lubrication not only improves the tool life and surface quality, it actually serves as an enabler or necessary prerequisite for the process.

7. Angle of tool tip

All the previous experiments were carried out on the vertical axis computer numerical control machine milling machine where the deformation of sheet takes place in vertical direction. Here one of the new analytical investigations related to the reduction of deformation force is discussed. This new idea is based on the effect of some angle (Figure 6) of tool for the deformation of the sheet. The angle of the tool tip is set to 50^0 with special attachment for both cases (ball end and conical end tool) and the rest of process parameter has been taken as previous experimentation.

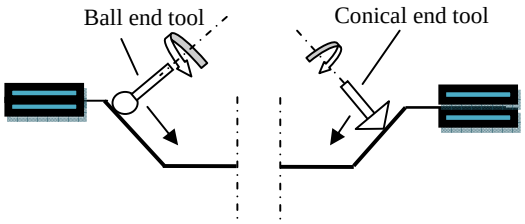

Fig 6. Angle of tool tip in Microforming

The result found that the deformation force greatly reduced for the thinning of sheet but the rate of deformation for both cases was very slower than previous experiment due to less contact area between the tool tip and sheet metal. As compared to the angle of tool, conical end tool needs less deformation force than the ball end tool.

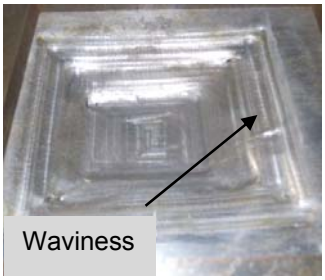

Fig7. Formation of wave using conical end tool

In the case of ball end tool the contact area at tool-sheet interface was more than the conical end tool. As result, the more area was deformed at the same rate of deformation as compared to the conical end

tool. As concern to surface finish, conical end tool produces more waviness (Figure 7) on the surface of the part than ball end tool.

8. Conclusion

Incremental Forming is most suited to manufacture small batches and, sometimes, unique components. An accurate process design is not possible due to a lack of knowledge and the inadequacy of the simulation tools.

In this study a simple way to monitor the effect of the forming forces on the deformation of sheet and the influences of the tool profile on the deformation process. As per experiment, the conclusion comes out that the more accurate shape is formed by the use of ball end tool rather than the conical end tool.

9. References

[1] G Ambrogio, J.R.Duflou,L. Filice and R. Aerens, “Some considerations on force trends in Incremental Forming of different materials”, 10th ESAFORM conference on material forming, AIP Conference Proceedings, vol. 907, pp 193–198, 2007

[2] J. Jeswiet, J.R. Duflou and A. Szekeres, “Forces in single point and two point incremental forming” Adv Mat Res 6–8:449–456, 2005

[3] A. Szekeres, M. Ham and J. Jeswiet, “Sheet metal 2007, force measurement in pyramid shaped parts with a spindle mounted force sensor” Key Eng Mater 344:551–558, 2007

[4] A. Petek, K. Kuzman and J. Kopac, “Forces and deformations analysis of incremental sheet metal forming” CAM3S, 11th Int J Adv Manuf Technology 46:969–982 981, 2010

[5] H. Iseki “an approximate deformation analysis and FEM analysis for the incremental bulging of sheet metal using a spherical roller” J Mater Process Technology 111:150–154, 2001

[6] W. Hongyu, C. Wenliang, and Lin Gao “Springback Investigation on Sheet Metal Incremental Formed Parts” World Academy of Science, Engineering and Technology, 2011

[7] J. Duflou, Y. Tunckol, A. Szekeres and P. Vanherck “Experimetal study on force measurement for single point incremental forming” Journal of Materials Processing Technology 189 pp 65-72, 2007

[8] C. Henrard ,C. Bouffioux , P. Eyckens, H. Sol, J. R. Duflou, P. Van Houtte, A. Van Bael, L. Duchêne and A. M. Habraken “Forming forces in single point incremental forming: prediction by finite element simulations, validation and sensitivity”, Comput Mech, 2010

[9] M. Oraon, V. Sharma and S. Kumar “Effect of tool geometry in sheet metal Incremental forming” 27th National Convention of Production Engineers: National Seminar on Advancements in Manufacturing - Vision 2020, mar. 2012

[10] R. de Bruyn and N.F. Treurnicht “An investigation into lubrication strategies for the incremental sheet forming of Ti-6Al-4V” CIE42 Proceedings, Cape Town, South Africa , (2012

APPLICATION OF INFORMATION TECHNOLOGY IN ENTREPRENEURIAL MANAGEMENT

Matija Japundžić[1*], Marko Martinović[1] and Tomislav Kovačević[2]

[1]College of Slavonski Brod, Slavonski Brod, Croatia
[2]Student of Faculty of Economics in Osijek, Croatia
*Corresponding author e-mail: matija.japundzic@net.hr

Abstract
Modern business which includes a large amount of data and complex business processes require the free information systems is hardly possible to imagine such a business. It is a system that collects, stores, store, process and then submit the required information in the way that they are available to all users of an organization. Information technologies contribute greatly to saving time to perform increasingly complex tasks, while on the other hand a significant impact on the structure and increasing the knowledge of employees in such places. This paper presents the key elements of information operations and their role in everyday business.

Keywords:
IT technology; entrepreneurship; management

1. Introduction

Modern information technology is based on the use of computers and computer networks and modern IT methods and techniques. It is experiencing rapid development and has a major impact on all areas of work and life in developed societies. Its application is of vital importance for the survival of businesses in terms of increasing market competition, allows the improvement of public administration and public enterprises that are expected to exceed the quality of services and the like. Information technology allows the use and management of information that supports and enhances the business processes in order to efficiently realized business goals and achieves a competitive advantage. Interaction of information technology, information and data processing procedures and the people who collect and use the information makes the information system. In other words, the information system is a total of infrastructure, organization, people and procedures for collecting, processing, generation, storage, transmission, display, and distribution of the information available to them [1].

2. TASKS OF IT MANAGER

The manager is a person whose primary tasks arise from the management process. He plans, organizes work and business, engages in and leads people, controls the human, material and information resources. His goals are achieved by employing other people. The manager must be a leader [2].

Straightening of IT sector to business activities is necessary so that changes in IT systems would not disrupt business process or disable access to information, all with the effect of creating a competitive advantage. Effective communication is needed with the rest of the organization and accessibility, simplicity and constant support along with upgrade of IT systems for fast and easy use by end users in other parts of the organization such as the departments of finance, marketing, customer relationship management, procurement departments, etc. Good planning reduces of costs in carrying IT projects. Be the first to purchase the latest expensive equipment is not always the most effective way. Moore's Law guarantees that the longer you delay the IT procurement, the more you will get for your money. Waiting will additionally reduce the risk purchase of technological equipment that is not yet free from defects or that is doomed to rapid obsolescence. In some cases, moving the sharp edge of new technology does make sense. However, such cases are becoming rarer as IT capabilities are becoming more homogenized. The balance of team building and "outsourcing" or decisiveness in deciding which part of IT processes to deliver to the treatment outside of the organization and which to keep inside, in order to achieve results with minimal cost and still retain the confidence of its own quality staff and create a quality team. The ultimate task of quality and successful IT managers is to enable faster response of the constant changes in the market. How successful company copes with technological changes can have a significant impact on their overall performance and competitiveness [3].

Information technology improves operational efficiency by enabling:

a) Quick and inexpensive communication and data transfer
b) Fast and quality decision-making
c) Distributed use of databases
d) The outsourcing to the organizations that collect data for the company
e) Improving the quality and accelerate product development time

f) Effective analysis of information in the production process.

Management of IT infrastructures are increasingly complex due to the ongoing development of software and the short lifespan of hardware and required special security concerns of IT processes (protection against data loss and system failure due to a system crash, hacking or theft).
Benefits of IT in business organizations are:

a) Work in a group – virtual groups
b) The ability to work outside the office – teleworking
c) Non-hierarchical organization of work - supported by a centralized database, data warehouse and local tools for decision support
d) To opening business processes to external organizations

2.1. Information technology in governance and management

Successful management of information system results in optimum performance of information technology, and ultimately adds value to the business [1]. Enterprise (or Institution) information system must meet two basic functions: information based on development of products (or service provision), business or management and for documentation. Every information system is set up with a deliberate purpose, striving to carry out the tasks set [4]. With the support of IT, management is significant improved since the management application of IT has received timely, complete, high-quality information.

2.2. Information technology and controlling

Information technology enables better data storage, which again used for further analysis, control and making better and more timely decisions. Quality control system and management system is achieved by the mechanism of feedback [5]. Feedback is a set of activities which governs the functioning of the system with the aim of achieving the desired goal of the system The output from the system is compared with the desired results, planned standards and the differences between desired and actual output is analyzed. If there is a difference, feedback, which becomes input to the system, is generated and returned to the process to achieve that outputs be as close to standard. Impact on the system can be as varied as: repairing the functioning of a single process, the introduction of control parameters for one or more processes, the introduction of new processes, ending old processes, a higher level of controlling the environment input.

2.3. Information technology in the planning process

Planning formulate objectives of the business system and develop plans to achieve the objectives. Planning is one of a decision support system, aimed at high management. IT is used in the planning process and most often in production planning, where there are different plans for production with known capacities and their commitment to other products, the necessary raw materials and optimizes production at the required criteria.
Planning (strategy) makes the initial phase in the development of the information system (IS) when is created:
(a) The initial strategy, i.e. moment of identifying a problem or idea, when there is a reasonable justification for further action in accordance with the planned business objectives: (b) feasibility study, i.e., when clearly analyzing problem area, to identify the border areas (of the IS project), and finally complete the development strategy of the IS., i.e. its business objective and decision: whether to run or not the project of IS [4].
When planning and investing in information systems (IS), we consider six types of strategic issues: (1) alignment with business priorities, (2) IS architecture, (3) infrastructure of IS, (4) centralization versus decentralization, (5) outsourcing (analysis of whether and what to outsource), (6) international issues (compatibility, localization - especially for multinational companies) [6].

2.4. Information technology in the decision-making process

Decision support systems have begun to develop during seventies in the last century, when scientists began to recognize the important role of computer aided information system that supports managers in decision making. Information used in decision-making can arise from data in a business process (internal), resulting in the decision-making process, and outside of the business system (external). Deciding resolve:
a) Structured problems (structured decision) when the decision can be programmed
b) Semi-structured problems (semi-structured decision-making) except due process decision-making is necessary to apply the knowledge and experience
c) Unstructured problems (unstructured decision) decided by the people on the basis of relevant information
The main task of decision support systems is providing quality output information, i.e. information which are adjusted to the particular manager approach in the decision making process. This information should have a high degree of determination power, the appropriate form and scope, with the possibility of projection and forecasting [7].

3. Trends in Information Technology

Key trends in the development of information technology in business systems can be summarized as follows:

a) improving the technology reduces the cost of application of IT tools, but at the same time increasing the volume and complexity of the company's investment in IT equipment
b) gradually increasing the awareness of managers about the meaning and range of IT in the enterprise
c) the activities of which the success of some companies vitally depends in the market are themselves very dependent on IT

The most important trends in information technology are:

a) Computers - simpler and more natural data entry into an information system. Manage the computer operations by voice and handwriting received a strong impetus to the development of tablet PCs early 21st century. This was a decisive contribution to handwriting recognition technology and voice. The creation of the so-called. " digital ink " and its integration into the operating system was crucial to allow the use of the computer screen as a surface on which we write or draw [8],
b) Communication - a global computer network (LAN, MAN, WAN, PAN), Internet,
c) Software - One of the long-term trends in software is the development of decision support systems and knowledge based systems. Some of the important methods used are seeking optimal solutions, modeling and simulation of dynamic and expert systems, and increasingly are being used methods called Intelligent Computing : neural networks, fuzzy logic and genetic algorithms [8],
d) Data - besides the classic data files and databases, increased used of graphics, sound, video, image, spreadsheet, drawing, chart are emerged. Also intensively developing data warehouses in which data is stored from multiple data sources. Different methods in the field of knowledge discovery and data mining, for example, statistical methods, neural networks and genetic algorithms, allow you to find and connect to the appropriate data required for the preparation of business decisions [8].

4. Components of Information Technology

The basic structure of the information system is:

1. Circuits (Hardware)
2. Program applications (Software)
3. Human Resources (Lifeware)
4. Organizational procedures (Orgware)
5. Communication resources (Netware).

Hardware is, essentially, a computer with all the peripheral units that perform the collection, processing, storage and distribution of data to users. In his development process, computers pass through five basic periods, or five generations. The development of the first generation of computers began 1951 while developing computer fifth generation began in 1990 year. Today when paradigm of neutral networks (ANNs - Artificial Neural Networks) has emerged, some consider it to make a new, sixth generation of computers.
Modern computer hardware architecture is complied with these basic elements:

1. Device data input
2. Central unit (CPU)
3. Memory unit
4. Device data output
5. Control unit

Software - the application programs - instructions to enable correct and proper utilizing of hardware resources and smooth operation. The market offers variety number of specialized software products. These programs cover the entire business operations or particular business activities. For instance, accounting programs, retail and wholesale programs, etc.

One of the world-renowned producer of business software is enterprise SAP. Today the most popular suite of programs for business office usage is the Microsoft Office which includes: Word, Excel, Power Point, Access, Outlook, Front Page, Publisher, etc.
Lifeware - within the organization as a separate subsystem are called lifeware or human subsystem consisting of professional IT and end-user information system. The main prerequisite for the proper fulfillment of the role that information should be handled in a way that just meet people at different levels of knowledge, education, with different functions within the organization, as well as with different needs. This result will enable well established and structured information system supported by computer, which is designed to assist people in solving organizational problems [9].

There are two types of human resources, dealing with IS:

a) users of information system themselves - such as managers and executors of tasks in the enterprise
b) IT-professionals, employees who are professionally engaged in the application of information technology, and the development or maintenance of the IS, such

as system analysts, programmers, operators and other IS staff.

Orgware (organization) - the main task of any business system is the realization of short-term and long-term goals. Without organization, each system, even the one with the highest quality parts is not able to optimally achieve the goal. In larger systems, the business organization is becoming a critical factor in business.

5. Conclusion

Due to the large amount of investment in information technology, more significant has become ways in which companies invest and use IT. It can be said that the ability to successfully manage information technology gradually developed into one of the strategic advantages of a number of companies. Because of that, appropriate procedures are required and forms prescribed effective ways of investment and management of information technology in modern companies. Increasing number of companies have emerging trend, a need to involve IT in the strategic plans of the company and watching their IT investments through the prism of business applications and justification. In doing so, the decision on the need for investment in IT must take into account direct, indirect and qualitative effects of IT on the overall business of the company, which often makes it very difficult to make a decision on certain investments in information technology.

6. References

[1] HNB “Smjernice za upravljanje informacijskim sustavom u cilju smanjenja operativnog rizika” [Online]. Available: http://www.hnb.hr/supervizija/h-smjernice-za-upravljanje-informacijskim-sustavom.pdf [Accessed: 19-Apr-2013].

[2] S. Netahli, “Menadžment malog poduzeća”, U: Cvitan, O. (ur) Zbornik radova Veleučilišta u Šibeniku, (1-16) 2008.

[3] Geek u odijelu managera / IT management [Online]. Available: http://www.posao.hr/clanci/karijera/magazin/geek-u-odijelu-managera-it-management/315/ [Accessed: 25-May-2013].

[4] V. Šimović, “Uvod u informacijske sustave”, Golden marketing-Tehnička knjiga, Zagreb, 2009.

[5] M. Pavlić, “Informacijski sustavi”, Školska knjiga, Zagreb, 2011.

[6] J. Müller, “Upravljanje informacijskom tehnologijom u suvremenim tvrtkama te Hrvatska poslovna praksa korištenja informacijskih tehnologija”, Ekonomski pregled, Vol. 52/5-6 (587-612) 2001.

[7] K. Ćurko, “Skladište podataka – sustav za potporu odlučivanju”, Ekonomski pregled, Vol. 52/7-8 (840-855), 2001.

[8] V. Čerić, “Informacijska tehnologija i poslovanje”, [Online]. Available: http://element.hr/artikli/file/1377 [Accessed: 26-Apr-2013].

[9] O. Petrović, K. Jalšovec, “Neki problemi komuniciranja profesionalnih informatičara i korisnika”, Journal of Information and Organizational Sciences, No. 13, (133-140) 1989.

STUDY OF SHAPE MEMORY ALLOYS AND THE PHASE TRANSITION BY DMTA AND DSC MEASUREMENTS

Kis Dávid, Béres Gábor , Dugár Zsolt

and Hansághy Pál

Kecskemét College - Faculty of Mechanical Engineering and Automation, Hungary

* *Corresponding author e-mail: david.istvan.kis@gmail.com*

Abstract

The aim of this research is the examination of the DMTA technique to measure the phase transition temperatures of shape memory alloys. These parameters are difficult to detect by traditional material testing techniques, meanwhile quick and reliable results can be provided by DMTA measurements.

Keywords:

DMTA, phase transition, shape memory alloy, complex modulus, Nitinol.

1. Introduction

The shape memory alloys are shape memory intelligent materials. Their main functional property is the shape memory effect. It means, that a permanent macroscopic deformation of the specimen can be ceased after heating it above a certain temperature. The basis of the shape memory effect is the martensitic phase transition. The alloys are usually adjusted such, that they have martensitic phase in room temperature and their austenitic phase transition temperature is below 100 ^{o}C. When the deformed martensitic specimen is heated to its austenitic phase transition temperature, the grid transformation occurs, and the specimen recovers its original shape.

The problem of the production of shape memory alloys is the determination of the phase transition temperatures. The most important parameters of manufacturing these materials are the temperature range of shape memory effect and superelasticity.

There have been many examples of measuring transition temperatures of metallic materials by DSC method, which was technically designed for plastic specimens. This method has also become well known in metal technology for the last ten years. However, the DSC measurement can only provide relevant results in case of higher heating speed, which worsens the reliability of the results.

The other possible method to measure the phase transition temperatures of such materials is DMTA. Our goal was to study if more exact results can be recovered by DMTA measurements.The other part of our research was studying a special kind of shape memory alloy, the Nitinol. It can be used as a material of a new kind of actuator in prosthesis hands. These kinds of actuators are compact and silent, so they make it possible to build a moving prosthesis. To demonstrate what these actuators are capable of, a prosthesis hand was built based on our design.
[1, 3, 4, 7, 8]

Figure 1. The first prototype of the prosthesis hand which is actuated by Nitinol springs

2. Method

When a sinusoidal load is applied to a viscoelastic material (e.g.: polimers), a loss angle will exist between the load and the responding deformation. Its value will be between 0^{o} and 90^{o}. The complex modulus (E*) expresses the properties of viscoelastic materials. The real part is the storage (E') and the imaginary part is the loss modulus (E''). The ratio of loss and storage modulus (E"/E') is tand which describes the elasticity and the plasticity of the samples. When the value of tand is high the material acts more viscous, while low tand means a more elastic behaviour. The DMTA monitors the changes of tand as a function of temperature.

The main unit of a DMTA equipment is the furnace, the moving and the fix clamp. During the

measurement the temperature changes in the furnace, while stress activation is applied on the sample with the moving clamp. That creates a direct link between the material's chemical structure and mechanical properties. Meanwhile the drawback of DSC is that the change of mechanical properties can not be monitored.

[2, 6, 7]

3. Measurement results

The specimens were CuAlNi and CuAlNiMnFe rods in martensitic phase. The rods outer diameter were 2 mm and they were cut into 20 mm long pieces. A TA instruments Q800 DMTA and a TA Instruments 2920 Modulated DSC equipments were used in our experiments. Our research focused on the DMTA measurements and the DSC results came from the University of Miskolc, Faculty of Material Science. The test frequency was 5 Hz, the amplitude was 30 μm and the heating rate was 3 °C. The applied temperature range was between 0 and 200 °C. [2.] Figure 2 shows the DMTA measurement results for CuAlNi specimen. There is a local tand peak in the heating cycles at about 80 °C, which we consider to be in the austenitic transition temperature range. Other peaks can be seen in the cooling cycles at about 100 °C, which is considered to indicate the martensitic phase transition. The change in the tendency of tand indicates that these shape memory alloys showed "viscoelastic" behaviour.

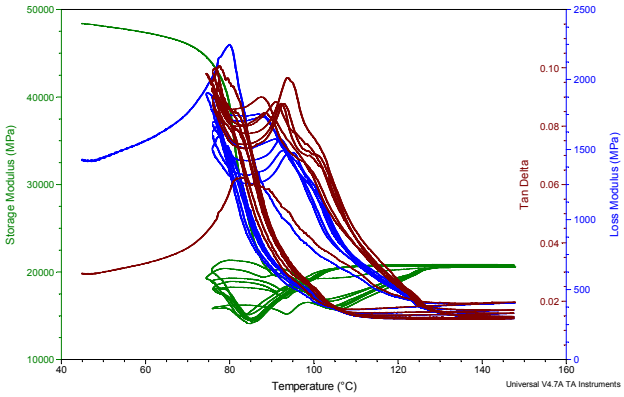

Figure 2. Recurrent heating and cooling cycles on CuAlNi specimen indicating the phase transition temperatures of the alloy

Figure 3 shows the DMTA measurement results for CuAlNiMnFe specimen. The aim of this measurement was to compare the results to DSC measurement results which were made in the University of Miskolc, Faculty of Material Science. The tand peak is at about 78 °C in heating cycles and 95 °C in cooling cycles.

The DSC curve of the same alloy showed the phase transformation approximately at the same temperatures. These results make DMTA measurement a potential new technique in the investigation of metals.

Discrepancies between the peaks of cooling cycles in case of DMTA and DSC measurements have been found. The reason is, that the specimen used in DMTA is approximately 50 times heavier than those used in DSC, which affects the thermal conductivity. We used liquid nitrogen to cool down the specimen in the DMTA furnace, which might have had an influence on the results, too.

[5]

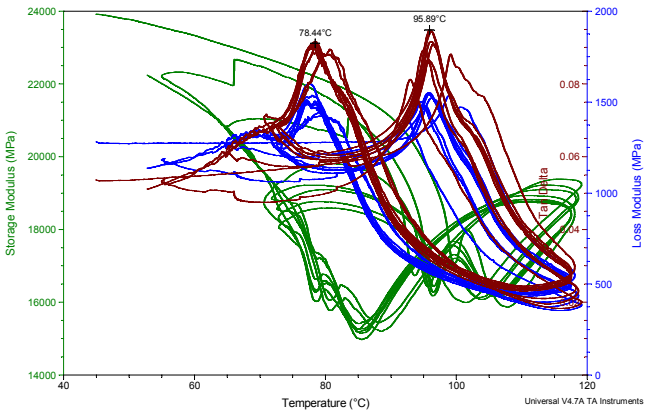

Figure 3. DMTA curves of CuAlNiMnFe specimen showing local peak at 95 °C during heating and at 78 °C during cooling

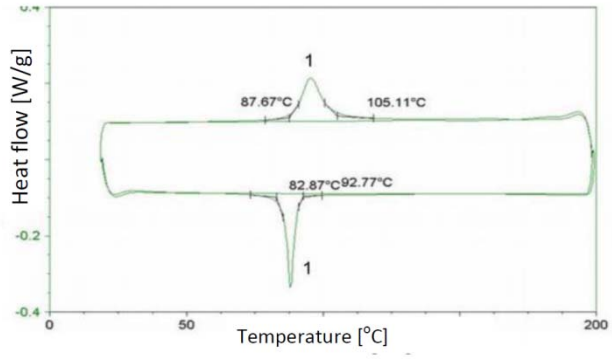

Figure 4. DSC curves of CuAlNiMnFe specimen showing local peak between 87 °C and 105 °C during heating and between 82 °C and 92 °C during cooling [2]

4. Acknowledgement

This research was supported by the European Union and the State of Hungary, co-financed by the European Social Fund in the framework of TÁMOP 4.2.4. A/2-11-1-2012-0001 'National Excellence Program'.

5. References

[1.] Ryklina, EP; Prokoshkin, SD; Khmelevskaya, IY: One-way and two-way shape memory effect in thermomechanically treated TiNi-based alloys, Article; Proceedings Paper, Materials Science and Engineering A-structural Materials Properties Microstructure and Processing, Vol. 481, pp 134-137, 2008

[2.] Benke, M; Mertinger, V; Daroczy, L: Investigations of Solid Phase Processes in CuAlNi Base Shape Memory Alloys, Proceedings Paper, ESOMAT 2009 - 8th European Symposium on Martensitic Transformations, Article Nr. 06003, 2009

[3.] Kiss Attila: Nikkel-titán (NiTi) alakemlékező ötvözet alkalmazása robotkezekben, Article, Fiatal Műszakiak Tudományos Ülésszaka, Vol. 2, pp 157-160, 1997

[4.] Huang, W: Modified Shape Memory Alloy (SMA) model for SMA wire based actuator design, Article, Journal of Intelligent Material Systems and Structures, Vol. 10, Issue 3, pp 221-231, 1999

[5] Tian, QC; Wu, JS: Characterisation of phase transformation in Ti50+xPd30Ni20-x alloys, Article, Intermetallics, Vol. 10, Issue 7, pp 675-682, 2002

[6] Foreman, J: Dynamic mechanical analysis of polymers, Article, American Laboratory, Vol. 14, Issue 1, pp 21-&, 1997

[7] Varhegyi, G; Groma, G; Lengyel, M: DSC Examination of Alloys, Article, Thermochimica Acta, Vol. 30, Issue 1-2, pp 311-317, 1979

[8] Bundhoo, V; Haslam, E; Birch, B; Park, EJ: A shape memory alloy-based tendon-driven actuation system for biomimetic artificial fingers, part I: design and evaluation, Article, Robotica, Vol. 27, pp 131-146, 2009

INVESTIGATION OF ALUMINIUM ALLOY 3003 BY DMTA TECHNIQUE

Béres Gábor, Dugár Zsolt, Kis Dávid, Hansághy Pál
Kecskemét College - Faculty of Mechanical Engineering and Automation, Hungary
* Corresponding author e-mail: gabberix@freemail.hu

Abstract
The researcher work pushes the borders of the application of a high efficiency equipment, in the matter of metals. With this equipment, which already testifies in the compound industry, a flasher query of some metal-related technological parameters could be easily available.
Towards the searching, we shaped aluminium-alloy 3003 samples, in different states, and accordingly we monitored the recrystallization. Following the shaping, the DMTA detected such microscopic transformations (as we expected), according to heating rate, whereby we could determine the specialities of the transformations.

Keywords:
DMTA, microscopic grindings, recrystallization, aluminium, shaping, loss factor, temperature difference

1. Introduction

The researcher team examines both the industrial metals (principally) as well as the high-tech materials and special metals (for example shape memory alloys) with DMTA equipment. Our current object is the monitoring of the recrystallization, in case of aluminium and the investigation of the influential factors of this process. The measurements' results, that the DMTA presented, had been compared with microscopic grindings.
It is well known, that the temperature of the recrystalliaztion is depend on the structure, and the shaping grade of the material [2]. For example the recrystallization in deformed aluminium with high purity could be completed at 150°C. for 50 sec. But that in deformed Al-0.01 at% Fe alloy would need more than 10 billion years at 150°C to complete the recrystallization [5].
Or Ito et al. have investigated that the recrystallization would appear obviously around 400 °C when the content of iron exceeds 0.01 wt% [5].
We measured that the difference between the recrystallization temperatures of cast and homogenized structure is only few degrees. The demonstration of such precision measures is more difficult with other processes. The recovery suppresses the recrystallization in DSC in case of aluminium alloys. The temperature monitoring with hardness analysis are also difficult because of the variation of the furnaces' constant temperature [3].
The literature research added up to that, we are not the first to examine metals with DMTA. Other (particularly Asian) researchers already determined metals' behaviour, which can't be measured with equipments of metal industry. In contrast with them, we would like to write up the measurement method, whereby the industrial materials would be easier defined.

2. Method

We studied aluminium alloy 3003 containing (in wt%) 0.58 Si, 0.62 Fe, 0.068 Cu, 1.09 Mn, 0.03 Mg, 0.006 Ti, 0.008 Zn, 0.007 Ni, the rest is Al [4]. The investigation based on two structures, a homogenized, and a cast one. The homogenization was carried out at 500°C over 8 hours.
Two homogenized structure samples were rolled on cold. One from 13mm to 12mm (q=0,92%) the other one from 3mm to 1mm (q=0,66%). Two more samples from the cast structure were also rolled on cold. One from 13mm to 12mm (q=0,92%) and the other from 3mm to 1mm (0,66%). The preperatory rolling happened on 500°C. It provided the base sizes (13mm and 3 mm) of the samples.
Previous operations were repeated with preperatory hot rolling on 400°C. This way, we could study the effect of the shaping temperature and the shaping grade for recrystallization.
For the DMTA measurements we used narrow sheets. We prepared it with cutting. The microscopic grindings also demand preparation. It consisted of the cutting, the resin embedding, the grinding and the etching of the samples.
In the course of the DMTA measurements we used two point bending method. The measurements were carried out in air. The heating rate was 3 K/min between room temperature and 450°C. The frequency of the σ stress was 5 Hz, the amplitude of the elongation was 10 μm.
In case of a visco-elastic material the σ bending stress is delayed to the deformation with delta angle (figure 1). In case of clearly viscous materials, like the water, the delay is 90°. Because the aluminium alloys are elastic materials, the σ bending stress and the deformation should have be in the same phase [6].

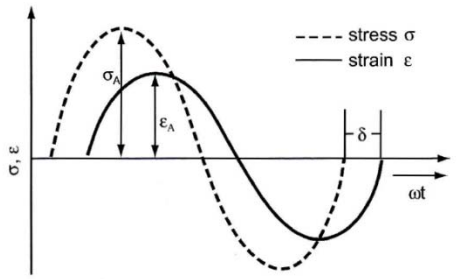

Figure 1. DMTA curve

In the curves of the DMTA the loss factor appeared. It means that in certain cases aluminium alloy 3003 also can show similar property than a visco-elastic material.

3. Results

Due to the recrystallization, the structure of the samples has changed. There are many forms to control this realignment. First we created microscopic grindings.
The microscopic picture of a rolled sample can be seen in figure 2. Due to the rolling, the grains stretch, the material hardens. Further shaping is more difficult [1].

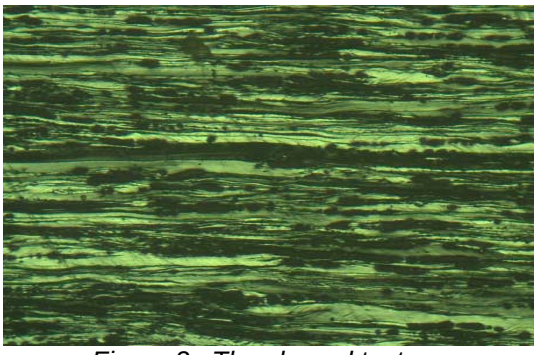

Figure 2. The shaped texture

With heat treatment, the material can be transformated again. New grains are produced, what are proof from the effect of the shaping [1]. It can be seen in figure 3. This is the essence of the recrystallization.

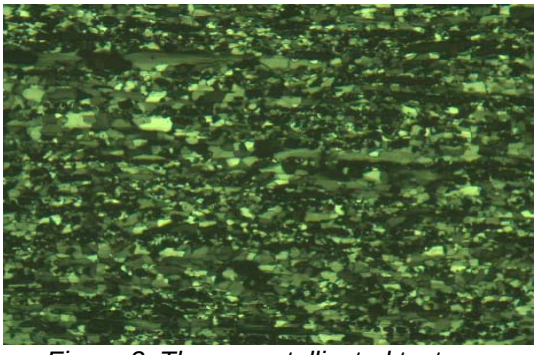

Figure 3. The recrystallizated texture.

The recrystallization is visible from the microscopic pictures, but the process is not able to followed in detail. In order to interpret the difference between the recrystallization temperatures, we used DMTA measurements.
First we examined the effect of the physical condition.

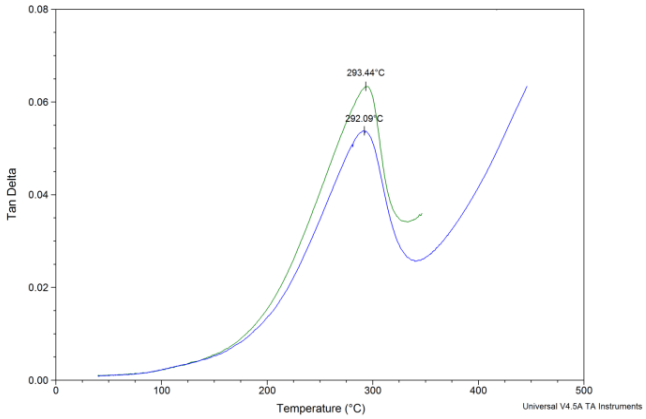

Figure 4. Cast (green curve) and homogenized (blue curve) samples

The difference between the cast and the homogenized samples is roughly one celsius degree. It is very little difference, yet we could measure with DMTA equipment.
Next to constant physical condition, we examined the effect of the shaping. The recrystallization took place at higher temperature, as the shaping grade larger. It is due to the different grain sizes formed during the deformation [2].
In our case, the difference between a 0,92% shaped and a 0,66% shaped samples, is roughly three celsius degrees.

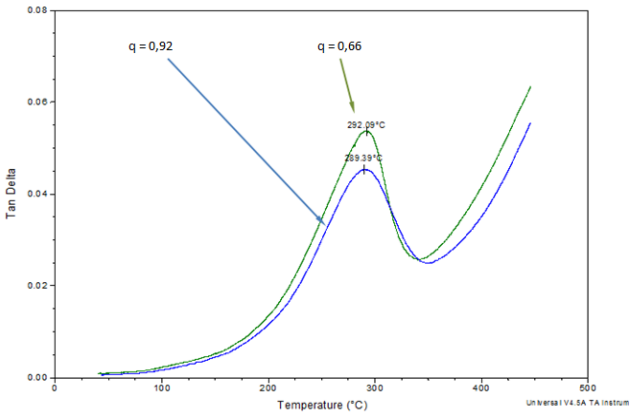

Figure 5. Diverse shaped samples (next to constant rolling temperature and physical compound)

The largest difference bertween the recrystallization temperatures was visible, if two of the parameters were different. Those parameters were the temperature of the hot rolling, and the grade of the colled working. The difference between the two temperatures is more than seven

degrees. This almost essential deviation is shown in figure 6.

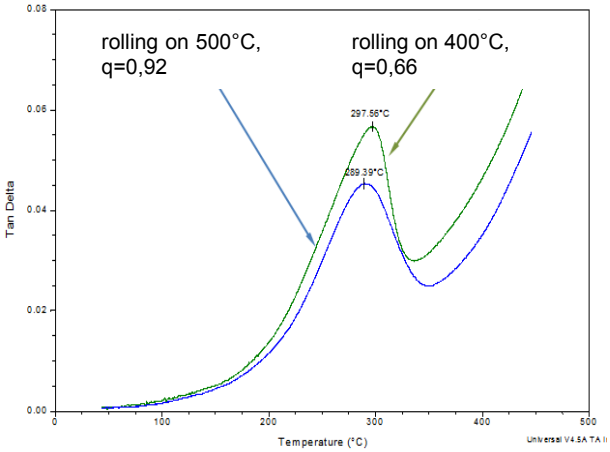

Figure 6. Homogenized samples on diverse temperetures and on diverse shaping grade

The realignment is well visible in all of the DMTA curves. It is assumed that the process of the recrystallization is able to follow up with thermo-dynamic investigations.

4. Conclusion

Recrystallization of aluminum alloy 3003 was investigated in different circumstances. To reveal the transformation we applied microscopic grindings and DMTA equipment.
Based on the results, we suceeded in demonstrating the appearance of the loss factor, with this new measurement process. Furthermore, it is observed, that the thermo-dynamic measurement process is a suitable method for monitoring recrystallization.

6. Acknowledgement

This research was supported by the European Union and the State of Hungary,co-financed by the European Social Fund in the framework of TÁMOP 4.2.4.A/2-11-1-2012-0001 ‘National Excellence Program’.

5. References

[1] George E. Dieter: Mechanical Metallurgy, SI Metric Edition 1988.
[2] William F. Hosford:, Robert M. Caddel: Metal Forming, Mehanics and Metallurgy, Cambridge University Press 2007.
[3] Raymond A. Higgins: Engineering Metallurgy, Applied Physical Metallurgy, Hodder Headline Group 1993.
[4] Metallic Materials Properties Development and Standardization, Office of Aviation Research Washington, D.C. 20591, 2003.
[5] George E Totten, D. Scott MacKenzie: Handbook of Aluminium Volume 1: Physical Metallurgy and Processes, Volume 2: Alloy Production and Materials Manufacturing
[6] Joel R. Fried: Polymer Science and Technology

5th International Scientific and Expert Conference TEAM 2013
Technique, Education, Agriculture & Management
Prešov, 4th to 6th November 2013

COMPRESSION MOULDING OF PNEUMATIC TYRE REGENERATE WITHOUT BINDER

Domagoj Ribar[1], Filip Jambrek[2] and Ana Pilipović[*3]

[1]Dok-ing d.o.o., Zagreb, Croatia
[2]Belupo d.d., Koprivnica, Croatia
[3]University of Zagreb, Faculty of Mechanical Engineering and Naval Architecture, Zagreb, Croatia
* *Corresponding author e-mail: ana.pilipovic@fsb.hr*

Abstract
Rubber is a material without which today's world would be unthinkable. The basic component for obtaining rubber is caoutchouc, which can be natural and synthetic. Before vulcanisation rubber is mixed with additives according to exactly defined recipe, which ensures certain properties of the finished product. A vulcanising agent is necessary for vulcanisation, usually sulphur, and it takes place over several hours at increased temperatures. The task of rubber is to connect all the ingredients together and to define the basic mechanical properties of the rubber product, such as elasticity and strength. Rubber can be recycled, and most often car pneumatics are recycled. The recycling product is wire, fabric and rubber powder. 5 – 10% polyurethane adhesive is added to the powder as binder, for better properties of the products made of recycled rubber. The problem arises in the selection of processing parameters of such regenerate without the addition of rubber. The paper has analyzed the selection of the processing parameters and mechanical properties were tested on the finished product in order to establish the difference in the moulding with and without binder.

Keywords:
Compression moulding, mechanical properties, pneumatic tyre, processing parameters, recycling

1. Introduction

Out of today's overall consumption of rubber about 38% is accounted for by natural rubber, and the remaining 62% are different types of synthetic rubbers. Out of this even more than 50% is used for the production of pneumatics which are required by the automotive industry, and air and transportation traffic. In the recent years there has been an increase in the need for the disposal of obsolete and discarded rubber products, mostly pneumatics, in order to protect the environment, and a number of measures have already been undertaken in order to increase the usability of the obsolete rubber products. [1,2]
Rubber materials are also called elastomer materials because no other material has such elastic properties. Apart from elasticity they feature an entire series of other favourable properties such as water- and airtightness, stability at high temperatures and to the impact of aggressive media, or retaining elasticity at very low temperatures. [1,2]

2. Butadiene rubber (BR)

Over 90% of butadiene rubber is applied in the production of pneumatics, whereas the rest is used for the production of seals or floor panels. [3,4]
Most of the butadiene rubber is obtained by emulsion polymerization. The activators which are applied are mainly titanium, cobalt, nickel, compounds of neodyne or alkaline-lithium compounds. Butadiene rubber is mainly applied in the compounds with natural rubber or styrene – butadiene rubber. Its advantages of processing are high strength, easier processing by pouring into the mould, shorter extrusion time. Butadiene rubber can be easily bound with all the non-polar rubbers. The ratio of the compound depends on the desired properties, and ranges from 30% to 50% of butadiene rubber. [3,4]
The mechanical properties of vulcanisates based on butadiene rubber are significantly lower compared to vulcanizates of natural or styrene-butadiene rubber, but in compounds with these rubbers the butadiene rubber can satisfy the technical requirements for high-quality vulcanisates. [3,4]

3. Recycling

The start of mechanical processing of waste pneumatics begins with the sorting of pneumatics. The pneumatics are divided into full profile pneumatics and tubeless pneumatics.
Full-profile pneumatics are subjected to a procedure in which they are grated up to the inner diameter. Such processing produces rubber buffings with no metal. The remainder of such peeled pneumatics taken to other collected pneumatics. The same procedure is applied to big truck pneumatics from which the tread layer without metal reinforcements is removed. [5,6]
The size of the buffings that can be obtained by this procedure: [6]

- 0 mm – 0.8 mm
- 0.8 mm – 3 mm
- 3 mm – 5 mm
- > 5 mm (*mulch*)

In the next step, using a hydraulic hook the wire cores are torn out, and transferred to the first mill that grinds them to a size of approximately 100 –

400 mm (figure 1). The pieces are further transferred to a series of mills that crash and separate the metal and fabric remains through several consecutive steps. [6]

Figure 1. Pneumatic tyre shreder [7]

Throughout the plant, through which the shredded granulate passes, there are on several places magnets that remove the metal particles, thus obtaining the granulate, i.e. powder, of high purity.
The size of the grains that are obtained by such a procedure is divided into: [6]

- Rubber powder 0 mm – 0.5 mm
- Rubber granulate 0.5 mm – 2 mm
- Rubber granulate 2 mm – 3.5 mm

The obtained granulate is further packaged for sales or transferred into silos from which it is transported to the mixers in which it is mixed with adhesive and paints before compression moulding. [6]
The annual capacity of pneumatics recycling in Croatia (car tyres from passenger and off-road vehicles, vans, and freight vehicles, buses, tyres of agricultural machines, tractors, fork-lifts, etc.) amounts to 23 000 tonnes of obsolete tires of all types.

4. Compression moulding of pneumatic tyre regenerate

This is a procedure in which the pre-heated preform is first placed into an open, heated mould cavity. This is followed by the closing of the press with a pressure, and the temperature and pressure are maintained in order to ensure the flow of the rubber compound (figure 2). [8]

Figure 2. Compression moulding

The preheating of preform is often very useful since it shortens the time of vulcanisation and facilitates the flow of the rubber compound. [2,8]
During the vulcanisation phase in the hydraulic cylinder high pressure (about 200 bar) needs to be turned on and uniform flow of the rubber compound in the mould cavity has to be ensured. Attempts are still being made to achieve the reduction of the vulcanisation time by raising the temperature of the mould cavity. [2,8]

5. Experimetal part

In the experimental part of the work a test has been made of direct moulding of the rubber powder without additives. The rubber powder is the recyclate of old car pneumatics. of the grain size of 0 – 0.5 mm. It mostly consists of butadiene rubber or styrene-butadiene rubber. In every application the granulate is mixed with polyurethane which serves as adhesive, and its stiffening produces a compact product. The objective of this experiment was to test whether the rubber granulate can be moulded into a compact entity without addition of adhesive.
The mould consists of three parts: the central frame into which the rubber powder is placed, and upper and lower plate which close the frame. The material for the production of mould is stainless steel which is additionally ground and polished in order to make the surfaces of the plates that close the frame as smooth as possible so as to avoid the sticking of the mould to the plates.
The moulding phases are:

- application of the lubricant *Sansil AC – 274* on the mould, due to the possibility of adhesive bonding of the mould to the mould plate;
- filling of the mould by the rubber powder;
- inserting of the mould into the press;
- closing of the press;
- short opening of the press in order to release gases from the mould;
- press time;
- opening of the press and taking out the mould;
- opening of the mould and taking out the moulding;
- cooling and cleaning of the mould in the preparation of the next cycle – mould cleaning is necessary in order to remove the residual rubber powder and the rest of the lubricant, thus achieving a smooth surface of the mould plate for the production of the next moulding, whereas cooling of the mould is necessary so that the new lubrication layer would remain in the liquid state during application.

For parameters are necessary to carry out the experiment. The initial parameters can be found in Table 1. The temperature, pressure and the pressing time are selected empirically, whereas the powder quantity has been selected computationally.

Table 1. Initial processing parameters

Processing parameters	Value
Temperature ϑ, °C	180
Pressure p, bar	250
Pressing time t, min	20
Mass of regenerate powder m, g	28

Calculating the necessary quantity of rubber powder was done by weighing 100 ml of powder, which amounted to 27 g, and then the density of powder was calculated, which amounts to 270 kg/m³. The product of the mould volume (V = 0.0000512 m³) and the density have yielded the mass necessary to fill the mould and this mass has been increased by 100%, which led to a mass of 28 grams.

$$m = V \cdot \rho = 0{,}0000512 \cdot 270 \quad (1)$$
$$m = 0{,}0138kg = 13{,}8g \quad (2)$$
$$m = 13{,}8 \cdot 2 = 27{,}6 \approx 28g \quad (3)$$

After pressing the sample under the initial parameters the conclusion has been made that the temperature of 180°C was not sufficient for full melting of the rubber powder since the sample crumpled and fractured by demoulding, and the mass of 28 grams was too small since voids remained in the sample (figure 3).

Figure 3. Moulding under the initial parameters

After having determined that the calculated mass of the powder of 28 g was not sufficient to achieve a compact moulding, the necessary quantity had to be determined through experiments. The time remained constant (20 min). The mouldings were tested with the following parameters:

1. ϑ = 180 °C, p = 250 bar, m = 28 g
2. ϑ = 220 °C, p = 250 bar, m = 40 g
3. ϑ = 240 °C, p = 250 bar, m = 35 g
4. ϑ = 200 °C, p = 300 bar, m = 35 g
5. ϑ = 200 °C, p = 200 bar, m = 42 g (figure 4)

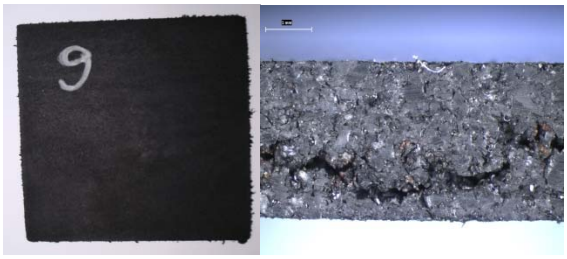

Figure 4. Moulding with m = 42 g, ϑ = 200 °C, p = 200 bar, t = 20 min

The mass of 42 g of rubber powder was obtained by setting the thickness frame at 4 mm to the 2 mm thick mould frame and additional weighing. Such procedure with two frames has proven to be necessary also for the uniform distribution of the powder in the mould since the not uniformly distributed powder caused holes in the sample. The testing showed a compact moulding of 42 g.

After having determined the necessary quantity of powder in order to obtain a compact sample, the impact of the moulding time had to be determined. For determining the moulding time a constant temperature of 200°C was determined, the pressure of 200 bar and the mass of 42 g, and the time changed. Selected were 10, 15, 20, 30 and 40 minutes. The testing determined that the minimal necessary moulding time was 20 min, and that there are no significant differences between moulding for 20, 30 and 40 min. In case of 10 and 15 minutes of time a "grainy" surface can be noticed, i.e. the moulding time was too short. The moulding time selected was 25 min.

In order to determine the limits of the moulding pressure the previously determined parameters have been selected: ϑ = 200°C, t = 25 min, m = 42 g. Testing was done with pressures of 150, 170, 190, 180 and 210 bar.

The pressures of up to 150, 170 and 190 bar have proven to be too low, since the moulding surfaces remained "grainy", and microscopic images showed voids in the structure. At pressure of 210 bar the moulding started to decompose during demoulding. The temperature of 200°C allows work with very narrow pressure range of 190-200 bar.

For further testing at different temperatures the following processing parameters have been selected: p = 200 bar, t = 25 min, m = 42 g. The temperature changes within limits ranging from 190°C to 240°C with increment of 10°C.

The temperature of 190°C proved to be too low since the moulding decomposed during demoulding and the "grainy" structure could be noticed, i.e. the rubber powder did not melt at that temperature. At temperature of 240°C the moulding also disintegrated and it was concluded that the temperature was too high, although it may be that the disintegration was also the result of a combination of excessive pressure and temperature. There is the possibility that with the application of lower pressure and a temperature of 240°C one could achieve a good result even with shorter moulding time.

Within limits from 200°C to 230°C the moulding structure did not change significantly. However, at 230°C the moulding had fewest voids (figure 5).

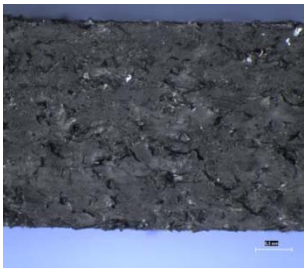

Figure 5. Moulding with ϑ = 230 °C, p = 200 bar, m = 42 g, t = 25 min

Since in the previous tests the moulding temperature of 230°C proved to be the best selection, and the best result was achieved precisely at this temperature, it is necessary to re-examine the limits of the moulding pressure precisely at the temperature of 230°C. Other parameters have remained the same (t = 25 min, m = 42 g, ϑ = 230°C). The testing was performed for the pressures of 150, 170, 210, 230, 250, 270, 300 bar.

At pressures from 170 – 300 bar no differences have been noticed, so that one may conclude that at a temperature of 230°C a much wider range of pressures can be applied than at lower temperatures. Figure 6 shows the moulding at a pressure of 230 bar.

Figure 6. Moulding with p = 230 bar, ϑ = 230 °C, m = 42 g, t = 25 min

After having determined that at a temperature of 230°C the rubber powder can be directly moulded with a wide range of pressures, it was necessary to test whether the moulding time would have impact on the moulding quality at the mentioned temperature, i.e. whether it was possible to shorten the time to 10 min. Other parameters are p = 230 bar, ϑ = 230°C, m = 42 g. Figure 7 shows the equally good structure as on the samples moulded for 25 min.

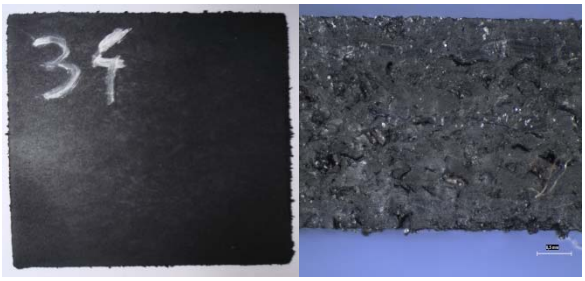

Figure 7. Moulding with p = 230 bar, ϑ = 230 °C, m = 42 g, t = 10 min

6. Discussion and comparison of mechanical properties with and without binder

It was determined by the experiment that at processing parameters of p = 230 bar, ϑ = 230°C, m = 42 g, t = 10 min a good moulding may be obtained in which the rubber powder was well fused. In comparison with the regenerate of the rubber pneumatics with the addition of polyurethane adhesive the tensile strength at break R_p was reduced, but the elongation at break ε_p increased (table 2).

Table 2. Tensile properties

	Tensile properties	
Processing parameters	R_p, MPa	ε_p, %
p = 230 bar, ϑ = 230 °C, m = 42 g, t = 10 min, without binder	1,97	124,22
with 35 % PUR binder	4,84	65,24
with 40 % PUR binder	6,36	93,23

7. Conclusion

The experimental part of the work showed that the rubber powder obtained by recycling of car pneumatics may be moulded without the addition of adhesive into a compact unit. The tensile strength at break was reduced by 67% in relation to the moulding with 40% of polyurethane adhesive, and therefore it is necessary to perform further research of the parameters of temperature and pressure with the aim of improving the properties as well as shortening of the moulding time.

8. Acknowledgement

This work is part of the research included in the project *Increasing Efficiency in Polymeric Products and Processing Development*, which is part of program *Rapid Production — From Vision to Reality* supported by the Ministry of Science, Education and Sports of the Republic of Croatia. The authors would like to thank the Ministry for the financing of this project. Authors also would like to thanks firm *Gumiimpex-GPR d.d.* and *TPK Nova* for some equipment.

9. References

[1] A. Ciesielski, “An Introduction to Rubber Technology, Rapra, Shawbury, 1999.
[2] M. Šercer, “Proizvodnja gumenih tvorevina“, Društvo za plastiku i gumu, Biblioteka polimerstvo, Zagreb, 1999.
[3] V.C. Chandrasekaran, “Rubber as a Construction Material for Corrosion Protection“, Wiley, Salem, 2010.
[4] W. Hoffman, *Rubber Technology Handbook,* Hansen publishers, Munich, 1989.
[5] J.S. Dick, “Rubber Technology, Compounding and Testing for Performance“, Hanser, Munich, 2001.
[6] http://www.gumiimpex.hr/en/cms/production/waste-tire-recycling/, 10.6.2013.
[7] http://www.seekpart.com/company/84039/products/20121213103910890628397352O.html, 12.6.2013.
[8] J.S. Dick, “How to Improve Rubber Compounds, Hanser, Munich, 2004.

INVENTORY MANAGEMENT: A PRACTICAL EXAMPLE FROM WOOD PROCESSING INDUSTRY

A. Katolik[1*], Z. Jurković[2]

[1]University of Applied Science in Slavonski Brod, Dr. Mile Budaka 1, 35000 Slavonski Brod
[2]Ivan Domac Secondary Commercial and Trade School, Vinkovci, A. Akšamovića 31, 32100 Vinkovci
** Corresponding author e-mail: andreja.katolik@vusb.hr*

Abstract
Inventory is a vital factor in the business operations of manufacturing and trade companies. The essence of inventory philosophy is to make sure that stocks do not fall below the minimum level or reach excessive quantity to prevent them from losing value with time. There are concepts, i.e., models available to be implemented by business entities that can provide for an efficient inventory management and facilitate business operations. This paper aims to present the theoretical framework of inventory management, discuss a real-life example of inventory management and offer possible solutions to the problem. The observed company's main activity is wood processing. One of the main problems of the observed company was the fact that it needed a more efficient inventory management because it often happened that it either had too much inventory or not enough to continue the production. Inventory management could be improved by using simple mathematical methods to determine the optimum order quantity for specific raw materials and the minimum inventory level for a product, as illustrated by a simple example. In addition to introducing essential structural changes to the management, in order to improve company's stock management it is proposed to implement advanced information technology which will help find the right planning and inventory control models.

Keywords:
Optimal stock management, stock models, business entity (company), management, production (manufacturing)

1. Introduction

Inventory is a vital factor in the business operations of a company. The term inventory (stock) means a quantity of goods (materials, own products, semi-finished and finished products) accumulated for the purpose of accommodating continuously temporally and spatially more or less distant production or personal consumption". [1] Another definition of stock says that it is "a buffer between the input and output of material goods". [2] In a contemporary business context, stock management is considered one of the major challenges companies have to deal with. [3] In the context of manufacturing industry, inventory refers to raw materials, component parts, work-in-process, supplies and finished products, whereas in the context of trade, inventory refers to wholesale and retail supplies. When stock levels are at their extremes this means that a company either has more than enough stock or that it is constantly on the verge of a stockout and keeps having to order new stock urgently. To be on the safe side, but also because of the market conditions, it would be beneficial to have enough raw materials, components, semi-finished products and finished products or supplies at the store at all times so that nothing gets in the way of the production and customers being served promptly. On the other hand, if assets are tied up in inventory and there is interest to be paid, the company's costs increase. Also, the prices of goods kept in stock may change on the market, which may have adverse effects. It is also uneconomical if there are production hold-ups due to the lack of raw materials and components. Should this happen, the incurred costs may far exceed the costs of keeping a larger stock. For reasons stated above, it is necessary to find a solution between the two extremes in order to make sure that the production is not disturbed or that there is enough stock at the store at the same time keeping the costs to a minimum. In any case stock should be kept at optimum levels. [4]

2. The importance of efficient stock management

Since the 1960s, all industrialized countries have witnessed a considerable progress in terms of efficient inventory planning and overall stock reduction. Stock management has been practiced since Biblical times. In times of shortages, those who had the largest stock of food and other subsistence goods had the greatest chance of survival. The belief that the larger the stock of goods the better prevailed until the 19th century. From the early 1900s to the 1970s, the supply and distribution were becoming more and more organized and the need to keep stock and the views about holding stock were changing. Expert practitioners were trying to find models and ways to plan and control inventory as efficiently as possible. The prevailing opinion at the time was that inventory holding was expensive. Since the 1970s, stock management has gained more and more attention in the developed industrial

countries. Stock holding has increasingly been seen as wasteful and efforts were made to reduce stock levels as much as possible. As a result, many companies worldwide reduced their stock levels which had significant economic effects not only on the companies themselves, but also on the country's economy as a whole. The effects of stock level reduction are so obvious that the share of stock in a country's gross domestic product is considered an important indicator for the efficiency of the economy of a country. Excessive funds committed to stockpiling increase costs unnecessarily and as a result reduce corporate liquidity and profitability of the invested capital. By reducing the level of inventory in the warehouse, the costs of production reduce as well, which has a positive effect on the competitiveness of the company in the market (especially foreign market). [3] Stock management begins by purchasing the raw materials and components and ends with storing the finished products which have not been delivered to customers. [3] It follows from the above that stock management is one of the most important tasks of the company management. The main goal is to keep stock at the lowest possible level, but at the same time sufficiently high to maintain the continuity of the production process. Poor stock management can pose a significant problem and, as has been already pointed out, may have a significant adverse impact on company's financial performance, including the return on net value and return on investment. [5] The development of information technology and the emergence of various planning and control models have greatly improved stock management.

Different inventory management methods and models are used to manage inventory efficiently, i.e., determine timely and adequate levels of inventory at minimal cost. [4] Inventory planning and control models include the following:

1. Traditional inventory planning and control system (Economic Order Quantity - EOQ)
2. Inventory planning and control system based on market conditions (Material Requirements Planning – MRP; Distribution Resource Planning - DRP)
3. Inventory planning and control system based on timely supply of goods for production and distribution (just-in-time - JIT)

The first model for determining the optimal order quantity or economic order quantity was developed in 1915 by Ford W. Harris. This model is also referred to as traditional inventory model. It is static and very simple. The underlying assumptions of this model are that the demand for goods is uniform and known in advance; the goods are ordered when they are out of stock; they are delivered on time and ordered in equal intervals, and no constraints are taken into account, such as the size of the warehouse, available financial resources, etc. Since then, the inventory theory has been constantly evolving, and the number of inventory management models today is so large that there is no uniform classification. [6]

Unlike traditional inventory planning and control system, where the required inventory level is maintained by replenishing the stock, the underlying assumptions of the inventory planning and control system based on market conditions are that the production, i.e., sales plan is known in advance and the material requirements for each product have been determined. When planning inventories based on this system, two techniques are used:

•Material Requirements Planning (MRP) and
•Distribution Requirements Planning (DRP). [3]

Inventory planning and control using the MRP model is based on the production planning and material requirements. Sophisticated computer programs or special mathematical methods are used to plan or forecast the required quantity of input materials (raw materials, components, semi-products and other goods required for production). This serves as the basis for planning and inventory control depending on the production, i.e., sales requirements. This is done by planning the quantity and type of input materials depending on the quantity of the main product planned to be produced or sold in a given period. The second technique, Distribution Requirements Planning (DRP), is based on demand forecasting. The most commonly used methods include moving average and exponential smoothing forecasting. Moving average method is simpler than exponential smoothing and consequently more frequently used. Moving average method is based on the average consumption or sales in several previous periods which is then taken as the basis for forecasting consumption or sales in the forthcoming period. [3] The objective of both planning and inventory control techniques is to reduce storage time, avoid the static concept of repeating fixed orders, avoid holding large quantities of safety stock and align production with demand. Planning and inventory control in the production and distribution using MRP and DRP systems enable complete control of the entire logistics system, from suppliers of raw materials and components to the finished product consumers. [3]

People have been using just-in-time (JIT) principle in various situations for quite some time. Whenever a person wants to achieve a major goal or task just in time, he/she must do some preliminary work just in time. In order to manufacture a certain product by following the JIT principle, it is necessary that parts ordered for the production of that product are delivered to the factory just in time so that production line workers can transform it into a finished product just in time.

This method of work reduces stock, accelerates movement of working capital, shortens the production process, eliminates the need for storage of materials, storage between production phases and storage of finished products. [3]

3. Real-life example of inventory management

One of the leading companies in the Croatian wood processing industry is Spačva d.d (joint stock company) from Vinkovci, whose main activity is wood processing and wood product manufacturing. This paper provides a summary of the problems this company is facing in terms of stock management. The observed business entity manufactures final products using mostly line production strategy. Production is planned on a monthly basis by creating the monthly production plan containing information about the name of the customer, shipping deadline, product name, unit measure, unit price, total quantity, and the number of hours needed for production of a single product. Due to company's current inventory management, inventory levels are often at their extremes and the company often has to deal with the lack of raw materials required for production. Before the economic crisis, the company piled inventories whose prices were subsequently not adjusted to market prices and were no longer readily marketable. The tied up inventory increased interest and other costs. As a result, the change in the value of stocked products has had long-term adverse effects. The problem can be resolved by determining the minimum level of inventory for all products, raw materials and components and reacting promptly when this level is reached, as well as by determining the optimal quantity of raw materials and components to be ordered. Based on the analysis of the current inventory management policy, it was concluded that the company had not taken into consideration the transaction motive in spite of the fact that, when it comes to keeping inventory, this would be advisable because it would lead to further cost reduction. The observed problem concerns the supply of raw materials and components for selected products. Furthermore, as already mentioned, since certain goods have occasionally not been available at a given time, this led to:
a) production delays or
b) production hold-ups.

Stock management problems were formulated on the basis of the data obtained from the observed business entity and do not refer to the calculation of the company's entire inventory, but rather to specific products. The following problem was formulated taking into account the underlying assumptions of the Economic Order Quantity (EOQ) model.

Problem 1. Optimum order quantity

Insulation glass manufacturer from Croatia regularly supplies its customer, Spačva d.d., with material required for door manufacturing. The mentioned company delivers to Spačva d.d. 3,147 units of insulated glass annually. The demand for glass units is fixed and known in advance. The manufacturer delivers this material on time. In case the delivery were not be made on time, the costs would be extremely high, both for the consumer and the producer. The unit price amounts to HRK 183.45, while the total holding costs amount to HRK 0.50 per unit. Lead time is 12 days.

Solution:

Carrying cost (*Cc*) =	0,50 kn
Ordering cost (*Cd*) =	183,35 kn
Demand (*D*) =	3147
Annual days =	300
Daily demand rate (*d*)=	10,49
Daily production rate (*p*)=	180
C =	1565,52
TC =	737,14044
Maximum inventory =	1474,2809

According to the above calculation, the annual optimum order quantity is approximately 1565,52 units of insulated glass.

Problem 2. Determining the minimum level of inventory

In 2012, the average annual usage rate of oak logs recorded by Spačva d.d., a manufacturer of oak products, was 2,924.73 "m3", and the average monthly usage rate of oak logs was 243.72 "m3". The time required to obtain the raw material (lead time) is 6 days. Spačva d.d. is operational 300 working days a year. In 2012, Spačva d.d. as a manufacturing company did not record any substantial fluctuations in comparison to the previous year. However, when it comes to the relationship between manufacturer and supplier, the factor that further aggravates the problem is (un)reliability of delivery of the goods ordered, because of already mentioned financial difficulties experienced by the company.

The formula for the calculation of the minimum inventory is as follows (Ferišak; 1983, p. 197):
Zmin = Q dn x V nab or Zmin = Qgod. x V nab. / D

Qdn – average daily usage
Qgod. – average annual usage
Vnab – time of order placement
D – number of working days in a year
Zmin – minimum inventory

Solution:

Zmin = 2,924.73. x 6 / 300
Zmin = 17,548.38 / 300
Zmin = 58.49 m3

In conclusion, according to the data supplied by Spačva d.d. Financial Department, minimum inventory level of oak logs that does not compromise the production process is 58.49 “m3”.
At the beginning of the economic crisis, due to the decline of finished product prices and the steady price of raw materials, the company accumulated stocks for which there was no buyer. The main problem lies in the fact that due to heavy liabilities the company does not receive the basic raw materials to accommodate its production capacity and is therefore not able to create a larger inventory, which prevents it from ensuring the safety and minimum stock. As mentioned in the theoretical part of this paper concerning inventory management, the financial impact of inventory is reflected in specific indicators that are evident on the company’s balance sheet and profit and loss account. Stocks significantly affect the financial performance of the company through the net profit; asset turnover and the rate of return on assets of Spačva d.d.; financial leverage and the net value of Spačva d.d. As a result, the company recorded negative growth performance, i.e., loss in the previous year. [8]
This investment will justify itself by providing good planning and inventory control models. Stock management can also be performed by establishing a normal level of customer turnover rate, by making sure that orders are not cancelled, and by reducing the quantity of inventory which is not in demand. Moreover, the observed business entity should use inventory planning and control model based on market conditions, i.e., the MRP model which would undoubtedly facilitate the process of inventory management. The implementation of this technique is possible because the production plan is known in advance. However, the precondition for introduction of this model is the implementation of computer programs and the required technology. In this way, the waiting time for goods used for standardised products can be reduced and the production aligned with demand.

4. Conclusion

It is common practice for manufacturing companies to stockpile. The essence of stock philosophy comes down to making sure that stocks do not fall below the minimum level or reach excessive quantity in order to avoid a situation where it would no longer be in demand. There are models available to be implemented by business entities that can provide for an efficient inventory management. According to the inventory theory, the most important question is when stocks need to be replenished and how much stock is required. Based on the analysis of the observed business entity, it was concluded that the company needed to establish a more efficient inventory management policy because it often happened that it either had too much inventory or not enough to continue the production. Inventory management could be improved by using simple mathematical methods to determine the optimum order quantity for specific raw materials and the minimum inventory level for a product, as illustrated by a simple example. In addition to introducing essential structural changes to the management, in order to improve company’s stock management it is proposed to implement advanced information technology which will help find the right planning and inventory control models. The MRP technique would undoubtedly facilitate the entire inventory management process. The implementation of this technique is feasible for several reasons, one of which is that the production plan is known in advance. Therefore, the most important thing for a company is to determine the optimum level of inventory between the two extremes – there should neither be too little nor too much stock. If either of these extremes is present, stocks will continue to incur large costs and this will ultimately have a significant negative financial impact on the company’s performance.

10. References

[1] Ferišak V. et al (1983.) Poslovna logistika, Informator, Zagreb
[2] Segetlija Z. (2008.) Uvod u poslovnu logistiku, 2. izm. i dop. izd., Ekonomski fakultet u Osijeku, ISBN 978-953-253-045-2, Osijek
[3] Šamanović J. (2009.) Prodaja, distribucija, logistika: Teorija i praksa, Ekonomski fakultet u Splitu, ISBN 978-953-281-012-7, Split
[4] Pavlović I. (2005.) Kvantitativni modeli i metode u poslovnom odlučivanju, Sveučilište u Dubrovniku i Sveučilište u Mostaru, Dubrovnik, 2005
[5] Lambert M. D. & Stock, R. J. (1993.) Strategic Logistics Management, Third edition, Irwin Homewood, ISBN 0-256-13687-4, Illinois
[6] Segetlija Z. (2011.) Logistika u trgovini Predavanja (hand out). Ekonomski fakultet u Osijeku, Osijek,
[7] Barković D. (2001.) Operacijska istraživanja, Ekonomski fakultet u Osijeku, ISBN 953-6073-51-X, Osijek
[8]Financial report Spačva, Available: zse.hr/UserDocsImages/financ/SPVA-fin2012-3Q-NotREV-N-HR.pdf (Accessed: 27-Dec-2013)

FUNCTIONAL PROPERTIES OF THE SURFACES AFTER TURNING OF NANO - TITANIUM

D. Stancekova*, A. Czan, J. Holubjak, J. Semcer

University of Zilina, Faculty of Mechanical Engineering, Department of Machining and Manufacturing Technology, Univerzitna 1,Zilina, 010 01, Slovakia
** Corresponding author e-mail: dana.stancekova@fstroj.uniza.sk*

Abstract
Nanomaterials: technology, properties and modeling accepted as poster Abstract The short abstract: The article is focused on the generation of functional properties of the surfaces for applications of precision machining of nanostructure titanium biomaterials technology by Equal Channel Angular Pressing (ECAP). A new method of extrusion ECAP provides new opportunities for functional properties surface of implants. The experiments are focused on the monitoring of the main technological features that ensure the functional properties of the surfaces, such as surface roughness, morphology, voltage conditions (residual stress), and dimensional strength. The results of the experiments contribute significantly to the formation of the exigent parts of implants which are made in the development of increasing demands with regard to functional properties.

Keywords:
biomaterials, properties, titanium materials, dental implants, surface roughness

1. Titanium and its importance in biomedicine

Materials used as permanent implants must be biocompatible, corrosion resistant, and compatible with tissue, with good durability and stretch. Titanium materials meet these requirements successfully. They are used to make prostheses, bone fixation materials such as nails, screws, nuts, sheets, and plates, dental implants and components for surgical treatment of bite and dental prostheses, covers for heart pacemakers and artificial heart valves, surgical instruments for cardiac surgery and eye surgery, and fast parts in centrifuges (Figure 1). [1]

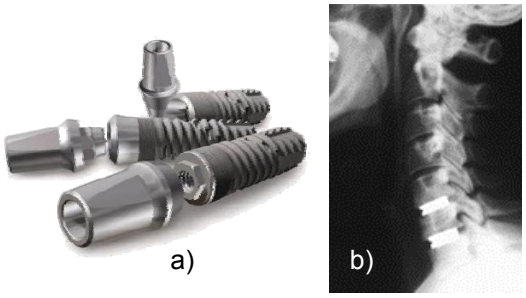

Figure 1. a) Titanium dental implant *[2], b) intervertebal titanium implant [3]*

2. Production of implants

According to the current and simple knowledge of nanostructured titanium we can conclude that this material has some useful features, and no material available in the medical field can compete with it. Gradually acquired orientations, in coopera-tion with foreign companies Timplant not reach the experience of the Czech Republic, which achieved over the past year clinical research nanostructured titanium Gr.2 and Gr.4. One of the reasons why little information about this material is available so far is that nTi is relatively novel, so it is not produced commercially and its price is very high, and there is probably still some time to go before titanium implant manufacturers acquire, develop, and manage implant manufacturing technology. [3]
Doctors who have used nano-implants are aware that they very quickly got world first in surgeries and thus may offer patients dental implant treatments, which are not yet available anywhere in the world. [3]

3. Proposal for a technological solution to the problem

The aim of this work is to determine the basic characteristics of the machining of new technology titanium materials used in the manufacture of implants by turning using removable cutting plates made of cemented carbide, which will be following machinability:

- in terms of dynamic machinability: the power conditions and size of the particles obtained by the cutting force in turning according to the cutting parameters and the cutting material used,
- in terms of the quality of the surface: the roughness of the machined surface due to the cutting parameters, the material, and replaceable cutting plates.

4. Turning titanium materials

Most of titanium materials are generally classified as hard-machining materials. The causes of the very poor machinability can be summarized as follows:

- high rigidity is maintained during machining, when there is a high temperature in the cutting zone, due to their refractoriness;
- the tool material is exposed to a highly abrasive effect due to the presence of very hard carbides in the workpiece;

- at high temperatures, a characteristic of machining of these materials is that chemical reactions occur when using conventional tool materials, leading to intense diffusion wear;
- machining of titanium alloys is often characterized by the creation of scab on the cutting edge, leading to the formation of a groove at the head of the instrument;
- poor thermal conductivity of titanium alloys results in the generation of high temperatures at the tip of the tool as well as a high temperature gradient in the tool;
- there is intensive friction in the contact chip and tool.

Given the above factors, titanium alloys cannot be machined under the cutting conditions that are commonly applied when machining steel [4]
The cutting speed is especially critical. The recommended cutting conditions for turning titanium alloys are listed in Table 4.2.1. The table shows that the fundamental difficulty in machining titanium alloys is associated with low cutting speeds and therefore a long cutting time. [4]
With regard to the accuracy of the geometric shape, dimensional accuracy, and surface quality of the workpiece, it is necessary to solve problems related to the machining of titanium materials and working conditions and to determine where the work will be done efficiently. [4]
Due to the high temperatures in the cutting zone and unfavourable distribution of the temperature field, cutting speeds are relatively low. Machining of titanium alloys is characterized by a high temperature zone located close to the cutting edge. Temperature is whether the cutting speed or the feed varies much more than is the case for steel.

Given these conditions in the cutting zone, the application of high speed steel tools for turning titanium alloys is limited. Their use is subject to the application of low cutting speeds that are unacceptable in terms of productivity. [4]

5. Machined titanium samples

When machining titanium samples according to the manufacturer's recommendations for cutting tools, used for hard turning dry environment, and thus prevent cracking.

The effects on the samples of cutting para-meters and material characteristics of each technology in the external longitudinal turning of commercially pure titanium, TiGr2, TiGr4 and TiGr5, were studied. The reference material chosen was titanium TiGr2. Titanium samples were machined with a diameter d = 5 mm and length L = 20 mm (Figures. 2a–d).

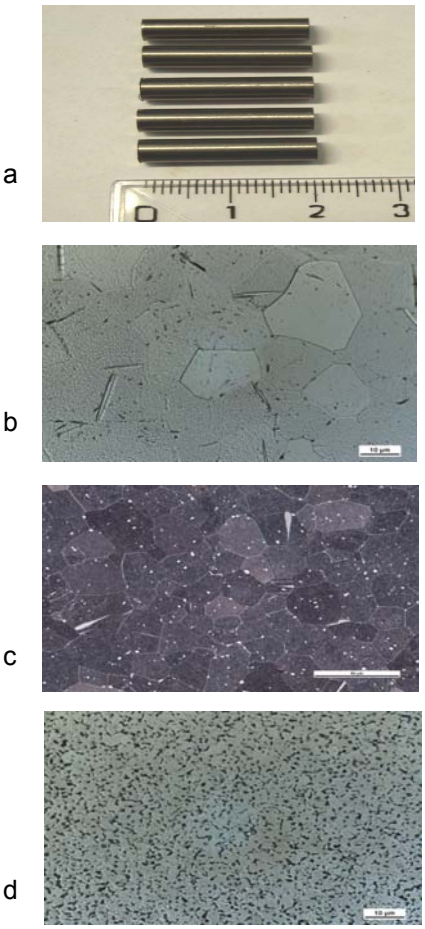

Figure 2 a - Appearance of sample, b - TiGr2,the microstructure of the material at 1000x magnification, etchant Kroll c - TiGr4, d - TiGr5

6. Measurement of cutting force components

Experimental tests were performed on the TiGr2, TiGr4, TiGr5 samples, and the effects of cutting parameters and material on the components of the cutting forces in outer longitudinal turning were observed. The results of the experimental measurements made using DASYLab (scheme shown in Figure 3).

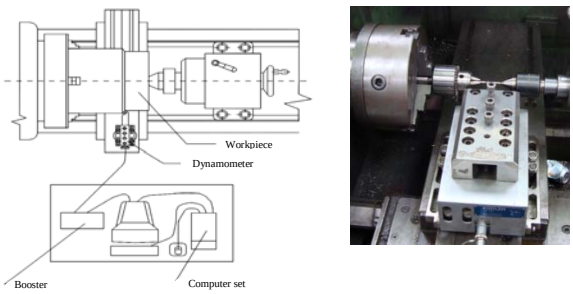

Figure 3. Scheme involving the measurement of cutting forces in turning

The structural equations are the basis for constructing three-dimensional graphs in two dimensions

6.1 Structural equations and three – dimensional graphs in printed view

As mentioned above, F_c denotes the main cutting force and is the component that most affects the process, is referred to as its evaluation.
Three-dimensional graphs in printed views for the tangential component of the cutting force F_c, constructed using structural equations (Figure 4).

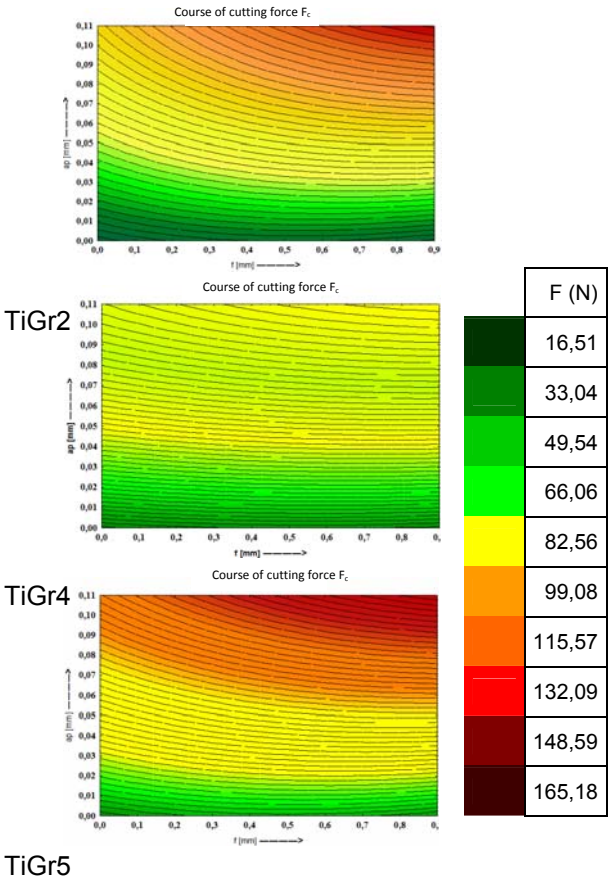

Figure 4. The resulting three - dimensional graphs in printed view for component cutting force F_c

6.2 Evaluation of cutting force measurements

Due to the demands on the machine, the smallest cutting forces are most suitable. For the evaluation of F_c, the reference sample material TiGr2 has a mean value of 41 N. The mean value of F_c was 53 N for the TiGr5 sample, 39 N for the TiGr4 sample.

7. Quality of machined surface

The status and quality of machined metal coating affect the fatigue strength, wear resistance, corrosion stability, quality of fit, and so on. The state and the quality of the surface layer are very important aspects, in particular for dynamically loaded parts.

7.1 Measurement of surface roughness

Surface roughness measurements of the samples of machined material were carried out on a Mitutoyo Surftest 301 (Figure 5.), which evaluated the characteristics of roughness Ra and Rz (Figure 6).

Figure 5. Digital Mitutoyo Surftest 301

Three-dimensional graphs of roughness Ra are shown in printed view in Figure 6.

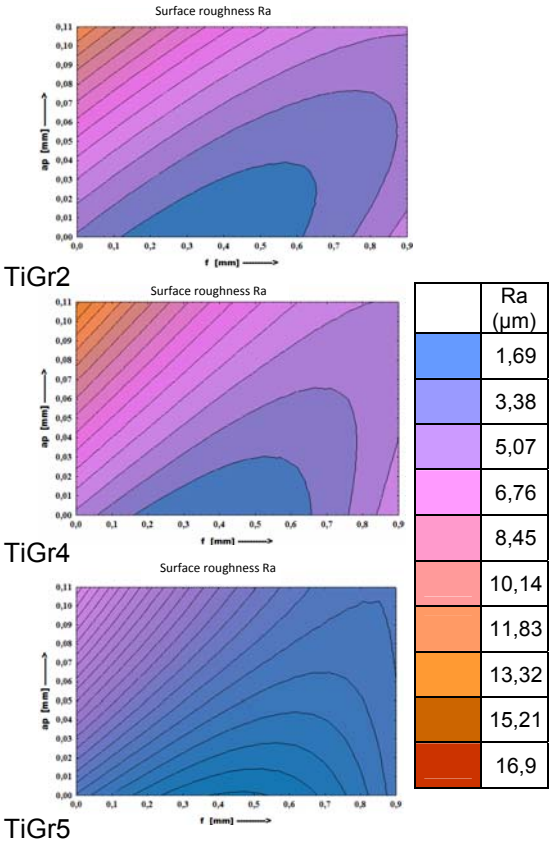

Figure 6. The resulting three - dimensional graphs in printed view for roughness Ra

7.2 Evaluation of surface roughness measurement

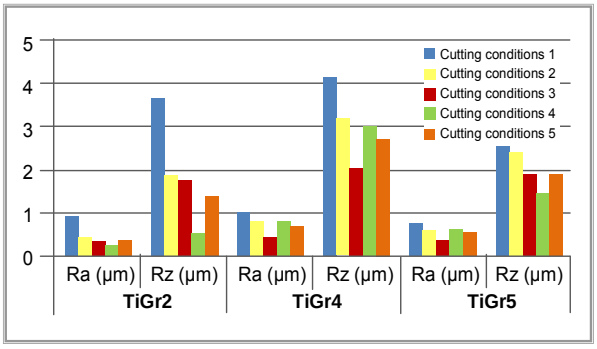

Figure 7. The resulting comparison of surface roughness of machined material

On the basis of the measured and recorded values of roughness, it can be concluded that the lowest

value of roughness Ra was obtained for the reference sample TiGr2 and the highest for the TiGr4 sample. From the comparison of surface roughness values it can be concluded that the most preferable surface roughness Ra is achieved using the cutting conditions a_p = 0,4 mm, f = 0,0035 mm, and n = 2200 min^{-1}.

8. Conclusion

In conclusion, we can be concluded that the dynamic machinability, surface quality, and shape of chip has a strong influence production of machined material as workpiece, microstructure, and chemical composition of the material.

The task of this work was to obtain information on the behavior of new materials introduced for the manufacture of dental implants by turning with an emphasis on their practical application. The resulting values of the components of cutting forces increased with increasing feed. Consequential values element cutting forces with by increasing the shift expand. Biggest effect on largeness element cutting forces has cutting depth a_p. From the measured values of the static components of the cutting forces, structural equations are constructed that are the basis for making three-dimensional graphs in two dimensions.

In tracking the quality of the surface, we found that the feed f has the greatest influence on the roughness. The roughness of implants should be between 0.8 and 1.4 microns. Compared to the reference material, TiGr4 material had the worst roughness. From the resulting comparison of surface roughness it can be concluded that the most preferable surface roughness Ra is achieved using cutting conditions of a_p = 0,4 mm, f = 0,0035 mm, and n = 2200 min^{-1}. The worst surface roughness was achieved with a depth of cut and a_p = 0,2 mm and feed rate f = 0,023 mm.

In the light of the tracking of dynamic machinability, we think that all new materials achieve poor machinability as reference materials. The worst machinability was achieved by TiGr5-0.73-made material, what is the meaning of, that has the 27% worse machinability as reference material. Closest to the reference material was the material TNT-65B/1, whose value of machinability was 0.93, so its machinability was about 7% worse than that of TiGr2 material.

On the basis of the measurement, evaluation, and knowledge it can be noted that the correct choice of cutting conditions may reduce static and dynamic load MTWP system, which can increase the efficiency, performance products and reduce production costs. Results and evaluation can be considered an appropriate basis for the research tasks at the Department of machining and manufacturing engineering as well as contribute to the solution of other works that are necessary for practical use in engineering production.

9. Acknowledgement

The article was funded by funds of grant project VEGA 1/0773/12 Implementation of technical ceramic material research to increase the innovation of hybrid products

This work is related to the project with the University of Zilina, 2009/2.2/04-SORO OPVaV number (26220220101). Name project is intelligent system for nondestructive evaluation technologies for functional properties of components of X-ray difractometry ". Main objective is to transform the new non-destructive technologies for knowledge transfer to industry practice in the evaluation of functional properties of the surface and subsurface layers of nondestructive techniques.

10. References

[1] http://deutschetitan.de/eng/profi/kbl/neu.html [Accessed: 15-Feb-2013].

[2] Information on http://www.smileclinic.sk/ zubne-implantaty/ [Accessed: 7-Jun-2013].

[3] Information on http://www.timplant.cz [Accessed: 24-Feb-2013].

[4] Vasilko, K.: *Obrábanie titánu a jeho zliatin*, účelová publikácia VŠDS Žilina, (2004).

[5] Czán, A. - Neslušan, M.: *Trieskové obrábanie ťažkoobrábateľných materiálov.* Rajecké Teplice: Andrej Czán, (2005). 156p.

[6] Kadnár, M.-Kadnár, J.-Hloch, S.- Valíček,, J. - Rusnák, J.: The designand verification of experimentalmachinefor realjournal-bearings testing. Technical Gazette 18, 95-98, (1/2011)

[7] Brychta J.-Sadílek, M.-Čep, R.-Petrů,J.: Progresivní metody v obrábění. Katedra obrábění a montáže, VŠB-TU Ostrava, (2012)

[8] Duplák, J. – Hatala, M. – Kratochvíl, J. – Sadílek, M.: *T-v_C dependence for sintered metal in standard ISO 3685.* Technologické inžinierstvo –Technological engineering, 6 – 9, 2/2010, (2011)

[9] Monka, P.; Monková, K. *Process plans design in relation to increasing of production efficiently*, Scientific Bulletin, 23, C, 239-244, (2009),

[10] Sajgalik, M. - Stancekova, D. - Jurky, M. - Kurnava P.: Application of thermovision systems and highspeed scanning for monitoring of dynamic processes in the cutting zone in turning of superalloys, volume 6 of Advanced manufacturing technologies (2012)

[11] Kouřil, K. –Čep, R.: The development of new axial tools with edges of various cutting materials on defined diameters for the machining of precision and high-precision openings.Technological engineering 1/2010, 43 – 44. (2010)

ADVANCED ENERGY SAVING HYDRAULIC SYSTEMS

M. Vašina[1*], L. Hružík[1] and A. Bureček[1]

[1]Faculty of Mechanical Engineering, VŠB - Technical University of Ostrava, Czech Republic
* *Corresponding author e-mail: martin.vasina@vsb.cz*

Abstract
The aim of the paper is to evaluate hydraulic systems in terms of energy savings. There are flow and pressure losses that have influence on total efficiency of hydraulic systems. The systems are compared from lower effective to energy saving. There are described advantages and disadvantages of the systems in this work. A part of the work is also focused on dynamic behaviour of energy saving Load-Sensing systems.

Keywords:
Hydraulic systems, efficiency, energy losses, dynamics, eigenfrequency.

1. Introduction

Hydraulic systems are applied in many spheres, e.g. as drives of excavators, cranes, hoists and loaders. These systems are mainly used to transmission of large forces at small sizes of equipment. Low wear, high service life, overload protection, a possibility to accumulate energy and automatic motion belong to some advantages of hydraulic systems. On the contrary, these systems have certain disadvantages, e.g. pressure and flow losses, leakages, liquid compressibility and dependence of liquid viscosity on pressure and temperature.
The purpose of the paper is firstly to compare hydraulic systems in terms of energy savings (i.e. from lower effective to energy saving systems). Dynamical properties of Load-Sensing system are investigated in the following part of the work.

2. Efficiency of hydraulic systems

The efficiency η [1] of hydraulic systems is defined by the ratio of the output power P_2 (i.e. the effective power of a consumer) and the input power P_1 (i.e. the power of hydraulic pump):

$$\eta = \frac{P_2}{P_1} \tag{1}$$

The power P is in general given by the product of the liquid flow Q and the pressure p:

$$P = Q \cdot p \tag{2}$$

There are different types of energy losses in hydraulic systems, e.g. pressure losses due to friction in lines, local pressure losses in throttle valves, flow losses in relief valves, energy losses in hydrostatic converters etc. There are taken into account only energy losses in throttle and relief valves in this work. Other energy losses are neglected in this case.

3. Energy saving hydraulic systems

Different connection methods of hydraulic systems and their energy balance are evaluated in this chapter.
The minimum efficiency is achieved in the case of the hydraulic system with the non-regulatory hydraulic pump HP (i.e. with the constant flow Q_1), the relief valve RV (i.e. with the constant pressure p_1) and the throttle valve TV which is used in order to adjust the flow Q_2 and thereby speed of movement of the hydraulic motor HM [1, 2]. The schematic diagram of this hydraulic system and its energy balance are shown in Fig. 1. There is dissipation of pressure energy in the relief valve and the throttle valve in this case. The loss flow Q_l on the relief valve is given by the difference of the input flow Q_1 and the output flow Q_2. For the above-mentioned reasons the efficiency of the hydraulic system is given by the equation:

$$\eta = \frac{Q_2 \cdot p_2}{Q_1 \cdot p_1} = \frac{Q_2 \cdot p_2}{Q_2 \cdot p_2 + (Q_1 - Q_2) \cdot p_1 + (p_1 - p_2) \cdot Q_2} \tag{3}$$

The maximum efficiency η_{max} = 0.38 is obtained at the pressure $p_2 = 2/3 \cdot p_1$. The flow Q_2 is changed as a result of a load change of the hydraulic motor. It is a further disadvantage of this system. This deficiency is solved by means of two-way throttle valve with pressure gradient stabilization [3].

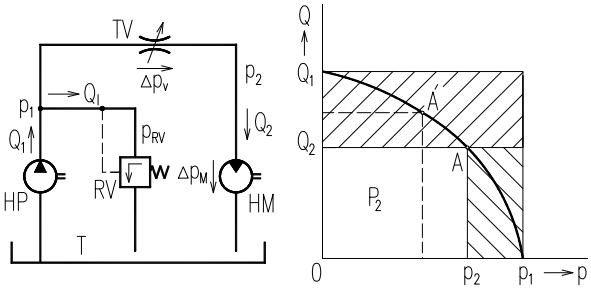

Figure 1. Schematic diagram and energy balance of hydraulic system with non-regulatory pump, relief valve and throttle valve

It is possible to obtain a higher efficiency by application of the three-way throttle valve and pressure gradient stabilization. In this case the throttle valve TV and the three-way pressure valve PV are arranged in parallel (see Fig. 2). The relief valve RV is only used to system protection against overload. The pressure gradient on the throttle valve Δp_v is constant and negligible, i.e. Δp_v = (0.5 ÷ 1.0) MPa. The efficiency of the system with the three-way throttle valve and pressure

gradient stabilization is in general achieved at higher loadings of the motor HM and is given by the formula:

$$\eta = \frac{Q_2 \cdot p_2}{Q_1 \cdot (p_2 + \Delta p_v)} \tag{4}$$

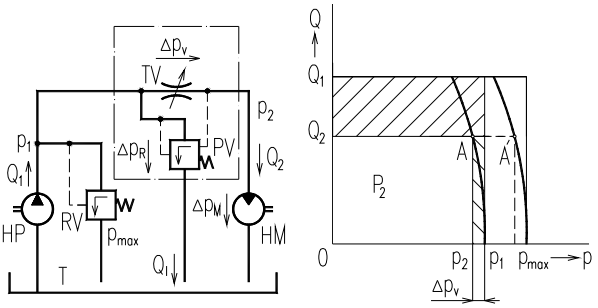

Figure 2. Schematic diagram and energy balance of hydraulic system with three-way throttle valve

The system with the hydraulic pump HP [2] with the pressure regulator PR and the throttle valve TV allows to achieve the efficiency η_{max} = 0.67. The schematic diagram and energy balance of this system are shown in Fig. 3. The transformation of pressure energy into thermal energy occurs in the throttle valve TV. The flows are equal (i.e. $Q_1 = Q_2$). For this reason the efficiency of the system is expressed by the equation:

$$\eta = \frac{Q_2 \cdot p_2}{Q_1 \cdot p_1} = \frac{p_2}{p_1} = \frac{p_2}{p_2 + \Delta p_v} \tag{5}$$

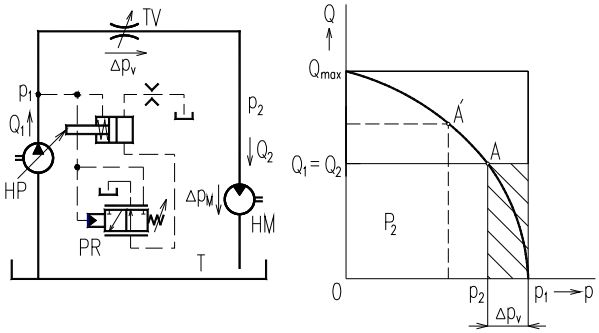

Figure 3. Schematic diagram and energy balance of hydraulic system with hydraulic pump with pressure control and throttle valve

Significant energy savings are obtained by means of Load-Sensing (LS) systems [4]. The example of LS system with the hydraulic pump HP and the flow regulator FR is shown in Fig. 4. The flows (i.e. $Q_1 = Q_2$) are adjusted by the control valve CV, most often by a proportional valve. For this reason the energy dissipation occurs only on the control valve with the pressure gradient Δp_v = (1 ÷ 2) MPa. The efficiency of this system is given as follows [1]:

$$\eta = \frac{Q_2 \cdot p_2}{Q_1 \cdot p_1} = \frac{p_2}{p_1} = \frac{p_2}{p_2 + \Delta p_v} = \frac{1}{1 + \frac{\Delta p_v}{p_2}} \tag{6}$$

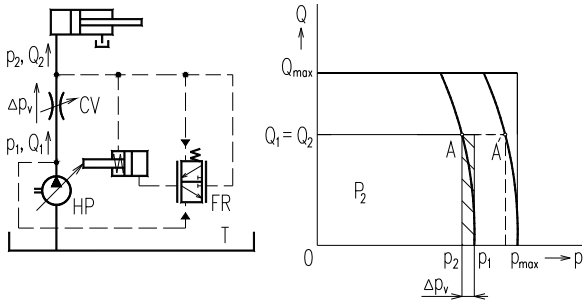

Figure 4. Schematic diagram and energy balance of Load-Sensing system

The maximum efficiency η_{max} = 1 is achieved at the system with the regulatory hydraulic pump and a programmable control system [2]. The flow of the system is controlled in terms of the angular displacement of the pump. Real and required values of the displacement are mutually compared by means of the control system. This hydraulic system is controlled without throttle elements. On the contrary, dynamic properties and limited application possibilities belong to disadvantages of the system.

4. Dynamical behaviour of LS system

Dynamics of hydraulic systems can be evaluated by means of experimental measurements, mathematical simulations or empirical formulas [3]. The eigenfrequency f_0 of hydraulic systems is a very important quantity in terms of dynamic assessment of the systems.

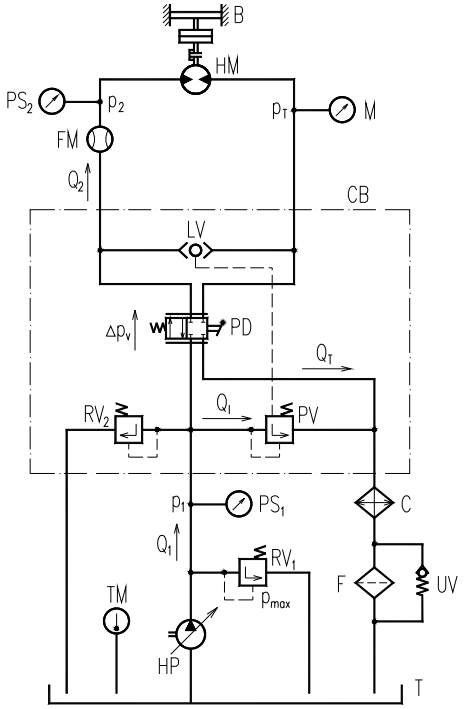

Figure 5. Schematic diagram of the investigated LS system

Dynamic properties were investigated on the energy saving open center Load-Sensing system, which is schematically shown in Fig. 5. The view of the system is shown in Fig. 6. The hydraulic pump HP is a pressure source of the system. The relief valve RV_1 is used in order to protect the LS system against overload. Hydraulic oil flows through the control block CB to the hydraulic motor HM and back to the tank T (see Fig. 5). The control block consists of the proportional distributor PD, the three-way pressure valve PV, the logical valve LV and the relief valve RV_2. The pressure loss on the distributor remains constant independent of load [5], i.e. Δp_v = (1 ÷ 2) MPa. The loading device of the motor consists of the brake B (from Škoda Felicia car). Oil flows in the output line through the cooler C, the filter F (or the unidirectional valve UV) to the tank T. The pressures p_1, p_2 and the flow Q_2 through the motor were evaluated by means of the measuring equipment M5000 Hydrotechnik. The pressure p_T was measured by the manometer M. The thermometer TM was used to oil temperature measurement. Dynamic properties of the LS system were solved for the oil bulk modulus $K = 7.34 \cdot 10^8$ Pa, the pressure p_2 = 8 MPa and the moment of inertia on the motor $J_M = 6 \cdot 10^{-2}$ kg·m^{-2}.

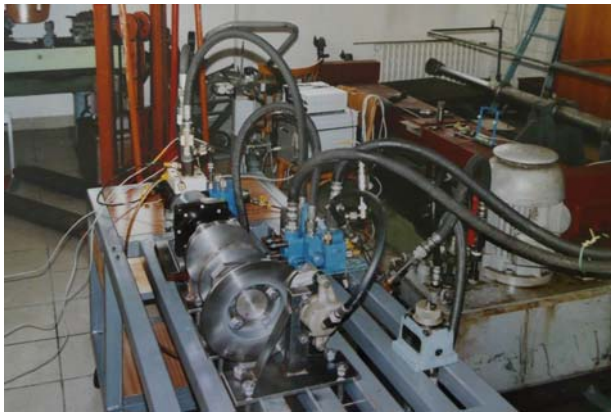

Figure 6. View of the investigated LS system

Experimental determination of dynamic properties of hydraulic systems can be realized by time-response characteristic (i.e. a unit step response), by response to a general input or by frequency characteristic (i.e. response to periodic input signal at various input signal frequencies).
The experimental measurement was performed by a step change of the motor load and for the oil flow $Q_2 = 3.33 \cdot 10^{-5}$ m^3·s^{-1}. For this reason, the pressures p_1 and p_2 were suddenly increased (see Fig. 7). It is evident, that the pressure loss on the distributor remains constant independent of load (i.e. $\Delta p_v = p_1 - p_2 \cong 1.4$ MPa). The eigenfrequency of the LS system under these operating conditions was obtained by means of Fast Fourier transformation [6, 7], which is applied for spectral analysis. The result of the analysis is the power spectral density G (i.e. a measurement of the energy at various frequencies). The frequency dependence of the power spectral density is shown in Fig. 8. The eigenfrequency f_0 of the investigated system is achieved at the maximum value of the power spectral density, in this case f_0 = 8.20 Hz (see Fig. 8).

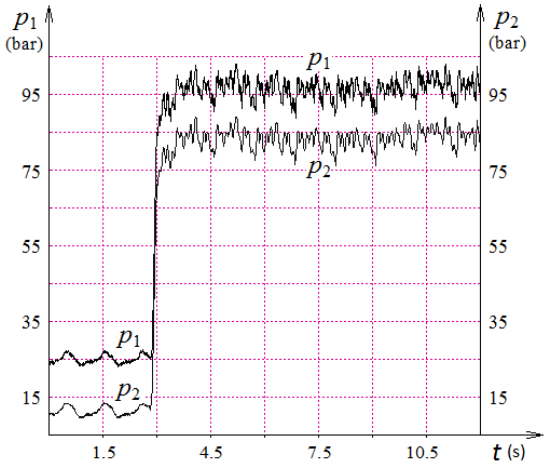

Figure 7. Time-response characteristics of pressures p_1 and p_2

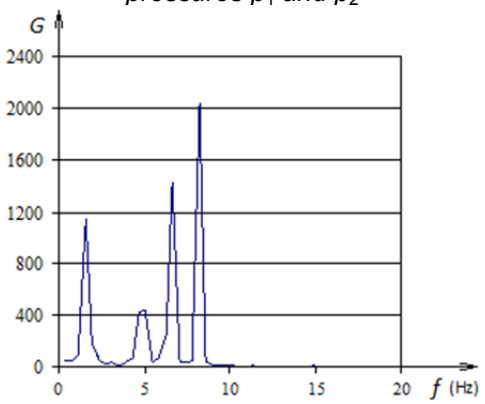

Figure 8. Frequency dependence of power spectral density

Dynamic behaviour of the system at the step change of the pressure p_2 and a constant slide valve opening of the proportional distributor is described by the following equations [3]:

$$m \cdot \frac{d^2x}{dt^2} + b \cdot \frac{dx}{dt} + k \cdot x = (p_2 - p_1) \cdot S \tag{7}$$

$$0 = -S_T \cdot x + Z_T \cdot p_1 + Z_v \cdot (p_1 - p_2) - S \cdot \frac{dx}{dt} \tag{8}$$

$$Q_2 = Z_v \cdot (p_1 - p_2) - S \cdot \frac{dx}{dt} \tag{9}$$

$$\frac{dQ_M}{dt} = \frac{p_2}{L_M} - \frac{\Delta p_{ML}}{L_M} - \frac{R_M}{L_M} \cdot Q_M \tag{10}$$

$$\frac{dp_2}{dt} = \frac{Q_2}{C_M} - \frac{Q_M}{C_M} - \frac{Z_M}{C_M} \cdot p_2 \tag{11}$$

Where: m – reduced slide valve weight (m = 0.21 kg), x – slide valve displacement, b – damping coefficient of slide valve (b = 100 N·s·m^{-1}), k – spring rate of slide valve (k = 15329 N·m^{-1}), S – slide valve area (S = 2.54·10^{-4} m^2), S_T – pressure valve sensitivity (S_T = 6.22 m^2·s^{-1}), Z_T – leakage permeability of pressure valve (Z_T = 6.4·10^{-10} N^{-1}·m^5·s^{-1}), Z_v – leakage permeability of distributor (Z_v = 1.2·10^{-11} N^{-1}·m^5·s^{-1}), Q_M – motor flow, Δp_{ML} – motor load, R_M – motor resistance to motion (R_M = 10^{10} N·m^{-5}·s), L_M – motor resistance to acceleration (L_M = 1.53·10^9 N·m^{-5}·s^2), C_M – motor capacity (C_M = 2.3·10^{-13} N^{-1}·m^5), Z_M – leakage permeability of motor (Z_M = 2.6·10^{-13} N^{-1}·m^5·s^{-1}).
The values of the above-mentioned quantities were experimentally obtained and are described in detail in [3]. The above-mentioned system of the equations Eq. 7 ÷ Eq. 11 was solved using Mathcad software by the Runge-Kutta 4th order method. Fig. 9 shows the time dependence of the input pressure change Δp_1 for the step change of motor load. The pressure p_2 was increased from 3 MPa to 8 MPa (i.e. Δp_{ML} = 5 MPa) in this case. It is visible that the pressure dependence is oscillating around the steady state value Δp_1 = 5 MPa with the time period $T \cong 0.124$ s. The eigenfrequency f_0 of the investigated LS system in the given working conditions is subsequently determined by reciprocal of the time period:

$$f_0 = \frac{1}{T} \cong 8.04 \text{ Hz} \tag{12}$$

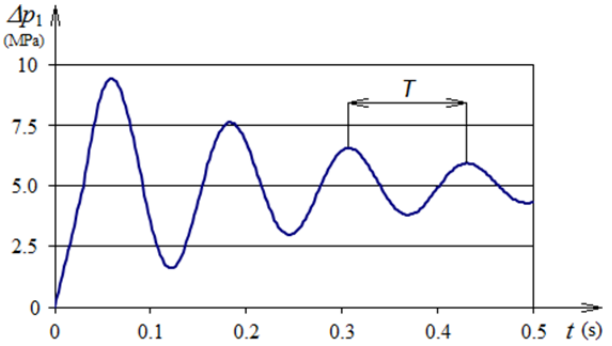

Figure 9. Time dependence of input pressure change

In the case of the investigated LS system, it is possible to determine the eigenfrequency f_0 by the empirical formula [3]:

$$f_0 = \frac{V_M}{4\pi^2} \cdot \sqrt{\frac{K}{J_M \cdot (0.5 \cdot V_M + V_1)}} \tag{13}$$

Where: V_M – geometric volume of motor (V_M = 39.36·10^{-6} m^3), V_1 – oil volume between motor and distributor (V_1 = 149·10^{-6} m^3). Substituting the quantity values to the Eq. 13, the eigenfrequency of the LS system f_0 = 8.49 Hz.

Table 1. Comparison of methods

Method	Measurement	Simulation	Formula
f_0 (Hz)	8.20	8.04	8.49

The eigenfrequencies obtained by three different methods are compared in Tab. 1. It is evident that their values are very similar.

5. Conclusion

The paper was focused on energy savings of hydraulic systems. Different systems were mutually compared in terms of their efficiency. Advantages and disadvantages of these systems were also summarized. A part of the paper was devoted to determination of the eigenfrequency of the open center Load-Sensing system by means of three different methods. A relatively large consensus was achieved between the experimental measurement and the mathematical simulation. For this reason mathematical simulations are more frequently applied to investigation of dynamic behaviour of hydraulic systems. Empirical formulas are used to an approximate determination of eigenfrequency values.

6. References

[1] E. Weishaupt, B. Völker, “Energiesparende elektrohydraulische Schaltungskonzepte,” *Ölhydraulik und Pneumatik*, no. 2, 1995.
[2] R. Püschel, “Leistungssteigerung durch Rexroth-Komponenten und –systeme am Beispiel Spritzgießmaschinen,” *Rexroth Information Quartelly*, no. 4, 1995.
[3] M. Vašina, “Energy saving hydraulic systems of lifting and loading equipment mounted on lorries,” *Doctoral thesis*, 2000.
[4] Z. Paszota, “Energy Saving in a Hydraulic Servomechanism System – Theory and Examples of Laboratory Verification,” *Brodogradnja*, no. 2, 2007.
[5] D. Lovrec, M. Kastrevc, S. Ulaga “Electro-hydraulic load sensing with a speed-controlled hydraulic supply system on forming-machines,” *The International Journal of Advanced Manufacturing Technology*, no. 41, 2009.
[6] V. Paar, N. Pavin, I. Basar, M. Rosandić, I. Luketin, S. D. Žinić “Spectral Densities and Frequencies in the Power Spectrum of Higher Order Repeat Alpha Satellite in Human DNA Molecule,” *Croatica Chemica Acta*, no. 1-2, 2004.
[7] M. Kušnerová, J. Foldyna, L. Sitek, J. Valíček, S. Hloch, M. Harničárová, M. Kadnár, “Innovative Approach to Advanced Modulated Waterjet Technology,” *Tehnički vjesnik – Technical Gazette*, no. 3, 2012.

INNOVATIVE PROJECT METHODS AND DEVICES IN TEACHING PROGRAMMING

Attila Pásztor[1*], Erika Torok[1] and Róbert Pap-Szigeti[1]

[1]Kecskemét College, Faculty of Mechanical Engineering and Automation, 10 Izsáki str., Kecskemét 6000, Hungary

** Corresponding author e-mail: pasztor.attila@gamf.kefo.hu*

Abstract

In our article we demonstrate the effects of using new pedagogical methods and innovative devices in teaching programming for beginners at Kecskemet College. Our experience shows that beginners face several problems in programming. In order to eliminate these negative effects new programmable robots are used such as Surveyor, RCX and NXT mobile robots in parallel with the traditional methods of teaching programming. We aborted the behaviorist teaching methods and added novel tools to our teaching practice and as a new constructive educational/teaching method using project methods has been introduced.

After a semester impacts were measured; how robots can be used in the changed learning environment; how the more effective teaching-learning process accompanied by new teaching strategies, learning management methods, forms of work and tools influenced the students' basic programming knowledge and skills; how their attitudes towards the subject and the programming self-image as a learning motive got modified.

Keywords:

project method, innovative devices, experiential learning

1. Introduction

Several factors influence the students' learning performance, the successfulness of learning and the adaptability of their acquired knowledge. Of course, the knowledge, the skills and abilities of students acquired earlier can have considerable effects on the obtainable knowledge. However, the individual differences of their preliminary knowledge are not sufficient to explain the individual differences of the knowledge acquired in the course of additional learning [1].

Learning theories respond to the current changes of the educational environment, and the basic mechanisms and processes of learning are described based on them. The different social, economic and technical backgrounds result in elaborating newer and newer theories, but in all cases, they are based on the psychological examination of individuals, groups and communities, so they have strong psychological definiteness.

The behaviorist learning concept was developed by Watson, Thordike, Pavlov and Skinner. The first computer-assisted teaching contents and methods were based on these concepts. The principal aim of behaviorists was the observation and description of behavioral processes [2], according to which the exterior, observable behavior is more important than understanding the inside, psychic processes.

Cognitive science endeavors to describe and explain the cognitive process and puts data processing in the centre. It tries to reveal the features of knowledge based on the analogy of computer systems. For example the LOGO programming language was developed by Papert. It is an educational program which can simulate problems and answers, too, to solve these problems.

Constructivist pedagogical approach took shape within the frameworks of cognitive psychology. According to the constructivist approach the student himself interprets the information affecting him based on his own experiences, develops and constructs his personal knowledge base and builds the mental representations of the world surrounding him for himself [3].

The behaviorist, cognitive and constructivist approaches in learning have led to the development of several methods for the learning environment supported by IT devices. One of them was the activity theory [4], according to which the full circle of the activities developed collectively creates the embedded knowledge essential for the solution of daily dilemmas. The essence of the project method, also called project pedagogy or project education, is to involve the student in the learning process intensively and to make him the central character of the learning process with the help of series of planned activities. Thus, the new knowledge of students emerges via experiences. With the help of this method, elaborated by Dewey and Kilpatrick, practical activities and experiences acquired through performing work gain considerable weight not only because of the result but rather because of performing experience-like activity carried out individually or in a group.

2. The problem statement

In the mandatory areas of Hungarian public education programming is not included in the curriculum. Many students entering higher education start to learn the elements of programming during their studies at the college. Most of our beginners are hard up in the learning of programming and they have multiple run-ups to successful exams. We can also observe a decrease in their interest for programming [5]. To empirically confirm our experiences a survey was carried out where the most important problems were:

- Professional programming languages offer a wide range of implementations, but as a consequence, they are complicated. The student's attention is focused rather on the programming languages than on solving the actual problem itself.
- Professional programming language environments do not really meet beginner programmers' needs, the features they offer do not provide support for new users, support is not provided in syntax error detection either, error messages and debuggers are not made for beginners but rather for professional programmers.
- In order to solve interesting problems students have to learn the language and the widespread use of large programs, which is impossible because of the short learning time.

Besides the problems of teaching-oriented programming, students also encounter other problems, e.g. difficult language structure, language syntax, machine control problems and using and controlling program development and debugging tools.

The results of this study have confirmed that new methods and tools should be applied to make the teaching of this subject more effective.

Researchers usually propose different approaches so that beginners could cope with programming difficulties and with the complexity of programming languages. Some of these proposals suggest teaching object-oriented paradigms instead of functional programming. Others suggest using the proper “programming language for beginners” with simple environment.

We wanted to introduce some tangible tools into teaching to boost our students’ motivation. We hoped that these tools would make the learning process more concrete, practical and effective. The programmable mobile robot, Mindstorms made by LEGO [6], seemed suitable to realize our aims. Programming the robots enables students to immediately develop skills at experiential level, thus preceding abstract thinking skills that are required during traditional programming.

It can facilitate the development of skills, and can deepen the level of understanding [7] [8]. At the same time the spectacular success in these learning situations can affect the development of students' motives, and the co-operation among students can strengthen students' social and communicative skills [9]. The enjoyable learning environment can create the feeling of the growth of knowledge, and can lead to flow. This state is called “flow” by *Csíkszentmihályi* [10]. The experience of flow may greatly increase the efficiency of learning, can create the level of activity needed for learning and can accelerate skill development [11].

3. Introduction of the new course, new pedagogical methods and new tools in teaching of programming

Because of the problems described in the introduction, a new subject has been introduced at KF GAMF Faculty, in which students get to know the basics of programming in a non-traditional way, with the help of LEGO RCX and NXT, and Surveyor programmable mobile robots [12].

In the case of the new subject *Programming model robots* we try to follow the teaching principles and the application of working methods and forms of constructive approach. Within the curriculum we spend just 20% of the lessons on traditional methods of knowledge transfer (teacher’s explanation, lecture). Later, the students usually work in groups of two or three and solve programming problems and tasks together. At this stage as a teacher, instead of the traditional teaching role, we support, encourage and coordinate the students’ work. We enhance the development of the task; provide access to useful resources, sample libraries and independent research necessary to be carried out for problem solving. The most prominent part of the students’ work is the project task performed in small groups. In the course of the project task the students are responsible for assembling a suitable robot to complete the task, write the algorithm and the program, compile their documentation, produce videos, images, and finally, present their tasks for the others and answer their questions. The evaluation of the project happens after the presentation prepared jointly. This time, in addition to the teacher's reflections, the peers’ evaluation and self-evaluation also play an important role.

4. Assumptions about the short-term effects

With the use of real devices we can activate and develop simultaneously the learning motives and enhance the acquisition of essential knowledge elements of programming [13] so the real tools make learning more enjoyable.

The knowledge and gaining a sense of joyful learning can establish flow, the state named by Csíkszentmihályi, which is a particularly strong motive. In addition, the graded, more and more

difficult exercises maintain proper challenges, they can activate the mastery motive which plays a fundamental role in the acquisition of skills and abilities, so the programming self-concept can be developed as a learning motive using programmable robots.
Experiences in robot programming, the sense of achievement in problem-solving can affect the students' beliefs about themselves, namely, tasks solved at the specific operational level have an impact on the development of abstract programming knowledge.
Learning programming at the abstract operational level often proves too difficult for beginner programmers. We assume that the concrete operational level of learning via physical tools can help with learning the abstract knowledge elements.

5. Conclusion

The course, therefore, means collaborative knowledge building [14] in which the knowledge-building strategies strengthen the understanding/interpretation process of creation. The individual's activities for personal understanding are associated with building social knowledge [15].
With the elaboration of the subject and with the help of the applied methodology we would have liked to move the listeners' attitude for programming and the programming self-concept as a learning motive into a positive direction, and this way, we wished to increase the efficiency of teaching.
The results show[16] that despite the short-period, the use of new tools and methods led to a significant advance in the students' self-concept. This is important in terms of further study because of the improved self-concept has a very strong effect on the further performance of the students [17][18].
Our analysis was primarily intended to clarify whether the course of mobile robots programming, the attitudes towards the topic and self-concept to mobile robots programming are long-lasting. We also wanted to explore whether the beneficial short-term changes can be transferred to other areas of programming.

6. Acknowledgement

This research was supported by the European Union and the State of Hungary, co-financed by the European Social Fund within the framework of TÁMOP 4.2.4. A/2-11-1-2012-0001 'National Excellence Program'.

7. References

[1] B.Csapó, "Az iskolai tudás felszíni rétegei: mit tükröznek az osztályzatok?", In: Csapó Benő (szerk.) Az iskolai tudás, Osiris Kiadó, Budapest. pp. 39-81. 1998.
[2] A.Ravenscroft,"Designing E-learning Interactions in the 21. Century: Revisiting and Rethinking the Role of Theory", European Journal of Education, 36. 2. pp.133-156, 2001.
[3] E. F. Strommen, and B.Lincoln, "Constructivism, Technology, and the Future of Classroom Learning", Education and Urban Society, 24. pp.466-476, 1992.
[4] J. Dewey, "Az iskola és társadalom", Lampel R. Kiadó, Budapest, 1912.
[5] R. Kiss and A. Pásztor, " Programozható robotok felhasználása a programozás oktatásban", Szakmai Nap, Kecskeméti Főiskola GAMF Kar, Kecskemét, 2006.
[6] Z. Istenes, "Learning Serious Knowledge while Playing with Robots", In: 6th International Conference on Applied Informatics, Eger, Hungary, 2004.
[7] J. Piaget, "Az értelem pszichológiája." Gondolat Kiadó, Budapest. 1993.
[8] J. Nagy "XXI. század és nevelés", Osiris Kiadó, Budapest, 2000.
[9] R. Pap-Szigeti, "Cooperative Strategies in Teaching of Web-Programming" Practice and Theory in Systems of Education, Vol 2. pp. 51-64, 2007.
[10] M.Csíkszentmihályi Mihály "Flow. Az áramlat. A tökéletes élmény pszichológiája", Akadémiai Kiadó, Budapest 2001.
[11] K.Józsa, Gy. Székely, "Kísérlet a kooperatív tanulás alkalmazására a matematika tanítása során", Magyar Pedagógia, 104. pp. 339-362, 2004.
[12] R. Pap-Szigeti, A. Pásztor, "A Lego programozható robotjaival segített programozás-oktatás beválás vizsgálata", Informatika a felsőoktatásban, Debrecen ISBN 978-963-473-129-0, pp.115, 2008.
[13] A. Pásztor, R. Pap-Szigeti, E. Török "Congruence Examination of NXT Robots in the Education of Programming at KF GAMF College", Practice and Theory in Systems of Education, Vol.3(3-4), pp.33-40, 2008.
[14] M. Scardamalia, C. Bereiter, "Knowledge Building", In Encyclopedia of Education. Macmillan Reference, New York, pp.1370-1373, 2003.
[15] G. Stahl, "Group Cognition: Computer Support for Collaborative Knowledge Building", MIT Press, Cambridge, 2006.
[16] A. Pásztor, R. Pap-Szigeti, E. Lakatos Török, "Effects of Using Model Robots in the Education of Programming", INFORMATICS IN EDUCATION An International Journal, 2010, Vol. 9, No. 1, ISSN1648-5831 pp. 133-140. 2010.

[17] A. Helmke, M. A. Aken, "The causal ordering of academic achievement and self-concept of ability during elementary school: A longitudinal study", Educational Psychology, 87, pp. 624-637, 1995.
[18] M. J. Niemivirta, "Academic achievement, self-concept and self-esteem: A longitudinal analysis of causal predominance", Paper presented at the 7th Eauropean Conference for Research on Learning and Instruction, Athens,Greece. 1997.

A NEW LOOK FOR DURABILITY BASED CUTTING TOOLS OF CEMENTED CARBIDE AND CERAMICS

Karol Vasilko [1*], Ján Duplák [2]

[1]Faculty of Manufacturing Technologies Technical University of Košice with seat in Prešov, Technical University of Košice, Slovakia
* karol.vasilko@tuke.sk

Abstract
Cutting property of tool materials is classically considered on the base of durability tests, the result of which is dependence of tool durability on cutting speed known as T-v_c dependence. It was first developed by Taylor in 1907 to evaluate the durability of high-speed steel [3]. This relation, which is interpolated by a line in double logarithmic coordinate system, has been used also for the observation of the durability of sintered carbides and cutting tools made of ceramics. As the experiments show, T-v_c dependence for such cutting materials is considerably different from the dependence for high-speed steel. However, they have not been examined thoroughly yet because they require complex experimental tests. In the strive to make the tests simpler, ISO 3685 standard was formed: Tool-life testing with single-point turning tools [5], which, however, prescribes to evaluate durability only in limited range of cutting speeds. The aim of this paper is a suggestion of the evaluation of tool durability by the dependence of the size of tool wear on cutting speed (VB = f(v_c) for constant machining time (τ_s). The dependence has the same predication value as T-v_c dependence and considerably shorter time is necessary for its formation [7].

Keywords:
Machining, cutting speed, tool durability

1. Introduction

The practice of material turning requires the knowledge of optimal cutting speed in concrete conditions of production of a part. This value should be derived from the maximum durability of actual tool. Exact determination of optimal cutting speed can be performed by a long-term test to obtain the dependence of durability on cutting speed. Such test is demanding on time and material. It requires to turn at constant cutting speed, cut depth and shift and to determine a range of diagrams of dependence of tool wear on time. Then a dependence of tool durability on cutting speed is derived from them to determine the criterion of tool blunting. Total T-v_c dependence is formed at the development of new cutting material or at the development of new cut material to determine its machinability. Cutting tools producers prefer shortened tests. The importance of knowing optimal durability from the viewpoint of maximum durability shows mainly in serial parts production where cutting conditions can be determined in long-term. In the conditions of small-lot production it is suitable to apply short-term operation tests (facing test, at cutting speed change by degrees, drilling test at constant force load ...). Suggested methodology presents a design for the realization of exact durability test on the base of the determination of dependence VB = f(v_c). If necessary, it is possible to form a dependence T = f(v_c) back from this dependence but in considerably shorter time. It is possible to state that the full long-term test for determining the dependence of durability gives the accurate results. However, it is very time consuming and consumption of worked material. On the other side current methodology to obtain T-v_c dependence, based on the application of this standard is fast, but very imprecise. Presented methodology, based on the obtained depending VB-v_c is an effective way to shorten time of the experiment, with the same accuracy of the results, which gives long-term test.

2. Test methodology

To draw a classical diagram of dependence of durability on cutting speed (T-v_c) requires a lot of time and material. It requires constructing a range of tool wear dependencies on machining time. After the determination of blunting criterion from it (VB_k) a diagram of dependencies T-v_c is constructed. To obtain reliable information about the course of tool durability it is necessary to perform an experiment in wide range of cutting speeds in comparison with recent practice. An example of such experimental diagram, constructed within the range of cutting speeds $5 \leq v_c \leq 1200$ m.min^{-1} is shown in Fig. 1. Considering great differences in durability values the diagram is constructed in double logarithmic coordinate system.

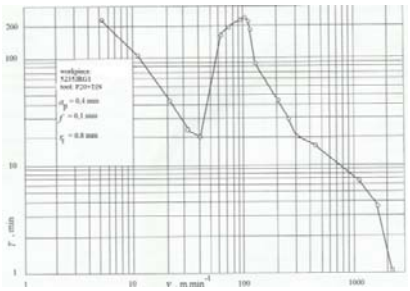

Figure 1. Experimental diagram of durability dependence for tools made of sintered carbide on cutting speed at VB_k = 0,3 mm [7]

Physical base of sintered carbide wear can be rationally explained on the base of such constructed diagram. At minimal cutting speeds (under 20 m.min^{-1}) cut material is in brittle state. The area of the contact of tool with segmented chip is short, there does not occur a wear groove on the face and wear on the back is small. The quality of machined surface worsens. Gradually, during the growth of cutting speed, the cutting temperature rises, cut material gets into plastic state, there occurs adhesion between machined and cutting material. Wear intensity grows it means that durability decreases sharply. In given case it reaches minimum at cutting speed 40 m.min^{-1}. At the same time the quality of machined surface improves. In Fig. 2 there is an experimental diagram of dependence of the highest height of unevenness of machined surface on cutting speed. This time it is with the use of ceramic cutting material. It can be seen that in the observed area the quality of machined surface is very good. It is interesting that the course of both diagrams is almost identical.

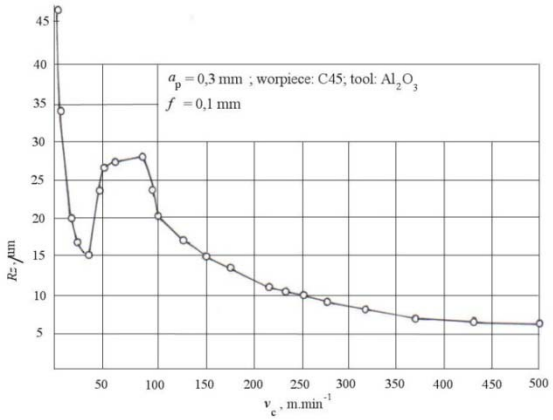

Figure 2. Experimental diagram R_z – v_c, obtained during turning with ceramic cutting tool [7]

During further growth of cutting speed we get into the area of built-up edge creation, it means intense adhesion between machined and cutting material. The built-up edge protects the tool from the direct contact with the chip, i.e. it protects it from wear. Machined material rigidity decreases further, therefore the tool durability of the tool grows considerably and reaches its maximum, in given case for cutting speeds about 100 m.min^{-1}. From Fig. 2 it can be seen that the quality of machined surface worsens at the same time. With further increase of cutting speed the tool durability decreases continually. Besides adhesion between the tool and machined materials there starts elements diffusion, which leads to fast tool wear. The largest drop of durability is recorded after crossing cutting speed 1000 m.min^{-1}. Vice versa, considering plastic state of machined material (cutting temperature reaches 1000°C) the quality of machined surface is very good. If average time for obtaining one point of the curve T-v_c is calculated at 60 min and continuous measurement of wear at every 5 minutes at one minute (totally 12 minutes for one point of the curve), a total time of test for 20 points is 864 minutes = 14,4 hours.

The essence of the test to obtain dependence VB-v_c is machining of reference workpiece at constant cutting speed at determined machining time (e.g. 15 min) and measuring the width of tool wear on rear area (VB) [3]. A range of values VB is obtained by the change of cutting speed and a diagram VB - v_c can be constructed. To construct complex diagram 20x15 = 300 min = 5 hours are necessary.

In Fig. 3 experimental diagram of dependencies VB-v_c obtained during machining of two kinds of steel with the tool of sintered carbide P20 is shown.

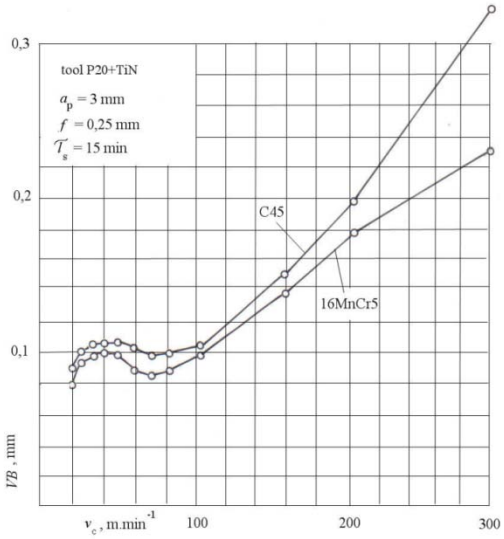

Figure 3. Experimental diagrams of dependencies VB - v_c [7]

The differences in values VB at selected cutting speed can serve for the comparison of the machinability of both materials.

3. Machining with tools made of sintered carbide

In Fig. 4 there are experimental diagrams VB-v_c obtained during machining with classical and coated sintered carbide P20. If it compared with Fig. 1 it can be said that it is in fact „inverse“ diagram of dependence T-v_c. Cutting speed, which corresponds with maximum and minimum wear intensity, i.e. tool durability, can be determined from it equally to Fig. 1.

(Values T_{max} and T_{min} are slightly shifted in comparison with Fig. 1 because different cut depth a_p has been used).

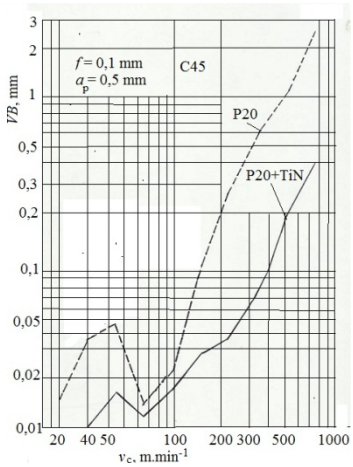

Figure 4. Experimental diagram of VB-v_c dependence obtained during machining with tools made of sintered carbide [6]

When comparing coated and not coated tools, coated tool shows quite considerable decrease of wear intensity. The areas of cutting speeds corresponding with tool durability maximum and minimum are identical. It can be concluded that diagram *VB*-v_c fully replaces diagram *T*-v_c.

4. Machining with tools made of oxidic ceramics

In Fig. 5 there are experimental diagrams of dependence *VB*-v_c obtained during machining with tool made of naked and coated ceramics Al_2O_3.

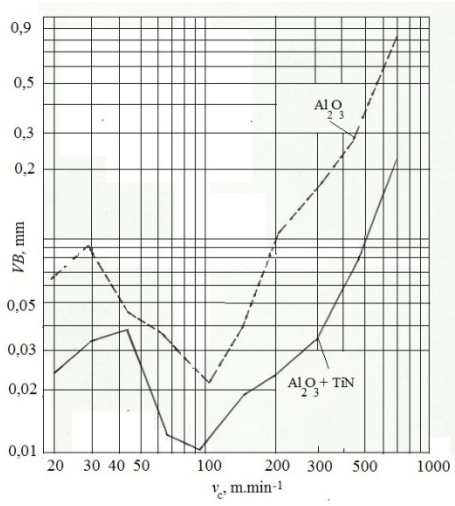

Figure 5. Experimental diagram of dependence *VB*-v_c obtained during machining with cutting ceramics [6]

Similarly to the case of sintered carbides, coated tools have considerably lower wear intensity. The area of the lowest wear intensity is identical, but cutting speeds, corresponding to the highest wear intensity, differ slightly. The diagrams clearly enable to determine optimal cutting speed which corresponds with the highest tool durability, similarly to diagram *T*-v_c.

5. Conclusion

The use of diagrams *VB*-v_c instead of *T*-v_c dependencies provides identical benefit for the practice of material machining. However, considerably shorter time and less machined material is required for their construction. In this phase the experiments concentrated only on referential machined material C45 and cutting materials P20 and Al_2O_3. Corresponding range of the same experiments in whole range of used cutting speeds is necessary to obtain similar diagrams for other kinds of material. Mentioned experimental results give a realistic assumption for a significant shorten of the time of the experiments, providing high accuracy of the dependece *VB*- v_c, respectively. *T*-v_c. Currently valid ISO 3685 should be reconsidered. Its application leads to an error in the selection of optimum cutting speed for specific machining conditions.

6. References

[1] D.A. STEPHENSON, J.S. AGAPIOU, “Metal Cutting Theory and Practice” London, New York: Taylor & Francis, 2005, 844 p. ISBN 0-8247-5888-9

[2] E.M. TRENT, P.K. WRIGHT, ”Metal Cutting” Oxford: Butterwoth –Heinemann, 2000, 446 p., ISBN 0-7506-7069-X

[3] F.W. TAYLOR, “On the art of cutting metals.“ Transaction of the ASME, 28 november 1906, pp. 31-279, 281-350

[4] I. MRKVICA, “Cutting ceramic by turning of nickel alloy Inconel”, Manufacturing Technology, 2012, Vol. 12, No 13, ISSN 1213-2489

[5] ISO 3685 Tool-life testing with single-point turning tools.

[6] J. DUPLAK, ”New analytical expression of *T*=f(v_c) dependence for different cutting materials”, PhD thesis, Prešov: FVT TU, 2013

[7] K. VASILKO, J. MÁDL, “The theory of machining“ Ústí n. Labem, 2012,, 526 s. ISSN 978-80-7814-460-8

[8] S.KALPAKJIAN, ”Manufacturing Engineering and Technology” New York: Addison – Wesley Publishing Company: 1989, 1199 p., ISBN 0-201-12849-7

[9] Z. PŘIKRYL, R. MUSÍLKOVÁ, “The theory of machining” Praha: SNTL, 198 s.

EVALUATION OF SURFACE ROUGHNESS AFTER MACHING OF COMPOSITE MATERIAL WITH WOOD REINFORCEMENT

Zuzana Hutyrová[1*], Marta Harničárová[2,3], Jan Valíček[2,4] and Matej Šomšák[1]

[1]Faculty of Manufacturing Technologies with a seat in Presov, Technical University of Kosice, Slovakia
[2]Institute of Physics, faculty of Mining and Geology, VŠB – Technical University of Ostrava, 17. Listopadu 15/2172, 708 33 Ostrava-Poruba, Czech Republic
[3]Nanotechnology Centre, VŠB – Technical University of Ostrava, 17. Listopadu 15/2172, 708 33 Ostrava-Poruba, Czech Republic
[4]RMTVC, Faculty of Metallurgy and Materials Engineering, VŠB – Technical University of Ostrava, 17. Listopadu 15/2172, 708 33 Ostrava-Poruba, Czech Republic
* zuzana.hutyrova@tuke.sk

Abstract
The major objective of this paper is to contribute to solve of problems of machining of composite materials (with reinforcement from natural fibers – wood flour and plastic matrix) and evaluation of parameters of surface. Turning was carried out with change of feed rate and cutting speed. Output of measured data (Rvk, Rk, Rp and Mr_1, Mr_2 – probability descriptors) is Abbott-Firestone curve and graphic projections of dependence of parameters Ra and Rz to cutting speed.

Keywords:
Wood plastic composite, machining, quality of surface roughness

1. Introduction

WPC (Wood Plastic Composite) present a new group of material emerging from a fusion of two different material – plastic matrix and natural fibers. These components are mixed under high temperature (T_{max}=200 °C) and pressed to different shapes. This material reflects the strong position at the market because of his: dimensional stability, production flexibility, minimum maintenance requirements and resistance to weathering or decay attack) [1], [2]. In spite of the technologies which directly ensure required shape it is, in many cases, needed to use the conventional ways of machining. The technical brochures of materials (from different manufacturers) indicate that wood based materials with plastic matrices can be easily machined and that they can be processed similarly as wood. The wood surface is generally specified by following parameters: statistical height descriptors (amplitude parameters: Ra, Rq, Rsk, extreme height descriptors: Ry, Rz), texture parameters (Sm), probability descriptors (Abbott-Firestone curve, Rpk, Rvk) and others analysis (autocorrelation, wavelets and fractals) [3], [4] .

2. Method and measured parameters

Tested material: composite material with wood reinforcement and plastic matrix (wood flour more than 70 % and HDPE with additives) which called Wood Plastic Composite – WPC. Samples were turning with tools with positive geometry and big tool nose radius 5 mm, tool cutting edge angle κ_r=45°, tool included angle ε_r=90°, side rake angle γ_f=0° (back rake angle and end clearance angle – tool A: γ_p=30°, α_p=10°; tool B: γ_p=20°, α_p=15°; tool C: γ_p=30°, α_p=15°). Conditions of the final turning process: feed rate f (from 0.1 to 0.61 mm) and spindle revolutions n (450; 900; 1400 min^{-1}), depth of cut ap=2.5 mm (constant). The machining was realized without cutting liquid (by using it, the unwanted enlargement of volume size of sample – so called swelling).

Table 1. Marking of samples of tool A, material for samples and angles tools

Marking of samples	f [mm]	n [min^{-1}]	v_c [$m.min^{-1}$]
A1	0.1	450	50.89
A5	0.61	450	50.89
A6	0.1	900	101.79
A10	0.61	900	101.79
A11	0.1	1400	158.34
A15	0.61	1400	158.34

Quantitative evaluation of average maximum height Rz (is the arithmetic mean value of the single roughness depths of the highest peaks and the lowest valley depth within a sampling length), roughness average Ra (is arithmetic average of the absolute values of roughness profile ordinates, Ra is the area between the roughness profile and its mean line, or the integral of absolute value of the roughness profile height over the evaluation length) and Abbott-Firestone curve (Fig. 1) gives a graphical representation of dependence of values of relative share of material on the position of the cut profile [5], [6]. The curve of share of material presents the share of material as a function of the cut level (according to DIN 4762). MITUTOYO series was used for measuring of roughness parameters, measuring length 7.5 mm (basic length 2.5 mm), profile R_ISO (filter type Gauss),

analyse software SURFPAK. The places with cracks were excluded due to the possibility of damage of the tip (probability descriptors were measured in three random places on the sample at the distance 40 mm from the head). The graphic projection for the particular tools was made from values of overall arithmetic averages (as average of averages in three random places).

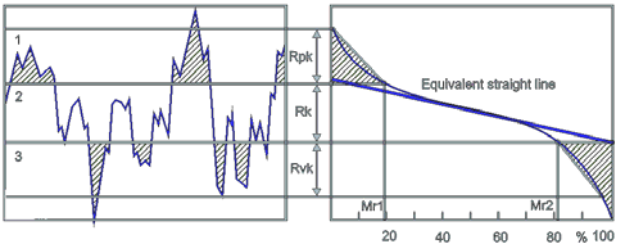

Figure 1. Graphical plotting of the supporting Abbott-Firestone curve (1 – apex area, 2 – core area, 3 – grooves area)

3. Results and discussion

At the feed rate f=0.1 mm (Fig. 2), the values of parameter Ra for tool marked as C, increase with increasing cutting speed. The values of Ra fall slightly at the average cutting speed (101.79 $m.min^{-1}$) and they then rise (for tools A and B). The courses at the dependence of the parameter of the highest height of the profile unevenness behave similarly (Rz – Fig. 3). At the feed rate 0.61 mm the values of parameter Ra (for the tools B and C – Fig. 4) decrease in the whole range of cutting speeds. For the tool marked as A the Ra values decreases at the cutting speed 101.79 $m.min^{-1}$ and it subsequently increases by more than 2.5 microns. A similar course can be seen for the parameter Rz – Fig.5 (but tool marked as C the values do not decrease in whole range of cutting speeds). At the maximum cutting speed value of the parameter Rz increases.

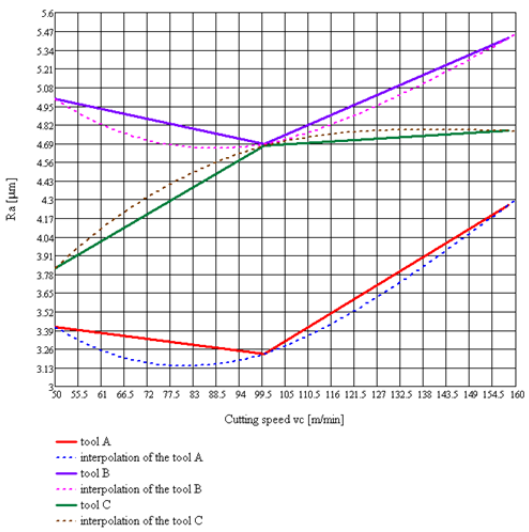

Figure 2. Graphical dependences of Ra on the cutting speed and feed rate of 0.1 mm

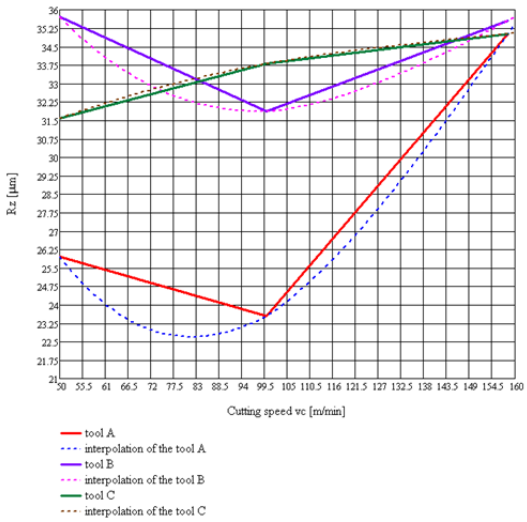

Figure 3. Graphical dependences of Rz on cutting speed and feed rate of 0.1 mm

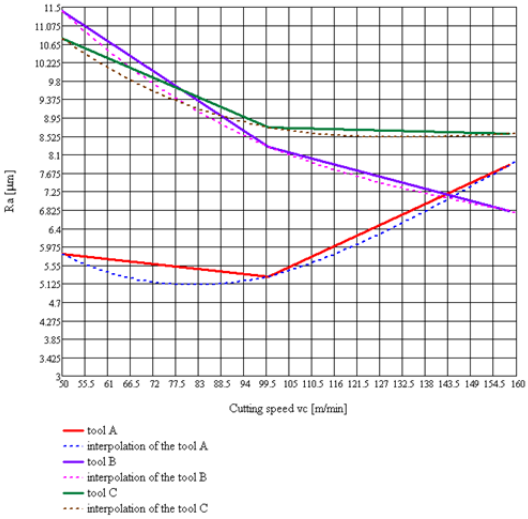

Figure 4. Graphical dependences of Ra on the cutting speed and feed rate of 0.61 mm

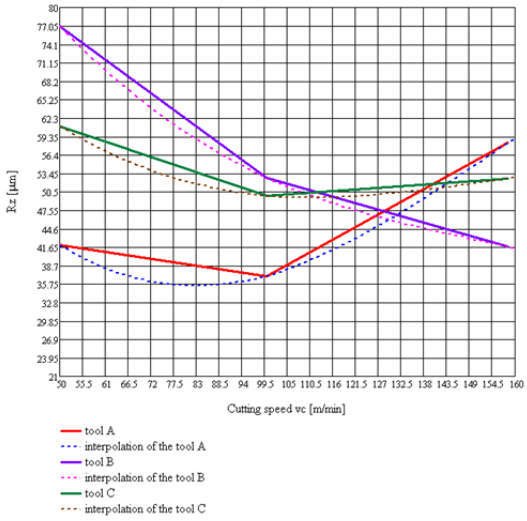

Figure 5. Graphical dependences of Rz on the cutting speed and feed rate of 0.61 mm

An apparent difference exists between the graphical representations of Abbott the curve for the minimal and for the maximal feed rate (Fig.6 and Fig. 7). In the case of minimal feed rate of 0.1 mm the bigger amount of material share is in the grooves (as evidence also by the record profile meter – Fig. 8 and Fig. 9).

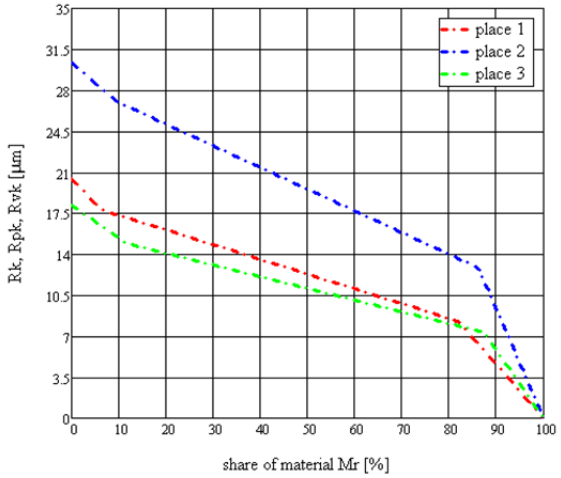

Figure 6. Abbott curve at three Places on the surface on the sample machined at the minimal cutting speed and feed rate of 0.1 mm

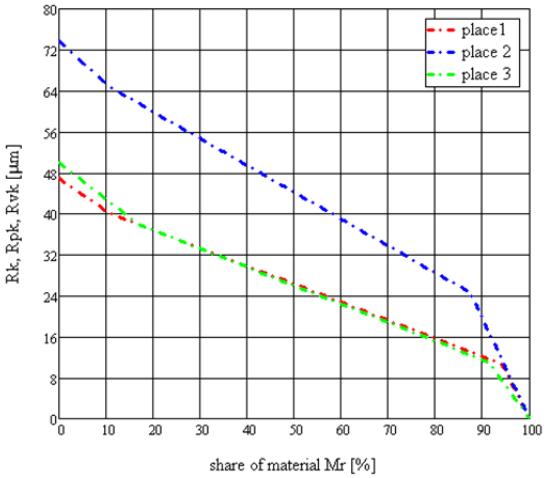

Figure 7. Abbott curve at three Places on the surface on the sample machined at the minimal cutting speed and feed rate of 0.61 mm

For example the sample C1 (Table 3 and Table 4), Place I – 17.991 % of material is in the grooves – bottom position of profile trace (calculated as the difference $100\% - Mr_2$), the sample C6, Place I – 14.748 % of material is in the grooves, etc. From the perspective of differences between individual Places we can see significant difference in the sample C11 between the Places I (area of grooves 17.741 %) and Place III (area of grooves – 7.895 %). At the feed of 0.61 mm the material share is more significant in the areas of peaks with the exception of the Place II on the sample C5, where the area of the peak height contains 11.242 % of material and the area of depth of grooves contains less than 13 % of material share ($100\% - 87.349\%$).

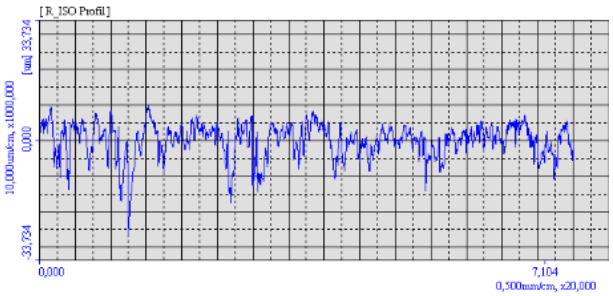

Figure 8. Record from the profile meter (sample C1 – f=0.1 m, v_c=50.89 m.min^{-1})

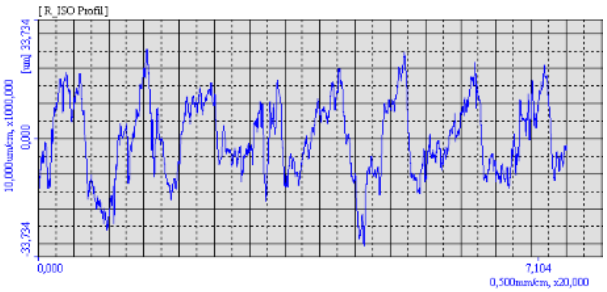

Figure 9. Record from the profile meter (sample C1 – f=0.61 m, v_c=50.89 m.min^{-1})

Table 3. Percentage of share of material within the core

C_x	Place I (Mr_1, Mr_2)	Place II (Mr_1, Mr_2)	Place II (Mr_1, Mr_2)
C1	6.487 % 82.009 %	9.688 % 86.244 %	11.589 % 87.512 %
C5	10.545 % 93.973 %	11.242 % 87.349 %	17.214 % 91.214 %
C6	7.78 % 85.252 %	10.32 % 81.868 %	13.192 % 90.148 %
C10	14.372 % 95,522 %	11.154 % 93.257 %	16.577 % 92.209 %
C11	9.357 % 82.259 %	12.174 % 85.147 %	7.066 % 92.105 %
C15	17.935 % 91.688 %	13.013 % 92.445 %	16.683 % 91.091 %

Table 4. Difference between Mr_1 and Mr_2

C_x	Difference in Place I (Mr_1, Mr_2)	Difference in Place II (Mr_1, Mr_2)	Difference in Place II (Mr_1, Mr_2)
C1	75.525 %	76.556 %	75.923 %
C5	83.428 %	76.107 %	74.0 %
C6	77.472 %	71.548 %	76.956 %
C10	81.15 %	82.103 %	75.632 %
C11	72.902 %	72.973 %	85.039 %
C15	73.753 %	79.432 %	74.408 %

4. Conclusion

When wooden particles are insufficiently encapsulated by plastic the formation of pores and cracks occurs, which made it necessary to divide the samples to zones and to avoid at measurement deliberately the zones with large cracks. It is clear that quality of surface roughness is dependant to feed rate (values of Ra, Rz increase with increased feed rate). The evaluation of the material share Place out difference of material share in the area of peaks and area of grooves (for the feed rate 0.1 mm and 0.61 mm). Shapes of the Abbott curve are different in individual places what is proof that the material is incompatible. The surface quality after the turning of material with wooden reinforcement is influenced by the ability of the matrix to encapsulate the wooden particle.

5. Acknowledgement

The authors are grateful for the financial support provided by the Regional material-technology research center (RMTVC), project No.CZ.1.05/1.1.00/02.0070 supported by the operational Programme "Research and Development for Innovations" funded by Structural Funds of the European Union and from the state budget of Czech republic and by the project Integrita No.Cz.1.07/2.3.00/20.0037.

6. References

[1] A. K. Bledyki, J. Gassan, D. "Composites reinforced with cellulose based fibres," *Progress in Polymer science*, no. 2, 1999.
[2] K. L. Pickering, G. W. Beckermann, S. N. Alam, N. J. Foreman "Optimising industrial hemp fibre for composites," *Compossites Part A: Applied Science and Manufacturing*, no. 2, 2007.
[3] U. Buehlmann, R. Lemaster, D. Saloni, "Wood Fiber-Plastic Composites: Machining and Surface Quality," *Proceedings of the 15th International Wood Machining Seminar*, 2011.
[4] J. Sandak, M. Negri,"Wood surface roughness – what is it," *Proceedings of the COST E35 - Workshop*, 2005.
[5] Z. Šomšáková, J. Zajac, P. Michalik, M. Kasina "Machining of wood plastic composite (pilot experiement)," *Materiale Plastice*, no. 1, 2012.
[6] J. Schmähling, F. Hamprecht, "Generalizing the Abbott-Firestone curve by two new surface," *Wear*, no. 11-12, 2007.

RETHINKING YOUTH ON SOME ISSUES IN RURAL AREAS OF THE COMMUNITY NIJEMCI, VUKOVARSKO-SRIJEMSKA COUNTY

Mirko Jokić[1*], Tomislav Kovačević[1] and Matija Japundžić[2]

[1]Student Management postgraduate University study, Faculty of Economics in Osijek
[2] College of Slavonski Brod, Slavonski Brod, Croatia
* *Corresponding author e-mail: zu.sv.lovre@vu.t-com.hr*

Abstract
Modern living conditions especially in urban areas require adjustment program primarily in the choice of appropriate content.
The concentration of population in cities is not a demographic point of view vantage equal development and imposes most of Croatian citizens with poor ecological conditions, but also Kinesiology view. Today it is mostly concerned with young people for a period of 20-30 years, who are leaving en masse from rural to urban centers. Without young people there is no progress and no future. It is therefore understandable that we talk and discuss on young people. But really, where are they today? What is their place in the village? Where to entertain after Sunday Mass or lunch? What to expect in the future? These questions are in fact some are angry. Provide answers to them is impossible. However, this does not mean that we can at least think about these issues and give some of our views. Maybe they did not have occurred in the history of so many changes as far as the life of young people in the last ten years. Young people never been exposed to various vices and challenges as today.

Keywords:
young, rural area, village, research, activity, problems

1. Introduction

There is a general belief amoung the scientists that rural area development is lagging behind urban enviroment in urban areas. There are many reasons for that. On the global plan there are known economic theories of the polarized development (Perroux, Mydral), that explains the creation and maintenance of the regional and national differences in development. Althoug inequialities are well known even in the pre-industrial period, industrialization and tertiarization of the economics are the main causes which are leading to bigger differences between regions developement [1]. We are familiar with the current situation of population in rural areas. Special focus was placed on population between 20 and 30 years of age. Since the start of recession few years back, young people are having difficulties with progress, finding a job and starting their own families. Generations of the young people are faceing with highest levels of unemployment, despite very high levels of qualifications and education. Nevertheless, education levels and early dropping the school are still the biggest problems (UN, 2011). Focusing on the formal qualifications as replacement for learning and development is not fair to the extent, depth and variety of different forms of learning that cotribute to the professional development and the acquisition of skills and competencies of career management. It should be more encouraged and focus should be placed on finding the most appropriate time for accepting different forms of learning and using qualifications in this process. With this short research we wanted to more closly examine the problems that occur in young people in rural areas and the reasons why the same abandon, and propose some solutions.

2. Method

The poll is created just for this research. It consists of 25 questions of different topics: social status of the family, education, free time, life in the countryside and employment, life in the city, violence, health problems, smoking, alcoholism, drugs, future of the young people and attitude on The Republic of Croatia.
Survey questions:

- Social status of the family, monthly income and number of unemployed
- Do you attend school/college, do you work?
- Free time you spend (with friends, taking care of somebody, helping your parents, at coffee bar, playing sports…)
- You live in the village/town, where is better life, do you want to live in the village/town in the future
- Where do young people have fun, what teenagers do for fun, What kind of entertainment do you like
- Violence in your village, and what kinds of violence are represented, how do others relate toward violence
- Health problems, reasons for that
- Do you play sports
- Do you smoke, drink alcohol, how often and in what quantities do you consider that normal, what do you think about drugs, is it present in your place
- How do you see your future

- Attitude on The Republic of Croatia.
- Would you like to leave RC and if so, what would be a reason?

Survey was carried in November 2012, on 60 respodents, those people are citizens of the Vukovarsko-srijemske County, Nijemci County, and their age is between 20 and 30 years. The survey lasted a month. Interviewees self-filled questionnaires at home.

3. Social status of the families

Young examinees are from rural area. 8 for them are living in the city – they were born and grown up there, and 52 of examinees are living in the village. More than 83.33% of the examinees are living with their parents, and 53.33% of the participants are living in the city as tenants, but their parents are helping them. The average monthly income of the families is 3000 – 4000 Kunas. In 80% of the examinees only one member is employed.

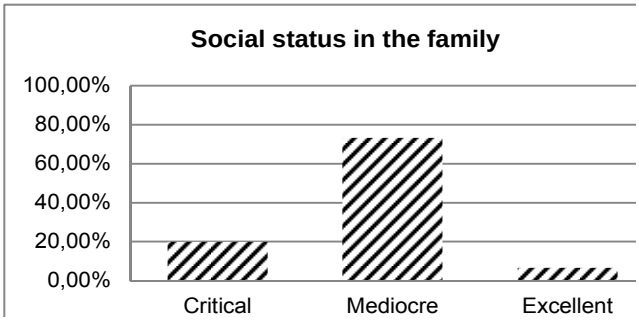

Figure 1. Social status in the families of the respondents

4. Free time respondents

Free time is a social phenomenon that requiers a thorough approach to all aspects of life. That is the time in which we recognize human as *homo univerzalis, homo ludens and homo faber* (Shaft, 1989). Because of that, a free time is an object of interest of the majority of Anthropological Sciences. In the past it was a reason for conflict between social classes as one of the human rights. Nowdays, especially in the future as futurists predict, it becomes segment of time which becomes wider and wider every day. So it simultaneously favors and threatens, as to individuals, so to whole societies [2]. Ninety percent of young people spend their free time socializing with friends, family, loved ones, while the smallest proportion of young people, only 10% of them, spends their free time on farming, as they are in rural areas, young people still avoid and neglect the natural resources of such areas. Here is one example: “I usually spend my free time drinking with my friends, playing poker or watching my 10 favourite sitcoms, or I sleep”. This is a bad example of spending free time, and one opposite to that said: “My free time is spent in going out, reading, learning computer skills or helping my parents in houseworks…” In this example we can see better utilization of time. This interviewee knows that free time should be used wisely and useful, young people should go out and have fun with friends in their free time, sometimes read something, spend some time on computer because technology is rapidly progressing, and young people should keep up with technology. One respondent, who voluntarily joined this research said that he doesn’t know how to use Microsoft Word. The research showed that the leisure of children and young people is not identical in duration, content or aspirations as compared to other social groups, because of it’s role in development of young individual who doesn’t own enough physical, psychic, intelectual or material strength to independently and sovereignly overpower in those fields of their own existence. [2].

5. Violence and experience with violence

None of the participants did not experienced any coarser form of violence, 43.33% had experienced domestic violence, but in a milder form during adolescence, in example, slapping children from their parents or beaten if they misbehaved, but now they are mostly just mutual verbal fights caused by dissagreement of one or more family members. Also, 25% of them don’t know if there is any violence present in their village, and those respondents who are familiar with the violence in their area, describe it as violence between the mostly male population in form of physical encounters, usually in bars or various social events, such as: “Fights caused by alcohol” and “Alcoholised minors fights”.

6. Young peoples health

The research is conducted on same proportion of males and females, 30 of them were girls, and 30 were boys. Interestingly, almost an equal number of boys and girls consumed narcotic substances, cigarettes and alcohol, cigarettes every day, and alcohol once or twice a week. Reasons and incentives for young people to start smoking are not simple. One of the most important factors for the initiation of smoking is that smoking is seen as a reflection of the maturity and independence. This illusion that adolescents attribute to adults who smoke, tobacco industry has carefully built and supported. There is no doubt that adults who smoke, as family members, famous actors, musicians, athletes and others that children, especially teenagers idolize and emulate, have a great impact on them [3]. The reasons why young people consume some of the psychoactive substances are: social peer pressure (27.7%) and curiosity (24.2%) (Croatian Institute of Public Health, 2007). The necessary multi-dimensional approach to the problem focus should be put on some of inappropriate family relations (poor

relationships with parents, lack of emotional warmth, conflict, poor relationships with family, etc.). A large number of children in 2007 (444) reach for hard drugs in attempt to "solve" or "forget" their everyday family life. Data refers to cases of children in the treatment system, so the dark numbers are certainly much higher. The fact that large number of juveniles who consume different types of alcohol daily, should be taken in account. [4]. Figure 2 shows the percentage of consumption of these substances.

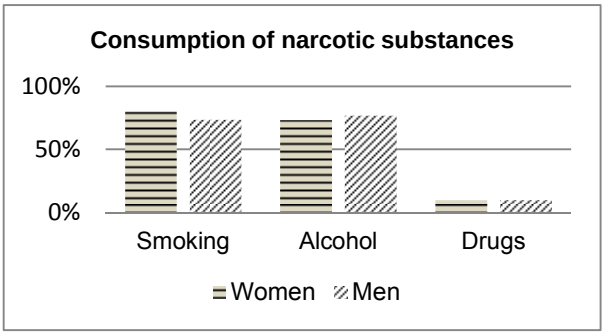

Figure 2. Consumption of narcotic substances by respondents (%)

The results shown in Figure 2, cause a lot of concern for the health of young people in rural areas. But there are even other health problems like mental health problems, obesity, various problems such as: problems with joints, the tonsils, allergies, migraines. One big problem which is related to the girls is the pregnancy. 10% of young girls in age of 18-20 years get pregnant, most of which are unplanned pregnancies. Also, the worrying fact is that even today, when various types of protection is available, very small number of young people are familiar with that or they are simply ignorant. Such a negative attitude of young people towards their health is actually the most important case in this study, because they began to destroy themselves and turned to bad habits because of the poor economic situation.

7. Life in village and employment

Quality of life of the local community is determined by level of development of the social, cultural and economic activities that provide opportunities for local people to satisfy their needs [5]. Numerous previous studies have shown that some of the reasons for leaving the village are poor infrastructure and inadequate traffic in villages, lack of public and other kinds of services, etc. [6] [7]. A very large percentage (83.33%) of respondents think that life in the countryside mediocre, and that life in the countryside doesn't provide a lot of options. They also listed the advantages and disadvantages of village and town, such as: "the village - it was impossible to find a job, it is still possible to produce enough food in village to be self-sufficient (although that has become very difficult)". The citiy – "in the city, mostly foreign capital and some of our "domestic", which is based on the consumption and sale, gives a better chance to find at least some kind of job". "Education, jobs, opportunities like various courses like dance or gym, gas stations that work 24/7. Those are very usefull things…and for the village I have no idea if you ask me about advantages", "The village is a smaller community, better people…", "In the city! Bigger chances for finding a job. In the village I have nothing to do!", "In the city… everything is at your fingertips, there are a lot more options for raising children, youth development, cultural, social and uplift in sport", "City, I love urban centers and the crowd in a weird way ... but I would like to have a weekend house in a quiet place…benefits of the city are: variety of activities, rich content of cultural events, a lot more content for children, schools, colleges, courses, sport clubs... and the village is better for farming and because of clean air, people who have the will and knowledge to cultivate various cereals, animals etc… should live in village, because it offers those advantages". Furthermore 51.66% of them still do not know what they actually want. They consider that the best way is to live in a village near the city, so that, as we stated in the survey: they can quietly live in the village, but also get everything they need for good life from town, such as playing sports, attend various courses, attend various social activities (Folk art Society, dance schools, music schools), work, college… Currently 88.33% of young respodnents are unemployed, while 48.33% have attended college, and 18.33% of currently employed are unsatisfied with their job. As the current economic situation in Croatia is questionable, getting job for young people without professional expirience is very difficult. Also, respondents have declared on this issue that there is a lot of corruption. They feel that they need to know certain people to help them to get easily employed, otherwise they think it makes no sense to look for a job. This is an example how the young people lose all hope and interest in finding any kind of work.

8. Education of the young people and vision of the future

96.66% of respondents has finished high school which means that only 3.33% did not attend secondary school, 48.33% is currently in further education (college, various courses), and only 8.33% of them have completed a university degree. So in this area, they are not bad, but certain consideration in relation to continue education after high school should be taken. Most of them have a too high expectations on vision of the future. In the near future, 90% of the respondents want to have a good job, excellent financial condition and high positions in society, also 80% want to have a family and to have a good health. Here are some examples that support this

statement: “I see myself as a master of construction, employed in a design office, I have a job and do what I like. I live with my current boyfriend in a house in the city or near the city and have a family ... we live happy and healthy life”, “I enjoy as an emperor, finished college, maybe get a job if I have to, women, children, mistress”.

9. Atittudes toward The Republic of Croatia

Different attitudes had been given regarding the regulation within the state, the economic situation, the opinion on the government, generally natural wealth and beauty of the Croatia. 8.33% of respondents are delighted with beauty and benefits of our state, but it is not all in beauty. It is very interesting that 80% of those who are satisfied with the economic situation have very harsh opinion towards goverment. Respondents believe that the top of Croatian society is corrupted and unfair, and that the wrong people are trying to lead the country. When we talk about division in politics a lilttle less than half of the respondents (43.44%) thinks that division on the parties is senseless thing and that we should all unite together and try to give our best to economically recover the country and that our young people could find job more easily. Furthermore, 36.66% believe that we have wrong role models. The majority of respondents (71.66%) responded that he/she was ready to leave Croatia looking for a job in hope for a better future, and this is what did they said: “The easiest way is to love country with full stomach, and send a donation to those who remained seated and hope that one day it would be better, same as their parents who live modestly hoped”. “Yes, we should go to the place where life is better, because we can not live only from love”. “What kind of attitude could I have when they themselves don’t know what they are doing, our government didn’t make anyothing except a lot of promises but none of them was fulfilled, I do not know can we actually be in a worse position!?”, “I think our country was/is lead by the selfish and damn people who only care about private interests”, “Republic of Croatia as a country is beautiful and has a beautiful sea and Slavonia, which is a land rich region... But the economic status of the country is zero”. Nothing from this country is not provided to anyone, only to those who are able to pick up and steal everything they can.

10. Conclusion

The results of the research have only confirmed the current situation among young people, which is well known in the state, but rather put aside. It's time for a serious undertaking and or providing assistence to young people (population between 20 and 30 years of age), while it is not too late, while young people still didn’t gave up on everything and became very pessimistic. The problem of today’s youth in rural areas is that majority of them are leaving from their areas to the regional centers (Zagreb, Osijek, Rijeka, Split), in search for job and higher living standards, and since recently, encouraged by poor socio-economic situation, they take risks searchnig for better standard abroad. Young people in village need support in all aspects of social life: they need the knowledge and ability to organize, increase the information flow, assistance in starting a small (family) business, help in establishing better relationships with parents and others who are active in their local communities. Some of the recommendations that the government should do to help young people stay in the village:

- Active employment measures should be focusing more on young people in the village,
- Proffessional assistance and support are required in inclusion of the unemployed in activities and programs (public works, self-employment schemes),
- Higher informativeness of young people, representatives of institutions on the objectives, content and measures of secondary education, which would be the task of local organizations, as well as mass media.
- Encourage them to refuse alcohol, cigarettes and drugs which aren’t doing any good for them, encourage them to keep the faith and believe more in themselves because it is the only way to find the right way for achieving their goals.

11. References

[1] “Nezaposlenost mladih: kriza našeg okruženja” [Online]. Available: http://ktl.jyu.fi/img/portal/23552/HR_youth_unemployment_concept_note_web.pdf?cs=1361521410 [Accessed: 10-Jun-2013]
[2] V. Mlinarević, V. Gajger, Slobodno vrijeme mladih - prostor kreativnog djelovanja, Međunarodna kolonija mladih Ernestinovo: 2003.-2008, (2010), p. 43-58.
[3] M. Kuzman, Adolescencija, adolescenti i zaštita zdravlja, MEDICUS, Vol.18, No.2, (2009), p. 155-172.
[4] J. Zloković, S. Vrcelj, Rizična ponašanja djece i mladih, Odgojne znanosti, Vol. 12 No.1, (2010), p. 197-213.
[5] Đ. Žutinić, D. Kovačić, I. Grgić, J. Markovina, Percepcija i kvalitete življenja i namjere o odlasku iz ruralnih sredina, Društvena istraživanja, Zagreb, (2010), 1-2, p. 137-159.
[6] Đ. Žutinić, N. Bokan, Village – Free Choice or Destiny for the Rural Youth (a study on the rural community of Vođinci), Sociologija i prostor, Vol. 46, No. 2, (2008), p. 143-160.
[7] M. Župančića, Infrastrukturna opremljenost hrvatskih seoskih naselja, Sociologija sela, Vol. 43, No. 3, (2009) p. 617-659.

GRAPES YIELD IN THREE YEARS OLD VINEYARD

Krešimir Horvat[1], Teuta Benković-Lačić[2*], Krunoslav Mirosavljević[2], Robert Benković[2] and Mirjana Brmež[3]

[1]bachelor of College of Slavonski Brod, Slavonski Brod, Croatia
[2]College of Slavonski Brod, Slavonski Brod, Croatia
[3]Faculty of Agriculture in Osijek, Kralja Petra Svačića 1D, Osijek, Croatia
* Corresponding author e-mail: tblacic@vusb.hr

Abstract
The paper analyzes grapes yield in a young three years old vineyard at the first harvest, with four grapes cultivars: Alphonse Lavallee, White Sultanina, Red Cardinal and Red Chasselas. After the analysis it can be concluded that the Red Chasselas cultivar had the highest number of grapes per vine, but also the lowest yield. The highest yield had the Aplhonse Lavallee cultivar. The average weight of one berry was the largest in the White Sultanina cultivar which had also the largest average volume of berries.

Keywords: grapevine, yield, berry

1. Introduction

One of the key points in planning and planting of new vineyard is grapes yield. Data on the grapes yield for certain cultivars can greatly help in choosing new cultivars. The growth rate of grape berries that affects the grapes yield depends on many elements but the varietal characteristic is the determining one [1]. The largest part of the berry is a meat and its ratio in grapes determines technological yield of certain cultivar.
Pruning is also one of the important factors in obtaining a particular grapes yield. Developed countries of Europe strive to achieve the expected grapes yield of 0.90 to 1.2 kg per vine, in order to increase the quality of the grapes. Grapes yield of about 3 kg per vine, depending on the cultivar and number of buds, cannot achieve a satisfactory quality of the grapes and therefore pruning is required to reduce the yield per vine. Basically, pruning reduces the number of buds per vine. Between the vines with a larger interspace a new vine should be planted to achieve the adequate training system [2].
Hanić et al (2011) conducted three-year experimental examination of the grapes yield, quality of the grapes and wine quality of Merlot cultivar. The study was conducted in the vineyards "NavIP - plantation", Leskovac (Serbia). The average grapes yield was 8.015 kg / ha and the sugar content was 22.81% with a total acidity of 6.74 g / l. Plantation was built on the Kober 566 basis with row spacing 3.5 m x 1.20 m which amounts to 2380 vines / ha [3].
Today there are many ways by which winegrowers are trying to increase the grapes yield and one of them is the use of growth hormones. Cardinal cultivars grown in Mostar wine region (Bosnia-Herzegovina) had the best response to two doses of gibberellin (GA3) at concentration of 10 ppm, which caused an increase in the height and width of the grapes as well as increase of entire mass of grapes and berries, in comparison to all other cultivars examined. The Cardinal cultivar yields from 1.92 kg to 2.37 kg per vine [4].
Medrano et al (2003) investigated the impact of irrigation on the yield of two grapes cultivars in Spain (Tempranillo and Manto Negro) [5]. Irrigation improved the grapes yield, especially for the Tempranillo cultivar. Also, the correlation between photosynthesis and grapes yield was significant for the Tempranillo cultivar. These results suggested a close relationship between water availability and grapes yield.
The aim of this study was to determine the grapes yield of certain cultivars in a young vineyard at the first harvest.

2. Method

Grapes yield in young vineyard was researched by the following cultivars: Alphonse Lavallee, Red Chasselas, White Sultanina and Red Cardinal. The yield was determined by using the following parameters:
a) the number of grapes per vine - (for each of four cultivars, four vines were examined);
b) the average weight of grapes for each variety - (average weight of ten grapes of each cultivar);
c) the average grape yield per vine;
d) the average weight of berries - (for each cultivar examined hundred berries were measured and the their average weight was calculated);
e) the average diameter of the berries - (for each cultivar examined hundred berries were measured and the average diameter of berries was calculated).

Vineyard where the research was conducted was raised in 2010 and the first harvest was done in 2012. The vineyard is located in the Brod Vinogorje in Slavonski Brod which belongs to the continental Croatian region, sub-region of Slavonia. The altitude of the vineyard is 98 meters and the position of the vineyard is southern exposure. Vineyard area is 50 m2. The planting distance between rows is 150 cm and within the

rows 100 cm. Grapevines cultivars planted in the vineyard are Alphonse Lavellee, Red Chasselas, Red Cardinal, White Sultanina, White Matilde and Osella. All cultivars were planted in breeding two-armed form. During the two years of the grapevine growth the standard work in the vineyard (such as mowing the grass, pruning and regulation of soil) was carried out. Fertilization was done in autumn 2011 with NPK 7-20-30 at a rate of 5 kg on the whole area of the vineyard and with manure (3 kg on the entire area of the vineyard). In spring 2012 fertilization with NPK 7-20-30 and manure fertilization were repeated, and manual hoeing of the soil to a depth of 15-20 cm was done in spring and summer of 2012. Plant protection with fungicide Bordeaux soup was performed in the spring, twice in 10 days before flowering, while at the same time tearing of laterals was carried out. During the vegetation season protection with fungicide Bordeaux soup and insecticide Basudin was carried out.

3. Results and Discussion

The Red Chasselas cultivar had the highest average number of grapes per vine (12.75) and the lowest number of grapes per vine (5.25) was for the White Sultanina cultivar. Total number of picked up grapes was the largest for the Red Chasselas cultivar, then for the Alphonse Lavalle and the Red Cardinal and the lowest number was for White Sultanina cultivar. Table 1 shows the results obtained from the analysis of the total number of grapes for each cultivar studied.

Table 1. Analyses of grapes numbers and weight

Cultivar	Total number of grapes	Average number of grapes per vine	Average weight of grapes (g)
Red Chasselas	51	12.75	78.04
White Sultanina	21	5.25	123.87
Red Cardinal	36	9	83.24
Alphonse Lavallee	48	12	118.43

After the analysis of grapes weight for each cultivar (Table 1) it can be concluded that the White Sultanina cultivar had the largest average grapes weight of 123.87 g but that weight is below the reported average of 250-450-800 g [2]. Red Chasselas had the lowest average grapes weight of 78.04 g. The average grape weight for Red Cardinal cultivar was 83.23 g and for the Alphonse Lavallee cultivar was 118.45 g. After investigation the average grape yield per vine was the largest for the Alphonse Lavallee cultivar and the smallest for the White Sultanina cultivar (Table 2).

Table 2.Average grapes yield per vine

Cultivar	Average grapes yield per vine (kg)
Red Chasselas	1.00
White Sultanina	0.65
Red Cardinal	0.75
Alphonse Lavallee	1.42

Table 3. Average berry weight

Cultivar	Average berry weight (g)
Red Chasselas	2.17
White Sultanina	3.63
Red Cardinal	2.02
Alphonse Lavallee	2.81

Average berry weight was the largest in the White Sultanina cultivar (3.63 g), while the lowest average weight of berries was for the Red Cardinal cultivar (2.02 g). After investigation of the average diameter of the berries, it can be concluded that the White Sultanina cultivar had the largest average diameter of berries (3.98 cm) and Red Chasselas had the smallest one (2.17 cm).

Table 4. Average berry diameter

Cultivar	Average diameter (cm)
Red Chasselas	2.17
White Sultanina	3.98
Red Cardinal	3.27
Alphonse Lavallee	2.97

4. Conclusion

This paper analyzes the contribution of four different grapevine cultivars and the average weight of grapes and berries in the three years old vineyard at the first harvest.
From the obtained results it can be concluded as follows:

• the Red Chasselas cultivar had the largest average number of grapes per vine (12.75), while in the White Sultanina it was 5.25 which is the lowest number of grapes in all four cultivars examined,

• the highest average grapes weight of 123.87 g was obtained for the White Sultanina cultivar, while the Red Chasselas had the smallest average grapes weight of 78.04 g,

• the Alphonse Lavallee cultivar had the highest yield per vine has a variety 1.42 kg, while the lowest yield per vine was observed for the White Sultanina cultivar (650 g),

• the average weight of one berry was the largest for the White Sultanina (3.63 g), while the lowest average weight of berries had the Red Chasselas (1.72 g),

• the White Sultanina cultivar had the largest average volume of berries (3.98 cm), and the Red Chasselas had the smallest average volume of 2.17 cm.

From the above analysis it can be concluded that the Red Chasselas cultivar had the highest number of grapes per vine, but also the lowest grape yield. The highest yield had the Aplhonse Lavallee cultivar which is a high yielding cultivar and these studies showed its varietal characteristic.

5. References

[1] Nikola Mirošević, Jasminka Karoglan Kontić: Vinogradarstvo, Zagreb, Nakladni zavod Globus, 2008.

[2] Available: http://www.agroklub.com/vinogradarstvo/rezidba-vinove-loze/762/, [Accessed: 31-Agus-2012].

[3] Elvedin Hanić, Senad Murtić, Nura Murtić, Agan Kojić, Mersija Delić, Milena Đurić: 46th Croatian and 6th International Symposium on Agriculture, Izvorni znanstveni rad, Opatija. Croatia, 2011.

[4] "Zotero Style Repository," *Roy Rosenzweig Center for History and New Media*. [Online]. Available: http://www.zotero.org/styles. [Accessed: 19-Mar-2012].

[5] Hipolito Medrano, Jose M. Escalona, Jose Cifre, Josefina Bota and Jaume Flexas: A ten-year study on the physiology of two Spanish grapevine cultivars under field conditions: effects of water availability from leaf photosynthesis to grape yield and quality, Funcional Plant Biology 30: 607:619

[6] http://www.batmanrw.bloger.hr/post/stolne - sorte-grozdja--sultanina-bijela/732115.aspx, 19.8.2012.

DEVELOPING A PHARMACEUTICAL BIOTECHNOLOGY COURSE AT A SOUTH AFRICAN UNIVERSITY

Roman Tandlich[1*], Denzil R. Beukes[1], Michael J. Naidoo[2] and Eva Tandlichová[3]

[1]Division of Pharmaceutical Chemistry, Faculty of Pharmacy, Rhodes University, P.O. BOX 94, Grahamstown 6140, South Africa
[2] Division of Pharmacology, Faculty of Pharmacy, Rhodes University, P.O. BOX 94, Grahamstown 6140, South Africa
[3] Department of English Language and American Studies, Comenius University, Gondova 2, 81806 Bratislava, Slovakia
** Corresponding author e-mail: roman.tandlich@gmail.com, r.tandlich@ru.ac.za.*

Abstract
The 2010-2012 instruction of Pharmaceutical Biotechnology at Rhodes University, South Africa is described in this article. In 2010, the pharmacy students achieved the best results in subject matter which was an extension of their foundational knowledge. Improvements in foundational knowledge on Pharmaceutical Biochemistry and Pharmaceutics are needed prior to the students taking the course. This is needed to improve the necessary fundamental knowledge and biotechnology instruction should be preceded by the start of clinical part of the pharmaceutical education. With Bachelor of Science students, module on intellectual property and fundamental of bioengineering must be run in third year of studies. This will maximize prepare the students' for understanding of the concepts of quality assurance and mathematical modelling in the biotechnology. Lectures and case studies if delivered step by step provide the best instruction format.

Keywords:
Tertiary education, case studies, bioengineering

1. Introduction

Up to 15 % of all pharmaceutical products are derived from biotechnology operations [1], i.e. biotechnology should be included in tertiary pharmacy curriculum [2]. This was not the case at Rhodes University prior to 2010 [3]. Graduates from the Science programme at the same institution often end up working in the pharmaceutical companies [3]. These are graduates from the Bachelor of Science Honours curriculum in the Department of Biochemistry, Microbiology and Biotechnology (designated as Department in further text). Before 2011, following topics were not covered sufficiently in the Department's curriculum: mathematical bioengineering, online monitoring and financing of biotechnological production. To address these curricular gaps, specialised courses/modules were introduced in the two academic units between 2010 and 2012. Course content, assessment and student feedback are below.

2. The 2010 Bachelor of Pharmacy Course

The 2010 final year class in Pharmacy was offered the "Applied Pharmaceutical Biochemistry and Biotechnology". Week 1 contained lectures on the recombinant DNA technology, selective culture media and biochemical identification of microorganisms. Two case studies took place where students were split into small groups. They were given assignments on topics such as antibiotic susceptibility of bacteria and its testing, microbial analyses of water and milk; and the nucleic acid and protein analyses. All groups presented particular case studies to their peers after preparation. Second week contained discussion on microorganisms as producers of the active pharmaceutical ingredients (APIs). Isolation of pure microbial cultures and product purification in biotechnology were covered. The subsequent topics were the microbial metagenomics and metabolic pathway engineering. Revision of chemotherapy and mechanism of action for antibacterial, antifungal, antiviral and anti-parasitic APIs followed. Safety/misuse of antibiotics was linked to genetics of resistance. Testing and quantification of antimicrobial activity of biotechnological products were dicussed using the review by Newman et al. [4].

In weeks 3 and 4, methods for quantifying microbial biomass and growth were introduced. Mathematical and operational differences between the batch, the fed-batch and the continuous bioreactors were explained. Microbial growth rate and maintenance coefficient were defined, along with nutritional requirements for the microbial production of selected API. Role of temperature and pH in biotechnological production were outlined. The next topic were tools and techniques for online and offline process monitoring. Scale-up of pharmaceutical production and treatment of pharmaceutical waste were discussed last. The case study by Elibol and Mavituna [5] was used to link the subject matter from week 3 to the students' knowledge obtained in weeks 1 and 2. After a three-day self-study period, two lectures were dedicated to critical analysis of the main assumptions of the mathematical model and quality of the experimental data. The course instruction was completed by and industrial tour

into Makana Meadery. Here the students were exposed to the biotechnological process development, continuous fermentation and service-learning.

In the first course week of 2010, each student was marked based on their group's performances in the following competences: understanding of the theory and application of biochemical/chemical concepts in biotechnology, practical application of such theory in presentations, the students' problem-solving abilities/reply to audience questions and creativity in the presentations. The final mark for week one was calculated for the given student as the average of their two case study marks. In weeks 2-4, summative assessment was based on one take-home test per week. The tested competences in week 1 as well as comprehension of genetic manipulation and engineering in pharmaceutical biotechnology, use of mathematical models in bioengineering, the quality assurance and intellectual property concepts, and extraction of information from service learning. Each student obtained three individual marks in weeks 2-4. The final course mark was calculated as an equal-weight average of marks from weeks 1-4.

3. The Bachelor of Science Honours Course

In 2011, the course was taught in the Department as part of the BSc Honours course in Biotechnology. In the first ten days, the focus was on topics from weeks 3 and 4 of the 2010 course. Then the case study by Geddes [7] on funding models in biotechnology was dicussed. This was done in a lecture and using self-study by the students. Then the students had five days to write an essay on the case study. They found the topic difficult to grasp and so another discussion on the subject was needed. Following this, the first draft essays were handed-in and returned with formative feedback to the students for revision. The same approach was applied to the case study by Sin et al. [8]. The formative assessment was aimed at developing the students' understanding of financing in biotechnology, comprehension and usage of mathematical models in biotechnology production and adherence to the intellectual property principles. At the end of the module, the students wrote a two-hour summative exam to be given a mark from the course.

In 2012, Pharmaceutical Biotechnology was taught in the Department as part of the "Pharmaceutical Biotechnology and Nanobiotechnology" Honours module. A quick undergraduate curriculum review was conducted prior to commencement of instruction. As a result, the 2012 module was arranged as a step-by-step demonstration of the relevant bioengineering principles and practical problems. The batch bioreactor, its modelling and operation were used as the starting point of instruction. The first case study was that of Mankad and Bungay [9]. The article was critically evaluated in class. The first formative essay took the form of a reviewer's report to the Journal of Biotechnology [10]. This is where the article had been published. The case study was read by the students overnight and then they wrote the reviewer's report over 45 minutes during the next day of instruction. This essay was marked using the peer assessment.

The second case study was the review by van Bodegom [11]. Microbial maintenance, its relationship to the growth requirements and basic cellular processes were lectured on in detail. Definition and measurement of the maintenance coefficient, the maintenance rate or the minimum substrate concentration was outlined. Critical concepts were discussed in the question and answer format drawing on students' prior knowledge. The third case study synthesized the student knowledge from the module. It covered the use of batch reactor in the production of the antibiotic actinorhodin [5]. Key equations for growth kinetics, utilisation of the growth and energy substrate, formation of the product and the dissolved oxygen concentration as a function of time were identified first. This was followed by the coverage of the model assumptions. Drawbacks of the analytical techniques were explained and the students were given additional resource for self-study.

4. Student feedback

Student feedback was sought via email and using open-ended questions. In 2010 and 2011, question 1: "Did you find the course well structured?". Question 2: "Which type of instruction did you prefer, lectures or case studies with self-study?". Question 3: "Which part of the course do you think are you most likely to apply during your career?". Question 4: Please feel free to provide additional and/or general comments you might have." Students could provide general suggestions with questions 1-3. The 2012 feedback include question 5, namely "Do you feel that the coverage of the mathematical aspects of the module was sufficient for your comprehension of them?". The respondence rates were as follows: 11.1 % in 2010, 37.5 % in 2011 and 22.2 % in 2012. The results are analysed in the next section.

5. Results and Discussion

The average mark for the 2010 elective course was 72 ± 3 %, while the individual week averages were as follows: 68 ± 4 % in week 1, 74 ± 5 % in week 2, 83 ± 8 % for week 3 and 65 ± 5 % for week 4. The Kruskal-Wallis analysis of variance by

ranks at 5 % level of significance (referred to as KW in further text) was used to analyse the individual week averages which weren't normally distributed. If any statistically significant differences exist among the averages from weeks 1-4, this would indicate that the students comprehended various lectured topics differently. All calculations were done using the Past 2.0 software package (Paleontological Museum, Oslo, Norway and Geological Museum, Copenhagen, Denmark) or Microsoft Excel (Microsoft, Johannesburg, South Africa). Eighteen students took the elective course in 2010. The KW statistic was equal to 41.94 (critical value = 9.49, p-value = 4.49×10^{-9}) [12]. Thus students' average mark was different in at least one of the course weeks.

The Jonckheere test for ordered alternatives was used to identify the possible trends in the average marks. The standardised value of the test statistic J was equal to -7.459 [13]. The critical value was equal to -1.650 for 5 % level of significance [12]. Therefore the summative week averages decreased as follows: week 3 > week 2 > week 1 > week 4 (p-value < 0.025). To confirm this trend, the averages from weeks 2 and 3 were log-transformed and analysed using the t-test with The test statistic was equal to 3.974. The critical value was 1.684-1.697 [12], i.e. the average in week 3 was higher than in week 2 (p-value = 0.0005). The same t-test was performed for the following average pairs: week 2 and 1; and week 1 and 4. The respective test statistic values were equal to 4.504 (p-value < 0.0001) for the former and 2.310 (p-value < 0.0001) for the latter. The critical value was again equal to 1.684-1.697 [12]. Thus the students probably achieved the best results in the weeks 2 and 3 of the 2010 course.

Mechanism of action of APIs forms the baseline knowledge of a pharmacy student [3]. Bioengineering aspects of the 2010 course were discussed through production of an antibiotic [5], so was the subject matter in week 2. Therefore the course content of weeks 2 and 3 was likely seen by students as an extension of their baseline knowledge. This familiarity probably stimulated the students' comprehension of the subject matter in weeks 2 and 3, i.e. indicating why the best week averages were reached in these weeks. In week 1, the instruction built on largely on the students' knowledge from Pharmaceutical Biochemistry, Pharmaceutics 3 and Pharmacology 3 [3]. Using the students' marks for the undergraduates who took the 2010 course, the following averages were calculated: 59 ± 7 % for Pharmaceutical Biochemistry, 55 ± 4 % for Pharmaceutics 3 and 66 ± 7 % for Pharmacology 3. The averages were log-transformed and t-tested against the average from week 1 of the course.

At 5 % level of significance, the average from Pharmaceutical Biochemistry was lower than the 2010 week 1 average (test statistic = -4.264, critical value = -1.333, p-value = 0.0004). The same was calculated for the Pharmaceutics 3 mark (test statistic = -10.556, critical value = -1.333, p-value < 0.0001). There was no statistically significant difference between the Pharmacology 3 average and the average mark from week 1 of the 2010 elective course (test statistic = -1.204, critical value = -1.333, p-value = 0.2397). Thus the students' insufficient fundamental knowledge from Pharmaceutical Biochemistry and Pharmacology probably did not facilitate comprehension of the subject matter in week 1 of the 2010 course. The 2010 course took place before the students' clinical training [3]. Thus the industrial tour required practical application of their theoretical knowledge, i.e. it could have been perceived as the first clinical experience. Thus their performance in the summative assessment from week 4 could have resembled the transition from pre-clinical to clinical stage of their professional career, which has been shown to be difficult for healthcare students [14]. Therefore the lowest course mark was most likely recorded in week 4.

In 2011, the overall average mark for the BSc Honours module was 75 ± 9 %. The topics averages (± one standard deviation) from the summative exam were as follows: 78 ± 6 % for principles of online monitoring, 71 ± 20 % for yield and maintenance coefficient comprehension, 78 ± 13 % for financing tenets, 70 ± 29 % for understanding of types of mathematical models of biological systems; and finally 79 ± 13 % for validity of theoretical assumptions of such models. The KW statistic value was equal to 0.6038 with the critical value of 9.49 (p-value = 0.9647) [12]. Thus the students performed equally well in all topics in the module. Lack of proper referencing and misunderstanding of the copyright/intellectual property issues were observed with all students in formative essays in 2010 and 2011. Educational interventions and discussion of issues of academic plagiarism were run with both classes. This resolved the problems.

The 2012 summative assessment was an essay on the antibiotic wastewater treatment which integrated all aspects of the course subject matter [3]. The average mark was equal to 68 ± 11 %. After log-transformation, this value was not statistically significantly different from the 2011 (the t-test for unequal sizes and variances, t statistic = 0.256, the p-value > 0.1000, the critical value = 1.895 at 5 % level of significance) [12]. Thus changes in the assessment format and instruction method did not lead to a statistically significant

decrease in student performance between 2011 and 2012. A bioentrepreneurship course and intellectual property took place in the BSc Honours course in 2012 and before the Pharmaceutical Biotechnology and Nanobiotechnology module. This probably led to improvement in the students' comprehension of intellectual property, as 89 % of the 2012 students did not have any issues with it.

All students in 2010 and 2012 found the course well structured, with the 2011 proportion at 67 %. The same proportions of respondents found knowledge of pharmaceutical biotechnology a valuable addition to their education. In 2010, 100 % of the respondents found lectures as the best mode of instruction. In 2011, 67 % of respondents stated this was a combination of case studies and formal lectures. In 2012, the instruction format model was perceived as easy to follow by all respondents, who also stated that bioengineering should be taught a year prior to the Honours course. One hundred percent of the 2010 respondents and 33 % of the 2011 ones stated that the logistical arrangements of the course were not good enough. In 2010, 50 % of the respondents stated that mathematical model manipulation or the entire subject matter of the course will contribute to the students' professional careers. In 2011, 33 % of the respondents stressed that they would use the following topics in their career: mathematical models of bioengineering processes, principles of scale-up and the bioengineering of the stem cell culturing.

6. Conclusion

Pharmaceutical Biotechnology curriculum must build on pharmacy students' foundational knowledge. Improvements are needed in pharmacy students' comprehension of Biochemistry and Pharmaceutics. Their biotechnology Instruction must take place after the start of their clinical training. With science students, modules on intellectual property and bioengineering must be run before the course. Optimum instruction is achieved through step by step combination of lectures and case studies.

7. Acknowledgement

The authors thank Dr. Garth Cambray for assistance with the 2010 industrial tour.

8. References

[1] S. Gaisser, M. Nusser, "The role of biotechnology in pharmaceutical drug design," *Zeitschrift for Evidenz, Fortbildung und Qualität im Gesundheitswessen*, 104, 732-737, 2010.

[2] M. H. Sosabowski, P. R. Gard, "International pharmacy education supplement: Pharmacy Education in the United Kingdom," *American Journal of Pharmaceutical Education*, 72, 6, Article 130, 2008.

[3] R. Tandlich, "Teaching, comprehension and assessment of Pharmaceutical Chemistry, Biochemistry and Biotechnology at Rhodes University," *Rhodes University*. Grahamstown, South Africa.

[4] D. J. Newman, G. M. Cragga, K. M. Snaderb, "The influence of natural products upon drug discovery," *Natural Product Reports*, 17, 215-234, 2000.

[5] M. Elibol, F. Mavituna, "A kinetic model for actinorhodin production by *Streptomyces coelicolor* A3(2)," *Process Biochemistry*, 34, 625-631, 1999.

[6] G. A. Cambray, "African mead: biotechnology and indigenous knowledge systems in iQhilika process development," *PhD dissertation*. Rhodes University, South Africa, 2005.

[7] D. Geddes, "Translational research – from gene to treatment: lessons from cystic fibrosis," *Clinical Medicine*, 5, 258-263, 2005.

[8] G. Sin, P. Ödman, N. Petersen, A. Eliasson Lantz, K. V. Gernaey, "Matrix notation for efficient development of first-principles models within PAT applications: integrated modeling of antibiotic production with *Streptomyces coelicolor*," *Biotechnology and Bioengineering*, 101, 153-171, 2008.

[9] T. Mankad, H. R. Bungay, "Model for microbial growth with more than one limiting nutrient," *Journal of Biotechnology*, 7, 161-166, 1988.

[10] "Guide for Authors," *Journal of Biotechnology.* [Online]. Available: http://www.elsevier.com/wps/find/journaldescription.cws_home/505515/authorinstructions [Accessed: 21-Jun-2012].

[11] P. Van Bodegom, "Microbial Maintenance: A Critical Review on Its Quantification," *Microbial Ecology*, 53, 513-523, 2007.

[12] D.C. Howell, "Fundamental statistics for the behavioral sciences," *Thomson Wadsworth*, New York, USA, 2007.

[13] A. Field, "Discovering Statistics using SPSS: Jonckheere's trend test," *Ilalas Blogbook*. [Online]. Available: sirpabs.ilahas.com/Andy Field - Discovering Statistics using SPSS, Second Edition/ Discovering Statistics using SPSS, Second Edition CD ROM/Jonckheere.pdf [Accessed: 30-Apr-2012].

[14] K. J. A. H. Prince, M. W. J. Van de Wiel, A. J. J. A. Scherpbier, C. P. M. Van der Vleuten, H. P. A. Boshuizen, "A qualitative analysis of the transition from theory to practice in undergraduate training in a public medical schoo,l" *Advances in Health Sciences Education*, 5, 105-106, 2000.

INNOVATION AND NEW PRODUCT DEVELOPMENT IN CROATIA

S. Knežević[1*], A. Kulaš[1] and L. Duspara[1]

[1] College of Slavonski Brod, Slavonski Brod Osijek, Croatia
* *Corresponding author e-mail: Sanja.Knezevic@vusb.hr*

Abstract
Today's enterprises in terms of a dynamic environment are faced with serious challenges such as global economy expansion, intense competition, severe struggle for markets, rapid technological changes, structural transformations, and so on. In order to respond to these challenges, enterprises need to constantly increase their productivity, improve the quality of products and services, develop new products and meet the requirements and desires of the environment. Innovations represent not only an initial point for growth and development but also a survival factor. Those enterprises that are able to respond rapid to changes by innovations and constantly introduce novelties are the only ones that can survive in the world today. This paper analyzes how high the innovations in Croatian enterprises are developed, and what are the main obstacles and innovation activities.

Keywords:
Innovation, new products, enterprises, Croatia

1. Introduction

Innovations today have a key position in the competitiveness of countries, regions and enterprises, and today's economy is characterized by a rapid and sustained competition on a global level. In order for Croatian enterprises to compete in such an environment, there is the need to develop a culture of innovation that supports understanding, creating and embracing innovation. Innovative enterprises are more competitive in the market because they provide a unique value. Today's enterprises are forced to invest in the development and innovation, because if they neglect them, they will be destroyed by the competitions that effectively innovate.

2. Innovations and new product development

Innovation is the application of new and improved ideas, procedures, goods, services, processes, which brings new benefit or quality used in applying. The main characteristics of innovations are changes. According to this, innovation is a specific tool of entrepreneurs, by which they use change as possibility for execution of different production and service activities. ''There are three main categories: product innovation, process innovation/service supply and managerial innovation.'' [1]

The term 'new product' can mean different things to different people. ''New products can be categorized:

- New to the world products or really new products
- New to the firms or new product lines
- Additional to existing product lines
- Improvements and revisions to existing products
- Repositioning
- Cost reductions'' [2]

Quality of enterprises is expressed in devising, development and realization of new ideas and products that are more profitable.
In Republic of Croatia, the concern of the innovation development carries Croatian Association of Innovators. ''Their mission is to promote innovative activities and the creation of attractive programs and actions, particularly care about the inclusion of animation and young innovators.'' [3]

3. Analysis of Croatian performance

Innovative performance of some country is a key driver of its economic growth and prosperity. The most innovative countries in Europe are shown in the table 1.

Table 1. The most innovative countries in Europe between 2008 and 2010 [4]

Number	Country	Percent of innovative enterprises
1.	Germany	79.3%
2.	Luxembourg	68.1%
3.	Iceland	63.8%
4.	Belgium	60.9%
5.	Portugal	60.3%
....	CROATIA	42.2%

Table 1 shows enterprises from industry and services reported innovation activity between 2008 and 2010. The survey was conducted in the EU-27 Member states so Croatia is not at the list.
Among all the participating countries, the highest proportions of enterprises with innovation activity were found in Germany, than in Luxemburg, Iceland, Belgium and Portugal. These are the top 5 countries. Croatia has 42.25 % of innovative enterprises.

According to research from 2006 conducted in Croatia ''44,6% of the respondents believe that the Croatia is slightly innovative, 36,9% believe is completely innovative, and 18,5% of respondents considered Croatia not innovative at all.'' [5]
Only limited numbers of enterprises in Croatia base their business on innovative products. ''As classic examples of local innovative companies are Pliva, which has developed its own antibiotic Sumamed, Podravka Vegeta with popular spice, HS Product developing and exporting its own firearms, and the cesspool that develops rigs and equipment for environmental protection.''[6]The total numbers of enterprises in Croatia which base their business on innovation are below in table 2.

Table 2. Enterprises in Croatia by innovation performance from 2008 to 2010 [7]

	Total	Innovators	Non-innovators	Share of innovators, %
Industrial enterprises	3 641	1 626	2 015	44,7
Service enterprises	6 427	2 126	4 300	33,1
Small enterprises	8 208	2 745	5 463	33,4
Medium enterprises	1 520	773	748	50,9
Large enterprises	339	234	105	79,0

Table 2 shows enterprises in Croatia divided according to the type and size of the enterprise and shows how many of them are innovators or non – innovators. In Croatia are over a ten hundred thousand enterprises. Although service enterprises are much more, industrial enterprises in Croatia have a more share of innovators (44,7 %) than service enterprises (33,1 %). That is 11,6% more than service enterprises. Enterprise size is the key factor for their innovation activities. The share of innovative enterprises increases with enterprise size. The most innovative are large enterprises, then medium- sized enterprises and at the end small enterprises. Increasing competitiveness is necessary basis of Croatian export growth, but also possibility of equal participation on open market under severe competitive pressures in the domestic market. In achieving this objective, the most crucial role has small and medium enterprises capable of continuously and dynamically adapt to market demands. Small and medium enterprises show worse results than large enterprises. However, promising information on the slight increase innovativeness of SMEs as shown in the following table 3.

Table 3. Growing enterprises in Croatia, according to the criteria of the new product development [8]

Criteria for the classification of growing enterprises	2010.	2011.
Enterprises that have new products that are new to everyone %	9,46	12,63
Enterprises that have new products which are new to some %	15,25	25,16
Enterprises that have new products that are new to anybody %	75,29	62,21

Table 3 shows the share of enterprises according to the criteria of the new product development. Share of enterprises that have new products that are new to everyone has increased by 33,50% from 2010 to 2011. Share of enterprises that have new products which are new to some has increased by 64,98 % and share of enterprises that have new products that are new to anybody has decreased by 17,38%. Share of product and process innovators in enterprises in Croatia are shown in table 4.

Table 4. Product and process innovators by type of innovation activity from 2008 to 2010 [7]

	Total	Product innovators	Process innovators	Product and process innovators	Ongoing/abandoned innovation activities
Industrial enterprises	35,6	4,6	9,5	20,0	1,4
Service enterprises	21,4	3,4	7,5	9,8	0,7
Small enterprises	22,6	3,4	7,3	11,3	0,7
Medium enterprises	39,3	5,2	12,0	20,1	2,1
Large enterprises	61,7	8,8	13,0	37,2	2,7

Table 4 shows that industrial enterprises have a larger share of all factors. They have 1,2 % more product innovators, 2 % process innovators, 10,2 % product and process innovators and 0,7% ongoing or abandoned innovation activities. As in table 2 the share of innovative enterprises increases with enterprise size. Most enterprises have higher proportion of process innovators than product innovators.''Based on the Summary Innovation Index, the EU Member States fall into the following four country groups: Innovation leaders, Innovation followers, Moderate innovators, Modest innovators.'' [9] The EU's innovation leaders are Sweden, Denmark, Germany and Finland. Austria, Belgium, Cyprus, Estonia, France, Ireland, Luxembourg, Netherlands, Slovenia and the UK are the Innovation followers. Czech Republic, Greece, Hungary, Italy, Malta, Poland, Portugal, Slovakia and Spain are Moderate innovators. Bulgaria, Latvia, Lithuania and Romania are Modest innovators. The performance of Innovation leaders is 20% or more above that of the EU-27, of Innovation followers it is less than 20% above but more than 10% below that of the EU-27, of Moderate innovators it is less than 10% below but more than 50% below that of the EU-27 and for Modest innovators it is below 50% that of the EU-27. Switzerland is the overall innovation leader, outperforming all Member States. For Croatia growth in innovation performance has been between 4,1% and 5,3%, well above that of the EU-27 in the same period. Conditions relating to Croatian innovation can be directly observed on the basis of the Global Innovation Index that is shown in table 5.

Table 5. Top 10 Leaders in the Global Innovation Indekx [10]

Rank	Country
1.	Switzerland
2.	Sweden
3.	Singapore
4.	Finland
5.	United Kingdom
6.	Netherlands
7.	Denmark
8.	Hong Kong (China)
9.	Ireland
10.	United States of America
42.	CROATIA

Table 3 shows top ten leaders in the Global Innovation Indeks in the year 2012. Second year in row Switzerland, Sweden and Singapore are ranked in top three places in the world rankings of innovation that includes a total of 141 countries and is based on the global innovation index. Among the 10 leading countries are also placed Finland on the fourth, the United Kingdom, on the fifth, the Netherlands, on the sixth, Denmark, on the seventh, Hong Kong, the eighth, Ireland, on the ninth, and the United States, on the 10th place. Among the 10 best-placed countries in the overall rankings dominated European countries. Croatia is ranked 42nd. Last year's ranking for Croatia is shown in table 6.

Table 6. Croatia's innovation in the Gobal Innovation Indeks [made by authors]

Year	Rank for Croatia
2012.	42
2011.	44
2010.	45
2009.	62

Table 4 shows ranking for Croatia in 2012. and in the past 3 years. 2009. Croatia is ranked 62 and that's the lowest rank. Croatia each year achieve better ranking. It is known that new products and innovations provide great competitive advantage. An investment in research and development contributes to greater profit, greater market share and companies' survival. One of the biggest obstacles to the realization of market innovation is the lack of money. The increase in overall investment in research and development and increasing the share of private sector investment in research and development in accordance with the objectives of the EU Croatia also has accepted as its national goal. But in terms of total outlays for research and development over the past few years Croatia recorded a trend of falling behind compared to the EU 27. ''Croatia has invested in research, development and innovation just 0.76 percent of GDP, while the average in developed countries is about three percent.'' [11] The World Intellectual Property Organization (WIPO) and INSEAD co-publish the top countries according to investments in research and development that is shown in table 7.

Table 7. Top 10 countries in the investments in research and development [12]

Rank	Country
1.	Israel
2.	Quatar
3.	Finland
4.	Island
5.	Denmark
6.	Japan
7.	Sweden
8.	Switzerland
9.	Singapure
10.	Korea, Rep.
42.	CROATIA

Table 7 shows top ten leaders in the investments in research and development in the year 2012. In the world country which invests the most in

research and development is Israel, followed by Quatar, Finland, Island, Denmark, Japan, Sweden, Switzerland, Singapore and Republic of Korea. Croatia is ranked 42th. Research, development and innovation should constitute the backbone of a healthy economy but unfortunately Croatia by gradually decreasing budget allocations that is shown in the table 8.

Table 8. Investments in research and development in Croatia [13]

Year	Budget allocations for research and development %
2010.	0,73%
2009.	0,83%
2008.	0,89%
2004.	1,05%

Table 8 shows the budget allocations for research and development in Croatia. In 2010 the allocation was only 0,73% of GDP, a year earlier in 2009 it was 0,83% of GDP, and in 2008 it was 0,89%. In 2004 it was 1,05% of the total state budget. Croatia needs to significantly increase its investment in research and development if wants to be part of competitive EU. Croatia by 2020 aims to raise the level of investment in research and development to 1,4 % of GDP.

4. Croatian Innovation Quotient

Croatian Innovation Quotient (CIQ) is a project focused on the research and evaluation of innovative Croatian enterprises. ''It covers the first research innovation capacities of Croatian enterprises for the systematic construction, management and effective implementation of innovative business practices, processes and models that lead to the creation of innovative products and services. CIQ have developed top Croatian experts, and based on the best international practices in the field of innovation.'' [14] According to research from 2011. 68% of enterprises in Croatia stated innovation as the highest or among the top three priorities of the business. It is a very good indicator for the future in Croatia business.

5. Conclusion

Enterprises, which at the present time do not recognize the necessity of constant change and the importance of creating innovative products and services, can be expected to be removed of the market. In modern business conditions, innovation is one of the main sources of competitive advantage. Croatian enterprises have a lot of space to improve its innovation. All listed data indicate that the innovative enterprises in Croatian are under-developed, and this situation negatively affects the competitiveness of the economy as a whole. Croatian enterprises must improve their systems and processes to create new products, but also seriously deal with changing innovation capacity as a basis for development. International experience suggests that enterprises should be in an environment that supports, encourages and promotes innovation for the development of a successful company. Exactly for this reason, constant development and investment in innovation must become a priority for every enterprise that wants to become more competitive and take their place in the market.

6. References

[1] Prester J. (2010.) Menadžment inovacija, Sinergija, Zagreb
[2] Crawford M., Di Benedetto A. (2006.) New product management,McGraw-Hill Irwin, eight editiond, New York
[3] Union of Croatian innovators, Available: http://www.inovatorstvo.com/?A=MED&IDGRU=MED#:ajaxCallback@4 [Accessed: 17-Aug-2013]
[4] Eurostat, Available: http://epp.eurostat.ec.europa.eu/cache/ITY_OFFPUB/KS-GN-13-001/EN/KS-GN-13-001-EN.PDF [Accessed: 30-Aug-2013].
[5] Poslovni dnevnik: Najinovativnije kompanije, Dnevnik d.o.o. Zagreb, 2011. str. 9
[6] Available: http://vijestigorila.jutarnji.hr/gorilopedija/lifestyle/ekonomija_i_pravo/inovacije_u_hrvatskoj [Accessed: 19-Aug-2013].
[7] Croatian bureau of statistics, Available: www.dzs.hr [Accessed: 19-Aug-2013].
[8]http://www.cepor.hr/SME%20godisnjak_2013.pdf [Accessed: 20-Aug-2013].
[9] European Commission, Available: http://ec.europa.eu/news/science/120208_en.htm [Accessed: 20-Aug-2013].
[10] The Global Innovation Index 2012 ,Available: http://www.wipo.int/export/sites/www/econ_stat/en/economics/gii/pdf/chapter1.pdf [Accessed: 19-Aug-2013].
[11] Available: http://www.tportal.hr/scitech/znanost/214787/Hrvatska-po-izdvajanju-za-znanost-na-zacelju-Europe.html#.UGnyPlG_10I [Accessed: 21-Aug-2013].
[12] Available: http://www.globalinnovationindex.org/gii/main/fullreport/files/Human%20capital%20and%20research.pdf [Accessed: 28-Aug-2013].
[13] http://www.sprint-ipa.org/Html/HR-Prijedlog%20mjera_Medjimurje_Krapina_Zagreb.pdf [Accessed: 02-Sep-2013].
[14] Croatian Innovation Quotient, Available: http://www.inovativnost.hr/ [Accessed: 05-Sep-2013].

NITROGEN LEACHING IN IRRIGATED AND N FERTILIZING CONDITIONS

[1]Monika Marković, [1]Jasna Šoštarić, [2]Božica Japundžić-Palenkić, [3]Marko Josipović, [4]Denis Cerjan

[1]Faculty of Agriculture of J.J. Strosmayer University in Osijek, Osijek, Croatia
[2]Department for horticulture, University of applied science in Slavonski Brod, Croatia
[3]Agricultural institute in Osijek
[4]Former university graduate student (master studies) Faculty of Agriculture in Osijek, Croatia

Corresponding author e-mail: **monika.markovic@pfos.hr**

Abstract
The field experiment was set up at the trial field of Agricultural institute in Osijek as split split-plot scheme in year 2012. The goal of study was to evaluate the effect of different irrigation and nitrogen fertilizers levels on nitrate-nitrogen leaching in maize filed. The experiment included three irrigation levels (A1= non irrigated; A2 = 60 to 100 field water capacity (FWC); A3 = 80 to 100 FWC) and three nitrogen fertilizers level (B1 = 0 kg N/ha, B2 = 100 kg N/ha, B3 = 200kg N/ha) with two replications. Lysimeters were set up at 80 cm depth on each irrigation and nitrogen fertilizers level (A, B, AxB). The water samples from lysimeters were taken three times during vegetation, after irrigation or precipitation. Maximum NO_3^- leaching out soil layer was 79.28 mg NO_3^- on plots irrigated with the highest amount of water (A3 = 80 to 100% FWC) and fertilized with maximum N (200 kg N/ha).

Keywords: Irrigation, N fertilizers, nitrogen leaching, lysimeters

1. Introduction

Nitrogen fertilization is one of the most important agricultural measures for achieving high and stable yields. If it is not properly conducted there is possibility of contamination of environment. While N provides large responses in crop yield and is an extremely valuable nutrient, it is the major nutrient of concern in water pollution, Davies [1]. The NO_3 leaching in to ground and surface water and accumulation in plant has harmful human effect [2]. Nitrate as N form is highly mobile and leachable. It has been as usual that excessive application of N leads to nitrate pollution of groundwater and surface water [3]. Nitrate leaching potentially depends on soil properties, crops and crop rotation, irrigation methods, management practices and climatic parameters [4, 5, 6, 7]. Irrigation practise should be planned and carried out in accordance to weather conditions and crop water requirements so that the loss of nitrate, water and soil pollution could be avoided [8].

2. Materials and methods

The research area is located at trial fields of Agricultural Institute in Osijek (45-46^{O}N - 18-19^{O}E), Osijek-baranja county, eastern Croatia. Trial was set up as split-plot method in year 2012. The main treatment is irrigation (A1= dry farming; A2 = 60 to 100% field water capacity (FWC); A3 = 80 to 100% FWC) and the second are three nitrogen fertilizers levels (B1 = 0 kg N ha^{-1}, B2 = 100 kg N ha^{-1}, B3 = 200 kg N ha^{-1}). The crop was irrigated with self moved sprinkler system. For the measuring of soil water content Watermark gypsum sensors (blocks) were used. The sensors were setup at two depths: 10-15 cm and 20-25 cm. The amounts of irrigated water applied thru irrigation system are presented in Table 1.

Table 1. Amount of irrigated water (mm)

	A2		A3	
	n	mm	n	mm
35*	5	175	7	245

*amount of water added in one irrigation; n = number of irrigation intervals; A2 = 60-100% field capacity; A3 = 80-100% FC

Nitrogen fertilization was conducted as follows: 2/3 of planned N quantities were added in autumn and before sowing (urea: 46% N) and the rest by two top dressings at early growth stages (calcium ammonium nitrate: 27% N). Area of sub plots was 78.4 m^2 (B = N fertilization) and 235 m^2 (A = irrigation practice). Lysimeters were set up at 80 cm depth on each irrigation and nitrogen fertilizers level (A, B, A x B) in two replicates. Lysimeters are open type: 80 cm wide x 80 cm long x 10 cm deep. The leachate was pumped by mechanical pump from Ebermayer's lysimeter reservoir 5 to 7 days after the rain or irrigation intervals; afterwards it was analyzed in laboratory in order to determine the content of nitrate (NO_3), nitrite (NO_2) and ammonium (NH_4^+) forms of nitrogen. Leachate sample where taken three times in vegetation period: May 30., September 5. and December 2. The rainfall (mm) and mean air temperature (^{o}C) during vegetation are presented with climate diagram according to H. Walter (Figure 1).

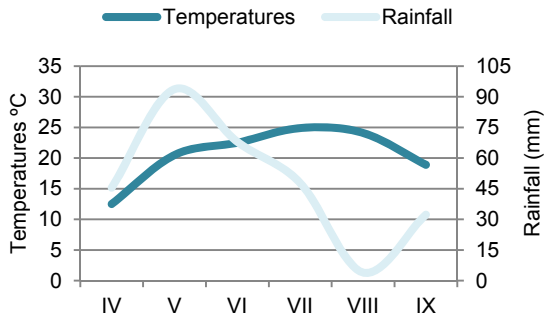

Figure 1. Walter climate diagram for vegetation 2012

In Figure 1. it can be noticed lack of rainfall during the vegetation season (June to September) which is the most important period for summer crops for water demands. Lack of rainfall should be restored with irrigation. Irrigation water is from well 37 m deep. Capacity of the well is 5 to 7 l sec^{-1}. The results of water analysis used for irrigation shown that water is suitable for irrigation with continual observing of water quality during vegetation period. Soil type at the trial field has been classified as eutric cambisol (Soil Survey Division Staff, 1993). Level of underground water was measured during the whole vegetation season (Figure 2). The level was below 280 cm during vegetation and had no impact on irrigation.

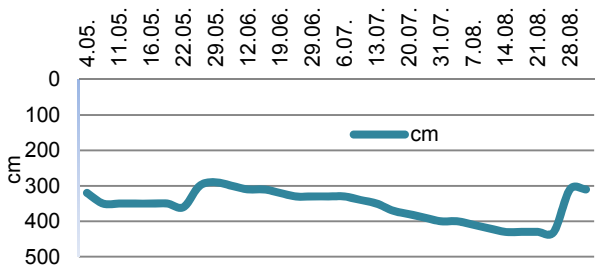

Figure 2. Level of underground water during vegetation 2012

The average values of selected physical properties of soil are presented in Table 2.

Table 2. Average values of selected physical properties of soil

	*Mechanical analysis (%)			P	AWC	AC	RAW
Depth (cm)	Sand	Silt	Clay	(%)	(%)	(%)	(%)
0-32	2,8	64,7	32,6	41,8	36,6	5,3	35,46
32-50	2,3	66,4	31,5	41,8	35,6	6,2	33,26
50-70	6,3	68,2	25,5	48,6	38,1	10,5	34,56
70-105	6,6	71,8	21,4	52,1	39,7	12,4	35,76
* = soil Survey Staff (1951, 1993); P = porous; AWC = available water capacity; AC = air capacity; RAW = readily available water							

3. Results and discussion

The minimal NO_3^- concentrations in water from lysimeters were measured at control plots of nitrogen fertilization as it was expected (B1 = 0 kg N ha^{-1}), 5.30 mg NO_3^-/l at A2B1 (May 30.). The maximal concentrations of nitrate in water were at plots fertilized with maximum amount of nitrogen fertilizers (B3 = 200 kg N/ha^{-1}). The maximal NO_3^- concentrations were 79.28 mg NO_3^-/l. The highest amount was measured at A3B3 plots as it was expected (September 3.).

During May NO_3^- concentration varied from 8.40 mg NO_3^-/l at A2B1 to 62.47 mg NO_3^-/l at A3B3. There was no percolate water at control irrigation plots (A1). Concentrations of nitrate above the maximum acceptable concentrations (MAC) were at A3B3 plots, meaning irrigated with maximum amounts of water (A3) and nitrogen fertilizers (B3). Nitrate concentrations for all plots are presented in Figure 3. In Republic Croatia MAC is below 50 mg NO_3^-/l.

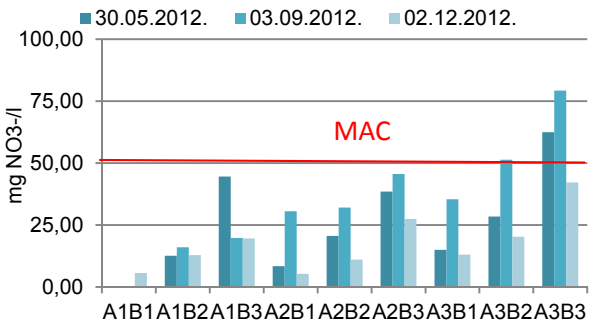

Figure 3. Nitrate concentrations for all plots (A, B, AxB)

In June NO_3^- concentrations were higher in compare to previous measurements in May. They varied from 15.98 mg NO_3^-/l at A1B2 plots to 79.28 mg NO_3^-/l at A3B3 plots. There was no percolate water at control irrigation plots (A1). Nitrate concentrations above the maximum acceptable concentrations (MAC) were at A3B3 plots (79.28 mg NO_3^-/l) but also at A3B2 (51.37 mg NO_3^-/l). In

September NO_3^- concentration varied from 5.30 mg NO_3^-/l at A2B1 to 42.20 mg NO_3^-/l at A3B3, although none of the concentrations were not above the MAC. Total amount of percolated NO_3^- in year 2012 is 6.54 kg NO_3^- ha^{-1} at B1 plots, 7.73 kg NO_3^- ha^{-1} at B2 and 31.59 kg NO_3^- ha^{-1} at B3 plots (Table 3).

Table 3. Monthly and yearly amount of leached nitrate (kg ha^{-1})

A	B	Year 2012 (kg NO_3^-/ha)			
		30.05.	03.09.	02.12.	Total
1	1	-	-	0,82	0,82
1	2	0,28	0,05	0,64	0,97
1	3	8,05	0,06	0,74	8,85
2	1	0,37	0,10	0,65	1,11
2	2	3,15	0,10	0,01	3,26
2	3	6,73	0,14	3,66	10,53
3	1	2,29	0,11	2,21	4,61
3	2	2,33	0,16	1,01	3,50
3	3	6,82	0,25	5,14	12,21
A1= dry farming; A2= 60-100% FWC; A3= 80-100 FWC; B1 = 0 kg N ha^{-1}; B2 = 100 kg N ha^{-1}; B3 = 200 kg N ha^{-1}					

There was positive and very strong and positive correlation between NO_3^-/ha and N fertilization (B) (r = 0.88**) during May. Very strong and positive correlation is between NO_3^-/ha and irrigation (A) (r = 08.2**). Both correlation are significant at **≤0.01. Results of correlation analysis are presented in Table 4, and regressions in Figures 4 and 5.

Table 4. Correlation analysis for amount of NO_3^-/ha and tested treatment

	A	B	A	B	A	B
	30. 05.		3. 09.		2. 12	
A	-		-		-	
B	0,00	-	0,00	-	0,00	-
NO_3^-/ha	n.s.	**0.88****	**0.82****	n.s.	n.s.	n.s.
A = irrigation; B = N fertilization; n = 18						

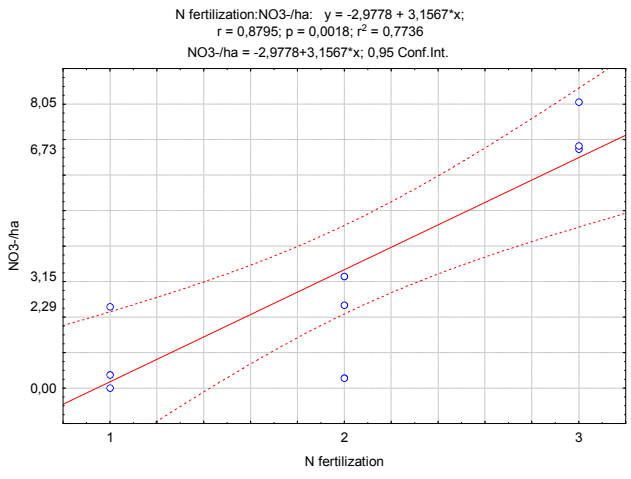

Figure 4. Regression for NO_3^-/ha and N fertilization

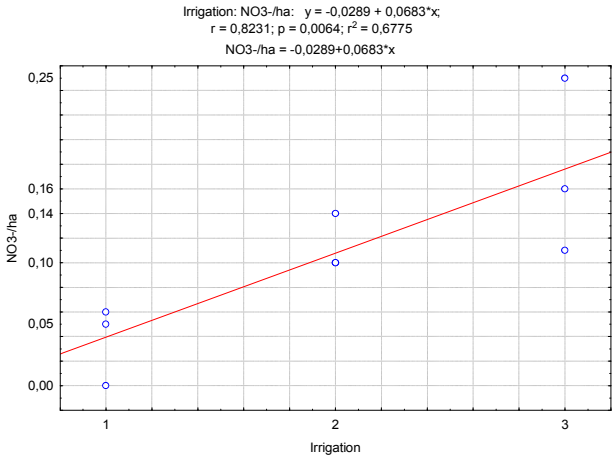

Figure 5. Regression for NO_3^-/ha and irrigation

4. Conclusion

The highest amount of nitrate concentration was at plots irrigated with the maximal water (A3= 80-100% FWC) and maximal nitrogen fertilizers (B3 = 200 kg N ha^{-1}. Concentrations above maximum acceptable concentrations were during May and September at plots fertilized with maximal N dosage and irrigation water. Correlation analysis showed very strong and positive connection between NO_3^- and N fertilizers and irrigation, depending of time of fertilization and irrigation.

5. Acknowledgments

The results published in this scientific paper are a part of research published as thesis of graduate student.

6. References

[1] Davies D. (2000): The nitrate issue in England and Wales, Soil Use Management, Vol. 16, pp 142-144

[2] Kristof K., Kampfl G., Heltai G., Nótas E., Algaidi A. (2007): Examination of NOx and CO2 production in agricultural soils. VI. Alps-Adria Scientific Workshop. Obervellach, Austria, 2007. 689-692

[3] Ajdary K., Singh D. K., Singh A. K. Khanna M. (2007): Modelling of nitrogen leaching form experimental onion field under drip fertigation. Agriculture water management, 89: 15-28.

[4] Nemeth T. (2006): Nitrogen in the soil-plant system, nitrogen balances. Cereal research communications 34(1). 61-64.

[5] Josipović M., Kovačević V., Šoštarić J., Plavšić H., Lović I. (2006): Influence of irrigation and fertilization on soybean properties and nitrogen leaching. Proceedings of 5th Alps-

Adria Scientific Workshop. 6-11 March, Opatija, Croatia.

[6] Nemcic Jurec J., Mesic M., Basic F., Kisic I., Zgorelec Z. (2007): Nitrate concentration in drinking water from wells at three different location in northwest Croatia. Proceedings of VI. Alps-Adria Scientific Workshop. Obervellach, Austria, 2007. 533-536.

[7] Bensa A., Rubinic V., Sever-Strukil Z. (2012): The effect of nitrogen fertilization on nitrate leaching under potato production. 3 international scientific symposium "Agrosym Jahorina 2012". pp 368-372

[8] Marković M., Josipović M, Šoštarić J., Brkić I., Krizmanić G., Plavšić H. (2011): Irrigation and N fertilization impact on maize yield (Zea Mays L.) and nitrogen leaching. Proceedings of 5. Croatian conference of Water, 18. – 21. 05. 2011., Opatija. 929-936.

CRANKSHAFT STRENGTH AND FATIGUE ANALYSIS

Ivan Žalac[1*], Dražan Kozak[1], Stipica Novoselac[2], Ivan Gelo[1], Željko Ivandić[1]

[1]Mechanical Engineering Faculty in Slavonski Brod, J. J. Strossmayer University of Osijek, Croatia
[2]AVL – AST d.o.o., Zagreb, Croatia
* *Corresponding author e-mail: izalac@sfsb.hr*

Abstract
This paper shows workflow for analyzing crankshaft strength and fatigue due to complex dynamic behavior. Crankshafts are subjected to multiaxial stress state with variable stress amplitudes during the lifetime. Such complex dynamic behavior needs to be analyzed with multi-body dynamic simulation (MBS). Crankshaft stress analyses with dynamic loadings were done with finite element method. Inputs for fatigue evaluation are stress tensors for critical crankshaft areas. Multiaxial high cycle fatigue evaluation were done with using basic unit load cases (BLCs), which are superimposed with linear static stress analysis load history, and with directly usage of displacements and rotations history from dynamic analysis. All main journals and crank pins have the same simple fillet radius. The aim of this paper is to check crankshaft fillets structural durability for infinite life. Results from both analyses are compared. Load history for nodes are displacements and rotations in time-domain for one engine cycle, i. e. 720°.

Keywords:
Crankshaft, fatigue, factors of strength, submodel

1. Introduction

In the internal combustion engine one of the most loaded parts is crankshaft. Conrod together with the piston, piston pin and a crank pin of the crankshaft translates the oscillatory motion of a piston to a rotational motion of a crankshaft. Main motions of a conrod and a piston in cylinder head are oscillatory motion and the rotation [1].
In this paper crankshaft strength and fatigue of the 4 cylinder inline diesel engine will be analyzed. Fatigue is a random process with extremely complex interactions and influences which vary between different materials and stress states. Fatigue life of similar specimens or structures under the same fatigue load spectrum can be significantly different [2]. Fatigue cracks initiate mostly at the surface of a structure material. Therefore, surface conditions are most significant for the fatigue behavior. In the crack initiation period, fatigue is a material surface phenomenon [2]. Combustion pressure in diesel engines can be two times higher than the combustion pressure of the gasoline engines. Pressure in these engines is growing with them. Parts of the crankshaft assembly needs to have optimized strength, stiffness and a mass. Crankshaft assembly is made from pistons, piston pins, conrods, crankshaft and a flywheel. All these parts are exposed to high loading amplitudes from combustion and inertial forces. Influence of these forces is reduced with the number of cylinders. On the other hand, torsional vibration sensitivity of a crankshaft increases with the crankshaft length [3]. For the strength analysis with superimposing of BLCs with linear static stress analysis load history there will be used the single web approach. These results will be compared with the results of strength for one single web which strength is analyzed with the dynamic load history.

2. Method

First analysis will be stress analysis with the dynamic load history based on dynamic MBS from AVL EXCITE Power Unit (PU) [4]. For dynamic analysis entire model of 4 cylinder inline diesel engine should be defined in EXCITE PU software workspace (Figure 1) and cylinder pressure loading should be applied.

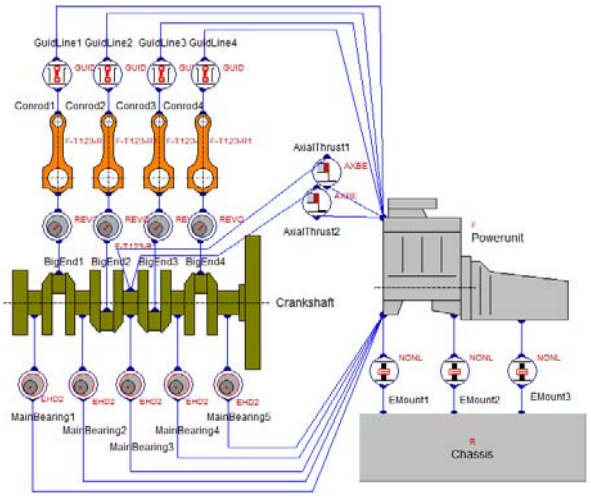

Figure 1. AVL EXCITE Power Unit workspace model

From earlier analyses of this type of engines it's well known that the most critical speed is at 3000 rpm, so only this speed will be used for this analysis. Also, it can be intended that most critical web will be web 8, due to its position next to the flywheel which has big inertia. Combustion pressure is highest for 3000 rpm's and it's shown on the Figure 2 [5].

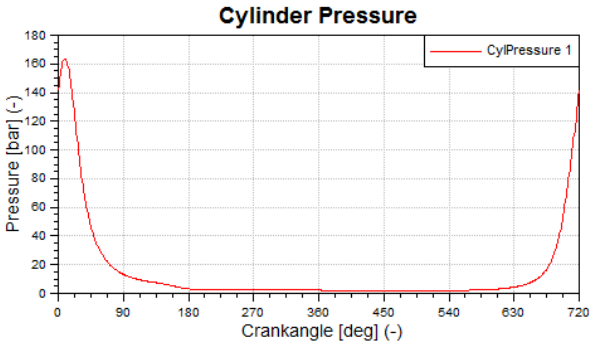

Figure 2. Cylinder pressure at 3000 rpm

Before doing dynamic analysis fillet geometry must be defined and it will be used in both types of analyses. Fillet shape and geometry is defined in the EXCITE PU tool Fillet Modeler. For these two analyses, the same simple fillet geometry will be used for all webs and for all of the main journal (MJ) and crank pin (CP) fillets. Figure 3 shows the shape and the geometry of fillets defined in the Fillet Modeler.

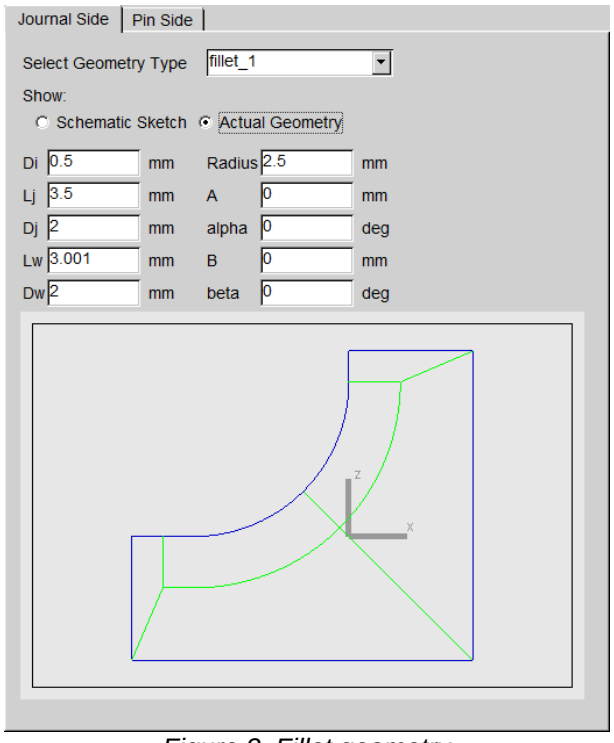

Figure 3. Fillet geometry

After defining the fillet shape, and sub-models geometry all fillet sub-models meshes will be automatically generated in the working directory of actual EXCITE PU case. Created sub-models will be only half of fillets circular direction (i.e. 180°) because maximum stress distribution due to dynamic loadings is always on one half. Also, with modeling only a half fillet for every CP and MJ sub-model calculation time and data size are reduced. For the second analysis BLCs tasks and the linear static stress analysis load history files should be prepared in EXCITE PU FEA tool. BLCs mean that one acting force has value of 1, and all other five basic unit loads have value of 0. Depending on the node position, is it on the CP or MJ side of the web, boundary conditions for the node on the opposite side of web are 0. Input files for BLCs analysis in Abaqus [6] and for the linear static stress analysis load history are written directly from the EXCITE PU FEA tasks.

Next step is Abaqus stress analyses. Fillets stress tensors for EXCITE Fatigue (fe-safe) [7] tool should be prepared. Material used for strength analysis is 42CrMo4 (SAE-4140), which is very often crankshaft material. This material according to DIN EN 10 083-1 (1996-10-00) [8] has the ultimate tensile strength of R_m = 1100 MPa, and the fatigue alternating strength for infinite life of σ_f = 495 MPa. Analysis with dynamic history of displacements and rotations were done in Abaqus and the safety factor is calculated in EXCITE Fatigue tool considering the surface roughness and taking the Neuber plasticity correction into account. Algorithm used for this analysis is stress – based Brown Miller Morrow algorithm.

Superimposing of BLCs results with load history files as a scaling factor was used in fatigue evaluation tool. Factor of strength (FOS) is calculated as a ratio between material fatigue strength and the load amplitude. If the loading amplitude is higher from the fatigue limit, FOS will have the value smaller than 1. That means that the crankshaft won't sustain defined number of cycles for infinite life, which is in this case $2N_f = 2 \cdot 10^7$ cycles [7].

First analysis was done for every 3° of a crank angle in 3rd engine cycle, which results with 240 steps. 3rd engine cycle was used because first two cycles are used for MBS dynamic simulation stability. Second analysis runs faster due to only 12 loading steps, 6 for unit load cases on CP side of the web, and 6 for the unit load cases on MJ side of the web. Figure 4 represents displacements and rotations load history for the node on web 8 MJ, and e.g. in the moment when maximum combustion pressure is applied at step 3 (green line) maximum displacement is approximately about -0.25 mm.

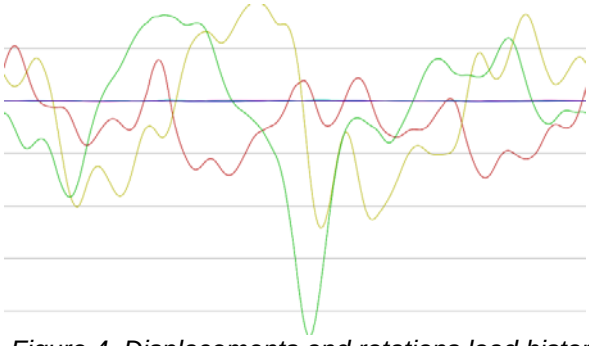

Figure 4. Displacements and rotations load history

3. Results

FOS results from the dynamic load history of web 1 MJ is shown on Figure 6 with minimum value of 1.34. Most critical node is also shown on this figure (node 800854). Comparison of these results with the results from the superimposed BLCs will be shown. Figure 5 represents the FOS of the fatigue analysis for dynamic load history.

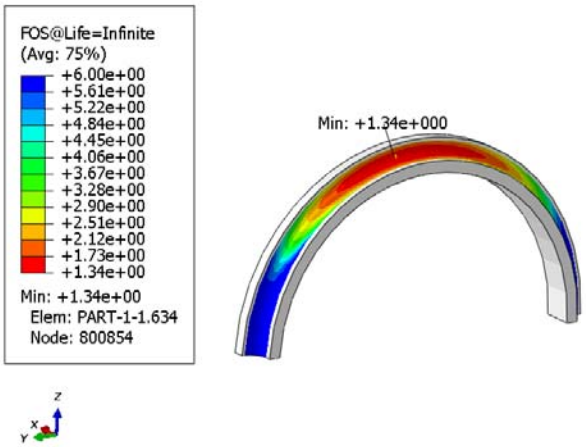

Figure 5. FOS for web 1 MJ from dynamic load history fatigue analysis

FOS from the superimposing of the BLCs (with the linear static stress analysis load history) for the web 1 MJ has the exactly same value as FOS from the dynamic load history. Critical node is the same, i. e. node 800854. Figure 6 shows the results from the fatigue analysis for this case.

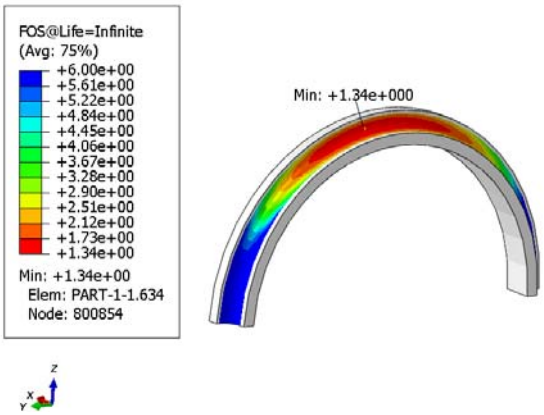

Figure 6. FOS for web 1 MJ from BLCs superimposed with linear static stress analysis load history with displacements and rotations

Lowest FOS in both cases appears around middle area of fillet sub-model. On all other CP and MJ sub-models critical node for all webs is also placed around the middle of fillet. FOS results for all webs are shown in table 1.

Table 1. FOS for all webs

	Web 1	Web 2	Web 3	Web 4	Web 5	Web 6	Web 7	Web 8
CP	1.06	1.44	1.13	0.92	1.34	1.16	1.19	0.86
MJ	1.34	1.64	1.31	1.59	0.91	1.23	1.47	1.03

4. Discussion

Fatigue analysis with superimposing of BLCs stresses with the linear static stress analysis load history gives the same FOS results in same critical node compared to the fatigue analysis with dynamic load history. Because analysis with BLCs has smaller number of steps, it takes less time to get the results of fatigue strength. Since the results for both cases are 100% the same, it is more appropriate to use method with superimposing of BLCs with linear static stress analysis load history.
Figure 7 shows the diagram with FOS values for all 8 webs.

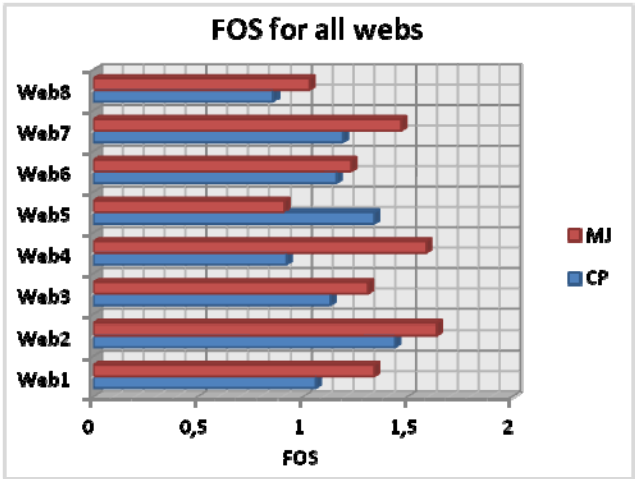

Figure 7. Diagram of FOS values for all webs

FOS results for all webs which are shown in Table 1 and Figure 7 are not sufficient for the crankshaft. Some of these results are lower than 1, which means that crankshaft cannot reach infinite life and that fatigue cracks will appear in finite life regime. Most of the fillets does not have sufficient fatigue strength for the loads from combustion pressure and inertial forces on 3000 rpm. More complicated shape of fillets should be used. Higher quality surface treatment also should be used to reduce the local stress concentrations and to improve fillets fatigue life for all webs.
Web with the smallest FOS is web 8 (FOS value of 0.86 for CP and 1.03 for MJ), what is expected, because this web is placed next to the flywheel in crankshaft assembly. Due to flywheels big moment of inertia compared to crankshaft inertia, gyroscopic effect are dominant which lead to very complex dynamic behavior with high stress amplitudes. It could be noticed that FOS for web 4 and web 5 also have the lower value than other

webs (except web 8). This is caused by the earlier mentioned crankshaft sensitivity for torsional vibration. For these types of crankshaft these webs are not critical. For the longer crankshafts torsional sensitivity will increase and fillets on these two webs would have smaller FOS values.

5. Conclusion

From these analyses following conclusions were made. Results of both analyses give the same results for FOS and critical node. Due to shorter evaluation time basic load cases method is very appropriate to use for design of engines from the concept phase. Used fillets in this analysis are simple and more complex and realistic fillets with higher quality of surface treatment should be used. Size influence and influence of statistics were not taken into account. Fatigue is an random process, and therefore influence of statistics in way of survival probability and cyclic material range of dispersion have significant influence which need to be taken into account for final and more detailed analyses.

6. Acknowledgement

Special thanks to the company AVL – AST d.o.o. Zagreb, Croatia for using their software and hardware resources with technical support during the work on this paper and master diploma thesis.

7. References

[1] MAHLE Gmbh; *Cylinder Components*; Stuttgart; Vieweg + Teubner; 2010
[2] Schijve, J.; *Fatigue of Structures and Materials*, 2nd edition, Springer, Netherland, 2009.
[3] Novoselac S.; *Numerical analysis of dynamic behavior of crankshaft of the big intermediate stroke IC engine*; Mechanical Engineering Faculty in Slavonski Brod, Slavonski Brod, 2012., 130 pages
[4] AVL Workspace v2013 - AVL EXCITE v2013, AVL List GmbH, Austria
[5] AVL EXCITE Power Unit v2013 installation example; 102 I4_Demo, AVL List GmbH, Graz, Austria
[6] Abaqus/CAE 6.12-3, Dassault Systems Simulia Corp., Providence, RI, USA
[7] EXCITE Fatigue (fe – safe) 6.3; Safe Technology Inc., 2012
[8] FKM - Guideline; *Analytical strength assessment of components in mechanical engineering,* 5th revised edition, English version, VDMA Verlag GmbH, 2003.

LEVEL OF INNOVATION IN CROATIA IN RELATION TO COUNTRIES IN THE REGION

A. Kulaš[1*], S. Knežević[1] and Z. Mirosavljević[2]

[1]College of Slavonski Brod, Slavonski Brod, Croatia
[2]Hrvatska elektroprivreda d.d., Slavonski Brod, Croatia
* *Corresponding author e-mail: anita.kulas@vusb.hr*

Abstract
Creativity is the essential source of all invention and innovation. It is derived from imaginative thought rather than from rational thought and it creates change. Innovation is closely associated with and flows out of creativity. Innovation represents a wide range of activities to improve firm performance, including the implementation of a new or significantly improved product, service, distribution process, manufacturing process, marketing or organizational method.
The aim of this work is to analyze the level of innovation in Croatia in relation to countries in the region.

Keywords:
Creativity, innovation, intellectual property, level of innovation

1. Introduction

The business world of the next several decades will be significantly different from the business world of the past. The changes underway, including demand for skilled talents, will provide the catalyst required to create a new way of working and challenge many of the fundamental assumptions that underlie the structure and design of today's organizations. It will need a new kind of leadership capability to reframe dilemmas, reinterpret options, and reform operations and to do so continuously. Recognizing the importance of creativity and innovation increasingly come to express in all human activities, especially in the field of management.

2. Fostering creativity and innovation

Knowledge and its use became a determining parameter of a new type of growth and development. It is regarded as a basic resource of modern organizations and the fundamental source of power. Organizations based on knowledge achieve competitive advantage and a continuous improvement. Only knowledge can create innovation, can improve production and supply and can maintain qualitative relationship with the market. Today, modern society search for creativity and innovation.

Creativity is based on the ability to combine previously disparate elements in new ways, which implies a need for a boarder focus and varied interests. Creativity arises through the confluence of the following three components: knowledge, creative thinking and motivation. Knowledge presents all the relevant understanding an individual brings to bear on a creative effort. Creative thinking relates to how people approach problems and depends on personality and style of thinking. Motivation is generally accepted as a key to creative production, and the most important motivators are intrinsic passion and interest in the work itself.
The way how to increase creativity uses multiple idea-getting techniques, including brainstorming, divergent thinking methods and other instructional approaches.
Innovation is the conversion of ideas and possibilities into tangible new products, processes, and opportunities. Innovation is required to create true value and to implement changes in how things are done. Innovation does not occur in isolation. It is driven by both creativity and learning [1]. The benefits of innovation occur in all aspects of the profit/loss statement: innovators drive additional sales volume, achieve price premiums and reduce costs through process improvements. In addition to the financial benefits, innovation goes hand-in-hand with sustainable development initiatives, as both require progressive leadership and an appetite for change, combined with a tolerance of experimentation and some risk.

3. Types of innovation

Innovation can basically be [2]:

1. a product innovation (e.g. new goods or services put on sale);
2. a process innovation, which changes the way a given good is produced within the firm or across a supply chain;
3. a behavioral innovation, when an organizational routine is replaced with new ones, including the main features of its "business model".

Quite often, the innovation turns out to be a mix of all three "pure" categories, as with the case of the introduction of a new product that require new productive competences and changes in the organization.

Innovation can also be:

1. a radical innovation (major novelty, a new view at old problems, knowledge is diversified with unprecedented use of analogy and tools developed in other industries, typical people are critical individualists or mission-oriented teams, organizations are outsiders or new entrants) and
2. an incremental innovation (minor improvements in existing products and processes, determination in solving problems within a given framework, knowledge is specific, people are front-line workers, organization is incumbent).

Top management holds the power to set the tone and thus plays a key role in whether a company will be innovative or not. Management must ask for technical innovation, demand it, encourage it, stimulate it, fund it and reward it. Management must want and be committed to creativity and be willing to sacrifice short term results for innovation.

4. Protecting intellectual property rights in a global economy

Many forms of protection of material goods have been developed during the history of human civilization, such as the methods of hiding, closing, keeping and monitoring. But the situation is different with the products of human mind. „Products of human mind are non-material goods, the value of which lies in their reproduction, use and presentation to other people, so they cannot be protected by hiding, closing, or other measures of physical protection [3].“ To protect that kind of products a corresponding system of legal protection of intellectual property has been developed.

Intellectual property includes industrial property rights and copyright and related rights.

„Copyright is the exclusive right of authors to dispose of their literary, scientific or artistic works, and works covering other fields of creativity; related rights relate similarly to the rights of performers, the producers of phonograms and broadcasting organizations [3].“

Industrial property includes patents, trademarks, industrial designs, geographical indications and designations of origin and topographies of semiconductor products.

Particular characteristics of a product may be protected by one or several different forms of intellectual property, which supplementing each other.

„A patent is an exclusive right granted for an invention – a product or process that provides a new way of doing something, or that offers a new technical solution to a problem. Patents provide incentives to individuals by recognizing their creativity and offering the possibility of material reward for their marketable inventions [4].“ Thereby, these incentives encourage innovation which improves the quality of human life. Patent protection is granted for a limited period, generally 20 years. But, it should be kept in mind that the process of patenting, especially abroad, requires pretty high expenses. In fact patent protection is being valid only on the territory of the country in which such right has been granted. Therefore the patents granted by the competent office of country to domestic and international applicants are valid only on the territory of that country. Patent protection on territories of other countries may be realized, first, by filing single application to the competent office of each country on which territory protection is required, second, by filing a uniform international application under the Patent Cooperation Treaty (PCT) for the contracting states, third, filing an application for the European patent with one of the competent offices of the EPO on one of the regional patent systems for member states of the European patent organization and current extension states [5].

A trademark is a sign that serves the specific and primary purpose of identifying the goods or services of a producer, thus allowing the consumers to distinguish goods or services of one producer from those of another [6]. Name, logo, emblem, label, or other distinctive characteristics of products and / or services it is possible to protect as the trademark. “Trademark protection ensures that owners of marks have the exclusive right to use them to identify goods or services, or to authorize others to use them in return for payment [4].“ Almost all countries all over the world register and protect trademarks. In fact, each national or regional office maintains a Register of Trademarks containing full application information on all registrations and renewals. To avoid the need to register separate applications with each national or regional office, WIPO administers an international registration system for trademarks. Trademark protection for the entire territory of the European Union may be realized by filing an application for a Community Trade Mark (CTM) directly to the competent office of the EU: Office for Harmonization in the Internal Market (OHIM) or through the Madrid System for the International Registration of Marks [7]. „From the moment of accession of the Republic of Croatia to the full membership of the European Union, the legal effects of all registered CTM and CTM applications will be automatically extended to the territory of the Republic of Croatia [8].“ Trademark protection is granted for 10 years, but it can be extend unlimited on the period of next 10 years.

Design is external appearance of some product or object. The design is what makes a product attractive, appealing and desirable. This contributes significantly to the sale of a product and increases its commercial value. The industrial

design is an industrial property right. Protected industrial design provides its owner the exclusive right to use or produce, supply, marketing, and import or export of products in which the industrial design is contained or to which the industrial design is applied. The owner of the industrial design may authorize other persons to use its design by providing temporary license or be fully transferable to another person [9]. Industrial designs protection is obtained only on the territory of the country in which such right has been granted. Protection of designs in the territories of other countries may be obtained by filing a single application with the competent office of each country on which territory protection is requested, by e-filing a uniform international application using the Hague System for the International Registration of Industrial Designs directly with the World Intellectual Property Organization (WIPO) (Croatia is a Member of the 1999.) and for the entire territory of the European Union by filing an application or e-filing for a Registered Community Design (RCD) directly to the competent EU Office: Office for Harmonization in the Internal Market (OHIM) or under the Hague System for the International Registration of Industrial Design. „Following the accession of Croatia to the full membership of the European Union, it will be possible to file a RCD application through the State Intellectual Property Office of the Republic of Croatia [10].“

Industrial designs are what make an article attractive and appealing; hence, they add to the commercial value of a product and increase its marketability.

5. Level of innovation in Croatia in relation to countries in the region

The following analysis shows the level of innovation in Croatia in relation to countries in the region for a period of 15 years. Figure 1 shows the level of registered patents in Croatia and neighboring countries.

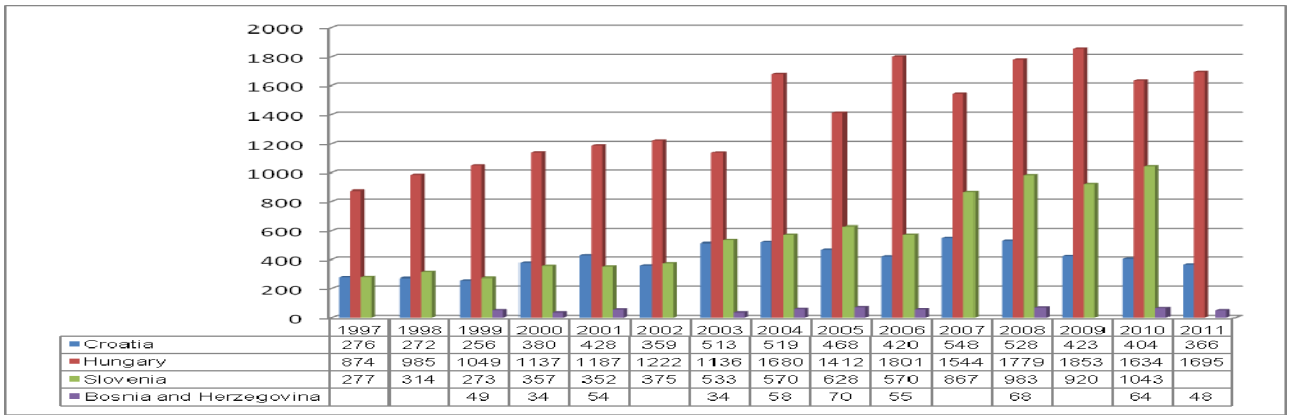

	1997	1998	1999	2000	2001	2002	2003	2004	2005	2006	2007	2008	2009	2010	2011
Croatia	276	272	256	380	428	359	513	519	468	420	548	528	423	404	366
Hungary	874	985	1049	1137	1187	1222	1136	1680	1412	1801	1544	1779	1853	1634	1695
Slovenia	277	314	273	357	352	375	533	570	628	570	867	983	920	1043	
Bosnia and Herzegovina			49	34	54		34	58	70	55		68		64	48

Figure 1. Level of registered patent in Croatia in relation to countries in the region [11]

The highest number of registered patents was in Hungary. During the period of 15 years, the number of patents in Hungary has doubled but in Slovenia has increased as much as 4 times. The number of registered patents in Croatia has varied during the period. The highest was in 2007. The minimum number of registered patents has recorded in Bosnia and Herzegovina.

The following is Figure 2 that shows the level of registered trademarks in the target countries.

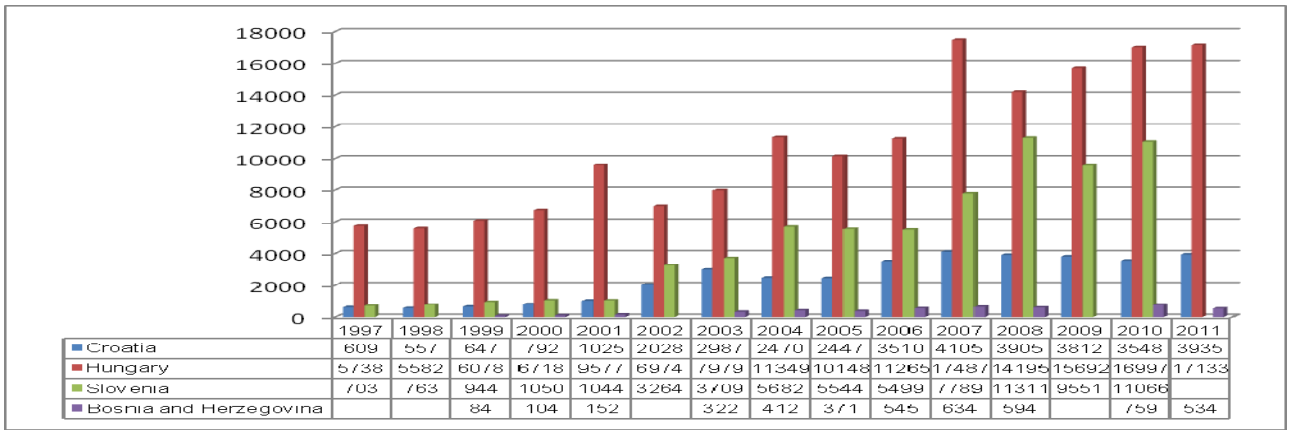

	1997	1998	1999	2000	2001	2002	2003	2004	2005	2006	2007	2008	2009	2010	2011
Croatia	609	557	647	792	1025	2028	2987	2470	2447	3510	4105	3905	3812	3548	3935
Hungary	5738	5582	6078	6718	9577	6974	7979	11349	10148	11265	17487	14195	15692	16997	17133
Slovenia	703	763	944	1050	1044	3264	3709	5682	5544	5499	7789	11311	9551	11066	
Bosnia and Herzegovina			84	104	152		322	412	371	545	634	594		759	534

Figure 2. Level of registered trademark in Croatia in relation to countries in the region [11]

In the same period, all the countries have recorded major increase, even up to 15 times. And here, the highest number of registered trademark has recorded in Hungary.

Below is a figure that shows the level of registered industrial design.

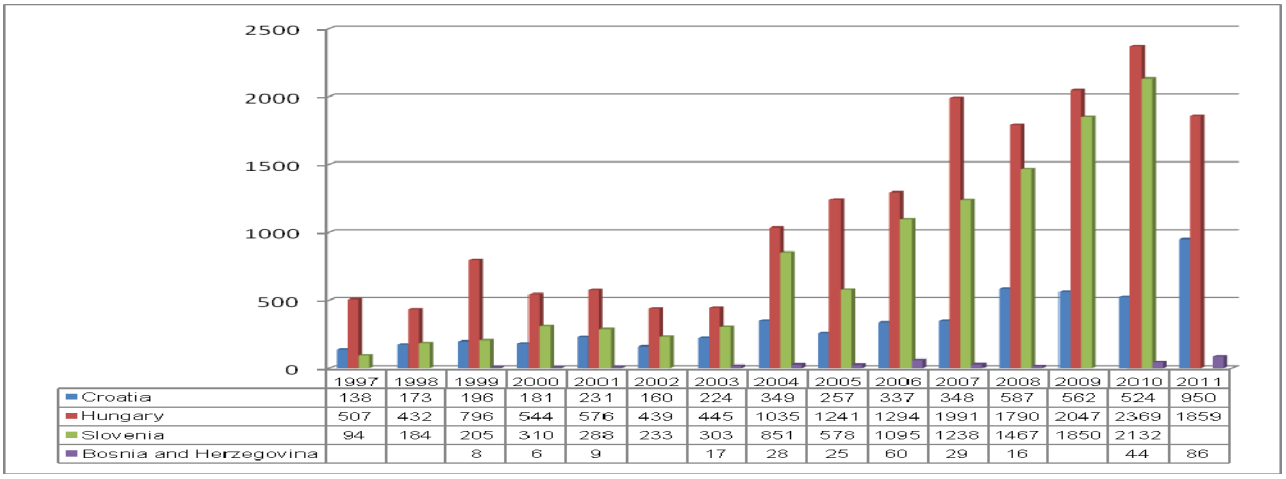

	1997	1998	1999	2000	2001	2002	2003	2004	2005	2006	2007	2008	2009	2010	2011
Croatia	138	173	196	181	231	160	224	349	257	337	348	587	562	524	950
Hungary	507	432	796	544	576	439	445	1035	1241	1294	1991	1790	2047	2369	1859
Slovenia	94	184	205	310	288	233	303	851	578	1095	1238	1467	1850	2132	
Bosnia and Herzegovina			8	6	9		17	28	25	60	29	16		44	86

Figure 3. Level of registered industrial design in Croatia in relation to countries in the region [11]

Figure 3 shows that during the observed period, level of registered industrial design in Croatia has increased nearly 7 times. However, the highest increase was recorded in Slovenia, whose number increased to a whopping 22 times. According to the data it is evident that the increase of registered industrial design in Bosnia and Herzegovina was to about 8 times.

6. Conclusion

Learning, creativity, and innovation provide organizations to survive and thrive. However, their value is often minimized when their potential is viewed in isolation. In today's economy, success often requires relentless attention to making effective changes and improvements. So, organizations must actively look for opportunities to create synergistic value by combining all three. Innovation in a business is more an imperative for survival than an option. Once you come to innovation, the issue of how to protect innovation as an intellectual property comes up. Intellectual property rights are like any other property right. Intellectual property rights reward creativity and human endeavor, which fuel the progress of humankind. So, it is very important to protect them. Many countries all over the world have intellectual property protection systems. But, with the increasing globalization of trade and rapid changes in innovation, it is important to extend them. WIPO plays a key role in helping these systems to develop through treaty negotiation.

Analysis of the level of innovation in Croatia in relation to countries in the region has showed that the most innovative country is Hungary, followed by Slovenia and Croatia. Bosnia and Herzegovina has a low level of innovation.

7. References

[1] http://www.banffcentre.ca/leadership/library/pdf/creating_value.pdf [Accessed: 28-Aug-2013]
[2] http://www.economicswebinstitute.org/glossary/innovate.htm [Accessed: 28-Aug-2013]
[3] http://www.dziv.hr/en/intellectual-property-protection/about-ip/ [Accessed: 27-Aug-2013]
[4] What is Intellectual Property?, World Intellectual Property Organization, WIPO Publication No. 450(E), ISBN 978-92-805-1555-0, http://www.wipo.int/export/sites/www/freepublications/en/intproperty/450/wipo_pub_450.pdf [Accessed: 27-Aug-2013]
[5] http://www.dziv.hr/en/intellectual-property-protection/patents/international-protection/ [Accessed: 27-Aug-2013]
[6] http://www.china-iprhelpdesk.eu/en/solution-centre/trademarks [Accessed: 27-Aug-2013]
[7] http://www.dziv.hr/en/intellectual-property-protection/trademarks/international-protection-of-trademarks/ [Accessed: 27-Aug-2013]
[8] http://www.dziv.hr/en/intellectual-property-protection/trademarks/trademark-protection-in-eu/ [Accessed: 27-Aug-2013]
[9] http://www.dziv.hr/hr/intelektualno-vlasnistvo/industrijski-dizajn/ [Accessed: 27-Aug-2013]
[10] http://www.dziv.hr/en/intellectual-property-protection/industrial-designs/international-protection-of-designs/ [Accessed: 27-Aug-2013]
[11] World Intellectual Property Organization (WIPO), Patents, Statistics, Intellectual Property Statistics, Statistical Country Profiles

IMPACT OF THE CUTTING PARAMETERS ONTO MICROHARDNESS OF AUSTENITIC STAINLESS STEEL SURFACE LAYER

Grzegorz Krolczyk[1], Stanislaw Legutko[2*], Piotr Nieslony[3] and Maksymilian Gajek[1]

[1]Faculty of Production Engineering and Logistics, Opole University of Technology, Poland
[2]Faculty of Mechanical Engineering and Management, Poznan University of Technology, Poland
[3]Department of Manufacturing Engineering and Production, Opole University of Technology, Poland
* *Corresponding author e-mail: stanislaw.legutko@put.poznan.pl*

Abstract
The objective of the investigation was to determine the technological surface layer (TSL) microhardness of 1.4541 austenitic stainless steel after turning of coated carbide tool point. The microhardness of TSL for various cutting speeds and feed of the turning process were compared. The study was conducted within a production facility during production of parts for electric motors and submersible pumps.

Keywords:
technological surface layer, microhardness, austenitic stainless steel, coated inserts, machining

1. Introduction

The austenitic stainless steels structure is a combination of good mechanical properties and good corrosion resistance. To utilize the useful properties of austenitic microstructure is necessary to study surface integrity of machined stainless steels. Surface integrity can be defined as a set of various properties (superficial and in-depth) of an engineering surface that affect the performance of this surface in service [1]. Achieving the desired surface quality is of great importance for the functional behaviour of a part [2]. To ensure better surface integrity, special attention must be paid to when choosing cutting parameters [3 – 6], tool material and geometry [7, 8] and tool coatings [9]. Surface integrity is important for the components adapting to high thermal and mechanical loads during their applications [10, 11]. One from surface integrity physical parameters is microhardness. According to Solomon and Solomon [12] in the case of materials with austenitic structure plastic deformation can induce transformation of austenite into martensite. The material properties of austenitic stainless steel is highly dependent on the transformation of the FCC system (Face Cubic Centered) in BCC system (Body Centered Cubic). The transformation may occur during the heat treatment or under the influence of mechanical deformation [13]. According to Kundrak et al. [14] turning performed at high speed is an intensive technology in terms of the heat generated in the process. The temperature of the workpiece material in the cutting edge area may reach the transformation temperature. Sasahara [15] demonstrated, using 0.45% C steel test material that, the feed rate did not affect the surface hardness for values between 0.05 and 0.4 mm/rev. Ezugwu et al. [16] demonstrated, that the cutting tool geometry in machining nickel-based alloys represents an important parameter in tool life and in the quality of the machined surface. Ezugwu and Tang [17] have found that machined surface obtained with the rhomboid shaped insert has a higher microhardness as compared to the round inserts. Javidi et al. [18] showed, that plastic deformation of the grain boundaries was found in the subsurface layer. They also confirmed that no significant variation in hardness was observed beneath the machined surface obtained by different cutting conditions. The study of surface parameters and cutting force in the turning of austenitic steels described Fernández-Abia et al. [19]. In their research did not provide the results of the influence of machining on microhardness of TSL (Technological Surface Layer). Such studies for 1.4306 steel presented Yan et al. [20], but without research the impact of cutting speed on microhardness of TSL.
This paper focuses on research problems related to the microhardness after turning by coated carbide tools. The main purpose of this study was to determine the effect of cutting speed and feed as a key process factor in controlling surface microhardness.

2. Machined material, cutting tool specification, microhardness measurements

The machined material was 1.4541 (DIN EN 10088-1) steel with a austenitic structure. The elemental composition of the machined material and technical details of the cutting tools are given in tables 1 and 2, respectively.

Table 1. Chemical composition of 1.4541 austenitic stainless steel

Element	C	Si	Mn	P max	S	Cr	Ni	Others
[%] at.	0,08	1,00	2,00	0,045	0,015	17,0 19,0	9,0 12,0	Ti:5xC to 0,7

Table 2. Cutting tool specification

Tool	Substrate	Coatings
MM 2025	Hardness: 1350 HV3 Grade: M25, P35	Ti(C,N) - (2 μm) (Top layer) Al2O3 - (1.5 μm) (Middle layer) TiN - (2 μm) (Bottom layer) Coating technique: CVD

Cutting tool inserts of TNMG 160408 designation clamped in the tool shank of ISO-MTGNL 2020-16 type were employed. Based on the industry recommendations a range of cutting parameters were selected: v_C = 50–150 m/min, f = 0,2 – 0,4 mm/rev, a_p = 1 mm. The study was conducted within a production facility. The research program was carried out on a lathe CNC 400 CNC Famot Famot - Pleszew plc.

The measurements of microhardness have been performed into the depth of material along a straight line perpendicular to the machined surface (radially). In the testing schedule, it was assumed that microhardness would be measured down to the depth for which hardness comparable to that of the core is obtained. The first point of microhardness measurement was located at the distance of up to 20 μm from the machined surface, depending on the profile hump or caving. The second measurement has been performed at the depth of 40 μm, the successive ones have been performed at 20 μm intervals till the hardness of the core was obtained. The microhardness measurements were effected by MHV-2000. The load of an intender was adopted in accordance with the standard PN-EN ISO 6507-1. The standard limits the time of the load increase until the required force F is obtained to 15 s. Therefore, the safe time of 10 s and the intender's load 0.49 N were assumed.

3. The experimental results and analysis

The TSL characteristics depends on numerous factors, technological parameters, stereometry and micro-geometry of a cutting edge, among others. In the process of the surface layer formation, the speed of machining is very important. It is a parameter which significantly determines the intensity of heat generated in the machining zone. It can be assumed that heat penetrating the surface layer of the machined material will influence the functionality of its surface, microhardness, among others. Therefore, the research focused on establishing an influence of the machining speed on the TSL microhardness.

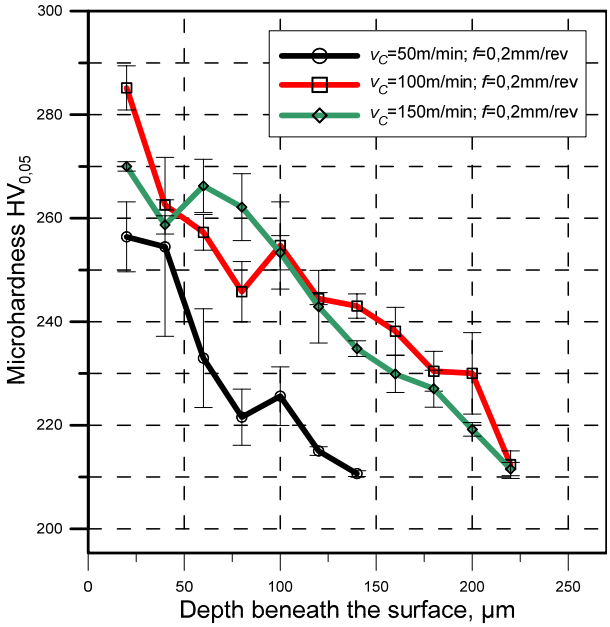

Figure 1. An influence of the cutting speed on the microhardness of surface layer after turning austenitic stainless steel (f = 0,2 mm/rev, a_p = 1 mm, dry cutting)

The findings of the research into an influence of the machining speed on the microhardness of the studied austenitic steel surface layer are presented in Figure 1. Turning took place with the use of an edge of cemented carbide covered with a coating with an intermediate ceramic layer, for the feed f = 0.2 mm/rev and the constant depth of machining a_p = 1 mm; dry machining. The results are presented in the form of graphs, as the arithmetic mean of three measurements of microhardness with standard deviation. The biggest values of microhardness were obtained for the speed v_C = 100 m/min. They were obtained for the layer closest to the machined surface, namely at the depth of up to 20 μm. In this case, microhardness was over 280 $HV_{0.05}$. For the speed of machining 150 m/min, the microhardness obtained in this area was by 15% smaller on average, whereas for

v_C = 50 m/min, the observed microhardness was smaller by 30%. Alongside departing from the surface, the TSL microhardness decreases, in the analyzed case reaching the hardness of the core at the depth of about 140 µm for v_C = 50 m/min and 220 µm for v_C = 100 and 150 m/min. In Figure 1, we can observe a monotonic and smooth decrease in the TSL microhardness values for v_C = 150 m/min, whereas microhardness for the remaining analyzed speeds of machining (v_C = 50 and 100 m/min) characterizes with a sharp angle of the drop of values to the depth of 60 µm. The reason for that may be a non-uniform deformation of the material, and thus the strengthening of austenite in the subsurface layer.

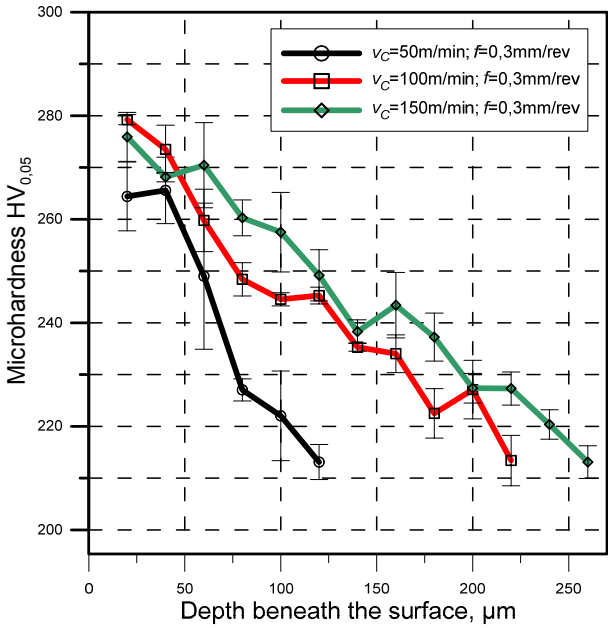

Figure 2. An influence of the cutting speed on the microhardness of surface layer after turning austenitic stainless steel (f = 0,3 mm/rev, a_p = 1 mm, dry cutting)

Figure 2 presents the results of the measurements of TSL microhardness as a function of machining speed after turning with the edge MM 2025, for the feed f = 0.3 mm/rev and the constant depth of machining a_p = 1 mm, also for the machining without the use of a cooling and lubricating substance. The biggest values of microhardness were obtained for the speed v_C = 100 and 150 m/min – at the level of 275 HV0,05, whereas TSL microhardness for a smaller speed of machining shapes at the level of about 265 $HV_{0,05}$. Alongside an increase in the speed of machining, microhardness after turning steel 1.4541 for the feed f = 0.3 mm/rev goes up, reaching hardness of the core at the depth of 120 µm for v_C = 50 m/min, 220 µm for v_C = 100 m/min and 260 µm for v_C = 150 m/min. For the speed of machining v_C = 100 and 150 m/min, we can observe a monotonic decrease in the value of TSL microhardness, whereas in case of the speed of machining v_C = 50 m/min, there are considerable fluctuations of changes in the values and their sharp drop. Bigger depth of hardening for an increase in the speed of machining is probably caused by a higher temperature in the machining process. Alongside an increase in the machining speed a bigger amount of heat is generated, and the heat penetrates the machined material deeper.

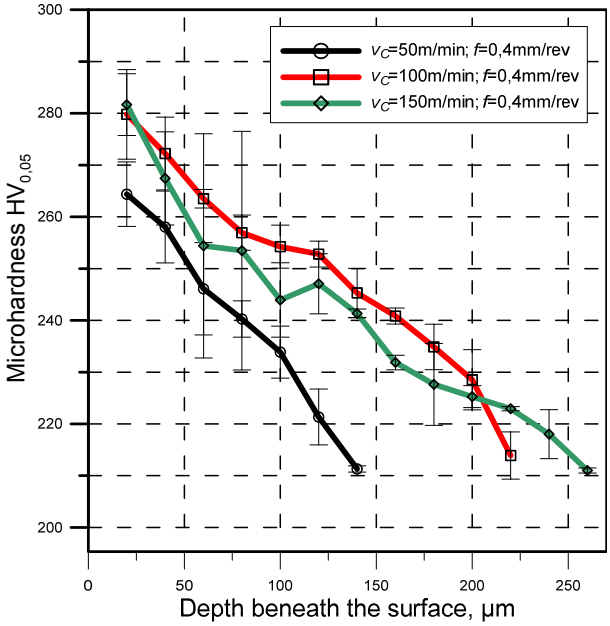

Figure 3. An influence of the cutting speed on the microhardness of surface layer after turning austenitic stainless steel (f = 0,4 mm/rev, a_p = 1 mm, dry cutting)

Another analyzed case illustrated in Figure 3 concerns the results of the TSL microhardness measurements for the variable speed of machining and constants f = 0.4 mm/rev and a_p = 1 mm. For the biggest studied feed, the depth of hardening shapes at the level of 140 – 260 µm, namely the range of the depth of hardening depth shapes in a similar way like for the average values of the analyzed feeds. The biggest average values of microhardness were obtained for the speed v_C = 100 and 150 m/min and they were equal to 280 $HV_{0,05}$. On the other hand, the smallest values of microhardness 265 $HV_{0,05}$ were obtained for the speed of machining v_C = 50 m/min. For the studied speeds of machining we can observe a monotonic decrease in the value of TSL microhardness. For the analyzed values of machining speed and the biggest feed, we can observe big fluctuation of changes in the biggest values of TSL microhardness within the range from the surface of the machined material to 80 µm.

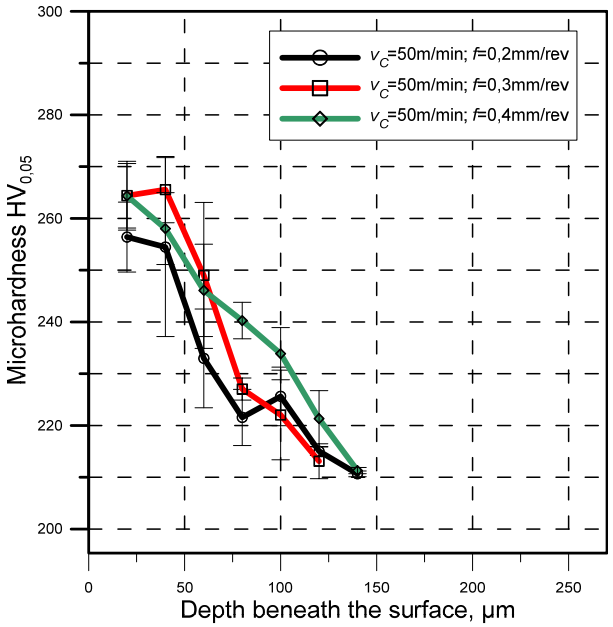

Figure 4. An influence of the feed on the microhardness of surface layer after turning austenitic stainless steel (v_C = 50 m/min, a_p = 1 mm, dry cutting)

Figure 4 presents an influence of feed on TSL microhardness for constant speeds and depths of machining (v_C = 50 m/min, a_p = 1 mm). The biggest values of microhardness were obtained for the feed f = 0.3 and 0.4 mm/rev, the smallest ones for f = 0.2 mm/rev. The microhardness values fluctuate within the range from 250 to 270 $HV_{0,05}$. The value of the hardening depth for constants v_C = 50 m/min and a_p = 1 mm for the analyzed feeds is 140 µm.

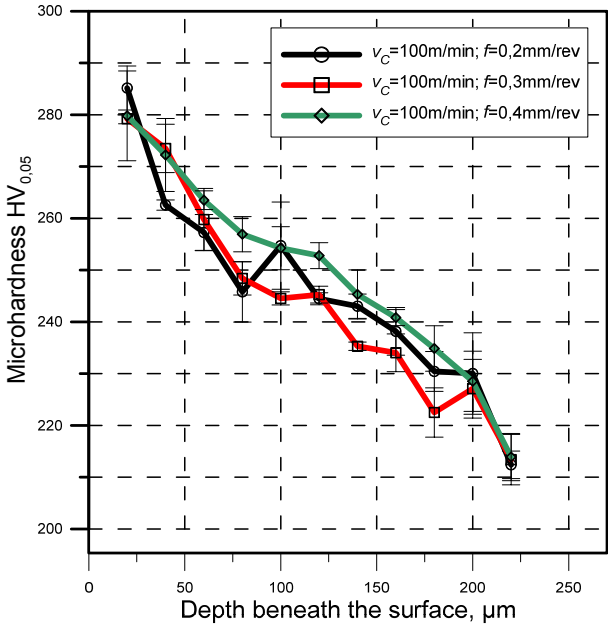

Figure 5. An influence of the feed on the microhardness of surface layer after turning austenitic stainless steel (v_C = 100 m/min, a_p = 1 mm, dry cutting)

Another analyzed case presented in Figure 5 concerns the measurements of TSL microhardness for variable feed and constants v_C = 100 m/min and a_p = 1 mm, analogously to the previously analyzed cases for machining without the use of a cooling and lubricating substance. For the discussed feeds within the range from 0.2 to 0.4 mm/rev no significant changes in TSL microhardness were observed, that is the depth of hardening for all the studied feed values was 220 µm. The initial measured value of microhardness situated under the machined surface of the studied austenitic steel is within the range from 270 to 290 $HV_{0,05}$. For the analyzed value of feed we can observe a monotonic and moderate drop of the value of TSL microhardness. Moreover, the results of the presented experiments characterize with small fluctuations of changes, which is proven by the standard deviation values. In the analyzed case, we can observe the lack of an influence of feed on TSL microhardness. There is no influence on the depth of hardening or the biggest value of microhardness $HV_{0,05}$.

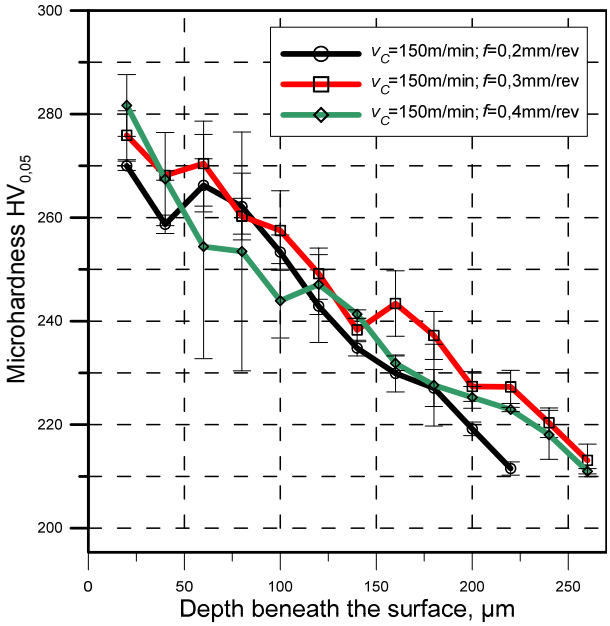

Figure 6. An influence of the feed on the microhardness of surface layer after turning austenitic stainless steel (v_C = 150 m/min, a_p = 1 mm, dry cutting)

The last analyzed case illustrated in Figure 6 concerns the measurements of TSL microhardness for variable feed and constants v_C = 150 m/min and a_p = 1 mm. For the biggest studied speed of machining, the microhardness values do not basically differ in the angle of the drop of values of microhardness $HV_{0,05}$ and the depth of hardening shapes on the similar level as for the value v_C = 100 m/min, namely at the level of 220 – 260 µm. The average value of the biggest

microhardness fluctuates as for v_C = 100 m/min within the range from 270 to 290 $HV_{0,05}$.

4. Conclusion

On the basis of the results of the experiments presented in the work, we can formulate the following conclusions:

1. An increase in the speeds of machining within the range from 50 to 150 m/min brings about an increase in the value of the maximum TSL microhardness of 1.4541 steel to 5% but raises the depth of hardening by an average value of 83%.
2. The depth of TSL hardening after turning austenitic steel 1.4541 with a edge of cemented carbide covered with a coating with an intermediate ceramic layer for the studied range of technological parameters reaches 260 μm.
3. Maximum microhardness for turning austenitic steel within the studied range of technological parameters reaches the value of up to 285 $HV_{0.05}$.
4. No significant influence of feed on the value of TSL microhardness of steel 1.4541 with austenitic structure was observed.
5. It would be necessary to conduct research into the TSL structure for the studied ranges of machining parameters, which would enable to present physical interpretation of the achieved results.

5. References

[1] Davim J.P., Surface integrity in machining, Springer-Verlag, London 2010.
[2] Hloch, S., Valíček, J., Kozak, D., Preliminary results of experimental cutting of porcine bones by abrasive waterjet, Tehnički Vjesnik - Technical Gazette, 18, 3, 467-470, 2011.
[3] Krolczyk, G., Gajek, M., Legutko, S., Predicting the tool life in the dry machining of duplex stainless steel, Eksploatacja i Niezawodnosc – Maintenance and Reliability, 15, 1, 62–65, 2013.
[4] Krolczyk, G., Gajek, M., Legutko, S., Effect of the cutting parameters impact onto tool life in duplex stainless steel turning process, Tehnički Vjesnik - Technical Gazette, 20, 4, 587-592, 2013.
[5] Krolczyk, G., Legutko, S., Gajek, M., Predicting the surface roughness in the dry machining of duplex stainless steel (DSS), Metalurgija, 52, 2, 259-262, 2013.
[6] Stoic, A., Pusavec, F., Kopac, J., Cutting disturbances influenced by variations in contact surface geometry, Machining Science and Technology, 13, 4, 516-528, 2009.
[7] Krolczyk, G., Legutko, S., Raos, P., Cutting wedge wear examination during turning of duplex stainless steel, Tehnički Vjesnik - Technical Gazette, 20, 3, 413-418, 2013.
[8] Grzesik, W., Zak, K., Surface integrity generated by oblique machining of steel and iron parts, Journal of Materials Processing Technology, 212, 12, 2586-2596, 2012.
[9] Yao, C.F., Jin, Q.C., Huang, X.C., Wu, D.X., Ren, J.X., Zhang, D.H., Research on surface integrity of grinding Inconel 718, International Journal of Advanced Manufacturing Technology, 65, 1019–1030, 2013.
[10] Axinte, D.A., Dewes, R.C., Surface integrity of hot work tool steel after high speed milling experimental data and empirical models, Journal of Materials Processing Technology, 127, 325–335, 2002.
[11] Grzesik, W., Bartoszuk, M., Nieslony, P., Finite difference method-based simulation of temperature fields for application to orthogonal cutting with coated tools, Machining Science and Technology, 9, 4, 529-546, 2005.
[12] Solomon N., Solomon I., Deformation induced martensite in AISI 316 stainless steel, Revista de Metalurgia, 46, 2, 121 – 128, 2010.
[13] Hilkhuijsen P., Geijselaers H. J. M., Bor T. C., Perdahcıoğlu E. S., Boogaard A. H., Akkerman R., Strain direction dependency of martensitic transformation in austenitic stainless steels: The effect of γ-texture. Materials Science and Engineering: A. 573, 100 – 105, 2013.
[14] Kundrak J.A., Mamalis G., Gyani K., Bana V., Surface layer microhardness changes with high-speed turning of hardened steels, International Journal of Advanced Manufacturing Technology, 53, 105 – 112, 2011.
[15] Sasahara H., The effect on fatigue life of residual stress and surface hardness resulting from different cutting conditions of 0.45%C steel, International Journal of Machine Tools and Manufacture, 45, 2, 131 – 136, 2005.
[16] Ezugwu E.O., Wang Z.M., Machado A.R., The machinability of nickel-based alloys: a review, Journal of Materials Processing Technology, 86, 1 – 16, 1999.
[17] Ezugwu E.O., Tang S.H., Surface abuse when machining cast iron (G-17) and nickel-base superalloy (Inconel 718) with ceramic tools, Journal of Materials Processing Technology, 55, 63 – 69, 1995.
[18] Javidi A., Rieger U., Eichlseder W., The effect of machining on the surface integrity and fatigue life, International Journal of Fatigue, 30, 10 – 11, 2050 – 2055, 2008.
[19] Fernández-Abia A.I., Barreiro J., Lacalle L.N.L.D., Martínez S., Effect of very high cutting speeds on shearing, cutting forces and roughness in dry turning of austenitic stainless steels, International Journal of Advanced

Manufacturing Technology, 57, 1 - 4, 61 – 71, 2011.

[20] Yan L., Yang W., Jin H., Wang Z., Analytical modelling of microstructure changes in the machining of 304 stainless steel, The International Journal of Advanced Manufacturing Technology, 58, 45 – 55, 2012.

FROM CONVEXITY TO INEQUALITY

Zlatko Pavić[1*], Vedran Novoselac[1] and Ivana Miloš[1student]

[1]Mechanical Engineering Faculty in Slavonski Brod, J. J. Strossmayer University of Osijek, Croatia
*Corresponding author e-mail: zpavic@sfsb.hr

Abstract
The article shows a development path in creating inequalities using convex and concave functions. It all starts with the Jensen inequality, which is then applied to the quasi-arithmetic means. At the end the power means are used as the most appropriate type of quasi-arithmetic means.

Keywords: convex function, Jensen's inequality, quasi-arithmetic mean, power mean

1. Introduction

The aim of the article is to present the simple way of deriving important and applicable inequalities. For this purpose we will use convex functions of one variable defined on the interval of real numbers. The starting point will be the Jensen inequality. We will rely on this inequality throughout the article. It can be argued that Jensen's inequality is dominant in the whole branch of mathematical inequalities.

The power means are used in the various applications. Therefore, the proof of the monotonicity of these means is fully implemented in four cases.

Throughout this article, we use an interval $\mathrm{I} \subseteq \mathrm{R}$ with the non-empty interior, a convex or concave function $f : \mathrm{I} \to \mathrm{R}$, and strictly monotone continuous functions $\varphi, \psi : \mathrm{I} \to \mathrm{R}$.

2. Jensen's Inequality

If $x_1, \ldots, x_n \in \mathrm{I}$ are points and $p_1, \ldots, p_n \in \mathrm{R}$ are non-negative coefficients of the sum $\sum_{i=1}^{n} p_i = 1$, then the linear combination $\sum_{i=1}^{n} p_i x_i$ is called convex, and it belongs to I. A function $f : \mathrm{I} \to \mathrm{R}$ is convex if it satisfies the inequality $f(p_1 x_1 + p_2 x_2) \le p_1 f(x_1) + p_2 f(x_2)$ for all binomial convex combinations in I. A function f is concave if its negative pair $-f$ is convex. The following is the famous Jensen's inequality.

Jensen's inequality. *Every convex function* $f : \mathrm{I} \to \mathrm{R}$ *satisfies the inequality*

$$f\left(\sum_{i=1}^{n} p_i x_i\right) \le \sum_{i=1}^{n} p_i f(x_i) \qquad (1)$$

for all convex combinations $\sum_{i=1}^{n} p_i x_i$ *in* I.

If a function f *is concave, then the reverse inequality is valid in (1).*

In 1905 (see [2]), Jensen was proved the inequality in (1) using the mathematical induction on the integer n. The graphic presentation of the Jensen inequality can be seen in Figure 1.

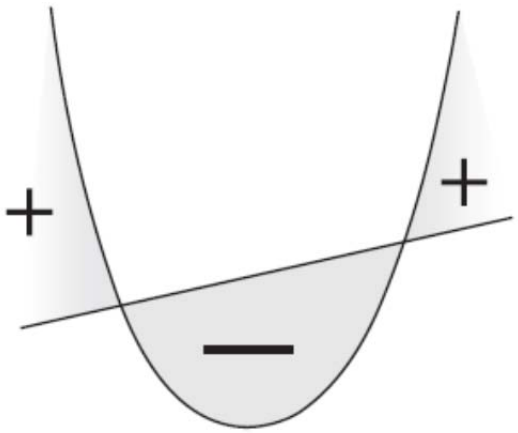

Figure 1. Graphic concept of Jensen's inequality

To demonstrate the application of Jensen's inequality take the function

$$f(x) = xe^x.$$

Relying on the second derivative $f''(x) = (x+2)e^x$, it follows that the function f is concave on the interval $(-\infty, -2]$, and convex on the interval $[-2, +\infty)$. Therefore, applying the Jensen inequality to the function f, we get that the inequality

$$(p_1x_1+\ldots+p_nx_n)e^{p_1x_1+\ldots+p_nx_n} \geq p_1x_1e^{x_1}+\ldots+p_nx_ne^{x_n}$$

holds for all convex combinations with $x_1,\ldots,x_n \in (-\infty,-2]$, and that the reversed inequality

$$(p_1x_1+\ldots+p_nx_n)e^{p_1x_1+\ldots+p_nx_n} \leq p_1x_1e^{x_1}+\ldots+p_nx_ne^{x_n}$$

holds for all convex combinations with $x_1,\ldots,x_n \in [-2,+\infty)$. If all $x_i=-2$, then the both sides of the above inequalities are equal to $-2e^{-2}$.

A general overview of convex sets, convex functions and its applications can be found in [4]. Many details of the branch of mathematical inequalities are written in [5].

3. Quasi-Arithmetic Means

In applications of Jensen's inequality we often use strictly monotone continuous functions φ and ψ such that ψ is convex with respect to φ (ψ is φ-convex), that is, $f=\psi\circ\varphi^{-1}$ is convex. This terminology is according to [5, Definition 1.19]. Similar notation is used for concavity.

Let $\varphi:\mathrm{I}\to\mathrm{R}$ be a strictly monotone continuous function. The φ-quasi-arithmetic mean of a convex combination $(x_i,p_i)=\sum_{i=1}^n p_ix_i$ in I is the point

$$M_\varphi(x_i,p_i)=\varphi^{-1}\left(\sum_{i=1}^n p_i\varphi(x_i)\right), \qquad (2)$$

and it also belongs to I since the convex combination $\sum_{i=1}^n p_i\varphi(x_i)$ belongs to $\varphi(\mathrm{I})$. Quasi-arithmetic means satisfy the invariant property $M_{a\varphi+b}=M_\varphi$ for every pair of real numbers a and b with $a\neq 0$.

Take a convex combination of the points $x_1,\ldots,x_n$ with the same coefficients. Applying the definition in (2) to the identity function, we get their arithmetic mean

$$M_{\varphi(x)=x}(x_i,1/n)=\frac{x_1+\ldots+x_n}{n} \qquad (3)$$

Using the logarithmic function, we have the geometric mean

$$M_{\varphi(x)=\ln x}(x_i,1/n)=\sqrt[n]{x_1\ldots x_n}, \qquad (4)$$

while using the reciprocal function, we have the harmonic mean

$$M_{\varphi(x)=x^{-1}}(x_i,1/n)=n\left(\frac{1}{x_1}+\ldots+\frac{1}{x_n}\right)^{-1}. \qquad (5)$$

Theorem of quasi-arithmetic means. *Let $\varphi,\psi:\mathrm{I}\to\mathrm{R}$ be strictly monotone continuous functions, and $(x_i,p_i)=\sum_{i=1}^n p_ix_i$ be a convex combination in I.*

If ψ is either φ-convex and increasing or φ-concave and decreasing, then we have the inequality

$$M_\varphi(x_i,p_i)\leq M_\psi(x_i,p_i). \qquad (6)$$

If ψ is either φ-concave and increasing or φ-convex and decreasing, then the reverse inequality is valid in (6).

Proof. We prove the case the function $f=\psi\circ\varphi^{-1}$ is convex on the interval $\mathrm{J}=\varphi(\mathrm{I})$, and the function ψ is increasing on the interval I.

In the first step, applying Jensen's inequality to the convex function $f:\mathrm{J}\to\mathrm{R}$ and convex combinations $\sum_{i=1}^n p_i\varphi(x_i)$ in J, we get the inequality

$$f\left(\sum_{i=1}^n p_i\varphi(x_i)\right)\leq\sum_{i=1}^n p_i f(\varphi(x_i)).$$

In the second step, assigning the increasing function ψ^{-1} to the above inequality, it follows the inequality

$$\varphi^{-1}\left(\sum_{i=1}^n p_i\varphi(x_i)\right)\leq\psi^{-1}\left(\sum_{i=1}^n p_i\psi(x_i)\right)$$

that represents $M_\varphi(x_i, p_i) \le M_\psi(x_i, p_i)$ which proves the theorem. □

The graphic representation of the quasi-arithmetic means M_φ and M_ψ in the case that ψ is φ-convex and increasing can be seen in Figure 2.

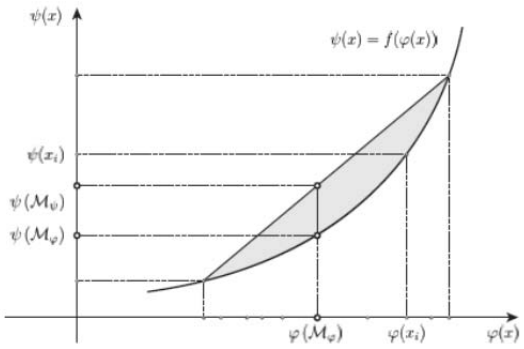

Figure 2. Quasi-arithmetic means for φ-convex and increasing ψ

The inequality in (6) can even be refined using the combinations of the functions φ and ψ as it is demonstrated in [3]. Briefly, let

$$\phi(x) = \alpha\varphi(x) + \beta\psi(x)$$

be a convex combination ($\alpha, \beta \ge 0$, $\alpha + \beta = 1$) of strictly monotone increasing or decreasing continuous functions $\varphi, \psi : \mathrm{I} \to \mathrm{R}$ such that $\varphi(\mathrm{I}) = \psi(\mathrm{I}) = \mathrm{J}$. Then we have

$$\phi^{-1}(y) = u(y)\varphi^{-1}(y) + v(y)\psi^{-1}(y)$$

where $u, v : \mathrm{J} \to \mathrm{R}$ are non-negative continuous functions such that $u(y) + v(y) = 1$ for every $y \in \mathrm{J}$. The above connections are presented in Figure 3.

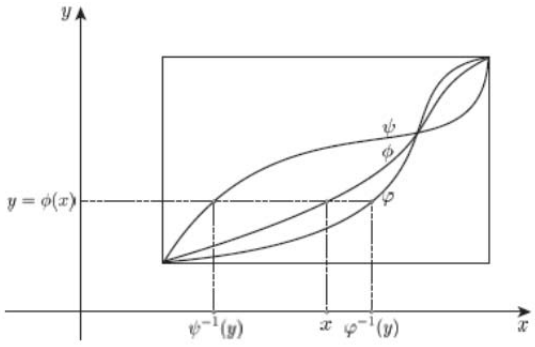

Figure 3. The convex combination of φ and ψ

In working with means and their inequalities we can rely on the book in [1] which offers basic ideas and information. Different types of quasi-arithmetic means were discussed in [3].

4. Power Means

The power functions $\varphi_r(x) = x^r$ for $r \ne 0$ and the logarithmic function $\varphi_0(x) = \ln x$ are strictly monotone and continuous on the interval $\mathrm{I} = (0, +\infty)$. Using the special case of the quasi-arithmetic mean defined in (2) with $\varphi_r(x) = x^r$ for $r \ne 0$ and $\varphi_0(x) = \ln x$, we get the power mean

$$M_n^{[r]}(x_i, p_i) = \begin{cases} \left(\sum_{i=1}^{n} p_i x_i^r \right)^{\frac{1}{r}} & \text{for } r \ne 0 \\ \exp\left(\sum_{i=1}^{n} p_i \ln x_i \right) & \text{for } r = 0 \end{cases}. \tag{7}$$

The power means satisfy a property of monotonicity which provides the whole collection of inequalities. This property reads as follows:

Monotonicity of power means. *Let $(x_i, p_i) = \sum_{i=1}^{n} p_i x_i$ be a convex combination in the interval $\mathrm{I} = (0, +\infty)$.*

If r and s are real numbers such that $r \le s$, then we have the inequality

$$M_n^{[r]}(x_i, p_i) \le M_n^{[s]}(x_i, p_i). \tag{8}$$

Proof. The inequality in (6) is applied to the power functions in four cases using the fact that the function $\varphi_r(x) = x^r$ is convex if $r \in (-\infty, 0] \cup [1, +\infty)$, and concave if $r \in [0,1]$. The function $\varphi_0(x) = \ln x$ is concave.

Case $r < s < 0$. Functions $\varphi(x) = x^r$ and $\psi(x) = x^s$ are strictly monotone decreasing with strictly concave composite function $f(x) = (\psi \circ \varphi^{-1})(x) = x^{s/r}$ because $0 < s/r < 1$.

Case $r < 0 = s$. Functions $\varphi(x) = x^r$ and $\psi(x) = -\ln x$ are strictly monotone decreasing

with strictly concave composite function $f(x) = (\psi \circ \varphi^{-1})(x) = -(1/r)\ln x$ because $-1/r > 0$.

Case $r = 0 < s$. Functions $\varphi(x) = \ln x$ and $\psi(x) = x^s$ are strictly monotone increasing with strictly convex composite function $f(x) = (\psi \circ \varphi^{-1})(x) = e^{sx}$.

Case $0 < r < s$. Functions $\varphi(x) = x^r$ and $\psi(x) = x^s$ are strictly monotone increasing with strictly convex composite function $f(x) = (\psi \circ \varphi^{-1})(x) = x^{s/r}$ because $s/r > 1$. □

The inequality in (8) can be refined using the convex combinations of the power functions and logarithmic function, see [3] for details.

Applying the inequality in (8) to three strictly monotone continuous functions $\varphi_{-1}(x) = \frac{1}{x}$, $\varphi_0(x) = \ln x$ and $\varphi_1(x) = x$ (two by two in pairs), we get the generalized (weighted) harmonic-geometric-arithmetic inequality

$$\left(\frac{p_1}{x_1} + \ldots + \frac{p_n}{x_n}\right)^{-1} \leq x_1^{p_1} \ldots x_n^{p_n} \leq p_1 x_1 + \ldots + p_n x_n. \tag{9}$$

5. Conclusion

The quasi-arithmetic means can be further applied to positive linear functionals and self-adjoint operators. The most important positive linear operator is the integral. For example, using integrals the harmonic-geometric-arithmetic inequality takes the form

$$\left(\int_{[a,b]} \frac{p(x)}{g(x)} dx\right)^{-1} \leq \int_{[a,b]} g(x)^{p(x)} dx \leq \int_{[a,b]} p(x) g(x) dx \tag{10}$$

where $[a,b] \subset (0,+\infty)$ is a bounded closed interval, $p : [a,b] \to \mathrm{R}$ is a non-negative continuous function with $\int_{[a,b]} p(x)dx = 1$, and $g : [a,b] \to [a,b]$ is a continuous function.

If we use more functions, then the above inequality grows up to

$$\left(\sum_{i=1}^{n} \int_{[a,b]} \frac{p_i(x)}{g_i(x)} dx\right)^{-1} \leq \prod_{i=1}^{n} \int_{[a,b]} g_i(x)^{p_i(x)} dx \leq \sum_{i=1}^{n} \int_{[a,b]} p_i(x) g_i(x) dx \tag{11}$$

where $p_i : [a,b] \to \mathrm{R}$ are non-negative continuous functions of the integral sum $\sum_{i=1}^{n} \int_{[a,b]} p_i(x)dx = 1$, and $g_i : [a,b] \to [a,b]$ are continuous functions.

6. References

[1] P. S. Bullen, D. S. Mitrinović and P. M. Vasić, *Means and Their Inequalities*, Reidel, Dordrecht, NL, 1988.

[2] J. L. W. V. Jensen, "Om konvekse Funktioner og Uligheder mellem Middelværdier", *Nyt tidsskrift for matematik. B.*, vol. 16, pages 49-68, 1905.

[3] J. Mićić, Z. Pavić and J. Pečarić, "The inequalities for quasiarithmetic means", *Abstract and Applied Analysis*, vol. 2012, Article ID 203145, pages 25, 2012.

[4] C. P. Niculescu and L. E. Persson, *Convex Functions and Their Applications*, Canadian Mathematical Society 2006.

[5] J. E. Pečarić, F. Proschan and Y. L. Tong, *Convex Functions, Partial Orderings, and Statistical Applications*, Academic Press, New York, USA, 1992.

ELIMINATION OF THE MEASUREMENT ERRORS CAUSED THROUGHOUT 3D MEASURING PROCESSES.

Ing. Michal Dúbravčík, PhD.[1*], Ing. Štefan Kender, PhD.[2]

[1]Faculty of Mechanical Engineering, – Technical University, Košice, Slovakia
** Corresponding author e-mail: michal.dubravcik@tuke.sk*

Abstract
Article is approaching the elimination methods of measurement errors, which are caused throughout 3d measuring processes by 3D measurement accessories; measurement of mechanical parts requires maximal precision; article describes possible inaccuracy of 3D measuring and the possibilities of errors generation; because of this errors it´s possible to interpret incorrect results, throughout the parts can be produced incorrect.

Keywords:
3D measurement systems, errors of measurement, elimination of errors, exact measuring

1. Introduction

The parts dimensions inspection must guarantee precise control of real dimensional parameters specified in the production documentation. These inspections must be made through the production process, as well as after the general part finalization. Precision of the final results depends on the suitable measurement/control method selection. Thanks early identification of incorrect dimensions done throughout the production process can we use some specific progress to perform the correction of these production errors right in the production process.

Mainly cases are about the control of sizeable parts, or multiple surfaces parts, where the selection of right measurement accessories important is. Exactly this for is the 3D measurement process effective. Through the use of these techniques it´s possible to measure various dimensions, that directly affected quality of the final part. For these measurement it´s profitable to use some contact 3D scanner benefits. There is measurement device FARO with laser scan probe FARO Laser ScanArm used on automotive production department of Technical university of Kosice. This device used a group of sensorial parts in its arms for exact determination of probe position in space [1].

3D measurement arm Faro serves for 3D contact measuring and digitalization of shaped and dimensional properties of produced parts, products, whole components, up-to assembling groups, and so it´s covering an area of all control measurements.

With help of Laser scanner probe, can be Faro arm used as full functional laser scanner. For contact measuring there are several specifically and shaped probes, which are making measuring easier. Probe selection primary depends on profile and character of the controlled dimension. It´s important to know if an outside or inside dimension are measured, eventually if it´s possible to measure surfaces/dimensions with use of one probe. Final accuracy depends on exact calibration of contact probe with measure arm.

Arm accuracy which we´ve used for set of control measurements is 0,036mm/each point. Every accessories of this type have exactly specified the maximum accuracy, following the certification process. For every new measuring process it´s important to calibrate the measuring probe to achieve the best accuracy [3].

2. Errors generated by 3D measuring

During the production process it´s important to control many of specified dimensions. For purpose of our experiment we´ve chosen 3D measurement accessories by Faro. Every measuring contains some measurement errors, which in final result decreases the relevance of final scores. To eliminate these errors, it's important to measure through the use of specific methods. In some cases also specific method show a offset of real dimension, because the process of measuring self-allocates an error. This error is in final result addend to error of the controlled dimension. Therefore it´s important to avoid the possibility of measuring errors generation. It can be done through properly chosen specific measuring method.

Our case shows the inspection of dimensional bigger welded steel frame, which is intended for production purpose of carrier unit. As it´s handle about jig for production, the dimensions must´ve been measured precisely. Any inaccuracy could have had bad impact onto whole series of produced steel constructions.

The goal of our measuring was the control of produced part´s dimensions according to drawing. (fig.1.) For example study we´ve chosen two dimensions - distance between two holes in direction X axis “vz9” and as supplemental

example we´ve been measured distance of two plains in Z axis direction - “vz3”.

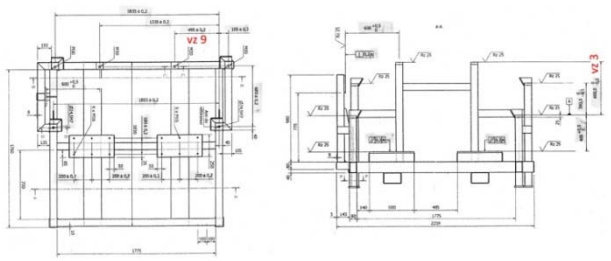

Figure 1: Measured dimensions vz9 and vz3

Specified dimensions values:
vz3 – 600.5 mm
vz9 – 495 mm

According to the correct verification of measuring progress, there had been done two independently measurements for two same parts. We´ve had done the 3D measurements by 3mm ball-probe contact method. The main problem of the exactness has been focused on 3D measurement of dimension between two 25mm holes.

Measurement method can be seen on fig.2. Simple description of the method: Through the progressive engaging of points in the measured hole, we enter the main shape of the object surface into software interface. After that we have to end the measurement through entering of reference point, which is situated inside the hole. That through we expressly confirm that we´re inside the hole, and the software takes the dimension´s compensation of contact probe with the calculation onto real dimension of measured hole.

Figure 2: cylinder / hole measuring method

Example of the hole measurement can be seen on fig.3.

Main problems of an exact measurement are about to a measuring of the holes. As seen on the next picture (fig.4), cylinder (H) created by software polyworks on the base of points we´ve entered from the hole surface isn’t perpendicular to the reference plane (A).

Figure 3: Finished part hole measuring

This effect is caused by small amount of initial points (minimum of these points is 6). The more of points we put through measuring arm, the more precisely the position of the hole against the reference plane will be. Anyway, this solution isn’t sufficient and so it´s important to be concerned about this problem in general.

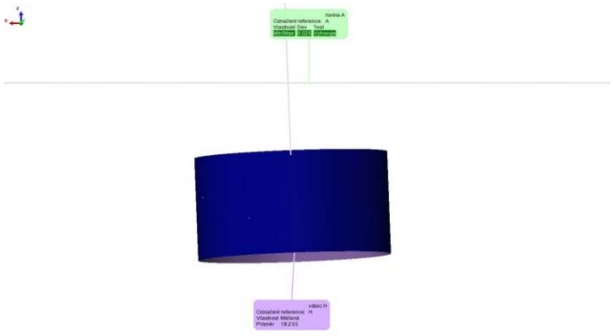

Figure 4: position of the cylinder H against the plane A

Second problem is the size, or the height of the hole/cylinder. It can’t be guaranteed that by putting the points through measuring device into the software, the first point and the last point of the measuring will be every time at the same distance from the hole/cylinder base. Other way said – the size and shape of the final measured plane, or body, in our case cylinder, depends on relative distance of the first and the last point from the set of scanned points from the inner surface of the hole.

Also important is the technique of points scanning. Some system of the scanning is needed. This system should supply an individual points those closed sequence created. This sequence should continuously subscribe the surface of the measured hole. The most appropriate progress is to use measuring gradually in spiral way. This ensures that the constituent part the surface will be described, and the software will have enough data to recounting and drawing the final plane. Number of scanned points depends on part complexity, applied method, and adequate accuracy [2].

Thereby progress we´ve scanned the measured cylinders of the controlled holes.

Because the Polyworks software doesn't need to scan more than six points (scanning of more than six points isn't of course limited), every measuring is individual, and the gravity centre of this way created cylinder is every time in different position/distance against the reference plane (fig.5).

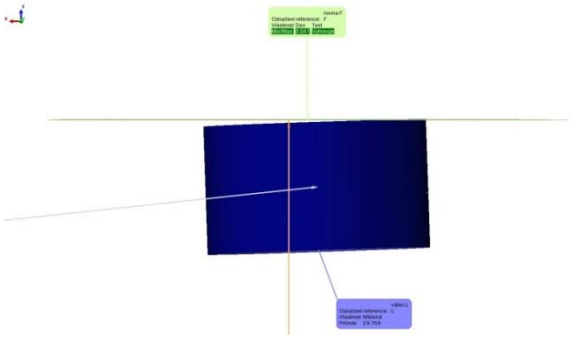

Figure 5: shorter distance of the cylinder L gravitational centre, against plane F

There can be a serious deviation of measurement by measuring trough this way. Software is measuring the distance of two points in a way of minimal distance of mass centre of two parts in chosen axis (fig.6). Different position of measured cylinder/hole in space regular causes distortion of measured dimensions.

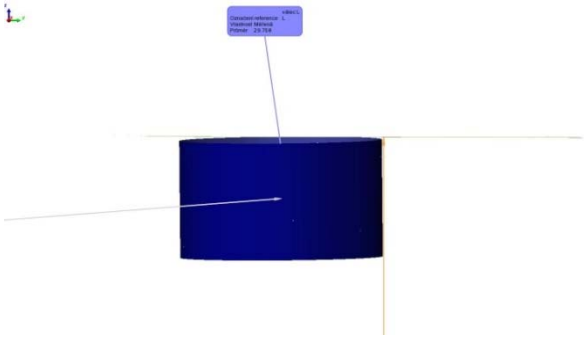

Figure 6: dimension leading to mass centre of chosen cylinder

This way created error is unacceptable (tab.1) (fig.7) and therefore it´s necessary to change the scanned parts measuring method.

Table 1: measured values after using standard method measuring the dimension between two holes

item	property	nominal	measured	tol+	tol-	deviation	test
vz3	distance Z	600,500	598,987	0,000	-0,100	-1,513	off-size
vz9	distance X	495,000	514,851	0,200	-0,200	19,851	off-size

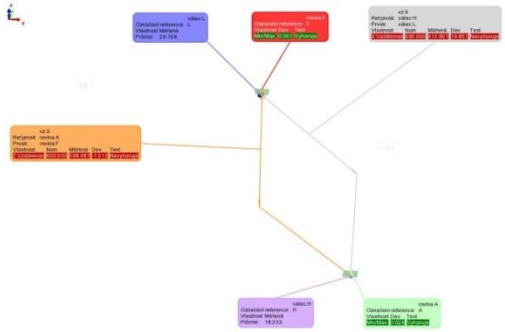

Figure 7: incorrect measuring view

3. Possible ways to eliminate the errors

As the easiest method to getting precise measuring of dimensions looks creation of help point, which can be created by intersection of cylinder and the reference plane. There is a purpose not to say that it´s negotiating about intersection of cylinder axis and a plane. An axis of cylinder, which isn't perpendicular to reference plane, regular isn't perpendicular also to the plane.

Polyworks offers opportunity to create point as a intersection of cylinder and plane. Using such a specific command, a point on specific plane is created, which commensurate the position of intersection of cylinder centre of gravity and the plane in 3D space.

A point created through intersection of cylinder axis and point as described above aren't identical, because of inaccuracy of the position of the cylinder to reference plane. For dimensions control is such a creating of help points necessary to an elimination of measurement errors caused by wrong demarcation of primal cylinders. Additional dimensions control runs through standard conditions and exactly definite directions of directional coordinate axis.

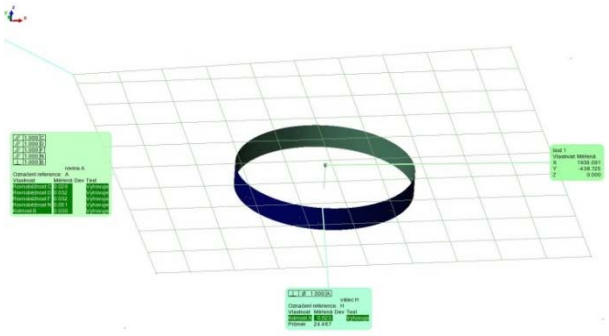

Figure 8: point "bod 1" created through suggested method

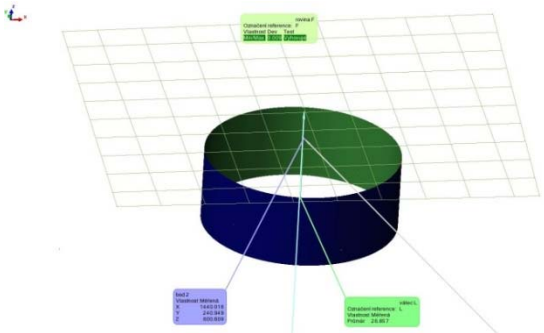

Figure 9: points "bod 1" and "bod 2" created through suggested method

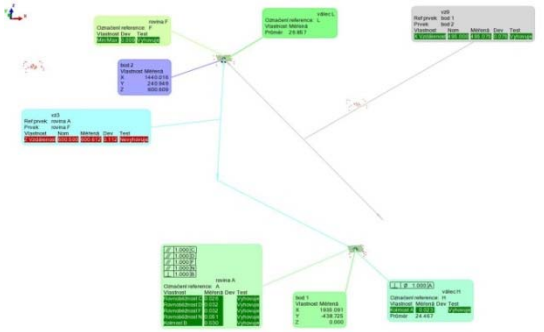

Figure 10: situation of measured dimensions after using new method of creating reference points

Table 2: measured values after using new method of creating reference points

item	property	nominal	measured	tol+	tol-	deviation	test
vz3	distance Z	600,500	600,612	0,000	-0,100	0,112	off-size
vz9	distance X	495,000	495,075	0,200	-0,200	0,075	OK

Through using of mentioned sequences we´ve achieved clear improvement of controlled dimensions value of dimension (vz3 and vz9) between two holes.

Measured value of vz3 without described method was vz3 = 598,987mm, what means deviation of -1,513mm for tolerance field 0 – 0,1mm. After application of us suggested method was the deviation 0,112mm.

Second value vz9 with specified dimension 495mm and the tolerance field ± 0,2mm was through primary method 514,851mm, what highly overlapping the tolerance field. The second measuring through our method showed that the real dimension is in the tolerance field. First value of vz9 was caused also by improper choosing of scanned points of cylinder/hole surface and throughout the general tilt of created cylinder to reference plane.

From described is clear, that using of us suggested method of measuring, is necessary for determination of dimensions between circular holes in space, because throughout are inaccuracy of establishing of convenient parameters for creating of geometrical part eliminated.

4. Conclusion

The Application of described methods for measurement errors elimination allows exact control of required dimensions and thereby it's avoiding the creation of incorrectness by complicated components production. Our study shows control and the methods of dimensions measuring of welded steel frame, which is intended for production purpose of carrier unit.

Only through precise control of initial dimensions of such a component type, allow producing dimensional high-class products. Any dimensional incorrectness of base frame will bring some error, which will be shift onto finale product and thereby make him a low-class product. Through summary of these partial errors can come to errors accumulation up to the condition, when the product will be a faulty piece and the production will be therefore overcharge.

Therefore it´s necessary to use such a methods and measurement progresses, which are able to identify any dimensional anomaly of real dimensions in compare with specified dimensions. This´ll allow full control about reciprocally affected dimensions.

9. Acknowledgement

Paper is the result of the Project implementation: Competency Centre for Knowledge technologies applied in Innovation of Production Systems in Industry and Services, ITMS: 26220220155, supported by the Research & Development Operational Programme funded by the ERDF.

10. References

[1] Application of reverse engineering techniques in mechanics system services / Michal Dúbravčík, Štefan Kender - 2012. In: Procedia Engineering : MMaMS 2012 : Modelling of Mechanical and Mechatronics Systems 2012 : November 6th-8th 2012, Zemplínska Šírava, Slovakia. - Košice : TU, 2012 Vol. 48 (2012), p. 96-104. - ISSN 1877-7058

[2] 3D skenovanie a meranie 3D meracími zariadeniami / Michal Dúbravčík, Štefan Kender - 2011. In: It-strojár. (2011), s. 1-4. - ISSN 1338-0761

[3] Využívanie meracích zariadení v strojárstve / Štefan Kender, Michal Dúbravčík - 2011. In: Transfer inovácií. Č. 21(2011), s. 216-220. - ISSN 1337-7094

THE GREENHOUSES SOIL HEATING BY GEOTHERMAL ENERGY

Mladen Bošnjaković[1*], Ivica Lacković[1], Ivan Grdić[2]

[1] College of Slavonski Brod, Slavonski Brod, Croatia
[2] Former Student of College of Slavonski Brod, Slavonski Brod, Croatia
* *Corresponding author e-mail: mladen.bosnjakovic@vusb.hr*

Abstract
The work represents the systems which use the sources of geothermal energy for heating greenhouses. The use of geothermal energy for conventional purposes is highly acceptable and is an excellent choice of energy source for the greenhouse design. Although the sources are not available in the whole area of the Republic of Croatia, they can be very useful and profitable on the locations where they have been found. The analysis of known technologies of greenhouse heating shows the advantages and drawbacks of some of them. The aim is to get to know the soil heating technology with geothermal energy which, by its further improvement, brings considerable economic benefits.

Keywords:
Geothermal energy, greenhouses, soil heating

1. Introduction

Many authors have discussed possibilities of geothermal energy application. Lund and others [1] talk about the areas of application of geothermal energy. Greenhouse heating, according to him, covers 7,5 % of the total use of geothermal energy.

Even though this percentage is small, using geothermal energy makes it possible to greatly reduce the heating costs. The application of thermo gens for floor and air heating of greenhouses of 500 m^2 demands the device of 109 kWh capacity, consumption of 12 l of fuel oil/h and with max. strength, in case the outside temperature is - 10° C, the stated daily temperature of plants 20° C, at night 16° C (tomatoes, peppers etc.). In this case, when calculating energy costs per kg of tomatoes and peppers in autumn-winter period and winter-spring period, it is 60 % - 65 % for continental part of Croatia. Due to constant increase of prices of oil products, this share will increase, and therefore, make the use of geothermal energy more interesting. Geothermal application as a renewable source of energy decreases environmental pollution as well as emission of CO_2.

2. Uses of geothermal energy in greenhouses

Heating of greenhouses is one of most common direct uses of geothermal energy. Greenhouses can directly use temperature of hot water ranging from 50 °C – 80 °C. The quantity of hot water required will depend upon the optimum growing temperature for the selected crop (Table 2.1), size of the greenhouse, and the lowest outside temperature expected in the area. The main advantage of geothermal energy used for heating greenhouses is its eco-friendly approach and lower prices than those of fossil fuels.

The main disadvantage of using geothermal energy for greenhouses is limited resource areas. Each greenhouse construction project includes drilling of the new geothermal well, which is very risky because of high costs of drilling that questions the profitability of the project. In order to avoid the mistakes, the greenhouse construction projects must be planned in the areas with existing sources of geothermal energy. Quality construction and installing quality equipment into the heating system will surely ensure high efficiency which is the main aim of starting such projects in the first place [4, 5, 6].

Table 2.1 Growing temperatures for typical greenhouse crops [8]

Produce	Day Time Temperature (°C)	Night Time Temperature (°C)
Peppers	20 - 30	16 - 20
Tomatoes	21 - 25	17 - 20
Cucumber	25 - 28	21
Lettuce	25	20
Poinsettias	21 - 27	19 - 22
Carnations	25	10
Geraniums	21 - 27	18

In practice there are three kinds of heating systems:

1. Coercive heat convection by recuperators under the greenhouse roof
   - at higher temperatures of geothermal water,
   - at lower temperatures
2. Surface heating – system on the ground
   - ribbed pipes
   - system of smooth pipes
3. Floor heating in combination with recuperators

In most geothermal applications, a heat exchanger is required to separate actual heating equipment from the geothermal fluid. This is because of the scaling and corrosion associated with most

geothermal fluids (7). Generally, the heat exchanger is placed between two circulating loops, the geothermal loop and the clean loop. The heat exchanger is placed between two circulation circles (the geothermal circle and the circle with clean water). The circle with clean water is a separate, closed system which is used exclusively for transmission of energy from geothermal water. As result of using the heat exchanger, the temperature drops depending on the exchanger type (Table 2.2).

Table 2.2 Heat loss depending on the heat exchanger construction

Exchanger type	Loss of water temperature
Plate construction	5 °C do 10 °C
Pipe- cover	15 °C do 20 °C
Non-commercial construction (home -made)	20 °C do 40 °C

Non-commercial exchanger construction is not recommended because often cause malfunction in the greenhouse heating system [4].

3. The soil surface heating

The first comprehensive researches into floor heating in greenhouses were conducted in 1972-74 and were focused on the use of low temperature sources, such as geothermal and solar energies. Technologies for plant growing and greenhouse heating had to be adjusted to use these energies. This resulted in learning that heating the soil instead of the air, together with lower energy input, achieves better growing results. Earlier ripening with the same or better appearance was spotted in many plants.
This knowledge started numerous experiments regarding changes in plant growing technologies. The habit of heating the entire area had to be changed, and the habit of heating the root system (growing plants in cooler environment) had to be adopted. Besides, soil heating requires about 30% less energy than air heating.

4. The ribbed tube system

Ribbed tubes are most commonly made of steel or copper, with fixed ribs made of aluminum or steel which may have a square, circular or rectangular shape. The comparison of prices of different rib materials and dimensions are presented in the table 4.1.

Table 4.1 The comparison of lengths and costs of ribbed tubes [5]

Combination of materials (tube/ribs)	Outer tube diameter (mm)	Number of ribs per meter	Price (€/m)
steel / aluminum	19,05 mm (3/4 in)	108	17,7
steel / aluminum	25,40 mm (1 in)	108	24,6
steel / steel	31,75 mm (1 ¼ in)	108	36,1
steel / steel	31,75 mm (1 ¼ in)	131	40,4
steel / steel	50,8 mm (2 in)	78	35,4
steel / steel	50,8 mm (2 in)	108	41,3

The tubes can be laid down in one, two or three lines. In this way the heat capacity can be increased based on the water temperature, number of lines of laid tubes, and number of ribs per meter (table 4.2).
After selecting the pipe length, the pressure drop has to be calculated. The total length of the pipes is related to the temperature gradient. The length of a single pipe will be limited by the permissible pressure drop.
When choosing the tubes it is essential to pay attention to quality, as poor quality tubes often lead to malfunction in the system.

Table 4.2 Heat transfer performance per tube meter regarding the water temperature [5]

Number of ribs	Number of lines	Water nominal value, ' kJ/h/m +						
		116 °C	110 °C	104 °C	99 °C	93 °C	88°C	82 °C
108	1	5.642,4	5.123,2	4.742,4	4.292,4	3.877,0	3.496,2	3.115,4
	2	9.727,1	8.896,3	8.169,4	7.407,8	6.715,5	6.092,4	5.365,5
	3	12.669,5	1.156,7	1.066,7	9.623,2	8.723,2	7.927,1	6.992,4
131	1	6.057,8	5.538,6	5.088,6	4.603,9	4.223,2	3.773,1	3.357,8
	2	10.142,5	9.242,5	8.515,5	7.684,8	6.957,8	6.334,7	5.573,2

The required length of ribbed tubes for heating plastic or glass greenhouses increases when the incoming water temperature drops. Thus, this way of heating is not the best choice for water below 65 °C, especially in colder areas [4, 5, 6].

5. The surface heating system using smooth tubes

In the past, tube materials were generally copper or steel. Because of corrosion and expansion problems with these materials, nonmetallic materials have seen increasing application in recent years. The most popular of these is polybutylene. This material is able to withstand relatively high temperatures (up to 80 °C) and is available in roll form for easy installation. PVC piping is only available in rigid form and is limited with respect to temperature. Polyethylene and similar materials are available in flexible roll form, but are (as PVC) generally limited in terms of temperature handling ability.
Tubes are smaller in diameter (25 mm), with wall thickness up to 4 mm. They are fitted directly onto the greenhouse floor, in parallel lines, taking into consideration the distance between the tubes. If the tubes are laid too close to one another, heating

efficiency decreases due to the reduced heating area potential (picture 5.1).

Picture 5.1 The heating system with smooth tubes [2]

Similarly, if the space between the tubes is too large, heating efficiency decreases, and the soil surface is not sufficiently heated.
The project of the heating system is based on the medium water temperature in the working area. Heat output from the floor occurs by two mechanisms: convection and radiation. The procedure for designing a floor system consists of:

- Determining the heat load for the greenhouse
- Calculating the required floor temperature to meet the load
- Calculating the required size, depth and spacing of the tubes

This system is applicable in greenhouses with plants which can stand higher temperatures at the level where the plant grows from the root into the stalk. An example of this heating system is growing tomatoes and peppers, as they can stand such heating conditions. This system is rarely used as the primary way of surface soil heating as the required tube length increases considerably in order to achieve the approximately equal heating power as with the ribbed tube system [4,5,6].

6. The floor heating combined with recuperators

This heating system includes the use of the greenhouse floor as a big radiator. The tubes, with circulating hot water, are buried in the ground. The floor system is of prime importance for heat production, and the recuperator is used to meet the need in the heating peak during colder months. The amount of heat required during colder months depends on the soil temperature, air temperature in the greenhouse, and also the average temperature of the unheated surfaces of the greenhouse (walls and the roof).
Tube spacing and size is dependent upon the available water temperature. Generally, depth is more a function of protecting the tubes from surface activity than system design. Since it is the purpose of the floor panel system to use the floor as a large radiator, it follows that the installation of the tubing should result in as uniform a floor surface temperature as possible. This is accomplished by two general approaches: (a) placing smaller diameter tubes at close spacing near the surface of the floor, or (b) placing larger tubes spaced further apart at a greater burial depth. The theory behind this approach is to reduce the difference between the distance heat must travel vertically (from the tube to the surface directly above it) and laterally (from each tube to the surface between the tubes).
It is important to point out that, because of the soil temperature increase in this heating system, one should make sure that the soil temperature does not rise above 30 °C. This soil temperature is much too high for most vegetables, whereas for some flowers, it can be suitable (picture 6.1).

Picture 6.1 Geothermal soil heating in the greenhouse [3]

Depending on the tube laying (picture 6.2), it is possible to ensure quality level of heat exchange with soil.

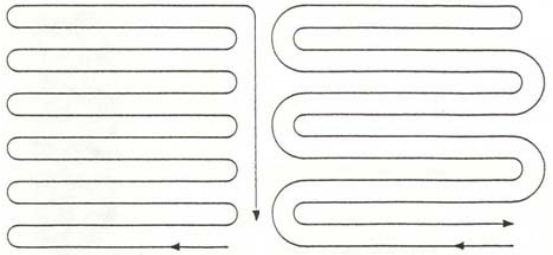

Picture 6.2 Single and double piping layout [5]

If the expected temperature drop is below 8 °C, single tubes are installed. In order to avoid the temperature drop (in circulation) above 8 °C, double loop tubes are installed, which will ensure the suitable temperature (within limits) for plant growth. Tubes should be buried deep enough because of the surface activities, the common depth being 50 to 150 mm [4, 5, 6].

7. Heating Control Systems

As daytime temperatures increase due to seasonal and/or daily temperature changes then the flow of geothermal water to the greenhouse heat exchangers would be cut back. Heat load requirements would be automatically adjusted using

signals from temperature sensing instrumentation. A regulation of the heat input into the greenhouse is achieved by bypassing a portion of the return cool fluid into the input leg of the heating system. A 3-way auto control valve, using data from temperature sensing instrumentation located inside and outside to the enclosure, controls the amount of fluid by-passed and thus the temperature of the circulating water through the heating pipes (Figure 7.1).

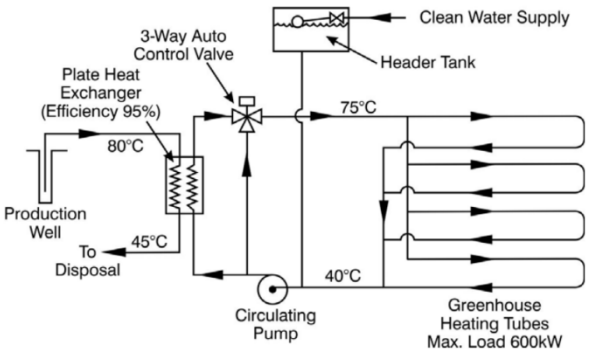

Picture 7.1 Schematic diagram of greenhouse heating system [8]

8. Conclusion

Thermal water temperatures and lower mineralization can be successfully used for irrigation and / or heating of greenhouses, which can only be heating the soil, air only, or the heating of soil and air. The use of thermal energy in greenhouses to reduce production costs, which amounts to 35% of the total costs of production. One of the major disadvantages of using geothermal water in greenhouses is the high investment cost. The solution of the problem is finding other consumers of geothermal water (eg for space heating or hot water), which would reduce the cost of heating greenhouses. The disadvantages of using geothermal energy for heating greenhouses is also limited areas where there is geothermal wells, which is sufficient for use in such projects, the cost of exploration and drilling wells is large, the high content of carbonates and iron in the water, and expensive geothermal water purification system.

9. Annotation

This paper is a part of Graduation Seminar of Ivan Grdić, Bachelor of College of Slavonski Brod.

10. References

[1] J. W. Lund, D. H. Freeston, T. L. Boyd, “Direct application of geothermal energy” 2005 worldwide review. Geothermics. 34(6). pp. 691-727.
[2] http://electrictreehouse.com/wp-content/uploads/2011/03/greenhouse_invernadero_1.jpg
[3] http://oe.confolio.org/scam/31/resource/186 [Accessed:19-Oct-2011.]
[4] M. Golub, “Iskorištavanje geotermijskih ležišta, Rudarsko-geološko-naftni fakultet”, Zagreb, 2008.
[5] K. Popovski, “Heating greenhouses with geothermal energy”, Faculty of Mechanical Enginering, Skopje, Makedonija, 1993.
[6] G. Ivanišević, R. Čepelak, “Prirodne mineralne vode u Hrvatskoj”, Hrvatske vode, Zagreb, 2003
[7] I. Grdić, “Upotreba geotermalne energije u svrhu zagrijavanja tla u staklenicima i plastenicima”, Završni rad, Veleučilište u Slavonskom Brodu, 2011.
[8] I. Thain, A. G. Reyes, T. Hunt, “A practical guide to exploiting low temperature geothermal resources”, GNS Science Report 2006/09

ANALYSES OF THE CHANGES IN SPECIFIC MOTOR ABILITIES OF FOOTBALL PLAYERS THAT ARE UNDER THE INFLUENCE OF A PROGRAMMED FOOTBAL TREATMENT

H. Sivrić[1*], M. Erceg[2] and M. Milić[3]

[1] College of Slavonski Brod, Slavonski Brod, Croatia
[2] University of Split, Faculty of Kinesiology, Croatia
[3] University of Split, Faculty of Kinesiology, Croatia
* *Corresponding author e-mail: Hrvoje.Sivric@vusb.hr*

Abstract
The main goal of this research was to determine the efficiency of a programmed football treatment on the changes in specific motor abilities of cadet level football players. A total of eight specific motor tests were applied on the examinees twice, in a time interval of four weeks and they were applied in order to evaluate: specific speed, strength, precision and agility. The results have clearly shown that the programmed football treatment, applied in a relatively short period of four micro cycles, affected mostly the changes in specific motor abilities in specific speed, strength, precision and agility. Given changes in this research are a consequence of the adaptation of the football treatment which has its basis in well programmed exercises for speed development, basic and specific agility, explosive and repetitive strength, coordination and precision.

Keywords:
Football, motor abilities, differences

1. Introduction

Football is one of the most popular sports today, so the attribute of being 'the most important secondary thing in the world' is clearly justified. Today's high-quality football requires powerful and durable athletes that have good motor and functional abilities (speed, explosive strength, aerobic and anaerobic capacity, coordination) and a sense for improvisation and collective playing. Being successful in football also depends on the ability of implementing individual characteristics of particular players into an entirety and building a coherent team [1]. The level of quality of competitive results of a single football team greatly depends on quality planning and training programming in particular periods, phases and micro cycles inside a year cycle [2]. A complex of anthropological characteristics and the specific ability of players to run the game i.e. control the game system and the concept; manage the tempo and the rhythm of the game and also his own bio energetic capacity and functional conditions during the game. All of the aforementioned features are responsible for being successful in football [3].
Informational, informational-motor and energetic component of managing and regulating process; all participate in dealing and realizing motor and partial situations in the game. Successfulness of football players is determined through the level and the structure of a great number of abilities, characteristics and skills. [4]. The hierarchy structure of successfulness in football contains three groups of factors. The first group consists of basic anthropologic features: health condition, morphological characteristics, basic functional abilities, basic motor abilities, intellectual abilities and personality characteristics. The second group consists of specific abilities and footballers knowledge. The third group consists of situational effectiveness and competition results. Motor and functional abilities represent the most important factors. Motor abilities comprise stamina, speed, strength, coordination, precision and flexibility. The foundation of these abilities lies in the effectiveness of the organic systems, especially nerve – muscle system which is responsible for the intensity, the duration and the regulation of movement.
The main goal of this research is to determine the effectiveness of a football treatment on the changes in motor abilities of cadet level football players, which were observed in two temporal points.
Partial goals of the research:

- to determine differences in the indicators in the initial testing, that are used for assessing motor abilities between cadets of FC "Orkan" and cadets of FC "Omiš";
- to determine the magnitude of quantitative changes in the indicators that are used for assessing motor abilities of FC „Orkan" football players;
- to determine the magnitude of quantitative changes in the indicators that are used for assessing motor abilities of FC „Omiš" football players;

• to determine differences in the indicators in the final testing, that are used for assessing motor abilities between FC "Orkan" and FC "Omiš".

2. Method

Examinee sample: the testing was done on a sample of 40 football players, members of cadets of FC „Orkan" and FC „Omiš", which train regularly three times a week and play competitive matches once a week. The examinee sample was divided equally between FC "Orkan" (20) and FC "Omiš" (20). FC "Orkan" and FC "Omiš" football players were treated according to the plan and programme made for cadet level, through 4 micro cycles, using different programmed football treatment. Testing was conducted on FC "Orkan" and FC "Omiš" playing grounds, with the help of experienced and educated surveyors.

Variable sample: variables sample that were chosen for assessing basic and specific motor abilities comprises the following battery tests: for evaluating basic motor abilities: SUD (standing long jump), SUV (standing vertical jump), 60 m (60 m sprint from a high start), 300m (300m sprint from a high start), 93639 BL (93639 sprint without a ball), KUS (side steps), ČUČ (squats), TRB (Sit ups-lifting the torso from a lying position). For evaluating specific motor abilities: 20 m SL (20 m sprint with dribbling), SUN (Foot kick strength), SUG (strength to head the ball), PN (Foot precision), PG (Head precision), PPN (Straight-line foot precision – vertical aim), STSL (Slalom running with dribbling), BTPP (Smi-circle running speed).

Methods for data processing: after the conducted measuring, the given results were entered into the Statistica programme for "Windows Ver.5.5". Basic statistic parameters were analyzed (arithmetic mean, standard deviation, minimum and maximum values of testing results, for NK "Orkan" and NK "Omiš". Distribution normalities have been tested using a Kolmogorov – Smirnov test. Reversely scaled variables can be seen in some of the following tables. They will be marked with **[a].** The differences between cadet level football players in the initial and final testing were determined with the help of a discriminative analyses. A degree of global and partial differences between the respective groups has also been determined. Changes between the initial and final testing for groups of football players have been analyzed by applying univariant variance analyses. A univariant variance analyses has also been conducted to determine the differences between the middle result values in groups of football players, from the initial to final testing of specific motor variables.

3. Results and discussion

Table 1. shows the basic statistic parameters of specific motor variables: arithmetic mean (AS), standard deviation (SD) and a KS-test of distribution normalities for football players of FC "Omiš" (20 players). As we can see in table 1., not one KS-test value exceedes the border value of the Kolmogorov-Smirnov test for the observed sample. We can therefore conclude that all the variables in the initial and final testing of football players, have a distribution for which can be noted that it doesn't significantly deviate from normal. It can also be noted that football players achieved better results in all the tests in the final testing (an increase of arithmetic mean values in all motor abilities test, i.e. a decrease in reversely scaled tests). This trend can also been seen in the area of minimum, i.e. maximum test result values. An insignificant decrease of standard deviation with most variables can be attributed to a greater increase (improvement) of minimum test values in the final testing.

Table 1. Descriptive statistic parameters of specific motor abilities – FC "Omiš"

Variab.	Initial			Final		
	AS	SD	KS	AS	SD	KS
M20L [a]	4,47	0,57	0,14	4,18	0,36	0,13
STSL [a]	12,45	0,63	0,13	12,15	0,5	0,17
BTPP [a]	10,52	0,44	0,16	10,17	0,27	0,13
PG	29,95	5,74	0,11	34	4,8	0,14
PN	29,9	5,42	0,11	33,6	4,03	0,13
PPN	20,65	2,11	0,16	21,85	1,69	0,14
SUN	4,6	1,27	0,17	5,6	0,88	0,7
SUG	9,84	1,57	0,1	10,49	1,43	0,11

Border value of the KS test for N=20 is 0,36

Table 2. shows the basic statistic parameters of specific motor variables : arithmetic mean (AS), standard deviation (SD) and a KS-test of normalities distribution of FC "Orkan" football players.

Table 2. Descriptive statistic parameters of specific motor abilities – FC "Orkan"

Variab.	INITIAL			FINAL		
	AS	SD	KS	AS	SD	KS
M20L [a]	4,17	0,31	0,14	4,1	0,27	0,12
STSL [a]	12,36	0,71	0,13	11,95	0,59	0,09
BTPP [a]	10,56	0,37	0,11	10,31	0,39	0,12
PG	29,2	6,3	0,1	31,4	8,39	0,15
PN	31,2	6,24	0,19	32,05	6,33	0,17
PPN	20,95	2,33	0,22	20,6	2,3	0,14
SUN	4,95	1	0,31	5	0,97	0,2
SUG	8,93	1,73	0,11	9,53	1,75	0,12

Border value of the KS test for N=20 is 0,36

As we can see in Table 2. not one KS-test value exceeds the border value of the Kolmogorov-Smirnov test for the observed sample. We can therefore conclude that all the variables in the initial and final testing of football players, have a distribution for which can be noted that it doesn't significantly deviate from normal. In the final testing, an increase of ability can also be noted (greater, i.e. smaller arithmetic mean values in negatively scaled tests) in all the variables, which was caused by programmed football treatment. This trend can also been seen in the area of minimum, i.e. maximum test result values. The variability of results in both initial and final testing are mostly even, i.e. there are no significant deviations in standard deviation values between the initial and final testing. Still, an increase of variability results can be noticed in precision assessment variables (PB and PG) and a decrease of variability in agility assessment variables and ball speed (STSL and M20L). An uneven influence of a programmed football treatment on all football players, in a specific motor space, is mostly reflected in the respective mentioned variables.
Table 3. shows multivariant and univariant indicators of differences between FC "Omiš" and FC "Orkan" football players, arithmetic mean (±SD) of motor variables and canonical discriminative analyses (F;CanR) in the initial and final testing.

Table 3. The discriminative analyses in the specific motor variables

Variab.	Initial		
	NK Omiš	NK Orkan	F
M20L [a]	4,47±0,57	4,17±0,31	0,47
STSL [a]	12,45±0,63	12,36±0,71	0,11
BTPP [a]	10,52±0,44	10,56±0,37	-0,1
PG	29,95±5,74	29,20±6,30	0,09
PN	29,90±5,42	31,20±6,24	-0,2
PPN	20,65±2,11	20,95±2,33	-0,1
SUN	4,60±1,27	4,95±1,00	-0,2
SUG	9,84±1,57	8,93±1,73	0,4
Centriods	*0,68*	*-0,68*	
CanR			*0,57*
Variab.	**Final**		
	NK Omiš	NK Orkan	F
M20L [a]	4,18±0,36	4,10±0,27	-0,2
STSL [a]	12,15±0,50	11,95±0,59	-0,2
BTPP [a]	10,17±0,27	10,31±0,39	0,24
PG	34,00±4,80	31,40±8,39	-0,2
PN	33,60±4,03	32,05±6,33	-0,2
PPN	21,85±1,69	20,60±2,30	-0,4
SUN	5,60±0,88	5,00±0,97	-0,4
SUG	7,20±1,43	9,53±1,75	-0,4
Centriods	*-0,82*	*0,82*	
CanR			*0,64**

F = discriminative function structure; CanR = cannonical discrimination coefficient; *p<0,05; **p<0,01; ***p<0,001

Based on the numeric parameters of the discriminative function (Can R=0,57 with a significance level of p>0,05), it can be seen that a statistically significant discriminative function can't be formed in the initial testing, in the motor characteristics area of two groups of football players. This means that football players didn't significantly differ in the initial testing, in the specific motor space. The discriminative function is defined with a positive projection of variables: M20L and SUG. The following variables are on the negative function pole: PN and SN. Other variables haven't been significantly projected on either of the function poles. The position of the group centroid (C:Omiš=0.68; C:Orkan=-0,68) defines FC "Orkan" football players, a group with better results in the initial testing in almost all the tests. It is possible to form a statistically significant discriminative function in the final testing (p<0,05) with a canonical correlation coefficient Can R=0,64. A different discriminative canonical analyses construction can be noticed. All the variables, except the BTPP, are projected on the negative function pole. The position of the group centroid defines FC "Orkan" football players as a group with better results in the final testing, in M20L, STSL, BTPP and SUG, while FC "Omiš" football players were better in other tests. Based on the given results, it can be concluded that FC "Omiš" and FC "Orkan" football players don't significantly differ in specific motor abilities in the initial testing. Moreover, in accordance with the results, we can observe that FC "Omiš" and FC "Orkan" significantly differ in specific motor abilities in the final testing. Table 4. shows measures univariate quantitative changes in specific motor variables between the initial and final measurement.

Table 4. Changes in specific motor variables

Variab.	FC OMIŠ		
	Init.	Final	F-test
M20L [a]	4,47±0,57	4,18±0,36	417,33*
STSL [a]	12,45±0,63	12,15±0,50	1057,42*
BTPP [a]	10,52±0,44	10,17±0,27	287,85*
PG	29,95±5,74	34,00±4,80	539,80*
PN	29,90±5,42	33,60±4,03	423,16*
PPN	20,65±2,11	21,85±1,69	581,45*
SUN	4,60±1,27	5,60±0,88	209,01*
SUG	9,84±1,57	7,20±1,43	363,41*
Variab.	**FC ORKAN**		
	Init.	Final	F-test
M20L [a]	4,17±0,31	4,10±0,27	365,85*
STSL [a]	12,36±0,71	11,95±0,59	375,54*
BTPP [a]	10,56±0,37	10,31±0,39	282,07*
PG	29,20±6,30	31,40±8,39	237,06*

PN	31,20±6,24	32,05±6,33	563,21*
PPN	20,95±2,33	20,60±2,30	570,82*
SUN	4,95±1,00	5,00±0,97	193,72*
SUG	8,93±1,73	9,53±1,75	143,76*

*F - test – univariant test value; p – significance level, *p<0,001*

By analyzing the indicators of partial changes (F – test) in the univariant variance analyses, it can be determined that significant changes occurred in all the measured variables of specific motor abilities of both groups of football players, in the period between the initial and final testing, which was anticipated. However, it's not possible to determine from these results, on which of the specific motor abilities of football players, did the programmed football treatment affect more significantly. Only further analyses in this paper will implicate the eventual effects of a football treatment on the specific motor abilities of FC "Omiš" and FC "Orkan" football players.

Table 5. presents measures univariate differences specific motor abilities between players of FC "Omiš" NK "Orkan". The difference in middle values between the final and initial testing for both groups have been calculated and displayed. The degree of changes in difference significance has been tested by applying the univariant variance analyses.

Table 5. Specific motor abilities differences (final - initial) of FC „Omiš" and FC „Orkan"

VARIABLES	x2-x1 FC Omiš	x2-x1 FC Orkan	F-test
M20L [a]	-0,29	-0,08	12,27**
STSL [a]	-0,30	-0,41	2,63
BTPP [a]	-0,34	-0,25	2,04
PG	4,05	2,20	1,76
PN	3,70	0,85	3,76*
PPN	1,20	-0,35	4,12*
SUN	1,00	0,05	11,08**
SUG	0,64	0,59	0,03

*x2-x1: arithmetic mean differences between the initial and final testing; F - test – univariant test of differences; *p<0,05; **p<0,01; ***p<0,001*

As it can be seen in the previous tables, the examinees from both groups have bettered their results in all specific motor abilities tests, in a period of four weeks. FC "Omiš" football players progressed more by comparison with FC "Orkan", in all of the tests, except the STSL variable. Based on these given results, it can be concluded that FC "Omiš" football players have progressed significantly more in M20L, PN, PPN and SUN tests. The programmed football treatment has significantly affected the development of specific motor abilities of football players of the cadet level, in a relatively short period of four micro cycles.

4. Conclusion

The given results point to how the results of FC "Omiš" and FC "Orkan" football players haven't significantly differed in a specific motor space in the initial testing, while there are statistically significant differences between the observed football players in the final testing. The results clearly show how significant differences occurred in all of the measured variables of specific motor abilities of both groups of football players, in the period between the initial and final testing, which was anticipated. FC "Omiš" football players progressed more by comparison with FC "Orkan" football players, in all the tests except the STSL variable. Based on these given results, it can be concluded that FC "Omiš" football players have progressed significantly more in M20L, PN, PPN and SUN tests. The programmed football treatment has significantly affected the changes of specific motor abilities (specific speed, strength, precision and agility), in a relatively short period of four micro cycles. Their increased involvement through this programmed football treatment has created positive changes that were manifested through increased values of all measured variables. Changes given in this research are a consequence of the adaptation of a football treatment which has its foundation in well programmed exercises for developing speed, basic and specific agility, explosive and repetitive strength, coordination and precision.

5. References

[1] B. Matković,B. Ivanković, „Funkcionalna dijagnostika vrhunskih hrvatskih nogometaša" u Hraski, Ž., i sur. (ur.) Znanstveno – stručno savjetovanje Trener i Suvremena dijagnostika, (str.117-121), 1999.

[2] D. Milanović, „Planiranje i programiranje kondicijskog treninga nogometaša" u ″Fitness″, Međunarodno savjetovanje o fitnessu, (str. II-70-II-77, 1996.

[3] M. Gabrijelić, „Neke situacione psihomotorne sposobnosti, potencijal i aktualno značenje za uspjeh djece u nogometnoj igri", Kineziologija 2, 1972.

[4] P. Dujmović, V: Mihačić, „Priručnik za nogometne trenere UEFA – B". 2004.

[5] M. Erceg, N. Zagorac, R. Katić, R., „The impact of football training on motor development in male children", Volume 32, Issue 1, , Pages 241-247 Faculty of Natural Sciences, Mathematics and Kinesiology, University of Split, Split, Croatia, March 2008.

[6] D. Dizdar, „Kvantitativne metode", Kineziološki fakultet u Zagrebu. 2006.

COMPUTER-AIDED DESIGN USING PROGRAMS ROBOT AND ADINA - COMPARISON

L. Kurzak[1], M. Major[1], I. Major[1*]

[1] Faculty of Civil Engineering, Czestochowa University of Technology, Poland
* *Corresponding author e-mail: admin@major.strefa.pl*

Abstract
In the paper the results of principal stress in the plate are presented produced by the two FEM programs ADINA and ROBOT. For the calculations a plate with external dimensions 6,00 x 5,00 m, with the longer plate side is attached both sided at the width of 15 cm, the axis of symmetry of the plate is supported by a column. The results of the calculations are presented in the form of contour lines (distribution) stress, in conclusion the results obtained are discussed.

Keywords:
ADINA, ROBOT, stress analysis, plate

1. Introduction

Fulfilling the conditions for bearing capacity and usage in the so-called structure maintenance are required within construction safety standards. To achieve these conditions complex and tedious calculations including time-consuming designer work, and time to achieve the expected results should be performed. Thus, computer-aided design using programs based on the finite element method, currently being the most effective and universal method to analyse the structure, are needed. There are two groups of FEM software commonly used in the structure modeling (comp. [2]). The first group allows you to perform calculations, the effect of which is to determine only the internal forces, stress, dislocations, etc., while the second one allows to supplement the above mentioned calculations with standardized criteria due to which the group forms basis for the effective structure measuring. The first group includes ADINA program (Automatic Dynamic Incremental Nonlinear Analysis), designed primarily for stress analysis in solids and both static and dynamic or flat and spatial structures [4]. The program also allows you to carry out various types of numerical simulations, linear modeling and highly non-linear behaviour of objects, taking into account large distortion, material nonlinearity and contact analysis [1]. The system consists of pre- and post-processor and computational modules:

- ADINA-IN – (preprocessor) data preparation module,
- ADINA – construction strength analysis module,
- ADINA-F - compressible and incompressible flow analysis module,
- ADINA-T – thermal field, electrostatic, porous media analysis module,
- ADINA-PLOT – (postprocessor) calculations results visualization module.

The second group comprises ROBOT Structural Analysis program [3] which is a tool for building and engineering structures calculations and analysis. The program allows calculation of any structure in accordance with the binding standards. It features efficient meshing tools, the option to use linear and non-linear analysis and a wide range of national measuring standards. The Calculating system package – ROBOT consists of computational modules which comprise:

- building and engineering structures modeling,
- structure analysis,
- reinforced concrete, steel and timber elements dimensioning.

In the paper, a comparative analysis of the stress and displacements results based on the program ADINA and ROBOT was made. Both programs have advanced computing environment with very high potential of computer-aided designing.

2. Computational assumptions

For the calculations a plate 0,15 m thick and the external dimensions of 6,00 x 5,00 m with a hole dimensions 3,00 x 1,40 m (Fig. 1).

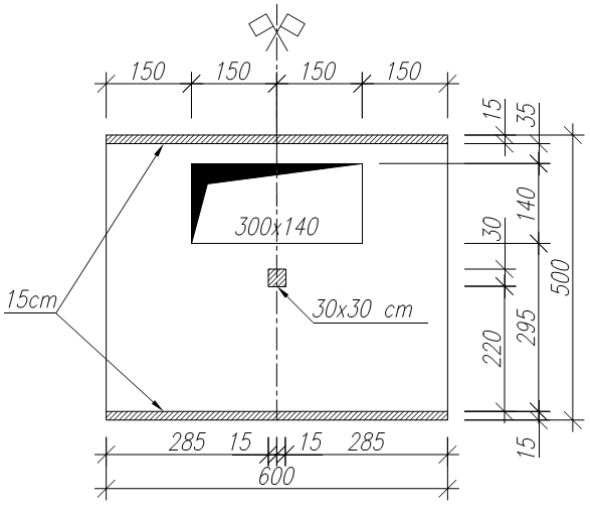

Figure 1. Support conditions and plate dimensions [cm]

The longer side of the plate is fixed both sided at the width of 15 cm. At the axis of symmetry the

plate is supported by an embedded column at the head, with dimensions of 0,30 x 0,30 m. The plate is supported by the column, which is located axially at a distance of 2,50 m from the attachment edge. Both attachments (linear on the walls and pointwise on the column) are not susceptible.
It has been assumed that the plate is made of concrete B25 (C20/25). The surface load "*q*" is 1,5 kN/m^2 and specific gravity of the plate „*g*" with bulk density 25 kN/m^3 has been assumed.(Fig. 2).

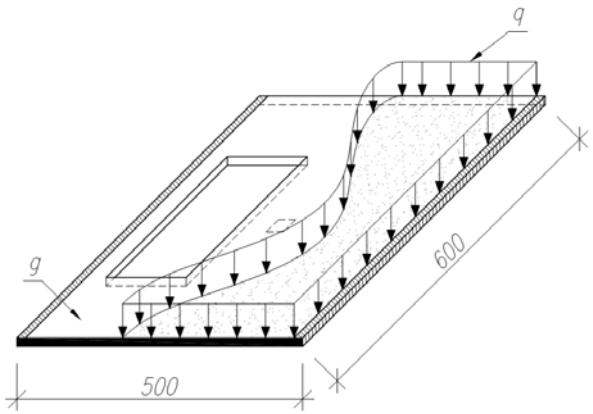

Figure 2. The load of the plate

3. Calculation model - FEM

The discrete model within ADINA (Fig. 3) and ROBOT (Fig. 4) programs has been achieved by dividing the area into the quadrangular elements (four-nodal) marking the plate edges every 10cm. The result is the homogeneous grid divided into squares almost throughout the surface being analysed.

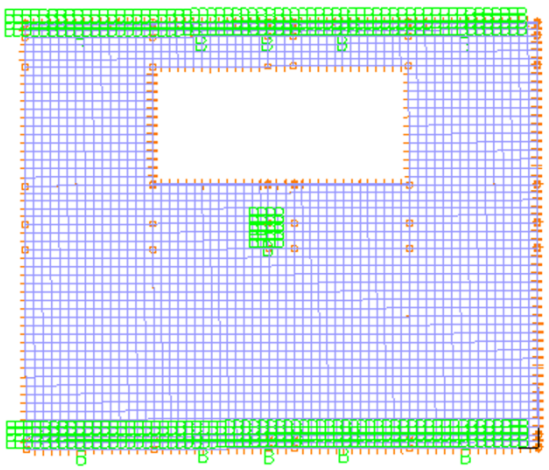

Figure 3. Discrete model of the plate in the ADINA program

The resulting model has made computer simulations of the work of the structure possible. In this case we consider the behaviour of the discrete mathematical model of the actual structure as a result of applied 1,5 kN/m^2 static load including the specific gravity of the plate 15 cm thick.

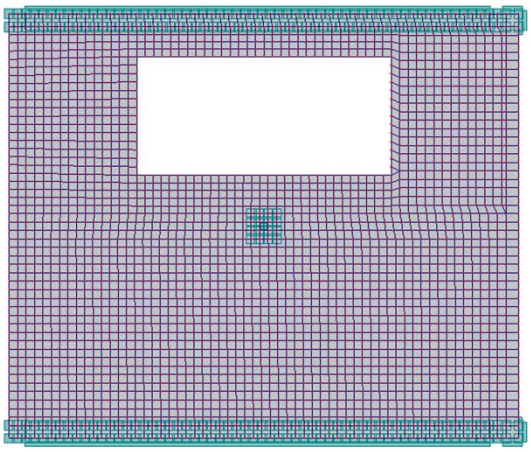

Figure 4. Discrete model of the plate in the ROBOT program

4. Analysis results of the ADINA and ROBOT programs

Figures 5 and 6 present the distributions of normal stress σ_X, while Figures 7 and 8 present distributions of normal stress σ_Y obtained respectively in the ADINA and ROBOT programs.

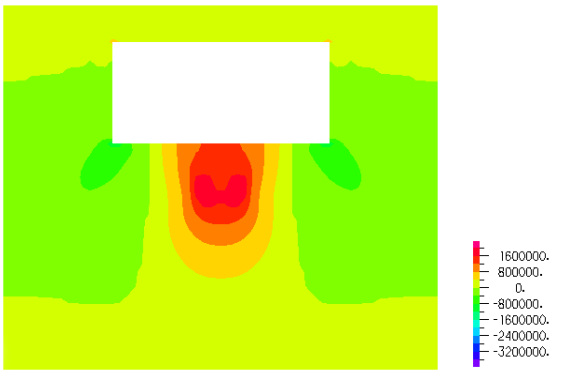

Figure 5. The σ_X stress distribution [Pa] in the ADINA program

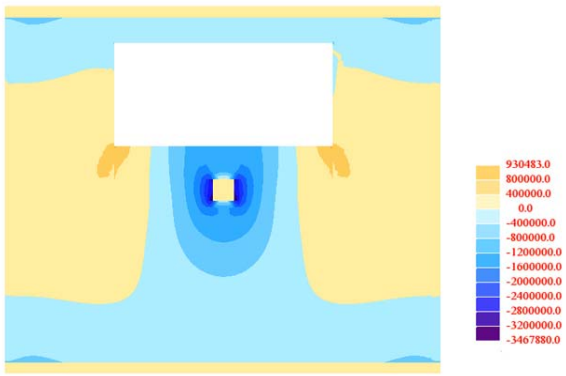

Figure 6. The σ_X stress distribution [Pa] in the ROBOT program

The normal stress σ_X in the ADINA program are formed in the range from ~1,0 GPa (extension) to ~2,1 GPa (compression) (see Fig. 5) and in the

ROBOT program it is from ~0,9 GPa to ~2,3 GPa respectively (Fig. 6). The reading from the distributions of the above stress values are different, and it is due to different divisions of the contour line of stress in both programs. Reading the stress values for specific points on the plate, these differences equalize, and one might say that identical values of the stress are obtained using both programs.
A similar solution has been received for the normal stress σ_Y (Fig. 7 and 8).

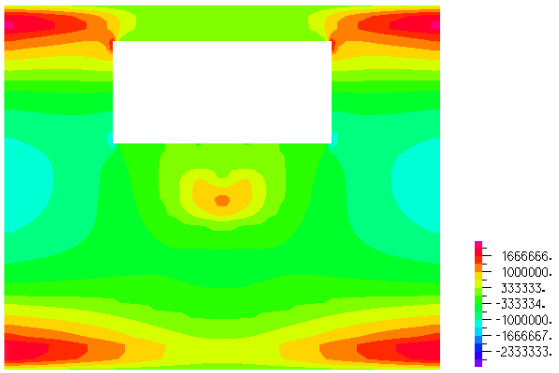

Figure 7. The σ_Y stress distribution [Pa] in the ADINA program

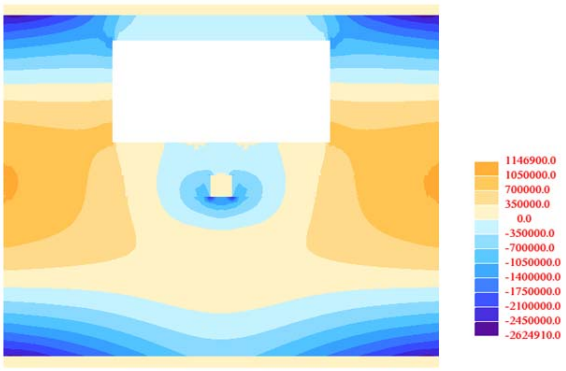

Figure 8. The σ_Y stress distribution [Pa] in the ROBOT program

The normal stress σ_Y in the ADINA program are formed in the range from ~1,2 GPa (extension) to ~2,0 GPa (compression) (Fig. 7) and in ROBOT it is from ~1,1 GPa to ~ 2,1 GPa respectively (Fig. 8).
Figures 9 and 10 show the distributions of displacements obtained respectively in the ADINA and ROBOT programs for plate attached both sides at the width of 15 cm, where at the axis of symmetry of the plate is supported by a column (see Fig. 1).
In the case of the ADINA program the greatest displacement obtained is 0,00078 m (Fig. 9), while in Robot it is 0,000729 m (Fig. 10). These differences are therefore small.

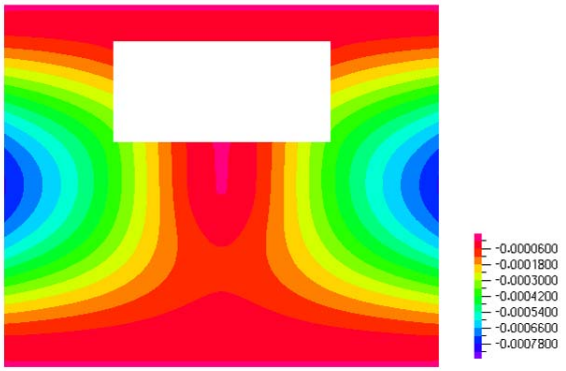

Figure 9. The displacements distribution [m] in the ADINA program

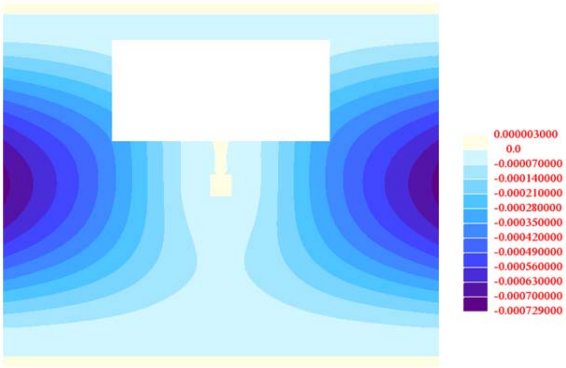

Figure 10. The displacements distribution [m] in the ROBOT program

5. Conclusion

The comparative analysis of stress states (in both tested models) showed little differences in principal stress distribution obtained in the two compared FEM programs - ADINA and ROBOT. No significant differences in the values of the stress generated by both programs were noticed. The applied loads (with the selected boundary conditions) brought the expected results. Also, the results for the displacements (displacement maps) obtained in the two programs have negligible differences in both distributions and values.

Comparison of the Figures 5 and 6 shows that the maximum stress is concentrated around the support column. Similarly, in Figures 7 and 8 it can be seen that the stress concentration is within the outermost sections of the attachments on the walls and at the support on the column. Comparison of figures 9 and 10 shows that the maximum deflection of the plate takes place in the middle of the free edges, which was a predictable outcome.
Declared edge attachment of the plate at a depth of 15 cm (see Fig. 1) is clearly marked on the graph of contour lines (distributions) in the ROBOT program. Also in this program, you can see the outline of the declared column and small concentrations in the distribution of stresses

around the column, resulting from the geometry of the cross section of the column and its attachment in the plate. In the ADINA program the distributions of principal stresses σ_X and σ_Y in the plate are much smoother both on the edge of the attachments on the walls and at the support on the column's head. In the attached edges at the width of 15 cm vertical displacements show zero values.
The comparative analysis showed that for the issues related to the structural calculations for plates, the ROBOT program is a more communicative environment for the designer. In comparison with the presented calculations the ADINA program is slightly less communicative, however, having a large spectrum of FEM calculations it provides the basis for the wider use as far as the calculation of building structures are concerned, including the vocational training being an integrated part within construction specialization. It is undoubtedly an important tool for shaping the awareness and skills of a future structure designer including a designer of building structures.

6. References

[1] M. Major, "Modelowanie zjawisk falowych w hipersprężystym materiale Zahorskiego", Wyd.PCzęst., 2013
[2] J. Awrejcewicz., M. Ciach, K. Włodarczyk, Finite element method analysis of non – linear behaviour of implants and stents, European Congress on Computational Methods in Applied Sciences and Engineering, ECCOMAS 2000, Barcelona, 11-14, 2000
[3] Robot Millenium 21.0 Podręcznik Użytkownika. Tom I i II, Autodesk 2008
[4] ADINA Tutorials, http://www.adina.com/tutorials.shtml

USING SCENARIO GENERATION FOR DECISION MAKING UNDER UNCERTAINTY

Tibor Vajnai[1,*], Olga Papp[1], Edit Csizmás[1] and Csaba I. Fábián[1]

[1]Institute of Informatics, Kecskemét College, 10 Izsáki út, 6000 Kecskemét, Hungary
* *Corresponding author e-mail: vajnai.tibor@gamf.kefo.hu*

Abstract
The objective of the present study is to develop advanced computational techniques to model complex electric power networks (smart grid). The problem requires the modelling of multidimensional random variables, and optimization based on the statistical model. Good calibration of the statistical model is very important because it is used for scenario generation which in turn feeds the stochastic programming optimizer.
The copula function is a flexible model describing collective behaviour of random parameters of the smart grid. Stochastic programming is used as a decision support tool.
In this paper we describe the above mentioned models and algorithms, and demonstrate their application using a financial data set.

Keywords:
stochastic dominance, scenario generation, copula, smart grid

1. Introduction

For the modelling of the collective behaviour of random parameters we can use Copula functions. With this aproach, we can separately consider the marginal behaviour of the random variables and the dependence between them.

Second Order Stochastic Dominanace (SSD) is a good tool to portfolio selection where the decision making process is based on risk-averse behaviour of the investor. However, the problem of finding SSD-efficient portfolios is computationally difficult.

2. Scenario generation

We used several scenario generation methods for randomly generating data for our model. The most complex method, namely the use of Copula functions has been chosen for modelling the collective behaviour of the random parameters [1]. Another scenario generation method is the one where we consider all random parameters to be independent of each other, thus we do not need to model the correlation between each pair of random variables.

This section focuses on the description of a special kind of copula functions, the Gaussian copulas [1],[5].

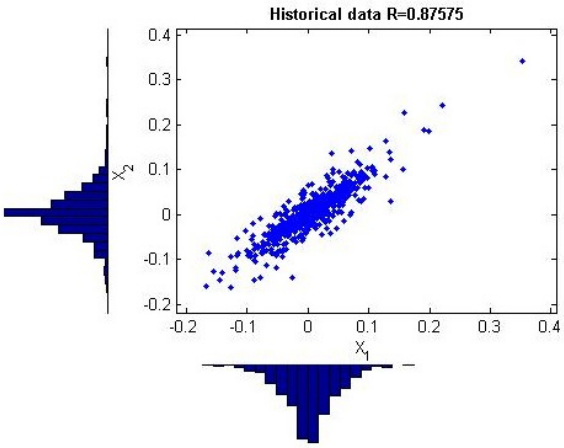

Figure 1. Samples from historical data. (N=710 ϱ =0,88)

Sklar in [12] proves that given an *m*-dimensional distribution function *F* with marginal distribution functions $F_{1,\dots}F_m$, there exists a function $C: \mathbb{R}^m \to \mathbb{R}$ for which $F(z_1, \dots, z_m) = C(F_1(z_1), \dots, F_m(z_m))$, $z_1,\dots,z_m \in \mathbb{R}$. Additionally, if the marginal distribution functions $F_1, \dots, F_m$ are continuous then this *C* function is unique. We call this *C* function a copula function. The copula method allows a large flexibility in modell selection.

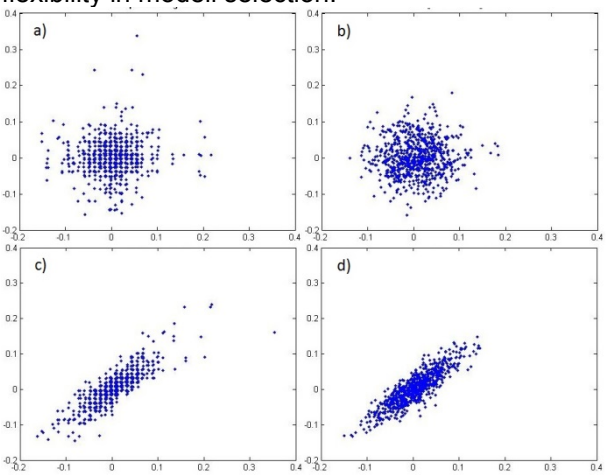

Figure 2. Samples (710) from independent modell with empircal (a) and lognormal (b) marginals Samples (710) from the Gaussian copula with correlation ϱ =0,88 with empirical (c) and lognormal (d) marginals

A Gaussian copula function is a special copula function with the following form:

$$C_\varrho\left(F_1(z_1), \dots, F_m(z_m)\right) = \Phi_{m,\varrho}(\Phi^{-1}F_1(z_1), \dots, \Phi^{-1}F_m(z_m))$$

where Φ is the one-dimensional standard normal distribution function and $\Phi_{m,\varrho}$ is the m-dimensional normal distribution function with expectation vector *0* and correlation matrix ϱ. In this paper we use gaussian copulae with empirical and lognormal marginals. The modell was calibrated with historical data sets.

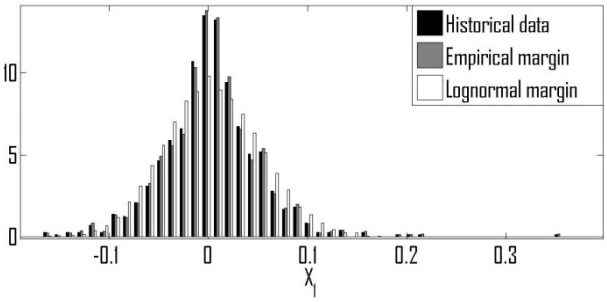

Figure 3. The X_1 marginal: normalised historical and 10 thousand simulated data

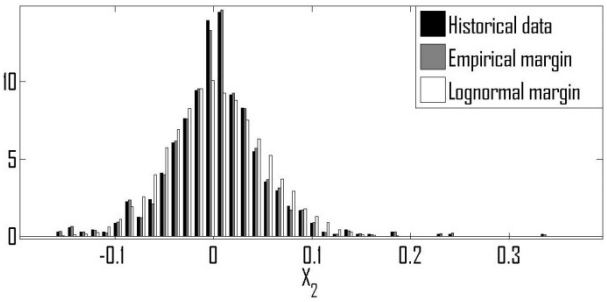

Figure 5. The X_2 marginal: normalised historical and 10 thousand simulated data

3. Stochastic dominance

Let's denote by *R* and *R'* random returns. Ω is a probability space with probability measure *P* and field of measurable sets $\mathcal{M}$. Let the random variables be integrable, that is *R, R'* $\epsilon \mathcal{L}^1 = \mathcal{L}^1(\Omega, \mathcal{M}, P)$.

Second-order stochastic dominance (SSD) can be defined by the three equivalent conditions below:

1. E(U(R)) ≥ E(U(R')) stands where *U* is a concave nondecreasing utility function with existing finite expected values.

2. $E([t\text{-}R]_+) \le E([t\text{-}R']_+)$ stands for each $t \in \mathbb{R}$

3. $\text{Tail}_\alpha(R) \ge \text{Tail}_\alpha(R')$ stands for $0 < \alpha \le 1$ and $Tail_\alpha(R')$ shows the unconditional expectation of the least α percent of the outcomes of *R*.

The concavity of the utility function at *(1.)* denotes the risk-averse behaviour. The equivalence of (*1.*) and (*2.*) can be found in [13]. The equivalence of (*2.*) and (*3.*) is found in [10]: here $Tail_\alpha(R)$ is considered a function of α, and $E([t\text{-}R]_+)$ a function of *t.* These functions are convex conjugates.

When (*1.*), (*2.*) or (*3.*) hold then we say that *R* dominates *R'* with respect to SSD, $R \succeq_{SSD} R'$. The corresponding strict dominance is $R \succ_{SSD} R'$, meaning $R \succeq_{SSD} R$ and $\neg (R' \succeq_{SSD} R)$.

In this computational study we focus on portfolio returns. Let the number of investment assets at the beginning of a determined time period be *n*. $\boldsymbol{x} = (x_1, \ldots, x_n) \in \mathbb{R}^n$ stands for a portfolio, that is the proportions of the portfolio value invested in the different assets.

R indicates the returns of the assets at end of the investment period. ***R*** is an *n*-dimensional random return vector. Our assumption is that the elements of ***R*** are in $\mathcal{L}^1$. If we consider ***R*** having realizations of different scenarios, then it can be described by a discrete distribution. Taking this assumption into account, the random return of an ***x*** portfolio can be defined by $R_x = x_1R_1 + \ldots + x_nR_n$.

Let $X = \{x \in \mathbb{R}^n \mid x \ge 0, x_1 + \ldots + x_n = 1\}$ denote the set of feasible portfolios. We say that a portfolio ***x**** is SSD-efficient if there is no feasible portfolio ***x*** for which $R_x \succ_{SSD} R_{x^*}$.

There are several SSD models we can review. We will examine two models, based on the SSD definitions (*2.*) and (*3.*).

Let us assume that a reference random return R_{ref} with discrete distribution is given. For example, this reference return could be the return of a benchmark portfolio or a stock index.

Using this reference return, Dentcheva and Ruszczyński [2] consider an SSD constrained portfolio optimization model according to the SSD definition (*ii.*):

$$\begin{gathered} \max f(x) \\ x \in X \\ R_x \succeq_{SSD} R_{ref} \end{gathered} \qquad (1)$$

In the above model *f* is a concave function, specifically, $f(x) = E(R_x)$. It is proven by the authors that when the random return vector has finite discrete distribution, the SSD relation can be defined by a finite system of inequalities. For the above assumption of finite discrete distributions, a duality theory is also developed by the authors, having the dual objects as concave nondecreasing utility functions.

Roman, Darby-Dowman and Mitra [11] describe a model according to definition (*3.*). Here, they assume having finite discrete distributions with equally probable outcomes. It is proven that the SSD relation $R_x \succeq_{SSD} R_{ref}$ can be described by a finite system of inequalities:

$$\text{Tail}_{i/S}(R_x) \ge \text{Tail}_{i/S}(R_{ref}), \forall\, i = 1 \ldots S \qquad (2)$$

In the above system *S* is the number of the equally probable scenarios. This model chooses an ***x*** portfolio whose return distribution R_x comes close to the reference return R_{ref} in a uniform sense. Uniformity is denoted by differences among tails. The *worst* tail difference is denoted by $\vartheta = min_{i=1\ldots S}(Tail_{i/S}(R_x) - Tail_{i/S}(R_{ref}))$.

If we maximize ϑ, we can consider the following multi-objective model whose Pareto optimal solutions are SSD efficient portfolios:

$$\begin{aligned} &\max \vartheta \\ &\vartheta \in \boldsymbol{R} \\ &x \in X \\ &\mathrm{Tail}_{i/S}(R_x) \geq \mathrm{Tail}_{i/S}(R_{ref}) + \vartheta \quad \forall i = 1 \ldots S \end{aligned} \tag{3}$$

The origin of the above model can be traced back to [6] and [7].
It often occurs, that the used reference distribution is not SSD efficient. In these cases the model improves until SSD efficiency is attained.
The model (3) has been implemented and tested on 51 real-world assets with data from 710 realizations.

4. Computational study

For the validity of comparison in this computational study we used the same historical data as in the previous works, namely: the data set contains weekly returns of *n*=51 stocks and the index of the FTSE 100 basket. This historical data reaches 944 weeks.
For each week each component's price and the stock index is given. Let s_0^t represent the stock index of the *t*th week and let s_k^t be the price of the *k*th asset.
Each week's return is computed in the following way: $r_k^t := (s_k^t - s_k^{t-1}) / s_k^{t-1}$, $0 \leq k \leq n$. Let $\boldsymbol{r}^t := (r_0^t, r_1^t, \ldots, r_n^t)$ and the data set $\mathcal{R} := \{r^t \mid t = 1 \ldots 944\}$.
For creating a proper test set we divided the data set randomly into two subsets H and T each representing 25% respectively 75% of the available data. We used the set H for generating sample data and performing in-sample tests and the set T for performing out of sample tests. Sizes of the subsets are 710 for the subset H and 236 for the subset T.
The division into subsets has been repeated independently six times and for each set H we generated sample data of 60000 using the empirical method combined with Gaussian Copula function and the method where we assumed the random variables to be independent of each other.
For each generated set and each set H we compared the optimal portfolios. For each pair of sets in-sample and out-of-sample tests have been performed.
Consolidated in-sample and out-of-sample results can be seen in Figures 7. and 8.

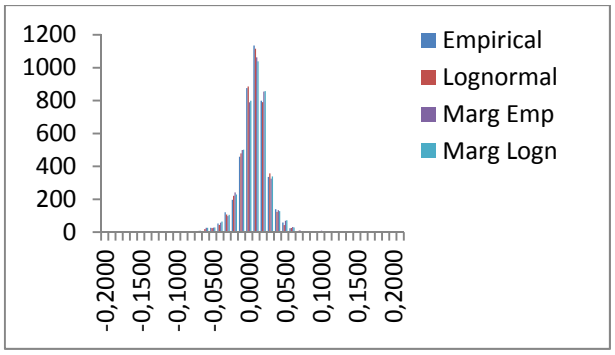

Figure 7. In-sample testing results

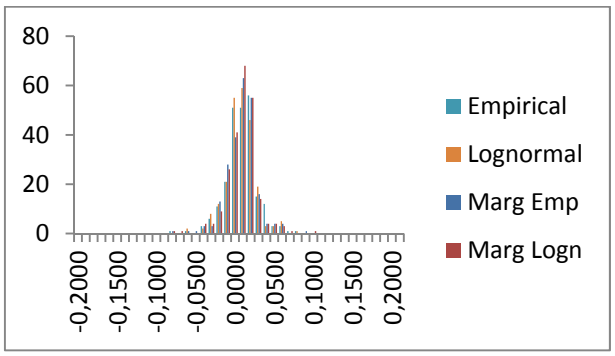

Figure 8. Out-of-sample testing results

As seen in the figures, the difference between the methods used is not significant. That results from the high number of scenarios, where the differences blend in.

5. Conclusion

We performed an analysis of different scenario generation methods for the financial risk-averse decision problem of selecting an optimal investment portfolio. The data used for our decision has been generated using different scenario generation methods. We conclude that the scenario generation method that takes into consideration the collective behaviour of the random variables and the model where these random variables are assumed to be independent do not result strongly different returns. However, the structure of the resulting optimal portfolios are entirely different: the first approach resulted in portfolios consisting of 31% of the available assets, whereas the second approach resulted in portfolios with over 98% assets from the available 51 ones.
Furthermore, he index distribution was dominated in all cases by the distribution of the optimal portfolio returns.
The approach is not sensitive to the independence of the random variables.
The presented approach is potentially useful for describing the statistical behaviour of smart grid stochastic parameters and optimizing the control of operation.

6. Acknowledgement
We would like to thank Gautam Mitra, Victor Zverovich and Diana Roman from Brunel University and OptiRisk Systems for providing us the data for testing.

This research and publication have been supported by the European Union and Hungary and co-financed by the European Social Fund through the project TÁMOP-4.2.2.C-11/1/KONV-2012-0004: National Research Center for the Development and Market Introduction of Advanced Information and Communication Technologies. This source of support is gratefully acknowledged.

7. References

[1] U. Cherubini, E. Luciano, and W. Vecchiato, "*Copula Methods In Finance", John Wiley and Sons,* 2006.
[2] D. Dentcheva and A. Ruszczyński, "Portfolio optimization with stochastic dominance constraints", *Journal of Banking & Finance* 30, 433-451, 2006
[3] C.I. Fábián, G. Mitra, D. Roman, and V. Zverovich, "An enhanced model for portfolio choice with SSD criteria: a constructive approach", *Quantitative Finance* DOI: 10.1080/14697680903493607, 2010.
[4] C. I. Fábián, G. Mitra, D. Roman, V. Zverovich, T. Vajnai, E. Csizmás, and O. Papp, "Portfolio Choice Models Based on Second-Order Stochastic Dominance Measures: An Overview and a Computational Study"*, Stochastic Optimization Methods in Finance and Energy,* 441-471*,* 2011.
[5] A.J. McNeil, R. Frey, and P. Embrechts, "Quantitative Risk Management"*, Princeton University Press*, 2005.
[6] W. Ogryczak, "Multiple criteria linear programming model for portfolio selection", *Annals of Operations Research* 97, 143-162, 2000.
[7] W. Ogryczak, "Multiple criteria optimization and decisions under risk", *Control and Cybernetics* 31, 975-1003, 2002.
[8] W. Ogryczak and A. Ruszczyński, "Dual stochastic dominance and related mean-risk models", *SIAM Journal on Optimization* 13, 60-78, 2002.
[9] O. Papp, E. Csizmás, C.I. Fábián, T. Vajnai, G. Mitra, D. Roman, V. Zverovich, "A computational study of scenario generation methods", *Applied Mathematical Optimization and Modelling. Extended Abstracts of the APMOD 2012 Conference (L. Suhl, G. Mitra, C. Lucas, A. Koberstein, and L. Beckmann, editors).* Vol 8 of the DSOR Contributions to Information Sytems. DS&OR Lab, University of Paderborn, 2012, pp. 89-94.
[10] O. Papp, E. Csizmás, C. I. Fábián and T. Vajnai: "A comparison of scenario generation methods with risk-averse decisions." *TEAM 2012, Proceedings of the 4th International Scientific and Expert Conference(Marija Zivic, Tomislav Galeta, editors).* Vol IV, Number 1, Mechanical Engineering Faculty in Slavonski Brod, Josip Juraj Strossmayer University of Osijek and Internationam TEAM Society, 2012. pp.219-222.
[11] D. Roman, K. Darby-Dowman and G. Mitra, "Portfolio construction based on stochastic dominance and target return distributions", *Mathematical Programming* Series B 108, 541-569, 2006.
[12] A. Sklar, "Fonctions de répartition à *n* dimensions et leurs marges", *Publications de l'Institut de Statistique de l'Universit de Paris* 1959/8, 229-231, 1959.
[13] G.A. Whitmore and M.C. Findlay, "Stochastic Dominance: An Approach to Decision- Making Under Risk", *D.C.Heath, Lexington, MA*, 1978.

TEACHING ENGLISH FOR SPECIFIC PURPOSES AT THE FACULTY OF MANUFACTURING TECHNOLOGIES

Rimma Bielousová

Faculty of Manufacturing Technologies of the Technical University of Košice with the seat in Prešov, Slovakia
Corresponding author address e-mail: rimma.bielousova@tuke.sk

Abstract
The author outlines a conception for English for Specific Purposes (ESP) course specially designed for the students of the Faculty of Manufacturing Technologies of the Technical University of Košice. The paper also emphasises the idea of „tailoring" study materials for technically oriented study branches and specialisations of the faculty.

Keywords:
tailored study materials, technical communication, English for Specific Purposes

1. Introduction

English for Specific Purposes courses worldwide are very often oriented towards development of reading comprehension. Undoubtedly, such an orientation is appropriate if the students' ideas of their future careers have more or less clear contours expecting that they will get a job in some engineering branch. Many of our future graduates can hardly predict the sphere of their professional activities. This reality has to be taken into account when formulating the principal course objective at the faculty – a proportional development of all language skills.

2. From general English to general technical English

In accordance with the current social trends, we should get rid of a rather one-sided view of an engineer as an expert in some scientific field using his English knowledge entirely for reading scientific literature. Engineering activities involve much broader repertoire. We suppose that, in general, the most common macro – activities, in which technicians, scientists, or business persons using English as a foreign language will likely find themselves, are: reading technical publications, handbooks, or journals to keep abreast of professional developments, writing technical publications and technical reports, giving presentations, contacts with business partners from abroad through business correspondence, telephoning, taking part in technical discussions at conferences, seminars, exhibitions and other technical meetings or international events, travelling, social and professional conversations with English-speaking clients and visitors. On the one hand, technical English has its own characteristic features: special terminology, passive voice constructions, etc. On the other hand, technical communication has much in common with everyday speech. Technical English is not only about graphs and figures. It would be much closer to the truth to say that technical English is about forming relationships with colleagues, customers and a variety of international contacts. It regards especially expressing agreement and disagreement, explaining, emphasizing, etc. Thus, it is the language which students are supposed to master when studying general English. A key difference between technical and general English consists in the language skills balance. If you make a mistake when writing, you can go back and check it. The same is with reading, but when you are speaking, you are under pressure and making mistakes when speaking can result in loss of face. Thus, we consider speaking to be a top priority skill. Our aim is to control the teaching process so that the process of learning the technical language was closely connected with the language of general English, i.e. using the forms of living speech: discussion, interview, presentation, etc. If any foreign language course is to fulfil its aim, it is necessary to determine precisely the content of the course (what the teacher and the students do) and how to reach the aim (teaching strategies and techniques for students' doing the tasks). This can be determined through an analysis of the macro-activities and micro-activities the students will be performing in the foreign language. The challenge lies in the definition of the curricula for foreign language courses and the use of a suitable textbook so that they satisfy the wide range of engineering specializations, and at the same time, in the most specific form they meet the requirements of the purposefully defined tasks. The principal goal of teaching English as a foreign language at the Faculty of Manufacturing Technologies of the Technical University in Košice is to develop communicative abilities (reading, writing, speaking, listening) of the engineering students through the topics which are related to engineering branches and specializations of the faculty and numerous macro-activities in which the future technicians and engineers may be involved in their professional careers. For this purpose Moodle Learning Management System has been adopted by the Technical University of Košice as

one of the e-learning platforms [1]. Having established the aim and content of the course, the next step is to select appropriate teaching materials that will be used in the course. There is a good choice of commercially prepared English textbooks for both Business and Technical English on the Slovak book market, but in spite of that we were not able to find a single textbook which suited our requirements for the following reasons:

a) too general or too specific books for our purposes;
b) impossible to find one common book for both Business English and Technical English teaching;
c) teacher's effort to tailor a "communication background" included in the English textbooks to the needs of students is a teacher's time - consuming and tiring job.

3. Language learning materials selection and development

Due to the lack of nationwide specialized English textbooks for technical universities in Slovakia and in an attempt to solve this problem we designed the textbook which since September 2011 has been used in ESP courses at the faculty [2]. The textbook includes teaching materials for both Business English and Technical English. It also includes a CD spoken by native speakers of English. The textbook was prepared according to the following criteria: proportional amount of Business English and Technical English, relevance of communicative information to the students' needs, adequacy to the language competence of most of the students, familiarity with the environment in which the language communication is going on (university, social and industrial background of the area or the country the students live in). Business English is given during one semester and it includes the following
macro-activities (and micro-activities): Finding a Job (Engineering jobs-descriptions, Job advertisements, A letter of application, Curriculum Vitae, Employment interview). Business Correspondence (Layout of a business letter, Letter of enquiry). Technical English course deals with specialized texts that relate to the students' particular study branches. The thematic range is relatively wide as in the second year of study students are not divided into groups according to their specialisations. This course deals with the following professionally relevant macro-activities: Environment, Giving Instructions, Describing Processes, Computers, Presentations, How Things Work, Traditional and Advanced Machining Processes, Engineering Materials, Manufacturing Technologies. The above mentioned macro-activities are accompanied by a series of functional micro-tasks commonly used in scientific or technical English and designed to help the students meet specific objectives, such as : giving instructions, describing a product, describing instruments, machines or appliances, describing parts of a system, describing a sequence of actions, classification, definition, functions. At the same time, the students are taught to do such tasks as how to agree or disagree, how to recommend, how to criticize and to evaluate, and to use structural or grammatical items: the passive, time adverbs, structures with participles, infinitive and gerund, relative clauses, expressions denoting purpose, cause and effect, etc. Texts used in the textbook are either authentic or simplified if authentic texts were too difficult to be used for the development of general reading ability. They are representative of the subject that the students are studying and are introduced in tandem with subject studies or after subject studies. According to the purpose they are used for, the texts can be divided into the following groups:

a) texts primarily used for reading (technical texts);
b) texts primarily used for speaking (Telephoning, Giving Instructions);
c) texts primarily used for writing (Business Correspondence, Finding a Job, Reports;
d) texts primarily used for listening (specially designed listening exercises).

The above classification of the texts, of course, does not mean that a mutual interference of individual language skills through a specific text is impossible. On the contrary, a purposefully designed set of exercises to each text is aimed at the integration of individual language skills. Actually, reading is seldom practised without writing or speaking, or, on the other hand, we hardly ever practise speaking without listening. A typical example of the development of all language skills (reading, writing, speaking, listening) is the topic Presentation where students use reading to acquire information, write a layout and notes to the presentation, present the presentation orally, and listen (and respond) to the questions of the audience. When developing exercises to each lesson of the textbook we concentrated on the following criteria:

a) gearing the goals of the exercises (through the content and techniques of the exercises) to the ultimate goals of the lesson and the teaching program;
b) the use of clear instructions to show the purpose of the exercises;
c) the use of variety of techniques to support the development of individual language skills as well as the use of English in real-life situations.

4. Conclusion

Those foreign language teachers who are faced with a need to create large bodies of teaching

materials for the students (and who of us is not?) know that this work is a time-consuming, exhaustive and frustrating process of self-training as teacher-preparation programmes in Slovakia do not include a specific training in the techniques of writing separate teaching materials or textbooks. Thus, the process is accompanied by trials and errors, by success or failure. While using the textbook, we may find out that some exercises do not work well, or some types of texts and exercises are missing, or the like. We rewrite the material or create the new one so the task seems to be never-ending. Preparation of a textbook in local conditions of the faculties or universities in Slovakia is even a more complicated process which verifies author's professional skills as well as his enthusiasm and pertinacity due to other problems (technical and financial) connected with the preparation of the textbook from the inception to the completion.

5. Acknowledgement

This paper is supported by KEGA, contract No. 013TUKE-4/2012 „Application of E-learning in Foreign Language Teaching at the Faculty of Manufacturing Technologies"

6. References

[1] M.Gluchmanová, "Blended learning in foreign language teaching",IETC -2013 :13th International Educational Technology Conference: Proceedings Book: May 13-15, 2013, Kuala Lumpur, Malaysia. – Kuala Lumpur: University of Malaya, P. 197-200,2013.

[2] R.Bielousová and M. Gluchmanová, "Essential English for Manufacturing Technicians", FVT TU, Prešov, 2011.

PROPAGATION OF DISTRUBANCES IN HYPERELASTIC BLATZ-KO MATERIAL

M. Major[1*], I. Major[2] and J. Różycka[3]

[1,2,3]Faculty of Civil Engineering at the Czestochowa University of Technology
** Corresponding author e-mail: admin@major.strefa.pl*

Abstract
The purpose of this paper is to discuss the approximate behavior of the propagation of surface of discontinuities in the form of transverse and longitudinal harmonic wave propagating in a composite made up of Blatz - Ko materials. In work in accordance with the assumptions discussed acoustic wave. The study adopted a composite consisting of two infinite material areas separated homogeneous layer with a thickness of d. Transition layer was filled a homogenous rubber, whereas extreme areas was filled foamed rubber of the same type. Numerical analysis was based on the work of [3], assuming successively the two extreme values in the range of Poisson's ratio (v), defined for homogeneous rubber.

Keywords:
Blatz-Ko material, acoustic wave, rubber-like layered composites, hyperelastic materials

1. Introduction

In this paper is considered the propagation of transverse and longitudinal acoustic waves propagating in the composite structure consisting with materials of Blatz-Ko. The composite consist of a homogeneous layer 1, a thickness d, separating the two infinite homogeneous material areas 0 and 2 as shown on Fig 1.

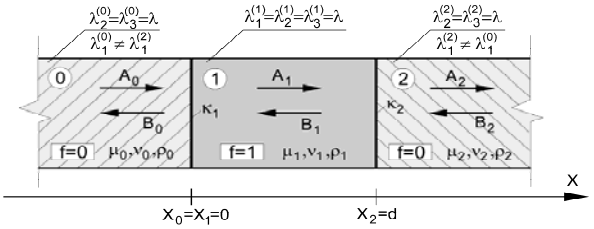

Figure 1. Composite structure with the transition layer (homogenous rubber)

The two extreme areas (0 and 2) were filled the same foamed rubber (f = 0), while the separating layer - homogeneous rubber (f = 1).Poisson ratio in foamed rubber undergoing infinitesimal deformation, according to the work [1], [2] assumes a constant value: v = 0.25, whereas in the case of homogeneous rubber this ratio is in a range 0.47 ≤ v ≤ 0.493. In this paper, was conducted an analysis of acoustic wave propagation at the upper values v ≤ 0.493 for homogeneous rubber and compared with the results obtained in [1] at the extreme lower value of Poisson ratio v ≤ 0.47.

2. Basic equations and equations describing the Blatz-Ko material

Constitutive equation describing the behavior of compressible porous elastomers, created as a result of experience is presented in the work of Blatz, Ko [1]

$$W(I_1,I_2,I_3)=\frac{\mu f}{2}\left\{I_1-3+\frac{1-2\nu}{\nu}\left[I_3^{\frac{-\nu}{1-2\nu}}-1\right]\right\}+\frac{\mu(1-f)}{2}\left\{\frac{I_2}{I_3}-3+\frac{1-2\nu}{\nu}\left[I_3^{\frac{\nu}{1-2\nu}}-1\right]\right\} \quad (1)$$

where: I_1, I_2, I_3 - invariants of the left Cauchy Green deformation tensor.
Appearing in the equation: μ - shear modulus, v - Poisson ratio relating to infinitesimal deformation. The value of the parameter f describing the share of pores in material is in the range 0 ≤ f ≤ 1.The literature, particular attention was paid to two models of the material, when f = 0 (foamed rubber) and f = 1 (homogenous rubbers). Equation (1) for the above two specific models of materials reduces to the following form:
for *f=0*:

$$W(I_2,I_3)=\frac{\mu}{2}\left\{\frac{I_2}{I_3}-3+\frac{1-2\nu}{\nu}\left[I_3^{\frac{\nu}{1-2\nu}}-1\right]\right\} \quad (2)$$

for *f=1*:

$$W(I_1,I_3)=\frac{\mu}{2}\left\{I_1-3+\frac{1-2\nu}{\nu}\left[I_3^{\frac{-\nu}{1-2\nu}}-1\right]\right\} \quad (3)$$

3. Conditions for propagation of acoustic waves propagating in a layered rubber-like composite.

It was assumed that the general motion associated with the propagation of a plane wave takes the form [3]:

$$x_1=\lambda_1^{(k)}X^r{}_1+u_1^{(k)}(X,t),\quad x_2=\lambda_2^{(k)}X^r{}_2,\quad x_3=\lambda_3^{(k)}X^r{}_3+u_3^{(k)}(X,t) \quad (4)$$

$X^r{}_1, X^r{}_2, X^r{}_3$ are the coordinates of the material, the upper index (k) is a variable defined in the layer k, whereas $\lambda_1^{(k)}, \lambda_2^{(k)}, \lambda_3^{(k)}$ are the main extensions of the static homogeneous deformation pre in the area k.

For foamed rubber and homogenous rubber layout of equations of motion reduces to two non-conjugated wave equations [3]:

$$u_{111}^{(k)} = \frac{1}{c_k^2} u_1^{(k)}, \quad u_{311}^{(k)} = \frac{1}{c'^2_k} u_3^{(k)} \tag{5}$$

where velocity of propagation of longitudinal waves for foamed rubber (f = 0) and homogenous rubber (f = 1), are respectively [3]:
for f=0

$$c_k^2 = \frac{\mu}{\rho_R^{(k)}}\left[3\lambda_1^{-4} + \frac{4\nu - 1}{1-2\nu}(\lambda_2,\lambda_3)^{\frac{2\nu}{1-2\nu}}\lambda_1^{-\frac{6\nu-2}{1-2\nu}}\right] \tag{6}$$

for f=1

$$c_k^2 = \frac{\mu}{\rho_R^{(k)}}\left[1 + \frac{1}{1-2\nu}(\lambda_2,\lambda_3)^{-\frac{2\nu}{1-2\nu}}\lambda_1^{-\frac{6-2\nu}{1-2\nu}}\right] \tag{7}$$

velocities of transverse wave present the following equation [3]:
for f=0

$$c'^2_k = \frac{\mu}{\rho_R^{(k)}}\frac{1}{\lambda_1^2\lambda_3^2} \tag{8}$$

for f=1

$$c'^2_k = \frac{\mu}{\rho_R^{(k)}} \tag{9}$$

It is assumed that the material k-1 in the left side of the plane $X_0 = X_1$ is foamed rubber (f=0), and k material lying in the right side is homogenous rubber (f=1). For two adjacent layers should be considered dependence of extensions of the main deformation $\lambda_1^{(k-1)}$, $\lambda_1^{(k)}$ in the form [3]:

$$\frac{\mu_k}{\mu_{k-1}} = \frac{(\lambda_1^{(k-1)})^{\frac{4\nu_{k-1}-1}{1-2\nu_{k-1}}}(\lambda_2^{(k-1)}\lambda_3^{(k-1)})^{\frac{\nu_{k-1}}{1-\nu_{k-1}}}}{\lambda_1^{(k)} - (\lambda_1^{(k)})^{\frac{-1}{1-2\nu_k}}(\lambda_2^{(k)}\lambda_3^{(k)})^{\frac{-2\nu_k}{1-2\nu_k}}} - \frac{(\lambda_1^{(k-1)})^{-\frac{1}{1-2\nu_{k-1}}}}{\lambda_1^{(k)} - (\lambda_1^{(k)})^{\frac{-1}{1-2\nu_k}}(\lambda_2^{(k)}\lambda_3^{(k)})^{\frac{-2\nu_k}{1-2\nu_k}}} \tag{10}$$

At the Poisson ratio for the foam rubber $\nu = 0{,}25$ for infinitesimal deformation [1], [2] and, assuming that the layer on the right side of the plane (homogeneous rubber) is subjected to homogeneous dilatation, where $\lambda_1^{(k)},\lambda_2^{(k)},\lambda_3^{(k)} = \lambda$ equation (9) takes the form [3]:

$$\lambda_1^{(k-1)} = \left\{\lambda^2 + \frac{\mu_k}{\mu_{k-1}}\left[\lambda^{-\frac{4\nu_k+1}{1-2\nu_k}} - \lambda\right]\right\}^{-\frac{1}{2}} \tag{11}$$

Considering the harmonic wave, propagating in the analyzed composite in the direction perpendicular to the layers, it is assumed the wave motion having the form [3]:

$$u_1^{(k)}(X,t) = A_k \exp i\omega\left(t - \frac{X - X_k}{c_k}\right) + B_k \exp i\omega\left(t + \frac{X - X_k}{c_k}\right) \tag{12}$$

$$u_3^{(k)}(X,t) = A'_k \exp i\omega^{'}\left(t - \frac{X - X_k}{c'_k}\right) + B'_k \exp i\omega\left(t + \frac{X - X_k}{c'_k}\right) \tag{13}$$

where: ω, ω'- the frequency of longitudinal and transverse waves; c_k, c'_k – velocity of propagation of longitudinal and transverse waves, A_k, B_k, A'_k, B'_k – reciprocally incorporated amplitude of the longitudinal. The relationship between the reciprocally incorporated amplitudes sinusoidal of longitudinal and transverse waves in the layer k-1 and k is [3]:

$$\begin{bmatrix} A_k \\ B_K \end{bmatrix} = M_k \begin{bmatrix} A_{k-1} \\ B_{k-1} \end{bmatrix}, \quad \begin{bmatrix} A'_k \\ B'_K \end{bmatrix} = M'_k \begin{bmatrix} A'_{k-1} \\ B'_{k-1} \end{bmatrix} \tag{14}$$

$$M_k = \frac{1}{2}\begin{bmatrix} (1+\kappa_z)\exp(-i\alpha_z) & (1-\kappa_z)\exp(-i\alpha_z) \\ (1-\kappa_z)\exp(-i\alpha_z) & (1+\kappa_z)\exp(-i\alpha_z) \end{bmatrix} \tag{15}$$

$$M'_k = \frac{1}{2}\begin{bmatrix} (1+\kappa'_z)\exp(-i\alpha'_z) & (1-\kappa'_z)\exp(-i\alpha'_z) \\ (1-\kappa'_z)\exp(-i\alpha'_z) & (1+\kappa'_z)\exp(-i\alpha'_z) \end{bmatrix} \tag{16}$$

where:

$$\kappa_k = \frac{\rho_R^{(k-1)} c_{k-1}}{\rho_R^{(k)} c_k}, \alpha_k = \omega\frac{X_k - X_{k-1}}{c_{k-1}} = \frac{\omega d_{k-1}}{c_{k-1}} \tag{17}$$

$$\kappa'_k = \frac{\rho_R^{(k-1)} c'_{k-1}}{\rho_R^{(k)} c'_k}, \alpha'_k = \omega'\frac{X_k - X_{k-1}}{c'_{k-1}} = \frac{\omega' d_{k-1}}{c'_{k-1}} \tag{18}$$

4. Numerical analysis

In paper assumed shear modulus of rubber homogeneous (f=1) μ_1 = 0,234MPa (comp[3]) and the foamed rubber $\mu_0=\mu_2$ = 0,221MPa. For foamed rubber used a constant value Poisson ratio, defined for infinitesimal values $\nu_0 = \nu_2 = 0{,}25$, while for the homogenous rubber assumed extreme values: $\nu_1 = 0{,}47$ [3] (case I) and $\nu_2 = 0{,}493$ (case II). It was assumed in the layer 1 (homogeneous rubber) the initial deformation in the form of homogeneous dilatation, where: $\lambda_1^{(1)},\lambda_2^{(1)},\lambda_3^{(1)} = \lambda$. After inserting the Poisson ratio for rubber homogeneous $\nu_1 = 0{,}47$ (case I) and (case II) to the equation (10), we obtain [3]:
for $\nu_1 = 0{,}47$:

$$\lambda_1^{(0)} = \left\{\lambda^2 + \frac{\mu_1}{\mu_0}\left[\lambda^{-4\beta} - \lambda\right]\right\}^{-\frac{1}{2\beta}} \quad (19)$$

$$\lambda_1^{(1)} = \left\{\lambda^2 + \frac{\mu_1}{\mu_2}\left[\lambda^{-4\beta} - \lambda\right]\right\}^{-\frac{1}{2\beta}} \quad (20)$$

For $\nu_1 = 0{,}493$

$$\lambda_1^{(0)} = \left\{\lambda^2 + \frac{\mu_1}{\mu_0}\left[\lambda^{-\frac{1486}{7}} - \lambda\right]\right\}^{-\frac{1}{2\beta}} \quad (21)$$

$$\lambda_1^{(1)} = \left\{\lambda^2 + \frac{\mu_1}{\mu_2}\left[\lambda^{-\frac{1486}{7}} - \lambda\right]\right\}^{-\frac{1}{2\beta}} \quad (22)$$

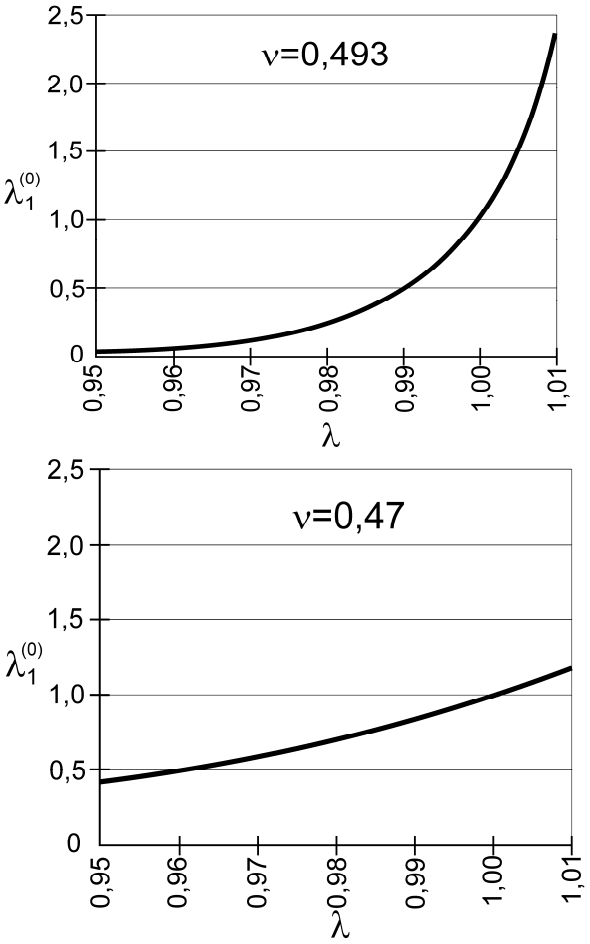

Figure 2. Graphs the relationship between the components of the deformation gradient in homogeneous and foamed rubber assuming two values Poisson ratio for homogeneous rubber

Complementing equation (6), (7), (8) and (9) with a value of Poisson ratios for the areas 0,1,2 we get:
for $\nu_1 = 0{,}47$:

$$c_1^2 = \frac{\mu_1}{\rho_R^{(1)}}\left[1 + 16{,}66\lambda^{-4\beta}\right], \quad c_1^2 = \frac{\mu_1}{\rho_R^{(1)}} \quad (23)$$

$$c_p^2 = \frac{3\mu_2}{\rho_R^{(2)}}\left(\lambda^2 + \frac{\mu_1}{\mu_2}\left[\lambda^{-4\beta} - \lambda\right]\right)^{\frac{1}{2\beta}} \quad (24)$$

$$c_s^2 = \frac{\mu_2}{\rho_R^{(2)}}\lambda^{-2}\left(\lambda^2 + \frac{\mu_1}{\mu_2}\left[\lambda^{-4\beta} - \lambda\right]\right)^{\frac{2}{2\beta}}, \quad \beta = 0{,}2 \quad (25)$$

For $\nu_1 = 0{,}493$

$$c_1^2 = \frac{\mu_1}{\rho_R^{(1)}}\left[1 + 71{,}429\lambda^{-\frac{1482}{7}}\right], \quad c_1^2 = \frac{\mu_1}{\rho_R^{(1)}} \quad (26)$$

$$c_p^2 = \frac{3\mu_2}{\rho_R^{(2)}}\left(\lambda^2 + \frac{\mu_1}{\mu_2}\left[\lambda^{-\frac{1486}{7}} - \lambda\right]\right)^{\frac{1}{2\beta}} \quad (27)$$

$$c_s^2 = \frac{\mu_2}{\rho_R^{(2)}}\lambda^{-2}\left(\lambda^2 + \frac{\mu_1}{\mu_2}\left[\lambda^{-\frac{1486}{7}} - \lambda\right]\right)^{\frac{2}{2\beta}} \quad \beta = 0{,}2 \quad (28)$$

The density of the foamed rubber is less than the density of homogeneous rubber and may change. Analysis was based on two values of density for the foam rubber $\rho_R^{(0)} = 0{,}9\rho_R^{(1)}$ and $\rho_R^{(0)} = 0{,}3\rho_R^{(1)}$, wherein the density of the rubber homogeneous: $\rho_R^{(1)} = 911\,\mathrm{kg/m^3}$.
Parameter of transition matrix of transverse wave κ'_R, that describes the jump surface of discontinuity in the layers of the composite for X=0 i dla X_2=d after substitution of velocity propagation is:
for $\nu_1 = 0{,}47$:

$$\kappa'_1(\lambda) = \left\{\frac{\rho_R^{(0)}\mu_0}{\rho_R^{(1)}\mu_1}\lambda^{-2}\left(\lambda^2 + \frac{\mu_1}{\mu_0}\left[\lambda^{-4\beta} - \lambda\right]\right)^{\frac{2}{2\beta}}\right\}^{\frac{1}{2}} \quad (29)$$

$$\kappa'_2(\lambda) = \left\{\frac{\rho_R^{(1)}\mu_1}{\rho_R^{(2)}\mu_2}\lambda^2\left(\lambda^2 + \frac{\mu_1}{\mu_2}\left[\lambda^{-4\beta} - \lambda\right]\right)^{-\frac{2}{2\beta}}\right\}^{\frac{1}{2}} \quad (30)$$

for $\nu_1 = 0{,}493$

$$\kappa'_1(\lambda) = \left\{\frac{\rho_R^{(0)}\mu_0}{\rho_R^{(1)}\mu_1}\lambda^{-2}\left(\lambda^2 + \frac{\mu_1}{\mu_0}\left[\lambda^{-\frac{1486}{7}} - \lambda\right]\right)^{\frac{2}{2\beta}}\right\}^{\frac{1}{2}} \quad (31)$$

$$\kappa'_2(\lambda) = \left\{\frac{\rho_R^{(1)}\mu_1}{\rho_R^{(2)}\mu_2}\lambda^2\left(\lambda^2 + \frac{\mu_1}{\mu_2}\left[\lambda^{\frac{1486}{7}} - \lambda\right]\right)^{-\frac{2}{2\beta}}\right\}^{\frac{1}{2}} \quad (32)$$

However, the parameter of transition matrix of longitudal wave κ_R, analogy after substitution of velocity propagation is:
for $\nu_1 = 0{,}47$:

$$\kappa_1(\lambda) = \left\{3\frac{\rho_R^{(0)}\mu_0}{\rho_R^{(1)}\mu_1}\frac{\left(\lambda^2 + \frac{\mu_1}{\mu_0}\left[\lambda^{-4\beta} - \lambda\right]\right)^{\frac{4}{2\beta}}}{1 + 16{,}66\lambda^{-4\beta}}\right\}^{\frac{1}{2}} \quad (33)$$

$$\kappa_2(\lambda) = \left\{ \frac{1}{3} \frac{\rho_R^{(1)} \mu_1}{\rho_R^{(2)} \mu_2} \frac{1 + 71{,}429\lambda^{-49}}{\left(\lambda^2 + \frac{\mu_1}{\mu_0}\left[\lambda^{-98} - \lambda\right]\right)^{\frac{49}{98}}} \right\}^{\frac{1}{2}} \quad (34)$$

for $\nu_1 = 0{,}493$

$$\kappa_1(\lambda) = \left\{ 3 \frac{\rho_R^{(0)} \mu_0}{\rho_R^{(1)} \mu_1} \frac{\left(\lambda^2 + \frac{\mu_1}{\mu_0}\left[\lambda^{-\frac{1498}{7}} - \lambda\right]\right)^{\frac{49}{98}}}{1 + 71{,}429\lambda^{-\frac{1498}{7}}} \right\}^{\frac{1}{2}} \quad (35)$$

$$\kappa_2(\lambda) = \left\{ \frac{1}{3} \frac{\rho_R^{(1)} \mu_1}{\rho_R^{(2)} \mu_2} \frac{1 + 71{,}429\lambda^{-\frac{1498}{7}}}{\left(\lambda^2 + \frac{\mu_1}{\mu_0}\left[\lambda^{-\frac{1498}{7}} - \lambda\right]\right)^{\frac{49}{98}}} \right\}^{\frac{1}{2}} \quad (36)$$

At the same extreme infinite materials (0 and 2), in the present case are identical $\kappa_2 = \kappa_1^{-1}$. According to the paper [5], in addition to appearing symmetry of reflection coefficients $r^{(0)} = r^{(2)}$, thanks to the symmetry of the placement of the materials in composition is introduced symmetry of transmission coefficient $t^{(0)} = t^{(2)}$. For the selected frequency ω'_n of the incident wave defined by $\omega'_n = \frac{(2n-1)\pi c_1}{4d}$ [3] formulas for the coefficients of reflection and transmission of transverse waves in composite accept as follows [3]:

$$r'^{(0)} = \sqrt{\frac{\left(\kappa'_1(\lambda) - (\kappa'_1(\lambda))^{-1}\right)^2}{8 + \left(\kappa'_1(\lambda) - (\kappa'_1(\lambda))^{-1}\right)^2}} \quad (37)$$

$$t'^{(0)} = \frac{2\sqrt{2}}{\sqrt{8 + 8 + \left(\kappa'_1(\lambda) - (\kappa'_1(\lambda))^{-1}\right)^2}} \quad (38)$$

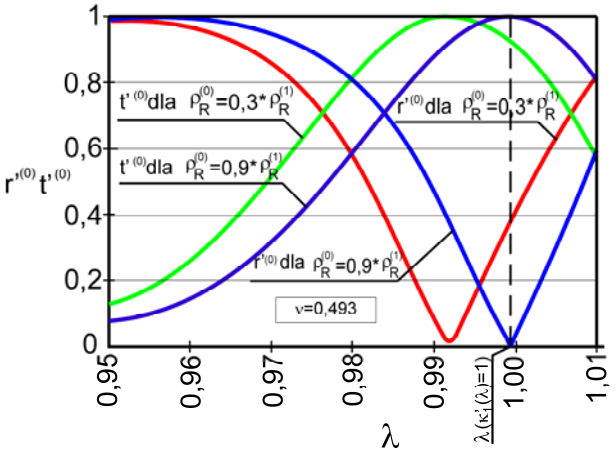

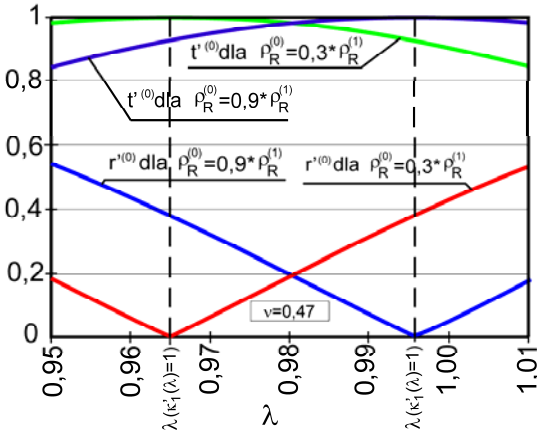

Figure 3. Graphs of reflection and transmission coefficients of the transverse wave r'(0) and t'(0)

5. Conclusions

Analyzing the graph of dependence between components of deformation gradient in rubber $\lambda_1^{(0)} = \lambda_1^{(2)}$ on the parameter λ (Fig 2.) shows that for the two values of shear modules μ for rubber homogeneous, small changes of value $\lambda = (0{,}95; 1{,}02)$ accompanied large fluctuations of value of the component $\lambda_1^{(0)} = \lambda_1^{(2)}$. Looking at the two graphs of Figure 2, you can see that these changes are much larger at the upper extreme values of Poisson ratio, that is v=0,493. For Depending $\kappa'_1(\lambda)$ found values of the deformation $\lambda(\kappa'_1(\lambda)=1)$. Consequently, for these values reflectance and transmission are equal: $r'^{(0)}(\lambda(\kappa'_1(\lambda) = 1)) = 0$, $t'^{(0)}(\lambda(\kappa'_1(\lambda) = 1)) = 1$ (Fig.3). The shown calculation of parameters serve broader researches and observing behavior of wave propagation in a layered elastic medium made of materials Blatz-Ko.

6. References

[1] Blatz P.J.,Ko W.L., Application of finite elastic theory to the deformation of rubbery materials, Trans. Soc. Rheol., 6 (1962) 223-251
[2] Beatty M.F. Stalnaker D.O., The Poisson function of finite elasticity,Journal of App. Mech.,53 (1986) 807-813
[3] Kosiński S., Fale sprężyste w gumopodobnych kompozytach warstwowych; Monografie Politechniki Łódzkiej, Łódź 2007
[4] Major M., Major I., Różycka J., Gumopododne materiały hipersprężyste - omówienie i kryteria praktycznego zastosowania, Zeszyty Naukowe Politechniki Częstochowskiej nr 167 Budownictwo z.17, Częstochowa 2012, s.134-145
[5] Wesołowski Z., On the dynamics of the transition region between two homogenous materials, J. TechnPhys 32 (1991) 293-312

BUSINESS ANALYSIS OF CROATIAN BANKS DURING THE FINANCIAL CRISIS

M. Vretenar Cobović[1*], M. Cobović[1] and K. Bratanić[2]

[1] University of Applied Sciences of Slavonski Brod, Slavonski Brod, Croatia
[2] Student
* *Corresponding author e-mail: maja.vretenarcobovic@vusb.hr*

Abstract
The authors analyse the business of two large banks in Croatia in the period of financial crisis. The goals of this paper were to investigate and analyse data on banks in the last three years and valorise them. Banking business is analysed by several parameters: bank assets, the share of total bank assets, profit before tax, capital adequacy ratio and regulatory capital.

Keywords: banking, big banks, business of banks, financial crisis, the parameters of business

1. Introduction

Banks are all those financial institutions that offer the widest range of financial services, primarily credit, savings and payment services and have the widest range of financial functions of any business firms in the economy [1, p. 189].
A credit institution is a legal entity that is from the competent authority received approval to operate, and whose business is to receive deposits or other repayable funds from the public and to grant credits for its own account [1, p. 189].
Activity banks occurs as a result of the exchange of surplus goods which means gearbox functions of banks, and the development of commodity-money relations generated cash surpluses (depository functions). Placing these funds by the forerunner bankers developed the credit function of banks.

2. Banking operations and performance indicators of banks

The most important functions of banks are the following: [1, p. 192-193]
- depository; development institute "depositum irregular" seeks the return of only a portion of deposits which the depositor entrusted the depositary enabling the depositary that this part has deposits in the form of loans,
- credit; commercial banks perform the function of financial intermediaries collecting deposits and offering them in the form of loans,
- payment function; this function performs the bank based on deposits as requested by the depositor where the bank will make the payment usually through money transfer, and less in cash,
- mediation function in payments; including payment services at home and abroad,
- function preservation value; initially they were real deposits, and later failed. This function is considered to be one of the oldest and influenced the development of banking,
- function of hedging; the bank under its structure, principles of business and management skills protect against risks to its customers,
- policy functions; banks are the most important form of the transmission mechanism of monetary policy and their actions directed towards the goal of ensuring stability in the financial and economic system,
- brokerage functions; bank this function is performed by offering investment services in the securities,
- commissioners' functions; applicable to asset management (the trust jobs),
- functions of cash; bank, according to the principles of banking operations, manage surplus cash of their clients,
- function of money creation and multiplication of deposits and
- function of the securities.

Based on its function, the banks operate as companies on the principles of liquidity, safety and profitability with the aim of making a profit.

The objectives of the banks as a joint stock company are: [1, p. 194]
- maximizing shareholder value; achieved growth in dividends and increased share capital. Maximization of profits and increases risks and is very important to determine what kind of profit the bank aims. Optimal target bank would achieve such a profit that provides short-term and long-term stability,
- perform basic functions; performing its basic functions, the bank creates the conditions for the maximization of shareholder value,
- achieve social goals; bank their actions achieve social objectives. These objectives are reflected in the equality of bank clients and their support placements to certain sectors (housing policy, policy development, exports, local communities, etc.).

Like the goals and operations of banks are different in character.

There are several different division of banking operations, depending on the principles, but the most common and most widely accepted division

of banking operations is a division of the balance sheet-analytical criteria.
In accordance with this criterion banking operations are divided into: [1, p. 209]
- passive banking operations
- active banking operations,
- intermediary (neutral) banking operations and
- own banking operations.

In active banking operations the bank is acting as creditors. These jobs along passive banking operations are the basis of the banking business, and the most developed and economically and financially most important active banking operations is lending.

Passive banking operations are also called business resources. By maturity, can be short term or long term, and the bank is acting as the debtor. The most common include accepting deposits.

Intermediary (neutral) banking operations are also called commission activities, because the bank is acting as commission agents or where the work done is taken the agreed fee that commission. Intermediary banking activities include: [1, p. 234]
- brokerage in payment transactions,
- preservation and management values (Depot operations),
- purchase and mediation in securities etc.

Own banking operations are those jobs that the bank performs in its own name and for its own account with the aim of make a profit. Common tasks include arbitration and stock speculation, and rarely occur in the form of industrial enterprises or participating in joint stock companies.

In addition to banking operations, the most important dimension of every bank is profitability and risk. Commercial banks tend to maximize wealth of shareholders, with acceptable risk. To achieve these goals it is necessary to monitor certain indicators of business. For this purpose are developed indicators of banking.
Indicators of banking business can be divided into indicators of profitability, capital ratios and the market indicators. The most important indicators of profitability, which is now used, are the return on equity - ROE and return on assets - ROA.

ROA is the primary indicator of managerial efficiency and indicates how management was capable of converting assets into net earnings. ROE, on the other hand, measures the rate of return that flows to shareholders of the bank [2, p. 159].

Calculated using the following formula [2, p. 158]

$$\text{return on equity (ROE)} = \frac{\text{net income after tax}}{\text{total proprietary income}} \quad (1)$$

$$\text{return on assets (ROA)} = \frac{\text{net income after taxes}}{\text{total assets}} \quad (2)$$

Other indicators are the net operating margin, net interest margin and non-interest margin. These are measures of efficiency, as well as measures of profitability, indicating how many were capable management and staff to maintain revenue growth as compared to the increase in costs [2, p. 159].

Net interest margin shows how the amounts realized interest income. It is calculated by dividing the difference in interest income and interest expenses to total assets:

$$\text{net interest margin} = \frac{\text{interest income-interest expenses}}{\text{total assets}} \quad (3)$$

Non-interest margin follows the amounts of non-interest income and is calculated by deducting non-interest expense from interest income and that amount is divided by the sum of total assets. This indicator was negative for most banks as they are non-interest expense generally higher than the fee income.
Net banking operating margin is calculated as follows:

$$\text{net operating margin} = \frac{\text{total operating revenue-total operating expenses}}{\text{total assets}} \quad (4)$$

Among other indicators, noteworthy indicator of employee productivity as well as an indicator of economic value added. Net profit per employee ratio is net income and total number of employees. Economic value added is net income reduced by the cost of capital as measured by the weighted cost of capital. This indicator gives a picture of the realized value at a given period and is a good indicator of the total value of the bank.

The most commonly used indicator of the capital is capital adequacy ratio, which determines the solvency and stability of the bank. It is the balance of regulatory capital to total assets. In other capital ratios include return on risk-adjusted capital - RORAC and risk-adjusted return on capital - RAROC.

Their goal is to identify the offerings and compare them with the capital [3, p. 187].

3. Business analysis of Privredna banka Zagreb d.d. and Zagrebačka banka d.d. during the financial crisis

Business of Privredna banka Zagreb d.d. (PBZ) and Zagrebačka banka d.d. (ZABA) was analysed through certain parameters.

Table 1 shows the assets of these banks in the last three years. Bank assets makes, the total assets including cash and deposits with the Croatian National Bank, deposits with financial institutions, treasury and treasury bills, securities and other financial instruments, loans to financial institutions and other clients, derivative financial assets, investments in subsidiaries and acquired companies, tangible assets, interest, fees and other assets and specific reserves for identified cumulative losses.

Table 1. Bank assets (in 000 HRK) [4]

Year	Privredna banka Zagreb d.d.	Zagrebačka banka d.d.
2010	67.937.204	96.159.942
2011	68.000.594 ↗	104.006.887 ↗
2012	68.951.902 ↗	104.397.458 ↗

ZABA of any bank in Croatia in recent years has the largest assets. Immediately behind it is PBZ. ZABA in the 2010 achieved growth in assets of 3.60%, while the PBZ achieved growth in assets of 4.42% which is the highest recorded growth of bank assets for the period. The 2011, compared to 2010, ZABA has achieved higher growth in assets of 4.56%, which is the equivalent of 8.16%. PBZ same year increased its assets by 0.09%. The 2012 ZABA increased assets by 0.38%, while the PBZ achieve asset growth of 1.40%.

Table 2 analysing the share of the observed banks in total banking assets.

Table 2. The share of banks in total bank assets (in %) [4]

Year	Privredna banka Zagreb d.d.	Zagrebačka banka d.d.
2010	17,07	24,16
2011	16,39 ↘	25,07 ↗
2012	16,91 ↘	25,61 ↗

ZABA notes continuous growth in total bank assets. The 2011, a growth of 0.91%, while the 2012 the share in total assets increased by an additional 0.54%. Share PBZ in total assets downward character, where it is possible to observe the impact of the financial crisis. In 2010 amounts to 17.07%. In 2011 decreased by 0.68%, while the 2012 grew by 0.52%, but again lower than in 2010.

Profit before tax two large banks is shown in Table 3.
Bank profits resulting income and expenses. Income side consists of interest income, fee and commission income, operating income before loss provisions and other non-interest income.
On the expenditure side are the interest costs, fees and commissions, non-interest expenses, general administrative expenses and depreciation expenses and provisions for losses.

Table 3. Profit before tax (in 000 HRK) [4]

Year	Privredna banka Zagreb d.d.	Zagrebačka banka d.d.
2010	1.035.505	1.558.596
2011	1.379.030 ↗	1.628.270 ↗
2012	972.452 ↘	1.150.850 ↘

Analysing the profit before tax is possible to observe that ZABA in the each reference year under review recorded the highest profit. The lowest income banks generated 2012, and the highest during the 2011. ZABA in 2011 recorded the profit increased by 15.31% compared to PBZ in the same year. PBZ in 2012 recorded the profit of 15.50% lower compared to ZABA in the same year.

Croatian National Bank (HNB) decides on the calculation of regulatory capital of credit institutions. According to the CNB, the capital adequacy ratio is calculated as the ratio between regulatory capital and total:

- the amount of risk-weighted exposure and
- initial capital requirements for market risk and operational risk multiplied by 12.5.

The rate of capital adequacy of credit institutions can not be less than 12%.

Table 4 shows the capital adequacy ratio of banks in the period examined by the bank.

Table 4. Capital adequacy ratio (in %) [4]

Year	Privredna banka Zagreb d.d.	Zagrebačka banka d.d.
2010	21,73	22,35
2011	21,48 ↘	21,72 ↘
2012	20,03 ↘	18,48 ↘

Analysing the capital adequacy ratio is evident from their constant decline for both observed bank. In 2010 and 2011 the higher capital adequacy ratio

had ZABA. However, PBZ in 2012 recorded a higher capital adequacy ratio of ZAB-e for 1.55%.

Regulatory capital is the amount of funds that the bank is obliged to maintain, and it guarantees the fulfilment of its obligations to creditors. It consists of core and supplementary capital, and is a decision on the definition of the Croatian National Bank.

Table 5 shown the regulatory capital of banks in the observed period.

Table 5. Regulatory capital (in 000 HRK) [4]

Year	Privredna banka Zagreb d.d.	Zagrebačka banka d.d.
2010	9.634.041	13.712.089
2011	10.221.626 ↗	14.254.795 ↗
2012	10.480.723 ↗	14.277.579 ↗

In the period from 2010 to 2012 ZABA had a higher regulatory capital of PBZ. During the 2010 the regulatory capital ZABA was higher for 29.74%. The 2011 was an increase of 28.29% and in 2012 ZABA had regulatory capital increased by 26.59%. It may also be noted that the regulatory capital of both banks grew every year.

4. Conclusion

Activity banks occurs as a result of the exchange of surplus goods. On these fundamental develops gearbox functions of banks. Further development of commodity-money relations resulting cash surpluses as basis for the development depository functions. Placement of funds by the forerunner bankers developed the credit function of banks.
As the activity of banks associated with money, they first appear in monetary economics, and later banking began to work as a system.
The objectives of banks as joint-stock companies are primarily maximizing shareholder value, and further the achievement of social objectives and the performance of its core functions.
Conducted research has shown that there are certain differences in the operations of the analysed banks in Croatia. These differences are reflected primarily in the amount of regulatory capital and the realized profit, and then in the amount of assets and shares in the total bank assets. Appear to be differences in the rate of capital adequacy.
Research has shown that Zagrebačka banka d.d., according to all analysed parameters, achieves better results as compared to Privredna banka Zagreb d.d.
Then is noticed that the assets of both banks grow over the period, despite the financial crisis, which is very important for the banking sector. Zagrebačka banka d.d. continuous growth in total bank assets, while the share of Privredna banka Zagreb d.d. in total bank assets has downward trend in the last two years, but it is not worrying.

Analysing the profit of banks was observed that the Zagrebačka banka d.d. in each reference year recorded higher profits compared to Privredna banka Zagreb d.d. Individually speaking, the biggest profits banks earned in 2011 and the lowest during the 2012. In addition, there has been a downward trend in the capital adequacy ratio of both banks, while regulatory capital is ever-increasing.

5. References

[1] Matić, B. (2011): Monetarna ekonomija, Ekonomski fakultet u Osijeku, Osijek
[2] Rose, P. (2003): Menadžment komercijalnih banaka, Mate, Zagreb
[3] Pavković, A.: Instrumenti vrednovanja uspješnosti poslovnih banaka. [Online]. Available: http://hrcak.srce.hr/index.php?show=clanak&id_clanak_jezik=41458. [Accessed: 12-Aug-2013].
[4] Hrvatska narodna banka. [Online]. http://www.hnb.hr/supervizija/hpokazatelji_poslovanja__bankovnih.htm. [Accessed: 12-Aug-2013].
[5] Matić, B.; Serdarušić, H.; Vretenar, M.: (2011): Impact of Financial Crisic on Credit Lending of Croatian Banks, Interdisciplinary Management Research VII, Faculty of Economics in Osijek, Croatia; Hochschule Pforzheim University, Osijek
[6] Vretenar, M.; Katolik, A.; Kulaš, A.: (2012): Residential Savings Experiences in Croatian Banks, Proceedings of the 4th International Scientific and Expert Conference TEAM 2012, Mechanical Engineering Faulty in Slavonski Brod, Slavonski Brod

ELONGATION OF RAGWEED MALE INFLORESCENCE IN DIFFERENT HABITATS DURING 2010

S. Antunović[1*], E. Štefanić[2] and S. Rašić[2]

[1]College of Slavonski Brod, Slavonski Brod, Croatia
[2]Faculty of Agriculture, J. J. Strossmayer University of Osijek, Croatia
* *Corresponding author e-mail: Slavica.Antunovic@vusb.hr*

Abstract
Ragweed (*Ambrosia artemisiifolia* L.) is an important agronomic and public health problem. In the Republic of Croatia it is mostly present in the continental part of the country. In agricultural production it reduces yield of many crops and it can cause allergies. Elongation of male inflorescence on 10 randomly selected plants of ragweed has been accompanied in five different habitats (sunflower, corn, soybean, ruderal habitat and stubble) during the 2010 growing season. According to the results it is almost identical in sunflower, corn and soybean. The lower value of the inflorescence length was established in ruderal habitat, while it was completely different in the stubble. Pearson's correlation coefficient between meteorological factors and elongation of ragweed male inflorescence has been calculated by statistical analysis. A statistically significant impact of the length of the day on the elongation of ragweed male inflorescence has been observed in all the investigated habitats during 2010.

Keywords:
Ragweed male inflorescence, elongation, different habitats, 2010

1. Introduction

Ragweed (*Ambrosia artemisiifolia* L.) is mostly distributed in the continental part of Croatia and represents a significant agronomic and public health problem. [1, 2] It has reduced yield of many crops in agricultural production. Results of Šubic's research showed that one ragweed plant per m^2 reduces the yield of sugar beet by 30%, five plants by 67%, and nine plants by 74%. [3] Kazinczi *et al* studied the effect of different ragweed density (1, 2, 5 and 10 plants per m^2) on the yield of sunflower and maize in the field conditions. The results have shown that an average yield loss in sunflower was 16%, and corn 30%. [4] Furthermore, ragweed releases abundance of aeroallergens pollen which can cause major problems for human health. [5] Bagarozzi *et al* report that its pollen contains a complex mixture of over 60 different proteins and many of them can cause allergies. [6] The disease is most commonly manifested as allergic rhinitis, allergic rhinitis with spastic bronchitis, allergic dermatitis, burning eyes, and even a possible feeling of suffocation. [7] The ragweed phenological observations contribute to good understanding of its ecology and biology. This knowledge can reduce ragweed competitiveness with the crop. According to numerous studies the most endangered habitats by ragweed are row crops (sunflower, corn and soybean), ruderal habitat and stubble. [8-11]

2. Method

The experiment was conducted during the 2010 growing season in Brod-Posavina County in eastern Croatia. According to the organization and implementation basis it was a field trial which has been based on phenological observations of ten randomly selected plants of ragweed in five different habitats: sunflower, corn, soybean, ruderal habitats and stubble. Also, the elongation of ragweed male inflorescence was monitored within phenological observations. After the emergence of inflorescence, measurements were performed every other day on selected and marked plants. The impact of meteorological factors on male inflorescence elongation was calculated by a statistical analysis (Pearson's correlation coefficient). This data was received from Meteorological and Hydrological Service, the monitoring station of Slavonski Brod. The applied meteorological factors were: the maximum and minimum daily air temperature, DTR, average daily air temperature, soil temperature, precipitation and length of the day.

3. Results and Discussion

Elongation curves of ragweed male inflorescences in the studied habitats during 2010 are shown on Figure 1. The first male inflorescences in crops and ruderal habitat were noticed in the first half of July. In the stubble they appeared one month later, in early August. Curve forms and achieved values are almost identical in all crops. The inflorescence elongation period and its values are somewhat shorter in the ruderal habitat. The graphical representation clearly separates the stubble as a completely different habitat compared to other studied habitats.

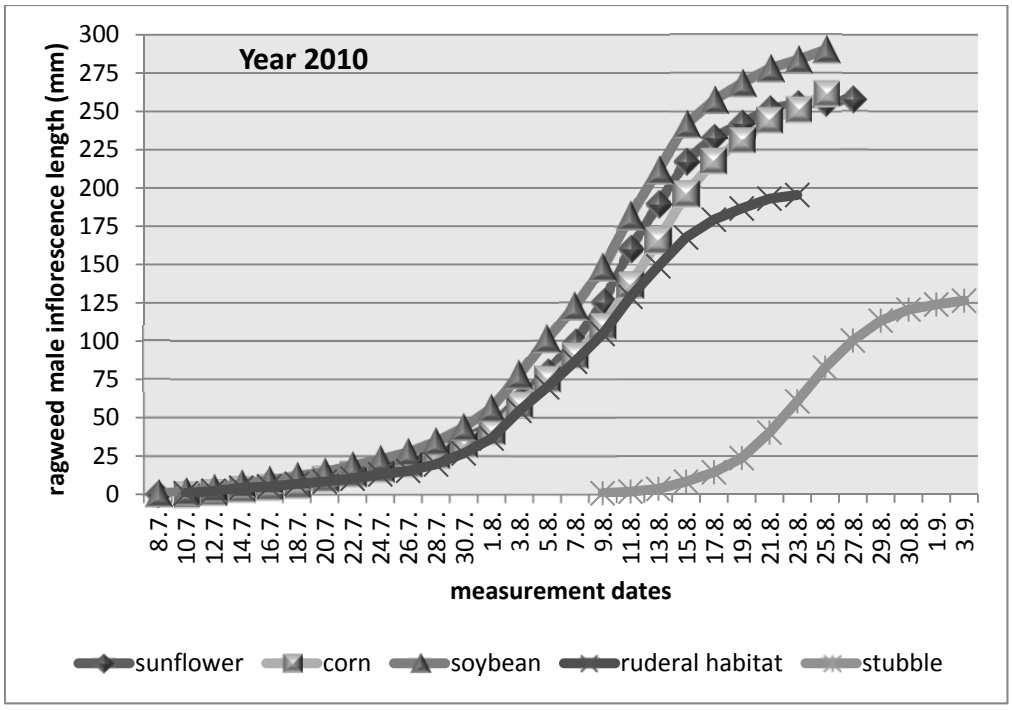

Figure 1. Flow of male inflorescence elongation in the studied habitats during 2010

The average length of ragweed male inflorescence, standard deviation (STD) and coefficient of variation (CV) for each studied habitats have been calculated by the results based on the measurements (Table 1.).

Table 1. Average value of ragweed male inflorescence length ($\bar{x}$), standard deviation (STD) and coefficient of variation (CV)

HABITAT	$\bar{x}$ (cm)	STD	CV (%)
Sunflower	25,46	4,47	17,56
Corn	26,18	3,32	12,68
Soybean	29,00	4,16	14,34
Ruderal habitat	19,54	7,76	39,71
Stubble	11,54	5,70	49,39

The highest values of average lengths in 2010 were in soybean, while the lowest were in the stubble. The inflorescence lengths in corn show the lowest dispersion with a CV of 12,68 %, and the largest one was in the stubble with a CV of 49,39 %. The Influence of meteorological factors on the elongation of ragweed male inflorescence was calculated by Pearson's correlation coefficient (Table 2).

Table 2. Pearson's correlation coefficient between meteorological factors and the ragweed male inflorescence elongation in the studied habitats during 2010

METEOROLOGICAL FACTORS / HABITAT	SUNFLOWER	CORN	SOYBEAN	RUDERAL HABITAT	STUBBLE
MAX. AIR TEM. (°C)	NS	NS	NS	NS	**-0,560****
MIN. AIR TEM. (°C)	NS	**-0,350***	NS	NS	**-0,661****
DTR	NS	**0,310***	**0,297***	NS	NS
MEAN AIR TEM. (°C)	NS	NS	NS	NS	**-0,702****
SOIL TEM. (°C)	NS	**-0,359****	NS	NS	**-0,660****
PRECIPITATION (mm)	NS	NS	NS	NS	NS
LENGHT OF DAY (hour:minute)	**-0,937****	**-0,950****	**-0,946****	**-0,928****	**-0,965****

NS – not significant
* – correlation is significant to 0.05
** – correlation is significant to 0.01

According to the results of statistical analysis the length of day was significant to 0.01, and had a negative impact on elongation of male inflorescence in all the habitats. This agrees with Allard's results which indicate that A. artemisiifolia L. is a typical short-day plant and its flowering begin with shorter length of the day after summer solstice. [12, 13] Buttenschøn et al confirm the similar and also say that ragweed is a short-day plant and its flowering is prompted by a dark period of about 8 hours. [14] Neither one of meteorological factors had an impact on the elongation of inflorescence in sunflower or the ruderal habitat. DTR was significant to 0.05 with a positive impact in soybean and corn. The minimum air temperature and soil temperature were significant, but with negative influence in corn. The stubble again stands out as a completely different habitat. With already mentioned length of day, maximum, minimum and average daily air temperature as well as soil temperature were significant to 0.01. The increase of these meteorological factors decreased the elongation of male inflorescence. Precipitation was not significant in any habitat in 2010.

4. Conclusion

Based on the results obtained by measuring the length of ragweed male inflorescence in five habitats (sunflower, corn, soybean, ruderal habitat and stubble) in the Brod-Posavina County during 2010 and the statistical analysis we can conclude the following:

• The first male inflorescence in the crops and ruderal habitat was observed in the first half of July, and in the stubble a month later, in early August.
• The elongation male inflorenscence curves in crops have an almost identical shape, period and achieved values. The shape of the elongation curve in ruderal habitat is the same but the elongation period and its value are slightly shorter.
• The highest value of the average length of male inflorescence in 2010 has been recorded in soybean, while the lowest was in the stubble.
• The lowest dispersion in 2010 shows the length of inflorescence in corn where the CV is 12.68%, while the largest is in the stubble with a CV of 49.39%.
• The length of the day among all meteorological factors had a statistically significant negative impact on elongation of ragweed male inflorescence in all habitats. The precipitation has not significant in any habitat.
• The stubble stands out as a completely different habitat in relation to other habitats. Except for the length of the day, the maximum, minimum and average daily air temperature as well as soil temperature had a negative statistically significant effect on the elongation of male inflorescence ragweed in this habitat.

5. References

[1] E. Stefanic, S. Rasic, I. Stefanic, Ragweed in Croatia – agricultural and public health problem. Abstracts of lectures. First International Ragweed Conference, Hungary (2008.), p. 30.

[2] S. Rašić, Ambrozija (*Ambrosia artemisiifolia* L.) - agronomski i javno-zdravstveni problem na području Baranje. Doktorski rad. Poslijediplomski sveučilišni interdisciplinarni znanstveni studij Zaštita prirode i okoliša. Sveučilište J. J. Strossmayera u Osijeku i Institut Ruđera Boškovića, Zagreb (2011.)

[3] M. Šubić, Utjecaj broja jedinki korovne vrste *Ambrosia elatior* L. na prirod korijena šećerne repe (*Beta vulgaris var. saccharifera* Alef.). Magistarski rad, Agronomski fakultet Sveučilišta u Zagrebu (2001.)

[4] G. Kazinczi, I. Béres, P. Varga, M. Torma, Competition between *Ambrosia artemisiifolia* and crops under field conditions. 2nd International Symposium „Intractable Weeds and Plant Invaders", Croatia (2008.), p. 16.

[5] M. Laaidi, M. Thibaudon, M., J.-P. Besancenot, Two statistical approaches to forecasting the start and duration of the pollen season of Ambrosia in the area of Lyon (France). Int J Biometorol (2003) 48:65-73.

[6] D. A. Jr Bagarozzi, R. Pike, J. Potempa, J. Travis, Purification and Characterization of a Novel Endopeptidase in Ragweed (*Ambrosia artemisiifolia*) Pollen. The Journal of Biological Chemistry, Vol. 271, No 42, Issue of October 18 (1996.) : 26227-26232.

[7] D. Gajnik, R. Peternel, Methods of Intervention in the Control of Ragweed Spread (*Ambrosia artemisiifolia* L.) in the Area of Zagreb County and the City of Zagreb. Coll. Antropol. 33 (2009), 4:1289-1294.

[8] E. Stefanic, A. Kocic, V. Kovacevic, Ragweed – a noxious weed and health problem in Croatia. Third European Symposium on Aerobiology, Worcester UK (2003.): 160

[9] Š. Týr, T. Vereš, M. Lacko-Bartošová, Occurence of common ragweed (*Ambrosia artemisiifolia* L.) in field crops in the Slovak Republic. Herbologia (2009.), Vol. 10, No 2, 2009, 1-9.

[10] R. Stanković-Kalezić, V. Jovanović, V. Janjić, Lj. Radivojević, Lj. Šantrić, J. Gajić-Umiljendić, Prisustvo ambrozije (*Ambrosia artemisiifolia* L.) u kukuruzu, soji i strništu na teritoriji Obrenovca. Zaštita bilja (2010.), Vol. 61 (2), No. 272, 119-128.

[11] G. Pinke, P. Karácsony, B. Czúcz, Z. Botta-Dukát, Environmental and land-use variables determining the abundance of *Ambrosia artemisiifolia* in arable fields in Hungary. Preslia (2011.), 83: 219-235.

[12] H. A. Allard, The North American Ragweeds and their occurrence in other parts of the world. Science, Vol. 98, No. 2544, (Oct., 1943), pp. 292-294.

[13] H. A. Allard, Flowering Behavior and Natural Distribution of the Eastern Ragweeds (Ambrosia) as Affected by Lenght of Day. Ecology, Vol. 26, No. 4, (Oct., 1945), pp. 387-394.

[14] R. M. Buttenschøn, S. Waldispühl, C. Bohren, Guidelines for management of common ragweed, *Ambrosia artemisiifolia*. (2009.) [Online]. Available: http://xwww.agrsci.dk/ambrosia/outputs/ambrosia eng.pdf. [Accessed: 14-Jan-2013].

APPLICATIONS OF CONVEX COMBINATIONS

Zlatko Pavić[1*], Maja Čuletić Čondrić[2] and Josip Matić[2student]

[1]Mechanical Engineering Faculty in Slavonski Brod, J. J. Strossmayer University of Osijek, Croatia
[2]University of Applied Sciences of Slavonski Brod, Slavonski Brod, Croatia
Corresponding author e-mail: zpavic@sfsb.hr

Abstract
The article demonstrates the application of convex combinations in determining the center of scalar quantity on a finite set. The same procedure can be applied to countable sets. The observing is extended to sets with uncountable number of points, more specifically, to sets with positive volume. In this continuous case, the barycenter of quantity function is defined using the integral method with convex combinations.

Keywords: convex set, convex combination, quantity center, quantity function barycenter

1. Introduction

In general case, the notation of convexity refers to vector spaces. Let us recall the geometric and analytic description of convex set. Let X be a real vector space. A linear combination

$$\sum_{i=1}^{n} p_i P_i \tag{1}$$

of points (vectors) $P_i \in \mathrm{X}$ and non-negative coefficients (scalars) $p_i \in \mathrm{R}$ of the sum $\sum_{i=1}^{n} \alpha_i = 1$ is called convex. Any convex combination with at least two positive coefficients can be expressed in the binomial form

$$\sum_{i=1}^{n} p_i P_i = p \sum_{i=1}^{k} \frac{p_i}{p} P_i + q \sum_{i=k+1}^{n} \frac{p_i}{q} P_i. \tag{2}$$

A set $\mathrm{C} \subseteq \mathrm{X}$ is convex if it contains the line segments connecting all pairs of its points. In other words, a set C is convex if it contains all binomial convex combinations $p_1 P_1 + p_2 P_2$ with points $P_1, P_2 \in \mathrm{C}$.

A convex hull $\mathrm{conv}S$ of a set $\mathrm{S} \subseteq \mathrm{X}$ is the smallest convex set that contains S, and it coincides with all binomial convex combinations $p_1 P_1 + p_2 P_2$ with points $P_1, P_2 \in \mathrm{S}$.

In this article, we consider the problems associated with our three-dimensional space R^3 identifying its points with radius-vectors. As is customary, we use the standard coordinate addition and coefficient multiplication.

The basic convex sets in R^3 are segments of the line, convex polygons in the plane, and convex polyhedrons in the space.

The book in [4] provides an exposition of the theory of convex sets and functions preferring extremum problems, while the book in [1] offers an overview of convex sets and functions promoting mathematical inequalities.

2. Quantity Center

Applying the convexity in the space R^3 we often use the analytic presentation of convex polyhedron.

Theorem A. *Let $\mathrm{C}(P_1,\ldots,P_n)$ be the convex polyhedron with vertices $P_1,\ldots,P_n \in \mathrm{R}^3$. Then a point $P \in \mathrm{R}^3$ belongs to $\mathrm{C}(P_1,\ldots,P_n)$ if, and only if, the convex combination equality*

$$P = \sum_{i=1}^{n} p_i P_i \tag{3}$$

holds for some coefficients $p_i \in [0,1]$ of the sum $\sum_{i=1}^{n} p_i = 1$.

If all the points P_i lie in the same plane, then Theorem A refers to analytic presentation of convex polygon, and if $n = 2$, Theorem A refers to analytic presentation of line segment.

Remark. *The convex combinations in (3) are unique only for a line segment ($n = 2$) and triangle ($n = 3$). If we have a quadrangle $\mathrm{C}(P_1, P_2, P_3, P_4)$, then we can choose the point P that belongs to the triangles $\mathrm{C}(P_1, P_2, P_3)$ and $\mathrm{C}(P_1, P_2, P_4)$, and does not belong to the edge $\overline{P_1 P_2}$. Using the vertices of these triangles, we have four-membered convex combinations so that*

$$P = p_1P_1 + p_2P_2 + p_3P_3 + 0P_4 = q_1P_1 + q_2P_2 + 0P_3 + q_4P_4.$$

Since the coefficients p_3 and q_4 are positive, the above convex combinations are different.

The concept of center is applied to the sets which contain finite or countable number of points. Such sets are also called discrete sets. Assume that a quantity q influences in some part of the space R^3. Let $\mathrm{P} = \{P_1, \ldots, P_n\}$ be a set of points $P_i(x_i, y_i, z_i)$, and $\mathrm{Q} = \{q_1, \ldots, q_n\}$ be a set of assigned non-negative quantity values $q_i = q(P_i)$ with positive $\sum_{i=1}^{n} q_i$.

The arithmetic mean of the quantity q on the set P is the convex combination number

$$\overline{q} = \frac{1}{n}\sum_{i=1}^{n} q_i, \tag{4}$$

and consequently $\overline{q}$ belongs to the convex hull of the number set Q.

The center of the quantity q on the set P is the convex combination point

$$\overline{P} = \frac{1}{\sum_{i=1}^{n} q_i}\sum_{i=1}^{n} q_i P_i = \frac{1}{\sum_{i=1}^{n} q_i}\left(\sum_{i=1}^{n} q_i x_i, \sum_{i=1}^{n} q_i y_i, \sum_{i=1}^{n} q_i z_i\right), \tag{5}$$

and consequently $\overline{P}$ belongs to the convex hull of the point set P.

Let us show the three basic examples of quantity centers: set center, mass center and expected position center.

Example 2.1. (Set Center) *Should be determined the center of the set of five points $P_1(-3,0,2)$, $P_2(0,4,6)$, $P_3(1,-7,0)$, $P_4(3,1,0)$ and $P_5(8,4,-9)$.*

Applying the formula in (5) with all $q_i = 1$, we get the center

$$\overline{P} = \frac{1}{5}\sum_{i=1}^{5} P_i = \frac{1}{5}\left(\sum_{i=1}^{5} x_i, \sum_{i=1}^{5} y_i, \sum_{i=1}^{5} z_i\right) = \frac{1}{5}(9,2,-1) = \left(\frac{9}{5}, \frac{2}{5}, -\frac{1}{5}\right).$$

Example 2.2. (Mass Center) *Let $P_1(0,0,0)$, $P_2(3,0,0)$, $P_3(0,6,0)$, $P_4(0,4,3)$, $P_5(0,0,3)$, $P_6(0,4,0)$ and $P_7(1,0,1)$ be particles with the associated masses $m_i = m(P_i) = x_i + y_i + z_i$. The center of the mass m on the given set of seven particles to be determined.*

According to the formula in (5) taking the mass m as the quantity q, we have the mass center

$$\overline{P} = \frac{1}{\sum_{i=1}^{7} m_i}\sum_{i=1}^{7} m_i P_i = \frac{1}{\sum_{i=1}^{7} m_i}\left(\sum_{i=1}^{7} m_i x_i, \sum_{i=1}^{7} m_i y_i, \sum_{i=1}^{7} m_i z_i\right) = \frac{1}{25}(11,80,32) = \left(\frac{11}{25}, \frac{80}{25}, \frac{32}{25}\right).$$

Note that the points P_1, P_2, P_3, P_4, P_5 are the vertices of the convex pentahedron, and the points P_6, P_7 belong to this pentahedron, as it shown in Figure 1. Therefore the center $\overline{P}(11/25, 80/25, 32/25)$ belongs to the pentahedron $\mathrm{C}(P_1, P_2, P_3, P_4, P_5)$.

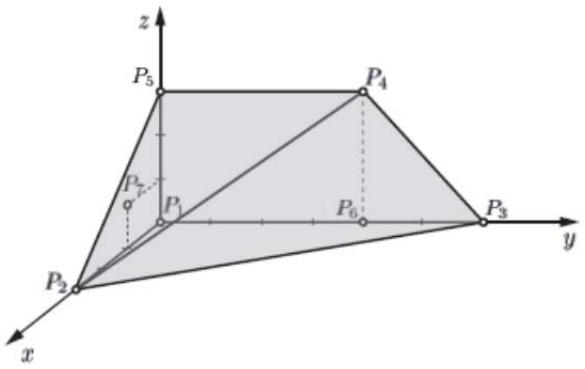

Figure 1. The convex hull of given points

Example 2.3. (Expected Position Center) *Should be determined the expected position center of the particles $P_1(-2,-1)$, $P_2(0,0)$, $P_3(2,-1)$ and*

$P_4(0,1)$ *with the associated absolute frequency values* $\nu_i = \nu(P_i) = x_i^2 + y_i^2$.

Using the formula in (5) with the frequency ν *as the quantity* q *acting on the plane, we get the expected position center*

$$\begin{aligned}\overline{P} &= \frac{1}{\sum_{i=1}^{4}\nu_i}\sum_{i=1}^{4}\nu_i P_i \\ &= \frac{1}{\sum_{i=1}^{4}\nu_i}\left(\sum_{i=1}^{4}\nu_i x_i, \sum_{i=1}^{4}\nu_i y_i, \sum_{i=1}^{4}\nu_i z_i\right) \\ &= \frac{1}{11}(0,-9) = \left(0,-\frac{9}{11}\right).\end{aligned}$$

The center $\overline{P}(0,-9/11)$ *does not belong to the quadrangle with vertices* P_1, P_2, P_3, P_4 *because this quadrangle is not convex.*

3. Quantity Barycenter

The concept of barycenter is applied to the sets with uncountable number of points. The barycenters have recently been considered in [2]. Let $\mathrm{V} \subset \mathrm{R}^3$ be a set with positive volume V, and $q : \mathrm{V} \to \mathrm{R}$ be a non-negative quantity as the Riemann integrable function $q = q(x, y, z)$ with positive integral $\iiint_{\mathrm{V}} qdV$ where $dV = dxdydz$. Given a positive integer n, let

$$\mathrm{V} = \bigcup_{i=1}^{n} \mathrm{V}_{ni}$$

be the partition of V with pairwise disjoint sets V_{ni} with volumes V_{ni} where every V_{ni} contracts to the point or vanishes in infinity as n approaches infinity. Note that $V = \sum_{i=1}^{n} V_{ni}$. For every $i = 1, \ldots, n$ we take the one point $P_{ni} \in \mathrm{V}_{ni}$ and quantity value $q_{ni} = q(P_{ni})$.

Quantity integral arithmetic mean $\overline{q}$ is the limit of the sequence of arithmetic means

$$\overline{q}_n = \frac{1}{V}\sum_{i=1}^{n} q_{ni} V_{ni}.$$

It is obvious that every arithmetic mean $\overline{q}_n$ is the convex combination of values q_{ni} with coefficients $p_{ni} = V_{ni}/V$. Letting n to infinity, it follows that

$$\overline{q} = \frac{1}{V}\iiint_{\mathrm{V}} qdV. \qquad (6)$$

Quantity barycenter $\overline{P}$ is the limit of the sequence of quantity centers

$$\begin{aligned}\overline{P}_n &= \frac{1}{\sum_{i=1}^{n} q_{ni} V_{ni}}\sum_{i=1}^{n} q_{ni} P_{ni} V_{ni} \\ &= \frac{1}{\sum_{i=1}^{n} q_{ni} V_{ni}}\left(\sum_{i=1}^{n} q_{ni} x_{ni} V_{ni}, \sum_{i=1}^{n} q_{ni} y_{ni} V_{ni}, \sum_{i=1}^{n} q_{ni} z_{ni} V_{ni}\right).\end{aligned}$$

It is evident that every quantity center $\overline{P}_n$ is the convex combination of centers P_{ni} with coefficients $p_{ni} = q_{ni} V_{ni} / \sum_{i=1}^{n} q_{ni} V_{ni}$. Applying the reflection moment, $n \to \infty$, we get

$$\overline{P} = \frac{1}{\iiint_{\mathrm{V}} qdV}\left(\iiint_{\mathrm{V}} qxdV, \iiint_{\mathrm{V}} qydV, \iiint_{\mathrm{V}} qzdV\right). \qquad (7)$$

Applying the above illustrated integral method with convex combinations (this method was also used in [3]) and Theorem A, we reach the conclusion:

Theorem B. *Let* $\mathrm{V} \subset \mathrm{R}^3$ *be a closed convex set with positive volume* V*, and* $q : \mathrm{V} \to \mathrm{R}$ *be a non-negative Riemann integrable function with positive* $\iiint_{\mathrm{V}} qdV$*. Then the barycenter* $\overline{P}$ *of the quantity* q *on the set* V *is expressed with the formula in (7), and it belongs to the set* V.

The three concrete examples of quantity barycenters follow.

Example 3.1. (Set Barycenter) *Should be determined the barycenter of the upper unit half ball* V *with the center at the origin.*

We use the formula in (7) with $q(x, y, z) = 1$. *Exploiting the symmetry of* V*, it follows that* $\iiint_{\mathrm{V}} qxdV = \iiint_{\mathrm{V}} qydV = 0$. *Replacing the*

Cartesian coordinates with cylindrical, it follows that

$$\iiint_{\mathrm{V}} qz\,dV = \int_0^{2\pi} d\varphi \int_0^1 r\,dr \int_0^{\sqrt{1-r^2}} z\,dz = \frac{\pi}{4}.$$

Since the volume $V = \iiint_{\mathrm{V}} dV = 2\pi/3$, *the barycenter is at* $\bar{P}\left(0,0,3/8\right)$.

Example 3.2. (Scalar Field Barycenter) *The scalar field* $q(x,y,z) = x+y+z$ *operates on the convex pentahedron* $\mathrm{V} = \mathrm{C}(P_1,P_2,P_3,P_4,P_5)$ *with vertices* $P_1(0,0,0)$, $P_2(3,0,0)$, $P_3(0,6,0)$, $P_4(0,4,3)$ *and* $P_5(0,0,3)$ *which is presented in Figure 1. The barycenter of the field* q *on the given pentahedron* V *to be determined.*

According to the formula in (7), the barycenter denominator is

$$\iiint_{\mathrm{V}} q\,dV = \int_0^3 dx \int_0^{3-x} dz \int_0^{6-2x-\frac{2}{3}z} (x+y+z)\,dy = 123,$$

and the barycenter numerators are:

$$\iiint_{\mathrm{V}} qx\,dV = \frac{1611}{20}, \quad \iiint_{\mathrm{V}} qy\,dV = \frac{5619}{20},$$
$$\iiint_{\mathrm{V}} qz\,dV = \frac{2781}{20}.$$

Using the above values, we get the barycenter $\bar{P}\left(537/820, 1873/820, 927/820\right)$.

Example 3.3. (Expected Position Barycenter) *Let* A *be the quadrangle with the vertices* $P_1(-2,-1)$, $P_2(0,0)$, $P_3(2,-1)$ *and* $P_4(0,1)$. *Should be determined the barycenter of the expected position of the random variable* $q(x,y) = x^2+y^2$ *on the quadrangle* A.

Adapting the formula in (7) to the quantity function of two variables, and denoting $dA = dxdy$, *we calculate the barycenter denominator*

$$\iint_{\mathrm{A}} q\,dA = 2\int_0^2 dx \int_{-\frac{1}{2}x}^{-x+1} (x^2+y^2)\,dy = \frac{5}{3},$$

and the barycenter numerators

$$\iint_{\mathrm{A}} qx\,dA$$
$$= \int_{-2}^0 dx \int_{\frac{1}{2}x}^{x+1} (x^3+xy^2)\,dy + \int_0^2 dx \int_{-\frac{1}{2}x}^{-x+1} (x^3+xy^2)\,dy = 0$$

and

$$\iint_{\mathrm{A}} qy\,dA = 2\int_0^2 dx \int_{-\frac{1}{2}x}^{-x+1} (x^2y+y^3)\,dy = -\frac{8}{15}.$$

After arranging we get the barycenter $\bar{P}\left(0,-8/25\right)$ *which does not belong to the quadrangle* A *since it is not convex.*

4. Conclusion

Using the measure and integral theory (a comprehensive approach to measure and integral theory can be found in [5]) we can generalize the basic formula of the previous section. Let μ be a measure on the space R^n, $\mathrm{V} \subset \mathrm{R}^n$ be a μ-measurable set, and $q : \mathrm{V} \to \mathrm{R}$ be the Lebesgue integrable quantity function with positive $\int_{\mathrm{V}} q\,d\mu$. Then the generalization of the barycenter formula in (7) reads as follows:

$$\bar{P} = \frac{1}{\int_{\mathrm{V}} q\,d\mu}\left(\int_{\mathrm{V}} qx_1\,d\mu, \ldots, \int_{\mathrm{V}} qx_n\,d\mu\right). \quad (8)$$

Relying on the barycenter formula in (8) we can also generalize Theorem B.

5. References

[1] C. P. Niculescu, and L. E. Persson, *Convex Functions and Their Applications*, Springer, New York, USA, 2006.
[2] Z. Pavić, "Convex combinations, barycenters and convex functions", *Journal of Inequalities and Applications*, vol. 2013, Article 61, pages 13, 2013.
[3] Z Pavić, and V. Pavić, "Applications of convexity on quantities and inequalities", *Far East Journal of Mathematical Sciences*, vol. 74, pages 269-287, 2013.
[4] R. T. Rockafellar, *Convex Analysis*, Princeton University Press, New Jersey, USA, 1972.
[5] W. Rudin, *Real and Complex Analysis*, McGraw -Hill, New York, USA, 1987.

CONTAINER CELL SIZE AS A FACTOR OF CABBAGE TRANSPLANT QUALITY

Božica J. Palenkić[1*], Vatroslava Kozak[2], Matija Japundžić[1] and Nataša R. Fajdetić[1]

[1] College of Slavonski Brod, Slavonski Brod, Croatia
[2] Former Student of College of Slavonski Brod, Slavonski Brod, Croatia
* *Corresponding author e-mail: Bozica.JPalenkic@vusb.hr*

Abstract
Production of vegetable transplants in protected areas is more safely then in an open area. The cost of this kind of production is higher therefore producers are trying to reduce it. One way of cutting the expenses is production the maximum quantity of transplants in certain protected area. The use of containers with larger number of seeding posts (cells) and lesser seeding posts volume (cell size) is the best way to reach that goal. The aim of this study was to determine the influence of different seeding posts volume (78 ml and 32 ml) on the cabbage transplants by measuring: number of leafs, leafs length, height of the transplants and average leaf surface area. Statistically very significant difference (P≤0.01) has been proved on the surface area and height of the transplants in the containers with lesser number of the seeding posts and bigger volume. The number of leafs and leaf length has been statistically significant in containers with lesser number of the seeding posts and bigger volume.

Keywords:
Cabbage (*Brassica oleracea* L. var. *capitata*), transplant, volume, container.

1. Introduction

Production of cabbage is usually done with the transplants although it could be done by sowing in the field [1]. Production of the transplants in protected areas (greenhouse) provides creation and control of the climate, feeding and other conditions needed for plant growth and development [2]. This kind of production is more reliable but it requests investments in appropriate production space and supporting objects [3]. Therefore trend among commercial producers of transplants is aiming to containers with more seeding posts which mean lesser volume per seed post. That way number of produced plants increase and needs for production space decrease [4]. The expenses also decrease because the costs of production are directly connected to the size and type of container used [5,6,7]. The aim of this study was to determine the influence of the volume of available substrate (volume of the seed post) on quality of the cabbage transplants (*Brassica oleracea* L. var. *capitata*) showed through indicator of growth with idea that the volume of the seed post will significantly influence on the quality of transplants.

2. Method

Cabbage transplants cultivar Ditmar produced in not heating greenhouse of College of Slavonski Brod by sowing (10.4.2013) in polystyrene containers of different cell size and with 40 or 104 seeding posts with the volume for root development 78 ml and 32 ml (Table 1). The plants emergence 10th day after sowing and 30th day the transplants has been transported to laboratory for growth indicator analyses. Forty transplants have been analyzed depending of the type of containers in which they have been developing. Measured indicators of growth have been: height of the transplant to the tip of the leaf (cm), average number of leafs, leafs length (cm) and leaf surface area of plant (cm^2). The leaf surface area of every transplant is determined by detaching leafs from the plant. Leaf surface area has been transcript on A4 size paper by following the contour of leafs with graphite pencil. Then that contour has been cut of from the paper, it weight measured and from the difference of mass and relation of the mass and surface the surface area of plant has been determined. The results have been statistically analyzed by PC applications StatSoft Statistica and Excell for determine the analyses of variance (ANOVA).

Table 1. Dimensions of polystiren containers used for sowing and growing cabbage transplants

Containers (seeding posts)	40	104
Dimensions (mm)	530x310x60	523.6x314.5x60
Surface (cm^2)	1643	1646.7
Cell size (mm)	Φ 55/33x55	Φ 33/23x50
Seeding posts volume (ml)	78	32
cm^2/ transplant	41.07	51.46

3. Results and Discussion

The size of seeding post determines volume of the substrate available to the plant during growth and development which can influence on the quality of the transplants. Filković et al. (2009) quote that the

most convenient growth indicators are height of the transplant, number and surface area of leafs [7].
The height of cabbage transplants measured to the tip of the plant differed depending of the type of container and size of the seeding post respectively. Plants developed in containers with openings of 78 ml has been in average 12.95 cm while in containers with 32 ml volume of seeding post average plant height was 9.69 (Figure1).

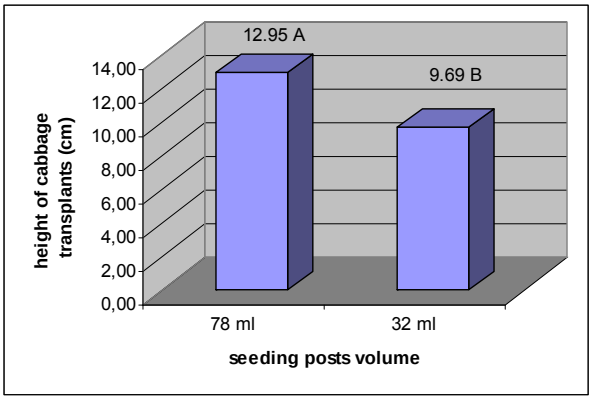

Figure 1. The height of cabbage transplants (cm) depending of seeding posts volume

Statistical analyzes showed very significant difference (P≤0.01) between haight transplants. Results similar to these announca Filković et al. (2009) where they investigate influence of volume of the seeding posts on quality of paprika transplants (*Capsicum annum* L.) and where volume of seeding posts had statistically significant influence on the height of transplant [7]. Topić et al. (2006) also determine that use of containers with bigger volume of seeding posts results with higher Pine tree transplants (*Pinus pinea* L.) [8].
Determining the number of leafs per transplant it has been perceived that the volume of seeding posts has an important role in it. The transplants in containers with 40 seeding posts and 78 ml substrate volume had in average 6.13 leafs and those from containers with 104 seeding posts and 32 ml substrate volume had 5.17 leafs in average (Figure2).
Increased number of leafs in transplants developed in containers with 78 ml volume of seeding posts is statistically significant in ratio to containers with higher number of seeding posts and lower seeding posts volume. The dependence of biomass and number of leafs to the volume of available substrate for developing transplants and their positive correlation determined Csizinszky and Schuster (1993), NeSmith and Duval (1998), Topić et al. (2006) and Filković et al. (2009.) [9,10,8,7].

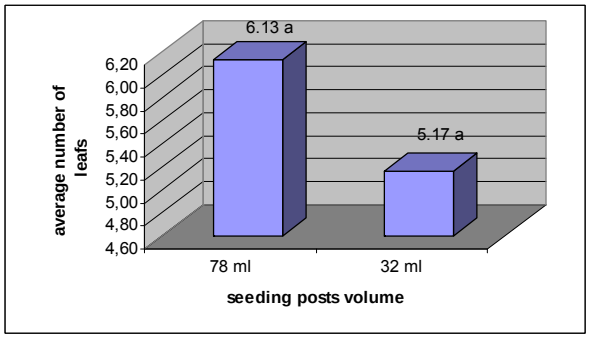

Figure 2. Average number of leafs depending of the volume of seed post

Analyze of the transplants on grounds of the leaf length showed that this parameter is bigger in transplants developed in containers with higher seeding posts volume and lesser number of seeding posts and it was 14.39 cm and in containers with more seeding posts and smaller seeding posts volume was 10.82 cm (Figure3).

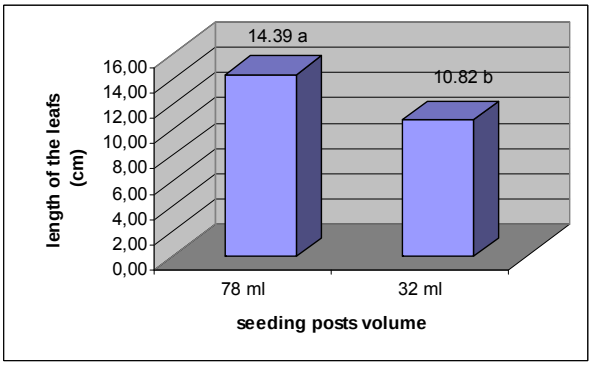

Figure 3. Leaf length of cabbage transplants depending of seed post volume

Analyzing the leaf length statistically significant difference (P≤0.05) has been determined between two types of containers. These results which are in accordance with numerous of investigations (Ne Smith and Duval 1998, Filković et al. 2009) implicate that increase of substrate volume, probably because of better root development, significantly influence on leaf length [10,7].
Average leaf surface area of all leafs in transplant developed in containers with higher seeding posts volume has been significantly higher (36.08 cm^2) than in those developed in containers with smaller seed post volume (13.91 cm^2), Figure 4.
Statistically very significant difference (P≤0.01) according to seeding posts volume has been noticed in transplants which developed in bigger seeding post volume. The effect of container size and restriction of root sistem perceived on cabbage Csizinszky and Schuster (1993) where it has been determined that reduction of root volume leads to restriction in leaf surface area [9].

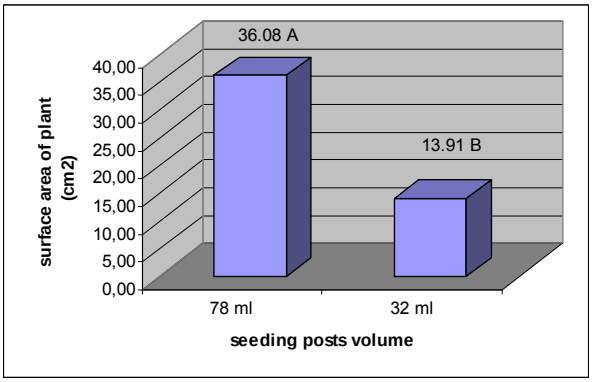

Figure 4. Average leaf surface area of all leafs (cm^2) of cabbage transplants depending of seed post volume

The transplants from containers with bigger seeding posts volume will probably have bigger cabbage crop which Marsh and Paul confirmed 1988 [6].

4. Conclusion

Based on conducted biometrical measuring it can be concluded:
-volume of seeding post significantly influenced on indicators of growth,
-the height of transplants is bigger in bigger seeding post volume,
-number of leafs, average length and leaf surface area also increased with volume of seeding post from 32 ml to78 ml.

5. Annotation

This paper is a part of Graduation Seminar of Vatroslava Kozak, Bachelor of College of Slavonski Brod.

6. References

[1] Z. Matotan, "Zeljasto povrće", *Neron d.o.o., Bjelovar,* 2008.
[2] N. Parađiković, Ž. Kraljičak, "Zaštićeni prostori-plastenici i staklenici". [Online]. Available: http://www.obz.hr/hr/pdf/poljoprivredni_info_pult/2010/Za%C5%A1ti%C4%87eni%20prostori-plastenici%20i%20staklenici.pdf [Accessed: 23-Aug-2013].
[3] R. Lešić, J. Borošić, I. Buturac, M. Herak-Ćustić, M. Poljak, D. Romić, "Povrćarstvo", *Zrinski d.d., Čakovec,* 2004.
[4] C. S. Vavrina, S. Olsen, J.A. Cornell, "An introduction to the production of containerized vegetable transplants", *Univ. of Florida, Gainesville, Coop. Ext. Serv., Bul. 302.,*1995.
[5] R. J. Dufault, Jr. Waters, "Container size influences broccoli and cauliflower transplant growth but not yield", *HortScience,* 20:682-684, 1985.
[6] D. B. Marsh, K. B. Paul, "Influence of container type and cell size on cabbage transplant development and field performance", *HortScience,* 23:310-311, 1988.
[7] M. Filković, Z. Lončarić, T. Teklić, B. Popović, K. Karalić, M. Vukobratović, D. Kerovec, "Volumen sjetvenog mjesta kontejnera i starost presadnica paprike: I. Utjecaj na kvalitetu presadnica ", *44th Croatian and 4th International Symposium of Agriculture,* 434-438, 2009.
[8] V. Topić, Z. Đurđević, L. Butorac, G. Jelić, "Utjecaj tipa kontejnera na rast i razvoj sadnica pinije (*Pinus pinea* L.) u rasadniku", *Rad. Šumar. Inst.,* Izvanredni broj 9:149-158, 2006.
[9] A. A. Csizinsky, D. J. Schuster,"Impact of Insecticide Schedule, N and K Rates, and transplant Container Size on Cabbage Yield", *HortScience,* 28(4):299-302, 2006.
[10] D. S. NeSmith, J. R. Duval,"The effect of container size", *HortTechnology,* 8(4):495-498, 1998.

DETERMINATION OF SEED VIGOR OF THE PEA

Božica J. Palenkić[1*], Andreja Serini[2], Matija Japundžić[1] and Monika Marković[3]

[1] College of Slavonski Brod, Slavonski Brod
[2]Former Student of College of Slavonski Brod, Slavonski Brod
[3]Faculty of Agriculture in Osijek, Osijek
Corresponding author e-mail: Bozica.JPalenkic@vusb.hr

Abstract
Seed producers regularly control seed before the distribution. Some of those methods are standard (standard germination – SG, germination energy – GE, 1000 grain mass) but some which would show reaction of the seed on unfavorable conditions in the field are not regular (cold test – CT, electrical conductivity – EC). The aim of this study was to investigate seed vigor of four cultivars of green pea by all early mentioned methods. Investigation has been conducted on College of Slavonski Brod with these cultivars: Telefon, Kelvedon Wonder, Wonder van America and Rondo. Standard seeds from local agricultural shop with expired date 2013 were used. The best results with 1000 grain mass, standard germination-SG and germination energy-GE had cultivar Rondo. Cultivar Rondo showed the worst germination on Cold test-CT. Increase of imbibition temperature (10 °C, 20 °C, 30 °C) result with increase of EC value (33.6 μS cm^{-1} g^{-1} and 45.2 μS cm^{-1} g^{-1}respectively). Results pointing on decrease of seed quality on relation between producer and user.

Keywords:
Pea (*Pisum sativum* L.), vigor, seed

1. Introduction

Good seed quality is one of the most important conditions for good crop results. Quality of seeds is a complex characteristic dependable on large number of factors. Seed quality consists of genetic, physiological, physical and health characteristics which are under agroecological conditions during vegetation and producing factors as well as period and conditions of storage [1]. Green pea vigor testing (ability of seed to germinate quickly and tolerate different environmental factors) is being conducted with different, according to Mc Donald (1975) physical tests (1000 grain mass), physiological tests (standard laboratory germination – SG, cold test - CT) and biochemical tests (conductometric measurements - EC) [2]. Standard germination test is an indicator of seed quality (under favourable conditions) and could be used for prediction of field emergence if soil conditions are nearly optimal [3,4].
In Republic of Croatia garden pea is sown in early spring when soil and air temperatures are low, with seed germination obtained by standard laboratory test is not in positive corelation with field emergence. In that case testing with cold test gives more precise results [5,6,7,8]. Today a routine vigor test for prediction of field emergence of green pea was developed by Matthews and Bradnock (1968) on the basis of Hibbard and Miller (1928) measurement of electrolyte leakage from plant tissues [9]. In field conditions soil flooded terain due to large quantitiy of rainfall can produce flooding stress, seed deterioration and loss of plant density. According to Sørensen et al. (1996) higher temperature of water in which seeds is immersed increase quantity of rinsed electrolytes from seed [10]. On the market in Republic of Croatia in garden shops and agricultural pharmacy smaller packages of standard seed of different cultivar can be found. Low price and availability of seed is first choice in garden production. The aim of this investigation was with different methods (standard germination – SG, germination energy – GE, 1000 grain mass, cold test – CT, electrical conductivity – EC) analyze the seed quality. Special attention has been on imbibition temperature during EC test.

2. Methods

During March 2012 on College of Slavonski Brod investigation of standard seed of four cultivar of green pea Woder van America, Kelvedon Wonder, Rondo i Telefon with declaration and with expired date 2013 has been conducted. Investigation comprises standard germination – SG, germination energy – GE, 1000 grain mass, cold test – CT, electrical conductivity – EC. Determination of water uptake during imbibition on 10 °C, 20 °C and 30 °C in termostat, followed measuring moisture level in seeds before imbibition (Sparex S.27470). Emergence testing was conducted by modified „rolled paper towels“ method. Four replications of 50 seeds were sown in filter- paper moistened with a quantity of water equal to 2.5 times the weight of the substrate [11]. The rolled papers were placed in polyethylene bages for moisture conservation and then incubated at 20 °C for 8 days according to the ISTA (1995) rules.
Seedling counts were made 8 days after sowing, results were expressed in percentage. Other tests were conducted as modified methods for soya bean according to Hampton i TeKrony, 1995, Panobianco, 2007 [9,11]. Determination of cold test results has been done on rolled filter-paper (modified „rolled paper towels“ method). Bulk electrical conductivity – fifty seeds of each replication were weighed (±0,01 g) and soaked in glass cups containing 250 ml deionized water, for 24 h. Afterwards, the electrical conductivity of the solution was determined through reading in a

conductivimeter (Cond 340i) and the values were expressed as μS $cm^{-1}g^{-1}$ of starting seed mass. After measuring of EC seeds were dried with filter-paper and its mass was determined on analytical scale (±0.01 g). On the bases of those results percentage of water uptake has been calculated in compare with seed mass before imerse.
All tests had 4 repetitions. Results were procesed by PC applications SAS for Windows (SAS Institute Inc., Cary, NC, USA), for variance determination (ANOVA) with F and LSD test.

3. Results and discussion

Mass of 1000 seeds of different green pea cultivars is between 130 – 350 g [12]. Tested green pea cultivars differed by seed size and at the beginning mass of all cultivars seed was determined. Cultivar Rondo had the highest seed mass (Table1).

Table 1. Quantity of moisture and 1000 seeds mass of green pea cultivars

Cultivar	1000 grain mass (g)	Seed moisture (%)
Telefon	284.2	12.2
Kelvedon Wonder	242	12.1
Woder van America	239.8	11.1
Rondo	320	11.5

Size and seed mass had positive correlation with seed vigor [2] and seed size had an impact on field emergence so it can be expected that green pea cultivar Rondo will have the best results on other vigor tests - GE and SG .
Tested seeds underwent standard germination test (SG) with germination energy test (GE) where cultivar Rondo scored the highest values (Table 2). Standard germination test has been conducted on optimal temperatures for germination it was expected that CT values would be inferior then the values of SG [13,14 cit. 10]. Eventually, CT results were superior for prediction of the field emergence when soil and air temperatures were low and presence of pathogens high [8].

Table 2. Effects of cultivar on seed germination and vigor parameters

Cultivar	Germination energy (%)	Standard germination (%)	Cold test (%)
Telefon	69.6^{A}	74^{A}	29^{A}
Kelvedon Wonder	46.4^{B}	49.2^{B}	13.5^{B}
Woder van America	45.2^{B}	50^{B}	$18.5^{A,B}$
Rondo	71.6^{A}	76.8^{A}	$7.5^{B,C}$

P<0,01

According to our CT results it was expected that Telefon would have better field emergence in extreme conditions. Minimal temperature for green pea seed emergence is from 1 °C to 2 °C which allows early sowing but during spring period oscillation of temperature and soil moisture are possible [12].
EC of green pea seeds largely depended of imbibition temperature (Table 3) with average value 33.6 μS cm^{-1} g^{-1} on 10 °C while on 20 °C and 30 °C it was higher but not statistically significant (45.2 μS cm^{-1} g^{-1} respectively 41.8 μS cm^{-1} g^{-1}).

Table 3. Effects of temperature and cultivar on seed electrical conductivity (μS cm^{-1} g^{-1}) and seed water uptake (%) after 24 h imbibition

Effect	Treatment	Electrical conduct. (μS$cm^{-1}g^{-1}$)	Water uptake (%)
Temperature (A)	10 °C	33.6^{B}	232.8^{B}
	20 °C	45.2^{A}	236^{B}
	30 °C	41.8^{A}	252.4^{A}
Cultivar (B)	Telefon	42.7^{A}	244.9^{A}
	Kelvedon Wonder	37.8^{B}	242.4^{A}
	Woder van America	$40.6^{A,B}$	237.2^{B}
	Rondo	$39.7^{A,B}$	237.2^{B}

P<0,01

Results of our investigation does not support some papers [Bradford, 2004. cit. 10;15] which qoute that low temperature, deppending of starting moisture content, enlarge imbbibition damage of seeds. Multiple increases of seeds EC determined numerous of investigators with different sorts. Five time increase of green pea EC showed Plenzer and Cieśla (2003) with increase of temperature from 282 K to 308 K [16]. In that paper highly significant influence of cultivar on seeds EC was showed as well so the biggest difference in EC on all imbibition temperatures was between Telefon and Kelvedon Wonder cultivars (42.7 μS cm^{-1} g^{-1} respectively 37.8 μS $cm^{-1}g^{-1}$). Generally, the EC values of green pea seeds weer high (Matthews and Powell, 1987; cit. Sørensen et al. 1996) [17] which leads to conclusion that seeds used in this study is with low vigor an therefore not suitable for sawing in unfavorable conditions.
In our study volume of water uptake in seeds after 24 hour imbibition showed high intensity of water absorption (Table 3). Seed samples had uptake between 232.8 % and 252.4 % of their starting

mass on all investigated temperatures. Increase of temperature caused higher water uptake with statisticaly very signifficant difference on 30 °C and other temperatures. Obtained results according to temperature and water uptake are similar with other investigations [18]. High values of EC and water uptake lead to conclusion that in case of flood or heavy rain, after sowing, there can fast water uptake, imbibition damage and electrolytes washing out.

Table 4. Response of cultivar on different temperatures from aspect seed electrical conductivity (μS cm^{-1} g^{-1}) and seed water uptake (%) after 24 h imbibition

Temp.	Cultivar	Electrical cond.	Imbibition
10 °C	Telefon	36.2^{A}	241.2^{A}
	Kelvedon Wonder	31.29^{A}	227.8^{B}
	Wonder van America	32.5^{A}	229.5^{B}
	Rondo	34.5^{A}	232.8^{B}
20 °C	Telefon	47.7^{A}	240.7^{A}
	Kelvedon Wonder	43.7^{A}	239.4^{A}
	Wonder van America	45.9^{A}	230^{B}
	Rondo	43.6^{A}	234.2$^{A, B}$
30 °C	Telefon	44.2^{A}	252.9$^{A, B}$
	Kelvedon Wonder	44.2^{A}	259.8^{A}
	Wonder van America	35.1^{B}	252.2^{B}
	Rondo	43.9^{A}	244.7^{C}

P<0,01

Green pea cultivars Telefon i Kelvedon Wonder absorbed significantly higher amount of water (244.9 %, 242.4 %, respectively) in order to Wonder van America and Rondo which absorbed equal amount of water (237.2 %). On grounds of EC results and percentage of water uptake it is hard to classified seed vigor and it is necessary to include more characteristics such as age of seed and genetics [10].

Separately analyzes reaction of each cultivar for water uptake and wash-out of electrolytes results are in table 4. The highest EC on temperature of 10 °C and water uptake had cultivar Telefon, therefore it is not suitable for sawing in flooded areas and low temperatures. Cultivar Kelvedon Wonder would show in such conditions smallest imbibition damage. Cultivars Kelvedon Wonder and Rondo on 20 °C would show smallest loss of electrolytes in spite of a large amount of water uptake. Highest tolerance to flood and elevated temperatures showed seed of cultivar Wonder van America with very signifficant smaller electrolytes wash-out then other cultivars.

4. Conclusion

Results of conducted research showed that seed of tested cultivars (Telefon, Kelvedon Wonder, Wonder van America and Rondo) had good mass of 1000 seeds but in all showed low germination (standard germination, germination energy and cold test). Electrical conductivity (μS cm^{-1} g^{-1}) and seed water uptake (%) after 24 h imbibition results with accent on imbibition temperature were high for green pea seeds. On the bases of such results it could be concluded that seed lost on quality and the vigor was weak. Seed vigor depends on production conditions as well as conditions and time of storage. During distribution of seeds in shops a lot of unpredictable and unfavorable factors can affect on decrease of seed vigor quality. The tests we described are easily available even to small producers and can be helpful in checking seed quality after manipulation on the way between producer and buyer. Such results are necessary to compare to declaration of producer because those tests were conducted in laboratories intended for seed testing.

5. Annotation

This paper is a part of Graduation Seminar of Andreja Serini, Bachelor of College of Slavonski Brod.

6. References

[1] A. Butorac, “Opća agronomija,” *Školska knjiga*, Zagreb, 1999.
[2] M. Milošević, M. Vujanović, Đ. Karagić, “Vigour tests as indicators of seed viability ”, *Genetica*, 42(1):103-118,2010.
[3] M. J. Duurant, R. J. Gummerson, “Factors associated with germination of Sugat beet seed in the standard test establishment in the field ”, *Seed science and technology*, 18:1-10, 1990.
[4] D. M. TeKrony, “Producing high quality soybean seed”, *Procedings of the twenty-fifth soybean seed research sonference*, 1995.
[5] J. Woltz, D. TeKrony, “Accelerating aging test for corn seed”, *Seed Technol.*, 23(1):21-34.
[6] B. A. Martin, O. S. Smith, M. O'Neil, “Relationships between Laboratory

Germination Tests and Field Emergence of Maize Inbreds ",*Crop Science,*28(5):801-805.
[7] J. Ferguson, "Report of seed vigour subcommitte", *Journal of Seed Technology*, 14:182-184.
[8] J. G. Hampton, "Vigour testing within laboratories of the International Seed Testing Association: a survey ", *Seed Science and Technology,* 20(1):199-203, 1992.
[9] J. G. Hampton, D. M. TeKrony, ISTA Vigour Test Committee, "Handbook fo Vigour Test Methods, 3rd Edition, *International Seed Testing Asociation*, 1995.
[10] I. Čičić, M. Špoljarević, B. J. Palenkić, L. Andrić, T.Teklić, "Electrical conductivity of soybean seed at different imbibition temperatures", *Sjemenarstvo,* 29(1-2):37-51, 2012.
[11] M. Panobianco, R. D. Vieira, D. Perecin, "Electrical Conductivity as an Indicator of Pea Seed Aging of Stored at Different Temperatures", *Sci. Agric.(Piracicaba, Braz.),* 64(2):119-124, 2007.
[12] I. Rapčan, G. Bukvić, S. Grljušić, T. Teklić, M. Jurišić ," Utjecaj agroekoloških uvjeta i starosti sjemena na prinos i kakvoću zrna stočnog graška", *Mljekarstvo,* 56(4):331-342, 2006.
[13] L. Andrić, T. Teklić, M. Vratarić, A. Sudarić, V. Duvnjak, "Soybean seed vigour and field emergence under influence of cultivar, seed age and planting date", *Cereal Research Commun*., 35(2):177-180, 2007.
[14] L. Andrić, D. Bešlo, H. Plavšić, "Lipid peroxidation and proline content in soybean seedlings under influence of germination conditions", *Cereal Research Commun*., 36 (1):1035-1038, 2008.
[15] G. G. Rowland, L. V. Gusta, "Effects of soaking, seed moisture content, temperature and seed leakage on germination of faba beans (Vicia faba) and peas (Pisum sativum)", Can. J. Plant Sci. 57:401-406, 1977., 30.4.2013.
[16] G. Plenzler, L. Cieśla, "Conductivity study of ions efflux from soaked pea seeds", *Acta Agrophysica*, 2(2):389-395, 2003.
[17] A. Sørensen, E. B. Lauridsen, K. Thomsen, "Electrical conductivity test – Technical note

IMAGE PROCESSING WITH TOPSIS METHOD

Vedran Novoselac[1*], Zlatko Pavić[2]
[1,2]Mechanical Engineering Faculty in Slavonski Brod, J. J. Strossmayer University of Osijek, Croatia
*Vedran.Novoselac@sfsb.hr

Abstract
The paper demonstrates the application of TOPSIS method in image processing. In many works on TOPSIS method stands as follows: "The basic principle is that the chosen alternative should have the shortest distance from the positive ideal solution and the longest distance from the negative ideal solution".

Keywords:
decision matrix, negative ideal solution, positive ideal solution, image processing

1. Introduction

Multi-criteria decision making. In a general sense, it is the aspiration of human being to make "calculated" decision in a position of multiple selection. In scientific terms, it is the intention to develop analytical and numerical methods that take into account multiple alternatives with multiple criteria.

TOPSIS (Technique for Order Preference by Similarity to Ideal Solution) is one of the numerical methods of the multi-criteria decision making. This is a broadly applicable method with a simple mathematical model. Furthermore, relying on computer support, it is very suitable practical method. The method is applied in the last three decades (on the history of TOPSIS see [2], [3]), and there are many papers on its applications (see [4], [5], [6], [7]).

Description of the problem. Given m options (alternatives) A_i, each of which depends on n parameters (criteria) x_j whose values are expressed with positive real numbers x_{ij}. The best option should be selected.

Mathematical model of the problem. Initially, the parameter values x_{ij} should be balanced according to the procedure of normalization. Suppose that a_{ij} are the normalized parameter values. Then each option A_i is expressed as the point $A_i(a_{i1},\ldots,a_{in}) \in \mathrm{R}^n$. Selecting the most optimal value $a_j^* \in \{a_{1j},\ldots,a_{mj}\}$ for every parameter x_j, we determine the positive ideal solution $A^* = (a_1^*,\ldots,a_n^*)$. The opposite is the negative ideal solution $A^\diamond = (a_1^\diamond,\ldots,a_n^\diamond)$. The positive and negative ideal solution are also denoted by A^+ and A^-. The decision on the order of options is made respecting the order of numbers

$$D_i^* = \frac{d(A_i, A^\diamond)}{d(A_i, A^*) + d(A_i, A^\diamond)}. \qquad (1)$$

The option A_{i_1} is the **best solution** if $\max\{D_1^*, D_2^*, \ldots, D_m^*\} = D_{i_1}^*$, and the option A_{i_2} is the **worst solution** if $\min\{D_1^*, D_2^*, \ldots, D_m^*\} = D_{i_2}^*$. The other options are between these two extremes. The maximum distance $D^* = \max_{i=1,\ldots,m} D_i^*$ is usually called TOPSIS metric.

2. Problem and formulas for applying topsis method

Problem. We examine m alternatives $A_1,\ldots,A_m$. Each alternative A_i respects n criteria $x_1,\ldots,x_n$ which are expressed with positive numbers x_{ij}. The criteria $x_1,\ldots,x_k$ are benefit (monotonically increasing preference), and criteria $x_{k+1},\ldots,x_n$ are non-benefit (monotonically decreasing preference). Weights w_j of the criteria x_j are given so that $\sum_{j=1}^{n} w_j = 1$. It is necessary to select the most optimal alternative.

Initial Table and Decision Matrix. For better visibility, the given alternatives, criteria and its weights are placed in the table (see Table 1).

Table 1. Initial table for TOPSIS method

CRITERIA	x_1 cr. 1	x_2 cr. 2	$\cdots$ $\cdots$	x_n cr. n
weights	w_1	w_2	$\cdots$	w_n
A_1	x_{11}	x_{12}	$\cdots$	x_{1n}
A_2	x_{21}	x_{22}	$\cdots$	x_{2n}
$\vdots$	$\vdots$	$\vdots$	$\ddots$	$\vdots$
A_m	x_{m1}	x_{m2}	$\cdots$	x_{mn}

The given numbers x_{ij} and their matrix

$$\mathrm{X} = \begin{bmatrix} x_{11} & x_{12} & \ldots & x_{1n} \\ x_{21} & x_{22} & \ldots & x_{2n} \\ \vdots & \vdots & \ddots & \vdots \\ x_{m1} & x_{m2} & \ldots & x_{mn} \end{bmatrix} \tag{2}$$

must be balanced, since the numbers x_{ij} present values of different criteria with different measuring units. One must also take into account the given weights w_j of the criteria x_j. First, the measuring numbers x_{ij} of the criteria x_j are replaced with the normalized or relative numbers

$$r_{ij} = \frac{x_{ij}}{\sqrt{\sum_{i=1}^{m} x_{ij}^2}} \tag{3}$$

belonging to the open interval $\langle 0,1 \rangle$. Then, according to the share $w_j x_j$ of the criteria x_j, the normalized numbers r_{ij} are replaced with the weighted normalized numbers

$$a_{ij} = w_j r_{ij} = w_j \frac{x_{ij}}{\sqrt{\sum_{i=1}^{m} x_{ij}^2}} \tag{4}$$

belonging to $\langle 0,1 \rangle$. The further data processing uses the weighted normalized decision matrix

$$\mathrm{A} = \begin{bmatrix} a_{11} & a_{12} & \ldots & a_{1n} \\ a_{21} & a_{22} & \ldots & a_{2n} \\ \vdots & \vdots & \ddots & \vdots \\ a_{m1} & a_{m2} & \ldots & a_{mn} \end{bmatrix} \tag{5}$$

If all weights w_j are mutually equal, in which case $w_j = 1/n$, the numbers r_{ij} can be applied in the matrix A as the numbers a_{ij}.

Working Table. The weighted normalized decision matrix A and all the data that will be calculated, we try to write in one table.

Table 2. Working table for TOPSIS method

CRITERIA	x_1^* cr. 1	$\cdots$ $\cdots$	x_n^* cr. n	d^* dips	$d^\diamond$ dins	D^* topm
A_1	x_{11}	$\cdots$	x_{1n}	d_1^*	$d_1^\diamond$	D_1^*
A_2	x_{21}	$\cdots$	x_{2n}	d_2^*	$d_2^\diamond$	D_2^*
$\vdots$	$\vdots$	$\ddots$	$\vdots$	$\vdots$	$\vdots$	$\vdots$
A_m	x_{m1}	$\cdots$	x_{mn}	d_m^*	$d_m^\diamond$	D_m^*
A^*	a_1^*	$\cdots$	a_n^*	A^*	$A^\diamond$	$d^* \sim d^\diamond$
$A^\diamond$	$a_1^\diamond$	$\cdots$	$a_n^\diamond$			

The coordinates a_j^* of the positive ideal solution $A^* = (a_1^* a_2^* \ldots a_n^*)$ are chosen using the formula

$$a_j^* = \begin{cases} \max\limits_i a_{ij} & \text{for} \quad j = 1, \ldots, k \\ \min\limits_i a_{ij} & \text{for} \quad j = k+1, \ldots, n. \end{cases} \tag{6}$$

If some alternative A_{i_0} is equal to A^*, then it is obvious that the alternative A_{i_0} is the best solution. If it is not, then we continue the procedure. The coordinates $a_j^\diamond$ of the negative ideal solution $A^\diamond = (a_1^\diamond a_2^\diamond \ldots a_n^\diamond)$ are chosen applying the formula

$$a_j^\diamond = \begin{cases} \min\limits_i a_{ij} & \text{for} \quad j = 1, \ldots, k \\ \max\limits_i a_{ij} & \text{for} \quad j = k+1, \ldots, n. \end{cases} \tag{7}$$

The numbers d_i^* of the column $d^* = (d_1^* d_2^* \ldots d_m^*)^{\mathrm{T}}$ as distances from the points A_i to the point A^*, which are calculated by the formula

$$d_i^* = d(A_i, A^*) = \sqrt{\sum_{j=1}^{n} \left(a_{ij} - a_j^*\right)^2}. \tag{8}$$

The numbers $d_i^\diamond$ of the column $d^\diamond = (d_1^\diamond d_2^\diamond \ldots d_m^\diamond)^{\mathrm{T}}$ are the distances from the points A_i to the point $A^\diamond$, which is calculated by the formula

$$d_i^\diamond = d(A_i, A^\diamond) = \sqrt{\sum_{j=1}^{n} \left(a_{ij} - a_j^\diamond\right)^2}. \tag{9}$$

The numbers D_i^* of the column $D^* = (D_1^* D_2^* \dots D_m^*)^{\mathrm{T}}$ are the relative distances of the points A_i respecting the points A^* and $A^\Diamond$, which is expressed by the formula

$$D_i^* = \frac{d_i^\Diamond}{d_i^* + d_i^\Diamond} = \frac{d(A_i, A^\Diamond)}{d(A_i, A^*) + d(A_i, A^\Diamond)}. \qquad (10)$$

If $\max\{D_1^*, D_2^*, \dots, D_m^*\} = D_{i_1}^*$, then we accept the alternative A_{i_1} as the **best solution**. If $\min\{D_1^*, D_2^*, \dots, D_m^*\} = D_{i_2}^*$, then we accept the alternative A_{i_2} as the **worst solution**.

3. Example of Image Processing using TOPSIS method

The significant growth of the Internet and high availability of large number of images in various white-black or colour types has increased the visual information in multimedia, which appear in everyday life, causing the need of image processing. This area has a topic of intense research in recent decades. Noise filtering in images is a classical and prevailing task in the subject of Image processing. Noises affect the image quality leading to the need of its reconstruction. For this purpose they are construct different types of filters which reconstruct corrupted image.

Original image can be presented as matrix

$$0 = \begin{bmatrix} o_{11} & o_{12} & \dots & o_{1N} \\ o_{21} & o_{22} & \dots & o_{2n} \\ \vdots & \vdots & \ddots & \vdots \\ o_{M1} & o_{m2} & \dots & o_{MN} \end{bmatrix} \qquad (11)$$

where $o_{ij} = (o_{ij}^1, o_{ij}^2, o_{ij}^3)$, $0 \le o_{ij}^1, o_{ij}^2, o_{ij}^3 \le 255$, denotes three dimensional RGB vector presenting pixel color at (i, j) position, $1 \le i \le M$, $1 \le j \le N$, where N, M represent a dimension of the image. Components are respectively the intensities of red (R), green (G) and blue (B) color intensity. In papper we use a widely *impulse noise* model with the noise probability (or noise ratio) ρ where noisy image is denoted as Y

$$\mathrm{Y} = \begin{cases} o_{ij}, & \text{with probability } 1-\rho \\ (\xi, o_{ij}^2, o_{ij}^3), & \text{with probability } \rho_1\rho \\ (o_{ij}^1, \xi, o_{ij}^3), & \text{with probability } \rho_2\rho \\ (o_{ij}^1, o_{ij}^2, \xi), & \text{with probability } \rho_3\rho \end{cases} \qquad (12)$$

where ρ_i denotes the channel corruption probabilities. Consequently, it follows that $\sum_i \rho_i = 1$. For this purpose we will set criteria weights to be $w_i = 1 - \rho_i$, hence we give a bigger influence to less corrupted channel.

Noise model defined by (12) will cause the random variation of brightness or color information. *Impulse noise,* sometimes called as a spike noise, are generally attended as an unexpected by product of image capture, where contaminated images will have dark pixels in bright regions and bright pixels in dark regions. When the image is contaminated by the fixed-valued impulse noise, well known as salt-and-pepper noise (NM1 - noise model 1), the noise value of the noisy pixel is equal 0 or 255, i.e. $\xi \in \{0,255\}$. For the random-valued impulse noise (NM2), the noise value of a corrupted pixel will be uniformly distributed between 0 and 255, i.e $\xi \in [0,255]$.

Filters in image processing are construct that they process a small image region

$$W_{ij} = \{y_{kl} : |k-i| \le \omega \ \& |l-j| \le \omega\}, \qquad (13)$$

centred around the pixel y_{ij} at (i,j)-th image position. Number ω in (13) represents a dimension of the sliding window, which is usually 3 or 5 (we used 3×3 sliding window), centred around the pixel y_{ij}. Goal of filter is to replace observed pixel with the result of filter which acts on the set of pixels within the window W_{ij}. Repeating the procedure for each pixel within the picture gets a new reconstructed image. Because of the easier notation, the set of vectors within the window will be marked with $W_{ij} = \{y_i = (y_i^1, y_i^2, y_i^3) : i = 1, \dots, 9\}$.

In order to adapt TOPSIS method to our problem of image filtering, where alternatives are consecutive pixels within the filtering window, it is necessary to modify the numbers x_{ij} in initial table as

$$x_{ij} = |y_i^j - \mathrm{med}_k\, y_k^j|, \ j = 1,2,3. \qquad (14)$$

After normalization we set positive ideal solution

$$a_j^* = \min_i a_{ij}, \qquad (15)$$

and negative ideal solution

$$a_j^\circ = \max_i a_{ij}. \qquad (16)$$

Reason of this modification is *impulse noise* characteristics, which acts as an outlier in sliding window with largest components value presented with (16), and the smallest value which presents observed pixel value presented with (15). As we mention, TOPSIS solution, i.e. proposed filter output $\hat{x}_{ij}$, will be alternative with maximum value of D_i^*.

For the measurement of the restoration quality we used mean squared error (MSE) expressed through the peak signal to-noise ratio (PSNR). The

PSNR is defined as

$$\text{PSNR}=20\log_{10}\frac{255}{\sqrt{\text{MSE}}}, \quad (17)$$

$$\text{MSE}=\frac{\sum_{i=1}^{M}\sum_{j=1}^{N}\left\|o_{ij}-\hat{x}_{ij}\right\|_2^2}{M\cdot N}. \quad (18)$$

Greater PSNR implicate better reconstruction quality.

We present performance of proposed method tested on well known colour test images Lena. Calculations-via PSNR was conducted via equal channel corruption implemented by (12), i.e. $\rho_1=\rho_2=\rho_3=1/3$. The visual quality results for Lena are presented in Figure 1. Figure 1(a) shows original Lena, while Figure 1(b), 1(c) shows the noisy image corrupted with 20% NM1 and NM2 respectively. Figure 4(d) shows the reconstruction results of standard VM-filter (Vector Median) [1]. Figure 4(e) shows the reconstruction results of proposed method. It can be easily observed that the filters suppress well impulses present in the image.

(a) (b) (c) (d) (e)

Figure 1.

The quantitative performances for NM1 in terms of PSNR are plotted in Figure 2. Analogous results were obtained for NM2. The given results show that the proposed method removes the impulse noise much better than the VM-filter.

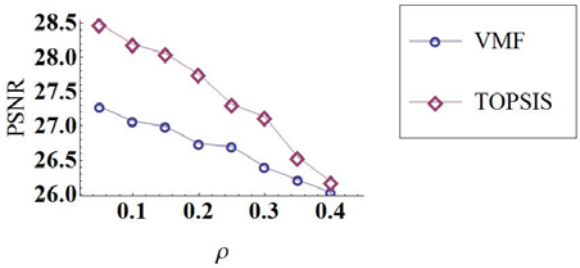

Figure 2.

4. Conclusion

In this paper we present a new approach to image processing where multi-criteria decision making is implemented. It is shown that TOPSIS method has good reconstruction properties in image colour denoising which are corrupted with impulse noise. Comparison with well known VM-filter [1] we have improved better reconstruction performances via PSNR reconstruction measurement.

5. References

[1] Dung Dang, Wenbin Luo, “Color image noise removal algorithm utilizing hybrid vector filtering”, Int. J. Electron. Commun (AEÜ), Vol. 62, No. 1, 2008, pp. 63-67.

[2] C. L. Hwang, Y. J. Lai, and T. Y. Liu, A new approach for multiple objective decision making, Computers and Operational Research 20, pp. 889-899, 1983.

[3] C. L. Hwang, and K. Yoon, Multiple Attribute Decision Making: Methods and Applications, Berlin Heidelberg New York, Springer-Verlag, 1981.

[4] Z. Pavić, and V. Novoselac, Notes on TOPSIS method, International Journal of Research in Engineering and Science, Volumen 1, Issue 2, pp. 601-618, 2013.

[5] G. H. Tzeng, and J. J. Huang, Multiple Attribute Decision Making: Methods and Applications, New York, CRC Press, 2011.

[6] J. Xu, and Z. Tao, Rough Multiple Objective Decision Making, New York, CRC Press, 2012.

[7] K. P. Yoon, and C. Hwang, Multiple Attribute Decision Making: An Introduction, California, SAGE Publications, 1995.

ILLUMINATION MODEL FOR THE CYLINDRICAL SURFACE AND RING-SHAPED LIGHT SOURCE

A. Kolcun[1,2*], V. Ferdiánová[1]

[1]Faculty of Science, University of Ostrava, Ostrava, Czech Republic
[2]Institute of Geonics, Ac. Sci. of Czech Republic, Ostrava, Czech Republic
* *Corresponding author e-mail: alexej.kolcun@osu.cz*

Abstract
Nowadays, ring-shaped light sources are very often used in combination with digital cameras. The presented paper analyses models of such light sources which are used for the illumination of the cylindrical surface. We can meet this situation e.g. when the borehole surface is monitored. As the motion of the camera is hand-controlled without any stabilization elements, resulting sliding motion is affected by strong instability. The purpose of this research is to eliminate the above-mentioned factors to reconstruct the borehole walls.

Keywords:
image processing, Phong's reflection model, video stabilization, borehole surface

1. Introduction

The borehole surface monitoring represents one of the methods, which enable to assess the mechanical state of massif, e.g. [3], [4], [5]. It is realized by a probe provided with a camera which is equipped with ring-shaped light source. The probe is attached to the end of a conductive stiff steel wire. In our case a simple camera without HW support of stabilization is used. The wire is hand controlled, so the obtained video record is charged by three forms of instability: 1. camera axis movement, 2. camera axis oscillating, and 3. unstable movement of the camera inside the borehole.
To compare the state of the borehole surface, before and after the realization of various experiments, it is advisable to keep the image information of the borehole in a standardized form − unfolded covering of the borehole surface. For this purpose it is necessary to stabilize the image.

The contribution of this paper consists in an analysis of the crucial part of stabilization, which is the finding the mutual position of the camera and borehole axes. We confine to the case where these axes are mutually parallel. The main idea of the solution is based on the analysis of the shape of the "eye of the borehole" i.e. of the dark part of the borehole surface, which is far away from the camera. In the paper various illumination models (local as well as global) are analyzed: the analysis is based on Phong's reflection model applied for ring-shaped light source. Lambert reflectance is used with a distance dependence between emitted and absorbed light. Resulting global illumination model is based on the radiosity method.

Figure 1. Camera − frontal view

Similar problem is solved e.g. in [6], however in that case the images of the video records are stabilized by hardware.

2. Formulation of the task

Let us consider the cylindrical borehole

$$x^2 + y^2 = R^2, \quad h_1 \le z \le h_2.$$

We use a simple model of the camera – central projection with the focus

$$F = \left(x_f, y_f, h_f\right) \tag{1}$$

and the projection plane z=0.
Camera has its own source of light – see Fig. 1. We can express it as a ring with the center (1) and radius l,

$$\left(x - x_f\right)^2 + \left(y - y_f\right)^2 = l^2, \quad z = h_f, \quad h_1 < h_f < h_2.$$

It is easy to show, that the projection of directrix

$$x^2 + y^2 = R^2, \quad z = h = const, \quad h_1 < h < h_2$$

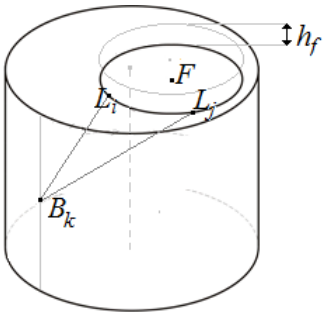

Figure 2. Light source with highlighted points L_i, L_j and illuminated surface with highlighted point B_k

is the circle with the centre C_h and radius r_h,

$$C_h = \frac{h}{h+h_f}(x_f, y_f, 0), \quad r_h = \frac{h_f}{h}R. \tag{2}$$

Fig. 3 shows an image of the video sequence where four thresholds (green, yellow, red and blue) of intensities are highlighted [2]. It seems that isoluxes, ie. the curves which connect the points with the same illumination level (black curves in Fig. 3) are the directricies. In this case we should find the position of the camera in the borehole according to (2)

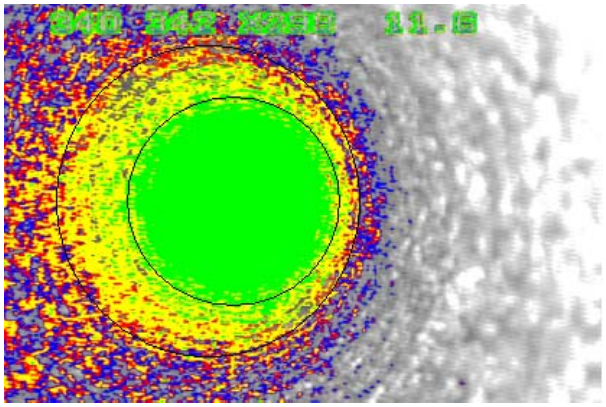

Figure 3. Image of the borehole with four highlighted thesholds of intensity

The aim of the paper is an analysis of relationship between the directricies and isoluxes – we shell formulate the conditions, when both curves are identical.

3. Local illumination model

We reduce our considerations to diffuse reflection only. It is based on Lambert's cosine law

$$i \approx \frac{\cos\varphi}{r^2}, \tag{3}$$

where i is light intensity, φ is angle between the observers´ line of sight and the surface normal. r is the distance from the light source to the area of illuminated surface. Instead of the "point light model" (3) we shall use the flat light model (4), where rate of the influence of pair of patches can be found as

$$F_{ij} = \frac{1}{\pi|B_i|}\int_{B_i}\int_{B_j}\frac{\cos\varphi_i \cos\varphi_j}{r^2}dB_j dB_i. \tag{4}$$

dB_i, dB_j are elementary patches, r is vector from dB_i to dB_j and φ_i, φ_j, are the angles between dB_i, dB_j and r respectively. (4) gives the proper amount of energy from a patch B_j to a patch B_i.
Fig. 4 shows the difference among various models of an elementary light source which is allocated on the borehole face (top, center of unfolded covering).

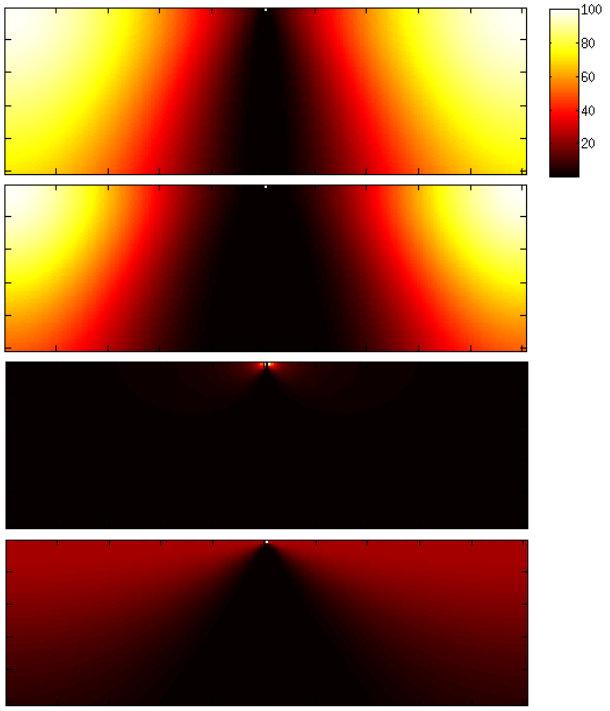

Figure 4.Unfolded covering of cylindrical face illuminated by various types of light (from the top to the bottom):point parallel, flat parallel, point omnidirectional (3),flat omnidirectional (4) light sources

Last one – flat omnidirectional light source is the best approximation of real illumination.

Fig. 5 compares the borehole illuminated by "simple-flat light" and "ring-shaped light", where flat omnidirectional light sources are used. We can see that even if the light source is located close to the axe of the borehole, illumination of the directrix in the distance *r* from the light source is changing in the range greater than 10% of maximal illumination.

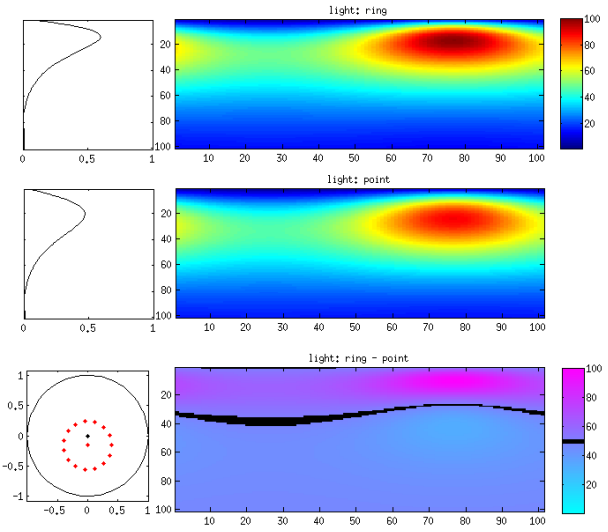

Figure 5.Unfolded covering of locally illuminated cylindrical face. Top: ring-shaped light source, center: point light source, bottom: difference between above mentioned light sources. Left: the difference of intensity (horizontal axe) vs. directrices (vertical axe). Left bottom: position of light sources (red) in the cylindrical borehole.

4. Global illumination model

Local model is valid, when faces in the scene do not affect each other. In our case of cylindrical surface, where reflected light from one patch affects the rest of patches, these have to be considered as secondary light-sources.

We use n-sided prism approximation of the cylindrical surface. So the face illumination can be expressed using the radiosity global illumination technique

$$\begin{pmatrix} 1-p_1F_{11} & -p_1F_{12} & \cdots & -p_1F_{1n} \\ -p_2F_{21} & 1-p_2F_{21} & \cdots & -p_2F_{2n} \\ \vdots & \vdots & \ddots & \vdots \\ -p_nF_{n1} & -p_nF_{2n} & \cdots & 1-p_nF_{nn} \end{pmatrix} \begin{pmatrix} x_1 \\ x_2 \\ \vdots \\ x_n \end{pmatrix} = \begin{pmatrix} e_1 \\ e_2 \\ \vdots \\ e_n \end{pmatrix} \qquad (5)$$

where x_i is the amount of desired global illumination of i-th patch, e_i, and p_i are it's emission and reflectivity respectively. F_{ij} are the form-factors (4).

Due to the cylindrical shape of the face, evaluating the values of form-factors F_{ij} is simple. Moreover we can see, that when both patches are in the same directrix, their mutual form-factors have the same value: so as we consider elementary patches and $\varphi_i = \varphi_j$, (Fig. 6), according to (4) we obtain

$$F_{ij} = \frac{\cos^2 \varphi_i}{\pi r^2} = \frac{\cos^2 \varphi_i}{\pi (2R\cos\varphi_i)^2} = \frac{1}{4\pi R^2}.$$

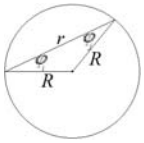

Figure 6.Configuration of the pair of patches in the same directrix.

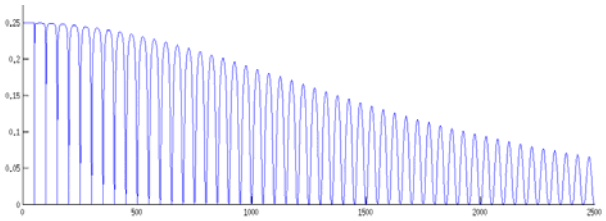

Figure 7. Form-factors F_{1i} for uniform discretization of the cylindrical face to 50x50 patches. One "period" in horizontal direction means set of elementary patches within one directrix.

The whole sequence of illumination computation can be expressed as follows:

1. Find local (primary) illumination on the cylindrical surface for the ring-shaped light.
2. Apply the global illumination method (radiosity) on primary illuminated cylindrical surface.

Fig. 8 shows the difference between locally and globally illuminated cylindrical face.

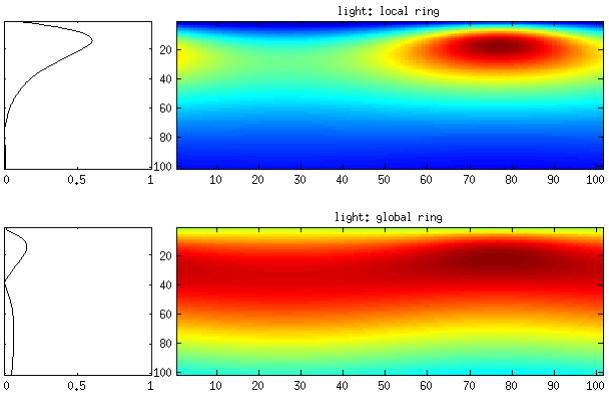

Figure 8.Unfolded covering of cylindrical face illuminated with ring-shaped light source from Fig. 5. Top: model of local illumination, bottom: model of global illumination. Left: the difference of intensity (horizontal axe) vs. directrix (vertical axe).

From Fig. 8 we can see that in the consequence of global illumination model, directricies in the cylindrical face are illuminated much more uniformly even from a small distance of the light source.

Figures below illustrate the behavior of the analyzed illumination models. We have used geometry configuration close to real proportions of camera and borehole: with $R=h$, $r/R=0.4$, $c/R=0.2$ where h − cylinder height, R − cylinder radius, r − light ring radius, c − the distance of light ring center from the center of the cylinder.
Instead of the continuous ring-shaped light, 15 flat light sources were used. Cylindrical surface was approximated with 80-sided prism and total number of faces is 1600. Faces with 50±3% of resulting maximal illumination value are highlighted.
We can see (and it is verified by various geometry configurations) that suggested illumination model leads to a simple and strong relationship between isolux-curves and directrices − the curves are identical.

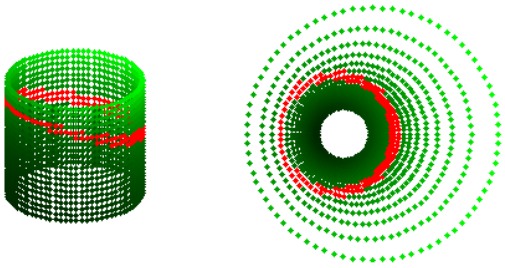

a) *b)*

Figure 3. 50% isolux (red line) for the Phong's illumination model. a) side-view, b) camera-view.

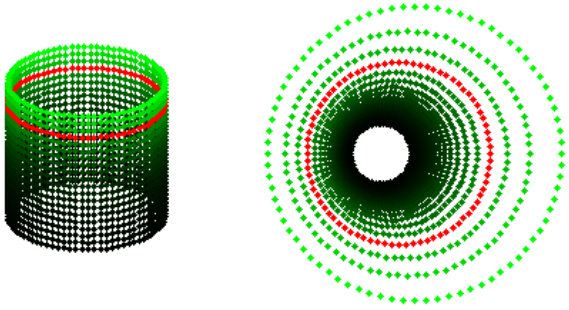

a) *b)*

Figure 4.50% isolux (red line) for our illumination model. a) side-view, b) camera-view

5. Conclusions and future work

The ring-shaped light source illuminating cylindrical face was analyzed for both cases - local and global illumination models. It is shown that in the case when both axes of light ring and cylinder are parallel, the isolux curve is the directrix of the cylinder.
Future work will be focused on general mutual position of the light source and analyzed cylindrical surface.

6. Acknowledgement

The presented work was supported by the projects:

- RVO: 68145535,
- Specific Research SP13/PřF/20132013 supported by the Ministry of Education, Youth and Sports of the Czech Republic.

7. References

[1] Ferdiánová, V., Hurtik, P., Kolcun, A.: "Reconstruction of the borehole wall using video records". In: *Conf. proc. Aplimat 2012*
[2] Hurtik, P.: Image stabilization of digital camera affected by torsional motion. MSc. Theses, University of Ostrava, 2011.
[3] Niu, C., Zhong F., Xu, S., Yang, C., Qin, X.: Creating Cylindrical Panoramic Mosaic from a Pipeline Video. In: *Conf. proc. CAD/Graphics 2011*, pp.171-175.
[4] Tan, Y.L., Ning, J.G., Li, H.T.: In situ explorations on zonal disintegration of roof strata in deep coalmines. *International Journal of Rock Mechanics & Mining* Sci 49 (2012), pp.113-124.
[5] Williams, J.H., Johnson, C.D.: Acoustic and optical borehole-wall imaging for fractured-rock aquifer studies, *J. of Applied Geophysics 55(2004)*, pp. 151-159.
[6] Zhang, Y., Hartley, R., Mashfort, J., Wang, L., Burn, S.: Pipeline Reconstruction from Fisheye Images, *J. of WSCG 2011*, pp. 49-57.

INEQUALITIES ON THE LINE AND PLANE

Zlatko Pavić[1*], Velimir Pavić[2] and Emina Dugančić[1]

[1]Mechanical Engineering Faculty in Slavonski Brod, J. J. Strossmayer University of Osijek, Croatia
[2]The Faculty of Graphic Arts, University of Zagreb, Croatia
Corresponding author e-mail: zpavic@sfsb.hr

Abstract
Applying the binomial and trinomial convex combination representations, the basic inequalities for convex functions of one and two variables are derived. The obtained results are generalized to more dimensions using simplexes.

Keywords: center of combination, binomial and trinomial convex combination, Jenesn's inequality

1. Introduction

Let X be a real vector space. A set $\mathrm{A} \subseteq \mathrm{X}$ is affine if it contains the lines passing through all pairs of its points (all binomial affine combinations in A, that is, the combinations $p_1P_1 + p_2P_2$ of points $P_1, P_2 \in \mathrm{A}$ and coefficients $p_1, p_2 \in \mathrm{R}$ of the sum $p_1 + p_2 = 1$). A function $f : \mathrm{A} \to \mathrm{R}$ is affine if it satisfies the binomial equality $f(p_1P_1 + p_2P_2) = p_1 f(P_1) + p_2 f(P_2)$ for all binomial affine combinations in A.

A set $\mathrm{C} \subseteq \mathrm{X}$ is convex if it contains the line segments connecting all pairs of its points (all binomial convex combinations in C, that is, the combinations $p_1P_1 + p_2P_2$ of points $P_1, P_2 \in \mathrm{C}$ and non-negative coefficients $p_1, p_2 \in \mathrm{R}$ of the sum $p_1 + p_2 = 1$). A function $f : \mathrm{C} \to \mathrm{R}$ is convex if it satisfies the binomial inequality $f(p_1P_1 + p_2P_2) \le p_1 f(P_1) + p_2 f(P_2)$ for all binomial convex combinations in C.

Using the induction, it can be proved that every affine function $f : \mathrm{A} \to \mathrm{R}$ satisfies the equality

$$f\left(\sum_{i=1}^{n} p_i P_i\right) = \sum_{i=1}^{n} p_i f(P_i) \qquad (1)$$

for all affine combinations in A, and that every convex function $f : \mathrm{C} \to \mathrm{R}$ satisfies the Jensen inequality

$$f\left(\sum_{i=1}^{n} p_i P_i\right) \le \sum_{i=1}^{n} p_i f(P_i) \qquad (2)$$

for all convex combinations in C. For an affine or a convex combination $P = \sum_{i=1}^{n} p_i P_i$ the point P itself is called the combination center, and it is important to mathematical inequalities.

Many details of convex functions and its applications can be found in [5] and [1].

2. Convex Combinations of the Line

The section shows the importance of convex combination centers in deriving inequalities. If $a, b \in \mathrm{R}$ are different numbers, say $a < b$, then every number $x \in \mathrm{R}$ can be uniquely presented as the affine combination

$$x = \frac{b-x}{b-a}a + \frac{x-a}{b-a}b. \qquad (3)$$

The above binomial combination is convex if, and only if, the number x belongs to the closed interval $[a, b]$. Given the function $f : \mathrm{R} \to \mathrm{R}$, let $f^{\mathrm{line}}_{\{a,b\}} : \mathrm{R} \to \mathrm{R}$ be the function of the line passing through the points $(a, f(a))$ and $(b, f(b))$ of the graph of f. Using the affinity of $f^{\mathrm{line}}_{\{a,b\}}$, we get

$$f^{\mathrm{line}}_{\{a,b\}}(x) = \frac{b-x}{b-a} f(a) + \frac{x-a}{b-a} f(b). \qquad (4)$$

If the function f is convex, then using the definition of convexity, we obtain the inequality

$$f(x) \le f^{\mathrm{line}}_{\{a,b\}}(x) \text{ if } x \in [a, b], \qquad (5)$$

and the reverse inequality

$$f(x) \ge f^{\mathrm{line}}_{\{a,b\}}(x) \text{ if } x \notin (a, b). \qquad (6)$$

By the end of this section we will use an interval $\mathrm{I} \subseteq \mathrm{R}$ with the non-empty interior I^0.

The following lemma represents a systematised version of [4, Proposition2], and deals with two convex combinations having the same center. Assigning the convex function to such convex combinations, we obtain:

Lemma 2.1. *Let* $a,b \in \mathrm{I} \subseteq \mathrm{R}$ *be points such that* $a \le b$. *Let* $\sum_{i=1}^{n} p_i x_i$ *be a convex combination with points* $x_i \in [a,b]$, *and* $\sum_{j=1}^{m} q_j y_j$ *be a convex combination with points* $y_j \in \mathrm{I} \setminus (a,b)$.

If the above convex combinations have the same center

$$\sum_{i=1}^{n} p_i x_i = \sum_{j=1}^{m} q_j y_j, \tag{7}$$

then every convex function $f : \mathrm{I} \to \mathrm{R}$ *satisfies the inequality*

$$\sum_{i=1}^{n} p_i f(x_i) \le \sum_{j=1}^{m} q_j f(y_j). \tag{8}$$

Using the above lemma we can derive the discrete form of the famous Jensen's inequality (discrete form in [2] and integral form in [3]).

Theorem 2.2. *Let* $a,b,a_1,b_1 \in \mathrm{I} \subseteq \mathrm{R}$ *be points such that* $a_1 < a < b < b_1$. *Let* $c = \sum_{i=1}^{n} p_i x_i$ *be a convex combination of the points* $x_i \in [a_1,b_1] \setminus (a,b)$ *with the center* $c \in (a,b)$.

Then there exist two binomial convex combinations

$$\alpha a + \beta b \text{ and } \alpha_1 a_1 + \beta_1 b_1$$

so that

$$\alpha a + \beta b = \sum_{i=1}^{n} p_i x_i = \alpha_1 a_1 + \beta_1 b_1, \tag{9}$$

and consequently, every convex function $f : \mathrm{I} \to \mathrm{R}$ *satisfies the inequality*

$$\alpha f(a) + \beta f(b) \le \sum_{i=1}^{n} p_i f(x_i) \le \alpha_1 f(a_1) + \beta_1 f(b_1). \tag{10}$$

Proof. We use (3) to calculate the coefficients $\alpha = (b-c)/(b-a)$ and $\beta = (c-a)(b-a)$ that satisfy $c = \alpha a + \beta b$. Also for α_1 and β_1. Now we need to apply Lemma 2.1 to both sides of the obtained equality in (9). □

The graphical representation of the equality in (9) and the inequality in (10) is shown in Figure 1.

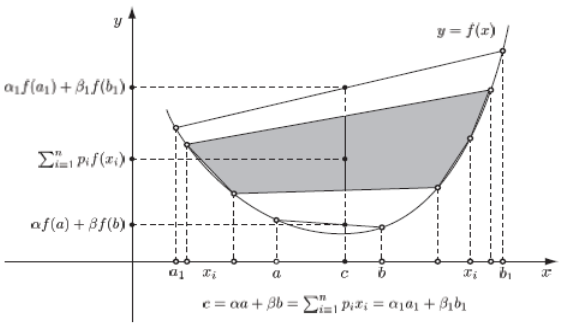

Figure 1. Line convex combinations with center c

The summarizing Jensen's functional of a function $f : \mathrm{I} \to \mathrm{R}$ for the given convex combination $\sum_{i=1}^{n} p_i x_i$ in I is defined with

$$J_{p_1 x_1 + \ldots + p_n x_n}(f) = \sum_{i=1}^{n} p_i f(x_i) - f\left(\sum_{i=1}^{n} p_i x_i\right).$$

If the conditions of Theorem 2.2 hold, we get the functional inequality

$$J_{\alpha a + \beta b}(f) \le J_{p_1 x_1 + \ldots + p_n x_n}(f) \le J_{\alpha_1 a_1 + \beta_1 b_1}(f).$$

3. Convex Combinations of the Plane

This section contains the main result, Theorem 3.2. We assume that R^2 is the real vector space treating its points as the vectors with the standard coordinate addition

$$(x_1, y_1) + (x_2, y_2) = (x_1 + x_2, y_1 + y_2),$$

and the scalar multiplication

$$\alpha(x, y) = (\alpha x, \alpha y).$$

If $A(x_A, y_A)$, $B(x_B, y_B)$ and $C(x_C, y_C)$ are the planar points that do not belong to one line, respectively the convex hull $\mathrm{conv}\{A,B,C\}$ is a real triangle, then every point $P(x,y) \in \mathrm{R}^2$ can be presented by the unique affine combination

$$P = \alpha A + \beta B + \gamma C. \tag{11}$$

The above trinomial combination is convex if, and only if, the point P belongs to the triangle $\mathrm{conv}\{A,B,C\}$.

Given the triangle with vertices A, B and C, the convex cone C_A with the vertex at A is the set spanned by the vectors $A-B$ and $A-C$ (similarly C_B and C_C; all three cones can be viewed in Figure 2), that is,

$$C_A = \{A + p(A-B) + q(A-C) : p, q \geq 0\}.$$

Given the function $f : \mathrm{R}^2 \to \mathrm{R}$, let $f^{\text{plane}}_{\{A,B,C\}} : \mathrm{R}^2 \to \mathrm{R}$ be the function of the plane passing through the points $(A, f(A))$, $(B, f(B))$ and $(C, f(C))$ of the graph of f. Due to the affinity of $f^{\text{plane}}_{\{A,B,C\}}$, it follows the equation

$$f^{\text{plane}}_{\{A,B,C\}}(P) = \alpha f(A) + \beta f(B) + \gamma f(C). \quad (12)$$

If f is convex, we get the inequality

$$f(P) \leq f^{\text{plane}}_{\{A,B,C\}}(P) \text{ if } P \in \text{conv}\{A,B,C\}, \quad (13)$$

and the reverse inequality

$$f(P) \geq f^{\text{plane}}_{\{A,B,C\}}(P) \text{ if } P \in C_A \cup C_B \cup C_C. \quad (14)$$

By the end of the section we will use a planar convex set $C \subseteq \mathrm{R}^2$ with the non-empty interior.

Lemma 3.1. *Let $A,B,C \in C \subseteq \mathrm{R}^2$ be points, $\Delta = \text{conv}\{A,B,C\}$, and $C_\Delta = C_A \cup C_B \cup C_C$ be the cone union. Let $\sum_{i=1}^n \alpha_i A_i$ be a convex combination of the points $A_i \in \Delta$, and $\sum_{j=1}^m \beta_j B_j$ be a convex combination of the points $B_j \in C_\Delta \cap C$.*

If the above convex combinations have the same center

$$\sum_{i=1}^n \alpha_i A_i = \sum_{j=1}^m \beta_j B_j, \quad (15)$$

then every convex function $f : C \to \mathrm{R}$ satisfies the inequality

$$\sum_{i=1}^n \alpha_i f(A_i) \leq \sum_{j=1}^m \beta_j f(B_j). \quad (16)$$

Proof. If the set $\text{conv}\{A,B,C\}$ is a real triangle, we can apply the proof of Lemma 2.1 using $f^{\text{plane}}_{\{A,B,C\}}$ instead of $f^{\text{line}}_{\{a,b\}}$ respecting the plane inequalities in (13) and (14). In other cases we use the chord line or the support line. □

Now we can prove the main theorem:

Theorem 3.2. *Let $A,B,C; A_1,B_1,C_1 \in C \subseteq \mathrm{R}^2$ be points such that*

$$\Delta = \text{conv}\{A,B,C\} \subset \text{conv}\{A_1,B_1,C_1\} = \Delta_1$$

with $\Delta^0 \neq \varnothing$, and $C_\Delta = C_A \cup C_B \cup C_C$ be the cone union. Let $P = \sum_{i=1}^n p_i P_i$ be a convex combination of the points $P_i \in C_\Delta \cap \Delta_1$ with the center $P \in \Delta^0$.

Then there exist two trinomial convex combinations

$$\alpha A + \beta B + \gamma C \text{ and } \alpha_1 A_1 + \beta_1 B_1 + \gamma_1 C_1$$

so that

$$\begin{aligned} \alpha A + \beta B + \gamma C &= \sum_{i=1}^n p_i P_i \\ &= \alpha_1 A_1 + \beta_1 B_1 + \gamma_1 C_1, \end{aligned} \quad (17)$$

and consequently, every convex function $f : C \to \mathrm{R}$ satisfies the inequality

$$\begin{aligned} \alpha f(A) + \beta f(B) + \gamma f(C) &\leq \sum_{i=1}^n p_i f(P_i) \\ &\leq \alpha_1 f(A_1) + \beta_1 f(B_1) + \gamma_1 f(C_1). \end{aligned} \quad (18)$$

Proof. First we determine the coefficients to get the equality in (17), then apply Lemma 3.1 to its both sides. □

The graphical representation of the equality in (17) can be seen in Figure 2.

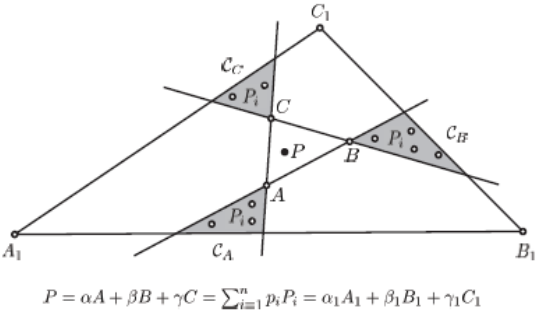

Figure 2. Plane convex combinations with center P

4. Conclusion

If $A_1,\ldots,A_{m+1}\in \mathrm{R}^m$ are points such that the vectors $A_1-A_2,\ldots,A_1-A_{m+1}$ are linearly independent, then the convex hull

$$\Delta=\operatorname{conv}\{A_1,\ldots,A_{m+1}\}$$

is called the m-simplex with the vertices $A_1,\ldots,A_{m+1}$. All the simplex vertices can not belong to the same hyperplane in R^m. Any point $P\in\mathrm{R}^m$ can be presented by the unique affine combination

$$P=\sum_{j=1}^{m+1}\alpha_j A_j. \qquad (19)$$

The combination in (19) is convex if, and only if, the point P belongs to the m-simplex Δ.

Given the m-simplex with vertices $A_1,\ldots,A_{m+1}$, let C_{A_1} be the convex cone with the vertex at A_1 spanned by the vectors $A_1-A_2,\ldots,A_1-A_{m+1}$ (similarly $\mathrm{C}_{A_2},\ldots,\mathrm{C}_{A_{m+1}}$), that is,

$$\mathrm{C}_{A_1}=\left\{A_1+\sum\nolimits_{k=2}^{m+1}p_k(A_1-A_k): p_k\in\mathrm{R},\ p_k\ge 0\right\}.$$

Given the function $f:\mathrm{R}^m\to\mathrm{R}$, let $f_\Delta^{\mathrm{hp}}:\mathrm{R}^m\to\mathrm{R}$ be the function of the hyperplane (in R^{m+1}) passing through the points $(A_j,f(A_j))$ of the graph of f. Applying the affinity of f_Δ^{hp} to the combination in (19), it follows

$$f_\Delta^{\mathrm{hp}}(P)=\sum_{j=1}^{m+1}\alpha_j f(A_j). \qquad (20)$$

If we use the convex function f, then we get the inequality

$$f(P)\le f_\Delta^{\mathrm{hp}}(P)\ \text{if}\ P\in\Delta, \qquad (21)$$

and the reverse inequality

$$f(P)\ge f_\Delta^{\mathrm{hp}}(P)\ \text{if}\ P\in\cup_{j=1}^{m+1}\mathrm{C}_{A_j} \qquad (22)$$

which can be proved in the same way as the inequality in (14).

By the end of the section we will use a convex set $\mathrm{C}\subseteq\mathrm{R}^m$ with the non-empty interior.

The generalization of Theorem 3.2 applies to m-simplexes:

Theorem 4.1. *Let $A_1,\ldots,A_{m+1};B_1,\ldots,B_{m+1}\in\mathrm{C}\subseteq\mathrm{R}^m$ be points such that*

$$\Delta=\operatorname{conv}\{A_1,\ldots,A_{m+1}\}\subset\operatorname{conv}\{B_1,\ldots,B_{m+1}\}=\Delta_1$$

with $\Delta^0\neq\varnothing$, and $\mathrm{C}_\Delta=\cup_{j=1}^{m+1}\mathrm{C}_{A_j}$ be the cone union. Let $P=\sum_{i=1}^{n}p_iP_i$ be a convex combination of the points $P_i\in\mathrm{C}_\Delta\cap\Delta_1$ with the center $P\in\Delta^0$.

Then there exist two $(m+1)$-membered convex combinations $\sum_{j=1}^{m+1}\alpha_jA_j$ and $\sum_{j=1}^{m+1}\beta_jB_j$ so that

$$\sum_{j=1}^{m+1}\alpha_jA_j=\sum_{i=1}^{n}p_iP_i=\sum_{j=1}^{m+1}\beta_jB_j, \qquad (23)$$

and consequently, every convex function $f:\mathrm{C}\to\mathrm{R}$ satisfies the inequality

$$\sum_{j=1}^{m+1}\alpha_jf(A_j)\le\sum_{i=1}^{n}p_if(P_i)\le\sum_{j=1}^{m+1}\beta_jf(B_j). \qquad (24)$$

5. References

[1] P. S. Bullen, D. S. Mitrinović, and P. M. Vasić, *Means and Their Inequalities*, Reidel, Dordrecht, NL, 1988.

[2] J. L. W. V. Jensen, "Om konvekse Funktioner og Uligheder mellem Middelværdier", *Nyt tidsskrift for matematik. B.*, vol. 16, pages 49-68, 1905.

[3] J. L. W. V. Jensen, "Sur les fonctions convexes et les inégalités entre les valeurs moyennes", *Acta Mathematica,* vol. 30, pages 175-193, 1906.

[4] Z. Pavić, J. Pečarić, and I. Perić, "Integral, discrete and functional variants of Jensen's inequality", *Journal of Mathematical Inequalities*, vol. 5, pages 253-264, 2011.

[5] J. E. Pečarić, F. Proschan and Y. L. Tong, *Convex Functions, Partial Orderings, and Statistical Applications*, Academic Press, New York, USA, 1992.

RECYCLING OF CORUNDUM PARTICLES - TWO-BODY ABRASIVE WEAR OF POLYMERIC COMPOSITES BASED ON WASTE

P. Valášek*, M. Müller

[1] Czech University of Life Sciences Prague, Faculty of Engineering, Department of Material Science and Manufacturing Technology
* *Corresponding author e-mail: valasekp@tf.czu.cz*

Abstract
Recycling of all materials should be supported by modern society. Material recycling is one of the most important ways of dealing with waste. One of material recycling possibilities is an inclusion of waste into primary matrices. A suitable ratio and a combination of waste particles influence in a positive way mechanical properties of the material in which they are dispersed and they decrease its price an example of mentioned material recyclation is a dispersion of corundum waste particles in the polymeric matrix. The combination of these types of matrix and filler gives birth to new polymeric particles composite - creates a qualitatively brand new material. As most important characteristics of the polymeric particle composites, one often lists resistance to abrasive wear, hardness, impact resistance and strength and, last but not least, their cost. This article deals mostly with the two-body abrasive wear resistance and hardness of polymeric particle composites with the waste Al_2O_3 as filler and two-component epoxy matrix.

Keywords:
Corundum, hardness, epoxy resin, porosity, tribology

1. Introduction

Composite materials satisfy with their properties more exacting needs of the modern engineering. Composite systems consist of two or more phases with different mechanical, physical and chemical properties, whose mutual interaction then influences the resulting characteristics and behavior. The individual phases influence the resulting characteristics of the material by their own characteristics and by the mutual interaction of the matrix and the filler. The filler can improve the value of mechanical properties like resistance to abrasive wear, hardness, impact resistance and can reduce the cost. To describe a polymeric particle composite as a material system it is necessary to specify, apart from the specifications of material components and their characteristics, the geometry of the supports in relation to the system. This geometry can be described by its shape, size and distribution of parts. [1-3]
All parameters influencing the characteristics of composite materials are related either to their structure, or to the relations between phases**.** It is important a mutual coherence of the system – a cohesion, an interaction in the interface of particles and the matrix and last but not least an adhesion of the system to a basis (as far as it is required).
By adding the corundum particles to the epoxy, we can influence a number of resulting characteristics. Satapathy et al. [4] found out in their experiments that for epoxy with primary corundum filler with particle size of 40-100 μm, the inclusion of corundum increased resistance to abrasive wear. Similar results were achieved by Basavarajappa et al. [5], who describe a significant positive influence of SiC micro-particles on the resultant three-body abrasive wear resistance of the polymeric matrices. Mohan et al. [6] used in their experiment also Si particles, they describe the improvement of tribologic properties of the polymeric composites filled with the particle size of the 20-25 μm. Valášek [7] uses in his experiments iron metal chips from processes of milling and machining for increasing an abrasive wear resistance of reactoplastics.
Epoxy resin as the matrix is brittle and prone to the initiation of cracks. The interface of microparticles and an epoxy resin can increase a proneness of the system to an initiation of cracks which shows itself with decreasing values of strength characteristics and an impact strength. Ku et al. [8] optimized the tensile and bending strength of epoxy and phenolic resins by adding microparticles of smaller sizes. Also Satapathy et al. [4] reached similar results with corundum particles at the tensile strength of epoxy resins.
Increasing other mechanical properties than the wear resistance of the material is described by Cerbu and Curtu [9], who mention using the recycled rubber together with the glass fibres at the epoxy resins – the presence of recycled rubber particles led to the increasing of the impact strength.
Particles composites distinguished for increased abrasive wear resistance are applied in the area of industry and agriculture at renovation of machine parts and in the area of connecting materials. [10-12]
During the process of the matrix hardening sedimentation occurs at particle composite systems. A control of particles distribution can be carried out by means of a reduction coefficient with using X-ray radiation. For interpretation of results

GD degree of grey and the equation (1) can be used:

$$\frac{GDL}{GDO} = e^{-\mu x} \quad (1)$$

where:
GDL… level of grey in place of ray going trough testing specimen,
GDO… level of grey for ray which did not go through testing specimen. [13]

Shots of the grey value (level) give information about the material and the reduction coefficient of X-rays in each point on the shot. Nowadays it exists an effort to correct other effects which would enable to convert the level of grey to values which are direct proportional to e.g. a local density of the material. [14]
The article deals with a polymeric particle composite based on abrasive waste in interaction with two-component epoxy resin. The abrasive waste is represented by abrasive corundum grain (Al_2O_3) with different grain sizes. This waste category belongs to the class 12 01 17 in the Czech waste catalogue. This group is not put in the attachment No. 5 of the Statute book 185/2001 about waste, therefore it is not a case of groups of dangerous waste and their handling is in the Czech Republic (as in the European Union) in no way limited by legislation. This manner of recycling is tolerant to the environment, creates new material and presupposes lower costs of the composite system**.** The production of this type of the waste is not negligible in the Czech Republic, as well as in EU countries (see Fig. 1). Almost 40% from the total amount of this waste was tipped – without possibility to use in the year 2011. [15] The tipping is not in accordance with EU priorities that is why the material using of this type of waste is still topical. An idea to use waste particles from blasting in the form of the epoxy resins fillers is protected in the Czech Republic by the utility pattern 22122 (Polymeric particle composite on basis of waste, authors Müller and Valášek).

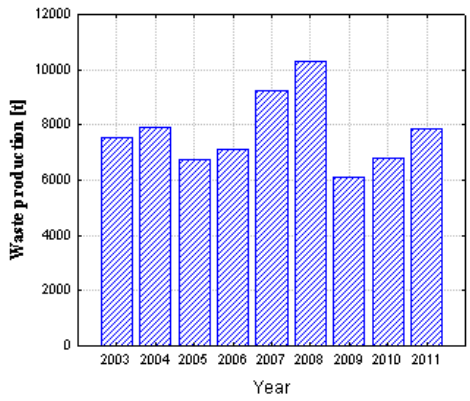

Figure 1. The production of waste from blasting in Czech Republic [15]

The aim of this experiment is to describe a behavior of the polymeric composite on the basis of waste corundum micro particles of various sizes depending on their changing ration and to compare chosen properties with industrially used polymeric materials (PA 6, Material S, Epros In). The experiment is based on a hypothesis coming from above mentioned references that microparticles will lead to a vehement increase of the abrasive wear resistance. The paper focuses namely on the two-body abrasion and the hardness.

2. Materials and methods

For carried out experiments the two-component epoxy resin ECO-EPOXY 1200/324 with the curing agent P11 (based on bisphenol A) was chosen. The curing time of this resin is 24 hours at 23 °C. The total curing occurs after 7 days. The filler was represented by the waste which did not show dangerous properties. As filler, the waste from mechanical surface preparations was used: waste abrasive particles from blasting – synthetic corundum of fractions F60 (284 ± 68 μm), F80 (153 ± 36 μm), F240 (47 ± 9 μm), F400 (15 ± 6 μm), and F800 (5.7 ± 1.1) μm. The synthetic corundum was taken from a sand blaster where common carbon steel sheets were blasted (grit blasted area corresponded to 820 cm^2). The microparticles size after the blasting proccess was measured on the stereoscopic microscope. Composite systems were prepared with filler volume percentage of 5, 10, 15, 20, 25 and 30%. The formulation of the filler part by volume eliminates the influence of the different density between the matrix (1.15 $g \cdot cm^{-3}$) and the filler (we worked with complete surface wettability of the grains with density of the corundum at 4.0 $g \cdot cm^{-3}$). The mixture of epoxy resin and microparticles was mixed mechanically in an ultrasound basin to prevent the emergence of air bubbles and to guarantee the mixture homogeneity. On purpose, other ways (e.g. vacuum) were not used for the testing samples preparation and this was owing to the linking up with the practice where the need to minimize costs for the preparation and application of these systems is assumed.
The two body abrasion was tested on a rotating cylindrical drum device with the abrasive cloth of the grain size P220 (Al_2O_3 grains) according to the standard CSN 62 1466. The testing machine with the abrasive cloth consists of the rotating drum on which the abrasive cloth is affixed by means of a bilateral adhesive tape. The testing specimen is secured in the pulling head and during the test it is shifted by means of a moving screw along the abrasive cloth from the left edge of the drum to the right one, (see Fig. 2). The testing specimen is in the contact with the abrasive cloth and it covers the distance of 60 m. During one drum turn of 360° it is provoked the testing specimen left above the

abrasive cloth surface. Consequent impact of the testing specimen simulates the concussion. The pressure force is 10 N. The mean of the testing specimens was 15.5 ± 0.1 mm and their height was 20.0 ± 0.1 mm. The mass decreases were measured on analytic scales weighing on 0.1 mg. The volume decreases were calculated on the basis of the found out volume and the density of the composite systems. The highest temperature value observed in the interface of the testing sample and the abrasive cloth was recorded by a contactless thermometer Testo 845.

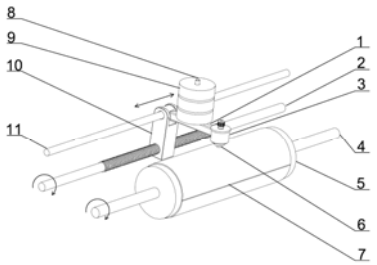

Figure 2. Schema of equipment for two-body abrasive wear testing

As guide for the hardness determination of the composite systems the standard CSN EN ISO 2039-1 was used. The testing specimens dimensions were of 35 x 25 x 9 mm. The hardness was measured in a bottom, respectively in a settled part of the specimen and it was because the fact that also the abrasive wear was found out in this part of the specimens. The distribution of the filler in the matrix caused by a gravitation force depends on its concentration, particles shape, a form etc. and it shows itself on the hardness values. [7] Because of the size of the filler, a ball of hard metal with the diameter D = 10 mm was used (see Fig. 3). The testing specimens were loaded using the force of 2.452 kN for the duration of 30 s. Average values stated in this paper do not contain extremes which would be set aside from the statistical data sets on the basis of normal distribution.

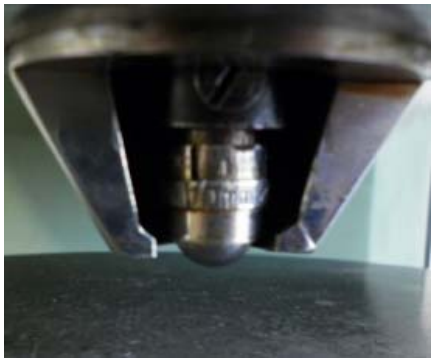

Figure 3. Hardness tester

The porosity was set on the base of the theoretical and real density difference which characterizes the quality of composite systems. When calculating the porosity, the theoretical density respectively, the matrix density 1.15 g·cm^{-3} and the corundum density 4.0 g·cm^{-3} where reasoned. The composite theoretical density ranges from 1.29 g·cm^{-3} to 2.01 g·cm^{-3}. The real density was calculated on the basis of exact sizes and weight of testing specimens (35 x 25 x 9 mm).

A statistical evaluation of results was carried out by means of a program Statistica – ANOVA, reliability level α = 0.05.

Results of the experiment were compared with commercially used polymeric materials:

- PA 6 – wear resistant polymeric material, density 0.93 g·cm^{-3}.
- Material S – wear resistant polymer, density 1.16 g·cm^{-3}.
- Epros In – two-component putty used for renovation of machine parts surfaces, density 1.7 g·cm^{-3}.

3. Results

The porosity values are graphically expressed by means of Fig. 4, a statistical evaluation of graphical presentation is visible in Table 1.

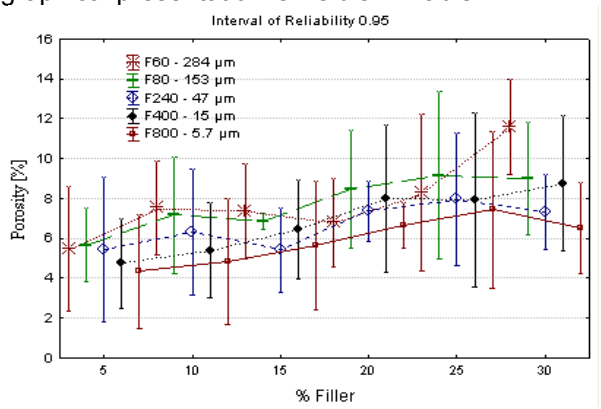

Figure 4. Porosity of composite systems

Air pores have already been found out by the optical analysis by the stereoscopic microscope in the unfilled resin whose real density corresponds to the density stated by the producer. The pores quantification would be difficult so that is why porosity of the unfilled resin was not presented in the graph.

Table 1. Statistical evaluation - ANOVA

Material	F(5;12)	p
F60 - 284 µm	10.1281	0.00
F80 - 153 µm	4.5835	0.01
F240 - 47 µm	2.8634	0.06
F400 - 15 µm	4.6268	0.01
F800 - 5.7 µm	2.9633	0.05

The hardness (HBW) of composite systems can be found in Fig. 5, representing the changes in hardness in individual percent concentrations of filler in the matrix (5% - 30%) in dependence on the used fraction. The fraction is represented in the graph by average particle sizes. The results are

graphically compared with PA 6, Material S and Epros In.

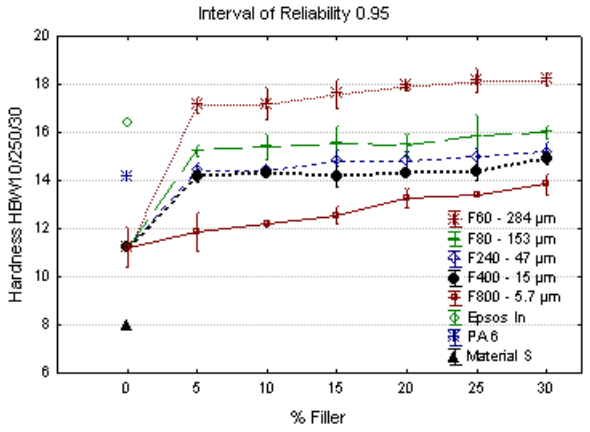

Figure 5. Hardness of composite systems

It is apparent from the graph that hardness decreases in correlation to the decreasing particle size. At the same time, hardness increases in correlation to the relative amount of filler in the matrix. The statistical evaluation arising from the graph is stated in Table 2.

Table 2. Statistical evaluation - ANOVA

Material	F(6;14)	p
F60 - 284 µm	412.8952	0.00
F80 - 153 µm	141.9302	0.00
F240 - 47 µm	172.8596	0.00
F400 - 15 µm	151.8804	0.00
F800 - 5.7 µm	62.0955	0.00

The highest values were recorded at 30% filler in the matrix with the F60 fraction (HBW 10/250/30 18.21). The variability of hardness, in the graph, can be explained by the unequal distribution of the filler in the matrix, caused for example by sedimentation or the potential contamination of the filler (resulting from the secondary nature of the raw material). The lowest value of hardness, (HBW 10/250/30 11.85) was recorded for the F800 fraction with 5% filler in the matrix. The hardness of resin without any filler was HBW 10/250/30 11.22.

Resistance to abrasive wear is apparent in the following Fig. 6. With the decreasing average particle size, the composite systems' resistance to abrasive wear also decreases.

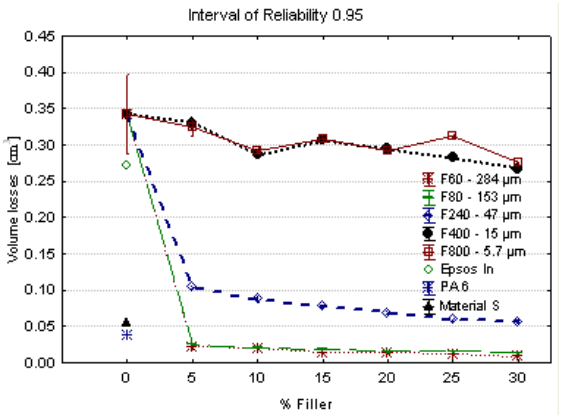

Figure 6. Volume loss of composite systems

The sample least susceptible to abrasive wear was the F60 fraction with 30% filler in the matrix, with the volume loss of only 0.009 cm^3. This volume loss is about 97% lower than the epoxy volume loss. The highest volume loss was recorded for the F800 fraction. The statistical evaluation following graph is stated in Table 3.

Table 3. Statistical evaluation - ANOVA

Material	F(6;14)	p
F60 - 284 µm	666.1652	0.00
F80 - 153 µm	655.3247	0.00
F240 - 47 µm	449.7013	0.00
F400 - 15 µm	30.5858	0.00
F800 - 5.7 µm	20.8826	0.00

The composite system cut and subsequent shot from the optical analysis of the phases of the composite worn area is presented in Fig. 7. This optical analysis could be carried out on used type of the stereoscopic microscope only till the used fraction size F240 that is why it is not presented more complex.

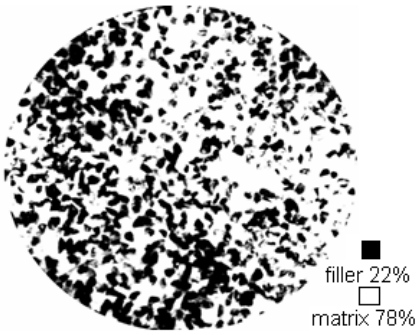

Figure 7. Optical analysis of phases of 5% filler concentration (F60)

4. Discussion

The conducted experiments confirmed the presumption based on the works of authors [1, 4, 6, 11, 12] who claimed that the inclusion of filler in the matrix of epoxy resin increases hardness and resistance to abrasive wear. The composite porosity was confirmed, the occurrence of air pores influences the mechanical properties of the composite in the negative way. The filler

sedimentation at lower concentrations at large middle sizes of particles was evident which confirms the conclusions of the authors [7, 13]. This fact leads in accordance with the experiment results to the conclusion that saturated systems are suitable from the wear resistance point of view – they excel in high wear resistance and they are not prone to the sedimentation (in the case of the experiment – concentrations 25%, 30%).
The resulting figures of hardness and resistance to abrasive wear depend upon the size of the filler particles. Based on the results of the experiment, it is safe to conclude that the ideal size of the filler particles most positively influencing the monitored characteristics of the systems at used abrasive cloth P220 would be the one found in the F60 and F80 fractions (average particle size 284-153 μm). Smaller particle sizes than these, the ones in F240, F400 and F800 fractions (47-5.7 μm), have a positive impact on both their hardness and resistance to abrasive wear, but their values are in lower order digits than those of the larger particles. The particle composites ability to resist to the abrasion at the abrasive cloth with bonded abrasivum depends on the size of used abrasive particles both at the composite systems and the abrasive cloth. This fact has to be considered at planning possible application areas for these composite systems.
Nowadays, on the basis of carried out experiments the implementation of these composite materials based on the waste corundum into the practice is taking place, and this is done in cooperation with czech agricultural companies. One of possible application areas is the renovation of parts of machines processing the soil (see Fig. 8). Following up the experiment prototypes of ploughing blades, land side and exchangeable parts of a moldboard were developed. Their functional steel surface was adjusted by these composite systems and nowadays partical tests are taking place (Fig. 9).

Figure 8. Prototypes of exchangeable parts of moldboard and land side with composite layer (F60, F80 a F240)

An advantage of filled polymeric materials based on the filler in the form of waste is their decreased adhesion when processing damp soil and connected arising friction influencing a consumption of fuels.

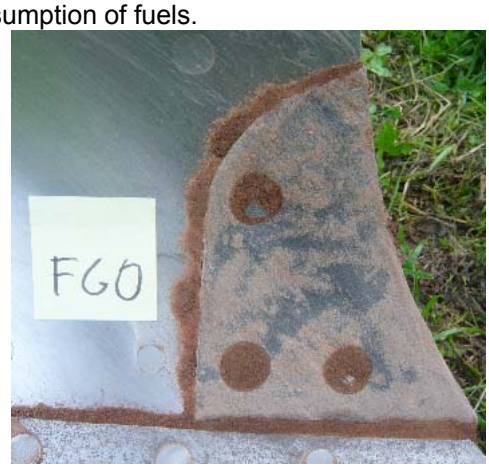

Figure 9. Practical tests - ploughing

From the experiment results it is visible that in the area of polymeric particle composites it is possible to replace the primary raw material (filler) by a secondary one. This possibility of recycling of synthetic corundum is very considerate to the environment and also saves costs necessary for the creation of a particle composite system.
The successful experiments confirmed the presupposition necessary for the application of polymeric particle composites with waste-based filler in industry and agriculture. Their high resistance to abrasive wear, increased hardness, low density and available costs predestine these systems for applications used for puttying, the renovation of mechanical parts and functional areas. What is not to be overlooked is also that with choosing the correct area of application, also different characteristics than hardness and resistance to abrasive wear are important, such as tensile strength and impact strength.

5. Conclusion

The hypothesis about considerable increase of the wear resistance and the hardness by the inclusion of hard inorganic particles based on the waste – corundum was confirmed:

- The composite with middle grain size 284 μm showed of 16% higher hardness and of 97% lower volume losses than the unfilled system.
- From the abrasive wear point of view the sufficient strength in the interface of the epoxy matrix and the waste filler was proved which did not lead to a delamination of particles during the experiment.
- This fact predetermines the polymeric matrix as a bearer of the material recyclation of particles waste.

6. Acknowledgement
This paper has been done when solving grant IGA TF.

7. References

[1] B.Ch. Kim, S. W. Park, D. G. Lee,"Fracture toughness of the nano-particle reinforced epoxy composite,". *Composite Structures,* vol. 86 , pp. 69-77, 2008.
[2] D. Gay, V. H. Suong, W. T. Stephen," Composite Materials – design and application," CRC Press LLC, 2003, 531 p.
[3] D. Vojtech, „Materials and their marginal status," VŠCHT, Prague, 2010.
[4] B.K. Satapathy, J. Bijwe,"Analysis of simultaneous influence of operating variables on abrasive wear of phenolic composites," *Wear*, 253, pp. 787-794, 2002.
[5] S. Basavarajappa, A.G. Joshi, K. Arun, A.P. Kumar, M.P. Kumar,"Three-Body Abrasive Wear Behaviour of Polymer Matrix Composites Filled with SiC Particles," *Polymer-Plastics Technology and Engineering*, 14, pp. 8-12, 2010.
[6] N. Mohan, S. Natarajan, S. P. Kumaresh Babu," The role of synthetic and natural fillers on three-body abrasive wear behaviour of glass fabric-epoxy hybrid composites," *Journal of applied polymer science*, 124, pp. 484-494, 2012.
[7] P. Valasek, M. Muller, A. Proshlyakov,"Effect of sedimentation on the final hardness of polymeric particle composites, *Research of. Agriculture Engineering*, 58, pp. 92-98, 2012.
[8] H. Ku, M. Trada, T. Cecil, et al.," Tensile Tests of Phenol Formaldehyde Glass-Powder Reinforced Composites: Pilot Study," *Journal of applied polymer science*, 116, pp. 10-17, 2010.
[9] C. Cerbu, I. Curtu," Mechanical haracterization of the glass fibres/rubber/resin composite material," *Materiale Plastice*, 48(1) pp. 93-97, 2011.
[10] P. Valasek, M. Muller,"Polyurethane resins filled with inorganic waste particles," *Manufacturing Technology*, 13, pp. 241-247, 2013.
[11] M. Muller, P. Valasek,"Abrasive wear effect on Polyethylene, Polyamide 6 and polymeric particle composites," *Manufacturing Technology*, *12*, pp. 55-59, 2013.
[12] M. Muller, P. Valasek, P. Novák, et al., "Aplikace návarů a kompozitů v oblasti technologie pěstování a sklizně cukrové řepy (Welding and composites applications in the field of technology growing and harvesting sugar beets)," *Listy cukrovarnické a řepařské (Sugar and sugar beet journal)*, 9, pp. 304-307, 2011.
[13] P. Valasek, A. Proshlyakov, M. Müller,"Využití RTG záření k určení vnitřní struktury technických materiálů – polymerních částicových kompozitů (Using X-ray to defining inner structure of technical materials – polymeric particle composites)," *Strojírenská technologie*, Vol. 17, No. 4, pp.266-270, 2012.
[14] D.H. Phillip, J.J. Lannutti," Measuring physical density with X-ray computed tomography," NDT&EInt., 30, 1997. pp. 339–350.
[15] Waste evidence [Online]. Available: http://isoh.cenia.cz/ groupisoh/fin.php. [Accessed 20-Jul-2013].

TEACHING ENGINEERING – A DIDACTICAL CHALLENGE

MMag. Sabrina Romina Sorko[1*], DI Gerhard Hanzl[2]

[1]FH JOANNEUM University of Applied Sciences, Industrial Management, Kapfenberg, Austria
[2]FH JOANNEUM University of Applied Sciences, Industrial Management, Kapfenberg, Austria
** Corresponding author e-mail: SabrinaRomina.Sorko@fh-joanneum.at*

Abstract
The Challenges of technical development for educationalists of our global information society can only be mastered by interactive and interdisciplinary didactical and educational methods. The objective of this article is to get a differentiated view on teaching of technical contents.

Based on integrated competence orientation of didactics and teaching - the content to be transferred can be divided into categories, which enables lecturers to use different proper didactical methods for every category in order to reach a maximum mobilisation level of students. These range from low activation methods such as listening to lectures up to highly activating general and technical teaching methods like simulation games or role plays. But the developed approach serves more or less only the teachers selection of teaching methods. The educational success however will also be influenced by environmental and situational factors concerning heterogeneity and group dynamics as well as different learning environments. Undoubted remains the importance of activation and motivation in the learning process of technical contents.

Keywords
Teaching methods, engineering education, competence orientation, didactical model

1. Introduction

The 21st century can be characterized with terms like technical progress, fast-pace or insecure professional careers and can be seen as a highly complex environment for people to be successful. The willingness to work hard and to fulfill all requirements is not enough anymore. Nowadays these are more or less the basic demands on employees. Key qualifications however are multidimensional competences that enable employees to use all their gathered knowledge for finding creative, holistic and therefore innovative solutions for daily work tasks [1].
Focusing on the engineering field, there is a second challenge education has to face. The massive technical progress of the last decades led to a highly complex working field which often frightens young people to start a professional career [2].
Taking this social and economic development into account, it is clear that new ways of teaching are necessary. Schools and Universities have to find proper ways to prepare motivated young people for the drafted working environment and to show them the opportunities the technical field provides.

2. Competence orientation

Within the last years, competence orientation and the hands-on model turned out to be appropriate teaching principals to face the discussed challenges. Competence based learning has become the key method of holistically teaching. The most common definition was formulated by *Weinert*, who points out the significance of multivariate learning outcomes. Therefore not only cognitive knowledge is important, but also social competences and the ability to adopt the individual competences for problem solving [3].

Especially in engineering education competence orientation plays a major role. Young engineers should be able to identify and analyse various industrial situations and create innovative technical solutions. Therefore independency, accuracy, responsibility and the ability to work in a team have to be trained [2].

Research shows, that with conventional teaching methods those competences can't be gathered. Although there are still topics that should be imparted classically, holistic approaches are necessary to train problem solving competences. Looking through the wide range of teaching methods, not all of them are capable to fit the described needs. Whereas there are loads of possibilities to classify teaching methods, this article focuses on the mobilisation level of students.
Depending on the behaviour of the students in class, teaching methods can be classified after their level of activation. If students assume a passive role during class, for example when only listening to a speech, those methods are on a low level of activation, whereas methods following competence orientation respectively the hands-on principle, leads students to work out different tasks actively. Simulation games or giving presentations are examples for that [4].

3. Engineering education

Nevertheless not only complex teaching methods are needed in order to ensure competence based learning. To provide an effective engineering education lecturers have to define a coherent didactical model including definitions of the teaching or learning targets, the particular content as well as adequate methods and media. In order to that in Germany the scientific concept of multi perspective engineering education has been established. This model does not describe the various fields of research but the different aspects of learning outcome [4]. Initial points of the concept are the four core objectives that should be taken into account similarly when planning engineering classes.

Action perspective emphasises the hands-on approach thus the need of using teaching methods where students have to actively work on technical tasks [2].
Second the knowledge perspective where the content plays the central role. Students must be able to identify, understand and combine the various technical fields as well as their integration [2].
After fulfilling the knowledge perspective, students should also be able to analyse technical situations and prepare effective solutions using their gathered competences. These abilities are called impact and evaluation perspective [2].
The fourth perspective emphasises the importance of preprofessional orientation [2].

The first two perspectives characterise the content dimension of engineering education and are therefore highly connected with the various engineering subjects that are taught. The third aspect stands for the social-human dimension of technical topics, which stated that engineering itself results out of human action and therefore affects society directly. The last perspective that was described could be seen as general teaching principle. Whenever young people are in learning-settings pointing out the practical use of the topics should be a permanent teaching guideline. Students have to realise the relevance of the content and get a clear overview of the various possibilities they have after finishing their education [5].
Summing up engineering is much more than a research field. Students have to be aware of the distinctive relation between technical topics and the impact technical actions have on society and our life.

4. Teaching methods for engineering education

Based on this cognition, it seems rather obvious that lecturers have to face some challenges. Subsequently they need to be supported didactically by planning their engineering classes. Depending on the main content a holistic concept fitting all the requirements pointed out before must be formulated. To support teachers in doing that, the Authors, in cooperation with some students of the degree program (International) Industrial Management at *FH JOANNEUM University of Applied Sciences* have conducted a matrix that gives an overview of different teaching methods. In addition it gives an idea for what type of technical content the particular methods are suitable.

The matrix is split up in two tables, one for low activating methods and one for high activating ones. The content categories are defined on base of the reduction model of *Lehner*. This model states that, depending on the available time, more or less content can be imparted [6]. Keeping that in mind it is necessary to define more, as well as less important topics. Regarding to technical classes the content can be divided as follows:

- basic knowledge in engineering
- in-depth knowledge in engineering
- add on business knowledge and
- add on general knowledge.

The last two categories are included, even though they are no engineering ones, because for some technical topics business or general knowledge is needed to understand the cross-linked impact of the topic.
The different methods are extracted from various literature such as W. H. Peterßen, “Kleines Methoden-Lexikon”, *Oldenbourg Schulbuchverlag*, 2009 or P. Baumgartner, “Taxonomie von Unterrichtsmethoden. Ein Plädoyer für didaktische Vielfalt”, *Waxmann*, 2011.

Table 1. teaching methods – low activation

content	level of activation	
	listening	experiencing
basic knowledge in engineering	• lecture • presentation • educational film	• excursion • fish bowl method • ball bearing method • mind mapping • POOL method
in-depth knowledge in engineering	• lecture • speech of an expert • educational film	• excursion • fish bowl method • ball bearing method • mind mapping • POOL method
add on business knowledge	• lecture • presentation • speech of an expert • educational film	• brainstorming • fish bowl method • ball bearing method • discussion • mind mapping • POOL method • circle discussion
add on general knowledge	• lecture • presentation	• brainstorming • fish bowl method • ball bearing method • discussion • mind mapping • circle discussion

As described, the level of activation is one possibility to cluster teaching methods from the students' point of view. According to the task they have to fulfill during class, low activation methods can be divided into listening and experiencing methods.
The first group includes teaching methods were students mainly have to listen to the lecturer or other media. Lectures, educational films or listening to a presentation are meant by that. To the second group methods such as excursions or discussions can be allocated.
The second table defines two different types of high activating teaching methods. Regarding to the hands-on principle students have to work actively on topics and gain practical experience.

Table 2. teaching methods – high activation

content	level of activation	
	general action	technical action
basic knowledge in engineering	• group puzzle • learning exhibition • circuit learning • mind mapping • freeze frame building • simulation game	• 4 step method • discovery learning • learning exhibition • simulation game
in-depth knowledge in engineering	• COOL concept • 4-corner-method • group puzzle • learning exhibition • circuit learning • mind mapping • simulation game • role play	• COOL concept • 4 step method • discovery learning • learning exhibition • simulation game • role play
add on business knowledge	• COOL concept • 4-corner-method • group puzzle • learning exhibition • circuit learning • mind mapping • freeze frame building • simulation game • role play	
add on general knowledge	• COOL concept • 4-corner-method • group puzzle • learning exhibition • circuit learning • mind mapping • freeze frame building	

Highly activating methods can be split concerning the type of action into general and technical ones. General action means that the students have to fulfill special tasks independently whereat those actions are primary not technical oriented. Examples are working out a presentation, working on a project or creating a mind map. The highest level of activation describes methods of technical action. These are tasks where students have to work manually to solve engineering problems. In those sessions, machines are built, materials are processed or entrepreneurial decisions are made.

The clearly represented tables support teachers of engineering classes in finding various proper teaching methods for their classes on the one hand and can on the other hand be seen as a thought-provoking impulse for structuring the teaching units and defining learning targets.

5. Discussion

When working with the shown model, some key factor has to be taken into account. Every group is different and has its individual dynamics. Here should be named at least the most important factors of influence that affect the choice of teaching methods.
Depending on the particular education and professional experience of the members of the learning group more or less specific topics can be worked on. According to that the level of activation has to be chosen. When the basic knowledge is already known, it is easier to continue with highly activating methods. Cause if not, first the basic understanding of the content must be gained [7].
Different professional qualifications lead to a certain level of heterogeneity of the group. Working with highly heterogeneous groups accompanies more complex teaching concepts in order to assure an adequate learning outcome of every student. The individual differences must be taken into account [7].
The third factor is the individual group dynamics which is different in every learning group. This leads to the phenomenon that using the same method for the same content can support the competences of one group very well however of another group quite badly.
Besides influencing factors linked with the students, also the learning environment plays a major role in the decision making process. Teaching methods have to be adjusted on the available resources such as duration of the class, room or budget [7].
Thinking about proper teaching methods is a multidimensional decision making process which should be done again for every learning group a lecturer have to work with even though the content is the same. The developed Matrix offers various possibilities for different types of content and thus helps educationists to prepare exciting, effective and holistic education.

6. Conclusion

The complex and dynamic content of engineering subjects need higher activation and motivation of students as well as teachers in order to provide holistically, competence oriented education. It is

reflected that technical education can be better supported by using action- and knowledge-based approaches simultaneously. Also the preprofessional orientation of teaching plays a major role because the relevance of learned content becomes increasingly a precondition of students' acceptance.

The main research of the Industrial Management Institute at FH JOANNEUM University of Applied Sciences was to adopt a differentiation of the content of technical lectures according to make use of the potential of various didactical methods. This approach can intensify students' activation and increase efficiency of teaching, though the result also depends on further social and environmental factors.

10. References

[1] K. Sonntag, "Kompetenztaxonomien und -modelle: Orientierungsrahmen und Referenzgröße beruflichen Lernens bei sich verändernden Umfeldbedingungen", *Nova Acta Leopoldina NF 100*, Nr. 364, 2009.
[2] B. Sachs, "Technikunterricht: Bedingungen und Perspektiven", *tu-Zeitschrift für Technik im Unterricht 26*, Nr. 100, 2001.
[3] F.E. Weinert, „Leistungsmessung an Schulen", *Beltz*, 2002.
[4] F.-J. Kaiser/H. Kaminski, "Methodik des Ökonomieunterrichts", *Klinkhardt*, 2011.
[5] W. Bienhaus, „Technikdidaktik – der mehrperspektivische Ansatz", *Pädagogische Hochschule Karlsruhe*. [Online]. Available: http://www.dgtb.de/fileadmin/user_upload/Materialien/Didaktik/mpTU_Homepage.pdf. [Accessed: 18-Sep-2013].
[6] M. Lehner, "Viel Stoff – wenig Zeit. Wege aus der Vollständigkeitsfalle", *Haupt*, 2009.
[7] A. Helmke, "Unterrichtsqualität und Lehrerprofessionalität", *Kallmeyer/Klett*, 2009.

BUCKET WHEEL EXCAVATOR SH630 AFTER OVERHAULING STRESS-STATE DIAGNOSTIC

N. Vukojević, F. Hadžikadunić*

Mechanical Engineering Faculty in Zenica, University of Zenica, Bosnia and Herzegovina
* *Corresponding author e-mail: hfuad@mf.unze.ba*

Abstract
An analysis of excavator SH630 type, manufactured by O & K Germany, which is used in the open pit mine in Lukavac is presented in this paper. For the purpose of the commissioning of this complex mining plant and confirming the correctness of activities performed on excavator repair one of the segments of the analysis is the measurement performance of the stress-deformation state of the vital parts of the excavator by strain gauges in working conditions, and analysis of measurement results. Stress analysis results showed that the main mast and pylon during normal working regime are not exposed to stresses that would in any way jeopardize their safety. Dynamic stress changes taking place around a relatively low medium stress with small stress amplitude, which is desirable from the standpoint of strength.

Keywords:
Bucket wheel excavator, stress-strain analysis, strain gauges.

1. Introduction

Excavator SH630 has a working wheel with buckets (1) which in the normal working process turns with 7 min^{-1}, and thus achieves the designed capacity of 1,000 t/h, Figure 1.

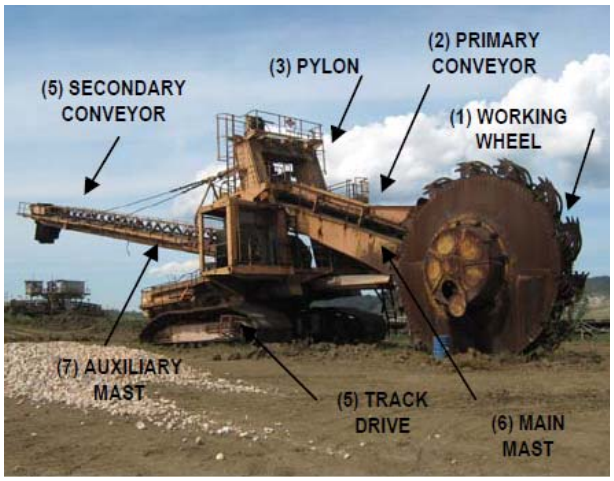

Figure 1. Excavator SH630 before overhaul

Working wheel is powered with 5 hydro-motor with gearing located at the operating point. The procedure of material digging is done by 14 buckets on the upper side of the working wheel with discharging through the openings in the structure where the excavated material over receiving hopper directs to the primary belt conveyor (2).

Figure 2. Excavator SH630 after overhaul

Working wheel and the primary conveyor over the main mast rely on the support excavator structure, so called pylon (3). Pylon is a welded steel frame which takes all the load and over a large circular support the load is transferred to the substrate. Pylon construction has the option of circular motion. The main mast is welded steel box-shaped construction which hanged with two shafts to the pylon, and over the hydraulic cylinder placed at the lower part of the pylon gets vertical movement. On the supporting structure there is also outpouring system through which the excavated material is directed to the secondary conveyor and transported further to the main system of transport for the material excavated from the mine. Construction of pylon is the main bearing structure through which all workloads are transferred to the substrate. Pylon is supported on caterpillars of the excavator which facilitate the movement of the entire system. The rehabilitation of the excavator is related to all vital parts of the steel structure, transport system, working wheel buckets and hydraulic system, Figure 2. Drive of the excavator is realized with electricity that powers the pump and the entire hydraulic system. On a steel frame main mast and pylons are provided measurements of stress-deformation state and acceleration during operation to assess the dynamic and static stability in terms of workloads.

2. Structural analysis and experimental results

Before experimental measurements an analysis of structure using the finite element method were done (not shown in the paper) in order to establish

a preliminary distribution of stress and strain on the structure as a help to define measuring points with strain measurements. The aim of the planned experimental measurements is to determine whether the structure is uniformly loaded and whether the stress intensity reaches a critical value. Based on the analysis of stress it has been shown that the zone transitions from horizontal to vertical load-bearing part of the structure is exposed to the highest pylons acting stresses. Operating force and force of bucket penetration in the ground, so called, cutting force, acting eccentrically in relation to the central axis of the main mast, and centrally in relation to the axis of the pylon, so that this displacement of the working force from the axis causes complex stresses, [1,2].

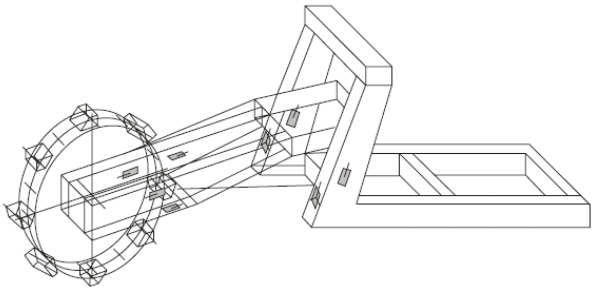

Figure 3. Scheme of measurement points

Complex excavator construction in static and dynamic sense requires that on the pillars of vertical pylon frame two measuring three-grid rosette gauges must be placed at the same position and one single-grid measuring gauges on the sides of the vertical pylon pillars on both sides. Measuring strain gauges are installed on identical positions on both vertical pylon pillars for comparison of results. Another significant part of the construction excavator is a main mast, which carries the working wheel and the primary conveyor. The main mast is welded box-shaped steel construction loaded with bending in two planes and to assess its behavior four strain gauges must be installed at the outer contour of the mast. Position of strain gauges are shown in Figure 3. Data acquisition was made for the characteristic working phases of the excavator, such as moving the excavator, idle operation phase, excavator rotation, digging with all necessary movements. Data acquisition was performed with rate of 5 [Hz] with 8-channel system "Spider 8-30" and the accompanying software, "Catman – Professional'' and strain gauge type 1-LY91-10/120 "HBM" Darmstadt, Germany. Data acquisition is done in "real-time" mode and software post-processing results are shown in sizes that define stress states. Measurements of strain were carried out in more specific working states of the excavator, which are common during operation, [3].

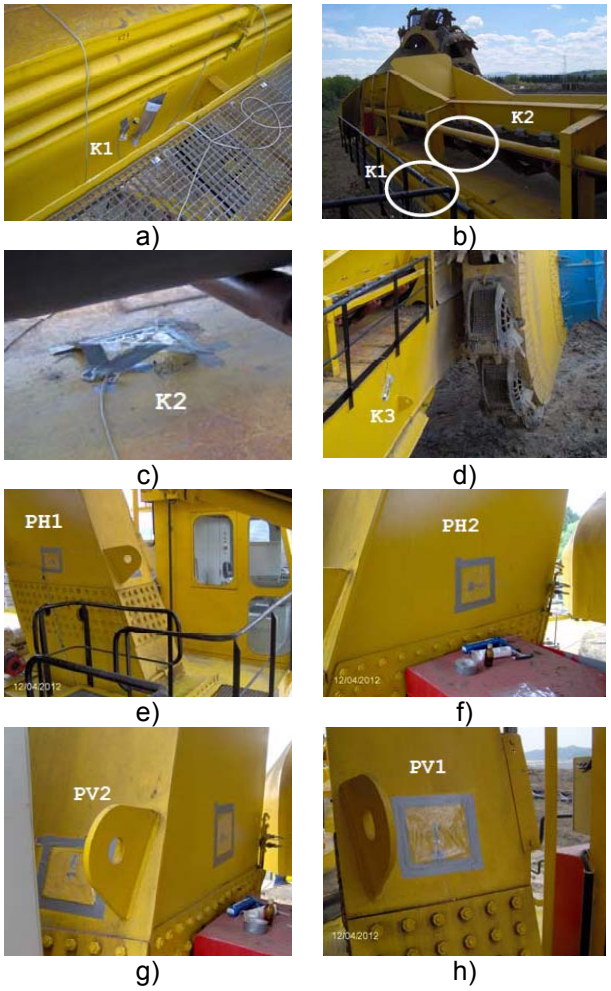

Figure 4. Measuring places on the main mast of excavator K1, K2 and K3: a) to d), the position of measuring places at a pylon PH1, PH2, PV1 and PV2: e) to h)

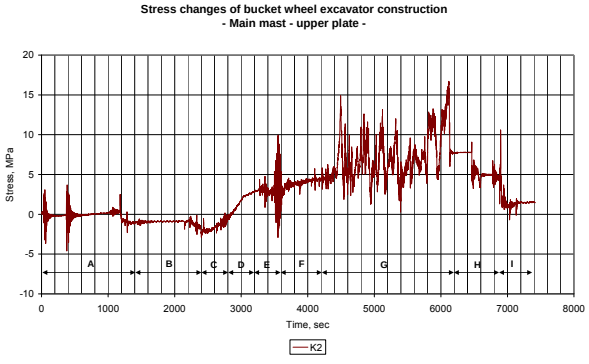

Figure 5. Diagram of stress changes - measuring place K2

This specific operating conditions are indicated in the graphs, Figures 5 to 9, and relate to: A-moving of excavator, B-mast rotation + rotor spinning without digging, C-belt conveyors turned on + increasing of wheel rotation speed without digging,

D-excavator rotating + conveyor belts turned on, E-moving forward without excavator digging + excavator rotation + lowering the working wheel, F-moving forward + rotation, G-digging + excavator rotation + mast lifting + mast lowering + normal operating regime of digging, H-mast lifting + belts turned on, I-working wheel works with no-load + excavator rotation + turning off.

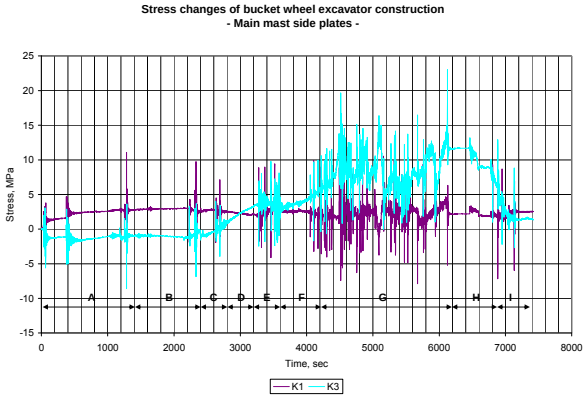

Figure 6. Diagram of stress changes - measuring places K1 and K3

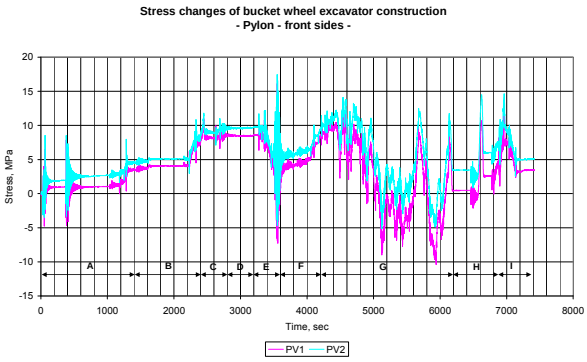

Figure 7. Diagram of stress changes - measuring places PV1 and PV2

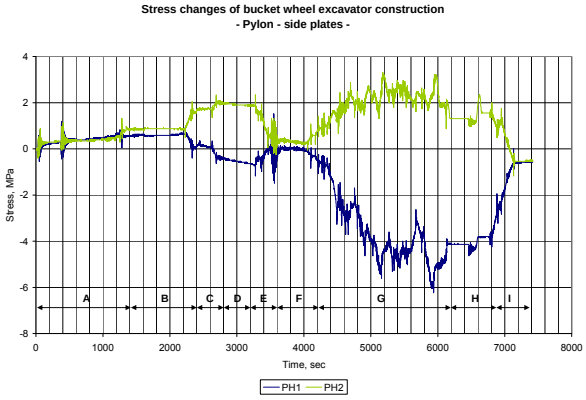

Figure 8. Diagram of stress changes - measuring places PH1 and PH2

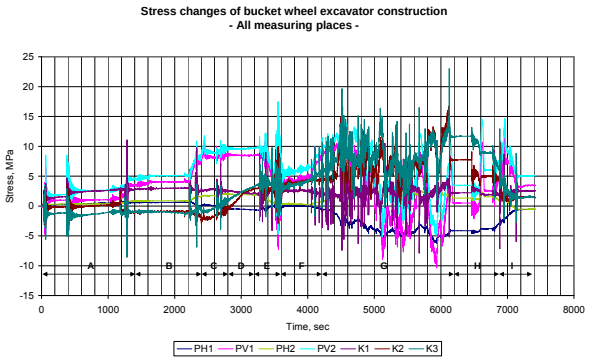

Figure 9. Diagram of stress changes - all measuring places

During the measurements, a change in pressure is followed within the system of working wheel. The usual range of registered pressure, during the measurements, was in the range 51 to 56 (bar). The highest level of pressure registered was about 80 (bar) corresponding to the highest measured stress. Because of that the projected maximum pressure in cylinder can reach 2.5 times higher value (up to 190 bar), which is caused by digging conditions (digging resistance), it can be expected that in such working conditions and maximum operating stress reaches a significantly higher value. As shown in Figure 9, it is clear that the character of the change in stresses at all points are of a stochastic (random) character. The highest measured tension character stress has a value of +23 MPa, and the highest measured pressure character stress is -10 MPa. Allowable stress for alternating variable load is σ_{allow} = 80÷100 MPa (S235). Maximum measured stress values correspond to the hydraulic pressure of about 80 (bar). For maximum design pressure in the cylinder of 190 (bar) it can be expected for stress to achieve proportional greater value σ_R = 60 MPa < σ_{allow}. The highest measured stress at the measuring point K2 is 17 Mpa, Figure 5. Stresses are mostly of tension character. Character of stress changes at measuring points K1 and K3 is the same, with the difference in intensity, Figure 6. The highest measured stress is the measurement of K3 and is about 23 MPa, while the maximum stress measured at the point in the K1 is about 10 MPa. After analysis of the stress character at the two measuring points, it is clear that there is presence of complex stresses - tension and bending, but it is bending to the left with a little more intensity. The dynamic nature of the changes is with low intensity and does not endanger the dynamic stability of the main mast. Stresses measured on vertical pillars of pylon at points of PV1 and PV2 have approximately the same intensity and character changes, Figure 7. All measured values vary between -10 MPa and 17 MPa.

The difference between the values PV1 and PV2 is higher than 2 MPa, which is negligible. This result indicates that there is no difference in the vertical deformations of the main pillars of the pylon. Maximum dynamic activity was observed in a field marked with "E" what is a period of excavator's moving and working wheel's lowering. Differences were detected in the sign of the measured stress at the measuring point PH2, where tensile stress occur, and at the measuring point PH1 – pressure, Figure 8. This difference suggests that there is a torsion of pylon pillars, which results in the fields marked with a "C", "G", "H" and "I", and these are precisely the operations in which the excavator rotation is performed and this phenomenon were expected.

For the goal of getting the whole excavator's diagnostic status under working dynamic conditions, some other measurements have been done as vibration measurements at bearings of rotating wheel and dynamic measurements with accelerators defining construction's frequencies, but not presented in this paper.

3. Conclusion

The construction of bucket wheel excavator is very complex and so static and dynamic states are. The assessment of those states must be based on several groups of measurements. In this paper only one field of interest is covered. The measured stress values at the specific measuring points are significantly less than the allowable stress for this type of construction. Dynamic stress changes, taking place around a relatively low medium stress with a small stress amplitude, are desirable in terms of strength. Stress change character fully agrees with the expected changes caused by normal excavator operations. Based on the measurements and analysis, it can be stated that the main mast and pylon, as the most important carrier of the excavator, during normal working regime are not threatened in terms of static and dynamic load capacity and strength.

4. References

[1] T. Maneski, D. Ignjatović, "Repair and reconstruction of bucket wheel excavators", *Journal of Structural Integrity and Life*, Vol.4, No. 1, 2004.
[2] D. Daničić, T. Maneski, "The structure failure of the discharge boom of bucket wheel excavator C700S due to dynamic effects", *Journal of Structural Integrity and Life*, Vol.12, No. 1, 2012.
[3] K. Hoffmann, "Eine Einfürung in die Technik des Messens mit Dehnungsme βstreifen", *Hottinger Baldwin Messtechnik GmbH*, Darmstadt, 1987.

THE ANALYSIS OF THE BROD-POSAVINA COUNTY FOREIGN TRADE EXCHANGE FOR THE PERIOD FROM THE YEAR 2008 TO THE YEAR 2012

B. Bolfek[1*], I. Blažević[1] and M. Tokić[1]

[1]College of Slavonski Brod, Dr. Mile Budaka 1, 35000 Slavonski Brod, Croatia
** Corresponding author e-mail: berislav.bolfek@gmail.com*

Abstract

In today's globalized conditions of business, country's foreign trade exchange is of great importance to its economy. The Republic of Croatia, according to its territorial constitution, is comprised of 21 counties, and the subject of this article is the analysis of foreign trade exchange of the Brod-Posavina County. According to the size and the number of residents, the Brod-Posavina County is in the middle of the mentioned 21 counties.

The main objective of this paper is to determine involvement and influence of some of the counties in foreign trade exchange through the level of openness by analyzing the secondary data gathered from the Croatian Chamber of Economy and the Central Bureau of Statistics. This paper analyzes the level of foreign trade exchange, import dependence, export development and the level of openness of the Brod-Posavina County.

Keywords: export, import, Brod-Posavina County

1. Introduction

The Brod-Posavina County has 2.034 km^2, what is 3,59% of the total size of the Republic of Croatia and as such is the 14th largest county in the Republic of Croatia. According to the population census from 2011, the Brod-Posavina County has 158.575 residents and is the 10th largest county according to number of residents in the Republic of Croatia.

In the Brod-Posavina County different economic activities are developed, such as metal processing industry, wood industry, construction, agriculture and trade (processing industry being the most developed).

Development of different economic activities enables foreign trade exchange of the Brod-Posavina County. The main objective of this paper is to analyze foreign trade exchange of the Brod-Posavina County in the period from 2008 to 2012 with special review of involvement and participation of counties through the level of openness.

The efficiency of a country on an international market is determined by the competitive capacity of all its business partners involved in its foreign trade business, respectively international exchange. It is essential to have competitive advantage what is the basis for achieving higher profitability [1].

On a global market, only those national economies, or its business subjects, that are capable of creating larger economic value in relation to its opponents can have competitive advantage [2].

2. Export of the Brod-Posavina County

Based on the data gathered from the Croatian Chamber of Economy, the economy of the Brod-Posavina County has been orienting on export and has marked a high rate of growth of export (Table 1) [3].

In accordance, the Brod-Posavina County has been 2nd in the year 2007 and 1st in the year 2008 for the rate of growth of export among the counties. In addition, the export has equalized with the import what is extremely positive, since on the national level the export covers only 60% of the import and this negative trend has been present for years.

Unfortunately, due to the recession the Brod-Posavina County has marked the decrease in the last three years. In 2012 the total export of the Brod-Posavina County has been 234.8 million USD, while import has been 264.9 million USD. This makes a total of negative balance of exchange of goods 30.1 million USD.

Table 1. The export of the Brod-Posavina County according to countries in the period from 2008 to 2012

DESCRIPTION	EXPORT (in USD)				
	2008.	2009.	2010.	2011.	2012.
TOTAL:	251.556.438	190.367.167	169.797.820	159.059.128	234.802.807
EU countries	202.787.635	147.983.303	123.739.853	108.163.092	151.077.897
EFTA counries	1.905.793	8.506.874	10.432.951	3.518.328	2.495.134
CEFTA countries	40.678.699	28.168.176	22.255.890	34.440.343	62.727.639
OPEC countries	572.947	1.963.890	832.755	548.389	81.434
Other EU countries	506.942	2.058.234	11.024.237	1.462.448	10.434.137
Other Asian countries	657.185	1.282.679	1.416.964	2.939.541	2.210.182
Other African countries	26.569	173.170	4.525	7.794.780	110.651
Other American countries	-	7.057	68.580	122.886	5.642.569
Ocean countries	-	-	22.065	69.321	23.164

3. Import of the Brod-Posavina County

Although the economy of the Brod-Posavina County is still burdened with problems (consequences of war destruction, problematic privatization of public property, permanent meaningful unemployment rate, difficult process of transition, decreasing industrial production, negative foreign trade balance…), in the last few years the tendency toward strengthening small and medium-sized enterprises and trades in personal ownership has been evident.

The County's foreign trade exchange is increasing, but the portion of the County's foreign trade exchange in the national foreign trade exchange is symbolic. The rest of the country is following the trend and increasing the loss (deficit) evident in higher rate of growth of the import in relation to the export.

Table 2. The import of the Brod-Posavina County according to countries in the period from 2008 to 2012

DESCRIPTION	IMPORT (in USD)				
	2008.	2009.	2010.	2011.	2012.
TOTAL:	223.691.975	161.594.776	143.248.387	214.320.931	264.935.967
EU countries	175.752.906	123.541.756	107.289.303	164.822.555	190.732.609
EFTA countries	2.303.399	5.507.920	2.115.747	6.164.933	8.428.513
CEFTA countries	26.786.001	19.253.619	10.663.646	17.825.526	45.869.187
OPEC countries	83.978	8.891	4.146.405	4.966.159	4.504.641
Other EU countries	738.843	586.203	1.035.845	1.204.099	1.556.719
Other Asian countries	10.874.812	6.484.028	15.480.169	13.781.491	10.996.656
Other African countries	3.215	180	100.802	292.473	137.129
Other American countries	564.353	1.177.136	2.360.032	5.163.896	2.679.918
Ocean countries	-	-	56.438	99.799	30.595

Based on the data from Table 2, gathered from the Croatian Chamber of Economy, it is evident that import has oscillated in the last 5 years [4].

In accordance, the import was much lower in the year 2009, while in years 2011 and 2012 there has been a tendency of growth. The total import for the year 2012 is 260 million USD. By far the largest import of the Brod-Posavina County is actualized from the EU countries, some of them are: Finland (44,5 million USD) and Germany (34,0 million USD), Italy (16,6 million USD) and Hungary (13,9 million USD). With all mentioned countries the Brod-Posavina County is making a deficit in foreign trade exchange.

The Brod-Posavina County entrepreneurs are actualizing foreign trade exchange with distant countries as well, such as Thailand, Taiwan, Singapore, the Republic of South Africa, United Arab Emirates, India, Korea, Singapore, Philippines, Vietnam, Aruba, Pakistan, Uganda and other. Germany is the most important foreign trade partner of the Brod-Posavina County since the exchange is the highest in both import and export. It should be mentioned that in 2009 the export to Germany was cut in half (- 44,1%) in relation to the year 2008, while the import to Germany in 2009 decreased for 31,4%.

4. The level of openness of the Republic of Croatia with special regard to the Brod-Posavina County

Foreign trade exchange of the Republic of Croatia is not equally distributed among its counties. In fact it is completely opposite, foreign trade exchange for the last ten years has been concentrated in five or six counties with the tendency of further growth of concentration. The level of openness is a very important segment or a part of foreign trade exchange of goods, and it can be calculated as a sum of total export and income within one year divided by the value of GDP.

The level of openness of the Republic of Croatia and its counties from 2005 to 2010 based on the data gathered from the Central Bureau of Statistics is shown in Table 3. [5]

Table 3. The level of openness of the Republic of Croatia and its counties in the period from 2005 to 2010

No.	Name of the county	2005.	2006.	2007.	2008.	2009.	2010.	Average
1.	Zagreb County	54.9	62.5	62.5	62.5	47.5	46.7	55.3
2.	Krapina-Zagorje	49.9	57.3	58.4	61.4	50.6	53.8	55.0
3.	Sisak-Moslavina	65.3	58.3	65.9	66.3	42.5	52.7	60.7
4.	Karlovac	37.7	34.2	35.7	34.6	31.3	31.4	34.6
5.	Varaždin	75.6	77.7	77.7	70.4	58.8	64.6	71.0
6.	Koprivnica-Križevaci	34.8	33.0	31.9	32.2	32.1	32.5	34.3
7.	Bjelovar-Bilogora	24.7	24.2	27.9	25.5	23.9	21.0	24.5
8.	Primorje-Gorski Kotar	32.6	35.5	36.1	41.4	27.6	32.2	35.6
9.	Lika-Senj	2.3	2.6	4.1	2.7	2.1	3.0	2.8
10.	Virovitica-Podravina	28.8	31.1	31.1	29.3	21.3	21.7	26.6
11.	Požega-Slavonia	25.6	30.5	31.9	26.0	23.7	27.0	26.7
12.	**Brod-Posavina**	**21.5**	**23.0**	**28.6**	**30.1**	**25.0**	**22.7**	**23.5**
13.	Zadar	23.3	26.9	24.9	21.5	17.8	18.6	23.2
14.	Osijek-Baranja	39.0	38.5	32.4	29.0	23.1	26.3	33.6
15.	Šibenik-Knin	40.1	47.5	42.1	44.1	30.3	45.6	38.4
16.	Vukovar-Srijem	22.9	27.9	27.9	25.4	23.9	27.3	22.2
17.	Split-Dalmatia	44.2	47.8	48.0	48.1	30.2	35.6	44.0
18.	Istria	70.9	71.7	73.4	70.4	54.3	61.6	69.9
19.	Dubrovnik-Neretva	12.7	12.7	12.2	11.0	6.9	6.6	10.9
20.	Međimurje	54.6	57.0	64.8	60.0	51.3	56.7	57.0
21.	City of Zagreb	100.3	106.2	106.7	106.5	84.7	84.9	97.0
Total the Republic of Croatia		61.6	64.8	65.0	64.2	49.8	52.4	59.7

The average openness of the Republic of Croatia for the mentioned time period is 59,7%. The most opened counties in the period from 2005 to 2010 are the city of Zagreb (97,0%), Varaždin (71,0%), Istria (69,9%) and Sisak-Moslavina (60,7%) counties.

Out of 21 counties only here mentioned four counties have above-average level of openness compared to the level of openness of the Republic of Croatia. As it is seen from the table, the total level of openness of the Republic of Croatia was the lowest in the year 2009 with only 49.8%, and the highest in the year 2007 with 65,0%.

The level of openness of the Brod-Posavina County is 23,5%, what is 36,2 percent lower than average openness of the Republic of Croatia in the

year in question. The lowest level of openness has the Lika-Senj County (2,8%) and the Dubrovnik-Neretva County (10,9%).

The Brod-Posavina County had the highest level of openness in the year 2008 (30.1), which was the last pre-recession year as well. Due to the recession, the level of openness has significantly lowered during the last two years. Looking at the average level of openness in the period 2005 to 2010 for all counties of the Republic of Croatia, the highest level of openness has the city of Zagreb (97.0), while the Brod-Posavina County takes 17th place with 23,5.

This means that the level of openness in the Brod-Posavina County is four times lower than the level of openness of the city of Zagreb. Furthermore, the Brod-Posavina County has 2,5 times lower level of openness than the average level of openness for the Republic of Croatia.

5. Conclusion

The results of analysis of the Brod-Posavina County export in the period from 2008 to 2012 show a significant decrease of export (24,32%) in the 2009 recession year in relation to the year 2008. Decreasing trend has continued throughout years 2010 and 2011 and stopped in the year 2012 which marked a growth of openness in relation to the two previous years. However, the export in the year 2012 is still lower for 6,66% than it was in the year 2008. As it is expected, throughout all analyzed years the most export has been to the EU member countries.

The results of analysis of the Brod-Posavina County import in the period from 2008 to 2012 are similar to the results of the analysis of export. In accordance, the decrease of import has been marked for years 2009 and 2010 in relation to the year 2008. In following years 2011 and 2012 the increase of import has been marked in relation to the previous two years.

The import for the year 2012 is 18,44% higher than in the 2008 pre-recession year. The most of the imported goods come from the EU member countries, while other countries take a small portion of the import.

In years 2008, 2009 and 2010 the Brod-Posavina County export has been higher than the import regardless the recession that has started in the year 2009 and continued till today. The Brod-Posavina County level of openness has been the highest in the year 2008, and with the recession it started to decrease in year 2009 and 2010.

Looking at the average level of openness for the period from 2005 to 2010, the Brod-Posavina County takes 17th place in relation to other counties. This means that the Brod-Posavina County has four times lower level of openness than the county that takes the first place, and 2,5 times lower level of openness in relation to the average level of openness for the Republic of Croatia.

Taking into account the size, the number of residents and the level of development of the economy, the Brod-Posavina County foreign trade exchange showed signs of recovery in the year 2012 in relation to the previous three years, in which due to the recession and the decrease of economic activities there was a negative trend of export and import.

10. References

[1] R. M. Grant, „Contemporary strategy analysis“, 7th ed., Wiley & Sons, United Kingdom, 2010.
[2] J.B. Barney, „Strategic Management and Competitive Advantage“, 2nd ed., Pearson Prentice Hall, 2008.
[3] „Robna razmjena s inozemstvom“, the Croatina Chamber of Economy, Sector for international relations, Zagreb, 2013.
[4] „Robna razmjena s inozemstvom“,the Croatina Chamber of Economy, Sector for international relations, Zagreb, 2013.
[5] „Statistika robne razmjene s inozemstvom Republike Hrvatske“, the Central Bureau of Statistics, [Online]. Available: http://www.dzs.hr/. [Accessed: 24-June-2013].

FRACTAL SHAPE IN FOUR DIMENSIONS

Maja Čuletić Čondrić[1*], Zlatko Pavić[2] and Mijat Jurišić[3]

[1]University of Applied Sciences of Slavonski Brod, Slavonski Brod, Croatia
[2]Mechanical Engineering Faculty in Slavonski Brod, J. J. Strossmayer University of Osijek, Croatia
[3]Student of University of Applied Sciences of Slavonski Brod, Slavonski Brod, Croatia
Corresponding author e-mail: Maja.CuleticCondric@vusb.hr

Abstract
In this paper we introduced the concept of fractals and fractal dimensions as well as their methods of computation in classical examples of fractals. Emphasis will be placed on a special form of fractal in space and the method using the resulting analog formats will be explained. One will stress the importance of area, the volume of fractals and the mathematical expressions obtained using real data. When designing fractal geometry, it is necessary to know the basis and the motive. If each base line replaces shape motives and that process continues to infinity, the result is a fractal. One can say that fractals are a set of points that have 3 important characteristics: self similarity, fractal dimension and the formation by iteration.
In this paper, comparison will be made between a known figures in the plane and in space. The various analogies we get to the figures in the fourth dimension, its area and volume.

Keywords:
fractal geometry, self similarity, simplex, pentachoron, four-dimensional space

1. Introduction

In mathematics, four-dimensional space ("4D") is an abstract concept derived by generalizing the rules of three-dimensional space. It has been studied by mathematicians and philosophers for over two centuries, both for its own interest and for the insights it offered into mathematics and related fields. Algebraically it is generated by applying the rules of vectors and coordinate geometry to a space with four dimensions. In particular a vector with four elements (a 4-tuple) can be used to represent a position in four-dimensional space. The space is a Euclidean space, so has a metric and norm, and so all directions are treated as the same: the additional dimension is indistinguishable from the other three.
In modern physics, space and time are unified in a four-dimensional Minkowski continuum called spacetime, whose metric treats the time dimension differently from the three spatial dimensions. Spacetime is thus not a Euclidean space.
A fractal is an object or quantity that displays self-similarity, in a somewhat technical sense, on all scales. The object need not exactly to exhibit the same structure at all scales, but the same "type" of structure must appear on all scales.

2. Simplex

In geometry, a simplex is a generalization of the notion of a triangle or tetrahedron to arbitrary dimension. Specifically, a *k*-simplex is a *k*-dimensional polytope which is the convex hull of its $k+1$ vertices. More formally, suppose the $k+1$ points $u_0,...,u_k \in R^k$ are affinely independent, which means $u_1-u_0,\ldots,u_k-u_0$ are linearly independent. Then, the simplex determined by them is the set of points

$$C=\left\{\theta_0 u_0+\ldots+\theta_k u_k \mid \theta_i \geq 0, \sum_{i=0}^{k}\theta_i=1\right\} \qquad (1)$$

For example, a 2-simplex is a triangle, a 3-simplex is a tetrahedron, and a 4-simplex is a 5-cell. A single point may be considered a 0-simplex, and a line segment may be considered a 1-simplex. A simplex may be defined as the smallest convex set containing the given vertices [7].
A regular simplex is a simplex that is also a regular polytope. A regular *n*-simplex may be constructed from a regular (*n* − *1*)-simplex by connecting a new vertex to all original vertices by the common edge length. In topology and combinatorics, it is common to “glue together” simplices to form a simplicial complex. The associated combinatorial structure is called an abstract simplicial complex, in which context the word “simplex” simply means any finite set of vertices.
A simplex, sometimes called a hypertetrahedron (Buekenhout and Parker 1998), is the generalization of a tetrahedral region of space to *n* dimensions. The boundary of a *k*-simplex has $k+1$ 0-faces (polytope vertices), $\frac{k(k+1)}{2}$ 1-faces (polytope edges), and $\binom{k+1}{i+1}$ *i*-faces, where $\binom{n}{k}$ is a binomial coefficient. An *n*-dimensional simplex can be denoted using the

Schläfli symbol $\frac{\{3,\ldots,3\}}{n-1}$. The simplex is so-named because it represents the simplest possible polytope in any given space.
The content (i.e., hypervolume) of a simplex can be computed using the Cayley-Menger determinant.
In one dimension, the simplex is the line segment $[-1,1]$. In two dimensions, the simplex $\{3\}$ is the convex hull of the equilateral triangle. In three dimensions, the simplex $\{3,3\}$ is the convex hull of the tetrahedron. The simplex in four dimensions (the pentatope) is a regular tetrahedron ABCD in which a point E along the fourth dimension through the center of ABCD is chosen so that $EA = EB = EC = ED = AB$. The regular simplex in n dimensions with $n \geq 5$ is denoted α_n. If $p_0, p_1, \ldots, p_n$ are $n+1$ points in R^n such that $p_1 - p_0, \ldots, p_n - p_0$ are linearly independent, then the convex hull of these points is an *n*-simplex.

Figure 1. 0-simplex and 1-simplex

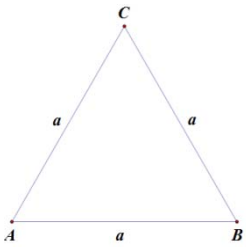

Figure 2. 2-simplex or triangle

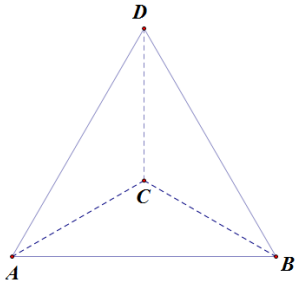

Figure 3. 3-simplex or tetrahedron

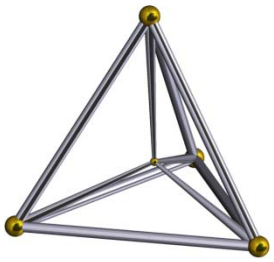

Figure 4. 4-simplex or pentatope

3. Fractals in plane and space

A fractal is an object or quantity that displays self-similarity, in a somewhat technical sense, on all scales. The object need not exactly to exhibit the same structure at all scales, but the same "type" of structure must appear on all scales. The fractal dimension is strictly greater than topological [1].
Koch's curve is based on length iteration, Koch's snowflake on triangle iteration.
Figure 5 and 6 show and describe the process of creating the above mentioned set of fractals [5].

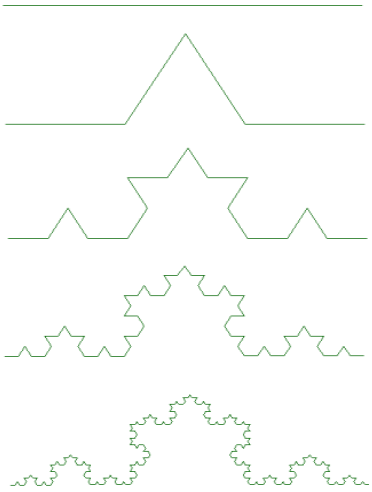

Figure 5. The construction of Koch's curve

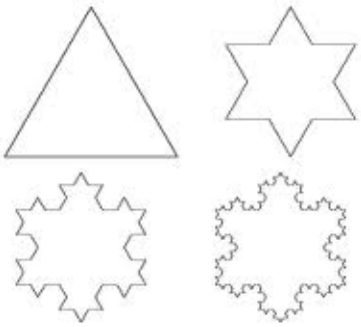

Figure 6. The construction of Koch's snowflake

The interesting thing about Koch's snowflake is its perimeter that gets bigger after each iteration thus growing into infinity.
Formulas for perimeter *n*-th geometrical object is:

$$O_n = 3 \cdot 4^{n-1} \cdot \frac{1}{3^{n-1}} = 3 \cdot \left(\frac{4}{3}\right)^{n-1} \quad (2)$$

A sequence O_n is divergent because it is a geometrical sequence with a quotient $\varepsilon = \frac{4}{3} > 1$.
This means that the perimeter of geometrical objects $K_1, K_{2,} \ldots, K_n$ grows indefinitely when $n \to \infty$.
Thus, Koch's curve is a curve of an indefinite perimeter.

The area of the n-th geometrical object is:

$$P_n = P_{n-1} + 3 \cdot 4^{n-2} \cdot \frac{1}{9^{n-1}} \cdot \frac{\sqrt{3}}{4} = \\ = \frac{\sqrt{3}}{4} + \frac{3\sqrt{3}}{20}\left[1 - \left(\frac{4}{9}\right)^{n-1}\right] \quad (3)$$

A sequence (P_n) is convergent and has a limit:

$$P = \lim_{n \to \infty} P_n = \frac{\sqrt{3}}{4} + \frac{3\sqrt{3}}{20} = \frac{2\sqrt{3}}{5} \quad (4)$$

The area of geometrical objects $K_1, K_{2,} \ldots, K_n$ converges towards a number when $n \to \infty$.
According to that, the snowflake is a closed curve that closes a definite area [4].
In a previous paper for a TEAM2012 the tetrahedron is very interesting for us. The tetrehedron is a regular polyhedron that has 4 vertices, 6 edges and 4 sides (equilateral triangles). A pyramid with three sides having all edges of equal length is called a tetrahedron. The net of a tetrahedron has 4 equilateral triangles, one triangle representing the base and the other three triangles forming the sides of the tetrahedron.
Connecting plane and space, it is possible to come to an analogy.
An equilateral triangle in a plane has its analogue in space which is the tetrahedron.
In a plane perimeter and area are calculated, in space area and volume.
If the edge of a tetrahedron has length *a*, the formula for the area is:

$$A = 4 \cdot \frac{a^2\sqrt{3}}{4} = a^2\sqrt{3} \quad (5)$$

The formula for the volume of a pyramid is :

$$V = \frac{B \cdot h}{3} \quad (6)$$

Seen the fact that the studied tetrahedron is a threeside pyramid *B* is the area of the base i.e. the area of an equilatera triangle and *h* is the height of the tetrahedron.
After substituting and editing get a final expression for the volume of the tetrahedron:

$$V = \frac{\frac{a^2\sqrt{3}}{4} \cdot \frac{a\sqrt{6}}{3}}{3} = \frac{a^3\sqrt{2}}{12} \quad (7)$$

The volume of the tetrahedral body can be expressed by the geometric series with initial terms $\frac{\sqrt{2}}{12}a^3$ and ratio $\frac{3}{8}$:

$$V = \sum_{n=0}^{\infty} 3^n \cdot \frac{\sqrt{2}}{12}\left(\frac{a}{2^n}\right)^3 = \frac{2\sqrt{2}}{15}a^3 \quad (8)$$

The area of the tetrahedral body can be expressed by sum of the separated member $\frac{\sqrt{3}}{4}a^2$, and the geometric series with initial terms $\frac{9\sqrt{3}}{16}a^2$ and ratio $\frac{3}{4}$:

$$A = \frac{\sqrt{3}}{4}a^2 + \sum_{n=0}^{\infty} 3^n \cdot \frac{9\sqrt{3}}{16}\left(\frac{a}{2^n}\right)^2 = \frac{31\sqrt{3}}{16}a^2 \quad (9)$$

4. Pentatope

The pentatope is the simplest regular figure in four dimensions, representing the four-dimensional analog of the solid tetrahedron. It is also called the 5-cell, since it consists of five vertices, or pentachoron. The pentatope is the four-dimensional simplex, and can be viewed as a regular tetrahedron ABCD in which a point E along the fourth dimension through the center of ABCD is chosen so that $EA = EB = EC = ED = AB$. The pentatope has Schläfli symbol $\{3,3,3\}$. It is one of the six regular polychora.
The skeleton of the pentatope is isomorphic to the complete graph K_5, known as the pentatope graph [6].

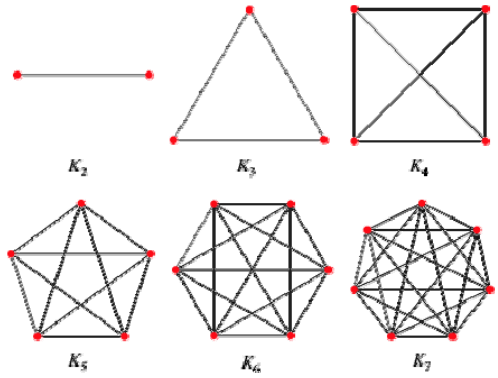

Figure 7. Complete Graph

The pentatope is self-dual, has five three-dimensional facets (each the shape of a tetrahedron), 10 ridges (faces), 10 edges, and 5 vertices. In the above figure, the pentatope is shown projected onto one of the four mutually perpendicular three-spaces within the four-space obtained by dropping one of the four vertex components.

A complete graph is a graph in which each pair of graph vertices is connected by an edge. The complete graph with *n* graph vertices is denoted K_n and has $\binom{n}{2}=\frac{n(n-1)}{2}$ (the triangular numbers) undirected edges, where $\binom{n}{k}$ is a binomial coefficient. In older literature, complete graphs are sometimes called universal graphs.

We use the 4-simplex (5 vertices) in R^4 with enge of the length *a.*

The volume of the 4-simplex body can be expressed by the geometric series with initial terms $\frac{\sqrt{5}}{96}a^4$ and ratio $\frac{1}{4}$:

$$V=\frac{\sqrt{5}}{96}a^4+4\cdot\frac{\sqrt{5}}{96}\left(\frac{a}{2}\right)^4+4\cdot\frac{\sqrt{5}}{96}\left(\frac{a}{2^2}\right)^4+\ldots$$
$$=\sum_{n=0}^{\infty}4^n\cdot\frac{\sqrt{5}}{96}\left(\frac{a}{2^n}\right)^4=\frac{\sqrt{5}}{96}a^4\sum_{n=0}^{\infty}\left(\frac{1}{4}\right)^n \qquad (10)$$
$$=\frac{\sqrt{5}}{96}a^4\cdot\frac{4}{3}=\frac{\sqrt{5}}{72}a^4$$

The volume of all 3-faces of the observed body can be expressed by the sume of the separated member $\frac{\sqrt{2}}{12}a^3$, and the geometric series with initial $\frac{\sqrt{2}}{6}a^3$ and ratio $\frac{1}{2}$:

$$A=\frac{\sqrt{2}}{12}a^3+\frac{\sqrt{2}}{6}a^3+4\cdot\frac{\sqrt{2}}{6}\left(\frac{a}{2}\right)^3+4^2\cdot\frac{\sqrt{2}}{6}\left(\frac{a}{2^2}\right)^3+\ldots$$
$$=\frac{\sqrt{2}}{12}a^3+\sum_{n=0}^{\infty}4^n\cdot\frac{\sqrt{2}}{6}\left(\frac{a}{2^n}\right)^3= \qquad (11)$$
$$=\frac{\sqrt{2}}{12}a^3+\frac{\sqrt{2}}{6}a^3\sum_{n=0}^{\infty}\left(\frac{1}{2}\right)^n$$
$$=\frac{\sqrt{2}}{12}a^3+\frac{\sqrt{2}}{6}a^3\cdot 2=\frac{5\sqrt{2}}{12}a^3$$

5. Conclusion

The results obtained by iteration and geometric construction shows that the basis and motive given shape divided into infinity. Koch's snowflake in a simple way to demonstrate one of the known properties of fractals. Infinitely long boundary encloses the final area. Tetrahedron and pentatope followed by analogy. The body that has a finite volume and finite area. On this basis, we conclude that using virtual reality finds that humans in spite of living in a three-dimensional world can without special practice make spatial judgments based on the length of, and angle between, line segments embedded in four-dimensional space.

The geometry of four-dimensional space is much more complex than that of three-dimensional space, due to the extra degree of freedom.

The purpose of this is to present heuristics or ars inveniendi, which is important in mathematics, and not only in mathematics.

6. References

[1] K. Falconer: Fractal Geometry, Wiley, 1990.

[2] M.J. Donahue, An Introduction to Mathematical Chaos Theory and Fractal Geometry, Duke University, 1997.

[3] V. Županović, D. Žubrinić, Fractal Dimension in Dynamics, University of Zagreb

[4] M. Paušić: Uvod u fraktale, Sveučilište u Zagrebu, Fakultet elektrotehnike i računarstva, Zagreb, 2004.

[5] Z.Bujanović: Matka, časopis za mlade matematičare, br.35, Zagreb, 2001.

[6] http://mathworld.wolfram.com

[7] http://en.wikipedia.org/wiki/Main_Page

ANALYSIS AND TESTING OF WATERJET ABRASIVE RECYCLEABILITY

Miroslav Duspara[1*], Tomislav Palatinuš[1*], Marija Stoić[2], Davorin Kramar[3], Antun Stoić[1]

[1]Mechanical Engineering Faculty in Slavonski Brod, J. J. Strossmayer University of Osijek, Croatia
[2]University of Applied Sciences of Slavonski Brod, Slavonski Brod, Croatia
[4]Faculty of Mechanical Engineerig, Ljubljana, Slovenia
* *Corresponding author e-mail: Miroslav.Duspara@sfsb.hr*

Abstract

Abrasive waterjet cutting is unconventional machining process which uses mixture of water and abrasive to cut material. There are, of course, pure waterjet cutting, without the addition of abrasives, but considering the characteristics of such a jet, it can be applied to soft materials, such as paper, plastics, rubber, wood, textiles, etc.
When we talk about the abrasive water jet, it is possible to cut a lot stiffer materials, because of the added abrasives. Used for cutting various kinds of metals, such as aluminum, steel, various alloy steels, copper, titanium, stainless steel and many others, while the non-metal can cut concrete, stone, granite and other materials.
It is often used for making machine parts, tools, and steel intended for heat treatment because the abrasive waterjet cutting does not heat the workpiece, as the water cools the material while cutting it.
When cutting with abrasive waterjet one of the biggest costs of the procedure is the cost of abrasives, so this paper explains the results of recycling of spent abrasives.

Keywords:
Abrasive, waterjet, recycling, garnet, reuse

1. Introduction

The aim of this paper is to present the results obtained experimentally recycling of spent abrasives Barton garnet. Calculations of the commercial viability of the procedure were made to companies Konid process parameters. Given the widespread use of the procedure abrasive water cutting, and consequently a large abrasive consumption, recycling the same not only brings economic benefits, but is also environmentally friendly, and greatly reduces the storage of large amounts of abrasives and returns it back to production.

2. Problem and goal

The goal of the experiment was to examine the possibility of recycling blast from the "sludge" that occurs after cutting abrasive waterjet. According to the assumptions companies Konid process within the sludge, there is a 50-80% unused and reusable abrasive. What creates the problem are the abrasive particles that are used when cutting. In contact with the material which they cut at high speed and pressure, they decay and burn up due to friction. They fall on the bottom of the machine in form of a fine powder, which has the possibility of clotting, with other similar particles, and that is what causes a problem with the reuse of sludge. If the sludge would be returned into cutting process, cutting would be possible, but due to clotting, nozzle would be blocked. Sludge also contains remnants of cut materials, such as metals, polymers, etc. In recycled abrasive remnants of cut materials are not harmful, as long as they don't block the nozzle, affect on the quality of the cut, or are outside of recycled abrasive dimensions.
Figure 1. shows why only a small part of the abrasive is being used. Since the nozzle has a circular opening, in contact with the material are just abrasive particles that are on the front edge of the circle so it is clear that the actual contact with the material has only a small percentage of abrasives.

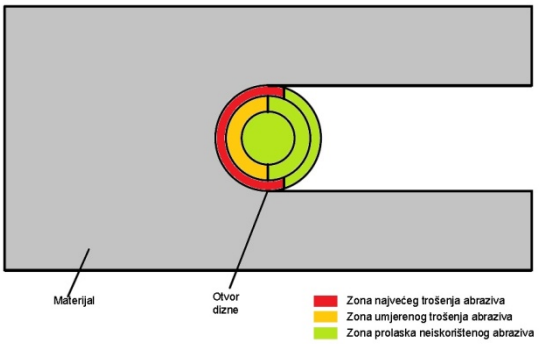

Figure 1. Abrasive usage zones

The experiment was created to remove the large remnants of cut materials, and then all of the used abrasive particles that can cause clogging of the nozzle. It also removes all unknown particles that do not correspond to abrasives granulation.

3. Microscopic analysis

In order to determine the difference of used and recycled blast at the microscopic level, was conducted microscopy samples, and compare the size and shape of grains.

The purpose of microscopic analysis was to determine the amount of spent abrasive in the sludge after a cut, and to determine the size and shape of the original grain abrasives in compare to recycled.

Figures 2. and 3. show us dry sludge, and it is obvious that the grains of unused abrasive are covered with more than 20% of white, spent abrasive grains, so the aim of the experiment the was to remove spent abrasive grains as much as it was possible.

Figure 2. Dry sludge

Figure 3. Dry sludge magnification 200X

Figures 4. and 5. show clotted used abrasive. Microscopy of this segment was conducted to determine whether there is enough usable abrasive in the clotted used abrasive to make recycling of this particle profitable. The assumption was that there is not enough usable abrasive, as it is obvious,grainis of usable abrasive are almost not visible, and microscopic analysis confirmed that about 90% of clotted used abrasive is unusuable.

Figure 4. Clotted used abrasive

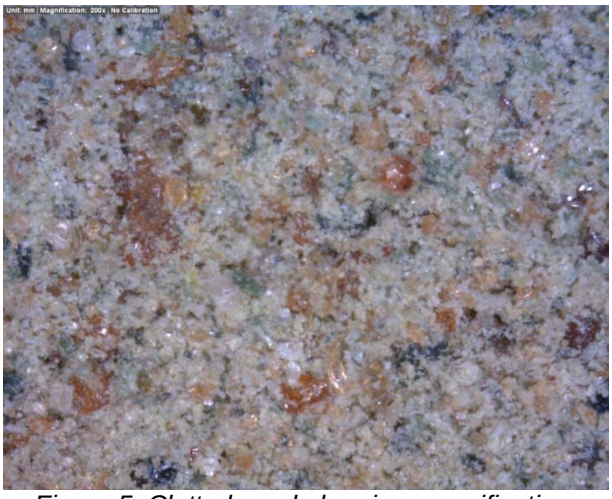

Figure 5. Clotted used abrasive magnification 200X

Figures 6. and 7. shows us recycled abrasive, grain shape and their average size. As can be seen in comparison with Figures 8. and 9., the share of small white grains of spent abrasive is invisible, which means that the recycled abrasive is almost identical to original by the presence of impurities.
Looking at the structure of the grain, it can also be concluded that the edges remained sharp, which is the main feature of abrasives. The only difference that occurred was in the grain size. While the original abrasive have an average grain size of about 300 micrometers, with the recycled value is about 200 micrometers, from which we can conclude that after cutting abrasive grit decreased by one.

Figure 6. Recycled abrasive

Figure 7. Recycled abrasive magnification 200X

Figure 8. Original abrasive

Figure 9. Original abrasive magnification 200X

4. Ecological anaylisis

In Croatia there is no registered facility which would carry out the recycling of spent abrasives after water cut, which means that all the abrasive, being once used is thrown away. Considering there are no specialized landfills for this kind of material, method and type of disposal depends on the companies. Such a system would greatly reduce the uncontrolled disposal of used abrasives, which would have a positive environmental impact. The amount of environmentally harmful polymers, metals and non-metals also depends on companies and if they are disposed of together with used abrasive can have very harmful effects on the environment, so this solution is not only desirable but necessary.
In Croatia, there are about 20 waterjet machines. Using Konid process data on a minimum monthly consumption of 1.5 t abrasives, and multiplying it with the number of machines in Croatia comes to the amount of at least 30t of used abrasive thrown monthly. With accurate data for each company, this amount could be doubled. On an annual basis it is at least 360t. Taking into account the data obtained from experiments on rudimentary recycling of 75%, it is concluded that in Croatia is yearly thrown about 270t of reusable abrasive, and about 90t of used abrasive and remnants of cut materials.
Further analysis would be desirable to examine the properties of the used abrasive, and to examine the possibility of its use for other purposes, such as building, and get a hundred percent recyclable abrasives.

5. Economical analysis

Cost-effectiveness of this procedure is extremely high. For calculations is also used number of 20 machines. There are three main factors in the abrasive water jet cutting, such as electricity, water

and abrasive. Calculation of these factors gets the share price of abrasives in the total consumption during cutting.
Waterjet machines use around 25kWh of electrical energy, 240 l/h of water, and around 30 kg/h of abrasive. Recalculated, that would be 2,5kn for water, 17,5kn for electricity and 90kn for abrasive. During the experiment, it was used around 25 kWh of electrical energy and around 250l of water to get 40kg of recycled abrasive, so the cost of recycling 40kg of abrasive is around 40kn. Same amount of original abrasive costs around 120kn.
Figures 10. and 11. shows percentage of costs in waterjet machining using mentioned factors.

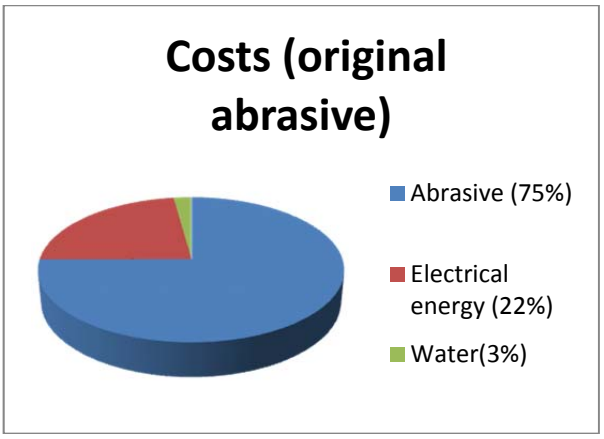

Figure 10. Costs of cutting using original abrasive per hour

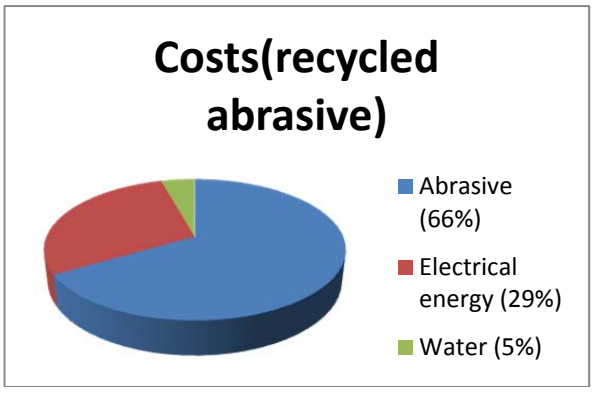

Figure 11. Costs of cutting using recycled abrasive per hour

This analysis gives a clear picture of the profitability of recycling of abrasives. When such a procedure is carried out in the framework of a recycling plant, it would also be cost-effective to separate remains of cutted material, and sell it as raw material. Calculations were made with worst possible numbers, so there is huge space for improvement.

6. Conclusion

Waterjet industry is growing industry. Thereby grows and abrasive producing industry, although at this level it is still "young" industry which is probably main reason to the lack of recycling plant or machinery. Given that fact, it is concluded that it is an ideal time to introduce the recycling of used abrasives. Not only because of the increasing use of machines for abrasive water cutting, but also to preserve the environment and reduce exploitation of precious ore. Furthermore, recycled abrasive can significantly reduce the price of products made by waterjet cutting. Therefore, there is considerable scope for increasing the competitiveness of this type of treatment and the increasing use both in Croatia and in the world. Recycling on the way that is shown in this paper, would allow the smaller companies consumption of recycled abrasives. Due to the growing need to preserve the environment, this procedure should be used to improve solve the disposal of used abrasive, and also to make a profit.

Acknowledgement

Authors would like to thank Company Konid proces from Zagreb and its director Davor Filjas, for their unweaving support in the experimental part of the work.

7. References

[1] T. Palatinuš: Analysis and testing of waterjet abrasive reciclability, Final thesis for first Bologna cycle Mechanical engineering faculty
[2] Hloch, Sergej; Valiček, Jan; Stoić, Antun; Kozak, Dražan; Samardžić, Ivan; Novak - Marcinčin, Jozef; Modrak, Vladimir: *Rezanje mlazom vode*, Strojarski fakultet u Slavonskom Brodu Sveučilišta J.J. Strossmayera u Osijeku, 2011.

PRE-BANKRUPTCY SETTLEMENT IN CROATIA

M. Stanić[1*],S.Knežević[1] and M. Stanić[2]

[1]College of Slavonski Brod, Slavonski Brod Osijek, Croatia
[2] Faculty of Economics in Osijek, Osijek, Croatia
Corresponding authore-mail: Milan.Stanic@vusb.hr

Abstract
Pre-bankruptcy settlement has lately become one of the solutions for enterprises who can't pay out their debt. However many small business owners still refuses to initiate pre-bankruptcy settlement although they are obliged to that. Noncompliance with an obligation to initiate the proceedings exposes a debtor to misdemeanor fines. Those who can but who are not obliged to initiate procedure are enterprises that have no employees and those whose assets are low or with low value. Enterprises refuse to initiate procedure because of insecurity, where they cannot be sure about an amount of debt. After adoption of decision for opening of the procedure creditors are called to name their claims towards debtor. Those claims can be much higher than the debtor had reported (interests, penalties, foreclosure etc.)

Keywords:
Pre-bankruptcy settlement, creditors, debtor, Croatia.

1. Introduction

Pre-bankruptcy settlement procedure was assumed to be more flexible and more effective than standard bankruptcy. Main aim of the procedure is to provide continuous business for enterprises with financial distress, with expectations that debt will be paid from future incomes. As opposed to that bankruptcy usually leads to sell-of debtor's assets which are in most cases insufficient to pay off all creditors. Creditor's consideration should be given to terms of settlement and restructuring plan because they provide terms and deadlines for future debt pay off. The pre-bankruptcy settlement procedure is a procedure conducted to retrieve liquidity and solvency for debtor, the Act also regulate obligation to start procedure.

2. The Act

Pre-bankruptcy settlement is defined within the Act on Financing and Pre-bankruptcy Settlement (The Act) which entered into force in 1 October 2012 and within Act on Amendments to the Act on Financing and Pre-bankruptcy Settlement in 30 June 2013.

3. Pre-bankruptcy settlement procedure

Pre-bankruptcy settlement procedure can be conducted over legal entity, sole trader and artisan. Procedure can be initiated only by debtor's Proposal for initiation of the procedure. Under the Act, companies are required to initiate settlement procedure when:

- within 60 days cannot establish condition of liquidity with financial restructuring outside from pre-bankruptcy settlement
- is late more than 30 days in respect of its payroll obligations

There are two types of procedure:

- Summary pre-bankruptcy procedure (amount of claims is not higher than 2.000.000,00 Kuna's, and debtor employs less than 30 employees. Those two conditions must be cumulatively fulfilled)
- Standard pre-bankruptcy procedure (every case in which previously two conditions for initiation summary procedure are not fulfilled)

Pre-bankruptcy procedure is intended to be quick and under the jurisdiction of the Settlement Council should be completed within 120 days, unless Advisory council approves extension of deadline for procedure's closer for at most 90 more days. Summary procedure must be completed within 100 days from procedure opening. The proposal for initiation of the procedure shall be transferred to Financial agency by direct delivery or by mail. On web page of Financial agency can be found initiation form. The proposal for initiation of the procedure may also be submitted in an incomplete form, but debtor will be summoned to supplement the documentation necessary for a decision on the opening of procedure. In case debtor fails to supplement required documentation on time, council will reject the request to open procedure, and Financial agency will ex officio initiate bankruptcy procedure. Pre-bankruptcy settlement cannot be carried over financial institutions, credit unions, investment funds, credit institutions, insurance and reinsurance companies, leasing companies, institution for payment and electronic money institutions. Procedure, also, cannot be carried over Republic of Croatia, fund financed by Croatian Government budget, pension and disability funds, Croatian Institute for Health Insurance, Croatian Institute for Pension Insurance and local and regional governments. Pre-bankruptcy settlement cannot be carried also over debtor against who is already opened bankruptcy

procedure, unless if bankruptcy procedure over debtor is initiated before The Act became valid, but only if the bankruptcy procedure had not been open until Proposal for initiation of the Pre-bankruptcy procedure. If proposal for initiation bankruptcy procedure had been open before The Act was brought debtor is allowed to propose initiation of the Pre-bankruptcy settlement. Decision suspending the bankruptcy procedure must be delivered to Financial agency in order to continue Pre-bankruptcy procedure. Pre-bankruptcy settlement is a procedure in which debtor will try to restore liquidity and solvency, without ceasing business and without changing person authorized to represent the debtor. If the settlement outcome in negative way and creditors do not agree with terms, Financial agency ex officio will initiate bankruptcy procedure, which will be aimed only toward complete liquidation and termination of the debtor and remove from the registry.

4. Authorities in procedure

Authorities in procedure are: Settlement Council and Pre-bankruptcy settlement Commissioner.
Settlement council has a formal role, their task is to: lead procedure, bring solutions and conclusions, publish decisions and other documents on Financial agency's website, submit a proposal to institute bankruptcy procedure against debtor, name Commissioner, give instructions to Commissioner and supervise his work. As it was already told Commissioner is named by Settlement council from bankruptcy trustee list. His tasks are: questioning the credibility of the documentation submitted by debtor, reviewing submitted claims, supervising debtor's financial business, notifying Council if debtor makes payments opposite to The Act, supervising payoff of costs of the procedure, supervising fulfillment of debtor's obligations towards creditors in contest of pre-bankruptcy settlement and performing other duties as requested by the presiding council.
When we speak about creditors, in order of deciding on a financial restructuring plan they are divided into three groups. One of the groups is consisted of public administrations and companies with majority state ownership. Second group is consisted from financial institutions and third group are other creditors. Creditors make decision by voting about the plan. They are allowed to vote in writing voting form which must be delivered to Settlement council, no later than beginning of hearing to vote. Creditors who's claims are determined have right to vote. Plan is considered accepted if is voted by creditors whose claims exceed half of value of established claims for each group of creditors, or if is voted by creditors whose claims exceed 2/3 of the value of all established claims.

5. METAL KOLOR d.o.o. company

Metal Kolor d.o.o is established in 21 August 1996. It was registered for activities: anticorrosive protection, metallization, construction, design and supervision.
Company suffered significant drop of income, increase of unpaid claims from clients, what led to company's inability to complete its financial obligations. Due to bank account blockade, company lost millions worth job, what was last hope that accumulated debt could be paid. As a result of blocked bank account longer than 60 days, company has submitted a request to initiate pre-bankruptcy settlement.
Calculation of lack of liquidity in the day 31 May 2013:

a) Due receivables 2.345.694,09
b) Due liabilities:
towards state 2.611.811,59
towards suppliers 1.323.501,65
towards banks 154.650,00
net wages 94.333,82
other liabilities 1.252.462,00

lack of liquid assets 3.091.054,97

Table 1. Profit and loss account [authors]

Year	2011	2012	2013
Operating income	13.651.788	7.278.726	202.604
Operating costs	13.289.986	6.225.225	248.838
Costs of materials	2.482.016	1.402.819	121.486
Other costs	1.449.619	1.036.210	123.186
Financial income	179.420	553	12
Financial costs	499.546	638.520	217.652
INCOME	13.831.208	7.279.279	202.616
COSTS	13.789.532	6.863.745	466.490
Income after taxation	41.676	415.534	
Loss			263.874
Tax	29.702	185.162	
Income of the period	11.974	230.372	

Table 2. Balance [authors]

Year	31.12.2011	31.12.2012	31.05.2013
ASSETS			
Long-term	164.215	151.600	151.600

Short-term	7.161.770	18.777.003	17.879.505
Receivables	1.139.255	3.187.014	2.345.694
TOTAL	7.289.092	18.928.603	18.031.105
LIABILITIES			
Capital	4.232.301	4.462.673	4.255.799
L.-term	599.608		
Financial inst.	147.737		
Other	451.871		
Short-term	2.557.183	5.486.637	5.436.748
Loan		154.650	154.650
Suppliers	2.172.122	1.302.150	1.323.501
Taxes	186.428	3.998.392	2.611.811
Wages	161,825	31.445	94.334
Deferred income		8.338.603	8.338.558
TOTAL	7.289.092	18.928.603	18,031.105

6. Financial restructuring description

Main duty for Debtor is to create financial restructuring plan. In Plan, company requests from Ministry of Finance to write-off liabilities for taxes and contributions in amount of 40% and to write-off interests. Besides that, company plans to settle 60% of the remaining obligations with interest of 4.5% per year in 60 monthly installments.

Also, for claims from suppliers and other creditors, for which they have writ of execution, company seeks to waive legal interests and their claims in the amount of 40%. Also they seek to achieve postponement of remaining debt for 4 years.

Main aims from this financial restructuring plan is to unblock bank accounts and to decrease of liabilities due which will allow company to continue business operation and from profit in next year settle all overdue debts. In addition, company started intense talks with potential partners about terms of joined market appearance, which will lead to employment of 30 people and maintaining of business operations.

As opposite, opening of bankruptcy procedure, would almost certainly result of company's inability to continue business operations. Also it could not add any new employees, every already started or planed job activity would had to be canceled. As a result it would lead to inability for creditors to settlement from current operations, but only from the assets of the company. which is not sufficient for the settlement of all company's liabilities. Therefore, company's management suggests opening of Pre-bankruptcy settlement.

In accordance with the plans of financial restructuring, company will in period from 2013 to 2017 achieve total profit of 22.450.000 Kuna.

In this period, total amount of net profit will be approximately 4.432.000,00 Kuna. This amount will be enough and will ensure company's ability to pay all its debts in time.

Debtor has made this plan in order to satisfy all creditors, or at least majority that is necessary for the plan to pass and for the settlement to be made. Figures must be inside of perimeters from The Act. Now, it is creditors part to decide whether will company survive with planned activities, or is company in problems so huge, that any kind of settlement could not help it. In other words, they have to decide is this plan bather for them than the Bankruptcy process.

Table 3. Calculation table 2013[authors]

Assets	31.05.	Restructuring effects	31.12.
Share Capital	24.000		24.000
Retained profit	4.495.673		4.495.673
Curent income	-263,874	2.075.105	1.811.231
Capital	4.255.799		6.330.904
Long-term liabilities		2.955.951	2.955.951
Short-term liabilities			
-loans	154.650		154.650
suppliers	1.323.501	(1.323.501)	-
-empl.	94.334		94.334
-taxes	2.611.811	(2.455.103)	156.708
-other	1.252.452	(1.252.452)	
Total short-term liabilities	5.436.748	-	405.692
Total Capital and liabilities	9.962.547	-	9.692.547

If creditors agree with plan it will mean cutting:

40 % of liabilities to Ministry of Finance to amount of 1.044.724 Kuna, 40 % of liabilities towards suppliers to amount of 529.400 Kuna, and 40% of others short-term liabilities to amount of 500.981 Kuna. The income from depreciation allocated amounts total 2.075.105 Kuna.

60% of taxes and contributions is transferred to long-term debt (payment in installments), amount of which is 1.410.379 Kuna. Also 60 % of debt toward suppliers is transferred to long-term debts amount of which is 794.101 Kuna. Same way, 60 % of other short-term liabilities will result in amount

of 751.471 Kuna. Total transfer towards long-term liabilities is 2.955.951Kuna.
After conducting of financial restructuring plan short-term liabilities is reduced for 5.031.056 Kuna and now it amounts 405.692 Kuna. This amount could be covered by receivables dues from customers.
It is evident that in case of conducting financial restructuring plan company will become solvent and will be able to continue business operations.
Dues to Tax Administration for taxes and contributions company is planning to pay in 60 monthly installments plus interest of 4.5 % per year. Those dues will be decreased for 40 % for taxes and contributions and 100 % for interests. Liabilities towards suppliers and other short-term liabilities will, after decrease of 40 %, be paid within four years. Unblocking of bank account is prerequisite for company's ability to pay late wages its employees and ability to provide necessary materials to continue business operations. In order to ensure proper production facility, company's management is in talks about potential association with company that owns proper facility, in order to prevent new loan and also to strengthen market position.

Table 4. Planed Balance sheet on 31 December 2017 [authors]

Year	2017
ASSETS	
LONG-TERM ASSETS	6.964.000
Land and buildings	5.313.000
equipment	1.500.000
Participating interests	151.000
SHORT-TERM ASSETS	1.900.000
Stocks	150.000
Receivables from customers	800.000
Cash	950.000
TOTAL ASSETS	8.864.000
LIABILITIES	
Capital	6.800.000
Share capital	24.000
Retained profit	6.776.000
Profit	864.000
LONG-TERM LIABILITIES	500.000
SHORT-TERM LIABILITIES	700.000
TOTAL ASSETS	8.864.000

7. Conclusion

Metal Color d.o.o. fell into the problems of illiquidity and insolvency, primarily because of inability to collect its receivables. After that came deep recession and deep crisis of construction sector in Croatia. With restructured obligations and continuing with business operations, company will rebuild its liquidity and solvency. This is logical conclusion from Pre-bankruptcy settlement plan and information, analysis and reports presented in this paper.
Despite the difficult business situation due to business cooperation contract already concluded, based on references about expected jobs, we are sure that with measures from financial restructuring plan there is a high perspective for continued business operations and opening new job places.
It is unquestionable that bankruptcy procedure would result with stop of business operations, and therefore no job places and termination o all already started or planed business operation. This scenario would lead to deletion from the register and sell-of of all assets with limited settlement towards creditors.

8. References

[1] Act on Financial Operations and Pre-Bankruptcy Settlement, Narodne novine d.d br. 108/12, 144/12, 81/13, 112/13.
[2] Bankruptcy Act, Narodne novine d.d. br 44/96. 29/99, 129/00, 123/03, 82/06, 116/10, 25/12, 133/12.
[3] Financial and Operating Restructuring Plan for Metal Kolor Company, Available: http://predstecajnenagodbe.fina.hr/pn-public-web/predmet/search [Accessed: 16-Sep-2013].

MEASUREMENT AND NUMERICAL SIMULATION OF HYDRAULIC HOSE EXPANSION

L. Hružík[1*], A. Bureček[1] and M. Vašina[1],

[1]Faculty of Mechanical Engineering, VŠB - Technical University of Ostrava, Czech Republic
* *Corresponding author e-mail: lumir.hruzik@vsb.cz*

Abstract
The paper deals with measurement and evaluation of volume expansion of hydraulic hoses. Modulus of elasticity of a hose is determined on basis of experimental measurement of oil volume change inside the investigated hose. The oil volume change after oil expansion for a given pressure and a concrete hydraulic hose is verified on numerical model using Matlab SimHydraulics software. Furthermore, time dependencies of pressure decreases in consequence of oil expansion from pipe and hose are measured and numerically simulated.

Keywords:
Hydraulic oil, hydraulic hose, bulk modulus, air bubbles.

1. Introduction

Hydraulic line is mainly created by pipe and hose in hydraulic systems. This line together with hydraulic oil creates a spring system. Total elasticity of the system has a negative influence on dynamic properties of hydraulic systems. For this reason it is necessary to take into account this undesirable effect in design of hydraulic systems. There are more frequently used preliminary mathematical simulations at the present time. The simulations make it possible to get a better idea of hydraulic system behaviour for designers. Furthermore, it is possible to eliminate system deficiencies in primary system design. Therefore it is necessary to investigate elasticity of hydraulic oil and hydraulic hoses. Wall deformation of a hydraulic hose depends on its structure [1]. The hose consists of inner tube, steel braids and outer layer. Its resultant elasticity is mainly influenced by a number of steel braids. Young´s modulus of elasticity is an important parameter of hydraulic hoses. The modulus is experimentally determined by static tensile testing [2]. The result of these destruction testing is the dependence of tensile stress σ on strain rate ε. The hose modulus of elasticity can be determined by another method, in the concrete by nondestructive pressure method. It is a big advantage of this method. For the reason the investigated hose can be subsequently used in hydraulic circuits.

2. Description of experimental equipment

The schematic diagram of the experimental equipment is shown in Fig. 1. The hydraulic pump HP is a pressure source of the system. The hydraulic aggregate consists of the check valve CV, the valve V, the relief valve RV, the manometer M, the tank T and the heater H too. The hydraulic system also consists of the steel pipe for oil bulk modulus measurement, the measured hose, the stop valves SV1 ÷ SV6, the measuring tube MT, the measuring points MP1 and MP2, the pressure sensors PS1 and PS2 and the measuring equipment M5050 (see Fig 1).

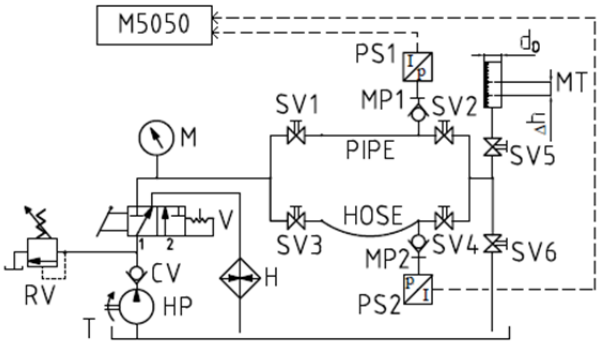

Figure 1. Schematic diagram of experimental equipment

Pipe and hose dimensions, that are necessary for calculation, are the following:

1. PIPE – length l_P = 1.6 m, outside diameter D_P = 0.03 m, inside diameter d_P = 0.022 m, wall thickness s_P = 0.004 m, Young´s modulus of elasticity $E_P = 2.1 \cdot 10^{11}$ Pa, Poisson ratio ν_P = 0.3.
2. HOSE – length l_H = 1.568 m, outside diameter D_H = 0.0234 m, inside diameter d_H = 0.016 m, wall thickness s_H = 0.0037 m, number of steel braids n = 2.
3. Measuring tube MT – inside diameter d_0 = 0.0098 m.

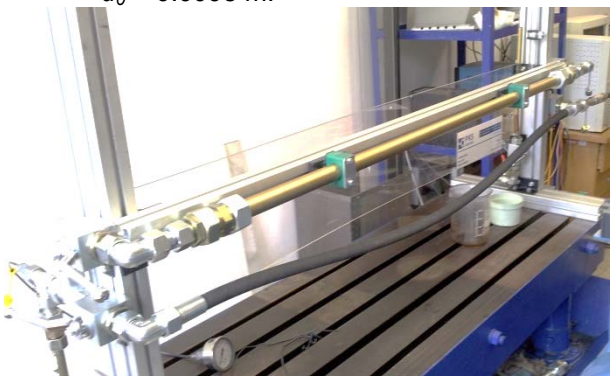

Figure 2. View of experimental circuit

The measurement of oil volume change during compression and subsequent oil expansion into the measuring tube MT was performed at first. Oil bulk modulus of elasticity K_O [3] was subsequently determined on basis of the following measuring procedure: The required oil pressure was adjusted by the relief valve RV. The valve V was adjusted to the position 2 and the valve SV2 was subsequently closed. The valve SV6 was closed after achieving of the pressure, which was adjusted by the relief valve RV. Furthermore, the valve SV5 was open. It was necessary to ensure sufficient amount of hydraulic oil in the measuring tube MT in order to measure the level difference Δh after oil expansion. In the next phase, the valve SV1 was closed and the valve SV2 was open. The working pressure was decreased to atmospheric pressure by the value Δp. The compressible oil flows into the tube MT. For this reason the oil level was increased by the value Δh. The same measuring procedure is also applied to determination of the modulus of elasticity of the investigated hose. In this case, the valves SV1 and SV2 are replaced by the valves SV3 and SV4.

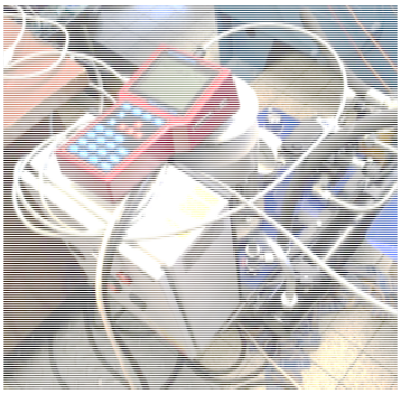

Figure 3. Measuring equipment M5050

3. Bulk modulus of system with oil and hydraulic hose

The capacity of oil/pipe system $C_{O,P}$ is given by the sum of the oil capacity C_O and the pipe capacity C_P:

$$C_{O,P} = C_O + C_P \tag{1}$$

The oil bulk modulus K_O is expressed by the formula [4]:

$$K_O = \frac{1}{\frac{\Delta V_{O,P}}{V_{O,P} \cdot \Delta p} - \frac{d_P}{E_P \cdot s_P}} \tag{2}$$

The capacity of oil/hose system $C_{O,H}$ is given by the sum of the oil capacity C_O and the hose capacity C_H:

$$C_{O,H} = C_O + C_H \tag{3}$$

The hose modulus of elasticity E_H is experimentally determined by the equation [4]:

$$E_H = \frac{1}{\left(\frac{\Delta V_{O,H}}{V_{O,H} \cdot \Delta p} - \frac{1}{K_O}\right) \cdot \frac{s_H}{d_H}} \tag{4}$$

The experimentally obtained values of the oil bulk modulus K_O and the hose modulus of elasticity E_H depending on the pressure gradient Δp are shown in Fig. 4 [5].

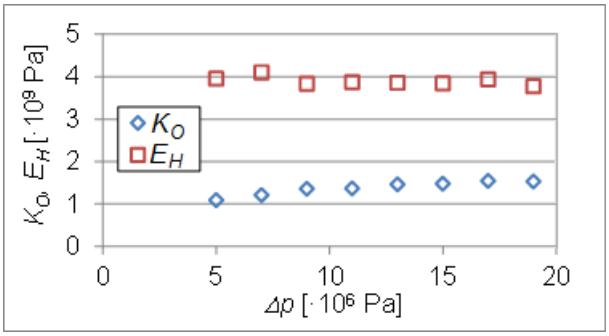

Figure 4. Dependence of oil bulk modulus and hose modulus of elasticity on pressure gradient

4. Mathematical model

The mathematical model (see Fig. 5) was created using Matlab SimHydraulics software [6].

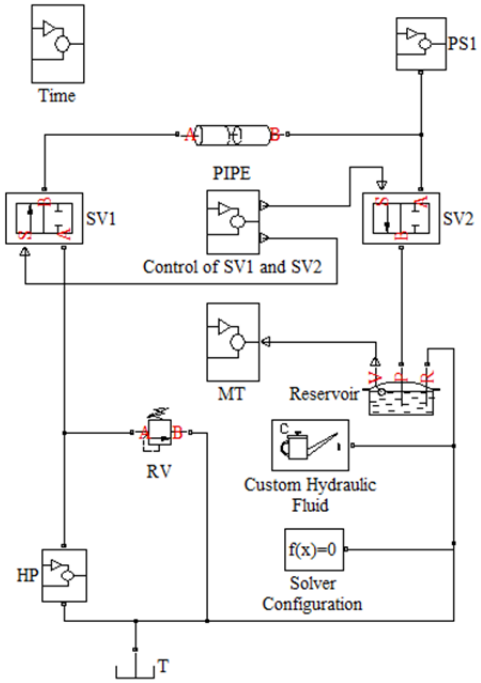

Figure 5. Mathematical model created in Matlab SimHydraulics software

The hydraulic pump HP is a pressure source. Oil flows through the stop valve SV1, the pipeline PIPE, the stop valve SV2 to the Reservoir. In the case of closing of the valve SV1 or the valve SV2, the oil flows through the relief valve RV. The circuit also consists of the blocks for valve control (i.e.

Control of SV1 and SV2), the block PS1 for pressure measurement, the solver block (i.e. Solver Configuration) and the block for liquid definition (i.e. Custom Hydraulic Fluid). The block Time was used in order to adjustment of the scanning time interval Δt = 0.001 s as in the case of experimental measurements. The pipeline PIPE was simulated as a segment pipeline [7].

5. Simulation of oil expansion in pipe

The expansion of compressed hydraulic oil in the pipeline PIPE was simulated by means of the created mathematical model (see Fig. 5). It was possible to evaluate the oil volume increase $\Delta V_{O,P}$, which is flowing from the PIPE to the measuring tube (i.e. Reservoir + MT). The simulated volume increase is subsequently compared with the experimentally obtained value depending on the pressure gradient Δp.

The mathematical simulation consists in setting of required parameters, i.e. the pressure gradient Δp, the oil bulk modulus K_O (including influence of air bubbles) according to Fig. 4 and the steel pipe modulus of elasticity E_P. The pipe elasticity is described by the static pressure-diameter coefficient $K_{P,P}$, which is defined by the formula [7]:

$$K_{P,P} = \frac{d_P}{E_P} \cdot \left(\frac{D_P^2 + d_P^2}{D_P^2 - d_P^2} + \nu_P \right) \qquad (5)$$

There is an agreement between the measured and simulated oil volume increases during oil expansion from the pipe (see Fig. 6).

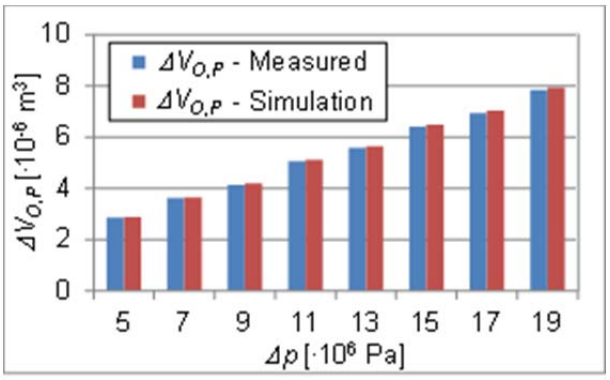

Figure 6. Comparison of simulation and experimental measurement of oil volume change $\Delta V_{O,P}$ after oil expansion depending on pressure gradient Δp

The pressure decrease during oil expansion depending on time was simulated and measured too. The measured time dependencies of the pressure p for the investigated pipe and hose are compared in Fig. 7. The green-labeled area (see Fig. 7) will be subsequently compared with the mathematical simulation. There are different pressure dependencies in defining of the oil bulk modulus in the case of homogenous liquid or polyphase mixture (i.e. oil with air bubbles) in this area. The bulk modulus K_O = 1.56·10^9 Pa of the homogenous liquid was defined including air bubbles influence. The polyphase oil/air bubbles mixture was defined by the oil bulk modulus K without air bubbles influence. Air content in oil was described by means of the volume fragment α. The bulk modulus $K_{O,PM}$ of the polyphase oil/air bubbles mixture depends on pressure as follows [7]:

$$K_{O,PM} = K \cdot \frac{1 + \alpha \cdot \left(\frac{p_a}{p_a + p} \right)^{1/n}}{1 + \alpha \cdot K \cdot \frac{{p_a}^{1/n}}{n \cdot (p_a + p)^{(n+1)/n}}} \qquad (6)$$

Where: K – oil bulk modulus without air bubbles (K = 1.79·10^9 Pa) [5], α – volume fragment of air bubbles content (α = 0.002) [5], n – polytropic coefficient, p – overpressure, p_a – atmospheric pressure.

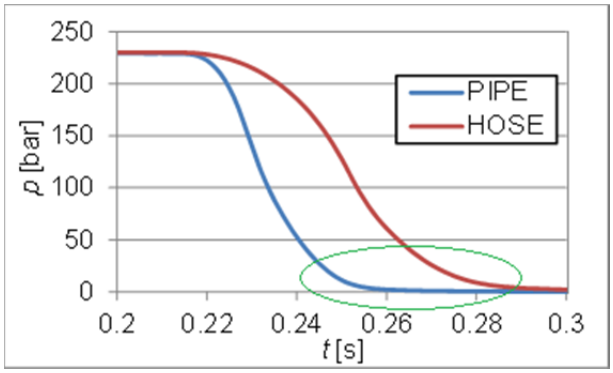

Figure 7. Measured time dependencies of pressure decrease during oil expansion from pipe and hose

Fig. 8 shows the experimentally obtained and simulated time dependencies of the pressure p during oil expansion from the pipe. It is evident that a better agreement is achieved in the case of the polyphase mixture (i.e. $K_{O,PM}$ - see Fig. 8). The volume of air bubbles is in general changed with the pressure in the model.

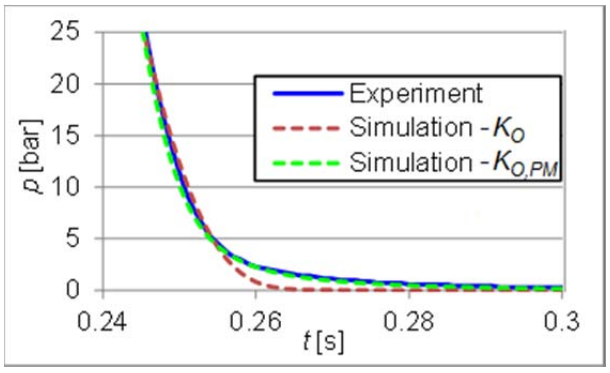

Figure 8. Time dependence of pressure decrease during oil expansion from pipe

6. Simulation of oil expansion in hose

This simulation was similarly performed as in chapter 5. Only the pipe was replaced by the hydraulic hose in this case. The mean value of the hose modulus of elasticity (i.e. E_H = 3.87·10^9 Pa) was determined from the experimentally measured values (see Fig. 4). The hose static pressure-diameter coefficient $K_{P,H}$ = 1.3·10^{-11} m·Pa^{-1} was calculated on basis of the hose modulus of elasticity E_H.

Fig. 9 demonstrates the comparison of the measured and the simulated oil volume increases $\Delta V_{O,H}$ after oil expansion from the hydraulic hose. For the simulation, the hose modulus of elasticity determined by two methods (i.e. during oil expansion from the hose and during oil compression in the hose) was used in this model. The modulus value $K_{P,HX}$ = 1.05·10^{-11} m·Pa^{-1} was calculated on basis of the experimentally determined value of the hose modulus of elasticity E_{HX} = 4.82·10^9 Pa by means of compression method [5, 8]. A bigger agreement between the experimental measurement and the numerical model is achieved using the static pressure-diameter coefficient $K_{P,HX}$ (corresponding to the volume increase $\Delta V_{O,HX}$), whose value was determined during oil compression in the hose.

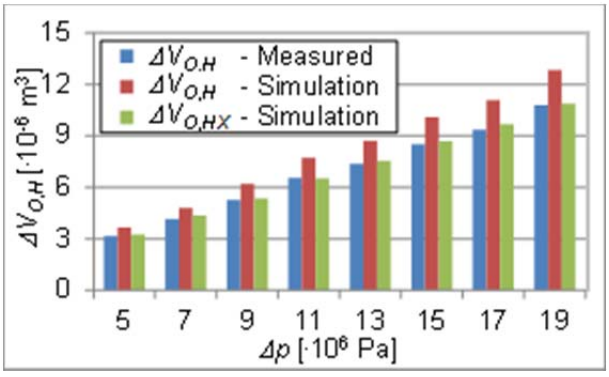

Figure 9. Comparison of simulated and measured values of oil volume change $\Delta V_{O,H}$ after oil expansion depending on pressure gradient Δp

Time dependencies of the pressure p were subsequently simulated for the investigated hose. They were compared with the experimental measurement (see Fig. 10).

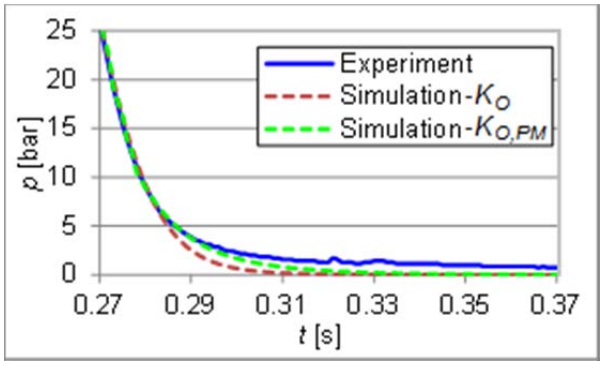

Figure 10. Time dependence of pressure decrease during oil expansion from hose

The oil bulk modulus was specified for the homogenous liquid and the polyphase mixture similarly as in the previous case (see chapter 5). A bigger agreement between the measured and simulated dependencies is achieved in the case of the supposed polyphase oil/air bubbles mixture (i.e. $K_{O,PM}$ - see Fig. 10).

7. Conclusion

The purpose of the paper was to describe the experimental equipment for determination of the oil bulk modulus and the hose modulus of elasticity. The mathematical model of the equipment was realized using Matlab SimHydraulics software. Oil volume increases after expansion of compressed oil in pipe and hose were simulated by the mathematical model. These oil volume increases were subsequently verified by experimental measurements. A better agreement in the case of the hose was obtained using the static pressure-diameter coefficient, which was determined by compression method. Furthermore, the measured and simulated pressure decreases during oil expansion from pipe and hose were compared in this work. Better results were achieved in case of the polyphase oil/air bubbles mixture.

8. References

[1] D. Lietze, “Requirements on the strength of rubber hoses assemblies for high pressure acetylene,” *Journal of hazardous materials*, no. 3, 1997.

[2] T. Štefić, A. Jurić, P. Marović, “Determination of modulus of elasticity for glass fibre reinforced polymers,” *Tehnički vjesnik – Technical Gazette*, no. 1, 2011.

[3] N. H. Scott, “An Area Modulus of Elasticity: Definition and Properties,” *Journal of Elasticity*, no. 3, 2000.

[4] L. Hružík, M. Vašina, “Nondestructive Testing for Experimental Determination of Elastic Modulus of Rubber Hoses,“ *Acta Hydraulica et Pneumatica 1*, p. 12-16, 2009.

[5] A. Bureček, “Fluid Structure Interaction in Case of Non-Stationary Flow,” *Doctoral thesis*, 2013.

[6] Y. A. Zhao, H. W. Du, Y. M. Li, X. Luo, G. Liu, “Impact of Low Hydraulic Pipeline upon Performance of Hydraulic Control System,” *Proceedings of International Conference of Mechatronics and Materials Processing*, p. 18-20, 2011.

[7] The MathWorks, Matlab Simulink User´s Guide, SimHydraulics User´s Guide, 2007.

[8] J. Kopáček, J. Šubert, “Objemový modul pružnosti pryžových hadic,“ *Strojírenská výroba 28,* no. 12, 1980.

CONTINUOUS IMPROVEMENT IN ENGINEERING EDUCATION: A CASE STUDY

M. E. Erdin[1*], C. Baykasoglu[1], and H. Aykul[1]

[1]Engineering Faculty, Mechanical Engineering Department, Hitit University, Turkey
* *Corresponding author e-mail: eminerdin@hitit.edu.tr*

Abstract
Increase in the number of educational institutions in engineering, growth of teaching staff and typical unrestrained education system dependent only to the supervisor academic member of the lecture lead to numerous efforts directed for the accreditation and quality standards searching of engineering programs in the world. In this study, the system established in Mechanical Engineering Department of Hitit University Engineering Faculty for the continuous improvement of the education quality and accreditation of the program is introduced, as a model to these efforts. System involves necessary regulations and improvements in a numerous fields from educational plan to infrastructure, corporation support and monetary resources to organization and decision making processes, etc. In the following years of actualization of continuous improvement system developed for the program, it is observed that there is a continuous improvement in the engineering education program outputs and major contribution in reaching determined program education objectives.

Keywords:
Engineering education, Quality, Accreditation, Continuous improvement

1. Introduction

Education is a cognitive effort which individuals conduct for detecting, understanding and supervising their environment solitarily or in groups [1]. Education is a production activity from this point of view. Education is an instrument for enlightenment and socialization as well as individualization. Higher education is an education and research activity which aims to manufacture production tools and raise professionals for realizing education phenomenon that will provide socialization of individuals. Quality standardization, equivalency and examination of quality and standards in engineering education is a usual subject at issue for many years in contemporary countries. As for international equivalency of engineering programs is a necessity which is imposed by globalization phenomenon, labor migration and transfer [2]. Analytical thinking ability, practical and good communication skills, creativity, leadership, entrepreneurship and innovativeness are particularly expected properties from an engineer [3, 4]. In addition to this, it is a noncontestable necessity that education programs of corporations which raise especially members of professions directly influential on human life and safety like engineering, etc. have to fulfil certain minimal requirements or standard quality properties.

Determining self-objectives of an engineering program in accordance with its mission, constituting education programs after appointing skills and qualifications, namely outputs, that its' graduates have to necessarily possess as part of these objectives, observing if determined objectives and assigned qualifications of the program are fulfilled with taking continuous feedback and carrying out necessary improvements on these basis constitute the principles of programs quality assurance. Quality assurance restructures and increases the productivity of an organization [5].

Output based education is gaining importance and most of the countries in the world are practicing this method [6]. In higher education, there is a common idea that raising qualified labor force is possible if a quality standard/assurance and continuous improvement model is provided and applied in every stage of education and all areas affecting education like physical and academic infrastructure, lecture plan, examination and evaluation system, human resources, research and publications, strategic planning, university-industry-society relations, etc.

In most of the countries in the world accreditation organizations continue their certification activities by taking ABET [7] (Accreditation Board for Engineering and Technology) as a model. Within them, a group of countries including USA, Australia, New Zealand, Republic of South Africa and England signed an agreement named Washington Accord [8] and acknowledge the other countries perfections given from local corporations in each country by accepting to nostrificate each other's accreditation systems. In Turkey, MUDEK [9] (Engineering Education Programs Evaluation and Accreditation Association) which is in the status of full member of Washington Accord since June 2011, is evaluating engineering education conducted in Turkish universities in undergraduate degree and accrediting related programs since 2003. MUDEK accreditation criteria are collected in main topics like students, education objectives,

program outputs, profession education, teaching staff, infrastructure, corporation support, monetary resources and discipline specific criteria (Figure 1).

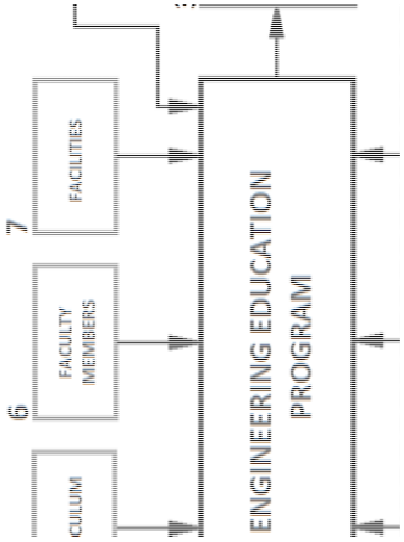

Figure 1. MUDEK Evaluation Criteria [9]

In this study, the system which is founded in 2011 for continuous improvement of the education quality and MUDEK accreditation process of the Mechanical Engineering Program of Hitit University Engineering Faculty is introduced. In general, system aims to provide 10 basic criteria and optimization of program outputs as a result. A continuous improvement is observed in the program outputs of Mechanical Engineering as a result of executing established system. This paper is organized as follows. Section 2 is devoted to continuous improvement system planning of the engineering education program and outputs of the quality system. Finally, results are presented in Section 3 and conclusion is made in Section 4.

2. Established continuous improvement system

Primarily, a quality system is constituted for managing undergraduate program continuous improvement studies healthfully that are conducted in our department. By means of activating this system where its short loop scheme can be seen in Figure 2 and long loop scheme can be seen in Figure 3, it is intended to carry the education activities in the department to a better level.

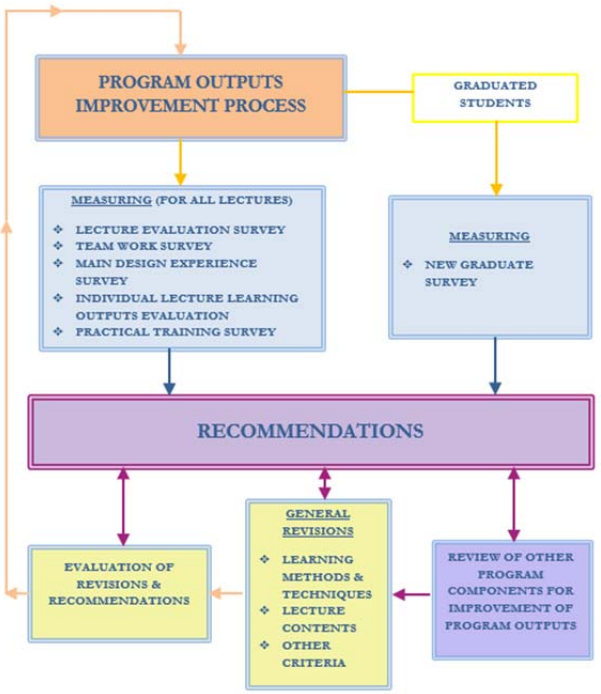

Figure 2. Short Loop Scheme of the Continuous Improvement System

These loops have cycle times of 1 semester/year in short term and 3 years in long term. The loops can be summarized as evaluation of activities conducted in the department via different tools on a regular basis, determining inadequacies, bringing forward improvement and solution proposals by arguing in different commissions, putting these proposals into practice and presenting evidences intended to improvement by tracking results. Improvements obtained from applied tangible precautions are tracked by evaluating surveys realized periodically in the quality and accreditation process.

Lecture efficiency measurement and evaluation survey, teamwork ability gaining survey, main design experience survey, instructor/assistant awareness and department evaluation surveys, supervisor evaluation survey, practical training surveys and lecture learning outputs evaluation of instructors are made in every semester/year involving all lectures in the short loop (Figure 2) with one year cycle time which is realized for measuring and improving program outputs. In addition, new graduate surveys are made every year for getting feedback from graduated engineers of the department. Afterwards, feasible revisions are argued and approved revisions are realized in lecture contents, learning methods/techniques and other criteria for improving program outputs in the light of obtained results.

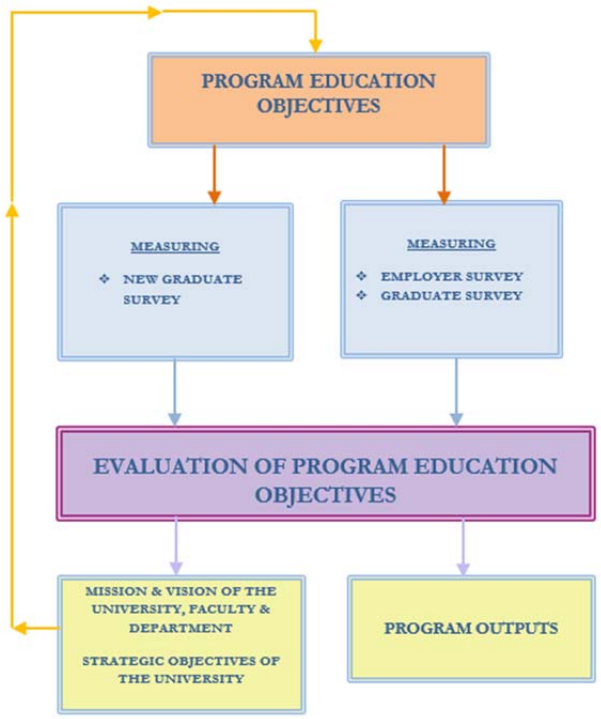

Figure 3. Long Loop Scheme of the Continuous Improvement System

Long loop (Figure 3) which has a cycle time of three years is executed for measuring achievement level of program education objectives. This loop includes long term evaluation of new graduate surveys and employer/graduate surveys. Program education objectives are reviewed and updated considering strategic objectives of the university and mission/vision of the university, faculty and department. In this context, subjects that are essential in realizing program education objectives are argued with the support of program outputs. All these processes are shared with the shareholders (students, department staff, graduates and sector representatives) in classes or special meetings.

In addition to department academic board, an advisory board which purveys members from all shareholder groups and various quality and accreditation work groups composed of department academic and related administrative staff are constituted for operating the system effectively. These work groups conduct their studies that are outlined in Figure 1-3 synonymously under the guidance of Department Quality and Accreditation Work Group. In summary, the continuous improvement system is carried out to increase the education quality in the department progressively.

3. Results

At the outset of the process, some critical alterations are realized according to the MUDEK Evaluation criteria such as revision of eight semester plan, documentation of lecture and examination files, etc. For example, lecture introduction forms are prepared for every lecture. Provided lecture learning and program outputs, teaching methods used in lectures and success measurement principles are specified in these forms. Lecture records are archived in Department Quality and Accreditation Archive Room in the end of every semester. These records include lecture introduction forms, lecture evaluation survey results and reports, answer keys, sample paper copies and statistics of exams, projects, homeworks, etc. and lecture statistics. These documents can be viewed by department shareholders. Various survey forms are used for measuring achievement level of all determined objectives. With the completion of loops, inadequacies of the education program are determined and solution offers are developed such as reconstitution of supervisory and practical training systems, specification of main design experience and team work ability principles, etc. as a result.

4. Conclusion

Today, quality concept is much more important than ever. It is also very important to provide evidence on quality of a product. Accreditation in education enables institutions to certify their education quality. At the same time, accreditation allows the continuous improvement of the quality, because it depends on a system which has to be evaluated periodically by an autonomous establishment. With the investigation of the system established in Mechanical Engineering Department, it is observed that there is a continuous improvement in the engineering education program outputs by comparing surveys made every semester/year periodically. Conducting such a system in an organization procures increase in the motivation of academic staff and all other shareholders.

5. Acknowledgement

Hitit University and Engineering Faculty administration are supporting quality and accreditation studies in every stage. Mechanical Engineering Department administration, academic staff and administrative staff are making a great effort in the process. The authors would like to appreciate all contributors.

6. References

[1] M. Talkhabi, A. Nouri, “Foundations of cognitive education: Issues and opportunities”, Procedia - Social and Behavioral Sciences, vol. 32, 385-390, 2012.
[2] J. A. Memon, R. E. Demirdöğen, B. S. Chowdhry, “Achievements, outcomes and proposal for global accreditation of

engineering education in developing countries", Procedia - Social and Behavioral Sciences, vol. 1, 2557-2561, 2009.
[3] M. M. N. Megat Johari, A. A. Abang Abdullah, M. R. Osman, M. S. Sapuan, N. Mariun, M. S. Jaafar, A. H. Ghazali, H. Omar, M. Y. Rosnah, "A New Engineering Education Model for Malaysia", International Journal of Engineering Education, 181, 11, 2002.
[4] S. Paramasivam, K. Muthusamy, "Study of Critical Success Factors in Engineering Education Curriculum Development Using Six-Sigma Methodology", Procedia - Social and Behavioral Sciences, vol. 56, 652-661, 2012.
[5] K. E. Torgersen, P. E. Torgersen, "Engineering education; The "P" word and continuous quality improvement", International Journal of Production Economics, vol. 52, 247-251, 1997.
[6] O. Akir, T. H. Eng, S. Malie, " Teaching and learning enhancement through outcome-based education structure and technology e-learning support", Procedia - Social and Behavioral Sciences, vol. 62, 87-92, 2012.
[7] http://www.abet.org/
[8] http://www.washingtonaccord.org/
[9] http://www.mudek.org.tr/

VIBRATION AND BUCKLING ANALYSIS OF STEEL FIBER REINFORCED ALUMINUM LAMINATED PLATES

A. Atmaca[1], C. Baykasoğlu[2*], M. E. Erdin[2] and H. Aykul[2]

[1]Vocational High School, Hitit University, Turkey
[2]Engineering Faculty, Mechanical Engineering Department, Hitit University, Turkey
* *Corresponding author e-mail: eminerdin@hitit.edu.tr*

Abstract
In this study, linear natural frequency and buckling load analysis of steel fiber reinforced aluminum laminated and isotropic aluminum plates are carried out by using the finite element method. Layers in the laminated plate $[0, \theta]_2$ are oriented in $[0, 15]_2$, $[0, 45]_2$, and $[0, 90]_2$ array. Free and clamped boundary conditions are taken into account in the analysis. The results show that the laminated composite plates have higher natural frequencies and buckling strength than isotropic aluminum plates in any ply orientation and ply orientation angle has influential effect on buckling loads. The results presented in this study could be useful for a better understanding of the mechanical behavior of fiber reinforced aluminum laminates and potentially beneficial for designers of these structures.

Keywords:
Composite Plates, Steel Fiber Reinforcement, Aluminum Matrix, Vibration, Buckling

1. Introduction

Metal matrix composites have been used in many applications for a long time due to their superior mechanical properties such as high ratio of stiffness to weight, fatigue life, corrosion and wear resistance [1, 3]. Fiber reinforced metal matrix composites combine the strength and rigidity of the fiber and ductility of the matrix [4-7]. In addition, compared with many fiber reinforced plastics, metal matrix composites are superior in their thermal performance [8, 9]. Aluminum matrix reinforced with steel fiber composites can be used in various components in automotive, aerospace and other industries.

The vibration and buckling of composite laminated plates are studied extensively in literature due to vibration and stability problems of these structures [3, 10-15]. The mode shapes of laminated plates have some specific characteristics that are different from isotropic plates due to high ratio of in-plane stiffness to transverse shear stiffness in laminated plates [16]. Computational tools such as finite element (FE) method are widely used in predicting mechanical behavior of laminated composites in literature [6, 10, 15]. Different scenarios can be easily applied by using FE method and optimum design of laminated composites can be achieved.

Mechanical properties of steel fiber reinforced aluminum laminated plates are already determined and elasto-plastic stress analysis are conducted in previous studies [7]. In this paper, linear natural frequency and buckling load characteristics of laminated plates which were manufactured in earlier studies [7] are examined. Different orientation angles and boundary conditions are considered in the analysis. The numerical model shows that the laminated composite plates have higher natural frequencies and buckling strength than isotropic aluminum plates in any ply orientations, the first vibration modes are prominently lower than the other ones and ply orientation angle has influential effect on buckling loads.

2. Structure of laminated plate and FE models

The steel fiber reinforced aluminum laminated plate mainly consists of three components: aluminum matrix, steel fiber and epoxy resin. Figure 1 and 2 show the arrangement of these components. Chemical composition and mechanical properties of these components can be found in [7].

Figure 1. Sample of manufactured composite plate [7]

A laminated square plate is considered in the analysis. The square composite plate models have the dimension of 50 × 50 × 3.2 mm (i.e., Figure 2) and have four plies of each with 0.8 mm thickness. Three different ply orientations are considered in the analysis: $[0, 15]_2$, $[0, 45]_2$ and $[0, 90]_2$. In numerical solutions, free (FFFF) and clamped (CCCC) boundary conditions are taken into account. For CCCC case, all the nodes on four edges are fully constrained. All models consisted of four-node quadrilateral shell elements with

reduced integration formulation in Abaqus. To obtain the best balanced accuracy and efficiency in numerical simulations, a standard convergence test is applied. Natural frequencies are computed in different mesh refinement levels and the acceptable mesh size is determined. Properties of the laminated plies are given in Table 1.

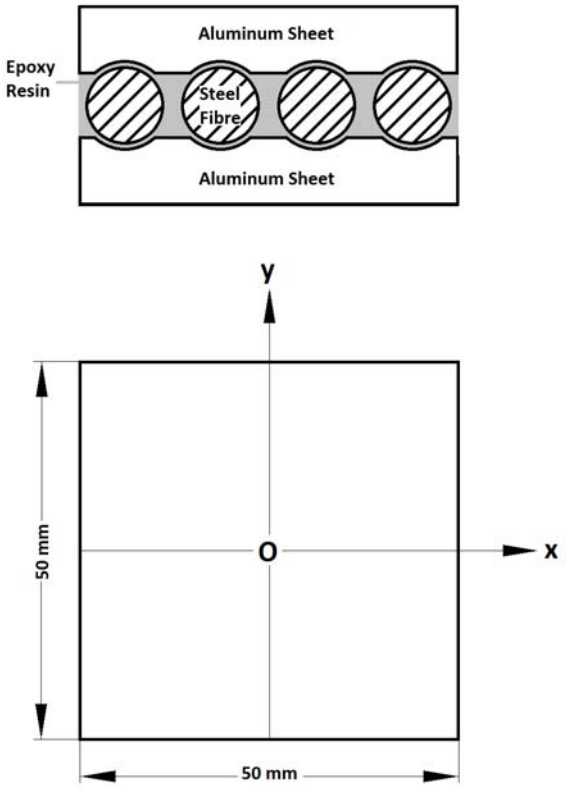

Figure 2. The components of composite plate

Table 1 Mechanic properties of laminate plies [7]

Property	X [MPa]	Y [MPa]	S [MPa]
Value	130	104	49
Property	ρ [kg/m^3)	v_{12} [-]	k [MPa]
Value	3550	0.33	2570
Property	E_1 [GPa]	E_2 [GPa]	G_{12} [GPa]
Value	110	87	41

Free undamped natural frequencies and corresponding mode shapes of the laminated plates can be obtained by solving the following eigenproblem

$$(\boldsymbol{K} - \omega_i^2 \boldsymbol{M})\boldsymbol{d} = \boldsymbol{0} \qquad (1)$$

where *K, M, d* and ω_i are the global stiffness matrix, global mass matrix, displacement vector and the natural frequencies, respectively. Similarly, critical buckling load and corresponding mode shapes are calculated by solving the following eigenproblem

$$(\boldsymbol{K}_0 - \lambda \overline{\boldsymbol{K}}_1)\boldsymbol{\psi} = 0 \qquad (2)$$

where K_0 is the global stiffness matrix, K_1 is the geometric stiffness matrix and ψ is the buckling-mode shape. The factor λ at which buckling occurs is designated as λ_{cr} and $P_{cr}=\lambda_{cr}P$ [17]. A frequency and buckling extraction procedure in Abaqus with Lanczos solver is used to determine the eigenvalues and mode shapes.

3. Computational results

Table 2 and 3 show the variations of the first three fundamental frequencies of steel fibers reinforced aluminum laminated plates oriented in $[0, 15]_2$, $[0, 45]_2$, $[0,90]_2$ and isotropic aluminum plates for FFFF and CCCC boundary conditions, respectively.

Table 2. First three fundamental frequencies of laminated and isotropic aluminum plates for FFFF boundary condition

	FFFF		
	Mode 1 (Hz)	Mode 2 (Hz)	Mode 3 (Hz)
$[0,15]_2$	4355	6198	7812
$[0,45]_2$	4296	6345	7764
$[0,90]_2$	4376	6277	7702
Aluminum	4051	6023	7612

Table 3. First three fundamental frequencies of laminated and isotropic aluminum plates for CCCC boundary condition

	CCCC		
	Mode 1 (Hz)	Mode 2 (Hz)	Mode 3 (Hz)
$[0,15]_2$	11147	21104	22759
$[0,45]_2$	11140	21450	22396
$[0,90]_2$	11118	21866	21866
Aluminum	10901	21529	21529

As seen from Table 2 and 3, the laminated composite plates have higher natural frequencies than isotropic aluminum plates as expected. The numerical model shows that the first vibration modes for every orientation are prominently lower than the other ones. In addition, orientation of plies hasn't got significant effect on vibrational frequencies. Figure 3 shows the first three vibration mode shapes of steel fiber reinforced aluminum laminated plates which oriented in $[0, 90]_2$ for FFFF and CCCC boundary conditions. The mode shapes of $[0, 15]_2$ and $[0, 45]_2$ laminated plates are also similar to those of $[0, 90]_2$ laminated plate that are not presented here for limited space.

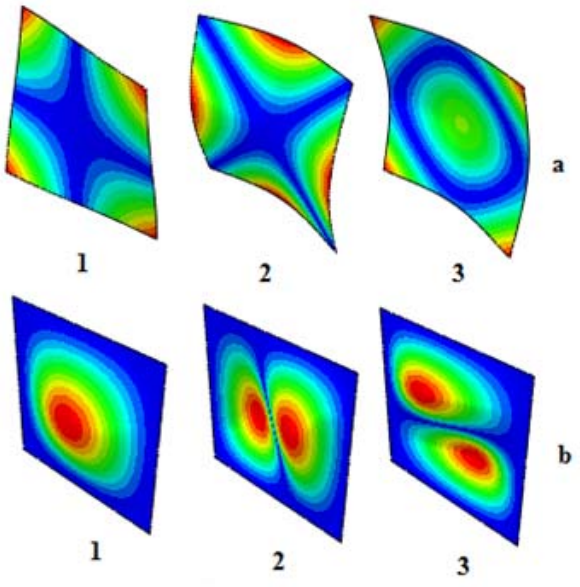

Figure 3. Vibrational mode shapes of $[0, 90]_2$ laminated plates: a) FFFF and b) CCCC boundary conditions

Table 4. First three critical buckling loads of laminated composite and isotropic aluminum plates

	Mode 1 (kN)	Mode 2 (kN)	Mode 3 (kN)
$[0,15]_2$	192.88	294.27	371.17
$[0,45]_2$	206.17	304.63	397.04
$[0,90]_2$	216.41	319.34	418.33
Aluminum	155.90	225.22	304.25

Table 4 shows the variation of first three critical buckling loads of steel fiber reinforced aluminum laminated plates which oriented in $[0, 15]_2$, $[0, 45]_2$, $[0, 90]_2$ and isotropic aluminum plates. In addition, Figures 4 shows first three buckling mode shapes of steel fiber reinforced aluminum laminated plates and isotropic aluminum plate. All the nodes on one edge are fully constrained, while the nodes on the opposite edge are only constrained in x and z directions and subjected to loads in buckling simulations. As seen from Table 4, the laminated composite plates have higher buckling strength than isotropic aluminum plates. Ply orientation angle has influential effect on buckling loads. Namely, $[0, 90]_2$ laminated plates buckling load is about 12 % higher than $[0, 15]_2$ laminated plates.

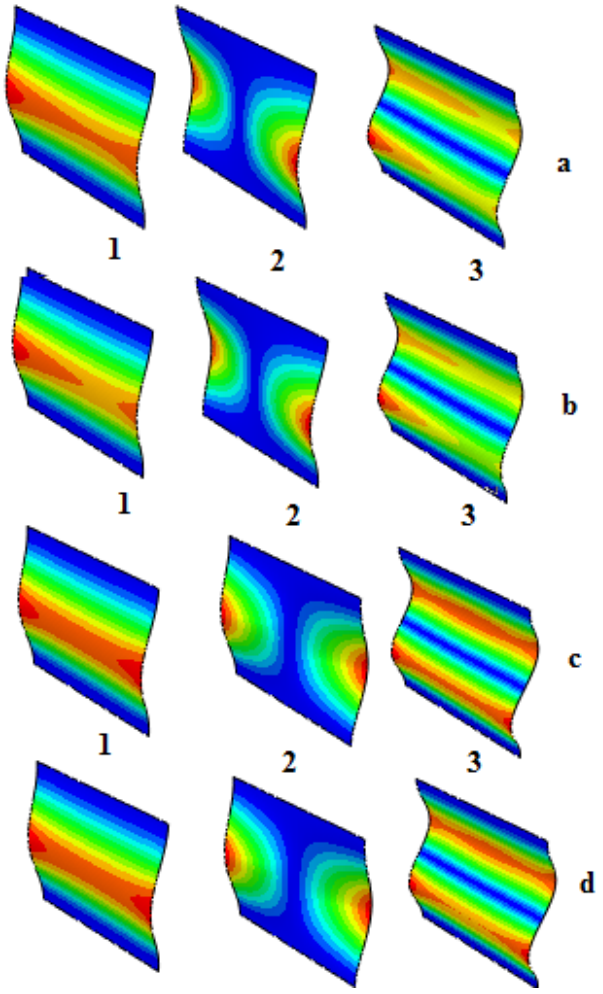

Figure 4. Buckling mode shapes of laminated and isotropic aluminum plates, a) $[0,15]_2$, b) $[0,45]_2$, c) $[0,90]_2$ and d) isotropic

4. Conclusion

In this paper, linear natural frequencies and buckling loads of steel fiber reinforced aluminum laminated plates are investigated by using the FE method. Layers in the laminated plate $[0, \theta]_2$ are oriented in $[0, 15]_2$, $[0, 45]_2$ and $[0, 90]_2$ are considered in the analysis. The results show that the laminated composite plates have higher natural frequencies and buckling strength than isotropic aluminum plates. Orientation of plies hasn't got significant effect on vibrational frequencies but has an important effect in buckling behavior. The results presented in this investigation could be

useful for a better understanding of the mechanical behavior of fiber reinforced aluminum laminates under different vibration and buckling load conditions. Thus, it will be beneficial for design of these structures. In future studies, we plan to investigate parametric analysis by using different thicknesses, dimensions and orientation angles with experimental validation.

5. References

[1] O. Sayman, S. Aksoy, "Elastic-plastic stress analysis of simply supported and clamped aluminum metal-matrix laminated plates with a hole", Composite Structure, vol. 53, 355-364, 2001.

[2] Y. Fu, J. Zhong, Y. Chen, "Thermal post buckling analysis of fiber-metal laminated plates including interfacial damage", Composites Part B: Engineering, vol. 56, 358-364, 2014.

[3] A. Shooshtari, S. A. Razavi, "Closed form solution for linear and nonlinear free vibrations of composite and fiber metal laminated rectangular plates", Composite Structures, vol. 92, 2663-2675, 2010.

[4] O. Sayman, "Elasto-plastic Stress Analysis in Stainless Steel Fiber Reinforced Aluminium Metal Matrix Laminated Plates Loaded Transversely", Composite Structures, vol. 43, 147-154, 1998.

[5] O. Sayman, H. Akbulut, C. Meriç, "Elasto-plastic Stress Analysis of Aluminium Metal Matrix Composite Laminated Plates under In-plane Loading", Computers & Structures, vol. 75 (1), 55-63, 2000.

[6] G. Alar, A. Ozel, S. Sen, R. Karakuzu, "Elastoplastic stress analysis of thick laminated metal-matrix composite plates by the finite-element method", Mechanics of Composite Materials, vol. 42 (4), 373-384, 2006.

[7] A. Atmaca, O. S. Türkbas, M. E. Erdin, H. Aykul, "Elasto-plastic Stress Analysis of Steel Fibre Reinforced Aluminum Metal Matrix Composite Plates", Journal of Manufacturing and Industrial Engineering, vol. 12, 12-16, 2013.

[8] C. Atas, O. Sayman, "Elastic-plastic stress analysis and expansion of plastic zone in clamped and simply supported aluminium metal matrix laminated plates", Composite Structures, vol. 49, 9-19, 2000.

[9] N. Arslan, M. O. Kaman, M. Duranay, "Elastic-Plastic Stress Analysis in Aluminum Metal-Matrix Composite-laminated Plates ($[0°/\theta°]_2$) Under Transverse Uniformly Distributed Load", Journal of Reinforced Plastics and Composites, vol. 23 (18), 2025-2045, 2004.

[10] B. G. Hu, M. A. Dokainish, W. M. Mansour, "Prediction of natural modes of laminated composite plates by a finite element technique", vol. 181 (5), 839-850, 1995.

[11] W. Zhen, Y. K. Cheung, S. H. Lo, C. Wanji, "Effects of higher-order global–local shear deformations on bending, vibration and buckling of multilayered plates", Composite Structures, vol. 82, 277-289, 2008.

[12] M. Cetkovic, D. J. Vuksanovic, "Bending, free vibrations and buckling of laminated composite and sandwich plates using a layerwise displacement model", Composite Structures, vol. 88, 219-227, 2009.

[13] W. Lanhe, L. Hua, W. Daobin, "Vibration analysis of generally laminated composite plates by the moving least squares differential quadrature method", Composite Structures, vol. 68, 319-330, 2005.

[14] S. Y. Kuo, L. C. Shiau, "Buckling and vibration of composite laminated plates with variable fiber spacing", Composite Structures, vol. 90 (2), 196-200, 2009.

[15] T. Ozben, "Analysis of critical buckling load of laminated composites plate with different boundary conditions using FEM and analytical methods", Computational Materials Science, vol. 45 (4) 1006-1015, 2009.

[16] Z. Wu, Y. K. Cheung, S. H. Lo, W. Chen, "Effects of higher-order global–local shear deformations on bending, vibration and buckling of multilayered plates", Composite Structures, vol. 82 (2), 277-289, 2008.

[17] T. J. R. Hughes, "The finite element method, linear static and dynamic finite element analysis", Prentice-Hall, 2000.

PROPERTIES OF THE COMPOSITE WITH THE PP MATRIX AND CELLULOSE FILLERS

J. Habr[1*], M. Borůvka[1], P. Lenfeld[1], L. Běhálek[1]

[1]*Technical University of Liberec, Department of Engineering Technology, Studentská 2, Liberec, 461 17*, Czech Republic
** jiri.habr@tul.cz*

Abstract
These days a rapid development of the applications pulls the automotive industry which by that creates continuous pressure for improving polymers and composite polymers utility properties. During the last years the polymers materials producers interest is focused on using natural materials which are thus from environmental and economical point of view major object of their interest. Nowadays it is possible to use natural material not only as composite matrixes (biopolymers) but also as fibres reinforcements thus substituting synthetic fibres. That is why this document is on research focused properties of the composite with the PP Matrix and Cellulose Fillers.

Keywords:
Composite, cellulose, PP matrix, mechanical properties

1. Introduction

These days a rapid development of the applications pulls the automotive industry which by that creates continuous pressure for improving polymers and composite polymers utility properties. During the last years the polymers materials producers interest is focused on using natural materials which are thus from environmental and economical point of view major object of their interest [1, 2]. Nowadays it is possible to use natural material not only as composite matrixes (biopolymers) but also as fibres reinforcements thus substituting synthetic fibres. Increasing interest about natural fibres is given mainly by their good mechanical properties, low density, biodegradability in the end of their life cycle and low production costs. These costs results mainly from the high power of the fibre plants and relatively low work in the countries where is possible to reap these plants several times per year. From the already mentioned factors results that price about getting natural fibres is three-times lower than for glass fibres, four-times lower than for aramid fibres and five-times lower than price for carbon fibre. With low price and easy accessibility of the natural fibres they can serve as a cheap and ecological addition to the reinforcing fibres which are used in the composites up to date [3]. Production development of the composite materials with the lingocellulose filler will be intended for using at problem mainly connected with the environmental protection. First of all it is about hazards with the waste accumulation from the plastic materials. To prevent these hazards will composite materials contain natural reinforcing components of the plant origin and biodegradable polymers obtained from the renewable resources. These materials (sometimes called as a “green composite”) fulfill requirements for the biodegradability after using in such manner not to be harmful for environment. Green composite can be used effectively in many applications with the short life cycles or for products designed for single-use or short-term use. Biodegradable matrixes can be made e.g. from the polysaccharide (starch, cellulose, chitin), proteins (casein, albumin, phytogen, silk) or polyesters (polyhydroxyalkanoates). To produce highly strength green composites is used e.g. cellulose fibres spinning by means of the fluid crystals. There is used cellulose dissolubility by phosphorous acid. Method is similar to the aramid fibres production as e.g. Kevlar is so by electrospinning. As a result there is material with the fluid crystal properties with cellulose chains oriented in the fibre direction. It was already measured that ultimate strength of these fibres varies about 1700 MPa which is as far the highest force (stress) measured for cellulose based fibres [4].

Plant fibres

Plant fibres are actually composite material which is designed by nature itself. Such fibres are reinforced by spire arranged cellulose microfibrils which are connected by amorphous lignin matrixes. Lignin keeps water in the fibres, acts as protection against biological attack on plant and also as a reinforcement which provides footstalk its good resistance against gravitational forces and wind. Hemicellulose contains in natural fibres acts as compatibilizer between cellulose and lignin. Most of the plant fibres consist of the cellulose, hemicellulose, lignin, wax and several different water soluble compounds. Cellulose, hemicellulose and lignin have the greatest portion. Natural fibres tensile ultimate strength depends on the sample testing length and plays a crucial role for effective reinforcement by polymer. By cotton fibres testing was proved that their ultimate strength heavily depends on their length. On the contrary this is not true e.g. at pineapple fibres where it doesn´t depend many on pineapple fibres length [4, 6].

Plant fibres are groups of the oblong thick-walled withered plant cells. Then element fibre is actually plant cell with typical length from 1 up to 50 mm and diameter about 10 – 50 μm. Cell-walls surround central lumen thus plant fibre is actually something as a microscopic tube. Fibres contain differently stratified structure compounds of the thin primary cell-wall which origins already during cellular growth and is surround by the secondary cell-walls. This secondary cell-wall consists of three layers (S1 – outer layer, S2 – middle layer and S3 – inner layer) and from that the thickest middle layer (80% of the total thickness) determinates fibres mechanical properties. This layer consists of the spire arranged cellulose microfibrils compounds of the long cellulose molecules chains [4, 6].

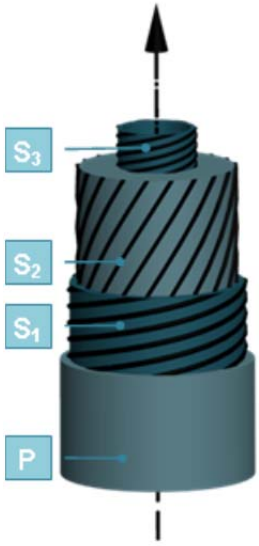

Figure 1. Elementary plant fibre structure (cell) [6].

Angle between central fibre axis and microfibril is called as the microfibril angle (MFA). Its value varies with the every fibre. Fibre force is increasing by increasing cellulose content and by decreasing angle of the spire arranged microfibrils regarding fibre axis (see fig. 2).

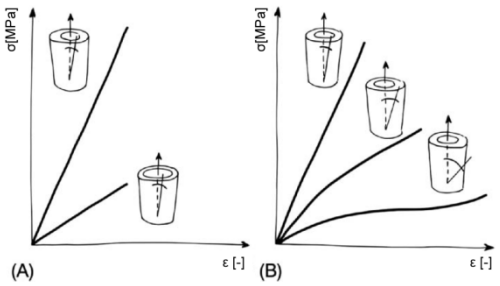

Figure 2. Schematic of the stress-strain curve for (A) high- and low-density fibres with the constant microfibril angle (MFA) and for (B) fibres with the different microfibril angles [5]

Chemical composition, structure and properties of cellulose fibres

Cellulose fibres are used as potential reinforcement material due to their many advantages. They are quite easy obtainable, have low density, are biodegradable, cheap, renewable, revealing low abrasion, have good mechanical properties and it is still just waste biomass. Surely, there are also their disadvantages. These fibres are hydroscopic, fibres quality is not always the same, have low thermal stability and compatibility with hydrophobic polymer matrix. Cellulose is the largest form of biomass affecting the Earth's surface and finds its application in many branches of the modern industry. Existence of the cellulose as a structural member of plant cell-walls was firstly detected by Ansalm Payen in the 1838. Cell-wall represents the functional structure for every kind of plants. Almost in its pure form cellulose can be found in the cotton fibres. Cellulose in wood, leaves and footstalks of plants occurs in the combination with the other materials like e.g. lignin and hemicelluloses is. Although it is entirely plant material, also some bacteria can produce it (Acetobacter xylinum) [4, 6]. Cellulose (α-cellulose) represents the main part of most plant fibres. It is natural linear macromolecule consists of repeating D-anhydride glucose components ($C_6H_{11}O_5$) connected by means of β-1,4 glycosidic bonds with the degree of polymerization about 10 000 (see fig. 3). Every repeating component contains three hydroxyl groups. Such hydroxyl group and their ability to create hydrogen brides play a crucial role at crystallization controlling and also determinate physical properties of these materials.

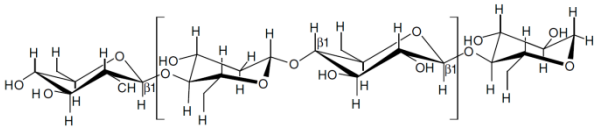

Figure 3. Structure of cellulose [6]

Cellulose is a polysaccharide with unique but simple structure. It is poly-dispersive, linear and syndiotactic polymer which creates thin and rigid, highly crystallic microfibrils. These microfibrils are insoluble in common organic solvents (it´s resistance against strong alkalis). On the other hand it is not resistance against acids and at hydrolysis it is split on the shorter chains (up to the monomers). Hemicellulose is a polysaccharide consists from the combination of five or six saccharide carbon atoms. Polymers chains are much shorter (degree of polymerization is from 50 up to 300) and branched, side-chains so determinate non-crystallic hemicellulose character. Hemicellulose serves as a supporting cellulose microfibrils matrixes. It is highly hydrophilous, soluble in alkalis and easily dissoluble by means of

acids. Lignin holds water in the fibres, acts as a protection against biological attack of given plant and also as reinforcement which gives the footstalk its rigidity and resistance against gravitation forces and wind. It is said to be complex, three-dimensional copolymer of aliphatic and aromatic compounds with high molecular weight. It features by high carbon content with low hydrogen content. It contains hydroxyl, methoxyl and carbonyl groups. In nature, lignin is amorphous and hydrophobic. It is thermoplastic polymer revealing higher glass transition temperature about 90°C and melting temperature c. 170°C. It resists to hydrolysis of acids, it is soluble in hot alkalic solutions and there quite fast oxidation of lignin [4, 5, 6]. Matrixes amorphous phase in the cell-wall is very complex and consists of hemicellulose, lignin and in some cases also pectin. Hemicellulose molecules are connected to cellulose by means of hydrogen bridges and act as agglutination agents among cellulose microfibrils. So they create cellulose/hemicellulose net which is said to be main construction element for plant fibres cells. Hydrophobic lignin net influences just such net properties as connecting agent which increases cellulose/hemicellulose matrix rigidity. Cell-wall composition differs by ration among cellulose, lignin/hemicellulose matrix and in the cellulose microfibrils orientation. Cellulose fibres properties are influenced by many factors as e.g. is variety of plants, climatic conditions, harvest-time, plant maturity, degree of soaking, debarking method and method how to get fibres, fibres modification and processing technology. So that to understand reinforced composite natural fibres properties is truly necessary to know mechanical, physical and chemical properties of these natural fibres.

2. Experiment

Experiment deals with the evaluation of the tensile and impact properties of the polymer composite with natural fibres. Composite is created by cellulose fibres with different content and sizes and as a compatibilizer are added two types of additives. Firstly was carried out polypropylene matrixes granulation with additives and 10, 20 and 30% content of cellulose fibres with different sizes. Testing samples were prepared by injection according to the international standards and subsequently were evaluated their basic mechanical properties. As a matrix was chosen material THERMOFIL PP E020M which is produced by Sumika Polymer Compound (see Tab. 1). It is unfilled polypropylene designed for injection technology and is typical of car door panels. It reveals excellent flow properties and low melting temperature. Such properties are truly very suitable for used cellulose fibres which lower melt flow rate and degrade under higher temperatures.

Table 1.: Properties of THERMOFIL PP E020M matrix

Property	Value	Unit
Volume Melt Flow Index	14,7	cm^3/10min
Tensile Modulus of Elasticity	1600	MPa
Yield Strength (Ultimate Strength)	27	MPa
Nominal Strain at Yield Strength	5	%
Tensile Stress at Fracture	16	MPa
Nominal Strain at Fracture	39	%
Charpy Impact Energy (+23°C)	9	KJ/m
Charpy Impact Energy (-35°C)	4	KJ/m
Flexural Modulus of Elasticity	1290	MPa
Flexural Strength	35	MPa
Hardness - Shore D	59	-
Melting Temperature	166	°C
Crystallization Temperature	125	°C

For preparation ***cellulose fibres (CF)*** was used knife-cutting mill RETSCH SM 300. As a input semi-products were used paper cellulose desks. From these desks were produce cellulose fibres by milling at 3000 rpm and screen with 0, 75 holes (see fig. 4).

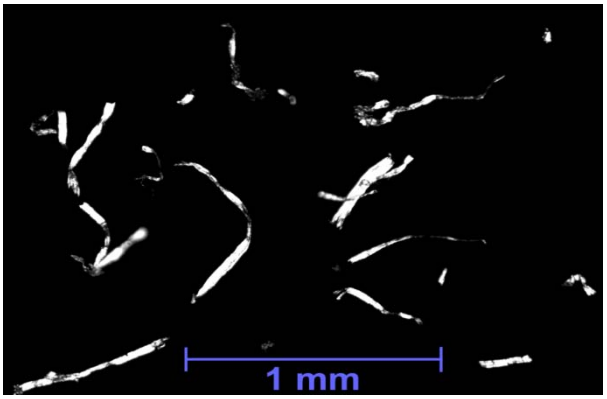

Figure 4. Cellulose fibres (CF) length distribution (CV) from microscope DM 2500 P (magnification 4x)

Microfibril cellulose (α- cellulose) was used with regard to possible using as additives for polymers matrixes in the company dealing with the development and production of parts for the automotive industry. It was delivered in the prepared state before processing thus no more modifications were not necessary.

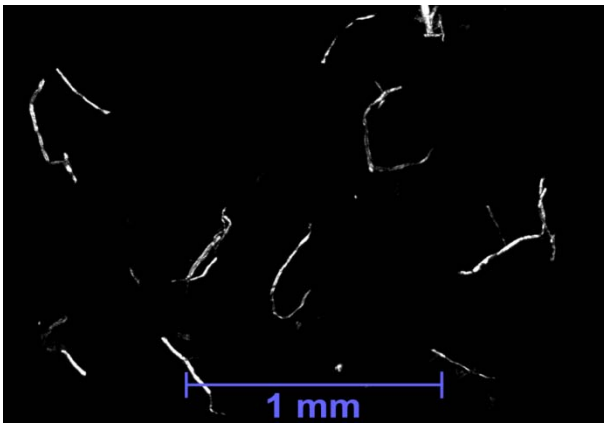

Figure 5. Length distribution of the α-cellulose fibres from the microscope Leica DM 2500 P (magnification 4x)

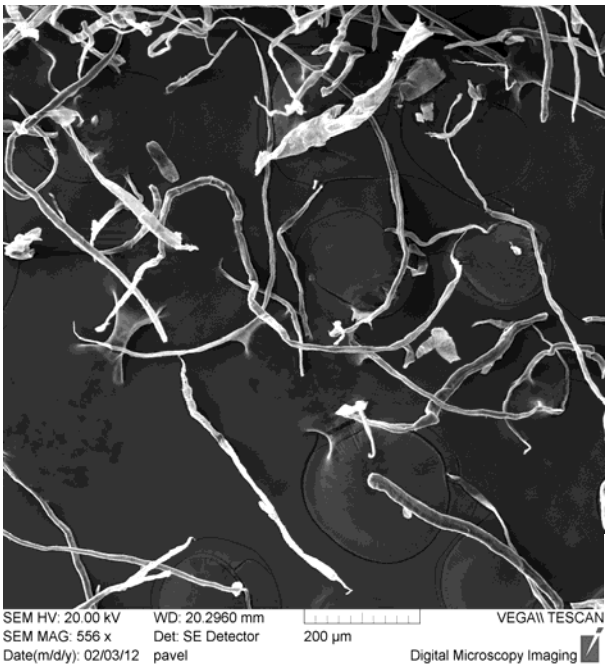

Figure 6. Image of the α- cellulose from the scanning electron microscope (SEM)

Compatibility of fillers with matrix is one of the crucial factor influencing final compostite properties both from the physical and from the chemical point of view (creation of the covalent bond between matrix and filler). To provide sufficient wettabillity of fibres by the polypropylene matrix and to achieve sufficient interphase compatibility were used following additives:

- ***Fusabond (MA-g-PP)***

Fusabond from the company DuPont is one of the most commonly used compound agent. This additive is on the basis of maleine anhydride (MA) which is by the producer bonded (grafted – g) with polyphonic chains which will be used as composite matrix (PP, PE and so on). Grafting is usually carried out by radical mechanism, as an initiator there is peroxide group which by the reaction with the PP chain creates free radical which subsequently reacts with the PP molecule at creation compound MA-g-PP. PP connected on the MA is during compoundation physically implemented into PP matrix by which there is complete interlacing of the PP matrix with natural fibres. Additive is delivered in the form of pellets.

- ***Struktol SA1012***

This additive is delivered in the form of pellets by company Struktol Company of America. It is added directly into compounder to polyphonic matrix and natural fibres. Struktol has a similar function as additive already mentioned above – FUSABOND (MA-g-PP). There is difference between free radical creations which enable connection of the polar and non-polar composite components. Covalent bond is created by the ion mechanism which is initiated by the additive hydrolysis.

As a output product there is granulate of the PP matrix, additives and cellulose fibres in the form of the cylindrical shaped granulates (see fig. 7).

Figure 7. Compound (composite granulate)of the polypropylene, cellulose fibres and additives

Charpy Impact Energy Evaluation

From measured and calculated average impact strength values were made graphs for the following dependences. Impact energy dependence on the 10, 20 and 30% content of the α-cellulose fibres for the additives FUSABOND and STRUKTOL at conditioning on the temperature 23°C (see fig. 8). Further there are impact energy dependences on the additive type for 20% α-cellulose and 20% milled cellulose fibres at temperatures 23° (see fig. 9).

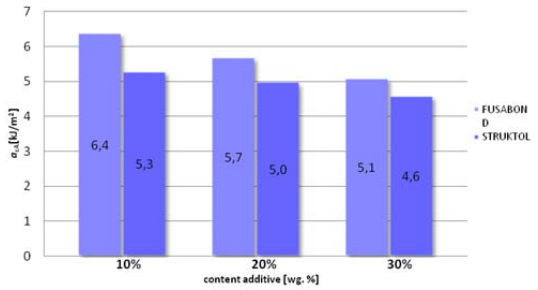

Figure 8. Impact energy dependence on the content of the α-cellulose fibres at different additives types at temperature 23°C

From the measured results and their average values at conditioning on the room temperature results that samples reinforced by α-cellulose fibres with the FUSABOND additive reveal higher impact energy values compared to results from STRUKTOL additive. Impact energy values are linearly decreasing for both used additives with the increasing fibres content. The highest impact energy results was achieved by the composite with FUSABOND additive and 10% α-cellulose filler.

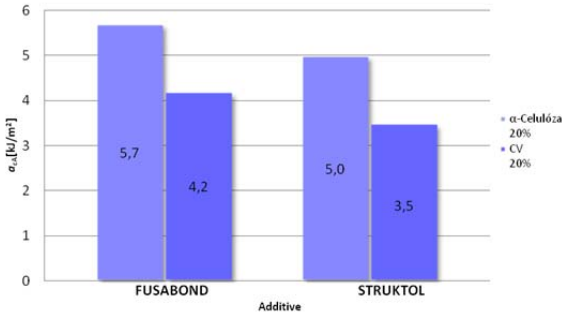

Figure 9. Impact energy dependence on the additive type for different cellulose fibres sizes at temperature 23°C

Impact energy is higher in the case of samples with the α-cellulose filler compared to the filler CV. Equally measured values for additive FUSABOND reveal compared to the additive STRUKTOL higher impact energy values at the conditioning on the room temperature. So FUSABOND according to the presumption create stronger bond and α-cellulose filler revelas better impact properties.

Tensile Properties Evaluation

From the ultimate tensile strength average values and fracture stress was made their dependence on the 10, 20 and 30% content of the α-cellulose fibres for the additive FUSABOND and STRUKTOL (see fig. 10 and fig. 12). Further there was made their dependence on the additive type for 20% α-cellulose and 20% milled cellulose fibres (see fig. 11 and fig. 13).

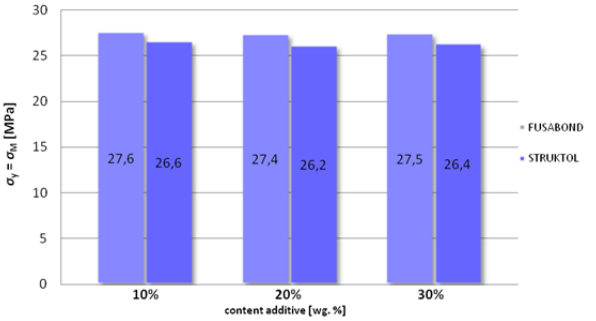

Fig. 10 Ultimate strength dependence on the α-cellulose fibres content for different additives types

From measured values is obvious that the maximal ultimate strength values was achieved by the additive FUSABOND. Tensile ultimate strength values are with regard to the different additive almost identical.

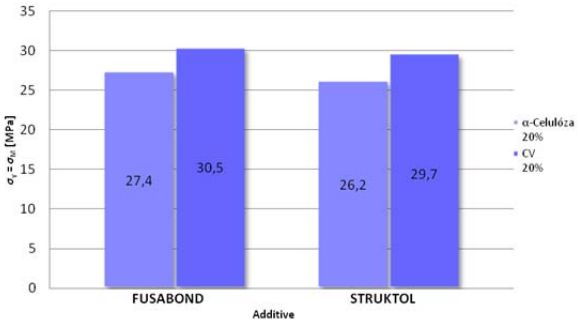

Figure 11. Ultimate strength dependence on the additive type for different cellulose fibres sizes

From th ecomparison of the ultimate strength for different fibres sizes revelaed better results the milled CV. The highest values wa achieved by using additive FUSABOND.

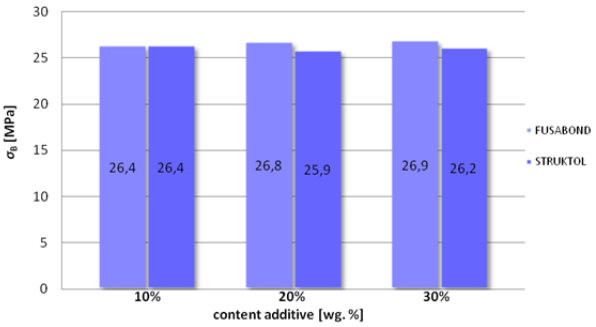

Figure 12. Fracture stress dependence on the α-cellulose content for different additives types

From measured fracture stresses values is clear that the highest strength value was achieved for the composite with the additive FUSABOND. Fracture stresses values are with regard to the different additivies contents almost indentical.

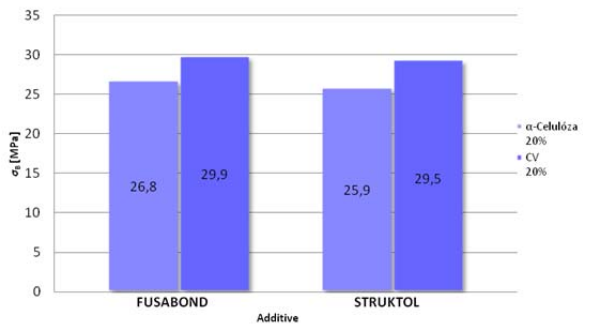

Figure 13. Fracture stress dependence on the additive type for different cellulose fibres sizes

From the comparison of the fracture stress for different fibres sizes can be found better results for the milled CV. The highest value was achieved for the additive FUSABOND.

Acknowledgments

This paper was written with research project SGS 28005 support.

3. CONCLUSION

From the measured values is clear that for the strength applications is more suitable additive FUSABOND which creates stronger bond between polymer and filler. Compared to additive STRUKTOL it revealed much better flow properties and could be applied e.g. for the thin-walled mouldings. With increasing α-cellulose fibres content in the matrix there is decrease of the impact energy and composite flow. In comparison to that there is increase of the mechanical properties as is e.g. ultimate strength. For using in praxis isn´t possible unambiguously recommend particular percentage content cause it depends on the final part application and processors requirements. From the fibres length point of view reveals better flow properties and impact energy (toughness) α-cellulose fibres. Milled cellulose fibres reveal higher mechanical properties values. For using individual cellulose fibres types in the praxis is then necessary to take into account also economical criterions. Paper cellulose with the price approx. 0,55 €/kg is much more cheaper than α-cellulose with its price about 3 €/kg.

REFERENCES

[1] *Materiálové inženýrství je nejen technická věda, ale i kus filozofie.* [online]. Available: http://www.mmspektrum.com [Accessed:14. 4. 2012]

[2] *World plastics consumption long term.* [online]. [Accessed: 24. 3. 2012]. Available: www.pardos-marketing.com

[3] *Cellulose based bio and nanocomposites – a review.* [online]. [Accessed:27. 2. 2009]. Available: < http://www.hindawi.com >.

[4] *Cellulose fibers*: *bio- and nano-polymer composites* [online]. New York: Springer, 2011, p. cm. [Accessed: 2012-05-21]. ISBN 978-364-2173-691.

[5] MÜSSIG, Jörg. *Industrial application of natural fibres*: *structure, properties, and technical applications* [online]. Editor Amar K Mohanty, Manjusri Misra, Lawrence T Drzal. Hoboken, N.J.: Wiley, 2010, xxi, 538 p. [Accessed:2012-05-21]. ISBN 978-047-0695-081.

[6] *Natural fibers, biopolymers, and biocomposites* [online]. Editor Amar K Mohanty, Manjusri Misra, Lawrence T Drzal. Boca Raton: Taylor, 2005, 875 s. [Accessed: 2012-05-21]. ISBN 978-0849317415.

[7] *Cellulose fibers*: *bio- and nano-polymer composites* [online]. New York: Springer, 2011, p. cm. [Accessed:2012-05-21]. ISBN 978-364-2173-691.

OMNIDIRECTIONAL CAMERAS IN CAR MOUNTED CAMERA SYSTEMS

Gábor Kátai-Urbán[1*] and Zoltán Megyesi[1]

[1] Faculty of Mechanical Engineering and Automation, Kecskemét College, Hungary
* *Corresponding author e-mail: katai-urban.gabor@gamf.kefo.hu*

Abstract
With the increasing need for reliable driver assistant systems, the car mounted camera systems become more and more studied. The main goal of these systems is to use visual information to detect dangerous situations and warn the driver. To reliable detect dangers in all direction around the car we apply multiple cameras with 360 degrees viewing angels (omnidirectional cameras) together with conventional cameras.
In this article we describe the main steps of the planning of a car mounted 3D camera system and we summarize the projection models of the omnidirectional cameras.

Keywords:
Image processing, Omnidirectional camera, Visual driver assistance

1. Introduction

Many modern car designs apply systems that provide the driver extra information about the surrounding (e.g. parking assist systems IPAS, APGS), warn the driver about possible problems (e.g. lane departure), or even actively change the movement of the car if an immediate danger is detected. Indeed, a major research effort is spent on developing better end more reliable systems to assist the drivers. These systems constantly monitor the surroundings of the vehicle to detect potentially dangerous situations at an early stage. In critical situations, these systems warn the driver to help avoid the accident or reduce the damage.
These systems utilize a wide range of sensors, often including one or more car mounted cameras.
The main difference between the applied systems is the selection of sensors and the targeted danger scenarios that are handled.
In this article we present the design of a Driver Assistance System that is based on visual information from a 3D camera system. The possibility of a dangerous situation can be indicated if we recognize and analyze certain visual clues. From the detection viewpoint, we categorize these clues into the following cases:

- road markings
- static objects
- moving objects
- scene behind blind spots

We address these cases separately. The main task of the **road marking analyzer** is to detect marks on the road pavement on front of the vehicle in 2-100 m. The most important related tasks are crosswalk detection and lane departure detection, but there are other possibilities. In general we can define danger zones on the images that are in the path of the vehicle, and analize the road texture.
The **static object detector** is for detecting statically located object in front of the car in a 2-50 m zone. These objects can be pedestrians standing near the crosswalks, or can be traffic signs.
The analysis of moving objects in the 3D space around the car is the task of the **moving object detector**. Moving objects can present a danger to the car from all direction, therefore visual information from 360° must be acquired. The detector computes trajectories of moving objects in zone 1-50 m.
The **blind spot reducer** aim to reduce the masking effects of the car body. For this, the light rays that are blocked by the chassis must be identified and analyzed.
The main component of this Visual Driver Assistance System is the camera system. To achieve the goals of the system, hybrid camera system to be used. The detection tasks in the front zone 2-100 m are requiring standard perspective cameras with smaller field of view and higher magnification. The object tracing tasks 360° around the vehicle in zone 1-50 m are requiring omnidirectional cameras with 360° viewing angle.

2. Omnidirectional cameras

The omnidirectional camera is an optical device consisting of a camera, lenses and/or mirrors which form an optical system with 360-degree horizontal field of view.
We consider only those systems, where light rays intersect in a single point. These systems are often called central projection systems.
Central omnidirectional camera systems are grouped in two main categories: dioptric and catadioptric systems.
Dioptric cameras consist of only lenses. Fisheye lenses has 180° or more field of view horizontally and vertically.
Catadioptric systems are formed as a combination of mirrors and lenses. There are four groups of central catadioptric cameras (see [2]).

Planar mirror: Placing polar mirror in front of a perspective camera, we can drive rays from other directions to the unused part of the image.
Elliptical mirror: The reflective inside of the elliptical mirror can be observed by a perspective camera. To achieve the single viewpoint the camera placed in the focal point (p) of the ellipsoid. The maximum viewing angel is 180°, because the side of the mirror blocks the rays if we use bigger elliptical mirror.
Parabolic mirror: The outer reflective sourface of a parabolic mirror reflect paralel rays. To detect these rays an orthographic camera must be applyed. The field of view can be chosen wider than 180°, but the special camera makes the system more complicated.
Hyperbolic mirror: The outer reflective surface of a hyperbolic mirror collects the rays in the external focal point. A perspective camera in this point can be used to detects these rays. With this simple configuration an omnidirectional camera can be formed with a viewing angel over 180°.

3. Projection model of omnidirectional cameras with hyperbolic mirror

Standard perspective cameras map scene point X from a line passing throw an optical center of the camera to image point x. This mapping can be described by

$$\exists \lambda \neq 0 : \lambda \mathrm{x} = \mathrm{P}\mathbf{X}, \qquad (1)$$

where $P \in R^{3\times4}$ is a projection matrix, $\boldsymbol{X} \in R^4$ is a scene point, and $\mathrm{x} \in R^3$ represents the scene point (see [4] and [5]). In this model the scene point could be anywhere on the line, even behind the camera. This case can be excluded during modeling perspective camera.
The real omnidirectional cameras with field of view over 180°, maps scene points in front of the camera to a point and the scene point behind the camera to a different point. Therefor the perspective camera model cannot be applicable to omnidirectional cameras. In this case one image point represents all scene points lying on a half-line which starts from the optical center. The direction of half-lines described by unit vectors, which are form a unit sphere. This spherical projection model can be described by

$$\exists \lambda > 0 : \lambda \mathrm{q} = \mathrm{P}\mathbf{X}, \qquad (2)$$

where $q \in R^3$ is a 3D unit vector representing an image point (see [1]).

Suppose that we observing a scene point X by a omnidirectional camera (See Fig. 1). The projection of the point X on the sphere represented by unit vector q''. There is a vector $p'' = (x''^T, z'')^T$ width the same direction as q'', which maps X to the sensor plane point u''. So that u'' is collinear with x''. The vector p'' can be written as

$$p'' = \begin{pmatrix} h(\|u''\|, a'')u'' \\ g(\|u''\|, a'') \end{pmatrix}, \qquad (3)$$

where g, h are functions of $R \times R^N \to R$ which depend on same parameters $a'' \in R^N$, and the distance $\|u''\|$ between the image point and the center of the image.

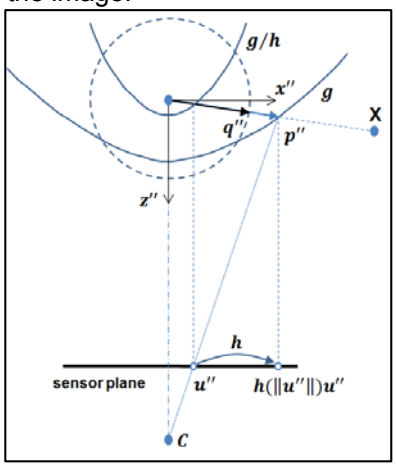

Figure 1. Hyperbolic mirror omnidirectional camera

The functions g, h are different for various omnidirectional camera types. Function g describe the shape of the mirror while h represents the projection of the camera.
In our case we designed a hyperbolic mirror, so we exactly know the shape of the mirror and the function g. Only the function h to be determined.

4. Planning of car mounted 3D camera system

To achieve the goals of the Visual Driver Assistance System, we design a car-mounted camera system. This system works while the vehicle moves and observes the scene around the car. The different kind of tasks require different visual information from the scene.
The first step of the camera system planning is to determine the suitable camera configurations: what type of lenses, mirrors and cameras should be used (see [3]). The viewing angle and the resolution are the main parameters.

For the first two tasks (road marking detection and static object detection), the cameras need to observe the scene in front of the car within 2-100 m.
The viewing angle of a standard perspective camera should be determined with calculations based on right-angled triangles (see fig. 2.)

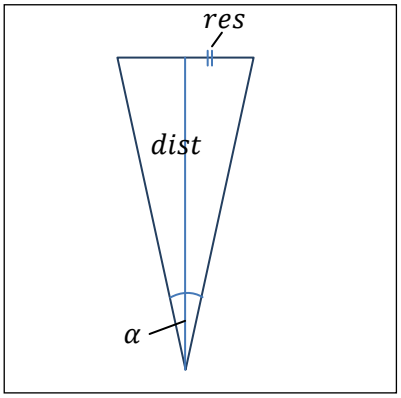

Figure 2. Viewing angle of a perspective camera

The calculation formalized as follows:

$$\alpha = 2 * arctg\left(\frac{pix * res}{2 * dist}\right), \quad (4)$$

where $dist$ is the distance from the camera center, pix is the pixel count of the camera CCD in the proper direction, res is the resolution which describes that the width of the pixel at this distance.
If we use 5 megapixel (2560x1920) cameras and the target resolution at the distance 100m is 2 cm/pixel, the horizontal viewing angle is :

$$\alpha = 2 * arctg\left(\frac{2560\ pix * 2\frac{cm}{pix}}{2 * 100m}\right) = 28.71° \quad (5)$$

To view the scene in 30° angle a 12 mm focal length lens is used.
In this subtask the distance of the detected objects is used, so a minimum of two cameras (stereo vision) is needed for the distance estimation.

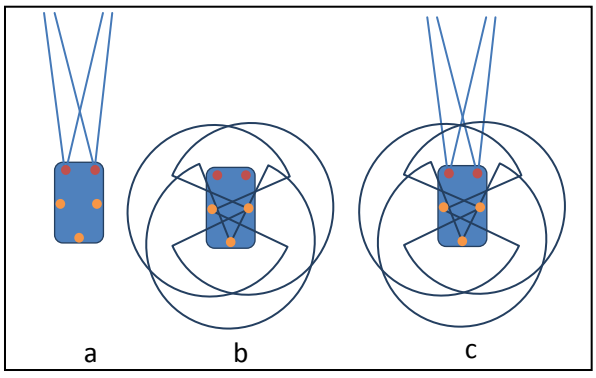

These two cameras placed in front of the car (see fig. 3/a).

Figure 3. Car mounted camera system

For the next two tasks (moving object detection and blind spot reduction), the whole scene around the car need to be observed. It is important to view critical regions from more than one cameras for reliable distance and speed estimation. In our design we use three omnidirectional cameras placed to the roof of the car (see fig. 3/b). One for the back view and two for the side views. The 360° horizontal viewing angel cameras observe the whole scene form 2-50 m around the vehicle.
We use 150 mm diameter hyperboloid mirror based omnidirectional cameras. The points on the surface of the mirror is described by

$$\circ\frac{x^2}{a^2} - \frac{y^2}{b^2} = 1. \quad (6)$$

The parameters a and b in case of our mirror are 107 mm and 90 mm respectively.
The perspective camera which observe the mirror should be placed in front of the mirror. The semi-major axis of the hyperboloid mirror and the projection center of the camera should be collinear. The distance of the camera center and the foci of the hyperboloid is twice the focal length of the hyperboloid. In our case the focal length is $f = \sqrt{a^2 + b^2} = 139.82\ mm$ and the distance is 279.64 mm.
The viewing angle of the standard perspective camera needs to be calculated. Similar as (4):

$$\alpha = 2 * arctg\left(\frac{150\ mm}{2 * 279.64\ mm}\right) = 30.03°. \quad (7)$$

To observe the mirror in 30° angle a 12 mm lens should be used.
Assuming a 10 megapixel (3840x2748) camera, the resolution at the mirror surface is $150\ mm/2748\ pix = 0.05\ mm/pix$. But the resolution of the scene what the mirror reflects is not calculated as easily. The resolution depends on the radius of the reflection point. At the middle of the mirror it is higher than at the edges (see fig. 4.)

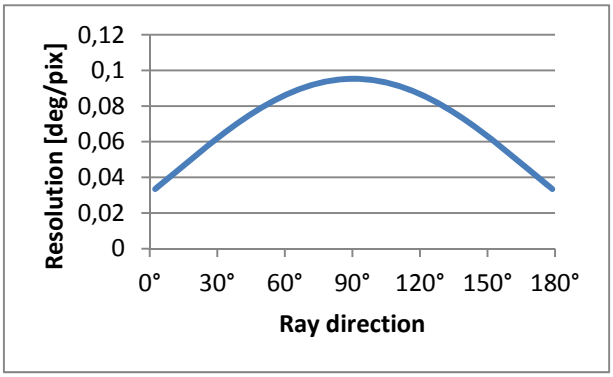

Figure 4. Scene resolution

For both types of optical systems standard perspective cameras are used to take pictures. We use IDS UEye UI-5490SE 10 megapixel industrial

cameras for the omnidirectional systems and UI-5480SE 5 megapixel cameras for the front views.

The designed optical system should be mounted on the top of the car. We planned a stand which can be mounted to roof rails (see fig. 5). The stand is constructed of aluminum profiles with flexible adjustable connection, so the camera positions can be changed to achieve the best settings.

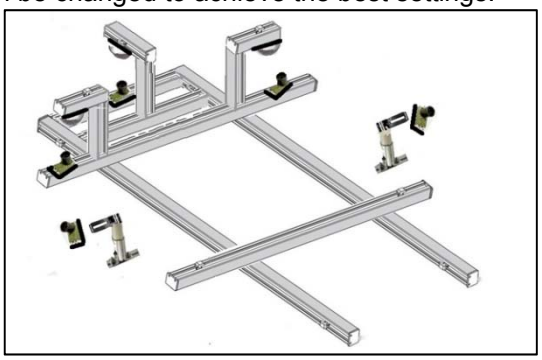

Figure 5. Car mounted camera stand

5. Conclusion and future work

In this article we presented the initial designs of a car mounted hybrid camera system that utilizes omnidirectional cameras. Our target with this setup was to have stereo visual information of the surrounding area in 360 degrees, while having good resolution stereo images of the front of the car.
We discussed the different type of omnidirectional camera systems and we summarized the projection model of the omnidirectional camera with hyperboloid mirror. We described the camera and lens selection criteria in detail.
We discussed the targeted software applications that all rely on stereo reconstruction. The stereo reconstruction algorithm will be produce real 3D information regardless of the speed of the vehicle. This 3D information will be used to reach our aims: detect road markings, detect static or moving objects and reduce blind spots.

6. Acknowledgement

This research is supported by TÁMOP-4.2.2.C-11/1/KONV-2012-0012: "Smarter Transport" - IT for co-operative transport system - The Project is supported by the Hungarian Government and co-financed by the European Social Fund.

7. References

[1] C. Geyer and K. Daniilidis, “A unifying theory for central panoramic systems and practical applications,” in European Conference on Computer Vision (ECCV), pp. 445–461, jun 2000.
[2] S. Baker and S. Nayar, “A theory of single-viewpoint catadioptric image formation,” International Journal of Computer Vision (IJCV), vol. 35, no. 2, pp. 175–196, 1999.
[3] Z. Zivkovic and O. Booij, „How did we built our hyperbolic mirror omnidirectional camera - practical issues and basic geometry“ , Technical Report IAS-UVA-05-04, Informatics Institute, University of Amsterdam, 2005.
[4] R. Hartley and A. Zisserman. Multiple View Geometry in Computer Vision. Cambridge University Press, second edition, 2004.
[5] Milan Sonka, Vaclav Hlavac, and Roger Boyle. Image Processing, Analysis, and Machine Vision. Thomson-Engineering, 2007.
[6] Sato, T.; Pajdla, T.; Yokoya, N., "Epipolar geometry estimation for wide-baseline omnidirectional street view images," Computer Vision Workshops (ICCV Workshops), 2011 IEEE International Conference on , vol., no., pp.56,63, 6-13 Nov. 2011

WIND ENERGY IN AGRICULTURE: A SIMPLE PREDICTIVE NOISE POLLUTION MODEL

A. Ruggiero[1*], J. Quartieri,[1] C. Guarnaccia[1], S. Hloch[2]

[1]Department of Industrial Engineering, University of Salerno, Italy
[2] Faculty of Manufacturing Technologies, of TUKE with a seat in Prešov |SK* *Corresponding author e-mail: ruggiero@unisa.it*

Abstract

This paper is mainly focused on noise pollution problems related to the use of wind turbines and deals about the mathematical analysis on the acoustical noise produced by wind turbines. The result has been validated with the aid of a predictive commercial software. The agreement between the analytical curve and the numerical one implicitly validates the assumptions of the presented procedure. In the software framework, more simulations have been performed, introducing the directivity of the source and simulating more turbines in a symmetric array, giving a first description of the results that can be achieved in terms of noise mapping in more complex configurations of wind farms.

Keywords:
Noise control, Wind turbine, Source Modeling, Noise propagation.

1. Introduction

It is well known that the wind power was used in agriculture through the ages: in the first millennium Persia, China, and Rome used blades on a vertical axis to mill grain; in the 1800s Americans invented the first self-directing, self-governing windmill for use in the Plains states, pumping water from wells for farmers and railroad stops to fill boilers; in the 1920s the farmers used the same machines hooked to generators to create electricity from wind. This largely ended by World War II with the Rural Electrification Act bringing power lines to rural areas. In the middle ages Europe developed horizontal axis machines to mill grain and pump water. In 2000 a whole new class of wind turbines – designed specifically to generate electricity, and based on lift rather than drag – allow farmers to make more money harvesting the wind above their land than from raising crops. This century is going to be characterized by the time of energy crisis. The lack of petrol, the still ongoing research on nuclear fission plants and the global warming are the main elements that lead to the development of green and renewable energies. In this framework, wind turbines are a relevant component of the complex scenario of the sustainable development. Wind turbines generate renewable energy and thus contribute to sustainable development. However, disturbance from wind turbines may be an obstacle for large-scale production ([1], [2]). Few studies have so far been directed to the prevalence of disturbance, and existing knowledge of annoyance due to wind turbines is mainly based on studies of smaller turbines of less than 500 kW ([3], [4]). Global wind power installed at the end of 2003 reached 39 GW according to American Wind Energy Association (2004), an increase of 26% in just one year. United States (7 GW) and Europe (29 GW) account for 90% of the cumulative capacity. In Sweden, more than 600 wind turbines are operating today with a total installed capacity of 0.4 GW, producing 600 GWh per year. They are placed in 84 of Sweden's 290 municipalities both along the coasts and in rural inland areas, concerning a number of people. The goal set up by the Swedish government for 2015 is 10 TWh, leading to an increase of 1600% from today. Most of new turbines could be probably situated off shore, but as the cost for building on land is considerably lower, the development on land is expected to continue. Already, turbines are being erected near densely populated areas. Some interviews conducted among 12 respondents living within 800 m of a wind turbine, and a register study of the nature of complaints to local health and environments authorities, indicated that the main disturbances from wind turbines were due to noise, shadows, reflections from rotor blades, and spoiled views ([5]). In particular, among these environmental polluting agents, acoustical noise must be considered. The turbines generate unwanted sound, both mechanical and aerodynamic. In the last years, with the advancement of technology, wind turbines became much quieter, but their noise is still an important source, to be considered in the site choice phase. In this framework, new technologies need to be developed in order to reduce the environmental impact of the wind turbines. Together with the technologies, a source and propagation modeling improvement could be helpful in order to understand the correct behavior of the noise produced by the wind turbine. In this paper, the authors analyze the properties of noise intensity function, from an analytical point of view, focusing on its slope when considering different dependences. In addition, in the last section, a comparison between the presented model and results obtained with a commercial predictive software are sketched, sharing lights to further investigations.

2. The Model

In this section, a wind turbine noise analysis is presented, starting from the construction of a simple model, based on the following assumptions:
1. The turbine can be, in a first approximation, considered as a point like source, with a subsequent spherical spreading of the noise.
2. Ground is considered completely absorbing.
3. Air absorption can be neglected over a short range.
4. The source sound power is assumed to be broad band.

Assumption 2 is supported from the fact that usually wind farms are designed and built in countryside environments. In general, since the aim of the paper is to highlight the mathematical properties of the noise intensity function and the possible impact on human activities, in a first study one can consider these ideal conditions, postponing a more detailed analysis to a further study.

The geometry of our approximated model is shown in Figure 2, where the source and the receiver position are highlighted, together with the relevant parameter of the model.

The first step of the procedure is to estimate the source sound power level L_{wA} (A weighted) of the turbine. In order to achieve this result, many procedures, both experimental and theoretical, can be used in an already operating wind farm. The L_{wA} as a function of the wind speed, for instance, can be obtained by means of a fit on noise emission data provided by datasheets of manufacturers, obtained according to IEC 61400-11. This does not diminish the value of the approach because the L_{wA} is an additive parameter that only affect the vertical shift of the curve.

Once the fit equation is obtained, it is easy to relate the source power level global emission to any wind speed value (in the range of the fit). These data can be used to evaluate the sound intensity level L_I at a certain distance r (see Fig. 1) from the source.

In the pointlike source and absorbing ground approximations, on can write:

$$L_I = L_{WA} - 20\log_{10}\frac{r}{r_0} - 11 - \alpha r \qquad (1)$$

where L_{wA} is the source power level, r_0 is the reference distance, chosen as 1 m and α is the air absorption coefficient.

The absorption of sound by the atmosphere can be obtained according to the calculation method described in "Acoustics - Attenuation of sound during propagation outdoors - ISO 9613-1:1993" and depends on the frequency, temperature, and humidity of the air. In a simple approach, a constant value can be assumed as follow:

$$\alpha = 0{,}005\, dBA/m \qquad (2)$$

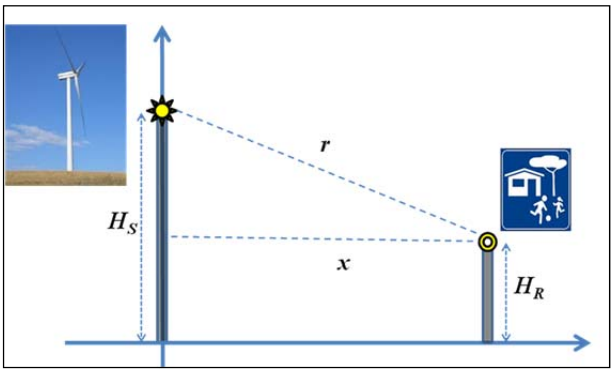

Figure 1: Geometry of the source and receiver configuration.

Obviously, within 100 m from the source, this attenuation can be neglected since it follows in the experimental uncertainty of any measurement.

With respect to the general propagation formula presented in ISO 9613, in this work some contributions, due for instance to ground reflection, screens, etc., are neglected since they are not relevant in this framework and can be easily implemented in a further study as simply additive terms.

Formula (1) is derived from the usual expression of a newtonian field (see for instance [6]**Error! Reference source not found.**) which gives the sound intensity I produced by a pointlike source in terms of source power W and distance source-receiver r :

$$\frac{I}{I_0} = \frac{W/W_0}{4\pi\left(r/r_0\right)^2} \qquad (3)$$

W_0, I_0, r_0 are reference values, used to make the logarithm argument dimensionless.

If one includes all the constant values and the source power W in a parameter K as follow:

$$K = \frac{I_0\, r_0^{\,2} W}{4\pi W_0} \qquad (4)$$

the sound intensity is:

$$I = K\frac{1}{r^2} \qquad (5)$$

Let us underline that, in this model, the parameter K is ruled only by the wind speed value, which is related to the power of the source.

Considering that (see Fig. 1):

$$r^2 = x^2 + \left(H_R - H_S\right)^2 = x^2 + H^2 \qquad (6)$$

with $H = H_R - H_S$, the sound intensity can be finally written as:

$$I = K\frac{1}{\left(x^2 + H^2\right)} \qquad (7)$$

Studying the Lorentzian-like function (7), one can easily find that it has a maximum in $x = 0$, with value $I_{max} = K/H^2$, and an inflection point in:

$$x = \frac{H}{\sqrt{3}} \tag{8}$$

where the second derivative is null.
Of course the 10 Log operator does not affect the properties on x axis, thus also the sound intensity level L_I has an inflection point.
By this result, one can affirm that there is a first region of proximity to the turbine in which the intensity level decreases slightly slower than the second region. The concavity, in fact, influences the slope of the sound intensity function.

3. An application of predictive software modeling

In this section, the authors will present an application of numerical methods for noise prediction, in an operating wind farm located in Postiglione, Salerno, Italy.
The software used for the simulation is CadnaA®, by DataKustik. The "Angle Scanning" and the inverse "ray-tracing" principles are at the basis of the software algorithm. The calculation grid is obtained dividing area under analysis in many small surfaces in which a receiver is placed at a variable height (in our case is 2 m). Each grid element releases many rays with a full angle coverage (omni directive) and these rays, eventually after many reflections, intercept the noise source. The path length of the single ray describes the attenuation of the sound wave coming from a certain noise emitter. In addition, specific receivers can be inserted in the map, with the possibility to export the results in a worksheet.
The turbines installed model is Vestas V52. The farm map under study is shown in Figure 2, in which the red circles represent the turbines position.

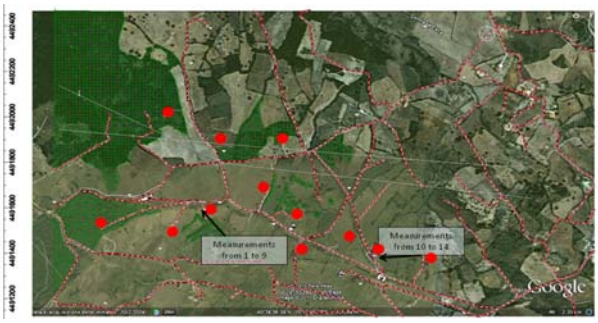

Figure 2: Map of the area of Taverne Vecchie (SA), Italy (Google map ©). Red circles represent the turbines.

Since the area is rural and the number of vehicles per hour is negligible, noise emitted by roads does not affect the prediction on turbines effect.
In order to perform the simulation, the source power is estimated considering the the annual mean wind speed data reported in [7]. The simulation parameters are resumed in Table 1.

Table 1. Simulation parameters in the case of constant source power

Hub height	65 m
Evaluation grid height	2 m
Grid square element	3 m x 3 m

Results from the simulation on the entire area of the wind farm are shown in Figure 3.

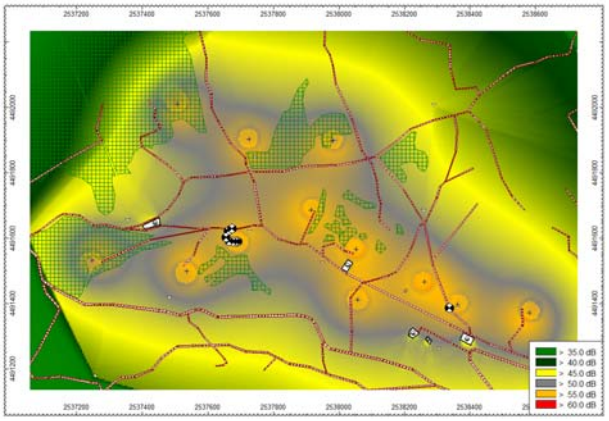

Figure 3: Simulation of Postiglione wind farm noise map. Annual mean wind speed for each turbine is used to set the source power.

Let us remind that the area under study is rural and is mainly devoted to agriculture. Thus, in order to estimate a potential danger on people working in the fields, a simulation of "high source power" condition is performed.
A 3 dBA increase of the source power of each turbine is simulated, mimicking a wind speed of about 9-10 m/s. The resulting noise map of the area is reported in Figure 4.
The results of the various simulations show that, in average wind speed conditions, the noise levels produced by turbines is under 60 dBA in all the area. Only when 9-10 m/s is set as wind speed, the zones under the turbine can be affected by levels around 60 dBA (red areas in Figure 7 and 8). Anyway, this levels occur only in the very proximity of the turbine, where usually no human activity is performed.

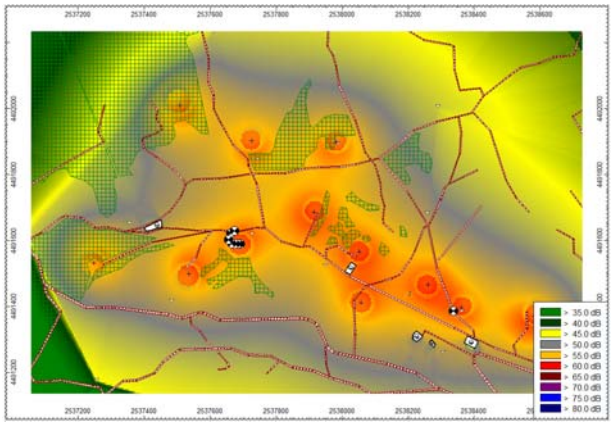

Figure 4: High source power condition noise map.

4. Conclusion

In this paper, a study on the impact of wind turbines in rural and agricultural areas is performed. In particular, the acoustical noise problem is analyzed by means of an analytical model and a predictive software approach.

The analytical model shows that the scaling of the noise level with the horizontal distance from the basis of the turbine, follows a Lorentzian function. Thus, the maximum value is obtained just under the turbine and an inflection point is present on the *x* axis, depending on the height of the hub.

Predictive software simulations show that the noise levels, in average wind speed conditions, are around 55 dBA in proximity of the turbines, and, of course, lower in the rest of the area.

In addition, a high wind speed condition, about 9-10 m/s, has been simulated in terms of high source power of the turbines. The increase in the noise levels is evident, but it seems to be compatible with daily human agricultural activity. Further studies on the frequency spectrum of the noise may be performed, in order to investigate the effect of possible tonal components.

5. References

[1] M. Rand, A. Clarke, "The Environmental and Community Impacts of Wind Energy in the UK", *Wind Engineering*, 1990, Vol. 14, No. 5, pp. 319-330.

[2] M. Wolsink, M. Sprengers, A. Keuper, T. H. Pedersen, C. A. Westra, "Annoyance from wind turbine noise on sixteen sites in three countries", *European community wind energy conference* 8-12 March 1993, Lübeck, Travemünde, 273-276.

[3] T. Ackermann and L. Söder, "Wind energy technology and current status: a review", *Renewable and Sustainable Energy Review* Vol. 4, Issue 4, 2000, pp. 315–374

[4] T.H. Pedersen, K.S. Nielsen, "Genvirkning af støj fra vindmøller" (Annoyance due to noise from wind turbines), *Report 150 [In Danish]. Copenhagen, Denmark: DELTA Acoustic & Vibration,* 1994.

[5] E. Pedersen, ''Storningsupplevelser fran vindkraft, forstudie" (''Experience of annoyance from wind turbines, a pilot study''), *Halmstad University, Sweden,* 2000.

[6] J. Quartieri, L. Sirignano, C. Guarnaccia, "Infinitesimal Equivalence between Linear and Curved Sources in Newtonian Fields: Application to Acoustics", *International Journal of Mechanics,* Issue 4, Vol.1, pp. 89-91 (2007).

[7] Trelettra Srl, "Final Wind Park Planning Report", *Report 01/2003,* 2003.

[8] Guarnaccia C., Mastorakis N.E., Quartieri J., "Wind Turbine Noise: Theoretical and Experimental Study", *International Journal of Mechanics*, Issue 3, Vol.5, pp. 129-137, ISSN: 1998-4448, 2011.

[9] Guarnaccia C., Lenza T.L.L., Quartieri J., *"*On the Propagation Model of Wind Farm Noise*", 4th International Meeting on Wind Turbine Noise, Rome, Italy,* 12-14 April 2011, ISBN: 978-88-88942-33-9, 2011.

[10] Guarnaccia C., Mastorakis N.E., Quartieri J., "A Mathematical Approach for Wind Turbine Noise Propagation"*, in "Applications of Mathematics and Computer Engineering", proceedings of the American Conference on Applied Mathematics (AMERICAN-MATH'11),* Puerto Morelos, Mexico, 29-31 January 2011, pp. 173-179. ISBN: 978-960-474-270-7 / ISSN (printed): 1792-7250, ISSN (electronic): 1792-7269, 2011.

[11] Ruggiero A., Senatore A., T.L.L.Lenza,, D'Agostino(P. On the determination of the uncertainty in environmental noise measurements. Proceedings of the 11th WSEAE International Conference on Acoustics & Music: theory and applications Iaşi (RO) June 13-15, 2010 WSEAS Pag.225-230 ISBN:9789604741922

PERFORMANCE OF THE WIRELESS DISTRIBUTION SYSTEM APPLIED IN A TRAFFIC INTERSECTION

Krisztián Medgyes[1*], Kálmán Bolla[2] , Edit Csizmás[3], Rafael Pedro Alvarez Gil[4], Tamás Kovács[5], Csaba Fábián[6], József Osztényi[7], Papp Olga[8]

[1,2,3,4,5,6,7,8]Kecskemét College, Izsáki út 10., H-6000 Kecskemét, Hungary
**medgyes.krisztian@gamf.kefo.hu*

Abstract
This work examines the possibilities of maintaining a vehicle based mobile ad-hoc network (VANET) by a Wireless Distribution System (WDS). We introduce and treat the performance limitations of this system. In our case the examined VANET is considered to be a communication system in a busy intersection of four-lane roads, and the WDS Base Station is located in the center of the intersection. The traffic simulation is based on the Intelligent Driver Model. Computer simulation measurements of the time average of the size of the WDS network is given in this paper. It was obtained that size of the network is growing together with the density of the traffic, but, due to the highly mobile radio stations (cars) and the relatively high connection time, it is limited to the order of magnitude of several times the radio coverage.

Keywords:
wireless networking, WDS, VANET, vehicle network

1. Introduction

Wireless communication plays an increasing role in numerous area of traffic control. Even if only a few cars are participating in an ad-hoc network, a very efficient information service can be rendered for the driver in case of overtaking or a nearby accident [1]. However, if it is possible to maintain a large network participating more tens or maybe hundreds of cars, a very effective control of the traffic-flow can be achieved, which helps to avoid traffic jams. Therefore, the performance of the implementable vehicle networks became a highly studied area in the last decade [1, 2, 3, 4].
In the present work we investigate the performance of the WDS [5] in a situation, where a Base Station is set in the center if a busy intersection of four-lane roads by computer simulations. We suppose that all of the simulated cars are carrying a WDS radio station and tries to connect to the large wireless network formed around the intersection.

2. The Wireless Distribution System (WDS)

Connecting two or more wireless (distribution) systems can have several practical reasons. Wireless systems can most easily be created from Bluetooth or Wi-Fi networks. From previous publications [1] it is seen that the Bluetooth technology cannot provide coverage of suitable range, although it has low energy-consumption, which is important when implementing it on robots.
Due to the significance of range, the answer to the problem can be the Wi-Fi standard with a greater and higher quality range than of a Bluetooth solution – though with a bigger consumption of energy.
Network connections can be classified into two categories based on the type of connection. One is the Ad-Hoc connection, where two devices connect to each other directly (without an AP). The other is, when more clients connect via an AP, the connection is called an infrastructure mode in a wireless network.
There are 3 well-known wireless network modes which enable clients and APs to connect to one sub-network. First, the Wireless Client Bridge mode, which, however, disables clients to connect directly to a wireless network and makes connection possible for a client only through a wired link to an AP. The second is the Wireless Repeater Bridge mode, where incompatibility problems (potential ARP problems) with certain programs or protocols (dependent on the MAC address) may occur due to the translation of the MAC address (Proxy ARP). The third is the WDS mode, which has the advantage of the WDS-method, that it is easy to create a continuous and long-range wireless network. The equipment on the vehicles (or other mobile agents) (APs) not only connects to the Base Station in an infrastructure mode, but also transmits its signals to the other APs connected (SSID Broadcast) as a WDS Client. Thus, networks of arbitrary rooted-tree graphs can be formed without using any repeater, where the Base Station is the root. Each client must have a radio connection that leads to the Base Station directly or through another client. Let us call this connection as “uplink”.
Besides, any such a client may have more radio connection to other clients that are connected to the network only through this client at hand. So each client must have strictly one uplink and more downlinks. Thus, networks of arbitrary rooted-tree graphs can be formed without using any repeater, where the Base Station is the root (see Figure 1).

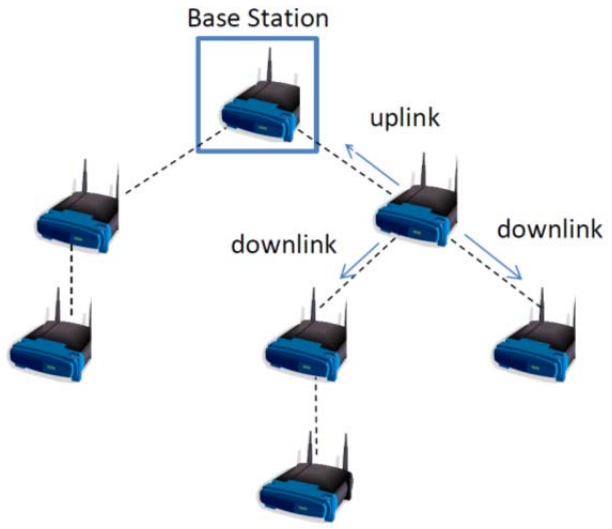

Figure 1. The typical rooted-tree graph of a WDS system

According to my measures, a client needs approximately 2 seconds to connect to the BASE STATON. (1,8 sec with use IEEE 802.11g 54 Mbps 2,4 GHz wireless adapter and 54 Mbps 2,4 GHz Access point).
To be more exact, any number of links (both wired and wireless) can connect to the points of the wireless backbone-network. For the installation of the WDS mode, all access points/devices to connect to the WDS master have to support the WDS client connection option.

Setting the WDS master:
• Select the WDS master mode in the menu of the wireless router.
• Set individual SSID network in the required field.
• Select an available radio channel.
• Note the MAC address of the WDS Master AP – it will be necessary during the setting of the clients.

Setting a WDS client:
• Select WDS client mode in the menu of the wireless router.
• Give the preset SSID in the required field.
• Give the preset channels of the WDS master.
• Give the MAC identification of the WDS master in the BSSID field.

From the encryption standards supported by the WDS, one can use the WEP and the WPA(1) standards. But irrespectively, one can use a MAC address filter, both for the connection points and the clients connecting to them. One should also consider the fact that in terms of WDS connections, the connection speed for communicating between two access points can only be the half of the connection speed of the access point at maximum.

Since the vehicles or mobile agents use little data exchange for communicating between each other, their requirements are profusely met by the wireless Wi-Fi.

3. The Intelligent Driver Model

In order to simulate realistic traffic each individual vehicle equipped with microscopic features which influence of traffic flow and produce homogenous and oscillating congested traffic, moving clusters and traffic jams. In our simulation application the driving model of Martin Treiber et al. [6] is chosen included a car-following (Intelligent Driver Model – IDM) and a lane changing model (MOBIL) [7]. Both models are collision free and simulate the human driving behaviour, too.
The used microscopic car-following model is called Intelligent Driver Model (IDM). IDM describes accelerations and decelerations of a vehicle in a collision-free way. The model inputs are the own vehicle speed (v), the bumper-to-bumper gap (s) to the leading vehicle, and the speed difference (Δv) of the own and leading vehicle. Finally the output is the acceleration (dv/dt) chosen by the driver for current traffic situation. IDM acceleration is given by

$$\frac{dv}{dt} = a\left[1 - \left(\frac{v}{v_0}\right)^{\delta} - \left(\frac{s^*(v,\Delta v)}{s}\right)^2\right] \qquad (1)$$

where

$$s^*(v,\Delta v) = s_0 + \max\left[0,\ \left(vT + \frac{v\Delta v}{2\sqrt{ab}}\right)\right] \qquad (2)$$

In this expression the desired speed (free acceleration) signed with v_0, maximum acceleration a, b is the maximum braking deceleration, and δ exponent is responsible for characterizing how the acceleration decreases with velocity. T means the desired safety time headway when other vehicles are followed, s_0 parameter is the minimum bumper-to-bumper gap to the front vehicle. For more details see [6].
Besides, the car-following model, lane changing behaviour is needed in order to get realistic description of traffic. In the real world multilane model faster vehicles take lane changing maneuvers to improve their driving positions by passing slower vehicles. The lane changing model of Martin Treiber [7] (MOBIL – Minimizing Overall Braking Induced by Lane change) satisfies two important criterions. First is the incentive criterion which is satisfied when the potential new target lane is more incentive then the old lane. Second safety criterion, the lane changing has to be performed safely, thus MOBIL also a collision free model.

The lane changing is executed when safety criterion is satisfied so that the effects of lane changing have to analyse. The deceleration of back vehicle (a_n) on new lane must be lower than a certain limit (b_{safe}) to guarantee the collision free changing. b_{safe} is the maximum safe deceleration of vehicles, as it is expressed by eq. (3).

$$\tilde{a}_n \geq -b_{\text{safe}} \tag{3}$$

After safety criterion the advantage of the target lane is computed from current neighbor vehicles (see eq. (4)). In this expression the politeness factor (p) means the degree of egoistic behavior, a_{th} is the lowest acceleration of any vehicle. In case of the expression is true the new lane is more attractive for the current vehicle. Ref. [7] describes lane changing model in more details.

$$\underbrace{\tilde{a}_c - a_c}_{\text{driver}} + p\left(\underbrace{\tilde{a}_n - a_n}_{\text{new follower}} + \underbrace{\tilde{a}_o - a_o}_{\text{old follower}}\right) > \Delta a_{\text{th}} \tag{4}$$

4. Computer simulations and results

In this work we used a simple traffic environment: a four-way intersection together with the four connected roads each with the length of 1000 meters. The roads consisted of four lanes on all of their length except the last 50 meters on the way to the intersection, where was an extra lane added for the traffic going to right. The scheme of the intersection and its turning lanes can be seen in Figure TN. Altogether N simulated cars where started from the four ends of the roads under 600 seconds uniformly distributed in time, so that equally N/4 cars started from each end. The destination of each car was chosen randomly prior to its start to be one of the other three road-ends, so that the traffic flow densities in the intersection from one road to the other three roads were equal (see Figure 2). The traffic in the intersection was controlled by a traffic-lamp system working in an "opposite-green-together" scheme as it is shown in Figure 3.

Meanwhile the traffic simulation the radio connections of the cars were also examined. A Base Station radio was fixed in the center of the intersection, and this advertised its SSID in its Radio Coverage, and it was supposed to accept an arbitrary number of connections with the nearby radio cars. According to the WDS system, this radio network originated from the Base Station was the only one in the simulation. The working algorithm of a car radio was also based on the

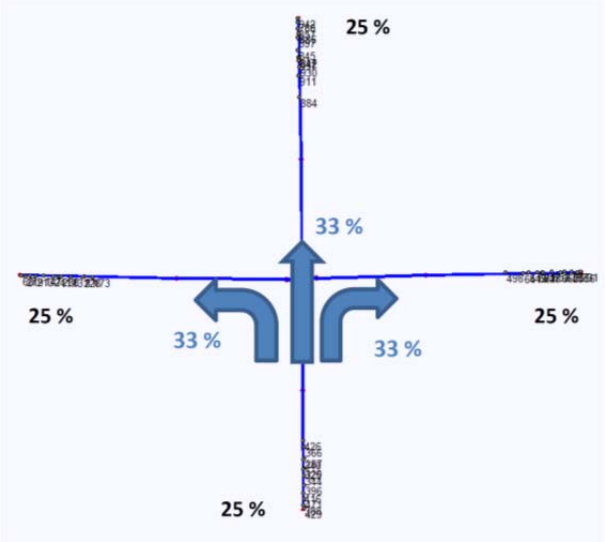

Figure 2.The main scheme of the simulated traffic environment.

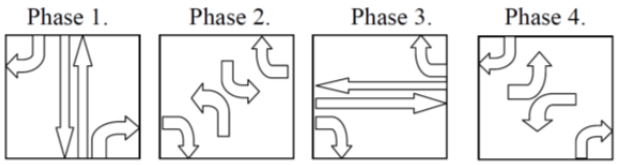

Figure 3. The opposite-green-together scheme of the applied traffic-lamp control.

WDS radio system. Corresponding to this, a car radio could connect to only one other radio as an uplink but could accept arbitrary number of connections as downlink. (An uplink connection leads toward, while a downlink leads away from the Base Station on the network tree) Besides, a radio could be in strictly one from the three following states:

1. Not connected;
2. Under uplink connecting process to another radio, which is part of the Base Station's network already;
3. Connected through an uplink to another radio, which is part of the Base Station's network already;

The algorithm of a car radio was as follows:
if it is in state 1 and there are radios within reach, then chose the closest of them and step into state 2 and start a connecting timer;

- **if** it is in *state 1* **and** there are radios within reach, **then** chose the closest of them and step into *state 2* and start a connecting timer;

- **if** it is in *state 2* **and** the connecting time is over **and** the radio chosen for connection is within reach, **then** connect to it as uplink and step into state 3; **if** it is not reachable anymore, **then** step back into *state 1*;

- **if** it is in *state 3* **and (** the radio to which it is uplinked is not reachable anymore **or** it stopped its downlinks**)**, then stop all of the downlinks of itself and step back into *state 1*;

It can be seen that the wireless network formed subject to this rules is a rooted tree, with the Base Station being the root, and if the uplink of a mobile car-radio is cut, then the whole branch, that was connected through this car will be cut from the network immediately. On the other side the building up of such a branch is much slower due to the connecting times needed for each uplink.
Meanwhile the simulations we examined the time-average and the variance of the distance of the furthest connected car, since these parameter inform us about the spatial range of the continuously changing ad-hoc network. Besides, we measured the rate of the connected cars compared to the total number of cars on roads at the moment. The parameters above were measured between the 100th and the 600th second after the start, so as to avoid the finite time effects of the simulations. (In the first 100 seconds the destination lanes and after the 600th second the starting lanes were empty). The connecting time and the radius of the radio coverage were taken to be 1.8 sec and 100 meters. The desired travelling speed of the cars was set to a fixed value for each car randomly selected from 40 km/h up to 60 km/h. The number of the cars (N) were chosen from the range of [150 ..1800]. With the help of this parameter the density of the traffic could be set, since, as it was mentioned before, all of the cars were started under 600 seconds. For example if N=1200 then 300 cars started from a source under 600 seconds, so one car started under two second. Calculated with 50 Km/h (13.89 m/s) average travelling speed, the spatial density of the traffic in this case was 1/27.78 car/meters. Note that there are two lanes for a specific direction, so this means 55.56 meters average follower's distance between the cars in one lane and 36 Km/car spatial traffic density on the two lanes leading in the same direction. For each value of N more simulations were run and finally the measured parameters were averaged.
The measured time averages of the network radius can be seen in Figure 4. It is shown by the data that the increasing traffic density results in an increasing network radius until the density reaches the value about 50 cars/Km. Above this value the radius does not grow further. This breakdown is caused by that the traffic lamp system retards the traffic and at this value of traffic density the lanes leading into the intersection are totally jammed by cars. However, it can be seen, that in the region below 50 cars/Km the network radius is in the range 200 – 600 meters, which means that in case of a non-jammed continuous traffic the communication range of the Base Station is extended to several times of its radius of radio-coverage (which is taken to be 100 meters in this work).
Even more interesting results are shown in Figure 5, where the time average of the ratio of connected cars is plotted against the spatial traffic density. The curve increases in the range 0—30 cars/Km and decreases in the range above 30 cars/Km. The reason of this behavior requires a more detailed theoretic investigation, which is outside the scope of the present work.

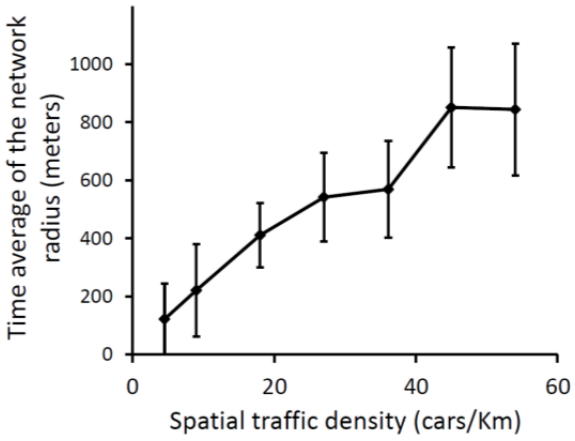

Figure 4.The measured time average of the radius of the network as a function of the spatial traffic density.

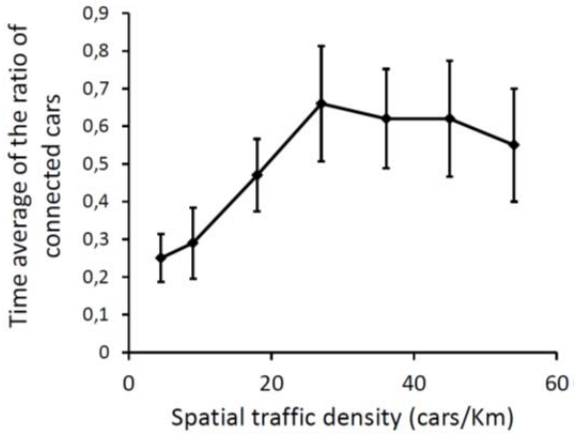

Figure 5. The measured time average of the radius of the network as a function of the spatial traffic density.

5. Conclusions

Based on the computer simulation result it can be concluded that the Wireless Distribution System with the parameters used here (connection time = 1.8 s and radius of coverage = 100 meters) is capable to extend the communication range of a Base Station situated in a busy traffic intersection. Provided that each car carries a WDS radio station, the time average of the radius of the communication network was measured as two to six times of the coverage radius of the base station under continuous (i.e. not jammed) traffic conditions. Besides, the increasing traffic density resulted in increasing network radius in a non-jammed traffic situation. It was obtained, however, that the time averaged ratio of cars connected to the network increases with the growing traffic density only in the range under 30 cars/Km.

6. Acknowledgement

This research is supported by TÁMOP-4.2.2.C-11/1/KONV-2012-0012: "Smarter Transport" - IT for co-operative transport system - The Project is supported by the Hungarian Government and co-financed by the European Social Fund.

6. References

[1] L. Briesemeister, G. Hommel: Role-based multicast in highly mobile but sparsely connected ad hoc networks, Mobile and Ad Hoc Networking and Computing, 2000

[2] M. Kafsi , P. Papadimitratos , O. Dousse , T. Alpcan , J.-P. Hubaux: VANET Connectivity Analysis IEEE WORKSHOP ON AUTOMOTIVE NETWORKING AND APPLICATIONS, 2008

[3] T. D.C. Little, A. Agarwal: An Information Propagation Scheme for VANETs, Proceedings of the 8th International IEEE Conference on Intelligent Transportation Systems, Vienna, Austria, 2005

[4] O. Tonguz, Wisitpongphan, N. F. Bai ; P. Mudalige: Broadcasting in VANET, Proc. of Mobile Networking for Vehicular Environments, p. 7-12, 2007

[5] K. Medgyes, T. Kovács: Mobile Ad-Hoc Network of Vehicles by Wireless Distribution System, 4th International Scientific and Expert Conference TEAM 2012

[6] M. Treiber, A. Hennecke, D. Helbing: Congested Traffic States in Empirical Observations and Microscopic Simulations, 2013.

[7] A. Kesting, M. Treiber, D. Helbing: General Lane-Changing Model MOBIL for Car-Following Models, 2007.

PRESSING FORCE CALCULATION FOR THE DEEP DRAWING OF END CAPS

B. Grizelj[1], M. Stoić[2*] and J. Cumin[1]

[1]Mechanical Engineering Faculty in Slavonski Brod, J. J. Strossmayer University of Osijek, Croatia
[2]College of Slavonski Brod, Slavonski Brod, Croatia
* *marija.stoic@vusb.hr*

Abstract
In this paper the basics of a deep drawing process for the production of a thick plate steam boiler end caps are shown. Also the analysis of stresses which appear in the deep drawing process are shown – bending stress, frictional stress and inner stress due to displacement of material are also shown. Afterwards some mathematical formulations are made in order to find total stresses which appear in the material during the forming process which are needed for the force calculation.

Keywords:
Deep drawing, thick plate, steam boiler

1. Introduction

The production of thick plate steam boiler end caps is usually performed in one or more work travels on hydraulic presses. The designer of hydraulic presses and the engineer responsible for deep drawing of products should be aware of the amount of deep drawing force in the process.
So far, the empirical and theoretical expressions have shown to have very different results. In order to examine deep drawing forces which appear in the deep drawing process, a tool shown in Figure 1. was used.

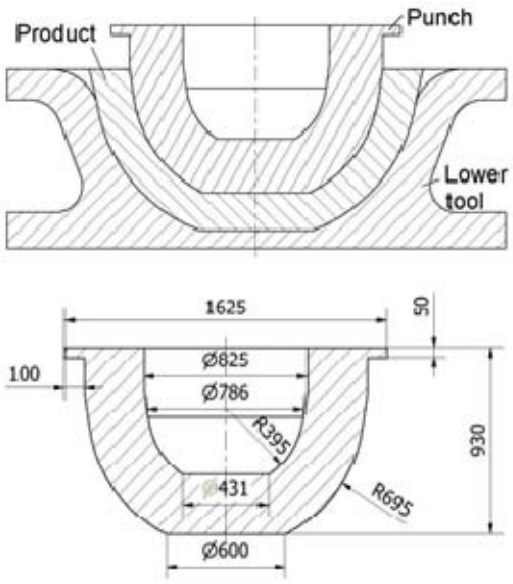

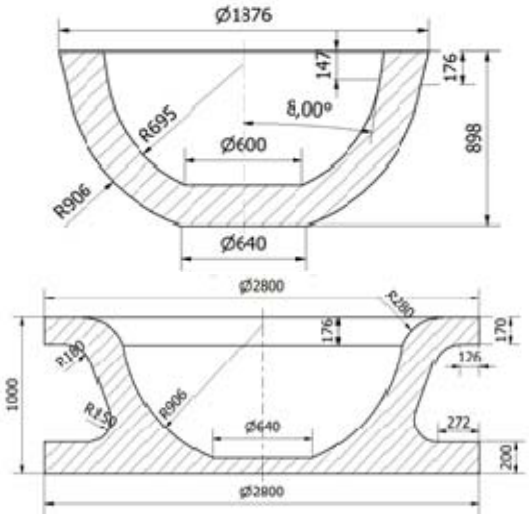

Figure 1. Experimental tool geometry and dimensions

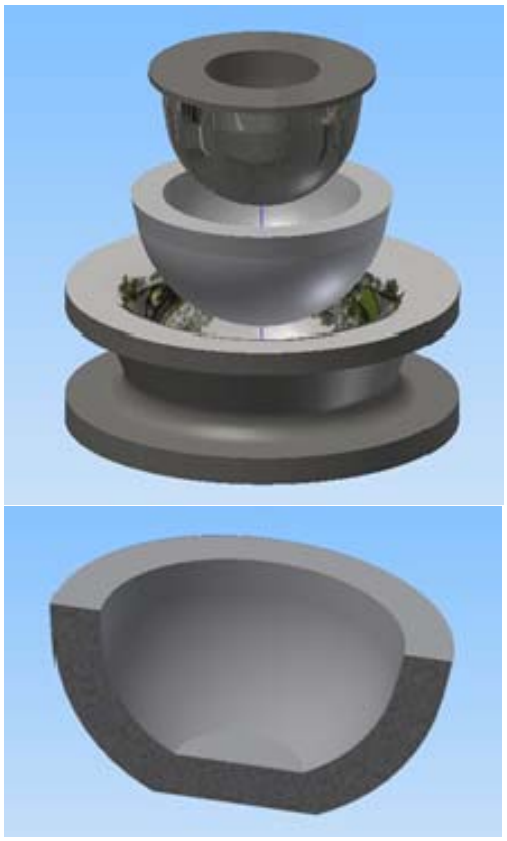

Figure 2. 3D model of experimental tool and deep drawn product

Deep drawing process is performed in such a way that first a thick metal plate (dimensions 2180 mm

in diameter and 210 mm thick) is heated-up to forming temperature, and then it is formed with tools under the pressure of hydraulic press.

2. Force calculation

In order to obtain the forming force needed for deep drawing process, it is necessary to understand which stresses act on infinitively small element which is shown in Figure 3 and Figure 4.

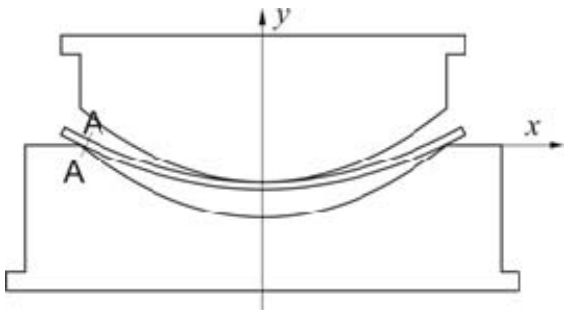

Figure 3. Schematic illustration of bending of plate with marked A-A section [1]

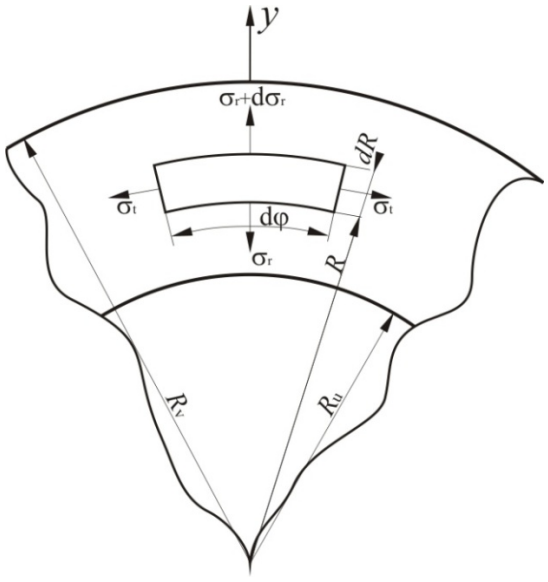

Figure 4. Stresses which act in marked section A-A form Figure 3. [1]

From Figure 3 it can be seen that section A-A is important for understanding stresses which act on the infinitive small element. This stresses are: plastic deformation stress σ_u, stress form friction over the edge σ_{fr} and bending stress σ_{bend} [1].
Total stress is calculated as:

$$\sigma_{tot} = \sigma_u + \sigma_{fr} + \sigma_{bend} \quad (1)$$

In order to obtain stress of plastic deformation □u it is necessary to use infinitesimally small element and forces acting on it which can be seen if Figure 4. [1].

From the condition that all forces in y direction are in equilibrium it can be written that:

$$\left(\sigma_r + d\sigma_r\right)\left(R + dR\right)s \cdot d\varphi - \\ -\sigma_r \cdot R \cdot s \cdot d\varphi + 2\sigma_t \cdot \sin\left(\frac{d\varphi}{2}\right) \cdot s \cdot dR = 0 \quad (2)$$

Since expression can be written for infinitesimally small angles and after dividing the expression (2) with thickness s it can be written [1]:

$$\left(\sigma_r + \sigma_t\right)dR + d\sigma_r \cdot R = 0 \quad (3)$$

In order to solve this differential equation (3) one additional expression must be introduced where kf is forming stress:

$$k_f = \sigma_r + \sigma_t \quad (4)$$

After combining expressions (3) and (4) the solution of differential equation can be found as [1]:

$$\sigma_u = k_f \cdot \ln\left(\frac{R_v}{R_u}\right) \quad (5)$$

During the forming process, a plate is moving over the filleted edge with respective radius r_M and this plate needs to overcome the force of friction. This results in the larger stress near inner radius R_u which consists from bending and friction stresses.

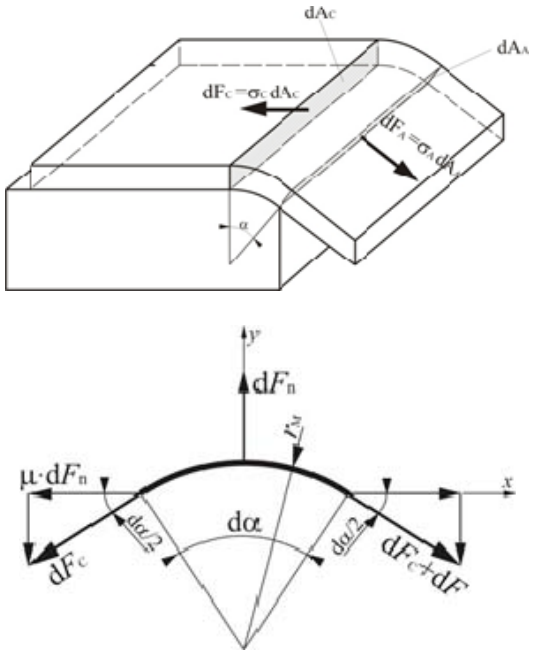

Figure 5. Schematic illustration of a plate moving over filleted edge of the tool and forces acting on the infinitesimally small element. [2]

If force dFA increases for amount dF=dFA-dFC there will be movement of sheet metal. By increasing the bending detail it can be shown that the forces which act on the bended surface looks like in Figure 5. Elementary band shown in Figure 5 has length dl=rM•dα [2].

From Figure 5, if all forces are set to be in equilibrium, and their values projected on x, and y axis, two equations can be written.

$$\sum X = 0$$
$$\left(dF_C + dF\right)\cdot\cos\frac{1}{2}d\alpha - dF_C\cos\frac{1}{2}d\alpha - \mu dF_N = 0 \quad (6)$$

$$\sum Y = 0$$
$$dF_N - \left(dF_C + dF\right)\sin\frac{1}{2}d\alpha - dF_C\sin\frac{1}{2}d\alpha = 0 \quad (7)$$

Since it can be written that:

$$\sin\frac{1}{2}d\alpha \approx \frac{1}{2}d\alpha$$
$$\cos\left(\frac{d\alpha}{2}\right)\approx 1 \quad (8)$$

Expressions (6) and (7) can be written as:

$$dF - \mu dF_N = 0 \quad (9)$$

$$dF_N - dF_C\cdot d\alpha = 0 \quad (10)$$

When this two equations are combined it follows that:

$$dF = \mu dF_C\cdot d\alpha \quad (11)$$

Total accession of force for the finite bending angle can be written as:

$$\int_{dF_C}^{dF_A}\frac{dF}{dF_C} = \mu\int_0^{\alpha} d\alpha \quad (12)$$

By integration of expression (12) it can be seen that the force of friction for one volumetric element at the end of the arc can be written as:

$$\Delta F = dF_A - dF_C = dF_C\left(e^{\mu\alpha} - 1\right) \quad (13)$$

Then it can be written that:

$$\sigma_{fr} = \frac{\Delta F}{\Delta A},\ \text{MPa}$$
$$\sigma_{fr} = \sigma_u\left(e^{\mu\alpha} - 1\right),\ \text{MPa} \quad (14)$$
$$\sigma_{fr} = k_f\cdot\ln\left(\frac{R_v}{R_u}\right)\left(e^{\mu\alpha} - 1\right),\ \text{MPa}$$

Bending stresses in the steam boiler cap will be positive in the outer tensile zone, and negative in the inner compressive zone in front of neutral plane.

This stress will increase with the thickness of the plate, and it will decrease with larger radius r_M.

Bending stress can be calculated with the following expression [2]

$$\sigma_{bend} = k_f\cdot\frac{s}{4r_M},\ \text{MPa} \quad (15)$$

This, combined with the expressions (1,5,12) leads to the following expression used for the calculation of total stresses in the material during forming [2]:

$$\sigma_{tot} = k_f\left(\ln\left(\frac{R_v}{R_u}\right)\cdot e^{\mu\alpha} + \frac{s}{4r_M}\right),\ \text{MPa} \quad (16)$$

Since total stresses are known, the forming force can be calculated with the following expression:

$$F_{tot} = A_A\cdot\sigma_{uk},\ \text{N}$$
$$F_{tot} = 2\cdot R_v\cdot\pi\cdot s\cdot k_f\left(\ln\left(\frac{R_v}{R_u}\right)\cdot e^{\mu\alpha} + \frac{s}{4\cdot r_M}\right) \quad (17)$$

There are several more expressions with which the forming force can be calculated and for the purposes of this work only two of them will be mentioned.

The expression for calculation of forming force according to DIN norm [3]:

$$F_{tot} = 2\cdot R_u\cdot\pi\cdot s\cdot R_m\left(\frac{R_v}{R_u} - b\right),\ \text{N} \quad (18)$$
$$b = 0{,}6\ \rightarrow\ \text{coefficient}$$

And the expression for the calculation of forming force according to Tomlenov [3]:

$$F_{tot} = \left(1{,}5\div 2\right)R_m\cdot\ln\left(\frac{R_v}{R_u}\right)\cdot\pi\cdot R_u\cdot s,\ \text{N} \quad (19)$$

According to Siebel's expression, the forming force can be calculated as [3]:

$$F_{uk} = 1{,}3\cdot\pi\cdot R_v\cdot s\cdot R_m\cdot\ln\left(\frac{R_v}{R_u}\right),\ \text{N} \quad (20)$$

3. Experiment

For the experiment, a steel plate of 2800 mm in diameter and 210 mm of thickness was used. During the forming plate was coated with graphite mixed with mineral oil. The temperature of heating of a steel plate was 1100°C and by the time the steel plate was mounted on the tool the temperature has dropped to 1040°C.

At the end of the forming process the temperature of the steel plate was 920°C.

The time needed for the plate to be extracted from the furnace and until the end of the forming process was 10-13 minutes. The forming process was performed in the 50 MN forming hydraulic press. In the production a 23 steam boiler caps were made, and maximal forming force was 28,6 MN.

Maximal difference of forming force in the production of 23 boiler caps was 2 MN.

Since material was heated to the medium temperature of 970°C, the forming stress and the tensile stress were assessed to 76 MPa according to the manufacturer data.

With the above mentioned data, and the use of Figure 1 (from which R_u = 695 mm, R_v = 906 mm), the forming force F_{tot} can be calculated.

From (17):

$$F_{tot} = 2 \cdot 906 \cdot \pi \cdot 210 \cdot 76 \left(\ln\left(\frac{906}{695}\right) \cdot e^{0,2 \cdot 1,57} + \frac{210}{4 \cdot 280} \right)$$

$$F_{tot} = 50022389 \text{ N} \approx 50 \text{ MN}$$

From (18):

$$F_{tot} = 2 \cdot 695 \cdot \pi \cdot 210 \cdot 76 \left(\frac{906}{695} - 0,6 \right) = 49037842 \text{ N}$$

$$F_{tot} \approx 49 \text{ MN}$$

From (19):

$$F_{tot} = 2 \cdot 76 \cdot \ln\left(\frac{906}{695}\right) \cdot \pi \cdot 695 \cdot 210 = 18477886 \text{ N}$$

$$F_{tot} \approx 18,5 \text{ MN}$$

From (20):

$$F_{tot} = 1,3 \cdot \pi \cdot 2 \cdot 906 \cdot 210 \cdot 76 \cdot \ln\left(\frac{906}{695}\right) = 31314033 \text{ N}$$

$$F_{tot} \approx 31,3 \text{ MN}$$

4. Conclusion

In this paper the basics of a deep drawing process for the production of a thick plate steam boiler end caps are shown. Theoretical analysis of stresses which appear in the deep drawing process are shown – bending stress, frictional stress and inner stress due to displacement of material are shown.

These stresses are described, and some mathematical formulations are made in order to find total stresses which appear in the material during the forming process.

Later the expression for the calculation of the forming force is shown. Also some other experimental formulations from the literature are presented.

These expressions were used for the calculation of the deep drawing force, and later the results were compared to the experimentally obtained force values in the production of boiler end caps.

The results show that the closest amount of force can be calculated with the expression (20). The difference in the results is from large amount of assumptions and simplifications used in the formulation.

Also some other forces exists in the forming process, and stresses which are caused by this forces needs to be further investigated by FEM methods in order to better understand the deep drawing process.

5. References

[1] B. Grizelj, "Oblikovanje metala deformiranjem" Strojarski fakultet u Slavonskom Brodu, 2002., pp 143-156.
[2] B. Grizelj, "Oblikovanje lima deformiranjem", Strojarski fakultet u Slavonskom Brodu, 2009., pp 169-190.
[3] M. Menzer, "Uber die mechanik des tiefziehens von Kesselboden", Dissertation, TU Clausthal 1975.
[4] K. Lange, "Umformtechnik", Springer-Verlag Berlin Heidelberg New York 1989.
[5] M. Planček, "Alati za tehnologije plastičnog deformisanja materijala", Novi Sad 2011.

BLENDED LEARNING EDUCATION IN THE CONTEXT OF ENGLISH TECHNICAL TEXTS

M. Gluchmanova

Faculty of Manufacturing Technologies of the Technical University of Kosice with a seat in Presov, Slovakia
Corresponding author e-mail: marta.gluchmanovar@tuke.sk

Abstract
The paper is focused on the basic manufacturing management terminology, such as the basic information about a company as an effective marketing tool, financial management, how is sale different from marketing, how leadership and management differ, change management, what is knowledge management, as well as market research. The author deals with the suitable technical texts concerning the manufacturing management study programme and the most useful exercises.

Keywords:
blended learning, technical text, management;

1. Introduction

Thoughts about use of new technologies show us some of the most varied and divided questions in foreign language education and classroom practice. On a far side of that divide are idealists who believe that new technologies can radically transform language education. To the idealists, digital tools provide means for viewing various media, collaborative network learning, and so forth. To others, new technologies are a great equalizer; nearly anyone can construct a level of product that a few years ago was only within the capacity of a few people with specialized training [1]. In my paper I suppose that new technologies have revolutionized our conception of knowledge – from something some people might have, to something which everyone should be able to find. The distinction has grown exponentially since the early days of the Internet. Before its inception, students relied on the foreign language education that was relatively fixed in its knowledge content. Computer-based foreign language learning in its various generations has acted to open up the world of knowledge to students and its most powerful variant, online blended learning, has become a catalyst that has enabled huge changes in what is learned and who is able to learn it [2].

2. Motivation for LMS

The important is to plan lessons taking into account the needs of all students regardless of their ability, culture, gender or motivation. For this purpose Moodle Learning Management System (LMS) has been adopted by the Technical University of Košice (Slovakia) as one of the e-learning platforms. Moodle is an open source LMS and has become very popular among teachers at the Faculties as a tool for creating online dynamic web sites for their students [3]. I suppose that The Faculty of Manufacturing Technologies will be successful with using Moodle in foreign language teaching to deliver foreign language online courses and to supplement traditional face-to-face classes (known as blended learning). Moreover, Moodle offers a wide variety of tools that can make foreign language course delivery more effective. It provides an easy way to upload and share materials, hold online discussions, give quizzes and surveys, and record grades. The term blended learning can be applied to a very broad range of foreign language teaching and learning situations. It can be commonly applied to a foreign language course where all the learners meet with the teacher in a face-to-face class, but in which the foreign language course includes a parallel self-study component such as a CD-ROM or access to web based English technical materials [4]. Use of these elements may be optional. It means that blended learning opportunities incorporate both face-to-face and online learning opportunities. The degree to which online learning takes place, and the way it is integrated into the teacher's plan, can vary across the faculties, institutes and the departments. The strategy of blending online learning with university-based instruction is often utilized to accommodate students' diverse learning styles and to enable them to work before or after school in ways that are not possible with full-time conventional classroom instruction. I suppose that online foreign language learning has the potential to improve educational productivity by accelerating the rate of learning, taking advantage of learning time outside of school hours, reducing the cost of instructional materials, and better utilizing teacher's time.
In this connection I ask questions: Why use technology in foreign language teaching? What opportunities does it offer? I suppose that using technology can be very motivating. Many students like using the computers, they prefer multimedia exercises as well as they can make their own choices as to how to work through the English technical online materials and technical texts.

3. Methodology and pedagogical consideration

In considering the use of electronic technical materials and learning environments, teachers should bear in mind: how the electronic technical material fits with the aims of the course, outcomes and objectives of the proposed learning experiences – Why am I using this technical material? What connections can I make between the electronic technical material and curriculum expectations? Next I suppose that connections between the electronic technical material and learning theory are very important – How does the resource match my beliefs about language learning?; connections between the electronic technical materials and student learning needs – How will my students engage with the resource? How does it support identified learning needs?; specific pedagogical practices needed to support the use of the electronic technical material during the foreign language teaching and learning experience – What information, skills and strategies do the student need to engage with the material? What explicit modeling and scaffolding of the necessary knowledge, skills and strategies do I need to offer? How will they be able to analyse, interpret, synthesise and evaluate the input provided by the electronic technical material?

The electronic technical materials available to support language teaching will continue to change and expand. What is critical, though, is that teacher have a clear rationale for the use of any technical materials within teaching and learning experiences [4].

English courses for specific purposes, especially for technical practices are aimed at preparing students who intend to get a job in technology. It presents them with English from a wide variety of technological fields and situations, develops their communication skills, and provide them with background in major technological concepts. For this reason I decided to choose the suitable and useful English technical texts for the students of Manufacturing Management study programme at the Faculty of Manufacturing Technologies in Presov and use them for blended learning education. I claim that knowing how to give and have the basic *information about a company* is very important for the students of manufacturing management. In a reading sections students meet a variety of technology-based texts. So they can start the basic information with reading an extract from the technical text concerning information about a company as an effective marketing tool. I suppose whatever the industry is, their company should tell the story online as interestingly and compellingly (and honestly) as possible. Customers want to know who makes the company and who is on the team. I stress that the ability to search a site is crucial. If a company does not have a clear, easy-to-navigate site, it is likely to lose the potential clients. All web users find pop-up windows very irritating. New online trends show that a presence on social networking sites and blogs is increasingly popular among customers. Social networking receives a continually stronger validation nowadays. For this reason, one of the most used pedagogical methodological step in teaching and learning is the reduction, it means the technical text is shortened in some way, for example – I can remove specific items (e.g. adjectives); combine sentences; remove clauses/sentences; rewrite in a different format; In the text above students can find the English equivalents of the given Slovak keywords, such as presvedčivý, kľúčový, vyskakovacie okno, tlačidlo, potvrdenie, pôsobivý, etc., or in the following exercises they can fill the gaps with a suitable word from the box, match English and Slovak collocations about describing a product, which seems to me very effective and interesting.

An extract from the text concerning the finance department and *financial management* is very useful for the manufacturing management students. In large companies, the finance activity is usually connected with a top officer of the company, such as the Vice President and Chief Financial Officer (CFO). Students should realize that the most important role of a financial manager is to create value from financial activities of the company. The financial manager should also analyze competitors and market trends and provide financial advice and support to colleagues and clients including both public and private sector organizations. Other main positions within a finance department are the treasurer and the controller who report to the financial manager. Treasurers direct their organization's budgets to meet its financial goals. Controllers oversee the accounting, audit, and budget departments. They also are in charge of preparing special reports required by regular authorities. It is necessary to emphasize that in the similar technical texts used the comparison/contrast means that points of similarity/difference must be identified between two or more texts, for example identify words/expressions common to both texts; identify words/phrases in one text which are paraphrased in the other; identify ideas common to both texts; identified facts present in one text and not in the other; compare grammatical/lexical complexity; Within the text above students can find the English equivalents of the given Slovak keywords, such as finančný manažér, peňažné toky smerujúce do spoločnosti, výplaty, záväzky, peňažné toky smerujúce von zo spoločnosti, pohľadávky, vedúci controllingu, riadenie peňažných prostriedkov v hotovosti, rozpočet, hlavný pokladník, etc. If students understand the accounting documents, they can write the headlines to the correct basic accounting documents, such as bill, invoice, purchase, order and receipt or

match a word from the left in Slovak language with a word from the right in English.

The students of manufacturing management should know *how is sale different from marketing***.** What is the difference between sales and marketing? This is a common question. It is important to explain them that marketing is a process for promoting products or services to a customer and sale is the activity of selling the product. For better understanding the students of manufacturing management should know that a strong marketing strategy implements: a process for discovering what customers want and targeting customer segments; a plan for developing the product or service; a method for determining pricing; a plan for promoting the product or service to the target markets. Once the product is successfully promoted to potential customers, the sales process takes place. I suppose that very useful will be to explain that an effective sales strategy includes: setting long-term sales goals; developing short-term objectives to reach the goals; creating an incentive plan for sales representatives to achieve objectives; understanding sales techniques for various customer types; utilizing marketing and promotional materials to reach the targeted customers; planning for maintaining relationships with existing customers and networking with potential customers. Both processes are essential to the success of positioning and selling products and services. Without a marketing strategy, there would be no products to sell. Without a sales strategy, products would not be sold. When the two work together, achieving sales goals and increasing the bottom line is the reward. In the context of the mentioned and similar technical texts interpretation, it means personal knowledge/experience, must be used to clarify and extend the meaning of the suitable and used technical text. Students should be able to formulate questions on the text beginning: what?, who?, where?, when?, why?, how?...; (What does this recall from your own experience?, What does this remind you of?, What associations does it have?). Students may practice understanding of the previous text by completing the dialogue with the expressions from the box, such as modern business, Sales Director, Sales Managers and Sales Representatives as well as study the words on one side, and then match them with the correct Slovak equivalent: dopyt a ponuka, presvedčiť, poučný, konečný súčet, požadovať, motivačný program, doslovne: vytváranie si kontaktov, etc.

In the following part I will point out *how leadership and management differ,* because successful management and leadership of team is critical to positive business results. There are fundamental differences between leadership and management and this fact must be emphasized to the manufacturing management students within the English course for specific purposes. The role of managers is to be tactical and direct in order to organize team activities to ensure the work gets done. It is important to recognize that not all high performing employees can take on the role of manager. It is also important to recognize that not all managers can be effective leaders. While managers focus on daily activities, the role of leaders is to produce change and motivation. They strive to understand what motivates their employees and work toward finding ways to inspire them intrinsically towards success and guide them through change. While leaders and managers ultimate goal is to present effective outcomes in the work produced, their approaches to get there are different. It is essential to have both roles within an organization. Management's organized and controlled approach to completion of tasks and leaderships motivation to reach the goals that these tasks are set to attain, provide the framework for a successful team. For practicing the suitable vocabulary in the given text I state that when the text is chosen according to some given criterion, then we speak about selection/ranking: students can choose the best text for a given purpose (e.g. inclusion in a teenage magazine); choose the most/least (formal, difficult, personal, complex…) text; choose the text most/least like the original version; choose words from a text to act an appropriate title. Students can complete the sentences with the suitable keywords such as managers, leaders, management and leadership as well as practice and choose the correct prepositions in the sentences concerning leadership and management.

In next part it could be stressed that *change management* plays an important role today, because the rate of change and development in the business world is always increasing. New competitors, new markets, new technologies, new products all result in an enterprise having to embrace change to remain successful. How can an organisation know when change is necessary? It is suggested that organisations should embrace change when they are doing well; they should not wait until things take a turn for the worse. It is doubtful that many organisations follow this advice. It is more likely that traditional indicators such as sales information can be used to decide when and what to change. How can an organisation achieve change? Financial and accounting information can help in the planning and implementation of change. However, I state that a key factor in the successful implementation of change is that organisations must "learn to learn", because the traditional top-down, authoritarian way of doing things is not flexible enough to cope with today's rapidly changing business environment. There are five factors that help make an organisation a "learning organisation": personal mastery – an employee's desire for lifelong learning to continually update that employee's set of job skills; the creative use of mental

models – all employees should question all aspects of a company's organisation; building a shared vision – the vision of the company's future must be positive, innovative, constantly evolving and something that all employees wish to achieve; team learning – employees need to think and learn together. Teams need to learn, not just individuals; systems thinking – this requires a wide vision across all sectors of an organisation. In fact the concept of "a sector" within a company is not useful. Activities in a company should be seen as a whole. It is also important to recognise patterns across an organisation, even in complex circumstances. If a company can become a learning organisation then it should be able to bring about successful organisational change. In the texts concerning change management teachers can work with the suitable technical texts which could be restored to an incomplete or defective text, this is called reconstruction - coherence/completeness, when appropriate words/phrases can be inserted into gapped text; reordered jumbled words, lines, sentences, paragraphs and so on or removed sentences/lines which do not "belong" in the text. Students study the text above and complete the suitable text with the correct form of some verbs or they can add the missing words to complete the summary of the article.

In the following part I ask question: What is *knowledge management*? I suppose that it should be very important for manufacturing management students to have more information about these facts. Organisations believe having better information leads to better decision-making. However, with greater access to information comes the problem of information overload – which pieces of information are important to make the best decision? The problems of selecting and obtaining the right information and the ability to use this information to make decisions which can give the organisation a competitive advantage gave rise to the field of knowledge management, or KM, and it is being adopted by more and more businesses today. In order to understand what knowledge management is, it is necessary to define what knowledge is. Knowledge can be defined as the know-how that comes from experience and understanding of a situation. For the time being, only humans, and not computers, can provide an organisation with the knowledge it needs to succeed and the combined knowledge that the employees of an organisation possess is often termed its intellectual capital. KM can be divided into 2 parts. The activity of obtaining the best information which often relies on technology such as having powerful computers to filter or store information, or good networks of communication so that knowledge can flow easily through organisation; and the more human side which focuses on employees exploiting the information in order to create competitive advantage for the organisation, perhaps by producing an idea which customers will want. Companies which nowadays adopt KM strategies believe that they will achieve better results because they harness the potential of both modern technological advances and good old-fashioned experiences. For practicing of used technical vocabulary in some cases the technical text must be expressed in a form different from the original without loss of essential meanings. It is called reformulation. Key words can be used to rewrite a text or students can rewrite it in a different style/mood. Knowing information about KM, students look at the sentences concerning knowledge management and decide whether they are true or false or they can match the parts of the sentences which provide a complete definition.

I state that if students want to have successful business, they need to know what their customers want or need. So we can speak about m*arket research.* People often think they know what their customers want, but they would not make assumptions. There are several ways to find out what they want. These practical methods can help students to get the feedback they need: Your employees often meet with your customers. Get feedback on what the customers ask for or what they complain about. Keep records of what customers are buying and not buying from you. For practising market research students can prepare comment cards with questions like: Were you satisfied with our services? How could we provide the perfect services? Are there any services you would like to see that do not exist yet? Know what your competition is selling. Perform surveys. Provide an incentive to the customers to encourage them to complete the survey. Students will get a wealth of information if they ask the right questions. A correspondence must be found between the technical text and something else – this is matching, for example match a text with a visual representation; match text with a title; match text with another text; match text with a voice/music; Students practise vocabulary by matching the collocations – which words collocate with market or marketing, for example market leader, market share, marketing campaign, marketing mix, marketing strategy and marketing agency. Next activity matches the English and Slovak verbs describing trends, such as "to reach a peak" - dosiahnuť vrchol; "to hit a low" - klesnúť na dno; "to boom" - prudko narásť; "increase tenfold" - vzrásť desaťnásobne, etc.

Considering the following exercises in online blending learning are e.g. to match the beginning of each phrase about success or strong interest from column A with its explanation in column B, such as: If the company is calling the tune, it is number one in the market; or If you kill two birds with one stone, you do two things at the same time. Next procedures and decisions only the teacher can properly make involved creating text.

The technical text is to be used as a springboard for the creation of new texts (for example students can write a parallel text on a different theme; use the same title but write a new text; add lines/sentences to the text to reshape it; combine these texts to create a new text). The next one is analysis, when the technical text is to be submitted to some form of language focused scrutiny (e.g. how many different tenses are used?, Which are most/least frequent?, How many content (or function) words does the text contain?, List all the words to do with (the sea, movement, ecology, etc.) in this text. The last one I would like to stress is project work – the text is used as a springboard for some related practical work with a concrete outcome. This text presents a particular point of view, prepare an article which either supports or disagrees with this point of view, collect ideas and examples to support their own point of view.

3. Conclusion

I state that the chosen technical texts give specific skills practice especially in reading and understanding. The ability to read and understand texts in English has never been more important in technology than it is today with the amount of written information available on the Internet, the majority of which is in English. A blended approach sees the role of teacher and technology as complementary. In conclusion, it can be seen that the term blended learning can have a range of meanings. We have defined it as referring to a language course which combines a F2F (face-to-face) classroom component with an appropriate use of technology. The technology can be integrated into the English language lessons, or be used by learners outside the classroom for further practice, and to complement the taught element of the course.

4. Acknowledgement

This paper is supported by KEGA, contract No. 013TUKE-4/2012 “Application of E-learning in Foreign Language Teaching at the Faculty of Manufacturing Technologies.“

5. References

[1] M. Ally, “Foundations of Educational Theory for Online Learning,” In: Anderson, T. & Elloumi, F. (Eds.) *Theory and Practice of Online Learning* (pp. 3-31). Athabasca University. Athabasca, Alberta.

[2] R. Bielousová, “On the issue of blended learning in foreign language teaching,” In: *SGEM* 2013 : 13th International Multidisciplinary Scientific Geoconference : Ecology, Economics, Education and Legislation: conference proceedings: vol. 2: 16-22 June, 2013, Albena, Bulgaria. Sofia: STEF92 Technology, Ltd, 2013. p. 469-474. ISBN 978-619-7105-05-6.

[3] R. Bielousová and M. Gluchmanová, “Essential English for Manufacturing Technicians,” FVT TU: Prešov, 2011.

[4] E.H. Glendinning, “Technology I.” Oxford: Oxford University Press, 2008.

THE POSSIBILITIES OF THE USAGE OF NEURAL STRUCTURES TO EVALUATE THE EXPERIMENT

Peter Michal[1*], Ján Pitel[1], Alena Vagaská[1], Miroslav Gombár[2] and Ján Kmec[2]

[1]Faculty of Manufacturing Technologies with a seat in Prešov, Technical University of Košice, Slovakia
[2]Faculty of management, University of Prešov, Slovakia
Corresponding author e-mail: peter.michal@tuke.sk

Abstract
Paper shows the possibility of using various types of neuron units (first order neural unit, second order neural unit, third order neural unit) for creation of prediction model that describes thickness of aluminium oxide layer during the process of anodic oxidation of aluminium. It also shows minimal range of training data for the learning process, so the neural unit can produce sufficiently reliable model.

Keywords:
Neural unit, prediction model, anodizing

1. Introduction

Pure aluminium and its alloys, as weight-reducing materials, are becoming more significant not only from technical, but also from technological and economical standpoint [1]. Mostly in aerospace and automobile industries, where light and sturdy structures are preferred [2]. Using these materials for moving parts presents a great challenge when high resistance to abrasion and wear is required. These tribological properties can be improved by anodic oxidation of components surface. Planned DoE experiment is one of the basic tools which helps to show the influence of input variable on outputs [3].The optimum selection of process conditions is an extremely important issue as these determine surface quality of the manufactured components[4]. The mathematical modelling of the process involves several parameters that may lead to difficult analytical solution [5]. On the other hand, use of artificial intelligence for evaluation of experiments results has its merits. Mainly because of faster and more reliable creation of prediction model for the studied process, compared to classic statistical methods [6].

2. Methods

Based on DoE, we have oxidized 46 samples of alloy EN AW 1050A. Chemical composition of electrolytes was in accordance with central composite design of experiment. Composition of electrolyte was influenced by amount of sulphuric acid in electrolyte (factor x_1), amount of oxalic acid in electrolyte (factor x_2) and amount of aluminium cations in electrolyte (factor x_3). Operating conditions were: electrolyte temperature (factor x_4), time of oxidation (factor x_5) and applied voltage level (factor x_6). Naming of observed factors and their levels in natural and coded scale are shown in Table 1.

Table 1. Factors level in nature and coded scale.

Factor		Factor level				
Code scale	***Natural scale***	-2,37	-1	0	+1	+2,37
x_1	H_2SO_4 [g.l^{-1}]	33,51	130	200	270	366,5
x_2	C_2H2O_4 [g.l^{-1}]	1,49	7	11	15	20,51
x_3	Al^{3+} [g.l^{-1}]	0,18	5	8,5	12	16,82
x_4	T [°C]	-1,78	12	22	32	45,78
x_5	t [min]	6,22	20	30	40	53,78
x_6	U [V]	5,24	8	10	12	14,76

We have measured the thickness of aluminium oxide layer on each sample after the oxidation. Layer thickness was measured in the area with surface current density 1 A·dm^{-2}.
We have used three types of neural units for the compile of prediction model: 1st order HONU (**H**igher-**O**rder **N**eural **U**nit) (linear neuron unit), 2nd order HONU (quadratic neural unit) and 3rdorder HONU (cubic neuron unit). These neural units compiled the prediction model based on adaptive optimization algorithm - Levenberg-Marquardt [6].

3. Results

We have gradually reduced range of training data during the neural unit's learning process. At first, we have used all of the 46 measurements of AAO (anodic aluminium oxide) layer thickness. The number of AAO layer thickness values was reduced by one with each subsequent iteration of the learning process. The lowest range of training data was 10 measurements of thickness. Table *2* shows learning error (sum of square errors for learning process for linear neural unit - sse_{LLNU}, quadratic neural unit - sse_{LQNU} and cubic neural unit -sse_{LCNU}) for each neural unit in select range of training data (number of training values - NoTV).

Table 2. Learning error of neural units

NoTV	sse_{LLNU}	sse_{LQNU}	sse_{LCNU}
46	480.48	100.82	0.88
40	464.59	47.60	$2.21 \cdot 10^{-2}$
35	430.74	28.17	$9.74 \cdot 10^{-11}$
30	388.22	10.46	$7.08 \cdot 10^{-11}$
25	321.53	1.75	$6.46 \cdot 10^{-11}$
20	298.42	1.11	$5.70 \cdot 10^{-14}$
15	284.64	$2.55 \cdot 10^{-13}$	$1.26 \cdot 10^{-14}$
10	61.33	$8.83 \cdot 10^{-23}$	$1.04 \cdot 10^{-23}$

From shown sums of squared errors (Table *2*), we can assume that each type of neural unit can produce more reliable prediction model with less training data.
However, process of verification denies this assumption. Table *3* shows sum of squared errors between measured and calculated values of AAO layer thickness for each neural unit. It can be concluded fromTable *3* that with decrease in amount of training data also decreases the reliability of prediction of AAO layer thickness. FromTable *3*it can also be concluded that CNU has the best prediction capability. It also shows that CNU is able of better prediction with 15 measurements of AAO layer thickness, as compared to LNU with all 46 measurements of AAO layer thickness.

Table 3. Sum of square errors for linear, quadratic and cubic neural unit

NoTV	46	35	23	15
LNU	480.48	494.30	614.43	664.16
QNU	100.82	1556.83	1954.48	657.03
CNU	0.88	10.19	284.75	328.32

Error! Not a valid bookmark self-reference.shows reliability of each neural unit for prediction of AAO layer thickness. Just as Table *3*alsoTable 4 shows that cubic neural unit has the best prediction capability.

Table 4. Adjustment for linear, quadratic and cubic neural unit

NoTV	46	35	23	15
LNU	62.73	61.70	54.71	48.64
QNU	92.77	63.38	69.75	63.34
CNU	99.93	99.24	79.18	74.71

Figure *1*, Figure *2* and Figure 3 show a comparison of measured and predicted AAO layer thickness values for linear, quadratic and cubic neural unit. Each unit used all of the 46 measurements of AAO layer thickness during the learning process. Straight lines of ideal (error-free) prediction were plotted in the graphs chart along the values of AAO layer thickness. Prediction of given neural unit is more precise the closer predicted points are to the line of ideal prediction.

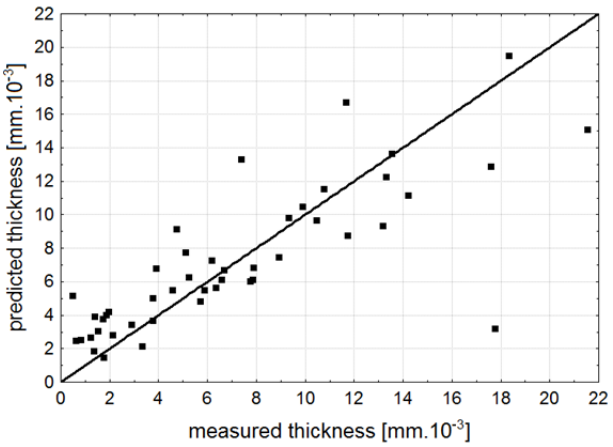

Figure 1. Validation of LNU for training process with 46 training data

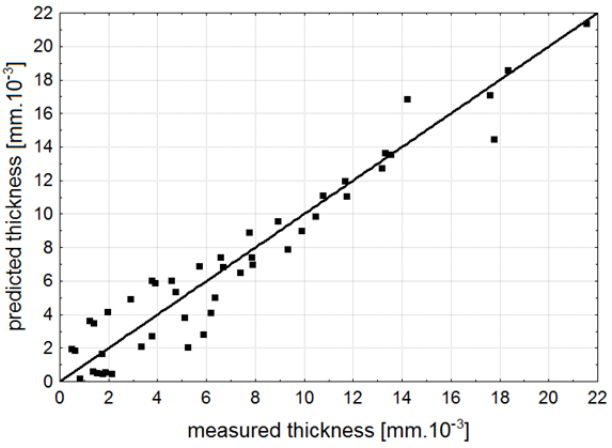

Figure 2. Validation of QNU for training process with 46 training data

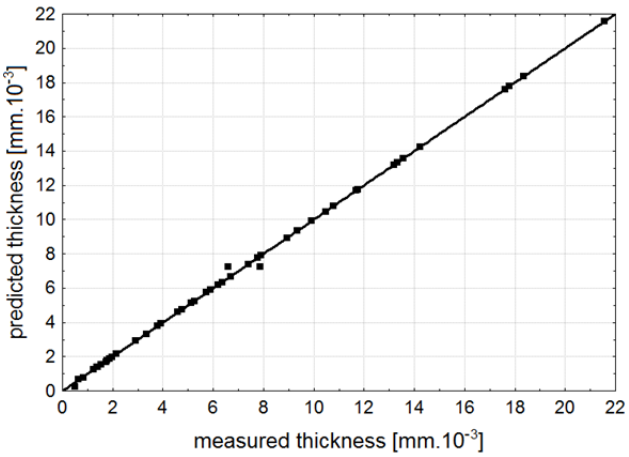

Figure 3. Validation of CNU for training process with 46 training data

Figure 3 shows that CNU was able to create almost perfect prediction model. Figure 2 shows that QNU was able to create a model with high prediction capability. However, this prediction model shows a considerable difference between measured and calculated AAO layer thickness. These differences are significant when the thickness of AAO layer is between 0.00 mm·10^{-3} and 6.00 mm·10^{-3}.Using tested prediction model foroptimalization of anodic oxidation of aluminium is possible but only under certain conditions. Linear prediction model created by LNU (Figure 3) shows significant error for all used values. Therefore, it is possible to use this prediction model only as indication to the AAO layer thickness. Use of this model for optimalization of aluminium anodizing is impossible.
Figure *4*, Figure *5* and Figure *6* show a comparison of computed and measured AAO layer thickness for linear, quadratic and cubic neural units, which used 35 values of AAO layer thickness during their learning process.

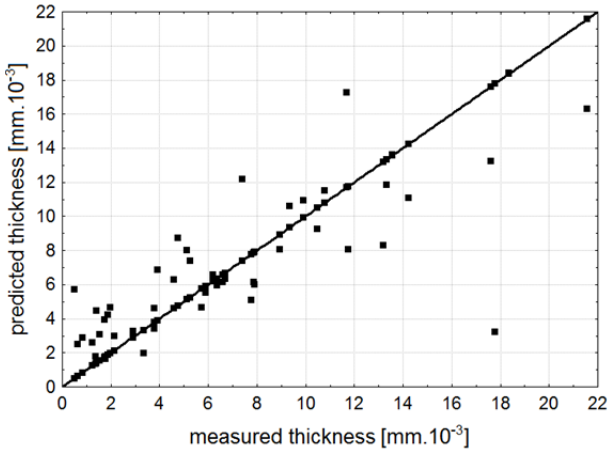

Figure 4. Validation of LNU for training process with 35 training data

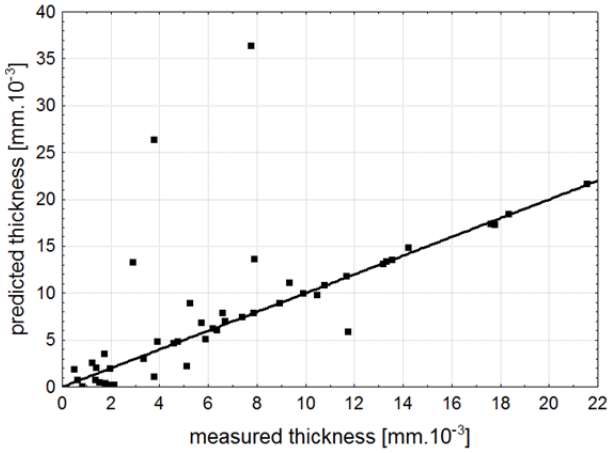

Figure 5. Validation of QNU for training process with 35 training data

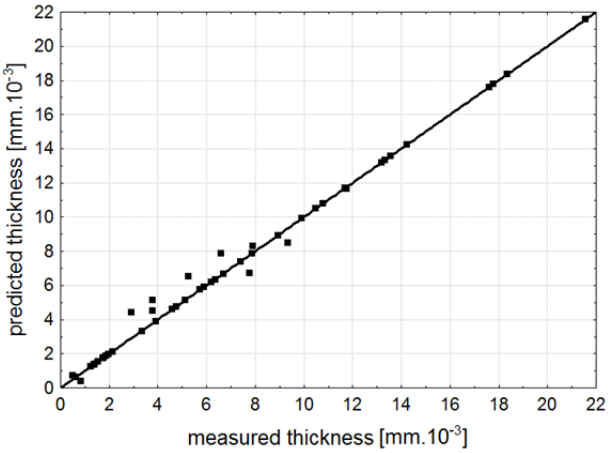

Figure 6. Validation of CNU for training process with 46 training data

Linear prediction model (Figure *4*) is still usable only for approximate calculations -it is the same as for model with 46 training values. Figure *5* shows that error for quadratic prediction model is too large (almost 25.00 mm·10^{-3}) for the model to be usable. Its accuracy is further reduced with a decrease in amount of training data. Cubic prediction model (Figure *6*) is still very reliable.
Figure *7* and Figure *8* show a comparison of measured and predicted AAO layer thickness for linear and cubic neural units, which used 23 values of AAO layer thickness during their learning process. Linear prediction model (Figure *7*) loses the capability to provide even an approximation– difference between measured and calculated AOO layer thickness was greater than 10 mm·10^{-3}. As shown on Figure *8*, cubic prediction model loses its high accuracy because CNU was unable to create a sufficiently accurate prediction model only from 23 values used as training data. Therefore, cubic prediction model can only be used for approximation.

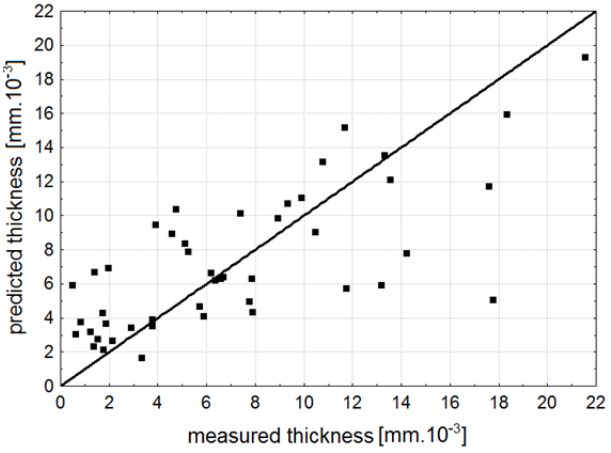

Figure 7. Validation of LNU for training process with 23 training data

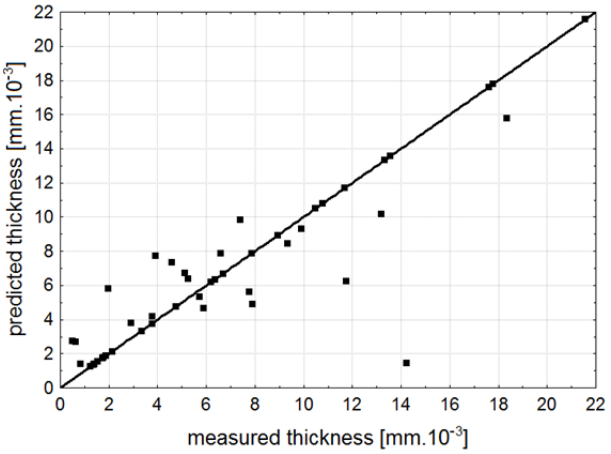

Figure 8. Validation of CNU for training process with 23 training data

Figure 9 shows measured and predicted values of AAO layer thickness, using model created by cubic neural unit that used 15 values of AAO layer thickness as training data. This model can be used only for approximation – it is the same as for model with 23 values used as training data (Figure 8).

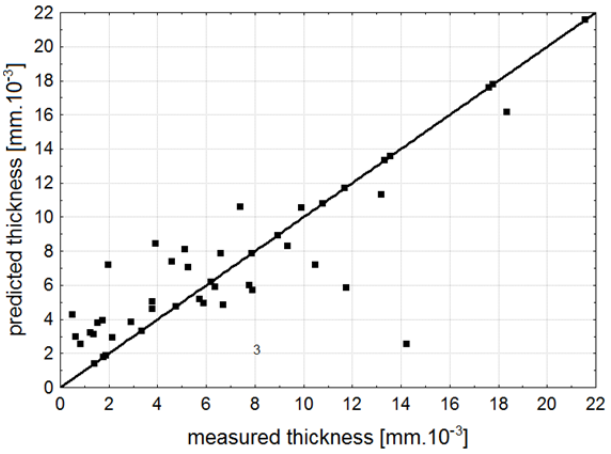

Figure 9. Validation of CNU for training process with 15 training data

Table 5 shows average computation error for the created AAO layer thickness using linear, quadratic and cubic neural units that used 43, 35, 23 and 15 values of AAO layer thickness as training data. If we consider results shown in Figure *1*toFigure *9*, we can conclude following. Prediction model is considered very accurate if the average error is ranging from 0.00 to ±0.50. Prediction model is considered accurate if the average error is ranging from 0.00 to ±1.50. Prediction model can be used only for approximation if the average error is ranging from 0.00 to ±3.50.Prediction model is considered unusable with average calculation error greater than ±3.50.

Table 5. Average error for linear, quadratic and cubic neural unit

NoTV	46	35	23	15
LNU	±3.23	±3.28	±3.66	±3.80
QNU	±1.48	±5.82	±6.52	±3.78
CNU	±0.14	±0.47	±2.49	±2.67

4. Conclusion

In conclusion, this paper shows that use of higher-order neural units has great potential for evaluation of experiments results. With properly selected range of training data, it is possible to create prediction models with reliability greater than 95.00 %. Such high reliability offers possibilities for off-line optimalization of examined production processes. The usage of developed prediction model allows us to reduce the operating cost and simultaneously create desired value of AAO layer thickness. Finally we can state, that it is possible to increase the corrosion resistance of treated components and extend their lifetime.

5. Acknowledgement

The research work is supported by the Project of the Structural Funds of the EU, Operational Programme Research and Development, Measure 2.2 Transfer of knowledge and technology from research and development into practice. ITMS code: 26220220103.

6. References

[1] J. Baumeister, J. Banhart, M. Weber, "Aluminium foams for transport industry", *Materials &Design*, vol. 18, pp. 217-220, 1997.

[2] L.A. Dobrzanski, M. Krupinski, J.H. Sokolowski,"Computer aided classification of flaws occurred during casting of aluminum", *Journal of Materials* Processing Technology vol.167, pp. 456-462, 2005.

[3] A. Vagaská, M. Gombár, J. Kmec, "Optimalizácia hrúbky zinkového povlaku lineárnym programovaním**",**in *Automatizácia a riadenie v teórii a praxi 2012*, Košice: TU, 2012,s. 64-1-9.

[4] K. Durmus, "Prediction and control of surface roughness in CNC lathe using artificial neural network", *Journal of Materials Processing Technology*, vol. 209, pp. 3125–3137, 2009.

[5] L.E. Zárate, F.R. Bittencout, "Representation and control of the cold rolling process through artificial neural networks via sensitivity factors",*Journal of Materials Processing Technology*, vol. 197, pp. 344–362, 2008.

[6] P. Michal, I. Bukovský, "Porovnanie možností použitia základných štruktúr neurónových sietí pre riadenie procesu anodickej oxidácie hliníka", in *Proceedings of the annual meeting New methods and procedures in automatic control, instrumentation and informatics,* Prague: CVUT, 2013, pp. 29-33.

THE CONTROL THE ACCURACY OF CNC MACHINE TOOLS BY SYSTEMS AXISET CHECK-UP AND BALLBAR QC20-W

D. Krchová[1], I. Kuric[2], A. Tofil[3]

[1]Faculty of manufacturing technologies with seat in Prešov, Technical university in Košice, Prešov, Slovakia*
[2] Faculty of mechanical engineering, University of Žilina, Žilina, Slovakia
[3]The Institute of Technical Sciences and Aviation, The State School of Higher Education in Chełm, Chełm, Poland
* denisa.krchova@tuke.sk

Abstract
The major objective of this paper is to refer to importance of diagnostics of machine tools. It analyses the current state of the newest control systems which are on the market. First, it´s described a system AxiSet Check-up with its benefits. Then, this paper describes a device-Ballbar QC20-W for analyzing the accuracy of CNC machine tools. It demonstrates testing and its 3- setup, scanning data and analysis.

Keywords:
Diagnostics, accuracy, machine tool, testing, measurement

1. Introduction

The right technical diagnostics of CNC machine relates to the length of its life and to the accuracy of machining part, too. Permanent control of technical condition prevents the failure factors that can cause a reduction in the life of machine parts of machine tools and workpiece inaccuracy.
Modern diagnostics and appropriate planning of repairs and service work is one of the elements which are ensuring safe and reliable operation of the machine tool, leading to cost-effective operation of all industrial facilities.
Running the machine tools in "errors" mode is risky and maintenance at strict intervals is unnecessarily expensive. In addition, another searching for errors is more time consuming than subsequent repair. The accuracy of machine tools can be verified by one of the diagnostic systems, which are presented below.

2. The control system AxiSet Check-up

The Renishaw company has extended its range of systems for calibration and testing machine, which is a leader on the market, by introducing AxiSet Check-up - *(Fig 1).*

Figure 1.The system AxiSet Check-up

It is a new cost-effective solution for checking the alignment and positioning performance of rotary axes. In just a few minutes, users of five-axis machining centres and mill- turn machines can identify poor geometry and machine alignment. These errors can cause delay of adjustment and production of non-conforming part.
Installation is quick and easy. When performing a test, a user can quickly locate a supplied calibration sphere within the machine tool's working envelope using a magnetic mount.
A touch probe is then programmed, using the supplied custom macro software, to automatically take reference measurements around the sphere *(Fig.2).*

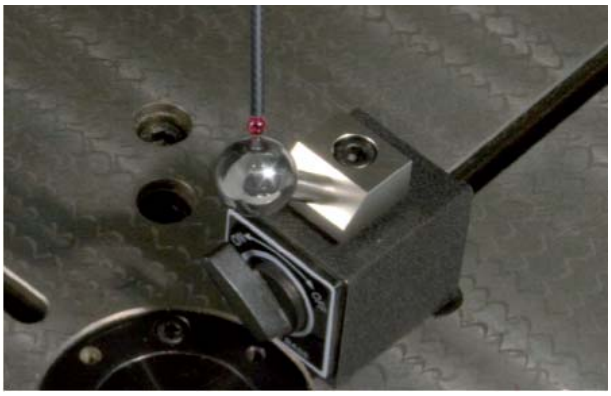

Figure 2.Reference measurement around the globe

The users have full control and can define their own test angles to ensure that the machine tools are tested in critical directions. To ensure maximum test accuracy, it is recommended to use high-precision strain-gauging sensor by company Renishaw.

Benefits of AxiSet Check-up:

- ✓ Ability to measure and deliver results of multi-axis machine performance in a matter of minutes.
- ✓ Ability to detect and report errors in rotary axis centre of rotation (pivot points) that are critical in 5 axis interpolation
- ✓ Fully automated probing tests provide accurate and consistent results, avoiding introduced errors associated with manual tests. *(Fig.3)*

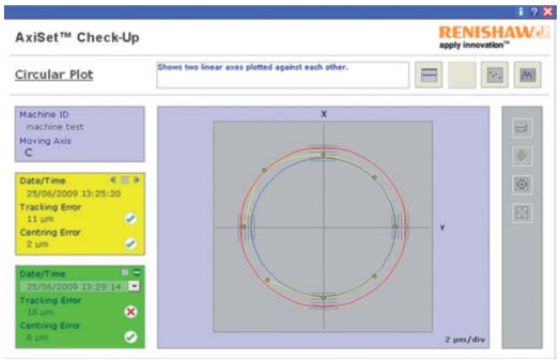

Figure 3.Pie graph

- ✓ Test angles set by a user allow machines to be tested at critical orientations *(Fig 4.)*

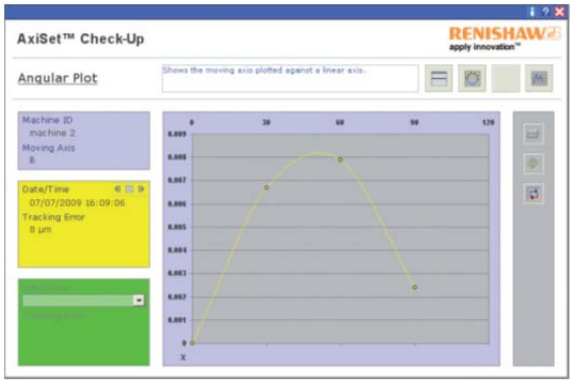

Figure 4.Angle graph

- ✓ Function of tolerances increase confidence before machining critical features.
- ✓ Functions of history and comparison allow performance to be tracked over time thus allowing trends to be monitored and maintenance scheduled *(Fig. 5)*

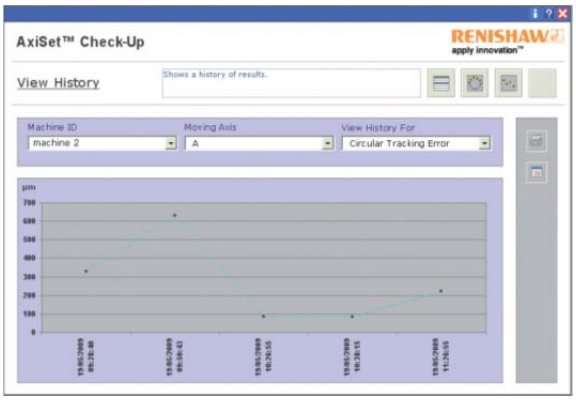

Figure 5.History graph

- ✓ Graphical reports combined with tolerance checking quickly identify changes in performance caused by collisions or settings errors.
- ✓ All graphical depictions are available in printed reports for record keeping and distribution.

3. The system Ballbar- analysis the accuracy of CNC machine tools

The calibration systems are used for diagnostics and control of machining tools. They evaluate deviations based on measured values in accordance with international standards such as ISO 230-4 and ASME B5.54. A device Ballbar is one of such system which has built-in length sensor.

The QC20-W ballbar is a completely new design featuring a linear sensor developed by Renishaw. This design is user-friendly and offers enhanced durability and allows the QC20-W to be used for testing even in "closed door" manufacturing where access for wiring can raise safety and procedural issues.

Ballbar system is practical and convenient device for analyzing the accuracy of CNC machine tools.

The new design also allows testing in 3 orthogonal planes through a single reference point *(Fig.6)*. A single, simple hardware set up means quicker testing and the ability to produce a representative volumetric measurement of positioning accuracy.

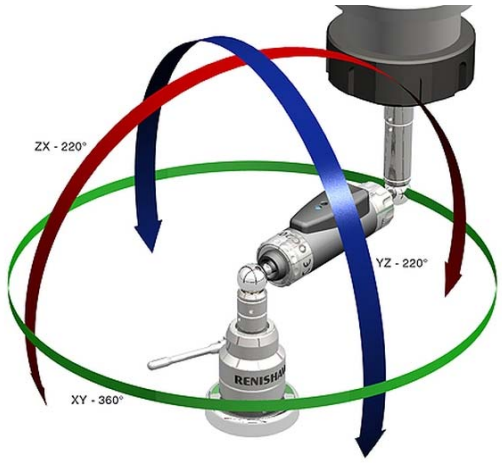

Figure 6.The wireless system Ballbar QC20-W-testing of a machine tool in 3 orthogonal planes through a single reference point

The QC20-W ballbar retains the principle of a simple CNC circular program, and powerful software. Together, these can quickly diagnose and quantify machine positioning errors including, servo mismatch, stick-slip errors, backlash, repeatability, scale mismatch and machine geometry as well as giving an overall circularity error value.

2.1 Testing

If the circular orbit is programmed on CNC machine and accuracy of positioning was perfect, then the path of machine tool corresponds with the programmed circular path. In practice, however, many factors of geometry of the machine tool, a control system and abrasion cause that the radius of circle declines from the programmed circle *(Fig.7).* If it is possible to measure the real circular path and compare it with the programmed path, the scale precision of CNC machine is obtained. This is the basis for testing by the telescopic system ballbars and ballbar QC20-W.

Figure 7.Testing by QC20-W ballbar with new function including of a partial arc

Testing system Ballbar consists of 3 simple steps:

- Setup:

The center pivot is placed on the machine table and spindle moves to the reference point and the „zero“ axis of test are set. The spindle moves to the initial position of the test and QC20-W is fixed between two magnetic kinematic joints. It is necessary to prepare a simple program for circular interpolation commands with G02 and G03.

Figure 8.Setup

- Scaning data:

1. Testing of a partial arc 220 °:

Before running the QC20-W, a plane which is vertical to XY plane needs to be tested. Now it is possible to accomplish tests in 3 orthogonal surfaces without repositioning the center pivot. The point is in the ability of system QC20-W to move along the path of the limited arc (220 °) at two levels. It leads to a modified analysis of the testing arc, but it also achieves a total value of circularity.
If these three tests are done around one point, it is possible to use a report of volumetric diagnostics which provides additional information faster previous systems.

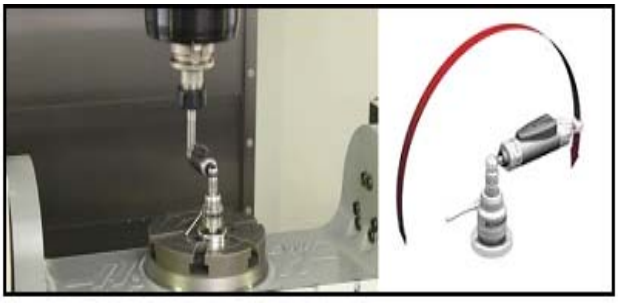

Figure 9.Testing of a partial arc 220°

2. Testing 360 °:

Standard test requires the machine tool to do a path of two consecutive circles – both clockwise and counter-clockwise. In practice, an additional arc is added before and behind the testing circle which enables an acceleration and deceleration of the machine tool. It is possible to choose the

testing radius of the test by lengthening bar-stock to reflect the size of the machine tool and sensitivity to specific problems (e.g. circles with a large radius are better for highlighting errors of geometry of the machine tool). The basic test is very fast if set correctly.

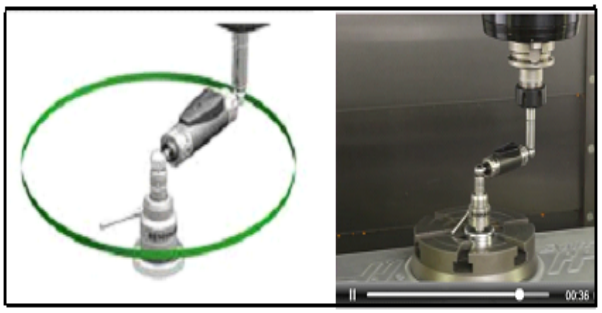

Figure 10.Testing 360°

- Analysis:

The user has a choice of several formats of reports in accordance to the international standards (e.g. ISO, ASME) and complex diagnostics - Renishaw (including volumetric analysis) with several different screen shots and references to the manual. Many reports may be adapted and the final result can be used for written messages using the function "copy and paste".

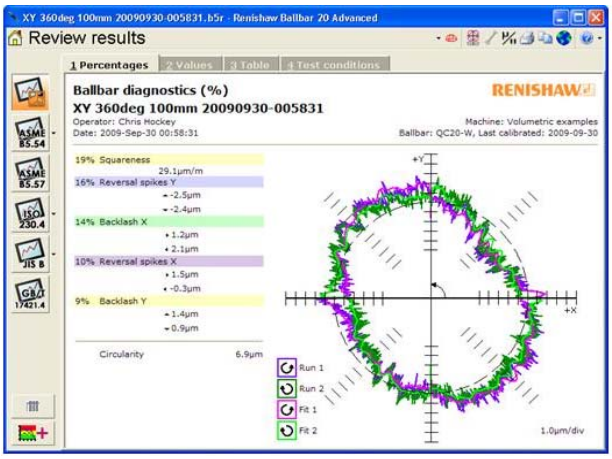

Figure 11.Table of measured values and final diagnostics

8. Conclusion

Dimensional and surface defects can be a result of a defective instruments, attired spindle or fixing work piece but the errors of a machine tool are usually attributed to the errors of the machine tool itself.

Problems are the results of geometric errors, dynamic errors and the feed rates of machine tool. Number of errors can be corrected in a few minutes – knowledge of type and their location required. It is irrelevant whether the machine tool is new or old because all devices tend to have errors. The secret of manufacturing without failures lies in the knowledge of accuracy and possibilities of production of own machine tools. It helps to plan production and make adjustments.

Therefore, it is important to check the accuracy of the machine tool regularly, and no less important it is to check it before machining.

Data were investigated by the machining test with subsequent control. That process was a time consuming and provides only a limited assurance, which was different than the standard workpiece.

The Ballbars systems, made by Renishaw, are dominant on the market for almost 20 years and this leading continues to this day by wireless ballbar QC20-W. This system is the fastest, easiest and most effective way of monitoring the state of machine tool. It enables rapid monitoring of state linear axis of machine tool.

The control system AxiSet Check-up, the newest product made by this company, enables rapid and automated control of rotary axis on the 5-axis machine tools.

Article was created in conjunction with the solution ITMS 26220220125 - Development and implementation of experimental simulation methods for optimization process at technological workplaces.

10. References

[1] "I. Ďurica, I. Kuric," *Diagnostics of CNC machines with renishaw equipment."* [Online]. Available: http://www.nordtech.ubm.ro/issues/2008/2008.01.28.pdf. [Accessed: 23-Sep-2013].

[2] "J. Dekan, J. Pilc," *Measurement of Circular Interpolation Specificity at Milling.* [Online]. Available: http://web.tuke.sk/fvtpo/journal/pdf12/4-pp-19-21.pdf [Accessed: 20-Sep-2013].

[3] "Český informačný portal," *Obráběcí stroje: Kontrola technickej diagnostiky CNC obráběcího stroje.* [Online]. Available: http://www.prumysl.cz/obrabeci-stroje-kontrola-technicke-diagnostiky-cnc-obrabeciho-stroje/. [Accessed: 22-Sep-2013].

[4] "Renishaw," *AxiSet™ Check-Up - Nový systém nabízí rychlou, automatizovanou*

kontrolu „zdravotního stavu“ víceosých obráběcích strojů. [Online]. Available: http://www.renishaw.cz/cs/1030.aspx. [Accessed: 23-Sep-2013].

[5] “Renishaw,” *Kontrolní systém AxiSet™ Check-Up.* [Online]. Available: http://www.renishaw.cz/cs/1030.aspx. [Accessed: 22-Sep-2013].

[6] “Renishaw,” *Bezdrátový systém Renishaw ballbar QC20-W pro diagnostiku přesnosti obráběcích strojů.* [Online]. Available: http://www.renishaw.cz/cs/1030.aspx. [Accessed: 20-Sep-2013].

[7] “J. Dekan, J. Pilc,” *Measurement of Circular Interpolation Specificity at Milling.* [Online]. Available: http://web.tuke.sk/fvtpo/journal/pdf12/4-pp-19-21.pdf [Accessed: 20-Sep-2013].

[8] “Renishaw,” *Proč používat systém ballbar Renishaw QC20-W?.* [Online]. Available: http://www.renishaw.cz/cs/proc-pouzivat-system-ballbar-renishaw-qc20-w--7871. [Accessed: 20-Sep-2013].

AN INVESTIGATION ON PROPER DRYING TIME IN CITRUS PROCESSING

G. Cuccurullo[1], A. Ruggiero[1*], S. Hloch[2]

[1]Department of Industrial Engineering, University of Salerno, Italy
[2] Faculty of Manufacturing Technologies, of TUKE with a seat in Prešov |SK
* Corresponding author e-mail: ruggiero@unisa.it

Abstract

The main parameters affecting drying time in lemon processing plants are investigated. Different coatings, air speeds and temperature were taken into account. Aiming to realize short time processing operations excessive air temperatures are usually employed, thus leading to loss in sensorial quality and a decrease in the fresh fruit shelf life. A further negative effect is unwanted energy consumption. In the above connection the proposed procedure aims to detect the proper end of the drying process. The novelty of the present approach stands in using IR thermography for surface temperature detection rather than air flow temperature. Suitable data reduction will allow to prepare a set of charts for reading the desired time extension depending on the chief process parameters. Preliminary results concerning the phisyco-chemical analysis during storage, showed that the pre treated lemons shelf-life and appearance were preserved thus showing the effectiveness of the proposed procedure.

Keywords: Citrus processing, drying time, thermography.

1. Introduction

It is well known that extending the time operation in citrus surface driers leads to marked loss of sensorial quality as well as to a decrease of fresh fruit shelf life and energy consumption. In the above connection, the present study aims to identify the proper lemon surface drying time by means of an innovative method based on the infrared thermography. Since the drying process is characterized by very high output of post-harvesting citrus lines and low quantity of water to be removed, the need to propose a new method arise from considering that the air temperature, which is commonly measured, reveals itself to be a scarcely sensitive parameter to the process completion. Thus, by providing a fine temperature control of the citrus surface both in time and in space by infrared thermography, it is possible to reduce the time/temperature treatment during the superficial drying to achieve both the desired dehydration degree and energy saving [1]. Operating in such a way makes possible to preserve the nutritional and sensorial properties of the fruits under process and to prolong lemons' shelf-life. IR thermography has scarcely been used in food drying operations, see for instance [2] and [3]. In particular, Fito et al, [3], used IR thermography applied to citrus surface drying but they used a different approach for detecting the end of the drying process.

They measured the wet bulb temperature, assumed to be the lowest temperature value at the very beginning of drying process, and established the end of drying process when the entire citrus surface was at a higher temperature than the wet bulb one. This criterion seems to be not completely adequate to establish the very end of the process. To overcome this difficulty, a simple idea is followed in the present study after the work performed in [4], that is having as a reference an uncoated lemon to detect the end of the process at hand.

2. Experimental setup and procedure

A pilot drying plant was specifically realized in order to realize lemon drying. It essentially consists of an infrared thermography equipment (FLIR P65); a channel 45 cm x 35 cm x 4 m, conveying air flow, long enough so to realize fully developed flow conditions; a fan and electric resistances enabling to control air flow and temperature. In particular a maximum temperature increase of 22°C @ the maximum flow rate corresponding to 3.5 m/s average velocity. Finally, spin rollers continuously rotating unwashed and uncoated lemons @ 25 rpm. Sorrento lemons, Citrus lemon, from Italy were obtained by local farmer; the fruits (of about 200 g), were washed and waxed: wax application consisted of coating the fruit with a commercially-available shellac-based wax on roller brushes, after the addition, respectively, of imazalil and nisin. Afterward the fruit were partially dried and stored at 10°C. Immediately prior to pre-treatment and at regular interval time the product quality was evaluated by measuring the following parameters: moisture content, weight loss, colour.

The coupling between the air fan and the channel size was such as to achieve a maximum air velocity of 3.5 m/s. In particular, having in mind typical values of air velocities in industrial plants, 1,

1.5 and 2 m/s air speeds were sought to perform testings. The electric resistance was such as to realize a maximum temperature increase of 25°C with respect to the ambient temperature for the maximum air flow. Experiments were performed setting the spin rollers speed at 20 rpm and fixing air flow temperature at 30°C, 40°C and room temperature. Continuous IR temperature detection @ 50Hz was allowed by inspecting inside the duct through a window 40 mm x 30 mm covered with a thin IR semitransparent sheet. Preliminary calibrations for fruit surface emissivity and window transmittance were carried on. The equivalent emissivity, taking in to account both lemon surface emissivity and window transmittance, resulted to be 0.95. The procedure essentially consisted in: 1) proper washing and coating of the fruits with wax film of different thickness; 2) fixing the spin velocity of the fruit to 20rpm; 3) starting the acquisition of the IR sequence of fruit surface temperature maps; 4) post treatment operations ; 5) data reduction.

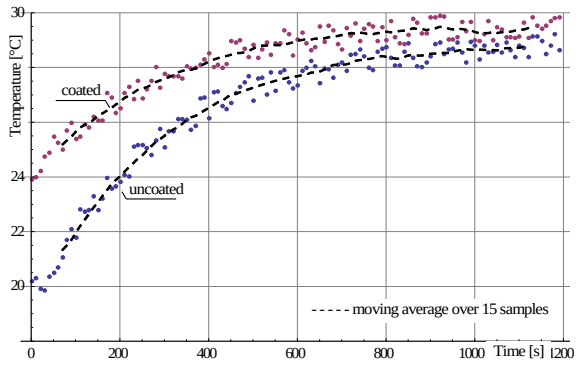

Figure 1 – min. temperature evolution for air @ 40°C, 1.5 m/s

The fruit volume was measured by immersion and its surface was calculated supposing to realize uniform deposition over the surface by using the sphere volume equation. The coating thickness was obtained measuring the weight increase after wax deposition. Care was taken in order to have practically the same coating by controlling spraying time and pressure over the rotating samples. Two coating thicknesses corresponding to 2.3·10-2 and 5.2·10-2 kg/m2 surface water were obtained. Post treatment operations included physico-chemical determinations such as weight loss percentage was estimated after each period of storage by weighting all samples, Colour measurements, Tristimulus reflectance colorimeter surface colour was measured using a reflectance colorimeter (Chromameter-2 Reflectance, Minolta, Japan), equipped with a CR-300 measuring head. Colour was measured using the CIE L* (lightness), a* (redness), b* (yellowness) scale.

3. Results and discussion

Measures of minimum temperature surface over lemons frontal area, featured by the same distribution of effective air velocities, were carried on both for coated and uncoated citrus exhibiting the same initial room temperature. A typical minimum temperature evolution of coated and uncoated lemons is represented in Figure 1 for air @ 40°C, 1.5 m/s, coating 2.3·10-2 kg/m2 where experimental data are adapted to moving average reference line to make easy the reading. It can be clearly seen the sudden initial temperature decrement featuring the waxed lemon due to evaporation. The temperature decrease in the early stage of the process aims to the wet bulb temperature. The addressed temperature decrement decreases while evaporation occurs with simultaneous sensible heat transfer with surrounding air. Then the slope of the curve decreases with decreasing the driving force inducing the evaporation, till to practically reach the one of the uncoated lemon which then acts as a reference. The reference lemon is assumed to be featured only by sensible heat transfer, assuming the peel drying to be negligible. Thus, the end of the film water evaporation on the fruit surface is assumed to be realized when the two slopes assume the same value. The drying time can be clearly inferred as almost 630 seconds. The occurrence of the same slope for both curves shows that essentially only sensible heat transfer takes place and thus it is the assumed to state the

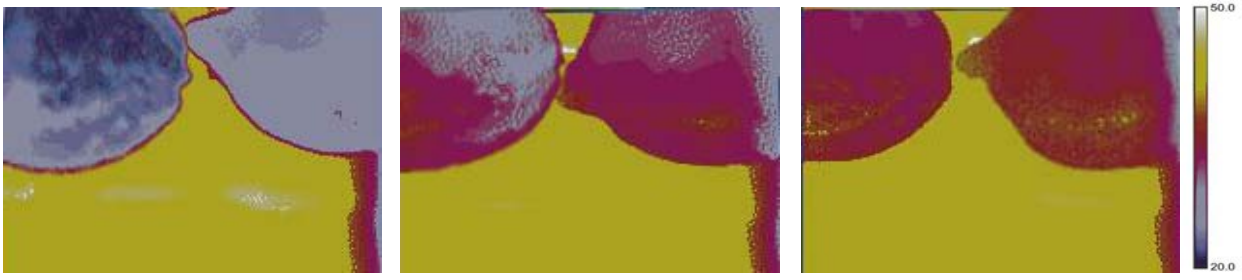

Figure 2 – lemon surface temperature development; images @ beginning, one half and at the process end (630 s)

end of the surface evaporation process. Data reduction provides the evaluation of the difference of the actual slope between the two curves and identifies, after suitable data smoothing, the drying time as the one for which the addressed difference is negligible. In figure 2 IR thermography pictures taken at the beginning, at one half and at the end of the drying process show qualitatively the same conclusions drawn above.

A first attempt chart related to $2.3 \cdot 10^{-2}$ kg/m2 coating thickness is reproduced in Figure 3. As expected, the chart shows that lower drying times are realized with increasing air velocity and temperature. The sensibility to air temperature appears to be much more marked than the one on air velocity. This latter decreases with increasing air velocity.

It is to underline that an easy model assuming exponential temperature/time variation cannot be adopted since the processing times are small when compared with the time constant of the system at hand. The very early stage of the drying process are well fitted with the seminfinite model, i.e. temperature increases with the time square root, but the time extend over which the model fits experimental data is not long enough to recover the end of the drying process. This explains the need of adopting Bezier fitting.

Controlling the minimum temperature over the selected area was chosen to be sure to "heat enough" all the samples to avoid the mould growth for the peel high water activity.

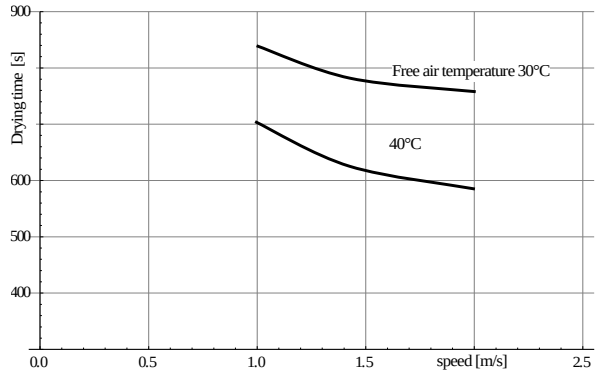

Figure 3 – drying chart

Finally, in order to check the effectiveness of the drying process, the pre-treated, dried, lemons aromatic profiles were analyzed during shelf-life obtaining quite satisfactory results. Moreover, to guarantee the safety and improve the shelf-life of such fruits, different pre-treatments complaint with consumers expectance are tested by employing natural fungicide compounds instead of chemical. The moisture content of the peel was of about 82.0%, while the moisture of the pulp was about 88.9%. Weight loss after 16 days of storage ranged from 8 to 10%, without remarkable differences among the different samples

As expected the wax coating improved the lemon appearance, by increasing the brightness values in all treated samples. After 16 days of storage at 10°C, the differences among the treated and untreated samples increased, confirming the positive effect of the wax coating on the lemon color.

4. Conclusion and future developments

A procedure to reveal the effect of air velocity and temperature and on waxing coating on the effective drying time has been proposed. It has been shown that shelf-life and appearance of the samples can be preserved in the respect of energy saving, i.e. with the minimum time operations compatible with an effective drying. Performing different experiments, charts of the effective drying time in dependence on the coating thickness, air temperature and velocity are to be obtained. Having in mind the possibility to realize on line process control by IR thermography, where coatings are not fine controlled in principle, the procedure could be of primary importance for feeding back a control strategy. Thus, further test are required to complete charts and new control strategies based on IR thermography can be set up on non homogeneous wax coatings.

5. References

[1] Fito, P., Asensio, S., Fito, P. J., Ortol_a, M. D., in IFT Annual Meeting. Surface drying kinetics in citrus fruits, Dallas, 1999.
[2] Workmaste, B. A., Palta, J. P., & Wisniewski, M., in: Journal of the American Society for Horticultural Science Ice, nucleation and propagation in cranberry uprights and fruit using infrared video thermography, 1999.
[3] P.J. Fito et al., in J. of food engineering, Control of citrus surface drying by image analysis of infrared thermography, pp. 287–290, 2004.
[4] Cuccurullo G., Sorrentino G., Cinquanta L., Di Matteo M., A procedure to control surface drying for improving citrus shelf life. XXIV Congresso Nazionale UIT sulla Trasmissione del Calore, Napoli, 2006.

MATERIAL ABRASIVE WATER JET CUTTING INVESTIGATION BY MEANS ACCOMPANYING PHYSICAL PHENOMENA

D. Kinik[1*], B. Gánovská[1], S. Hloch[1,2], J. Cárach[1], D. Lehocká[1]

[1] Faculty of Manufacturing Technologies of Technical University in Košice with the seat in Prešov, Slovakia
[2]Institute of Geonics Academy of Science of Czech Republic, v.v.i., Ostrava-Poruba
*daniel@kinik.sk, aksvonag@gmail.com, hloch.sergej@gmail.com

Abstract
The paper deals with the indirect ways of on-line monitoring of technological processes of cutting. The objective of the study is a design of on-line monitoring system for the cutting technology through an abrasive water jet. In cutting by the abrasive water jet two parallel phenomena are formed. The phenomena are represented by generated surface and vibrations. For the purpose of proving of the hypothetical assumptions on dependence of generated surface quality on vibrations the experiments utilizing stainless steel AISI 304 were performed. The experiments were realized at four diverse settings of cutting head traverse speed. The material vibrations were collected by means of two independent accelometers PCB IMI 607 A11. One of the accelerometers was oriented towards the cutting direction and the other in direction perpendicular to cutting. The generated topography of the material was measured by an optical profilometer FRT MicroProf. The collected data were evaluated by a virtual tool developed in LabView 8.5 in the form of vibration analyses being consequently mutually compared. Both phenomena proved to be dependent on common technological cause, i.e. on cutting head traverse speed. At the same time the study offers a theoretical design of the on-line monitoring system and of the future heading of the research in this field.

Keywords:
abrasive water jet, vibrations, monitoring, on-line, acoustic emission

1. Introduction

The paper was written pursuant to constant increase of quality and production requirements. The increase demands the system design which would produce high-quality products cheaply and fast. The fact is that quality is many times linked with the higher price level and thus fully flexible system able to eliminate purposeless production costs [1]. One of the alternatives of generation of such system or at least of getting closer to it is introduction of on-line monitoring into already existing conventional and unconventional technological processes. The abrasive water jet cutting (AWJ) ranks among the unconventional technological processes of material cutting [1], [3], [4], [6], [7]. This technological process is currently being pushed to the foreground since any available material is possible to be cut by the technology [2]. The advantages of AWJ technology rests not only in low impact upon environment, but in non-occurrence of temperature changes in the cutting point [5], [8]. As any other technological process even the AWJ technology is during cutting accompanied by the attendant phenomena such as vibrations or acoustic emissions. Therefore the aim of the thesis is focused on the analysis and comparison of data acquired through the experimental measurements of vibrations and of their utilization in theoretical design of feasible method of on-line monitoring of the given technological process.

2. Experimental study

The experiments were performed at a workplace of the company of DRC, s.r.o., v Prešove in cooperation with the company of Technická diagnostika, s.r.o. in Prešov. During the experiment stainless steel AISI 304 represented the cutting material. A workpiece in case of which the measurements were performed was a plated with dimensions of 100 mm x 150 mm x 12mm. In the course the experiment the plate was cut four times in total by the method shown in Fig.1

Figure 1. Cutting material - a workpiece

Collection of data inevitable for more profound analysis of vibrations was repeatedly performed several times. Two sensors placed directly on a workpiece (one was fixed axially - S1 and the other radially - S2) served as data collectors in the form of accelometers PCB IMI of series type of 607 A11 with an integrated cable. These sensors were connected to the measurement system of NI PXI. The system consisted of the measuring card PXI 4472B and was typical for the 8-channel simultaneous collection and 24 bit analogue and digital converter with the dynamic range of 110 dB. The frequency analyser SKF Microlog Gx-S was used for the performance of verification and calibration measurements in case of which the analysis of the measured data was realized through the program equipment of SFK Aptitude Analyst. Measurement of the profile parameters of surfaces generated by the particular technology was carried out by means of optical contactless method through the optical profilometer Microprof FRT by the producer Fries Research&Technology GmbH that allowed 3D evaluation of the surface. The obtained data were transferred to LabView 8.5 (MS Excel 2007), in which they were monitored and evaluated.
The experiment was performed under environmental and technological conditions presented in the following tables (Tab. 1, Tab. 2).

Table 1. Environmental conditions

Factors	Symbol [Quantity]	Value
Pressure	p [hPa]	1007
Temperature	C [°]	21
Air moisture	%	38
Altitude	[m]	280
Geographical position	-	49°00'00" 21°14'00"

Table 2. Technological conditions

Factors	Symbol [Quantity]	Value
Pressure	p [MPa]	350
Traverse speed	v [mm/min]	50; 75; 100; 150
Abrasive mass flow rate	m_a [g / min]	250
Material thickness (stainless steel)	b [mm]	12
Abrasive type (Barton Garnet)	*MESH*	80
Standoff	z [mm]	2
Focusing tube	d_f [mm]	0.8
Orifice	d_o [mm]	0.35

In the frame of the experiment it was inevitable to monitor and to record the change of formed vibrations at the point of sensor fixation in dependence on cutting conditions by the system of NI PXI. The following Fig. 2 shows a simplified development of the experiment to get the idea of the process.

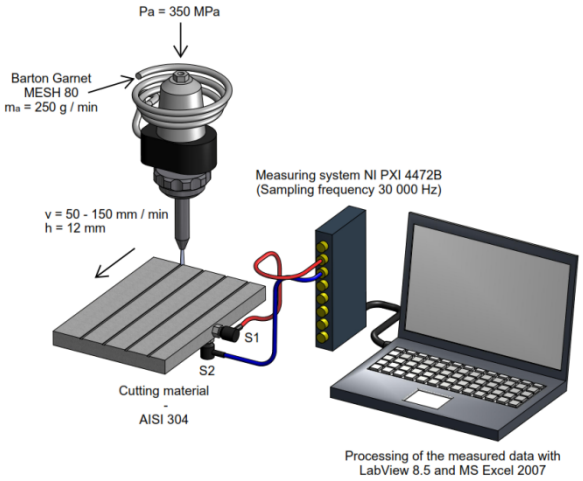

Figure 2. Simplified representation of the experiment

Four measurements were performed with diverse setting of traverse speed of cutting head (v = 50 mm/min, v = 75 mm/min, v = 100 mm/min, v = 150 mm/min).

3. Results and discussion

3.1 Analysis of the generated surface topography

As per graphic dependences it is clear that with the growing depth the overall numerical development of the individual roughness profile parameter of the generated surface changes as well. The phenomenon is caused by the fact that with the growing depth the jet acting upon the material gradually loses its energy and thus its higher curvature in larger depths occurs and at the same time surface quality in the particular depth lines declines.
Roughness parameters Ra, Rq, Rz were measured in 21 depth lines of the 20 mm long segment marked by green boundaries. The red boundary represents the end of the sample cutting (Fig. 3 A – Fig. 3 D). If the dependence of the surface profile parameters Ra, Rq and Rz on cutting depth at speed of v = 50 mm/min is compared with dependence of the surface roughness parameters Ra, Rq and Rz on cutting depth at speed of v = 150 mm/min (Fig. 3E, Fig. 3F) from the perspective of the influence of speed upon the development of the values of these

parameters, it might be stated that apart from the cut depth the development of the values of roughness parameters is significantly affected by speed at which the cutting head moves in the course of cutting.

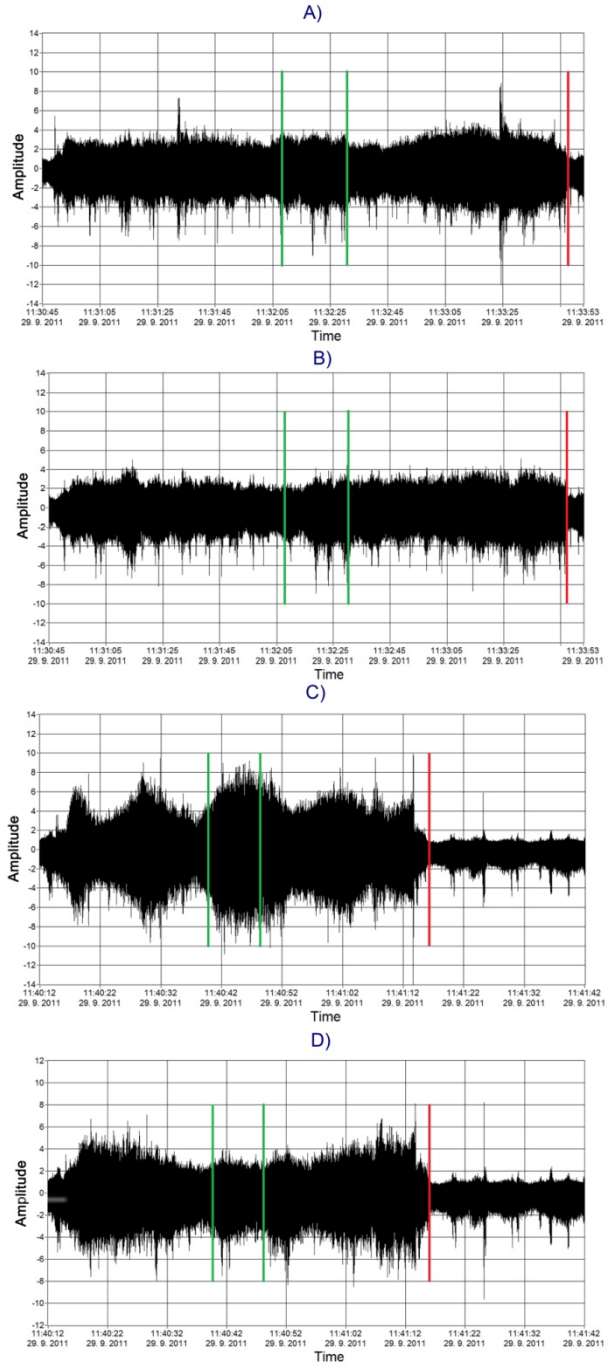

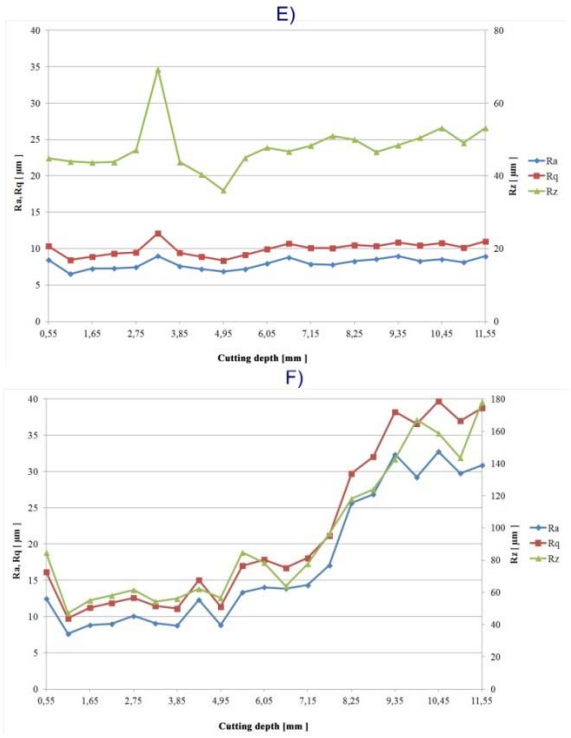

Figure 3. Time development of vibration signal:
A) at traverse speed of v = 50m/s - sensor S1
B)at traverse speed of v = 50m/s - sensor S2
C)at traverse speed of v = 150m/s - sensor S1
D)at traverse speed of v = 150m/s - sensor S2
Dependence of roughness profile parameters:
E) on cutting depth on traverse speed v = 50m/s
F) on cutting depth on traverse speed v = 150m/s

At speed of v = 50 mm/min it could be observed that the development of the aforementioned parameters is more linear contrary to the case in which the speed was set to the value of v = 150 mm/min. The phenomenon is possible to be explained from the point of view of interaction between a high-speed permeate and a workpiece. At traverse speed of cutting head of v = 50 mm/min the abrasive water jet disposed of sufficient amount of time to make the abrasive particles capable of even and intensive erosion of the material surface along the entire depth of cutting sample which is not applicable at traverse speed of v = 150 mm/min. The combination of higher traverse speeds of cutting head with larger depth of the cut causes disability of the jet to erode the material surface of cutting sample to satisfactory extent and that is in consequence demonstrated by the formation of striated zone the roughness of which is not sufficient from the perspective of input requirements for surface quality.

3.2 Analysis of formed vibrations

The elaborated time developments of vibration signals are divided into two groups. The first group includes the data measured by sensor S1 (Fig. 3

A, Fig. 3 C) which was fixed on the cutting material in axial direction and the second group contains the data measured by sensor S2 (Fig. 3 B, Fig. 3 D) fixed on the cutting material in radial direction. Through the comparison of these time developments at speeds of v = 50 mm/min and v = 150mm/min it is possible to state that at lower traverse speed of the cutting head the development of amplitude of vibration oscillations is more stable contrary to higher speeds and this fact opens the door for further research for the purpose of detection of utilizable vibration spectrum (inevitable is to determine the utilizable vibration spectrum both at lower and higher traverse speeds of cutting head) for the application of on-line monitoring of the particular technological process. Out of these time developments the changes of amplitude of vibration signal oscillations is obvious not only in dependence on the means of the sensor fixation but also in dependence on the traverse speed of cutting head.

4. Utilization of acquired knowledge for the solution proposal

The series of performed experiments was carried out with the aim to show connection between surface topography and vibrations. In dependence on acquired knowledge of the technology in question and pursuant to realized analyses the real existence of connection between vibrations and surface topography might be referred to. Such indirect connection is influenced by variant setting of traverse speed of cutting head as with the change of the speed setting the changes of intensity of amplitude of oscillations during vibrations occur as well as changes of surface topography quality. At low speeds the amplitude of oscillations is lower contrary to higher speeds. At the same time proved was the assumption that at lower speeds the surface topography is of higher quality than at higher speeds since at higher speeds the abrasive water jet did not possess sufficient amount of time to be able to erode the material surface equally along the entire depth of the cutting sample.

In case of proposal of on-line monitoring of AWJ technology inevitable is to be particular about selection of adequate feedback. The established feedback regulation is required to take into consideration the time delay resulting from the need of processing and evaluation of the measured data. The proposal of correct feedback is significant due to prevention of repeated regulation of traverse speed of cutting head at points in case of which it is not desired.

The thesis along with other existing studies and future research direction might provide certain basis for formation both theoretical and practical method of on-line monitoring of the AWJ technology. Such method of on-line monitoring is possible to be demonstrated from the theoretical point of view Fig. 4.

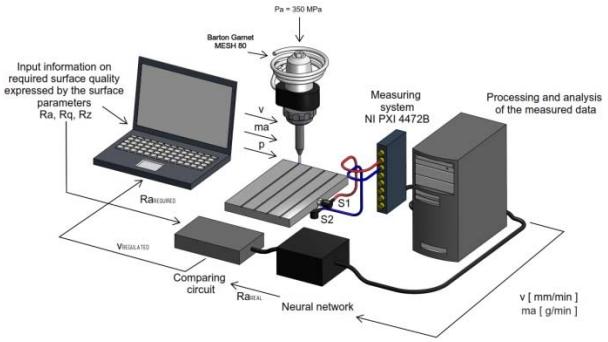

Figure 4. Simplified scheme of possible method of online-monitoring of the AWJ technology

5. Conclusion and the future research direction

Currently, the control of cutting process by AWJ technology is performed in so called off-line mode. In case of the off-line mode those are beforehand specified requirements for cutting quality of cutting material and the cutting quality is possible to be verified after material cutting. Although in the cutting by means of such technology the method of prediction of cutting material surface quality exists, it is still necessary to point out that only under certain conditions and due to diverse accompanying features of the technology and its complicated specification. At the same time through on-line control and regulation the working productivity shall increase and potential defect occurring in the course of the system operation shall be possible to be determined and thus the reject formation shall be prevented (saving of costs related to rejects).

On-line monitoring is possible to be performed with the particular technology only indirectly by accompanying phenomena such as vibrations or acoustic emissions. The endeavour of the thesis was pursuant to performed experiments focused on vibration measurement to detect dependence between traverse speed of cutting head (the cause) and formation of vibrations and to find out the extent of influence of the aforementioned traverse speed upon final surface roughness of cutting material.

According to the acquired knowledge the existence of real option of vibration utilization in introduction of on-line monitoring of the AWJ technological process can be confirmed. However, it is necessary to mention that in general the introduction and utilizable proposal of functional method of on-line control in practice require performance of a number of experiments focused on evaluation of vibrations with diverse variants of setting of input process factors because the formation of vibrations and final surface roughness are except for the examined cause of traverse

speed v [mm/min] influenced also by other factors, for instance, permeate pressure or abrasive type. Such experiments are also inevitable to be performed in case of other materials than was used in our experiment (stainless steel AISI 304) as formation and spread of vibrations along with the surface roughness depend even on material properties of the individual materials. At the same time it would be convenient to carry out the experiments in ideally isolated environment (under laboratory conditions) as well as in common environment (for instance, production hall in the proximity of main road) with the aim to reveal "strange vibrations – vibration zone"(main road vibrations, machine vibrations, etc.) that could negatively affect the development of on-line control and process regulation. With the idea of proposal of online control system a number of other open questions occur concerning, for instance, the appropriate proposal of feedback system since in on-line monitoring it is necessary to take into account even certain time delay of measured data processing and consequent repeated regulation of process quantities in occurrence of failure in the process.

Out of the aforementioned it is clear that the introduction of on-line monitoring into technological processes is not by far as simple as it might seem. In analysis of the measured data other outputs were gained as well which, however, were not possible to be presented in the thesis due to the required amount of text. These outputs along with the need of other experiments with the aim to design and apply on-line monitoring of technological processes into practice represent a challenge for further direction of the authors of the thesis. The processed data shall be monitored and evaluated further on. The direction of the future research and its results shall be presented in other thesis by these authors.

6. Acknowledgement

Experiments were carried out under the support of project science and research HydroMon - APVV 0207-12.

7. References

[1] Hloch, S.; et al.: Analysis of acoustic emission emerging during hydroabrasive cutting and options for indirect quality control. // International Journal of Advanced Manufacturing Technology, Vol. 66, 1-4(2013), pp. 45-48.

[2] Arola, D.; Ramulu, M. Material removal in abrasive waterjet machining of metals surface integrity and texture. // Wear 210, 1–2(1997), pp. 50–58.

[3] Hassan, A. I.; Chen, C.; Kovacevic, R. On-line monitoring of depth of cut in AWJ cutting. // International Journal of Machine Tools and Manufacture, 44, 6(2004), p. 595-605.

[4] Momber, A. W.; Mohan, R. S.; Kovacevic, R. On-line analysis of hydro-abrasive erosion of pre-cracked materials by acoustic emission. // Theoretical and Applied Fracture Mechanics, 31(1999), pp.1-17.

[5] Sharma, V.; Chattopadhyaya, S.; Hloch, S. Multi response optimization of process parameters based on Taguchi-Fuzzy model for coal cutting by water jet technology // International Journal of Advanced Manufacturing Technology, Vol. 56, 9-12(2011), pp. 1019-1025.

[6] Hloch, S.; Ruggiero, A. Online monitoring and analysis of hydroabrasive cutting by vibration. // Advances in Mechanical Engineering, vol. 2013, ID 894561, pp. 1-10.

[7] Hreha, P.; Hloch, S.; Peržel, V. Vibration emission as a potential source of information for abrasive waterjet quality process control. // International Journal of Advanced Manufacturing Technology, 61, 1-4(2012), pp. 285-294.

[8] Hloch, S.; Dissintegration of bone cement by continual and pulsating water jet. // Technical Gazette, 20, 4(2013), pp. 593-598.

INFLUENCE OF CONTACT MODELING IN NUMERICAL ANALYSIS OF AN AXIAL BELLOW

I. Losonc[1*], D. Kozak[1], F. Haas[2], D. Damjanovic[1]

[1]Mechanical Engineering Faculty in Slavonski Brod, J. J. Strossmayer University of Osijek, Croatia
[2]CAMPUS 02 University of Applied Sciences Graz, Austria
** Corresponding author e-mail: ilosonc@sfsb.hr*

Abstract
This paper presents the importance of correct modeling of contact surfaces in numerical analysis by the finite element method, using a software ANSYS Workbench. As a representative sample for analysis, axial expansion joint was used. The contact modeling method is based on the paper [1] where different software and a smaller expansion joint are used.

Keywords:
Numerical analysis, finite element method, modeling of contact, axial bellow expansion joint.

1. Introduction

The main goal of this paper is to point out potential mistakes that occur when modeling of contact in numerical analysis, and have a major impact on the result. Axial bellows expansion joints are tubular elements for pipelines compensation of axial stretching due to temperature change, pressure or physical movement. Theoretically, the expansion joint is one of the most sensitive parts of the pipeline.

2. Geometry and Load Conditions

The axial expansion joint's diameter is 400 mm, the overall length is 1145 mm, with a tube thickness of 10 mm, while the center part of the expansion joint, the bellow, is made out of two layers, and each with a thickness of 1 mm. Figure 1 shows dimensions of an axial expansion joint, and Figure 3 shows a 3-D model of it.

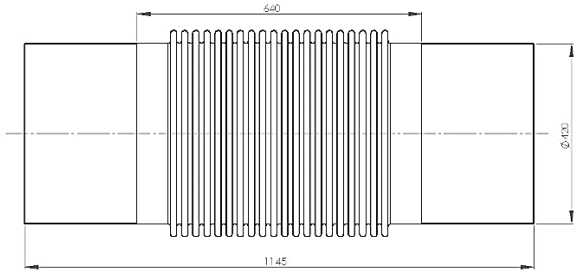

Figure 1. a) Dimensions of an axial expansion joint

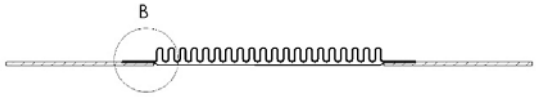

Figure 1. b) Cross section of an axial expansion joint

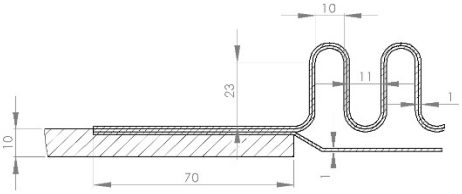

Figure 1. c) Detail dimensions of an axial expansion joint

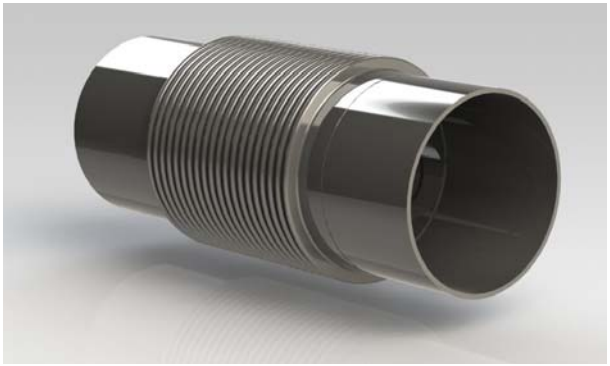

Figure 2. 3-D model of an axial expansion joint

The material properties are given in Table 1. Two different materials are used for expansion joint, one for tubular extension (St 37.0) and one for bellows (1.4541).

Table 1. Material properties of an expansion joint

Material	1.4541	St 37.0
Elasticity modulus, *E,* GPa	200	210
Poisson's ratio, ν	0,3	0,3
Yield stress, σ_y, MPa	465	295
Hardening modulus, *H,* MPa	1174	829
Coefficient of thermal expansion, α, $^{\circ}C^{-1}$	$1{,}85 \cdot 10^{-5}$	$1{,}2 \cdot 10^{-5}$

Working temperature of the expansion joint is 300 °C, inner pressure is p = 16 bar, while the prescribed axial displacement is 125 mm.

3. Preparing models for analysis

The problem was analyzed with three-dimensional elements using the software ANSYS Workbench. Since the model is axisymmetric, only a section of an axial expansion joint is used, not the whole expansion joint (Figure 3).

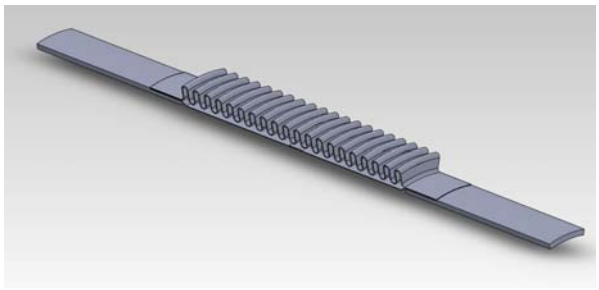

Figure 3. Axisymmetric section of expansion joint model for analysis

The final model consists of 256131 nodes and 37262 finite elements (Figure 4).

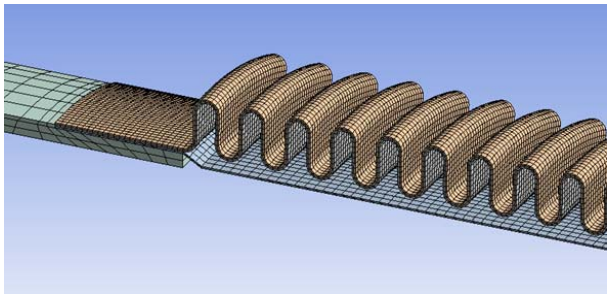

Figure 4. Part of a meshed model for analysis

4. Contact modeling

In finite element analysis, if two independent parts are present, there is no stiffness relationship defined between them, and the resulting stiffness matrices will be uncoupled – consequently, one part my pass through the other during the course of the simulation. Contact elements are required to define the interaction of two or more sets of meshes to prevent such penetration [2].

ANSYS contact technology offers many algorithms to control how the code enforces compatibility at a contacting interface.

The penalty method is a traditional algorithm that enforces contact compatibility by using a contact "spring" to establish a relationship between the two surfaces. This mathematical formulation is used in this analysis. The spring stiffness is called the penalty parameter or, more commonly, the contact stiffness. The spring is inactive when the surfaces are apart (open status), and becomes active when the surfaces begin to interpenetrate [3].

The penalty method introduces a force at the contact detection points that has penetrated across the target surface with the express purpose of eliminating the penetration. This method uses very simple formulas:

$$p = k_{\mathrm{n}} \cdot x_{\mathrm{n}} \qquad (1)$$

That is for contact detection points that penetrate across the target, and for open contact detection points following applies:

$$p = 0 \qquad (2)$$

Where p is contact pressure, k_{n} is the contact stiffness (penalty stiffness) which is a predetermined property of the contact element, and x_{n} is the penetration at the contact element [2].

Currently, auto-contact detection in ANSYS Workbench Simulation allows users to quickly set up contact (part interactions) between multiple entity types [4].

For correct modelling of an axial expansion joint, it is necessary to apply contacts at three areas: at inner part of the sliding tubes (Figure 5.a), which enables contraction without stress; at the bellow, at the boundary between the two layers, since the bellow is made out of two layers of sheet metal (Figure 5.b); and between inner part of the sliding tubes and bellows (Figure 5.c).

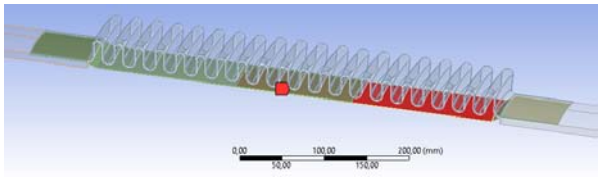

Figure 5. a) Contact between sections of a sliding tubes

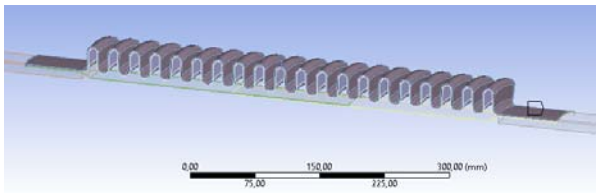

Figure 5. b) Contact between bellow layers

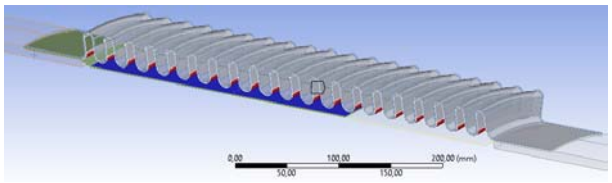

Figure 5. c) Contact between sliding tubes and bellows

For asymmetric behavior, the nodes of the Contact surface cannot penetrate the Target surface. This is a very important rule for contact as shown in Figure 5.c) [5].

Is very important to correctly determine what a Contact surface is and what a Target surface is, as shown in Figure 6.

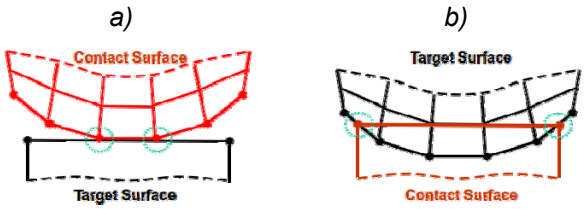

Figure 6. Different behavior of contact surface [5]

On the Figure 6.a, the top red mesh is the mesh on the Contact side. The nodes cannot penetrate into the Target surface, so contact is established correctly.

On the Figure 6.b, the bottom red mesh is the Contact surface whereas the top is the Target. Because the nodes of the Contact cannot penetrate into the Target, too much actual penetration occurs.

Therefore, if Contact surface is incorrectly defined the results will be like this one shown in Figure 7.

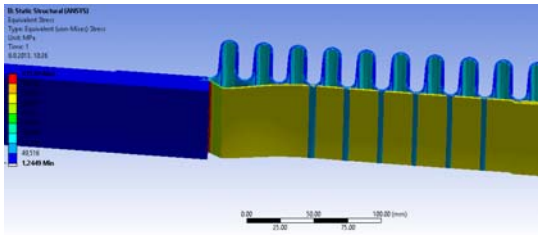

Figure 7. Results after incorrect defined contact surface

Rigid-body motion in which parts are not initially in contact is often a common convergence problem. Therefore, defining and verifying contact between parts is an important first step in the analysis. Initial contact status is easily checked in mechanical solutions from ANSYS, including whether or not parts that are thought to be in initial contact are truly touching [6].

To verify the contact surfaces it can be used a *Contact Tool*, as shown in Figure 8. Specific contact regions can be selected or deselected, and plotting/listing of only the contact or target side is possible from this worksheet.

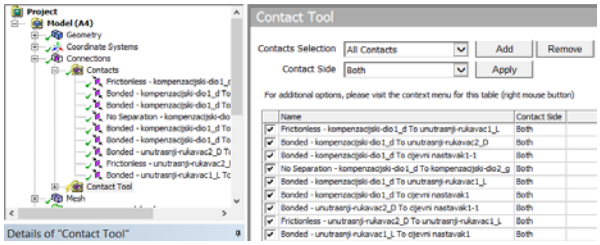

Figure 8. The contact tool can be used to check initial contact status

After Generate Initial Contact Results, initial contact information will be calculated and presented in tabular form, as shown in Figure 9.

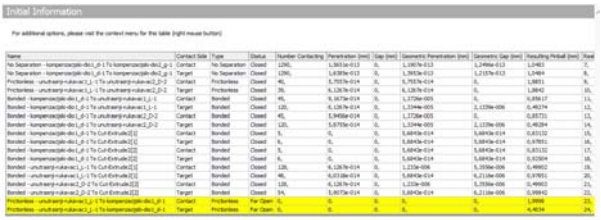

Figure 9. Types of contact are summarized, with potential problems highlighted in colors

The rows conveniently summarize the type of contact and highlight possible problems in different colors. Yellow indicates to frictionless or frictional contact pair having an initially open state, what is correct in this case.

5. FE Analysis

For the better simulation modeling of working conditions of a pipeline, of course it is necessary to define the boundary conditions of an expansion joint, what is shown on Figure 10.

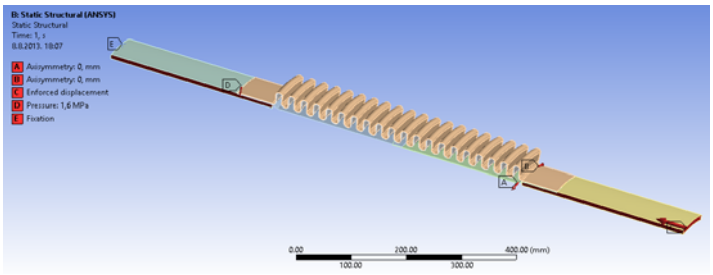

Figure 10. Boundary conditions of an expansion joint

In contact element analysis, apart from applied loads, is advisable to apply enforced displacement, which leads to better convergence. Hence, a 125 mm displacement is applied at the model one end in the axial compression direction. Other boundary conditions are axisymmetry on both sides, 16 bar pressure from the inner side, and a 300 °C temperature load on the whole expansion joint. The other side of a tube is fixed.

Analysis was carried out with finite element method using the ANSYS Workbench software. The problem was analyzed with three-dimensional axisymmetric elements. The elements used for contact model are as follows [7].

Solid186 – the element is defined by 20 nodes having three degrees of freedom per node: translations in the nodal *x*-, *y*-, and *z*-directions.

Conta174 – the element is used to represent contact and sliding between 3D surfaces. This element has three degrees of freedom at each

node: translations in the nodal *x*-, *y*-, and *z*-directions.

Targe170 – the element is used to represent various 3D "target" surfaces for the associated contact elements. The contact elements themselves overlay the solid, shell, or line elements describing the boundary of a deformable body and are potentially in contact with the target surface.

SURF154 – may be used for various load and surface effect applications. It may be overlaid onto an area face of any 3-D element. The element is applicable to 3-D structural analyses. Various loads and surface effects may exist simultaneously.

Figure 11 shows results after nonlinear static analysis. The highest von Mises stress, for contraction of 125 mm, is 426 MPa.

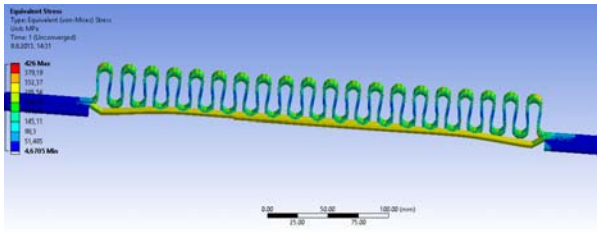

Figure 11. Von Mises stress distribution

Figure 12 shows deformed shape of an expansion joint where contact surfaces were defined correctly. It is evident that there is no more penetration of nodes into the surface, what is necessary target.

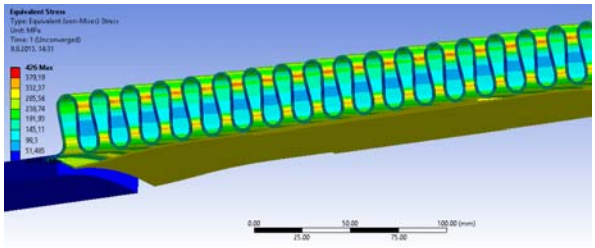

Figure 12. Results after correct defined contact surfaces

6. Conclusion

Analysis of axial bellows is ideal to show the importance of proper modeling of contact surfaces. It is essential to notice that with help from a predefined contact, it is possible to realistic model the axial expansion joint under working conditions, elevated temperature and working pressure. In that way, penetration of one layer of a bellow into another and interweaving of the inner part of a tube, is prevented.

7. References

[1] M. Brčić, M. Čanađija, "Stress and Strain Analysis of an Axial Bellow" *Engineering review*, Vol. 29, No 1, 2009.
[2] Sheldon Imaoka, "Contact Analysis Tips"; STI0902, January 2009.
[3] ANSYS, Inc. Technical Support, "Contact Defaults in Workbench and ANSYS", *ANSYS Solutions*, 2004.
[4] Siddharth Shah, "Nonlinear Simulation Provides More Realistic Results", *ANSYS Advantage*; Volume II, Issue 2, 2008.
[5] ANSYS, Inc. Proprietary: "Advanced Contact", *Lecture 4*, 2010.
[6] Sheldon Imaoka, "Analyzing Nonlinear Contact", *ANSYS Advantage*, 2009.
[7] Oday I. Abdullah and Josef Schlattmann, "Contact Analysis of a Dry Friction Clutch System", *ISRN Mechanical Engineering*, Vol. 2013, Article ID 495918, 9 pages, 2013.
[8] L. Morovič and P. Pokorny, "Optical 3D scanning of small parts", *Advanced Materials Research Vols*. 468-471, 2012.

INFLUENCE OF DOMINANT MECHANISM AND DIMENSIONAL CRITERION OF SEIZURE ON THE CHOICE OF WEAR PROTECTION PROCEDURE

Ž. Rosandić[1*], I. Samardžić[1], D. Krumes[1], I. Opačak[1], V. Marušić[1]

[1]Mechanical Engineering Faculty in Slavonski Brod, J. J. Strossmayer University of Osijek, Croatia
* *Corresponding author e-mail: zeljko.rosandic@sfsb.hr*

Abstract
Some characteristic examples, with the components worn by the abrasion and fatigue of the surface layer, were chosen. The analysis of structure, wear marks and hardness measurement were conducted on the components with clad layers. It was found that the abrasion influences on a decrease of installed capacity efficiency as the result of pronounced local damage of components due to wear, and that the fatigue results in seizure of components and losses due to seizure. The possible causes could be in the type and distribution of carbides and the matrix of clad layers. By introducing a dimensional criterion of seizure of components, the preconditions for investigating the possibilities of using the carbonitrided layers were created. Considering the properties of samples achieved by the high temperature carbonitriding with a variable C and N potential, some advantages of its use on the components with the dimensional criterion of seizure up to 0,2 ev. 0,3 mm were emphasized. It was concluded that the cladding of protective layers is recommended in the cases where the dimensional criterion of seizure is a few millimetres with the condition that carbides/carbonitrides are distributed as evenly as possible in the tough matrix. The high temperature carbonitriding, with a variable C and N potential, is recommended for the conditions where the dimensional criterion of seizure is up to 0,3 mm.

Keywords:
dominant wear mechanism, dimensional criterion of seizure, wear protection

1. Introduction

It is very common that in the processing industry, the wear of components cannot be avoided due to the fact that the medium, which is being processed, contains abrasive. Furthermore, the working pressures reach the values of a few tens up to a few hundreds bar. For example, this is the case in the sugar processing plant during pelletisation, in the oil processing plant during oil extraction, in the petro-chemical industry, etc.

Damage or seizure of components and equipment, among other things, can occur due to the fracture (breakdowns) and due to the wear. The breakdown is a completely unpredictable and often instantaneous occurrence. The wear is mostly a gradual, but still limiting phenomenon with regard to the life of components. In the selected examples, the abrasion is dominant, but due to the continuous flow of medium which is being processed, and high pressures, the fatigue of surface layer also appears. The wear by abrasion usually results in a decrease of installed capacity efficiency. The fatigue of surface leads to damage of the layer which results in seizure (breakdown). Therefore, the properties of existing original and possible alternative methods of wear protection were examined. A comparison was done on the example of clad layers where the dimensional criterion of seizure was a few millimetres, and the high temperature carbonitrided layers with a variable C and N potential, where the dimensional criterion of seizure was only a few tenths of millimetre, ev. 0,2 up to 0,3 mm. The aim is to create a basis for the further research in order to not only extend life, but also reduce the risk of fracture and thus contribute to an increase of the efficiency of components and equipment, as well as to reduce the direct and indirect tribological losses.

2. Analysis of Tribosystem

Figure 1 shows the dependence of wear intensity (I_w) and designed time (t_d) up to seizure [1].

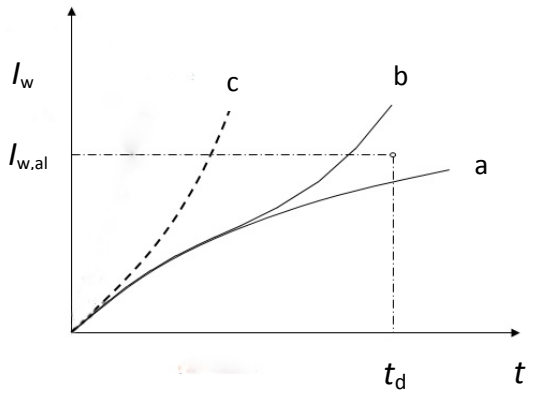

Figure 1. Dependence of wear intensity and designed time

It can be noticed that there are three curves in this diagram: (a) curve for normal wear, (b) curve for excessive wear, (which are usually mentioned in the reference books) [1, 2], and (c) curve for catastrophic wear (which was added) [3]. The catastrophic wear occurs when the wear of one element of tribopair causes sudden – unexpected and unusual damage of other elements of tribopair. In the end, this results in a breakdown. In order to create a basis for the research of defined topic, the components of worm presses for oil extraction (Figure 2 and Figure 3) and the matrices for pelletisation of sugar beets (Figure 4), were chosen.

a) b)

Figure 2. Damaged worm segments
a) first stage of damage of worm segments
b) catastrophically damaged worm segment

The most intensively worn surfaces of the worm segments are the front edge of screw and the corresponding portion of the upper surface of screw, and the dimensional criterion of seizure is approximately 3 to 4 mm [4, 5].

a) catastrophically damaged knife

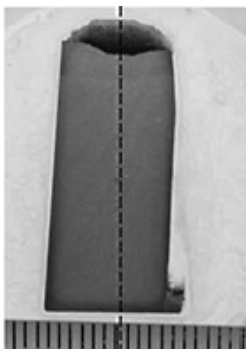

b) cross-section of knife

Figure 3. Clad knife of extraction cage (damaged due to use)

It should be pointed out that the most intensively worn surfaces of knives are the front edge (in the direction of rotation of worm) and the upper work surface, and the dimensional criterion of seizure is max. 0,2 mm. It can be noticed that the clad layer is “torn off” because of the fatigue. A possible reason for this is too much martensite, and too little of “tough” matrix that should keep the carbides - the carriers of wear resistance (by abrasion) - from “crowning off”.

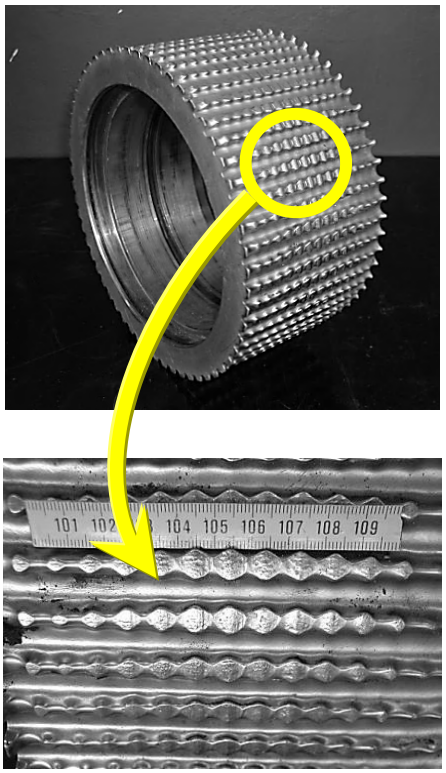

Figure 4. Matrix for pelletisation of suggar beets

A visual inspection, as well as the dimensional control and investigation of characteristic wear marks, were made. The clad parts were made with a protective layer of filler material (≈4 %C; ≈30 %Cr; ≈1 %Si) on the base material in class Ck 45. Hardness measurements of the upper (work) surface of selected samples determined the hardness values in the range between 51 and 57 HRC. Hardness measurement by HV1 method, at the cross-section of sample, determined that the thickness of clad layer is approximately 4,2 mm. The hardness of base material is approximately 26 HRC. The images of work surfaces show the dominant wear mechanisms. There are damages due to the mechanism of surface layer fatigue (Figure 5 a). Figure 5 b shows the particles of clad, just before falling out, in the area just beneath the worn surface.

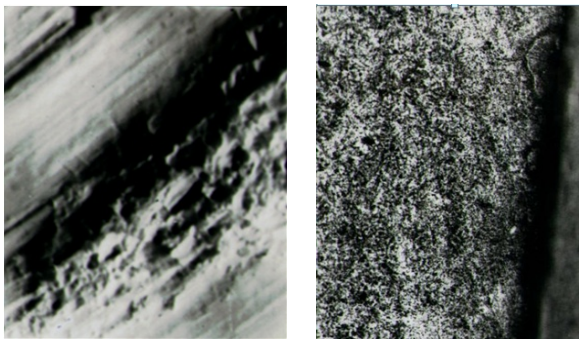

a) b)

Figure 5. Characteristic wear marks of clad: a) fatigue of surface layer, magn. ≈700X b) area just beneath the worn surface, magn. ≈300X

Selective abrasion can be seen (Figure 6 a, and 6 b) – manifested by the surface pores, pits and grooves. Furthermore, the higher the proportion of carbides (carbonitrides) harder than the abrasive, the less are these protective layers worn, and at a slower rate. However, it is important to emphasize that these carriers of wear resistance should be evenly distributed in the tough matrix [5].

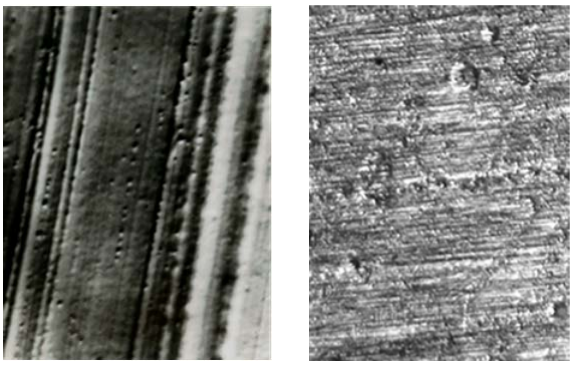

a) b)

Figure 6. Selective abrasion, magn. ≈500X

The emphasis of scientific approach to solving a problem of this type is put on the reduction of indirect losses and breakdown. The reason lies in the fact that a delay, due to the need to replace the damaged components, can take a few weeks, and the operation with the partially worn work surfaces of components leads to the reduced efficiency of installed capacity [6, 7].

3. Experimental Work

In the experimental part, the high temperature carbonitriding of the material for carburization 20MnCr5 was performed. The samples in the form of disc were put on the bolts M16, Figure 7. The process of high temperature carbonitriding was performed in the protective atmosphere of a furnace, rich with earth gas and ammonia, at the constant parameters of temperature (920 °C) for the duration of 10 hours. Different values of carbon potential (C_{pot}) and nitrogen potential (N_{pot}) were used. C_{pot} values were read directly on the measuring equipment which is part of the furnace. For Experiment 1, C_{pot} = 0,5 % C (Figure 8), and for Experiment 2, C_{pot} = 1,0 % C (Figure 9). N_{pot} values were regulated by the flow of ammonia. They were as follows: 10 % NH_3 for Experiment 1, and 5 % NH_3 for Experiment 2.

Figure 7. Samples prepared for carbonitriding

Figure 8 shows a diagram of furnace temperature and C_{pot}, as the result of Experiment 1.

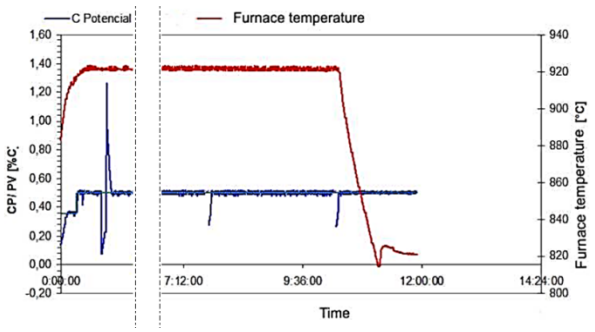

Figure 8. Parameters of high temperature carbonitriding – Experiment 1

Figure 9 shows a diagram of furnace temperature and C_{pot}, acquired on the available equipment as the result of Experiment 2.

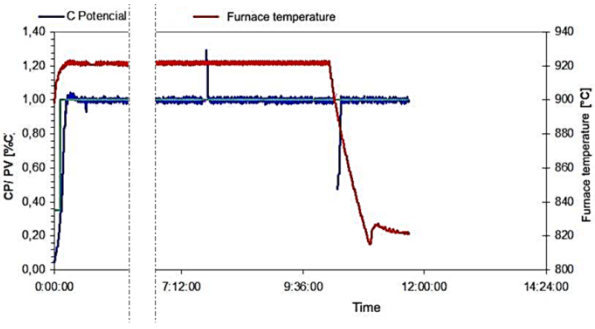

Figure 9. Parameters of high temperature carbonitriding – Experiment 2

Using HV1 method, the hardness measurement was performed at the cross-section of test samples (Figure 10). A characteristic dark edge (marked by the arrows) can be noticed on the surface layer of the test samples sealed in polymer.

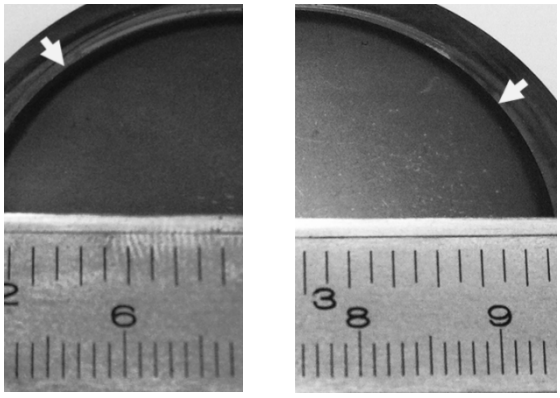

a) Experiment 1 *b) Experiment 2*

Figure10. Cross-section of high temperature carbonitrided samples sealed in polymer

Figure 11 shows the hardness measured at the cross-section of samples (high temperature carbonitrided for 10 hours). The achieved effective depth of carbonitriding was 1÷1,3 mm.

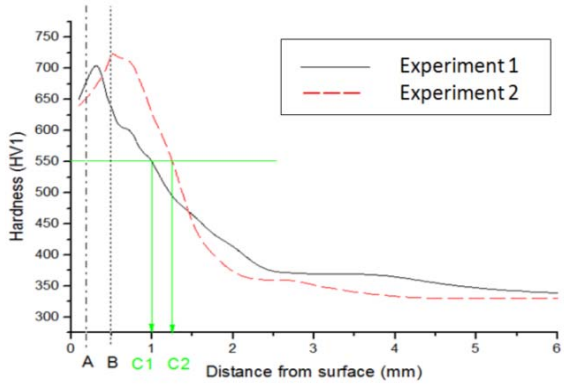

Figure 11. Hardness (HV1) at the cross-section of sample shown in Figure 10

Figure 12 shows a characteristic microstructure of the high temperature carbonitrided samples.

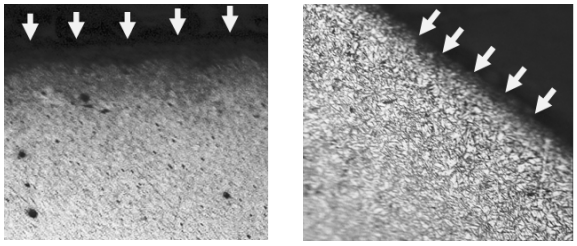

a) Experiment 1 *b) Experiment 2*

Figure 12. Characteristic microstructure of high temperature carbonitrided samples, 200x

Spot-like inclusions are evenly distributed along the entire cross-section of sample from Experiment 1 (Figure 12 a). The cross-section of steel, which was carbonitrided using the parameters from Experiment 2, indicates a rough, needle-like martensite microstructure (Figure 12 b).

4. Analysis and Conclusion

The presented results clearly indicate a great importance of the proper definition of the dominant wear mechanism and the dimensional criteria of seizure. The abrasion and surface fatigue, as the dominant wear mechanisms, should be taken into consideration, as well as the dimensional criteria of seizure, which can be different for some elements up to 10 times (from 0,2 mm up to 2 and 3 mm). This significant difference between the individual dimensional criteria of seizure demands the selection of appropriate wear protection, in order to reduce the wear intensity to the acceptable measure, while maintaining the optimal costs. Based on the monitoring of condition and the conducted investigations, it can be concluded that the choice of optimal procedure of wear protection directly depends on the dominant wear mechanism and the dimensional criterion of seizure. A basis for the further research was created with a goal of not only extending life, but also reducing the risk of fracture, in order to increase the efficiency of components and equipment, as well as to reduce the direct and indirect tribological losses.

10. References

[1] B. Bhushan, “Introduction to Tribology“, John Wiley & Sons, 2002.
[2] G. Rozing, D. Krumes, V. Marušić, ”Analiza prekomjernog trošenja vjedričnog elevatora”, HDO, 2009
[3] G. Rozing, M. Katinić, V. Marušić, “Neke specifičnosti utjecaja dominantnog mehanizma trošenja na pristup održavanju pužnih preša”, HDO, 2010.
[4] S.K. Gupta, “Technological Innovations in Major World Oil Crops“, Volume 2: Perspectives, Springer Science, LLC 2012.
[5] V. Ivušić, V. Marušić, K. Grilec: “Abrasion resistance of surface layers,“ Tribology Symposium: proceedings, Ronkainen, H., Holmberg, K., (ur.). VTT Technical Researche Centre of Finland, 1998.
[6] G. Fregapane, A. Gómez-Rico, A. M. Inarejosand Salvador, “Relevance of minor components stability in commercial olive oil quality during the market period“, 2013.
[7] M. N. Riaz, “Extrusion Processing of Oilseed Meals for Food and Feed Production“, Bailey's Industrial Oil and Fat Products, 2005.

APPLICATION OF JENSEN-SHANNON DIVERGENCE IN SMART GRIDS

Istvan Pinter[1*], Lorant Kovacs[1], Andras Olah[1,2], Rajmund Drenyovszki[1,3], David Tisza[1,2] and Kalman Tornai[1,2]

[1]Kecskemet College, Faculty of Mechanical Engineering and Automation,
Izsaki ut 10, H-6000 Kecskemet, HUNGARY
[2]Pazmany Peter Catholic University, Faculty of Information Technology
Prater utca 50/a, H-1083 Budapest, HUNGARY
[3]University of Pannonia, Department of Computer Science and Systems Technology,
Egyetem u. 10, H-8200 Veszprem, HUNGARY
* *Corresponding author e-mail: pinter.istvan@gamf.kefo.hu*

Abstract
A lot of problem in smart grids, such as automatic detection of appliance categories, customer categories or anomaly detection are rooting in segmentation of non-stationary time series into stationary subsequences. This problem is often referred to as Change Point Detection (CPT). In this paper an information theoretic measure: the Jensen-Shannon Divergence will be shown as promising candidate tool for solving CPT tasks in smart grids.

Keywords:
Smart grid, Change Point Detection, Jensen-Shannon Divergence

1. Introduction

Smart grid is new vision of future evolution of electricity systems. In contrast to the present grid, smart grid is adaptively managing the balance (supply and demand) of the system, and can handle the challenge of incorporation of renewable energy resources. These features are based on a two-way communication system and a SCADA (Supervisory Control and Data Acquisition) system from the top to the bottom.

The new system components imply new applications that require new signal processing methods as well. One of the relevant problems is the consumption management of an electricity customer that requires handling of traditional appliances as well. The smart meter has to have information about the type of the device connected to the grid even in the case of being not able to communicate its statistical parameters. Furthermore, the smart meter has to recognize the change of the appliance to another one. As a result the task of categorization is twofold: at first stationary segments in the time series of consumption data should be identified, and then a category detection algorithm should be performed. This is quite the same if the task is to categorize the customer in order to predict its behavior. Another task when stationary segments have to be detected is outlier detection, i.e. finding not reliable data in a huge dataset.

From a mathematical point of view the above mentioned problems have a common component: non-stationary time series has to be segmented into stationary ones, or by other words, change points in the signal should be identified. In this paper an information theoretic measure, the Jensen-Shannon Divergence (JSD) will be used for Change Point Detection (CPT) in a smart grid environment. It will be shown that the method is capable of detecting seasonality and category change in the time series.

The paper will be organized as follows: In Section 2. the JSD and its properties will be introduced. In Section 3. the generalized JSD and JSD-contour will be explained as a tool for CPT. In Section 4. numerical results will be presented, finally in Chapter 5. conclusions will be drawn.

2. The Jensen-Shannon Divergence

The JSD is an information theoretical measure to determine the distance of two discrete probability distributions [1,2,]. Let's denote $P = \{p_1, p_2, \dots, p_i, \dots p_K\}$ and $Q = \{q_1, q_2, \dots q_i, \dots q_K\}$ two discrete random distributions where p_i and q_i indicate the probability of the occurance of ith symbol in P and Q, respectively. In order to introduce the definition of the $JSD(P,Q)$, one needs the average distribution

$$A = \frac{P+Q}{2} = \{a_1, a_2, \dots, a_i, \dots a_K\}, \qquad (1)$$

where $a_i = \frac{p_i+q_i}{2}$. The JSD can be expressed by both the Kullback-Leibler Divergence and by the Shannon-entropy. Let's denote $KLD(P,Q) = \sum_{k=1}^{K} p_k log \frac{p_k}{q_k}$ the Kullback-Leibler Divergence [1], by which the JSD can be expressed as

$$JSD(P,Q) = \frac{D_{KL}(P,A) + D_{KL}(Q,A)}{2} \qquad (2)$$

Note that $KLD(P,Q) \neq KLD(Q,P)$, but $JSD(P,Q) = JSD(Q,P)$, and $JSD(P,Q) \geq 0$ furthermore $\sqrt{JSD(P,Q)}$ satisfies $\sqrt{JSD(P,Q)} \leq \sqrt{JSD(P,R)} +$

$\sqrt{JSD(R,Q)}$, hence it can be used as measure of distance.
The JSD can be expressed by the terms of the Shannon-entropy as well, gives as

$$JSD(P,Q) = H(A) - \frac{H(P)+H(Q)}{2} \qquad (3)$$

where $H(P) = -\sum_{k=1}^{K} p_k log p_k$. In the following section expression (3) is more convenient for our purposes, hence it will be used instead of (2).

3. The generalized JSD and the JSD-contour for CPT detection

The average distribution A in (1) can be seen as an averaged sum of the distributions P and Q, where the weights are 0.5. Let's introduce the weights $\omega_A, \omega_B > 0$, so that $\omega_A + \omega_B = 1$, than the average of the distribution is $A = \omega_P P + \omega_Q Q$ and using this new definition of the average distribution we arrive at the generalized JSD as

$$JSD(P,Q) = H\left(\omega_P P + \omega_Q Q\right) - \left[\omega_P H(P) + \omega_Q H(Q)\right] \qquad (4)$$

The purpose of this generalization is reducing the negative effect of unreliable estimates of the true statistical values by empirical ones using short segments.
The generalized JSD can be used for the segmentation of symbol-sequences introducing the idea of JSD-contour. Let us assume a symbol sequence $S = [s_1, s_2, ..., s_N] = [S_1, S_2]$ where $S_1 = [s_1, s_2, ..., s_{N_1}]$ and $S_2 = [s_1, s_2, ..., s_{N_2}]$ and the symbols take their values from a finite alphabet $s_i \in \{\alpha_1, ..., \alpha_k\}$. S_1 and S_2 will be referred to as left and right-series, respectively. Note that S_1 and S_2 are the real subsequences of the whole sequence S; our aim is to find the change point N_1. Let us denote an arbitrary segmentation of the whole sequence S by $S_l(n)$ and $S_r(n)$ where n stands for the segmentation point, and $n = \{1, 2, ..., N-1\}$. The relative frequencies of the symbols in a subsequence can be described by a K-element vector $P(n) = [p_1, p_2, ..., p_K]$ where $p_i = \frac{n_i}{n}$ and n_i is the number of occurrences of symbol α_i, and $Q(n) = [q_1, q_2, ..., q_K]$. The JSD-contour is a sequence of the generalized JSDs for all the possible segmentations $n = \{1, 2, ..., N-1\}$.

$$JSDC(S) = [JSD(1), JSD(2), ..., JSD(N-1)]$$

where

$$JSD(n) = H(\omega_P P(n) + \omega_Q Q(n)) - [\omega_P H(P(n)) + \omega_Q H(Q(n))]$$

In [3] it has been proven, that the sharpest peak in the JSD-contour can be observed, if the weighting factors are set as

$$\omega_P = n/N \text{ and } \omega_Q = \frac{N-n}{N}, \qquad (5)$$

respectively. This choice is reasonable to suppress the uncertainty of the relative frequencies in the case of short subsequences. However there is further reason: In the case of (5) the distribution of the JSD(n) (since it is a random variable because of the usage of relative frequencies) can be calculated, and can be used to evaluate the distance of the distribution of two subsequences.
In Figure 1. results of a numerical example can be seen. A sequence of length of 2500 has been generated by concatenating of two subsequences: the left sequence consists of 500 while the right sequence of 2000 symbols. The distributions of S_1 and S_2 were $P = [0.3, 0.7]$ and $Q = [0.5, 0.5]$, respectively (i.e. binary example). From these distributions 1000 sequences were generated. For each the JSD-contour has been calculated which are depicted by blue curves. The mean of the JSD-contours is indicated by red.

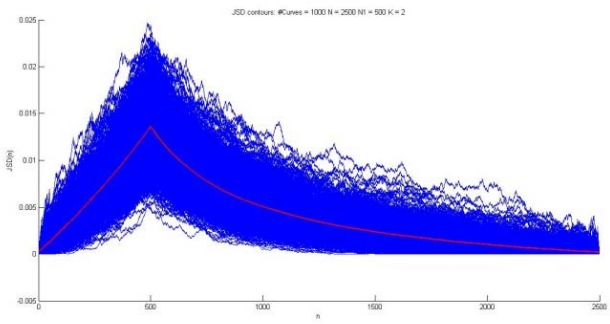

Figure 1. JSD-contour of 1000 randomly generated binary sequences (blue) and the mean of the contours (red)

In Figure 2. the distribution of the detected CPT by the JSD-contour can be seen for the same example. Note, that the true CPT of $n = 500$ is estimated with the largest probability and the variance is relatively low.

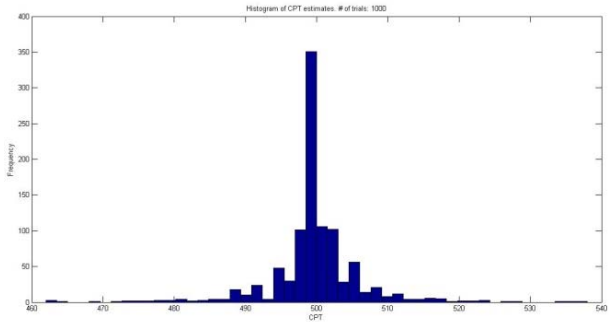

Figure 2. The histogram of the index of the maximum of the JSD-contour

4. Numerical results

In this section we test the performance of the JSD-contour based segmentation technique on real consumption data of households. In the numerical experiments the following assumptions has been made

- measurements are available from Smart Meters
- the non-stationary data series are composed from stationary sub-sequences
- the numerical measurement values can be mapped to a usable alphabet.

The original measurements were sampled by 12-bit AD-converter, resulting in an alphabet of $\mathbf{2^{12} = 4096}$ elements. We recognized that the JSD-contour based CPT detection does not perform satisfactory in the case of large alphabets. Therefore re-quantization of the measured sequence has been performed using a histogram-based method with histogram bin-width $\boldsymbol{h}$ and for number of bins $\boldsymbol{K}$ as

$$h = \frac{max - min}{\sqrt[3]{N}}$$

$$K = \left\lceil \sqrt[3]{N} \right\rceil$$

As a source of real data we used the UCI Machine Learning Repository [5]. In the database there are seven time-series available from December 2006 to November 2010. The sampling interval is 1 minute, the registered measures are global active power, global reactive power, voltage, intensity, sub-metering 1 (kitchen), sub-metering 2 (laundry), sub-metering 3 (water heater, air-conditioner).
As a test sequence for detecting the CPT we used artificially concatenated segments. Two scenarios has been tested:

- seasonal change (using winter-summer data of global active power);
- load profile change (using the data of sub-meters).

In Figure 3. and 4. The concatenated sequence can be seen with seasonal change point. The vertical magenta bar indicates the (artificial) change point. The JSD-contour is the red curve. In both cases the maximum of the JSD-contour seems to be a good estimation of the change points. The relative errors of the true change points and the approximated one are below 0.005. The relative error of the change point detection is measured by

$$e = \frac{|n_0 - \hat{n}_0|}{\hat{n}_0},$$

where n_0 is the artificial CPT, and $\hat{n}_0$ is the estimate of it by the maximum of the JSD-contour.

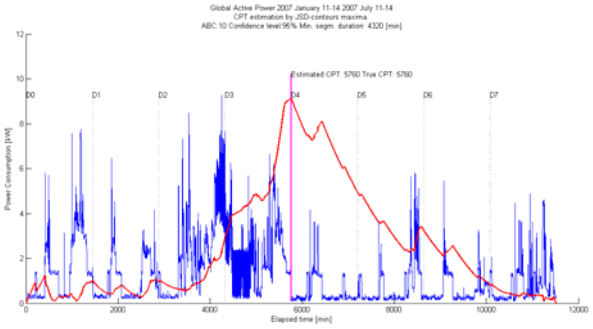

Figure 3. Concatenated seasonal data: left sequence January 11-14 2007, right sequence July 11-14 2007 (global active power)

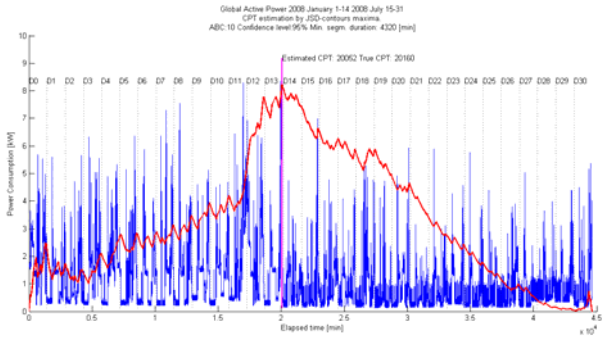

Figure 4. Concatenated seasonal data: left sequence January 1-14 2008, right sequence July 15-31 2008 (global active power)

In Figure 5.-7. The concatenated sequence can be seen with the change point coming from different sub-metering devices (but from the same time interval). In these cases the relative errors are below 0.03.

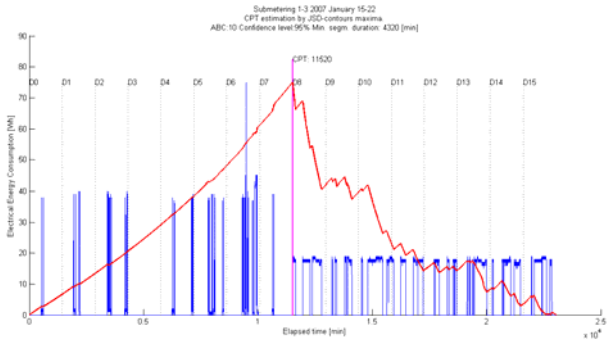

Figure 5. Concatenated home appliance data: left sequence: January 15-22 2007 ,sub-metering 1, right sequence: same days, sub-metering 3 (energy consumption)

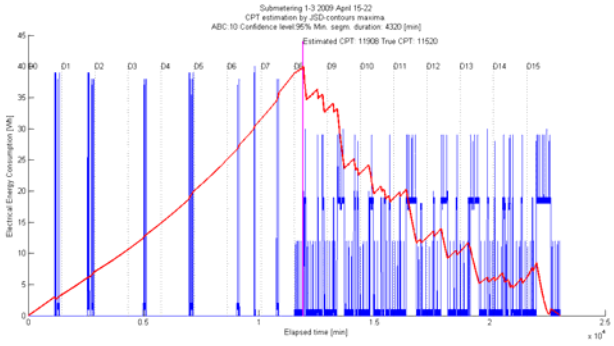

Figure 6. Concatenated home appliance data: left sequence: April 15-22 2009, sub-metering 1, right sequence: same days, sub-metering 3 (energy consumption)

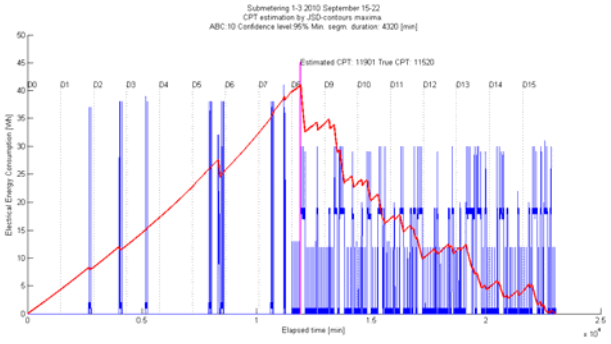

Figure 7. Concatenated home appliance data: left sequence: September 15-22 2010, sub-metering 1, right sequence: same days, sub-metering 3 (energy consumption)

5. Conclusions

This paper introduces the Jensen-Shannon Divergence Contour, which is capable to perform the segmentation of non-stationary sequences by an off-line manner. Extensive numerical analysis of real consumption data for the case of seasonal and category of appliance change point has been done. The results prove that the method can solve CPT problems in a smart grid environment.

6. Acknowledgement

This research and publication have been supported by the European Union and Hungary and co-financed by the European Social Fund through the project TÁMOP-4.2.2.C-11/1/KONV-2012-0004: National Research Center for the Development and Market Introduction of Advanced Information and Communication Technologies. This source of support is gratefully acknowledged.

7. References

[1] I. Csiszár, J. Körner: „Information Theory - Coding Theorems for Discrete Memoryless Systems“, Akadémiai Kiadó, Budapest, 1981.

[2] I. Deák: „Random Number Generators and Simulation“ Akadémiai Kiadó, Budapest, 1990.

[3] I. Grosse, P. Bernaola-Galván, P. Carpena, R. Román-Holdán, J. Oliver and H. E. Stanley: „Analysis of symbolic sequences using the Jensen-Shannon divergence“, Physical Review E, Volume 65, 2002, 041905 pp. 65-81.

[4] Lucien Birge and Yves Rozenholc: „How many bins should be put in a regular histogram', ESAIM: Probability and Statistics February 2006, Vol. 10. pp. 24-45.

[5] Bache, K., Lichman, M.: „UCI Machine Learning Repository“, Irvine, University of California, School of Information and Computer Science, [http:/archive.ics.uci.edu/ml], 2013

STATISTICAL INVESTIGATION OF GPS-BASED LOCALIZATION OF VEHICLES

Rajmund Drenyovszki[1], Lorant Kovacs[1*], Krisztian Barsony[1], Istvan Pinter[1] and Bence Csak[1]

[1] Kecskemet College, Faculty of Mechanical Engineering and Automation,
Izsaki ut 10, H-6000 Kecskemet, HUNGARY
* *Corresponding author e-mail: lorant.kovacs@gamf.kefo.hu*

Abstract
As part of an intelligent traffic management system development project we are building an in-vehicle GPS module for algorithms requiring position information. The aim of this paper is to present our statistical approach which is used to investigate the estimation of GPS receivers accuracies and to elaborate signal processing methods to improve precision.

Keywords:
GPS differential error, GPS location, covariance matrix

1. Introduction

Users of intelligent traffic management systems are growing worldwide. Traffic information is used not only by vehicle drivers but they are also available for public transport users, pedestrians and cyclists [1]. From the viewpoint of traffic and transportation the role of European integration is even more valuable. The need to develop cooperative intelligent traffic systems and services is increasing, applications use cross border data more extensively. Broad set of technical solutions are available that enable us to build intelligent traffic management systems so it is time to develop algorithmic solutions to solve the most relevant problems posed by our society. As many universities and research centers, Kecskemet College also joined the research activities related to intelligent traffic system developments. The "Smarter Transport – ICT support for cooperative traffic systems" (TÁMOP-4.2.2.A-11/1/KONV) project is about driver assistance and sustainable traffic solutions for vehicles, where vehicles communicate with each other (vehicle-to-vehicle) and with infrastructure elements (e.g. roadside units). In our project we are working on research fields that need GPS data processing.

Proactive pollution reduction with ad hoc networks capable of vehicle-to-vehicle and vehicle-to-infrastructure communication

Reducing environmental impact is feasible with preventive algorithmic solutions. On the one part technological basis for algorithmic developments are present in cars in the form of embedded systems (more specifically Electronic Control Units), on the other part researchers need to elaborate vehicle-to-vehicle and vehicle-to-infrastructure communication solutions to be able

to control traffic in a whole. It is possible to reduce environmental impact with reactive actions. Vehicles can send desired destination information prior to the trip, or in case it is not available, habitual route information can be communicated to a central traffic control system. Pre-trip knowledge about traffic can help the system to make optimal decisions so that preventing polluted gridlocks becomes possible. To reach these aims we need to collect GPS location information, learn habitual route behaviors and build adequate knowledge base.

Development of novel driver assistant systems with ad hoc networks capable of vehicle-to-vehicle and vehicle-to-infrastructure communication

One of the most effective ways to make traffic safety better is the improvement of the efficiency of driver assistant systems. Communication also opens up new ways towards the development of totally new kind of services in this field. One potential application can be the forecasting of risky situations based on database of drivers' profiles and motion and velocity vectors of nearby vehicles. Driving profiles are learned from vehicle dynamics and GPS location information. The driving assistant can send alert signals to own and nearby vehicles drivers according to the GPS data, forecasted vehicle path and dynamics.

Vehicles providing environmental data as mobile sensors platforms, data acquisition and communication tools

In case of vehicle-to-infrastructure communication capability, data coming from on-car sensors can be transmitted to central systems and much more information can be gathered from the environmental parameters as ever before in a distributed manner. If the system receives precise GPS positions, it can generate maps containing environmental parameter data and can make GSM/radio coverage measurements which can support several applications as background information.
We can see from the descriptions of our project aims that our main task is to collect and process the location data coming from GPS devices. First

of all we make measurements with multiple GPS receivers to be able to estimate GPS location errors with statistical investigations. Development of an intelligent traffic management system requires the elaboration of differential accuracy of GPS localization. If we can define a statistical method to improve the precision with multiple GPS receivers, we can build systems like collision avoidance which demand 1-2 m precision or better. This paper aims to rely on pure GPS data, and does not use sensor fusion techniques, which are available in the literature [2], most frequently using data coming from an accelerometer or gyroscope.
Sources of errors in GPS are from the differences of satellite positions, orbital fluctuation, multipath, relativistic and atmospheric effects, clock and rounding inaccuracies [3]. In consideration of the error sources and with attention on our application fields, following properties of measurement situations are the most important: accuracy-speed dependence, radius of trajectory, effect of multipath (high building, vs. rural environment) and weather conditions. In our measurements 3 different types of GPS receivers were installed in a car. It is important to note that these devices are not capable to use EGNOS system to make positioning more precise. The primal issue is that on a moving vehicle the exact GPS position is not available, so we do not have a fixed position as a reference point. The only opportunity to make implications is to use differential signal from multiple GPS receivers. In the followings the reader can find our model, evaluation of the measurement data and our final conclusions.

2. The model

In this paper an effective signal processing method will be introduced in order to improve the precision of GPS-based localization of vehicles. The base of the method comes from statistical analysis of the signals of multiple receivers. In the model the following assumptions were made:

- sensor fusing techniques such as combining the GPS signal with the signal of accelerometers are excluded;
- We can access only the global output of the GPS receiver devices (we cannot reach the raw data of time measurements);
- Possibly signal processing elements have been applied in the receiver devices – the algorithms are not known for us;

In the mathematical model we assume generally N receivers that measure a series of position in a synchronized way. For the sake of simplicity, without any loss of generality, we assume N=3. Let us denote the signal of the ith receivers by X_i as follows

$$\begin{aligned} X_1 &= X_0 + \mu_1 + \xi_1 \\ X_2 &= X_0 + \mu_2 + \xi_2 \\ X_3 &= X_0 + \mu_3 + \xi_3 \end{aligned} \tag{1}$$

where X_0 denotes the exact position, μ_i is the DC offset of the ith receiver and ξ_i represents Gaussian measurements noise with zero mean and σ_i standard deviation

$$\begin{aligned} \xi_1 &\sim N(0, \sigma_1) \\ \xi_2 &\sim N(0, \sigma_2) \\ \xi_3 &\sim N(0, \sigma_3) \end{aligned} \tag{2}$$

respectively. The measurement noise of the different receivers are assumed to be independent, and hence uncorrelated:

$$E(\xi_i \xi_j) = 0 \tag{2.1}$$

The basic problem is, that in the case of a moving vehicle, we have no information about the exact position X_0, therefore we can elaborate the statistical properties of difference sequences. In order to do this we define the following variables:

$$\begin{aligned} d_{12} &= x_1 - x_2 = \mu_1 - \mu_2 + \xi_1 - \xi_2 \\ d_{23} &= x_2 - x_3 = \mu_2 - \mu_3 + \xi_2 - \xi_3 \\ d_{31} &= x_3 - x_1 = \mu_3 - \mu_1 + \xi_3 - \xi_1 \end{aligned} \tag{3}$$

Using the properties of Gaussian random variables [4] the statistics of the difference signals are

$$\begin{aligned} d_{12} &\sim N(\mu_1 - \mu_2, \sigma_{12}) \\ d_{23} &\sim N(\mu_2 - \mu_3, \sigma_{23}) \\ d_{31} &\sim N(\mu_3 - \mu_1, \sigma_{31}) \end{aligned} \tag{4}$$

where

$$\begin{aligned} \sigma_{12}^2 &= \sigma_1^2 + \sigma_2^2 \\ \sigma_{23}^2 &= \sigma_2^2 + \sigma_3^2 \\ \sigma_{31}^2 &= \sigma_3^2 + \sigma_1^2 \end{aligned} \tag{5}$$

respectively. Furthermore we can calculate the covariance matrix **K** of the difference signals, where by definition

$$\boldsymbol{K} = \begin{bmatrix} E(\tilde{d}_{12}^2) & E(\tilde{d}_{12} \cdot \tilde{d}_{23}) & E(\tilde{d}_{12} \cdot \tilde{d}_{31}) \\ E(\tilde{d}_{23} \cdot \tilde{d}_{12}) & E(\tilde{d}_{23}^2) & E(\tilde{d}_{23} \cdot \tilde{d}_{31}) \\ E(\tilde{d}_{31} \cdot \tilde{d}_{12}) & E(\tilde{d}_{31} \cdot \tilde{d}_{23}) & E(\tilde{d}_{31}^2) \end{bmatrix} \tag{6}$$

and

$$\tilde{d}_{12} = d_{12} - E(d_{12}) = \xi_1 - \xi_2$$
$$\tilde{d}_{23} = d_{23} - E(d_{23}) = \xi_2 - \xi_3 \quad (6.1)$$
$$\tilde{d}_{31} = d_{31} - E(d_{31}) = \xi_3 - \xi_1$$

are the centralized difference variables. The expectations in the covariance matrix can be easily calculated as

$$E(\tilde{d}_{12}^2) = E((\xi_1 - \xi_2)^2) = E(\xi_1^2 - 2\xi_1\xi_2 + \xi_2^2) = \sigma_1^2 - \sigma_2 \quad (7)$$

$$E(\tilde{d}_{12} \cdot \tilde{d}_{23}) = E((\xi_1 - \xi_2)(\xi_2 - \xi_3)) = E(\xi_1\xi_2 - \xi_2^2 - \xi_1\xi_3 + \xi_2\xi_3) = -\sigma_2^2 \quad (8)$$

where we used the assumption that the measurement noises are uncorrelated. As a result

$$\mathbf{K} = \begin{bmatrix} \sigma_1^2 + \sigma_2^2 & -\sigma_2^2 & -\sigma_1^2 \\ -\sigma_2^2 & \sigma_2^2 + \sigma_3^2 & -\sigma_3^2 \\ -\sigma_1^2 & -\sigma_3^2 & \sigma_1^2 + \sigma_3^2 \end{bmatrix} \quad (9)$$

3. Measurement results

For validation of the model described in Section 2 the signal of three different GPS receivers has been registered in urban environment installed in a car. Since the exact trajectory of the vehicle is not known, only the differential data were used for calculations. The types of the receivers that were used are

- Sony Ericsson Xperia sk17i Mini Pro
- Garmin GPS18x-5Hz
- Bluetooth connected G-Sat BT-328

All the GPS receivers has been sampled by 1 Hz sample frequency. The measurement time was approximately 11 minutes resulting altogether 668 coordinate data per receiver.
We made difference calculations separately for the latitude and longitude coordinates, because the Gaussian assumption can be used only for coordinate data (the Euclidean distance is a positive valued random variable, with chi-square distribution [5] in the case of Gaussian coordinate-data.)

Results for latitude coordinates

In Figure 1 the difference signals as a function of time can be seen, while in Table 1 we summarized the statistical parameters of the difference signals. We used the following notations:

- d_{12}: Xperia-Garmin
- d_{23}: Garmin-Bluetooth
- d_{31}: Bluetooth-Xperia

Note, that there is a nonzero mean, i.e. a constant offset between the receivers. In the case of the Xperia-Garmin difference, this offset is almost 5 meters. The standard deviations are approximately 3-5 meters, but the maximum of the differences is of approx. 40 m. For more information see Figure 2 which depict the histograms of the difference signals. We also performed chi-square hypothesis test to validate the normality of the difference signals, the H0 hypothesis of normality should be rejected with a negligible probability (see Table 1), i.e. the Gaussian hypothesis for the measurement uncertainty validated by our measurements.

	d_{12}	d_{23}	d_{31}
mean	4.8024	-1.4500	-3.3524
standard deviation	3.0778	4.4750	5.3314
prob. of H0 reject.	8.36e-143	0	2.38e-241

Table 1. Statistics for latitude difference values

The covariance matrix of the difference signals can be used to estimate the individual uncertainty of the receivers, as explained in Section 2, the covariance matrix for the latitude data is

$$\mathbf{K} = \begin{bmatrix} \mathbf{9.4727} & \mathbf{-0.5369} & \mathbf{-8.9358} \\ \mathbf{-0.5369} & \mathbf{20.0254} & \mathbf{-19.4885} \\ \mathbf{-8.9358} & \mathbf{-19.4885} & \mathbf{28.4243} \end{bmatrix}$$

from which the estimation of the individual standard deviations of the receivers are

$$\sigma_{Xperia} = \sqrt{8.9358} = 2.99m$$
$$\sigma_{Garmin} = \sqrt{0.5369} = 0.73m$$
$$\sigma_{Bluetooth} = \sqrt{19.488} = 4.41m$$

As one can see, the accuracy of the three receivers are very different (regarding the latitude coordinate), Garmin has the smallest standard deviation of 0.73 m.

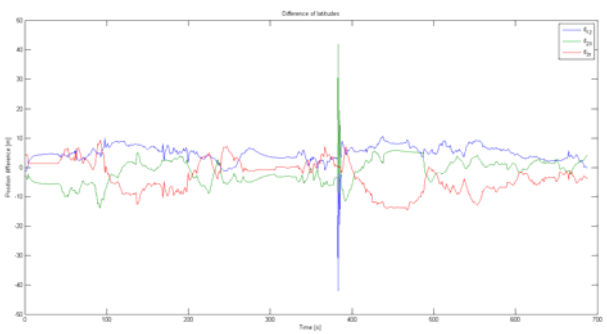

Figure 1. Differences of latitude coordinates

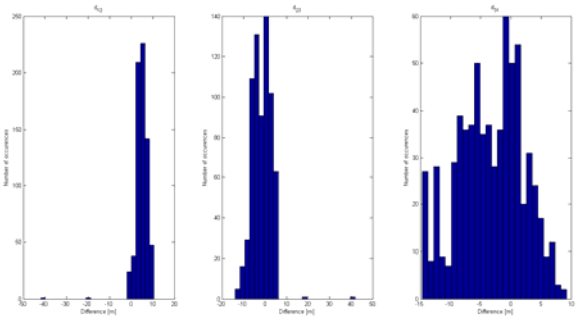

Figure 2. Histograms of differences of latitude coordinates

Results for longitude coordinates

In Table 2 there are the descriptive statistics of the longitude coordinate data. The offset is much lower for longitude (<0.5m). The hypothesis of normality can be accepted by a high probability for the longitudes as well. In Figure 3 and 4 the difference signal and the histograms of longitude data are depicted, respectively.

	d12	d23	d31
mean	0.4969	-0.4580	-0.0388
standard deviation	4.8955	9.2832	7.8148
prob. of H0 reject.	1.81e-005	4.64e-163	3.80e-029

Table 2. Statistics for longitude difference values

The covariance matrix:

$$\mathbf{K} = \begin{bmatrix} 23.965 & -24.536 & 0.5702 \\ -24.536 & 86.178 & -61.64 \\ 0.5702 & -61.64 & 61.0719 \end{bmatrix}$$

from which the standard deviations of the individual receivers:

$$\sigma_{Xperia} = \sqrt{0.5702} = 0.75m$$

$$\sigma_{Garmin} = \sqrt{24.536} = 4.95m$$

$$\sigma_{Bluetooth} = \sqrt{-61.64} = 7.85m$$

Note, that for the longitude coordinate the Xperia has the lowest standard deviation of 0.75 m, and (as well as for latitude) Bluetooth shows the poorest performance.

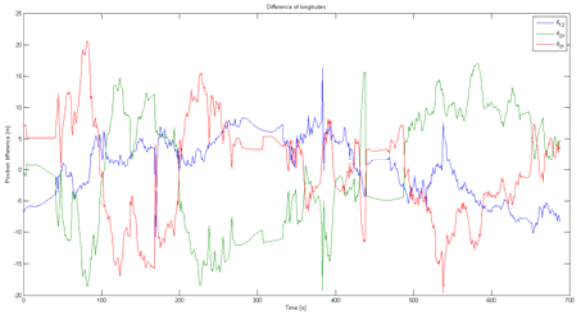

Figure 3. Differences of longitude coordinates

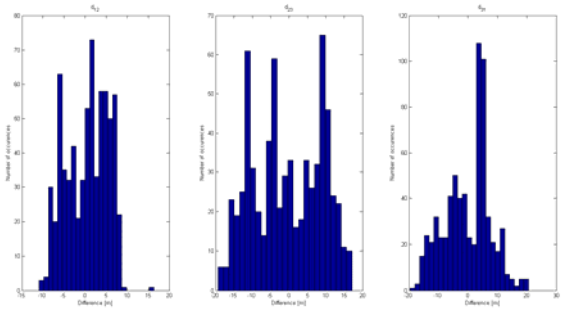

Figure 4. Histograms of differences of longitude coordinates

As a conclusion one can see, that in the case of this three type of receivers the longitude coordinate data should be read from the Xperia, while the latitude from the Garmin receivers, having smaller variance than can be reached by averaging.

4. Conclusion and future work

In this paper we introduced statistical investigation to recognize the statistical behavior of commercial GPS receivers. The Gaussian nature of the uncertainty of the measurement has been proven. Using the special form of the correlation matrix, a method has been introduced to estimate the individual accuracy of the receivers by differential measurements. In the future, for the sake of statistical reliability much more data point will be required. For control more receivers from the same type should be incorporated. The accuracy as a function of different parameters related to mobile vehicle applications (such as velocity, shape of trajectory, rural vs. urban environment) should be systematically detected.

5. Acknowledgement

This research is supported by TÁMOP-4.2.2.C-11/1/KONV-2012-0012: "Smarter Transport" - IT for co-operative transport system - The Project is supported by the Hungarian Government and co-financed by the European Social Fund.

6. References

[1] J. Pfister, B. Horváth, T. Kulpa, T. Tvrzsky, "GSP-technical feasibility and achieve results"

[2] C. Hide, T. Moore, M. Smith, "Adaptive Kalman Filtering for Low-cost INS/GPS". The Journal of Navigation, 56, pp. 143-152, 2003

[3] "Sources of Errors in GPS," [Online] Available: http://www.kowoma.de/en/gps/errors.htm [Accessed: 10-Sept-2013].

[4] J. Wu, "Some Properties of the Gaussian Distribution", 2004

[5] E. Hung, L. Xiao, R. Y.S. Hung, "An Efficient Representation Model of Distance Distribution Between Uncertain Objects", Comp. Int., Vol. 28, Issue 3, pages 373-397, Aug 2012.

COMPARSION OF FLAT AND ROUND NOZZLE USING FOR DISINTEGRATION OF PMMA BY PULSATING WATER JET TECHNOLOGY

D. Lehocká[1*], S. Hloch[1,2], J. Foldyna[2], P. Monka[1], K. Monková[1],K. Colic[3] and K. Brezíková[1]

[1]Faculty of Manufacturing Technologies with seat in Prešov – Technical University of Košice, Slovakia
[2]Institute of Geonics Academy of Science of Czech Republic, v.v.i., Ostrava Poruba, Czech Republic
[3]University of Belgrade, Innovation Center of Faculty of Mechanical Engineering, Belgrade, Serbia
* Corresponding author e-mail: lehocka.dominika@gmail.com

Abstract
Paper deals with comparsion of flat and round nozzle using of disintegration of PMMA by pulsating water jet. As a bone cements were used PALCOS R+G. Samples were prepared by vacuum mixing. Experiments with pulsating water jet were done using two types of nozzles - flat and round. Influence of pulsating water jet factors on volume removal rate was studied. Results will serve for understanding of pulsating water jet interaction and PMMA, in order to use results for possible surgery technique, for easy removal of cemented femoral stem from femoral channel during revised surgery. Results show that pulsating water jet will be possible focuses as a tool for medical purposes, but further detailed research is needed.

Keywords:
pulsating water jet, PMMA - bone cement, volume removal

1. Introduction

Achievement of implantation of total hip joint replacement and its long-term life depends on many factors, which include: the correct surgery indication, patient preparation, proper realization of the surgical operation, the surgeon's experience, technical equipments, conditions in the operating room and the post-operative care [1], [2], [3]. The components of endoprosthesis have to withstand the cyclic loading for many years, what satisfies to the weight of the human body at least three to five times. Implantation of metal, ceramic or plastic substitutes into the human body can cause many problems that lead to the failure of total endoprothesis [1], [4], [5].

At the failure of total endoprothesis, the reimplantation is needed, what means that the freed endoprothesis is replaced [6] and that is why the bone surgery requires the precise technique. Classic division even today uses conventional instruments. In the past, there were chisels and handsaws, currently there are used pneumatically operated saw and high speed milling cutter. Bone, however by responds very sensitive to the temperature and time of its actuating. The aforementioned tools cause irreversible damage of bone tissue in femoral canal working [1], [7], [8], [9], [10], [11].

Unfortunately, number of degenerative joint diseases (osteoarthritis) is constantly increasing in the last period, what represents a significant medical, economic and social problem in regard of diseases importance, therapeutic complications and relatively frequent disability of person [1], [3]. In order to be the replacement of damaged prosthesis allowed, it is necessary to destroy the interface between the bone and a femoral stem, where the interface is formed by bone cement - polymethylmethacrylate (PMMA). The traditional tools (such as drills or oscillating saws) are used for the destruction. However, there are a large number of disadvantages associated with the utilization of these tools, such as high risk of fragmentation, cracking and various other complications connected with reimplantation of total hip joint [1].

Authors Hloch, et al. [12] studied experimental examination of PMMA disintegration by water jet. They investigated the mechanical properties of PMMA disintegration using plain and pulsating water jet. The research showed that disintegration of PMMA by pulsating water jet is better choice and it has better mechanical properties as disintergration by plain water jet.

The main goal of the experimental investigation described in this paper was to determine the influence of selected factors of pulsating jet (pressure and stand-off distance) on the volume removal of PMMA.

2. Material and Methods

In order to verify the possibilities of PWJ application in bone cement disintegration, the experiments were performed on experimental materials called Palcos R+G. PMMA was prepared under the vacuum and it was prepared in accordance with the manual for mixing. After mixing the powder and liquid components created a flowable substance that was injected into a mold where it hardened. Following the removal of samples from mold, PMMA were ready to carry out experiments [1].

In this article were compared 2 samples of Palcos R+G to illustrate the experiments with flat and round nozzle (Table 2 and Table 3)

The tests were performed at the Institute of Geonics of the ASCR in Ostrava – Poruba. The 2D X-Y cutting table PTV WJ2020-2Z-1xPJ with inclinable cutting head specially designed for cutting with water jet was used for disintegration tests of PMMA. Technological set up consisted of plunger pump Hammelmann HDP 253 (max. operating pressure of 160 MPa, maximum rate of 67 l/min) and a robot ABB IRB 6640-180//2.55 Master for handling of water jet cutting head. Pulsations were generated by ultrasonic device Ecoson WJ-UG_630-40. Technological conditions of tests are listed in Tab. 2. Depth of the traces, created by PWJ, was measured over an area 4x4 mm using an optical profilometer MicroProf FRT (Figure 1b). Experimental test were performed with flat and round circular nozzles and following factors combination [13]:

- at flat nozzle (Figure 1a); sample D1) with a diameter 0,8 mm, it was performed 6 tests of material removal by PWJ. The distance of the nozzle and material varied between 3-7 mm. One test will incorrect setting was done [13].
- at round circular nozzle (Figure 1a); sample D2) with a diameter 0,7 mm, it was performed 4 tests of material removal by PWJ. The pressures varied from 8 MPa to 20 MPa with an increasing step 4 MPa and the nozzle stand-off from material was at a distance of 2 mm in all 4 tests [13].

Table 1. Characteristics of experimental material [13]

Trade name	Mark	ATB	Weight	Colour	Consistence	Type of mixing
Palacos R+G	D1, D2	yes	40 g	green	dense	vacuum

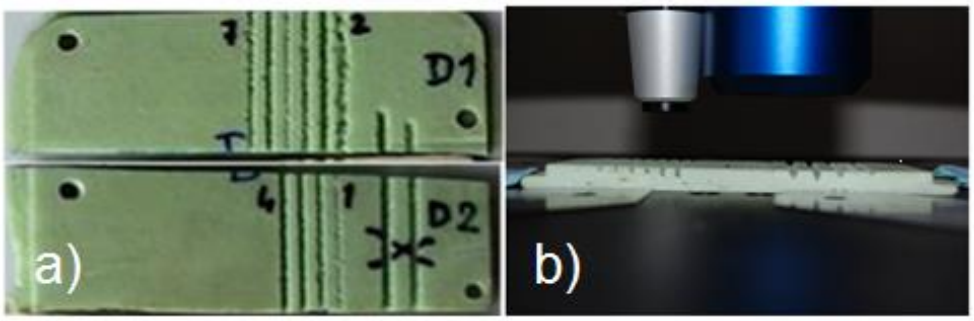

Figure 1 a) Samples D1, D2 Palacos R+G mixed in vacuum; b) Measurement of the sample by optical profilometer Micro Prof FRT [13]

Table 2. Tests on PMMA by means of flat nozzle [13]

Parameters for group of samples no. 1							
Nozzle type flat, splash angle 10°		Equivalent nozzle diameter 0,8 mm	Feed rate 60 mm/min	Frequency of pulsations 40 kHz		Position of the face of sonotrode A 12 mm	
Run		2	3	4	5	6	7
Pressure (MPa)		20	20	16	12	12	8
Jet type		Pulsating	Pulsating	Pulsating	Pulsating	Pulsating	Pulsating
Stand-off distance (mm)		Incorrect set up	7	7	7	4	3
Volume material removal from the area 4x4 mm (μm^3)	D1	$-1{,}68 \times 10^{10}$	$-2{,}13 \times 10^{10}$	$-1{,}80 \times 10^{10}$	$-3{,}35 \times 10^{9}$	$-1{,}40 \times 10^{10}$	$-9{,}40 \times 10^{9}$

Table 3 Tests on PMMA by means of round nozzle [13]

Parameters for group of samples no. 2					
Nozzle type round, sapphire		Equivalent nozzle diameter 0,7 mm	Feed rate 60 mm/min	Frequency of pulsations 40 kHz	Position of the face of sonotrode A 0 mm
Run		1	2	3	4
Pressure (MPa)		8	12	16	20
Jet type		Pulsating	Pulsating	Pulsating	Pulsating
Stand-off distance (mm)		2	2	2	2
Volume material removal from the area 4x4 mm (μm3)	D2	$-1,17x10^{10}$	$-1,11x10^{10}$	$-1,11x10^{10}$	$-6,21x10^{9}$

3. Results and Discussion

On the basis or carried out experiments, the disintegration tests on PMMA are described the tables (Table 2 and Table 3). When individual parameters varied (nozzle type, nozzle diameter, feed rate and stand-off distance of the nozzle from the material), the changes in volume material removal occurred, too. Total 10 tests of material disintegration tests were performed at various pressures and stand-off distance of the nozzle from material. Six tests (Table 2) shows the selected groove on sample of PMMA (Figure 1a), which were created at a the pressure of 12 MPa and using flat nozzle (Table 4). These grooves varied depending on the change of the stand-off distance between the nozzle and material (4 and 7 mm) [13].

Table 4 The comparison of material removal using of flat nozzle at the lift change [13]

Factors no. 1	Groove no. 5		Factors no. 1	Groove no. 6
pressure, jet type	lift		pressure, jet type	lift
pressure 12 MPa, pulsating	SOD 7 mm		pressure 12 MPa, pulsating	SOD 4 mm
Sample mark	Volume material removal (μm^3)		Volume material removal (μm^3)	Sample mark
D1	$-3,35x10^{9}$	>	$-1,40x10^{10}$	D1

In the second comparison, the variability in volume material removal was observed with the change of operating pressure round nozzle type. In the table below (Table 5) is showed grooves on PMMA samples, which were created at a fixed stand-off distance 2 mm between the nozzle and target material. The depth of the grooves varied depending on the change of operating pressure 12 MPa and 16 MPa [13].

Table 5 The comparison of material removal using of round nozzle at the lift change [13]

Factors no. 2	Groove no. 2		Factors no. 2	Groove no. 3
pressure, jet type	lift		pressure, jet type	lift
pressure 12 MPa, pulsating	SOD 2 mm		pressure 16 MPa, pulsating	SOD 2 mm
Sample mark	Volume material removal (μm^3)		Volume material removal (μm^3)	Sample mark
D2	$-1,11x10^{10}$	<	$-1,27x10^{10}$	D2

In the first series of measurements, when using flat nozzle (Figure 2), at the pressure 12 MPa and at the stand-off distance 7 mm between the nozzle and material, the samples showed higher removal of material compared to the same pressure and stand-off 4 mm). From given measured sample values result that the highest volume removal of PMMA was under the actuating of pressure of 8 MPa and at the stand-off distance of flat nozzle 3 mm. These conditions appear to be best suited for disintegration of PMMA, but additional measurements will be needed. Grooves stand-off recorded in Figure 3 were compared at constant parameter of round nozzle - 2 mm. The maximum volume removal of

material was, in this series of measurements, observed at a pressure of 20 MPa. However it will be necessary to carry out next measurements, which will confirm this finding.

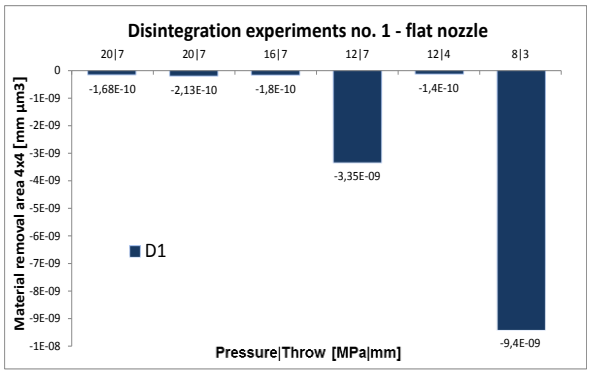

Figure 2 Graphical presentation of tests no.1 on PMMA at flat nozzle

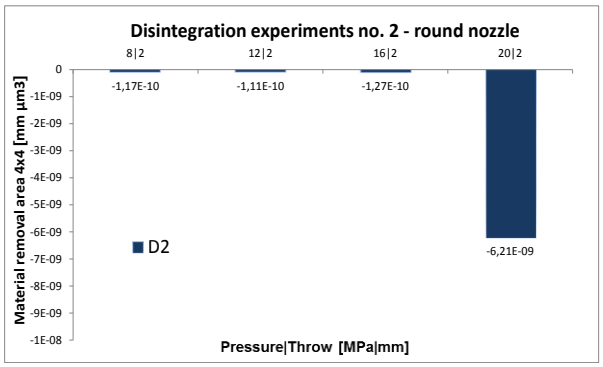

Figure 3 Graphical presentation of tests on PMMA at round nozzle

4. Conclusion

The results obtained in this part of work will serve as a aid for next experimental investigation of PWJ using within PMMA disintegration. Obtained data will be a valuable source of information needed in the continuing research.

The importance of this investigation is evident, especially from the view of science and research, at which a man's life should be in the first place. This research directs towards to the finding of the ways how to improve a person's life, specifically in simplifying surgical procedure and less destructive interference with the human body at reimplantation of total replacement of endoprothesis. Easier convalescence of a person after surgery represent another man´s life improvement.

5. Acknowledgement

This work was supported by the Slovak Research and Development Agency under the contract No. APVV-207-12.

Experiments were carried under the support Institute of clean technologies for mining and utilization of raw materials for energy use, reg. no. CZ.1.05/2.1.00/03.0082 supported by the Research and Development for Innovations Operational Programme financed by the Structural Funds of the European Union and the state budget of the Czech Republic, and with support for the long term conceptual development of the research institution RVO:68145535.

6. References

[1] S. Hloch, et al., „Hydroabrasive cutting in orthopedics“, Prešov 2011. ISBN 978-80-970623-4-7.

[2] A. Majerová, „Preoperative and early postoperative rehabilitation care for patients after total hip replacement“, In. Rehabilitácia. vol. 33, 2000, no. 1, p. 11-23. ISSN 0375-0922. (in Slovak)

[3] E. Novotná, K. Modranská, „Quality of human life after an accident skeletal system,“ In. Revue ošetrovateľstva. vol. 12, 2006, no. 3, p. 143. ISSN 1335-5090. (in Slovak)

[4] A. Sosna, et al., „Basics of orthopedics,“ Praha: Triton, 2001. ISBN 80-7254-202-8.

[5] A. Sosna, et al., „Hip arthroplasty. Guide the patient's period of operation, rehabilitation and other life,“ Praha: Triton, 1999.

[6] L. Nečas, et al., „Slovak arthroplastic register – analysis 2003-2008,“ 2009.

[7] A. Eriksson, et al., „Heat caused by driling cortical bone. Temperature measured in vivo in patients and animals,“ Acta Orthop Scand, 1984, vol 55(6), pp. 629-31.

[8] O. García, et al., „The Influence of the Size and Condition od the Reamers on Bone Tepmerature During Intramedullary Reaming.“ The Journal of Bone and Joint Surgery (Americian) 86:994-999 (2004).

[9] A. Goran, et al., „Thermal osteonecrosis and bone driling parameters revised.“ Arch Orthop Trauma Surg, 2008; 128:71-77.

[10] M., T. Hillary, I. Shuaib, „Tepmerature effects in the driling of human and bovine bone,“ In. Journal od Materials Processing Technology. Vol. 92-93, 1999, pp. 302-308.

[11] V. Modrák, „Some specifics of the design technology of water jet method.“ In. Machining technology in automated engineering production: Anniversary volume from conference. Košice: DT ZSVTS, 1993.

[12] S. HLOCH, et al.: „Disintegration of high fatigue G bone cement and Palacos R+G® by pulsating water jet,“ CIM 2013: Computer Integrated Manufacturing and High Speed Machining. International Scientific Conference on Production Engineering, Biograd, Croatia. Zagreb: Croatian Association of Production Engineering, 2013. ISBN 978-953-7689-02-5.

[13] K. Brezíková, „Analysis of the causes affecting the proces of removing material by pulsating water jet,“ Bachelor thesis, Technical University of Košice, Faculty of Manufacturing Technologies, Prešov, 2013.

STATISTICAL EVALUATION OPTIONS AT MACHINING OF COMPOSITES

J. Líska[1*], I. Jámbor[2*]

[1]Kecskemét College, Faculty of Mechanical Engineering and Automation, Kecskemét, Hungary
[2]ACTA NON VERBA, s. r. o.
1 liska.janos@gamf.kefo.hu, 2*ijambor@anv.sk*

Abstract
Main application areas of composites we can mention as: automotive industry, reactor technique, chemical industry, entertainment industry and sports-related industries. Today, composites are used not only with flat surfaces and free form surfaces, but materials with round surfaces, too. They have to be machined (turned) that assembled with metal parts can be built-in. We used a GFRP (Glass Fibre Reinforced Plastic) part with round surface. During the experiments we measured: the cutting temperature by infrared camera and we measured surface roughness too. We evaluated the results statistically and graphically by the help of SPSS software and Excel. Our goal is to help the development of composite-material industry and to define the required parameters at turning.

Keywords:
Composite, Turning, Linear regression model, Coefficient of determination, Stability

1. Introduction

The composite materials, or the composites, are the construction materials made of two or more components with significantly different physical and chemical properties. Combinating this two components we create a new material with unique properties that cannot be reached by none of these components separately neither by simply summarization [1,2].

As a composite it can be understood such a material that meets following conditions:

- Was made artificially,
- Consists of at least two chemically different components,
- The components have homogenous distribution throughout the volume from the macroscopic point of view,
- Consequential properties of composite are different from the properties of the individual components

These conditions exclude the natural materials (eg: wood as associated material to lignin matrix, reinforced by celluloid fibres, further bamboos, bones, etc.)

At present time the composite materials can be divided by a type of matrix and by a production method [1,2].

Division by a type of matrix is following:

- Polymers,
- Metallic,
- Ceramic [1,2].

The glass in the Mohs scale of hardness neighboures with cemented carbide, carbide of silicon and with boron carbide. Therefore all the materials besides PCD (polycrystalline diamond) will be intensively worn by the machining of glass reinforced composite materials [1,2].

The filler of the composite materials can be oriented differently so the material is anisotropic. The process of machining influences a binder too, as the carrying-off heat is poor and “sticks” the function surfaces of the cutting tool, mainly the cutting face [1,2].

It is possible to machine the reinforced composites on the standard metal or alternatively wood processing machine tools without cooling, but with sucking dust and chips [1,2].

Very low carrying-off heat of the machined material (glass reinforced composite) causes that the heat is not getting through to the chip and the work piece so extensively as by the metal machining. Therefore it must be carried-off by tool. This significantly increases the tool wear. To use the cooling system is not possible, alternatively only in few rare cases [1,2].

It is possible to use cemented carbide with high quality coat or diamond (PCD).

As the composites are low resistant to temperatures (100 to 300 °C) they are not constant and so the cutting conditions need to be adjusted not to reach the critical temperature [1,2].

The physical properties of the fibre and the basic material are completely different and together with the fibre orientation predestinate the cutting power and machinability of composite material [1,2].

2. Experimental part

Experiments in mechanical engineering are planned by the help of full-factorial design of experiment, which says, that for investigation of machining process is applicable the “black box” [1].

We designed an experiment with combination of three variables of minimum, middle and maximum values (1. Table).

During the experiments we use conventional turning machine SU50/1500 Combi, the diameter of workpiece were Ø96mm, the cutting material

was PCD insert and the cutting (v_c) speed were 200 m/min.

The aim of this section is to find a mathematical model between the input and output parameters along cutting composite materials. From technical viewpoint, the following inputs (independent or explanatory variables) were specified:

- depth of cut - *ap* [mm]
- main cutting edge – K_r [º]
- feed – *f* [mm/rev.]

For the outputs (dependent variables):

- surface roughness depth – *Ry* [µm]
- cutting temperature – *T* [°C]

were selected.

1. Table Technological parameters and results

No.	a_p [mm]	K_r [º]	f [mm/rev.]	R_y [µm]	T [°C]
1.	0,5	45	0,1	26,038	85,5
2.	0,5	45	0,15	41,996	89,5
3.	0,5	45	0,2	65,747	96,6
4.	0,5	60	0,1	17,787	81,1
5.	0,5	60	0,15	18,146	78,5
6.	0,5	60	0,2	19,881	83,9
7.	0,5	90	0,1	26,546	67,9
8.	0,5	90	0,15	28,98	76,7
9.	0,5	90	0,2	33,301	69,3
10.	0,75	45	0,1	25,924	89,4
11.	0,75	45	0,15	33,048	99,1
12.	0,75	45	0,2	51,71	104
13.	0,75	60	0,1	11,154	93,8
14.	0,75	60	0,15	14,23	102
15.	0,75	60	0,2	17,081	99,4
16.	0,75	90	0,1	25,528	78,8
17.	0,75	90	0,15	24,882	86
18.	0,75	90	0,2	29,433	82,9
19.	1	45	0,1	34,916	96,6
20.	1	45	0,15	33,503	110
21.	1	45	0,2	55,158	108
22.	1	60	0,1	10,724	88,2
23.	1	60	0,15	12,408	97,1
24.	1	60	0,2	16,34	105
25.	1	90	0,1	24,339	73
26.	1	90	0,15	28,669	89
27.	1	90	0,2	33,567	93,6

3. The statistical evaluation of results

We will consider 3 different models. First the linear:

$$y = b_0 + b_1 x_1 + b_2 x_2 + b_3 x_3 \quad (1)$$

Afterwards the exponential and polynomial:

$$y = b_0 b_1^{x_1} b_2^{x_2} b_3^{x_3} \quad (2)$$

$$y = b_0 x_1^{b_1} x_2^{b_2} x_3^{b_3} \quad (3)$$

The two latter can be easily transformed into linear by logarithmization (along our investigation, the 10 based logarithm was used).

For the calculations, mainly the SPSS software was used, for its advantageous features, namely that from a set of input variables it can choose the subset determining the output variable the best. With other words, it finds the optimal regression function. This procedure has 2 commonly used approaches, the Backward and the Stepwise method. We used the latter, which continuously builds new variables into the model, according to certain criteria.

During the construction of the model several possible input variable sets were tested and for each of them, the coefficient of determination was calculated. This coefficient is to show how much % of the uncertainty for the dependent variable (the variance) can be dispersed given the input variables. Although it is not very exact, but it is common to say: how precisely the input variables determine the dependent ones.

Obviously, along the work, it was always tested that the conditions of the linear regression (normality of the error term, homoscedasticity, etc.) are fulfilled.

Models for the roughness depth

At first, the correlation matrix was determined between all input and output variables.

2. Table Correlation Matrix

	ap	K_r	*f*	*Ry*	*T*
ap	1				
K_r	0	1			
f	0	0	1		
Ry	-0,10	-0,74	0,41	1	
T	0,53	-0,40	0,35	0,24	1

From Table 2., several observations can be made:

- the input variables are obviously not correlated
- the roughness is negatively correlated with the K_r angle, and, though less strongly, but also negatively correlated with the feed
- the correlation between the roughness and the depth of cut is negative, but very weak

Let us now consider the investigated models. From the set of models tested, the following proved to be the most appropriate:

$$Ry = 10^{-14.15} 0.83^{Kr} 62.6^{f} a_p^{-0.223} K_r^{11.52} \quad (4)$$

The coefficient of determination of the corresponding linear model was 0.91, indicating that 91% of the variance of the dependent variable can be eliminated given the independent variables. For simplicity, in the sequel we will also say that the input variables determine the model in 91%.

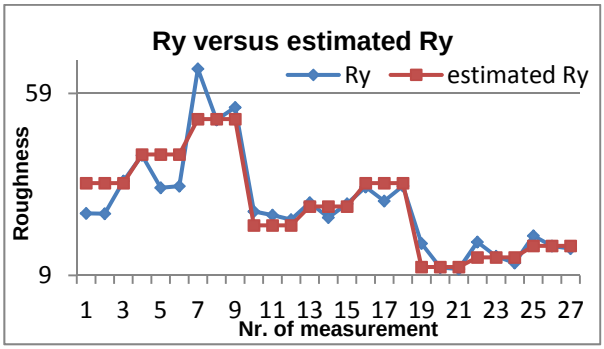

Figure 1. The 1st model for Ry

Visibly, the fit is fairly good. Nevertheless, in equation (4), the order of magnitude of the term $Kr^{11.52}$ makes the model instable for input variables – even a small change in K_r changes a lot, that is why the constant has to be so small, to compensate this phenomenon.

Therefore, it is a straightforward idea to find a model which might be slightly less well determined, but more stable. Indeed, the following model satisfies this:

$$Ry = -623.4 - 3.53Kr + 132.5f + 485.8\log K_r \quad (5)$$

This model has a few advantages compared to the previous one. First, it does not have coefficients with a huge order of magnitude. Second, it does not have the term *ap,* which makes it simpler. On the other hand, we had to pay the price of this, the coefficient of determination dropped to 0.8. However, an 80% determination is still considered as good.

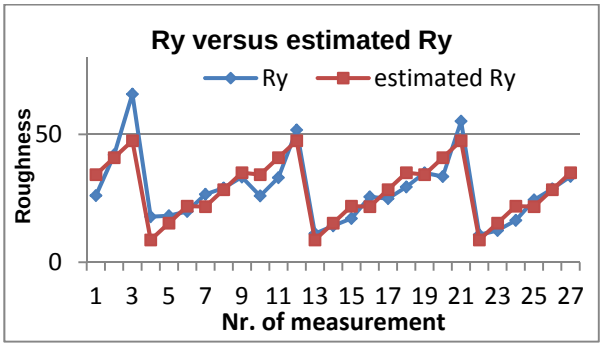

Figure 2. The 2nd model for Ry

From the graph, we can also ascertain that the fit is remarkably good with this simplified model as well.
Nevertheless, if we recall the correlations in Table 2., the *Ry* is in positive correlation with the feed but in negative with the K_r. The former is justified in equation (5) as well, but the latter contradicts with it.

This anomaly provided the thought for further simplification, eliminating the logarithm term from the equation.

$$Ry = 40.28 - 0.41K_r + 132.51f \quad (6)$$

The coefficient of determination now is 0.72, which is about 7-8% decrease compared to the previous, but in exchange this way the model is much simpler and, in addition, in accordance with the correlations in Table (2).

Further, it shows reasonable fit, see the following figure.

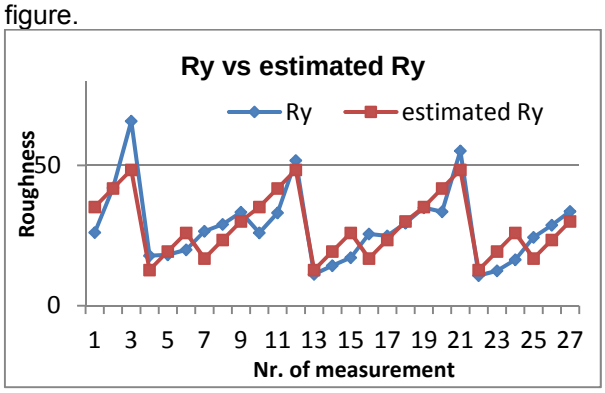

Figure 3. The 3rd model for Ry

Models for the cutting temperature

Based on Table 2, we can announce that the temperature is in moderate positive correlation with the depth of cut and in a little weaker but still positive correlation with the feed. Further, there is a moderate negative correlation between the K_r angle and the cutting temperature. Considering the significance levels (SPSS provides them), we can say that the relationship with the feed is not significant (p value 7%), while it is with a_p and K_r.

Our first model for the temperature is as follows:

$$T = 1200.6 + 4.8K_r - 776.3\log K_r + \\ + 49.8\log ap + 33.5\log f \quad (7)$$

The goodness of fit of the model can be observed on Figure nr. 4.

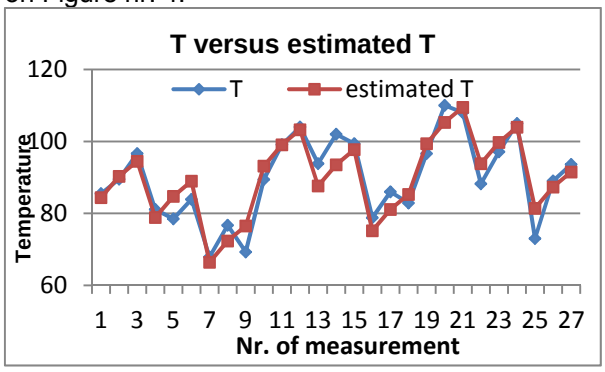

Figure 4. First model for T

The fit is indeed fairly good as expected from the high value (r^2=0.865) of the coefficient of

determination. It has to be noted here that the Equation 7 somewhat contradicts the correlation matrix presented in Table 2., because based on the equation the cutting temperature is in opposite relationship with the a_p and the f, as opposed to the correlation. We should not forget, though, that the correlation is measuring the strength and direction of the linear relationship. In case of a U-shaped relationship the correlation is zero, for example.

Our next model for the cutting temperature is inspired by the previous one. Since in Equation (7), most of the input independent variables are present with their logarithms, let us take the logarithm of the dependent variable as well. This argument led to the next relationship:

$$T = 10^{7.56} \cdot ap^{0.24} \cdot K_r^{-3.93} \cdot f^{0.16} \cdot 1.058^{K_r} \quad (8)$$

This model consists of the same explanatory variables as the previous one, but with different coefficients, of course. The independent variables determine the temperature in 85.9%, being the coefficient of determination 0.859.

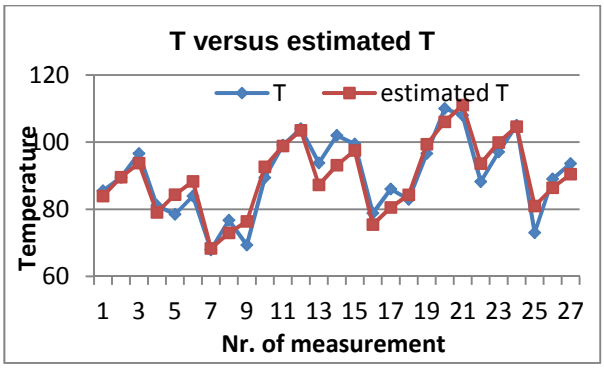

Figure 5. The 2nd model for T

The visual fit of the model is also remarkably good. Nevertheless, the equation is destabilized by the factor $K_r^{-3.93,}$ as the order of magnitude of this term is around 10^{-7} and 10^{-8}, for the possible K_r values we considered. That is why the constant term has to be so huge, to compensate this phenomenon.

For our last model, let us turn back to the 1st (at Equation (7) and remember that, according to the correlations, the relationship between the cutting temperature and feed was not significant (p-value being 7%). Inspired by this, let us find a relationship which neglects the feed as independent variable.
That provides us with the equation:

$$T = 1172.37 + 49.76 \log ap - \\ - 776.32 \log K_r + 4.8 K_r \quad (9)$$

Slightly contradicting the correlation matrix, according to this equation, there is a positive relationship between the cutting temperature and the depth of cut. On the other hand, the T and the K_r have a relationship, which coincided with the one indicated by the correlations.
The coefficient of determination in this case is 73%, about 10% less than any of the previous – that is the price we had to pay for simplifying the model.

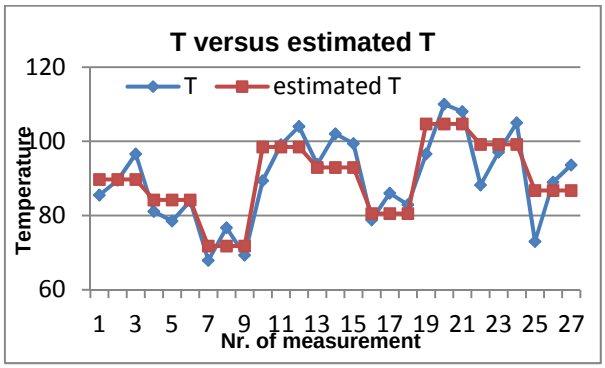

Figure 6. The 2nd model for T

From the graph it is well-seen that the fit is fairly good. Further, in this case the model does not contain as high destabilizing factors than in Equation nr 8.

4. Conclusion

We can conclude that third model is applicable for surface roughness. If the goal is simplicity and stability, the third model (Equation no. 6) is recommended. The Stepwise algorithm did not take the depth of cut among the independent variables estimator, but I managed to find a suitable model for the roughness.
At investigation of cutting temperature is not so clear. Here the best fit has the first model and it is also the most stable, because there are no members order of magnitude. However, the other two models give very similar determination coefficient.

5. References

[1] TÁBORSKÝ, L., ŠEBO, P.: Konštrukčné materiály spevnené vláknami. Alfa 1982.
[2] LÍŠKA, J., KODÁCSY, J.: *Tool wear and cutting temperature at machining of composties.* International conference ISAAT 2011. Stuttgart.
[3] Dr. Fridik László, Válogatott fejezetek a gépgyártás-technológiai kísérletek tervezése témakörből - Kézirat., Nemzeti tankönyvkiadó

THE EXPERIMENTAL VERIFICATION OF AGING INFLUENCE ON COMPOSITES PROPERTIES

Ľudmila Dulebová[1*], Emil Spišák[1], Volodymyr Krasinskyj[2]

[1]Faculty of Mechanical Engineering in Košice, Technical University of Košice, Slovakia
Lviv Polytechnic National University, Lvov, Ukraine
* *Corresponding author e-mail:* ludmila.dulebova@tuke.sk

Abstract
The contribution deals with the influence of degradation to possible changes in selected mechanical properties of composites. Experiment arose out of collaboration with company that uses following materials to produce covers for electrical devices. The change of materials properties was investigated by tensile test and Charpy impact test in standard environment and after aging in UV chamber.

Keywords:
Composites, thermoplastics mechanical properties, polymer degradation, plastic additives

1. Introduction

It would be difficult to imagine our modem world without plastics. One of the key factors which make plastics attractive for engineering applications is the possibility of property enhancement through fiber reinforcement. Both thermoplastics and thermosets can reap the benefit of fiber reinforcement although they have developed in separate market sectors. This situation has arisen due to fundamental differences in the nature of the two classes of materials, both in terms of properties and processing characteristics. Glass fibers are the principal form of reinforcement used for plastics because they offer a good combination of strength, stiffness and price. [1] [2]

With the growing standard of living accumulates demand for synthetic polymeric materials. With this demand thus arise questions concerning the behavior of these substances in the environment.

Degradation (aging) of plastics can be defined as a set of chemical and physical processes in the plastics and gradually leading to irreversible changes of their properties. We distinguish natural and artificial aging. [3] The term natural aging means the slow ongoing change of plastics properties by light, air, carbon dioxide and water. These changes, first limits and ultimately make impossible to further use of plastic product. At most plastics are aging appearing by yellowing and embrittlement. The cause of degradation of plastics and shortening of their life are physical, chemical and physico-chemical effects of environment and biological degradation of polymers. Artificial aging is the aging of plastics in artificial conditions. [4]

Material lifetime is the period during which practically important properties are maintained at the sufficient level for the proper function of the product. [1] It depends on the material properties and on the conditions under which the product is used. Self-degradation of polymers can occur as a result of exposure to light radiation polymer's surface, temperature, cold, chemical compounds or microorganisms. [4] The surface of the polymer can be disturbed and with the subsequent diffusion of the outside environment towards inside of the polymer. The polymer can react with the environment. As a result these reactions may also occur to diffusion on the surface of polymer or to their release into the environment from the polymer. [5]

Objective of the experiment in the present contribution was to verify effect of UV radiation to modify the mechanical properties of selected composites filled with glass fiber (GF) used in the electronics industry. From the range of mechanical properties, the tensile properties and Charpy impact toughness were listed as verification values to determine changes of properties in the standard environment and after their exposure in the UV chamber. Experiment arose out of collaboration with company that uses following materials to produce covers for electrical devices. [6]

2. Experimental work

For experiments were used four types of materials including:

- Slovamid 6 GF 30, in experiments labeled A,
- Slovamid 6 GF 25 FRA, in experiments labeled B,
- Makrolon 9415/Z, in experiments labeled C,
- Starex HR 0370 W 91564, in experiments labeled D.

Material Slovamid 6 GF 30 - is chemically strengthened polyamide PA6 with 30% glass fiber and with the content of thermoplastic kaoutchouc. Main applications are impacted moldings and moldings with high strength applied in automotive, electrical, engineering and consumer goods industry. With the increasing content of GF also the toughness, bending and tensile strength increase as well as the heat application increases up to 250°C and the shrinkage decreases.

Material Slovamid 6 GF 25 FRA – is chemically strengthened polyamide PA6 with 25% glass fiber with halogen flame retardant. Main features are flammability in accordance with UL 94 V0 at 1.6mm, glow wire at 960°C, CTI 300. In application for the electrical industry remain products protectors, coil forms, covers, and terminals.

Material Makrolon 9415/Z – is polycarbonate PC with medium viscosity suitable for extrusion and injection molding. Material is chemically strengthened with 10% standard glass fibers and contains flame retardant grade and easy mold release agent.

Material Starex HR 0370 W 91564 - is acrylonitrile butadiene styrene (ABS) suitable for injection molding and contains flame retardant. Main applications areas are automotive, engineering and electrical industry.

The test specimens used in experiments for determining the tensile properties of plastics were manufactured in the multiple ISO-type form of type A with the Z-type of sprue. Impact toughness tests were made on test specimens that were injected in the multiple ISO form. Defective samples were excluded and all test specimens used in the experiments did not reveal any deficiencies. For the production of samples injection molding machine Arburg – Allrounder 320C was used.

Tensile properties of tested materials were evaluated according to STN EN ISO 527-1,2 and test specimen of type 1A was used for tests. Tensile test was performed on the test machine TIRA-test 2300. Sample was pinned to jaws of the ripper and was loaded with the force until the disruption. Five (5) samples from each type of material and for the each environment were tested.

Determination of Charpy impact strength was performed according to STN EN ISO 179-1. The test is based on the detection of the consumed energy to break the test piece by falling rotary hammer and was performed by Charpy's hammer PS V500. Ten (10) test specimens of each type of material and for the each environment were tested according to standards.

Artificial aging test with fluorescent UV lamps was performed in UV chamber according to STN EN ISO 4892-3, while the exposure time was set to 28 days at 12 hours cycles for the all tested materials. Subsequently, tensile test and the Charpy impact strength test were performed to detect changes in the properties of these materials.

2.1 Experimental results

Dependence of the average measured values of tensile strength (σ_M) of tested samples in standard environment and after the degradation in the UV chamber is shown in Figure 1.

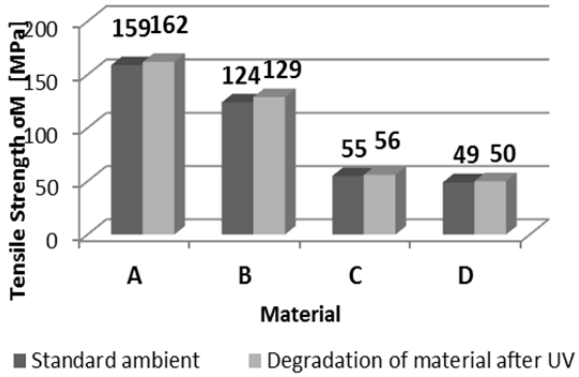

Figure 1. Comparison σ_M of tested materials

Dependence of average measured values of relative elongation (ε_M) of tested materials in the standard environment, but also after the degradation in the UV chamber is shown in Figure 2.

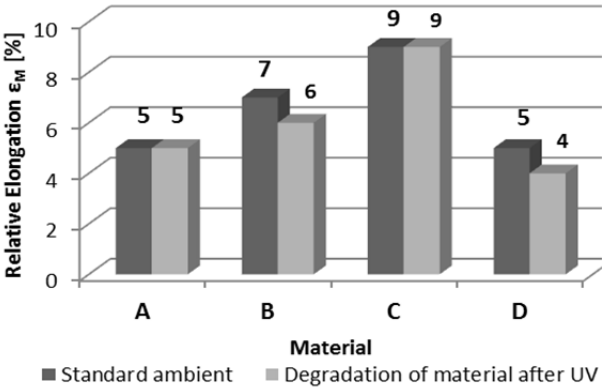

Figure 2. Comparison ε_M of tested materials

Fracture surfaces of test specimens of tensile test were also observed on the scanning electron microscope JEOL JSM - 7000F, Japan.

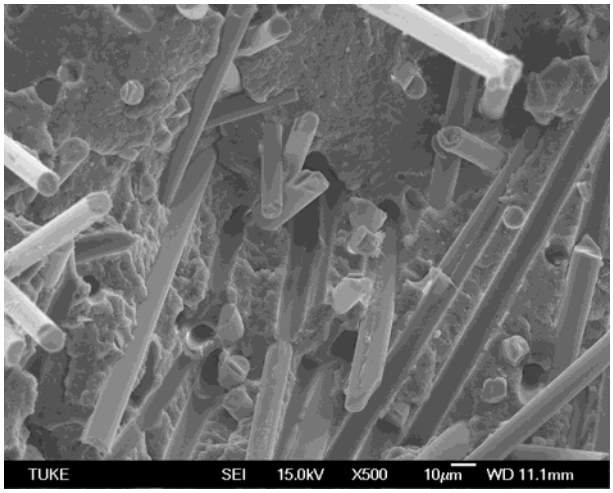

Figure 3. The fracture area of material PA6/GF30

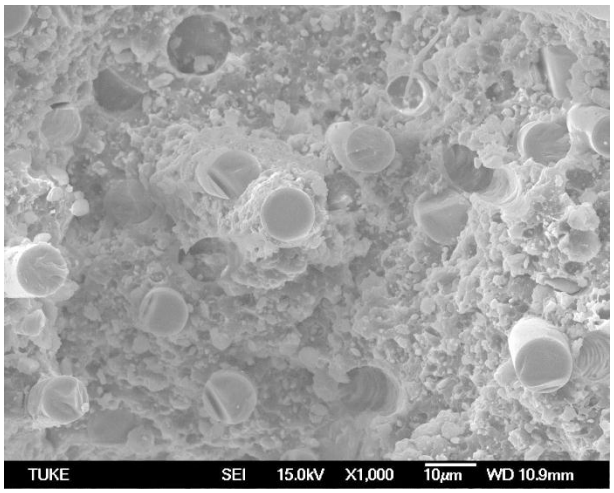

Figure 4. The fracture area of material PA6/GF25

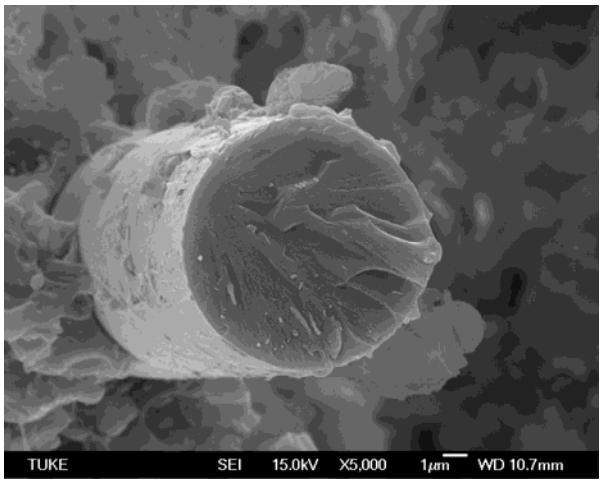

Figure 5. The fracture area of glass fiber of material PA6/GF25

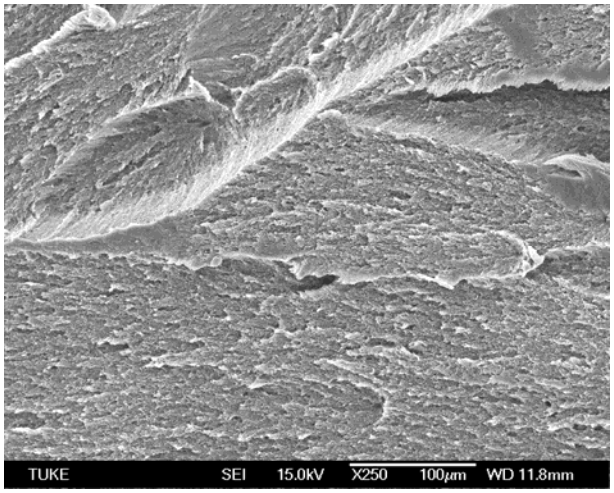

Figure 6. The fracture area of material ABS

Figure 3 to Figure 5 shows the surface fracture of a polymer composite, reinforced with different percentages of glass fibers in the material after tensile test. Holes after ripped fibers are marked with arrows. In glass fiber there was a cracking of fibers and the crack slowly expanded. The ridges and stream characterizes the direction of fracture development. Surface breach of the material ABS after tensile test is shown in Figure 6.

Dependence of the average measured values of Charpy impact toughness in a standard environment, but also after the degradation in the UV chamber is shown in Figure 7. Complete penetration of all tested specimens was performed.

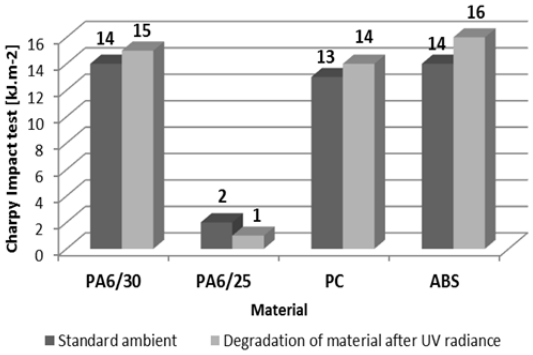

Figure 7. Comparison of the Charpy impact toughness of tested materials

The Figure 8 shows the fracture surface after the Charpy test of material Starex (ABS) with inclusion and detail to it (Figure 9). That inclusion caused the growth of the crack. It is necessary to thoroughly clean the screw and the injection tool - injection mold before further injection of material.

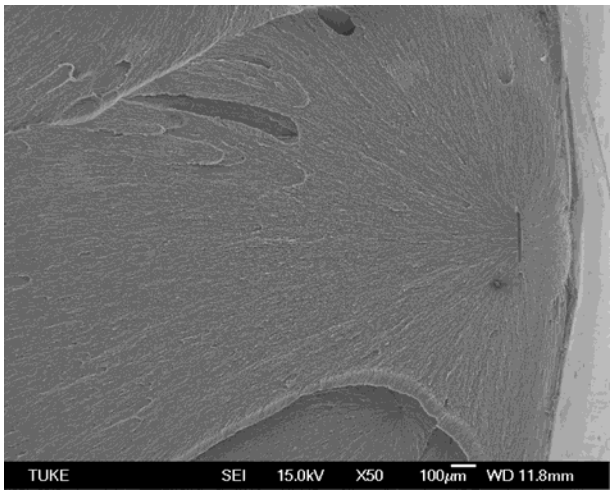

Figure 8. The fracture area of material ABS with inclusion

3. Conclusion

The aim of paper was to study the impact of degradation to mechanical properties for specific values of strength, elongation and impact toughness after aging in UV chamber with four types of materials.

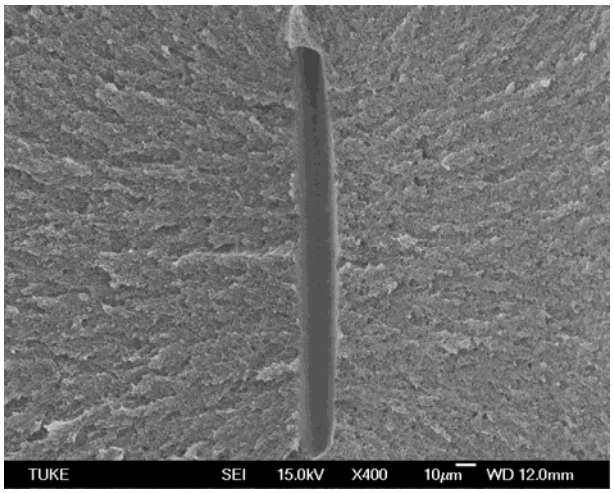

Figure 9. The fracture area of material ABS with inclusion - detail

Based on experimental tests above, the following conclusions were determined:

- The highest tensile strength (162 MPa) was measured at material Slovamid 6 GF30 after exposure to the UV chamber. The tensile strength after the degradation in the UV chamber was increased only at material Slovamid 6 GF 25 in about 5 MPa, which is a negligible value. σ_M value measured in two environments at material Makrolon hasn't changed. We conclude that artificial aging in UV chamber did not affect the σ_M value of the tested materials.
- The highest elongation value was measured at material Makrolon - 9% in the standard environment and also after that artificial aging in UV chamber did not affect the ε_M value of the tested materials.
- The impact toughness after the aging in UV chamber for each tested material increased only by negligible amount (1- 2 $kJ.m^{-2}$). At material Slovamid 6 GF25 was detected value of impact toughness a_{CN}= 2 $kJ.m^{-2}$, which is consistent with material list. The average value of other materials ranged from 13 $kJ.m^{-2}$ to 16 $kJ.m^{-2}$. At Charpy impact test, the values did not changed after the degradation in the UV chamber. Thus, aging in UV chamber had no effect on the impact toughness of materials.

Mechanical properties of composites depends on many parameters, from which are the most important properties of the matrix and reinforcement, type or length of the fiber reinforcement, the volumetric proportion and arrangement of reinforcement and cohesion with the matrix surface. Fiber composites always exhibit a preferential orientation. The bearer of the strength is reinforcing fiber, which is anchored into the matrix only by the friction force.

According to the tests carried out we can conclude that products made from the tested material and exposed to UV radiation do not significantly change their properties and may be exposed to the external environment.

Acquired knowledge in this paper is only part of the broad field of engineering plastics testing. Mentioned experiments require further study of changes in the structure of plastic material as well as complement of other technological tests according to applications of the investigated materials in practice.

4. Acknowledgement

This paper is the result of the project implementation: Technological and design aspects of extrusion and injection moulding of thermoplastic polymer composites and nanocomposites (PIRSES-GA-2010-269177) supported by The international project realized in range of Seventh Frame Programme of European Union (FP7), Marie Curie Actions, PEOPLE, International Research Staff Exchange Scheme (IRSES) and VEGA No. 1/0600/13.

5. References

[1] Greškovič, F., Dulebová, Ľ., Varga, J., *Technológie spracovania plastov*. Vstrekovanie. TU v Košiciach, Strojnícka fakulta. 200 s. ISBN 978-80-553-0369-7

[2] A.L.N. da Silva et al. *Mechanical and rheological properties of composites based on polyolefin and mineral additives.* Polymer Testing 21 (2002) 57–60

[3] Džoganová, Z., Herczner, P., Badida, M., *Impact assessment of mechanical properties of degraded pet bottles in selected environmental degradation*, In: SGEM 2012 , PP. 331-337. ISSN 1314-2704, Albena, Bulgaria, June, 2012, Sofia

[4] Encyclopedia of polymer science and technology/ *Degradation to magnetic polymers*. Vol. 6, 3rd ed. Hoboken: Wiley-Inter science, 2003. p. 735. ISBN 0-471-28781-4 (v. 5-8)

[5] Förtsch W., Franz H.E., Friedrich K. *Microfractographic Aspects of Interfaces in Creep under Fatigue Loading*, Proc.28th Risø International Symposium on Materials Science: Interface Design of Polymer Matrix Composites – Mechanics, Chemistry, Modeling and Manufacturing, Risø National Laboratory, Roskilde, Denmark,2005.

[6] Dulebová, Ľ., Greškovič, F. *The influence of amount of filler on mechanical properties for elektro products*. Mechanika z. 80. No. 273 (2010), p. 59-64. - ISSN 0209-2689

THE CHANGE OF CORROSIVE RESISTANCE OF THIN TINPLATES AFTER PLASTIC DEFORMATION

E. Spišák [1*], J. Majerníková[2]

[1]Technical University of Košice, Košice, Slovak Republic
[2]Technical University of Košice, Košice, Slovak Republic
* *emil.spisak@tuke.sk*

Abstract
Nowadays thin tinplates are processed predominantly by compression moulding. At the production of two-piece tins (lid and cap with flange) various types of stresses and deformations of thin wrapping sheet occur. From the viewpoint of material stress, the least appropriate scheme is the one containing tension stress. In this contribution we have tested the corrosive resistance of thin tinplates after the biaxial tensile test (Bulge test). Corrosive resistance was evaluated after various time spans (corresponding to 3 years). Samples were deformed in three deformation levels (approx. 5%, 10% and after deformation). For the purpose of this test, samples made from continually annealed, batch annealed, once reduced and twice reduced sheets were used.

Keywords:
Thin Tinplates, Corrosion, Cracking of Meat Tins

1. Introduction

Nowadays thin tinplates belong among the most important production and export goods of the biggest metallurgical companies. Within the last three years the production of these plates in U.S. Steel Košice has boosted to more than twice the quantity before and currently it makes more than 300 thousand tones of thin tinplates per year. In the last years the development of these plates led to a significant reduction of thickness (from thickness of 0.26 mm to 0.14 – 0.18 mm) and considerable reduction of tin coating thickness from the former 11 and more gram/m^2 (hot-dip tinning) to the current 1 – 2 gram/m^2 (electrolytic tin coating) [1]. There is a significant change in the treatment of thin tinplates for the production of wrappings [2, 3]. Currently the majority of produced wrappings are of so called two-piece metal wrappings made by drawing round, square, oval, etc. caps and tin lids that are mutually connected by flanging. The current technology of drawing for the purpose of caps production lays extensive demands on the plastic properties of thin tinplates. With this drawing process there are considerable plastic deformations of steel material, as well as tinned layer. These days even prominent manufacturers feel the pressure of quality demands on tinplates. Thicknesses of tinplates need to be reduced while maintaining the required elongation [5]. There are increasing requirements as to the inner and outer cleanness of bands, as to their close dimensional tolerances and ideal planeness. Requirements for surface microgeometry are tightening. In this contribution the intention was to point out the relation between the size of plastic deformation and corrosive resistance of thin tinplates.

2. Method

For the experimental research we used materials once reduced continually annealed with marking TH 435 CA, thickness 0.24mm and twice reduced batch annealed with marking TS 550 BA, thickness 0.16 mm. Mechanical properties of applied sheets discovered by the uniaxial and biaxial tensile test are shown in Table 1. Graphic relation between tension and deformation at biaxial tensile force test of tested materials are presented in Figures 1 and 2. Once reduced continually annealed sheet showed higher elongation as well as lower yield of point and tensile strength(Figure 1) in comparison with twice reduced batch annealed sheet (Figure 2).

Table 1 Mechanical properties of examined materials

	Tensile test			Biaxial test		
Material	Re [MPa]	Rm [MPa]	A_{50} [%]	Re [MPa]	Rm [MPa]	A_B [%]
TH 435 CA ⊥	468	447	28.1	342	506	14.6
TH 435 CA ‖	453	448	25.5			
TS 550 BA ⊥	525	534	2.6	535	587	6.3
TS 550 BA ‖	523	531	3.,1			

Figure 1 T Dependence stress-strain of material TH 435 CA, thickness 0.24 mm

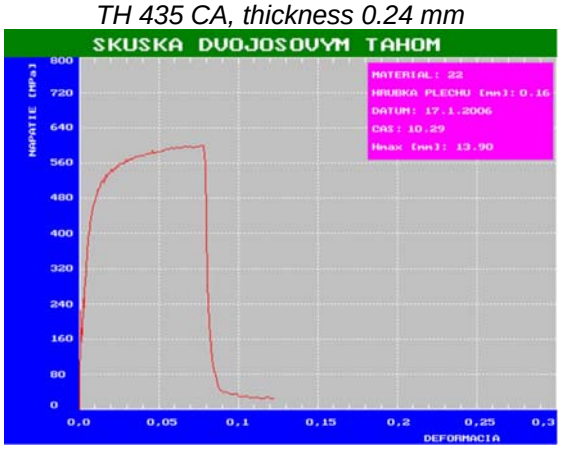

Figure 2 T Dependence stress-strain of material TS 550 BA, thickness 0.16 mm

After approx. 3% (5%) and after 6% (10%) deformation the tested materials were placed into corrosive chamber with salt fog at the temperature 20°C. Action time of the corrosive environment corresponded with the average period of 3 years in real conditions. The corrosive treatment of tested materials was evaluated both visually and metallographically. Figures 3, 5 and 7 show sheets from steel TS 550BA after 3%, 6% deformation and breakage. Figures 4, 6 and 8 show sheets from steel TH 435CA after 5%, 10% deformation and breakage.

Figure 3 Sheet TS 550 BA after 3% deformation

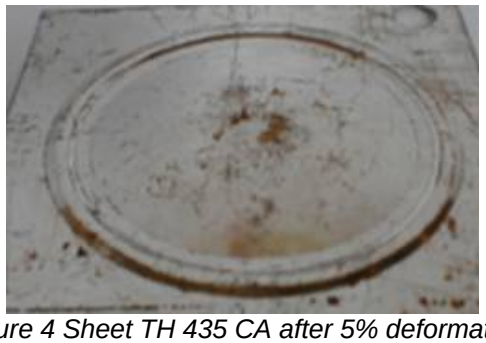

Figure 4 Sheet TH 435 CA after 5% deformation

Figure 5 Sheet TS 550 BA after 6% deformation

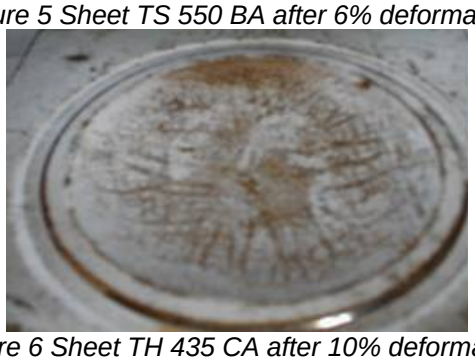

Figure 6 Sheet TH 435 CA after 10% deformation

Figure 7 Sheet TS 550 BA after breakage

Figure 8 Sheet TH 435 CA after breakage

3. Results

Sheets from steel TS 550 BA were distinguished by a higher yield of point, higher breaking strength

and lower elongation (rupture occurred at approx. 8% deformation), but the deformation process ran without any significant slip planes in the entire deformed volume. In case of continually annealed sheet TH 435 CA we measured a higher elongation, lower yield of point and lower tensile strength, but the sheet deformation showed a considerable inhomogenity in form of significant slip planes (Figures 9 and 10).

Figure 9 Sheet TS 550 BA after breakage before corrosion

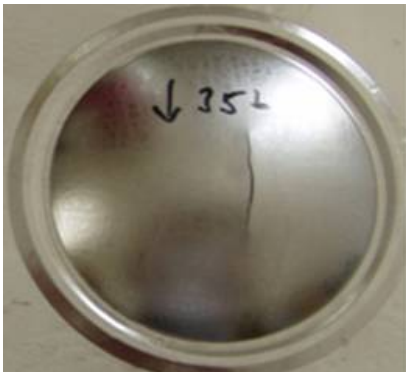

Figure 10 Sheet TH 435 CA after breakage before corrosion

With sheets batch annealed the corrosion became evident on a larger area, though it was more uniform and did not do significant damage to the base material. As with sheet continually annealed, the corrosion collected right on the place of local deformations (slip planes), (Figures 6 and 8). This corrosion damaged the tin protective layer and a rather significant corrosion of base material occurred (Figures 11 and 12).

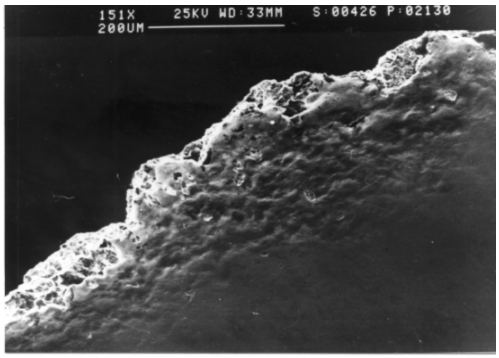

Figure 11 Sheet corrosion near to material breakage

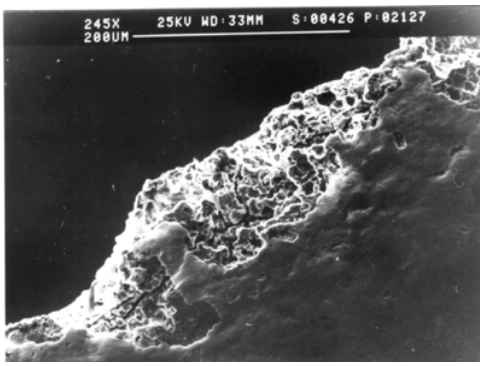

Figure 12 Secondary corrosion cracks

4. Discussion

Teams of experts started to be concerned with the issue of breaking of tinned meat in the sixties of the 20th century. This phenomenon came to be seriously significant with long-term storage of tins and, in fact, has partially persisted to these days. The mentioned problem was even more obscure, as meat and meat products were categorized as the least aggressive filling by all the authors in accordance with the contemporary expert literature. Considerably more works were dedicated to breaking of tinned meat that contained fillings releasing hydrogen sulphide (e.g. green bean). According to these sources, sulphides are rather effective accelerators of hydrogen diffusion in steel [4, 5, 7, 8]. Hydrogen then accelerates the electrolytic corrosion. In particular it is manifested on those places that are concurrently deformed and contain internal tension. It is assumed that the reasons for unsystematic occurrence of FeS are found in steel production faults. The effect of diffused hydrogen on the corrosion process is an especially significant accelerator of non-metallic inclusion and carbide occurrence. As for continually cast steel the effect of hydrogen is significantly lower [6].

In case of tinned meat it is the interaction of wrapping and filling, which are mostly associated only with the occurrence of dark iron sulphides and tin on the inner tin surface. With the case of the above breaking, theoretically two types of corrosive cracking could apply herein:

a) sulfitic – material embrittlement by diffusing hydrogen released on steel surface, or tin coating by hydrogen sulphide,

b) stress-corrosion cracking with the mechanism of anodic dissolution of metal, in this case some substances released from meat or additives, above all NH3, amines and Cl-, but also NO2-, carboxyl acids, residues of pesticides, etc.

These facts, however, needed to be unambiguously proven and demonstrate that tinned meat cracking occurring with long-term storage is not caused merely by low-quality sheet, but it is a corrosive-mechanic process, indeed. For the above to apper, only two conditions are necessary and sufficient:

1. specific minimum level of residual tensile stress,
2. specific corrosive environment.

As for tinned meat both the above conditions [4] have been fulfilled. There was significant residual tensile tension on lid and bottom curvature radii and the filling made for long-term storage contained significantly more chlorides. The above mentioned assumptions were proven on several types of tinned meat, which at the time of research were not damaged. The example of such tin cap with apparent corrosion and local thinning in the radius of lid curvature is present in Figure 13. The lid was damaged by corrosion nearly over the entire thickness.

On Figure 14 it is evident that except for primary corrosive rupture in the lid there are further secondary corrosive ruptures that are being expanded, which in turn could cause material rupture. In Figure 15 there is the part of lid damaged by corrosion which serves as clear evidence of intercrystallic corrosion spreading over the edges of base material grains. The above spreading was further enhanced by a partial decarburization of the thin steel sheet surface prior to its tinning, where the enlargement of grain in surface layers [6] had occurred.

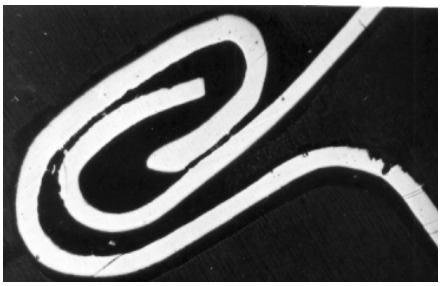

Figure 13 Lid of the tin damaged by corrosion

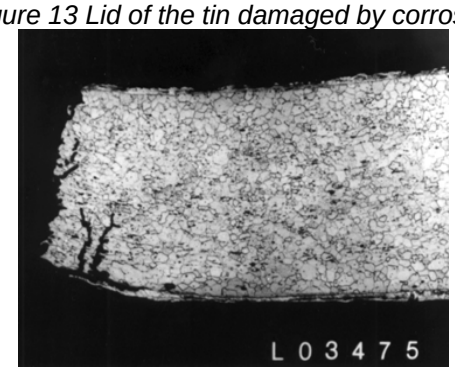

Figure 14 Missing tin layer in the area of breakage

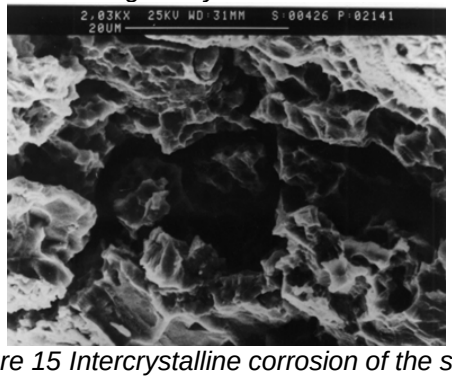

Figure 15 Intercrystalline corrosion of the sheet

5. Conclusion

On the basis of experiments performed with tested corrosive resistance of plates continually annealed and batch annealed, once or twice reduced, we can observe that as for sheets batch annealed twice reduced even at lower plastic properties and higher yield of point and tensile strength there is a uniform plastic deformation, thus also to uniform thinning of protective tin layer. The corrosion was more uniform and did not affect the base material to a large extent. The plates continually annealed were distinguished by lower yield of point, lower tensile strength and higher elongation, yet their deformation with biaxial stress was characterized by inhomogenity (significant slip bands). In the places of their significant slips there is a considerable thinning of protective tin layer, increase of their porosity, and as a result loss of anti-corrosive effects. If such sheets are used for the production of tin wrappings, the effects of corrosive activity of the tinned meat filling can result in significant corrosion of the tin lid, later even to its damage.

9. Acknowledgement

This contribution is the result of the project implementation: č.1/0396/11- Research and optimalization of evaluation methods of strength and plastic properties of thin tinplates.

10. References

[1]E. Spišák: Odksztalcalnosc blach ocynowanych, Rudy i metale nieželazne, Volume 40 (1995), No.11, pp.499-501.
[2] E. Spišák, F. Greškovič, J. Slota: Evaluation of plastic properties of tinned steel sheets, Rudy Metale, Volume 42 (1997), No.11, pp. 510-512.
[3] E. Spišák, J. Slota: Hodnotenie plastických vlastností tenkých oceľových plechov, Acta Mechanica Slovaca, No. 3 (1998), pp.39-44.
[4] E. Spišák, A. Hrivňák, F. Greškovič: Vlastnosti a podmienky spracovania obalových plechov, Strojírenská výroba, No.11-12 (1993), pp. 33-35.
[5] L. Sobotová, E. Spišák: The Influence of Production of Thin Tinplate Steel on its Formability, Journal of Materials Processing Technology, Volume 34 (1992), pp. 411-417.
[6] M. Šlesár, J. Billy, P. Marek, E. Zárubová: Vzťah mikročistoty, technológie valcovania a kvality povrchu tenkých plechov, Plechy vyšších technických parametrov, Stará Lesná(1994), pp. 6.
[7] C. Jung: Creasteel – An asset for steel packaging innovation, Metal bulletin and Tinplate Technology, 8th International Tinplate Conference, Paris (2004).
[8] D. Gade: D and I CAN: Tribological behaviour of tinplate during ironing, Metal Buletin and

Tinplate Technology, 8th International Tinplate Conference, Paris (2004).

IMPORTANCE OF THE OPTIMAL BATCH SIZE

Romana Hricová

Technical University Košice, Faculty of Manufacturing Technologies with the seat in Prešov, Bayerova 1, 08001 Prešov, Slovak republic
Corresponding author e-mail: romana.hricova@tuke.sk

Abstract
The paper deals with calculation of batch load. Its aim is to propose an effective solution of optimal production batches. The problem by optimization of production batches, should be result of right adjustment and production volume increase it the firm.

Keywords:
batch, company, scheduling

1. Introduction

A production management system is a much more complex part of the company that it is to be embedded in than is usually perceived by its staff. It is not just a new technological investment, but a component which has to fit the company's culture. It has to be embedded in a network of other technologies, companies and individuals through which it will be exploited. A production management system cannot be fully utilized unless it will become an equivalent part of the organization and treated in the same manner as other resources in the company.

2. Batch Scheduling

Batch scheduling is a technique involving the determination of optimum batch size and a schedule for the completion of such batches on a set of facilities. The batch sizes are determined by comparing set-up (or charge) costs with holding or inventory costs. The schedule is determined by reference to these batch sizes. The technique is concerned with both scheduling and inventory management. [1]
Among the standard direction of production management belong:
- running production time,
- production lead,
- stock of work-in-process
- standard work plan
- rate of quality-class products.

Manufacturing throughput time is the sum of the setup time, processing time, inspection time, moving time and waiting time.
Manufacturing throughput time begins by the first operation and ends by enlistment of product to the storage of final products. Its duration is affected by technical-economical and technical-organizational conditions. The basic ways of its calculation are given in Table 1.

Table 1. Basic ways of calculation of production cycle

Production cycle	Relation
One operation for one product item	$T_c = \frac{t_i}{I}$ T_c - total length of production cycle I – number of components which are treated together in workplace
Batch for one operation	$T_c = \frac{b_s \times t_k}{W \times I} + t_{pe}$ b_s – batch size W – number of workplaces where the operation runs simultaneously
Total for one item	$T_c = \sum_1^b T_w + \sum_1^b T_b + \sum_1^b T_{wa} + \sum_1^b T_a$ T_w – working time of the component T_b – time of inter-workshop breaks T_{wa} – waiting time for completion before assembly T_a – assembly time

There are several factors influencing batch size. Those have opposite-acting influence very often. Decreasing batch causes:
- increase of work productivity and rate of technological operation,
- simplification of operative production management,
- decrease of fixed costs.

On the other hand the increase of batch size causes:
- extension of average manufacturing throughput time,
- decrease of production tolerance to changes and failures.

3. Optimal Size of Production Batch

Capacity approach figures out the minimum batch as:

$$b_s = \frac{t_{pe}}{\alpha \times t_i} \quad (1)$$

α – coefficient ensuring that t_{pe} will not exceed the so-called maximum acceptable rate. It is chosen for a certain components group with the same production conditions. Coefficient is in the interval <0.02; 0.12> and for example:
for big and complicated components – α = 0.04
middle-size components – α = 0.05
small components – α = 0.08
automated production – α = 0.10
Cost approach - also called optimization approach as it solves compromise between fixed cost dispraise for one piece and increase of batch size. On the contrary, with increase of fixed costs, total costs and capital fixture increase.

$$b_s = \sqrt{\frac{2 \times C_{pe} \times Q_p}{C_i \times C_s \times t}} \qquad (2)$$

C_{pe} – costs of preparation and finishing,
Q_p – planed production quantity in pieces or kilograms,
C_j – costs of one item in SKK,
C_s – storage costs.
t - period of the year depends on Q (for year period t = 1).

Standard frequency of batches approach – batch is corrected for standard year frequency following the calendar rhythm of the planning of production set.

Method of static batches divides produced items and components to value-significant and non-significant. Value non-significant products are mass-produced and their batch size is stable and constant in time. Value significant products are produced in smaller quantity and a predefined batch is corrected by allowance (which is predefined too), what approximate batch quantity to real planned need for a period. The result of the method is a basic batch as an interval from minimum to maximum batch quantity, which should not be exceeded.

4. Batch Size from Modern Approaches Point of View

Material Requirements Planning (MRP I) – is concerned primarily with the scheduling of activities and the management of inventories. It is particularly useful where there is a need to produce components, items or sub-assemblies which themselves are later used in the production of a final product. MRP was developed step by step and every step is hierarchical distant to previous one by taking out of lacks.
1st degree - the Master Production Schedule is based on known or forecast demand for a specified future period, e.g. the forecasting period. The schedule shows how much of each end item is wanted and when the items are wanted. It is in effect the delivery of the "due date" schedule for each product expressed in terms of both quantity and timing. The period over which this demand expressed will depend on the type of product concerned and the capacity planning procedures used by the organization.
2nd degree – Detailed Scheduling and Loading – is particular schedule of production tasks for individual workplaces with a time advance of one day up to one decade.
3rd degree – Economic Order Quantity – optimal batch depends only on total costs. Stationary frequent production with constant times and costs for rebuilt of production equipment is assumed.
4th degree - Sequencing – the determination of the best order for processing a known set of jobs through a given set of facilities in order, for example, to minimize total throughput time, minimize queuing, minimize facility idle time…
5th degree – MRP I – a technique by which known customer demand requirements are "exploded" to produce "gross" parts, components or activity requirements. These "gross" requirements are compared with available inventories to produce "net" requirements, which are then scheduled within available capacity limitations. MRP is for scheduling and also for inventory management and capacity management.
6th degree – MRP II – Manufacturing Resource Planning – represents an extension of the features of the MRP system to support many other manufacturing functions. The most important functions of MRP II are: Master Production Scheduling (MPS), Rough Cut Capacity Planning (RCCP), Capacity Requirement Planning (CRP), Production Activity Control (PAC).
7th degree – Optimized Production Technology (OPT) – is the focus on "bottleneck" operations. OPT rules are:
- balance flow, not capacity,
- the level of utilization of a non-bottleneck is not determined by its own potential but by some other constraint in the system,
- activation and utilization of a resource are non-synonymous,
- an hour lost at a bottleneck in an hour lost for the total system,
- as hour saved at a non-bottleneck is a mirage,
- bottleneck govern both throughput and inventories,
- the transfer batch may not, and often should not, be equal to the process batch,
- the process batch should be variable, not fixed,
- schedules should be established by looking at all of the constraints simultaneously. Lead times are the result of a schedule and cannot be predetermined.

5. How to Reduce the Batch Size

1. Possibility how to reduce the batch size is to limit what worker puts into it. The firm can limit number and size of requirements that workers are

grouping together. The inputs limiting is the simplest method but also the cheapest one. [2]
2. Many companies can make huge advances in cutting their cycle time very simply by focusing on what they out into the batch in the first place, although this approach has not any significant effect on overall cost. Smaller change sets reduce queued work (e.g. pending deployments).
3. Improves flows as smaller change sets reduce the probability of unpredictable, costly value stream blockages.
4. Improved feedback – smaller change sets shrink customer feedback loops, enabling product development to be guided.
5. Improved overheads – smaller change sets reduce transaction costs by encouraging optimizations, with more frequent releases necessitating faster tooling.
6. Improved efficiency – smaller change sets reduce waste by narrowing defect feedback loops, and decreasing the probability of defective code harming value-adding features. [3]

6. Advantages of Small Batch Size

In general, reducing batch size is one of the most powerful techniques available for improving the flow. When firms reduce batch size they can deploy more frequently, because reducing batch size drives down cycle time. [4]
Among other advantages of small batch size belong:
1. Small batches bring faster feedback.
2. Small batches mean problems are instantly localized.
3. Small batches reduce risk.
4. Small batches reduce overhead.

7. Conclusion

The purpose of the article was to analyze the importance of batch load in the firms. Many small firms try to manufacture their product in as large of batch sizes as are possible. The reasoning behind this is the potential for economies of scale. By producing in large batch sizes, the small business can reduce their variable costs and obtain bulk discounts from material suppliers. While these seem like valid reasons on the surface, there are additional costs and hindrances that arise from producing in large batches. Firstly with large batches comes the need to carry inventory. Secondly when materials are purchased in bulk to obtain discounts, this material must be stored in the warehouse. In addition, once the finished product is complete, it must be stored as well. With these inventories comes a great deal of cost.
Firms produce in large batches also limit the own ability to meet customer demand through flexibility. This is not a problem if a company produces one or two products, but for a business with several different products it is a major issue.
With smaller batches firm has increased flexibility and reduced inventory.

8. References

[1] Hill, T.: Manufacturing Strategy Text and Cases - second edition.The McGraw-Hill Companies, Inc. 1994. ISBN 0-256-10666-5
[2] “Batch Size Matter – Flow faster delivery” [Online]. Available: https://www.valueflowquality.com/resources/Batch-Size-Matters-SAMPLE.pdf [Accessed: 25-Sep-2013].
[3] “Release More With Less” [Online]. Available: http://www.stephen-smith.co.uk/release-more-with-less/. [Accessed: 25-Sep-2013].
[4] Goldman, A.: Small Batch Versus Large Batches. [Online]. Available: http://www.gaebler.com/Small-Batches-Versus-Large-Batches.htm [Accessed: 25-Sep-2013].

DURABILITY AND WEAR OF EXCHANGEABLE COATED CUTTING INSERTS AFTER MACHINING THE NI-625 ALLOY

Tomáš ZLÁMAL[1*], Jana PETRŮ[1], Marek SADÍLEK[1], Marek PAGÁČ[1], Josef BRYCHTA[1], Juraj SUROVSKÝ

[1]Faculty of Mechanical Engineering, VSB – Technical University of Ostrava, Czech Republic
* tomas.zlamal@vsb.cz;

Abstract
This contribution deals with machining and design of suitable cutting materials, cutting geometry and conditions for machining the Inconel 625 nickel superalloy. The experimental part proposes three various types of exchangeable inserts, describes the process of machining Inconel 625, and determines the influence of tool back wear on roughness of machined surface. The conclusion lists knowledge, analysis and recommendations from machining of Inconel 625 for practice and determines durability and wear of the tool cutting wedge.

Keywords:
Turning, special alloys, surface integrity, wear

1. Introduction

In connection with technical development within machine industry there are requirements to improve user properties and parameters of machined parts. Increasing demands for quality, dependability and especially service life of products currently drive the development and use of new materials with state-of-the-art properties. The term “superalloy” designates materials, including Inconel 625, that are heat resistant, heat proof and corrosion-resistant even under increased temperatures. On the other hand there is a number of machining problems during machining of these superalloys that do not normally occur, while machining carbon steels. Also requirements for specific technologies and methods of machining differ significantly according to proposed areas of use. During machining by classic chip methods superalloys demonstrate worsening machinability, which directly affects productivity and economy of the whole production. [1, 2]

2. State of the machining of superalloys

Machining technology underwent huge development in the last two decades that has been displayed by its massive use in industrial practice. A fundamental part within machine industry production is chip machining, to which a whole series of experimental method analyses is linked to. Development in the area of superalloy splinter machining unambiguously targets increase of productivity during machining. Superalloys can be classified as difficult-to-machine materials due to their specific properties. Although these alloys are not exceptionally hard, their high strength at higher temperatures and high toughness have fundamental influence on their machinability. Thus machining of superalloys based on nickel is highly problematic for all machining operations. Also demands for technologies, cutting machines, tools, cutting materials and cutting conditions are highly specific from the point of view of superalloy machinability.[2, 3]
A large number of experts occupied themselves with machining of nickel superalloys, which produced several monographies and professional contributions listed in the Scopus and Sciencedirect databases. Authors like M. Neslusan [2] and A. Czan [2] or K. Vasilko introduced findings that concern these problems in their publications. Also several contributions with the topic of machining and machinability of nickel superalloys were published in the Tehnički Vjesnik (Technical Gazette) journal, however, only very little was published about machining of the Inconel 625 superalloy. This experimental activity was based on not quite known process of Inconel 625 superalloy machining.

3. Ni-625 Experimental machining

The targets of this research were to experimentally verify suitability of use of proposed cutting materials, cutting geometry, Inconel 625 superalloy cutting conditions, to determine types and mechanisms of cutting tool wear, and to determine roughness of machined surface. Finding of suitable material and cutting conditions was taking place during longitudinal turning of the Inconel 625 superalloy.
The Inconel 625 material is a corrosion-resistant superalloy based on Ni-Cr that is characterized by high strength during very low and very high temperatures, primarily due to the strengthening effect of nickel and molybdenum. Its chemical composition does not influence only mechanical properties and corrosion resistance, but also areas of its use. [4, 5]

Chemical composition and mechanical properties of Ni-625. [4]

Ni……58 % min.	S….0,015 % max.
Cr……20-23 %	Al……0,4 % max.
Fe…...5 % max.	Mn…..0,5 % max.

Mo…...8-10 % C…….0,1 % max.
Nb…..3,15-4,15 % Co.....1 % max.
Si……0,5 % max. Ti…….0,4 % max.
P…….0,015 % max.

Density.....8,44 [g·cm^{-3}]
Tensile strength……862 [MPa]
Yield strenght.....448 [MPa]
Elongation.....50 [%]
Hardness Brinell.....200 [HB]

For machining of difficult-to-machine materials, nickel superalloys and thus also Inconel 625, it is recommended to use high powered and highly rigid machines. The horizontal CNC machine Mori Seiki SL - 403, see Fig. 1, that provides maximum machining speed stability and necessary rigidity, while being highly accurate, was used.

Figure 1. Mori Seiki SL – 403[9]

4. Selection of cutting tool

Due to specific properties that lead to worse machinability, while machining nickel superalloys, it is important to select tool material and cutting tool geometry correctly. It is important primarily due to very high strength during increased temperatures, toughness, low heat conductivity and tendency of the surface to harden during the machining process. During selection of the cutting tool the character of loading of the tool cutting wedge was decisive. Primarily high strength of cutting wedge was required, therefore it was suitable to use sintered carbide tools with higher cobalt content or fine-grained carbide ones for machining of nickel-based alloys. The cutting geometry must meet tool requirements for sufficient strength of cutting wedge, smooth cutting action without vibrations, and maximum tool durability with minimum wear. Also technological requirements concerning accuracy and quality of machined surface needed to be taken into account during selection of the tool geometry.

Three exchangeable inserts made from coated sintered carbide were used for machining of the Inconel 625 material:

- The insert from the IC 807 tool material marked CNMG 120408 – TF. The IC 807 material consists of tough sub-micron substrate. The coating (Ti, Al)N is laid on the insert by the PVD method with following SUMO TEC special processing. This material is suitable for machining nickel alloys during low to medium speeds.[6]

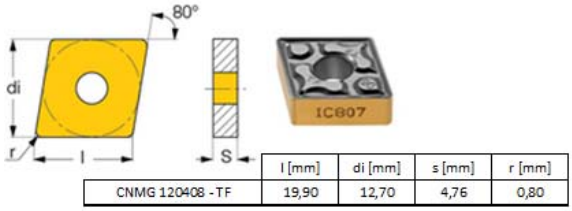

	l [mm]	di [mm]	s [mm]	r [mm]
CNMG 120408 - TF	19,90	12,70	4,76	0,80

Figure 2. CNMG 120408 – TF[6]

- The insert from the GC 1115 tool material marked CNMG 120408 – SMR. The GC 1115 material consists of thin PVD coating with very good adhesion that is coated on fine-grained substrate with high strength at increased temperatures and good resistance against plastic deformation.[7]

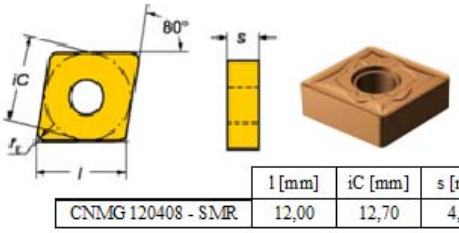

	l [mm]	iC [mm]	s [mm]	r_ε [mm]
CNMG 120408 - SMR	12,00	12,70	4,76	0,80

Figure 3. CNMG 120408 – SMR[7]

- The insert from the TM4000 tool material marked CNMG 120408 – M5. The TM4000 material is intended for nickel alloys and operations from finishing to heavy rough machining. It has the Duratomic coating, Ti (C, N) + Al_2O_3, whose advantage is resistibility against back wear and creation of build-ups.[8]

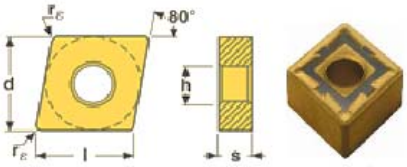

	l [mm]	d [mm]	s [mm]	r_ε [mm]
CNMG 120408 - M5	12,90	12,70	4,76	0,80

Figure 4. CNMG 120408 - M5[8]

During selection of cutting parameters we used values recommended by insert manufacturers, while maintaining comparable conditions for

machining. The following cutting parameters were proposed for rough cutting operations with processing liquid in order to verify cutting ability and durability of the proposed inserts:

- Cutting depth a_p = 2.5 mm,
- Feed per revolution f = 0.3 mm,
- Cutting speed v_c = 50 m.min^{-1}.

5. Results and discussion

From the point of view of efficient nickel superalloy machining it was difficult to determine individual cutting tool wear mechanisms. These materials belong among difficult-to-machine materials that create articulated chip during machining, which results in the creation of large highly dynamic cutting forces. Due to very low heat conductivity and high strength, high temperatures occur during machining. The high strength, mechanical hardening and adhesion result in notch shaped wear at the maximum cut depth level, while extremely abrasive environment is created for the cutting tool edge at the same time. Machining of nickel alloys generates high amount of heat, there is occurrence of significant mechanical hardening, and the material easily sticks to the cutting edge creating a build-up.

The measurement of back wear of exchangeable cutting inserts was done by micrometric method by the direct measurement of linear dimensions in individual sections to previously set wear value of VB_B = 0.3 mm. Determination of the roughness parameters Ra and Rz was done using the Surftest SJ - 210 roughness meter. Roughness was measured in longitudinal direction (parallel to movement direction) always in three places turned by 120°.

- L_i = 50 mm……..machined length
- i = 5…….....number of passes
- VB_B = 0.3 mm....previously set wear value

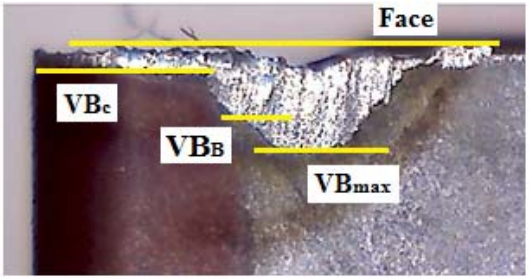

Figure 5. Wear of inserts - CNMG 120408 - TF

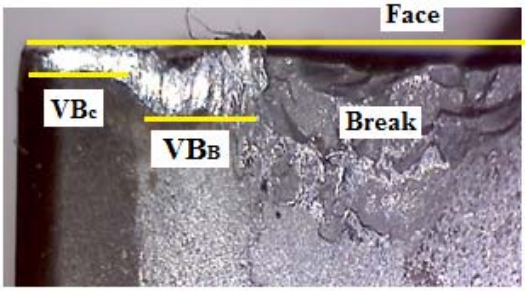

Figure 6. Wear of inserts - CNMG 120408 - SMR

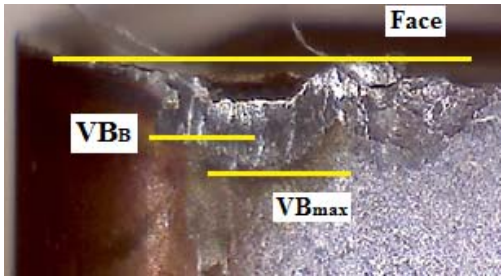

Figure 7. Wear of inserts - CNMG 120408 - M5

Table 1. The obtained values

	CNMG 120408 - TF			CNMG 120408 - SMR			CNMG 120408 - M5		
i	VB_B [mm]	Ra [µm]	Rz [µm]	VB_B [mm]	Ra [µm]	Rz [µm]	VB_B [mm]	Ra [µm]	Rz [µm]
1	0,16	2,44	6,89	0,11	2,19	8,76	0,23	2,96	11,28
		2,15	8,57		2,26	9,57		2,85	10,15
		2,32	7,64		2,07	8,54		2,66	10,30
$\bar{x}$		**2,30**	**7,70**		**2,17**	**8,96**		**2,82**	**10,57**
2	0,18	2,37	9,16	0,13	2,26	11,65	0,28	3,35	13,58
		2,46	10,16		2,36	9,14		3,45	13,30
		2,63	9,58		2,28	10,27		3,48	14,45
$\bar{x}$		**2,49**	**9,63**		**2,30**	**10,35**		**3,43**	**13,78**
3	0,22	3,17	12,15	0,22	2,75	13,30	0,33	4,12	16,59
		2,87	11,85		2,98	14,14		3,87	17,27
		2,93	12,26		3,12	13,49		3,95	17,92
$\bar{x}$		**2,99**	**12,09**		**2,95**	**13,64**		**3,98**	**17,26**
4	0,25	2,97	13,69	0,25	3,47	17,66	0,38	4,20	19,52
		3,15	14,23		3,27	15,33		4,27	20,36
		3,27	11,13		3,36	16,85		4,23	19,16
$\bar{x}$		**3,13**	**13,01**		**3,37**	**16,61**		**4,23**	**19,68**
5	0,30	3,33	13,65	0,34	4,17	18,74	0,51	4,87	21,36
		3,16	14,87		3,85	19,22		4,62	21,60
		3,27	14,79		3,92	18,33		4,74	21,17
$\bar{x}$		**3,25**	**14,44**		**3,98**	**18,76**		**4,74**	**21,38**

- Calculation of machine time:

$$T_{as} = \frac{L_i}{f \cdot n} \quad (1)$$

Where: T_{as} - machine time [min],
L_i - machined length [mm],

f - feed per revolution [mm],
n - number of revolutions [min^{-1}].

- Amount of cut-off material:

$$V = v_c \cdot a_p \cdot f \cdot T_{as} \quad (2)$$

Where: V - amount of cut-off material [mm^3],
v_c - cutting speed [$m \cdot min^{-1}$],
a_p - cut depth [mm],
f - feed per revolution [mm],
T_{as} - machine time [min].

Table 2. Evaluation of results (VB_B = 0,3 mm)

VBD	T_{as} [min]	V [mm^3]	Ra [µm]	Rz [µm]
CNMG 120408 - TF	8	300000	3,25	14,4
CNMG 120408 - SMR	7,35	275625	3,8	17,85
CNMG 120408 - M5	3,75	140625	3,6	14,6

Graph 1. The process of insert wear

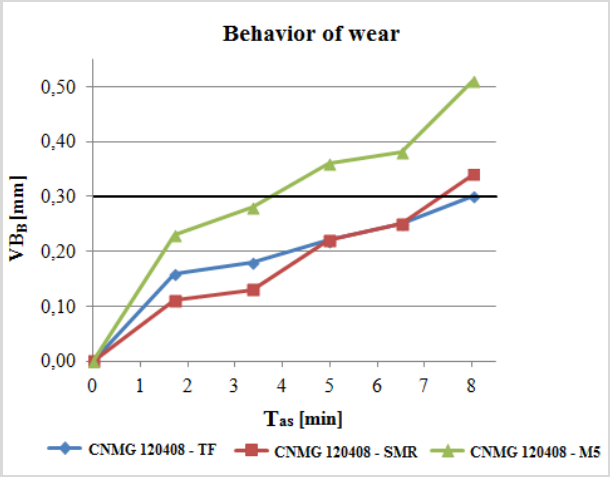

Graph 2. Volume of removed material

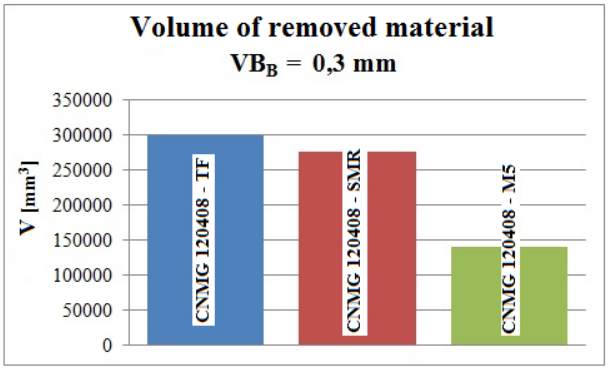

Figure 8. Machined material Inconel 625

Graph 3. The value of surface roughness parameter Ra

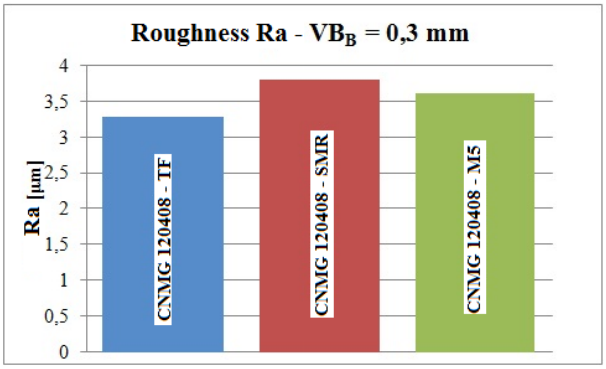

Graph 4. The value of surface roughness parameter Rz

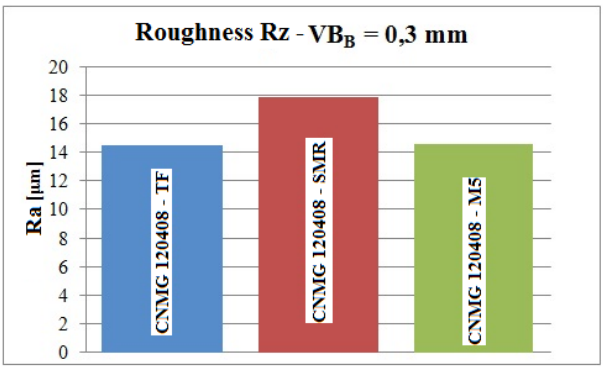

6. Determination of tool-wear mechanisms

The tool wear occurred during machining of Inconel 625 by exposing the insert to high mechanical and heat loads. The cutting edge wear was characteristic by the creation of a notch at the back at the location of tool exit from the stroke. This was caused primarily by the tool cutting edge going into stroke at the hardened layer of material, whose mechanical properties, especially hardness, are different from the basic material. The

assumption was that the notch at the back occurred through the process of sticking of machined material to the cutting edge and consequent tearing of the tool cutting material. An accompanying process was creation of burrs at this location. This phenomenon is characteristic for machining of nickel alloys using low cutting speeds, where the machined material is pushed in front of the tool insert edge.

7. Conclusions and the direction of future research

A goal of this experimental activity was to analyze the status of nickel superalloy machining, and to verify by experiment and to propose the way, by which we could easily and efficiently machine these materials. For this we first need to propose a tool, cutting material, cutting geometry and cutting conditions. Exchangeable cutting insert made from coated sintered carbide intended for machining of nickel superalloys were used for machining.

Under the set cutting conditions the main evaluation criteria were durability and amount of wear at the back of cutting tool and achieved roughness of the machined surface. Machining results and suitability of use of individual exchangeable cutting insert were influenced primarily by specific properties of the machined material, tool cutting material and the type of coating. The achieved results show that the insert marked CNMG 120408 – TF from the IC 807 tool material was the most suitable.

8. Acknowledgement

Article has been done in connection with project Increasing of Professional Skills by Practical Acquirements and Knowledge, reg. no. CZ.1.07/2.4.00/17.0082 supported by Education for Competitiveness Operational Program financed by Structural Founds of Europe Union and from the means of state budget of the Czech Republic and by project Practical competence and professional qualifications improvement in the area of technical education, reg. no. CZ.1.07/2.4.00/31.0162 financed by Structural Founds of Europe Union and from the means of state budget of the Czech Republic

9. References

[1] J-E. Stahl, *METAL CUTTING – Theories and models*. Sweden: Division of Production and Materials Engineering. Lund University Sweden, 2012. 580 s. ISBN 978-91-637-1336-1.

[2] M.Neslušan; A. Czán, *Obrábanie titánových a niklových zliatin*. Žilina: Žilinská univerzita v Žilině / EDIS, 2001. 189 s. ISBN 80-7100-933-4.

[3] A.Maurotto, and all. *Comparing machinability of Ti-15-3-3-3 and Ni-625 alloys in UAT*. 5th CIRP conference on High Performance Cutting 2012 [Online]. [Accessed 2013-10-01] Available: http://www.sciencedirect.com

[4] Specialmetals.com [Online]. c2009. *Machinig Special Metals.* [Accessed 2013-10-01]. Avaliable:http://www.specialmetals.com/documents/machining.pdf

[5] E.O. Ezugwu, et al., *The machinability of nickel-based alloys: a review*. Journal of Materials Processing Technology 86 (1999) 1–16. School of Engineering Systems and Design, South Bank University, 103 Borough Road, E.O. London, SE1 0AA, UK

[6] Iscar s.r.o. *ISO Turn*. [Online], [Accessed 2013-10-02]. Available: http://www.iscar.com/Ecat/familyhdr.asp?fnum=60&app=970&mapp=IS&GFSTYP=M&lang=EN&type=1

[7] Sandvik Coromant s.r.o. *Soustružnické nástroje - Všeobecné soustružení.* [Online], [Accessed 2013-10-02]. Available: http://www.sandvik.coromant.com/sitecollectiondocuments/downloads/global/catalogues/cs-cz/turn_a.pdf

[8] Seco Tools s.r.o. *Soustružení.* [Online], [Accessed 2013-10-02]. Available: http://www.secotools.com/CorpWeb/Downloads/seconews2_2011/MN/turning/Turning%202012_CZ_LR.pdf

[9] DMG/Mori Seiki. SL - 403. [Online], [Accessed 2013-10-02]. Available: http://www.dmgmoriseikiusa.com/sl-series/sl-403

GREYWATER COMPOSITION AND TREATMENT IN A COASTAL AREA OF SOUTH AFRICA

Nosiphiwe P. Ngqwala[1], Bongumusa M. Zuma[2], and Roman Tandlich[1*]

[1]Division of Pharmaceutical Chemistry, Faculty of Pharmacy, Rhodes University, P.O. BOX 94, Grahamstown 6140, South Africa
[2] Flux Development Scientists, 10 Samson Street, Vincent, East London 5200, South Africa
* *Corresponding author e-mail: roman.tandlich@gmail.com, r.tandlich@ru.ac.za.*

Abstract
The PozzSand® fly ash in combination with lime is tested for possible application in greywater treatment in coastal areas of South Africa. This was done in a two-phase study. Firstly, the physical, chemical and microbial composition of greywater from a donour household was assessed over six weeks. Then the fly-ash-lime filter tower was used to treat the greywater. The baseline NH_4^+ concentrations ranged from 0.51 to 2.4 mg/L, while analogical PO_4^{3-} concentrations ranged from 0.54 to 2.0 mg/L. The NO_3^- concentration interval spanned from 0.39 to 2.4 mg/L. The chemical oxygen demand varied between 630 and 1580 mg/L. The Cl^- concentration was recorded to range from 0.13 to 48 mg/L. The SO_4^{2-} concentrations ranged from 110 to 380 mg/L. The faecal coliform concentrations varied between 0 and 490 colony-forming units per 100 mL. Turbidity ranged from 2.7 to 620 nephelometric turbidity units, while pH was inside the interval from 7.80 to 8.50. Electrical conductivity values ranged from 190 to 1980 μS/cm. The maximum removal efficiency in greywater treatment was recorded for faecal coliforms and it stood at 100 %. The fly ash filter tower system was able to remove up to 92 % of PO_4^{3-}. Further experiments are curently underway to modidy the FLFT system to manage the pH of the effluent, while maintaining the treatment efficiency observed in this preliminary study

Keywords:
greywater reuse; PozzSand®; fly ash-lime-filter tower,

1. Introduction

Water scarcity is a global phenomenon [1], [2]. Pressure on drinking water resources is higher in developing countries due to faster population growth and higher rates of urbanisation [3]. South Africa is a member of the G20 group as an emerging economy [4]. It has reached a medium level of human development as indicated by the Human Development Index [5], but is still considered a developing country [6]. At least part of the country has a semi-arid climate, with a high geographical variability of precipitation exists [7]. Climate and service delivery considerations often cause limitations in drinking water supply [8]. South Africa will likely reach physical water scarcity by 2025 [9], mainly due to the water-intense activities such as mining and agriculture. Wastewater treatment for reuse has been seen as one of the possible solutions to this problem [10].

The rationale is the treated wastewater could be recycled and used in activities where drinking water quality is not required, e.g. toilet flushing or irrigation. This would reduce the freshwater consumption in areas with water shortages, e.g. coastal zones. Limited efficiency of wastewater treatment and skills shortages in the sector [10], as well as lack of sanitation infrastructure [2], often prevent such effort. Reactive filters are low-cost sanitation systems where wastewater percolates down a system of layered materials and in-situ treatment takes place through precipitation and straining [11]. It can be implemented in decentralised settings from low-cost materials such as wood chips, coarse sand and gravel [12]. The mulch-tower (MT) system is an example of such as reactive filter [12]. It has previously been to provide partial treatment of greywater in South Africa, but lacked the ability to remove phosphates and indicator microorganisms from greywater [9]. PozzSand ® is a conditioned and low grade fly ash from the pulp and paper mill industry [10]. Replacing the mulch layer in the MT with a combination of PozzSand® and lime has been shown to sterilise greywater and remove phosphates and COD [10]. The Fly Ash Lime Filter Tower (FLFT) system developed by Zuma [10] is tested in this study for the treatment of the greywater from coastal areas of South Africa.

2. Materials and Methods

The study started with characterisation of greywater and then treatment was performed using the methods of Zuma [10]. Greywater was obtained from one donour household in the coastal town of Kleinemonde, Eastern Cape Province of South Africa. For sample collection, 500 or 1000 ml Schott bottles (Sigma-Aldrich, Johannesburg, South Africa) were washed in 10 % hydrochloric acid (Sigma-Aldrich, Johannesburg, South Africa), commercial detergent and MilliQ water (Millipore/Merck, Port Elizabeth, South Africa). These were then sterilised in the Model RAU-53Bd REX MED autoclave (Hirayama Manufacturing, Tokyo, Japan) at 121 °C/kPa for 15 minutes. The samples were collected as described by Tandlich

et al. [13]. Samples placed on ice after collection and transported to the laboratory at 4 °C. There all microbiological, physical and chemical analyses were completed within 48 hours of collection. The baseline greywater composition was measured over a six-week period, while the preliminary treatment assessment was measured over a two-week period.

Greywater samples were analysed for concentrations of ammonium (NH_4^+), phosphate (PO_4^{3-}), nitrate (NO_3^-), chloride (Cl^-), sulphates (SO_4^{2-}), COD and faecal coliforms (FC). Turbidity, electrical conductivity (EC) and pH of the samples were also determined. Unless stated otherwise, all quantitative analyses were performed according to Standard Methods [14]. Besides SO_4^{2-}, the concentrations of ions and COD determination were determined using the relevant kits as purchased from Merck Pty. Ltd. (Johannesburg, South Africa). Spectrophotometric measurements were performed using the Shimadzu 1200 UV/VIS spectrophotometer (Shimadzu, Johannesburg, South Africa). The EC and pH of the greywater samples were measured using the portable testers from Hannah Instruments (Port Elizabeth, South Africa). FC was determined using the membrane filtration technique [14] on the m-FC agar (Merck Pty. Ltd., Johannesburg, South Africa). Cells were trapped on the 47 mm GF-6 membrane filters (pore size 0.45 μm, Spellbound Labs, Port Elizabeth, South Africa). Turbidity (Tur) was measured using the Lutron TU-2016 portable turbidimeter (Test and Measurement Instruments CC, Johannesburg, South Africa). The SO_4^{2-} concentrations were determined using the United States Environmental Protection Agency (EPA) method 375.4 [15]. Sterile plastic Petri dishes were purchased from EC Labs (Port Elizabeth, RSA). Duplicate measurements for all samples were conducted.

The FLFT system was built according to the specifications provided by Zuma [10] and the system outline was analogical to that of the MT system as published by Zuma et al. [12]. The only difference was the exchange of the wood chips layer for the 5:3 (v/v) PozzSand ® and lime mixture. Bathroom greywater composition and preliminary assessment are assessed in this study. The treatment performance was tested by obtaining samples of the untreated greywater (the influent) and the treated greywater (the effluent).The reactor was fed twice a day with 3 litres of greywater in the morning and 2 litres in the afternoon. The influent and effluent samples were collected as composite fractions of individual feedings. Analyses on the influent and effluent were performed analogically as stated for the baseline greywater characterisation. Efficiency of treatment was assessed by calculating the percentage of removal for each parameter as defined in Eq. (1).

$$PR = 100 \times \frac{C_{\text{influent}} - C_{\text{effluent}}}{C_{\text{influent}}} \quad (1)$$

In Eq. (1), *PR* is the percentage removal, while $C_{\text{influent,effluent}}$ are the concentrations or values for a given parameter in the influent (subscript influent) and the effluent (subscript effluent). The *PR* values are dimensionless while the units for a given parameter are listed in the Results and Discussion section (see below).

3. Results and Discussion

Data from the baseline greywater characterisation and the preliminary treatment are summarized in Tables 1 and 2. Baseline characterisation of the greywater is necessary due to high variability of its composition among the various sources [12], [13] The NH_4^+ concentrations ranged from 0.51 mg/L recorded in week 6 up to 2.4 mg/L recorded in week 3. The PO_4^{3-} concentrations ranged from 0.54 mg/L recorded in week 3 up to 2.0 mg/L recorded in week 1. At the same time, the NO_3^- concentration interval spanned from 0.39 mg/L recorded in week 5 up to 2.4 mg/L recorded in week 1. The concentration of organic matter was measured as the COD content. It varied between 630 mg/L in week 4 and 1580 mg/L in week 2. The Cl^- concentration was recorded to range from 0.13 mg/L in week 4 and 48 mg/L in week 6. The SO_4^{2-} concentrations were shown to be inside the following interval: 110 mg/L (week 1) and 380 mg/L (week 4).

The FC concentrations were below the detection limit of 0 colony-forming units per 100 mL of greywater (CFUs/100 mL) during the first three weeks of the baseline study. Then the concentrations increased to between 150 CFUs/100 mL in week 5 and 490 CFUs/100 mL in week 6. The TUR values varied between 2.7 nephelometric turbidity units (NTUs) for week 4; and 620 NTUs in week 2. The minimum pH value was measured in weeks 3 and 4, with the respective value of 7.80. The maximum pH value was, on the other hand, recorded in week 1 when it stood at 8.50. Finally, the EC values ranged from 190 μS/cm in week 5 and 1980 μS/cm in week 1. No EC value could be obtained in week 4 due to instrumental problems. The greywater values from Kleinemonde are comparable to those measured in Port Alfred (also a coastal area) by Tandlich et al. [13]. At the same time, the values span a narrower interval than recorded by Zuma et al. [12].

Table 1. Physicochemical and microbial quality of bathwater greywater in Kleinemonde, Eastern Cape Province of South Africa.

Para-Meter	W1[a]	W2[a]	W3[a]	W4[a]	W5[a]	W6[a]
NH_4^+ (mg/L)	1.9	2.2	2.4	0.52	2.1	0.51
PO_4^{3-} (mg/L)	2.0	1.6	0.54	1.3	1.0	1.0
NO_3^- (mg/L)	2.4	2.1	1.6	0.58	0.39	1.4
COD$\times10^3$ (mg/L)	0.80	1.58	1.18	0.63	1.36	1260
Cl^- (mg/L)	3.5	4.7	6.3	0.13	3.9	48
SO_4^{2-} (mg/L)	110	190	171	380	250	190
FC (CFU/ 100 ml)	0	0	0	250	150	490
Tur (NTU)	550	620	590	2.7	170	100
pH	8.50	8.30	7.80	7.80	8.00	8.20
EC (μS/cm)	1980	1970	1810	ND[b]	190	1240

[a] W represents week in question
[b] Not determined due to instrumental problems with the EC tester.

Between the background characterisation and greywater treatment, increases were recorded in levels FC, Tur, NO_3^- and NH_4^+. At the same time, the concentrations of SO_4^{2-} and COD decreased significantly. Such variability has been reported for greywater in South Africa before [12]. Spike in the concentrations of FC, Tur and NH_4^+ indicate that a sewage pipe might have been broken in the vicinity of the tap water supply into the donour household [16]. The FLFT system was able to decrease the higher influent concentrations and the percentages of the removal are shown in Figure 2. The minimum *PR* value was observed in week 1 for Cl^- when no removal, but a 1 % release of Cl^- from the FLFT system was recorded in week 1 of treatment. At the same time, the maximum removal efficiency of 100 % was recorded FC in week 1. Contrary to the MT system [12], the system was able tom remove 78 and 92 % of the PO_4^{3-} influent concentration, respectively. The *PR* for FC was 99 and 100 % in both weeks of the sampling. The COD and NO_3^- removals were maintained as observed in MT system. Thus the problems of the original reactive filter system, namely MT, were addressed by the FLFT modification. Therefore the PozzSand® fly ash in combination with high purity lime is a potentially effective material for the treatment of greywater.

Table 2. Treatment efficiency of the greywater using the modified fly ash filter tower.

Samples	Influent		Effluent	
Para-meter	W1[a]	W2	W1	W2
NH_4^+ (mg/L)	54	47	34	27
PO_4^{3-} (mg/L)	2.0	2.1	0.45	0.17
NO_3^- (mg/L)	55	25	9.0	1.8
COD (mg/L)	50	51	7.4	0.98
Cl^- (mg/L)	31	25	32	3.3
SO_4^{2-} (mg/L)	5.2	6	1.9	1.3
FC (CFU/100 ml)	1000	720	0	5
Tur (NTU)	85	98	1.7	2.0
pH	9.2	7.9	12.8	12.0
EC (mS/cm)	1960	1940	1720	1771

[a] W represents week in question

Problem arise from highly alkaline pH values of the FLFT effluent which ranged from 12.0 to 12.8 (see Table 2). The high pH will sterilise the greywater and remove all the indicator/pathogenic microorganism [10]. However, it will also result corrosion of piping during irrigation operations, as well as lead to the destruction of the soil structrue upon discharge [17]. Thus further experiments are currently underway to modidy the FLFT system to manage the pH of the effluent, while maintaining the treatment efficiency observed in this preliminary study.

4. Conclusion

Therefore the PozzSand® fly ash is a potentially effective material for the treatment of greywater from coastal areas of South Africa. Complete removal of indicator microorganisms was recorded and high phosphorus removal is also encouraging. Further experiments are curently underway to modidy the FLFT system to manage the pH of the effluent, while maintaining the treatment efficiency observed in this preliminary study.

5. Acknowledgements

Authors thank the Water Research Commission of South Africa (grant no.K5/2011/3) for funding the study in part. The National Research Foundation of South Africa is acknowledged for providing funding for first author's PhD degree.

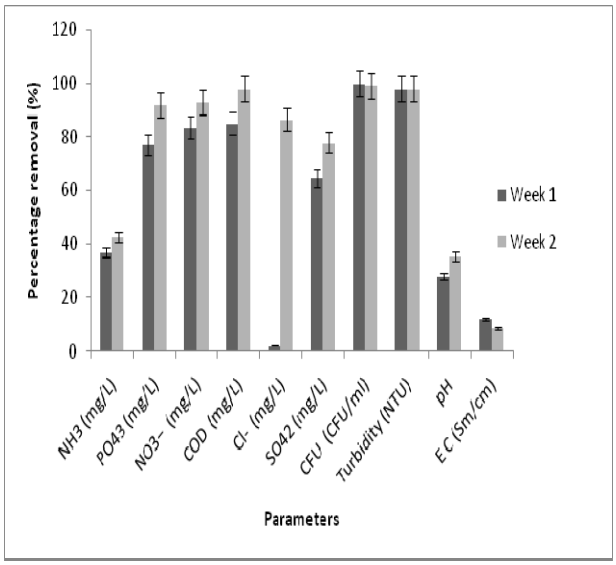

Figure 2. Treatment efficiency of the fly ash-lime filter tower for bathroom greywater from Kleinemonde, Eastern Cape, South Africa.

6. References

[1] D. Seckler, R. Barker, U. Amarasinghe, "Water scarcity in the twenty-first century," *International Journal of Water Resource Development*, 15, 29-40, 1999.

[2] K. Carden, N. Armitage, K. Winter, O. Sichone, U. Rivett, J. Kahonde, "The use and disposal of greywater in the non- sewered areas of South Africa: part 1—quantifying the greywater generated and assessing its quality," *Water SA*, 33(4), 425-432, 2007.

[3] N. Rodda, K. Carden, N. Armitage, H. M. du Plessis, "Development of guidance for sustainable irrigation use of greywater in gardens and small-scale agriculture in South Africa," *WRC 40-Year Celebration Special Edition* 37, 5, 2011.

[4] L. Boulle, "The Republic of South Africa and the G20: Its Political, National Interests and Priorities as Member of the Process", *Konrad Adenaur Stifftung*. [Online]. Available: http://www.kas.de/upload/dokumente/2011/10/G20_E-Book/chapter_14.pdf [Accessed: 1-Oct-2013).

[5] "United Nations Human Development Index," *United Nations*. [Online]. Available at: http://hdrstats.undp.org/en/indicators/103106." html [Accessed; 23-Jul-2012].

[6] R. Tandlich, T. G. Chirenda, C. S. Srinivas, "Gender aspects of disaster management in South Africa," *Journal of Disaster Risk Studies*, 5(4): Article 84, 2013.

[7] J. C. Stager, P. A. Mayewski, J. White, B. M. Chase, F. H. Neumann, M. E. Meadows, C. D. King, D. A. Dixon, "Precipitation variability in the winter rainfall zone of South Africa during the last 1400 yr linked to the austral westerlies'" *Climate of the Past*, 8, 877-887, 2012.

[8] M. N. B. Momba, Z. Tyafa, N. Makala, B. M. Brouckaert, C. L. Obi, "Safe drinking water still a dream in rural areas of South Africa. Case Study: The Eastern Cape Province," *Water SA*, 32, 715-720, 2006.

[9] R. Tandlich, B. M. Zuma, J. E. Burgess, K. Whittington-Jones, "Mulch tower treatment system for greywater re-use. Part II: destructive testing and effluent treatment," *Desalination*, 242, 1-3, 57-69, 2009.

[10] B. M. Zuma, "The efficacy and applicability of the low-cost adsorbent materials in wastewater treatment," *Rhodes University*, Grahamstown, South Africa.

[11] I. Tsalakanidou, "Potential of reactive filter materials for small-scale wastewater teatment in Greece," *KTH Architecture and Built Environment*. [Online]. Available: http://www2.lwr.kth.se/Publikationer/PDF_Files/LWR_EX_06_1.PDF [Accessed: 2-Oct-2013].

[12] B. M. Zuma, R. Tandlich, K. Whittington-Jones, J. E. Burgess, "Mulch tower treatment system Part I: Overall performance in greywater treatment," *Desalination*, 242, 1-3, 38-56, 2009.

[13] R. Tandlich, B. M. Zuma, S. A. Dyongman, A. Slaughter, "Characterization of greywater from selected sites in South Africa for potential reuse in irrigation" *IASTED International Conference on Water Resource Management*, Gaborone, Botswana, 8-12-Sep-2008.

[14] American Public Health Association, American Water Works Association, Water Environment Federation, "Standard methods for the examination of water and wastewater," *American Public Health Association*, Washington, DC, USA.

[15] "Sulphate (Turbidimetric). Method #: 375.4," *Cornerstone Laboratory*. [Online]. Available: http://www.cornerstonelab.com/EPA-Methods/100-400/375_4.PDF [Accessed: 3-Feb-2012].

[16] A. J. Ribbink, "The Impact of climate change on food security among coastal communities of Keiskamma, in the Eastern Cape, South Africa," *Final Project Report for 2011 START Grants for Global Change Research in Africa*. [Online]. Available: http://start.org/download/gec11/ribbink-final-report.pdf [Accessed: 7-Oct-2013].

[17] "South African Water Quality Guidelines: Irrigation," *Department of Water Affairs and Forestry*, Pretoria, South Africa, 1996.

EXPERIMENTAL ANALYSIS OF WELDED PIPING BRANCH JUNCTIONS UNDER INTERNAL PRESSURE

Mato Kokanovic*, Tomislav Baskaric[1], Jelica Busic[1], Zeljko Ivandic[1], Drazan Kozak[1]

[1]Mechanical Engineering Faculty in Slavonski Brod, J. J. Strossmayer University of Osijek, Croatia
* *Corresponding author e-mail: Mato.Kokanovic@sfsb.hr*

Abstract
This paper presents a procedure for calculating the welded piping branch according to EN 12952-3, which defines the shaping and method of calculation of such components. In the experimental part of the paper stresses are measured the under internal pressure of 0-420 bar. Stresses were measured using strain gauges.

The analysis of the calculated stresses and with the help of experimental methods for Y-shape pipe branch can conclude that the calculations according to standards are pretty strict compared to the real stresses that occur in real-world conditions.

Keywords:
piping branch, EN 13445-3, HRN EN 13480-3, EN 12952-3, measuring strains, piping

1. Introduction

Considering that pipe branches and connectors are components of power and process plants and other piping systems that are considered very dangerous, there are regulations that define the rules for the design elements of welds such as branches and pipe fittings. In Croatia, the following regulations are used for the construction of these elements:

HRN EN 13445-3
HRN EN 13480-3
HRN EN 12952-3

2. Calculation of welded piping branch junctions

For sample calculation was selected the Y-shape branch (Figure 1) and it is made of a material P235GH-TC2. Nominal diameter of pipe is ø88,9 mm and a pipe wall thickness is 8 mm with welded seams. The angle at which the pipes branching is 90 ° and the branches were analyzed considering the load of internal pressure in the range of 0-420 bar. We analyzed the case of application branches at room temperature.

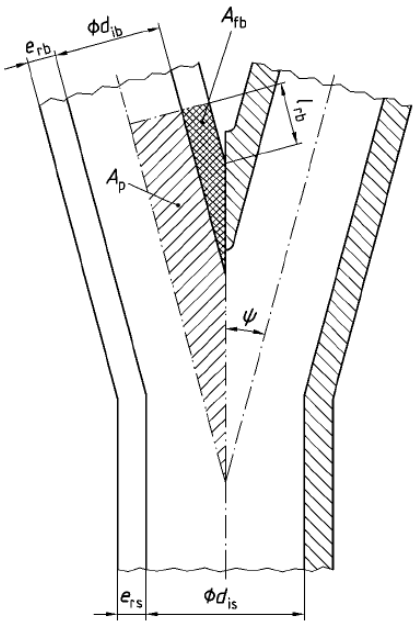

Figure 1. Y shape branch made by welding or forging [6]

Calculation of these branches described in regulation EN 12952-3 [6] according to Figure 1, which stipulates $\psi \geq 15°$. For the analyzed branch angle is $\varphi = 90°$ and the condition $\psi = \varphi / 2 \geq 15°$ is fulfilled.
This calculation is based on the fact that the pressure vessels material can create greater or equal reactive force compared to the one that gives the load due to internal pressure. Reactive force in the material vessel is obtained from the product of the average allowable stresses for the material pressure vessels and surface cross-sections exposed to this stress. Loading force is the product of pressure acting on the vessel and the cross-sectional area of the pressure vessel. When calculating the observed cross-section of branch is in the axial plane of branch and therefore the expression for the calculation of stress is as follows:

$$f_a = p_c \cdot y \cdot \left(\frac{A_p}{A_f} + \frac{1}{2} \right) \leq f_s \qquad (1)$$

Where is:
p_c - calculation pressure, MPa

y - factor for branches with $\psi > 45°$, while for the branches with $d_o \leq 102\,\text{mm}$ and $15° \leq \psi \leq 45°$ it is calculated according to the formula:

$$y = 1 + 0{,}005 \cdot (45° - \psi) \tag{2}$$

$$A_{fb} = e_{rb} \cdot l_{rb} + \frac{e_{rb} \cdot \frac{e_{rb}}{\tan\psi}}{2} = e_{rb} \cdot l_{rb} + \\ + \frac{e_{rb}^2}{2\tan\psi} = e_{rb} \cdot \left(l_{rb} + \frac{e_{rb}}{2\tan\psi} \right) \tag{3}$$

$$A_p = \left(\frac{d_{ib}}{2} + e_{rb} \right) \cdot l_{rb} + \frac{\left(\frac{d_{ib}}{2} + e_{rb} \right)^2}{2\tan\psi} = \\ = \left(\frac{d_{ib}}{2} + e_{rb} \right) \left(l_{rb} + \frac{\frac{d_{ib}}{2} + e_{rb}}{2\tan\psi} \right) \tag{4}$$

$$l_{rb} = \min\left\{ \sqrt{(d_{ib} + e_{rb}) \cdot e_{rb}}\,; l_{b1} \right\} \tag{5}$$

Where is:
e_{rb}, e_{rs} - pipe wall thickness

$$e_{rb} = e_{nb} - c_1 - c_2 \tag{6}$$

$$e_{rs} = e_{ns} - c_1 - c_2 \tag{7}$$

Where is:
e_{nb} and e_{ns} - nominal pipe wall thickness
c_1 - addition for the rolling tolerance of pipes (± 12%)
c_2 - addition for corrosion and erosion (1 mm)
f_s - allowed stress, and is calculated by:

$$f_s = \min\left\{ \frac{R_e}{2{,}4}\left(\frac{R_{p0,2}(T)}{2{,}4} \right), \frac{R_m}{1{,}5} \right\} \tag{8}$$

For material P235GH-TC2 yield strength at room temperature is $R_e = 235\,\text{MPa}$, and the tensile strength is $R_m = 450 - 550\,\text{MPa}$. According to the above formula allowed stress in branch is $f_s = 97{,}92\,\text{MPa}$.
The results of calculations are given in Figure 4. Analysis of these results shows that according to EN 12952-3 maximum allowed pressure is 84 bar. If the pressure rises above the allowed, plastic deformation should occur at a pressure of 204 bar and at 390 bar the strain in the material achieves the value of limit tensile strength.

3. Measuring strains on Y shape branch

On the Y-shape branch analyzed in the previous section we measured strains using strain gauges. Load during the measurement was internal pressure 0-420 bar.
Display of measurement points on the experimental Y-shape branch is shown schematically in Figure 2. For measuring the strains on test points 1 to 7 are used rosettes type 0 ° / 45 ° / 90 °, while on measuring point 8 used two strain gauges placed perpendicular to each other in a way to measure deformation in the axial and circular direction.

After the measured strains, we calculated the amounts of principal stresses. For the measurement of 1-7 where we used rosettes 0 ° / 45 ° / 90 °, amounts of principal stresses are calculated according to the formula:

$$\sigma_{1,2} = \frac{E}{2 \cdot (1 - \nu)} \cdot (\varepsilon_a + \varepsilon_c) \pm \\ \pm \frac{\sqrt{2} \cdot E}{2 \cdot (1 + \nu)} \sqrt{(\varepsilon_a - \varepsilon_b)^2 + (\varepsilon_c - \varepsilon_b)^2} \tag{9}$$

For measuring point 8 the main stresses are calculated according to:

$$x^2 y^2 + A x_2 - 2Bxy = 0 \tag{10}$$

$$\sigma_1 = \frac{E}{1 - \nu^2} (\varepsilon_1 + \nu \cdot \varepsilon_2) \tag{11}$$

$$\sigma_2 = \frac{E}{1 - \nu^2} (\varepsilon_2 + \nu \cdot \varepsilon_1) \tag{12}$$

For principal stresses calculation of the material P235GH-TC2 used value for the modulus of elasticity is $E = 206\,\text{GPa}$ and Poisson factor is $\nu = 0{,}3$.
After calculating the principal stresses, equivalent stresses are calculated according to the theory of maximum energy density of strain distortion for plain stress (energy theory HMH):

$$\sigma_{ekv} = \sqrt{\sigma_1^2 + \sigma_2^2 - \sigma_1 \cdot \sigma_2} \tag{13}$$

Measurement results and calculated values of equivalent stresses HMH theory are shown in Figure 4.

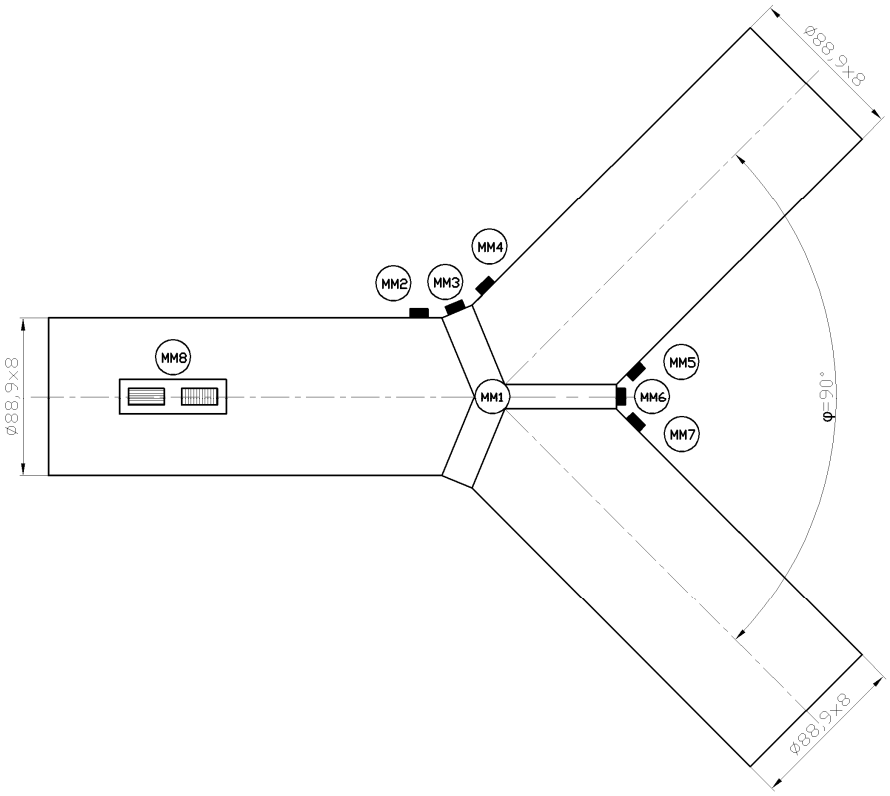

*Figure 2. Schematic presentation of the measuring points on the experimental Y-*shape *branch (*MM - *measuring point*)

*Figure 3. Strain gauges on the experimental Y-*shape *branch (*MM - *measuring point*)

If we compare stresses obtained according to EN 12952-3 with equivalent stress (HMH) obtained experimental (Figure 4) we can conclude that the analysis according to the above regulations are much stricter than the real conditions, which may explain the tendency towards safety as structural elements of pipe branch apply to very dangerous places in power and chemical plants.

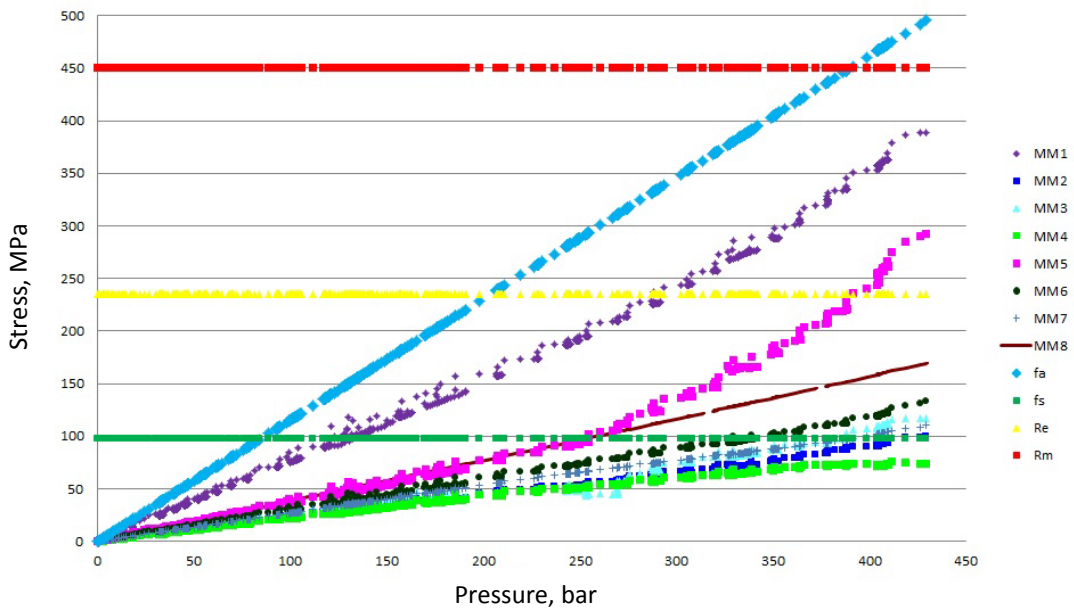

Figure 4. Equivalent stresses calculated by EN 12952-3 and measured equivalent stresses on Y-shape branch (MM - measuring point, fa - strain due to internal overpressure, fs - allowed stress in the branch material, Re – yield stress of branch material, Rm - tensile strength of branch material)

4. Conclusion

The analysis of the calculated stresses and with help of experimental methods for Y-shape pipe branch can conclude that the calculations according to standards are pretty strict compared to the real stresses that occur in real-world conditions.

Because there is a difference between measured stresses and the calculated according to the regulations, there is enough space for exploration and eventual optimization methods for calculating such elements of pressure structures in order to reduce the wall thickness, which would ultimately bring savings in production facilities and pipelines which contain this structural elements.

5. References

[1] Karl – Heinz Decker : *Elementi strojeva; Golden marketing-Tehnička knjiga,* Zagreb, 2006., 597.- 614. str.

[2] Eduard Beer : *Priručnik za dimenzioniranje uređaja kemijske procesne industrije*; Hrvatsko društvo kemijskih inžinjera i tehnologa , Berislavićeva 6.Zagreb, 1994., 125.-129. str.

[3] Milovan Živković, Taško Maneski : *Termomehanički naponi cevovoda i posuda*; Savez mašinskih i elektrotehničkih inžinjera i tehničara Srbija (SMEITS) Kneza Miloša 7, 11000 Beograd , 11.-20. str

[4] HRN EN 13445-3 *„Neložene tlačne posude - 3. dio: Konstrukcija (EN 13445-3:2002)“;* Hrvatski zavod za norme, Zagreb, 2002.

[5] HRN EN 13480-3 *„Metalni industrijski cjevovodi - 3. dio: Projektiranje i proračun (EN 13480-3:2002+A1:2005+A2:2006)“*;Hrvatski zavod za norme, Zagreb, 2005.

[6] HRN EN 12952-3 *„Vodocijevni kotlovi i pomoćne instalacije – 3. dio: Konstrukcija i proračun dijelova pod tlakom (EN12952-3:2001)“* ; Hrvatski zavod za norme, Zagreb, 2006.

[7] *Ivo Alfirević: Nauka o čvrstoći 1;* Izdavačka radna organizacija, Tehnička knjiga, Zagreb, Juršićeva 10, 1989., 92-96 str.

CHOICE OF A UNCONENTIONAL CUTTING TECHNOLOGY FOR THE DISINTEGRATION OF COMPOSITE MATERIALS

A. Andrej[1], M. Šomšák[1], L. Krausová[1], J. Carách[1], F. Murgaš[1,2], J. Nemcova[1], K. Colic[3] and M. Milosevic[3]

[1]Faculty of Manufacturing Technologies of Technical University of Košice with seat in Prešov, Slovakia
[2]SOR Libchavy spol. s r.o., Libchavy, Czech Republic
[3] University of Belgrade, Innovation Centre of the Faculty of Mechanical Engineering, Belgrade, Serbia
Corresponding author e-mail: andrej.andrej@tuke.sk

Abstract
The paper deals with selecting the most appropriate unconventional method of the disintegration of composite materials. Specifically, it deals with the disintegration of the bone cement also known as Poly (methyl methacrylate) (PMMA). Analytic Network Process (ANP) method was used to select the most appropriate technology of the disintegration. The interdependencies and linkages between the various criteria of each technology have been taken into account.

Keywords:
Composite material, Bone cement, Analytic network process, Non-traditional machining processes

1. Introduction

The main goal of this paper is to find the most favourable method for the cutting of composite material (namely bone cement). This material is known as PMMA – Poly (methyl methacrylate).
ANP method was defined relatively recently, in 1996, the method of AHP Thomas L. Saat. These include other multi-criteria decision-making methods that help improve the quality of decision-making and thus the process becomes more efficient and more transparent. The basis ANP method is a mathematical calculation [4].
PMMA material is used over 50 years, mainly in clinical practice. It features excellent biomechanical properties, long-term stability and tolerance by the human body and the possibility of the application through a thin needle. Mixing the liquid and powder components forms a liquid substance that solidifies in about 8-10 minutes to a firm and hard cement. During the solidification, the material core can be heated to up to 62° Celsius. However, the temperature decreases towards the material edge, and reaches a maximum of 42° Celsius, which means that it doesn't cause heat damage to neural structures [4, 8]. PMMA is used to repair dentures, repairs of bone and skull defects in humans, in total hip joints replacement, etc.
Currently there is a new type of bone cement, which is characterized by good viscosity. This reduces the risk of cement leakage outside the reserved area during the application [8, 9].
Often however, a failure of an implant in the body (in the bone), joined by the bone cement, occurs. As an example a re-implantation of a total hip replacement due to its failure. In such cases it is necessary to destroy the connection and replace the implant. Therefore, there is an attempt to find a most optimal method of disintegration of the PMMA, to avoid a possible risk of infection, damage to neural structures, or similar.
The 3D optical strain and displacement analysis using digital image correlation method, represents a useful experimental approach that helps to better understand of full displacement/strain fields of loaded biomaterials and denture structures [5-7].

2. Comparison of progressive cutting technologies

Traditional working methods use a "classic" cutting tool and mechanical energy to cut the material. But, unconventional methods use other forms of energy in various chemical and physical events.
Below are defined the special features of these advanced methods:

- material removal does not depend on the mechanical properties (such as hardness, toughness, strength, machinability , etc.).
- cutting force does not work on site of the separation of particles; the cutting resistance is not formed, therefore the worked pieces are not deformed
- less heat passes into the worked piece during the particles removal, because the cutting of the particles is micro sized with a large number of sites and the frequency of elementary removals is high .
- the entire surface of the worked piece is machined at the same time
- when micro working Nano sizes of 10-9 mm are obtained
- the size of the worked piece is defined by the energy base equipment (102 - 103kW)
- the energy consumption during material removal is greater and removal rate is much lower than in traditional processes

Comparison and selection of the most appropriate method was implemented from the following cutting technologies. Specifically, we focused on these nine unconventional methods shown in Figure 1.

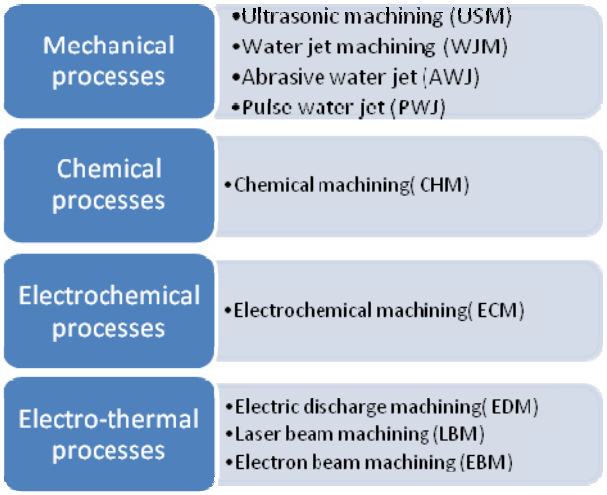

Figure 1. Compared technology cutting

3. Defining defects

When choosing the most appropriate cutting technology in-between the above-mentioned nine methods, the deficiencies that may arise from fragmentation of bone cement will play a big role. These shortcomings need to be defined and focused on. The selected technology should minimize these flaws to acceptable levels. The deficiencies are broken down into three areas (Figure 2.), namely in social, technological and economic fields.

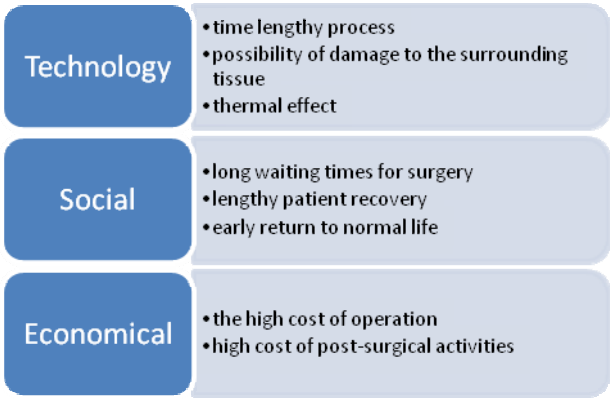

Figure2. Defined defects

The aim is to find a cutting technology, which minimizes technological shortcomings, such as that the cutting will be done without damaging the surrounding tissue, that there is no heat effect in the actual disintegration of bone cement and the overall process will not be time consuming.
Minimizing these shortcomings should result to a shorter surgery; the patient would remain shorter time under anesthesia, thus the risk of infections and other complications would be minimized. Patient's quality of life will depend primarily on: reduction of waiting time for surgery; elimination of post-surgery complications; also a shorter recovery and quicker return to normal life [1, 4].

4. ANP method and process solutions

The ANP (analytic network process) method is one of the multi-criteria decision-making methods that support the user in choosing the best option from the available options [4]. This method presents the problem as a network of criteria, sub-criteria and alternatives, but it can only be applied if the criteria, sub-criteria and alternatives are dependant.
The advantages of the ANP method are particularly straightforward methodology; a network structure of the decision-making process for greater understanding of the problem; possibility of combining the results with other methods; the ability to include the qualitative decision criteria in the decision process; and also that the method has been verified in real cases..

The calculation method and procedure ANP

To find the most appropriate cutting technology of bone cement, it is necessary to follow the decision criteria, which must contain certain sub-criteria. The main criteria for cutting composite materials are process performance, divisibility, performance and operational requirements. The sequence of steps ANP method was set as follows:

I. building a hierarchical structure for the material of bone cement
II. pairwise comparison of individual criteria
III. designation of the degree of importance of individual technologies based on five criteria
IV. pairwise comparison of criteria and sub-criteria
V. dependence between the different technologies
VI. developing an overall resultant matrix w_p and summary results W_{ANP}

I. The preparation of a hierarchical structure

Figure 3 shows in a hierarchical structure individual unconventional cutting technologies with their criteria and sub-criteria. These are: ultrasonic machining (USM), water jet machining (WJM), abrasive water jet (AWJ), pulse water jet (PWJ), chemical machining (CHM), electrochemical machining (ECM), electric discharge machining (EDM), laser beam machining (LBM) and electron beam machining (EBM) [2, 4].

II . Pairwise comparison of individual criteria

Pairwise comparison of individual criteria, namely: MA - material, DI - divisibility, PP - Process

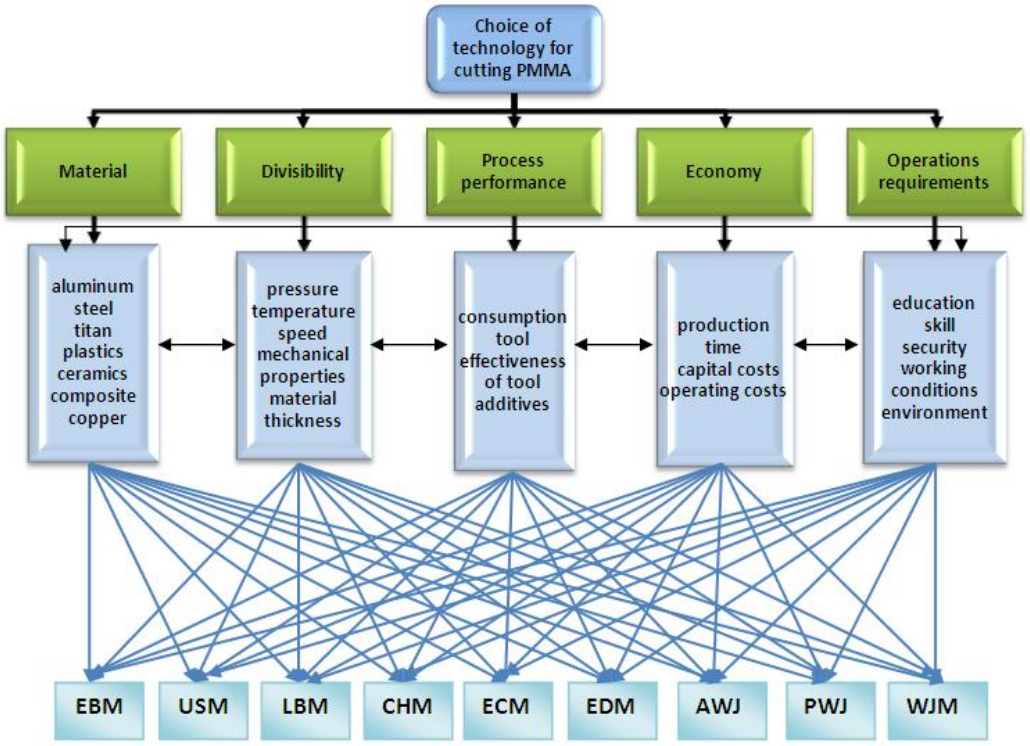

Figure3.Requirements for cutting PMMA in a hierarchical structure ANP

Performance, EC - Economy and Trade - operations requirement . In the table 1 (Table 1) the decision maker chose values on the Saaty scale 1-9, where 1 means that the criteria are equally important. Fractions represent the reversed (inverse) value [4].

Table 1. Paired comparison criteria

	MA	DI	PP	EC	OR	Geomean	W_1
MA	**1**	4	7	7	7	4,2410	0,5356
DI	1/4	**1**	6	6	6	2,2206	0,2804
PP	1/7	1/6	**1**	2	2	0,6248	0,0789
EC	1/7	1/6	1/2	**1**	2	0,4735	0,0598
OR	1/7	1/6	1/2	1/2	**1**	0,3589	0,0453
						7,9189	**1,0000**

In this table in the column entitled to "GEOMEAN " is a geometric mean calculated by the formula (1), with a total value of 7.9189.

$$G = \sqrt[n]{x_1.x_2...x_n} \qquad (1)$$

Where :
G is the geometric mean of the line
n is the radical of the conjunction of the values
x_1 , x_2, ..., x_n are the values assigned to the criteria

In the column labeled, "w_1" is calculated the weight of each criteria (2), which is calculated as the geometric mean of the outcome of each line dividing by the sum of the final resultant average. Their total sum must be equal one.

$$w_{tj} = \frac{x_g}{\sum\left(x_{g1} + x_{g2}...x_{gn}\right)} \qquad (2)$$

Where :
w_{ij} is the calculated weight of each criterion in line
x_g is the geometric mean of the matrix row
x_{g1} , x_{g2} ... x_{gn} is the sum of all geometric means

III . Construction of the importance stage

Decision and designation of the degrees of importance took place on the basis of theoretical knowledge and subjective view of the decision maker. The results are presented in table (Table 2). It should be noted that if this table was made by someone else the results could differ because other maker's opinions may be different.

Table 2. Degree of importance processes

	MA	DI	PP	EC	OR
A1 (EBM)	7	3	1	3	8
A2 (USM)	9	7	3	4	8
A3 (LBM)	7	3	8	3	3
A4 (CHM)	7	5	3	3	1
A5 (ECM)	3	5	4	1	1
A6 (EDM)	3	3	1	3	8
A7 (AWJ)	9	8	7	4	7
A8 (PWJ)	9	9	9	7	9
A9 (WJM)	9	7	7	4	7

The final values of importance are then recalculated according to the formula (2), where the results are the values representing the dependence of importance of unconventional technologies based on 5 criteria. These values of weights will be used in further calculations in the form of matrices (figure 4.).

$$w_{21}=\begin{pmatrix}0{,}1111\\0{,}1429\\0{,}1111\\0{,}1111\\0{,}0476\\0{,}0476\\0{,}1429\\0{,}1429\\0{,}1429\end{pmatrix}\quad w_{22}=\begin{pmatrix}0{,}0600\\0{,}1400\\0{,}0600\\0{,}1000\\0{,}1000\\0{,}0600\\0{,}1600\\0{,}1800\\0{,}1400\end{pmatrix}\quad w_{23}=\begin{pmatrix}0{,}0233\\0{,}0698\\0{,}1860\\0{,}0698\\0{,}0930\\0{,}0233\\0{,}1628\\0{,}2093\\0{,}1628\end{pmatrix}\quad w_{24}=\begin{pmatrix}0{,}0938\\0{,}1250\\0{,}0938\\0{,}0938\\0{,}0313\\0{,}0938\\0{,}1250\\0{,}2188\\0{,}1250\end{pmatrix}\quad w_{25}=\begin{pmatrix}0{,}1538\\0{,}1538\\0{,}0577\\0{,}0192\\0{,}0192\\0{,}1538\\0{,}1346\\0{,}1731\\0{,}1346\end{pmatrix}$$

Figure 4. The resulting scales matrix

IV . Pairwise comparison of individual criteria and sub-criteria

To create a pairwise comparison of individual criteria and sub-criteria is the same as in section II. with the difference that the comparison is not carried in respect of all criteria, but only one. Gradually, the weights of pairwise comparison w_{31} to w_{35} are calculated. These are summarized in a next matrix, which multiplied by the resulting weights w_1 according to formula (3), obtains the value of w_c. This represents the result of the overall balance between the weights of all possible interdependencies among criteria and sub-criteria weights and the resulting pairwise comparison of the five criteria. Image (Figure 5)

$$w_3.w_1 = w_c \qquad (3)$$

$$\begin{pmatrix}0{,}5089 & 0{,}2865 & 0{,}2014 & 0{,}1562 & 0{,}1852\\0{,}2571 & 0{,}5492 & 0{,}1875 & 0{,}1852 & 0\\0{,}1145 & 0{,}1002 & 0{,}5518 & 0 & 0{,}1562\\0{,}0680 & 0{,}0641 & 0 & 0{,}6586 & 0\\0{,}0515 & 0 & 0{,}0593 & 0 & 0{,}6586\end{pmatrix}\times\begin{pmatrix}0{,}5356\\0{,}2804\\0{,}0789\\0{,}0598\\0{,}0453\end{pmatrix}=\begin{pmatrix}0{,}3865\\0{,}3176\\0{,}1400\\0{,}0938\\0{,}0621\end{pmatrix}$$

Figure5. The total scales the resulting matrix

V. Dependence between different technologies

We continue by calculating the resulting weights w_{41} to w_{45} . Using them we express the resulting relations between the alternatives of unconventional methods of cutting in respect of each criterion individually. Implementation process is similar to that in sections I., II. , III. and IV. except for the fact that dependence is not expressed with regard to the criteria, but with regard to a technology with certain criteria. We gradually multiply the resulting weights w_{41} to w_{45} with weights w_{21} to w_{25} and reach weights w_{p1} to w_{p2}. These results matrices are further allocated to the final resultant matrix w_p.

VI . Developing an overall resultant matrix w_p and summary results W_{ANP}

The resulting total matrix w_p drawn from the resulting matrix of weights w_{p1} to w_{p2} has when normalized values shown in the following figure (figure 6).

$$w_P=\begin{pmatrix}0{,}0042 & 0{,}0182 & 0{,}0199 & 0{,}1202 & 0{,}0392\\0{,}0245 & 0{,}0547 & 0{,}1137 & 0{,}1445 & 0{,}0638\\0{,}0316 & 0{,}1059 & 0{,}0619 & 0{,}1121 & 0{,}1505\\0{,}0316 & 0{,}0623 & 0{,}1137 & 0{,}1121 & 0{,}0163\\0{,}0188 & 0{,}0710 & 0{,}0885 & 0{,}0292 & 0{,}0163\\0{,}0188 & 0{,}1059 & 0{,}0199 & 0{,}0741 & 0{,}1312\\0{,}0547 & 0{,}1293 & 0{,}1095 & 0{,}0874 & 0{,}1166\\0{,}0668 & 0{,}2244 & 0{,}2268 & 0{,}2161 & 0{,}2690\\0{,}0788 & 0{,}2282 & 0{,}2461 & 0{,}1042 & 0{,}1971\end{pmatrix}$$

Figure 6. The resulting total matrix w_P

The final step is to calculate the matrix w_{ANP} that is expressed by multiplying the derived weights w_p and w_c using formula (4). The image (figure 7.) shows calculated value.

$$w_P.w_C = W_{ANP} \qquad (4)$$

$$\begin{pmatrix}0{,}0042 & 0{,}0182 & 0{,}0199 & 0{,}1202 & 0{,}0392\\0{,}0245 & 0{,}0547 & 0{,}1137 & 0{,}1445 & 0{,}0638\\0{,}0316 & 0{,}1059 & 0{,}0619 & 0{,}1121 & 0{,}1505\\0{,}0316 & 0{,}0623 & 0{,}1137 & 0{,}1121 & 0{,}0163\\0{,}0188 & 0{,}0710 & 0{,}0885 & 0{,}0292 & 0{,}0163\\0{,}0188 & 0{,}1059 & 0{,}0199 & 0{,}0741 & 0{,}1312\\0{,}0547 & 0{,}1293 & 0{,}1095 & 0{,}0874 & 0{,}1166\\0{,}0668 & 0{,}2244 & 0{,}2268 & 0{,}2161 & 0{,}2690\\0{,}0788 & 0{,}2282 & 0{,}2461 & 0{,}1042 & 0{,}1971\end{pmatrix}\times\begin{pmatrix}0{,}3865\\0{,}3176\\0{,}1400\\0{,}0938\\0{,}0621\end{pmatrix}=\begin{pmatrix}0{,}0239\\0{,}0603\\0{,}0744\\0{,}0594\\0{,}0460\\0{,}0588\\0{,}0930\\0{,}1658\\0{,}1594\end{pmatrix}$$

Figure 7. Expression of matrix W_{ANP}

Finally, to select the most unconventional cutting technology for cutting the PMMA bone cement, a graphical dependence is created (figure 8.), where we can see the result of the ANP calculation methods.

5. Conclusion

The selection of the most appropriate technology for unconventional disintegration of PMMA bone cement was based on ANP methods and calculations and the water jet cutting technology was selected, specifically the cutting by pulsating water jet. This technology has many advantages compared to other technologies, such as: the use of low pressure (8-20 MPa), less water

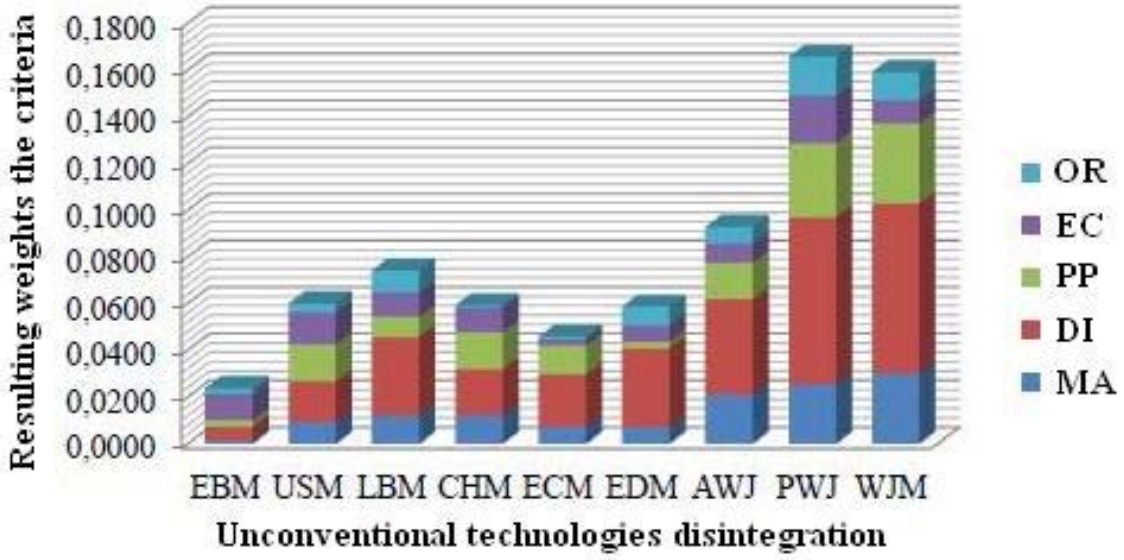

Figure 8. The resulting graph ANP method

consumption and the associated lower power requirement. Despite the pressure pulsations a continuous stream of water exits the nozzle, which, however, due to the pulsation of the variable has axial velocity component. Therefore, there is a continuous water jet disintegrates to partial clusters of water and thus acts as a pulsating current. Sufficient water pressure, which is able to divide a bone cement is based on the experimental work of prelector Hloch et al. dealing not only with this issue. Pulsating water jet is one of the gentlest processes of cutting technology using water flows in such a case of cutting. The very process of disintegration of bone cement takes place so that the flow of water creates a slot without damaging surrounding tissue. The disrupted cement is taken from the point of cutting by integrated extractor into a receiver container. The big advantage is also the small diameter of the stream, only 0.5 mm, which is very practical for cutting in small spaces.

Based on all these data, as well as decision by ANP method the most appropriate and least intrusive way of cutting the bone cement is pulsating water jet technology.

This work was supported by the Slovak Research and Development Agency under the contract No. APVV-207-12".

6. References

[1] S. Hloch, et al., „ Hydro abrasive cutting in orthopedics," Prešov 2011, ISBN 978-80-970623-4-7.

[2] I. Maňková, „Progressive Technologies," Košice: Faculty of Mechanical Engineering TU Košice, ISBN 80-7099-430-4.

[3] S. Hloch, J. Valíček, „Factors influence the surface topography created by cutting Hydroabrasive," Prešov 2008. ISBN 978-80-553-0091-7.

[4] L. Krausová, „ Application of ANP on the choice of technology for the disintegration of composite materials," Prešov, Master's thesis, Faculty of Manufacturing Technologies of Technical University of Košice with seat in Prešov, 2013.

[5] A. Sedmak, M. Milosevic, N. Mitrovic, A. Petrovic, T. Maneski: "Digital image correlation in experimental mechanical analysis", Integritet i vek konstrukcija (Structural Integrity and Life), Vol.12, No1, pp.39–42, 2012.

[6] N. Mitrovic, M. Milosevic, A. Sedmak, A. Petrovic, R. Prokic-Cvetkovic: „Application and Mode of Operation of Non-Contact Stereometric Measuring System of Biomaterials", FME Transactions, Vol. 39, No 2, pp. 55-60, 2011.

[7] I. Tanasic, Lj. Tihacek-Sojic, A. Milic Lemic, M. Djuric, N. Mitrovic, M. Milosevic and A. Sedmak: Optical aspect of deformities analysis in the bone-denture complex, Collegium Antropologicum, 36, 1:173–178, 2012

[8] „Bone cement" [Online]. Available: http://www.vertebroplastika.sk/kostny-cement [Accessed: 19-Sep-2013]

[9] M. Zezula, „ Analysis of the flow properties of bone cement during curing. Master's thesis. Brno: Faculty of chemistry, Brno University of Technology, 2010.

PRODUCTION OF MISCANTHUS X GIGANTEUS ON THE LANDFILL

Snežana Kirin[1], Aleksandar Sedmak[2], Snežana Trmcić[3], Goran Dimic[4], Zeljko Simovic[5]

[1] Innovation Center of Faculty of Mechanical Engineering, University of Belgrade, Serbia
[2] University of Belgrade, Faculty of Mechanical Engineering, Belgrade, Serbia
[4] Faculty for Management of SMEs, University „Privredna Academia“, Novi Sad, Serbia
[5] Public Community Enterprize, Čačak, Serbia
* *Corresponding author e-mail: asedmak@mas.bg.ac.rs*

Abstract

The possibility of establishing energy plantations in landfills, other degraded areas and unused land, has been analyzed, having in mind land recovery and biomass to be used as an energy source. It has been predicted that Miscanthus × giganteus plant, due to its high energy potential, can become important raw material for the biofuel of second generation, like e.g. bioethanol, especially because it can grow even in a landfill. In this paper the example has been shown, indicating that Miscanthus × giganteus plant can be produced on the landfill, and used as an alternate energy source for heating of business offices. The presented results proved that increasing energy efficiency and solving environmental problem can be done simultaneously.

Keywords:
Energy plantations, Miscanthus×giganteus, landfill, sustainable development

1. Introduction

Increase of production lead to increased exploitation and exhaustion of natural resources. Upon exhausting these resources, without recovery and recultivation, it was common to turn to new natural resources. These areas are, thereby, left without the possibility of further exploitation. This situation leads to thinking about creating of a sustainable development concept, i.e. sustainability.

The concept of sustainable development is based on economic and ecological starting points, hence we can define sustainable development as the kind of development that fulfils the needs of present generation without endangering future ones.

This paper presents an example of establishing of biomass as a renewable source of energy. This biomass would be used as fuel for heating of offices in the public utility company “Komunalac” Čačak, improving the company’s energy efficiency. The experiment is in accordance with the concept of sustainable development.

2. Materials and methods

The experiment of establishing biomass was performed on a degraded area of Prelići landfill in Čačak, run by Public Community Enterprise “Komunalac”. The experiment was approved and supported by the Department of ecology and environmental protection, Municipality Čačak.

Energy plants have many positive features. These plants have positive effects on the environment, the ecology and environmental protection since they serve as a means of recovery of degraded areas, in this case for the recultivation of Prelići landfill. Calorific value of energy plantations reach 15000 - 20000 KJ/kg (dry mass), compared to the calorific value of lignite-coal, cca 10500 KJ/kg. When considering return on investment one should keep in mind that these plantations can be exploited for up to 20 years.

Miscanthus x giganteus plant is fast-growing perennial hybrid grass. It was created by crossing Miscanthus x Sacchariflours (diploid) with Miscanthus x sinesis (tetra–ploid). Miscanthus X giganteus resembles wild sorghum and Italian reed, with the main difference being that it can grow up to 4 meters in height, with lush foliage, and with its tree interior made of parenchyma, providing relatively high strength. Planting and developing is done from a rhizome, i.e. its subterranean organs, which do not spread uncontrollably onto adjacent surfaces. By photosynthesizing, Miscanthus X giganteus provides significant biomass energy.

Figure 1. Miscanthus x Giganteus

It is recommended to plant Miscanthus x giganteus at soil temperatures below 10 ^{0}C.

As for hibernation, when temperatures are lower, it is recommended to go with deeper planting or covering with a protective layer of straw, [2].

Planting of this plant requires preparation of the soil. Plowing up to 30 cm is recommended.

Vegetative reproduction by rhizomes or plantlets from plantations is very expensive, [3]. Another options are to use plants that grow from mechanically divided rhizomes, manually divided rhizome fragments or plantlets micro-propagated within the tissue culture. In the majority of experiments, performed in the EU, young plants were used, transplanted directly onto freshly cultivated soil, with the density of 1-3 plants per m^2. Rhizomes can be made from 2-3 years old plants, which will reduce the costs in comparison to micro-propagating.

The method for mechanical dividing of rhizomes in the field, called macro-propagation, was initially developed in Denmark, [4]. According to this method, planting sites for plantation production are cultivated with a rotary tiller after their second or third year, prior to the removal of rhizomes, in order to tear the rhizomes into 5-15 cm long fragments. Rhizome fragments are then gathered using a potato or bulb digger. Rhizomes and their fragments are immediately gathered and planted to prevent them from drying out. Planting is performed using manual or semi-automatic potato planters.

As plants age, the aboveground biomass starts to develop faster after the third year in every aspect. The full miscanthus x giganteus plantation is achieved between the second and fifth years, depending on climate conditions. Maximum yield is usually achieved during the second year in southern EU countries, and during the fifth in the north.

Water content is important when considering storing of harvested plant. High percentage of moisture will cause the growth of mold and mildew and might lead to spontaneous combustion. The safe storing of miscanthus x giganteus is possible after drying the product up to 15% moisture in the field or a ventilated warehouse. When complete drying is not possible in the field, additional drying is needed immediately after harvesting (if moisture percentage is above 25%) or during storing (if it is below 25%), if there is a ventilation. Moisture percentage above 25% can lead to self-heating of stored material, with risks of spontaneous combustion if there is no ventilation, [5].

Upon developing and assessment of various parameters and references, procurement of rhizomes was undertaken. For this experiment 28000 rhizomes of Miscanthus x giganteus were purchased and planted on Prelići landfill. At the same time several other experimental sites were planted for a comparative analysis.

Out of these 28000, 26130 rhizomes were planted at Prelići. The remaining 1870 rhizomes were planted on experimental planting sites, for the purpose of research and promoting of biomass with different soil properties and different height elevation, a shown in Table 1.

Table 1. The list of miscanthus trial planting sites

No	Planting site	Area, 100 m^2	Number of rhizomes	Elevation, m	Planting orientation	Level of germination, %
1.	Zablaće	2	250	230	S	80
2.	G. Gorevnica	1	120	317	S-E	80-90
3.	Rošci 1	3	380	593	S-W	80
4.	Rošci 2	2	250	762	-	-
5.	Sime Sarage	1	120	242	W-E	90
6.	Slatina	2	250	263	W	60-70
7.	Trbušani	2	250	257	S-W	80

Prior to planting and due to large amounts of weeds, the landfill was treated with total herbicide, while other planting sites were not. Planting on all locations was performed manually.

Mechanical planting on the landfill was not possible, because of the existence of large quantities of waste, soil and humus covering the waste.

Communal waste is no longer deposited on that part of the landfill. It should also be mentioned that attempts were made to plant poplar in that part of the landfill, but were unsuccessful, since the all of the plants dried.

Locations used for the plantations have different properties; hence soil analysis was performed for these planting sites and compared to the soil found at the Prelići landfill.

The soil analysis of the landfill and other locations where miscanthus x giganteus was planted determined that there is no need for additional fertilization in order to increase the yield. Also, soil acidity was within the limits of tolerance for miscanthus x giganteus. For the purpose of soil research, cooperation was established with the “Institute for Fruit Growing”, Čačak.

Figure3. Miscanthus x giganteus, June, 2012, at Prelići landfill site

3. Experimental results

It is important to mention that the year 2012 was extremely dry, reducing referent yield values to 70-80%. Therefore, this year will be referenced as the zero years for the future analysis. Control of planting sites in November 2012 has proved that the rhizomes have not dried. Soil that was analyzed was collected from the depths up to 30 cm, weighing around 1,5 kg. Soil was analyzed in terms of acidity, and contents of calcium-carbonate ($CaCO_3$), humus, nitrogen (N), phosphorus-pento–xide (P_2O_5) and potassium oxide (K_2O).

The chemical analysis indicated that the soil value of the landfill is equivalent to the soil value of other planting sites, with some differences, but within the optimal limit.

Table 2 shows the trunk heights and diameters of plant, after two months of plantation.

Table 2. Analysis of height and trunk diameter parameters measured during 14-22.6.2012.

Location	Trunk height cm	Trunk diameter cm
Prelići landfill	12,11	0,52
G. Gorevnica	18,06	0,45
Trbušani	8,15	0,37
Rošci 1	7,62	0,37
Slatina	17,12	0,46
Zablaće	16,98	0,59
Sime Sarage	21,15	0,59

Measuring was performed on marked plants, which are used as samples. This table shows that no rhizomes adapted to the Rošci 2 location, which suggests that miscatnhus x giganteus should not be planted on elevations above 600 meters.

4. Economic evaluation

Based on the calculated lower average values of yields of 340 t/ha for the energy plant miscanthus, for the exploitation period of 20 years, it was concluded that 680 tons of miscanthus x giganteus produced on the area 2 ha could replace 250 tons of coal, 280,000 litres of oil or 280,000 m^3 of heating gas.

Predicted expansion of plantation would lead to significant savings in conventional energy sources.

The price of establishing Miscanthus x giganteus plantations for research purposes and transition into the second stage, “heating”, by processing into briquettes and pellets is 2,725 Eur/ha (all costs are included in this price). Expansion of plantations from the current 2 ha of planted rhizomes in the following years would be performed out of its own resources.

Internal rentability rate of the project is 20%, being higher than the interest rate on the market. Recovery period of funds is 7 years.

The economic component of the project, performed by using dynamic criteria, shows that the project is economically justified.

Based on Table 3, under the assumption that the total life of the plantations is 20 years, for a given initial investment for establishing plantations in the first year, we can see the expected annual return, the income of planted area, as well as revenue after expansion plantation from 2 to 4 ha.

The initial investment was 5,448 Euro. Net present value with a discount rate of 8% is 32,083 Euro, with a discount rate of 12%, 21,414 Euro. The internal rate of return of the project is 20%, so the program is effective because this rate is higher than the interest rates on the market.

Table 3. Income for 2 ha and 20 Years of Yield

Exploitation Year	Investment for 2 ha per Year (Eur)	Yields t/ha	Income for 2 ha (Eur)
1.	5,448	0	0
2.	512	3-5	780-1,300
3.	512	5-10	1,300-2,600
4.	512	10-20	2,600-5,200
5.	512	10-20	2,600-5,200
6-15	512	23	5,980
16	512	20	5,200
17.	512	20	5,200
18.	512	20	5,200
19.	512	10-20	2,600-5,200
20.	512	10-20	2,600-5,200
Total	15,176		87,880-100,100

4. Conclusions

Based on everything that was presented in this paper, the hypothesis about establishing energy plantation production on a landfill, as well as other locations, can be confirmed.

Research determined that there are certain issues with forming of energy plantations. Heavy dependence on water has been observed, since landfill soil is made of various building, animal, communal and industrial waste, making it very porous. Therefore, assessment of yield must be approached very carefully and it is not possible to make accurate conclusions during the first year.

5. References

[1] Clifton-Brown J Jones MB, 1997, The thermal response of leaf extension rate in genotypes of C4-grass Miscanthus: an important factor in determining the potential productivity of different genotypes. *Journal of Experimental Botany*, Vol. 48, No. 313: 1573-1581

[2] Jørgensen U (1995): Genotypic variation in dry matter accumulation and content of N, K and Cl in *Miscanthus* in Denmark. *Biomass and Bioenergy*, Vol. 12, No. 3: 155-169.

[3] Lewandowski I (1998): Propagation method as an important factor in the growth and development of *Miscanthus x giganteus. Industrial Crops and Products*, Vol. 8, No. 3: 229-245.

[4] Jørgensen U (1997): Macro propagation of Miscanthus. In: Fachagentur Nachwachsende Rohstoffe e.v., editor. Symposium Miscanthus. *Schriftenreihe "Nachwachsende Rohsstoffe"*, Vol. 6: 27-30

[5] El Bassam, N., Huismann, W., 2001, Harvesting and Storage of Miscanthus. In: *Miscanthus for energy and fibre* (Eds MB Jones and M Walsh), James & James, London, pp. 86-108,

.

INFLUENCE OF WELDING PARAMETERS ON IMPACT TOUGHNESS OF FRICTION STIR WELDED Al-ALLOY

Abdsalam Eramah[2],Andrijana Djurdjevic[1], Srdjan Tadic[1], Aleksandar Sedmak[2], Srdja Perkovic[3]

[1] Innovation center of the Faculty of Mechanical Engineering, KraljiceMarije 16, Belgrade, Serbia
[2] University of Belgrade, Faculty of Mechanical Engineering, KraljiceMarije 16, 11000 Belgrade, Serbia
[3] Military Technical Institute, Ratka Resanovića 1, 11030 Belgrade, Serbia
Corresponding author-mail: asedmak@mas.bg.ac.rs

Abstract

Friction Stir Welding is a nonconventional, frictional welding process dominantly applied on plate-shaped parts. Activation energy-heat, necessary for the weld creation, is generated on the frictional contact between the specialized welding tool and base material. The amount of the generated heat depends from numerous parameters (technological, tribological), dominant being angular rotation of the welding tool, welding speed and geometry of welding tool. Beside special geometry of the welding tool, Friction Stir Welding has numerous advantages over other welding procedures: energetically is very efficient, it is eco-friendly process, welds are of great quality etc. Intensive researches and industrial application in aero, space, naval and railway systems made Friction Stir Welding competitive with other welding techniques. This paper is giving analysis of parameters that influence impact toughness of the Friction Stir Welding process. Experimental confirmation of the analysis has been presented on welding of aluminium-magnesium alloy 5803.

1.Introduction

Friction Stir Welding (FSW) is a solid state joining process that uses (combined) influence of the heat and the mechanical work for the weld creation [1].

From its invention in December 1991 until present days, FSW is successfully developing and finding application in various technological branches [2]-[4]. This is predominantly influenced by numerous advantages of the FSW over other welding procedures: absence of the melting phase during FSW leads to no hot-cracks and no porosity and, furthermore, minimal distortion of the weld (geometrical stability) is achieved.

In FSW, key parameters for the successful welding and quality gaining are the heat and stirring/mixing the by heat softened material of base metal. Heat is generated at the intimate tribological contact between the welding tool and base metal [1] used for the preheating of the base metal and lost over air and contact between base metal and backing plate.

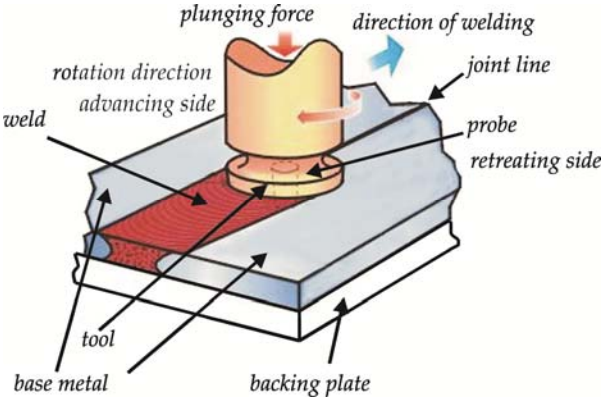

Figure 1. Scheme of the FSW

The contact between welding tool and base metal is highly frictional and the most of the generated heat is frictional. However, the amount of the heat generated by the deformation should not be neglected [1]. The input (generated) heat depends on technological parameters (welding rate, rotation of the welding tool – rotation rate, geometry of the welding tool, duration of the welding process etc.), tribology parameters (friction coefficient, contact pressure) and thermo-mechanical properties of the welding tool and the base metal (thermal conductivity, hardness, yield strength etc.). Parameters of FSW that can be directly affected by user with the goal of efficiency increase are just technological parameters; proper selection of these parameters results in productivity, quality and the efficiency increase of the FSW.

Welding rate is transversal velocity of the welding tool and it depends on mechanical properties and height of the base metal. Welding rate is directly affecting the material deposition – stirring/mixing. For example, if height of the base metal increases, welding rate must decrease [6].

Experimental investigations have shown that imperfections-less FSW products are developed if ratio of the rotation rate ωand the welding rate v(also known as welding stepω /v) has some specific values [7]-[8].

2. Experiment

Chemical composition of the investigated alloy is given in Table 1. It is a non-heat treatable, 5xxx family alloy member designed for automotive panels and marine vessel constructions. Material has been supplied in the form of hot-rolled and fully annealed plate with d=6mm thickness. It was cut and machined into the strips 260x45mm. Two strips made a single pair for FSW butt-joints. Before each welding experiment, every pair of strips was firmly clamped on the stainless steel backing plate.

All welding experiments were performed on a FSW-adapted laboratory milling cutter equipped with accurate displacement control, i.e., the depth of penetration, rotational and traverse speed were kept constant during welding cycle. The welding parameters are listed in Table 2. In total, 4^3 welding parameters were examined. The tool, made by tool steel H13, had a ∅25mm shoulder and left threaded cone probe of 5,5 mm height.

In order to evaluate impact toughness of the friction stir weldments, Charpy impact test specimens were machined. Dimension of specimens were 10x5x55 mm^3 with 45^o v-notch of 2 mm depth and 0.25 mm root raius. Notches were machined at the bottom side of welded plates, precisely along the welding line of weldements.

Charpy impact tests were carried out at room temperature using insrumented impact pendulum. The pendulum was equipped with load cells positioned on a striker edge. Measuring device was connected to high-speed data acquisition with response time in terms of mili-seconds. This instrumented system enabled to collect instantaneous load and strain gauge data from pendulum during the "fracture opening time". Typical impact fracture time had lasted 2.6 x 10^{-3} seconds and, within this period, 2600 measuring points, load – time – deflection, were recorded into the accompanied digital oscilloscope. These digital signals were transfered into a personal computer for post-processing analysis of the fracture behaviour.

TABLE 1. CHEMICAL COMPOSITION OF THE 5803 ALLOY

Alloy	Chemical compositopn, mass %							
	Mg	Mn	Fe	Cu	Si	Zr	Cr	Al
5083	6.8	0,51	0,20	0,04	0,09	0,11	0,032	Bal.

TABLE 2. APPLIED FSW PARAMETERS

Rotational speed, (rpm)	500	600	700	800
Traverse speed, (mm/min)	75	100	125	150
Tilt angle,(^{o})	1	2	3	4

To understand the fracture behaviour, surfaces of fractured specimens were examined under JEOL JSM-3860 scanning electron microscope (SEM) and Nikon optical magnifier.

3. Results

Charpy impact load vs. deflection data are shown in Figures 1 and 2. Each figure shows two curves obtained by impact testings of identicaly welded specimens. Erratic appereanceof sharp peaks on curves are the result of high sensitivity voltage measurement, and should not be connected with any phisical phenomena. Simple areal integration of the curves and dividing it by cross sectional area of the specimen provides the impact toughness values (J/cm^2) of the tested specimens. Impact toughness values, inserted in Figures 1 and 2, show almost identical values although the rotational speeds were ω=500 and 700 rpm, respectively. Similar behaviour was found for other specimens that might led to misleading conception about fracture toughness of the investigated alloy.

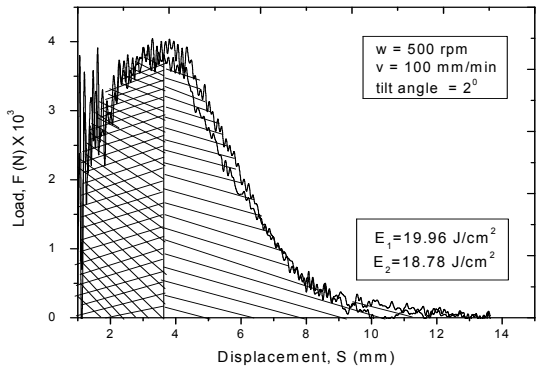

Fig.1. Load-deflection curves, ω=500 rpm

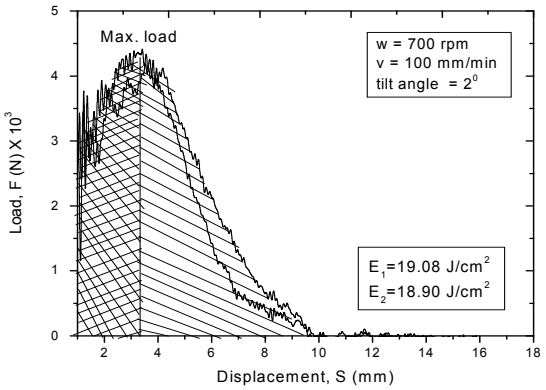

Fig.2. Load-deflection curves, ω=700 rpm

Force-deflection curves, derived from impact tests can be split into an up-to-peak load (cross-hatched area on Figs.1 and 2) which is, typically, associated with energy to initiate crack. After the peak load, dropping off in force relates to crack propagation with accompanying energy dissipation in this phase. Relative ratio of this two phases indicates the ability of material to sustain plastic deformation during fracture process. Detailed, but still preliminary analysis in this work have revealed that rotational and traverse speed mainly influence the energy of crack propagation phase. But, the crack initiation phase remains almost intact unaffected.

Total fracture energy (which is the area under the entire force-deflection curve) dependency on rotational and transverse speed is presented on Figures 3 and 4, respectively. Diagrams are presented in a confidence band form, due to certain scattering of results. However, statistical analysisrevealed “FSW processing window”, at least if the maximal impact energy is of concern.

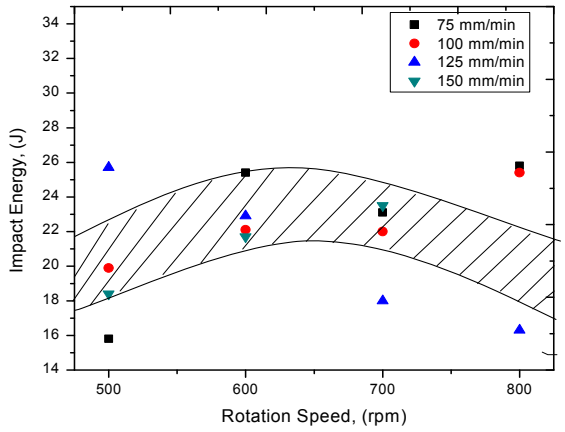

Fig.3. Influence of rotational speed on fracture energy

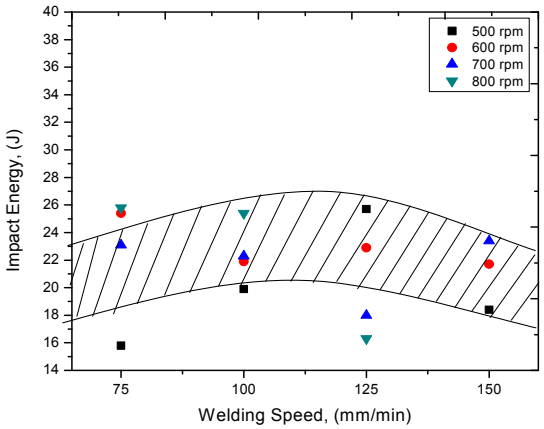

Fig.4. Influence of welding speed on fracture energy

Optical image of the representative fracture surface is shown in Figure 5. Although it seems to be typical for this kind of investigations, several features deserves to be emphasized: (i) the crack initiation (arrowed) at the bottom of the notch, (ii) area deformed by hammer impact, on the opposite side of notch, with noticeable lateral expansion, (iii) shear lips indicative of ductile tearing in final phase of fracture, and (iv) between them, crack propagation zone. All the examined specimens, regardless of the welding conditions, dispose the same features, with only distinction in relative area ratio among the specified zones.

SEM fractographies of the same broken specimen are presented in low (Fig. 6) and high (Figs. 7, 8) magnifications. Roughened, dimpled topography indicates ductile fracture behaviour. The presence of tear ridges (Fig.7) indicates ductile behaviour due to ability to sustain the impact load after microvoid coalescence had begun. However, within the stiring zone, Fig.8, internal defects can appear as a consequence of insufficient stirring around the pin. It is not yet quite clear how does it affects fracture behaviour.

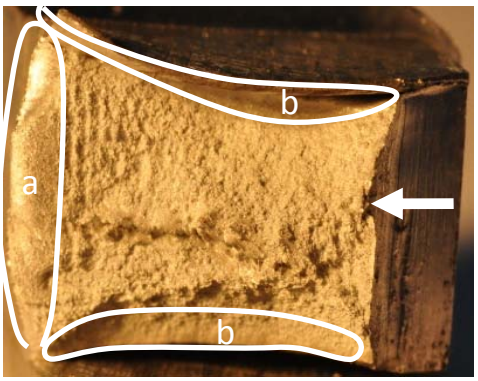

Fig.5. Optical fractography of the specimen

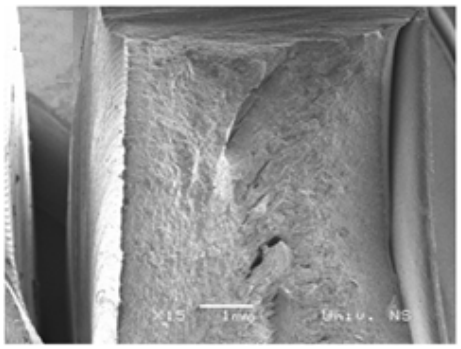

Fig.6. SEM fracture surface morphology

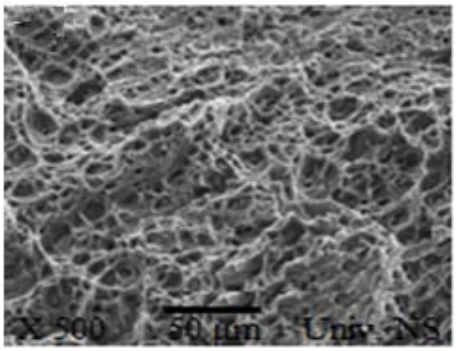

Fig.7. Dimples and tear ridges in the stir zone, SEM

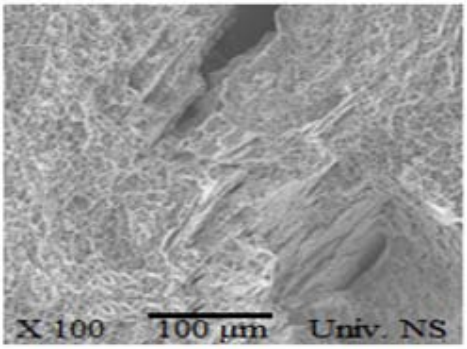

Fig.8. Defects due to insufficient stirring, SEM

4. Discussion

This paper disposes preliminary results of the extensive investigation in the FSW of aluminium alloys. Presented results revealed two phenomena that deserves to be clarified. First, the influence of welding variables on crack opening phase in Charpy impact tests while the crack initiation phase remains unaffected. It is not quite clear, at the moment, is it consequence from some intrinsic fracture behaviour. However, it might be speculated in terms of more trivial circumstances, i.e., the position of the notch on the impact test specimens. In particular, notches were machined on the bottom side of the specimens, at the position beneath the pin of the welding tool. This position seems to be the least affected by stirring process. This speculation is supported by the fact that internal defects, in all examined specimens, were concentrated in the mid of stirring zone.

It has been considered that the friction heat flow is a very important factor for FSW because the microstructure in the stir zone is strongly influenced by the friction heat flow. There are two main mechanisms for friction heat flow during FSW. One is the friction heat flow from the shoulder, and the other is that from the pin. However, it has been reported that the friction heat flow from the pin is considerably small in comparison with that from the shoulder [9]. The friction heat flow from the shoulder during FSW, Q, can be evaluated by [10]:

$$Q = \frac{4}{3}\pi^2 \mu P \omega D_{sh}^3 \qquad (1)$$

where μ is the friction coefficient, ω is the rotational speed, P is the applied pressure, and D is the shoulder diameter. However,the FSW tool moves during FSW by traverse speed v. Thus, the friction heat flow during FSW is evaluated by Q/v. In addition, it can be quantified that

$$\frac{Q}{v} \propto \frac{\omega D_{sh}^3}{v} \qquad (2)$$

since the applied pressure and friction are not technicallymanageable variables, [11].

The heat input (generated by the friction between tool shoulder and welded metal) increases with increase in tool rotational speed and decreases with welding speed. Low heat input causes irregular metal flow and improper stirring around the tool pin due to insufficient plasticization of the material. On the other side, high heat input causes the turbulent metal flow around the tool pin due to over-plasticization of welded material under the tool shoulder. Both these welding conditions produced defective welds with detrimental internal defects. Only the delicate balance of variables in Equation 2 reveal optimal processing window in FSW.

5. Conclusions

The influence of FSW parameters on the impact fracture toughness was examined in this study. Rotational and traverse speeds were examined in terms of load-deflection curves obtained by instrumented impact tests. It was found that absorbed fracture energy depends on these variables. Fractography analysis has been found to be consistent with these results.

6. Acknowledgment

Financial support by Serbian Ministry for Science and Technology is gratefully acknowledged. One of the authors, A.Eramah, is thankfull to Libian Government for his PhD grant. SEM facility is to prof. Dr K.Gerić.

7. References

[1] Mijajlović, M, Milčić, D, Stamenković, D, Živković, A: Mathematical Model for Generated Heat Estimation During Plunging Phase of FSW Process, Transactions of Famena, Faculty of Mechanical Engineering and Naval Architecture, Zagreb, Croatia, XXXV-1/2011, April 2011, pp 39 - 54, ISSN 1333-1124, UDC 621.791.1.

[2] Thomas W. M. et al 1991 Friction stir butt welding International Patent Application No PCT/GB92/02203; THOMAS W. M. et al 1995 Friction stir butt welding GB Patent Application No 9125978.8; THOMAS W. M. et al 1995 Friction stir butt welding UP Patent No 5 460 317.

[3] O. T. Midling, J. S. Kvale: Industrialisation of the FSW Technology in Panels Production for the Maritime Sector in Proceedings of the First International Symposium on Friction Stir Welding, Thousand Oaks, CA, June 1999.

[4] Friction Stir Welding – Applications,http://www.twi.co.uk/ j32k/ getFile/fswapp.html

[5] Y. Sato, M. Urata, H. Kokawa: Parameters controlling microstructure and hardness during friction-stir welding of precipitation-hardenable aluminum alloy 6063. Metallurgical & Materials Transactions A, 33(3):625–635, 2002.

[6] Dong P, Lu F, Hong JK, Cao: Analysis of Weld Formation Process in Friction Stir Welding, 1st International Symposium on Friction Stir Welding @ Thousand Oaks, Cal June 1999.

[7] T. Shinoda: Effect of Tool Angle on Metal Flow Phenomenon in Friction Stir Welds, 3rd International Symposium on Fricion Stir Welding, Kobe Exhibition Centre, Port Island, Kobe, Japan, 27-28 September 2001.

[8] Živkovic, A: Influence of friction stir welding tool geometry on properties of welded joint of

alloys Al 2024, PhD thesis, University of Belgrade, Faculty of Mechanical Engineering, 2011.
Z.Y. Ma, R.S. Mishra, M.W. Mahoney, and R. Grimes: Mater. Sci. Eng., A, 2003, vol. 351, pp. 148–53.
[9] P. Periyasamy, B. Mohan, and V. Balasubramanian, J.of Mat. Eng and Perf., 21(11) 2012. pp.2417-2428.
[10] A.Eramah, PhD Thesis submitted at the Faculty of Mechanical Engineering, University of Belgrade, 2013..

RISK MANAGEMENT OF A WORKPLACE IN THE OPEN PIT MINE

Snežana Kirin[1], Igor MIljanovic[2], Aleksandar Sedmak[3]

[1] Innovation Center of Faculty of Mechanical Engineering, University of Belgrade, Serbia
[2] Faculty of Mining and Geology, University of Belgrade, Serbia
[3] Faculty of Mechanical Engineering, University of Belgrade, Serbia
** Corresponding author e-mail: snezanakirin@yahoo.com*

Abstract

The new standard highlights a set of principles that organizations must follow to achieve effective risk management. Risk management of a work-place in mining industry has been analysed and main risks have been identified.

Keywords:

Risk management, mining industry, hazards

1. Introduction

Risk is now defined in terms of the effect of uncertainties on objectives. The new standard highlights a set of principles that organizations must follow to achieve effective risk management. For risk management to be effective, organizations at all levels need to ensure that their risk management program:

- Creates and protects value;
- Is an integral part of all of the organization's processes;
- Forms part of decision making;
- Explicitly expresses uncertainty;
- Is systematic, structured and timely;
- Is based on the best available information;
- Is tailored to the organization fit;
- Takes human and cultural factors into account;
- Is transparent and inclusive;
- Is dynamic, iterative and responsive to change;
- Facilitates continual improvement of the organization.

The core of new approach is the consideration of risk management as the key activity, associated with all decisions, the goal being to prevent consequences and exploit opportunities at all levels, from strategic and project management, to support basic processes.

2. Risk management in mining industry

Mining is an industry with great importance from an economic point of view, and from the aspect of protecting and preserving the environment and regional development. At the European level, mining and related industries generate about 10% of raw materials for other industries. Mine industry of Europe has a total annual production of about 3 billion tons of material, which put emphasis on the quantity of material produced. The process of quality improvement can be seen as a series of steps necessary to achieve quality improvement in an organization.

In the countries of Central, Eastern and Southern Europe, the mining industry has significant effect on society at large, because in these countries in the mining industry work a total of about 900,000 employees. Although the mining industry in Europe is steadily declining, it remains an important economic factor. Compared with other regions of the world, mining European countries lose their significance, partly due to the geological characteristics of the remaining mineral deposits, and because of smaller producers of minerals that are specific for the European market, they lose competitiveness at the global level, but partly because of the extensive and strict regulations.

The mining industry is a heterogeneous structure in both the environmental and technical sense and in terms of international connectivity. However, having all this in mind, all segments of the mining industry expect similar challenges in the future, as a result of the internationalization of markets and increased expectations from the standpoint of environmental and economic standards.

Technological advancement and progress in the field of management systems can greatly affect the capacity of professionals when in terms of development and implementation of standards for the safe and efficient management of the system and operation of mining equipment and machinery. According to the systemic concept, the ideal working environment would have the right equipment, competent staff, functional and control systems in fully familiar environment. In real systems, threat to the smooth functioning of the mining unit, connected to the basic characteristics of mining with incomplete or insufficient precision of a determination parametric data or uncertainty about future activities and events, as a result of the impact of complex and stochastic nature of geological, technical, technological, market, economic, political, environmental and other factors.

3. Surface coal mine

Risk analysis of this economic-business system is of particular importance considering the need for

continuous and reliable electricity supply of economy and population (defined voltage, frequency and other characteristics and thermal energy (appropriate characteristics), as well as in terms of the rational and efficient use of natural resources.

Excavated coal is used for combustion in power plants. For continuous operation of power plants that are supplied with coal from this deposit, the annual need is about 6 millions of tons of coal, and an additional 500,000 t/year of bulk lime of coal for household consumption.

Limitation for this capacity of surface mine is derived based on the following criteria:

- Supply of thermal coal in the amount of 6 x 10^6 tons per year,
- The supply of consumer carbon amount of 0.5 x 10^6 tons per year,
- Geological reserves and coal quality,
- Full exploitation of geological reserves in the deposit,
- Geological boundaries bearings, and
- Achieving optimal length of working the mine floor and the dump.

In addition to these basic criteria for the restrictions of the open pit, one should pay attention to influence of the position of existing infrastructure: power plants, protected natural areas, rivers and settlements.

4. Risk management of a worplace in surface coal mine

Effective and integrated risk management sits at the heart of true business sustainability. More and more papers are related to the synergistic effect of integrating risk and quality management while improving the performance of both systems.

Risk assessment (professional) in the workplace is seen as a process which, taking into account all aspects of work and working conditions, determines the risk of injuries or damage to the health of the employee. The law defines the other definitions necessary to implement the assessment of occupational risks.

Workplaces with high risk is the position determined by the act of the risk assessment on which, in addition to a fully or partially implemented measures, in accordance with this law, there are circumstances that may endanger the safety and / or health of the employee.

Based on the identified hazards and risks in the workplace and work environment, and the estimated risk of possible injury, occupational disease or illness in connection with the work shall be taken to eliminate risks to ensure safe and healthy working employees.

In the coal open pit mines in Serbia, there is a risk analysis of individual jobs and registration of incidents. Risk analysis is done qualitatively and partly quantitatively assigning risk values from 1 to 100. Qualitative and quantitative risk analysis classifies risks into five categories:

- 0-20 low risk
- 21-40 permissible risk
- 41-60 moderate risk
- 61-80 increased risk
- 81-10 high risk

Qualitative-quantitative risk analysis is performed according to the model shown in Figure 1.

According to the regulations on the previous and periodical medical examinations of employees in workplaces with high risk ("Off. Gazette of RS" br.120/07) an employee is sent to the control of periodic medical examinations for 12 months.

5. Hazard identification – diagram of sources

In our mining companies risk is mainly accessed by organizational unitspartially.The risk to the safety and human health where the main risks are identified: coal dust, noise, working the night shift, inexperience in manipulation with machinery and equipment. It should also be noted that working in extreme temperature conditions can affect the safety and health of people. If health effects arise from exposure to coarse particles, such as from mining activities, the following symptoms are likely to be: cough, wheeze, or worsening of asthma, increased need for medications (egg: puffers, antibiotics), increased breathlessness. Some recent research suggests that heart problems, such as angina and heart attacks may also be associated with coarse particle pollution. The main sources of increased risk (p>60) were identified and presented in Figure 2.

Mechanical hazards are identified as: lack of security due to rotating or moving parts; freely moving parts or materials, internal transport and movement working machines or vehicles and moving equipment for the work; dangerous instruments of labor, which can produce an explosion or fire; inability or limitations the timely removing from the place of work; exposure detention, mechanical shock, and the coincidence of other factors that may occur as a mechanical source of danger.

Identified hazards related to the characteristics of the job are working at height or depth; dangerous surfaces (floors, surfaces, contact surfaces) that have sharp edges, spikes, rough surface, protruding parts, work in confined, limited or dangerous area; physical instability of the workplace, problems due to the compulsory use of the means and equipment for the personal protection at work; the efforts or physical strains; non-physiological position of the body; the psychological workload; responsibility, appropriate knowledge and skills; responsibility for the rapid changes in work procedures; intensity of work; conflicts; lack of motivation to work; inadequate or unsuitable methods of operation, and other hazards that may arise in relation to the characteristics of workplace and working methods.

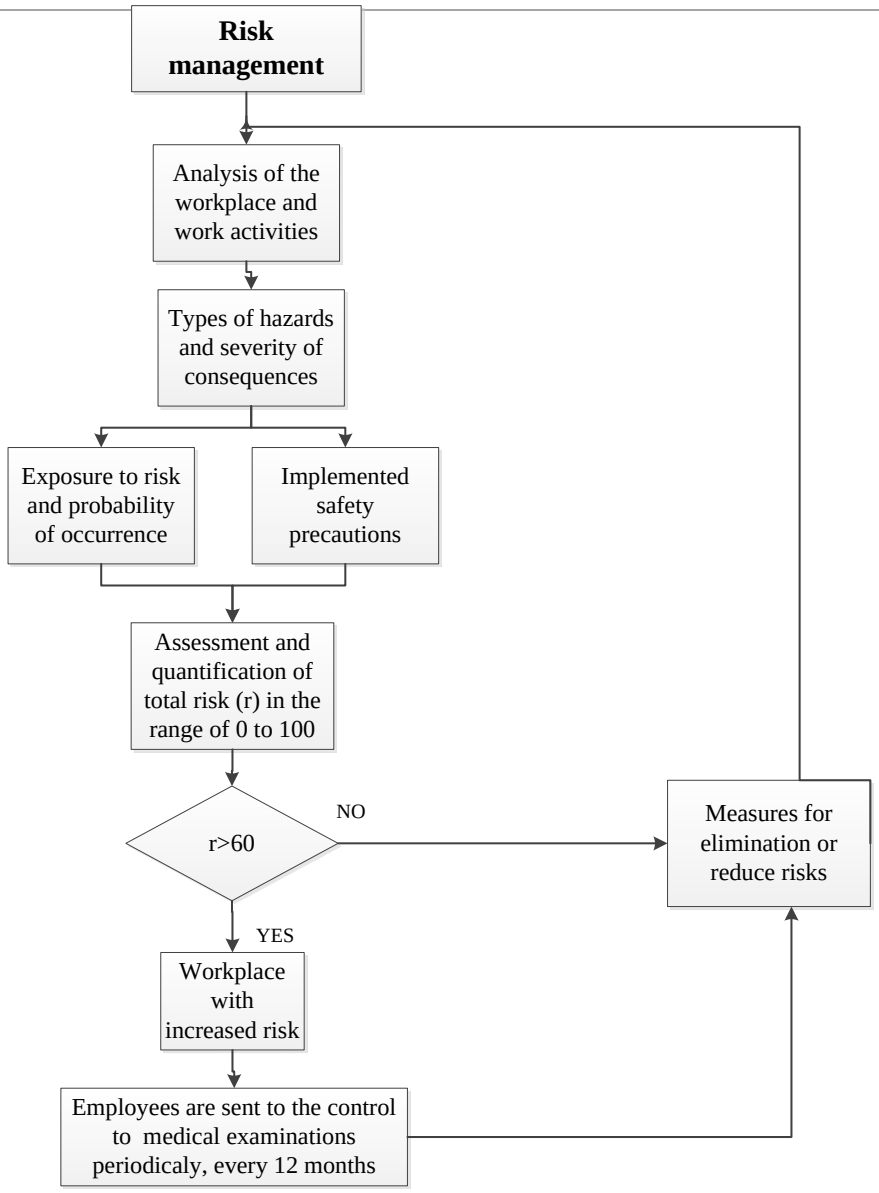

Figure 1 Risk management in the worplace

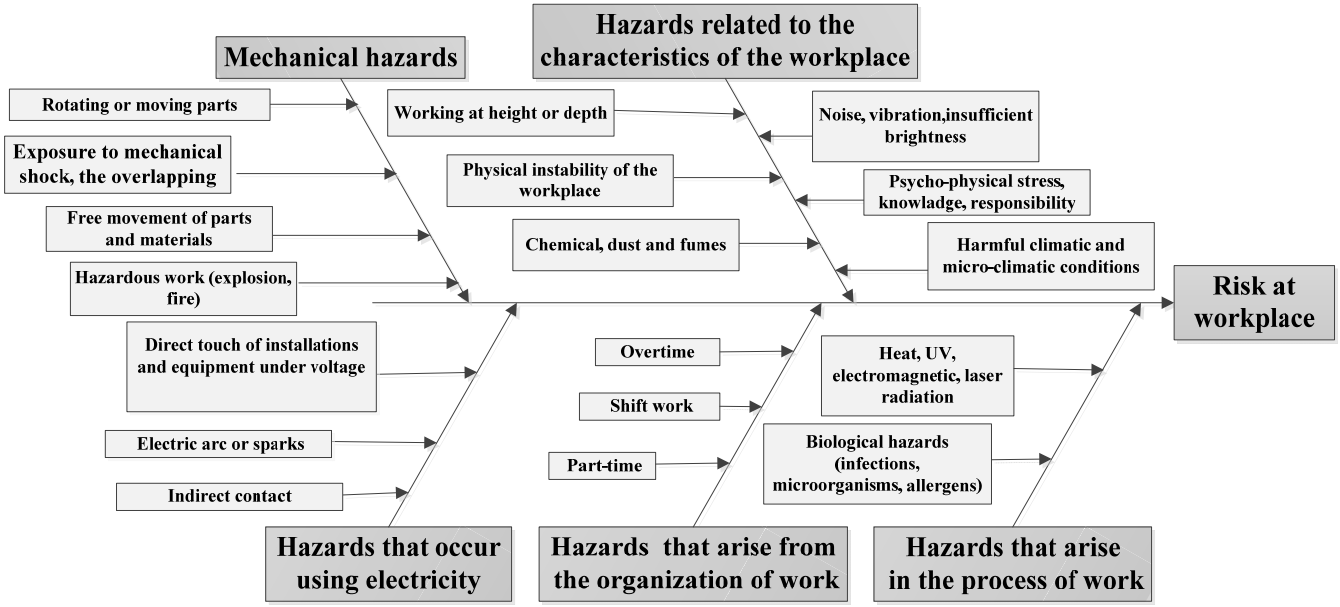

Figure 2. The sources of the increased risk in the workplace in the open pit mine

Hazards that occur using electricity are the direct contact of installation and equipment under voltage; against indirect contact; against thermal effects that develop electrical equipment and installations (overheating, fire, explosion, electric arc or sparks) from lightning and effects of atmospheric discharge, from electrostatic charges and other hazards that can occur in connection with the use of electricity.

Hazards related to the organization of work as overtime, shift work extensive and long work with a physical or mental stress

Hazards that arise or occur in the process of work are biological hazards (infections, microorganisms, allergens), the harmful effects of non-ionizing radiation (thermal radiation), UV radiation, electromagnetic radiation, laser radiation and other hazards that occur in the work process, and that may be the cause of injuries, occupational disease, or diseases related to work

4. Conclusions

From Figure 2 it can be seen that the main identified hazards in the workplacein the open pit mine are: physical (vibration), biological hazards, infections, exposure to allergens and microorganisms, the possibility of slipping or stumbling (wet or slippery surfaces), work at height or depth,non-physiological body positionduring work, the Noise, physical instability of the workplace, the effort or physical strains, work in a confined space and hazardous - opportunity slip or stumbling (wet or slippery surfaces), direct contact with the installation and equipment under electrical voltage, the psychological burden (monotony or stress), hazardous climatic conditions, microclimate, chemical hazard, dust and fumes, unsuitable - insufficient brightness, Inadequate or unsuitable methods of operation and Hazards caused by other persons.

From the foregoing, it can be concluded that the operation of the open pit mines, despite the improved technology, is still the work in the presence of high risk for the health and safety of people and that there is a constant need to reduce the level of risk.

It is especially important to monitor the work process, especially in the introduction and promotion of new technologies that bring new risks to be identified and managed.

5. References

[1] Snežana Kirin, Milena Josipović Pejović, Aleksandar Petrovski: Integralni pristup upravljanju rizicima u rudarstvu; 39. Simpozijum o operacionim istraživanjima, SYM-OP-IS 2012, Tara

[2] Snežana Kirin, Aleksandar Sedmak, Tamara Sedmak, Modern mining industry management – synergy of Quality and risk based approach, BALKANMINE 2013 Vth JUBILEE BALKAN MINING CONGRESS 2013 – Ohrid, Macedonia

[3] Slobodan Vujić, Snežana Kirin, Igor Miljanović, Milena Josipović Pejović: Upravljanje rizicima u rudarstvu-površinska eksploatacija uglja, 39. Simpozijum o operacionim istraživanjima, SYM-OP-IS 2012, Tara, 2012, septembar 2012;

[4] Maria Popescu, Adina Dascalu, Considerations on Integrating Risk and Quality Management, Annals of “Dunarea de Jos” University of Galati Fascicle I. Economics and Applied Informatics, Years XVII – no1/2011, ISSN 1584-040,

.

INNOVATIVE STRATEGIES FOR DISTRIBUTION PROCESS ON FMCG AND A CASE STUDY

Ö. Vayvay[1*], Z. T. Şimşit[1], A. Tarım[1], E. G. Veran[1], G. Demirözen[1], Ş. Uzun[1]

[1]Department of Industrial Engineering, Faculty of Engineering, Marmara University, Istanbul, Turkey
** Corresponding author e-mail: ozalp@marmara.edu.tr*

Abstract
In today's changing world, the only thing that doesn't change is "change" itself [1]. In this fast moving business world conditions, companies should create innovative strategies to survive among its rivals. This project is about increasing efficiency in the processes of a FMCG company and was implemented in company' traditional channel of Sales Operations. By channel-based analysis, measuring problem for some indicators is realized in Traditional Channel. In order to solve measuring problem, new sales channel was created by considering revenue and the number of sales points. Sales representatives were assigned to this channel and training program for sales representatives was improved. In addition, sales incentive program was enhanced for sales representatives and customers to motivate for reaching sales target.

Keywords:
Innovation, sales operations, traditional sales channel,

1. Introduction

"Increases in global competition, customer requirements, and environmental and governmental regulations suggest that many firms for future success and economic survival require dramatic changes. Firms across a wide range of industries have reengineered major business processes.in the pursuit of continuous improvement."[2]
In today's ever-changing world, the only thing that doesn't change is 'change' itself [1]. In a world increasingly driven by the three Cs (Customer, Competition and Change), companies are on the lookout for new solutions for their business problems. [3].
Nowadays, some of the more successful business corporations are using Business Process Reengineering (BPR). "Reengineering is the fundamental rethinking and radical redesign of business processes to achieve dramatic improvements in critical, contemporary measures of performance such as cost, quality, and service and speed [3]."
Business Process Reengineering is a discipline which was first appeared at the beginning of 1990's. In 1990, Michael Hammer, a former professor of computer science at the Massachusetts Institute of Technology (MIT), published an article in the Harvard Business Review, in which he claimed that the major challenge for managers is to obliterate non-value adding work, rather than using technology for automating it [4]. Reengineering is the term fundamental rethinking of the processes and to reform the spoiled system with the new well-engineered system.
Hammer's claim was that most of the work being done does not add any value for customers. For that reason these works or studies should be removed, not accelerated through automation. Instead, companies should reconsider their processes in order to maximize customer value, while minimizing the consumption of resources required for delivering their product or service. Following the publication of the fundamental concepts of BPR by Hammer (1990) [4], Davenport and Short (1990) [5], published a detailed article about BPR. Many organizations have reported dramatic benefits gained from the successful implementation of BPR [6]. In today's business world, BPR is one of the useful tools that companies used to achieve dramatic improvements. For that reason in both real life and academic researches, there are several studies and discussions about BPR and its implementation for a long period of time.
At BPR, there are 5 major phases. The first phase is preparing for BRP. You need to build a across functional team and then to identify customer driven objectives. At the final level of phase one, developing a strategic goal is crucial. The second phase is Map and Analyze as-is Process. Creating activity models is the first level of this phase. Then you should create process models. Later, you should simulate and perform these models. After that, identifying disconnects and value adding process is the last left level about this phase. Other phase is about the designing the process. The first step is very important part of this phase, benchmarking. The remaining headings about of this part are design and validate to be process and perform trade-off analysis.
On the other hand, despite the significant growth of BPR, not all organizations can achieve remarkable results with using BPR. Having BPR repeatedly at the top of the list of management issues in annual surveys of critical information systems reflects executives' failure to either implement properly or acquire the benefits of BPR [7]. To implement reengineered processes is the one of step of BPR. This phase starts from involving implementation

plan. Then you should simulate and implement the transition plans. As a result, the implementation process is complex, and needs to be checked against several success/failure factors to ensure successful implementation, as well as to avoid implementation pitfalls [6]. Hammer and Champy (1993) [3] estimate that as many as 70 percent do not achieve the dramatic results they seek. This mixture of results makes the issue of BPR implementation very important.

BPR has great potential for increasing productivity through reduced process time and cost, improved quality, and greater customer satisfaction, but it often requires a fundamental organizational change [6]. Today's fast moving business world day by day, tehre are incredibly new developments in technology. Demand and markets are becoming much more dynamic than before. With BPR, organizations are able to analyze the fundamental business processes and systems, restructure them periodically such that they can be flexible to future redesigns [8]. However, in such a situation of survival, mostly organizations ignore to work properly on the elements of BPR and results in failure [9]. BPR is ideal for every firm in both public and private sectors and is equally applicable in service and production firms. But these system requires time and proper planning before introducing and implementing otherwise there are great chances of failure [9].

2. Methodology

The XXX Company is a multinational consumer goods company and one of the world's largest producer of household cleaning products and a major producer of consumer healthcare and personal products.

The company runs a number of graduate programmers, in most of its markets. Once hired, graduates tend to work for a couple of years as a trainee in the country in which they were originally employed, followed by a posting overseas for those who have excelled during initial training. Graduate trainees start off in one of the firm's business areas: Marketing & Sales; Supply Chain; Research & Development and Information Systems.

In this study first step is the examination of existing situation of XXX Company at traditional channel. In the current state analysis part, several analyses used to understand the existing conditions both market and company. Firstly, Channel based distribution spends and revenues were analyzed in two categories, business share percentages by net values and trade investment percentages. Then, scatter plot was prepared which is presented in figure 1. Main sales channels were compared with their gross sales and net revenue and their percentages.

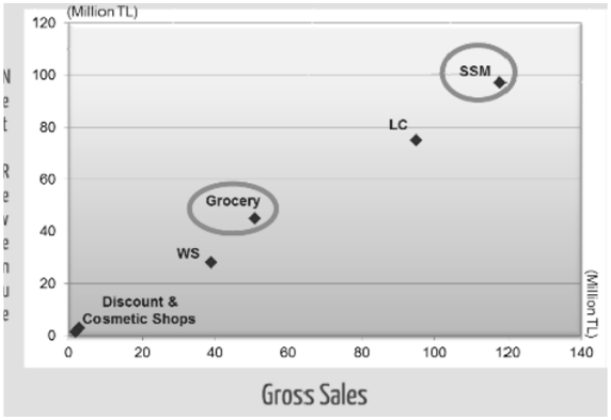

Figure 1.Channel based distributions

According to scatter plot with gross sales and net revenues parameters, selected super market (SSM) and local chain (LC) should be chosen. However LC has been already optimized very well, so this channel was ignored. Grocery is the most profitable channel after LC. For that reason, Grocery channel was chosen instead of LC. The main reason that SSM is not the only chosen channel is because of excessive sales points on Grocery channel.

Second step was distributer visits. XXX Company has 15 distributors all over Turkey. These distributors stores and distributes company' products by their own sales representatives. As the part of this project, distributors in Adana, Mersin, Maraş and İstanbul were visited to gain information about field sales operations. From the meeting reports, most sales representatives (SR) of distributors know their region very well and they are close with grocery owners. When we look at their sales targets, it is obvious that they are about to reach their sales target amounts. In addition, since they don't sell only XXX Company' products they are not fully loyal to the XXX Company.

As third task, SWOT analysis is used to identify strengths and weaknesses [10] and to understand the competition in FMCG. In figure 2, SWOT analysis is represented. According to analysis, it is shown that Turkey has some problems about SR"s, budgeting and analysis in sales points. However, as FMCG is close to innovative strategies and consumers shopping behavior is still traditional type (preferring traditional accounts), creating innovative strategy by choosing the problems in sales channels will be the solution.

At this phase of this project, we analyzed top100 customers for every distribution region. There are 15 distributions within 21 distribution regions at XXX Company Turkey. At the end of this study, we have seen that gross sales of top 100 customers from distribution region, 2100 customers, is 93% of the gross sales of distribution channel. As a result of this analysis we saw that we should focus on these 2100 customers more closely. Since, it is

clear that these samples of customers form the most valuable customers for distributor operation.
In addition to these analyses, SR groups are examined and the structure of company investigated. According to current state, company has two sales representative groups, SR and mixed distribution SR. SR group reports directly to the distribution manager and mixed distribution SR Group reports to Company Area Manager.

Figure 2.SWOT Analysis

3. Results

After current state analyses, main problems are obtained and some innovative solutions created. The main point of the sales operations problems is about SR. In current condition, SR structure is not good enough fır the XXX Company. So, new structure for sales operations is proposed which is presented in figure 3.

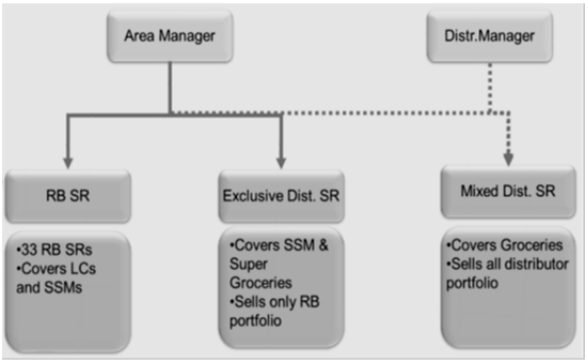

Figure 3.New structure of the XXX Company' sales tree

The new system that we improved there will be new SR group who will be reporting to Area Manager. In addition, at this strategy the key point is that The Exclusive SR Group is going to sell only XXX Company Portfolio.
By adopting this strategy, we consider to change the Go to Market Strategy of company. In previous structure, SR's were selling not only products of XXX Company but also they were selling products of competitors. Moreover, we aim to be a more employee involved and employee empowered company.
So as a first step of solution, all over Turkey, it has been asked to area managers "How many exclusive SR do you need?" After needed work force was obtained a training program developed. Therefore, our project team and Company' HR Department prepared a training program. In addition, the results of distributor visits, it is clear that SR's are talented but they are needed to be educated. By visiting sales field region and taking opinions of regional sales managers, inadequacies were determined and the program content was formed. According to this program, there will be at least one conference for supermen (sales representatives of Super Grocery Channel) in which contains trainings and group activities to provide continuous training and motivation. Apart from training, local sales management booklets were prepared. On 7th of April, the 1st Annual Supermen Conference was conducted in Antalya. In this conference supermen were trained about company culture, project, brand strategies, competitive work environment, importance of 4P (price, place, product, promotion) analysis and planogram and effective communication techniques [11].
For keeping the sales representatives motivation high, incentive programs are very useful. There are two types of incentive program to bring sales representatives more aggressive and efficient job of selling. One of them is Financial Incentive and the other one is Nonfinancial Incentive [12]. For this project, we focused on the financial incentives to stimulating the sales force for effective selling. When we applied the issue for our project we observed our case from 2 different perspectives. One of them is sales representatives by customary way and the other one is customer perspective.
Sales representatives" incentive program system was categorized on following 3 categories which are gross sales per customer, number of invoiced sales point that is called strike, and number of SKU (Stock Keeping Unit) sold per customer. For each category we gave a goal to sales representative every month. According to these categories if the sales representative can reach this goal, we will give him a determined amount of money.
For customer incentive program, we classified our customers according to their gross sales capacities to identify them. If customers increase their gross sale capacities incrementally by 30 %, 20% or 10%, they will be able to gain 3%, 2% or 1% of total gross sales. In addition ıf customer upgrade to upper level and stays this level at least 2 months, they will be able to gain extra 5% of total gross sales just for one time. In figure 4, the gross sales capacities of customers are represented.

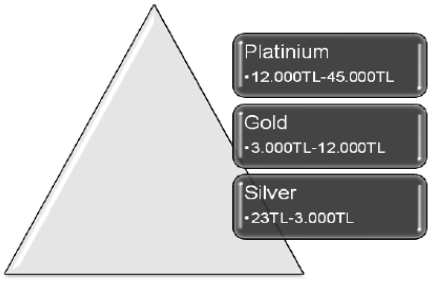

Figure 4.The gross sales capacities of customers

SR's were only one part of the sales operations problem. So we evaluated distribution channels by number of sales criteria and Grocery channel has excessive number of sales points. All channels contain variety of customers range from 100 TL gross sales to 10.000 TL gross sales per month. We thought that we should add a new channel between Grocery and Selected Super Market channel since this channel has too many customer. We will attain profitable customers from top 100 customer analysis. The new and old system of sales point is presented in figure 5.

Existing Channels	Number of Sales Points
Local Chain	47
Selected Super Market	822
Grocery	14883
Wholesalers	159
Cosmetic Shops	123
TOTAL	**16034**

New Channel Structure
Local Chain
Selected Super Market
SuperGrocery
Grocery
Wholesalers
Cosmetic Shops

Figure 5.Old and the new version of sales points

5. Conclusion

It can be said that we analyzed the existing situation at company's traditional channel. We faced reporting and measurement problem on channel-based analysis. To solve this measurement problem, we improved innovative strategies to monitor key performance indicators. In addition, with the aim of increasing quality and customer satisfaction, the new exclusive sales representative group has been added to the company's sales structure.

Since we have not conclude the project yet, the results cannot be shown exactly. However, the Company will use a system which was improved by us. The scorecard contains the following criteria; (i) gross sales, (ii) net revenue), (iii) trade spend and finally (iv) strike.

In Conclusion, the firm adopted this strategy for long term. As a result of the strategy, the firm will be able to examine sales field and competitors with better reporting. Therefore, they will take competitive advantage on sales field. In addition, since this strategy increases sales representatives" quality and engagement, the company will be able to provide better service to customers. By increasing customer loyalty, the company will be able to reach sales targets in long term.

6. References

[1] S. Muthu, L. Whitman, and S. Hossein Cheraghi , "Business Process Reengineering: A Consolidated Methodology" Proceedings of The 4th Annual International Conference on Industrial Engineering Theory, Applications and Practice , pp.17-20, 1999

[2] A. Lockamy, W. Smith, "A strategic alignment approach for effective business process reengineering", International Journal of Production Economics, Vol 50., No 2,3 , p. 141-153, 1997

[3] M. Hammer , J. Champy "Reengineering the corporation: a Manifesto for Bus,ness Revolution" , Harper Collings, 1993

[4] M. Hammer , "Re-engineering Work: Don't Automate, Obliterate", Harvard Business Review, pp. 104-112, 1990

[5] T. H. Davenport, J. E. Short, "The New Industrial Engineering : Information Technology and Business Process Redesign", Sloan Management Review, pp. 11-27, 1990

[6] M. Al-Mashari , M. Zairi, "BPR implementation process:an analysis of key success and failure factors", Business Process Management Journal, Vol.5 No.1, pp.87-112, 1999

[7] A. Alter, "Re-engineering tops list again", Computerworld, Vol. 28 No. 5, 31, p. 8., 1994

[8] A. Anand, S. Fosso Wamba and D. Gnanzou, "A Literature Review on Business Process Management, Business Process Reengineering, and Business Process Innovation" , The 9th International Workshop on Enterprise & Organizational Modeling and Simulation, 2013

[9] M.N. Habib, "Understanding critical success and failure factors of Business Process Reengineering", International Review of Management and Business Research, Vol.2/1, 2013

[10] B. N. Jyothi, "Object Oriented and Multi-Scale Image Analysis: Srengths, Weeknesses, Oportunities and Threats – A Review", Journal of Computer Science, , p. 706-712, 2008

[11] A. G. Churchill,Jr., N. M. Ford, S. W. Hartley, O. C. Walker,Jr. "The Determinants of Salesperson Performance: A Meta Analysis", Journal of Marketing Research,p.117, 1985

[12] D. J. Dalrymple , W. L. Corn , Sales Management Concepts and Cases "Leading and Motivating the Sales Force", p. 551-611, 1995

SOME RESULTS OF TANGENTIAL TURNING WITH AN ABRASIVE WATER JET

J.Cárach[1], P. Hlaváček[2], K. Vasilko[1], J. Klich[2],S. Hloch[12]

[1]Faculty of manufacturing technologies of Technical university of Košice with a seat in Prešov, Slovakia
[2]Institute of Geonics Academy of Science of Czech Republic, v.v.i., Ostrava Poruba, Czech Republic
* Corresponding author e-mail: jan.carach@tuke.sk

Abstract
This article deals with the visual comparison of the finished surface of sandstone using the tangential abrasive water jet. The continual abrasive water jet with turning was used with the constant pressure of 400 MPa for all sections of turning and with a depth of cut of 2mm. The abrasive particles were added to the water jet in the amount of 400 g.min^{-1}. The traverse speed (v_f = 60, 30, 10 mm.min^{-1}) was gradually changing at a constant speed of rotation of workpiece n = 30min^{-1}.
The down turning method was used on sample number 1. and the conventional method of turning was applied on sample number 2., whereby the direction of rotation of the circular workpiece of the sandstone with a diameter 50mm was against the tool, which was the abrasive water jet.

Keywords:
turning, abrasive water jet, rotation, workpiece, sandstone

1. Introduction

The machining of extra hard and brittle materials, to this day, causes problems associated with the reaching of the required quality indicators, economic efficiency and the overall effectiveness of the process. The machining of such materials by employing the conventional methods, does not always have to fulfill the requirement of the eco-friendly technology and the efficiency of the technological device and tool. A suitable technological method is Abrasive Water Jet (AWJ), also known as “tool-less machining”. So far, in the case of turning, the water jet has not been applied yet. [5]
It is necessary to focus the research on exploring the dependencies between input factors influencing the process of material separation and the quality of the surface created by hydro-abrasive machining of a semi-finished product.
In addition, there is also a need of optimization and rationalization of the process from an economical point of view.
It is important to setup the technological process so that there will be a minimal need to use another technology to apply the finishing touches on the workpiece.

2. State of the Art

The Technology of hydro-abrasive cutting is a process of material removal using a high-speed water jet in which abrasive particles are injected. [1]
Implementation of this method using turning, gives us a real possibility not only to cut sheet materials, but also to machine rotating semi-finished products of a different structure and shape. Because it is not possible to direct the water jet perpendicularly to a product, the method of tangential turning was used. [7]
The water jet is generated in a cutting head, where it is changed from the high-pressure water to a high-speed water jet (cca 1000 m.s^{-1}). The high-pressure water jet goes through the water-nozzle and through a mixing chamber, where the abrasive particles are added into the water jet and regulated by passing through the focusing tube. [1]
The workpiece is held by a power chuck and makes the main rotary movement, and the AWJ tool makes the translatory movement (*Fig. 1*.).

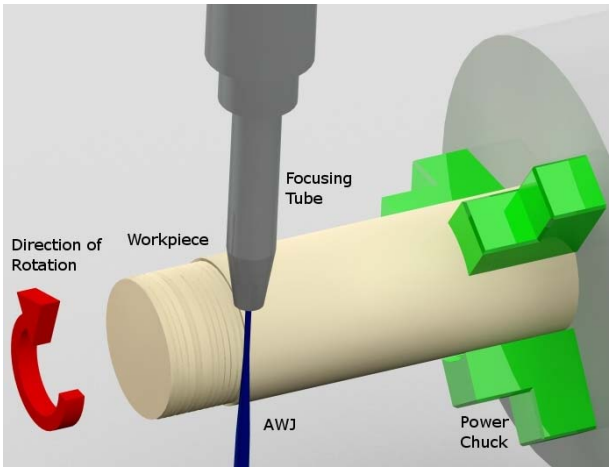

Figure 1. The Method of an Abrasive Water Jet Turning

The turning abrasive water jet process, presents a method of material removal without the heat-affected zone, with relatively small cutting power (the power is under 40N) on a workpiece. [2]

3. Materials and Methods – Experimental Set Up

In the implementation of the experiment, the semi-product a circular bar made of sandstone was used as a workpiece.

Sandstone is a sedimentary rock created by sand hardening. Its composition differs, the most common and most-represented element as for volume, is quartz. The color depends on the amount and nature of the constituents. It is a very brittle, hard and porous material. [3]

The experiment was performed on the 2D X-Y cutting table PTV WJ2020-2Z-1xPJ with an inclinable cutting head. The head is specially designed for cutting with abrasive water. The water jet was used for turning of the sandstone workpiece with a diameter of 50mm. The water pressure was generated by PTV75-60 pump with two pressure intensifiers (max. flow of 7,8 l.min^{-1} at 400 MPa). The workpiece was clamped between the jaws of the device to allow the rotation of the workpiece (*Fig. 2*.). [4]

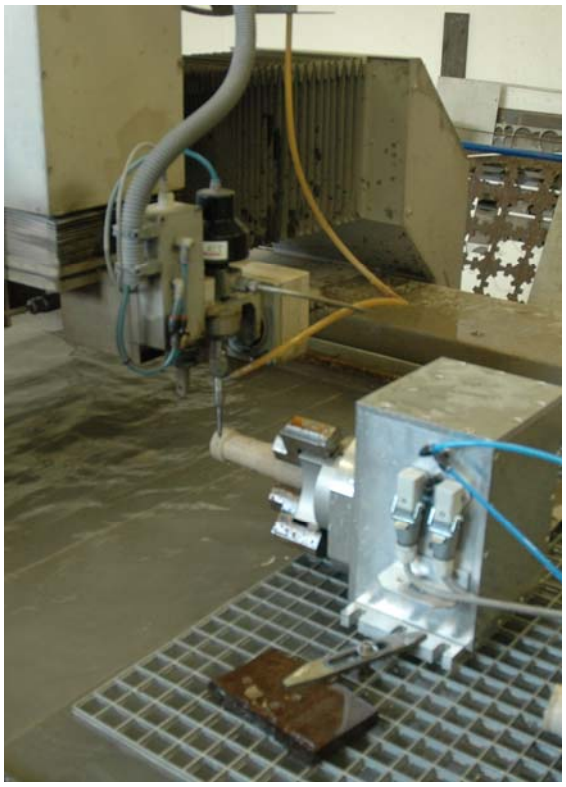

Figure 2. Device with Workpiece by the Experiment

The values of technological parameters (*Table 1.*) of the abrasive water jet turning were set identically for both methods, the only changes that were made were to the traverse speed of the tool and the direction of the rotation of the workpiece.

Table 1. Experimental Set- Up for Abrasive Water Jet Turning

Factors	Sign	Value	Base value
Pressure	p	400	MPa
Orifice diameter	d_o	0,33	mm
Focusing tube diameter df	d_f	1,02	mm
Depth of cut	a_p	2	mm
Stand off distance	b	25	mm
Abrasive mass flow rate m_a	M_a	400	g.min^{-1}
Workpiece diameter	d_w	50	mm

By the use of the down turning method, the workpiece performes a movement of parallel rotation in the sense of rotating in cohorence with the direction of the abrasive water jet (*Fig. 3*).

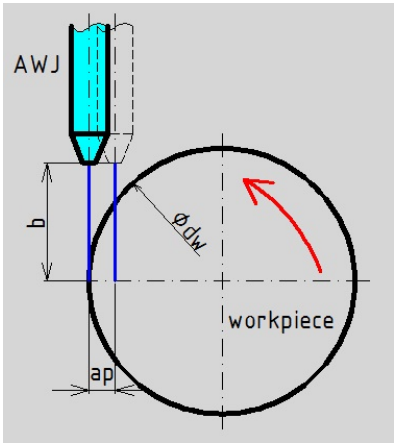

Figure 3. Down Turning

Contrarily, by conventional up turning, the workpiece performs rotative movement against the direction of the abrasive water jet (*Fig. 4*).

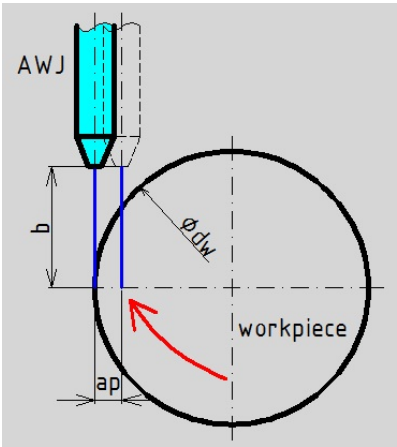

Figure 4. Conventional Up Turning

The removal of the material takes place when the abrasive water jet comes into contact with the rotating workpiece. At this point, the AWJ strikes the surface of the sandstone and through the microerosive process, particles of material are displaced. (*Fig. 5*). [6]

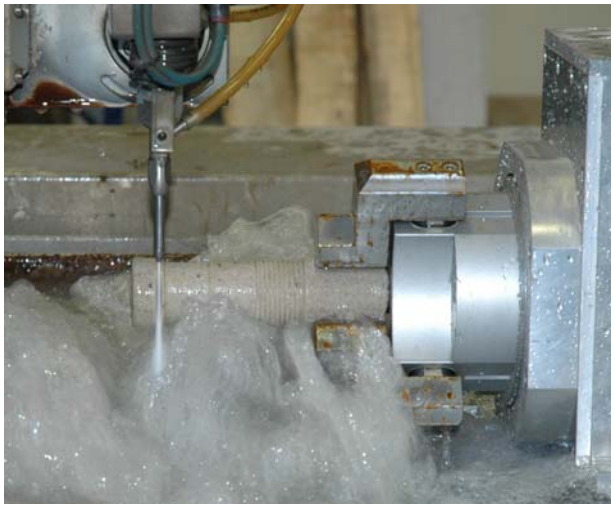

Figure 5. The Process of Volume Removal

The setting of technical parameters was the same for the down and convetional up turning method. Only the value of the traverse speed of the abrasive water jet, moving axialy with the axis of the workpiece was changed. (*Tab. 2.*).

Table 2. Experimental Set- Up for Down and Conventional Up Turning

Down Turning			
Factors	**7.**	**8.**	**9.**
Speed of rotation; n, min^{-1}	30	30	30
Depth of cut; mm	2	2	2
Traverse speed v_f; mm.min^{-1}	60	30	10
Conventional Up Turning			
Factors	**10.**	**11.**	**12.**
Speed of rotation; n, min^{-1}	30	30	30
Depth of cut; mm	2	2	2
Traverse speed v_f; mm.min^{-1}	60	30	10

4. Results and Discussion

At first, the Abrasive Water Jet Turning of samples was used with the parallel rotation of the workpiece. After the replacement of the sample, the conventional up turning method was used with contra-rotation of the workpiece against the AWJ. (*Fig.6*, *Fig. 7*).

The first visual comparison was made comparing the individual sections for each sample separately, the only difference was in the traverse speed of the AWJ. (*Fig. 6,7*).

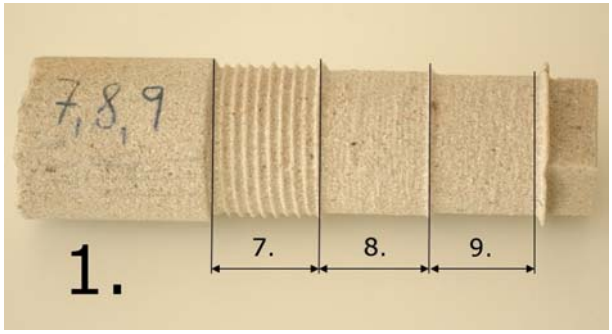

Figure 6. Sample Machined by the Down (Hydro-abrasive) Turning

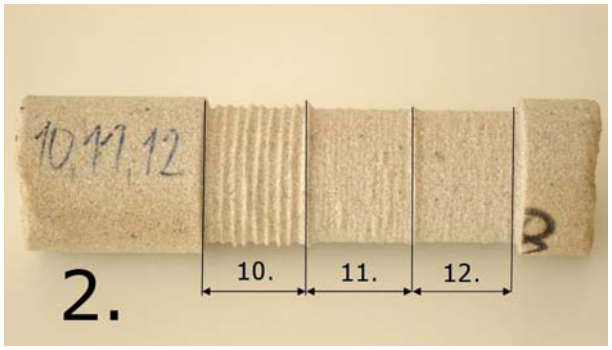

Figure 7. Sample Machined ByThe Conventional Up (Hydro-abrasive) Turning

The comparison between the down turning and conventional up turning methods, were made for sections A, B and C with equal values of traverse speed (*Fig. 8*).

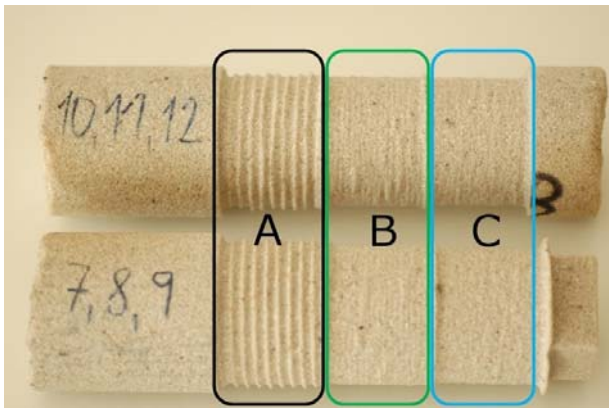

Figure 8. Section for Comparison of Samples of the Down and Conventional Up Turning Method Making Use of the AWJ

In order to reach a higher quality of visual comparison of the sections with equal values of traverse speed of the tool, detailed pictures were taken (*Fig. 9,10,11*). These pictures show details

of the surface of the sandstone for the down and conventional up turning methods.

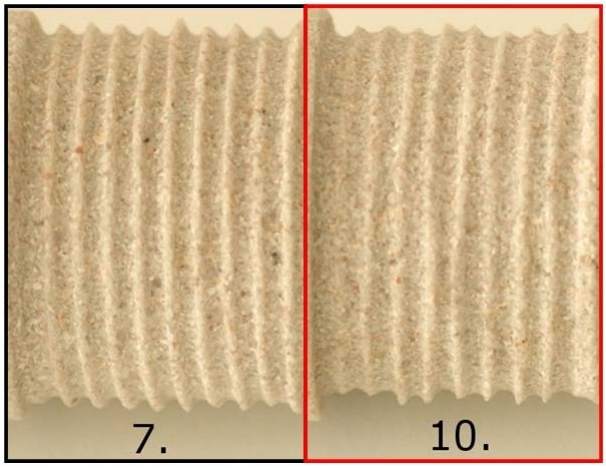

Figure 9. Detail of Section A

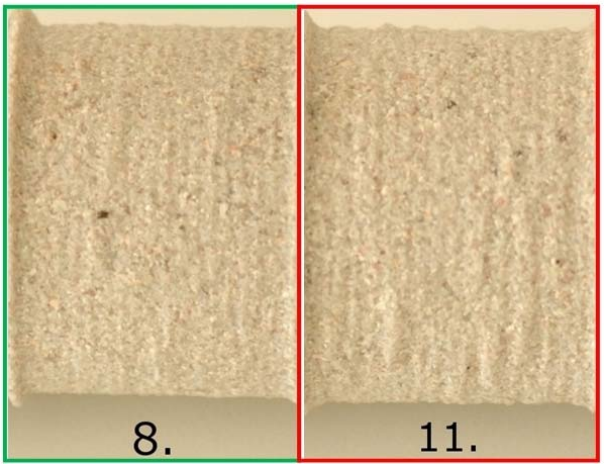

Figure 10. Detail of Section B

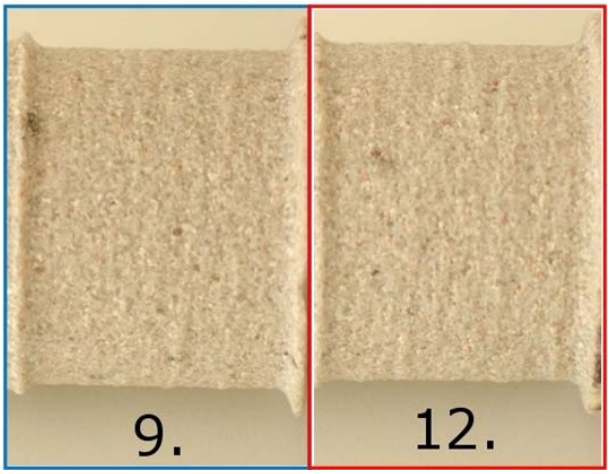

Figure 11. Detail of Section C

The visual comparison of samples was made at first for each sample separately, based on the impact of deceleration of traverse speed of the AWJ on the quality of surface of the sandstone.

By the visual comparison of individual sections (*Fig. 6*) of the sample, it can be stated that with accelerating traverse speed of the abrasive water jet, increase of roughness, higher irregularity of machining and higher waviness of the surface of sandstone occur. The same goes for the convetional up turning method (*Fig. 7*).

The comparison between the down and conventional up hydro-abrasive turning was made by the use of the method of visual comparison of the sections with equal values of traverse speed of the AWJ. It can be seen (*Fig. 9*) that by the parallel rotation of the workpiece, a relatively equal removal of the material of sandstone occurs.

Moreover, approximtelly parallel lines and waviness of machined surface were created by the AWJ. On the contrary, by the conventional up turning method, the uneven lines with variable waviness occured.

When the traverse speed changed from 60 $mm.min^{-1}$ to 30 $mm.min^{-1}$ (*Fig. 10),* the more evenly machined surface of sandstone can be seen as by the use of the convetional up turning method. At the lowest traverse speed, (*Fig. 11*) the quality of the machined surface of sandstone is on the level of the lowest waviness. The down turning method shows more moderate transitions caused by movement of the AWJ as it is by the conventional up turning method.

5. Conclusion and Future Direction of Research

With the visual comparison of down turning method and conventional up turning method of a sandstone worpiece with a diameter of 50mm and by the use of abrasive water jet technology and by the selected experimental conditions, it can be concluded that the direction of rotation of the workpiece to the tool, influence the final quality of surface wavines of the sandstone workpiece.

The influence of the traverse speed of the abrasive water jet was another factor which will influence the final quality, this was also demonstrated. It was used with the visual comparison method as well.

For further research of maching, using the abrasive water jet method, turning the sandstone workpiece is important to research as well as the influence of several other factors, such as: the frequency of rotation of the workpiece, the angle of the tool to the workpiece, the stand off distance, the abrasive mass flow rate and the material used for the abrasive partlicles, the number of passes and the depth of the cut.

Both the process and the technology involved in the Turning Abrasive Water Jet method, is very efficient. This makes it highly suitable for both removing materials, as well as the machining of high strength, brittle materials with special properties.

It is necessary to set this process up so that it will not only pre-treat the material, but possibly do the

finishing as well, without the requirment of any other technology. This would have a possitive impact on the efficiency of turning with the Abrasive Water Jet.

6. Acknowledgemet:
This work was supported by the Slovak Research and Development Agency under the contract No. APVV-207-12. Experiments were carried under the support Institute of clean technologies for mining and utilization of raw materials for energy use, reg. no. CZ.1.05/2.1.00/03.0082 supported by the Research and Development for Innovations Operational Programme financed by the Structural Funds of the European Union and the state budget of the Czech Republic, and with support for the long term conceptual development of the research institution RVO: 68145535.

7. References

[1] HLOCH, Sergej – VALÍČEK, Jan: "*Influence of Factors on Surface Topography Created by Abrasive Water Jet Cutting",* Faculty of manufacturing technologies of Technical university of Košice with a seat in Prešov, Prešov, 2008, ISBN: 978-80-553-0091-7

[2] AXINTE, A.D. – STEPANIAN, P.J. – KONG, C.M. – MCGOURLAY, J. :"*Abrasive waterjet turning – An afficient method to profile and dress grinding wheels*". In: International Journal of Machine Tools and Manufacture, Volume 49, Issues 3-4, March 2009, Pages 351-356

[3] Sandstone. [Online]. Available: *http://sk.wikipedia.org/wiki/Pieskovec.* [Accessed: 28-Sep-2013]

[4] HLOCH, S. et al.: "*Disintegration of bone cement by continuous and pulsating water jet*". In: Technical Gazette, Reading, no. May 2013, Pages 593-598

[5] HLOCH, S., VALÍČEK, J., HREHA, P., BEDNÁR, S., PERŽEL, V., LATOVÁ, A.: "*Online-identification of Hydroabrasive Cutting by Using Acoustic Emission and Vibration"*, Faculty of manufacturing technologies of Technical university of Košice with a seat in Prešov, Prešov, 2011, ISBN: 978-80-553-0698-8

[6] MANU, R – BABU, R.N.: "*An erosion-based model for abrasive waterjet turning of ductile materials"*. In: Science Direct, *Wear 266* (2009) 1091-1097 Available: http://www.springerimages.com/Images/RSS/1-10.1007_978-1-4419-7302-3_9-15. [Accessed: 28-Sep-2013].

[7] VASILKO, K., STROJNÝ, M.: "Progressive Methods of Turning*"*. Bratislava, ALFA, 1967.

THE STUDY OF JOB SATISFACTION WITH THE PHASE OF LIFE CYCLE OF COMPANY

Snezana Kirin[1], Milan Mitrovic[2], Sinisa Borovic[2], Tatjana Janovac[2], Ljuba Barovic[2], Vukašin Petrović[3]

[1] Innovation center of the Faculty of Mechanical Engineering, Belgrade, Serbia
[2] University Privredna Akademija, Faculty for Management of SMEs, Belgrade, Serbia
[3] Prima international school, Belgrade, Serbia
Corresponding author-mail: snezanakirin@yahoo.com

Abstract

There is strong evidence that employees who experience high level of satisfaction are also more productive. It is also known that internal and external factors affect job satisfaction. The aim of this study was to investigate the relationship between internal factors, such as satisfaction with the content of work, conditions of work, and relationship with colleagues and managers, with life stage of company.

Keywords: job satisfaction, life stage of company

1. Introduction

Motivation and satisfaction of employees has become the basis of stability of a modern organization. Dissatisfied workers may not provide the growth and development of the organization and the presence of dissatisfaction is an important indicator of future problems. Understanding the issues of motivation and job satisfaction is essential for the design of the workplace, organizational culture, reward system, system improvement and management style.

The phenomenon of the life cycle has long been known not only in biology but also in many other scientific disciplines. There are several theories of the life cycle of companies, which are only partially coincide. Phases of the life cycle of companies come and go one by one by predetermined order. For different theorists have different views on the number of life cycle stages of companies. The more stages to the detailed management strategies can be developed in them. The research presented in this paper was applied according to the following classification:

- Phase foundation and development ("go-go")
- Phase early age (adolescence)
- Phase full maturity (top form)
- Early Stage of bureaucracy
- Phase bureaucracy
- Late Phase bureaucracy ("death" of the company).

The foundation and development phase is the period when the company was born and the company is in a growth phase. During the phase of early youth, organizations recognize that there is life outside of their founders. Isak Adizes stated [1]: 'In many ways similar companies teenager trying to become independent of the family." It is the beginning of movement the organization to success. The transition between the “go-go” stage and adolescence is difficult, because there was a need for delegation of authority, change of leadership and setting new goals. Top form represents optimal state in the life cycle of when it achieves a balance between the organization's ability to keep its processes under control and its flexibility. Early stage of the bureaucracy is the beginning of falling performances. The aim of this paper is to explore the dimensions of job satisfaction with social aspects depending on the life stage of company.

2. Research Methodology

The survey was conducted in eight companies that are diverse in their activities, ownership rights, qualifications, education and age structure.

The survey was conducted during working hours, at workplace of respondents, using a questionnaire in which it used a Likert scale. The sample contained 125 of respondents. Complexity of the impact of factors that affect job satisfaction and their activities was highlighted through a questionnaire.

Information on the respondents and their personal characteristics are meant to provide data that we considered most relevant to the research problem, and relate to the following five variables: Gender, Level of Education, The age, Years of service, Activities of the company,and Type of employment. The main hypothesis was:

H0: Job satisfaction depends on the phase of the life cycle of the company.

Data were processed by the appropriate mathematical and statistical procedures. The basic plan of the research methodology is based on the correlation between the variables of the general level of education, work experience, education, gender, employment type (independent) and job satisfaction, relationships, relationships with colleagues and superiors, satisfaction with work conditions (dependent variable).

For the analysis of job satisfaction in the organization of content, satisfaction with rewarding work, relationships with colleagues, managers and overall relationships depending on the phase the life cycle the organization was applied a single-factor analysis of different groups, ANOVA with additional tests.

In order to find the mutual relationship between job satisfaction and life cycle stages of the company we have observed Pearson's correlation.

Statistical data analysis was performed using the algorithms embedded in software applications Microsoft's "Excel" and "SPSS for Windows".

2.1. Place and conditions of research

The conditions in which firms operate at the time of this research can be called unstable because it is a period of economic crisis during the last phase of a long transitional period of privatization and restructuring. Deindustrialization and decline of activities of the Serbian industry and economy is the process that takes nearly a quarter century and is characterized by: narrowing of industrial production; devastation of industrial capacities; reduced productivity in the industrial sector; out-of-date industrial equipment and technologies; decline in the competitiveness of major industries and companies, especially those with export ambitions; decreased the share of industrial sector in GDP of Serbia; decline in export activities; reduction of the number of employees in the industrial sector.

Independent variables

Organization size is observed through four categories: up to 50 employees, 51 to 100 employees, 101 to 1000 employees, over 1000 employees

Activity of the organization is viewed from the two categories: Production and Service.

Average incomes are given in 7 categories from the smallest to the largest.

The sample investigated whether the hypotheses was influenced by the Gender of the respondents (male and female).

Four categories of the age structure of the respondents were analysed: Up to 30 years, 31 to 40 years, 41 to 50 years, and over 50 years.

Level of education was observed by the five categories: Primary school, Three-year secondary school, Four-year high school, College degree, University degree.

Length working experience was determined by the four categories: 5 years, 6 to 10 years, 11 to 20 years, over 20 years.

Type of employment was observed in four categories: full-time, part-time, freelance, and volunteers.

The ownership structure of the company is presented through three categories: stock company, Limited Liability Company, and state ownership.

Dependent variables

With the aim to highlight the influence of phase of the life cycle of the company, the following was analyzed: satisfaction with the content of job; satisfaction with working conditions (workplace equipment, hours of operation); satisfaction with rewarding the work; satisfaction with relationships with colleagues and managers; satisfaction with working atmosphere; all in relation to phase of the life cycle of the company.

3. Results and discussion

To answer the question: Does the results of measurements satisfaction of: job content, award system, relationships with colleagues, relationships managers and human relations, are different in general, depending on the phase of an organization is we did a statistical analysis ANOVA (one factor). One of the assumptions of factorial analysis, ANOVA is that the variances of groups being compared are similar. In order to do determine, is used the Levin's test of homogeneity of variance that is reduced to testing the null hypothesis:

H0: variances are equal (there is no strong evidence that the differences in the variances of the different phases of the life cycle of the company significant).

H1: the variance differences are significant.

After the analysis we obtained:

• Significant differences in the mean values of the dependent variable "satisfaction with job conditions" between the phases of adolescence and bureaucracy

• Significant difference in satisfaction with job conditions between the phases "top form "and the bureaucracy.

For of the dependent variable "satisfaction with rewarding system," we obtained:

• a significant difference between satisfaction with the rewarding system in the "phase foundation and developement" and during the phase "top form" and

• significant differences between satisfaction with rewarding system in phase "top form" and the last stage of the life cycle of the company.

Figure 1 indicates that employees are most contented with their colleagues at work, being fairly balanced throughout all phases of the life cycle of the company. which can be interpreted as belonging to a nation of collectivist dimension of culture, [2].

Satisfaction with management is highest in the initial stage - foundation and development stage, when it is the greatest enthusiasm, and then drops significantly during adolescence to increase under top form and stage of bureaucracy when there are already developed of procedures for work and when are established ways of working.

Satisfaction with interpersonal relationships is satisfactory with what is highest in the beginning, when the expectations are highest, to the lowest value reached under top form when it is expected that the company operates at full capacity and when it is expected that all other parameters follow that development.

They expressed mostly balanced satisfaction with the content of work which shows that employees are generally realistically assessed what will work. Slightly higher values of satisfaction of the content of

the work reported in the foundation and development stage phase and the phase of the bureaucracy.

Satisfaction with the conditions in the workplace is the highest in a bureaucracy stages when there are already developed working procedures and when are established ways of working.

Satisfaction with the rewarding system resembles the letter „U“ and it is the highest in the initial stage. After that it is shown disappointment because wages do not follow growth and development of the company. In stages when the company is in the most advanced position workers expressed dissatisfaction with the system of rewarding.

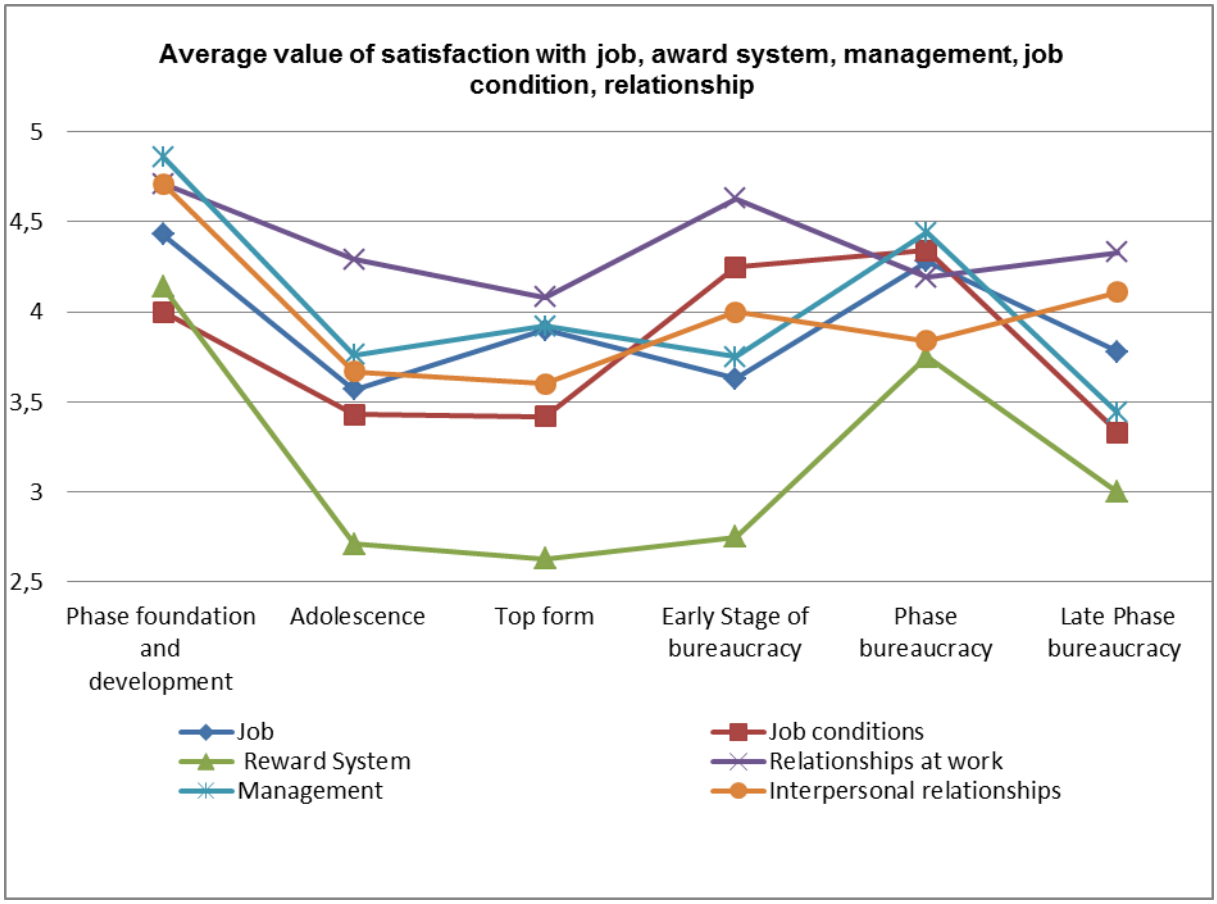

By applying the Pearson correlation between the independent and dependent variables we did not get the relationship between the factors of job satisfaction and life stage of company. We have got weak correlation between satisfaction of conditions of work and activities of the company, and the weak correlation of satisfaction with reward system and activities of the company.

By observing correlation of dependent variables we obtained a strong correlation of satisfaction with job content, satisfaction with working conditions and satisfaction with reward system. We also received a strong correlation of satisfaction with relationships with managers and colleagues.

4. Discussion and conclusions

From all the above mentioned in the survey it can be concluded that hypothesis H0, that job satisfaction depends on the phase of the life cycle of the company, has been proved.

It is shown that in the first, „foundation and developement“ phase of the life cycle of company satisfaction is present with work content, relationships with colleagues and managers, working conditions and rewarding system and overall interpersonal relationships.

At the stage of adolescence, there has been decline of enthusiasm, and consequently' satisfaction. The most prominent is neutral attitude towards job content, and occasionally appearing dissatisfaction and satisfaction with job content. In this stage neutral attitude towards to conditions of work (equipment of the workplace, working hours, etc.) is expressed. It is also evident mark of neutral opinion on the issue of remuneration, and is present both satisfaction and dissatisfaction totally rewarding work. In this phase is predominant solid content with colleagues. Also predominates satisfaction with the relationships between people although there are cases of and discontent. At this stage, conflicts occur mostly rarely, have them occasionally, and rarely occurring frequent conflicts that affect the business of the organization.

At the stage of life cycle of the organization, which is denoted by the "top form" is the most pronounced satisfaction with work content. At this stage dissatisfaction with the job content is very little present. In this phase we have a full range of satisfaction / dissatisfaction with working conditions. When the organization is operating at full capacity, it is normaly that employees expected that other working parameters follow the development of the organization. Since this is usually not the case at this stage, dissatisfaction is the most pronounced with rewarding system. In this stage satisfaction with colleagues, managers and overall relationships between people is evident, though fully dissatisfaction with relationships is rarely present as well.

At this stage amount of occasional conflicts is the largest by far which can be explained by the intensity of the job. A smaller number of respondents expressed the rare occurrence of conflicts and the lowest number of respondents expressed the existence of frequent conflicts that affect the business of the organization.

After a phase of top form, in the early stage of the bureaucracy, there is a drastic decrease in satisfaction with job content which could be explained by disappointment in job possibilities. Also, much smaller number of respondents expressed satisfaction with working conditions. As far as satisfaction with rewarding system is concerned, the neutral position is presented most often, which is different from the opinion in the top form phase, but still dissatisfaction is more present. In relationships with colleagues and interpersonal relationships no dissatisfaction is present, whereas in relationships with the managers satisfaction is more prevalent, but with the appearance of some discontent.

As regard conflicts they are less pronounced than in the phase of top form and there is balanse of those who believe that conflicts rarely occur, and those who believe that they occur occasionally.

At the stage of the bureaucracy satisfaction with the content of work has grown, compared to the early phase of the bureaucracy, after a period of adjustment. At this stage satisfaction with rewarding system is evident, as well as with relationships with colleagues and managers, and human relations. Anyhow, dissatisfaction with working conditions is present, which can be interpreted by the obsolescence of equipment throughout the life cycle of the company.

At this stage the amount of occasional conflicts is far the largest, with somewhat fewer respondents identified the rare occurrence of conflicts and the least of them existence of frequent conflicts that affect the business of the organization.

In the late stage of the bureaucracy satisfaction with job content is present, as well as neutral attitude towards the content of work, but there is dissatisfaction with job content. As far as conditions of work ar the concern, very few respondents have expressed complete satisfaction. They have indicated, on a smaller scale, dissatisfaction and satisfaction with rewarding system and neutral opinion. When considering rewarding system, there are all levels of satisfaction / dissatisfaction. Their intensity is small, and the shape reminds of normal distribution. In relationships with colleagues there is no dissatisfaction, while the relationship with managers and interpersonal relationships in general, satisfaction is more present, but with the appearance of discontent. It should be noted that at this stage all procedures for the job are defined and elaborated in written form.

In this phase occasional conflicts occur mostly, while a relatively small number of respondents pointed out to the rare occurrence of conflicts and some of them existence of frequent conflicts that affect the business. When observing differences in mean values of individual dependent variables at different stages of the life cycle of company, the significant difference is obvious between the mean value of the variable "satisfaction with working conditions", between the phases adolescence and the phase of „the bureaucracy“ and the phase "top form" and the „bureaucracy“. For the dependent variable "satisfaction with rewarding work," there is significant differences between satisfaction with rewarding system in the phase "top form" and phase which is the last stage of life cycle of the company.

Acknowledgment

Financial support by Serbian Ministry for Education, Science and Technology is gratefully acknowledged (Project 33044).

References

[1] *Managing Corporate Life Cycles, 2nd Edition* by Ichak Adizes. Published by the Adizes Institute. © 2004.

[2] International Differences in Work Related Values, Hofstede G., Beverly Hills, CA: Sage Publicarions

CLAMPING EFFECT ON THE WELDING DEFORMATION OF MONEL PLATES

Y. Javadi*[1], S. Hloch[2]

[1]Department of Mechanical Engineering, Semnan Branch, Islamic Azad University, Semnan, Iran.
[2]Faculty of Manufacturing Technologies with seat in Prešov, Bayerova 1, Prešov, Technical University in Košice, Slovakia
* *Corresponding author e-mail: yasharejavadi@yahoo.com*

Abstract
Welding of nickel-based super alloys is increasingly used in the industry to manufacture important components of the jet engine, marine industries, chemical processing, etc. In this study, a 3D thermo-mechanical finite element analysis is employed to evaluate deformations caused by the tungsten inert gas (TIG) welding of Monel 400 (Nickel-Copper alloy) plates. The finite element (FE) results related to the deformations have been verified by using common dimensional measurement tools. Two welded plates are experimentally prepared (with and without using clamp) to investigate the clamping effect on the welding deformations. It has been concluded that employing the clamp decreases the deformations significantly.

Keywords:
Monel; Nickel Alloy Welding; Finite Element Welding Simulation; Welding Deformation.

1. Introduction

Monel is a trademark for a series of nickel alloys, mainly composed of nickel (up to 67%) and copper, with some iron and other trace elements. MONEL alloy 400 is a solid-solution alloy that can be hardened only by cold working. It has considerable strength and toughness over a wide temperature rangeand exceptional resistance to many corrosive environments. Monel 400 is widely used in many industries, especially marine and chemical processing.
The conventional welding processes could be used to produce high-quality joints in nickel alloys. However, some of the characteristics of nickel alloys necessitate employing somewhat different techniques than those used for commonly encountered materials such as carbon and stainless steels [1]. Welding procedures for nickel alloys are comparable to those used for stainless steel with some practical considerations [1].
Welding processes, as essential production processes in the industry, produces undesired deformations at a significant level. Welding deformations are the results of non-uniform thermal expansions and solidifications caused by the welding processes. The thermal expansion characteristics of the nickel alloys approximate those of carbon steel so essentially the same tendency for welding deformations can be expected.The finite element (FE) method has been used since the early 1970s to predict stresses and deformations produced by the welding processes [2]. Lindgren [3-5] in three parts has reviewed the development in the finite element welding simulation: the increased complexity of the models [3], development of material modeling [4] and computational efficiency [5].
By developing calculation capabilities of the computers, many numerical studies have been conducted to analyze the deformations by employing three-dimension (3D) FE models. For example, a 3D model has been used by Sattai-far and Javadi [6] to predict the welding deformations of stainless steel pipes. They investigated influence of welding sequence on the welding distortions. They concluded that the welding deformations could be accurately predicted by 3D model. They also showed that selecting a proper welding sequence leads to considerable decreasing in the welding deformation.
The main goal of this study is evaluation of the welding deformation in the Monel plates to investigate clamping effect on the deformations. The FE simulation of the welding process is also employed. Good agreement is achieved in comparing the FE simulation results with those obtained from the deformations measurement. Experimental measuring and also FE simulation confirm the decreasing trend of welding deformations in the clamped Monel plates.

2. Theoretical Background

Numerical analysis of the welding deformations needs to take account of the mechanical properties of welds. The coupling among heat transfer, microstructure evolution and thermal stresses also influences the process. From the thermo-mechanical point of view, the heat input can be assumed as a volumetric or surfaced energy distribution. The fluid flow effect, which leads to homogenizing the temperature in the molten area, can be taken into account by increasing the thermal conductivity over the melting temperature. Heat transfers in solids are described by the heat equation as following:

$$\rho \frac{dH}{dt} - div\,(k\nabla T) - Q = 0 \quad (1)$$

$$k\nabla T.n = q(T,t) \quad \text{On } \partial\Omega_q \quad (2)$$

$$T = T_p(t) \quad \text{On } \partial\Omega_t \quad (3)$$

In Eq. (1-3), ρ, k, H, Q and T are density, thermal conductivity, enthalpy, internal heat source and temperature respectively. In Eq. (2), n is the outward normal vector of domain $\partial\Omega$ and q is the heat flux density that could rely on temperature and time to model convective heat exchanges on the surface; and T_p is a prescribed temperature.
The heat input is represented by an internal heat source. In this study, the double ellipsoid heat source pattern presented by Goldak and Bibby [7] is employed to simulate the heat source in the FE model. The moving heat source is modelled by a user subroutine in the ANSYS commercial software. Material modeling has always been a complicated stage in the welding simulation because of material data lack at elevated temperatures. Some simplifications and approximations are normally employed to overcome this problem. These simplifications are necessary due to both lack of data and numerical difficulties when trying to model the actual high-temperature properties of the material. The elevated temperature properties of Monel 400 (used in the welding model of this study) are extracted from Yegaie et al. [8]. The FE problem is formulated as a successively coupled thermo-mechanical analysis. First, a nonlinear thermal analysis is performed to find the temperature history of the entire domain. Then, the results of thermal analysis are applied as thermal body loads in a nonlinear mechanical analysis, which determines residual stress and deformations. The FE models for both thermal and mechanical analysis are the same. The general-purposed FE program ANSYS is used for the analysis. A full Newton-Raphson iterative solution technique with direct sparse matrix solver is employed to reach the solution. During the thermal analysis, the temperature and temperature dependent material properties are quickly changed. Hence, the full Newton-Raphson technique with using modified material properties is believed to give more accurate results. The common "Element Birth and Death" technique is used to model the deposited weld. A complete FE model is generated in the start of the analysis while all elements representing the deposited weld (except elements for the tack welds) are deactivated by assigning them a very low stiffness. During the thermal analysis, all the nodes of deactivated elements (excluding those shared with the base metal) are fixed at the room temperature till the birth of the corresponding elements. Deactivated elements are reactivated sequentially when the welding torch arrives over them. The basic FE model and mesh size is shown in Fig. 1.

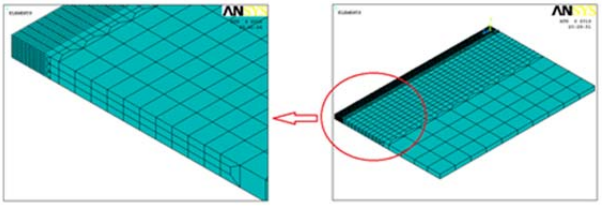

Figure 1. FE model selected in this study

3. Experimental Procedures

3.1 Sample description

In this study, the plates from Monel® 400 are welded to investigate the welding deformations. Two 220×150×6 mm plates are welded in V-groove (90° included angle) by employing tungsten inert gas (TIG) welding process. Multi-pass butt-weld joint geometry is used while the welding procedure specifications (WPS) are listed in Table 1. The plates are tacked weld in two points while clamping is used during the welding process of Plate 2 (no clamp is used for Plate 1). It is not practical to test non-flat surfaces in the ultrasonic stress measurement hence; the weld reinforcement is removed by employing a 30000 rpm hand grinder machine. However, a water-cooling system is employed to control the grinding temperature and prevent producing new thermal stresses.

Table 1. WPS for Monel welding process

Sample	Pass No.	Ampere (A)	Voltage (V)	Clamping
Plate 1	1	100	20	No
	2	110	20	
	3	120	20	
Plate 2	1	100	20	Yes
	2	110	20	
	3	120	20	

3.2 Measurement of the welding deformations

The deformations are measured to compare the Plate 1 and Plate 2 in order to find the effect of using clamp on deformations produced by the welding process. The angular shrinkage (Fig. 2) is the most important deformation type, which is considered in this study.

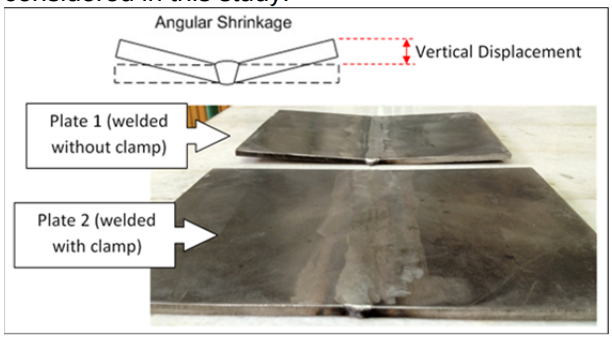

Figure 2. Angular shrinkage produced after the welding of Monel plates

It is obvious that a considerable amount of angular shrinkage is produced in Plate 1, which is welded without using of the clamp.

4. Results and Discussion

4.1 Deformation measurement results

The angular shrinkage is accurately measured by employing a coordinate-measuring machine (CMM). The angular shrinkage of Plate 1 is measured by employing a CMM. The measurement is fulfilled on the surface of plate in Z=110 mm, which is middle of the weld line. The results are shown in Fig. 3, which shows that the maximum of vertical displacement is produced in left corner of the plate and is equal to 7.32 mm.

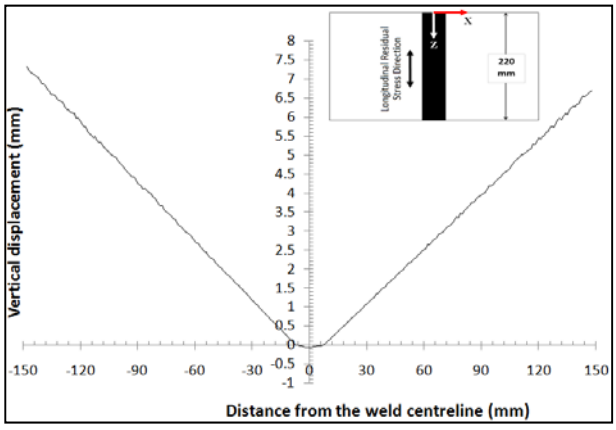

Figure 3. Angular shrinkage (Plate 1; in Z=110 mm)

4.2 Influence of using the clamp

The effect of clamping is investigated by comparing the deformation measured on Plate 1 (no clamp) and Plate 2 (with clamp). The comparison results, shown in Fig. 4, shows that using clamp during the TIG welding of Monel plates leads to considerable decreasing the deformations. By using clamp, the angular shrinkage decreases from 7.32 mm into 1.61 mm. Hence, the angular shrinkage of clamped plates welding is less than a quarter of no clamp sample.

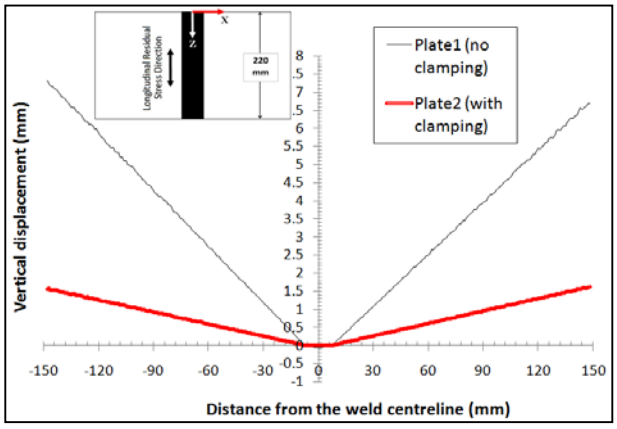

Figure 4. Clamping effect on the welding deformations

5. Conclusions

The main goal of this study is evaluation of the welding deformation in the Monel plates to investigate the clamping effect on the deformations. According to the achieved results, it can be concluded that:

1) The reasonable agreement was achieved in comparing the FE simulation with the results obtained from the welding deformations measured by using the CMM.
2) The angular shrinkage of Plate 2 (welding with clamp) is less than a quarter of Plate 1 (no clamp using). It confirms that employing the clamp significantly decreases the deformations in the Monel welding.

6. References

[1] Special Metal Corporation (SMC), 2003. Publication Number: SMC-055. http://www.specialmetals.com
[2] Hibbit, H.D., Marcal, P.V., 1973. A numerical thermo-mechanical model for thewelding and subsequent loading of a fabricated structure. Comput. Struct. 3, pp. 1145–1174.
[3] Lindgren, L.E., 2001. Finite element modeling of welding. Part 1: Increased complexity.J. Therm. Stresses 24, pp. 141–192.
[4] Lindgren, L.E., 2001. Finite element modeling of welding. Part 2: Improved materialmodeling. J. Therm. Stresses 24, pp. 195–231.
[5] Lindgren, L.E., 2001. Finite element modeling of welding. Part 3: Efficiency andintegration. J. Therm. Stresses 24, pp. 305–334.
[6] Sattari-Far, I., Javadi, Y., 2008. Influence of welding sequence on welding distortions in pipes. Int. J. of Pressure Vessels and Piping.85, pp. 265–274.
[7] Goldak, J., Bibby, M., 1988. Computational Thermal Analysis of Welds. Modeling of Casting and Welding Processes. 4, pp. 153–166.
[8] Yegaie, Y.S., Kermanpur, A., Shamanian, M., 2010. Numerical simulation and experimental investigation of temperature andresidual stresses in GTAW with a heat sink process of Monel 400 plates. Journal of Materials Processing Technology. 210, pp. 1690-1701.

CLAMPING EFFECT ON THE WELDING RESIDUAL STRESSES OF MONEL PLATES

Y. Javadi[1*], S. Hloch[2]

[1]Department of Mechanical Engineering, Semnan Branch, Islamic Azad University, Semnan, Iran.
[2] Institute of Geonics AS CR, v. v. i. , Studentska 1768, Ostrava-Poruba, 708 00
* *Corresponding author e-mail: yasharejavadi@yahoo.com*

Abstract
Monel is a trademark for a series of nickel alloys, mainly composed of nickel (up to 67%) and copper, with some iron and other trace elements. Welding of nickel alloys is increasingly used in the industry to manufacture many important components of the jet engine, marine industries, chemical processing, etc. In this study, a 3D thermo-mechanical finite element (FE) analysis is employed to evaluate residual stresses caused by the tungsten inert gas (TIG) welding of Monel 400 (Nickel-Copper alloy) plates. Residual stresses obtained from the FE analysis are then employed as verification of ultrasonic stress measurement results. The ultrasonic stress measurement is based on acoustoelasticity law, which presents the relation between the acoustic waves and the stress of material. The ultrasonic stress measurement is carried out by using longitudinal critically refracted (L_{CR}) waves, which are longitudinal ultrasonic waves propagated parallel to the surface inside the tested material. Two welded plates are experimentally prepared (with and without using clamp) to investigate the clamping effect on the welding residual stress. By utilizing the FE analysis along with the L_{CR} method (known as the FEL_{CR} method), the distribution of longitudinal residual stress could be achieved. It has been shown that employing the clamp considerably increases the longitudinal residual stresses of Monel plates.

Keywords:
Monel; Nickel Alloy Welding; Finite Element Welding Simulation; Ultrasonic Stress Measurement; Welding Residual Stress.

1. Introduction

Monel is a trademark for a series of nickel alloys, mainly composed of nickel (up to 67%) and copper, with some iron and other trace elements. It has considerable strength and toughness over a wide temperature range and exceptional resistance to many corrosive environments. Monel 400 is widely used in many industries, especially marine and chemical processing.

The conventional welding processes could be used to produce high-quality joints in nickel alloys. However, some of the characteristics of nickel alloys necessitate employing somewhat different techniques than those used for commonly encountered materials such as carbon and stainless steels [1].

Residual stresses are defined as remaining stresses inside the material after manufacturing process, in the absence of any external loads or thermal gradients. The engineering properties of industrial equipment can be considerably influenced by residual stresses. There are different methods available for stress measurement including three major categories: destructive, semi-destructive and non-destructive methods.

Welding residual stresses of Monel 400 plates were investigated by Yegaie et al [2]. By developing the TIG welding with a heat sink process, they concluded that the high temperature region was only limited to the vicinity of heat source and the maximum temperature of the sample was much lower than that of conventional TIG welding process leading to a lower residual stresses and even compressive stresses near the weld zone. Korsunsky and James [3] also analyzed the welding residual stress of nickel alloy. They used high-energy synchrotron X-ray diffraction for stress analysis in nickel super-alloys and succeeded to evaluate the stresses nondestructively.

The finite element (FE) method has been used since the early 1970s to predict stresses and deformations produced by the welding processes [4]. Lindgren [5-7] in three parts has reviewed the development in the finite element welding simulation: the increased complexity of the models [5], development of material modeling [6] and computational efficiency [7].

By developing calculation capabilities of the computers, many numerical studies have been conducted to analyze the residual stresses and deformations by employing three-dimension (3D) FE models. For example, a 3D model has been used by Sattai-far and Javadi [8] to predict the welding deformations of stainless steel pipes.

Ultrasonic stress measurement is a nondestructive method based on the linear relation between ultrasonic wave velocity and the material stress. This relation is called asacoustoelastic effect, which expresses that flight time of the ultrasonic wave changes with the stress. Crecraft [9] showed that the acoustoelastic law could be used to measure stress of the engineering materials. He employed transversal ultrasonic wave while longitudinal critically refracted (L_{CR}) waves are recently used for stress measurement. The L_{CR} wave is a longitudinal ultrasonic wave propagated parallel to the surface. Egle and Bray [10] showed

that the L_{CR} wave sensitivity to the stress is highest among the other types of ultrasonic waves. The ultrasonic stress measurement is capable of measuring through-thickness stresses nondestructively which was also confirmed by Javadi et al. [11]. They also compared the results with FE welding simulation and called the combination of FE simulation and the L_{CR} waves as the FEL_{CR} method, which is considered also in this study.
The main goal of this study is evaluation of the welding residual stress in the Monel plates to investigate clamping effect on the residual stresses. The FE simulation of the welding process is also employed to complete the FEL_{CR} method. Good agreement is achieved in comparing the FE simulation results with those obtained from the ultrasonic stress measurements. It means that the FEL_{CR} could be successfully used in residual stress measuring of the Monel plates.

2. Theoretical Background

2.1 L_{CR} method

Different experimental setups could be employed for residual stresses measurements fulfilled by the L_{CR} waves. As a common configuration, three ultrasonic transducers with same frequency are utilized. To produce the L_{CR} wave, the longitudinal wave is produced at the first critical angle by a transmitter (sender) transducer, and then propagates inside and parallel to the surface of tested material. Two receiver transducers assembled in different distance from the sender finally detects the wave. The reason of employing two receiver transducers is decreasing the environmental effects, like ambient temperature, on the wave velocity. More experimental details of the L_{CR} waves could be found in several previous studies [11-20]. The relation between travel-time measured by the L_{CR} wave and the corresponding uniaxial stress is developed by Egle and Bray [10] to be:

$$\Delta\sigma = \frac{E}{Lt_0}(t - t_0) \qquad (1)$$

In Eq. (1), $\Delta\sigma$ is stress change, E is the elastic modulus and L is the acoustoelastic coefficient (known as acoustoelastic constant) for longitudinal waves propagated in the direction of the applied stress field. The acoustoelastic constant would be measured by the uniaxial tensile test carried out over the specimens extracted from the investigated material. Also, t is travel-time of the L_{CR} wave, which is experimentally measured on the tested material while t_0 is travel-time related to the stress-free sample. Measuring the acoustoelastic constant along with the weld induced change in travel-time leads to determination of the stress changes caused by the welding process.

2.2 Finite element welding simulation

Numerical analysis of the welding residual stresses and deformations needs to take account of the mechanical properties of welds. The coupling among heat transfer, microstructure evolution and thermal stresses also influences the process. From the thermo-mechanical point of view, the heat input can be assumed as a volumetric or surfaced energy distribution. The fluid flow effect, which leads to homogenizing the temperature in the molten area, can be taken into account by increasing the thermal conductivity over the melting temperature. Heat transfers in solids are described by the heat equation as following:

$$\rho \frac{dH}{dt} - div\,(k\nabla T) - Q = 0 \qquad (2)$$

$$k\nabla T.n = q(T,t) \quad \text{On} \quad \partial\Omega_q \qquad (3)$$

$$T = T_p(t) \quad \text{On} \quad \partial\Omega_t \qquad (4)$$

In Eq. (2-4), ρ, k, H, Q and T are density, thermal conductivity, enthalpy, internal heat source and temperature respectively. In Eq. (3), n is the outward normal vector of domain $\partial\Omega$ and q is the heat flux density that could rely on temperature and time to model convective heat exchanges on the surface; and T_p is a prescribed temperature.
The heat input is represented by an internal heat source. In this study, the double ellipsoid heat source pattern presented by Goldak and Bibby [21] is employed to simulate the heat source in the FE model. The moving heat source is modelled by a user subroutine in the ANSYS commercial software.
Material modeling has always been a complicated stage in the welding simulation because of material data lack at elevated temperatures. Some simplifications and approximations are normally employed to overcome this problem. These simplifications are necessary due to both lack of data and numerical difficulties when trying to model the actual high-temperature properties of the material. The elevated temperature properties of Monel 400 are extracted from Yegaie et al [2].
The FE problem is formulated as a successively coupled thermo-mechanical analysis. First, a nonlinear thermal analysis is performed to find the temperature history of the entire domain. Then, the results of thermal analysis are applied as thermal body loads in a nonlinear mechanical analysis, which determines residual stress and deformations. The FE models for both thermal and mechanical analysis are the same. The general-purposed FE program ANSYS is used for the analysis. A full Newton-Raphson iterative solution technique with direct sparse matrix solver is employed to reach the solution. During the thermal

analysis, the temperature and temperature dependent material properties are quickly changed. Hence, the full Newton-Raphson technique with using modified material properties is believed to give more accurate results.
The common "Element Birth and Death" technique is used to model the deposited weld. A complete FE model is generated in the start of the analysis while all elements representing the deposited weld (except elements for the tack welds) are deactivated by assigning them a very low stiffness. During the thermal analysis, all the nodes of deactivated elements (excluding those shared with the base metal) are fixed at the room temperature till the birth of the corresponding elements. Deactivated elements are reactivated sequentially when the welding torch arrives over them. The basic FE model and mesh size is shown in Fig. 1.

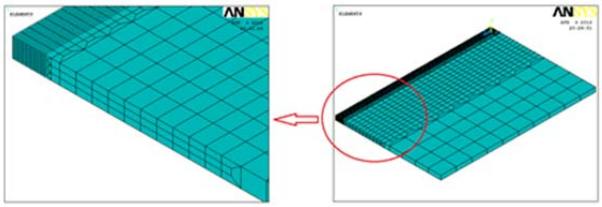

Figure 1. FE model selected in this study

3. Experimental Procedures

3.1 Sample description

In this study, the plates from Monel® 400 are welded to investigate the welding deformations. Two 220×150×6 mm plates are welded in V-groove (90° included angle) by employing tungsten inert gas (TIG) welding process. Multi-pass butt-weld joint geometry is used while the welding procedure specifications (WPS) are listed in Table 1. The plates are tacked weld in two points while clamping is used during the welding process of Plate 2 (no clamp is used for Plate 1).

Table 1. WPS for Monel welding process

Sample	Pass No.	Ampere (A)	Voltage (V)	Clamping
Plate 1	1	100	20	No
	2	110	20	
	3	120	20	
Plate 2	1	100	20	Yes
	2	110	20	
	3	120	20	

3.2 Measurement devices

The most important step in ultrasonic stress measurement is measuring time of flight (TOF) related to the L_{CR} wave while the corresponding equipment is shown in Fig. 2. Employing an ultrasonic portable box, laptop and ultrasonic transducers fulfills TOF measurement. A moving mechanical table is also used to move the transducers over the investigated plates with proper accuracy and stability. The ultrasonic portable box is equipped with an analogue to digital (A/D) converter, which is controlled by synchronization between the pulser signal and the internal clock. The ultrasonic wave is produced at the first critical angle by the transmitter transducer, passing from the wedge and then propagates as the L_{CR} wave inside the material. Based on the Snell's law, the first critical angle related to the ultrasonic wave passing from the Plexiglas wedge and propagating in the Monel material is calculated equal to 31.5˚ which should be considered in machining process to construct the wedge. Two receiver transducers assembled in different distance from the sender while the frequency of all the transducers is equal to 2 MHz finally detect the L_{CR} wave.

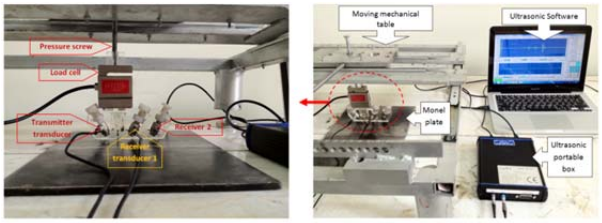

Figure 2. Ultrasonic TOF measurement devices

According to Eq. (1), the acoustoelastic constant (L) is also needed to be measured in other to evaluate the stress. The standard uniaxial tensile test is employed to evaluate the acoustoelastic constant while a changed form of Eq. (1) could be used for the calculations:

$$L = \frac{E}{\Delta\sigma \times t_0}(t - t_0) \qquad (5)$$

Tensile test specimens are extracted from the Monel plates to be exposed to the tensile test. During the tensile test, the TOF measuring devices are employed while the transducers are assembled on the tensile test specimen in order to measure flight-time (t) of the L_{CR} wave. However, stress relief treatment is already needed to determine the stress-free flight-time (t_0) by TOF measurement. By employing a tensile test standard machine, the tensile test (σ) is increased step by step; meanwhile the flight-time (t) is measured in each step. The elastic modulus (E) could also be measured by using the tensile test results or obtaining from the material properties tables. As a result, the acoustoelastic constant (L) would be calculated based on Eq. (5).

4 Results and Discussion

4.1 Longitudinal residual stress

The longitudinal residual stresses are analyzed by FE welding simulation and measured by ultrasonic method while the results are shown in Fig. 3. All the results are obtained for a plane perpendicular

to the weld line of Plate 1 in Z=110 mm while the FE model is run for only one side of the plate with symmetry assumption. The results are considered as the surface stresses, which are obtained in 2 mm depth from the surface. The 2 mm depth is related to the penetration depth of 2 MHz transducers producing the L_{CR} waves. It should be noticed that the L_{CR} ultrasonic method measures average of stresses in the 2 mm depth hence, the average of stresses in 0-2 mm from the surface are also considered in obtaining the FE simulation results.

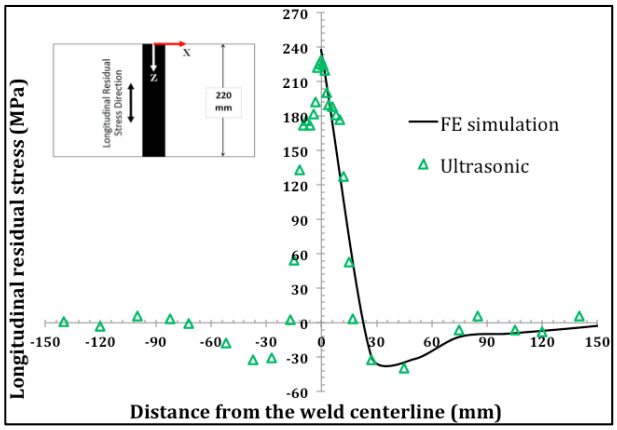

Figure 3. Longitudinal residual stress evaluated by FE and ultrasonic method (Plate 1; in Z=110 mm)

According to the results shown in Fig.3, the difference between the residual stresses measured by the ultrasonic method with those obtained from the FE simulation does not exceed than 10 MPa, which is produced in the weld centreline. It means that the ultrasonic and FE simulation results have reasonable agreement, which is the confirmation of FEL_{CR} potential in stress evaluation of Monel plates.

4.2 Influence of using the clamp

The effect of clamping is investigated by comparing the residual stress measured on Plate 1 (no clamp) and Plate 2 (with clamp). The comparison results, shown in Fig. 4, confirm that using clamp during the TIG welding of Monel plates leads to considerable increasing the longitudinal residual stress. By using clamp, the peak of longitudinal residual stress increases from 229 MPa to 253 MPa. It means that, welding Monel plates by using clamp leads to about 10 percent increase in the residual stress. It can also be concluded that the ultrasonic stress measurement using the L_{CR} waves (which is used for comparing Plate 1&2) has enough resolution to distinguish less than 25 MPa changing in the longitudinal residual stresses caused by the clamp usage.

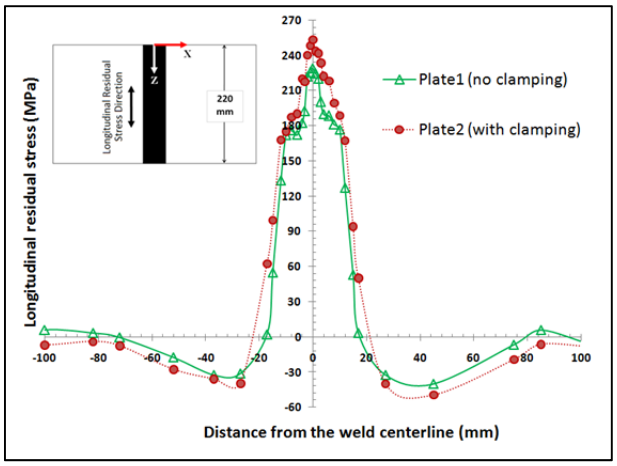

Figure 4. Clamping effect on the longitudinal residual stress (Z=110 mm)

5. Conclusions

The main goal of this study is evaluation of the welding residual stress in the Monel plates to investigate the clamping effect on the residual stresses. The FEL_{CR} method (which is the combination of finite element welding simulation with the L_{CR} ultrasonic stress measurement) is employed to reach this goal. According to the achieved results, it can be concluded that:

1) The reasonable agreement achieved in comparing the FE simulation with the ultrasonic stress measurement showing that the FEL_{CR} method has good potential to be employed in residual stress measurement of Monel plates.
2) The ultrasonic stress measurement using the L_{CR} waves has also enough resolution to determine the clamping effect on the longitudinal residual stresses.
3) The welding process of Monel plates by using clamp leads to about 10 percent increase in the longitudinal residual stress.

6. References

[1] Special Metal Corporation (SMC), 2003. Publication Number: SMC-055. http://www.specialmetals.com
[2] Yegaie, Y.S., Kermanpur, A., Shamanian, M., 2010. Numerical simulation and experimental investigation of temperature andresidual stresses in GTAW with a heat sink process of Monel 400 plates. Journal of Materials Processing Technology. 210, 1690-1701.
[3] Korsunsky, A.M., James, K.E., 2010. Residual Stresses Around Welds in Nickel-based Superalloys. Journal of Neutron Research. 12, 153-158.
[4] Hibbit, H.D., Marcal, P.V., 1973. A numerical thermo-mechanical model for thewelding and subsequent loading of a fabricated structure. Comput. Struct. 3,1145–1174.
[5] Lindgren, L.E., 2001a. Finite element modeling of welding. Part 1: Increased complexity.J. Therm. Stresses 24, 141–192.

[6] Lindgren, L.E., 2001b. Finite element modeling of welding. Part 2: Improved materialmodeling. J. Therm. Stresses 24, 195–231.
[7] Lindgren, L.E., 2001c. Finite element modeling of welding. Part 3: Efficiency andintegration. J. Therm. Stresses 24, 305–334.
[8] Sattari-Far, I., Javadi, Y., 2008.Influence of welding sequence on welding distortions in pipes. Int. J. of Pressure Vessels and Piping.85, 265–274.
[9] Crecraft, D.I., 1967. The Measurement of Applied and Residual Stresses in Metals Using Ultrasonic Waves. J. Sound. Vib. 5, 173-192.
[10] Egle, D.M., Bray, D.E., 1976. Measurement of Acoustoelastic and Third-Order Elastic Constants for Rail Steel. J. Acoust. Soc. Am. 60, 741-744.
[11] Javadi, Y., Akhlaghi, M., Najafabadi, M.A., 2013. Using Finite Element and Ultrasonic Method to Evaluate Welding Longitudinal Residual Stress through the Thickness in Austenitic Stainless Steel Plates. Materials and Design. 45, 628–642.
[12] Javadi, Y., Pirzaman, H.S., Raeisi, M.H., Najafabadi, M.A., 2013. Ultrasonic inspection of a welded stainless steel pipe to evaluate residual stresses through thickness. Materials and Design. 49, 591–601.
[13] Javadi, Y., Najafabadi, M.A., 2013. Comparison between contact and immersion ultrasonic method to evaluate welding residual stresses of dissimilar joints. Materials and Design. 47, 473–482.
[14] Javadi, Y., Najafabadi, M.A., Akhlaghi, M., 2012. Residual Stress Evaluation in Dissimilar Welded Joints Using Finite Element Simulation and the LCR Ultrasonic Wave. Russian Journal of Nondestructive Testing. 48, 541–552.
[15] Javadi, Y., Afzali, O., Raeisi, M.H., Najafabadi, M.A., 2013. Nondestructive Evaluation of Welding Residual Stresses in Dissimilar Welded Pipes. Journal of Nondestructive Evaluation. 32(2), 177-187.
[16] Javadi, Y., Pirzaman, H.S., Raeisi, M.H., Najafabadi, M.A., 2013. Ultrasonic Evaluation of Welding Residual Stresses in Stainless Steel Pressure Vessel. Journal of Pressure Vessel Technology (ASME). 135(4), 041502: 1-6.
[17] Javadi, Y., Najafabadi, M.A., Akhlaghi, M., 2013. Comparison between Contact and Immersion Method in Ultrasonic Stress Measurement of Welded Stainless Steel Plates. Journal of Testing and Evaluation (ASTM). 41(5), 1-10.
[18] Sadeghi, S., Najafabadi, M.A., Javadi, Y., Mohammadisefat, M., 2013. Using ultrasonic waves and finite element method to evaluate through-thickness residual stresses distribution in the friction stir welding of aluminum plates. Materials and Design. 52C, 870-880.
[19] Javadi, Y., 2013. Ultrasonic Measurement of Hoop Residual Stress in Stainless Steel Pipes. Journal of Manufacturing and Industrial Engineering.1-2, 1-6.
[20] Javadi, Y., Hloch, S., 2013. Employing the L_{CR} Waves to Measure Longitudinal Residual Stresses in Different Depths of a Stainless Steel Welded Plate. Advances in Materials Science and Engineering. Article ID 746187. http://dx.doi.org/10.1155/2013/746187.
[21] Goldak, J., Bibby, M., 1988. Computational Thermal Analysis of Welds. Modeling of Casting and Welding Processes. 4, 153–166.

APPLICATIONS OF WELD POOL DYNAMICS AND GAUSSIAN DISTRIBUTION IN SUBMERGED ARC WELDING

N.K.Singh[1*]

[1]Mechanical Engineering Faculty in ISM, Dhanbad, India

** Corresponding author e-mail: nks221@yahoo.co.in*

Abstract
The aim of the paper is to derive an analytical solution to predict the transient temperature distribution on the plate during the process of Submerged Arc Welding(SAW). An analytical solution was obtained from the 3D heat conduction equation. The main energy input that is applied on the plate is taken as the heat lost from the electric arc. The electric arc is assumed to be a moving double central conicoidal heat source which follows approximately the Gaussian distribution. The kinetic energy of filler droplets, electromagnetic force and drag force (i.e. weld pool dynamics) were considered as input to the process for finding out weld bead geometry. It was observed that the predicted values are in good agreement with the experimental results. The heat affected zone(HAZ)width calculation was also done with the help of analytical solution of the transient 3D heat conduction equation.

Keywords:
Submerged Arc Welding, Weld Pool Dynamics, Gaussian Heat Distribution, Transient temperature distribution, HAZ, Microstructure

1. Introduction

In arc welding processes, distributed moving heat sources are generally applied. Due to heating and convective and radiative cooling process in welding processes, the temperature field changes with time and space. Two methods dominate in the literature for modeling transient temperature distribution on welded plates. One is numerical solution (finite difference method, finite element method etc.)[7].Another is analytical solution [1-5,8], which described further in the present work, where integration transformations and Green's function method are applied.

Nguyen et al.[5] presented analytical solution for the transient temperature field of the semi infinite body subjected to 3-D power density of a dynamic heat source (such as semi-ellipsoidal and double ellipsoidal heat source). However, the results are not satisfactory with the single semi-ellipsoidal 3-D heat source with respect to the double ellipsoidal one.Nguyen et.al is only correct when both semi-ellipsoids are equal.

Winczek [8] described an analytical solution for the transient temperature field of half infinite body caused by volumetric heat source with changeable direction of motion. In his work, analytical temperature field was approximated by straight segments for volumetric heat source with trajectory considering temperature changes caused by next transitions (increase in temperature connected to action of heat source and self cooling of areas heated up earlier).

But Rykalin [1] pointed out that a heat flow model needs to be considered for the factors mainly variable thermal properties, temperatures of phase transformation, the magnitude of heat and characteristics of heat distribution, plate geometry, convection and surface depression in the weld pool.

In present wok, an analytical solution was derived considering all modes of heat transfer for the transient temperature field of the welded plates subjected to 3-D power density of a moving heat source (double central conicoidal heat source).

Major process control parameters (i.e. current, voltage, travel speed, stick out, electrode wire diameter, polarity etc.) involved in Submerged Arc Welding operation which forms the heat input function and the shape of heat source is varied with change of major process control parameters. This is the main motivation for considering a central conicoidal heat source. Parameters controlling the heat source are obtained through the measurement of weld pool geometry. The derived analytical solution has good agreements with the measured experimental values. In previous works, particular shape of heat source (i.e. elliptical heat source) has been chosen but practically in SAW process the shape of heat source may change with the change of input parameters. It (consideration of Central Conicoidal Heat Source) is the basic difference of the present

work with respect to the previous works and it delivers better results. The prediction of HAZ width has been made with the help of three dimension transient temperature distribution equations and validation through the analysis of microstructure and change in hardness has been carried out.

Very few researchers discussed on weld pool dynamics [6].In present work, prediction of weld pool geometry was also made by applying weld pool dynamics concept.

2. Transient Temperature Distribution

Only When heat source is moving with constant speed v from time t'=0 to t'=t, the increase of temperature during this time is equivalent to the sum of all the contributions of the moving heat source during the travelling time as

$$T-T_0=\int_0^t \frac{1}{2}\times\frac{Q_0}{\frac{2}{\rho c\pi^{\frac{3}{2}}[4\pi\alpha(t-\tau)]^{\frac{3}{2}}}}\times\frac{\sqrt{a^2a'^2b^2}}{\sqrt{a^2+a'^2}}\times$$

$$\left[\frac{1}{2}\times\frac{Q_0 d\tau}{\frac{2}{\rho c\pi^{\frac{3}{2}}[4\pi\alpha(t-\tau)]^{3/2}}}\times\frac{\sqrt{a^2a'^2b^2}}{\sqrt{a^2+a'^2}}\times\left[\frac{e^{-\frac{by^2}{[1+4b\alpha(t-\tau)]}}}{[1+4b\alpha(t-\tau)]^{\frac{1}{2}}}\times\right.\right.$$

$$\frac{e^{-\frac{cz^2}{[1+4c\alpha(t-\tau)]}}}{[1+4c\alpha(t-\tau)]^{\frac{1}{2}}}$$

$$\left.\left\{\frac{e^{-\frac{a^2[x-v(t-\tau)]^2}{[1+4a^2\alpha(t-\tau)]}}}{[1+4a^2\alpha(t-\tau)]^{\frac{1}{2}}}+\frac{e^{-\frac{a'^2[x-v(t-\tau)]^2}{[1+4a'^2\alpha(t-\tau)]}}}{[1+4a'^2\alpha(t-\tau)]^{\frac{1}{2}}}\right\}\right] \quad (1)$$

Here $T, T_0, Q_0, \rho, \alpha$,are temperature at point x,y,z at time t,initial tmperature,heat input of heat source,density,thermal diffusivity respectively anda',a",b,c are central conicoidal heat source parameters,

3. The Prediction of Weld Bead Penetration

Weight of liquid droplet (W):

$W = \rho \times V \times g$ (2)

Electromagnetic force:

The electromagnetic force **F,** results from the interaction between the current flow and the induced magnetic field in the weldment, and is equal to the vector product of the current density**,** **and** the self induced magnetic flux, **B':**

F = J×B' (3)

Where **J** is current density

Magnitude of Electromagnetic force along z direction:

The current density on the weld pool surface obeys a Gaussian distribution and can be described by the following function:

$$J_z = \frac{2I}{\pi\sigma_j^2} e^{\left(-\frac{2r^2}{\sigma_j^2}\right)} \quad (4)$$

Where J_z is the vertical component of the current density, I is the current, r is the radial distance from the arc location, and σ_j is the effective radius of the arc.

Magnitude of electromagnetic force per unit volume along z direction is given by,

$$F_z=\frac{\mu_m I^2}{4\pi^2 r^2 t_0^2}\left[1- e^{\left(-\frac{2r^2}{\sigma_j^2}\right)}\right](z) \quad (5)$$

Where μ_m = 8.75×10 $^{-4}$ H/m is the magnetic permeability of the material, t_0 is the thickness of the welded plates (= 20 mm).

So, total electromagnetic force along z direction throughout weld pool volume,

$$F_{z,\,total} = \int_0^l \int_0^{\pi} \int_0^{\left(\frac{w^2}{8}\cos^2\theta+\frac{l^2}{8}\sin^2\theta\right)^{1/2}} F_z\, r\,dr\,d\theta\,dl$$

Considering the of weld pool geometry equation

$$\frac{x^2}{w^2/8}+\frac{y^2}{l^2/8}+\frac{z^2}{a^2/8}=1.$$

l = length of welded plates along x axis.

$y=\frac{r}{\sqrt{2}}\cos\theta$, $z=\frac{a}{\sqrt{2}}\sin\theta$.

Where θ makes an angle with y .

So,

$$F_{z,\,total} = [\log(\tfrac{w^2}{3}) + \log(\tfrac{a^2}{3})]\times\frac{0.5\pi\mu_m I^2}{4\pi^2 r^2 t_0^2}\times(B/2)l$$

[Here, B = weld bead width] (6)

Drag Force F_{drag} is given by

$$F_{drag} = C_{ds}\times\frac{1}{2}\times\rho_g\times v_g^{\,2}\times\left(\frac{\pi D_d^2}{4}\right)$$ (for each liquid droplet) (7)

Where C_{ds} is the drag coefficient of a sphere, ρ_g is density of liquid droplet v_g is velocity of droplet,D_d diameter of droplet and

$$C_{ds} = \frac{24}{R_e}+\frac{6}{\sqrt{1+R_e}}+0.4$$

R_e is Reynolds number. Here,D_d =1.5mm and the droplet velocity immediately above the base metal isv_g = 0.604 m/s, [18]ρ_g=density of liquid droplet=6900kg/m^3,μ=Dynamic Viscosity=0.006kg/ms.

$$\text{Reynolds Number, } Re = \frac{\rho\times v_g\times D_d}{\mu} \quad (8)$$

$$\text{So, } R_e = \frac{\rho\times v_g\times D_d}{\mu} = 1041.9,$$

So, C_{ds} =0.58, which are similar to the reported experimental value [18].

So total drag force will be equal to sum of drag force of each liquid droplet

Energy gained by the liquid droplets,
E_{one}= Wh + ($F_{z,\ total}$) P + Heat gained by liquid droplets (E_{two}) (9)
Heat gained by liquid droplets is given by
$E_{two}=\int_{T_0}^{T_m} m_l c_p(s)\, dT + m_l \Delta q + \int_{T_m}^{T_d} m_l c_p(l)\, dT$ (10)

Where, m_l = mass of liquid droplets, T_m = melting point of droplet which can be depicted from fig.2.

Δq =latent heat of fusion = 2.47×10^5J/kg, T_0=initial temperature of electrode = 308K, T_d = final temperature of liquid droplet = 2400K, $c_p(l)$ = 520 J/kg-^{o}C, $c_p(s)$ = 465 J/kg^{o}C and h = 25 mm.

Calculation of Penetration(P):
Form law of conservation of energy we can write,
E_{one}= $F_{drag,\ total}$ P + E_{three}
or,
Wh+ ($F_{z,\ total}$) P + E_{two}= $F_{drag,\ total}$ P + E_{three}

Or $$P=\frac{F_z + Wh - E_2}{F_{drag,total} - F_{z\,total}} \quad (11)$$

Where, E_{three} = E_s + E_{wm} + E_c

E_s = Energy required for deforming the spherical shape of droplet due to surface tension

E_{wm} = Heat input in the portion of welded plates which is melted due to heat interaction between liquid droplets and welded plates

E_c = Heat flow from liquid droplets in conductive and convective heat flow mode

Calculation of value of E_s, E_{wm}, m_{wm}:

E_s = surface tension of liquid droplet (= 1900 mN/m) × increase of surface area due to deformation of shape of droplet (increase of surface area of liquid droplet is 2.48 times of its initial surface area,

And,
$E_{wm}=\int_{T_0}^{T_m} m_{wm} c_p(s)\, dT + m_{wm} \Delta q + \int_{T_m}^{T_d} m_{wm} c_p(l)\, dT$ (12)

(Where m_{wm} = mass of the portion of welded plated which is melted due to heat interaction between liquid droplets and welded plates and other values are same as liquid droplets (eqn.No-9) & as shown in figure-2C) and

m_{wm} = density of liquid droplets × (difference of volume of weld pool just below the Z = 0 plane and volume V groove of welding; assuming density of liquid droplet and welded metal are equal)

4. Conclusion

1. Weld bead penetration is primarily affected by heat input, gravity force, electromagnetic force, drag force of liquid droplet which can be depicted from fig.2.
2. Heat distribution on welded plate is central conicoidal shape for Submerged Arc Welding process and parameters of this heat source can be measured from the dimension of bead geometry.
3. Transient temperature distribution on welded plate can be calculated with the help of Gaussian central conicoidal heat distribution technique.
4. In this study, analytical solutions for the transient temperature field of a semi infinite body subjected to 3-D power density moving heat source (such as double central conicoidal heat source, which is first time attempted in this work) were found and experimentally validated. The analytical solution for double central conical heat source was used to calculate transient temperatures at selected points on a mild steel plates which are welded by taking x- axis along welding line, origin is starting point of welding, y-axis is perpendicular to welding line and z-axis towards plate thickness. Both analytical and experimental results (as shown in fig 1)from this study have shown that the present analytical solution could offer a very good prediction for transient temperatures near the weld pool, and could simulate the complicated welding path. Furthermore, very good agreement between calculated and measured temperature data indeed shows the creditability of the newly found solution and potential application for various simulation purposes, such as thermal stress, residual stress calculations and microstructure modeling.

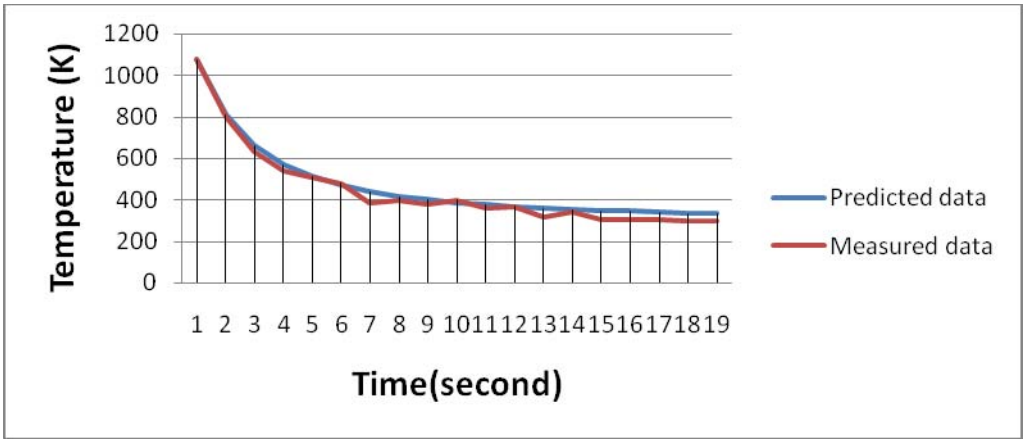

Figure 1.Comparison of Predicted and Experimental transient temperature distribution at point x=0, y=6.5cm, z=0.

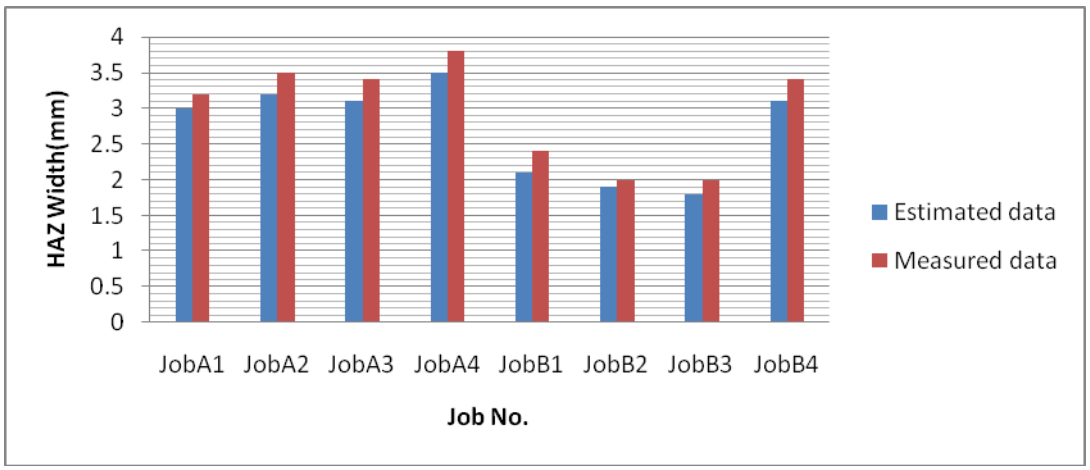

Figure 2.Comparison of predicted and estimated data of HAZ width

5. References

[1] Rykalin NN,Nikolaev AV.Welding Arc heat Flow: *Welding in World*. 1971;9(3/4):112-132.

[2] Eager TW,Tsai NS.Temperature fields produced by traveling distributed heat sources.*Welding Journal* 1983;62(12):346-355.

[3] Jeong S K, Cho H S. An analytical solution to predict the transient temperature distribution in fillet arc welds.*Welding Journal.* 1997;76(6):223-232.

[4] Goldak J, Chakravarti A and Bibby M. A Double Ellipsoid Finite Element Model for Welding Heat Sources. *W Doc*. 1985;No.212:603-685.

[5] Nguyen NT, Ohta A, Suzuki N and Maeda Y. Analytical Solutions for Transient Temperature of Semi-Infinite body Subjected to 3-D Moving Heat Source. *Welding Journal* accessed August,1999:265-274.

[6] Kumar A, Deb Roy T. Calculation of three dimensional electromagnetic force field during arc welding. *Journal of Applied Physics.* accessed July, 2003;94(2):1267-1277.

[7] Goldak J, Chakraborty A and Bibby M. A new finite element model for welding heat sources, Metallurgical Transactions B, 1984;15B:299-305.

[8] Winczek J.Analytical solution to transient temperature field in a half-infinite body caused by moving volumetric heat source. *International Journal of Heat Mass Transfer.* 2010;53:5774-5781.

ON SOME ASPECTS OF DYNAMIC ANALYSIS OF ROTOTRANSLATION TYPE SERVO LINEAR ACTUATOR

V. NASUI [1*], N, UNGUREANU[1], R. COTETIU [1], M. UNGUREANU[1], A. COTETIU[1]

[1] Faculty of Engineering, North Univ Center of Baia Mare, Technical University of Cluj-Napoca, Romania
* *Corresponding author e-mail: vasile.nasui@ubm.ro*

Abstract
There are going to be presented some of the original achievements of units elements of practice of the telescopic linear be actuator type with the possibly of application using it on the in the industry of the machine-tools and of the robots. We are also analyzing some parameters of dynamic quality that influence their technical characteristics as a mechatronic produce making them compatible with here requirements of such intelligent machines. The paper presents an analysis of rotation-translation systems that can be programmed and the project of an equipment of translation with a system of transforming the movement of rotation in movement of translation using a screw with balls. There are presented the main constructive variants, the model of kinematics, dynamics and the calculus with the working conditions.

Keywords:
Electro mechanic linear actuators, mechatronic, dynamic quality, optimal synthesis, motion control

1. Introduction

The technical and technological evolution towards the integration in mechatronic included the stages of development of the module of linear acting of the actuator type marked by the integration of the microprocessors. The new generation of modern machine and installations requires powers and very high speeds; the precision of regulating the position and but also a rational coordination of the composing individual action.
The development of the mechatronic technology within this context contributed to the development of the actuators as elements of execution capable with this which have besides the cinematic chain, energetic and informational material. The modular mechanical actuators represent a new concept in mechanical transmissions of various types and destinations that efficiently replace classical systems mechanically, hydraulically and pneumatically activated. These provide the optimal solution for the construction of quantitative and qualitative mechanical transmissions due to a wide range of usage, high efficiency, cinematic, dynamic capacities and high precision.
The linear actuators are used to the mechanic servo systems of positioning as systems of transmission and analogical servos stems of following of the position.
The technical system of the linear actuator perfected through this method has a few basic characteristics expressed by particular indicators such as: adjustable acting, high precision, and efficiency portent capacity, a rank of high speeds, numerical control etc. The actuator have a complex structure, the mechanical part being composed of certain elements which ensure a high kinematics and dynamic precision, and the commanding part being represented by a computer-led system, based on appropriate software. The main component parts of an actuator are represented in Figure 1, including the electric engine of acting, the transmission itself, the filling and the control devices: 1- planetary reducer; 2 - asynchronous electric engine and 3 - static converter of frequency. The linear actuator is composed of a motor turning a screw in which the nut on screw is not allowed to rotate. This allows linear motion o*n* the nut for the length of the screw. A position at some point along the screw is commanded by the user and the motor turns the screw until the nut reaches that position. The motor rotates the drive screw by a synchronous timing belt drive, worm gear drive, or a coupling direct inline drive, connected from the motor shaft to the screw. Thrust is transmitted from the drive nut, to the translating tube. One type is the electromechanical actuator, which converts the torque of an electric rotary motor into linear mechanical thrust. For the moment of training the screw, we need the average force with we load the system, the pace of the screw and the efficiency which the screw on rolls offers. The function of coordination and mechanic timing is replaced with the electronic alternative, using a new concept of dynamic regulation, which improves the performances of the system.

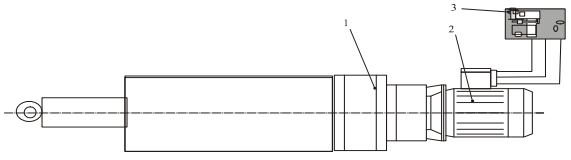

Figure 1. The linear actuators with converter

The linear actuator as a mainly electromechanic servomechanism in the industry of the machine-tools and of the robots has an important role in the evolution and its applications, with a direct dependence on their performances. Their synthesis represents an issue that is always approached and developed in the literature of specialty and in the recent research. The research of the control system of the movement of the actuator to characterize the dynamic answer can be simplified by introducing concept of operational

function of transfer in the theory of the automat systems.
The ideal dynamic behavior of a component within the control system of the movement can be defined in a single equation representing the system of null order, deducted in a differential equation of two order (the D' Albert's principle where the elements of accumulation and dissipation of energy of the type are missing.

$$y_e = k \cdot x_i \quad (1)$$

For the automat regulator of the proportional type, the following relation exists:

$$U_c(t) = k_{RA} \cdot U_r(t) \quad (2)$$

were k_n is the amplifying factor;
The transfer function will be

$$H_{RA} = \frac{U_C}{U_R} \quad (3)$$

The general solution of differential equation is obtained after solving the characteristically equation corresponding on the basis equation of the order which is homogeneous,

$$\alpha D^2 + \beta D + \gamma = 0 \quad (4)$$

where D expresses the differential generator d(df).
If the equation is transcribed by introducing the differential operator D and by defining in general the input signal Xi, as a series of the derivatives of different orders is obtained by treating continuously the equation, the report between of output and input results:

$$\frac{X_e}{X_i}(D) = \frac{\lambda^n + \mu D^{n-1} + \gamma D^{n-2} + \ldots}{\alpha D^2 + \beta D + \gamma} \quad (5)$$

This relation indicates operational function of transfer and the representation of the block schemes of the control systems or when the dynamic answer is established.
By analyzing these preoccupations through the ant saturation synthesis of the movement control of the actuators results the necessity of its extension and generalization for the actuators used in the automat regulating systems. From the constructive and functional points of view, the actuators have certain cinematic and dynamic restrictions that have to between into account so as not to cause significant degradations of the performances of the controlled system regarding its stability and friability.

2. The optimal synthesis of linear actuators

The optimal synthesis of their servomechanisms has to fit the requirements of stability, precision, transitory avower etc., using a compromise between the allowable size of the stationary loops and the desired degree of stability functional. The servomechanisms used to machine tools are usually equipped with reactions loops of speed and for position, and their functioning is characterized by the transfer function of the engine mechanism burden system.

The characteristics of all composed elements have a special importance because it influence differently the functional parameters, resulting there in the appropriate introduction of some new criteria extra appreciations in the case of mechatronic products, presented further (Fig.2).

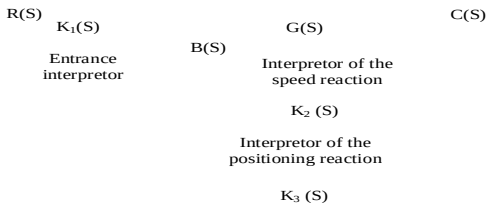

Figure 2. The block pattern of a positioning system

The sensitivity is a measure of the dependence of the characteristics of the system on one of its particular element. For the automatic systems with reactions loops we define the sensitivity of the system. S_k^m towards an element k global transfer function,

$$M(S) = \frac{C(S)}{R(S)} = \frac{K_1 \cdot G(S)}{1 + K_2(S)}, \quad (6)$$

where: R(S) is changed into the entrance signal; G(S)-transfer function of te direct way; K(S)-transfer function of te reaction; C(S)-changed into te getting aut signal.
According to the relation 1 and 2 we illustrate that any change in the parameters and characteristics of the interpreters k_1, k_2, k_3 is reflected in the change of the function of global transfer of the system. From the analysis it results that the error of the direct way (the transforming mechanism) is divided by 1+ K_2G, while the error owing to the reaction is added directly to the function of global transfer of the system we can conclude that from the point of view of the sensitivity, the error induced in the system on the direct way is less critical that the error introduced in the system from the reaction.
In the study of the modern mechanical transmissions dynamics, the transitory phenomena are inherent, reason for which parameters as mechanical impedance become extremely important in correlation with the mechanical efficiency. Knowing mechanical impedance is important, taking into account its influence on energy consumption as well as its effect on the dynamical parameters and feasibility especially in the transitory regimes.
In the present calculation methods of efficiency the impact of the inertia forces is neglected, as premises which satisfactorily describe reality outside the transitory regime and of the neglected friction from the rotation coupling compared to those of gearing [7]. The raise of the design calculation precision and the best choice of driving is done by correctly establishing the dynamic coupling inertial caused and by the evaluation of losses by friction which leave unchanged the angular speed transmission law but modify the force transmission law [3].
For the transitory running regime, efficiency can be calculated more precisely by the correct determination of the two loss coupling components

from the reducers, including the dynamic coupling, according to relation:

$$\eta_t = \frac{M_t}{M_t + \Delta M_c + \Delta M_a}, \quad (7)$$

The maximum driving moment necessary to overcome inertia produced when we have accelerations is calculated basing on a relation in mechanics at the mechanical system in Fig. 3. [4].

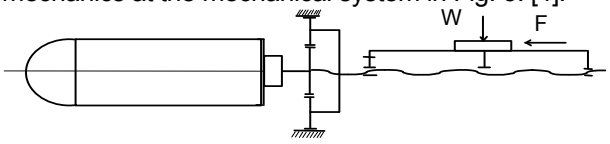

Figure 3. Rototranslation cinematic model system

$$M_a = I_A \cdot \dot{\omega} + M_M + \left(K \cdot \frac{F_0 l}{2\pi} + \frac{Pl}{2\pi\eta} + M_B \right) \cdot i \quad (8)$$

where: I_A - the system inertia moment, [daN mms^2]; ώ - the motor angular acceleration, [rad/s^2]; I_a ώ^2 - acceleration moment necessary to overcome inertia; M_M - internal friction moment in motor,[daN m]; F_0 - initial precompression force, [daN]; P - the final axial force, [daN]; M_B - friction moment in bearings, [daN m]; i - reduction ratio.

The relation gives the inertia moment of the motor driven system:

$$I_A = I_M + I_{R1} + i^2 \cdot \left[I_{R2} + I_S + \frac{W}{g} \left(\frac{i}{2\pi} \right)^2 \right] \quad (9)$$

where: I_n is the motor inertia moment, [daN mms2]; I_{R1},I_{R2} - gears inertia moment; I_S - screw inertia moment.

This measure of mechanical resistance to movement can be considered mechanical impedance, not only from the force point of view but also from the resistance moment point of view.

Thus, according to the definition of impedance [2]:

$$Z = \frac{F}{v} \quad \text{or} \quad Z = \frac{F}{\dot{x}} \quad (10)$$

where: F is the applied force; v - the speed resulted in the point of force application

Replacing v = ω r, there results:

$$Z = \frac{F}{\omega \cdot r} \quad (11)$$

where: ω is the tangential angular speed; r - rotation radius.

The consideration leads us to the observation that there is interdependence between efficiency and impedance in the situation of the dynamic regimes of modern mechanical transmissions when we take into account the inertial effect we also consider the mechanical impedance according to relation (1) by the help of the resistant moment.

3. Programmable motion control systems

An actuator's function is to provide thrust and positioning in machines used for production or testing. One type is the electromechanical actuator, which converts the torque of an electric rotary motor into linear mechanical thrust (Fig.4).

The motion control system's purpose is to control any one, or combination, of the following parameters: position, velocity, acceleration, torque.

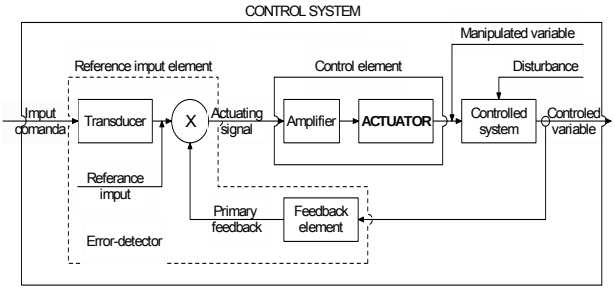

Figure 4. The block diagram of a feedback control system with actuators

Many motion control systems are integrated into a larger system. Various computer-based devices, such as programmable controllers, stand-alone industrial computers, or mainframe computers serve to link and coordinate the motion control function with other functions.

Thus, a more integrated motion control system would appear as shown below: the assembly of the process of developing new products, covering the conception aspects, manufacture and the link between them.

The application of a specific command causes a corresponding signal at the input through action input transducer. The result is an unbounded increase in controlled variable and loss of control by the command source. In order to develop and optimization pattern according to very strict engineering requirement it is necessary the introduction of a number of performance criterion and the formulation of some appropriate objective functions.

These restraints refer the achievement to the possibility of achieving technical performances referring to the parameters of functional geometrical precision. These are essential in the case of using positioning systems from robots, machine-tools computer controlled, specific to transitory conditions with frequent speeding and braking, starting and stopping at a. fixed point

The vector to be optimized, that will satisfy the constrains: contact stress; basic static and dynamic axial load (daN), - static axial rigidity daN/μm; - safety factor for outer speed; - the efficiency (0,80 – 0,99); - life duration (10-20.000 hours); - the position precision ($\sum \Delta p_{max} / l$);

This results a characteristic of functioning specific to each measure of translation unit according to the dimension and the step of the moving screw with which it is equipped. These restraints refer the achievement to the possibility of achieving technical performances referring to the parameters of functional geometrical precision. These are essential in the case of using positioning systems

from robots, machine-tools computer controlled, specific to transitory conditions with frequent speeding and braking, starting and stopping at a. fixed point. A block diagram of the system (Fig. 1) is shown below in Figure 5.

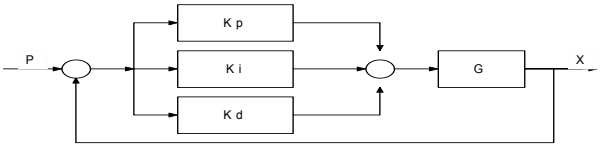

Figure 5. The continuous control block diagram

We observe that the equations are the same; therefore, we can establish correspondence among the analogous parameters which allow solving electrical circuit's dynamics problems by the theoretical and experimental methods. According to Relation 1, the idealized equation for continuous control algorithm is,

$$f(t) = k_p E(t) + k_i \int_0^t E(t)dt) + k_d \frac{d}{dt}[E(t)] \quad (12)$$

where: F(t) is the output of the controller at time *t;* k_p – the proportional gain constant; k_i - the integral gain constant; k_d – the derivate gain constant; E(t)- the error at time t.

The block diagram of the control system in the continuous control form is shown in Fig.5. For small sample times this equation can be turned into a difference equation by discretization. The derivate term is replaced by a first-order difference equation and the integral term is approximated using trapezoidal integration. This equation required storage of past errors.

The intermediate equation can be transformed into a recursive equation where only the previous output, current error, and last two errors must be stored. The final equation then takes the form

$$F(t) = F(t-1) + k_1E(t) + k_2E(t-1) + k_3E(t-2) \quad (13)$$

where: F(t - 1) is the previous control output; E(t - 1)- the previous error; E(t-2)- the error proceeding E(t-1).

The Lab VIEW program allows the selection of real numbers for gain constants. These constants, along with the sample frequency, are converted into K_1,K_2,K_3 according to the formula shown above.

$$k_1 = k_p + \frac{Tk_i}{2} + \frac{k_d}{T}, \quad k_2 = -k_p - \frac{2k_d}{T} + \frac{Tk_i}{2},$$

$$k_3 = \frac{k_d}{T}, \; T = \frac{1}{f} \quad (14)$$

4. Conclusion

Development of modern servo positioning system type with elements of mechatronic drive technology requires the introduction of additional control parameters should verify dynamic performance and a new concept of optimal synthesis. The result of the research we can value immediately any system of linear movement because it has as a basis the newest techniques of modeling in the field. These have as an objective the developing of new system of electro-mechanic linear actuator type as well as perfecting the existent ones in a very short time and in highly energetic and economic conditions. The applicative and experimental researches viewed the practical checking and the making up of the theoretical patterns used in the output and also convergences to the ways of approaching the problems to reality.

The conception and its manufacture assisted on the computer has as application field the assembly of the process of developing new products, covering the conception aspects, manufacture and the link between them. This research is part of the modern preoccupations regarding the improvement of new systems of linear acting and of numerical modeling using algorithms and programs of numerical computation and virtual instrumentation.

5. References

[1]. Adrian, Olaru s.a. - Dynamic robotilor industrial, Editura BREN, Bucuresti, 1999.
[2]. Demian,T. s.a. The Basic of Designing the Apparatus of Fine Mechanic, Ed. Tehnica 1986
[3]. Borangiu, Th.. *Advanced Robot Motion Control*. Editura Academiei Romane, Bucuresti, 2003.
[4]. Galis M.,Popescu S.,Pop C.,Ciupan C., Design of Machine Tools. Editura Transilvania Press, 1994
[5]. Gâlca, A. Study on the Using of Transmissions of the Field of Worm Gears in Servosystem. Bucuresti, Edit. Tehnica.1995
[6]. Ispas, C.,Predincea, N. Ghionea, A: Constantin, G Maşini-unelte, Editura Tehnică, Bucureşti, 1998.
[7]. Montgomery, D.C., Design of Analysis of Experiments, 4th Edition, John Wiley & Sons, New–York, 1996.
[8]. Mohora, C., Cotet, E., Patrascu, G. Simularea sistemelor de productie. Editura Academiei Romane, 2001.
[9]. Popa, A. Controlul digital al sistemelor mecatronice. Editura Orizonturi Universitare Timisoara, 2002.
[10]. Năsui, V., Actuatori liniari electromecanici.Editura RISOPRINT Cluj Napoca 2006.
[11]. Nasui,V. Pay,G. Basis of the Optimization of the Mechanic Efficiency. Editura Universităţii de Nord. Baia Mare 2000.
[12]. *** LINACT/LabVIEW. -Linear Actuator. The University of Alabama. 2004.

DRILLING DEVICE IN APPLICATION WITH EDUCATIONAL ROBOT

T. Šarić[1*], D. Pezer[1], G. Šimunović[1] and M. Flanjak[2]

[1]Mechanical Engineering Faculty in Slavonski Brod, J. J. Strossmayer University of Osijek, Croatia
[2]Harburg-Freudenberger Belišće d.o.o, Radnička 5, Belišće, Croatia
* *Corresponding author e-mail: tsaric@sfsb.hr*

Abstract
The possibility of connecting the educational robot system and the pneumatic equipment in the Laboratory for Computer Integrated Manufacturing to increase the quality of education of students, was explored in this paper. The problems were analyzed, and the objectives in the realization of integration of robot and pneumatic equipment (in the design of automated device for drilling) were set. The method of forming assembly support was proposed, and the algorithmic and software solution for the given technological problem were given.
In the experimental part of the paper, the proposed assembly was tested. According to the accepted solution, a simulation of software solution on the pneumatic control system (FluidSIM-Festo) was conducted. The proposed solutions were tested and connected into an integrated unit, i.e., the robot operation was synchronised with the electro-pneumatic equipment.

Keywords:
Robot, Programming, Drilling device

1. Introduction

Since the global market requires the high quality products at reasonable prices, production must be competitive and it can be achieved by increasing the level of automation, flexibility and reliability of production systems. Flexibility can be achieved among other things also with the application of robots in the manufacturing processes. Through their educational process for the engineering professions, the students have to learn the theoretical basis and confirm it through the exercises (experimental work). The theoretical theses are confirmed through the simulation of proposed solutions and in the laboratory conditions through setting and implementation of exercises. This paper aims to show a comprehensive approach that is implemented in the design of automated electro-pneumatic device integrated with the educational robotic system. In this paper, the available equipment of the Laboratory for Computer Integrated Manufacturing was used. In the Laboratory, various researches [1] and exercises are conducted.

2. Educational robot and software

SCORBOT-ER 4u is a robotic system developed and designed for the educational process, as the equivalent of industrial robotic systems. The open structure of the robot arm (Figure 1) and the internal mechanism enable students easy exploring and studying of the construction of robots. The robot is a vertical structure, and with a gripper, it has six degrees of freedom, and can be programmed in an equivalent way as the industrial robots [2]. The robot can be used as an independent educational system or as a part of an integrated system with different components for the solution of defined technological tasks. The features of this robot (such as speed, repeatability, etc.) make it suitable for independent work and for integration into automated work cells (such as robotized welding, serving of CNC machine tools, sorting, measuring, palletizing, etc.).

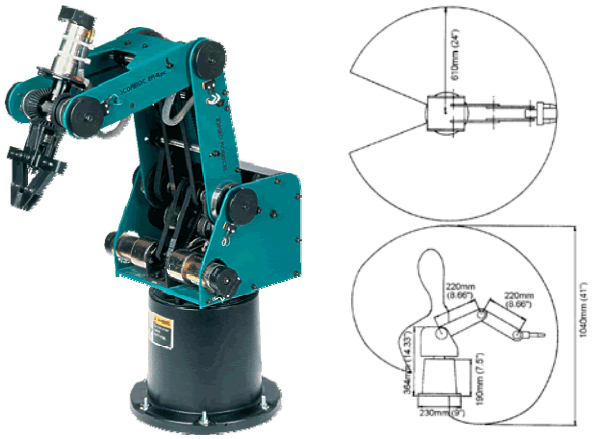

Figure 1. Robot Scorbot-ER 4u in manipulative space

SCORBASE is a software package that enables robot programming and its control. The software package provides numerous advantages, among which only a few are emphasized, such as: Control and display of conditions in real time of all working axes, gripper, and two peripheral axes, all the digital and analog inputs and outputs. The commands with associated attributes for programming are defined at three separate levels (L1, L2, Pro) according to the level of complexity, which allows students a gradual introduction with the commands and adequate dynamics of acquisition of knowledge in programming and control with the robotic system for different weights of given tasks.
Scorbase commands were grouped into three folders (Figure 2) and these are [3]:

a) Group for control and management of axes
b) Group for management of program
c) Group for defining the state of the inputs and outputs

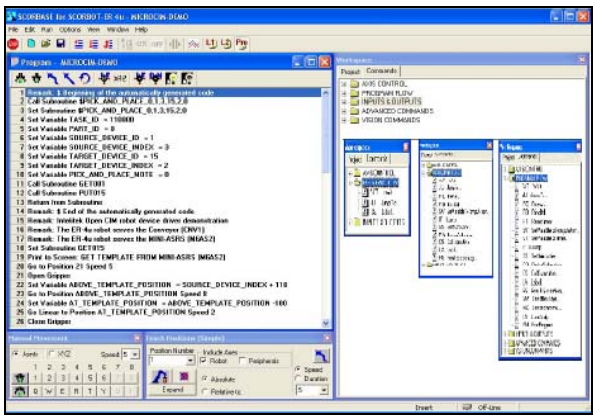

Figure 2. Graphical interface of the SCORBASE program

The interface is dynamic and it changes according to the type of work that is performed, and the same user can shape the appearance of the interface to make the operation more comfortable and user oriented.

3. Experimental

In the experimental part of the work, the technological solution of defined tasks was designed. Within the given task, an automated drilling of prismatic parts (Figure 3), using the elements of electro-pneumatics with the design of the receiving device, as well as serving, using the available robot, should be solved.
Robot Scorbot-ER 4u was used for feeding of raw materials (Figure 3.a) and dispatching of workpieces (Figure 3.b), while clamping and simulation of drilling was done on the Festo didactic equipment.

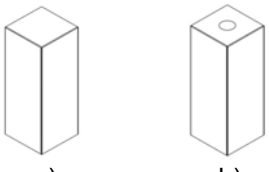

a) b)

Figure 3. Raw material - a) and workpiece - b)

The robotic system and the didactic equipment connected to each other make the educational automated device for drilling and enable the independent production of products. The designed software support must enable the control of robotic system, as well as the monitoring and control of electro-pneumatic cycles. The simulation of the processes of orientation, clamping and horizontal drilling was performed on a didactic equipment using the selected elements of pneumatic and electro - pneumatic control.

The electro - pneumatic and relay control scheme for a defined technological task was designed and simulated in Festo FluidSIM [4,5] (Figure 4).

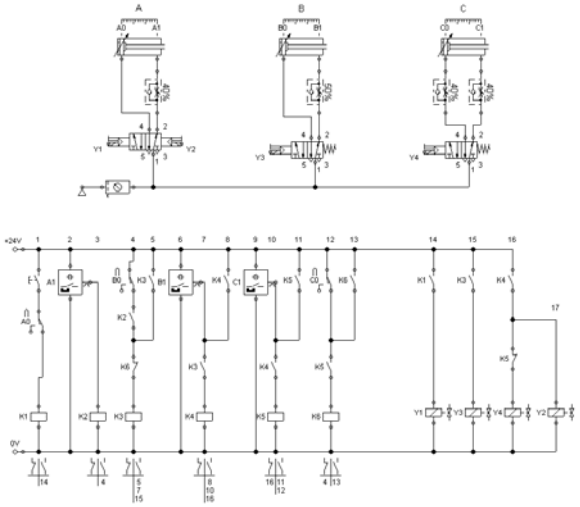

Figure 4. Electro and relay control scheme

The synchronization of operation of pneumatic cylinders is shown at the path – time diagram (Figure 5). The diagram shows the speed of the cylinder piston rod, as well as the relationship for movement of more cylinders (cylinder A – Orientation, cylinder B – Clamping, cylinder C – Simulation of drilling).

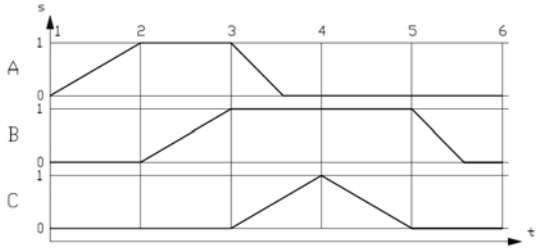

Figure 5. Path – time diagram

Figure 6 shows a designed device on the table with all used electro-pneumatic elements, relay with additional equipment, and the space for clamping and drilling of the workpiece.

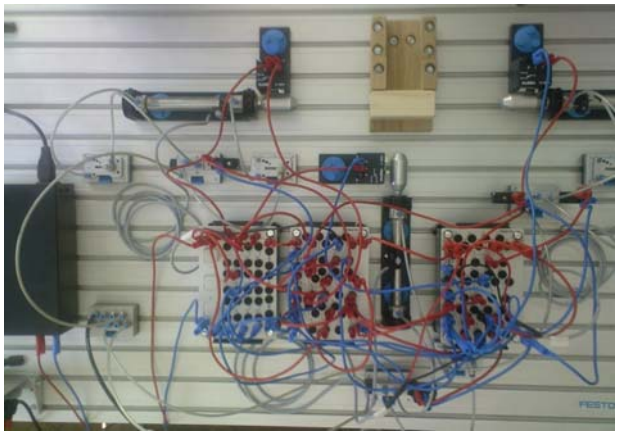

Figure 6. Designed electro-pneumatic device for drilling simulation

In the design of control program for the robot, it is necessary to pay special attention to the defining of the system's surroundings. During orientation, clamping and simulation of drilling (active pneumatic cylinders) robotic gripper must be at a safe distance from the machining process (avoiding possible collisions), which is achieved by creating a spatial schedule plan of the robot workspace within which the movement of the robot is performed (Figure 7). After designing the spatial schedule, the working cycle of robot with the characteristic positions, is defined (Figure 8).

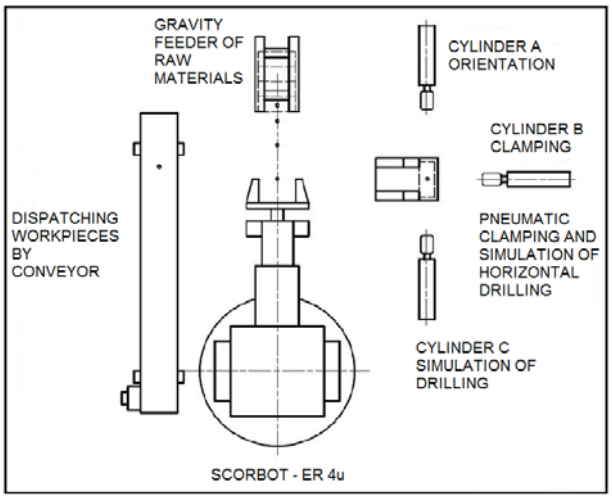

Figure 7. Schematic display of spatial schedule for designed system

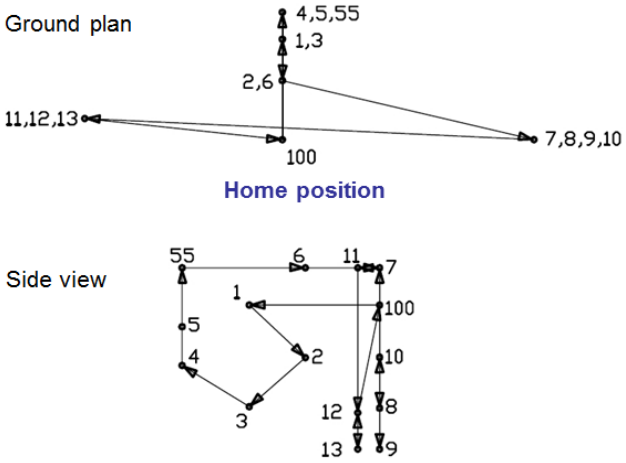

Figure 8. Designed scheme for the working cycle of drilling simulation

The working cycle of robot can be described as follows: A robot takes a raw material from the gravity feeder (Figure 9), and transfer it to the clamping device (Figure 10). The control unit of robotic system then gives the signal to the relay which drives the electro-pneumatic cycle that consist of orientation, clamping and simulation of horizontal drilling of raw material. Upon completion of the cycle, the sensor for cylinder status activates the relay which sends a signal to the control unit of the robot system and starts the operation of robot. The robot takes the workpiece, transfers it and places it on the conveyor belt (conveyor) (Figure 11) which transfers it into a fictional production process or the storage.

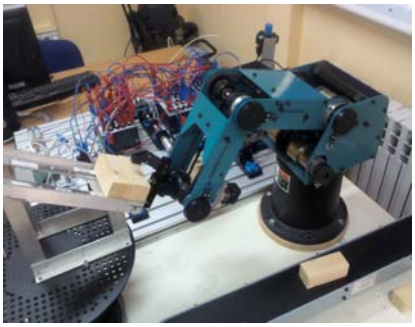

Figure 9. Raw material acceptance

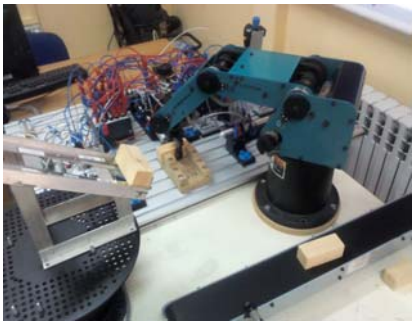

Figure 10. Disposal of raw material – Taking of the workpiece

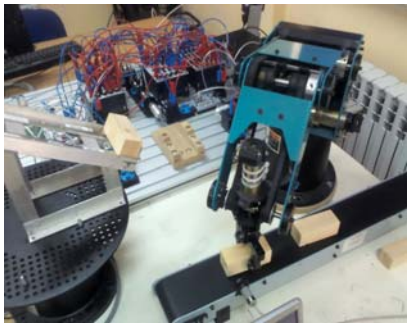

Figure11. Disposal of the workpiece on the conveyor belt

The synchronization of the robot operation – control unit and automated device for drilling during designing of program for robot control and periphery was analyzed and an algorithm of solution was given (Figure 12).
After the designing of electro-pneumatic device for the simulation of drilling and making of the program for the defined task, the testing in a real laboratory environment followed (shown in Figures 6, 9,10 and 11).

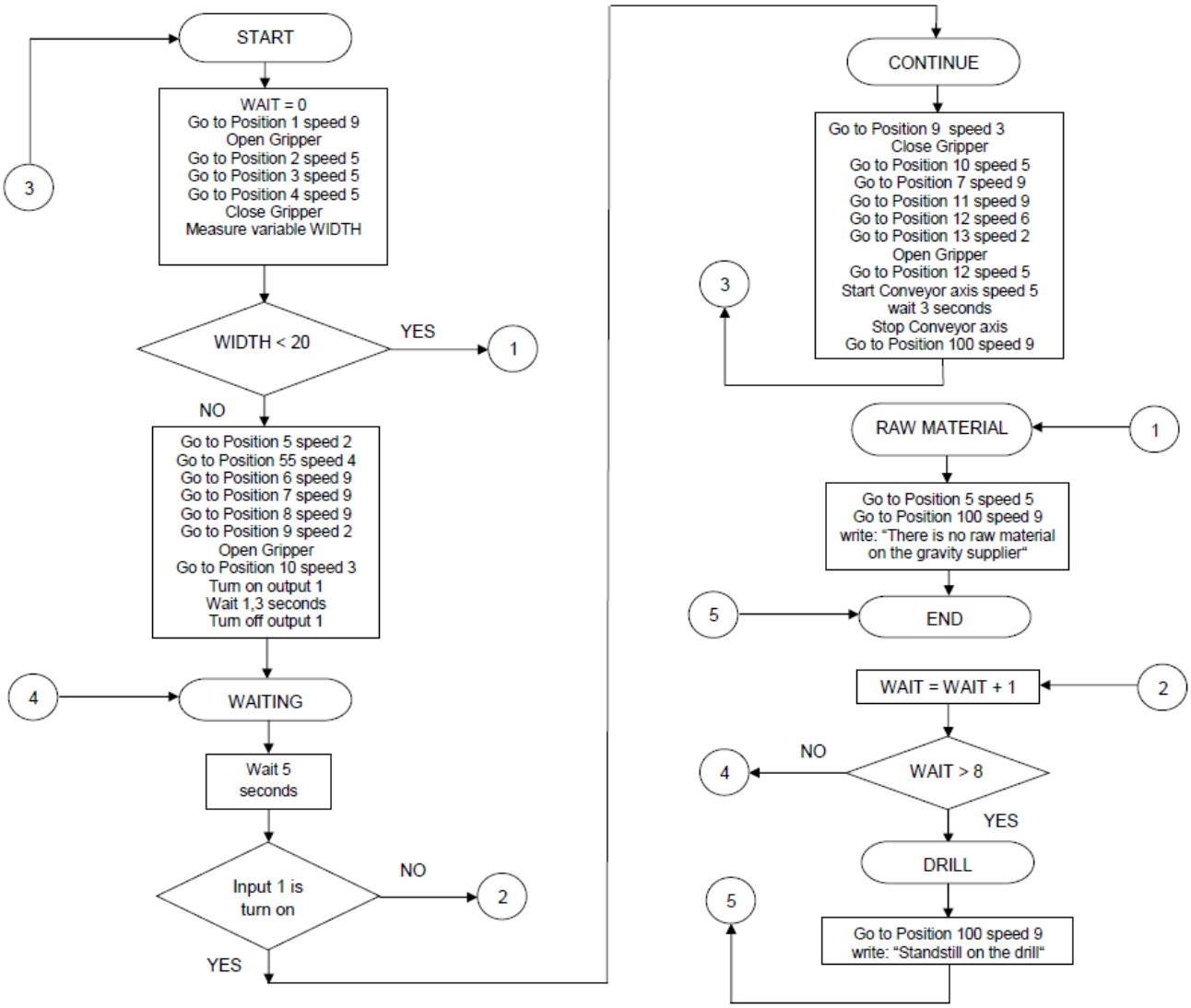

Figure 12. Algorithm of solution of defined technological tasks

4. Conclusion

In this paper, on the selected technological task, a technological solution using the robotic system Scorbot-ER 4u and electro-pneumatic equipment, was elaborated and presented. In the laboratory environment, the procedure of design and simulation of operation of solutions on the didactic equipment was performed. The design and testing of proposed solution gives students the opportunity to better acquire knowledge in the field of robot programming. The proposed solution enables the continuation of work on the proposed assignment in the direction of implementation of new theoretical and practical knowledge, and it helps to better prepare students for the labour market.

5. References

[1] T. Šarić, G. Šimunović and R. Lujić, "Researching and designing of hardware and software supports for an educational flexible cell," *Technical Gazette* vol. 15 no.3, p.p. 21-28, 2008.

[2] "Scorbot ER-4u User Manual," *Manchester, Intelitek*, 2001.

[3] "Scorbase for ER-4u User Manual," *Manchester, Intelitek*, 2001.

[4] "FluidSIM Pneumatics User`s Guide," *FESTO*, 2004.

[5] "FluidSIM Pneumatics", ver. 3.6, *Festo*, 2004.

SPENT MUSHROOM (*AGARICUS BISPORUS*) COMPOST

N. Romanjek Fajdetić [1*], B. Japundžić Palenkić [1], K. Ciprić [1] and M. Japundžić [1]

[1]University of Applied Sciences of Slavonski Brod, Slavonski Brod, Croatia
* *Corresponding author e-mail: nrfajdetic@vusb.hr*

Abstract
Spent mushroom compost is a viable and useful by-product of mushroom farming. After the mushroom crop is harvested, this organic material is steam treated to eliminate any pest, pathogens and weed seeds and then removed from the environment space. After the substrate has been pasteurized, it is referred to as spent mushroom compost. The material has been found to be good nutrient sources for agriculture because of its nutrient-status. It has a high cationic exchange capacity, and is very rich with macronutrients (N, P, and K) and micronutrients. It can be available fresh from the mushroom farm, or weathered by further composting. Spent mushroom substrate should be decomposed for at least 12 months either by natural weathering in pits or aerobic/anaerobic recomposting before use because it contains a lot of salt and unstable organic material. Spent mushroom compost contains about 1-2% nitrogen, 0,2% phosphorous and 1,3% potassium. In general, a good, organic compost, if used properly, can improve plant growth in poor or marginal soils.

Keywords:
Key words: spent mushroom compost,

1. Introduction

Generally mushroom growing is an eco-friendly activity as it utilizes the wastes from agriculture, poultry, brewery etc. and in turn produces fruit bodies with excellent and unique nutritional and medicinal attributes. [1]
Agaricus bisporus is more commonly known as the white or button mushroom. Compost for cultivation is prepared from mixture of organic materials horse and chicken manure, straw and gypsum. After composted and pasteurized this substrate is inoculated by button mushroom mycelium. Nitrogenous substances and calcium sulphate are added to ensure a selective substrate for optimal development of the mushrooms. The second main component in button mushroom production is 5 cm thick casing soil that is made of mixture of black peat moss and lime and covers mushroom compost. These products are formed into a rich organic media that serves as the nutrient source for mushrooms. The environmental conditions in the growth rooms are then manipulated to encourage fungal mycelium growth and produce mushrooms. After three flushes the substrate is exhausted or "spent" of its potential to produce mushrooms. The substrate is then subjected to a

steam treatment and removed from the growing houses. [2]

After the substrate has been pasteurized, it is referred to as mushroom compost. At that point, it can go on to be composted further either by active or passive. [3] Compost is considered „spent substrate" when one full crop of mushroom has been taken and further extension becomes unremunerative.[4] Spent mushroom substrate is a high nutrient, low odour, and weed free way to incorporate organic matter into your soil, reduce some nitrogen leaching potential in vulnerable areas and provide both macro and micro-nutrients to crop. [2] The diversified uses of spent mushroom substrate in managing agriculture, environment and recycling energy have come in light recently and because of which its name has been changed from spent mushroom substrate to "used mushroom substrate". The material has been found to be good nutrient sources for agriculture because of its nutrient-status. It has a high cationic exchange capacity, a measure of the amount of nutrients a medium can hold and a slow mineralization rate retains its quality as an organic matter. It can be available fresh from the mushroom farm, or weathered by further composting. Both types of spent mushroom substrate should have an earthy odour and be free of an ammonia or rotten egg sulphur smell. The particle size should be uniform and it should be fairly homogenous and resemble soil.

Moisture contents between 30 and 50% are easiest to evenly field apply and incorporate.
Dry matter between 40-60%
pH between 6-8
Carbon to nitrogen ratio that is generally below 30:1, which means it will give up nitrogen rather than tie up available nitrogen.

The nitrogen is about the same total value as dairy manure; only more of the nitrogen is in the organic form and is more slowly released over time. Studies in vegetables in the US have shown that there is less nitrogen leaching from spent mushroom substrate than from commercial fertilizers. As for the phosphorus and potash values, they are actually higher per ton than raw

dairy manure. This is not unexpected since the composting process tends to concentrate mineral nutrients. It contains appreciable amounts of iron, manganese, zinc and boron. The addition of spent mushroom substrate in nutrient poor soil improves its health by improving the texture, water holding capacity and nutrient status. Spent mushroom substrate incorporation in soil leads to an increase in both pH as well as the organic carbon content .[5] The experiments carried out for studying the effect of spent mushroom substrate on several crops have shown that the dry matter content of plants increases with incorporation of increasing amount of weathered or unweathered spent mushroom substrate in soil.[6] The phosphorus and potassium requirements of the crop plants can be fully met by incorporating 5% of spent mushroom substrate by volume, while nitrogen requirement by 25% of spent mushroom substrate by volume .[7] Spent mushroom substrate not only improves soil health but also helps in the turf establishment which, however, depends on the rate of spent mushroom substrate application in soil .[8] The aged mushroom compost is preferable over the fresh compost. [9] Spent mushroom substrate should be decomposed for at least 12 months either by natural weathering in pits or aerobic/anaerobic recomposting instead of disposing off in open on road side.

Passive composting
With passive composting, the process proceeds naturally with no further turning or addition of raw materials. Since the compost is not turned, it is best to mix the compost well in order to make a homogeneous mixture that leads to a more rapid decomposition process.

Active composting
Active composting is a process in which the compost windrow is actively turned to promote aeration, better mixing, and a more rapid decomposition process. Actively prepared compost takes less time to mature and is turned regularly to maintain high temperatures for more consistent and efficient composting. Since the process of turning compost can release odours, it is best to select a time of day for turning that is least inconvenient for neighbouring residences. Keeping track of wind direction can also help with selecting a proper time to turn compost. [10]
Similarly, the doses of recomposted SMS for various crops should be worked out on the basis of total nutrient (N.P.K.) requirement of the respective crop and the nutrient status of the soil/SMS. The recomposted spent mushroom substrate can be used singly as basal application or in combination with inorganic fertilizers. [11]
Spent mushroom substrate makes the soil suitable for raising vegetables. [5] Weathering in open for two to three years make spent mushroom substrate more suitable for either complete or partial substitution of growing media for flowers, vegetables, fruits, saplings, ornamental shrubs and other horticultural plants of economic importance. [12] In general, good, organic compost, if used properly, can improve plant growth in poor or marginal soils. This is because compost amended into those soils will improve the structure of clay soils, reduce surface crusting and compaction and therefore improve drainage, increase beneficial soil microbial activity, and provide nutrients to plants which can reduce the need for fertilizer. Overall, compost can be very beneficial to the soil, and mushroom compost is no exception. [13]

Mushroom compost has high water and nutrient holding capacity and exhibits no nitrogen draw down problems.

It can be used as fertilizer and soil amendment for farming, and supports plant growth in a variety of plant applications such as corn, pumpkin, tomato and potato yields and brassicas.

Mushroom compost supports plant growth of mulch hays from orchard grass, timothy, reed canary grass, tall fescue and brome grass.

It can be used as fertilizer and soil amendment for lawn care and landscaping; Mushroom Compost supports plant growth and inhibits artillery fungus.

Mushroom compost is therefore most useful on acid soils that are low in organic matter, where the liming effect of the chalk is an added benefit to soil fertility. It is not recommended for neutral, alkaline or chalky soils which would be made excessively alkaline by the addition of further chalk. Mushroom compost is excellent on the vegetable garden. Vegetable crops usually grow best when the soil not acid and where the soil is alkaline. Brassicas (cabbage, broccoli, cauliflower, kohlrabi, brussels sprouts and kale) are less likely to be infected by clubroot disease. Mushroom compost use should be avoided where ericaceous plants such as rhododendrons, camellias, azaleas and heathers are being grown, as these plants need acidic growing conditions and are chalk-hating. In ericaceous beds, leaf mould is preferable as mulch and soil improver, being pH neutral (broad leaves) or acidic (pine needle leaf mould) in its nature. [14]

The electrical conductivity is usually higher in spent mushroom compost than in soils, and is generally over 4 dS/m. [15] Many plants are sensitive to high level of salt in the soil. Problems due to high salt levels can result when too much spent mushroom compost is applied to the soli, or when plants are grown directly in spent mushroom

compost. Conductivity gradually goes down due to leaching during the fifth and sixth months of weathering, and stabilizes after twelve months. Most of the salts originally present in the spent mushroom compost are released during the first year of weathering. It should not be applied to young plants because they are particularly sensitive to high salt levels and ammonium. [16]

The best time of application to soil is from autumn to early spring. It should not be applied in the summer because this stimulates late season growth. It is usually applied in broadcast or in bands. Broadcast application provides a uniform effect through the orchard. Application in bands permits the use of lower doses of spent mushroom compost. After application it should be incorporated into the soil in order to prevent nitrogen loss.

Good agricultural practice dictates that no more than 250 kg/ha of nitrogen is sufficient where there are no problems with water quality, and no more than 170 kg/ha where are present water quality problems. When applied at a rate of 10 tons/ha, spent mushroom compost supplies approximately 80 kg/ha. As fertilizer it is more expensive than mineral fertilizers in terms of the nutrient content per unit weight. But nutrients are released slowly over longer time, and plants can use them more effectively. There are the other benefits such as increasing organic matter, water capacity, microbial activity, higher soil temperature and decreasing soil compaction. The benefits are not possible to see first year after applying, then in subsequent years.

Spent mushroom compost could be used as mulch to prevent weeds and to raise the soil temperature. Also it is used as alternative pesticide in form of compost tea (liquid extract of spent mushroom compost prepared by mixing one part of compost with four parts of water. The composition of compost is very variable and for this reason there are conflicting reports on the efficacy of using compost tea to control diseases.

2. Conclusion

Spent mushroom compost is extremely good source of nutrients for any kind of plants. It is more expensive than mineral fertilizers but it releases nutrients much longer. Beside that there are many others benefits as biological, physical and chemical soil improver. Growers have to be aware of the fact that benefits of using this fertilizer are visible for several years after application, but not during the first year after application.

3. References

[1] [Online]. Available: http://www.nrcmushroom.org/Folder_Recycling_SMS_Folder.pdf [Accessed: 20-Feb-2013].
[2] [Online]. Available: http://www.omafra.gov.on.ca/english/crops/hort/news/orchnews/2007/on-1207a5.htm [Accessed: 24-Feb-2013].
[3] [Online]. Available: http://www.americanmushroom.org/pdfs/MshrmSubstr.pdf [Accessed: 28-Feb-2013].
[4] Wuest PJ, Fahy HK and Fahy J (1995). Use of spent mushroom substrate (SMS) for corn (maize) production and its effect on surface water quality. Compost Science and Utilization. 3(1): 46-54.
[5] Kaddous FGA and Morgans AS (1986). Spent mushroom compost and deep litre fowl manure as a soil ameliorant for vegetables. In Proc. of Surface Soil Management Rotorua, New Zealand, pp. 138-147.
[6] Chong C, Cline RA, Rinker DL (1987). Spent mushroom compost and papermill sludge as soil amendments for containerized nursery crops. Combined Proceedings - International Plant Propagators Society 37: 347-353.
[7] Maher MJ (1991). Spent mushroom compost (SMC) as a nutrient source in peatbased potting substrate. Mushroom Science XIII (Part II): 645-650
[8] Landschoot P and McNitt A (1994). Improving turf with compost. Biocycle 35(10): 54-57.
[9] Lohr, V.I., D.L.Coffey(1987). Growth responses of seedlings to various rates of fresh and aged spent mushroom compost. HortScience 22(5):913-915
[10] [Online]. Available: http://www.americanmushroom.org/pdfs/MshrmSubstr.pdf [Accessed: 06.Mar-2013].
[11] [Online]. Available: http://www.nrcmushroom.org/Bul-SMS.pdf [Accessed: 08.Mar-2013].
[12] Beyer M (1996). The impact of the mushroom Industry on the environment. Mushroom News 44(11): 6-13.
[13] [Online]. Available: http://www.mushroomcompost.org/faqs.htm [Accessed: 10.Mar-2013].
[14] [Online]. Available: http://www.mushroomcompost.org/ [Accessed: 10.Mar-2013].
[15] [Online]. Available: www.hri.ac.uk/recoveg [Accessed: 12.Mar-2013].
[16] Uzun I.2004. Use spent mushroom compost in sustainable fruit production. Journal of Fruit and Ornamental Plant Research, vol.12

NEW SYSTEM FOR NONCONTACT CALIBRATION OF GAUGE BLOCKS

S. DVOŘÁČKOVÁ[1*], J. SOBOTKA [2*], P.BRDLÍK [2*], O. CÍP [3*], F. DVOŘÁČEK [4*]

[1]Technical University of Liberec, Department of Manufacturing Technology, Liberec 1, Czech Republic
[2]Technical University of Liberec, Department of Engineering Technology, Liberec 1, Czech Republic
[3]Institute of Scientific Instruments, Academy of Sciences of the Czech Republic, Kralovopolska 147, 612 64 Brno, Czech Republic
[4]Czech Metrology Institute, Regional Inspectorate of Liberec, Slunecna 23, Liberec, 460 01, Czech Republic
stepanka.dvorackova@centrum.cz

Abstract

The paper deals with the new system for contact–less calibration of gauge blocks (further only GB) with possibility of full automatization (optical measuring system is added by automatic exchanger of GB with capacity up to 126 pieces with nominal length from 0,5 up to 100 mm). The system combines laser interferometry and low-coherency interferometry – nevertheless under the new approach. The method rests in admeasurement of GB nominal length from both sides by means of combination light from continuous laser and pulse generator of wide–spectrum coherent light. In this paper will be described new system for calibration GB including method using these days according to ISO 3650.

Keywords:

Gauge Block,Calibration, Interferometer.

1. Introduction

For calibration GB are according to standard ISO 3650 used two basic methods. First uses laser calibration (or multiwave interferometry) for calibration – interferometry method. In this case is GB wrung on the reference plane and chosen interferometry technique is measured distance from reference plane to GB free side (nominal length of GB). Part of the laser interferometer – NPL TESA AGI 300s with applied GB is shown in fig. 1.

Figure 1. Laser interferometer measuring chamber for calibration GB (NPL TESA AGI 300 – Czech metrological institute)

The second method is based on the comparison of calibrated GB nominal length and reference gauge length – comparative method. In this case is used double-sided contact method by incremental length sensors. Measuring comparative system – TESA UPC is shown in fig. 2.

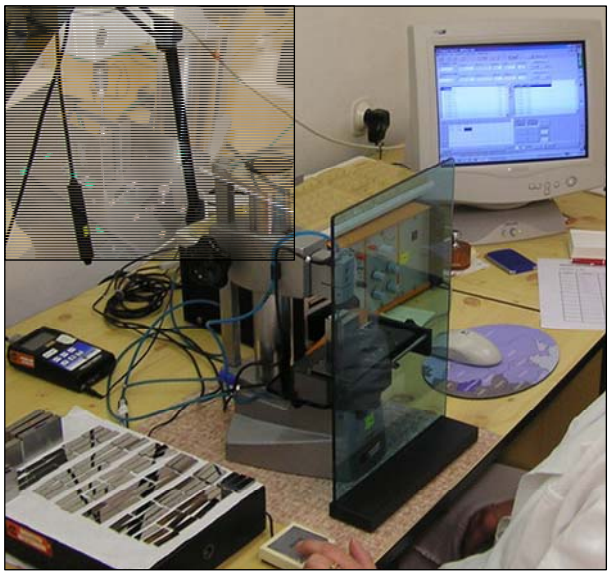

Figure 2. Comparative system for calibration GB (TESA UPC–Czech metrological institute)

New system for contact-less calibration of BG offers another option to both methods mentioned above – moreover it is contact-less system with possibility for full automatization. Such measuring system combines laser and low-coherency interferometry – still as newly developed system in comparison to similar systems. This method rests in admeasurement of GB nominal length from both sides by combination of light from continuous laser and wide-spectrum coherent lightpulse generator. Measuring system is shown in fig. 3.

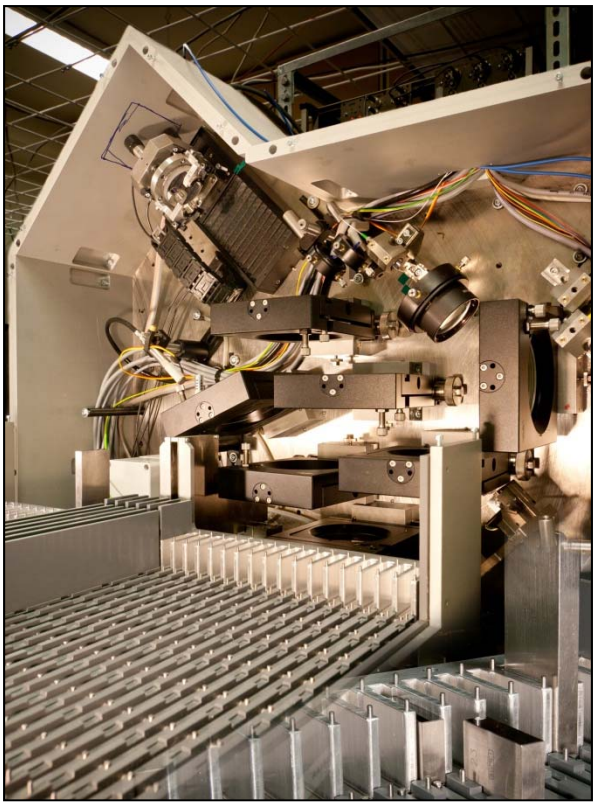

Figure 3. System for contact-less calibration of GB

2. Experimental Setup

Schema of the measuring setup is shown in fig. 4. The presented optical setup combines a Michelson interferometer and a Dowell interferometer [9], placed in the reference arm of the Michelson interferometer. The beam of white (wide-spectrum) light from the source is divided by semi-permeable Mirror 1 on two parts. Such created measuring beam of Michelson interferometer passes the pair of compensating plates CP, CP2 and reflects on the reference plate RS. Reference beam of the Michelson interferometer presents primary beam for Dowell interferometer. By Mirror 2 is split into two counter-rotating beams passes Dowell interferometer – triangle created by Mirrors 2, 3 and 4. Part of these beams is reflected by measured GB face, non-reflected part of counter-rotating beams passes along GB. So finally there are totally five beams in the output of interferometer and these beams are able for mutual interfere. According to low-cohesion interferometry principles is valid that there is interference of measuring and reference beam just under the balance state of interferometer. In the case of described experimental system it is possible to observe interference on the output of interferometer for positions of reference plate RS marked in the fig. 4 as P1', P2' and P3'. When reference plate RS is adjusted into position P2', there is interference of reference beam and part of measuring beam reflected from GB side P2. For reference plate position P3' there is interference of reference beam and part of measuring beam reflected from GB side P3. Position of reference plate P1' matches to interference of reference beam with part of measuring beam passes along gauge block. This state is equal to system configuration with mirror placed in position P1. For measuring gauge block length represents the position P1 (eventually P1') reference position given by experimental system configuration. Information about the mutual distance of measuring positions P1', P2' and P3' is taken from measurement by means of radiation HeNe laser (633 nm) which is using principles of conventional laser interferometry. Beam from HeNe laser is combined with white-light with the help of fiber optics on the output of measuring system.

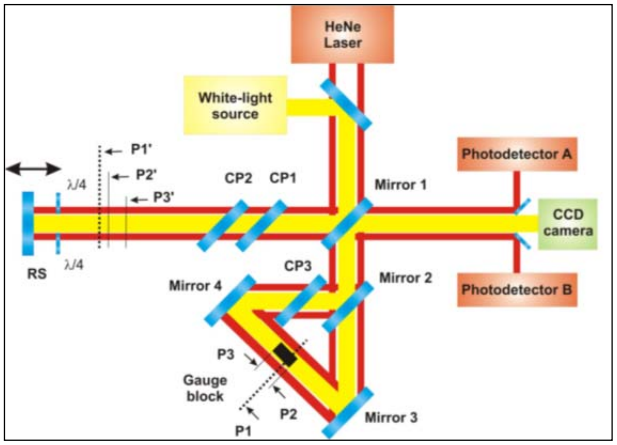

Figure 4. Optical setup for gauge blocks measurement. CP1, CP2 and CP3 are compensating plates, RS is a reference surface, λ/4 is a retardation quarterwave plate.

In Fig. 5 the picture recorded by camera on the output of measuring system is schematic demonstrated.

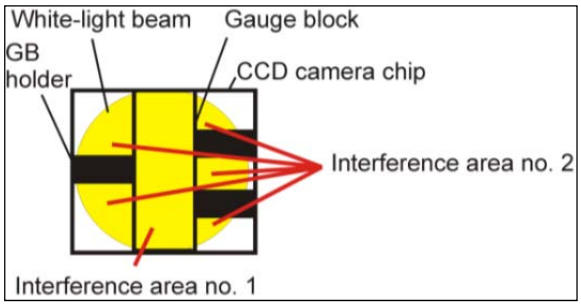

Figure 5.Schematic visualization of picture recorded by camera on the output of measuring system.The zone of interference 1 is valid for locations P2' a P3', the zone of interference 2 then for location P1'.

For better imagination of measuring principle, the example of obtained experiment result is shown in Fig. 6. This result of GB measurement shown three locations of white light mentioned above. The gauge block length (GBL)is then specified from equation (1):

$$GBL = \left|P1' \quad P2'\right| + \left|P1' \quad P3'\right| \qquad (1)$$

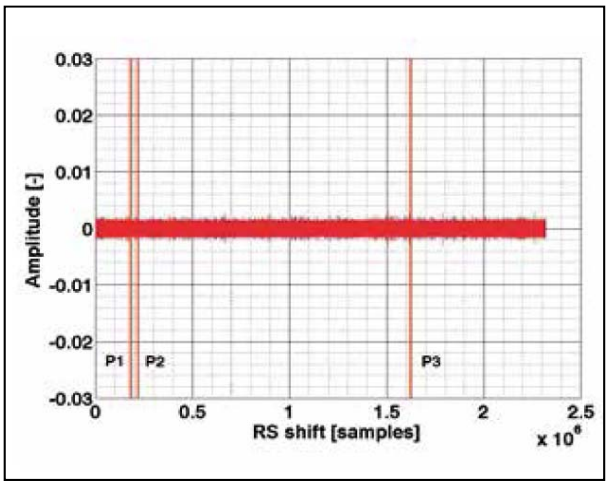

Figure 6.The example of BG measuring result

The same record which give the information about different positions of interference signal central point on side of GB then made possible by deeper analyze to explore sides of GB which can lead to detection of possible defects (Fig. 7).

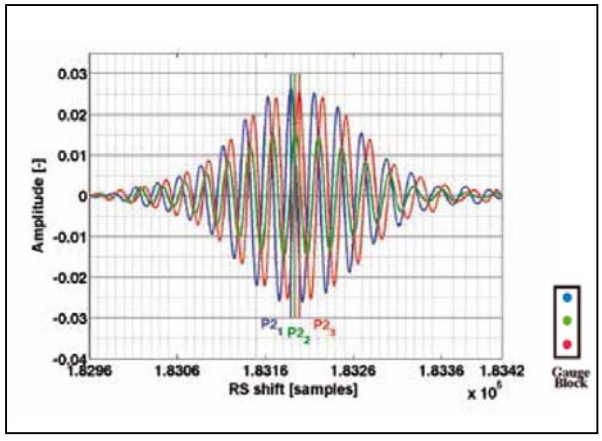

Figure 7.Detailed outlook on the recorded signal in P2 measuring position which makes possible to analyze GB side.

The described optical system was created with help of three-inches optics which enables to use stream about diameter 35mm and thus to measure whole area surface of GB. The gauge block is during measurement fixed on three-point holder (Fig. 4 and Fig. 5). The holder position is before every measuring automatically setup by piezoelectric screws with goal to reached maximal contrast of interference bands. Accordingly, the holder of reference surface is using the similar system where piezoelectric screws ensured reference surface undesirable tilt correction during measurement.

The optical assembly is completed by group of sensors for monitoring temperatures in different parts of system. It helps to correct temperature dilatations during measurement. Next important sensor ensures detection refractive index of air which is necessary for measuring of length with laser interferometer within the magnification range in tens of nanometers.

The automatic feeder was designed and created for presented system. This feeder could contain up to 126 pieces of GB within the range GB lengths from 0,5 mm to 100 mm. It enables full automatic calibration of the whole GB set with maximal possible elimination of undesirable influences which could appear by changing of GB [9 – 12].

3. Conslusion

This paper presents a new principle for contact-less gauge block measurement using a combination of low–coherence interferometry and laser interferometry. The experimental setup combines a Dowell interferometer and a Michelson interferometer to ensure a gauge block length determination with direct traceability to the primary length standard. This setup was designed for contact-less complex gauge block analysis providing information about gauge block length, gauge block surface profile (e.g. indication of scratches) and by analysis of the interference fringes shape, also about the gauge block edge flatness distortion. The designed setup is supplemented by an automatic handling system designed for a set of 126 gauge blocks (0,5 mm to 100 mm) to allow the automatic contact-less calibration of the complex gauge block set without a human operator.

A new system for contact-less calibrations of GB is currently tested and developed in terms of research project TA03010663. The system will be further (after attestation and certification) placed on workplace of Czech Metrologic Institute where will be with Czech producer of precision mechanics and precision engineering used for calibration of GB huge amount. The system will be offered into the international metrology development program.

4. Acknowledgement
This paper is related to the investigation on the Research Projects TA03010663: Advanced systems for length calibration gauge blocks and surface inspection of end standards, which are supported by the Technological Agency of the Czech Republic.
The paper was supported in part by the Project OP VaVpI Centre for Nanomaterials, Advanced Technologies and Innovation CZ.1.05/2.1.00/01.0005.

5. References

[1] Doiron, T.; Beers, J. The gaugeblock handbook. *NIST Monograph 180 with Corrections 2005*, 1–143.Reference source.
[2] Decker, J.E.; Miles, J.R.; Madej, A.A.; Siemsen, R.F.; Siemsen, K.J.; de Bonth, S.; Bustraan, K.; Temple, S.; Pekelsky, J.R. Increasing the range of unambiguity in step–height measurement with multiple–wave length interferometry – application to absolute long gauge block measurement. Appl. Opt. 2003, 42, 5670–5678.Reference source.
[3] Bönsch, G. Automatic gauge block measurement by phase stepping interferometry with three laser wavelength. *Proceedings of Conference on Recent Developments in Traceable Dimensional Measurements 2001,* 4401, 1–10. Reference source.
[4] Khavinson, V.M. Ring interferometer for two–sided measurement of the absolute lengths of end standards. Appl. Opt. 1999, 38, 126–136.
[5] Ishii, Y.; Seino, S. New method for interferometric measurement of gauge blocks with out wringing onto a platen. *Metrologia 1998*, 35, 67–73.
[6] Abdelaty, A.; Walkov, A.; Abou–Zeid, A.; Schödel, R. PTB'S prototype of a double ended interferometer for measuring the length of gauge blocks. *Proceeding of Simposio de Metrologia 2010,* SM 2010–S2C–2, 1–6.
[7] Buchta, Z.; Mikel, B.; Lazar, J.; Číp, O. White–light fringe detection based on novel light source and color CCD camera. *Measurement Science and Technology 2011*, 22, 094031–6.
[8] Ikonen, E.; Kauppinen, J.; Korkolainen, T.; Luukkainen, J.; Riski, K. Interferometric calibration of gauge blocks by using one stabilized laser and a white–light source. Appl. *Opt. 1991*, 30, 4477–4478. Reference source.
[9] Dowell, J.H. British patent No. 555672 1943.
[10] Číp, O.; Petrů, F. A scale–linearization method for precise laser interferometry. *Meas. Sci. Technol. 2000*, 11, 133–141.Reference source.
[11] Číp, O.; Buchta, Z.; Petrů, F.; Lazar, J. On–line monitoring of the refraction index of air for ultra–precise length measurement in the nano–world. *Proceedings of 8th IEEE Africon Conference 2007*, 8, 294–298.
[12] Lazar, J.; Číp, O.; Čížek, M.; Hrabina, J.; Buchta, Z. Suppression of air refractive index variation in high–resolution interferometry. Sensors2011, 11, 7644–7655.

THE INFLUVENCE OF CARBOXYL DIOXIDE COOLING ON MECHANICAL PROPERTIES OF BLOW MOLDED PRODUCTS

P.BRDLÍK

[1]Technical University of Liberec, Department of Engineering Technology, Liberec 1, Czech Republic.
pavel.brdlik@tul.cz

Abstract
This article presented deals with cooling problems of blow molding process. The problems consist in differences in cooling rate on interface wall of mould/ polymer/ blowing air. These differences could cause a non-uniform structure throughout the wall thickness, as well as changes of density, molecular orientation, birefringence, shrinkage or even warpage. The way how to reduce this negative effect is possible search out in degrease of the thermal difference in wall distribution. It mean increase cooling ability of internal cooling system. In last decade several techniques have been developed which solve just this problem. One of the very efficiency one is the injection of inert gas. The main aim of this article is exploring impact heat transfer ability changes on mechanical behavior of polymer materials which is crucial parameter for most of product.

Keywords:
Carboxyl dioxide, mechanical behavior, blow molding, internal cooling, polyolefin.

1. Introduction

The production of hollow products using blow-molding technology is a non-stationery, non-isothermal process where thermal energy is removed via the external cooling system of the mold and the gaseous medium of internal cooling system. When the cooling systems are compared, the efficiency is significantly different. The mold cooling system is more efficient than the internal system [1]. This is because the commonly-used blowing medium, air, usually has very low heat transfer ability. It leads to non-even thermal conductivity at the polymer/ mold interface and the air/ polymer interface [2]. Result could be a non-uniform structure throughout the product regarding wall thickness, as well as changes of density, molecular orientation, mechanical properties and many else [2], [3]. The way how to reduce this negative effect is possible to found in degrease of the thermal difference in wall distribution. Consequently, an improving the cooling ability of inner surfaces should ensure more uniform structure and a decrease in potential warpage or distortion in the mold. In last decade several techniques have been developed which solve just this problem [4]. One of them is the exchange of air during the cooling or exhaust phase with an air stream (circulated air). Another, much more effective technique is to apply a very cold medium, such as deep-cooled air, the injection of a mixture of water droplets with pressurized air or the injection of inert gas [4].

From the above introduced theories it is obviously that internal cooling could influence the nature of the products. Hence experimental measurements were taken to explore the changes of the microstructure and mechanical properties of products by connecting a progressive internal cooling system to the common blow molding process.

2. Experiment

When the introduced internal cooling variants are compared, it is clear that the biggest cooling effect is achieved by using the injection of inert gas [5] and therefore can produce the most obvious results. It is reason why to investigate the influence of internal cooling on microstructure and consequently on mechanical properties, the liquid carbon dioxide injection system was chosen. The mechanical properties were evaluated with help of tensile strength and deformation characteristics. The next important decision laid o selection of test material and product. From the polymers used, polyolefin was selected. This is because polyolefin is by far the most common material in the production of hollow products. Two variants were selected. The first one is a common linear, high-density semi-crystal copolymer called PE-Liten BB 29 and the second one is a homopolymer, PP-Mosten EH 0.1. The 0,3 liter container with 1,2 mm average wall thickness (figure 1) was chosen for planed experiment. This product make possible created the normalized test specimens (ČSN EN ISO 527-2), type 1BA. Production was carried out on classic single station, pneumatic blow molding machine GM 250 at G D K spol. s.r.o.. The specimens were loaded uni-axial tensile stress on tensile tester machine Housnfield H 10 KT.

Figure 1. Chosen product with test specimens place of taken

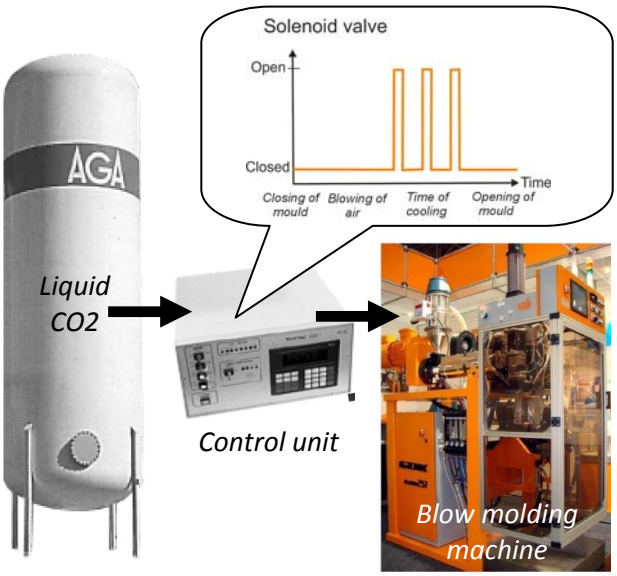

Figure 2. The liquid CO_2 injection system connection

Table 1. The experiment setting of measurement

Material	Melt temperature	Cooling temperature of mold	Critical cycle time of blow molding setting	Cooling time of blow mold cooling system	Machine time	Injection time of liquid CO2	Increase of efficiency
PP	190 °C	4°C	22s	16s	4s	8s	30%
PE-	190 °C	4°C	22s	16s	4s	8s	30%

The concept of the planned experimental is next. In first part, the common blow molding process running at the maximum production limit was measured. The melting temperature was set at 190 °C for all the measurements, which made the evaluation more transparent. Furthermore, the temperature of the circulated water of the external cooling system was set at 4°C for all cases. This was the lowest temperature to achieve the maximum cooling effect and does not lead to sweating of the mold. Next, the carbon dioxide cooling system was connected to the common blowing process (the sheme of coonection is shown in figure 2). Thermographic pictures and test specimens were taken from each setting to additionally analyze the mechanical properties. Concretely values of setting blow machine and CO_2 injection system are shown in table 1.

3. Results and Discussion

This part of article deals with evaluation and discussion of created experiment. In the first step, the reached cooling efficiency of carbon dioxide is presented. Consequently, the influence internal CO_2 cooling on mechanical properties is evaluated.

3. 1 The Efficiency of CO_2 Cooling System

The evolution of cooling efficiency was analyzed by taken thermographic pictures, fig. 3.

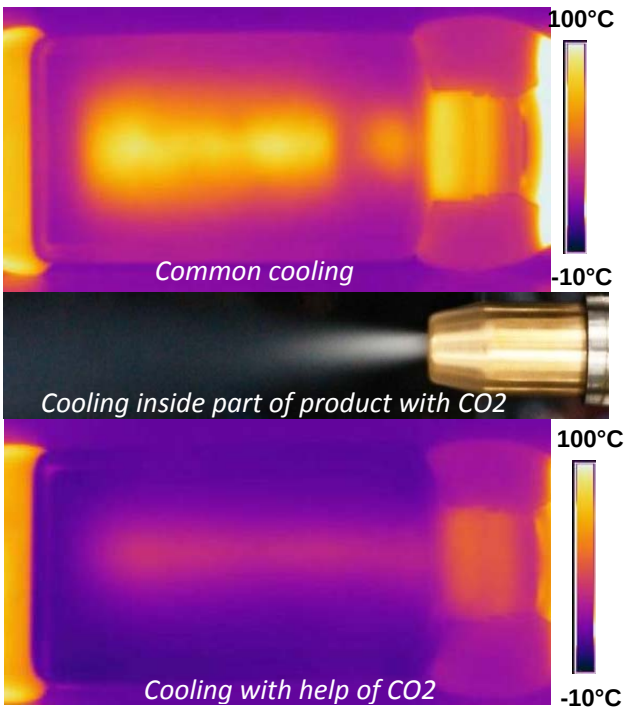

Fig. 3 Thermographic pictures of experiment setting

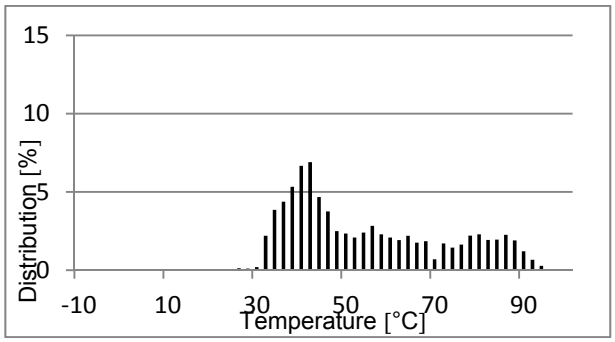

Figure 4. Distribution of temperature by common cooling

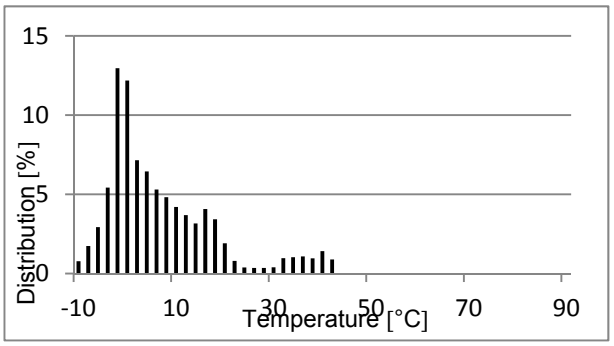

Figure 5. Distribution of temperature by cooling with help of carboxyl dioxide

From the radiometric pictures (figure 3) and graphs of distribution of the temperature (figure 4 and 5), the considerable cooling effect of carbon dioxide is clear. The improvement in cooling ability led to a demooulding temperature decrease. The averege temperature dorped about 50°C, maximal temperature about 40°C. This degrease of critical demoulding temperature made posssible to 30% increasing of productivity.

3. 2 The Mechanical Behavior

The theoretically and eperiment research say that mechanical properties are predetermined among others their structure. The microstructure of the polymer is composed of deposited (crystals) and amorphous fragments. Their rate is specified as percentage of crystalline. The quantity of fragments created is mainly influenced by the ability of the material to crystallize, but the thermal-kinetic conditions also have a considerable impact [6]. For example, if slower cooling is applied, it gives the spherolites more time to grow than with faster cooling. The result is creation less, but bigger spherolites than in case of more intesive cooling variant [6]. For our experiment it means that with lower efficiency of cooling should increase area of spherolits and so percentage of crysltallinity.

For the evaluation of mechanical properties of semi-crystal polymers, it is necessary to know that crystal fragments have different mechanical properties from amorphous ones. Their closer ordering leads to higher adhesive forces [6]. Consequently, the increasing percentage of crystals leads to increased strength, mechanical stiffness and hardness by several degrees of toughness. The amorphous segments are possible to imagine as joints about which the crystals can rotate by deformation. It contributes to improving toughness and elongation [6].

How does influence connection of progressive internal cooling system microstructure and so on mechanical properties of polymers? From the theoretical statement introduced above, it can be assumed that the percentage of crystalline will degreas and the spherolites would be smaller. Probubly the easiest test for detection of crystalline changes is the determination of the density. The crystal fragments contain macro-molecules which are closer together than the macro-molecules in amorphous locations. Consequently these areas have a higher density [6]. The increase in density then clearly indicates an increase in the percentage of crystals. Therefore, the densities of both materials were measured. The results (tab. 2) confirmed introduced theory. Higher densities were obtained in less efficiency cooling variants. Therefore, it is possible to say that the connection intensive internal cooling evoked small degrease of percentage of crystalline for both polyolefin.

Table 2. The measured densities by experimental cooling variants

Material	Cooling variant	Density [$Kg.m^{-3}$]	Standard deviation [$Kg.m^{-3}$]
PE	Common cooling	901,9	0,6
	Cooling with CO_2	899,8	0,7
PP	Common cooling	944,0	1,0
	Cooling with CO_2	941,7	1,1

Table 3. Tensile test results

Material	Cooling variant	Yeld Point in tension [MPa]	Standard Deviation [MPa]	Ultimate Strength [MPa]	Standard Deviation [MPa]	Deformation of Yeld Strength [%]	Standard Deviation [%]	Deformation of Ultimate Strength [%]	Standard Deviation [%]	Modulus of elasticity [-]	Standard Deviation [-]
PE	Common cooling	16,0	0,2	28,1	0,7	10,8	0,1	821,0	53,7	420	19
	Cooling with CO_2	15,7	0,6	28,9	1,1	10,5	0,3	880,1	26,9	504	22
PP	Common cooling	25,6	1,5	9,2	1,0	36,9	2,6	679,9	56,5	617	150
	Cooling with CO_2	26,3	0,7	8,5	0,6	37,1	2,3	671,7	57,0	679	202

With regard to above mentioned theories and results it possible says that examined test specimens from production process without connection cooling system should reach the highest value of tensile strength but the lowest values of deformations. Results of uniaxial - tensile test didn´t confirmed this premise, as can be seen in the table 3. Altought there are some differences between the results, differences are very small and could be with relation to reached values of standard deviations neglected. The last evaluated parameter was the modulus of elasticity. The reached results confirmetd theorie, that material with higher percentage of crystallinity should get higher values of modulus of leasticity. But it is important to note that also here the standard deiviation is very large.

4. Conslusion

The essential goal of this work is focused on the investigation of the influence of carboxyl dioxide cooling on mechanical properties of blow modled products. Theoretical research states that increase of internal cooling could evoked change in microstructure of semicrystalic polymer. Consequently, the chenge of mechanical properties could by noted too. The presented resutls showed samll change of microsturcture (different percentage of crystalline) but with relation to standart deviation the chages of mechanical properties is not possible to declare.

For production company it means that the cooling effect of CO_2 had not significant influence on mechanical behavior. Improving the cooling ability of inner surfaces then could bring increase productivtiy (in our experimetal settign 30%) without negative effect on product cvality. The cvality could theoreitcal increase becouse it is ensured more more uniform thermal distribution on both sides of plastic article and conseqentely decreases potential warpage or distortion in the mold. Therefore, the effect of internal cooling is possitive. But but question is how the mechanical properties are changed by production larger products with thicker wall? Becase the differences in morphology increas with increasing product thickness.

5. Acknowledgement

This paper was prepared due to the financial support from Student Grant Contest project 28005 **(SGS 28005).**

6. References

[1] ROSAT, D. V. - ROSAT, A.V. - DIMATHIA, D.P. (2004). C. H. Verlag. *Blow Moulding Handbook*. Hanser Gardner Publications. Munich, Germany p. 237-243, ISBN 1-3446-22017-8

[2] KALYON D. M., JEONG S. Yu. Microstructure Development in Blow Molded Amorphous Engineering Plastic. Journal of Plastic, Rubber and Composites Processing and Applications. vol .15, no. 2, p. 95-101, 1991, ISSN 0959-8111.

[3] TAN, S.B, HORNSBY P.R, MCAFEE M.B, KEARNS M.P., MCCOURT M.P. Internal Cooling in Rotational Molding – a Review. Journal of Polymer Engineering and Science. vol . 51, p. 1683-1692, 2011, ISSN 1548-2634.

[4] HUNKAR, D. B. Coolin Blow –Molded Bottles From the Inside Out. Journal of Plastic Engineering. vol . 29, p. 25-27, 1973, ISSN: 0091-9578

[5] JORG, CH. (2006). Carbon dioxide cooling method may take the waiting out of plastic parts. Journal of Automotive Engineering. p. 40-41, ISSN 2008-9899.

[6] KREBS, J. Teorie zpracování nekovových materiálů. Liberec: Technická univerzita v Liberci, p.20-30, 48-55, 90. 2006, ISBN 80-7372-133-3.

CADMIUM AND STRONTIUM CONCENTRATIONS IN OATS (*Avena sativa* L.) GRAIN AS AFFEXCTED BY LIMING

Iljkić Dario, Kovačević Vlado, Rastija Mirta

Faculty of Agriculture of J.J. Strosmayer University in Osijek, Kralja Petra Svačića 1d, 31000 Osijek, Croatia
* *Corresponding author e-mail:* **diljkic@pfos.hr**

Abstract
The stationary field trial of liming by dolomite powder (0, 5, 10 and 15 t ha^{-1}) was started in spring 2003. The field trial was conducted in four blocks each of 370 m^2 area. Each block was divided in four subplots of 92.5 m^2 which represented four replicates. Oats was grown on the experimental site in the 2011 growing season. Aim of this study was testing subsequently effects of liming in the growing season 2011 on oats (grain yield, cadmium and strontium concentrations in grain).Using the highest lime rate resulted by oats yield increase by 16% (6.26 and 7.25 t/ha, for the control and 15 t/h of dolomite, respectively). Also, harmful elements cadmium and strontium in grain were significantly decreased as affected by liming (0.79 and 0.59 mg Cd/kg, 1.71 and 0.73 mg Sr/kg, respectively.

Keywords: liming, oats, grain yield, cadmium, strontium

1. Introduction
Oats (*Avena sativa* L.) is high valuable food in human and livestock nutrition. Among the cereals, oats are the richest sources of calcium, phosphorus and iron, as well as the vitamins thiamine, riboflavin and tocopherol [1]. However, these advances of oats are insufficiently using in human diet in Croatia. The harvested area of oats for the 2001-2010 decade period in Croatia has been only about 21308 ha/year [2]. Oats growing area in Croatia was considerably reduced in comparison with the periods of the sixties (53340 ha), and seventies (38488 ha) of the last century [3] and it is in accordance with the global decreasing trend of oats growing areas [4]. In general, oat plants require more water and are relatively tolerant to cool, cloudy weather and acid soil. Heavy metals contaminations becoming serious problem for the health status of human population. Aim of this study was testing liming effects on grain yield and cadmium (Cd) and strontium (Sr) concentrations in grain of oats.

2. Materials and methods
The field experiment with increasing rates (0, 5, 10 and 15 t/ha) of dolomite powder (56% CaO + 40% MgO) application was started at the beginning of May of 2003 on the acid soil (pH in 1n KCl 3.74) in Badljevina (Pakrac municipality, Pozega-Slavonia County). The field trial was conducted in four blocks each of 369.6 m^2 area ordered in sequence of treatments from 0 to 15 t/ha. Each block was divided in four subplots of 92.4 m^2 which represented four replicates. In the next years (2004-2011) the experiment was fertilized differently, dependent on the field crop, in level of the ordinary fertilization. Crop sequence for the 2003 - 2009 was as follows: maize (2003 – 2005) – spring barley (2006) – maize (2007). These results were elaborated in the previous study (Kovacevic and Rastija, 2010). Winter wheat was grown for the 2009/2010 growing season and the results were shown in the study by Iljkic et al. (2011). The spring oats (the cultivar *Baranja* – Bc-Institute Zagreb) was grown on the experiment site in the 2011 growing season. Grain yields, grain composition (P, K, Mg, Fe, Mn, Zn and Zn concentrations) of oats, cropping practices and weather characteristics were elaborated in the previous study [5].
The grain samples of oats were taken from the portion of grains collected from 1-m^2 area of trashed seeds and prepared for chemical analyses by grinding. The total amounts of the individual elements in grain samples were determined using inductively coupled plasma (ICP) after their microwave digestion by concentrated HNO_3+H_2O_2. These analyses were made by Jobin-Yvon Ultrace 238 ICP-OES spectrometer in the laboratory of the RISSAC, Budapest. The data were subjected to the analysis of variance (ANOVA) and treatment means were compared using t-test and subsequent least significant difference (LSD) at the 0.05 probability level.

3. Results and discussion
In general, liming was useful soil management practice on the acid soil, because grain yields of the field crops were considerably increased compared to the control. However, the nutritional value of oats grain with aspect of manganese, zinc and copper status were the lower. These properties are in close connections with liming effects on the soil pH increases from very acid (3.74) to nearly neutral value of 6.36 (Table 1). Liming with dolomite in spring 2003 subsequently affected on grain yield of oats in the 2011 growing

season. Effects of liming on the nutritional value of oats grain with aspects of nutrients composition was positive regarding increases of P and Fe status, while concentrations of Zn, Mn and Cu in grain were decreased by liming. These effects were mainly in accordance with effects on soil pH on nutrient availabilities (Tables 1 and 2). Also, contents of harmful elements cadmium and strontium in grain (Table 2) were significantly decreased as affected by liming (0.79 and 0.59 mg Cd/kg, 1.71 and 0.73 mg Sr/kg, for the control and 15 t/ha of dolomite, respectively).

Table 1. Impacts of liming on soil pH, grain yield, Cd and Sr status in grain of oats

	Dolomite (t ha^{-1}) 2003				LSD
	0	5	10	15	5%
	Grain of oats (mg/kg in dry matter): the growing season 2011				
Cadmium	0.79	0.79	0.67	0.59	0.10
Strontium	1.71	1.43	0.92	0.73	0.18
	Grain yield of oats				
t ha^{-1}	6.26	6.25	6.96	7.25	0.55
	Soil pH (October 2004)				
pH in KCl	3.74	4.90	5.71	6.36	0.37

Table 2. Grain composition of oats [5]

Element	Dolomite (t ha^{-1}) 2003				LSD
	0	5	10	15	5%
	Grain of oats (mg/kg in dry matter): the growing season 2011				
P	3242	3897	3792	4202	302
K	5048	4805	4648	4859	ns
Mg	996	1303	1266	1283	152
Fe	57.3	60.4	60.4	66.6	6.3
Mn	85.0	67.8	46.2	39.3	6.7
Zn	30.8	28.6	22.9	19.8	3.0
Cu	4.84	4.76	3.81	3.35	0.42

Table 3. Grain yields of field crop [5] [6][7]

Crop and year	Dolomite (t/ha) 2003				LSD
	0	5	10	15	5%
Grain yield (t/ha)					
Maize 2003	6.75	7.49	7.53	7.76	0.93
Maize 2004	9.82	11.76	12.29	12.01	0.68
Maize 2005	3.72	8.05	9.35	8.72	0.90
Barley 2006	2.70	2.94	2.86	3.24	0.30
Maize 2007	3.60	4.04	4.72	5.40	0.72
Wheat 2010	2.92	3.44	3.34	3.24	0.40

Liming had mainly considerable effects on yields of the other tested field crops, especially maize, in this stationary field experiment (Table 3).
In the some previous studies in Croatia, also considerable effects of liming on decreases of Cd and the other harmful elements in grains of the field crops were found [8] [9][10][11]][12].

4. Conclusion

In general, liming was useful soil management practice on the acid soil, because grain yields of the field crops were considerable increased compared to the control. However, Mn, Zn and Cu contents were lower. The harmful elements cadmium and strontium in grain of oats were significantly decreased as affected by liming.

5. References

[1] „Corn Agronomy-Where science meets the field“(Online) Available: crop.agronomy.wisc.edu/crops/oat.(Accessed: 30-July-2013.).
[2] http://faostat.fao.org/site/567 (Harvested Area of Oats in Croatia).
[3] Statistical Yearbooks of Croatia, The State Bureau for Statistics, Zagreb (Online). Available: http://www.dzs.hr/
[4] crop. agronomy.wisc.edu/crops/oat.
[5] D. Iljkic, V. Kovacevic „Impacts of liming on soil status, yield and nutritional value of spring oats“. In: Proceedings, of the 48th Croatian & 8th International Symposium on Agriculture .17-22 Febr. 2013 Dubrovnik (Maric S. and Loncaric Z. Editors), Faculty of Agriculture, Univ. J.J. Strosmayer in Osijek, p. 484 – 488.,2013.
[6] D. Iljkic, M. Rastija, G. Drezner, K. Karalic, R. Sudar „Impacts of liming with dolomite on the wheat yield“. Proc. of Intern. Conference „Soil, Plant and Food Interactions“, 6–8 Sept. 2011, Faculty of Agronomy, Mendel University in Brno, Czech Republic, p. 141-146.,2011.
[7] V. Kovacevic, M. Rastija „Impacts of liming by dolomite on the maize and barley grain yields“, Poljoprivreda , Vol 16, No 2: 3-8., 2010.
[8] V. Kovacevic, D. Simic, I.Kadar, D. Knezevic, Z. Loncaric „Genotype and liming effects on cadmium concentration in maize“. Genetika, 43 (3): 607-615., 2011.
[9] V. Kovacevic, A. Vragolovic „Genotype and environmental effects on cadmium concentration in maize“. Journal of Life Sciences, USA 5 (11): 926-932., 2011.
[10] L. Andric, M. Rastija, T. Teklic, V. Kovacevic „Response of maize and soybeans to liming“, Turkish Journal of Agriculture and Forestry 36: 415-420., 2011.
[11] V. Kovacevic, A. Sudaric, M. Antunovic „Mineral Nutrition. In: Soybean Physiology and Biochemistry“ (edited by Hany A. El-Shemy). InTech Publisher, p. 389 – 426 November 2011.

[12] V. Kovacevic, I. Kadar, J. Koncz, I. Brkic, D. Banaj "Cadmium and lead status in corn hybrids grown on acid soil of Eastern Croatia", Poljoprivreda/Agriculture 8 (1): 10-14., 2002.

THERMAL PROPERTIES EVALUATION OF COMPOSITE WITH PP MATRIX AND α-CELLULOSE FILLER

M. Borůvka[1*]

[1]*Technical University of Liberec, Department of Engineering Technology, Studentská 2, Liberec, 461 17*, Czech Republic
** Martin.Boruvka@tul.cz*

Abstract

This paper deals with the evaluation of thermal properties of injection molded parts based on synthetic PP matrix reinforced by α-cellulose filler. Growing demands and requirements for these 'green' materials constantly increasing. Materials in plant and animal kingdom are entirely based on composite principle and cellulose is the most common organic compound affecting the Earth's surface which finds its application in many branches of the modern industry. Using differential scanning calorimetry (DSC) were evaluated thermal properties of PP/α-cellulose composites, depending on the different percentage content of α-cellulose within the weight ratio of 10% up to 30%. In recent studies we observed that hemp and banana fibres work like natural nucleating agents and due to this fact we evaluate thermal properties of PP/α-cellulose composites.

Keywords:
Natural fibres, cellulose, DSC, thermal properties

1. Introduction

Materials in plant and animal kingdom are entirely based on composite principle. These natural composites were created for a specific purpose, a specific strain and the desired function, with ingeniously crafted structure [1]. Synergy between strong-stiff fibres and flexible matrix allows the construct composites with high strength, stiffness and toughness. These composites exceed everything, what was previously achieved by treatment of conventional materials, and therefore they are given as much attention. They indicate the direction of technology development in all scientific fields, especially in the aviation, aerospace and automotive industries.

Nowadays it is possible to use natural material not only as biopolymers but also as fibres reinforcements. Pressure on the application of such materials is constantly increasing (Fig. 1), not only due to the economic situation resulting from constantly increasing price of oil, not only due to the possibility of influencing the final and utility properties of the products, but also in terms of climate change resulting from almost unresolved recycling existing parts of synthetic plastics, synthetic plastics incineration and landfilling. With increasing filler content decreases also the volume of consumed synthetic plastics and therefore, also dependent on the petroleum products [2].

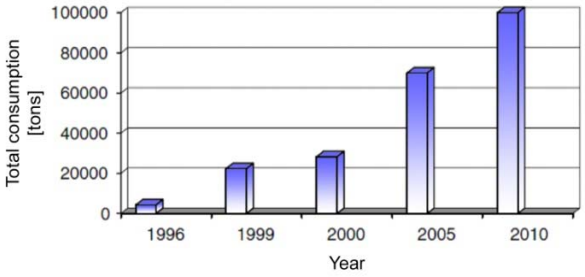

Figure 1. Growth in consumption of natural fibres in western Europe [2].

The advantage of natural fibres compared to the conventionally used fibrous material is their low weight, low abrasion, better electrostatic properties, better vibration absorption and noise reducing properties, CO2 neutral, biodegradability and especially low price. There are also disadvantages like low thermal stability, wettability and compatibility with the hydrophobic polymeric matrix [3].

Such fibres are reinforced by helically arranged crystalline microfibrils of cellulose, which are connected by amorphous lignin matrixes. In most plants fibres are cellulose microfibrils oriented at an angle to the normal fibre axis called the microfibrillar angle (MFA) (see Fig. 2).

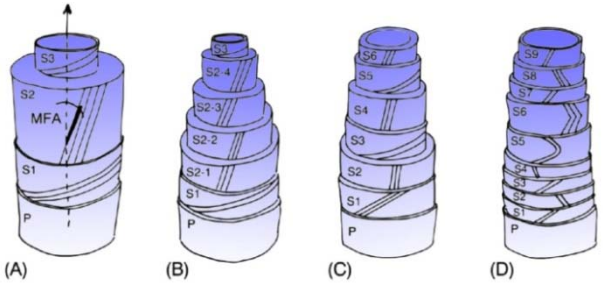

Figure 2. Schematics of possible cell wall organisation in (A) wood fibres, (B) bast fibres, (C) monocotyledonous plant fibres (bamboo) and (D) seed fibres. Black lines indicate orientation of cellulose microfibrils [1].

Cell-wall represents the functional structure for every kind of plants [4]. Each microfibril is a string of cellulose crystallites, linked along the chain axis by amorphous domains (Fig. 3) [5]. Microfibrils have typical diameter of about 10−30 nm and are made up of 30 to 100 cellulose molecules in a extended chain conformation [2].

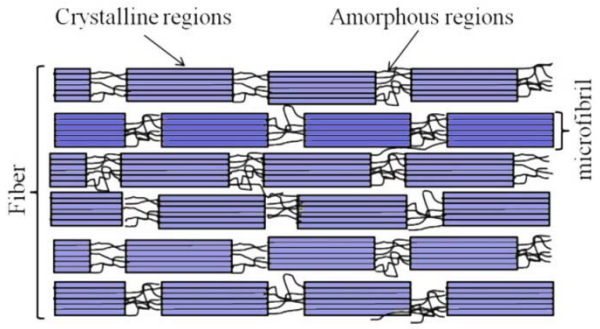

Figure 3. Schematic diagram of the semicrystalline cellulose fibre physical structure [5].

Using progressive elimination of less oriented parts leads to nanofibres with a raising degree crystallinity (as far as 100% e.g. whiskers). Raman spectroscopy technique has been used to measure the elastic modulus of native cellulose crystals, with a reported value of approximately 143 GPa [5].

2. Method

Firstly we prepared the composites by adding the α-cellulose microfibrils (Fig. 4) in to synthetic PP matrix (Tab. 2) within ratio 10, 20 and 30 (wt. %) (wt. % - percentage by weight).

All natural fibres are hydrophilic from its natural essence and primary objective transverse is lignocellulosic structure that contains a strongly polarized hydroxyl groups. For the use of natural fibres as reinforcement of polymeric matrixes are important their mechanical properties and a high-quality interfacial interface. The combination of non-polar hydrophobic polymer matrix and polar hydrophilic natural fibres creates poor interface with low adhesion of both components.

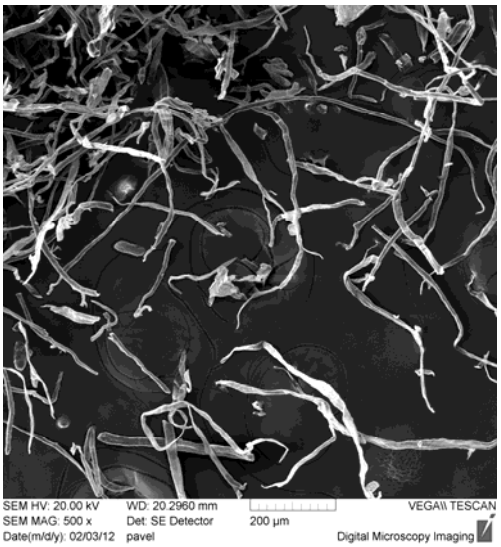

Figure 4. Image of the α- cellulose from the scanning electron microscopy (SEM)

Table 2. Properties of THERMOFIL PP E020M

Properties	Value	Unit
Volume Melt Flow Index	14,7	cm^3/10min
Tensile Modulus of Elasticity	1600	MPa
Yield Strength (Ultimate Strength)	27	MPa
Nominal Strain at Yield Strength	5	%
Tensile Stress at Fracture	16	MPa
Nominal Strain at Fracture	39	%
Charpy Impact Energy (+23°C)	9	KJ/m
Charpy Impact Energy (-35°C)	4	KJ/m
Flexural Modulus of Elasticity	1290	MPa
Flexural Strength	35	MPa
Hardness - Shore D	59	-
Melting Temperature	166	°C
Crystallization Temperature	125	°C

That implies poor wettability of fibres by polymeric matrix. Therefore is needed a specific coupling agents to enhance the compatibility between filler and matrix. For this experiment were used Fusabond (DuPont) 4 (wt. %) and Struktol SA1012 (Struktol company of America) 3 (wt. %). Fusabond is based on the maleine anhydride (MA) which is by the producer grafted (g) with PP chains which will be used as composite matrix. Grafting is usually carried out by radical mechanism at creation compound MA-g-PP. PP connected on the MA is during compoundation physically implemented into PP matrix by which there is complete interlacing of the PP matrix with natural fibres. Struktol has a similar function. The difference is in free radical creations, which enable connection of the polar and non-polar composite components. Covalent bond is created by the ion mechanism initiated by the additive hydrolysis.

For fabrication composite pellets was used twin screw extruder (Fig. 5) flowed by water bath and pelletizer. Output product was composite compound. Coupling agents and α-cellulose was dosed directly into the melting chamber of extruder in the recommended position by external device, working on the gravimetric principle. The reason for dosing fibres in the front parts of the extruder (near granulation head) is to prevent excessive shear stress of fibres during compounding melt composite and thus their damage or thermal degradation.

In the previous operation extruded string passed through a water bath. Natural fibres absorb moisture causing reversible and non-reversible swelling. Due to this fact it was necessary to dry granulated composite in stationary laboratory oven.

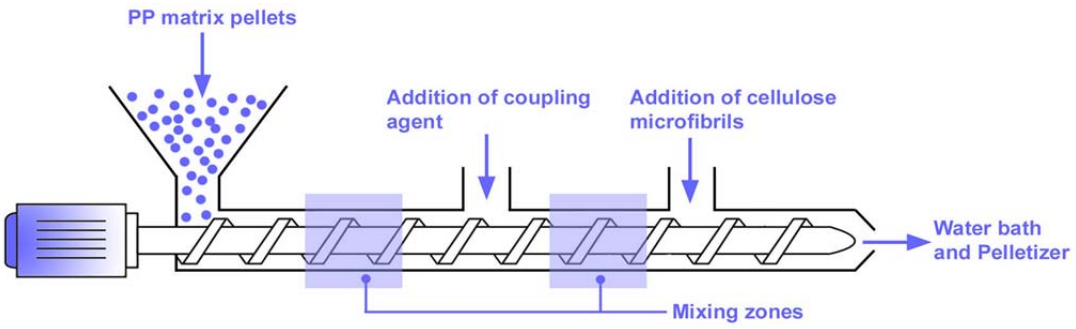

Figure 5. Schematic of compounding procedure

From composite pellets were for the subsequent evaluation of thermal composite properties injected on injection molding machine the multipurpose test specimens according to ISO 3167.

Study of thermal properties and crystallization was carried out with a DSC 6 Perkin Elmer (Fig. 6) which was calibrated against an indium standard. As a reference, was used an empty aluminium pan. For injection moulding thermal history evaluation in relation to the amount of micro-fibrillated cellulose (MFC), the samples amount was 10 mg and analysis run at 10 °C.min-1 heating/cooling ramp in one heating-cooling cycle in a nitrogen atmosphere (flow rate 50 ml.min-1). Inert atmosphere also ensures exhaust performances rising at warming of sample and increases the quality of measuring.
From the DSC thermograms we studied effect of micro-fibrillated cellulose on crystallization of PP and thermal properties such as endothermic melting temperature (Tm), melt crystallization temperature (TC), melting enthalpy (ΔHm) and melt crystallization enthalpy (ΔHC).

Figure 6. DSC 6 Perkin Elmer

3. Results and discussion

Typical DSC thermogram of thermoplastic polymers are shown in Fig. 7. Extremes (peaks) in termograms determine melting and crystallization temperature, area below peaks then represent difference between melting enthalpy (ΔHm) and melt crystallization enthalpy (ΔHC).

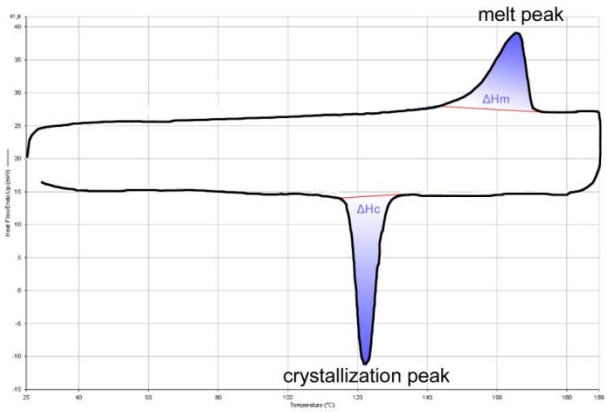

Figure 7. Schematic DSC curve for thermoplastic polymers

DSC thermograms of PP/α-cellulose composites with 10, 20 and 30 wt. % content of microfibrills and 4 wt. % of Fusabond coupling agent are shown in Fig. 8.

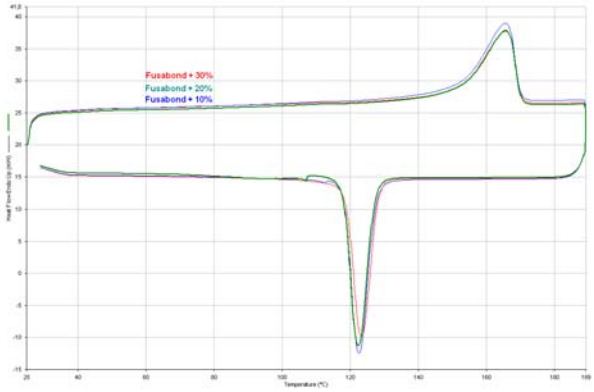

Figure 8. DSC results for PP/α-cellulose composites with Fusabond coupling agents

DSC thermograms of PP/α-cellulose composites with 10, 20 and 30 wt. % content of microfibrills and 3 wt. % of Struktol coupling agent are shown in Fig. 9.

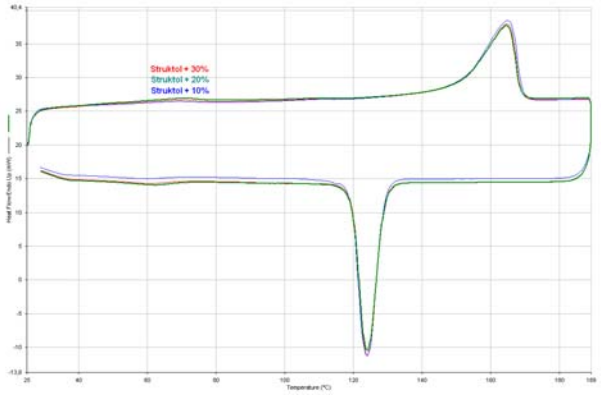

Figure 9. DSC results for PP/α-cellulose composites with Struktol coupling agents

Observed melting temperature (Tm) (Fig. 10) and melt crystallization temperature (TC) (Fig. 11) is summarized in following figures.

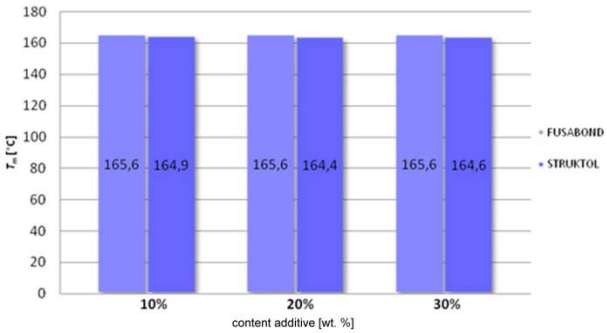

Figure 10. Melting temperature dependence on the content of the α-cellulose fibres at different additives types

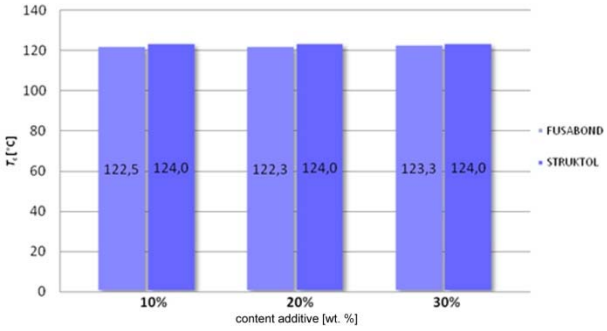

Figure 11. Melt crystallization temperature dependence on the content of the α-cellulose fibres at different additives types

In comparsion between THERMOFIL PP E020M data sheet and measured PP/α-cellulose composites samples is obvious that composites crystallize approximately at same temperature as matrix. This implies that there is no speed-up crystallization, α-cellulose doesn't work like natural nucleating agent and thus there is no improve in material properties of matrix.

Melting enthalpy (ΔHm) is approximately same for increasing content of α-cellulose, that implies same degree of crystallinity.

4. Conclusion

In spite of that α-cellulose doesn´t work like natural nucleating agent causes the addition of MFC in a polymer matrix following benefits and economics contributions. With increasing filler content increases also dimensional stability of moulded part and decreasing shrinkage. Reducing the technological times by shorten the cooling time due to the lower volume of the polymer matrix. Improving the mechanical properties of the final composites by adding MFC filler. With increasing filler content decreases also the volume of consumed synthetic plastics and therefore, dependent on the petroleum products. The lower price of natural fibres compared to the increasing price of petroleum products also reduces the final price of the composite below the price of non-filled plastics and finally achieving environmental aspects.

5. Acknowledgement

This paper was written with research project SGS 28005 support.

6. References

[1] MÜSSIG, J. (2010). *Industrial application of natural fibres: structure, properties, and technical applications.* Wiley, Chichester, West Sussex, U.K, ISBN 978-047-0695-081

[2] Mohanty, A. K. - Misra, M. – Drzal, L. T. (2005). *Natural fibers, biopolymers, and biocomposites.* Taylor & Francis, Boca Raton, ISBN 978-0849317415

[3] AKIL, H.M. - OMAR, M.F. - MAZUKI, A.A.M. - SAFIEE, S. - ISHAK, Z.A.M. - ABU BAKAR, A. Kenaf fiber reinforced composites: A review. *Materials & Design*, vol. 32, 8-9, p. 4107-4121, ISNN: 0261-3069

[4] KALIA, S. - DUFRESNE, A. - CHERIAN, B. M. - KAITH, B. S. - AVÉROUS, L. – NJUGUNA, J. – NASSIOPOULOS, E. (2011). Cellulose-Based Bio- and Nanocomposites: A Review. *International Journal of Polymer Science,* vol. 2011, p. 1-35, ISSN: 1687-9422

[5] KALIA, S. – KAITH, B. S. – KAUR, I. (2011). *Cellulose fibers*: *bio- and nano-polymer composites*. Springer, Berlin, ISBN 978-364-2173-691.

MILLING OF COMPOSITE MATERIALS

Líska Katalin[1*], Líska János[1] and Dávid Babicz[2]

[1]Kecskemét College, Izsáki út 10, Kecskemét, Hungary
[2]Slovak University of Technologies, Bottova 23, Trnava, Slovakia
* liska.katalin@*gamf.kefo.hu*

Abstract
Paper describes the process of machining of composite materials. Also deals with ability to machine composite materials, selection of appropriate instruments, tools and wear problems during machining. At this paper was prepared experiment, which deals with the milling of the composite material. The experiment was designed for investigation of delamination and surface rougness of composite materials with different cutting parameters [1].

Keywords:
Composite materials, influence, milling, surface roughness, delamination,

1. Introduction

Development of composite materials still progresses and still appears new materials, which has better mechanical and chemical properties. Current development in material field is conditioned by increasing of material and energy shortage or by global material and energy saving principles. Composite materials as other materials, have their own disadvantages. One of these disadvantages is their problematic machining [1].

2. Composite materials

Composites are mixed materials, created by physical connection of simple materials. Represents a qualitative change in contradiction solution between desired properties and options of homogeneous material. Selecting the combination of used materials is always a compromise, which is based on the requirement for the final properties of components. The failure to satisfy the other properties can cause lower lifetime of component, increasing of of critical sections, etc. [2].

Currently, exists a large number of polymer-based composites, which number increases every year. These materials are formed by combining of the reinforced material (filler) and macromolecular substances, to improve the mechanical properties. The article deals with two types of composites, such as: composite with epoxy matrix and glass fiber – GFRP and composite with epoxy matrix and carbon fiber – CFRP [2].

Polyester matrix composites/glass fiber (GFRP) are the cheapest and most used materials. The last innovation is using of thermoplastic as a material for producing of matrix, either in form of fabric from cheap polypropylene and glass fiber, or as expensive high temperature thermoplastic. The GFRP products are used to thin electronic circuit boards to masts of ships, for the body and interior panels of automobiles, furniture and fittings [2].

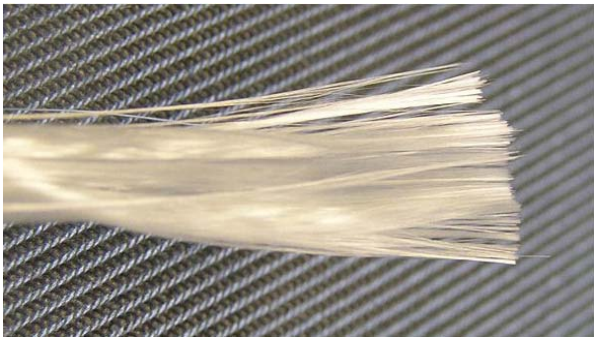

Figure 1. Glass fiber composite [4]

Composites with epoxy matrix and carbon fibers (CFRP) looks as follows: carbon fiber remains from extremely thin fibers with diameter 0,005-0,010mm. Several thousand carbon fibers are twisted and together forms a roving, which can be used themselves or woven into fabric.

The density of carbon fiber is significantly lower than the density of steel. Is ideal for applications, which requires low weight. Composite materials are very popular in aircraft industry, construction engineering, military and motor sports [3].

Figure 2. Carbon fiber composite [5]

3. Accompanying phenomenas during the composite machining

Machining of composite materials requires a revision of existing methods, tools, settings and in some cases in necessary to invest to new machines and preparations. All new type of composite material [6].

Cutting conditions at composite materials varies significally from cutting conditions of metals. The edge of composite material breaks off – very often cuts off by epoxy resin and breaks, cuts fibers. The

main rule at machining of composites is using of very sharp cutting blades, which ensures incision and minimize the possibility of tool friction to the workpiece. The tool wear should be kept to a minimum, because smaller changes of tip geometry can lead to the heat-increasing in cutting zone and to the breaking open of it, which may affect the level of production quality [6].
One of the biggest problems at composite machining is the method of chip-formation. Chips are created in different sizes and different kinds. Therefore method of chip removing from working area is very important method. Where is important to adjust the tool geometry to properties of composite, is important to ensure smooth tool-cut and to minimize the tool vibration. To achieve the required performance, the safety of machining and good results, is needed to adjust and optimize various processes of machining by the type of composite material. Area of composite material machining is constantly evolving, therefore should be used special cutting tools for machining of different types of composites.
Furthermore, is necessary to establish properly cutting parameters for the given operation and ensure the proper tool-clamping [6].

4. Delamination at milling

Conventional tools with one-direction helix are not applicable for contour milling of composites with aramid fibers. The reason is, that by the impact of axial cutting forces releases scraps from fibers on the top layer (delamination). Preparing of milling tool with straight teeth reaches high machining quality at the beginning, but after short cut path begins quickly release fragments of fibers on both upper layers [5].

5. Experiments and results

The aim of the experiments was to investigate values of delamination and surface roughness of machined surface. The machined surface is functional surface. At machining we used composite material with polymer matrix. Concretely it was composite with epoxy matrix and glass-fibre (GFRP) and composite with epoxy matrix and carbon fibre (CFRP) [1].

Figure 3. Machined workpiece - material CFRP [1]

Figure 4. Machined workpiece - material GFRP [1]

For experiment we used machining machine Tomill 250 3D CNC and tools from company Seco. We choosed tool with marking JC 840 (840060R050Z4.0-dura). This tool is specially created for machining of composites [1].

Figure 5. Milling machineTomill 250 3D CNC

We measured delamination by the help of optical measuring machine Mitutoyo QuickVision Elf Pro, what You can see on Fig. 6.

Figure 6. Mitutoyo SV- 3100 with joystick

Surface roughness was measured, too, it was measured on measuring machine Mitutoyo SV-C 3100. Machine for measuring of surface roughness You can see on Fig. 7.

Figure 7. Measuring machine for surface roughness Mitutoyo SV-C 3100 [8]

Experiments were carried out at Kecskemét College, Faculty of Mechanical Engineering and Automation. Goals of experiments were to find values of delamination and surface roughness of machined surface [1].

Figure 8. Cutting of grooves to material GFRP [1]

Experimental results are presented in following tables:

Table 1. Cutting parameters and values of delamination at milling of material GFRP [1]

Number in ranking	v_c (m/min)	f_z (mm)	Delamination
1.	60	0,15	1.1230
2.	60	0,05	1.0682
3.	110	0,15	1.0598
4.	110	0,05	1.0435

You can see the machined grooves on Fig. 9.

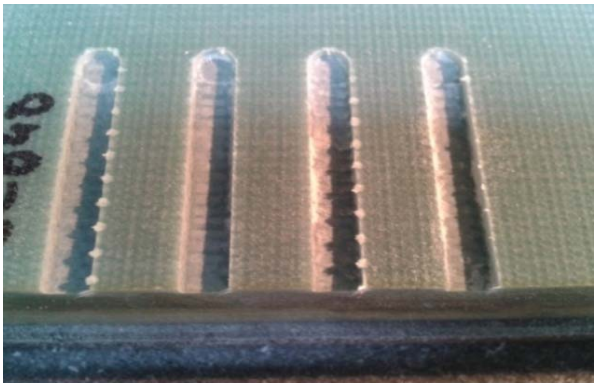

Figure 9. Created grooves to material GFRP [1]

From measured values we found, that the lowest value of delamination at milling of GFRP was created at cutting of fourth groove.
For material CFRP we received the following values:

Table 2. Size of delamination at cutting parameters [1]

Number of ranking	v_c (m/min)	f_z (mm)	delamination
1.	60	0,15	1.0727
2.	60	0,05	1.0536
3.	110	0,15	1.0504
4.	110	0,05	1.0459

At milling of CFRP we received similar results to results at machining of GFRP. The lowest value of delamination was created at machining of fourth groove and conversely, the highest value of delamination was created at cutting of first groove [1]

Figure 10. Created groove at CFRP [1]

We measured surface roughness at different cutting parameters by the help of measuring machine Mitutoyo SV-C 3100, on materials GFRP a CFRP [1]

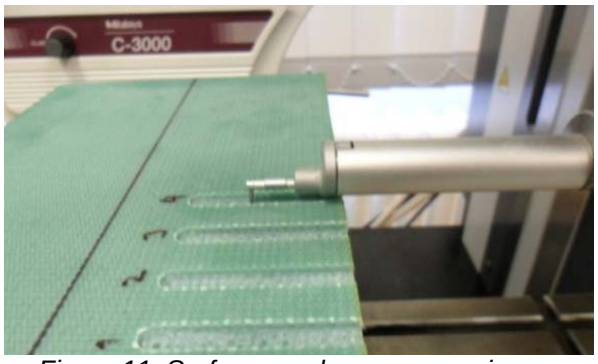

Figure 11. Surface roughness measuring on material GFRP

Data, which You can see in following tables, presents processed values of individual grooves of composite material.

Table 3. Results of surface roughness measurements at material GFRP

GFRP	1. groove	2. groove	3. groove	4. groove
Ra (µm)	3,547	2,732	2,552	2,621
Rq (µm)	4,466	3,530	3,198	3,280
Rz (µm)	21,565	18,928	16,521	16,907
Rt (µm)	34,214	34,419	24,165	23,748

Table 4. Results of surface roughness measurements at material CFRP

CFRP	1.groove	2. groove	3. groove	4. groove
Ra (µm)	2,625	1,872	2,120	1,658
Rq (µm)	3,306	2,455	2,685	2,182
Rz (µm)	16,434	15,171	14,196	12,796
Rt (µm)	26,814	24,175	64,383	21,387

6 Conclusion

Cieľom mojej práce bolo oboznámiť sa s problematikou frézovania kompozitných materiálov

The goal of paper was to get know the problematic of composite material milling.

From experiments we found, that delamination is most dependent on cutting speed (v_c) and feed per tooth (f_z). We learned, that by increasing of cutting speed and decreasing of feed the delamination has decreased.

Also were founded, that delamination at material GFRP has bigger values, as at material CFRP.

In second part of experiment we dealed with measuring of surface roughness of composite material at different cutting parameters.

Each groove was measured three times in order to get more accurate results. We measured four values: Ra (average surface roughness), Rz (roughness height), Rt (maximum height profile) and Rq (medium quadratic deviation profile).

The highest value of surface roughness was created at higher value of feed per tooth (f_z) and lower values of cutting speed (v_c). However, we can say, that material CFRP at same parameters has lower values of surface roughness than material GFRP.

The biggest effect for surface roughness from factors has the material, smaller effects have feed per tooth (f_z) and cutting speed (v_c).

7. References

[1] D. Babicz, “Frézovanie kompozitných materiálov,“ MtF STU Trnava, 2012.
[2] “Kompozity s epoxidovou matricou a sklenenými vláknami (GFRP),“ ... [Online]. Available: http://www.matnet.sav.sk/index.php?ID=1114. [Accessed: 3-January-2012].
[3] ... [Online]. Available: http://wikipedia.infostar.cz/c/ca/carbon_fiber_1.html. [Accessed 3-January-2012].
[4] ... [Online]. Available: http://en.wikipedia.org/wiki/MATLAB. [Accessed 10-January-2012].
[5] ... [Online]. Available: http://www.automoto.sk/clanok/185877/uhlik-chce-byt-materialom-buducnosti. [Accessed 8-January-2012].
[6] J. Líška, “Obrábanie kompozitných materiálov“, Dissertation thesis, STU MTF, Trnava, June 2010.
[7] J. Líška, “Obrábanie kompozitných mariálov“, Project of dissertation thesis, STU MTF, Trnava January 2009.
[8] ... [Online]. Available: http://www.mitutoyo.co.uk/MitProd/mtopr.nsf/UNIDS/937007168C234F52802571FC0048FD2C!Opendocument. [Accessed 3-February-2012].

MOTION FOR WORKPLACE DECOMMISSIONING OF DISCARDED MUNITION WITH TECHNOLOGY OF WATER JET

J. Ferko[1], M. Šomšák[1] , J. Cárach[1], S. Hloch[1], S. Radchenko[1], A. Andrej[1] and F. Murgaš[1,2]

[1]Faculty of manufacturing technologies of Technical university of Kosice with seat in Prešov, Slovakia
[2]SOR Lipchavy spol.s.r.o, Lipchavy, Czech Republic
** Corresponding author e-mail: matej.somsak@tuke.sk*

Abstract
The presented paper deals with the decommissioning of discarded ammunition using progressive water jet technology. In the handling and decommissioning of explosive substances, ammunition and grenades, the life and health of people is at great risk. Therefore, this article tries to design a workplace for the decommissioning of ammunition, where one process itself does not directly participate in the disposal. This would minimize the threat to the life and health of humans to an acceptable level. A design for a complete workstation of ammunition decomposition using water jet technology, manipulators, robots, as well as decommissioning individual components is described.

Keywords:
Water Jet, Ammunition, Safety improvement, Delaboration of Ammunition, Design of workplace

1. Introduction

At present in Slovakia, according to the information available, more than 98% of ammunition from the Cold War is at end of its life. Overall, 90% of all military munitions must be discarded. The term ammunition includes that for small arms, but also artillery, mortar and air bombs. On the territory of our country today there can be found ammunition from World War II, which also needs to be securely disposed of. The fact that Slovakia is one of the world leaders in the disposal of explosives and ammunition indicates the commitment of our bomb squad in foreign missions. Decommissioning of ammunition at the end of its life is dangerous to the life and health of people, which is why it is necessary to pay close attention to this issue. The presented proposal of a modern workplace for decommissioning single medium calibre artillery ammunition using water jet technology should reduce the risks arising from the nature of the process of decommissioning.

2. Analysis of the current situation

At the present time there are several methods of decommissioning of ammunition (Table 3). Detonation outdoors, which is performed now transporting hazardous material for decommissioning is becoming less frequent. Dumping in the sea is used when the ammunition is stored in barrels. It is also used for the disposal of old mines, which are placed in hard rock with a depth is up to 900 metres. Newer methods include decommissioning by cutting with a circular saw, laser, plasma burning in furnaces and water jet cutting. Precisely the latter technology will form the basis of the work.

Water jet cutting is a progressive technology that is widely used in various industries. The cutting performance of pure water flow is increased by adding abrasive particles. The basic technology advantages include:

- The use of a fast moving jet of water does not create dust
- In the cutting process, material is not affected by heat and deformation of the workpiece surface
- The opportunity to start and finish the process of cutting in any place and time
- Water jet cuts up the material in any direction, achieving a high precision shape
- Possibility of cutting multi-component composite materials, hard and soft materials
- In the section there arise only minimal losses
-There is no direct contact with the workpiece and does not need to consolidate. [2], [3]

In figure 1 we can see an experimental cutting of a single medium calibre artillery shells in the Czech-Slovak conditions using water jet technology. Table 4 shows the cutting conditions used in the experiment. Risk Assessment for the original and newly proposed work has been conducted using the Failure mode and effects analysis (FMEA), which works with five classes of probability determining the likelihood of an undesirable event, which are listed in Table 1. Determination of result of unwanted events is the next step in the FMEA. They are arranged into five categories according to the severity of occurrence of an event according to Table 2. Consequence of risk indicates the severity of harm, economic damage, environmental and health damage, or loss of life that may result from the action of adverse events that the factor causes. The procedure for the application of this method is the following. The first step is to define all the problems and points in the production process, for example using Ishikawa diagram. Subsequently, with each there is associated a value for the probability of the occurrence and an estimate due to the problems to create a point matrix. [4]

Table 1. Table of probability values for FMEA

Probability	Points	Frequency	Time exposure of risk
Improbable	1	The emergence of the phenomenon almost excluded	Almost impossible threat
Random	2	The emergence of the phenomenon nearly expelled or impossible	Very rare threat
Probable	3	The phenomenon occurs during the lifetime of the device	Rare threat
Very probable	4	The phenomenon occurs during the lifetime of the device several times	Common threats
Pernament	5	The phenomenon occurs during the lifetime of the device most often	Continuous threat

Table 2. Table of consequences estimation

Value	The severity of the consequences
1	Injury without incapacity for work
2	Injury with incapacity
3	Severe injury requiring hospitalization
4	Severe injury requiring hospitalization, which can caused invalidity
5	Injury causing death

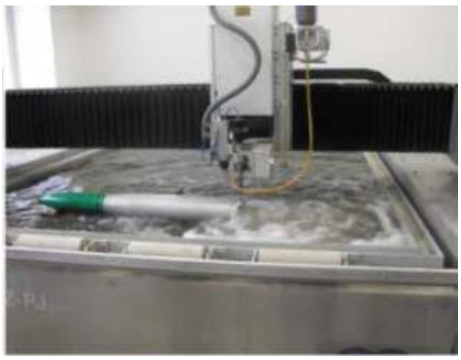

Figure 1. Experimental cutting of artillery ammunition [7]

Table 3. Ammunition disposal methods

Traditional methods of disposal of ammunition
Detonation outdoors
Dumping in the sea
Disposal in old mines
New methods of disposal of ammunition
Water jet cutting
Laser cutting
Circular saw cutting
Plasma burning in furnaces

Table 4. The conditions of the experiment used in cutting a single artillery ammunition

Factors	Experimental range
Pressure p $[MPa]$	350
Traverse speed v $[mm.min^{-1}]$	15
Abrasive mass flow rate m_a $[g.min^{-1}]$	300
Water nozzle diameter d_o $[mm]$	0,33
Focusing tube diameter d_f $[mm]$	0,8
Stand off $[mm]$	3
Number of passes	1
Angle of cut φ [°]	90
Type of abrasive	Barton garmet
MESH	80
Characteristic of multiplier	PTV-37-60 PUMP
Type of multiplier	Double-acting
Performance $[kW]$	37
Oil pressure $[MPa]$	20
The maximum pressure $[MPa]$	415
Amplification ratio	20 x
Max. water flow rate $[l.min^{-1}]$	3,68
Material thickness $[mm]$	10
Consumption to cutting one shot with bag - cartridge	
Time of cutting $[min]$	73,3
Water consumption per 1 shot $[l]$	269,8
Consumption of abrasives for 1 shot $[kg]$	22

Table 5 shows the classification of risks and their subsequent categorization. In the left column are the risks to which there is assigned a quantified value for the probability and consequence. Using these values, it is possible to create a matrix of risks, which for this case is illustrated by the point shown on Figure 2. The numerical values on the horizontal at the top of the image represent the value of the probability of occurrence of the risk The vertical on the left shows values representing the value as a result of the risk. Each cell of the matrix consists of three numbers. The top is the product of the probability and as a result, in the middle the Roman numeral represents the risk category, and the lower number represents the risks. RwCells are colour coded, whereby the green colour represents a small risk and red the highest risk. From these is apparent the necessity of eliminating human presence from the decommissioning of ammunition as well as the improvement of its methods of decommissioning. [3], [4]

	1	2	3	4	5
1	1 I Number of identified risks 0	2 I Number of identified risks 0	3 II Number of identified risks 0	4 II Number of identified risks 0	5 II Number of identified risks 0
2	2 I Number of identified risks 2	4 II Number of identified risks 3	6 III Number of identified risks 1	8 III Number of identified risks 0	10 IV Number of identified risks 0
3	3 II Number of identified risks 3	6 III Number of identified risks 3	9 IV Number of identified risks 2	12 IV Number of identified risks 1	15 V Number of identified risks 0
4	4 II Number of identified risks 1	8 III Number of identified risks 2	12 IV Number of identified risks 1	16 V Number of identified risks 0	20 V Number of identified risks 2
5	5 II Number of identified risks 0	10 IV Number of identified risks 0	15 V Number of identified risks 0	20 V Number of identified risks 1	25 V Number of identified risks 0

Figure 2. Point matrix of risk assessment of ammo delaboration [7]

3. Design of the workplace for the decommissioning of ammunition

In order to achieve a reduction in the risk of explosion and damage to the health or life of people, an alternative to current decommissioning workplaces has been proposed. The building is built from reinforced concrete walls, which are covered with protective armour. The roofing is made of lightweight materials and constructed so that the explosive power of a possible explosion will be directed to the roof, the destroyed parts of which will not cause great material damage to the surroundings. The floor is antistatic, all the machinery is grounded, and the space is heated to the desired temperature of 18-25 °C. The building has a code security system and after the commencement of the process of decommissioning, it will not allow any person to enter. The building is at a distance from other structures in order to show that a possible explosion would not cause damage or endanger persons working in them.

Table 5. FMEA the current stage of decomposition

Risk	Probability	Conse-quence	Points	Cate-gory
Wound	3	1	3	II.
Falls, fractures, bruises	2	2	4	II.
Eye damage	3	2	6	III.
Stumble, slipping	2	1	2	I.
Death	4	5	20	V.
Invalidity	3	4	12	IV.
Damage of health	3	2	6	III.
Burns	4	3	12	IV.
Concussion	3	2	6	III.
Strikes	3	1	3	II.
Lacerations	2	1	2	I
Damage of the skin	3	3	9	IV.
Damage to the human body	3	3	9	IV.
Fire	5	4	20	V.
Breathing problems	2	2	4	II.
Electrical shock	2	2	4	II.
Psychologi-cal stress	4	1	4	II.
Damage of hearing	4	2	8	III.
Headaches	3	1	3	II.
Damage of the machine	4	2	8	III.
Environ-mental pollution	2	3	6	III.
Munitions blast	4	5	20	V.

A plan view of the workplace is shown on Figure3. The entry to supply ammunition is located on the left of the hall A. The quantity of ammunition prepared for decommissioning should be limited in case an unexpected event such as a chain explosion or unpredictable damage occurs. At the bottom right there is a space for the removal of parts decommissioned. The walls between halls A and B are safety walls because only in part B does there occur decommissioning.

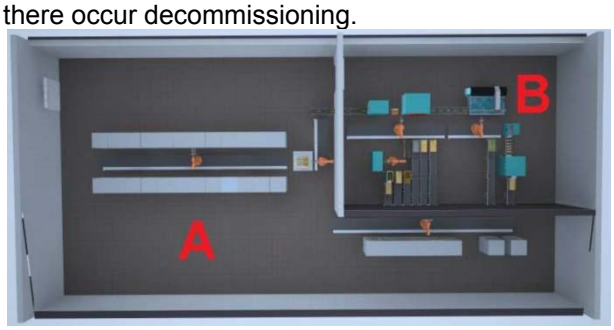

Figure 3. View of the proposed workplace [7]

The main features of entrance hall A are two robots moving along a running gear, a manipulation table, a conveyor belt and tanks with standardized pallets (Fig.4). Robot No. 1 picks up a pallet of ammunition from the right tray, moves it along the running gear to the manipulation table, where it is exchanged for an empty pallet and put it back in the left pallet tray. Robot No. 2 (Fig.5) takes ammunition from the palette to manipulation table and places it on the conveyor belt going towards the hall B.

Figure 4. Containers with pallets and robot No.1 [7]

Figure 5. Containers with pallets, handling table and robot No.2 [7]

In Figure 6 there is a view of Hall B. Above right you can see the truck, which gets ammunition for the decommissioning workplaces. Below left, the decommissioning process is ending and ammunition is returned to Hall A.

Figure 6. Preview into the hall B [7]

The first step in decommissioning ammunition, is cleansing is from preservatives. There is provided equipment for degreasing (Fig. 7), served by the handling robot, which picks up artillery shells and moves them to the bottom of the device. After degreasing, the ammunition is highlighted in the upper part, which is dried in a stream of air from the nozzles.

Figure 7. Degreasing machine [7]

On the front cover of decommissioning machine (Fig. 8) is red armour. The manipulation robot places the ammunition into the machine and grabs special keys from the manipulation table to the left by which a machine in the actual decomposition process separates the detonator from the missiles and ignition screw from the case. There is also a separate copper ring at the bond between a case and projectile. At the end of liquidation process, the closed armoured cover has been opened, the robot manipulates the individual components. To the left there are three tanks, two of which, for the detonator and ignition screw, are for reasons of safety, made of wood. In the third container there are stored copper hoops. To the right of the machine the projectile is place on the conveyor towards the device for water jet cutting and the bag - cartridge on the side conveyor, leading to another decommissioning station. At the water jet workplace (Fig. 9) a robot grabs the ammunition and takes it from the conveyor to the machine holder. Over the holder is an arm, on which it is placed the cutting head and vibration sensor. After completion of the cutting, the manipulation robot grabs both halves of the projectile and inserts them

into the machine for washing out or steam smelting (Fig. 10). Here in the closed area is carried out the process of washing out (smelting). The explosive material, after filtration is placed into crates. Then it moves into the opening on the left side of the machine for drying (Fig. 11).

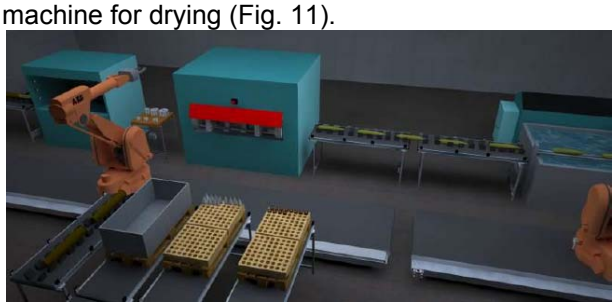

Figure 8. Delaboration machine [7]

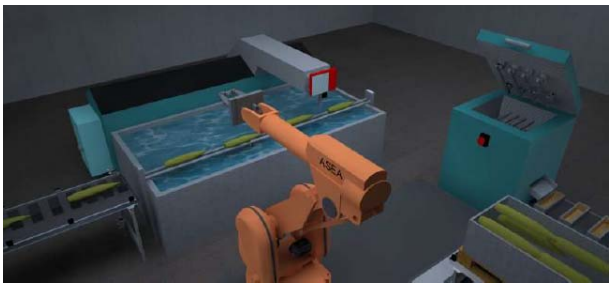

Figure 9. Workplace of cutting with technology AWJ [7]

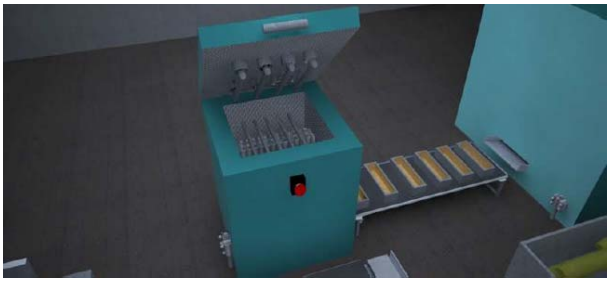

Figure 10. Workplace for extracting projectile blasting cartridges [7]

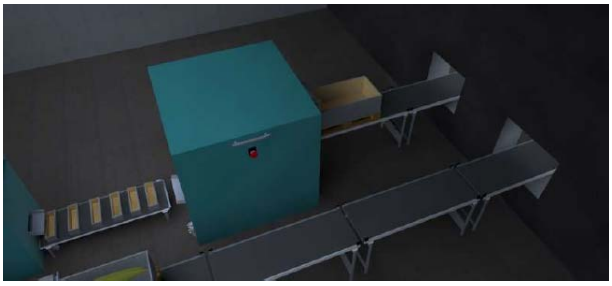

Figure 11. Workplace of drying explosive material [7]

Bag - cartridges from the decommissioning machine travel by conveyor to the robot, which empties its powder filling (Figure 12). The bag - cartridge is then placed on the holder and its primer is removed. The bag - cartridge is moved to storage and the powder is placed into the crusher, where, after crushing, it is stored in the reservoir.

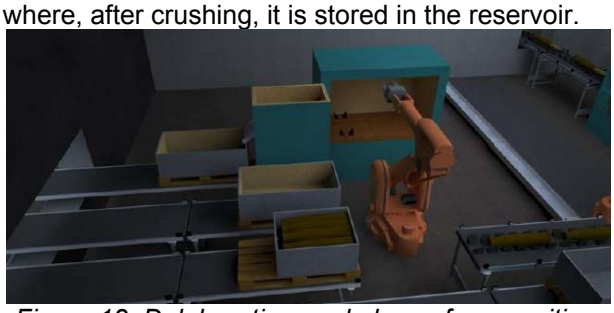

Figure 12. Delaboration workplace of ammunition [7]

All components and materials decommissioned move back into hall A, where manipulation robots move them into the prepared storage boxes (Figure 13).

Figure 13. Offtake workstation - Hall A [7]

Analysis of the evaluation and quantification of risks to new workplace is located in Table 5 and the risk matrix shown on Figure 14.

	1	2	3	4	5
1	1 **I** Number of identified risks **2**	2 **I** Number of identified risks **8**	3 **II** Number of identified risks **0**	4 **II** Number of identified risks **1**	5 **II** Number of identified risks **1**
2	2 **I** Number of identified risks **7**	4 **II** Number of identified risks **1**	6 III Number of identified risks **1**	8 III Number of identified risks **0**	10 IV Number of identified risks **1**
3	3 II Number of identified risks **0**	6 III Number of identified risks **0**	9 IV Number of identified risks **0**	12 IV Number of identified risks **0**	15 V Number of identified risks **0**
4	4 II Number of identified risks **0**	8 III Number of identified risks **0**	12 IV Number of identified risks **0**	16 V Number of identified risks **0**	20 V Number of identified risks **0**
5	5 II Number of identified risks **0**	10 IV Number of identified risks **0**	15 V Number of identified risks **0**	20 V Number of identified risks **0**	25 V Number of identified risks **0**

Figure 14. Point matrix of risk assessment of ammo delaboration for the new workplace [7]

Table 6. FMEA the new workplace of decomposition

Risk	Probability	Conse-quence	Points	Cate-gory
Wound	2	1	2	I.
Falls, fractures, bruises	1	1	1	I.
Eye damage	1	2	2	I.
Stumble, slipping	2	1	2	I.
Death	1	5	5	II.
Invalidity	1	4	4	II.
Damage of health	1	2	2	I.
Burns	1	2	2	I.
Concussion	2	2	4	II.
Strikes	2	1	2	I.
Lacerations	2	1	2	I.
Damage of the skin	2	1	2	I.
Damage of the human body	2	1	2	I.
Fire	2	3	6	III.
Breathing problems	1	2	2	I.
Electrical shock	1	2	2	I.
Psychological stress	2	1	2	I.
Damage of hearing	1	2	2	I.
Headaches	1	1	1	I.
Damage of the machine	1	2	2	I.
Environ-mental pollution	1	2	2	I.
Munitions blast	2	5	10	IV.

5. Conclusion

Decommissioning damaged or end-of-life ammunition is still dangerous with currently used techniques. There is a risk of damage to the machine, the environment or human health. The worst is the high risk of death. Therefore, based on new knowledge, a workplace for the decommissioning of ammunition without human presence has been designed and machines are managed online from a safe distance. The building, where the process takes place, is situated in an area where accidental explosion of ammunition would cause the least possible environment pollution. The Failure mode and effects analysis for risk assessment has shown that the newly proposed workplace significantly reduces the risk involved in the decommissioning of ammunition. Safety and protection of human health is paramount. This work was supported by the Slovak Research and Development Agency under the contract No. APVV-207-12

6. References

[1] O.Híreš, M. Hatala, S. Hloch : "Cutting of metal materials with circular saw, water jet and plasma arc". 1.edition. Ostrava: Jiří Pustina, 2007.

[2] S.Hloch, J. Valíček, P. Hreha. et al.: "On-line identification of hydroabrasive cutting using acoustic emission and vibration". 1.edition. Prešov: Faculty of manufacturing technologies of TU of Kosice with seat in Prešov, 2011. 126 p. ISBN: 978-80-553-0698-8

[3] Et all: New trends in technology laboration and current aspects of decomposition and utilization of ammunition. 1.edition. Trenčín: KONŠTRUKTA-Industry, a.s., 2003. 250p. ISBN: 80-88914-96-5

[4] M.Korecký, V. Trkovský: Risk Management projects focusing on projects in industrial enterprises. 1.edition. Praha: Grada Publishing, a.s., 2011. 584p. ISBN: 978-80-247-3221-3

[5] V.Smejkal, K. Rais: Risk management in companies and other organizations. Grada Publishing a.s.,2006. 300p. ISBN: 80-247-1667-4

[6] J. Kmeč: Proposed method of disposal of discarded munitions with water jet. Master's thesis, Prešov: Faculty of manufacturing technologies of TU of Kosice with seat in Prešov, 2011. 58p.

[7] J. Ferko: Use water jet technology in the process of reverse logistics processing discarded munitions with minimal human intervention. Master's thesis, Prešov: Faculty of manufacturing technologies of TU of Kosice with seat in Prešov, 2013. 58s.

GREEN SUPPLY CHAIN SYSTEM: A CASE STUDY FROM INDIAN INDUSTRIES

Sanjeev Kumar[1*], Somnath Chattopadhyaya[2] and Vinay Sharma[3]

[1] *Professor, Mechanical Engineering Department, IIMT College of Engineering, Greater Noida, India,*
[2] *Associate Professor, ME&MME Department, Indian School of Mines, Dhanbad, India,*
[3] *Professor, Production Engineering Department, Birla Institute of Technology, Mesra, Ranchi, India,*
** Corresponding author e-mail: sanjeevkg9@gmail.com*

Abstract:
As industries attempt to move forward towards environmental sustainability, management/senior level managers must extend their efforts to improve environmental practices across their supply chain and for improving environmental performance of processes in accordance with the requirements of environmental regulations green supply chain system has emerged as a proactive approach. This research examines the consistency approach that determines the practice and implementation of green supply chain in Indian industries. Expanding on some earlier work, this paper explores the green supply chain pressures, initiatives and performance of the green supply chain using an empirical analysis of 119 industries within India. Issues are analyzed through the survey results. The results for the practice and implementation of green supply chain in industry investigated in this work generate a model for decision makers who can prioritize those approaches for implementing green supply chain system in Indian industries.

Keywords:
Green Supply Chain System, Survey, Communality Scores, Indian industries.

1. Introduction

Supply chain management has become a very important competitive approach for industries in this environment. Green supply chain is the process of incorporating environmental criteria into industrial procurement decisions and long-term relationships with suppliers **(**Gilbert, s et al. 2001) [3]. India is one of the most industrialized countries in the world. Now a day's researchers and enterprises have become more conscious towards environmental related issue. Supply chain management is the coordination and management of a complex network of activities involved in delivering a final product to the consumer. All stages of a product's life cycle will influence a supply chain's environment burden, from resource extraction, to production, reuse, recycling, or disposal. (Ninlawan C et al. 2010) [8]. Beyond this definition with adding the "green" component, it refers to green supply chain management which is defined as "green-procurement, green-resources, green-design, green-accounting, green-production, and green-logistics". "Green Supply Chain Management, including product design, material sourcing and selection, manufacturing processes, delivery of the final product to the consumers, and end-of-life management of the product after its useful life". Green Supply Chain Management has emerged as an important tool to achieve industrial profit and market share objectives by improving ecological efficiency and mitigating environmental risks (Gunasekaran A, et al. (2001) [4]. The assessments presented here are based on parts of the data and information collected through the execution of the Competitive Strategies and Best Practices Benchmarking Questionnaire from Indian industries. Using various literature in the field of green supply chain, a number of parameter has been introduced that may be used to help evaluate practices in this area. This study aims at assessing the green supply chain in the manufacturing industries in India on an empirical basis. The entrepreneurs have started implementing effective and integrated environmental criteria into their practices and onto their strategic planning agenda. Given the theoretical and practical importance for developing a green supply chain practices implementation measurement scale, a study based on an empirical survey of Indian industries has been undertaken.

Paper consists of six sections. After this introduction, in Section 2, a short review of the relevant literature helps to establish a link among environmental management, supply chain management, and organizational performance. Section 3 states the objective of the study. Following the research methodology (Section 4), the results and extracted factor of green supply chain parameters are presented in section 5. Finally, conclusions in section 6.

2. Literature review

Working with green supply chain means to work in the interface of those areas because the green supply chain is totally linked to environmental protection. Currently, there has been a great deal of interest in the field of research work regarding whether or not environmental management practices can improve enterprises performance. There are very few studies of performance measurement in the field of green supply chain. Approaches to Green Supply Chain (GSC) practice

and implementation have been identified by researches; are outlined below.

Zhu et al. (2008) [11] studied that development and scale of GSCM with Chinese manufacturers. The models of GSCM practices and adaption were tested by confirmatory factor analysis. The results suggested that the models were reliable and valid. Hsu and Hu (2008) [2] stated that supplier management plays the very important and crucial part of implementing Green Supply Chain Management, the customer-supplier relationship affect Green Supply Chain Management implementation to address the related issue. A system devised by Handfield et al. (2002) [6] to measure environmental practice of suppliers using multi attribute utility theory. Horvath, 1999 [7] devised system to assess supply chain management for telecommunication sectors in telephone and telegraph communication and services. Zsidisin and Hendrick (1998) [13] identified GSCM factors-hazardous materials, investment recovery, product design, supply chain relationship and determined their existence with exploratory factor analysis (EFA). Ninlawan C et al., 2010 [8], conceptualize GSCM practices implementation as encompassing 11 different dimensions of practices including Internal environmental management, Eco purchasing, Eco-design, Cooperation with customers, Investment recovery, Environmental, Positive economic, Negative economic, Market, Regulatory, Competition for Electronics Industry in Taiwan. Relationship between Green Supply Chain Management practices implementation and performance were investigated by Zhu and Sarkis (2004) [10] focusing the moderating effects of quality and lean practices. Gunasekaran et al. (2004) [5] introduce six metrics for measuring SCM capability and performance. Metrics are based on the following SCM processes: plan, source, make/assemble and delivery/customer. Sarkis (2003) [9] devised framework for Green Supply Chain Management practices adaptation to evaluate alternatives methods used by the companies which will effect relationship with suppliers and consumers. Bowen et al. (2001) [1] analyzed the implementing pattern and derive three types of green supply chain management. First; adaptation to supplier management activities by collaborating with supplier to eliminate packaging and recycling initiatives. Second; attempt to recycle supplied packaging. Third and last proactive approaches towards environmental criteria in risked sharing, evaluation of customer performance and joint clean technology programs with supplier. Zhang and Zhiwei (2009) [12] have developed a fuzzy based analytical hierarchy process (AHP) for evaluation of performance of green supply chain, taking into consideration the characteristics and influencing factors of green supply chain.

This study aims to examine the measurement model of green supply chain practices implementation focusing on its 14 underlying factors (consist 105 underlying dimensions) and a measurement scale for it. These factors and the scale are represented in the form of questionnaire items, for measuring the different facets of green supply chain practices implementation, enabling industries to evaluate their strength and weakness in the course of implementing these practices.

3. Objective

To study Supply Chain of SME of India based on different environmental aspect and legislation.
Development of manufacturing strategies and managerial for effective implementation of Green Supply Chain in Indian SME.

4. Research methodology

A survey instrument was developed based on the previously reviewed literature and a series of extensive interviews with different stakeholders/managers/supervisors/environmental expert/expert from the field of supply chain. On the basis of review, a preliminary questionnaire was framed considering all the objectives and the present study embodied. A quantitative methodological approach was used for this study. Quantitative research utilizes deductive logic. The research starts with an abstract idea, followed by a measurement procedure, and ends with empirical data, capable of being analyzed by statistical methods representing the abstract ideas.

Research design refers to “those group of small worked-out formulas from which prospective researchers can select or develop one or more that are suitable for their specific research goals and objectives”. A survey design (Figure-1), as plan for the investigation has been followed.

Figure 1: Research Design

The Competitive Strategies and Best Practices Benchmarking Questionnaire have been developed. The questionnaire consists of total 14 factors with 105 underlying dimensions. The model aims to explore possible near future developments in the competitive strategies of the companies by addressing their competitive priorities,

manufacturing objectives and action plans. Information is collected through the 105 dimensions. Performance and outcome measures are asked to be reported as point values. Industries performance strategies will depend upon their aggregate score. The competitive strategy factor is designed along the lines of a process model of manufacturing strategy. The model aims to explore possible near future developments in the competitive strategies of the companies by addressing their competitive priorities, manufacturing objectives and action plans. The target respondents of our survey were requested to indicate, using a five-point Linkert scale (1-Below average/Completely disagree, 2-Average/ Rarely agree, 3-Good/ Partly agree, 4 –Very good/ Rather agree, 5- Excellent/Completely agree), the extent to which they perceived their companies implementing each of the dimensions of GSCM practices. In every case, a higher scale score indicated the use of better quality management practices. The respondent's score on each statement were summed together to measure his or her perception toward Green Supply Chain efficiency.

4.1. Scale procedure and Reliability Analysis:

Item analysis was conducted for each of the 105 statements between the highest and lowest group through a "**mean score**" and "**t-test**". Based on the results, 105 items were found significantly differentiating the two groups and thus were retained for the reliability analysis. The reliability of the scale was examined through reliability tests, to measure the internal consistency of the items and, one to measure the temporal stability of the scale. Factor Analysis in Green Supply Chain statements was applied to find out the underlying factors and their importance. The data is analyzed by using SPSS. The data validity for Factor Analysis was tested with the help of Kaiser-Meyers-Olkin (KMO) measures of sampling adequacy, Communality Scores of all statements.

5. Score Analysis

5.1. Comparative analysis of Green Supply Chain factors

Table: 1 and Figure: 2 explain about the comparative analysis of effective of green supply chain factors on the basis of industry. 14 supply chain factors considered in study and each factor has its own importance for effective green supply chain performance. It has been taken 119 industries as a whole in the diversified areas. As per the literature review & experts view, used linkert scale in this questionnaire, where '1' employs below average & '5' employs excellent. Each scale signifies how these factors for an industry for effective green supply chain factors. While analyzing the industry, it has been found that the most important factors which leads to effective supply chain is customer co-operation (2.427) followed by human & technological resources (2.263) and operational performance (2.230) & the least important dimension factor as the proceed is the stakeholders (1.599) followed by vendor management (1.655) & eco accounting (1.668). There are certain other factors which the industries precede not much important for effective green supply chain in their industry but these factors must be taken seriously by the management, that supply chain management effectively monitored.

Table 1. Comparative analysis of effective (Mean Score) of Green Supply Chain factors

FACTOR	DESCRIPTION	MEAN SCORE	RANK
1	Eco Procurement	1.806	8
2	Eco-Accounting	1.668	12
3	Eco-Logistics Design	1.792	10
4	Eco-Product Design	1.980	6
5	Eco-Manufacturing	1.963	7
6	Marketing & Communication	1.798	9
7	Economic Performance	2.220	4
8	Environmental Performance	2.139	5
9	Customer Co-operation	2.427	1
10	Human and Technological Resources	2.263	2
11	Internal Environmental Management Performance	1.790	11
12	Operational Performance	2.230	3
13	Stakeholders	1.599	14
14	Vendor Management	1.655	13

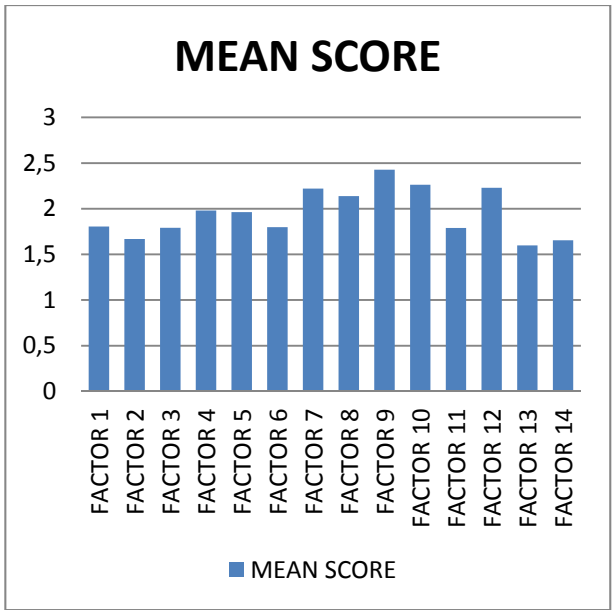

Figure: 2- Comparative analysis of effective (Mean Score) of Green Supply Chain factors

5.2. Comparative Analysis Of Mean Score Of Factors As Per Size Of Employee Wise In Indian Industries

Table: 2, 3, 4, 5 and figure: 3 explain the comparative analysis of factor on the basis of number of employee engaged in the industry. It has been taken '4' group in this study, where the group '1' consist the industry whose employee size is less than 50, then group'2' consist employee size between 50-100, group'3' consist employee size is 100-200, group'4' consist employee size 200-500 in their industry. The objective of this table is to find out whether the green supply chain factor is related or affected as per the size of the employee concern. We have taken null hypothesis that there is no significant difference of the green supply chain factors which has equal number of employee engaged in the industry. For these scores have been calculated the competitive mean score with**'t' value**. Considering null (0) hypothesis that no significant differences of green supply chain factors on the basis of employee wise. An alternate hypothesis there is significant differences of green supply chain factors on the basis of employee. From the table it is clear that out of 14 factors all 14 factors have't' value more than '2'. It means that our null hypothesis of these 14 factors is rejected. Here "p" is the probability of acceptance (The p-value is a numerical measure of the statistical significance of a hypothesis test. It tells how likely it is that sample data have responded even if the null hypothesis is true. By convention, if the p-value is less than 0.05, it is concluded that the null hypothesis can be rejected).

Table: 2- Comparative analysis of effective (Mean Score) of Green Supply Chain factors employee wise

Employee size: Less than 50

FACTOR DESCRIPTION	MEAN SCORE	RANK	t	p
Eco Procurement	1.64	9	23.348	0.00
Eco-Accounting	1.49	12	18.325	0.00
Eco-Logistics Design	1.70	8	27.952	0.00
Eco-Product Design	1.81	6	25.661	0.00
Eco-Manufacturing	1.80	7	32.025	0.00
Marketing & Communication	1.52	11	17.048	0.00
Economic Performance	1.94	4	41.606	0.00
Environmental Performance	1.91	5	34.127	0.00
Customer Co-operation	2.46	1	23.466	0.00
Human and Technological Resources	2.00	3	39.878	0.00
Internal Environmental Management Performance	1.55	10	22.978	0.00
Operational Performance	2.06	2	37.866	0.00
Stakeholders	1.36	14	16.899	0.00
Vendor Management	1.42	13	16.917	0.00

The table: 2 explain the group whose employee size is less than 50. When analyzing the green supply chain factors where employee size is less than '50', it has been observed that the most important factor is customer cooperation (2.46) followed by operational performance (2.06), human & technological resources (2.00) and the least important factor is stakeholders (1.3647) followed by vendor management (1.42),eco accounting (1.49). The biggest mean difference among the industry is found customer cooperation and the lowest is stakeholders. It means all the industry whose employee size is less than 50 as we have targeted are equally performed well in stakeholders followed by vendor management , eco accounting but they are more different in customer cooperation followed by operational performance, human & technological resources. 't' value of all the 14 factors, we have examine is more than '2' therefore the null hypothesis is rejected. Therefore it can be generalized that there is significant differences of all the 14 factors among the industries whose employee size is less than 50. Therefore for the management point of view they should give more strengthen on stakeholders, vendor management and eco accounting for improving green supply chain factors.

Table: 3- Comparative analysis of effective (Mean Score) of Green Supply Chain factors employee wise

Employee size: Between 50-100

FACTOR DESCRIPTION	MEAN SCORE	RANK	t	p
Eco Procurement	1.73	9	17.593	0.00
Eco-Accounting	1.59	13	10.455	0.00
Eco-Logistics Design	1.78	6	14.689	0.00
Eco-Product Design	1.74	8	25.655	0.00
Eco-Manufacturing	1.71	10	28.845	0.00
Marketing & Communication	1.76	7	12.071	0.00
Economic Performance	2.14	2	18.740	0.00
Environmental Performance	2.01	5	14.691	0.00
Customer Co-operation	2.16	1	19.781	0.00
Human and Technological Resources	2.10	3	17.262	0.00
Internal Environmental Management Performance	1.71	11	12.583	0.00
Operational Performance	2.01	4	25.423	0.00
Stakeholders	1.49	14	14.474	0.00
Vendor Management	1.66	12	11.812	0.00

The table 3 explains the group whose employee size is 50 to 100.

When analyzing the green supply chain factors where employee size is between 50-100, it has been observed that the most important factor is customer cooperation (2.16) followed by economic performance (2.14), human & technological resources (2.10) and the least important factor is stakeholders (1.49) followed by eco accounting (1.59), vendor management (1.66). The biggest mean difference among the industry is found customer cooperation and the lowest is stakeholders. It means all the industry whose employee size is between 50-100 as we have targeted, are equally performed well in stakeholders followed by eco accounting, vendor management but they are more different in customer cooperation followed by economic performance, human & technological resources. 't' value of all the 14 factors, we have examine is more than '2' therefore the null hypothesis is rejected. Therefore it can be generalized that there

is significant differences of all the 14 factors among the industries whose employee size is between 50-100. Therefore for the management point of view they should give more strengthen on stakeholders, eco accounting, and vendor management for improving green supply chain factors.

Table: 4- Comparative analysis of effective (Mean Score) of Green Supply Chain factors employee wise

Employee size: Between 100-200

FACTOR DESCRIPTION	MEAN SCORE	RANK	t	p
Eco Procurement	1.47	9	15.100	0.00
Eco-Accounting	1.35	13	11.619	0.00
Eco-Logistics Design	1.51	8	20.111	0.00
Eco-Product Design	1.81	6	18.642	0.00
Eco-Manufacturing	1.72	7	17.631	0.00
Marketing & Communication	1.28	14	10.885	0.00
Economic Performance	2.07	2	24.300	0.00
Environmental Performance	1.83	5	31.058	0.00
Customer Co-operation	2.17	1	19.357	0.00
Human and Technological Resources	2.00	4	23.905	0.00
Internal Environmental Management Performance	1.43	11	13.873	0.00
Operational Performance	2.02	3	31.853	0.00
Stakeholders	1.43	10	12.572	0.00
Vendor Management	1.41	12	11.872	0.00

The table 4 explains the group whose employee size is 100 to 200.

When analyzing the green supply chain factors where employee size is between 100-200, it has been observed that the most important factor is customer cooperation (2.17) followed by economic performance (2.07), operational performance (2.02) and the least important factor is marketing & communication (1.28) followed by eco accounting (1.35), vendor management (1.41). The biggest mean difference among the industry is found customer co-operation and the lowest is marketing & communication. It means all the industry whose employee size is between 100-200 as we have targeted are equally performed well in marketing & communication followed by eco accounting, vendor management but they are more different in customer co-operation followed by economic performance, operational performance. 't' value of all the 14 factors, we have examine is more than '2' therefore the null hypothesis is rejected. Therefore it can be generalized that there is significant differences of all the 14 factors among the industries whose employee size is between 100-200. Therefore for the management point of view they should give more strengthen on marketing & communication, eco accounting, and vendor management for improving green supply chain factors.

Table: 5- Comparative analysis of effective (Mean Score) of Green Supply Chain factors employee wise

Employee size: Between 200-500

FACTOR DESCRIPTION	MEAN SCORE	RANK	t	p
Eco Procurement	2.05	10	16.644	0.00
Eco-Accounting	1.93	11	11.147	0.00
Eco-Logistics Design	1.91	12	11.343	0.00
Eco-Product Design	2.25	7	14.750	0.00
Eco-Manufacturing	2.25	6	17.647	0.00
Marketing & Communication	2.14	8	10.559	0.00
Economic Performance	2.45	4	19.042	0.00
Environmental Performance	2.45	5	17.768	0.00
Customer Co-operation	2.60	2	14.321	0.00
Human and Technological Resources	2.63	1	13.454	0.00
Internal Environmental Management Performance	2.09	9	10.973	0.00
Operational Performance	2.50	3	14.660	0.00
Stakeholders	1.83	14	9.579	0.00
Vendor Management	1.86	13	8.884	0.00

The table 5 explains the group whose employee size is 200 to 500.

When analyzing the green supply chain factors where employee size is between 200-500, it has been observed that the most important factor is human & technological resources (2.63) followed by customer cooperation (2.60), operational performance (2.50) and the least important factor is stakeholders (1.83) followed by vendor management (1.83), eco logistics design (1.91). The biggest mean difference among the industry is found human & technological resources and the lowest is stakeholders. It means all the industry whose employee size is between 200-500 as we have targeted are equally performed well in stakeholders followed by vendor management, eco logistics design but they are more different in human & technological resources followed by customer cooperation, operational performance. 't' value of all the 14 factors, we have examine is more than '2' therefore the null hypothesis is rejected. Therefore it can be generalized that there is significant differences of all the 14 factors among the industries whose employee size is between 200-500.Therefore for the management point of view they should give more strengthen on stakeholders, vendor management and eco logistics design for improving green supply chain factors.

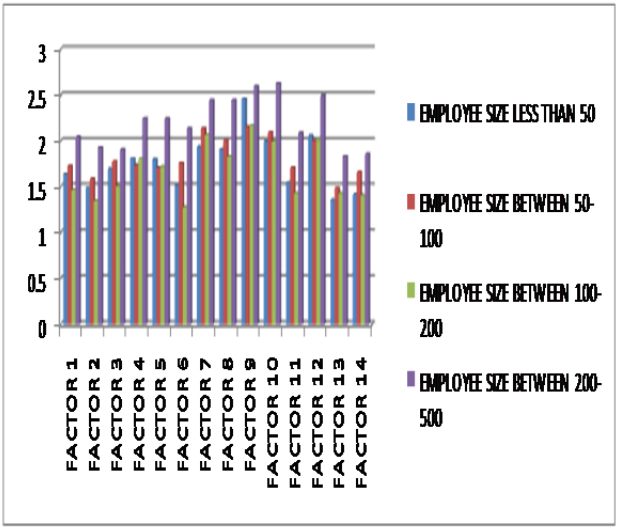

Figure: 3- Comparative analysis of effective (Mean Score) of Green Supply Chain factors employee wise

5.3. Extracted dimensions of green supply chain parameters through Factor Analysis

Factor Analysis (Factor analysis is a statistical procedure used to uncovered relationship among many variables) is applied on responses provided by the respondents. Factor Analysis is a set of techniques which by analysing the correlation between variables, reduces their number into few factors that explained much of original data more economically.

5.4. Validity Test for Sample Adequacy

The KMO measure of sampling adequacy is an index used to examine the appropriateness of factor analysis. High values (between 0.5 and 1.0) indicate factor analysis is appropriate and factor analysis explains about the sample taken for research is adequate or not. The value of Kaiser-Meyer-Olkin (KMO) which is a measure of sample

adequacy is found to be 0.720. This indicates that Factor Analysis test has proceeded correctly and the sample used is adequate as the value of KMO is more than 0.5.

5.5. Communality Scores of All Statements

The communalities for all the variables (dimensions) calculated. It has been considered 105 statements/dimensions from the SERVQUAL questionnaire with 105 positive influence statements in the study. The communalities score emphasize the importance of the statements according to the choices of the respondents. The most high impact statement is "Updating the current and proposed environmental regulations and legislation that may impact on business (0.900) followed by Support for green supply chain management from junior & middle level managers/executive (0.883), Recovery through sale of old/obsolete equipment (0.883), Environmental issues are regularly shared by vendors (0.878), Environmental performance is an important criteria in vendor selection (0.875) and the most least impact statement is Selection and use of energy efficient equipments and fixture for electrical, mechanical and lighting application (0.593) followed by Minimization of solid waste (0.610), Environmental costs associated with operations and processes (e.g. monitoring and abatement equipment, waste disposal etc.) are taken care (0.633) , Reduction in cost of energy consumption (0.658) and Reduced inventory level (0.663).

Range of communality score	0.900-0.593

It has been calculated communality score for all 105 statements. All the 105 statements retained for this study because the communality score of these statements are greater than 0.5.

6. Conclusion

The environmental performance of Indian industries and their long term commitment to managing their environmental impacts must be increased and supported through simple, effective and strategic support systems. The empirical results suggest that all 105 items are critical attributes of the 14 underlying factors of Green Supply Chain Management practices implementation. 119 enterprises have participated from different sectors from different region of India. In order to determine the importance of the factor and approaches, the judgment collected from respondents generated the normalized local and global weights for approaches to implementing Green Supply Chain Management. The results of priority weights determined the relative importance of individual factor and approaches and in turn recognized the points on which organizations should put their efforts throughout the process of Green Supply Chain Management implementation. In addition, the result could represent the general status of Green Supply Chain Management implementation in Indian industries, importance of approaches to GSCM implementation as shown in table 1,2,3,4 and 5. Indian industries are now on their path towards formal environmental management and sustainability.

6. References

[1] Bowen, F. E.; Cousine, P. D.; Lamming, R. C.; Faruk, A. C., Explaining the gap between the theory and practice of green supply. Greener Manage. Int., 35, 41-59, 2001.

[2] C. W. Hsu; A. H. Hu, Green supply chain management in the electronic industry, Int. J. Environ. Sci. Tech., 5 (2), 205-216, 2008.

[3] GILBERT, S., Greening Supply Chain: Enhancing Competitiveness Through Green Productivity pp 1-6. Tapei, Taiwan,2001.

[4] Gunasekaran A, Patel C & Tirtiroglu E ,Performance measures and metrics in a supply chain environment. International Journal of Operations & Production Management 21(1/2): 71–87,2001.

[5] Gunasekaran A, Patel C & McGaughey RE, A framework for supply chain performance measurement. International Journal of Production Economics 87(3): 333–347,2004.

[6] Handfield, R., Walton, S., Sroufe, R., Applying environmental criteria to supplier assessment: A study of the application of the analytical hierarchy process. European Journal of Operational Research 141, 70–87, 2002.

[7] Horvath, A., Supply chain environmental assessment of the telecommunications sectors. Intemational Symposium on Electronics & the Environment, San Francisco, Califomia, 146-150, 1999.

[8] Ninlawan C., Seksan P., Tossapol K., and Pilada W.,The Implementation of Green Supply Chain Management Practices in Electronics Industry, Proceedings of the International Conference of Engineers and Computer Scientists,Hong Kong, vol.III, March 17-19, 2010.

[9] Sarkis, J., A strategic decision making framework for green supply chain management. Journal of Cleaner Production 11 (4), 397–409, 2003.

[10] Zhu, Q., Sarkis, J., Relationships between operational practices and performance among early adopters of green supply chain management practices in Chinese manufacturing enterprises. Journal of Operations Management 22 (3), 265–289, 2004.

[11] Quinghu Zhu, Joseph Sarkis and Kee-hung Lai, Confirmation of a measurement model for green supply chain management practices implementation, International Journal of Production Economics, Vol.III, Issue 2, pp 261-273, 2008.

[12] Zhang, Xiaoyu and Zhiwei, Zhao, Green supply chain and its performance based on fuzzy and AHP and measurement system, 978-1-4244-4589, 2009.
[13] Zsidisin, G.A., Hendrick, T.E., Purchasing's involvement in environmental issues: A multi-country perspective. Industrial Management and Data Systems 7, 313–320, 1998.

THE FORMING OF THE BRIDGE STRUCTURE FOUNDED ON RC PILES AND SOLUTION SEISMICS STRENTHENING MIDDLE FRAME

Boris Folić[1], Simon Sedmak[1], Mladen Ćosić[2], Đorđe Lađinović[3]

[1] Innovation Center of Faculty of Mechanical Engineering, University of Belgrade, Serbia
[2] Marka Milanovića 17, 15300 Loznica, doktorant on Faculty of Civil Building, University of Belgrade, Serbia
[3] Faculty of Technical Science, University of Novi Sad, Serbia
* *Corresponding author e-mail: boris.folic@gmail.com*

Abstract

Presented in this paper is a brief overview of building of an existing overpass along with several possible ways of using seismic reinforcing of the central frame and certain criteria of choice. The calculation of the existing bridge-overpass using non-linear dynamic analysis (NDA) via time history (TH) while taking into account dynamic interactions between the foundations and soil is also given in this paper. In a soil-pile-structure system, the structure is modeled by using p-y curves for sand, as a link element, according to Reese model. The order of appearance of plastic hinges was analyzed.

Keywords:: seismic strengthening, nonlinear dynamics analysis, dynamics soil pile interaction, link elements soil-pile

1. Introduction

This paper will analyze a number of possibilities of seismic reinforcing of a bridge or overpass structure. Common requirement for bridge structures is that, for the a given level of seismic activity, the columns are allowed to take damage, but should not collapse and that the road plate-beam most remain undamaged, i.e. the bridge should remain functional and capable of being used for transportation even after the earthquake. In case of building, the order is reversed.

Bridge columns founded on piles are built either as massive, in cases where the appearance of plastic hinges is allowed, or as frame columns when plastic hinge opening is expected in beams below the road plate level.

The projected level of seismic activity is given according to a country's regulations (NAD) and is accompanied by a map of seismic intensity, for a corresponding return period. The choice of structure concept, type of founding and its calculation and detailing is directly affected by the significance factor, behavior factor, geomechanical conditions, etc.

2. Building of construction

The overpass was designed as a double-spanned prefabricated monolithic structure, with spans of 2x24 m=48 m. Upon finishing the usual preparations, building of the bridge begins by making HW bored piles. Piles are made in a steel pipe, and concreted on site. Piles of outer frames are encircled by wing walls, because when the bridge is finished, an access causeway is made within the wing. The causeway is made of nearly identical material as the soil beneath the pile, in order to avoid shear forces in the pile.

Upon finishing the central frame piles, its ends are cut short and cube shaped transition elements with 1.30 m sides are made for the purpose of connecting the overlapping reinforcement of piles and columns. Diameters are 1.20 m for piles and 0.90 m for columns.

Prefabricated supports with spans of 16.30 m, according to the project, temporarily rely on a heavy scaffold, after which the planking is placed and the reinforcements are positioned in the monolithic part above the piles of outer and central frames. The structure is then monolithized by concreting on site. The pedestrian walk represents an integral part of the outer prefabricated support. Once the structure is finished, roadsides, separating zones and asphalt surfacing are made.

2.1. Dynamic model used for calculation

Central frame system consists of four piles with a diameter of 1.20 m, which continue into circular columns with a diameter of 0.90 m, using cube shaped connecting elements with 1.30 m sides. Columns are connected at the top by a monolithic beam with height of 1.15 m and width of 8m. The beam continuation including the pedestrian walk is taken into account only as substituting load. Axial distance between the columns is 4.15 m. Pile length is 14.50 m (which is only 30 cm longer than the real one). Clear height of columns is 6.48 m-1.15/2 m = 5.90 m, since the offset function for rods is enabled, which corresponds to the actual length. The soil is modeled using bilateral link elements with p-y curves, which respond to pressure only. In this way, the central frame is formed for calculating effects of earthquake in the transverse direction of the bridge.

2.2. Seismic reinforcing of the structure

This section will briefly cover some of the methods for seismic reinforcing of frames, during

and after their construction, with a critical review of a specific case. These methods include:

- Reinforced tie beams between columns,
- Reinforced tie beams, subsequently pre-stressed,
- Metal, steel bracings of various shapes,
- FRP (carbon fiber reinforcements).

Each of these methods of reinforcement should be subjected in detail to following criteria:

- Feasibility-durability-maintenance
- Building costs, maintenance and repairs of damages caused by earthquakes
- Aesthetic criteria.

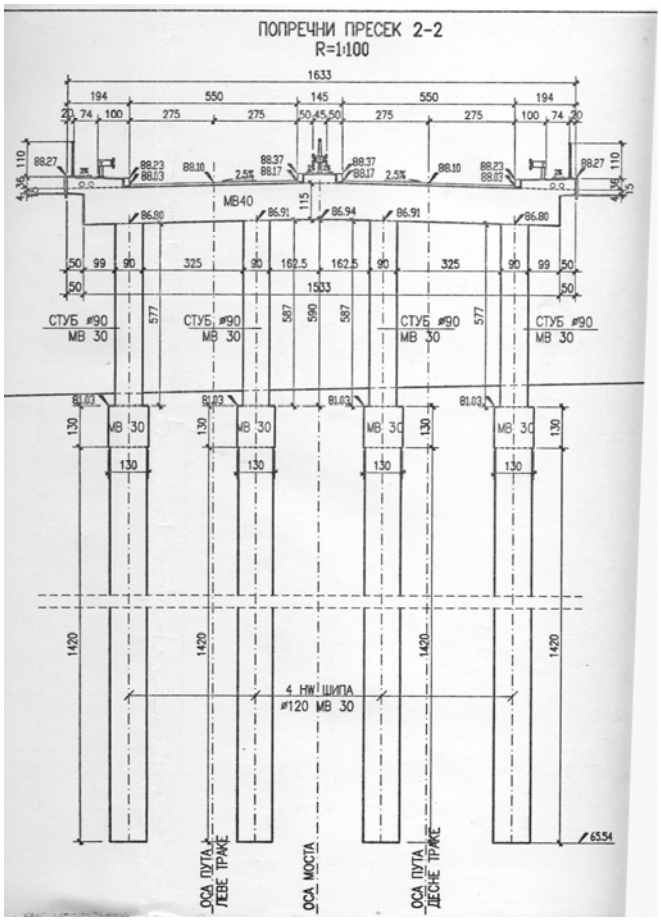

Figure 1. Middle frame cross section.

2.3. Reinforced tie beams between columns

In figure 3, a reinforced tie beam is added between reinforced cubes in the digging, with bilateral planking. The tie beam is made with an overhang in the middle. The overhang is equal to the maximum deflection (around 1,5-2cm), although in this case of a more rigid beam, slightly higher values could be allowed. The overhang is introduced for at least two reasons. One of these reasons is to program the opening of plastic hinge I in the middle of the span, which increases the amount of energy consumed during an earthquake in statically indeter–minate structures. The second reason is to program the beam overshoot, according to the analogy with a shallow arc, in order to prevent even–tual subsidence of the surrounding soil. After the overshoot the beam reaches the lower position and three plastic hinges are opened in a single beam, which allow it to rely on the compacted fill layer of gravel. When the beam comes in contact with the gravel, the friction between the gravel and the beam becomes active. Subsoil beneath the gravel with thickness d≈10 cm is partially reinforced, i.e. cemented. Gravel is also partially cemented, along with the layer of soil above the reinforced tie beam. This reinforcement is mild form so that it could enable the consupmtion of seismic energy in this part of the structure-soil. New layers must not be completely reinforced, since this would have a counter-effect, since the basic idea is for the energy to be first consumed by the tie beam and its surrounding area.

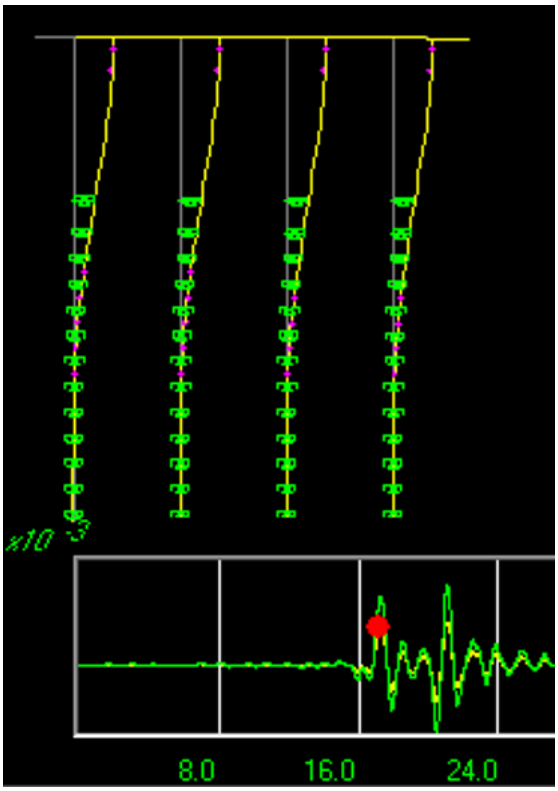

Figure 2 Vrance 1986 Focsani scale at 0.50g. Forming of the first plastic hinge in column at 15.90 sec, bat forming plastic hinge in pile at 17.00 sec

Dimensions of the tie beam are usually deter-mined in relation to the intensity of the normal force in columns and the transverse force in the tie beam. Tie beams are typically very rigid structures whose purpose is to equalize, as much as possible, the displacements of foundations at the level between groups of piles. Stiffness of tie beams is such that it causes them to break before the foun-dation pillows do, therefore dissipating a part of the seismic energy.

Assumed dimensions of tie beams in this case are b/h=60/40cm, 60/60cm and 80/70cm. Greater beam dimensions would result in stiffness values closer to those of columns, which is unfavorable. Next step includes the drawing of reinforced beam details in scale, so that the realistic image of dimensions can be obtained.

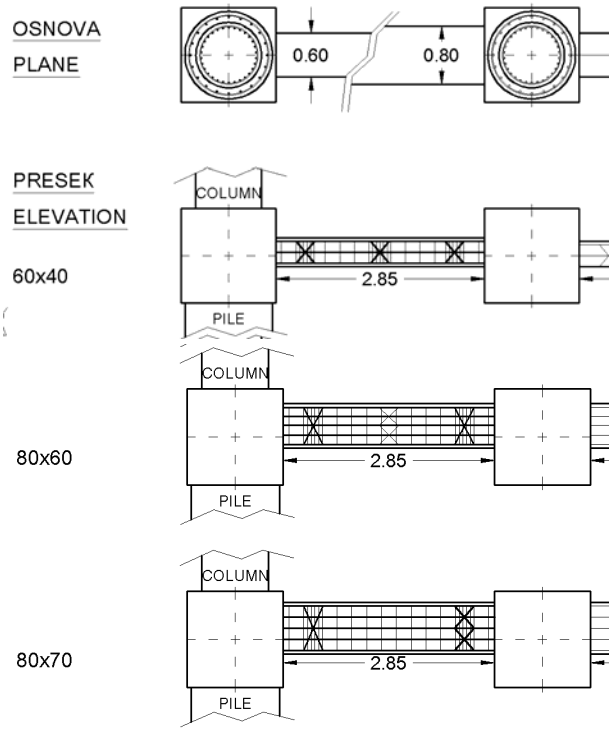

Figure 3 Plane and cross-section of the tie beam.

Even though the axial distance is 4.15m, taking into account that the cube dimension is 1.30m, the remaining length for the tie beam is only 2,85m. This suggests the following reasoning: the central hinge can only be placed for a beam with the height of 40cm. The length plastic hinges can be partially influ–enced by choosing the reinforcement bar diameter, its type and positioning and the shape and dimen–sions of the concrete cross-section. It is necessary to tighten plastic hinges using stir-ups or spirals. This tightening can be performed using FRP technology.

Anchoring of the tie beam is achieved through the reinforced cube, the part of the pile that is cut short and where reinforcement is continued. It is certainly easiest to place anchors in the cube, once the planking is set up, prior to concreting, since this makes it easier to achieve the projected anchor re-inforcement position and anchoring length. Subse-quent adding of anchors requires additional atten-tion and effort, as well as boring of inclined anchor holes, partial chiseling and coating with SN bond and epoxy. This solution does not disturb the appe-arance of the structure, since it is not visible and is performed above groundwater level. It is harder to check the state of tie beams after the earthquake, since it requires excavating.

The system was run in SAP2000 software with link friction between beams and soil. Assumed friction coefficient is less than tan(40)=0,84. Further investigations and fitting of this model are required in accordance to the correlation of the chosen reinforcement principle.

2.4. Pre-stressing of tie beams

Pre-stressing can be performed using cables according to IMS technology. It is necessary to bore the reinforced cubes, so that cables can pass through them (4Φ7 ori 6Φ7mm cables). Anchors should be protected by using reinforced „roses“. Cables and holes should be injected upon tightening and anchoring.

2.5. Metal bracings

Steel bracings can be made above soil level in many different ways. When choosing the solution, the aesthetic criteria is of great importance, since trans–portation takes place under the overpass as well. Bracings can be made as K shaped, X shaped, double X shaped or a combination of various sha-pes with different spans, etc. Cross-section can be circular, square, rectangular, etc. Material can be black steel, galvanized black steel, stainless steel, aluminum, etc. These bracings are readily available for inspections during structure state monitoring.

Even though bracings are not exposed directly to rain, since they are located beneath the road plate, they are still exposed to indirect effects of rain, snow and de-frosting salt because of vehicles, and in rare cases because of wind. Hence, if tube-box black steel profiles are used, it is necessary for them to be hermetically welded to face plates.

2.6. Comments on NDA TH of the central frame

Regardless of the fact that p-y curves were once a significant contribution to the non-linear analysis of interactions, certain degree of caution is required when applying this method, for both Reese or API method, or any other similar methods. It is first re-quired to be careful with soil sensitivity parameters and then it is required to examine the stability of results in relation to the variation of specific soil pro-perties. Further recommendation includes the appli-cation of models for higher-order soils or with connections between piles along soil layers, in addition to the p-y curves.

During the NDA scaling of records for Vrance 1986 station Focsani, above 30g after the appearance of plastic hinges in the central frame, separation of pile heads occurred. This directly means that, if during THNDA, drifts are observed for a single column, without including the displacement of pile heads, we will not be able to see local failures in the structure, at lower scaling levels, hence results could be inter–preted in a wrong way. It is recommended to monitor TH, the timeline of earthquake response of at least one column in continuity with the pile.

Taking into account that the actual structure is located in northern Serbia, in Vojvodina, earth–quake records from Romania from 1977 and 1986, with epicenter in Vrance, with varying locations and directions were adopted as representative. Regard–less of the possibility for these records to have same values of PGA (peak ground acceleration) during accelerogram scaling, they cause variable individual effects of relatively similar structures, depending on the amplitude frequency composition.

Figure 4 shows the plastic multi-linear model of Takeda soil. Even though this model is good at simulating the hysteresis gap effects in soil, it is better to adopt a plane soil model with plastic behavior for a model with reinforced tie beams. Program SAP 2000 can not do this directly, instead it requires non-linearity to be established using link elements in plane model nodes during the connecting of FEM soil with the structure. (ABAQUS software enables the analysis of non-linear elasto-plastic behavior of plane soil elements.)

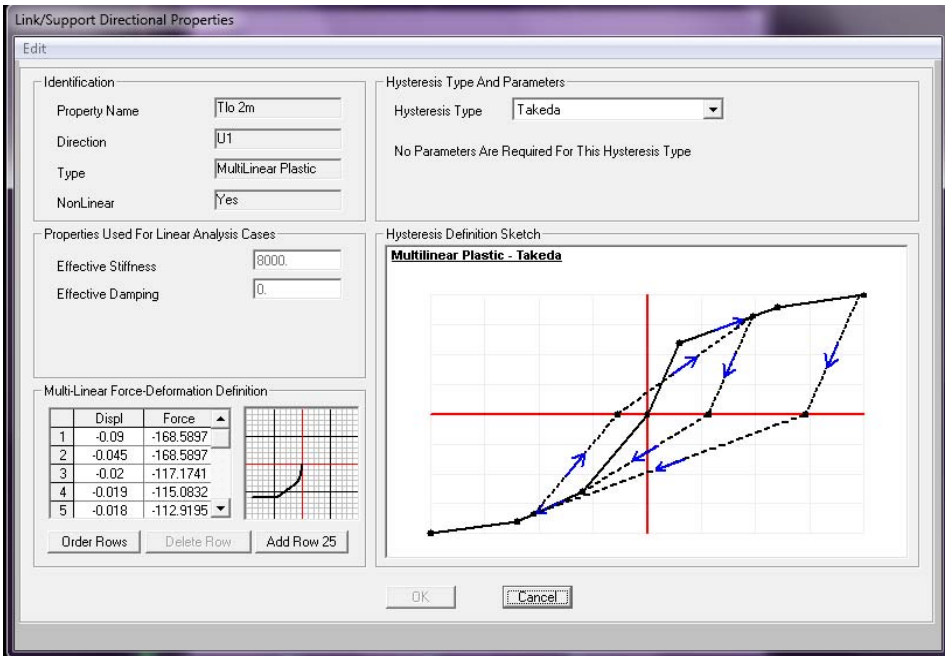

Figure 8. Solid model. P-y multi-linear

3. Conclusions

Analysis of structure vulnerability and determination of significance factor for bridges should not only be governed by individual consideration of an object. It is necessary to create criteria for the flow of traffic and transport in emergency conditions. In these cases it is possible for a single structure, made for multiple buildings and locations, to have varying levels of significance in ensuring protection and functionality, even under very similar conditions and the assumption that they are located on roads of the same priority and traffic intensity.

Acknowledgements

This research was financially supported by the Ministry of Education and Sciences Republic of Serbia within the Project TR 36017.

References

[1]. EC 8. (euroccode 8) published by Građevinski fakultet Univerziteta u Beogradu. IMK.
[2] Finn W.D.L., Fujita N.: Piles in liquefiable soils: seismic analysis and design issues. Soil Dynamics and Earthquake Engineering 22 (2002)
[3] Meymand P. J.: Shaking Table Scale Model Tests of Nonlinear Soil-Pile-Superstructure Interaction In Soft Clay. University of California, Berkeley. 1998.
[4] Миловић, Д., Ђого. М.: Проблеми интеракције тло-темељ-конструкција. САНУ, огранак Нови Сад, 2009.
[5] Panetsos P., Liolios A.: Seismic Vulnerability Functions for a Bridge Case of Egnatia Motorway. Aseismic design and construction in Egnatia Odods. Thessaloniki 2010
[6] Prakash S.: Soil Dynamics. McGraw-Hill Book Company. New York 1981.
[7] Ruwan Rajapakse. Pile Design and Construction Rules of Thumb
[8] Suarez, V.: Implementation of Direct Displacement Based Design for Pile and Drilled Shaft Bents. NCSU. October. 2005.
[9] Theoretical Manual for Pile Foundations. ERDC /ITL TR-00-5. Novembar 2000. Vulcanhamer. net

DIGITAL IMAGE CORRELATION IN EXPERIMENTAL STRAIN ANALYSIS OF WELDED JOINTS

Nenad Milošević[1], Miloš Milošević[1*], Simon Sedmak[1], Uros Tatic[1], Nenad Mitrović[2], Sergej Hloch[3], Ratko Jovičić[1]

[1]University of Belgrade, Innovation Centre of the Faculty of MechanicalEngineering, Belgrade, Serbia,
[2]University of Belgrade, Faculty of MechanicalEngineering, Belgrade, Serbia,
[3]Faculty of Manufacturing Technologies of Technical university of Košice with seat in Prešov,Slovakia
Corresponding author-mail: mmilosevic@mas.bg.ac.rs

Abstract
Behavior of welded joints in local areas and their mutual influence is a major challenge for designers of welded structures. The possibility of determining the value of the local displacement/strain makes Digital image correlation (DIC) a very suitable technique for testing of welded joints. Development of DIC methodology in experimental local strain analysis with use of Aramis software for 3D displacement/strain measurement of welded joint is presented in this paper.

Keywords:
Digital image correlation, strain analysis, Aramis software, welded joints, stiffness.

1. Introduction

Strain measurement in engineering practice can be done in several ways. General classification could be divided to contact measurement, i.e. direct measurements (extensometers, strain gauges) and non-contact strain measurement using appropriate equipment, mainly camera and software for processing results [1-11]. Non-contact testing methods are rapidly evolving and developing different ways of testing based on the same principle, like DIC (Digital Image Correlation), stereography, stereometry). Non-contact deformation studies are suitable for standard applications (calculation of stresses, strength, etc.), and for non-standard, such as, measuring during non-destructive testing (NDT). Determining the deformation capacity of welded joints is complex due to the structure of the compound, which can be seen as a combination of the three areas. These three areas are: base material (BM), heat affected zone (HAZ) and weld metal (WM). Procedure for testing the properties of these areas, which include cutting the entire specimen in a particular field, such as is done in the contact investigation and provides results for observed area. The analysis of welded structures also requires the determining of the deformation capacity of the entire weld with all areas of the joint. DIC method is solution to the problem of determining the quantitative properties of materials at the local level in the welds, without excluding mutual influence zone of the welded joint. DIC is a simple and quick technique for the determination of a large number of data on the tested components. The measurement is based on a comparison of a series of images that were obtained over a period of microseconds to several years, depending on the time of experiment. DIC process is divided into three modules. The first module is responsible for the grid generation, the other for the actual correlation, i.e. correlation of images and the third for post-processing. Some of the advantages of this test method are: non-contact method allowing tests of large objects and objects with complex geometry, calibration techniques that provide high accuracy and the analysis with post-processing which allows for an experiment to get more kinds of results. This method is possible in 2D and 3D measurement, depending on the number of cameras used.

2. Material and test procedure

For the purposes of this study, specimens with parallel sides that were previously welded with MAG process using CO_2 as a shielding gas, were made. Specimen material is Č0361 (S235JRG2) whose chemical composition is shown in Table 1.

Table 1.The chemical composition of base material

C	Si	Mn
max 0,2	max 0,55	max 1,4
S	Cr	Mo
max 0,045	max 0,3	max 0,08

Table 2. The mechanical properties of base material

Nominal thickness (mm)	to 100 mm	100-250 mm	250-500 mm
Re (MPa)	215	175	165
Rm (MPa)	340	340	340
A-longitudinal %	24	23	23
A-transversal %	17		

Materials with these characteristics area low alloy carbon steel with fine weldability and there was no need for preheating or post weld heat treatment. Specimen sketch with characteristic dimensions is shown in Figure 1.

As seen in figure 1, the elevations are not ground in order to simulate the real exploitation situation as closely as possible. Figure 2.shows the defining of small measuring zones in the characteristic area of a welded specimen. After welding, the specimen was minimally processed, i.e. only the surface was cleaned so that following measurements would be easier to perform.

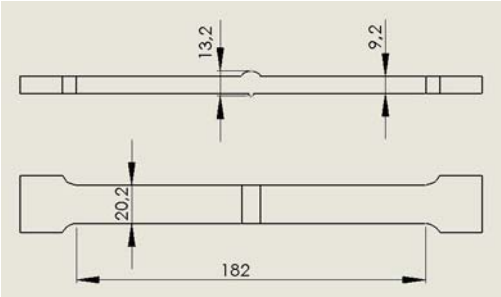

Figure 1. Specimen dimensions

Not removing the portion of the weld metal from the face and the back side has of great influence on the accuracy of the experiment, especially if we bear in mind that the certain stress and strain concentration occurs at the face and the base of the seam. After completing the tests, post-processingis performed. During this test data were analyzed in Excel and the results are presented in chart form that is suitable for further analysis, which includes stresses and strain values.

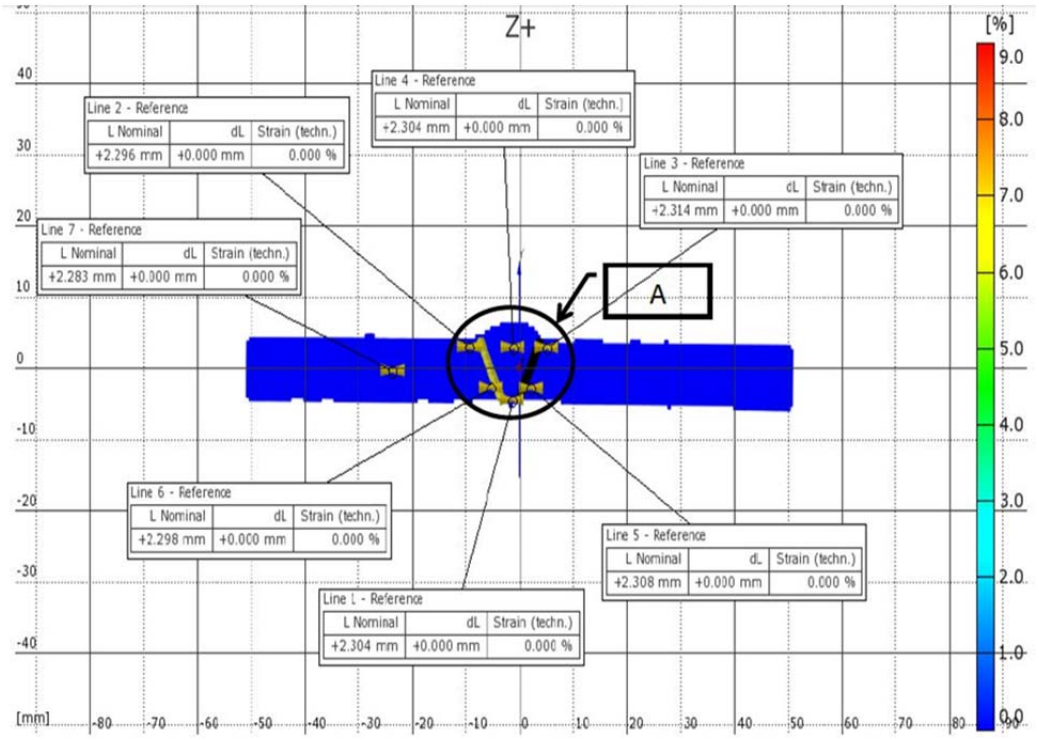

Figure 2. The positions of small measuring zones in the weld

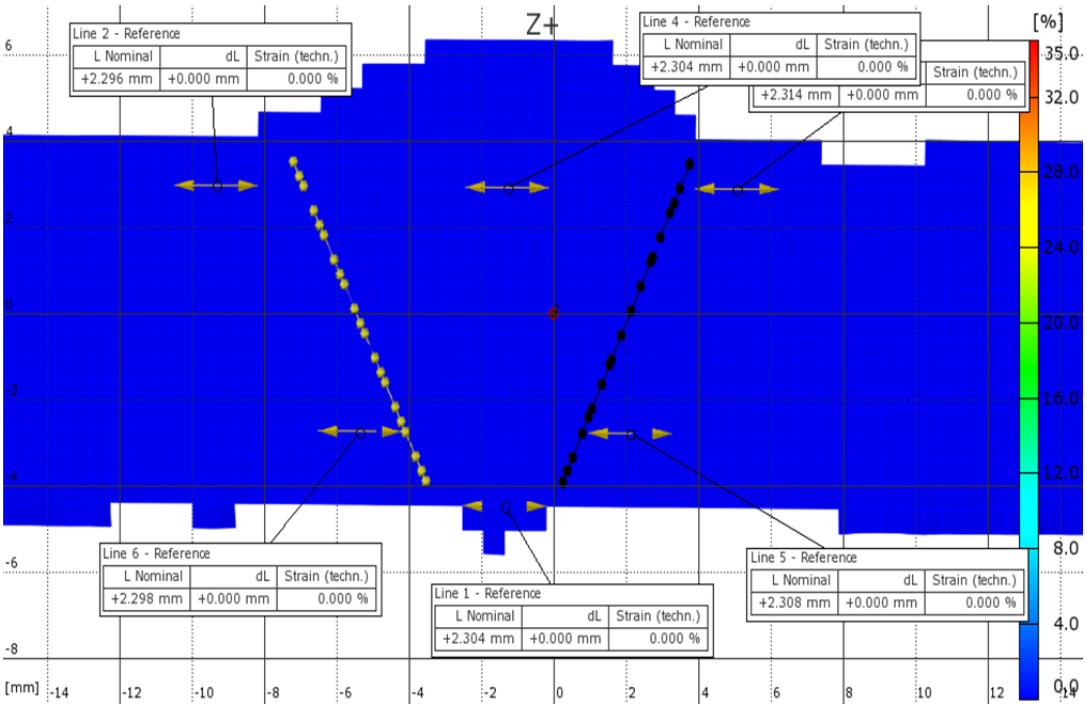

Figure 3. Observed zones position (Detail A from Figure 2)

From Figure 2 it can be seen that the measuring zones areof varying lengths, around 2.3 mm. It can also be seen that the technical strain is the property that will be monitored, in order to compare the deformation capacity of these areas. Technical deformation of small measuring zones which are monitored are obtained using the tools of Aramis called "point-point distance", which in this case defines the length of the measuring zone. Yellow and black lines that can beseen in Fig. 2 represent the fusion line on each side of the weld and mark the boundary between the areas of WM and HAZ's. Figure 3 shows the detail A from Fig. 2. From Figure 3 one can gain insight into the precise positions of six measuring zones that are placed in WM and HAZ.

3. Results and discussion

Aramis software registers elongation as it truly is, while strain is calculated from the changes in the distance between two points. Value of the strain that is displayed on the local level is actually real strain and does not depend on the chosen reference length of the grid. Figure 4 shows stress-strain diagram for welded joints obtained from tensile testing.

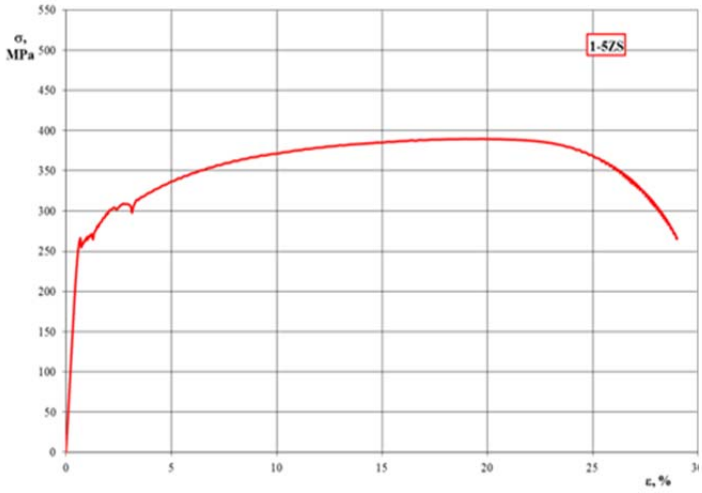

Figure 4.Stress-strain diagram for welded joint

Determining of deformation capacity of local zones is done by obtaining the actual values of stress and strain in interested fields. From diagram shown in Figure 5, after the linear approximation, the elastic strain zone was obtained as a straight line, whose slope represents the stiffness of these zones. As in a case of elasticity module, determining the tangent of the angle between the horizontal axis and the stress-strain line is used to determine the stiffness of the measured zone. Hereinafter, the slope that determines the stiffness zone, i.e. its deformation ability will be marked as S ("slope"), Figure 5.

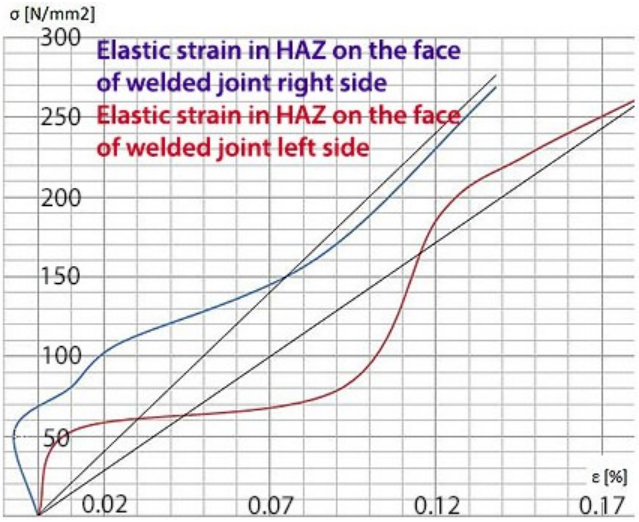

Figure 5. Linear approximation of elastic strain zones on right and left side in HAZ

It is clear from the diagram that the yielding appears at a stress of approximately 260 MPa and strain of approximately 0.67%. It is also seen that the maximum stress is 390 MPa, and the total strain is approximately 29%. In order to obtain a complete picture of the distortion of specimen and the small measuring zones, this diagram was compared with the values obtained bythe software, Figure 6. Yield point on the stress-strain diagram (Figure 4) is used as the first characteristic point. The appearance of the strain fields at the point of yielding is shown in Figure 6. It can be concluded from strain fields, that the most significant strain occurred in the base metal and HAZ with the root, i.e. the back side of the weld. Values of strain as shown in the figure are consistent with the values that are characteristic forthe diagram obtained from tensile testing, since the maximum strain at the point of yieldingis between 0.6 and 0.7% and for the tensile testing diagram, it is approximately 0.67%.

4. Conclusions

This study shows that in the elastic deformation domain, face of the weld deforms more than the root, causing the pressure in the HAZ (in cause of tensile test). This is a consequence of different degrees of interference in the face and the root of weld, geometry, shape of joint which is in this case V or greater weight of the weld face side. In the initial phase of testing, the presence of bending stress leads to compressive stresses in the weld root, resulting in increased facial strain in relation to this area. Local deformation capacity using DIC method is obtained in accordance with the welded joint geometry.

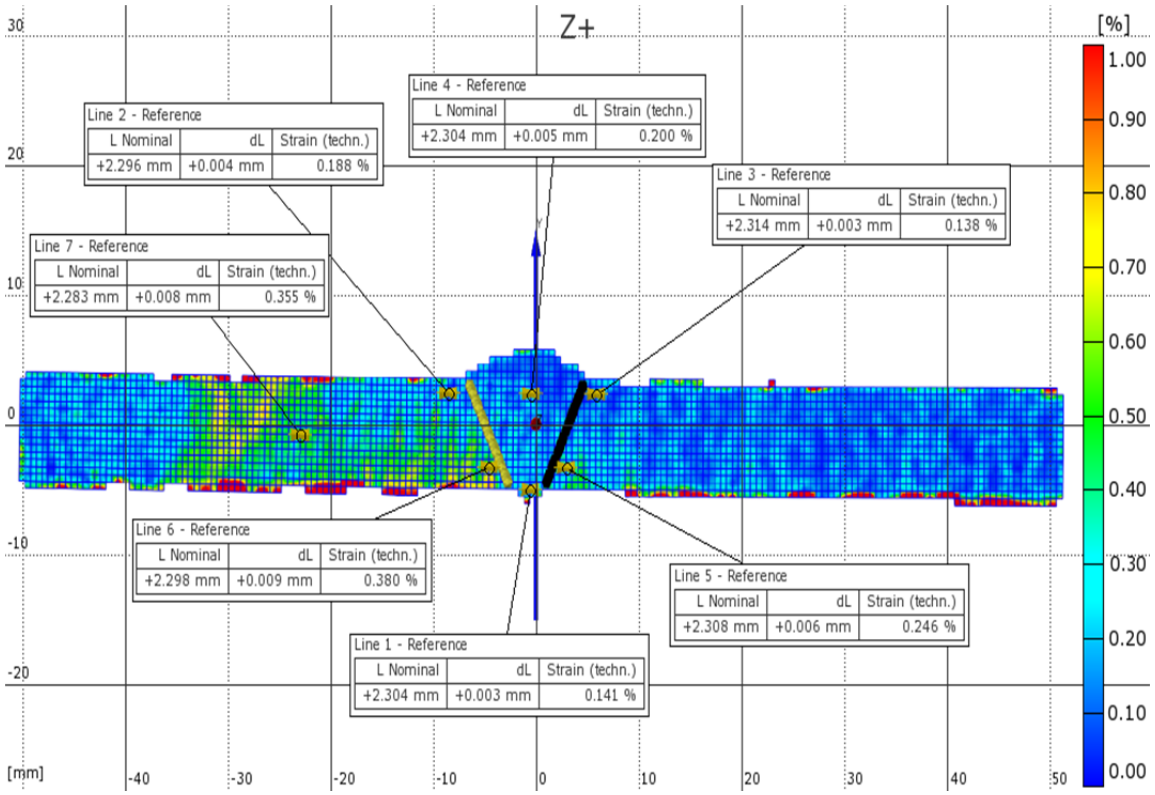

Figure 6. Strain field of the welded joint

5. References

[1] Tanasic I, Tihacek-Sojic Lj, Milic Lemic A, Djuric M, Mitrovic N, Milosevic M and Sedmak A: Optical aspect of deformities analysis in the bone-denture complex, Collegium Antropologicum, 36 (2012)

[2] Milosevic M., Miletic V., Mitrovic N., Manojlovic D., Savic-Stankovic T., Maneski T.: "Measurement of local deformation fields in dental composites using 3D optical system", Chemicke Listy 105, s751 - s753, 2011.

[3] Jovicic R., Sedmak A., Colic K., Milosevic M., Mitrovic N.: "Evaluation of the local tensile properties of austenite-ferritewelded joint", Chemicke Listy 105, s754 - s757, 2011.

[4] Miletic V., Manojlovic D., Milosevic M., Mitrovic N., Savic Stankovic T., Maneski T.: "Analysis of local shrinkage patterns of self-adhering and flowable composites using 3D digital image correlation", Quintessence Int 2011;42(9):797-804

[5] Lj. Tihacek Sojic, A. Milic Lemic, I.Tanasic, N. Mitrovic, M. Milosevic, A. Petrovic, Compressive strains and displacement in a partially dentate lower jaw rehabilitated with two different treatment modalities, Gerodontology 2012, 29(2):e851-7;

[6] M.Milosevic, N.Mitrovic, R.Jovicic, A.Sedmak, T. Maneski, A. Petrovic, T. Aburuga, Measurement of local tensile properties of welded joint using Digital Image Correlation method, Chemicke Listy 106, pp. 485-488, 2012.

[7] N. Mitrovic, M. Milosevic, N. Momcilovic, A. Petrovic, A. Sedmak, T. Maneski, M. Zrilic, Experimental and numerical analysis of local mechanical properties of globe valve housing, Chemicke Listy 106, pp. 491-494, 2012.

[8] Sedmak A., Milosevic M., Mitrovic N., Petrovic A., Maneski T.: "Digital image correlation in experimental mechanical analysis", Integritet i vek konstrukcija (Structural Integrity and Life), Vol.12, No1, pp.39–42, 2012.

[9] I. Tanasic, Lj. Tihacek-Sojic, A.Milic-Lemic, N. Mitrovic, R. Mitrovic, M. Milosevic and T. Maneski: Analysing Displacement in the Posterior Mandible using Digital Image Correlation Method, J Biochip Tissue chip S1:006, 2011.

[10] Tanasic I, Tihacek- Sojic Lj, Milic Lemic A, Mitrovic N, Milosevic M, Mitrovic R and Maneski T, Strain Behavior in the Restored Edentulous Mandible Bone. J Bioengineer & Biomedical Sci 2:107, 2011.

[11] Mitrovic N., Milosevic M., Sedmak A., Petrovic A., Prokic-Cvetkovic R.: „Application and Mode of Operation of Non-Contact Stereometric Measuring System of Biomaterials", FME Transactions, Vol. 39, 2, page 55-60, 2011.

[12] H.J.K. Lemmen, R.C. Alderliesten, R. Benedictus, J.C.J. Hofstede, R. Rodi, The power of Digital Image Correlation for detailed elastic-plastic strain measurements Faculty of Aerospace Engineering, Delft University of Technology, P.O. box 5058, 2600 GB Delft, The Netherlands, 2008.

ENTERPRENURIAL MANAGEMENT OF SMALL HOTELS OFFER IN CONTINENTAL CROATIA

Lena Duspara[1*], Ivana Blazevic[1]

[1] University of Applied Sciences of Slavonski Brod, Slavonski Brod, Croatia
* *Corresponding author e-mail: lena.sigurnjak@vusb.hr*

Abstract
Development of tourism in Croatia in the past had been based on building huge hotels which were working only during short summer seasons and on massive scale of guests that meant only the number in the series, competition approach to the development of tourism. It has been focused on the growth of a network of small family hotels opened through the year with far better service. With the change of the political situation in the country and turning towards the market economy, the former touristic product stopped being competitive or profitable, thus the hotels suffered from heavy losses, as they have to be more flexible and high-grade competitive.
To prevent the accumulation of losses and declining of hotels, the Republic of Croatia has turned to the development of small family hotels and creating of a trendy touristic product that is not based only on the sun and sea. Entrepreneurial managers have the main role in this development, these who are able to create a new quality, supplement a new value to the product and meet the needs of their gusts in any aspect with their creativity and innovations.
Since the developing potentialities of tourism have not been used up, but there are greater differences between possibilities and realization in the continental part of Croatia than along Adriatic coast, it is reckoned the continental part of Croatia is about to see its touristic development carried by small hotel managers.

Keywords:
small hotels, management, touristic offer, planning, quality

1. Introduction

Continental tourism has been present in European countries for decades, but in the last few years in the Croatian gets a more prominent position. However, if small hotels want to be successful- could maximize their profits- they need a quality management whose role in achieving business results and improve the performance of small hotels is most important. Management is like any other profession continuously changing and adapting to the evolving business and social environment whose main characteristic is variability.
In global environment, successful are only those companies that have ability to quickly learn and use the available information to create new products and increase the quality of existing products and services. Only such enterprises are able to adapt to constant change and continuous learning can beat competitors to satisfy their customers and create some new trends. Specifics and special hotel activities and determine the necessary size of the hotel management features are critical to successful hotel business, and in this paper will be presented the necessary characteristics, knowledge and skills and the importance of entrepreneurial management for successful business and increase of competitiveness of small hotels offer in continental Croatian.

2. Entrepreneurial management in small hotels

It is time of great and rapid change in the global and social level as well as on the economic front. Turbulence and uncertainty of the environment is growing, and disaffiliation change means stagnation, backwardness and decay. The new era poses new challenges and requires new skills necessary for these challenges, and there is no doubt that in this process of transformation prominent place belongs to the knowledge of management, without which it is impossible to imagine the modern business world.
Management is the phenomenon of the twentieth century and one of the three revolutions with car industry and telecommunications, which have changed the way of life around the world. “Factors that determine the diversity of hotel management in the legal and economic standards: cultural and historical heritage, religion, tourist market, capital structure and ownership, diversity of tourism resources limited form of hotels and hotel companies, ratio of technical knowledge and general education”[1]. Specificity resulting from the two key determinants of the economy: “seasonal restrictions on operations and the nature, function and technology services provided”[2].
It is extremely important to clearly identify specific areas of management in small hotels and at the same time is especially important to consider: “role of marketing, quality management, importance and usage of information technology, relationship between planning and performance, strategic management and growth of the company and development of entrepreneurship”[3].

It could be concluded that the activities of hospitality nurtured specific form of management while taking into account specific components and providing hotel services such as: “immateriality - hotel services are largely intangible, they cannot be stored (service-nights); uno-actu-principle, service and consumption occur simultaneously (service rates immediately provided and consumed by the guests); integration of external factors that could provide the service the customer must come to the place of service (service can be provided only in the presence of guests); obligation to participate, to be a part in the success of your stay in a tourist destination, building, etc. (their wishes should be adequately communicated); consumption at the point of service, guests must arrive product consumption follows the place of service; package combines the things and services (lump journey consists of transportation/service provision/nights /providing a service/food /making stuff); basic and additional services, the overall catering consists of primary and secondary services; high comfort to the parts of the product, the various elements of the tourism product influence each other reciprocally (bad or good hotel affects the overall travel picture)” [4].

3. Functions of entrepreneurial management in small hotels

Small, medium and large businesses have five basic functions: planning, organizing, staffing, leading and motivating and controlling. These functions depend on the size of the company, only differ in the comprehensiveness, complexity and diversification to individual holders of such a small hotel, the holder of these managerial functions are combined in one person - the owner.

The plan is the basis for the operation of each entrepreneurship. It is not surprising, because like in all everyday situations-how many times was seen as a housewife and her husband in the hand holding a piece of paper that says what they want or they can buy. Planning determine the tasks which can be accomplished in a limited time in order to achieve the desired goals, so this management function requests from the manager that knows the opportunities in the external environment, your potential guests but also the potential limitations to be able to put together a realistic and efficient business plan.

The function of the organization involves the development of an organizational structure through the design and distribution of tasks, specify a range of control and distribution of the leading roles in the company. It tends towards the formation of the structure of relationships and authority that enables effective coordination of all functions and business efforts.

When the entrepreneur made a business plan and organizational chart following step is to choose a frame that is able to implement his ideas into action. Selecting the required personnel or staffing is an essential function of management that largely determine the success or failure of enterprises, which is particularly pronounced in the catering business, where the human factor is crucial for the quality of work, and includes the: “job analysis, personnel planning, acquiring staff, their introduction into the business, motivating staff, their constant training, promotion and progression”[5].

Conduct appears as one of the basic management functions, which means the process of impact on people so that they are willing to contribute to the achievement of common goals. This means understanding and exploitation of knowledge, skills, capabilities and other features motivating people, not manipulating. “Controlling is monitoring, checking and judgment decisions, procedures, measures and results achieved with respect to the plan and to set goals that indicates the measurement and correction activities and behaviors identified in the plan, to ensure the achievement of the objectives" [6].

4. Characteristics of small hotel entrepreneurial management in continental Croatia

Any enterprise including small hotels should be used for business planning to build a business orientation, and help to bridge the difference between where is currently located, and a future state where they want to be over a certain period of time. Accordingly, the plan as a result of planning that helps management in creating a desired future, and as such is not only an instrument but also to guide the execution of all business tasks that lead to management goals. So, no serious entrepreneur should invest money in any business venture if not previously explored the market and based on the information obtained can be planned and anticipated operating results. Figure 1.below shows source of funding small hotels.

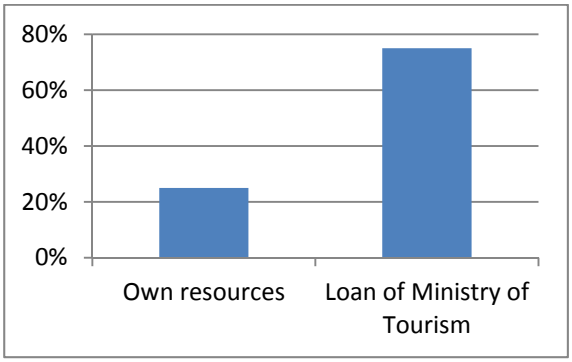

Figure 1. Source of funding small hotels

Figure1. shows that „75% of small hotels are financed by the Ministry of Tourism of the loan because it enables easier operations and increase

competitiveness but encourages new investment to build a new class hotels, and only 15% of the hotel uses its own funds“ [7]. A business plan is documents that detail the entrepreneurial idea and gives an estimate of future business and financial developments during the project. A business plan is used to test the idea that this would reduce the investment risk and increase success. A business plan is the most convincing proposal for financing entrepreneurial projects.
Managers, who are also the owners of small hotels in the continental Croatian financed the construction of its facilities mainly through credit lines to the Ministry of Tourism "Incentives for Success" and had to do a study in which they presented a business plan and return the object. In figure 2. is shown the structure of business of small hotels in continental Croatia.

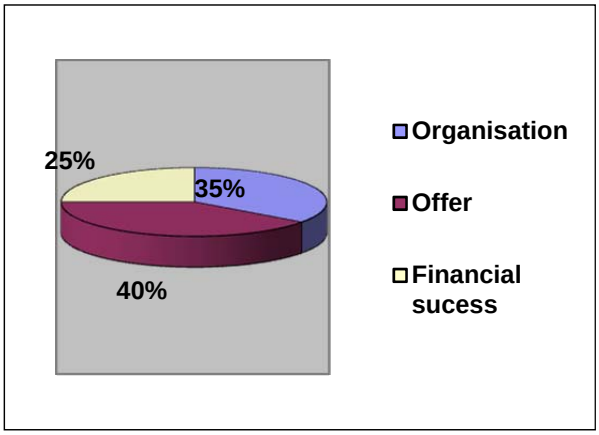

Figure 2. The structure of the business

Owners of small hotels in the continental Croatian, aware of their strengths and weaknesses, optimism for the more successful business built on the fact that it is currently a bit in this area and would therefore work is currently supposed to be for everyone, and eventually when you overcome the initial problems in the business hopes that the quality and range of reach small hotels in other areas Croatian.
Personnel in the hotel industry with its peculiarities in the breadth of general education, knowledge and necessary skills of verbal and nonverbal communication, etiquette, foreign language skills and knowledge of related technologies which are attended by, raise each employee who works in the hotel industry at the level of the required forms of education, and search and temporary adjustments and learning the specifics of the hotel where works.

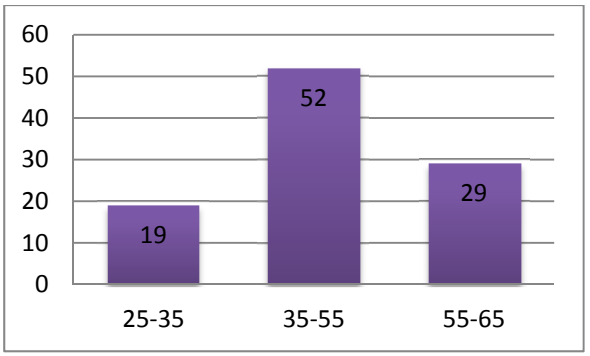

Figure 3. Age managers in small hotels continental Croatia

Figure 3. shows that most hotel managers employed at the age of 35-55 years because they possess certain knowledge and skills necessary for performing of the required work, and only 19% of them are employed in the age of 25-35 years.
Competition and constant technological changes in all areas of human life and work made transform and thrive, in order to increase the diversity, variability, dynamism and choice. In such a global environment, successful organizations are those that are able to change, learn, develop and utilize all available information in order to create inventive products and services. Therefore, the most important task on the way to the future stimulation, recognition and management of innovation and its potential application in all areas of life and work. „Inventive management in tourism is a set of knowledge and ability to quickly adapt to change, and the power of selection, the importance of certain events, in order, at any time, the hotel staff was able to react in a way, that the manager personally, or executors, meet the needs of the customer, as expected and that will make tourists happy“ [8].
Structure of the personnel management of small hotels in the continental Croatian are managers who are also the owners of small hotels men aged 35-55 years and possess a high school diploma or higher, speak English and German and are IT written. All owners of small hotels are opening small hotels primarily to expand the range of offerings of their enterprises or products to which products easier to sell and presented to the market and thus rounded out its offerings.
In strong competition and increasing demands of consumers quality has become a fundamental factor for survival in the market, profitability and overall development of the country's economy and its individual businesses and companies. Access to quality has evolved from the concept related to the quality of products and services related to the concept of management, so today management is based on the principles of „Total Quality Management's (TQM), which ensures the achievement and maintenance of quality, increased flexibility, efficiency and effectiveness of

operations“ [9]. TQM system is completely oriented to the market, driven by the customer, the customer is king in a system full of quality, because the process begins with the customer and ends with the customer. Advantages and disadvantages of implementing of small hotels in implementing of TQM are next. Advantages: the organizational structure is simple, which makes introduction of quality easier; it is easier to explain the program to all of the quality system and gain confidence in the system; every employee is in constant contact with the product and service and hotel guests and has a clearly defined tasks and responsibility; employees often work different jobs and are more connected to each other and more familiar with the hotel business; trainings and education is much easier to organize; connection between management and employees is higher; faster and easier to notice threats and weaknesses and also to detect and satisfy the desires of guests. Some of disadvantages of small hotels in implementing of TQM: education of employees is usually lower than in big hotels; training times of employees are organized less because for managers it could mean the loss of working hours of employees and owners workouts often treated only as an expense; managers and owners of small hotels often do not have a market vision and strategy, and the TQM have in reserve; in small hotels lack of knowledge often provides resistance to TQM and all the news and new ideas in general; the owner, his knowledge and culture dominate the management of a small hotel, so all depends on his understanding of TQM; lack of co-operation and understanding of the owner and the manager makes the introduction of TQM.

On the performance of the small hotels in continental Croatia is largely affected by leadership that management and other factors, both internal and external, which are shown in Figure 4.

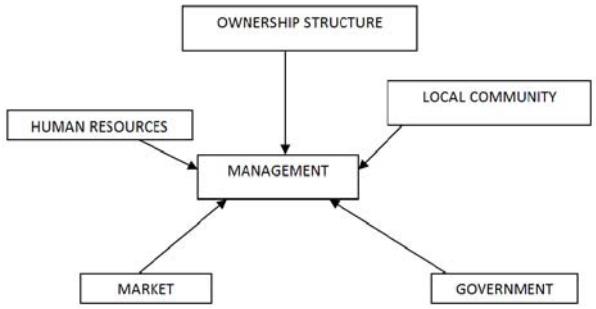

Figure 4. Factors that influence on success of a small hotel management

Figure 4. includes the most important connections and relationships between factors that affecting the performance of the management of small hotels: government, local communities, human resources, market and ownership structure.

5. Conclusion

Small hotels increase the level of service in the Croatian tourist offer and also improve the quality of the destination and provide business not only during the summer time, but also during a whole year. In small hotel guests can enjoy the intimate atmosphere, better service, more attention and individual approach, and it now wants a uniqueness that gives the unique experience of staying in a resort.

Family-run hotels open all year round are the future of Croatian tourism and currently there are only about 120 which, in the judgment of the National association of small and family-run hotels, ten times less than the need. Therefore after Croatian accession to the European Union, Croatia should work for at least a thousand small family hotels, similar to those that are tourist reborn European powers like Italy or Austria.

Opportunities for tourism development in Croatia are far from being exploited, but the differences between the features and what has been achieved in continental Croatian is significantly greater than its Adriatic part is therefore logical to expect that the continental Croatian yet to experience its powerful tourism development carried by entrepreneurial managers of small hotels.

6. References

[1] Cerović, Z., 1993. „Poduzetništvo i menagment čimbenici uspješnog poslovanja hoteljerstva“, Doktorska disertacija, Hoteljerski fakultet Opatija, Opatija 1993

[2] Marković, S. 1969. „Problem optimalne organizacije poduzeća u turističkoj privredi“, Ekonomski pregled, No. 3-5, Zagreb

[3] Morrison,A., Thomas,R.: „ The future of small firms in the hospitality industry“, International Journal of Contemporary Hospitality Management, 1999. Vol.11, No.4.

[4] Pavia,N.: „Management in the Function of Catering offer Develepment“ 2 international Scientific Conference „ Economics and Ecology in Function of Tourism Development“, Opatija-Bratislava, 1999

[5] Deželjin. J.: «*Upravljanje ljudskim potencijalima*», Organizator, Zagreb, 1996

[6] Grupa autora: „*Poduzetnički menadžment-izazov, rizik, zadovoljstvo*“, Sveučilište u Rijeci, HITA Zagreb, Zagreb.,2002.

[7] www.dzs.hr (26.8.2013.)

[8] Cerović. Z.: «*Hotelski menadžment*», Fakultet za turistički i hotelski menadžment Opatija, Opatija 2003.

[9] Holjevac. I. A.: « *Upravljanje kvalitetom u turizmu i hotelskoj industriji*», Fakultet za turistički i hotelski menadžment Opatija, Opatija 2002

THE IMPACT OF EU FUNDS ON RAISING THE QUALITY OF VOCATIONAL EDUCATION IN BROD-POSAVINA COUNTY

A. Vukasinović[1*], L. Vukojević[1] and I. Blažević[2]

[1] Brod-Posavina County , P. Krešimira IV br.1 35 000 Slavonski Brod, Croatia [2]College of Slavonski Brod, Dr. Mile Budaka 1, 35000 Slavonski Brod, Croatia
** Corresponding author e-mail: anica.vukasinovic@gmail.com*

Abstract
Vocational education provides acquiring of professional competencies that are required on the labor market. In the process of adjustment of the Croatian education system to the systems of developed countries which economies are based on knowledge, sustainability and inclusion, an investment into development of relevant, contemporary competence in vocational education is necessarily required. In the knowledge society vocational skills and competencies are as important as academic ones. Thereby, it is important to take into account about the compliance of the education system at all levels of the needs at the labor market in order that today's students could find their place in a competitive and demanding labor market tomorrow. The current budget allocation for education in Croatia have been reducing year after year, in contrast to developed countries, with a total allocation which significantly exceeds allocations of RH and what consequently reflects on the quality of the entire education system, particularly the vocational education. The current system of vocational education in the Republic of Croatia covers 70,9 % of the total secondary school population, i.e. 135,930 students in 290 schools. Enhancing of such system requires additional funding except decentralized funds that are received by the local governments from the state budget and provide the assurance of minimum financial standards of secondary education. One way of ensuring the quality of vocational education in Croatia is in using of EU funds that promote the mobility of students and teachers from vocational education, training and acquiring the necessary knowledge, skills and competencies. In this work we are going to analyze the impact of EU funds on the raising of the quality of vocational education in Brod-Posavina County.

Keywords: vocational training, labor market, quality, competencies

1. Introduction

On the development of the educational system there is a great impact of investments: in human capital, equipment, infrastructure, development programs, etc. The higher budget allocations for education contribute to the quality and competitiveness of the education system. The quality of the education system in Croatia does not monitor the quality of education systems in developed countries because of reduced spending on education. This is particularly evident in vocational education. New technologies introduce a whole range of new processes and new products in every aspect of life.

Today's labor market is influenced by changes in technology more than ever. According to statistics of the labor market, career opportunities in the fields covered by the new technologies are not only the fastest growing, but also one of the leading fields of professions. Education has a major responsibility to respond to the constant technological advance, and vocational education - through raising competence of teachers and students as well as improving of the quality of professional practice as the basic foundation of the existing as well as the future production and running economy. The substantial assistance offers the EU funds through various projects. Brod-Posavina, as the founder of vocational secondary schools in its area has actively participated in the contests for specific projects aimed at improving the vocational education in its area.

2. Vocational education in the world

The sudden increase in youth unemployment in many developed and developing countries is conditioned by the global recession. The number of young people who have not found their place in the labor market and did not have the resources and motivation to continue their education has significantly increased. The share of young people (age 18-24 years) in 2011. ranges from 4% (Netherlands) to 20% (Italy and Greece) in Europe, 12% in Australia and New Zealand, 15% in the U.S.[1]. In developing countries, the percentage is even higher, ranging from 20 to 25%.

Vocational education and training provide the skills necessary to work and to achieve a successful professional career [2] [3]. However, in developing countries there is a gap between the knowledge and skills that young people have acquired by education and the labor market needs, which is necessary to reduce in order to influence on a high unemployment rate [4]. Experiences show that the

vocational education system especially in Central Europe is far from desirable because it characterizes a clear division between education and work [5].

Namely, according to the employer's statements it is hard to find young people with the necessary technical knowledge and skills. The importance of vocational education varies considerably from country to country around the world, as well as the organization itself. The solution is the introducing of the effective system of vocational education as an important pillar of transformation into knowledge-based economy. However, before that, it is important to solve the issue of financial allocations for education that are mainly budgetary and on which depends the quality of the education system, and thereby the vocational education.

According to data from the United Nations Educational, Scientific and Cultural Organization (UNESCO), Cuba is with 12.9% consumption of total GDP, which it allocates for the education sector in the first place in the world. Until now it was considered that such primacy belongs to the Scandinavian countries and New Zealand, but the first place had to be ceded to the land which copes with the problems caused by the financial and economic sanctions. It should be noted that Iceland allocates 7.8% of the total GDP, Sweden 7.3%, New Zealand 7.2%, Norway 7.3% and Finland 6.8%.

3. Investment in vocational education in Croatia

Vocational education in Croatia, training and development as an activity which enables the development and acquisition of competencies required to obtain vocational qualifications is regulated by the Vocational Education Act, and special regulations and the law which regulates the activity of secondary education.

The aim of vocational education is to enable students for acquiring of basic and vocational competencies for obtaining the qualifications that are necessary on the labor market, then for further education and lifelong learning and in function of personal development and economic and general development of the society as well as enable international comparability of acquired vocational qualifications and the development of the open curricula.

The relevant ministry has adopted the Strategy for Development of Vocational education and Vocational Education Act with the aim of flexibility of vocational education to the needs of students and the labor market through modernizing of the content, methods of vocational education and assurance of the continuing education opportunities. The Agency for Vocational and Adult Education has been since its establishment actively involved in the implementation of numerous international and bilateral projects in the field of vocational education and training: CARDS 2002, 2003, 2004, Instrument for Pre-Accession Assistance (IPA), MATRA, SKILLS @ WORK in order to improve the quality of vocational education in the Republic of Croatia by additional funding.

The share of budget allocations of RH for Ministry of Science, Education and Sports from GDP is decreasing, but not just in the next year, by projections of the Government of RH, but also in the future years. If this accomplishes, there will be a reduction of the budget share for the Ministry of Science in GDP, from 3.6% in the year 2011. to 3.2% in the 2013., 3.05% in the 2014. and 2015. to the low 2.95%.

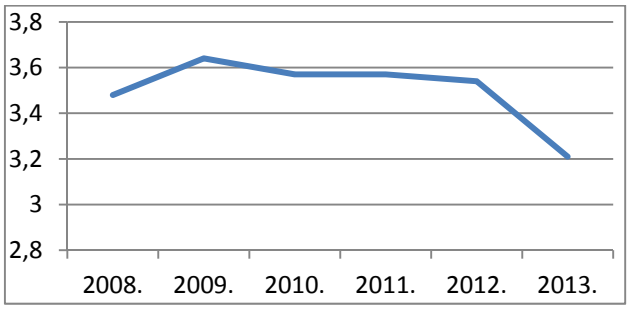

Figure 1. Budgetary allocations for the Ministry of Science [6]

Table 1. Shares for decentralized functions as a percentage of income tax [6]

Shares for decentralized functions	Cities and districts	City of Zagreb	Counties
Secondary schools		2.2%	2.2%

4. Using of the EU funds in raising the quality of vocational education in the Brod-Posavina County

The quality of vocational education in the area of Brod-Posavina County is determined primarily by proportional allocation for secondary education in the Budget of Republic of Croatia, which is then distributed to the local and territorial (regional) governments (Brod-Posavina County) that are the founders of the secondary schools in its area. The founders of secondary schools establish the investment priorities.

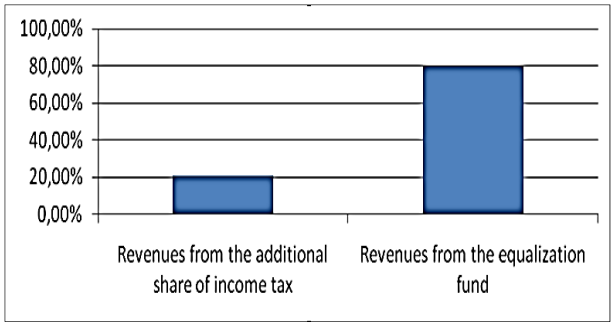

Figure 2. Decentralized functions of secondary education Brod-Posavina County in 2012. – the structure of income [7]

In 2012. Brod-Posavina County, due to the very low GDP per capita and fiscal capacity, realized 79.56% of the revenues for assurance of ensuring minimum financial standards of secondary schools from Funds Settlement (12.121.226,00 HRK) and only 20.84% of revenues from the additional share of income tax (3.191.782,59 HRK).

So the original budget revenues of Brod-Posavina County do not contribute to the improvement of the education system in its territory or in any segment, but only maintaining the minimum standards.

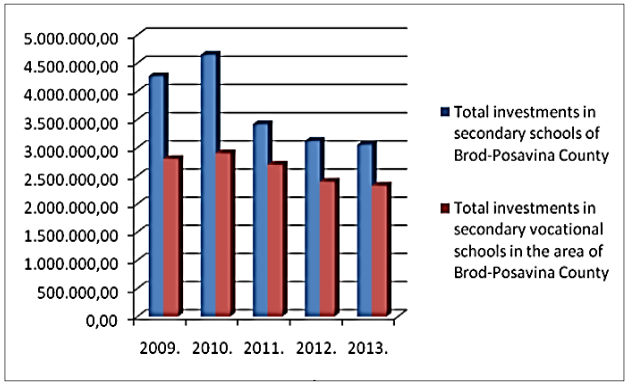

Figure 3. Investment in secondary education in the Brod-Posavina in the period 2009 to 2013 [8]

Although, realistically Brod-Posavina County does not have enough funds from the original budget with which it would improve the operation of secondary schools in its area, it invests almost 71% of the total funds received from the Funds Settlement (State Budget) into vocational schools in its area. However, all of these funds are not sufficient for effective vocational education in Brod-Posavina County and for increasingly demanding needs of the labor market. The opportunities for improvement of vocational education are in the use of EU funds.

Brod-Posavina County has invested considerable efforts in building the institutional capacities that are necessary for effective absorption of the EU funds, and devoted a special attention exactly to the raising of the quality of vocational education. Thus, in the period 2007-2013 through the CARDS and IPA programmes, the secondary schools in the area of Brod-Posavina County realized EU projects of total value 28.883.000,00 HRK, what is a very significant amount, especially if it is compared with the total investment from the budget of the county.

The most important results of these projects are the built infrastructure, equipped laboratories and practicums, raised knowledge level of vocational and other professors, as well as the knowledge level of students of vocational schools and harmonization of vocational training and labor market needs.

5. Conclusion

By strategic thinking in establishing of guidelines, development and competitiveness of the Croatian economy, the education has to be made as a priority segment investment, because the investment in education and training for creation of new knowledge and skills provides obtaining of competencies required at the labor market, reducing of the unemployment rate of young people, as well as the development of the entire economy. The education system has a difficult task, to train young people for the challenges posed by the knowledge society. The role of vocational education and training in this part is crucial. In searching of new forms of financing all stakeholders have to be involved; founders of educational institutions, schools, business entities, international institutions. The part of vocational schools in Brod-Posavina County has already successfully used the resources available in the pre-accession funds, and even the next year EU structural funds will be available and will give the opportunity to vocational schools of Brod-Posavina County in meeting the European standards and achieving the goals that are set in the regional, national and European strategies.

6. References

[1] OECD, Employment Outlook, United Kingdom, OECD Publishing, Paris, 2012.
[2] G. Quintini, S. Martin, “Starting well or losing their way? The position of youth in the labour market in OECD countries”, OECD Social, Employment and Migration Working Papers 39, Paris, 2006.
[3] J. Middleton, A. Ziderman, A. V. Adams, “Skills for Productivity: Vocational Education and Training in Developing Countries.” New York: Oxford University Press, 1993.
[4] R. Almeida, J. Behrman, D. Robalino, “The right skills for the job?: Rethinking training policies for workers”, World Bank

Publications, World Bank, Washington, DC., 2012.
[5] T. Matkovic, "Recent developments in the education system and school-to-work transitions in Croatia", Working Paper 138., Mannheimer Zentrum für Europäische Sozialforschung, 2008.
[6] Ministry of Finance, [Online] Available: http://www.mfin.hr/hr/raspodjela-poreza-na-dohodak-temeljem-zakona-o-financiranju-jlprs [Accessed: 21-Jul-2013]
[7] Ministry of Science, Education and Sports, 2012.
[8] Documents of Brod-Posavina County

USING OF THE EU FUNDS IN BROD-POSAVINA COUNTY IN THE PERIOD 2006-2013

L. Vukojević[1*], V. Bartolović[2] and M. Martinović[2]

[1]Brod-Posavina County, P. Krešimira IV br.1 35 000 Slavonski Brod, Croatia
[2]College of Slavonski Brod, Dr. Mile Budaka 1, 35000 Slavonski Brod, Croatia
* *Corresponding author e-mail: lvukojevic@gmail.com*

Abstract
Since 2001. the Republic of Croatia has been allowed to participate in various EU programmes that provide opportunities for financing the development needs of local and regional government, for what until then its own funds were not sufficient. Brod-Posavina County has recognized the need of strengthening of human capacity and creating its own "pipelinestockpile" of project proposals and that is why in 2005. with technical assistance from foreign consultants, it develops strategic development documents and establishes the Department of Development and EU integration. In the period of 2006 - 2013, Brod-Posavina County, as an applicant, a partner or through the provision of technical assistance has participated in the preparation and implementation of 102 projects with a total value of 61 million EUR. In the period 2006-2009. from that were financed under CARDS, PHARE, SAPARD, INTERREG and other programmes of foreign aid, and in the period 2009-2013 mobility programmes and 42 projects under IPA have been financed.
In the process of preparing for the absorption of structural and cohesion funds, Brod-Posavina prepared "supply" of 224 project proposals, distributed in 4 strategic development objectives.

Keywords: European Union funds, Brod-Posavina County, development objectives

1. Introduction

Financing local development projects through EU funds presupposes the existence of their built institutional and human capacity. Pre-accession funds are intended for the candidate countries in order to implement political, economic and institutional reforms that are required for EU accession, to prepare for effective programming, implementation and management of the Structural and Cohesion Funds [1]. Brod-Posavina County is one of the counties that have been started with the process very early and with the application of the new methodology in a short time have managed the achieving of significant results.

The starting point in defining the development goals was a creation of the Regional Operational Programme for the period 2005-2012., the establishment of the Department of Development and EU integration, and work on the preparation and implementation of projects before IPA (CARDS, PHARE, SAPARD, INTERREG, PSGO). In the same period of time employees of the Department of Development and EU Integration in collaboration with the Centre for Development and with the help of consultants of Dutch company Ecorys held more than 450 meetings with potential applicants of the projects.

As the Brod-Posavina area was affected by the war it received for the development of this document financial and technical assistance of the European Commission through the CARDS programme, which served as an instrument of support and implementation of the Stabilisation and Association Agreement [2].
After basic and detailed SWOT analysis of Brod-Posavina County's vision and goals, priorities and measures for the realization of the vision were defined, according to the methodology and principles of operating in the European Union. In the process of defining the strategy it was used participative "bottom-up" approach. As a basic development objectives there were set:
• Strengthening the economy in a manner leading to significant and lasting reduction in unemployment
• Provide infrastructure required for the expansion of businesses and the sound management of the environment
• Enhanced development of the educational system in a manner that is relevant to the economy
• Development of social infrastructure aiming to improve the position of vulnerable groups [3].

2. Methodology

For the purpose of this work, analysis of the following were made: Regional Operational Programme of Brod-Posavina County 2005 - 2012, County Development Strategy of Brod-Posavina from 2011. to 2013., data and projects that Brod-Posavina applied in observed period, the values of contracted funds, according to the IPA pre-accession assistance and other resources, and there are presented the perceived benefits and challenges during the mentioned process.

3. Results

ROP is created with the aim to enable to Brod-Posavina County efficient use of the pre-accession EU funds (CARDS, ISPA, PHARE, SAPARD,...) and EU structural funds, as soon as they would be available for Croatia. After defining the ROP

strategy and criteria for selection of projects that will be financed, the supply of 250 project proposals from all spheres of social life has been collected [2].

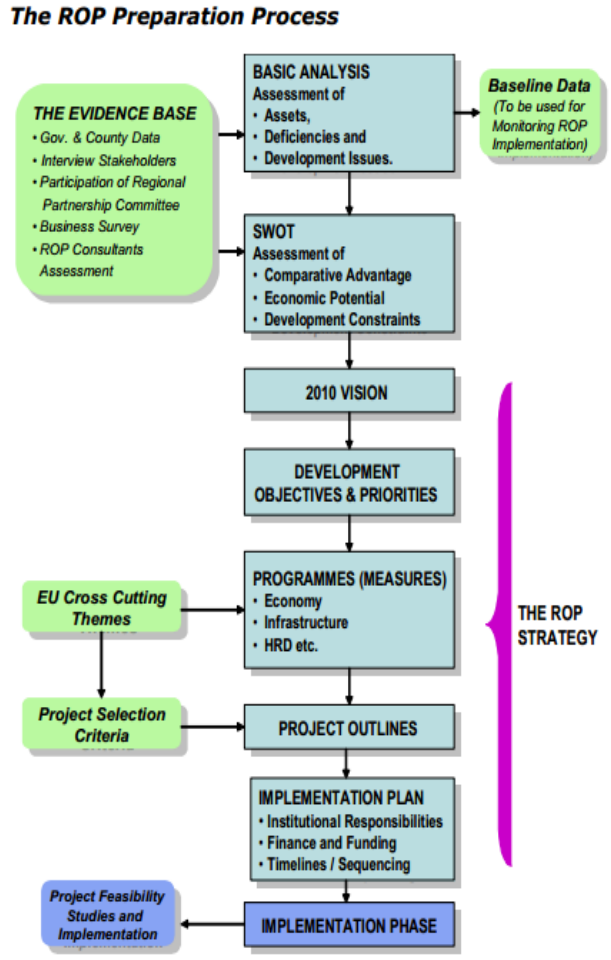

Figure 1. The process of developing ROP, Source: Regional Operational Program Brod-Posavina County 2005-2012 [3]

Projects that Brod-Posavina nominated on the contest programme CARDS 2004. are highly ranked by the Ministry and the European Commission because they contribute to economic and social development, and refer to the following priorities and measures:

a) Local Employment Partnerships value of contracted projects: 1,405,000 HRK

b) Environmental protection and sustainable development of the value of contracted projects: 730,000 HRK

c) Investment in business infrastructure and the education system - the value of contracted projects: 22,700,000 HRK

d) The SAPARD program - Value of approved projects: 6,723,535 HRK

e) PHARE program - The value of approved projects: 365,000 HRK

f) INTERREG - The value of approved projects: 4,600,000 HRK

g) Other programs:

PSGO - a project of social and economic recovery of areas of special state concern. The value of approved projects: 29,445,288 HRK.

EIB European Investment Bank. The value of approved projects: 59,657,448 HRK

Table 1. Recap - sources of funding (EU and others) in BPŽ in the period 2006-2009 [6]

Nr.	SOURCE OF FINANCING	Number of projects	Amount in HRK
1.	EUROPEAN PROGRAMMES	11	36.523.535
2.	PSGO	27	29.445.288
3.	EIB	18	59.657.448
	TOTAL	**56**	**125.626.271**

Although in the initial period of using EU funds were noted numerous problems and shortcomings, such as insufficient and nonconforming purpose of projects, insufficient number of personnel with the necessary knowledge and skills for preparation and application of projects EU funds, the lack of legislation in the field of regional development, analysis of the capacity of counties and development agencies, which were 2007. conducted by the Ministry and the Institute for International Relations, ranked Brod-Posavina County in the top by value implemented projects and by preparation of human capacities for the preparation and implementation of projects [4].

Brod-Posavina has made significant efforts in education and informing to help preparing for the significant resources that have been available since 2007. under the pre-accession IPA (Instrument for Pre-Accession Assistance) and consist of five components:

IPA I: Transition Assistance and Institution Building - supports activities directed on construction and strengthening institutional framework that is related to the adoption and implementation of the EU acquis. The users of this component are government bodies, bodies in the public domain, non-governmental organizations, the business community and other non-profit entities.

IPA II: Cross border cooperation - supports activities related to cross-border cooperation with Member States and beneficiary countries of the IPA, and is based on a multi-year program of cross-border cooperation. The users of these components are border regions, i.e. counties with land and maritime borders of Croatia.

IPA III: Regional Development - supports infrastructure projects in the sectors of environment protection and transport as well as programs for enhancing the competitiveness and regional development. The users are government

bodies, public and research institutions and the business community.
IPA IV Human Resources Development - supports measures directed to motivating of employment, education, training and social inclusion, as a precursor to the European Social Fund (ESF). Users are government bodies, public institutions, social partners and non-governmental organizations.
IPA V: Rural Development (IPARD) - supports preparations for participation in the common agricultural policy and rural development. Users are local governments, farms and other physical / legal entity [5].

In the period 2009 - 2013 Brod-Posavina County as an applicant, a partner or technical assistance has participated in the preparation and implementation of 43 projects total value 335.319.000 HRK, that have been financed by the various components of the IPA and other EU programs (Mobility, PHARE 2006) [6].

Table 2. Recap – The utilization of EU funds in Brod-Posavina County in the period 2009 – 2013 [6]

Nr.	Name of the programme	Number of projects	The value of the project, HRK
1	IPA II	3	7.600.000,00
2	IPA III	3	241.850.000,00
3	IPA IV	15	20.327.000,00
4	IPARD	15	63.147.739,16
5	OTHER (PHARE 2006, mobility)	7	2.394.700,00
	Total	**43**	**335.319.439,16**

If we observe the value of projects by individual components of IPA programme, IPA component III has the largest share Regional competitiveness, but very significant is also IPA component IV - Human Resources Development, because the large number of nominated and implemented projects significantly increased the absorption capacity of potential applicants in Brod-Posavina County.

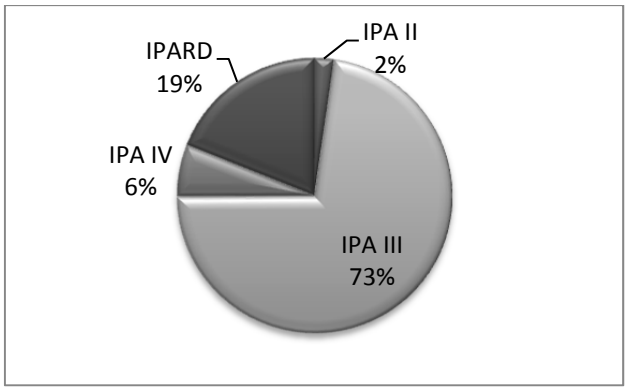

Figure 2. Utilization of EU funds per IPA component in Brod-Posavina County [6]

4. Discussion
Total value of contracted projects in the observed period is 460 945 710 Kn. In the structure of financing European funds participate with 81%, the projects approved under the program of social and economic recovery of Areas of Special State Concern (PSGO) funded by World Bank loans participate in the amount of 6% and the projects financed by the European Investment Bank in the amount of 13%.

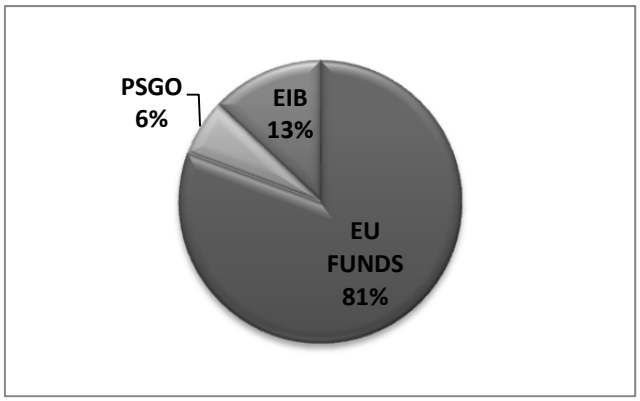

Figure 3. Recap of funding sources of contracted projects in the period of 2006–2013 [6]

In the period of preparation for Croatia's entry into the EU and using of Structural Funds, Brod-Posavina County has developed medium-term strategic document called the County Development Strategy 2011-2013.

After conducted analysis, the following strategic development goals are identified:

1. Strengthening of the economy in a way that leads to a significant and continuous increase in employment and quality of working places.

2. Environmental protection as a basis for sustainable development and economic activities.

3. The continued development of the education system in accordance with the needs of the economy

4. Improving the quality of life, development of social infrastructure and improving the position of vulnerable groups [7]

5. Conclusion

EU grants in the Brod-Posavina represent one of the major drivers of regional development, especially if we consider relatively weak capacity of the original budget and the inability of financing development projects from its own resources or from resources from the central state. Except the financial benefits, through participation in the pre-accession funds of the EU in Brod Posavina County a new methodology is introduced which is based on the strategic development planning partnership approach and continuous monitoring of achievement of objectives. Pre-accession funds also were used for the building of institutional capacities which were necessary for effective absorption much more abundant structural funds.

6. References

[1] M. Belić, G. Ćorić, B. Peurača, G. Stojanović, A. Tonč, „EU fondovi – Vodič kroz europske fondove 2008.-2013.", 2008.
[2] S. Novota, I. Vlašić, R. Velinova, K. Geratliev, O. Borissova, „Europski fondovi za hrvatske projekte, Priručnik o financijskoj suradnji i programima koje u Hrvatskoj podupire europska unija", 2009.
[3] Brodsko-posavska županija (BPŽ), „Regionalni operativni program BPŽ 2005 – 2012", 2005.
[4] Institute for International Relations, Zagreb., Ministry of the Sea, Tourism, Transport and Development, „Overall analysis of existing capacity in counties and CDAs for the preparation and implementation of projects financed from international sources", 2007.
[5] Središnji državni ured za razvojnu strategiju i koordinaciju Europske unije, „Programi Unije", 2009.
[6] The report of the Board for Development and EU integration of Brod-Posavina County

BIOMECHANICS OF DENTAL IMPLANTS WITH 3D FEA

Eda Ozyilmaz[1*], Halil Aykul[2]

[1]Amasya University Technology Faculty, Department of Mechanical Engineering, Amasya, Turkey
[2]Hitit University Engineering Faculty, Department of Mechanical Engineering, Corum, Turkey
* *Corresponding author e-mail: eda.ozyilmaz@amasya.edu.tr*

Abstract
Applying appropriate stress through the teeth is considered essential for maintaining the homeostasis of the jaw. The aim of this study was to clarify the effects of forces applied via endosseous implants on internal structures of the jaw. This numerical study was carried out using three – dimensional finite element method (FEM). Human mandible model is transferred from CT. Solid models of implants were built up in Solid Works and then transferred to a mesh model in FEM (ANSYS) to perform a stress analysis. The results showed that the maximum stress and deformation values are concentrated on the implant and abutment interfaces.

Keywords: Finite Element Analysis, Dental Implants, Fully Edentulous, Mastication Force, Micro Movements

1. Introduction

The Recent studies have clearly shown the effectiveness of endosseous implants as one of the treatment options in the field of prosthodontics [1, 2]. Implants of various shapes and properties are being developed, and procedures and techniques are becoming more diversified. From the standpoint of anatomy, interesting structural changes occur in mandibular trabecular bone due to functional pressure following long-term use of endosseous implants. Moreover, the motivation of this work was a planned integration of structural analysis into a computer aided design/computer aided manufacturing (CAD/CAM) software. CAD/CAM for dental restorations is a commonly used method of production [*3*].

On the other hand, the use of finite element analysis in dental biomechanics has been submitted to a significant increase during the last decades. Some authors [*4*-6] often carry out very simplified finite element models instead of using realistic ones. Thus, regarding these models the results are being quite different and non reliable because of not being able to have loading conditions that is similar to real one. Therefore, if reliable results want to be obtained from the analysis, we have to design more carefully and realistic models. Sufficiently fine meshes have to be used in peri-implant zones [*6*-7]. Boundary conditions need also to be modelled very accurately in order to obtain real interactions. For example, the precise modeling of muscular actions during mastication is required to avoid significant errors in the stress and strain distribution [8].

2. Method

The commercial software package ANSYS 14.5 was used for the finite element analysis. The STL data was imported, and a curvature-based mesh was created. The finite element model was generated by 95390 nodes and 54292 tetrahedral solid elements. The three dimensional model of the mandible were scanned with the use of Next engine laser scanner to obtain more realistic design and results. To get the accurate geometry of the prosthesis and mandible, a computed tomography exam was carried out on the patient. 3D model of dental implants were designed with Solid Works 2013 for each kind of teeth models. In order to see the effects of mastication forces then we transferred 3D geometry to Ansys Workbench to make analysis on stress distributions. The geometry was meshed with Ansys Workbench Meshing tools to have realistic results. The dimensions of designed dental implants for incisor and molars are given in Table 1. In this analyze, incisor dental implants are taken into consideration. The dental implants are shown in Figure 1.

Table 1. The dimensions of implants

	Lower Diameter (mm)	Great Diameter (mm)	Pitch (mm)	Total length (mm)
Type 1 (molars)	3.2	5	0.5	15
Type 2 (incisors)	2	3	1	17

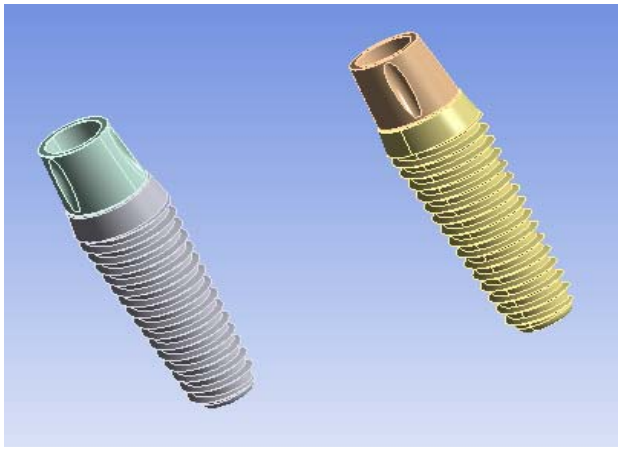

Figure 1. Designed Dental Implants

The material properties used in analysis are given in table 2.

Table 2. The Material Properties

	Modulus of Elasticity (MPa)	Poisson's Ratio (v)	Shear Modulus (MPa)
Titanium 6Al-4V	103 400	0.35	38296
Cortical Bone	13 700	0.30	5269,2
Trabecular Bone	1 370	0.30	526,92
Plate Mucosa	680	0,45	234,48
Dental Porcelain	70,000	0,17	29915

After the modeling process of dental implants and mandible, all threads during mesh generation process must be meshed very carefully for having more reliable results (Fig 2).

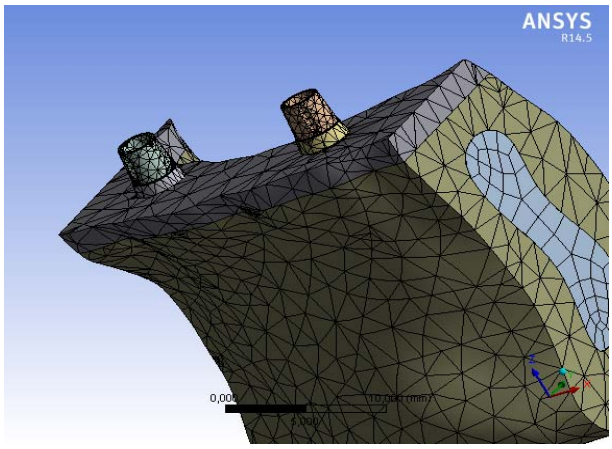

Figure 2. Meshed view

In order to analyze effects of mastication forces to human mandible and implant fixture, we applied the loadings which was equal to 150 N. The placement of loading can be seen in Figure 3.

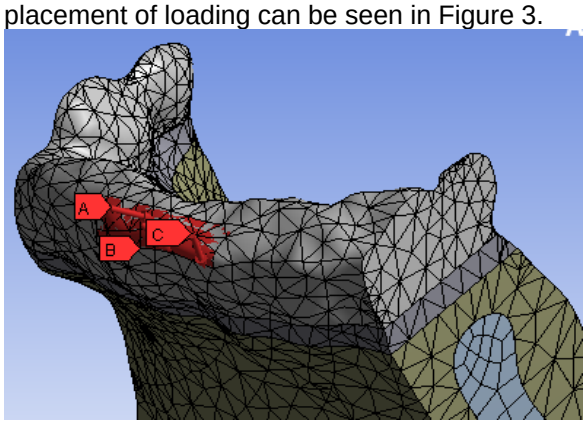

Figure 3. Applied Forces

3. Results

The distribution of equivalent stresses and total deformation in the mandible and implant components are presented in this study. The finite element analysis revealed different tensile stress concentration zones in the connectors. The results are obtained for mandible, implant, abutment and their connection regions. Total deformation results just for implants can be seen from Figure 4. It can be observed that the deformations are concentrated on implant abutment connection region.

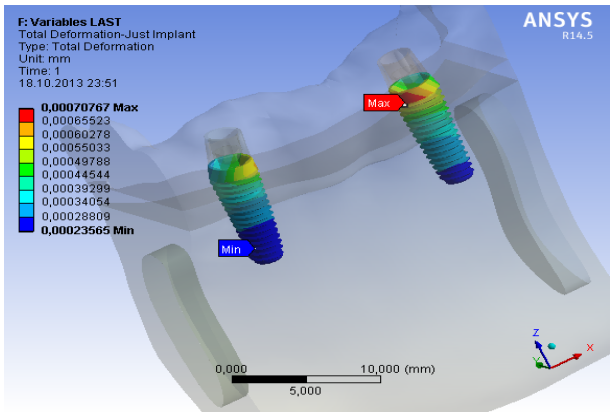

Figure 4. Total Deformation Results Just for Implants

When we look for the equivalent stress of just implants, It can be seen that the maximum stresses are at the connection region of implant and abutment (Figure 5).

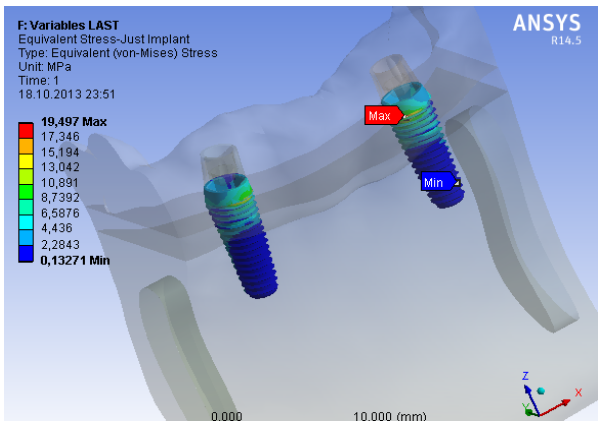

Figure 5. Equivalent Stress Results Just for Implants

The results of total deformation for abutments and equivalent stress for mandible is given in Figure 6 and 7. It is very significant that the maximum stresses and deformations are being observed on the connection points of implant, abutment and mandible.

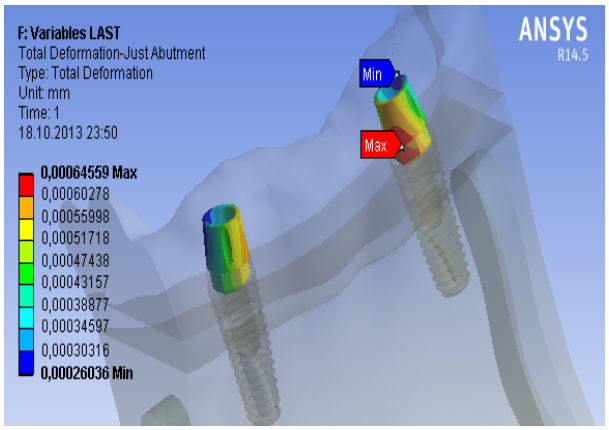

Figure 6. Total Deformation Results Just for Abutments

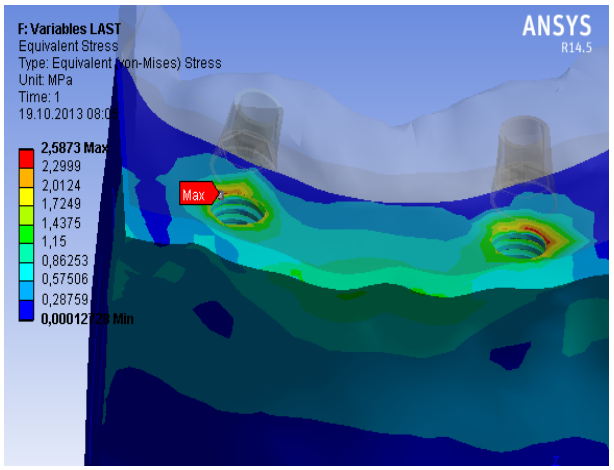

Figure 7. Equivalent Stress Results Just for Mandible

The maximum total deformation and equivalent stress for full body, full dental implant, just dental implants, just abutments and mandible are given in Table 2.

Table 2. The Results of Analysis for different parts

	Total Deformation (mm)	Equivalent stress (MPa)
	Maximum	Maximum
Full Body	0,0021769	24,444
Full Dental Implant	0,00070767	19,497
Just Implants	0,00070767	19,497
Just Abutments	0,00064559	14,495
Mandible	0,00085685	2,5837

4. Discussion

This study was carried out in order to analyze static behaviors of dental implants under 150 N loading with use of three dimensional finite element methods. It can be understand from the results that the implant-abutment and implant-mandible connection regions are the most important parts. The maximum deformations and equivalent stresses are concentrated both regions. The mechanical behavior of bone is difficult to model because of its anisotropic structure. And also there are some other reasons such as age, sex and type of bone which makes it more difficult to model. Due to these reasons, the mechanical properties of bone are being used as isotropic in most of studies. Consequently, we made all our investigations and observations as our bone properties are isotropic.

The highest stresses are observed especially on the neck of dental implants. When we compare the results for all components, it can be seen that the maximum equivalent stress on implants are 19,497 MPa and abutments are 14,495 MPa. The maximum values are generally concentrated on the connection points of implant and abutment. The design of these parts are really important for long-term durability of dental implants. These results are also supporting the view of importance on micro movements between implant and abutment during chewing activities.

5. Conclusion

A mandible was analyzed by Micro-CT and dental implants designed on Solidworks to prepare a finite element model of the mandible, including implants and the surrounding internal microstructures. Based on this model, mechanical analysis was conducted by the three dimensional finite element method. The results showed that stress distribution was seen in the trabecular bone around the implants. It became clear that loading is transmitted to mandibular internal structures via implants and stress is dispersed along internal trabecular alignment.

Maximum stress values are observed at implant-abutment interfaces. The design of these interfaces must be done very carefully in order to eliminate micro movements. On the other hand, the dentists should be take care on these parts during implantation period. In addition to these preventions, patients must be very careful on their oral health to use their implant lifelong. Even a small piece can cause micro movements and bone losses depending on this.

6. References

[1] Brånemark, P.I., Engstrand, P., Ohrnell, L.O., Grondahl, K., Nilsson, P., Hagberg, K., Darle, C. and Lekholm, U. Brånemark Novum:a new treatment concept for rehabilitation of the

edentulous mandible. Preliminary results from a prospective clinical follow up study. Clin. Implant. Dent. Relat. Res. 1:2-16, 1999.

[2] Bornstein, M. M., Lussi, A., Schmid, B., Belser, U.C. and Buser, D.Early loading of nonsubmerged titanium implants with a sandblasted and acid-eched (SLA) surface: 3-year results of a prospective study in partially edentulous patients. Int. J. Oral Maxillofac. Implants 18:659-666, 2003.

[3] Petrie, C.S. and Williams, J.L. Comparative evaluation of implant designs-influence of diameter, length, and taper on strains in the alveolar crest. A three-dimensional finite element analysis. Clin. Oral Implants Res. 16:486-494, 2005.

[4] Satoh T, Maeda Y, Komiyama Y. Biomechanical rational for intentionally inclined implants in the posterior mandible using 3D finite element analysis. International Journal of Oral & Maxillofacial Implants 2005; 20: 533–9.

[5] Las Casas EB, Ferreira PC, Cimini CA Jr, Toledo EM, Barra LP, Cruz M. Comparative 3D finite element stress analysis of straight and angled wedge shaped implant designs. International Journal of Oral & Maxillofacial Implants 2008; 23: 215–25.

[6] Natali A. N, Pavan P. G., Numerical approach to dental biomechanics. In: Natali AN, editor. Dental biomechanics. London: Taylor & Francis; 2003, p. 211–39.

[7] Natali A. N, Pavan P. G., Ruggero A. L., Analysis of bone-implant interaction phenomena by using a numerical approach. Clinical Oral Implants Research 2006; 17: 67–74.

[8] Röhrle O., Pullan A.J., Three-dimensional finite element modeling of muscles forces during mastication. Journal of Biomechanics 2007; 40: 3363–72.

DESCRIPTION OF TECHNOLOGY AND FACTORS INFLUENCING MATERIAL REMOVAL BY ABRASIVE WATER JET TURNING

J.Cárach[1], S. Hloch[12], P. Hlaváček[2], J. Klich[2], A. Andrej[1] , D. Lehocká[1] and M. Šomšák[1]

[1]Faculty of manufacturing technologies of Technical university of Košice with a seat in Prešov, Slovakia
[2]Institute of Geonics Academy of Science of Czech Republic, v.v.i., Ostrava Poruba, Czech Republic
* Corresponding author e-mail: jan.carach@tuke.sk

Abstract
This article deals with the analysis of the technological factors influencing material removal by the abrasive waterjet turning. The preparation of semi-finished products and the machining with the abrasive waterjet is lately gaining in importance. This technology brings new possibilities and advantages against the conventional methods of cutting and machining of metal sheets and high strength materials with special properties.

Keywords:
Abrasive water jet, turning, technology, factors.

1. Introduction

With the increasing requirements on qualitative and economic indicators of production, new technological processes and methods are put into practice. Consequently, through the technological advancement of these processes, the research and development of technology, management, monitoring and control of technological parameters are improved as well. Nowadays, there is also an indisputable importance of eco-friendly technologies promoting the recycling of input and output raw materials and energies in the process of production. The AWJ offers a good alternative here.

2. State of the Art

Since 1900 the water jet has been commercially used in the machining of materials. Through the adding of abrasive particles, this method could be successfully used not only for the cutting of sheet materials, but also for the machining of semi-finished, complex shaped products. The material removal without heat-affected zone and with the high-precision of micro-cutting, represents a suitable method for cutting and machining of such materials, where the use of conventional methods can be problematic. [1]

The importance of the machining with the abrasive water jet (AWJ) is remarkable especially when used on composite materials, extra-firm and hard materials with special properties, used chiefly in the aerospace industry. [2]

The AWJ turning is an alternative to conventional turning, using the tool with a defined cutting edge, and offers a variety of applications of this technology for turning, milling, cutting, creating threads and holes in high strength materials (such as composites, ceramics, glass and stone). AWJ turning still does not completely fulfill the requirement of precision, because at the higher values of traverse speed, it often comes with the increase of roughness, the higher waviness of the surface, to the disunity in diameter for a given length and the compromising of the roundness of a workpiece. [7]

3. Mechanism of Material Removal

The material removal is realized through the mutual interaction of solid abrasive particles dispersed in the high-speed water jet with the rotating surface of a workpiece. Through the contact of an abrasive particle with the surface of the workpiece, the deformation and subsequent hardening of material occur. [7]

The impact of a succeeding particle causes further splitting and chipping of material, the resulting cracks spreading quickly in brittle materials. The washing out of these particles leads to further material removal. [3]

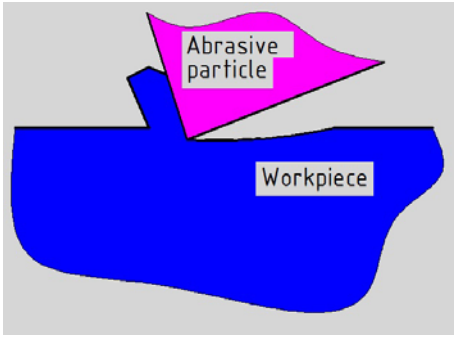

Figure 1. Contact of Abrasive Particle with the Workpiece

To reach an even material removal at the whole length of the machined surface, the correct values of technological parameters must be set. Similarly as with conventional turning, there is also a tool, performing a movement needed for the controlled material removal, the AWJ. [7]

4. The Priciple of Abrasive Water Jet Turning

With conventional up turning, the main rotatory movement is made by the workpiece and the tool with a defined cutting edge, makes a translatory movement. The same principle works by the AWJ turning as well, but in this case the tool, represented by the abrasive water jet, enables very fine removal of the material. This method, if the low tolerances are kept, also allows us to machine semi-finished products with a great length and small diameter. [2]

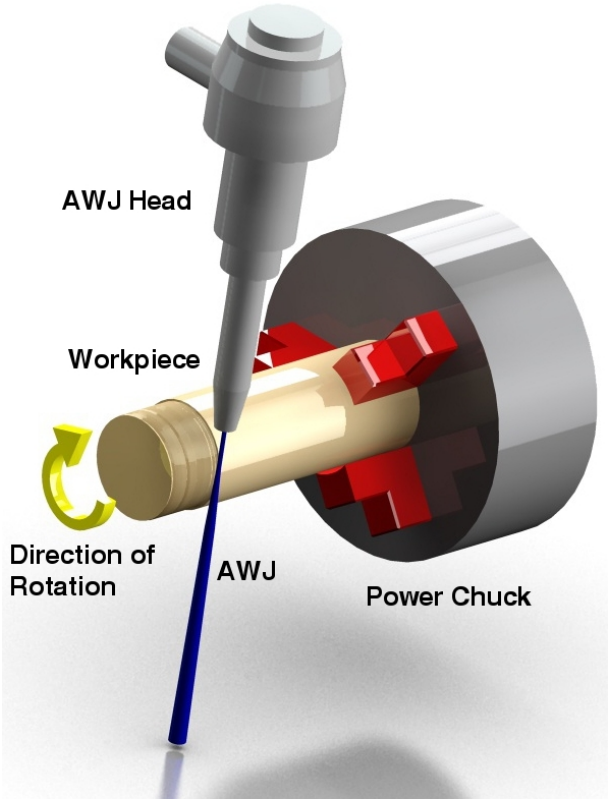

Figure 2. 3D Model of AWJ Turning

The significant advantages of this technology are relatively small cutting power (the power is under 40N) and the cold material removal (no heat-affected zone), enabling the machining of special materials (heat-sensitive alloys and composites), where conventional methods cannot be used. [9]

5. The Abrasive Materials

To enhance the efficiency of material removal, the Indian, Bengali and Australian garnet, olivine or corundum are used as the abrasive materials. The wear of the water focusing tube, caused by the use of abrasive materials for the hydro-abrasive cutting, subsequently leads to the worsening of the precision and the cutting quality. The advantage of using a natural garnet, is in its ability to break up into small grains with sharp edges. Moreover, this abrasive material does not chemically react with the workpiece. The size of grains is approximately 0,18 to 0,35 μm. For its durability, the garnet is suitable for recycling and may be used repeatedly in several cycles.[5]

Figure 3. A Natural Garnet [6]

6. Setting the Position of the Tool to the Workpiece

For the AWJ turning the machine for cutting of sheet materials, with the addition of a device for rotation and clamping of the workpiece is used. The correct setting of the technological parameters, affecting the final quality and precision of the machined surface, is of great importance here.

To set the right position of the workpiece and the AWJ,a radial mode and an offset radial mode can be used. Usually, the radial setting with the offset centre is used. [8]

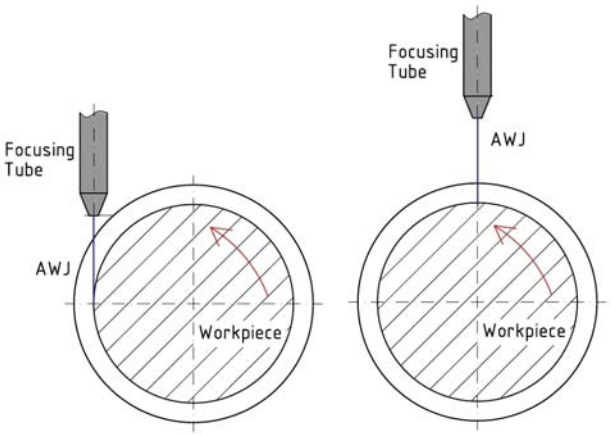

Figure 4. A Position of AWJ to the Workpiece [8]

The technological tool and workpiece alignment is usually realized similarly as with conventional turning. The rotating workpiece is clamped in the power chuck and the tool rotates parallel with the axis of rotation, whereby it is always moving closer to the required diameter of the workpiece, towards the center of rotation.
With down turning, (Fig. 5) the workpiece rotates in coherence with the direction of the AWJ, whereas in the conventional up turning method, (Fig.6) the workpiece performs a rotatory movement against the rotation of the AWJ.

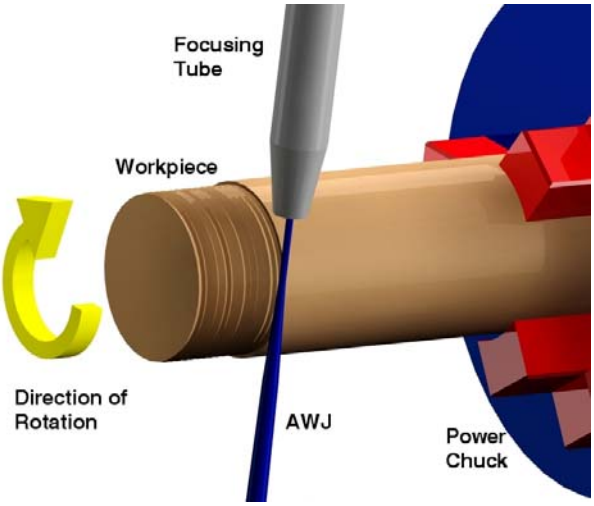

Figure 5. AWJ Down Turning

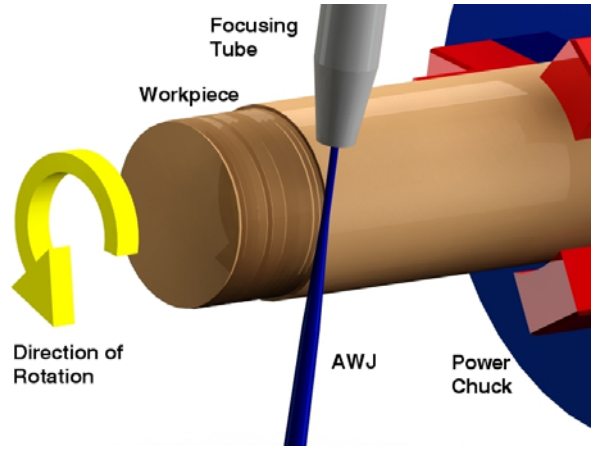

Figure 6. AWJ Conventional Up Turning

7. Factors Influencing the Material Removal

The qualitative indicators of a machined surface are influenced by many factors, such as technological, hydraulic, mixing and abrasive. Foremost it is the matter of:
The traverse speed - the higher value of traverse speed, the lower amount of abrasive particles, coming into contact with the machined material in a given time.
Tilt angle of the focusing tube - it is an angle between the axis of the AWJ and the surface of workpiece. According to the newest studies, the setting of the angle impacts the quality of machined surface.
The elevation – the distance between the surface of the machined material and the opening of the focusing tube.
The number of transitions – with the higher number of transitions, the higher depth of cut can be reached under the same conditions. Further on in process, the increase in depth of the cut declines, this is due to the resistance of the walls which prevents the penetration of the stream and its erosive effects.
The pressure – at the higher values of pressure, the higher values of the traverse speed and the depth of cut may be used as well.
The diameter of water nozzle – after leaving the nozzle, the abrasive material is added to the water jet and then runs through the focusing tube. To reach the required output speed of the AWJ, the right combination of diameters of the water nozzle and the focusing tube is necessary.
The length and diameter of focusing tube - determine the ability to focus the water jet with abrasive particles directly on the point of cut. With focalization comes the loss of energy, through the contact of abrasive particles with walls of the tube.
The abrasive - the qualities of an abrasive impact on the speed of material removal and on the possibility of repeatability and recycling.
The abrasive mass flow – the higher volume of particles, included in the water jet, can provide a higher impact on the machined surface. With the exceeding of optimal volume of abrasive particles, the kinetic energy of the stream declines, because of collisions, because of this, the depth of cut is reduced as well.
The material of workpiece – chemical properties and mechanical qualities of a workpiece. [10]
The speed and the direction of rotation of the workpiece – the factors influencing the waviness and the evenness of removed material.

A study from Zhong and Han, examining the influence of technological factors on the quality of the surface by hydro-abrasive turning of glass, stated that a lower traverse speed of abrasive water jet and higher rotation of the workpiece lead to the reduction of roughness and waviness of machined surface.[2]

8. Rationalization of AWJ Turning

The possibilities for rationalization directly lead towards the requirement to reach the most optimal qualitative indicators, in order to increase the economic efficiency, the effectivity of process and the speed of machining. The research should follow these goals:

- to increase the quality and productivity of machining,
- to gain the optimal settings of technological factors,
- to reduce the need of additional machining (operations),
- to increase the yields,
- to reduce the risks. [11]

With Hydro-abrasive turning it is necessary to focus on the optimization of the machining of a specific material together with the search for relationships between the setting of an angle and position of the cutting head, pressure, traverse speed and mass flow of the abrasive. For this reason it is necessary to choose criteria of input factors for a planned experiment. [10]

9. Conclusion and future direction of research

The technology of the turning with the abrasive water jet, without a heat-affected zone at the point of material removal, offers considerable advantages in pre-machining of composite, extra-firm and hard materials. For this reason, it is important to focus the research and the development of this technology on the improvement of qualitative indicators and on the increase of efficiency. The research, the development and the rationalization of the abrasive water jet turning may bring significant advantages and savings in comparison with other conventional methods, especially by the machining of so called "difficult-to-machine" materials. [4]

10. References

[1] HLOCH, S. – VALÍČEK, J.: "*Influence of Factors on Surface Topography Created by Abrasive Water Jet Cutting",* Faculty of manufacturing technologies of Technical university of Košice with a seat in Prešov, Prešov, 2008, ISBN: 978-80-553-0091-7

[2] ZOHOURKARI, I. – ZOHOOR, M. "*An Eerosion-based Modeling of Abrasive Waterjet Turning*" In: World Academy of Science, Engineering and Technology 38 2010. [Online]. Available: http://www.waset.org/journals/waset/v38/v38-65.pdf. [Accessed: 27-Sep-2013].

[3] ŤAVODOVÁ, M. " *The quality of the cut surface after abrasive water jet cutting*" In: Acta facultatis Technicae Zvolen- Slovakia. 2011 [Online]. Available: http://www.tuzvo.sk/files/FEVT/fakulta_fevt/tavodova-akta-fevt-2-2011-4.pdf [Accessed: 27-Sep-2013].

[4] UHLMANN, E. – FLÖGEL, K. – KRETZSCHMAR, M – FALTIN, F. "*Abrasive waterjet turning of high performance materials*" In: SciVerse ScienceDirect, 5th CIRP Conferenceon High Performance Cutting 2012

[5] KARKOVÁ, M. – SOBOTOVÁ L. " *Abrasive materials used in AWJ cutting of material technology*", Katedra environmentalistiky, Transfer inovácií 25/2013. [Online]. Available: http://www.sjf.tuke.sk/transferinovacii/pages/archiv/transfer/25-2013/pdf/146-149.pdf. [Accessed: 28-Sep-2013].

[6] Abrasives, Available: http://www.pan-abrasives.com/abrasives. [Accessed: 28-Sep-2013].

[7] MANU, R – BABU, R.N. "*An erosion-based model for abrasive waterjet turning of ductile materials*" In: ScienceDirect, Wear 266 (2009) 1091-1097 Available: http://www.springerimages.com/Images/RSS/1-10.1007_978-1-4419-7302-3_9-15. [Accessed: 28-Sep-2013].

[8] LI, W – ZHU, H. et al. "*An investigation into the radial-mode abrasive waterjet turning process on high tensile steels*" In: International Journal of Mechanical Sciences. May 2013

[9] AXINTE, A.D. – STEPANIAN, P.J. – KONG, C.M. – MCGOURLAY, J. "*Abrasive waterjet turning – An afficient method to profile and dress grinding wheels*" In: International Journal of Machine Tools and Manufacture, Volume 49, Issues 3-4, March 2009, Pages 351-356

[10] HLOCH, S. – VALÍČEK, J. – HREHA, P. – BEDNÁR, S. – PERŽEL, V. – LATOVÁ, A.: "*Online-identification Hydroabrasive separation using acoustic emission and vibration*", Fakulta výrobných technológií TU v Košiciach so sídlom v Prešove, Prešov, 2011, ISBN: 978-80-553-0698-8

[11] SZOMBATHYOVÁ, E.- KRAUSZOVÁ, A. "*Ways to streamline the work of manual assembly*" In:Transfer inovácií 11. 2008. [Online]. Available: http://www.sjf.tuke.sk/transferinovacii/pages/archiv/transfer/11-2008/pdf/71-73.pdf. [Accessed: 28-Sep-2013].

1.PN moulds & wire tools parts

We moulding Your idea

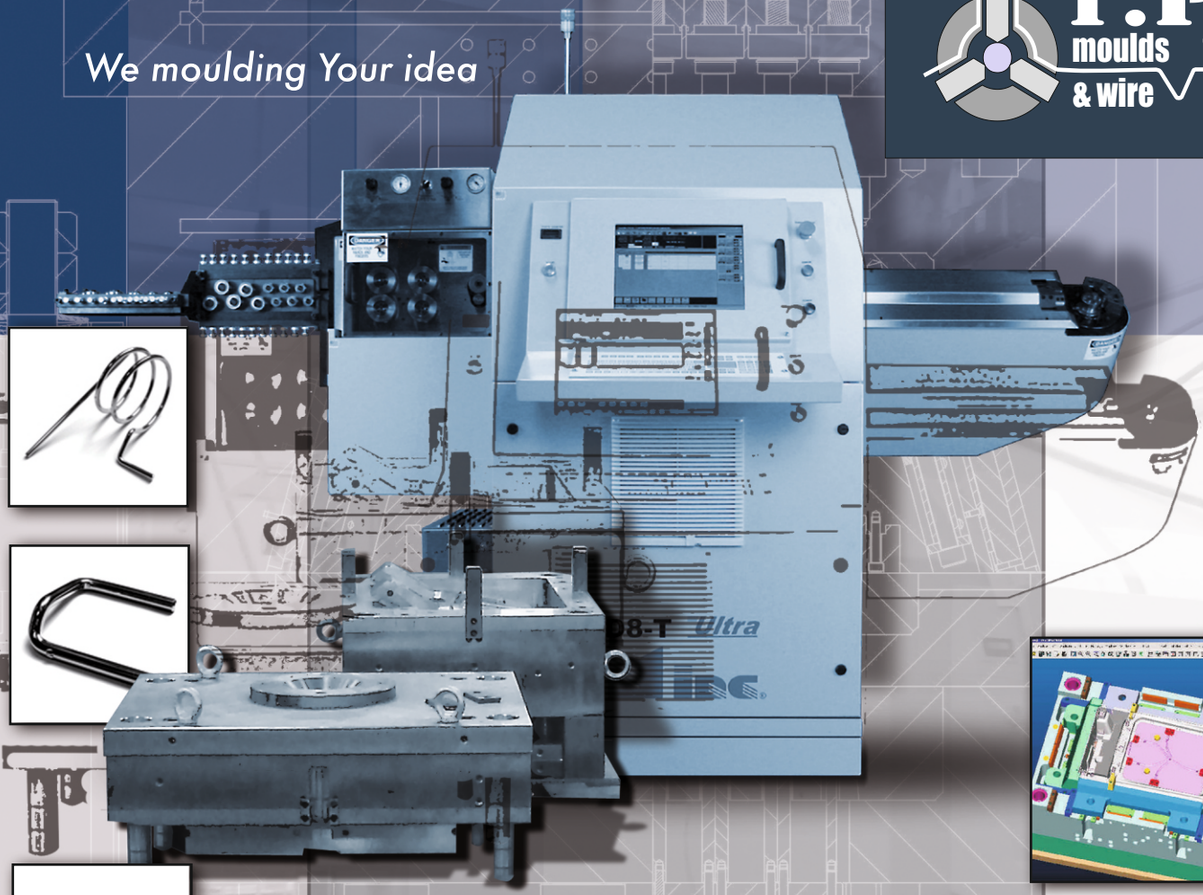

Company profile

1.PN is a private company, the main production program, of which is represented by the production of tools, injection molds for thermoplastics and dies, and shears and bending tools.
Using its more than 50 years of experience in the production of special tools, we provide our customers with professionalism in our collaboration, problem solving and in accommodating the production lead times with the support of modern technologies, software equipment and a team of highly qualified workers. As of 2008 we started serial production on a new CNC 3D wire bending machine.

The main objectives of the company are:

- Investing in the modernization of technologies and software in order to reduce the production lead times and to increase the quality and effectiveness of the production.
- Firmly establishing itself on its intended markets in cooperation with the electro-technical and automotive industries.

Within the vision of searching for possibilities of providing customers with a wider range of services in the area of design and development of plastic parts, production tooling necessary for serial production and finally the realization of such products, 1.PN and LPH Vranov n/T, s.r.o. entered into a mutual agreement on strategic collaboration.

References

Pressings from both molds and tools produced at 1.PN are used, directly or indirectly, by our customers, in assembly lines and plants of several companies, i.e.:

Our customers:

Whirlpool, VOLVO, XEROX, HELLA, SIEMENS, BOSCH, VW, GLOBAL GARDEN PRODUCTS

Contact

1. prešovská nástrojáreň, spol. s r.o.,
Ľubochnianska 2407/2
080 06 PREŠOV-ĽUBOTICE,
SLOVAK REPUBLIC
www.1pn.sk
info@1pn.sk
Phone: +421.51.7485052
Fax: +421.51.7485050

100 95 75 25 5 0

STORE – ARCHIVE – WARDROBES – MAILBOXES

MERCATOR DMS
Spol. s r.o. - G.m.b.H.
EXPORT - IMPORT

Furnishing for your storeroom, archive of a working place, cloakroom and a workshop

PROPOSAL, REALIZATION, GUARANTEE

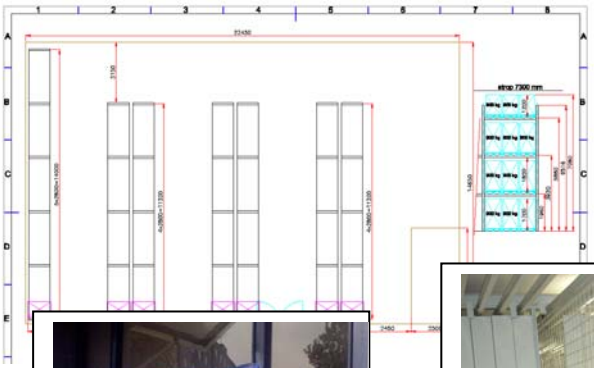

www.MERCATOR.sk
+421-2-63532160
mercator@mercator.sk

Certified by ISO 9001:2000
Certified by ISO 14001:2004
Certified by ISO /TS 16949:2002

LPH Vranov n/T, s.r.o.
PLASTIC PARTS & ASSEMBLY

LPH a.s.
PLASTIC PARTS & ASSEMBLY

Company profile

The company LPH Vranov n/T, s.r.o. has been operating in the manufacture of plastic products since 1989. The main activity of the company is injection molding of plastic components, including the sub-assembly and assembly of additional units. LPH is a limited liability company funded 100% by Slovak capital. LPH supplies its products and services to four continents around the world (Europe, Central America, South America and Australia). The new independent production plant of LPH a.s. situated within the Industrial Park Poprad - Matejovce started with serial production in October 2007.

Quality

- Metrology equipment (Mitutoyo, Mettler)
- Statistical methods for scoring




Services offered

- Design and project development
- Testing and verification of designed parameters
- Molds and tools design and production
- Metrology
- Production and measurements of samples
- Pre-serial production
- Validation
- Serial production
- Assembly / sub-assembly
- Stocking
- Transport and delivery

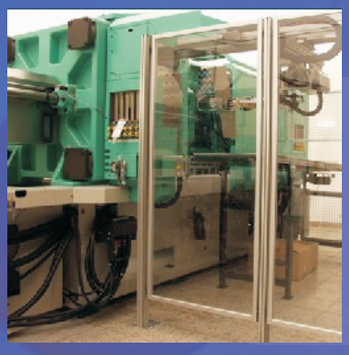


Our priorities

- Flexibility
- Development of new technologies
- Cost reduction
- Quality
- Advantageous prices
- Complexity

New activities

- Vacuum coating (by aluminum)
- Special chroming through painting
- Investment into new technology - (incl. 2K)

References

THE DOCUMENT COMPANY XEROX
Whirlpool
HELLA
MAGNA MAGNA MIRRORS
KŘIŽÍK
CONTITECH®
PUNCH
ParkettWorld
WILDEN
REGADA
STIGA
ALPINA
CASTELGARDEN
Mountfield

Contact

LPH Vranov n/T, s.r.o.
Pod dolami 838
093 02 VRANOV NAD TOPĽOU
SLOVENSKÁ REPUBLIKA

Tel.: +421.57.486 04 28
Fax.: +421.57.486 04 17
Email: lph@lph.sk
www: www.lph.sk

LPH a.s.
Priemyselná ul.
059 51 POPRAD - MATEJOVCE
SLOVENSKÁ REPUBLIKA

Tel.: +421.52.418 08 12
Fax.: +421.52.418 08 15
Email: info@lph-as.sk
www: www.lph-as.sk

www.lph.sk **www.lph-as.sk**

Complex Solution Under One Roof...

Title: **TEAM 2013 Proceedings**
Editors: LEHOCKÁ DOMINIKA
CÁRACH JÁN
KNAPČÍKOVÁ Lucia
HLOCH SERGEJ
Publisher: TEAM Society, Slavonski Brod, Croatia
Print: STEVEPRESS, Ltd., Prešov

ISSN: 1847-9065